NASA CR- 152113

AN INVESTIGATION OF WING BUFFETING RESPONSE AT SUBSONIC AND TRANSONIC SPEEDS: PHASE II F-111A FLIGHT DATA ANALYSIS

VOLUME II - PLOTTED POWER SPECTRA

David B. Benepe, Atlee M. Cunningham, Jr.,
Sam Traylor, Jr., and W. David Dunmyer

Prepared under Contract No. NAS 2-7091 by
GENERAL DYNAMICS CORPORATION
Fort Worth Division
Fort Worth, Texas

for

AMES RESEARCH CENTER
NATIONAL AERONAUTICS AND SPACE ADMINISTRATION

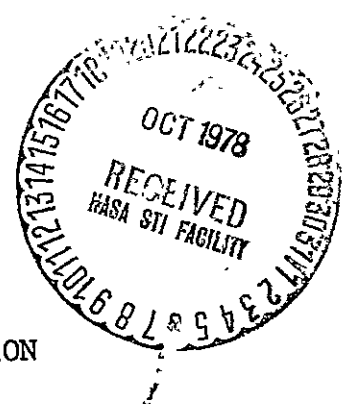

TABLE OF CONTENTS

LIST OF TABLES

LIST OF TABLES, Continued

LIST OF FIGURES

LIST OF FIGURES (Continued)

LIST OF FIGURES (Continued)

LIST OF FIGURES (Continued)

SUMMARY

A detailed investigation of the flight buffeting response of the F-111A was performed in two phases. In Phase I stochastic analysis techniques were applied to wing and fuselage responses for maneuvers flown at subsonic speeds and wing leading-edge sweep of 26 degrees. Power spectra and rms values of response were obtained for·

(1) vertical accelerations at the wing tips, the center of gravity and the pilot's seat,

(2) lateral accelerations at the center of gravity and the pilot's seat,

(3) vertical sheat, bending moment and torsional moment at 4 spanwise locations on the right variable sweep wing panel.

In Phase II the analyses were extended to include maneuvers flown at wing leading-edge sweep values of 50 and 72.5 degrees at subsonic and supersonic speeds and the responses examined were expanded to include vertical shear, bending moment, and hingeline torque of the left and right horizontal tails.

This volume presents plotted power spectra for all of the flight points examined during the Phase II flight data analysis. Detailed descriptions of the aircraft, the flight instrumentation and the analysis techniques are given.

Measured and calculated vibration mode frequencies are also presented to assist in further interpretation of the PSD data

The major conclusions of the investigation are:

(1) The structural response to buffet during moderate to high-g maneuvers is very complex. Many natural symmetric and antisymmetric natural vibration modes (and perhaps asymmetric modes) can be excited to significant levels of response.

(2) An array of different types of sensors and locations of the sensors is needed to adequately describe the structural response during buffet investigations.

(3) The modal content of the response varies with sensor type and location and also can vary with angle of attack, wing sweep and Mach number. The variations in modal content are attrituted to the variations in the spatial extent and phase relationships of the separated flows.

(4) At low wing sweep there are significant differences in the variations of rms response with angle of attack for different Mach numbers. The largest magnitudes of response were measured during flight

conditions where shock induced flow separations were present.

(5) In general, the rise in rms response with angle of attack becomes smaller as wing leading edge sweep is increased.

(6) The buffeting loads on the wing are small relative to the maneuver loads at the most inboard measuring station but become larger near the wing tip. The larger relative rms values of response near the tip are attributed to higher frequency modes and thus should be considered important from a fatigue standpoint with respect to secondary structure

The data obtained in this investigation were used to help formulate and evaluate a method of predicting buffeting response which uses wind tunnel measurements of the fluctuating pressures on a "rigid" wing as the input forcing function.

The entire investigation is documented in eight reports which are listed below.

Benepe, D. B., Cunningham, A. M., Jr., and Dunmyer, W. D.. An Investigation of Wing Buffeting Response at Subsonic and Transonic Speeds: Phase I F-111A Flight Data Analysis.

Volume I - Summary of Technical Approach, Results and Conclusions, NASA CR-152109.

Volume II - Plotted Power Spectra, NASA CR-152110.

Volume III - Tabulated Power Spectra, NASA CR-152111

Benepe, D. B., Cunningham, A. M., Jr., Traylor, S., Jr., and Dunmyer, W D.· An Investigation of Wing Buffeting Response at Subsonic and Transonic Speeds· Phase II F-111A Flight Data Analysis.

Volume I - Summary of Technical Approach, Results and Conclusions, NASA CR-152112.

Volume II - Plotted Power Spectra, NASA CR-152113.

Volume III - Tabulated Power Spectra, NASA CR-152114.

Cunningham, A. M , Jr., Benepe, D. B., Watts, D., and Waner, P. G.· A Method for Predicting Full Scale Buffet Response with Rigid Wind Tunnel Model Fluctuating Pressure Data.

Volume I - Prediction Method Development and Assessment, NASA CR-3035.

Volume II - Power Spectral Densities for Method Assessment, NASA CR-3036.

SYMBOLS

Note: Quantities are presented in the International System of Units (U.S. customary units in parenthesis). The work was performed using U.S. customary units.

b	wing span - m, (ft)
$B.M._{DES}$	design value of wing bending moment, N-m, (in - lb)
c.g.,C.G.	"center of gravity"
f	frequency, hertz
f_o	spectral base frequency or analysis bandwidth, hertz
F_Z	wing vertical shear as measured by strain gages - N, (lb)
g	gravitational acceleration
M	Mach number
M_X	Wing Bending Moment as measured by strain gages N-m, (in - lb)
M_Y	Wing torsional moment - N-m, (in - lb)
n_{max}	maximum maneuver load factor - g's
S	theoretical wing area (leading and trailing edges of swept panel extended to airplane centerline m^2, (ft^2)
T	length of input frame in spectral analysis - seconds
T_1	start time of interval for spectral analysis - seconds
T_2	stop time of interval for spectral analysis - seconds
ΔT	time interval used for spectral analysis = T_2-T_1,sec
V_{DES}	design value of wing vertical shear, N, (lb)
y	lateral acceleration g's
z	vertical acceleration g's

SYMBOLS (Continued)

α	indicated angle of attack referenced to wing manufacturing chord plane
α_{max}	maximum indicated angle of attack - deg.
α_{nom}	nominal angle of attack representing time interval ΔT
α_1	indicated angle of attack at time T_1, deg
$\Delta\alpha$	increment in indicated angle of attack during time interval ΔT, deg
β'	indicated sideslip angle, deg
σ_a	rms value of acceleration fluctuations - g, rms
$\sigma_{V_{max}}$	maximum rms value of wing vertical shear fluctuations - N, rms, (lb, rms)
$\sigma_{BM_{max}}$	maximum rms value of wing bending moment fluctuations - N-m, rms, (in - lb, rms)
Ψ_T	average rms value determined from power spectral analysis

ABBREVIATIONS

Alt	altitude
Asym	antisymmetric
B.M.	bending moment
Cross-PSD,XPSD	Cross power spectral density
dB	decibel
Dyn Press	dynamic pressure
FM	frequency modulation
H_z	hertz
hor,hori	horizontal
in-lb, IN-LB	inch-pound
inb'd	inboard
L	left
lb,LB	pound
L/H	left hand
LWT	left wing tip
m	meter
N	newton
N-m,N-M	newton-meter
outbd	outboard
P.S.	pilot seat
PSD	power spectral density
R	right
R/H	right hand

ABBREVIATIONS, (Continued)

rms	root-mean-square
RWT	right wing tip
Sym	symmetric
TOR	torsion
W.S.	Wing Station for strain gage measurements

SECTION 1

INTRODUCTION

A detailed investigation of the structural response of an F-111A aircraft to buffet during moderate to high-g maneuvers was accomplished in two phases. In Phase I (References 1, 2, 3) the response characteristics with the variable sweep wings set at a nominal leading-edge sweep of 26 degrees were examined for the seven maneuvers described in Table 1.

Power spectra and rms values of response were determined for 19 different measurement items consisting of vertical accelerations at the wing tips, the center of gravity and the pilot's seat, lateral accelerations at the center of gravity and the pilot's seat and vertical shear, spanwise bending moment, and torsional moment at 4 different spanwise stations on the right wing.

The conclusions reached from the Phase I Study were:

(1) The structural response during buffet is very complex. Many natural vibration modes both symmetric and antisymmetric can be excited during a maneuver in which flow separation occurs on the wings.

(2) The spectral content of the response varies with the type of sensor, the location of the sensor and in some cases with angle of attack.

Table 1

PHASE I FLIGHT MANEUVERS

FLT	RUN	MANEUVER	WING SWEEP DEG	NOMINAL FLIGHT CONDITIONS		
				MACH	ALTITUDE	GROSS WEIGHT
48	6	Windup Turn	26.6	.70	7,559 m (24,800 ft)	294,472 N (66,200 lb)
77	S&C-R	Windup Turn	25.6	.80	6,035 m (19,800 ft)	266,004 N (59,800 lb)
78	5	Pullup	26.2	.80	3,780 m (12,400 ft)	327,389 N (73,600 lb)
79	9R	Pullup	26.7	.80	1,494 m (4,900 ft)	323,386 N (72,700 lb)
60	10	Roller Coaster	26.6	.87	8,382 m (27,500 ft)	307,817 N (69,200 lb)
78	4	Pullup	26.3	.87	3,688 m (12,100 ft)	330,503 N (74,300 lb)
70	2	Pullup	26.8	86	1,494 m (4,900 ft)	328,800 N (73,800 lb)

(3) The variations of rms values of response with angle of attack can be quite different for different values of Mach number. The largest measured responses occurred under conditions where shock-induced flow separations occurred on the wing. In particular the torsional response was significantly higher than anticipated on the basis of previous buffet studies.

(4) The magnitudes of the wing bending and wing shear responses at the most inboard measurement station are small relative to the maneuver loads. Near the wing tip the buffet loads are a much larger percentage of the maneuver loads.

(5) Horizontal tail vibration modes appear to make significant contributions to the fuselage responses.

In Phase II the structural responses at nominal wing leading-edge sweeps of 50 and 72.5 degrees were analyzed. Vertical shear, bending moment and hingeline torque at the root of the left and right horizontal tails were analyzed in addition to the 19 measurement items examined in Phase I. All 25 items were studied for six maneuvers listed in Table 2. In addition the horizontal tail responses were analyzed for two wind up turn maneuvers from the Phase I Study as listed in Table 2.

Volume I (NASA CR-152112) summarizes the Phase II investigation in detail. This Volume (NASA CR-152113) presents plotted power spectra for all of the flight points and instrumentation items analyzed in the Phase II study. Sufficient information about the aircraft, the flight instrumentation and the analysis techniques is presented to allow the reader to perform additional

Table 2

PHASE II FLIGHT MANEUVERS

Flight	Run	Maneuver	Wing Sweep	Nominal Flight Conditions		
				Mach	Altitude	Gross Weight
61	R227	Windup Turn	49.1	.80	8,382 m (27,500 ft)	330,948 N (74,400 lbs)
51	S38/150	Slowdown Turn	49.5	1 25 - 1.13	10,912 m (35,800 ft)	278,903 N (62,700 lbs)
48	4	Windup Turn	49.8	1.20	9,053 m (29,700 ft)	261,111 N (58,700 lbs)
48	7R1	Windup Turn	72.2	.89	7,559 m (24,800 ft)	265,559 N (59,700 lbs)
48	5	Windup Turn	72.2	1.20	9,083 m (29,800 ft)	274,455 N (61,700 lbs)
59	S132R	Slowdown Turn	72.2	1.31 - 0.96	8,382 m (27,500 ft)	274,900 N (61,800 lbs)
77	S&GR*	Windup Turn	25.6	.80	6,035 m (19,800 ft)	266,004 N (59,800 lbs)
48	6*	Windup Turn	26.6	.70	7,559 m (24,800 ft)	294,472 N (66,200 lbs)

*Phase I Selections

analyses if desired. Volume III (NASA CR-152114) presents tabulated PSD data.

SECTION 2

AIRCRAFT DESCRIPTION

The test aircraft was F-111A Number 13. A drawing showing the general features of the aircraft is presented in Figure 1. Detailed geometry associated with the aircraft and its components appears in Table 3. The aircraft has a variable sweep wing and a convention was adopted early in the development program that all aerodynamic coefficients would be referenced to geometric characteristics at a specific wing sweep, namely, $\Lambda_{LE} = 16$ degrees. The variations of some key geometric characteristics of the wing with wing leading-edge sweep angle are presented in Figure 2.

Although the aircraft is fitted with a high-lift system consisting of multisegment leading-edge slats and multisegment double-slotted trailing-edge flaps, these devices were in their retracted positions for all maneuvers analyzed in this study.

Two-segment upper surface spoilers on each wing are used at low wing sweeps in addition to differentially controlled all-movable horizontal tails to achieve roll control.

The aircraft has a three-axis stability augmentation system which was operational on all maneuvers analyzed in this investigation.

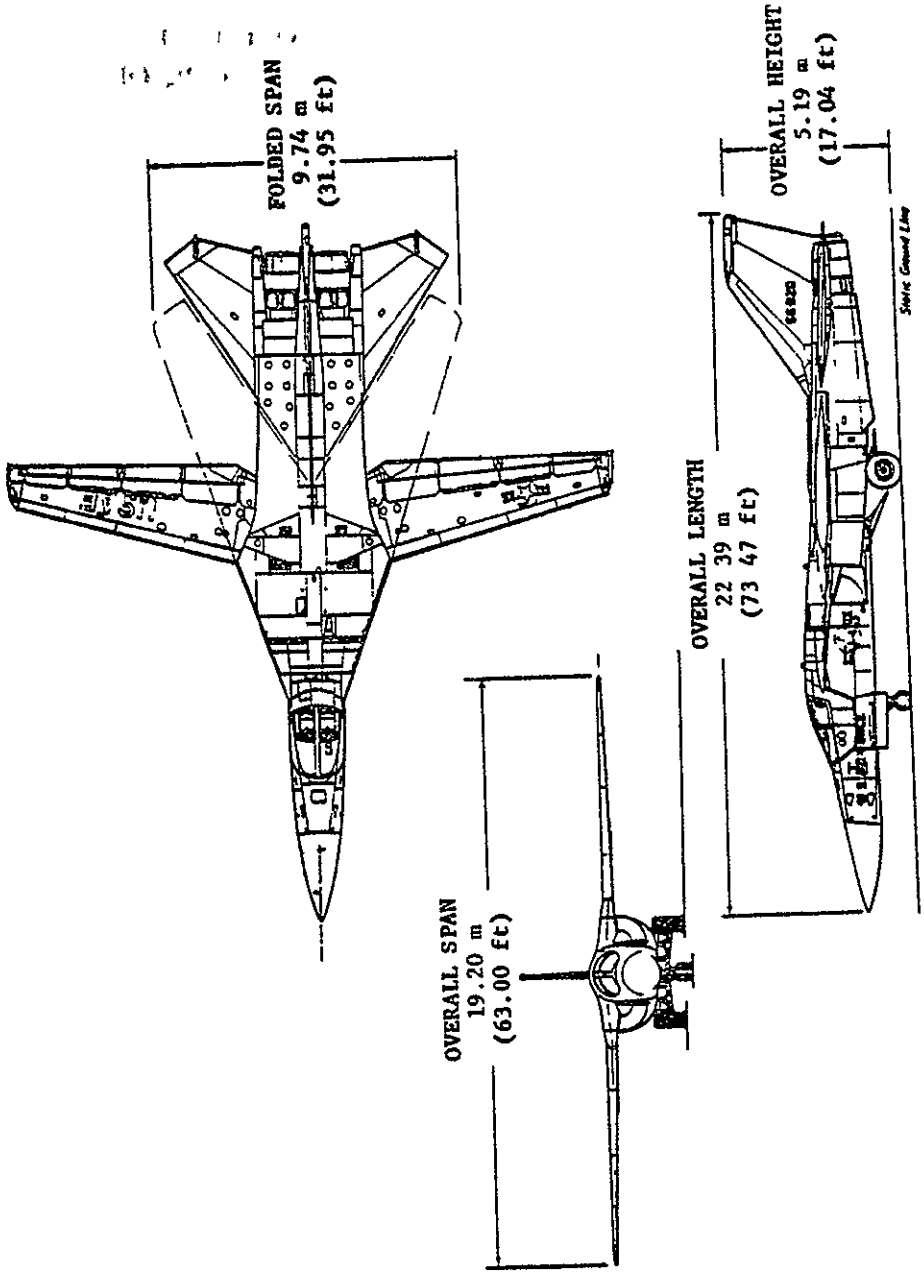

Figure 1 F-111A THREE-VIEW

TABLE 3

PHYSICAL CHARACTERISTICS OF THE
F-111A AIRPLANE (NUMBER 13)

Wing –	
Airfoil section, at pivot	NACA 64A210 7 (modified)*
Airfoil section, tip	NACA 64A209 8 (modified)*
Sweep, deg (leading edge)	16 to 71 5
Incidence, deg	1
Dihedral, deg	1
Span, area, mean aerodynamic chord	(See fig 2)
Leading-edge slats	
Area (planform projected), $ft^2(m^2)$	60 7(5 64)
Span percent of exposed wing-panel span	96 5
Deflection, maximum, deg	45
Trailing-edge flaps	
Type	Double Slotted Fowler
Area (aft of hinge line), $ft^2(m^2)$	117 8(10 94)
Span, percent of exposed wing-panel span	
Deflection, maximum, deg	37 5
Spoilers	
Area (planform projected), $ft^2(m^2)$	28 6(2 66)
Span ft(m)	11 8(3 6)
Deflection, maximum, deg	45
Wing pivot	
Distance from airplane nose, ft(m)	40 18(12 25)
Distance from airplane centerline, ft(m)	5 86(1 79)
Horizontal tail (all movable) –	
Airfoil section	BICONVEX
Incidence, deg	1
Dihedral, deg	-1
Sweep at leading edge, deg	57 5
Span, ft(m)	29 3(8 93)
Area (exposed), $ft^2(m^2)$	174 3(15 74)
Area (movable), $ft^2(m^2)$	154 2(13.92)
Aspect ratio	1 42
Mean aerodynamic chord (exposed), in (cm)	137.5(349.3)
Deflection, maximum, deg	
As elevators	
Trailing-edge up	(approx) 25
Trailing-edge down	(approx) 10
As ailerons (total)	(approx) ±15
Surface stops	
Trailing-edge up	(approx) 31
Trailing-edge down	(approx) 16
Vertical tail –	
Airfoil section	BICONVEX
Sweep at leading edge, deg	55
Span, ft(m)	8 9(2 71)
Area, $ft^2(m^2)$	111 7(10 09)
Aspect ratio	1 42
Mean aerodynamic chord, in (cm)	159 3(404 6)
Rudder	
Span, ft(m)	7 8(2 38)
Area, $ft^2(m^2)$	29 3(2 65)
Deflection, maximum, deg	±30
Speed brake –	
Area, $ft^2(m^2)$	26.5(2 39)
Deflection, maximum, deg	77
Ventrals –	
Area (total), $ft^2(m^2)$	25(2 26)
Power plants –	
P & W TF30-P-3 engines	2

* $\Lambda_{LE} = 16°$

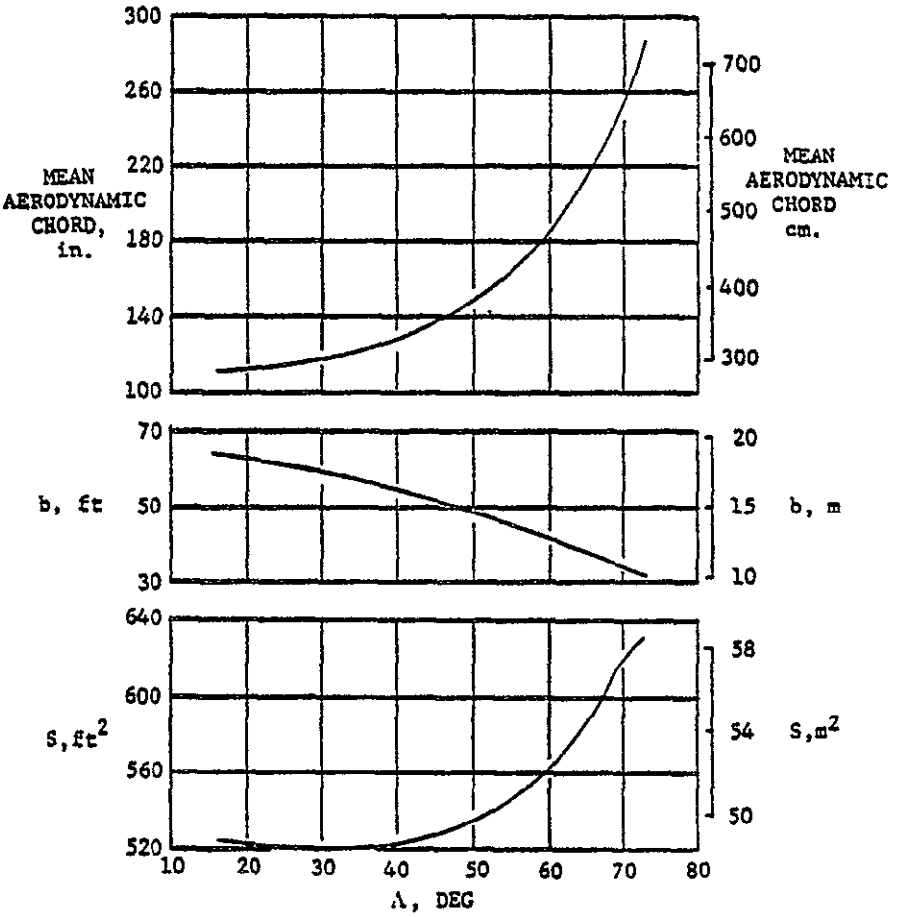

Figure 2 F-111A WING GEOMETRY AS A FUNCTION OF WING-SWEEP ANGLE

SECTION 3

AIRCRAFT INSTRUMENTATION

The instrumentation system installed in the aircraft consisted of two 30 track and one 14 track FM analog magnetic tape recorders and various transducers throughout the airplane. IRIG B time reference signals were recorded on each tape recorder to provide time correlation. The general locations of the accelerometers pertinent to the buffet study are shown in Figure 3. The actual locations in terms of aircraft geometry references are listed in Table 4.

The characteristics of the accelerometers most of which were commercially available units are indicated in Table 5. The accuracies quoted refer to the nominal flat frequency response up to the limit frequency quoted. No calibration data exist above the quoted limit of flat frequency response, however, the natural resonant frequencies are well beyond 100 herz for all of the accelerometers.

The locations of the wing strain gage sensors pertinent to the buffet study are shown in Figure 4. Shear, bending moment and torque were measured at each of the four indicated wing stations on the right wing.

The locations of the strain gage sensors for the horizontal tail loads measurements are shown in Figure 5. Vertical shear bending moment and hingeline torque were measured at the

Figure 3. ACCELERATION MEASUREMENTS

Table 4

ACCELEROMETER LOCATIONS

ITEM CODE	MEASUREMENT	LOCATION					
		FUSELAGE STATION		WATERLINE		BUTT LINE	
		METERS	INCHES	METERS	INCHES	METERS	INCHES
AB018	c.g. vertical	12.996	(511.64)	4 740	(186.62)	0	0
AB019	c.g. vertical	12.996	(511 64)	4 740	(186.62)	0	0
AB020	c.g. lateral	12.996	(511.64)	4.740	(186 62)	-.023	(- .89)
AF009	Pilot seat vertica	6.462±.127	(254 40±5.0)	4.245±.127	(167 12±5 0)	-.133	(-5 25)
AF010	Pilot seat lateral	6.462± 127	(254.40±5.0)	4.245±.127	(167.12±5.0)	-.133	(-5.25)
AW001	Left wing tip - vertical	Front spar station 9.500 meters (374 inches)					
AW002	Right wing tip - vertical	Wing span station 9.157 meters (360.5 inches) @ $\Lambda_{LE} = 16^{\circ}$					

Table 5

ACCELEROMETER CHARACTERISTICS

ITEM CODE	MEASUREMENT	NOMINAL FULL SCALE RANGE*	SPECIFIED ACCURACY % FULL SCALE**	SPECIFIED FLAT FREQUENCY RESPONSE TO HZ.	RESONANT NAT. FREQ HZ	FLIGHTS
AB018	C.G Vertical	-3.5 to +6 5	±5	25	Not Available	48, 60
AB018	C.G. Vertical	±15	±3	42	530	70, 77, 78, 79
AB019	C.G. Vertical	±10	±5	325	--	ALL
AB020	C.G. Lateral	±7.5	±5	275	--	ALL
AF009	Pilot Seat Vertical	±10	±3	32	400	ALL
AF010	Pilot Seat Lateral	±7.5	±5	275	--	ALL
AW001	Left Wing Tip Vertical	±25	±5	500	--	ALL
AW002	Right Wing Tip Vertical	±25	±5	500	--	ALL

*The actual range calibrated varied from these nominal values.
**Over range of flat frequency response and at all temperatures between -70° and +250°F

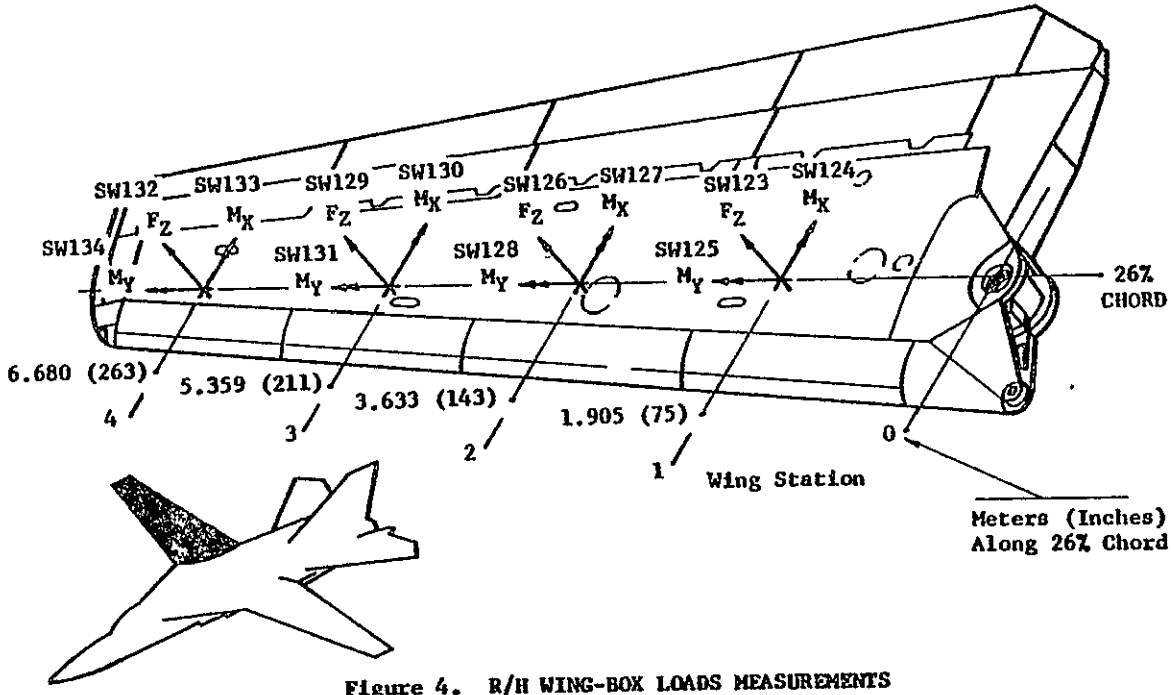

Figure 4. R/H WING-BOX LOADS MEASUREMENTS

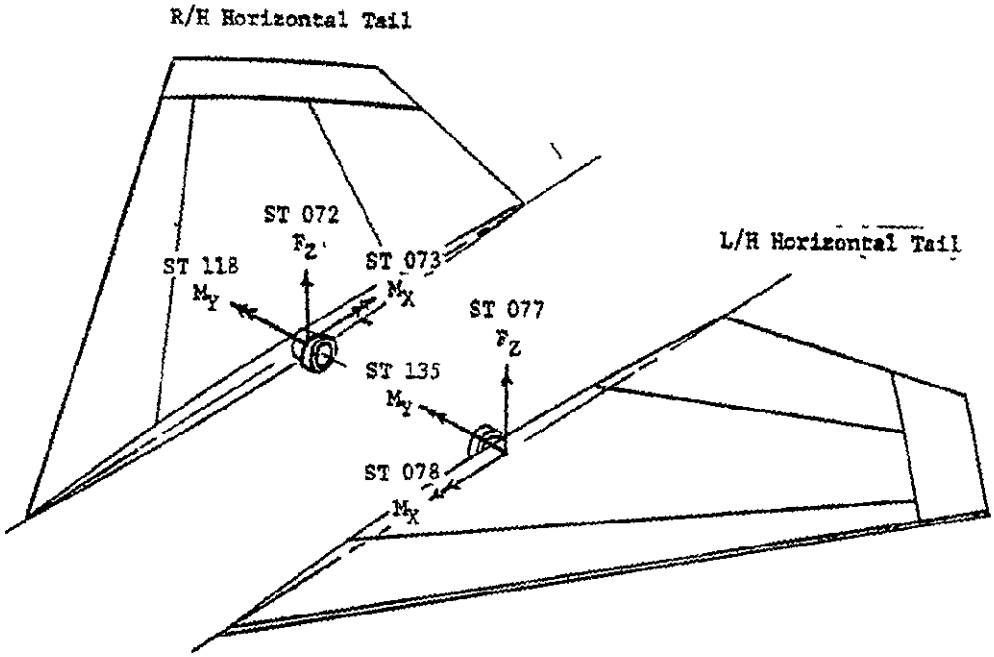

Figure 5. HORIZONTAL TAIL LOADS MEASUREMENTS

root of both the left and right horizontal tails. The sensitivities of the wing and tail loads measurements were goverened by the fact that the loads were to be measured during maneuvers at load factors up to the maximum capability of the aircraft. As a consequence the signal-to-noise ratios for the present buffet studies were lower than is desirable. The calibration slopes for each channel of information are shown in Table 6.

In several cases the frequency response upper limit for the measurements was set by the subchannel characteristics of the flight recording system. Table 7 lists the appropriate nominal limit frequency of subchannel arrangements for each flight selected for detailed analysis.

Other pertinent measurements such as angle of attack, Mach number, altitude, fuel remaining, horizontal tail position and spoiler position were also recorded on the FM tapes.

TABLE 6

CALIBRATION SLOPES — UNITS/PERCENT OF BANDWIDTH

ITEM	MEASUREMENT	S I. UNITS	U S. CUST. UNITS	FLT 48		FLT 59-61		FLT 70		FLTS 77, 78		FLT 79	
				S.I	CUST	S.I.	CUST.	S I	CUST	S I	CUST	S.I.	CUST
AW001	LWT-Vert	g's	g's		50304		50304		33578		33578		33578
AW002	RWT-Vert	g's	g's		50232		50232		33322		33322		.33322
AB018C	CG-Vert	g's	g's		130		130		10690		.10313		18339
AB018F	CG-Vert	g's	g's		.010		.010		---		---		---
AB019	CG-Vert	g's	g's		20142		20142		20172		.20172		20172
AB020	CG-Vert	g's	g's		.05129		05129		.05052		05052		.05052
AF009	P.S -Vert	g's	g's		15306		15306		29280		29280		29280
AF010	P.S.-Lat	g's	g's		10232		.10232		.10128		10128		.10128
AB015	Ang Roll	rad/sec^2	rad/sec^2		.53569		.53569		.3012		3012		.3012
AB016	Ang. Pitch	rad/sec^2	rad/sec^2		32175		32175		.0998		0998		0998
SW123	Shear-W S 1	N	lbs	8011	1801	8011	1801	11770	2464	11770	2464	11926	2681
SW124	B M -W S 1	m-N	in-lbs	22517	202896	22517	202896	37110	334383	37110	334383	37393	336937
SW125	TOR -W S.1	m-N	in-lbs	4136	37264	4136	37264	3913	35263	3913	35263	3969	35767
SW126	Shear-W S.2	N	lbs	5124	1152	5124	1152	9475	2130	9475	2130	9608	2160
SW127	B.M -W S 2	m-N	in-lbs	9981	89935	9981	89935	9828	88557	9828	88557	9897	89181
SW128	TOR -W S.2	m-N	in-lbs	1251	11268	2501	22535	2798	25215	2798	25215	2834	25539
SW129	Shear-W.S 3	N	lbs	2358	530	2358	530	3479	782	3479	782	3523	792
SW130	B.M.-W S 3	m-N	in-lbs	2800	25228	2800	25228	4160	37481	4160	37481	4197	37821
SW131	TOR.-W S 3	m-N	in-lbs	1008	9084	1008	9804	964	8690	964	8690	982	8847
SW132	Shear-W S 4	N	lbs	801	180	801	180	1561	351	1561	351	1588	357
SW133	B.M -W S.4	m-N	in-lbs	393	3541	393	3541	758	6835	758	6835	765	6896
SW134	TOR.-W S 4	m-N	in-lbs	188	1694	188	1694	344	3100	344	3100	349	3142
DH001C	α	deg	deg		875		875		875		875		875
DH001F	α	deg	deg		080		080		080		080		080
DH002F	β	deg	deg		080		.080		080		080		080
DW001	L Inbd Spoil	deg	deg		60		.60		60		60		60
DW002	R Inbd Spoil	deg	deg		60		.60		60		60		60
DW003	L Outb Spoil	deg	deg		60		60		60		60		60
DW001	R Outb Spoil	deg	deg		60		.60		60		60		60
DT003C	L Hor T	deg	deg		.88		.88		.88		.88		88
DT004C	R Hor T	deg	deg		.88		88		88		88		88
PD016F	Mach	---	---		.0034		0034		0034		0034		0034
PD004F	Alt	m	Ft	15 24	50	15.24	50	---	---	---	---	---	---
PH022F	Alt	m	Ft	---	---	---	---	12 192	40	12 192	40	12 192	40

Table 6 (Concluded)

ITEM	MEASUREMENT	S.I. UNITS	U.S. CUST. UNITS	FLT 48		FLTS 59,60,61		FLT 70		FLTS 77,78		FLT 79	
				S.I	CUST.	S I.	CUST.	S.I.	CUST.	S I	CUST	S I	CUST
ST072	R/H H.T. SHEAR	N	lbs	5249	1180	5249	1180	8051	1810	8051	1810	8051	1810
ST073	R/H H.T BEND. MOM.	M-N	in-lbs	5512	49663	5512	49663	6978	62874	6978	62874	-	-
ST073S	R/H H.T. BEND. MOM.	M-N	in-lbs	-	-	-	-	-	-	-	-	5256	47363
ST0118	R/H H.T TORQUE	M-N	in-lbs	2377	21416	2377	21416	2443	22014	2443	22014	2458	22151
ST077	L/H H.T. SHEAR	N	lbs	4466	1004	4466	1004	4466	1004	4466	1004	4497	1011
ST078	L/H H.T. BEND. MOM.	M-N	in-lbs	3485	31402	3485	31402	6970	62804	6970	62804	4860	42185
ST135	L/H H.T. TORQUE	M-N	in-lbs	2134	19233	2134	19233	2134	19233	2134	19233	2148	19357

Table 7

FLIGHT RECORDER FREQUENCY RESPONSE CHARACTERISTICS

ITEM CODE	FLIGHTS 48-61		FLIGHTS 70-79	
	IRIG CHANNEL	FILTER FREQ. - HZ	IRIG CHANNEL	FILTER FREQ. - HZ
AW001	8	45	11	110
AW002	12	160	12	160
AE018	14	330	11	110
AE019	9	59	8	45
AE020	14	330	9	59
AF009	11	110	12	160
AF010	12	160	10	81
SW123	10	81	7	35
SW124	11	110	8	45
SW125	12	160	9	59
SW126	13	220	10	81
SW127	8	45	11	110
SW128	9	59	12	160
SW129	10	81	13	220
SW130	11	110	6	25
SW131	12	160	7	35
SW132	13	220	8	45
SW133	8	45	9	59
SW134	9	59	10	81
ST072	11	110	11	110
ST073	12	160	13	220
ST118	13	220	10	81
ST077	8	45	12	160
ST078	9	59	11	110
ST135	8	45	9	59

SECTION 4

BASIC DATA PROCESSING METHODS

During the Loads Demonstration Flight Program, the FM analog magnetic tapes containing raw flight test data were processed by automated processing techniques. The data were first played out on strip chart recorders for instrumentation verification. Next, the data were digitized at sample rates of up to 20 samples per second under computer control. Either 10 or 20 samples per second were used for the data pertinent to this study. The digitized data were then scaled, calibrated and output in computer listings and computer tapes for additional processing on an IBM System/360. Second generation computer runs were made to obtain corrected flight condition data such as gross weight, Mach number, altitude, dynamic pressure and fuel distribution at 1-second intervals.

Microfilm records of the computer listings from the original flight program data reduction were used in the present program to make plots of angle of attack, normal load factor, Mach number and dynamic pressure as functions of flight time and to identify the gross weights and altitudes for the selected flight maneuvers. The Mach number, altitude and dynamic pressure data include corrections for position error. The angles of attack from the basic reduction are indicated angles and do not include the effect of

upwash at the nose boom. A correction formula to account for the upwash is

$$\alpha_T = 0.318 + 0.931\,\alpha \text{ (degrees)}.$$

It was not considered fruitful to apply this correction in the various plots presented in this report because corrections to the wing angle of attack due to structural flexibility are much larger in magnitude and can only be approximated. Both corrections were considered in selecting the time intervals for the stochastic analysis in Phase II in order to obtain agreement with existing wind tunnel model data insofar as possible.

Time histories were made of about 30 items of instrumentation measurements which were considered pertinent to the buffet study. Examples of each of the strip chart records have been previously presented in the Phase I report (Reference 1). These records were used to aid in the process of selecting the maneuvers for the Phase II Study. The records for the Phase II Study maneuvers were in general too large to be legibly reproduced on an unfolded page.

SECTION 5

FLIGHT CONDITIONS FOR DETAILED ANALYSIS

In the Phase II Study the major criterion for selecting the particular flight maneuvers was matching insofar as possible conditions of wing sweep, Mach number and angle of attack for which wind tunnel data already existed. It was considered important to use maneuvers for at least two additional wing sweeps and at both subsonic and supersonic speeds. The four wind up turn maneuvers listed in Table 2 were selected on that basis.

A question had arisen in the Phase I Study with respect to the character of the structural responses as deduced from relatively short time samples. The two slowdown turn maneuvers listed in Table 2 were chosen to examine whether or not short time samples and longer time samples gave consistent results.

Variations of angle of attack, load factor Mach number and dynamic pressure with flight time are presented in Figure for each of the selected maneuvers.

Table 8 lists the segments of each maneuver selected for detailed analysis. In most cases the time duration of the records (ΔT) is one second, but some longer records were used. The table also lists the indicated angle of attack at the start

a) FLIGHT 61, R227, WINDUP TURN.

Figure 6. FLIGHT CONDITIONS FOR SELECTED MANEUVERS

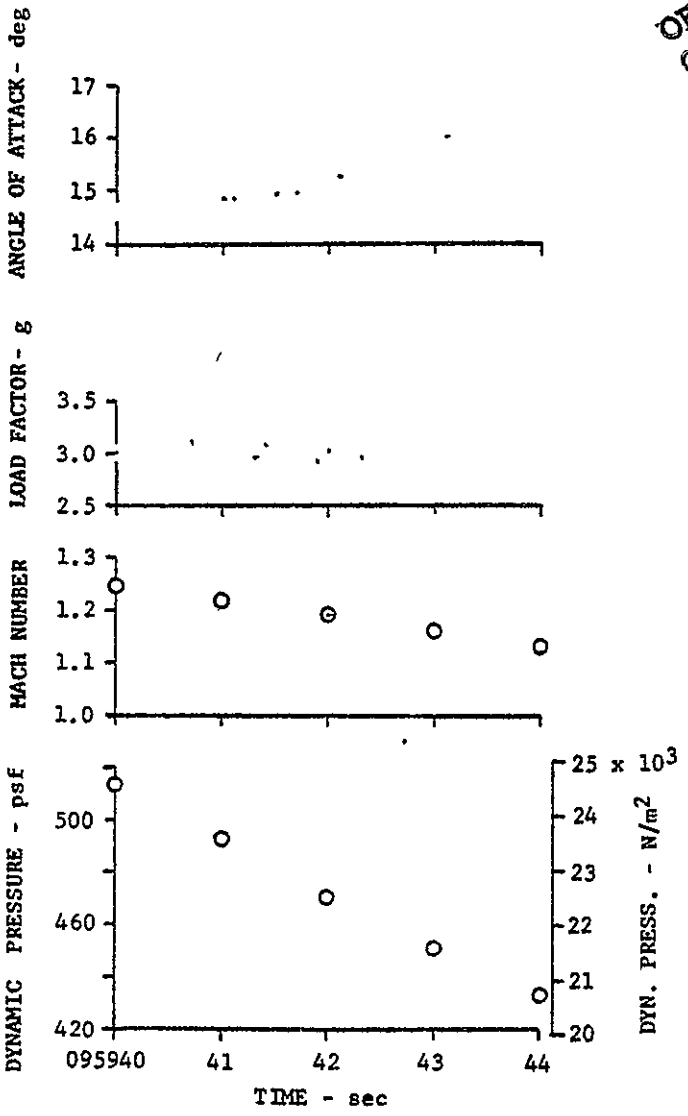

b) FLIGHT 51, S38/150, SLOW DOWN TURN

Figure 6. Continued

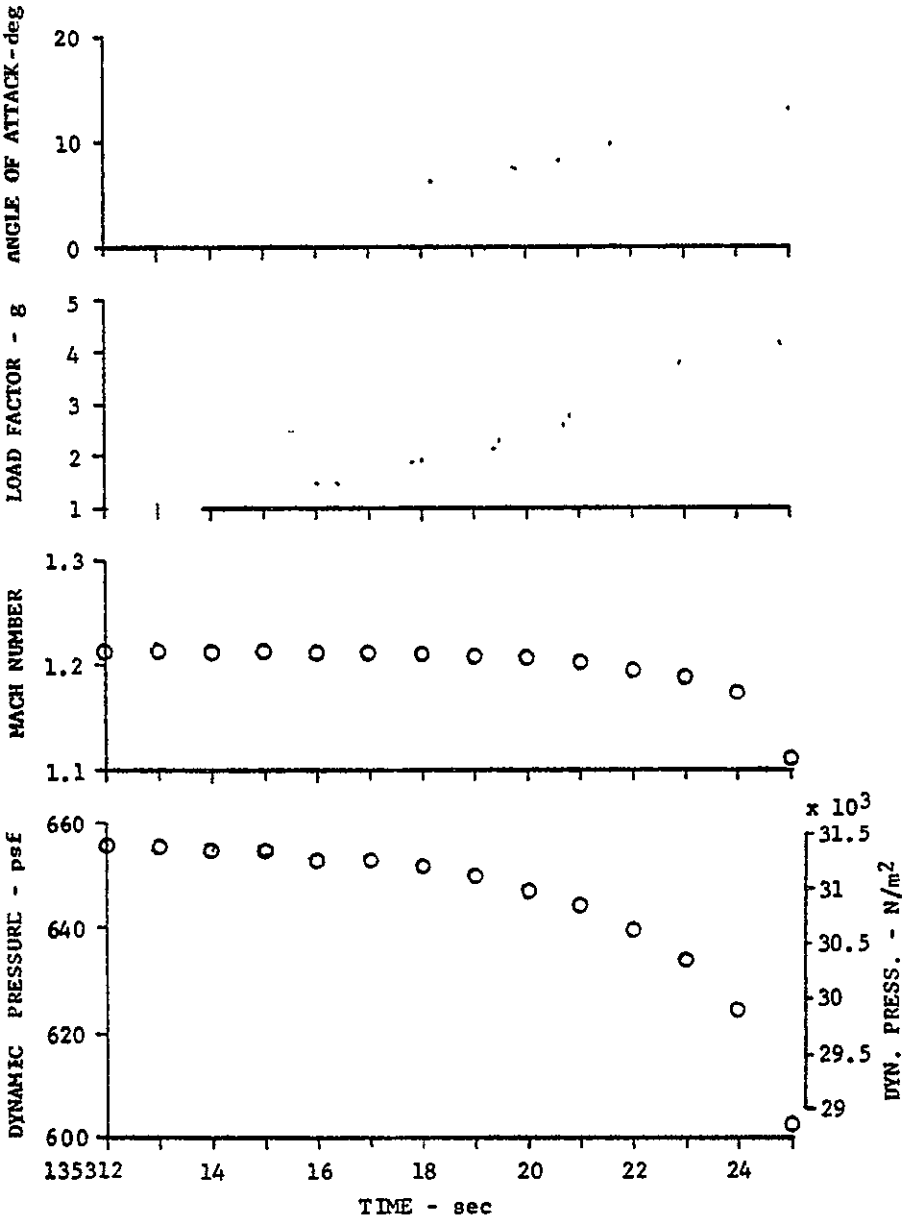

c) FLIGHT 48, Run 4, WINDUP TURN

Figure 6. Continued

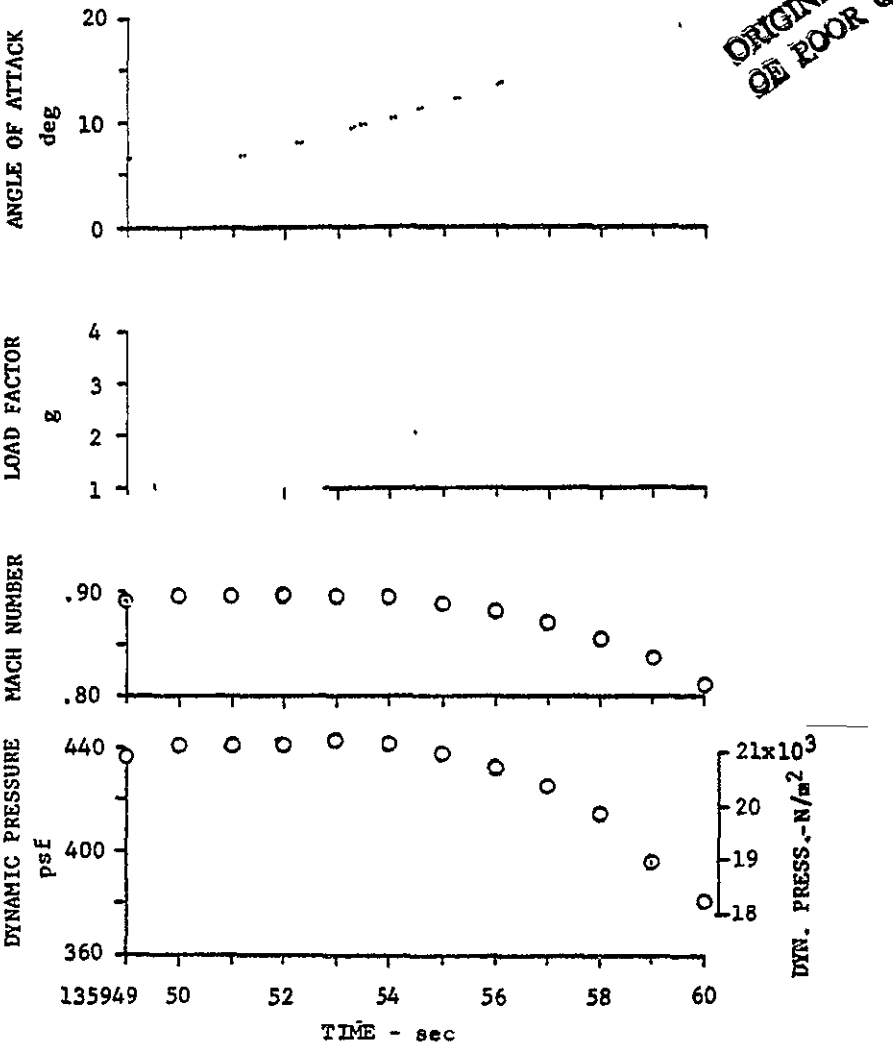

d) FLIGHT 48, RUN 7R1, WINDUP TURN

Figure 6. Continued

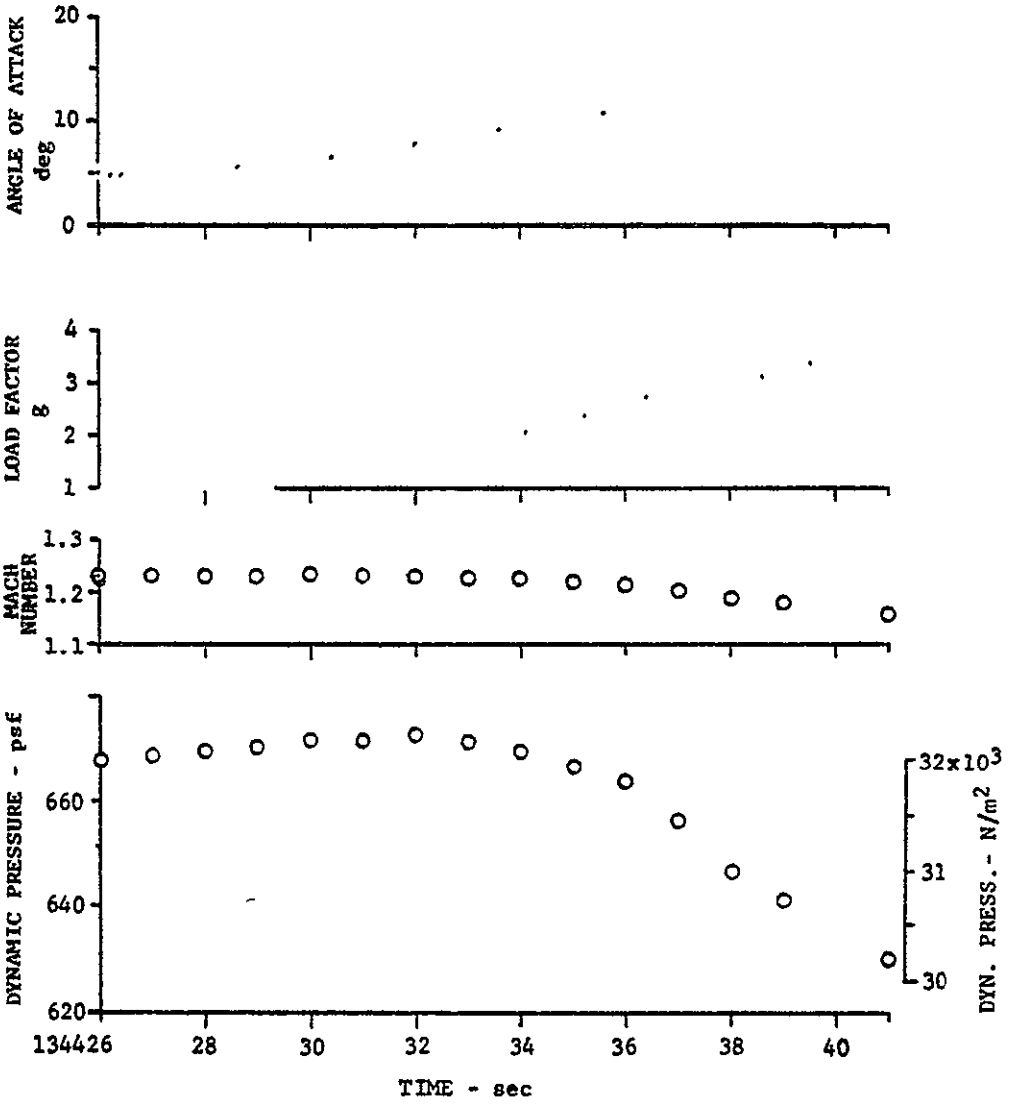

e) FLIGHT 48, Run 5, WINDUP TURN

Figure 6. Continued

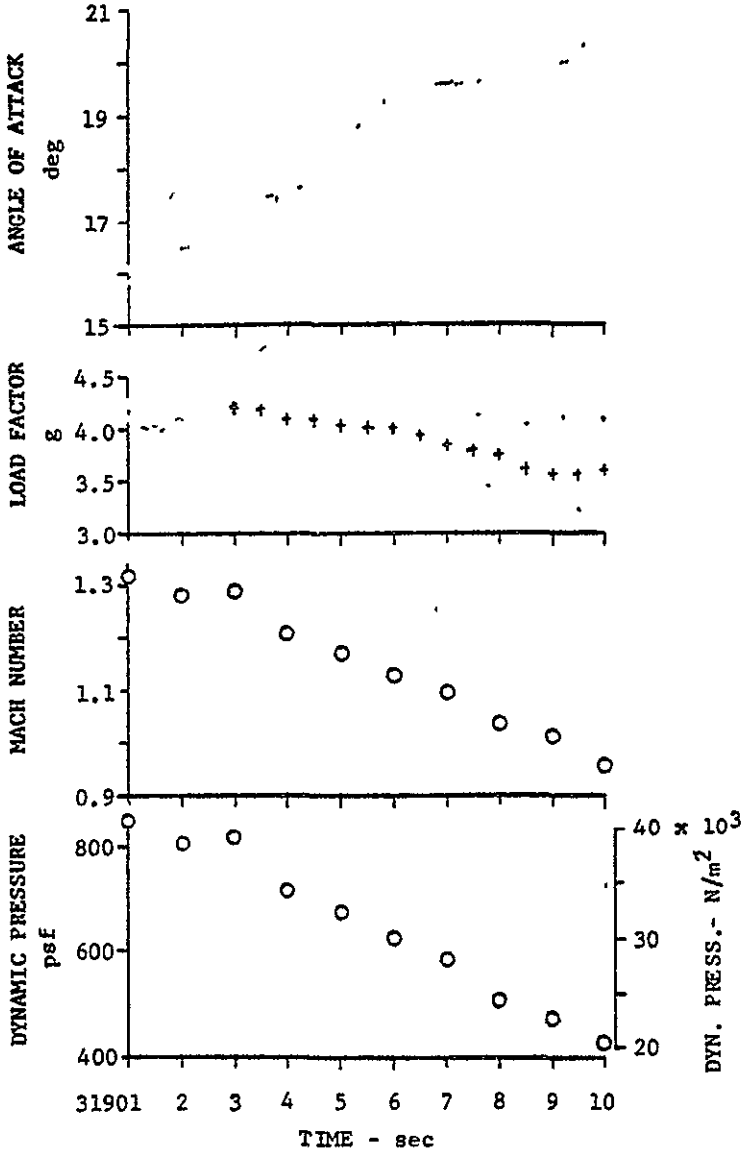

f) FLIGHT 59, Run S132R, SLOW DOWN TURN

Figure 6. Continued

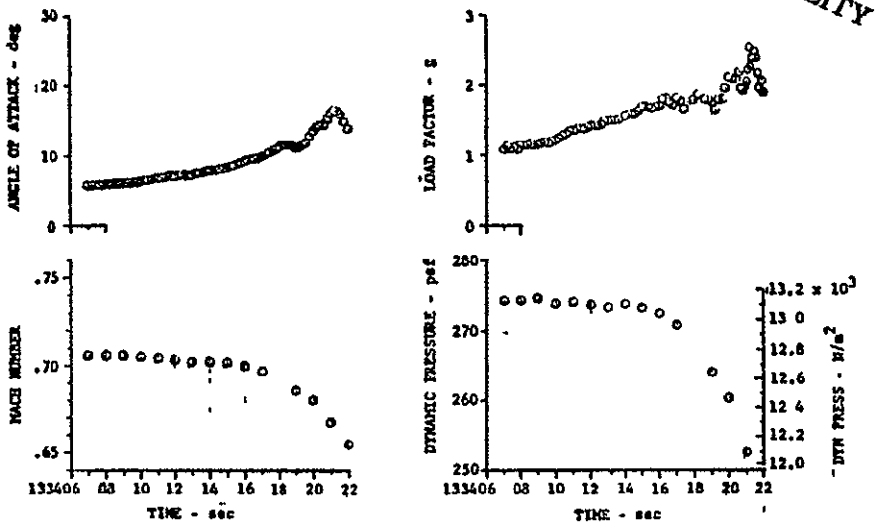

(g) FLIGHT 48, RUN 6, WINDUP TURN

Figure 6. Continued

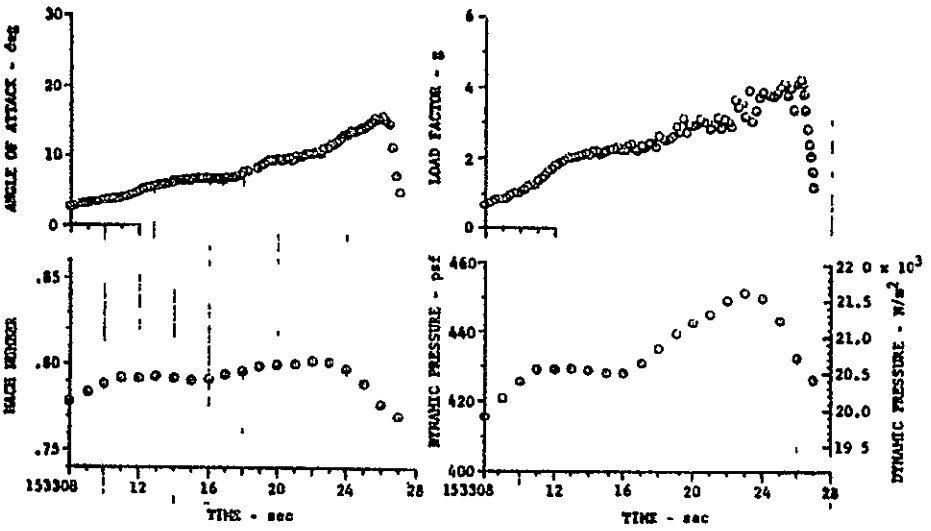

(h) FLIGHT 77, RUN S&C-R, WINDUP TURN

Figure 6. Concluded

Table 8

FLIGHT POINTS SELECTED FOR STOCHASTIC ANALYSIS

Flight	Run	Point	Start Time T_1	Stop Time T_2	ΔT (SEC)	α_1 (DEG)	α_2 (DEG)	α_{max} (DEG)	α_{nom} (DEG)	$\Delta\alpha$ (DEG)	PSD PLOT Fig. No.
61	R227	1	110107 9	110108 9	1	7 10	9 25	--	8 05	2 15	8
		2	110108 4	110109.4	1	8.05	10.10	--	9.25	2 05	9
		3	110109 7	110110 7	1	10.10	10 80	--	10 42	0 70	10
		4	110110 6	110111 6	1	10 60	12.70	--	11.65	2 10	11
		5	110112 0	110113 0	1	12 90	14 60	14 60	13.75	1.70	12
51	S38/150	1	95940 0	95942 0	2	14 55	15 12	--	14 85	0.75	13
		2	95943 0	95944 0	1	15 95	16 45	--	16.25	0 50	14
		3	95940 0	95944.0	4	14 55	16 45	--	15.12	1.90	15
48	4	1	135315 7	135316 7	1	4.70	5 50	--	4.95	0.80	16
		2	135320 7	135321 7	1	8.20	9.80	--	8.90	1.60	17
		3	135322 8	135323 8	1	12 10	13 70	--	12.95	1 70	18
		4	135323 9	135324 9	1	13 70	13 90	15 0	14.3	1.30	19
48	7R1	1	135951 7	135952 7	1	7 15	8 65	--	8.00	1 50	20
		2	135952 7	135953 7	1	8.65	10 00	--	9 40	1.35	21
		3	135954 3	135955 3	1	10 75	12.20	--	11.62	1.45	22
		4	135956 8	135957.8	1	14 15	16.15	--	15.15	2 00	23
		5	135958 55	135959 55	1	17.90	18 90	19 35	18.70	1.45	24
48	5	1	134426 2	134427.2	1	4.80	4.80	--	4.80	$\pm$0.1	25
		2	134432 3	134433.3	1	8 00	8 80	--	8 41	0.80	26
		3	134436 2	134437 2	1	11.30	12 70	--	12.10	1.40	27
		4	134439 65	134440 65	1	14.95	16 75	--	15.95	1 80	28
59	S132R	1	31901 0	31903 0	2	15 95	17.55	--	16 75	1.60	29
		2	31903.0	31905 0	2	17.55	18 13	--	17 75	0.63	30
		3	31907 0	31909 0	2	19 55	19.60	20 00	19 80	0 45	31
48	6*	3	133415 0	133416.0	1	8 72	9 55	--	9.1	0.83	32
		4	133416 7	133417 7	1	9 70	10 75	--	10 2	1 05	33
		5	133417 3	133418 3	1	10 30	11 75	--	11.1	1 45	34
		6	133419 0	133420 0	1	11 15	13 55	--	12.3	2.40	35
		7	133420 3	133421 3	1	14 25	16 60	--	15 3	2.35	36
77	S&C-R*	7	153311 0	153313 0	2	4 22	5 98	--	5.1	1.76	37
		8	153315 5	153317 5	2	7 00	7.32	--	7.1	0.32	38
		9	153318 5	153320 5	2	8.45	9.65	--	9.2	1.24	39
		10	153322 35	153324 35	2	10 85	13 40	--	12.2	2.55	40
		11	153324 35	153326 35	2	13.40	15.35	15 55	14.8	2.15	41

* Phase I selections used in Phase II for consistency

of each record (α_1), at the end of each record (α_2) and in a few cases the maximum angle of attack occurring during the record (α_{max}). A nominal angle of attack (α_{nom}) has been assigned to each data segment which is used later to plot trends in the variations of instrument responses with angle of attack. Also included in Table 8 is a key to the Figure numbers for the plotted power spectra for each flight point which are presented in Section 7.

SECTION 6

STOCHASTIC ANALYSIS TECHNIQUES

The analysis techniques used in this study are compatible with American National Standard (ANS S2.10-1971) recommended methods for analysis and presentation of shock and vibration data. A quick-look examination was performed on each time-history measurement to determine the data classification, degree of stationarity, record length and recoverability.

Measurements

Data reduction was performed on the following data:

1. Shear, bending moment and torsion at four wing stations, (12 measurements).
2. Shear, bending moment and hingeline torque at the root of both left and righ horizontal tails (6 measurements)
3. Two wing tip accelerometers (verticals)
4. Two c.g. vertical and one c.g. lateral accelerometers.
5. Pilot's seat vertical and lateral accelerometer.

The stochastic analysis performed on these items was limited to power spectral densities (PSD) and average rms values for each data sample. A total of 660 PSD's were processed in Phase II.

In addition a few narrow band time histories were made for selected wing instrumentation items.

Special-Purpose Processing

A block diagram of the special-purpose stochastic equipment is shown in Figure 7. The FM signal is discriminated to recover the analog signal. Band-pass filters at 3 H_z and 100 H_z (48 dB per octave) were used to reject unwanted frequencies and to minimize aliasing effects on the sampled data. The data is calibrated at this point. The T/D 100 analyzer was used to compute the PSD's. The stochastic algorithm utilized by the T/D 100 to perform this function is discussed below.

Prior to the Phase II Study the equipment was modified to achieve a direct interface with an SEL-810A mini-computer which then permitted direct recording of the output of the T/D-100 on magnetic tape. The tapes were then used as input to a plotting routine.

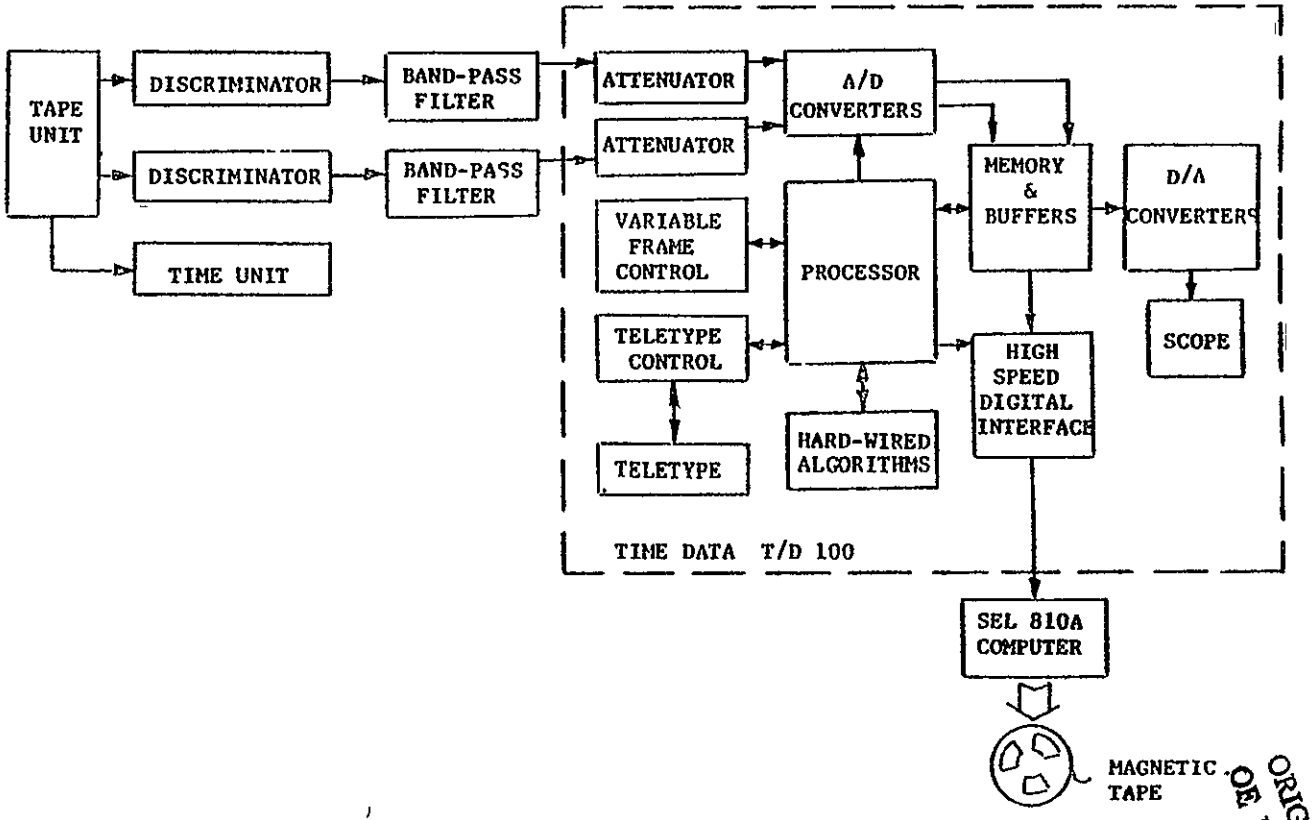

Figure 7. STOCHASTIC SPECIAL-PURPOSE EQUIPMENT

Auto-Spectral Density (PSD)

The T/D 100 computes the PSD coefficients by first approximating the complex Fourier transform of the input signal. The Fourier transform of the time-domain input function x(t) is given by:

$$G(jf) = \int_{-}^{+} x(t)(\cos 2\pi ft - j \sin 2\pi ft)\, dt \qquad (1)$$

where $j = \sqrt{-1}$. Since the time-domain input is sampled and quantitized in the analyzer, and only a finite number of samples are available, the finite transform is used, and separated into its real P(f) and imaginary Q(f) components can be written as follows:

$$P_T(f) = \int_{-T/2}^{T/2} x(t) \cos 2\pi ft \; dt \qquad (2)$$

$$Q_T(f) = \int_{-T/2}^{T/2} x(t) \sin 2\pi ft \; dt \qquad (3)$$

where T is the length of the input frame, which is assumed to be centered about time t=0.

Replacing the continuous input, x(t), with a set of 2N+1 discrete samples at intervals of $t_o = \frac{1}{2N}$, and replacing the sinusoidal functions by corresponding values, the continuous integrals may be expressed as the sum of products:

$$P(kf_o) = \sum_{n=-N}^{+N} x(nt_o) \cos \left[2 \quad kf_o(nt_o) \right] \tag{4}$$

$$Q(kf_o) = -\sum_{n=-N}^{+N} x(nt_o) \sin \left[2 \quad kf_o(nt_o) \right] \tag{5}$$

where k is a series of 2N integers and f_o is the base frequency which is equal to $\frac{1}{2T}$.

The PSD coefficients $\left[S(kf_o) \right]$ are then computed from (4) and (5) by the equation:

$$S(kf_o) = \left| P(kf_o) \right|^2 + \left| Q(kf_o) \right|^2 \tag{6}$$

Average rms (Ψ_T)

The average rms of the input signal is calculated from the PSD coefficients $\left[S(kf_o) \right]$ by the following equation:

$$\Psi_T = \sqrt{f_o \sum_{k=0}^{2N} S(kf_o)}$$

where $f_o = \frac{1}{2NT}$ is the base frequency or analysis bandwidth.

SECTION 7

PRESENTATION OF DATA

During the course of the Phase II study, approximately 660 power spectral diversity plots were obtained. These data have two primary uses. First they permit identification of the significant model contributions through comparison with measured and calculated and antural vibration modes of the aircraft. Second, they provide the data base for assessment of prediction methods.

The spectral content of the structural responses is related to the natural vibration modes. Summaries are presented of the natural vibration mode frequencies as determined from ground vibration tests and also as calculated using a finite element representation of the aircraft structure for each wing sweep These data are useful for interpreting the power spectra

Natural Vibration Modes

The measured natural vibration modes and their associated frequencies are presented in Tables 9 through 11 for wing sweeps of 26, 50, and 72 5 degrees. These data were obtained during extensive ground vibration tests conducted on aircraft in the F-111 development program and are taken from References 4 and 5. In addition, calculated modes were determined for

Table 9

MEASURED F-111A NATURAL VIBRATION MODES, $\Lambda_{LE} = 26^{\circ}$

Predominant Mode (Airplane No. 12 Tests)	Frequency - Hz			
	Fuse Empty, Wing Empty		Fuse. Full, Wing Empty	
	Symmetric	Antisymmetric	Symmetric	Antisymmetric
Wing First Bending	5.2	7.6	5.1	7 1
Fuselage First Vertical Bending	8 6	---	8 0	---
Fuselage First Lateral Bending	---	---	---	8.7
Wing Fore and Aft Bending	7 9	9.3	8.8	8.7
Wing Second Bending	16.9	29.2	17 8	29 0
Wing-Horizontal Tail	---	16.2, 17.5	---	17 5
First Wing Torsion	25 2	25.4	25 7	26.1
Horizontal Tail First Bending	13.6	13 3	13 8	13.1
Horizontal Tail Fore and Aft	15.2	15.3	16.3	16.2
Horizontal Tail Pitch	34.4	37.3, 31.0	30.9	29.5, 36.1
Vertical Tail Bending	---	9 9	---	9.6
Vertical Tail Torsion	---	28.0	---	11.7
Rudder Rotation	---	32.7	---	28.3
Rudder Torsion	---	45.0	---	44.8
Rotating Glove				
Leading Edge Bending	27.4			
Yaw	44 3			
Pitch	50.9			
Aft End Bending	63.8			
Spoiler Modes (From Airplane No. 1 Tests)				
Spoiler No. 1			46,56,62	53,60
Spoiler No. 2			55,65,72	68

Table 10
MEASURED F-111A NATURAL VIBRATION MODES, $\Lambda_{LE} = 50^{\circ}$

PREDOMINANT MODE AIRPLANE NO. 12 TESTS	Frequency - HZ Fuse Full Wing Empty Symmetric	Fuse Full Wing Empty Antisymmetric	Fuse Full Wing Full Symmetric	Fuse Full Wing Full Antisymmetric
Wing First Bending	5.0	6.6	4 1	6.0
Fuselage First Vertical Bending	8.0	-	7.9	-
Fuselage First Lateral Bending	-	8.9	-	8 9
Wing Fore and Aft Bending	8.7	7.3	5 8	5 2
Wing Second Bending	17.5	28.9,30 6	13.0	26.1
Wing - Horizontal Tail	15.8	16.5	-	14.7
Wing First Torsion	26.4	26.1	23.8	24.5
Horizontal Tail Bending	13.3	12.8	13.1	11.9
Horizontal Tail Fore and Aft	16.3	16.6	16.2	16.5
Horizontal Tail Pitch	21.4,33.7	29.8,35.9	31.8,35 6	29.3,36.5
Vertical Tail Bending	-	9.7,11.5	-	9.7,11.6
Vertical Tail Torsion	-	27.6	-	27.5
Rudder Rotation	-	32.0	-	32.6
Rudder Torsion		45.0		45.4
Airplane 13 Tests (Close Tolerance Hor. Tail Bushings)				
Horizontal Tail First Bending	13.3	12.8	-	-
Horizontal Tail Fore and Aft	16.9	17.0	-	-
Horizontal Tail Pitch	34.2,39.0	37.9,43.2	-	-
Horizontal Tail Second Bending	-	47.2,52.4	-	-

Table 11
MEASURED F-111A NATURAL VIBRATION MODES, $\Lambda_{LE} = 70^{o}$

PROMINANT MODE AIRPLANE NO. 12 TESTS	Frequency - HZ			
	Fuse Full Wing Empty		Fuse Full Wing Full	
	Symmetric	Antisymmetric	Symmetric	Antisymmetric
Wing First Bending	5.0	5.8	3.8	4.9
Fuselage First Vertical Bending	8.0	-	7.8	-
Fuselage First Lateral Bending	-	9.0	-	8.3
Wing Fore and Aft Bending	8.0	7.3	5.6	5.6
Wing Second Bending	17.4	30.0	12.9	26.4
Wing - Horizontal Tail	16.1	16.6	-	14.4
Wing Torsion	26.2	27.1,28.7 29.4,31.0	23.7	24.5
Wing - Flap	-	-	-	29.4,29.6
Horizontal Tail Bending	13.3	12.6	-	-
Horizontal Tail Fore and Aft	16.2	16.5	-	-
Horizontal Tail Pitch	31.8,35 2	29.6,36.3	-	-
Vertical Tail Bending	-	9.7	-	-
Vertical Tail Torsion	-	27.7	-	-
Rudder Rotation	-	31.9	-	-
Rudder Torsion	-	44.5	-	-

specific flight conditions for use in the prediction method development and evaluation portions of the contracted investigation. The calculated modes are presented in Tables 12 through 19. Further discussion of the analytical effort appears in References 6, 7 and 8.

Power Spectral Density Plots

All power spectral density data obtained during the Phase II investigation are presented in this Section in plotted form. For ease of use the data are arranged in the following way.

Each figure number represents a data set which corresponds to a given Flight Number, Run Number and Point Number as listed in Table 8. Each Phase II data set consists of 7 pages of accelerometer data, 4 pages each of the wing shear, wing bending moment and wing torsion data, and 2 pages each of horizontal tail shear, bending moment and torsion data For the Phase I maneuvers each data set has only the 6 pages of horizontal tail data since the wing and fuselage power spectra appear in Reference 2.

The format for each PSD plot is the same. The ordinates are normalized by the sum of the measured PSD values taken over the range from 1 to 100 Hz. The numerical value of this sum appears as the scaling factor listed above each plot.

Table 12

CALCULATED F-111A SYMMETRIC VIBRATION MODES

$\Lambda_{LE} = 26^{\circ}$ GW = 266,044N (59,800 lb)

Mode No.	Mode Description	Frequency - Hz
1	First Wing Bending	4 794
2	First Fuselage Vertical Bending	7.013
3	Horizontal Tail Bending + Sec. Wing Bend. + Sec. Fus. Bend.	13.930
4	Horizontal Tail Bending + Second Wing Bending	14.828
5	Second Wing Bending	17.010
6	Third Fuselage Bending + Wing Torsion	22.853
7	First Wing Torsion	24.064
8	Horizontal Tail Second Bending	27.521
9	Third Wing Bending	30.666
10	Horizontal Tail Torsion	33.893
11	Fuselage Fourth Bending + Second Wing Torsion	37.573
12	Second Wing Torsion	39.229

Table 13

CALCULATED F-111A SYMMETRIC VIBRATION MODES

$\Lambda_{LE} = 26^{\circ}$ GW = 293,138N (65936 lb)

Mode No.	Mode Description	Frequency - Hz
1	First Wing Bending	4.792
2	First Fuselage Vertical Bending	6 870
3	Wing - Horizontal Tail (in-phase) + Sec Fuse Bending	13 894
4	Wing - Horizontal Tail (out of phase)	14 721
5	Second Wing Bending	17.110
6	Third Fuselage Bending + Wing Torsion	22.665
7	First Wing Torsion	24 024
8	Horizontal Tail Second Bending	27.197
9	Third Wing Bending	30 446
10	Horizontal Tail Torsion	33.884
11	Fourth Fuselage Bending + Wing Second Torsion	37.551
12	Second Wing Torsion	39 076

Table 14

CALCULATED F-111A SYMMETRIC VIBRATION MODES

$\Lambda_{LE} = 50^{o}$ GW = 331,392N (74,515 lb)

Mode No.	Mode Description	Frequency - Hz
1	First Wing Bending	4.908
2	First Fuselage Vertical Bending	6.736
3	Wing - Horizontal Tail (in-phase) + Fuselage Second Bending	13.529
4	Wing - Horizontal Tail (out of phase)	15.218
5	Second Wing Bending	16 762
6	Third Fuselage Bending + Wing Torsion	21.836
7	First Wing Torsion	24.217
8	Horizontal Tail Second Bending	25.987
9	Third Wing Bending + Horizontal Tail Pitch	31.293
10	Horizontal Tail Pitch	33.869
11	Horizontal Tail Bending + Third Wing Bending	37.618
12	Wing Second Torsion + Horizontal Tail Pitch	39.377

Table 15

CALCULATED F-111A SYMMETRIC VIBRATION MODES

Λ_{LE} = 72 5 GW = 268,673N (60,419 lb)

Mode No.	Mode Description	Frequency - Hz
1	First Wing Bending	4.849
2	First Fuselage Vertical Bending	6.913
3	Wing - Horizontal Tail (in-phase) + Fuselage Second Bending	14.391
4	Wing - Horizontal Tail (out of phase)	15.425
5	Second Wing Bending	17.794
6	Third Fuselage Bending + Wing Torsion	22.927
7	First Wing Torsion	24.571
8	Horizontal Tail Second Bending	27.448
9	Third Wing Torsion + Horizontal Tail Pitch	31.927
10	Horizontal Tail Pitch	33.898
11	Second Wing Torsion	39.260
12	Horizontal Tail Torsion	39.856

Table 16

CALCULATED F-111A ANTISYMMETRIC VIBRATION MODES

$\Lambda_{LE} = 26^{o}$ GW = 266,044N (59,800 lb)

Mode No.	Mode Description	Frequency - Hz
1	First Wing Bending	7.417
2	First Fuselage Lateral Bending	8.119
3	Vertical Tail Bending + Wing Bending	10.887
4	Horizontal Tail Bending + Wing Bending	12.290
5	Second Fuselage Lateral Bending	15.720
6	Wing - Horizontal Tail	18.510
7	Third Fuselage Lateral Bending	21.947
8	Wing Torsion + Bending	22.983
9	Wing Torsion + Horizontal Tail Pitch	25.081
10	Vertical Tail Torsion	25.678
11	Vertical Tail Torsion + Second Wing Bending	26.029
12	Second Wing Bending	27.179
13	Fuselage Lateral Bending + Second Wing Bending	31.249
14	Horizontal Tail Pitch	31.990
15	Fuselage Lateral Bending + Second Wing Torsion + Hor. Tail Torsion	36.377

Table 17

CALCULATED F-111A ANTISYMMETRIC VIBRATION MODES

$\Lambda_{LE} = 26^{o}$ GW = 293,138N (65,936 lb)

Mode No.	Mode Description	Frequency - Hz
1	First Wing Bending	7 284
2	First Fuselage Lateral Bending	7.863
3	Vertical Tail Bending	10.699
4	Horizontal Tail Bending + WingBending	12.078
5	Second Fuselage Lateral Bending	15 663
6	Wing - Horizontal Tail	18.183
7	Third Fuselage Lateral Bending	21.636
8	Fuselage Lateral Bending + Wing Bending	22.586
9	Wing Torsion + Horizontal Tail Pitch	24.647
10	Vertical Tail Torsion	25.260
11	Vertical Tail Torsion + Second Wing Bending	25 595
12	Second Wing Bending	26 881
13	Fuselage Lateral Bending + Second Wing Bending	29.033
14	Horizontal Tail Pitch	31.460
15	Fuselage Lateral Bending + Second Wing Torsion + Hor. Tail Pitch	35.189

Table 18

CALCULATED F-111A ANTISYMMETRIC VIBRATION MODES

$\Lambda_{LE} = 50^{o}$ GW = 331,392N (74,515 lb)

Mode No.	Mode Description	Frequency - Hz
1	First Wing Bending	6.917
2	First Fuselage Lateral Bending	7.795
3	Vertical Tail Torsion + Wing Bending	10.844
4	Horizontal Tail Bending + Wing Bending	12.290
5	Second Fuselage Lateral Bending	15.070
6	Wing - Horizontal Tail	17.815
7	Horizontal Tail Pitch + Vertical Tail Torsion + Wing Bending	21.185
8	Third Fuselage Lateral Bending	22.354
9	Wing Torsion + Horizontal Tail Pitch	23.794
10	Vertical Tail Torsion	25.264
11	Vertical Tail Torsion + Second Wing Bending	25.915
12	Fuselage Lateral Bending + Second Wing Bending	27.925
13	Second Wing Bending	29.479
14	Horizontal Tail Pitch	31.698
15	Fuselage Lateral Bending + Second Wing Torsion + Hor. Tail Torsion	34.660

Table 19

CALCULATED F-111A ANTISYMMETRIC VIBRATION MODES

Λ_{LE} = 72.5° GW = 268,673N (60,419 lb)

Mode No.	Mode Description	Frequency - Hz
1	First Wing Bending	6.036
2	First Fuselage Lateral Bending	7.973
3	Vertical Tail Bending + Horizontal Tail Bending	10 739
4	Horizontal Tail Bending + Wing Bending	12.385
5	Second Fuselage Lateral Bending	16.542
6	Wing - Horizontal Tail (out of phase)	17.408
7	Wing - Horizontal Tail (in-phase)	20.631
8	Vertical Tail Torsion + Wing Torsion	23.599
9	Third Fuselage Lateral Bending + Vertical Tail Torsion	24.085
10	Vertical Tail Torsion	25.462
11	Vertical Tail Bending	25.973
12	Fuselage Lateral Bending + Wing Torsion	29.300
13	Wing Second Bending	30.429
14	Horizontal Tail Pitch	31.581
15	Fuselage Lateral Bending + Wing Second Bending + Hor. Tail Torsion	36.404

The format for the scaling factor is.

$$SF = .XXX \pm Y\ (Z)^{**2}$$

where

.XXX is a decimal value

Y is the power of 10 by which the decimal value must be multiplied.

Z is the basic unit of the scaling factor.

$**^2$ represents the fact that the units are squared.

Where appropriate, scaling factors are presented in both S.I. and U.S. Customary units

The values plotted at frequencies of 0 to 1 Hz are used to set the scales for the automatic plotting routine and do not represent actual data When a symbol appears on the lower bound of a plot for frequencies greater than 1 Hz, it actually represents the fact that measurement was below the dynamic threshold of the analysis equipment. Finally, although data are plotted at all frequencies from 2 to 100 Hz on all the plots, the upper frequency limit of valid data varies. Table 7 should be consulted for the frequency limit appropriate for each item and flight.

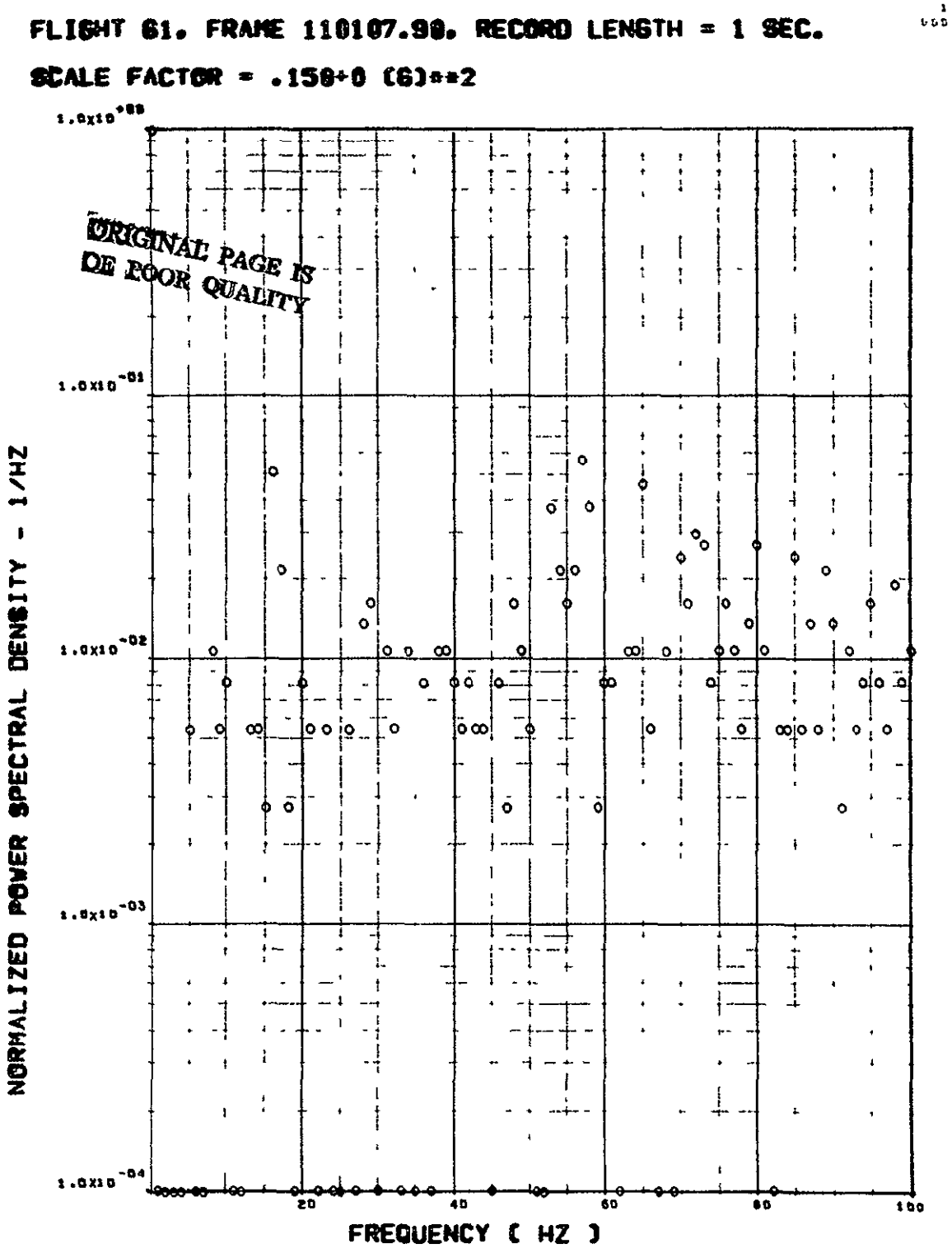

Figure 8. Power Spectra - Flight 61, Run 227, Point 1 T_1 = 110107 9, ΔT = 1 Sec, α_{Nom} = 8.05 deg, $\Delta\alpha$ = 2.15 deg.

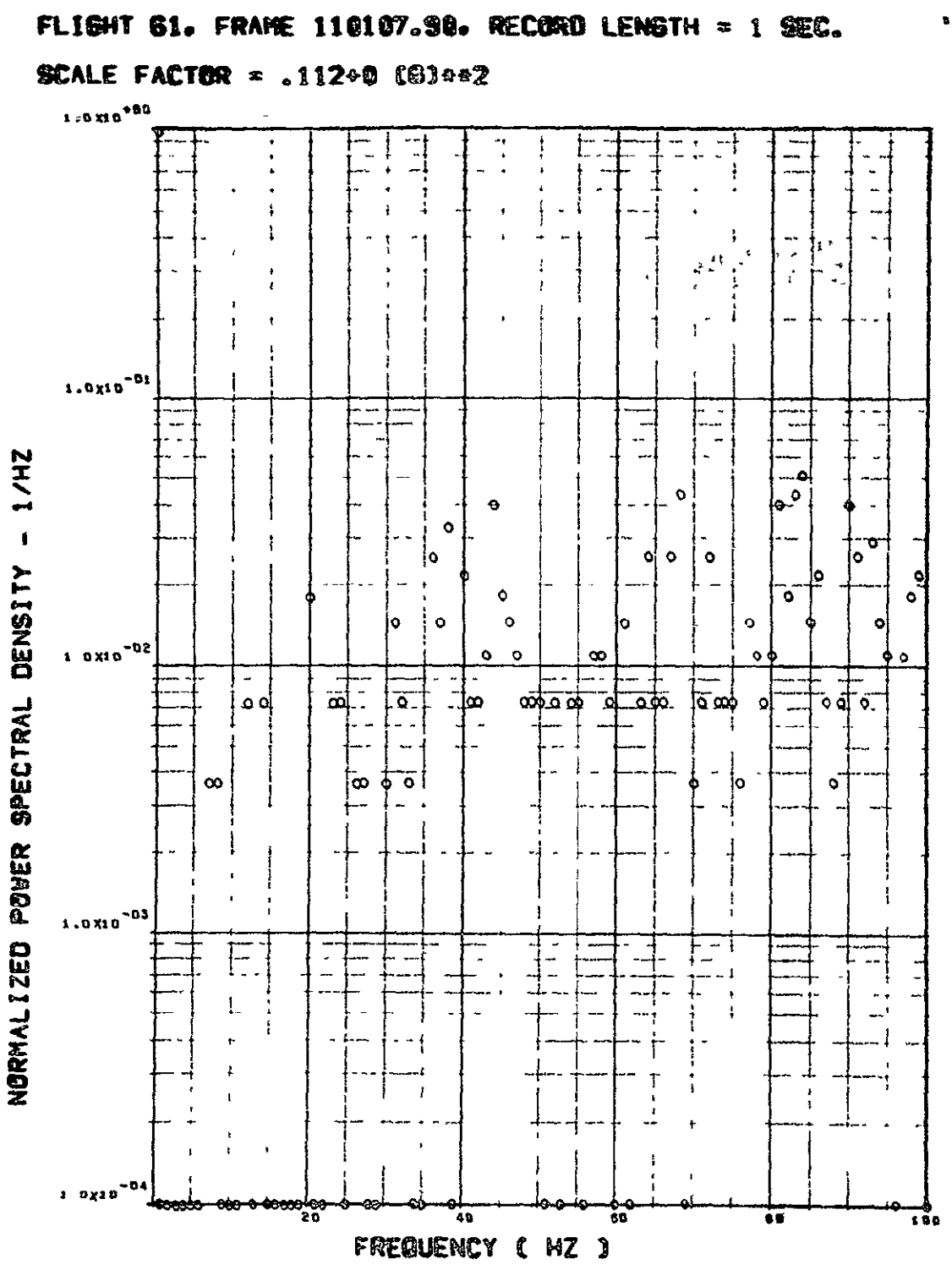

Figure 8. Continued

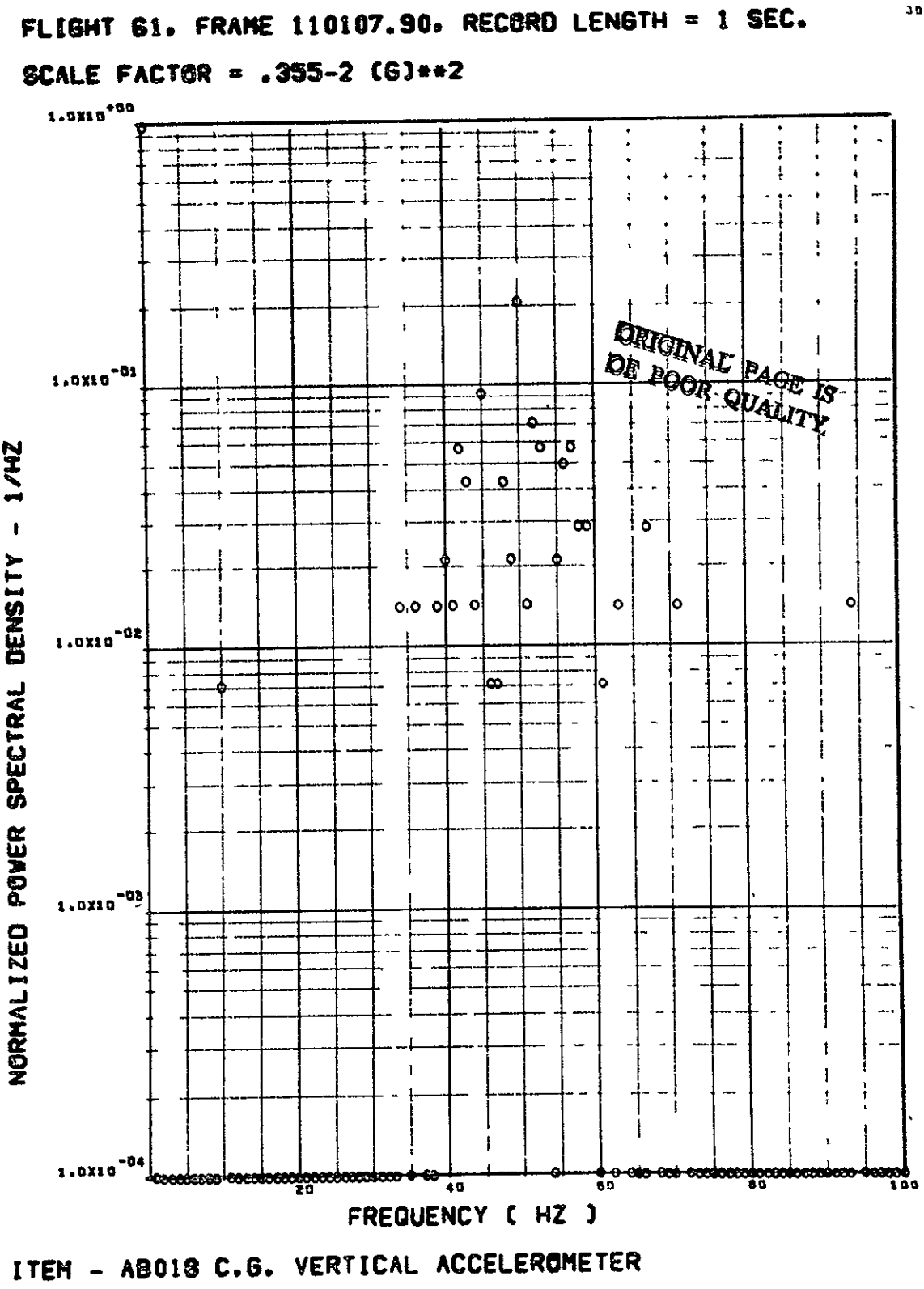

Figure 8. Continued

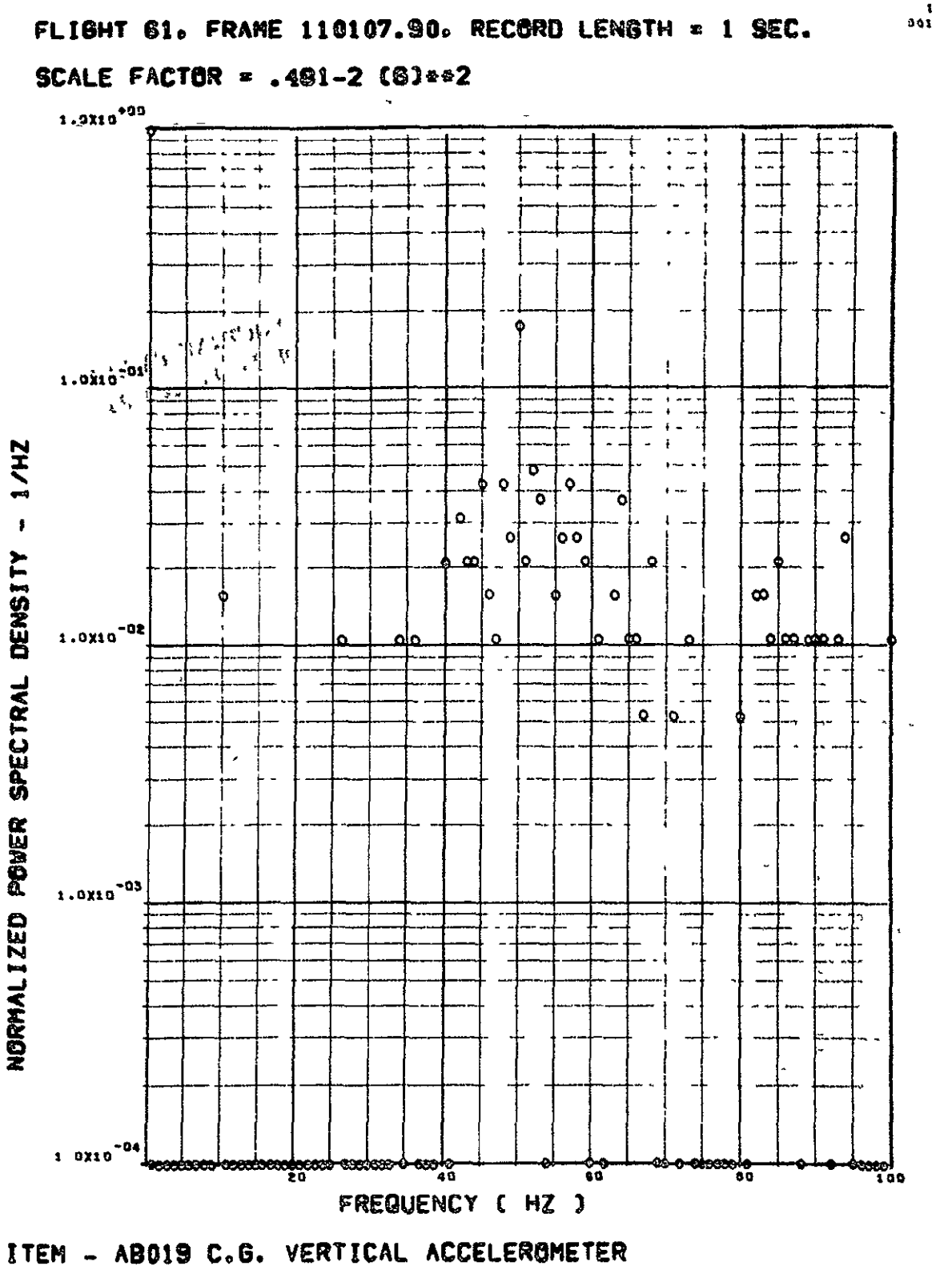

Figure 8. Continued

FLIGHT 61. FRAME 110107.90. RECORD LENGTH = 1 SEC.

SCALE FACTOR = .188-2 (6)**2

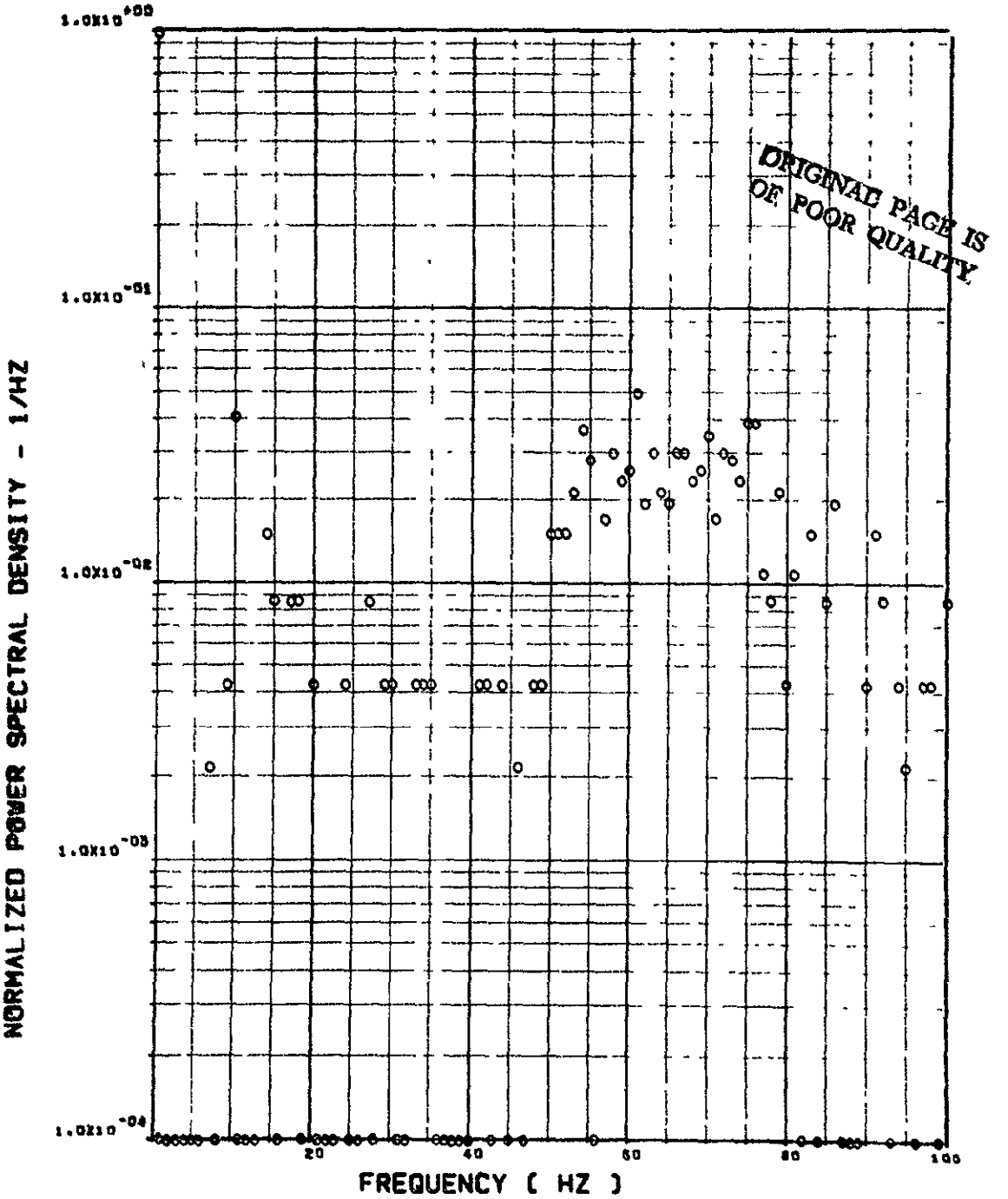

ITEM - AF009 PILOT'S SEAT VERTICAL ACCELEROMETER

Figure 8. Continued

FLIGHT 61. FRAME 110107.90. RECORD LENGTH = 1 SEC.

SCALE FACTOR = .646-3 (G)**2

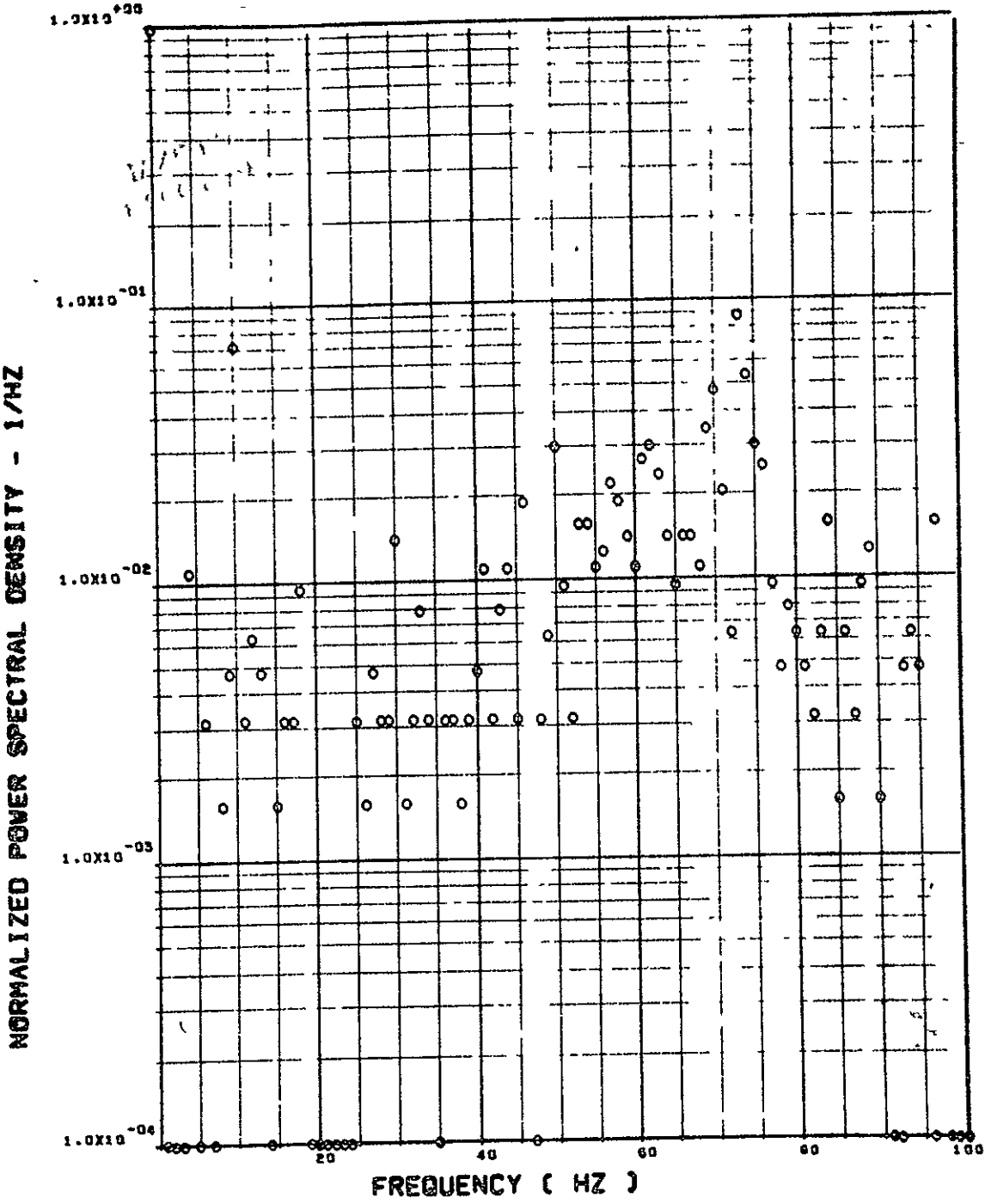

ITEM - AF010 PILOT'S SEAT LATERAL ACCELEROMETER

Figure 8. Continued

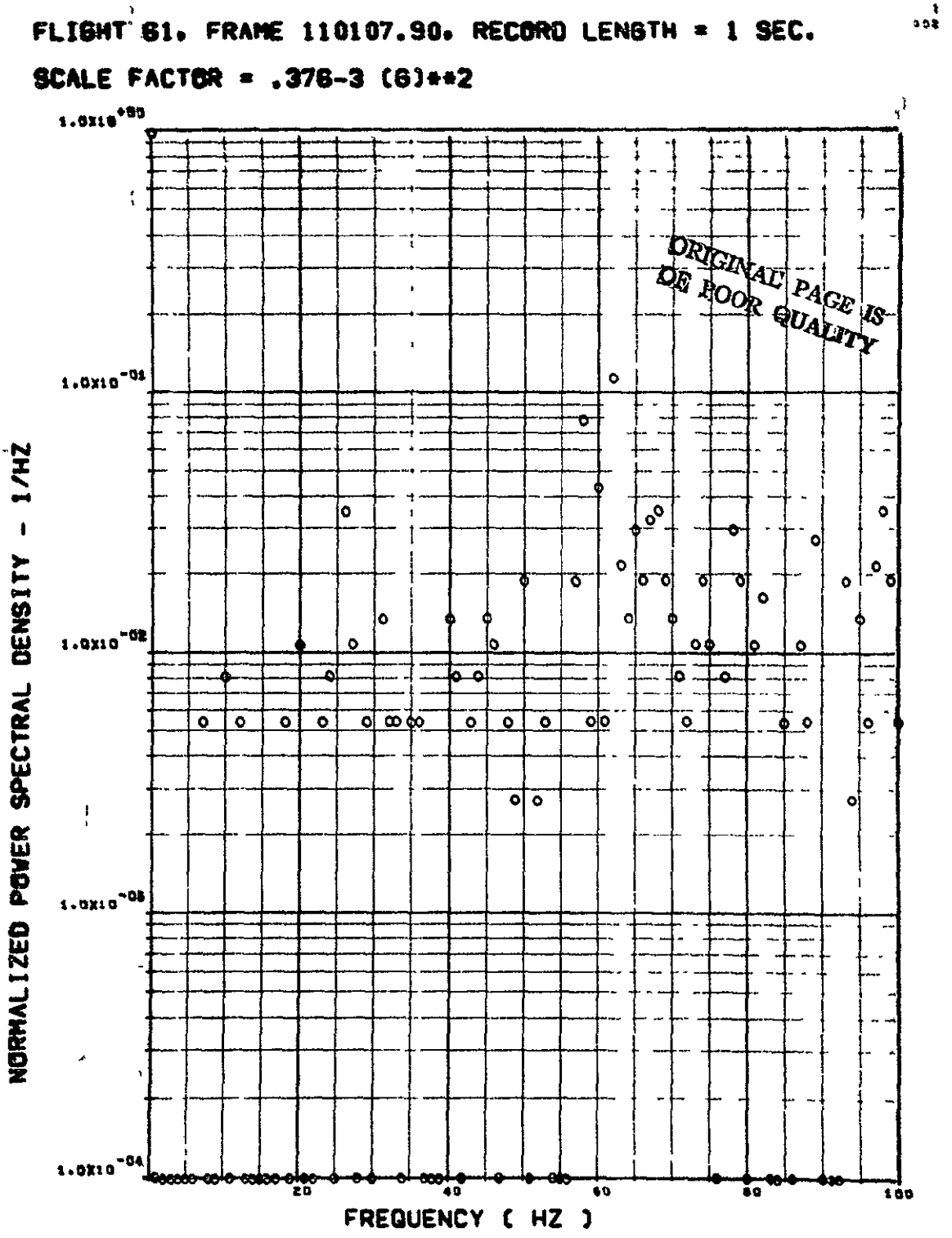

Figure 8. Continued

FLIGHT 61. FRAME 110107.90. RECORD LENGTH = 1 SEC.

SCALE FACTOR = .270+6 (N)**2 =.136+5 (LB)**2

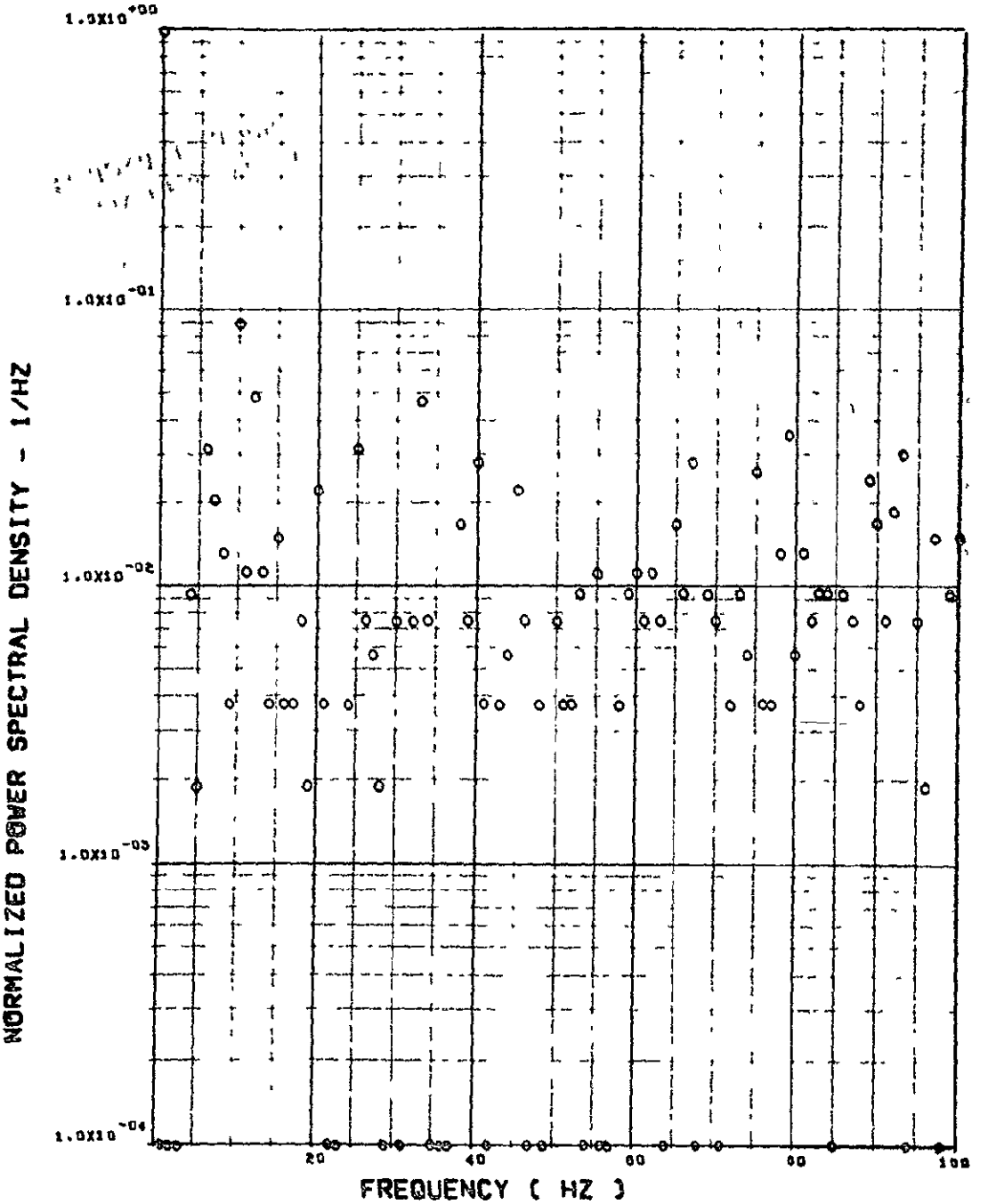

ITEM - SW123 SHEAR AT WING STATION 1

Figure 8. Continued

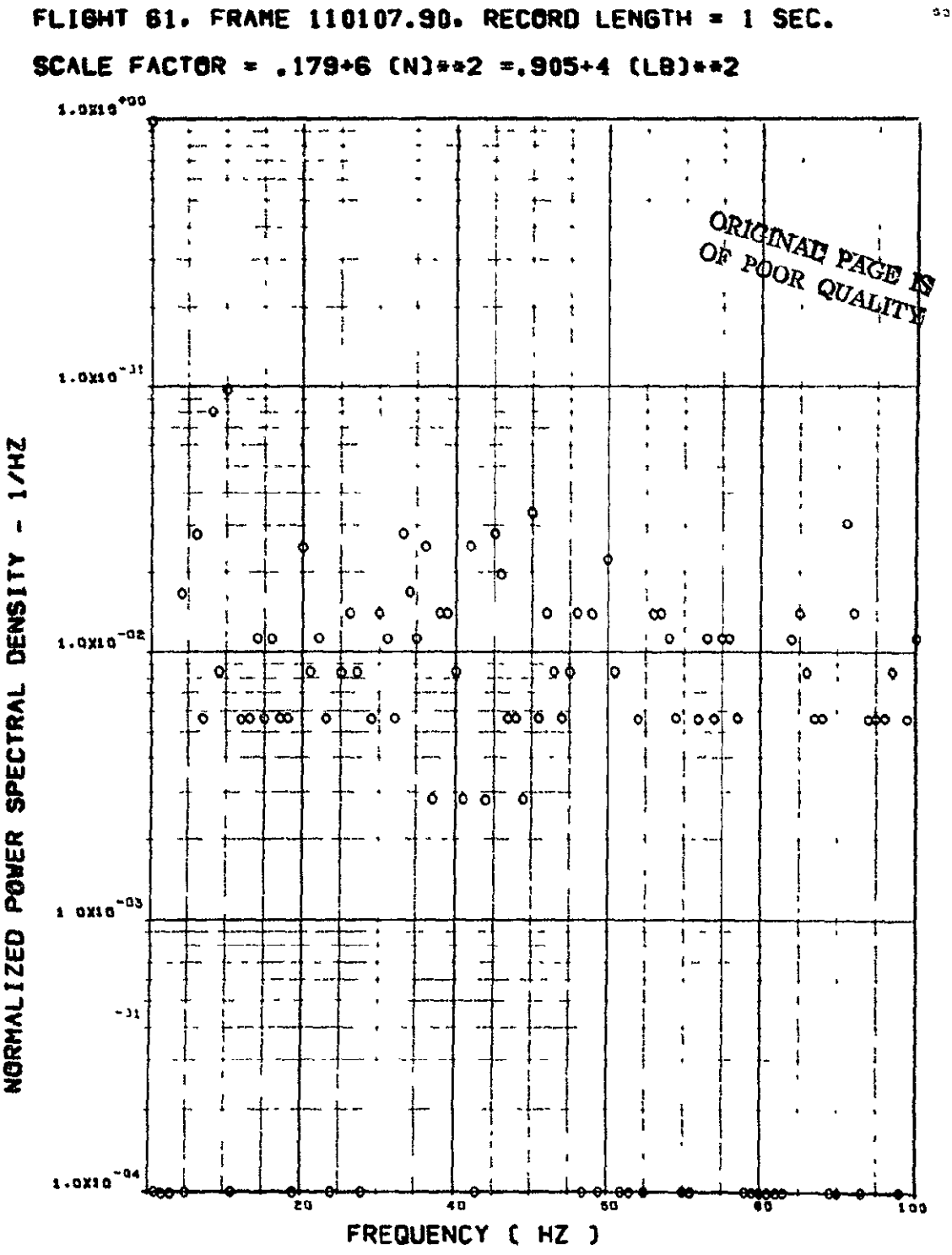

Figure 8. Continued

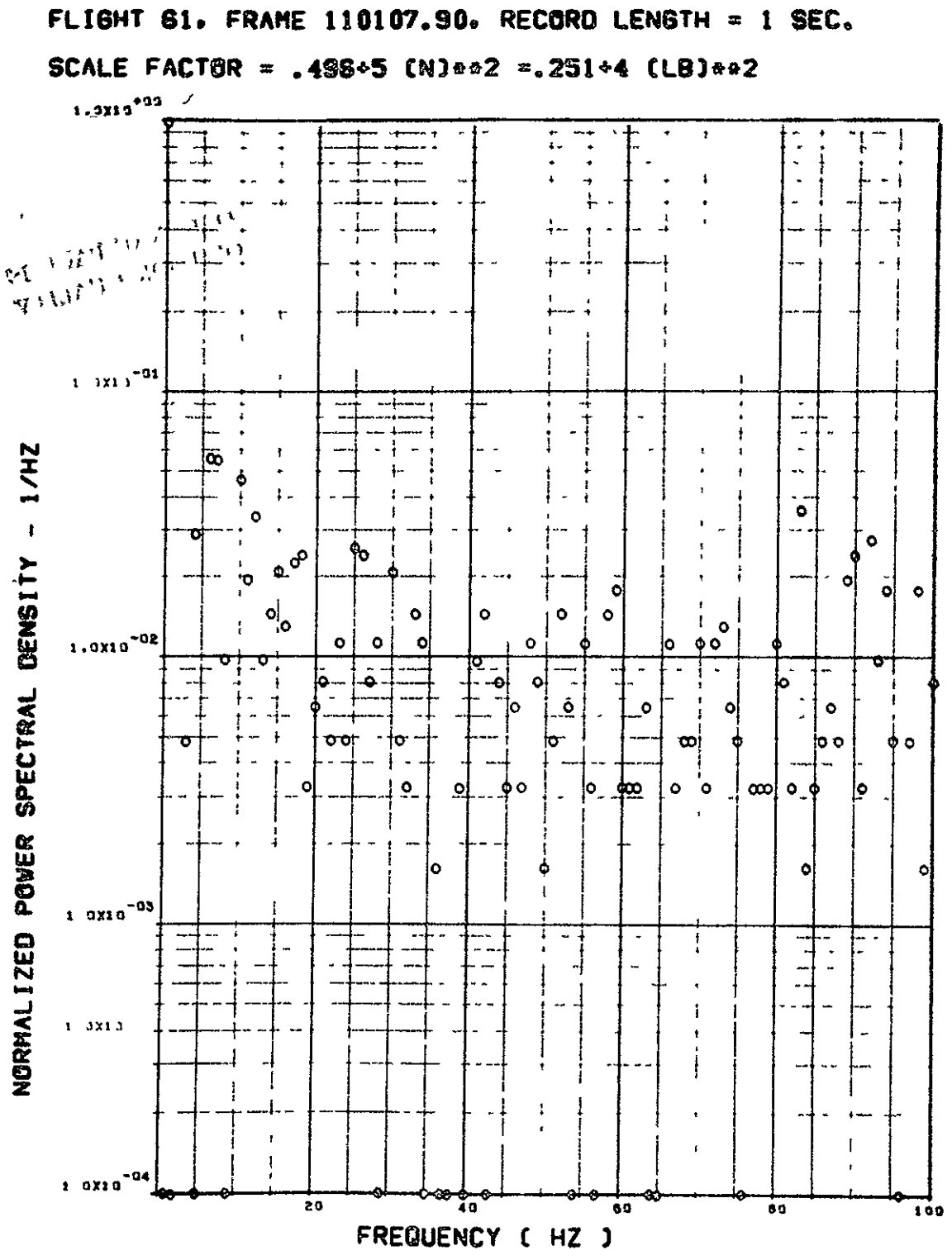

Figure 8. Continued

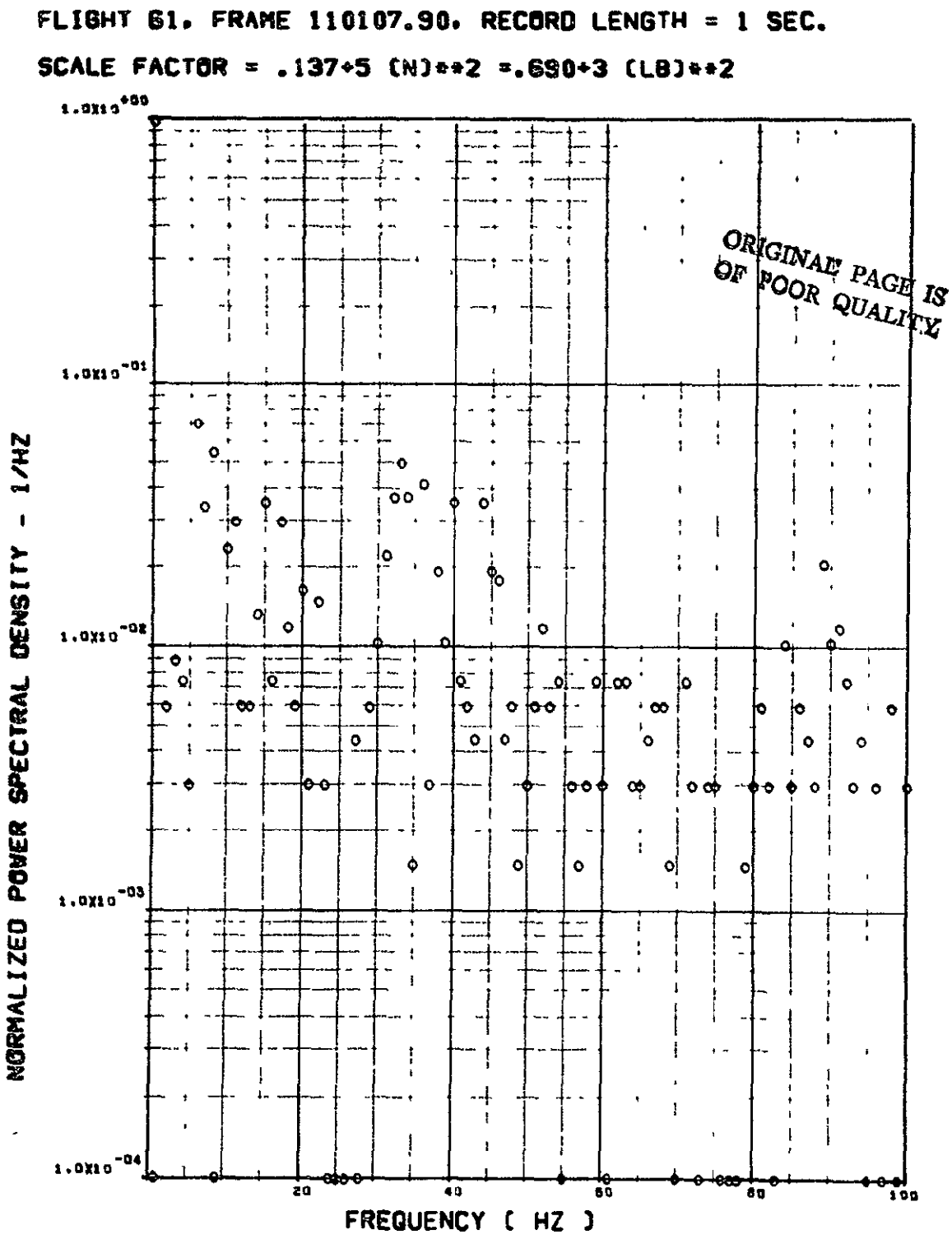

Figure 8. Continued

FLIGHT 61. FRAME 110107.90. RECORD LENGTH = 1 SEC.

SCALE FACTOR = .183+7 (M-N)**2 =.149+9 (IN-LB)**2

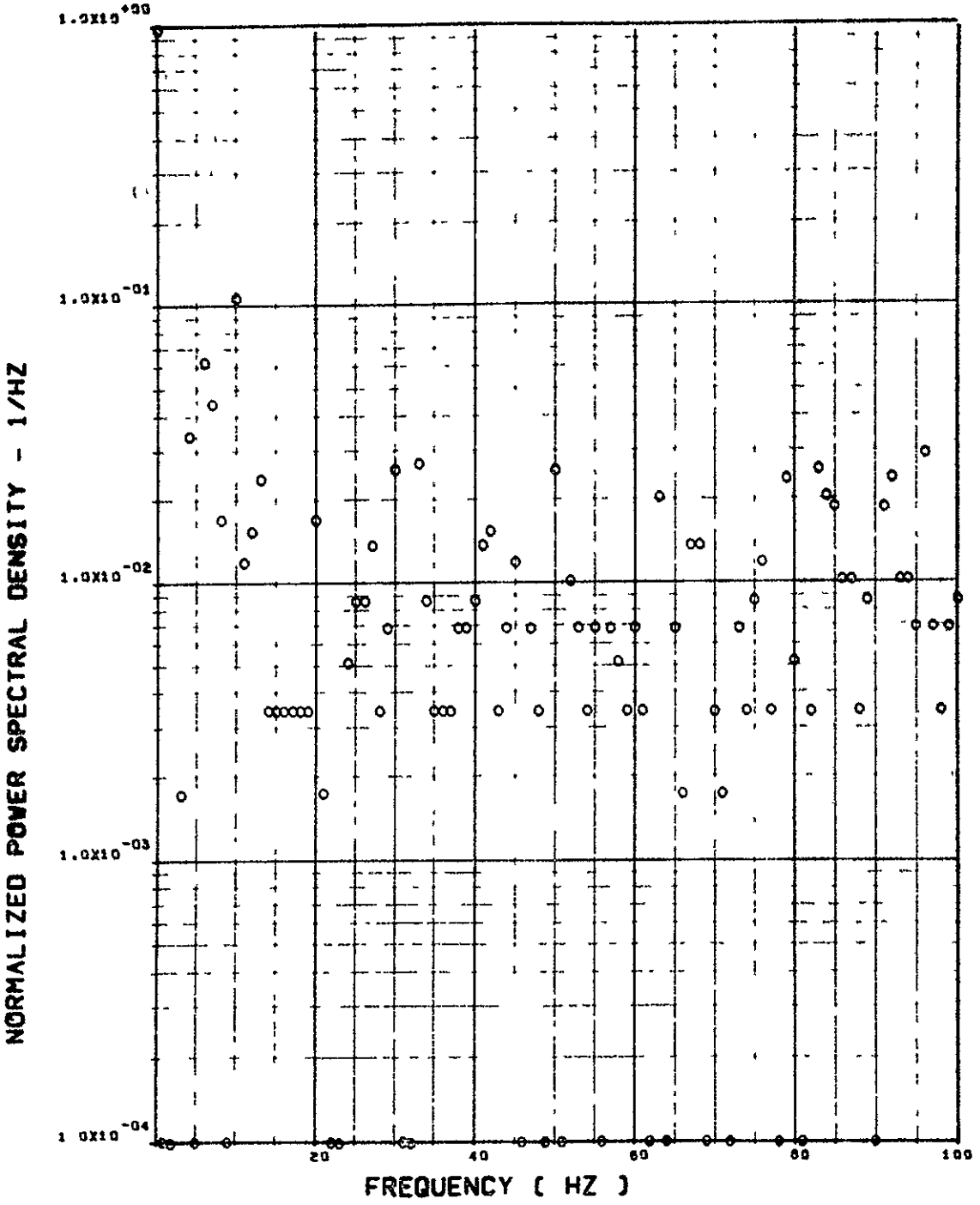

ITEM - SW124 BENDING MOMENT AT WING STATION 1

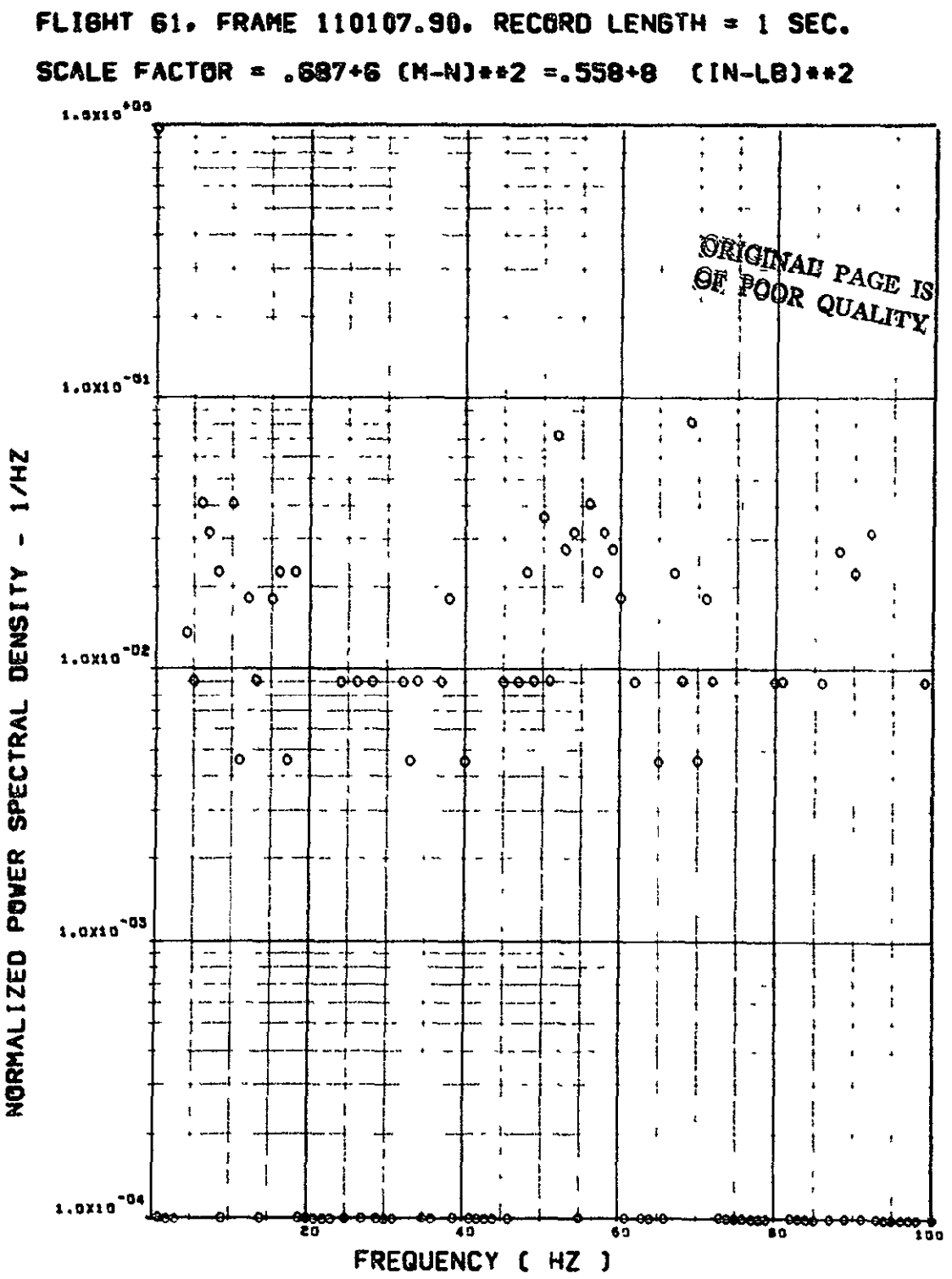

Figure 8. Continued

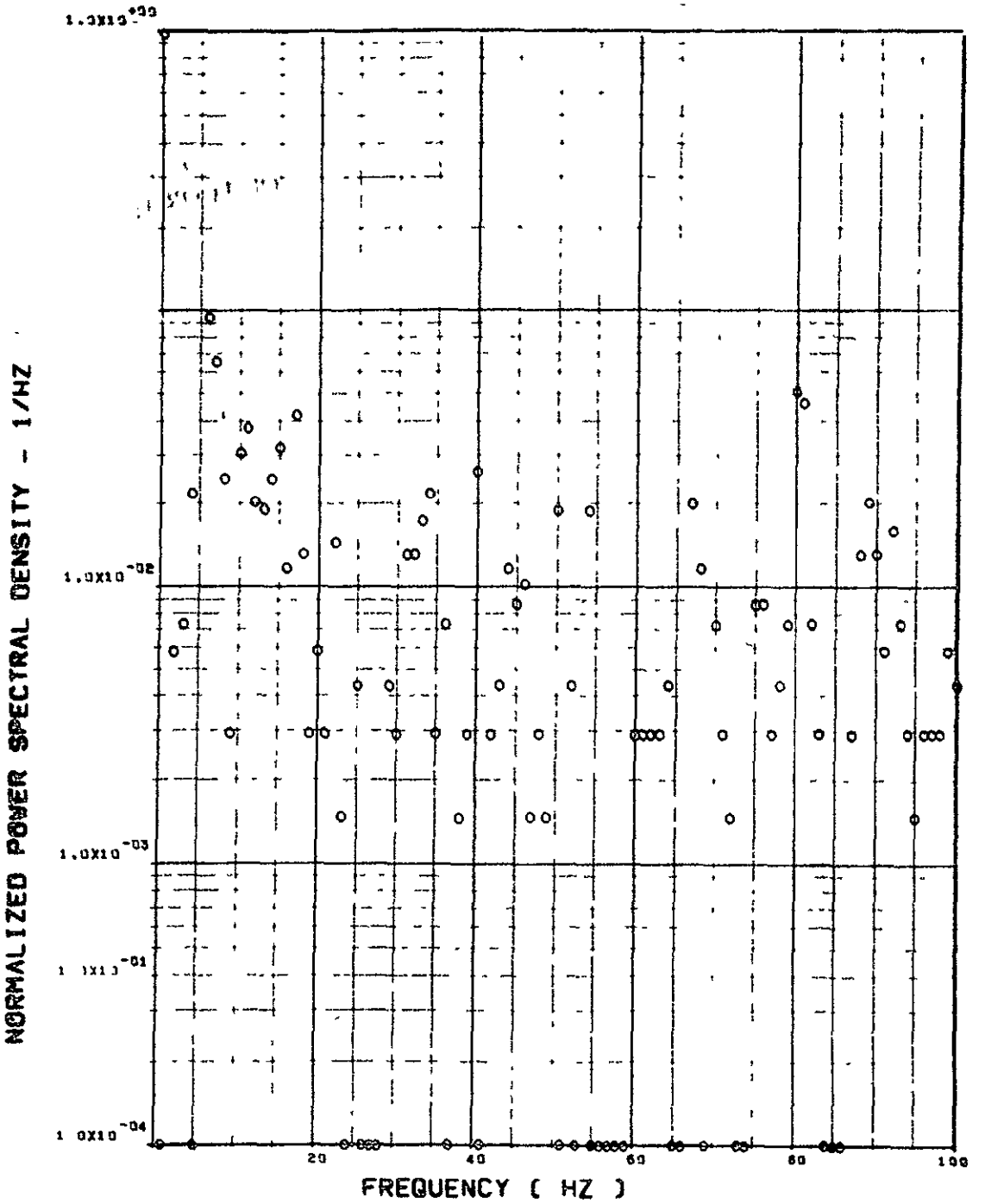

Figure 8. Continued

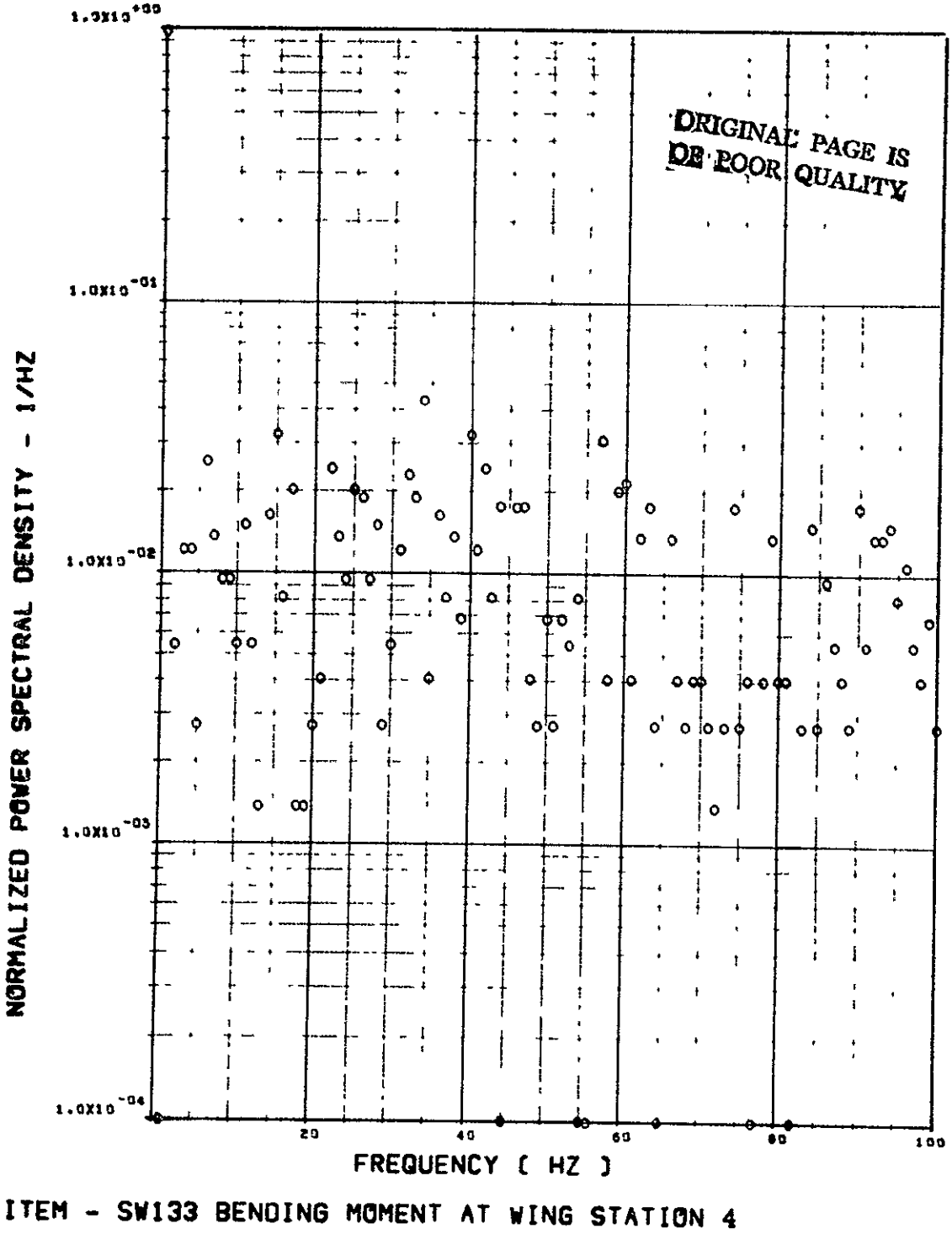

Figure 8. Continued

FLIGHT 61. FRAME 110107.90. RECORD LENGTH = 1 SEC.

SCALE FACTOR = .123+6 (M-N)**2 =.997+7 (IN-LB)**2

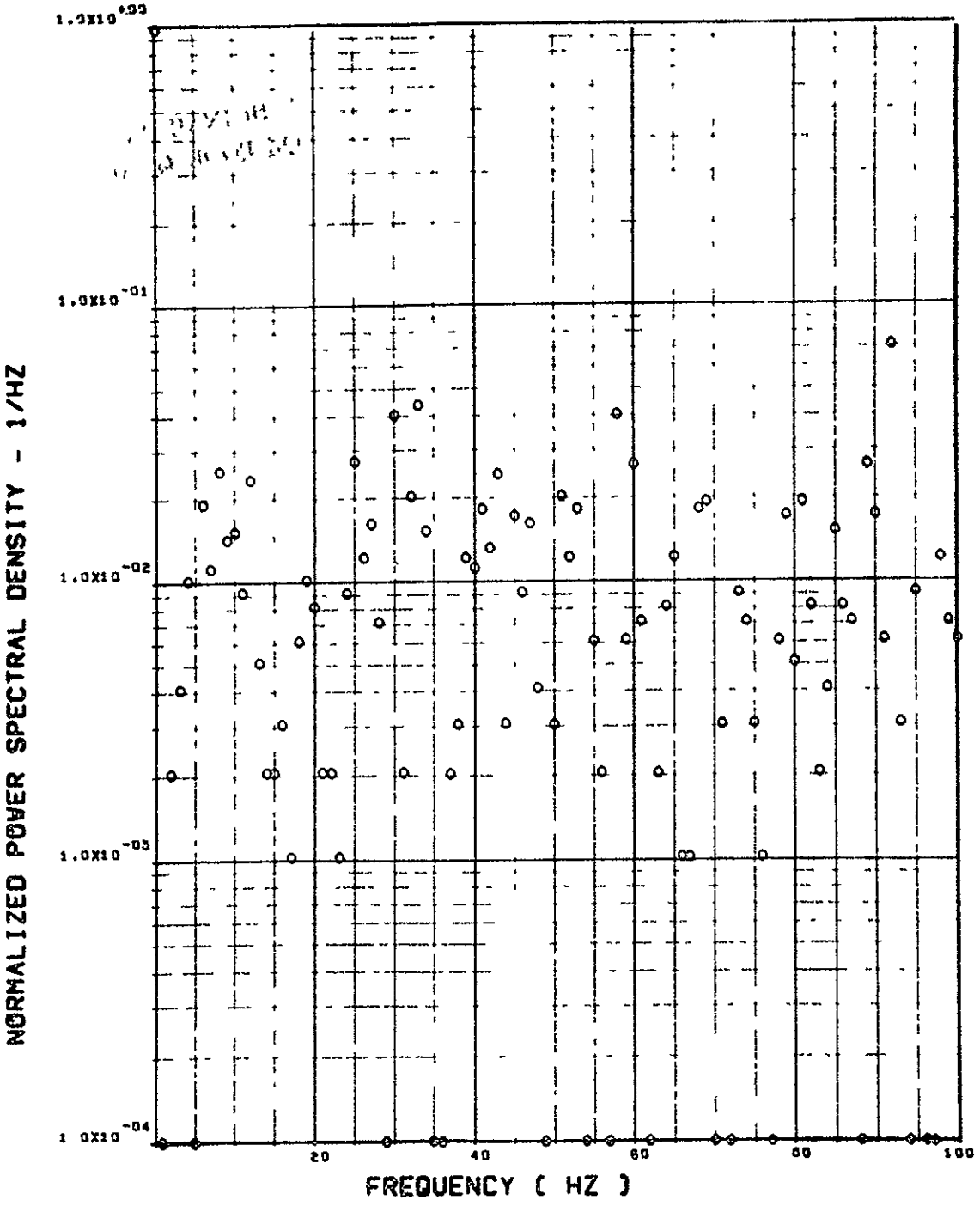

ITEM - SW125 TORSION AT WING STATION 1

Figure 8. Continued

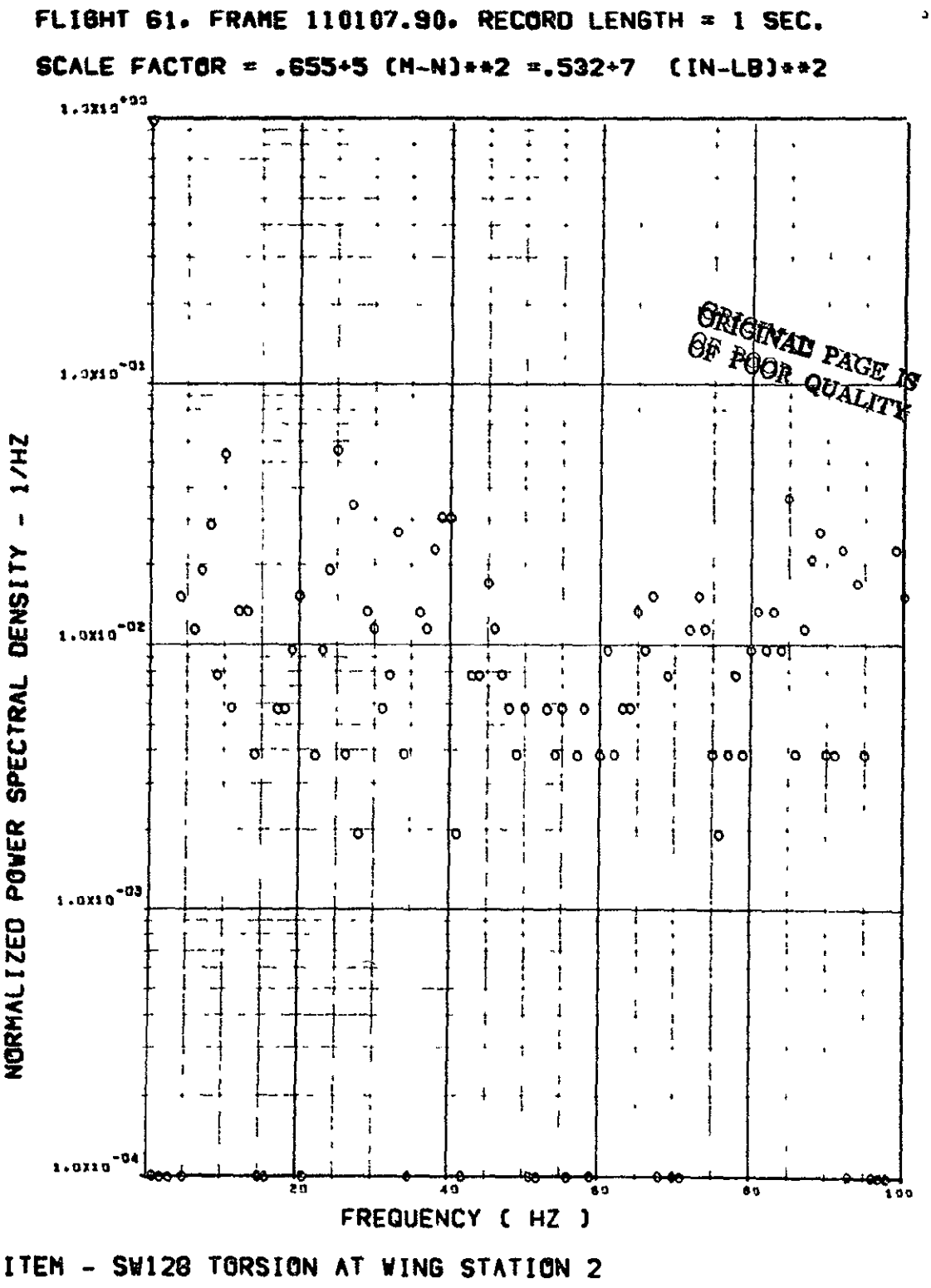

Figure 8. Continued

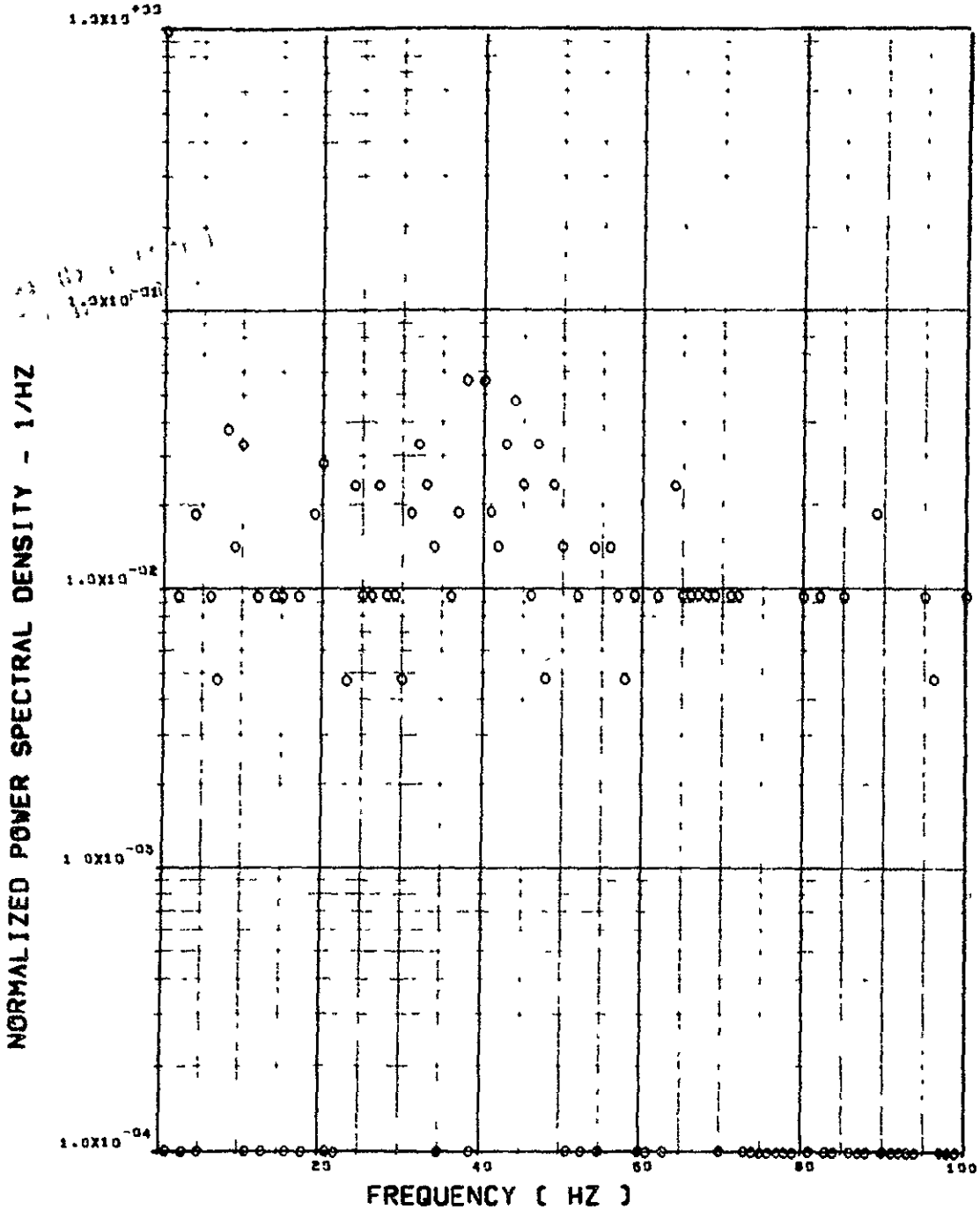

Figure 8. Continued

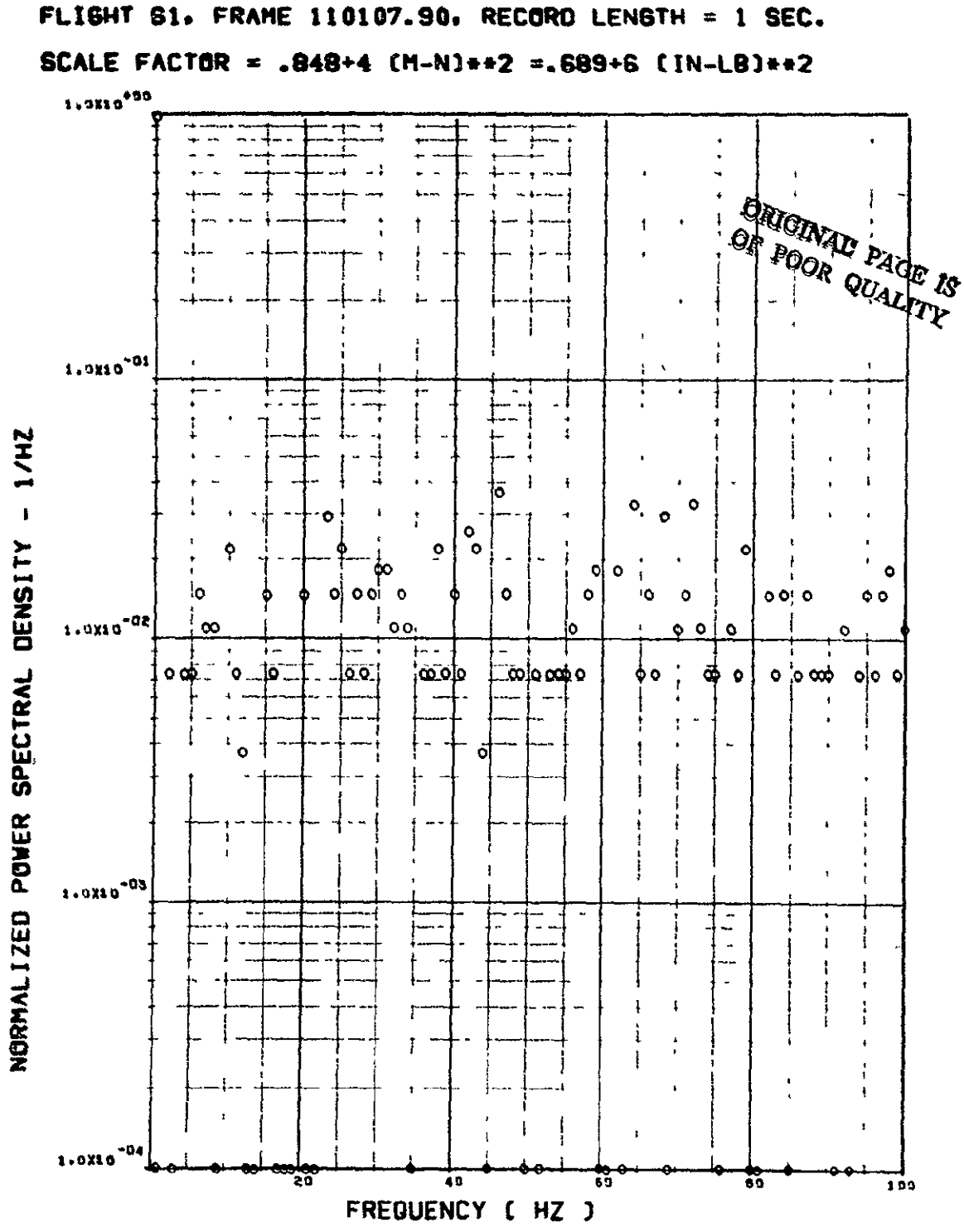

Figure 8. Continued

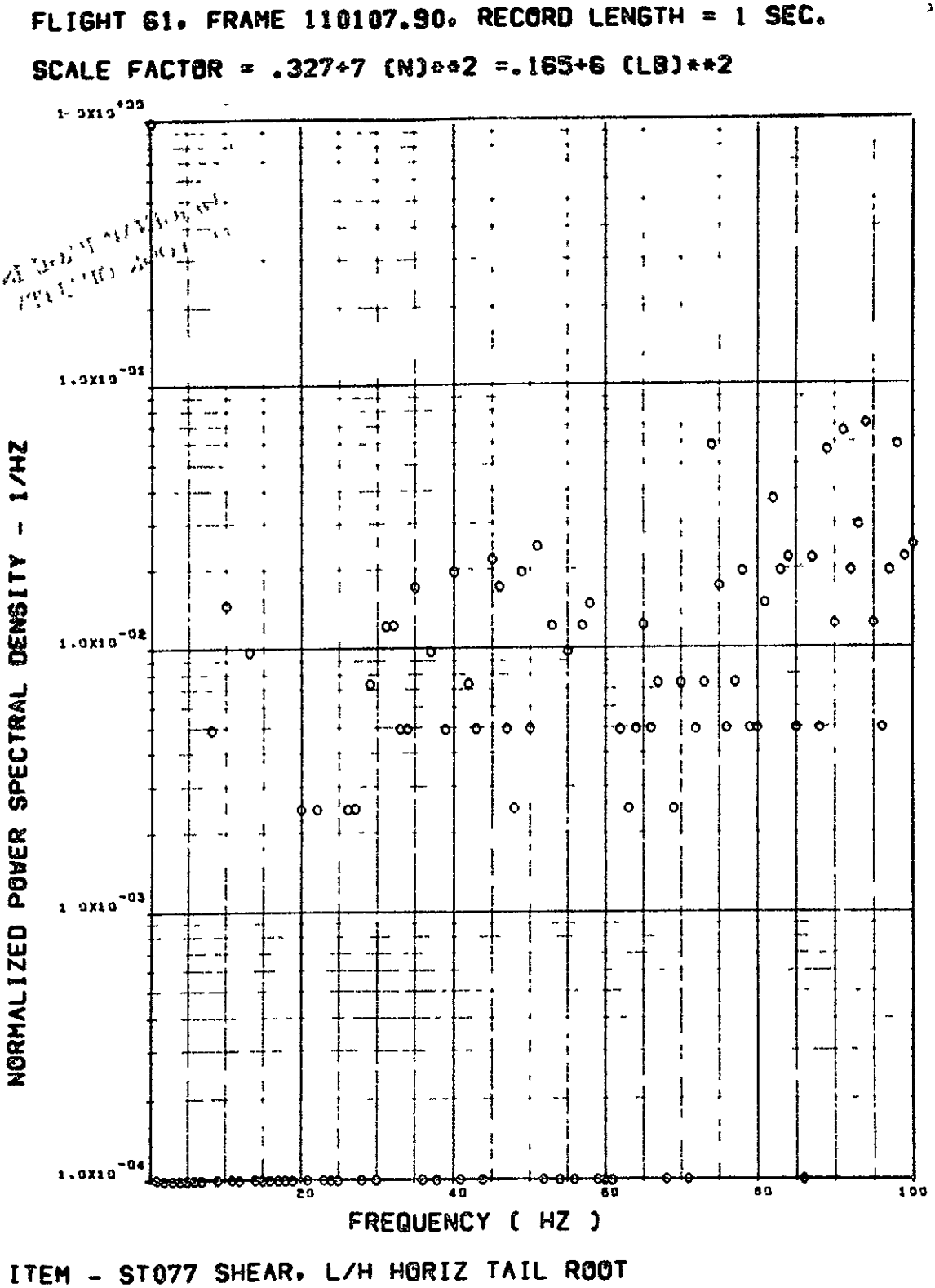

Figure 8. Continued

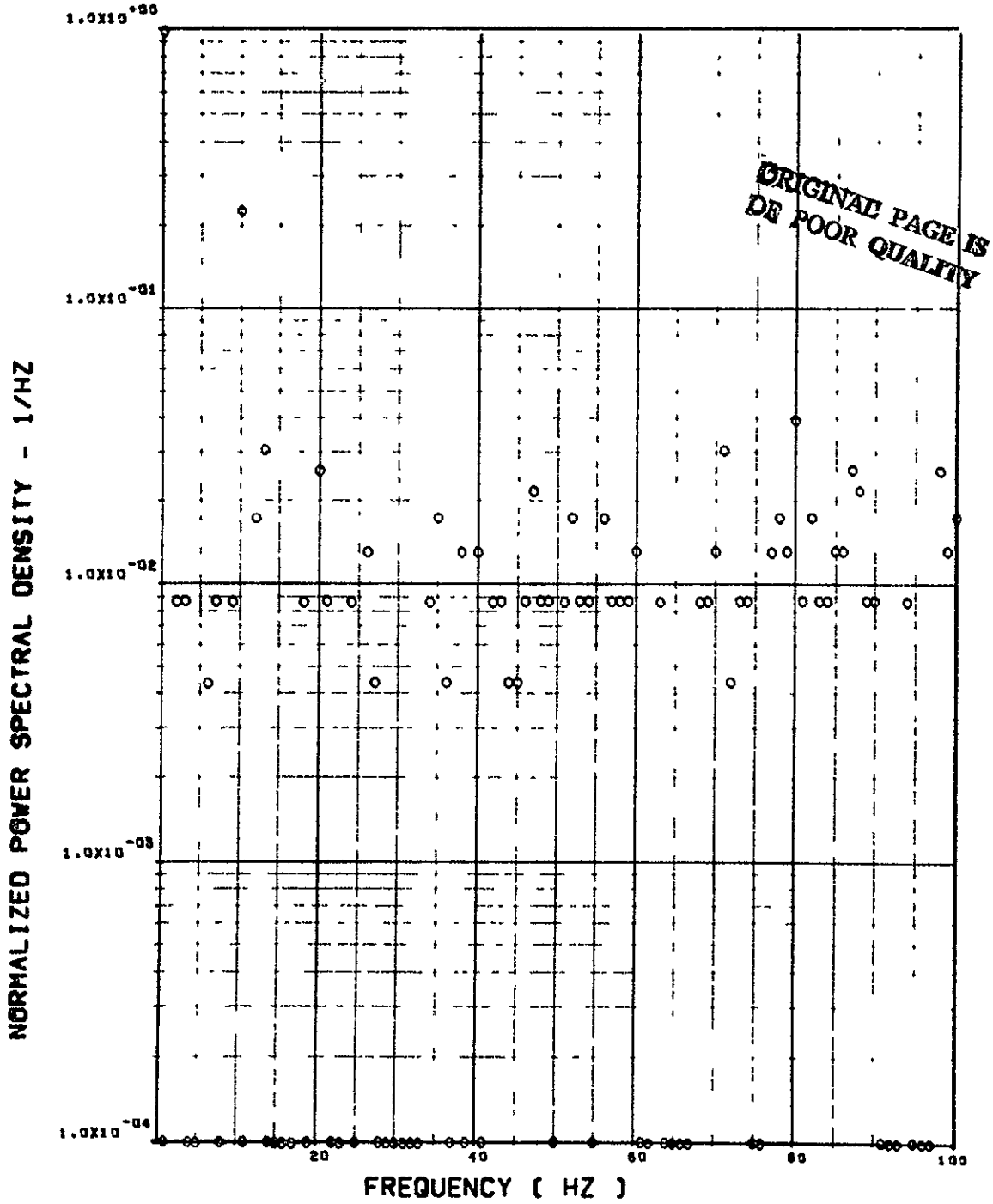

Figure 8. Continued

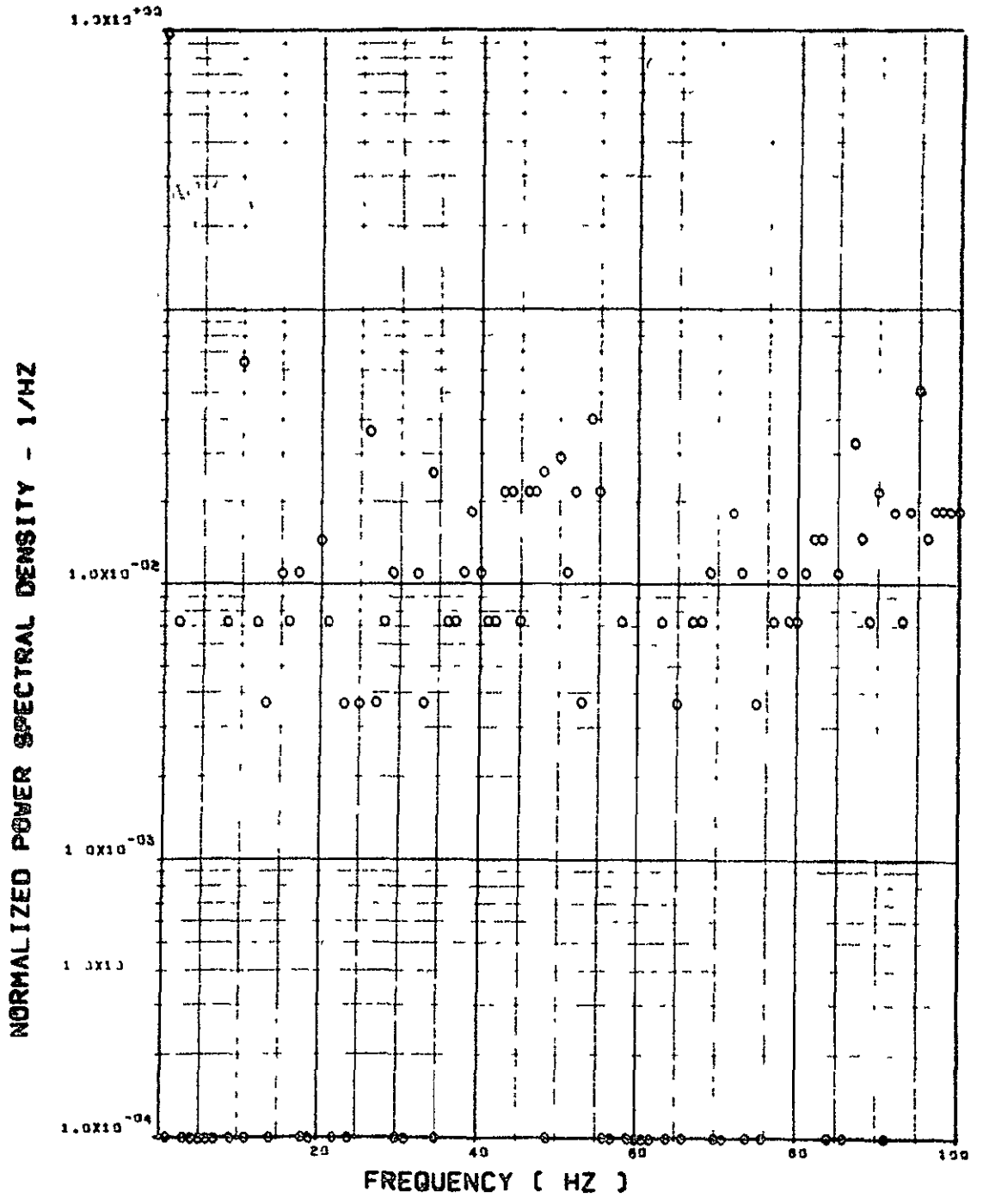

Figure 8. Continued

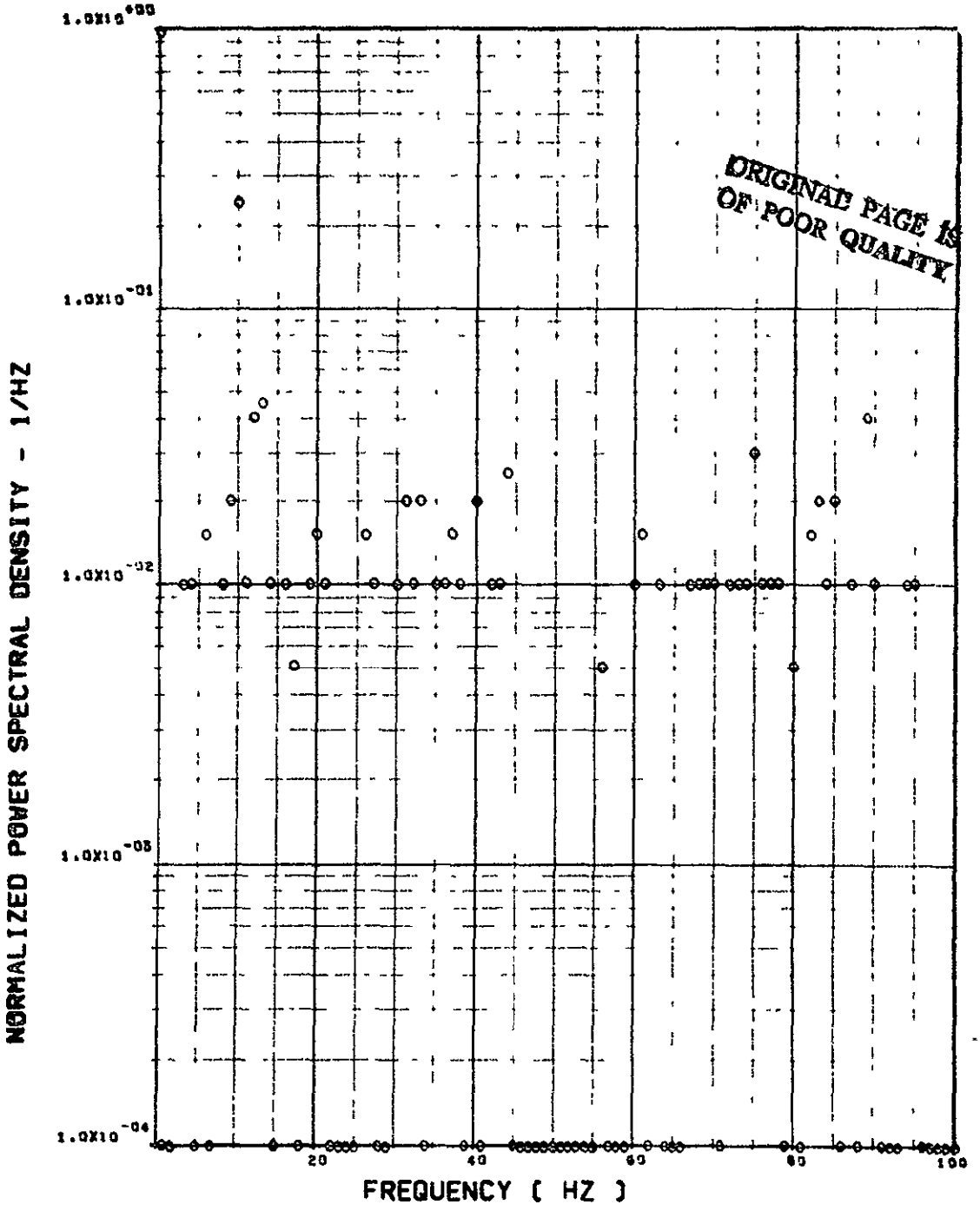

Figure 8. Continued

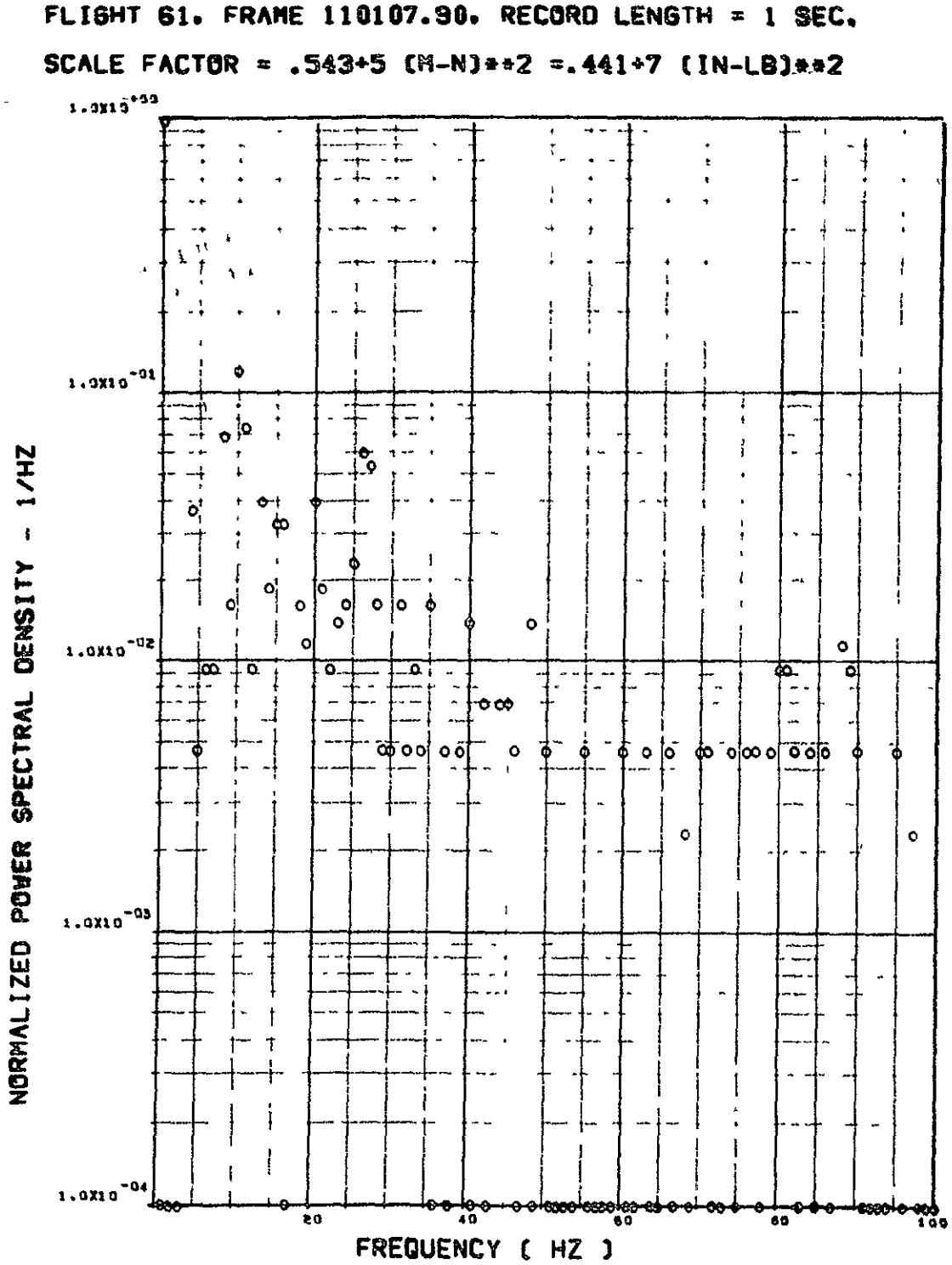

Figure 8. Continued

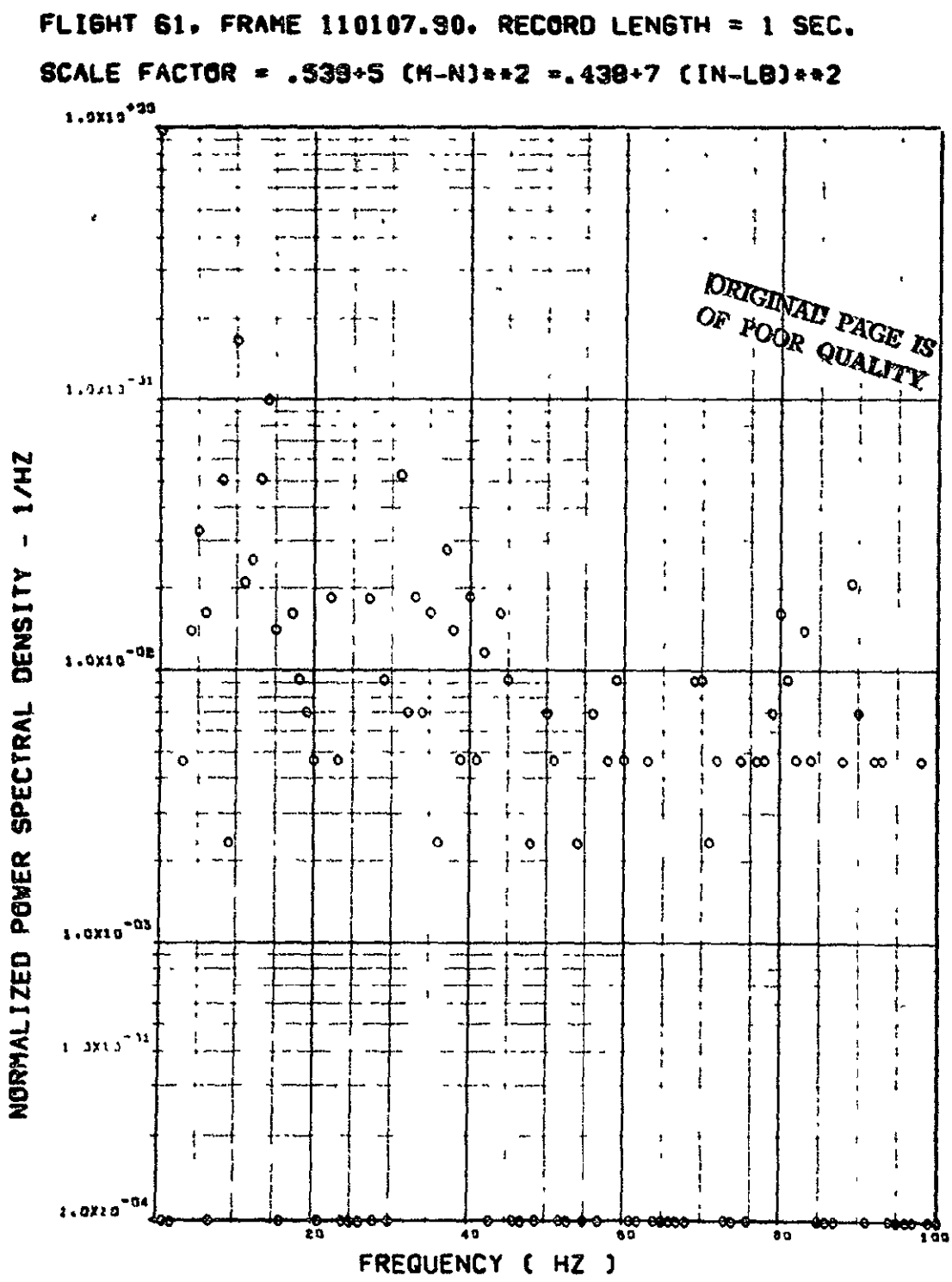

Figure 8. Concluded

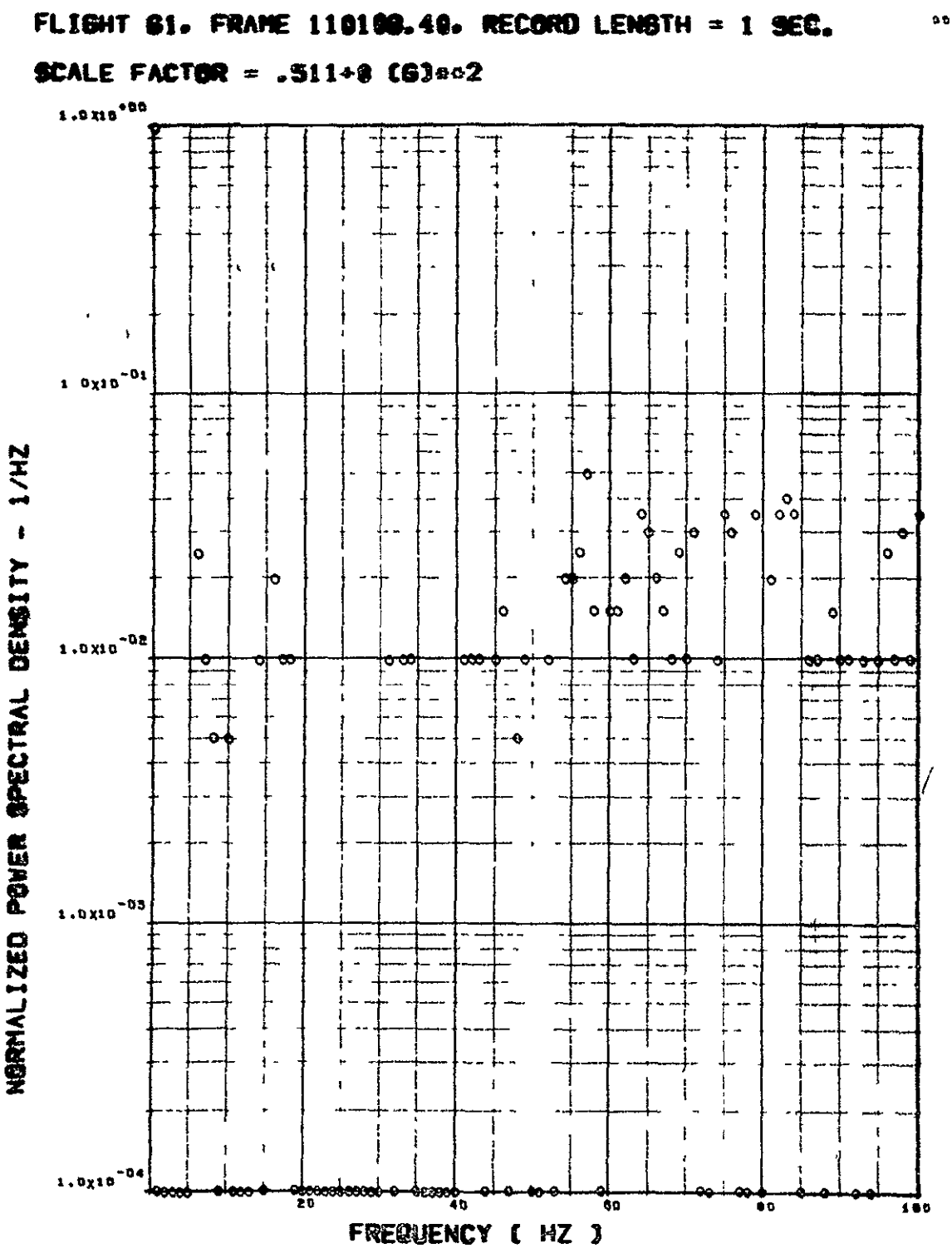

Figure 9. Power Spectra - Flight 61, Run 227, Point 2 T_1 = 110108.4, ΔT = 1 Sec, α_{Nom} = 9.25 deg, $\Delta\alpha$= 2.05 deg.

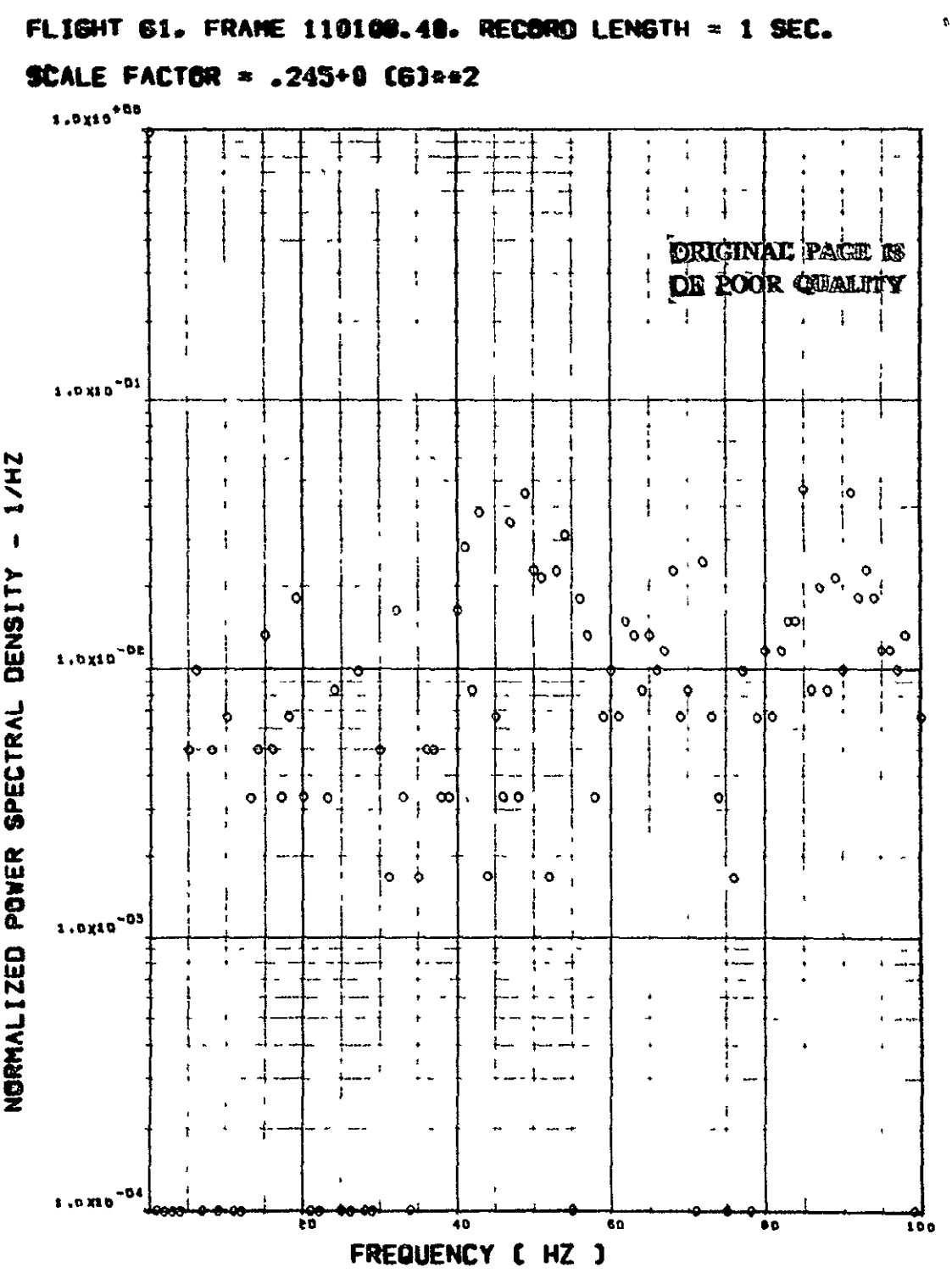

Figure 9. Continued

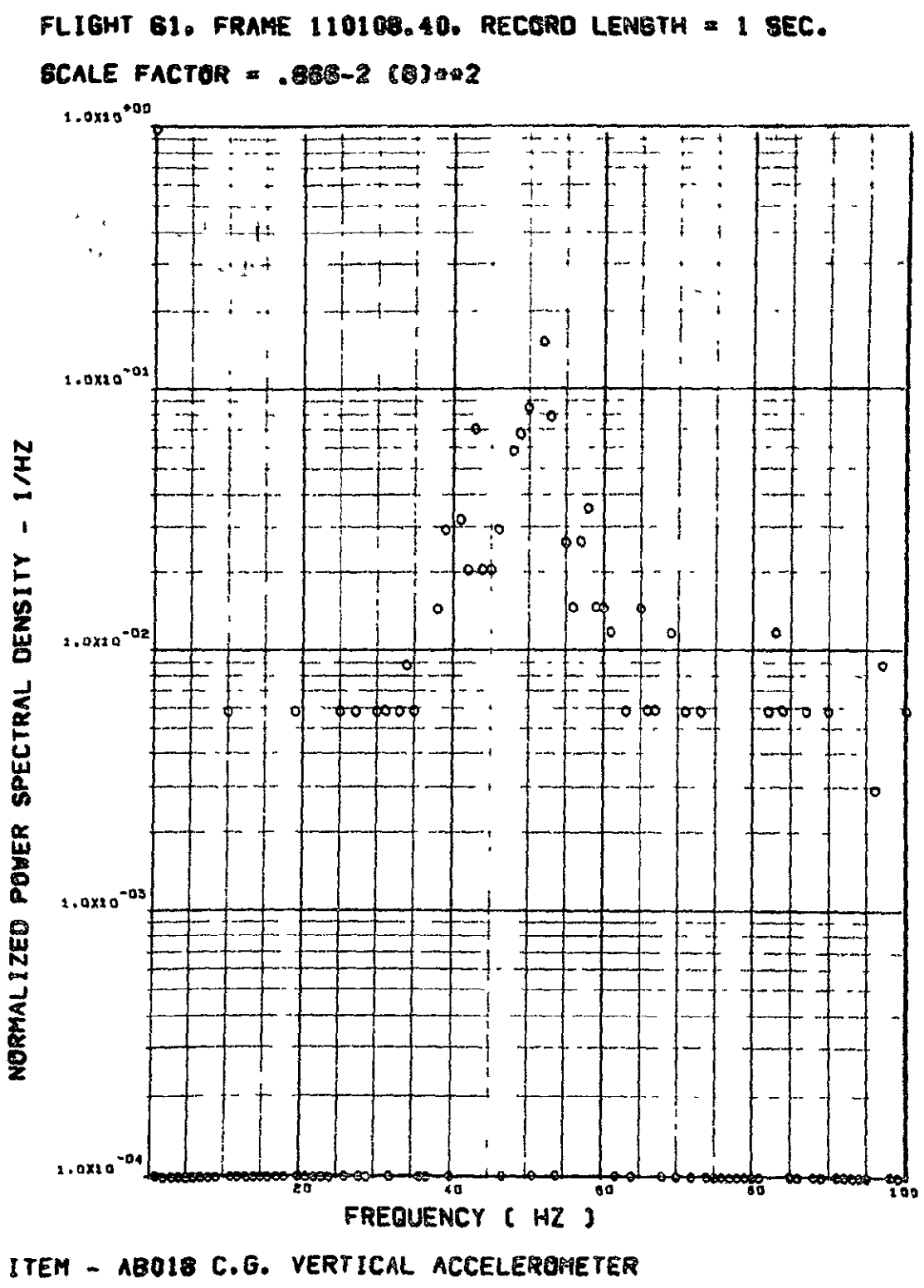

Figure 9. Continued

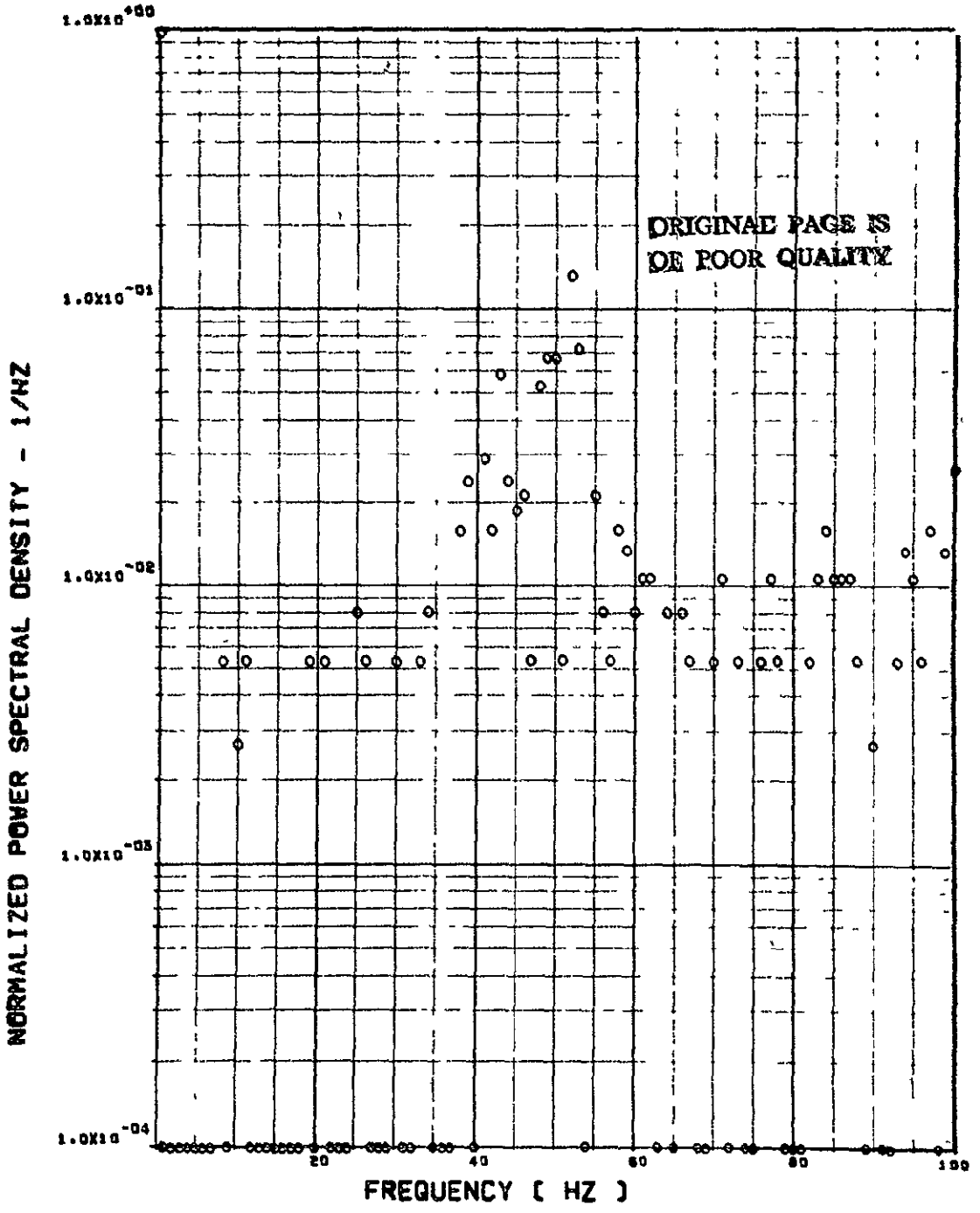

Figure 9. Continued

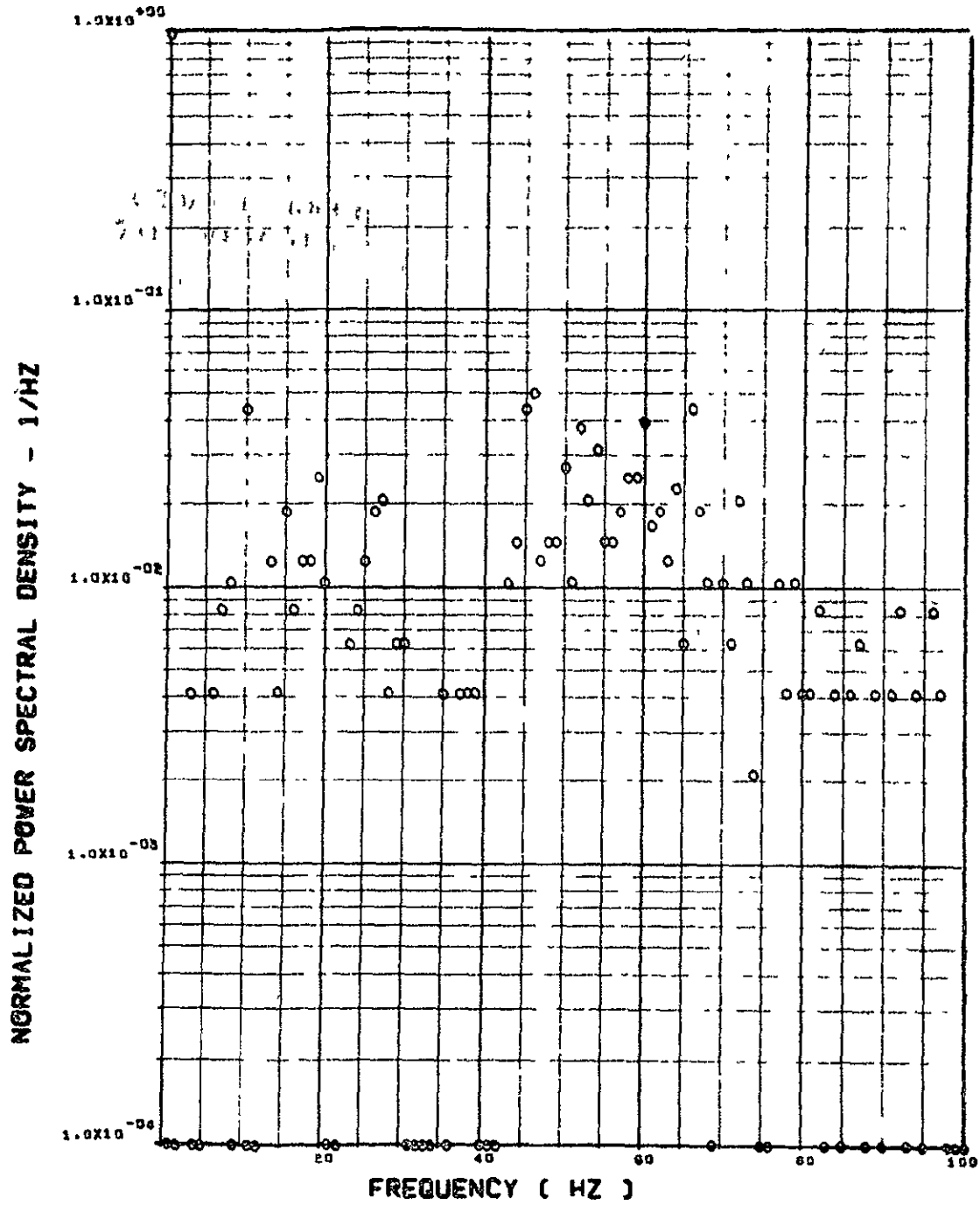

Figure 9. Continued.

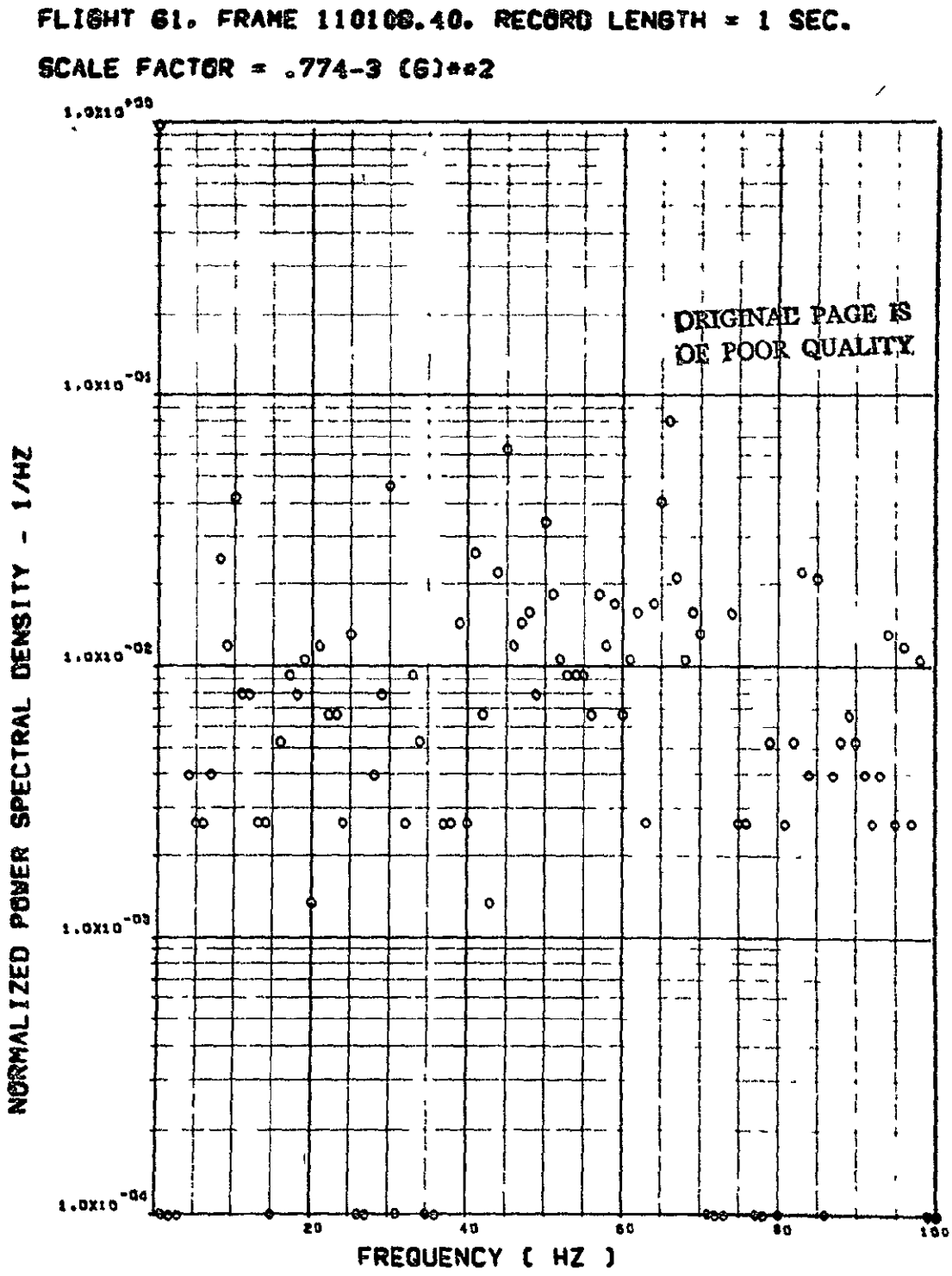

Figure 9. Continued

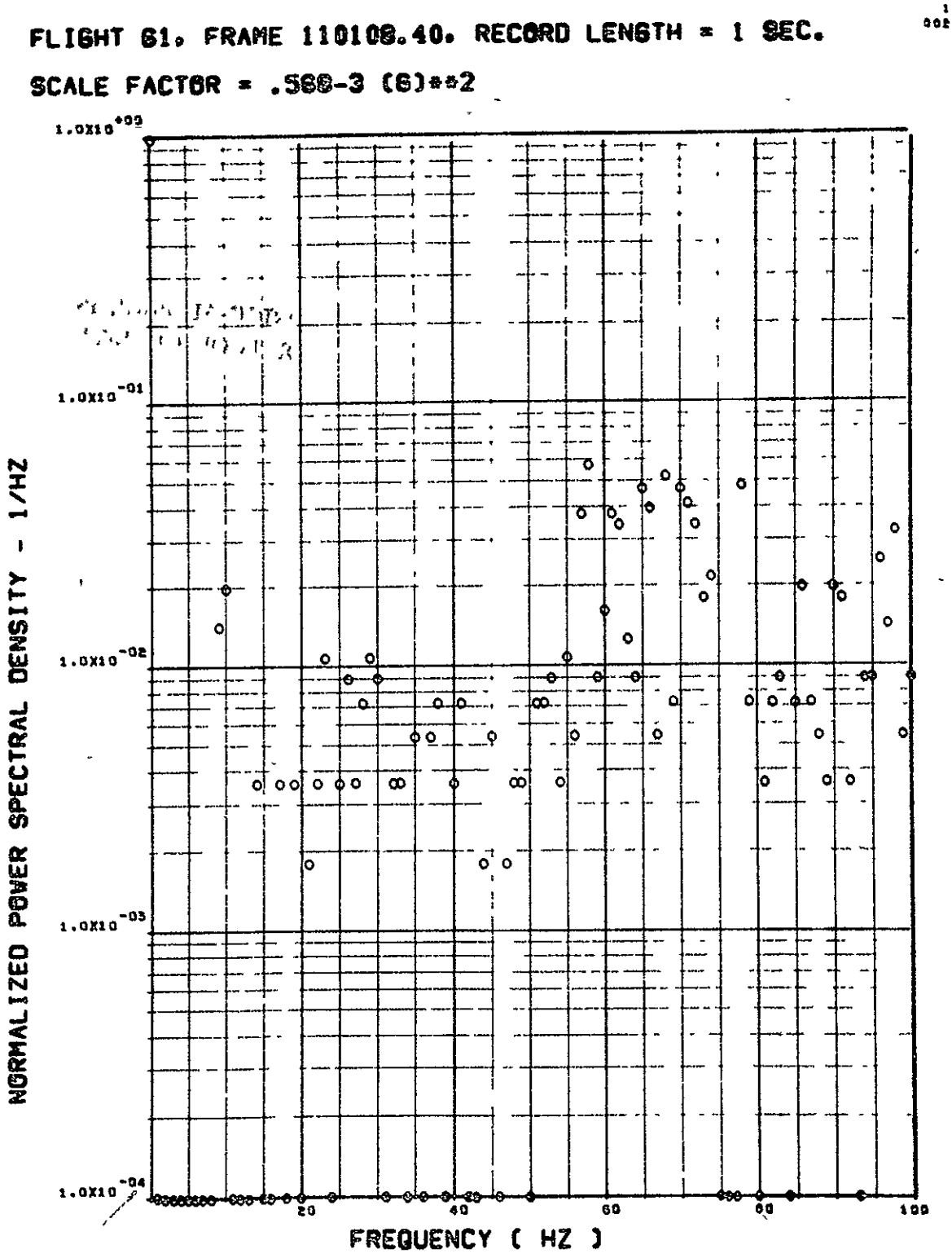

Figure 9. Continued

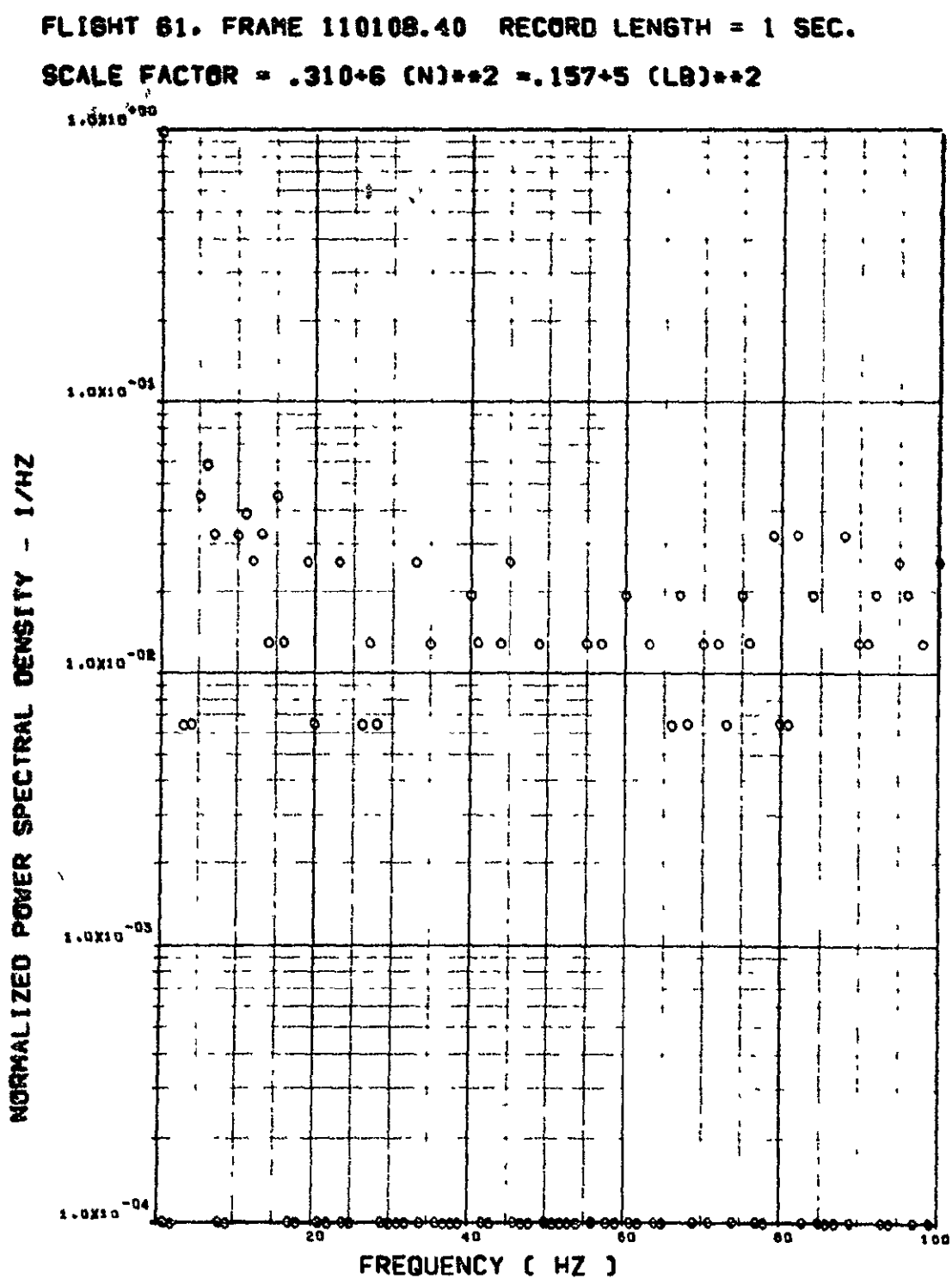

Figure 9. Continued

FLIGHT 61, FRAME 110108.40, RECORD LENGTH = 1 SEC.

SCALE FACTOR = .328+6 (N)**2 =.166+5 (LB)**2

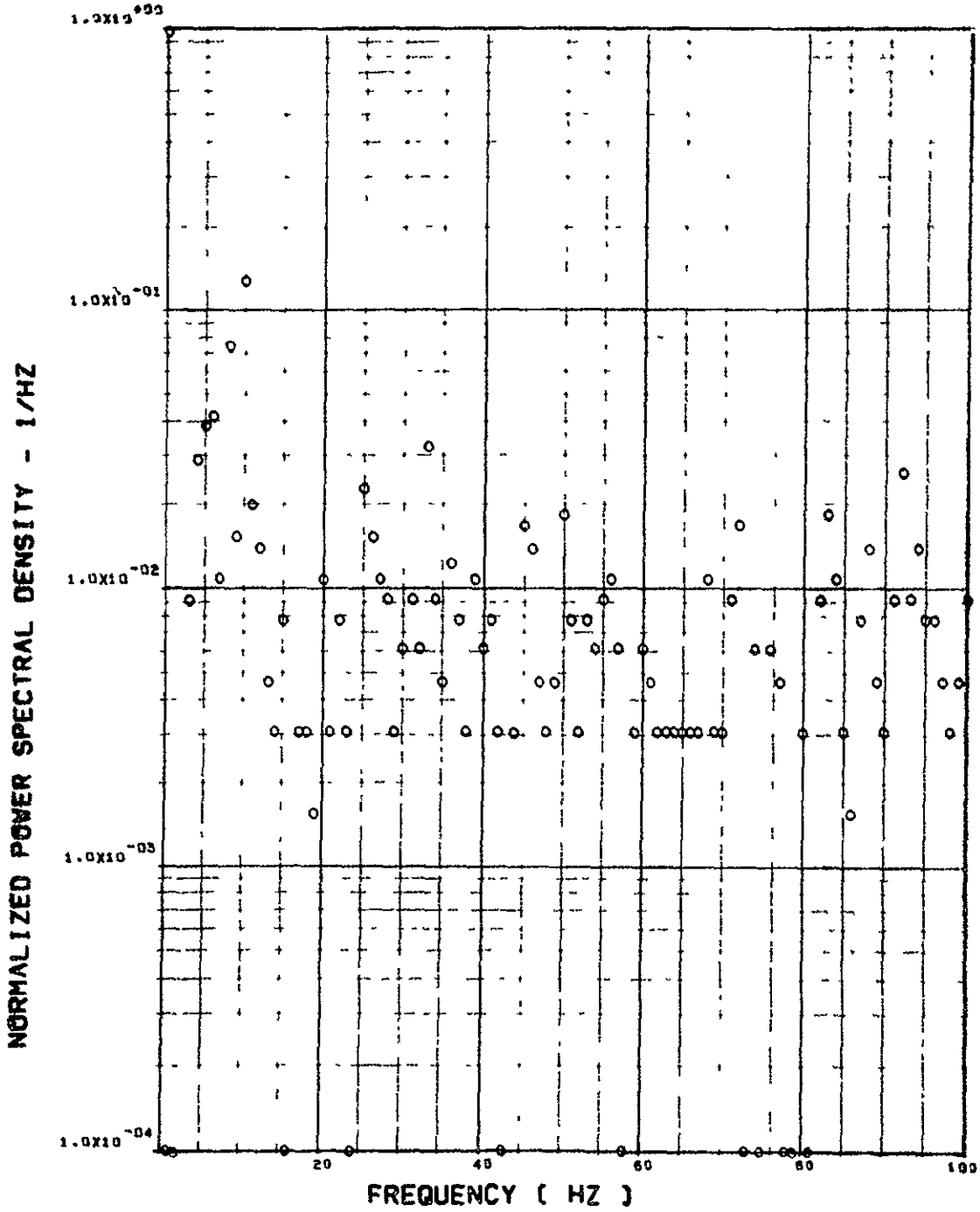

ITEM - SW126 SHEAR AT WING STATION 2

Figure 9. Continued

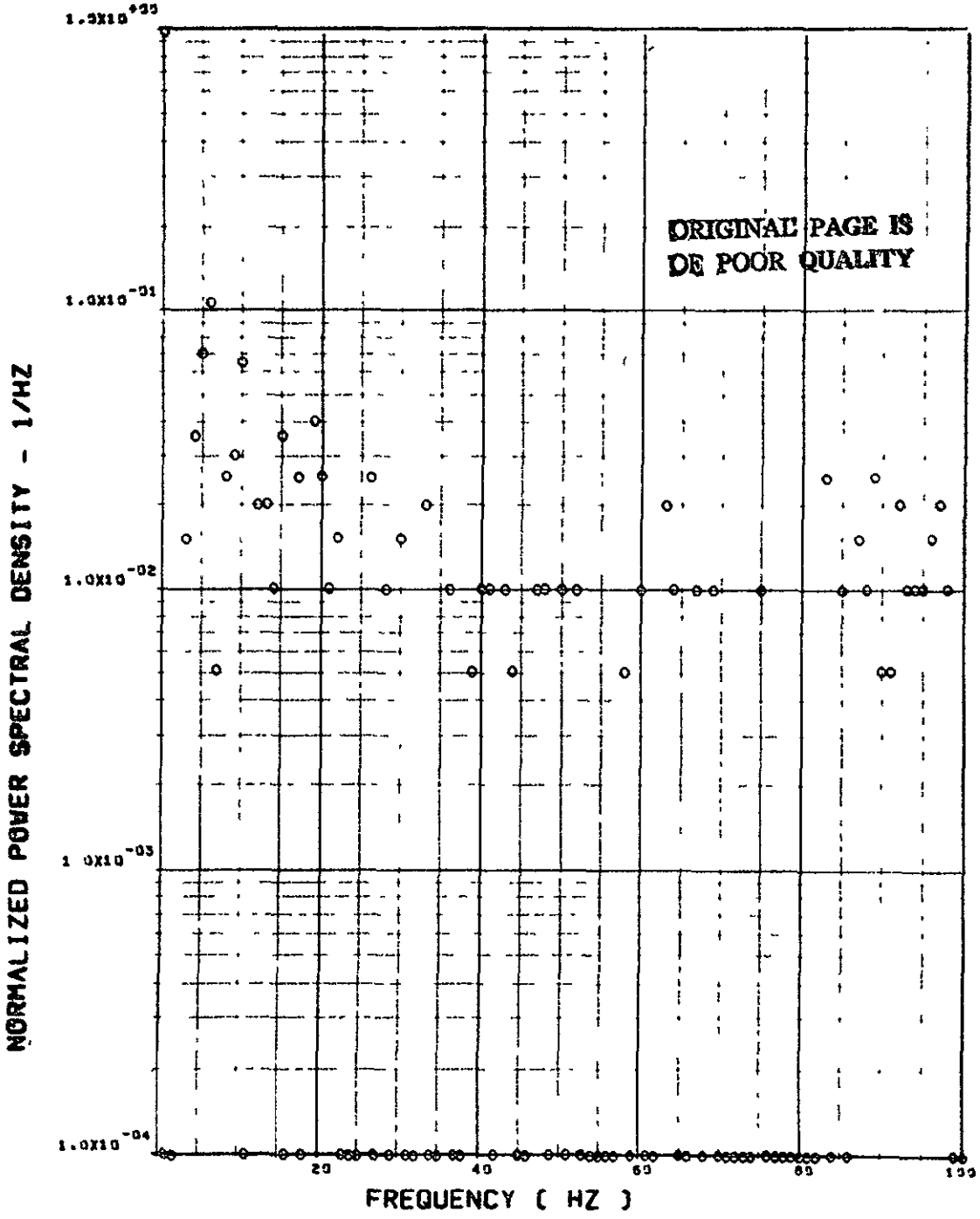

Figure 9. Continued

FLIGHT 61. FRAME 110108.40 RECORD LENGTH = 1 SEC.

SCALE FACTOR = .364+5 (N)**2 =.184+4 (LB)**2

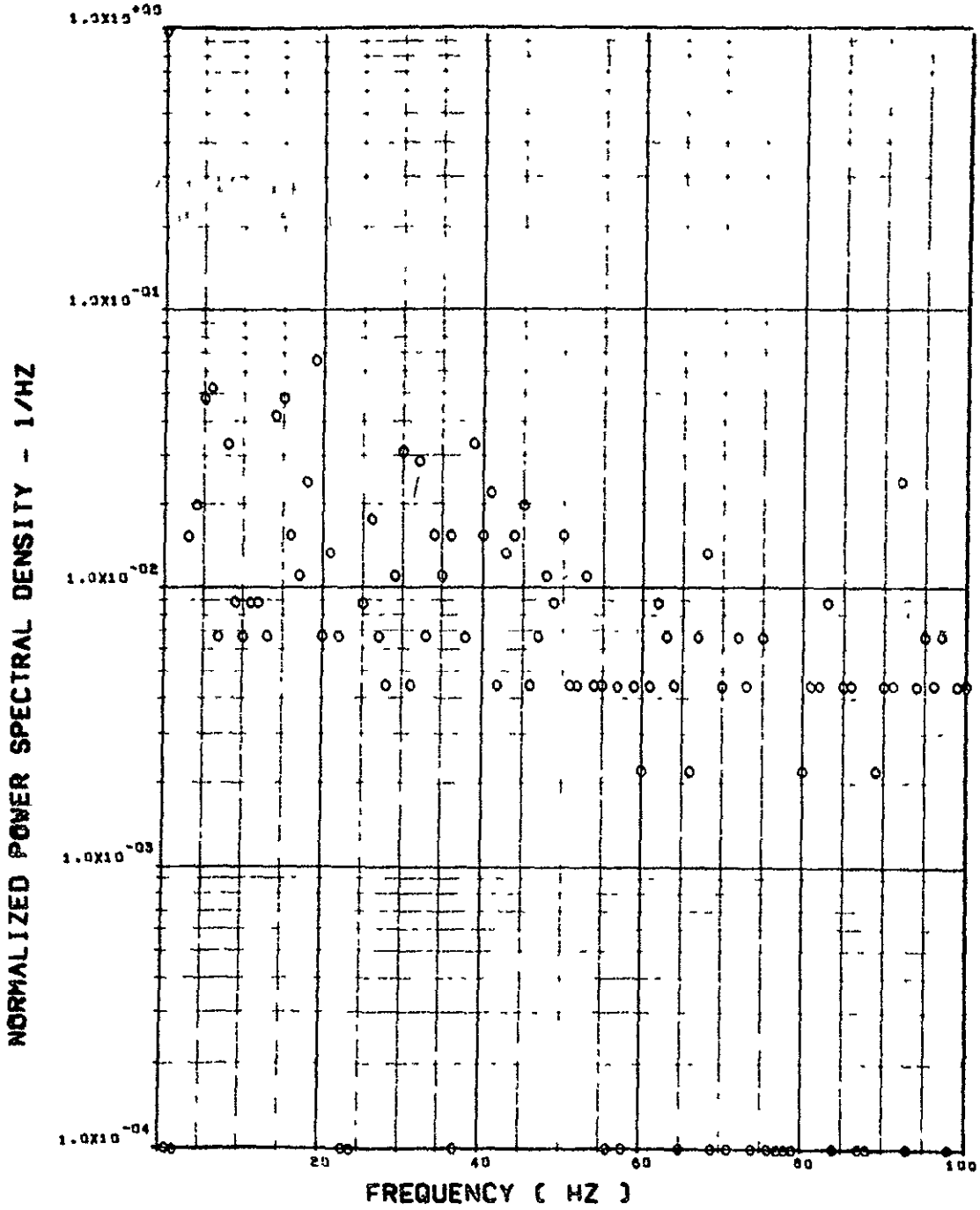

ITEM - SW132 SHEAR AT WING STATION 4

Figure 9. Continued

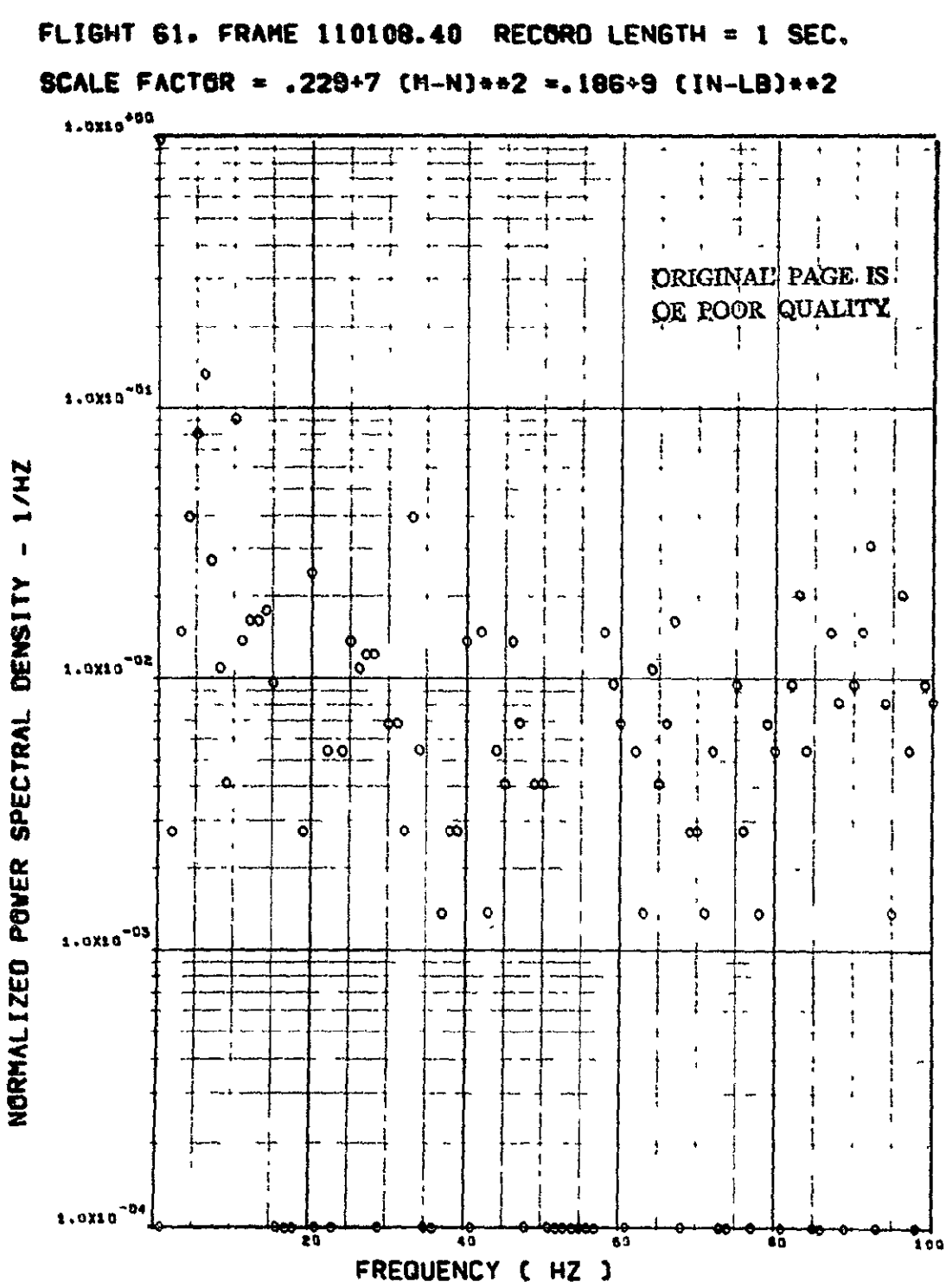

Figure 9. Continued

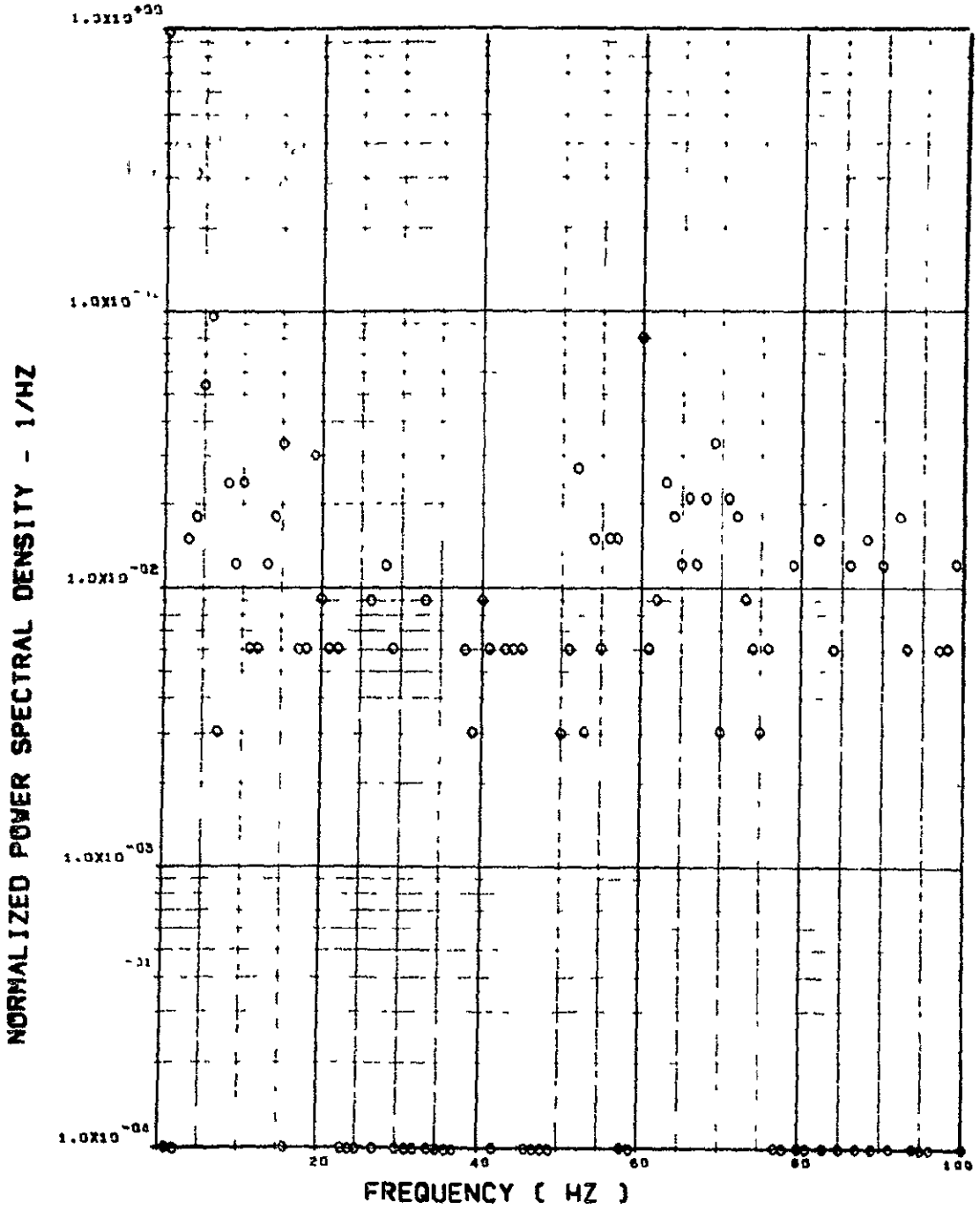

Figure 9. Continued

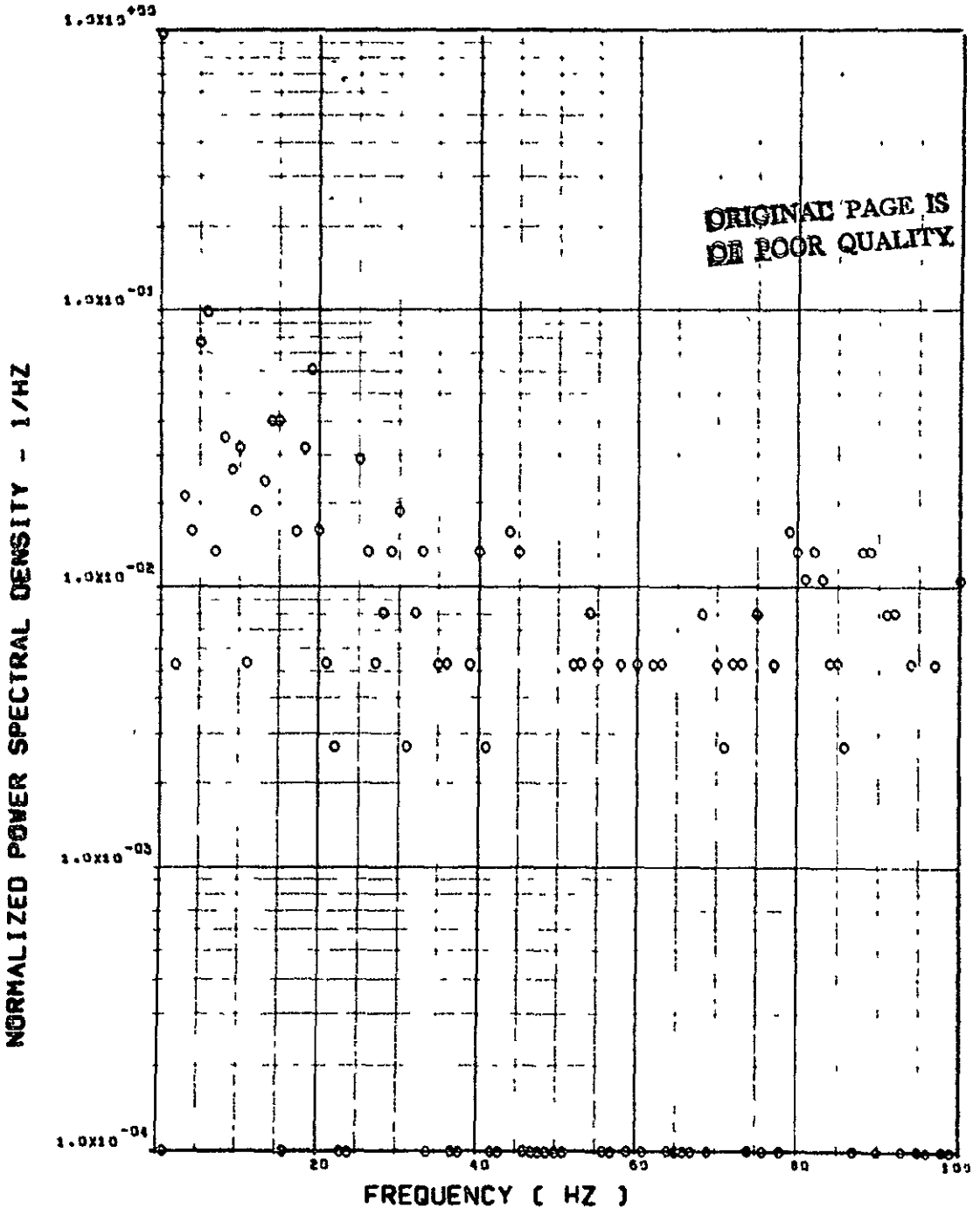

Figure 9. Continued

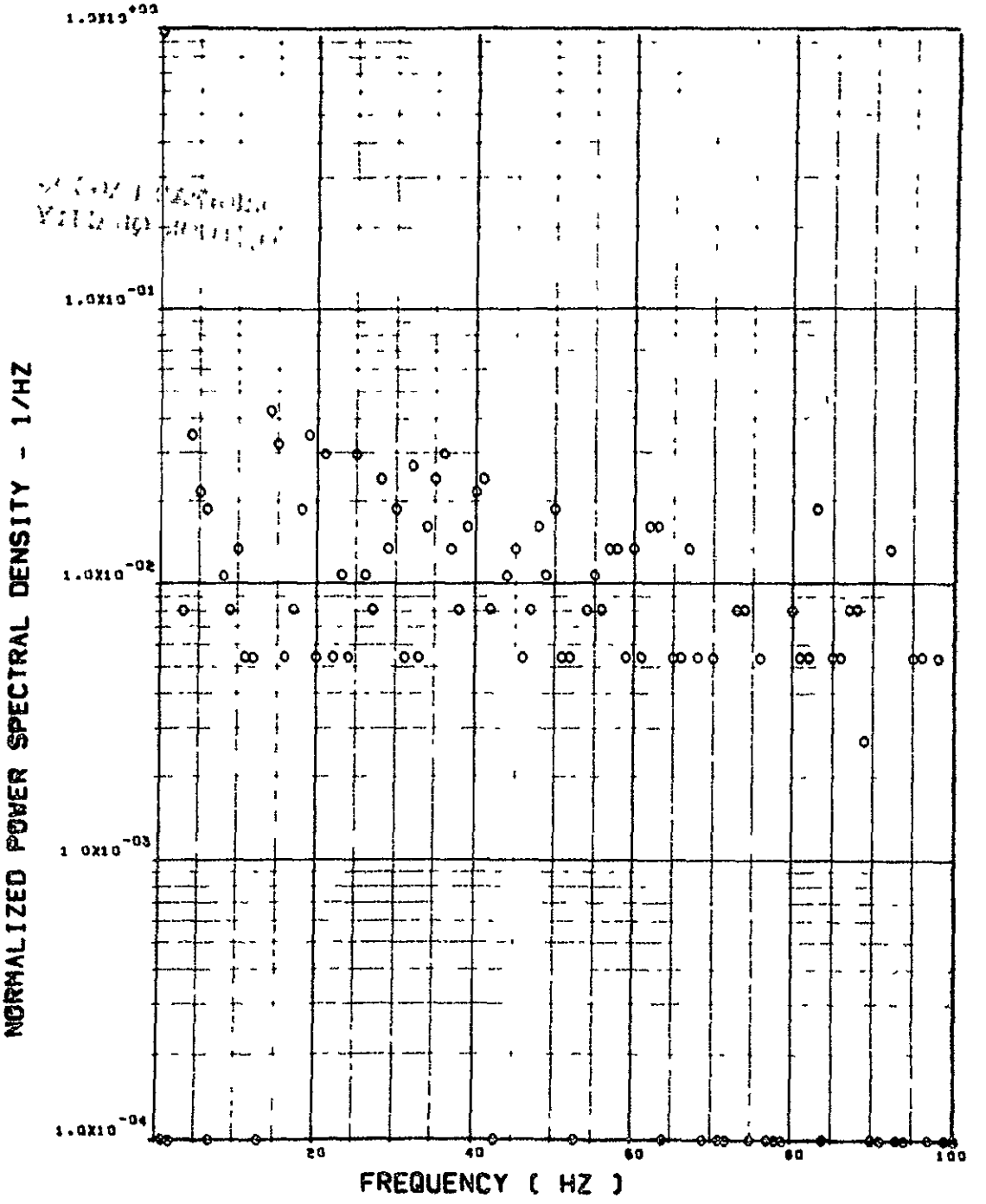

Figure 9. Continued

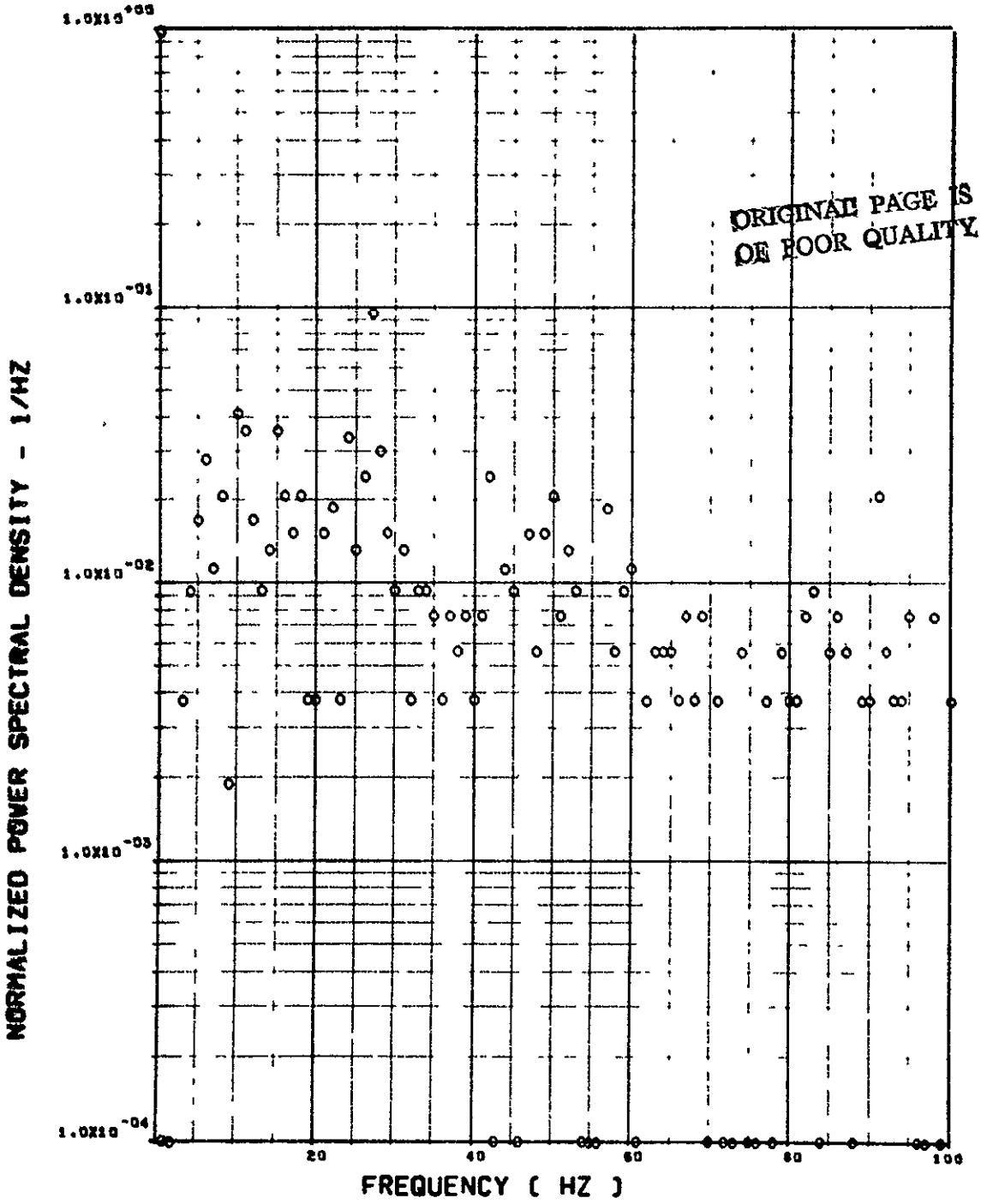

Figure 9. Continued

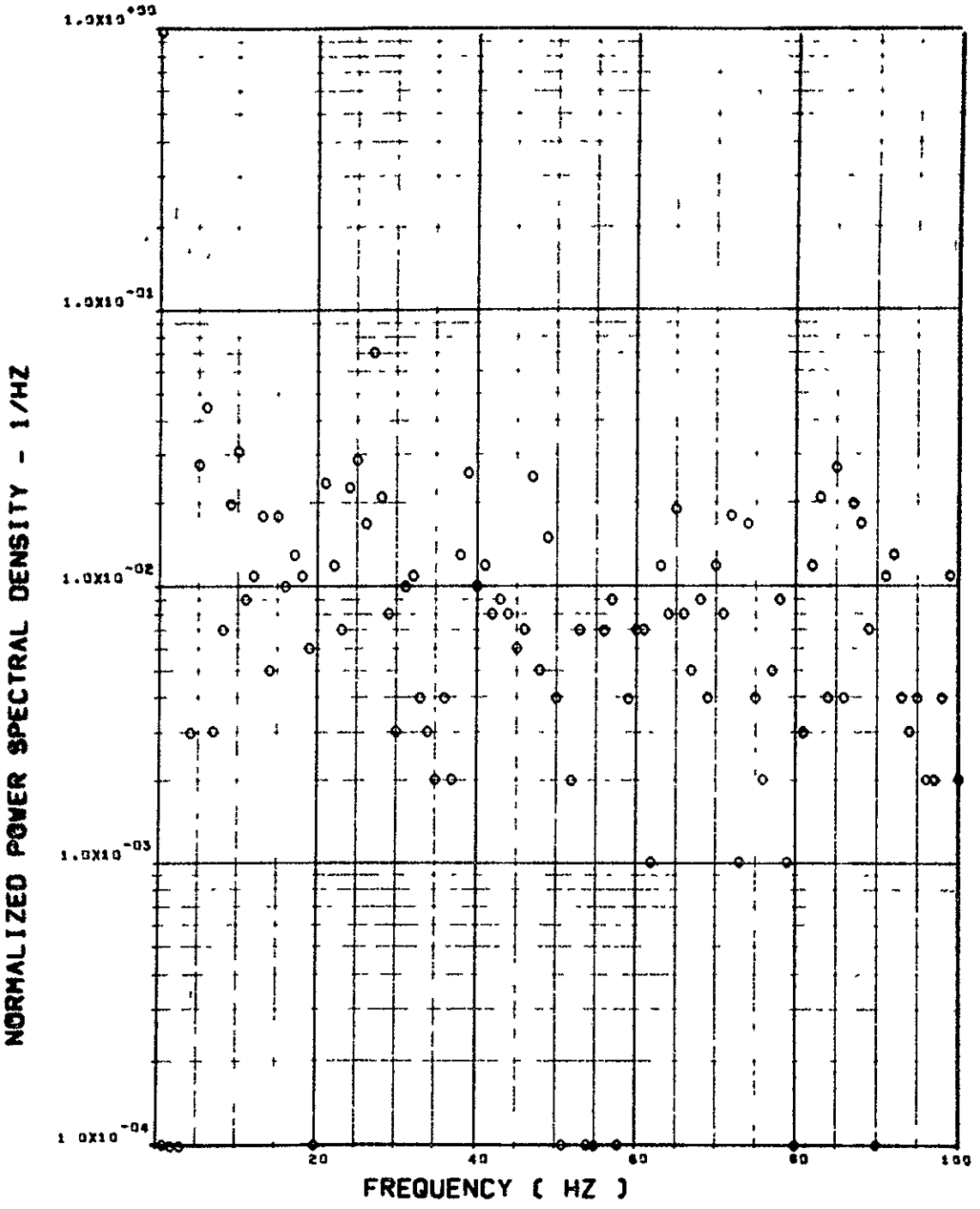

Figure 9. Continued

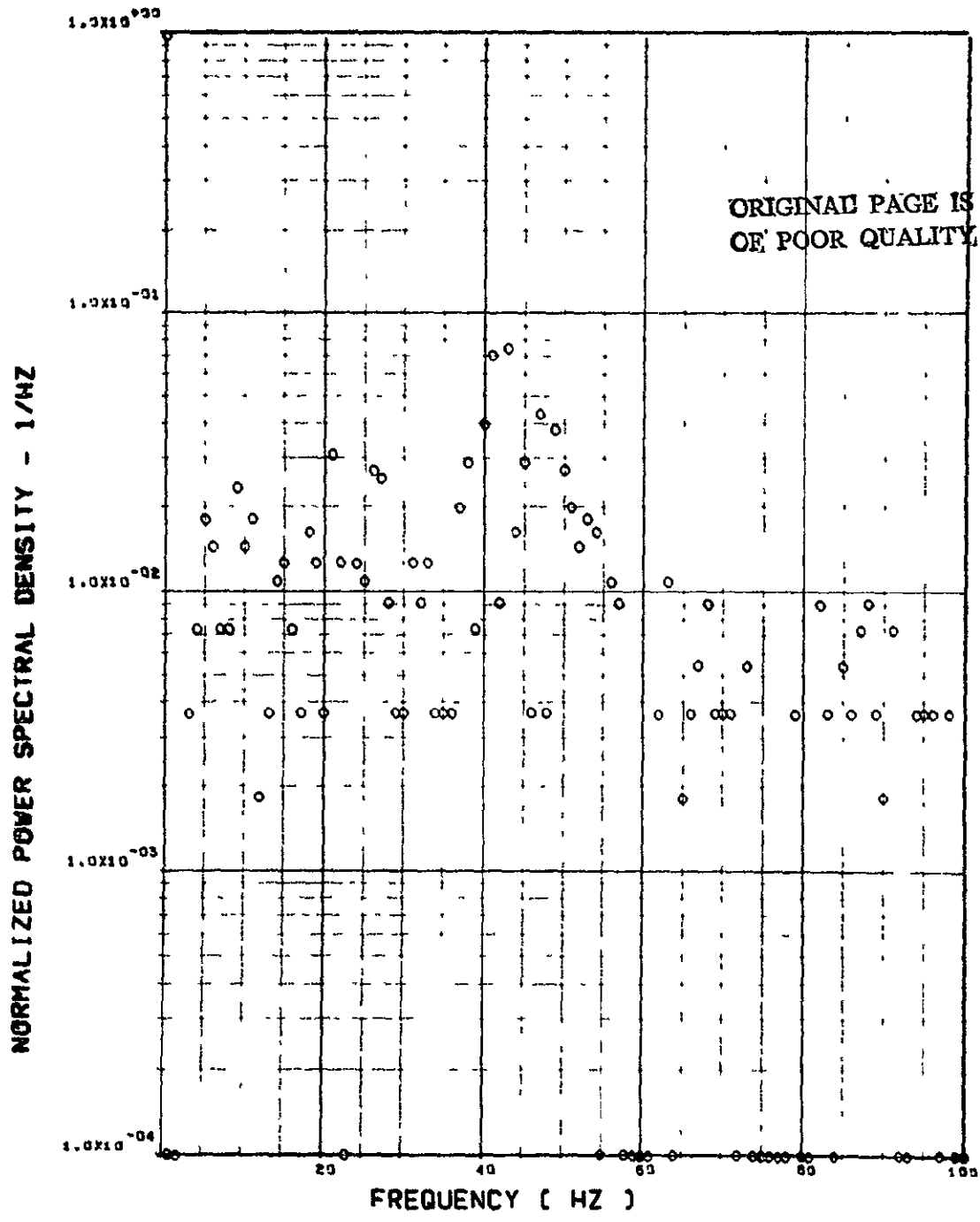

Figure 9. Continued

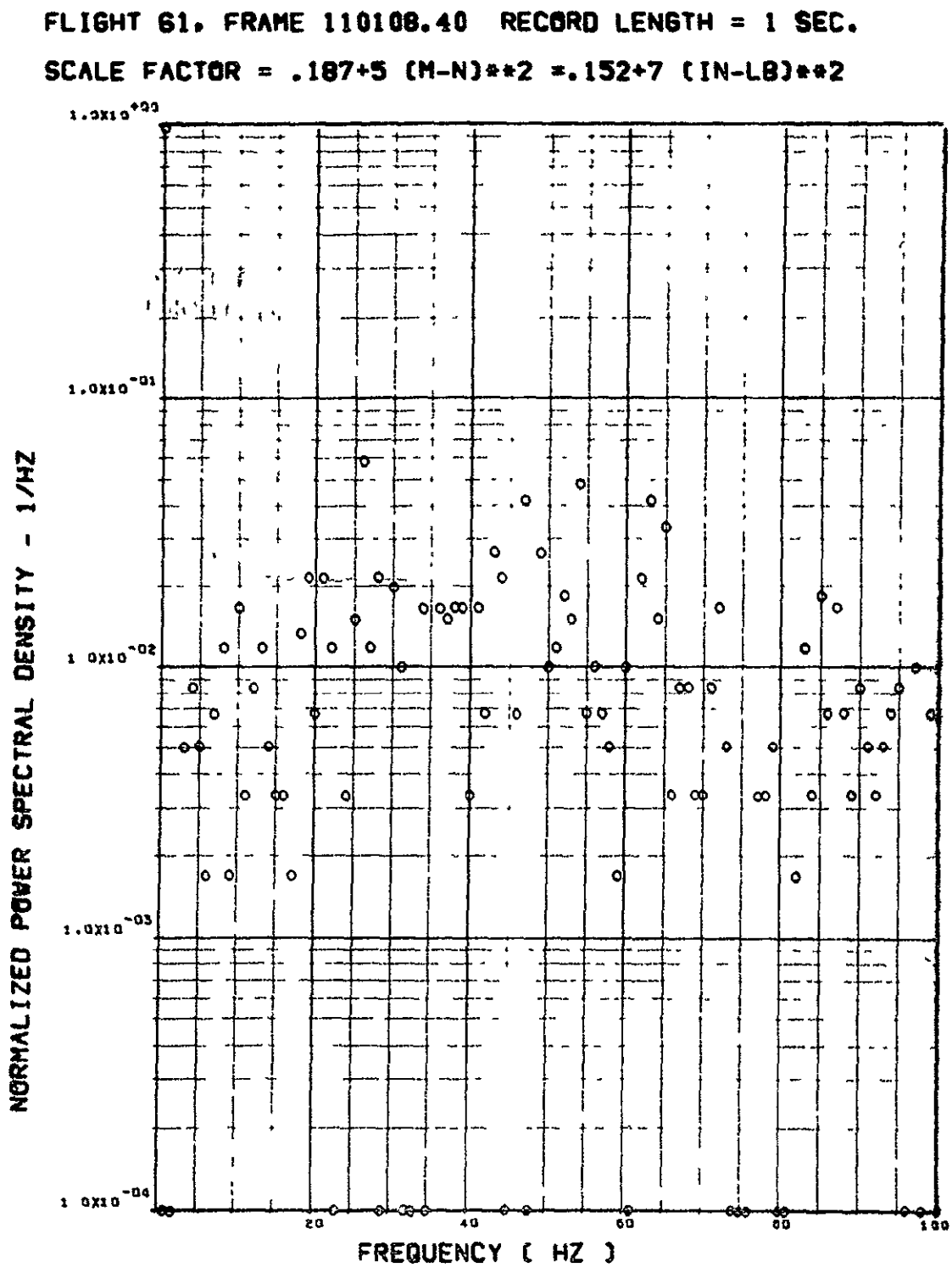

Figure 9. Continued

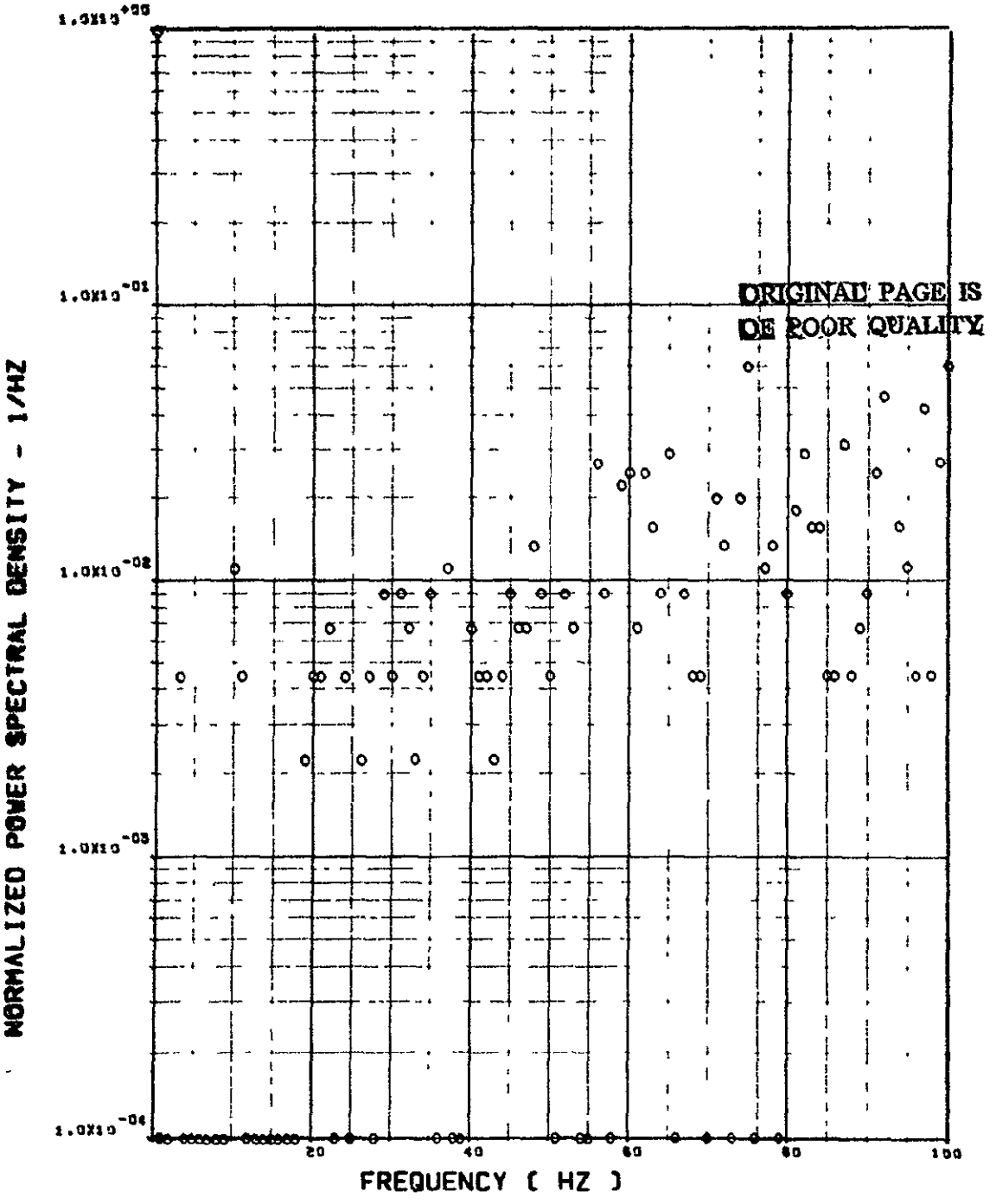

Figure 9. Continued

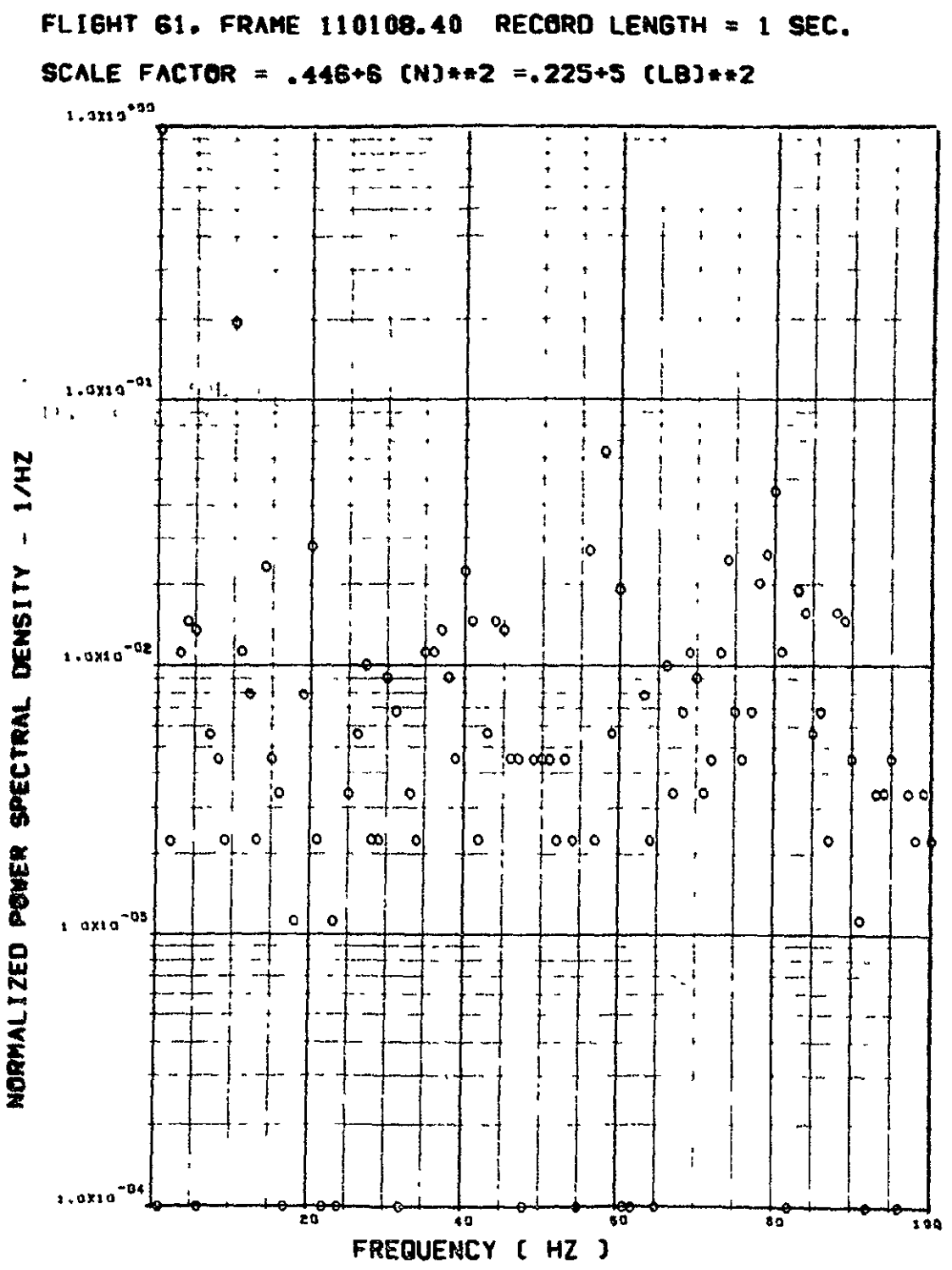

Figure 9. Continued

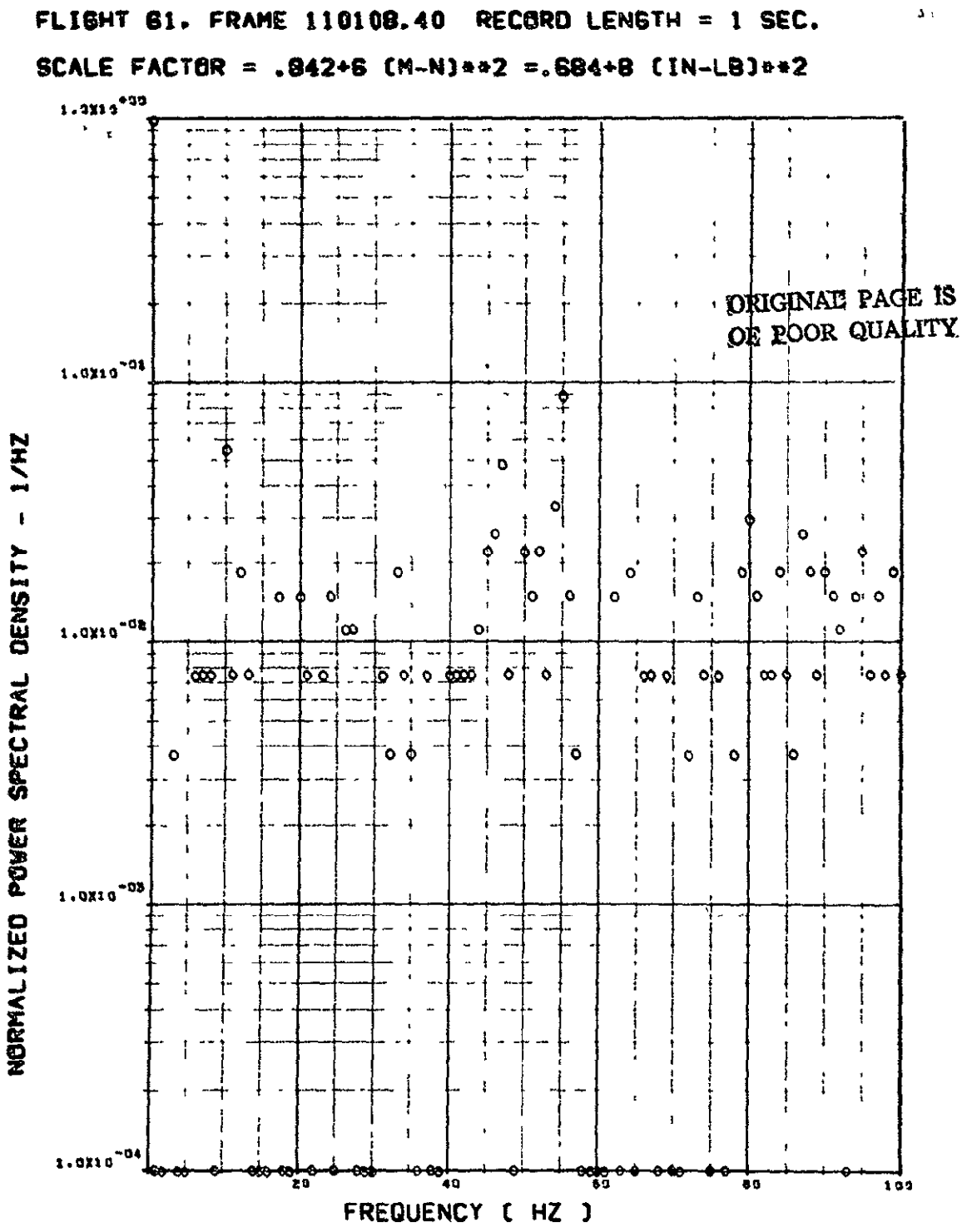

Figure 9. Continued

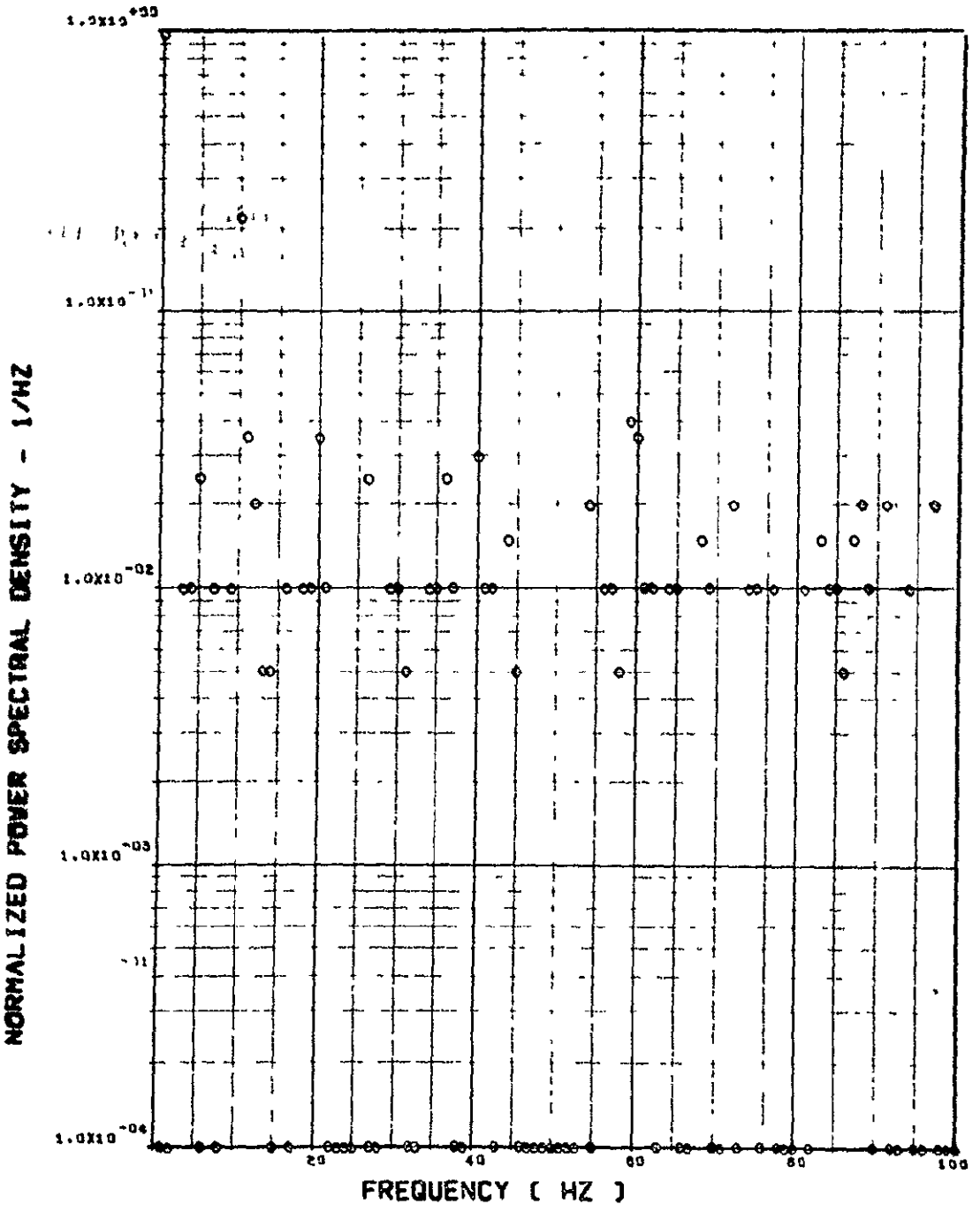

Figure 9. Continued

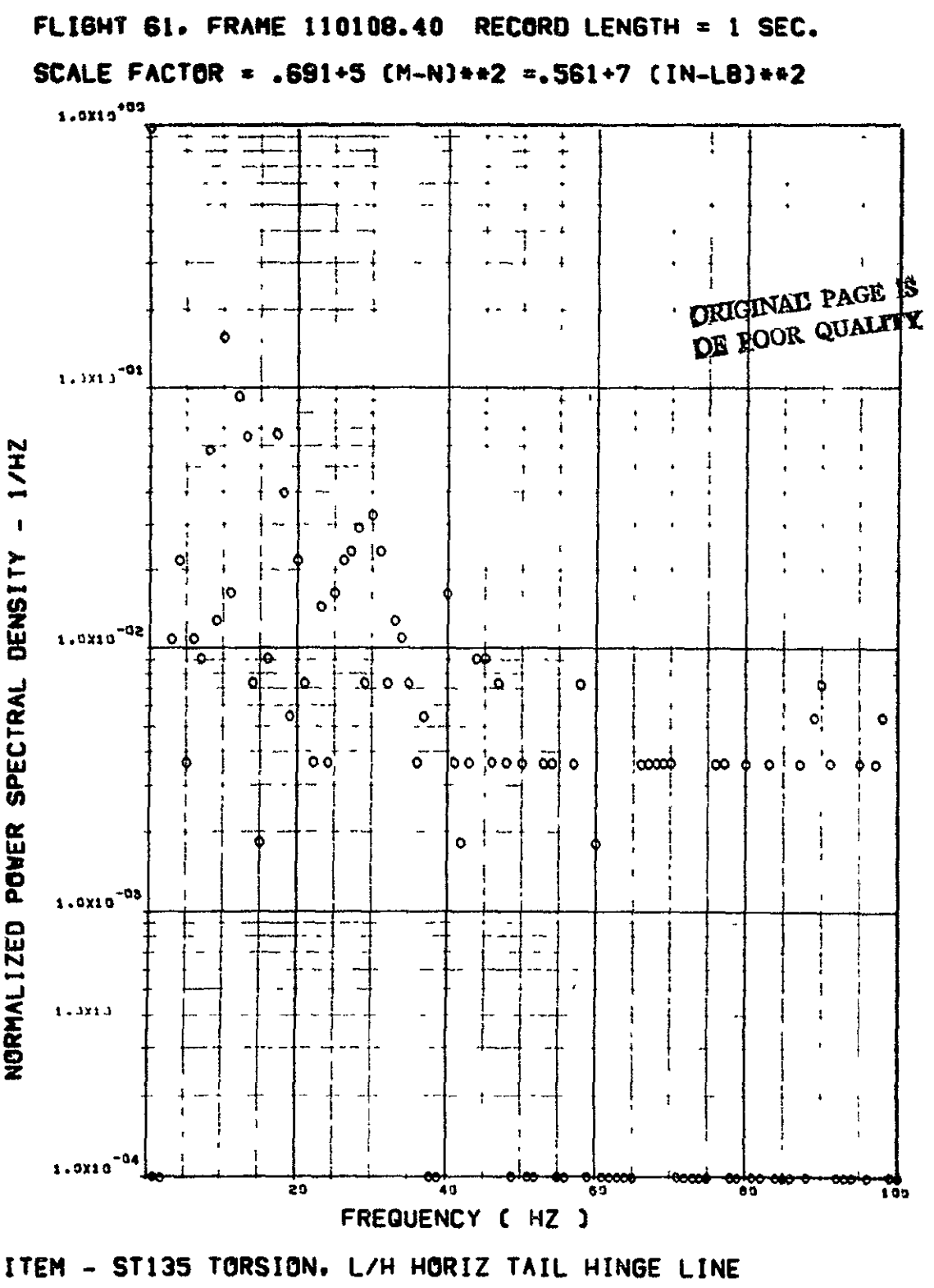

Figure 9. Continued

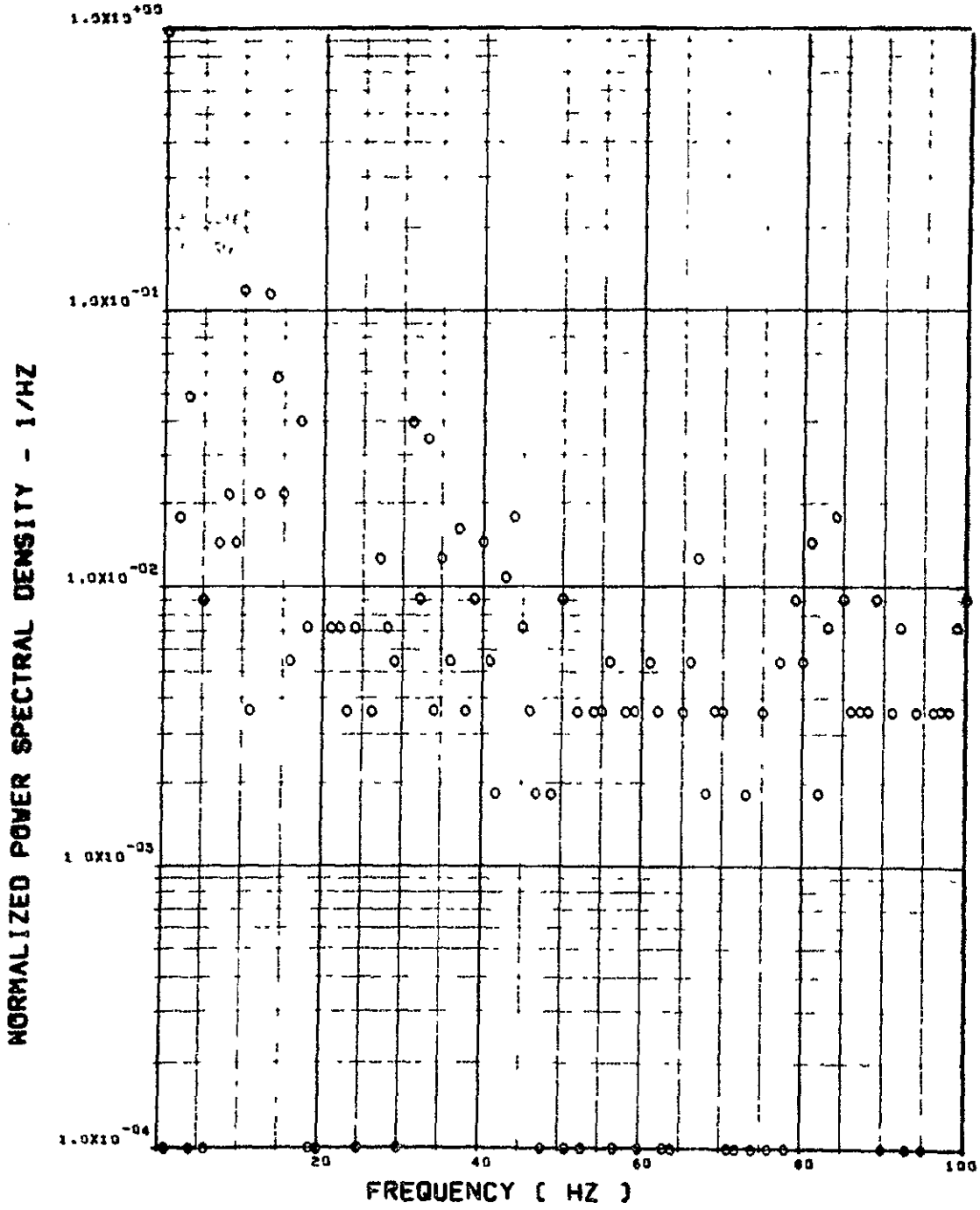

Figure 9. Concluded

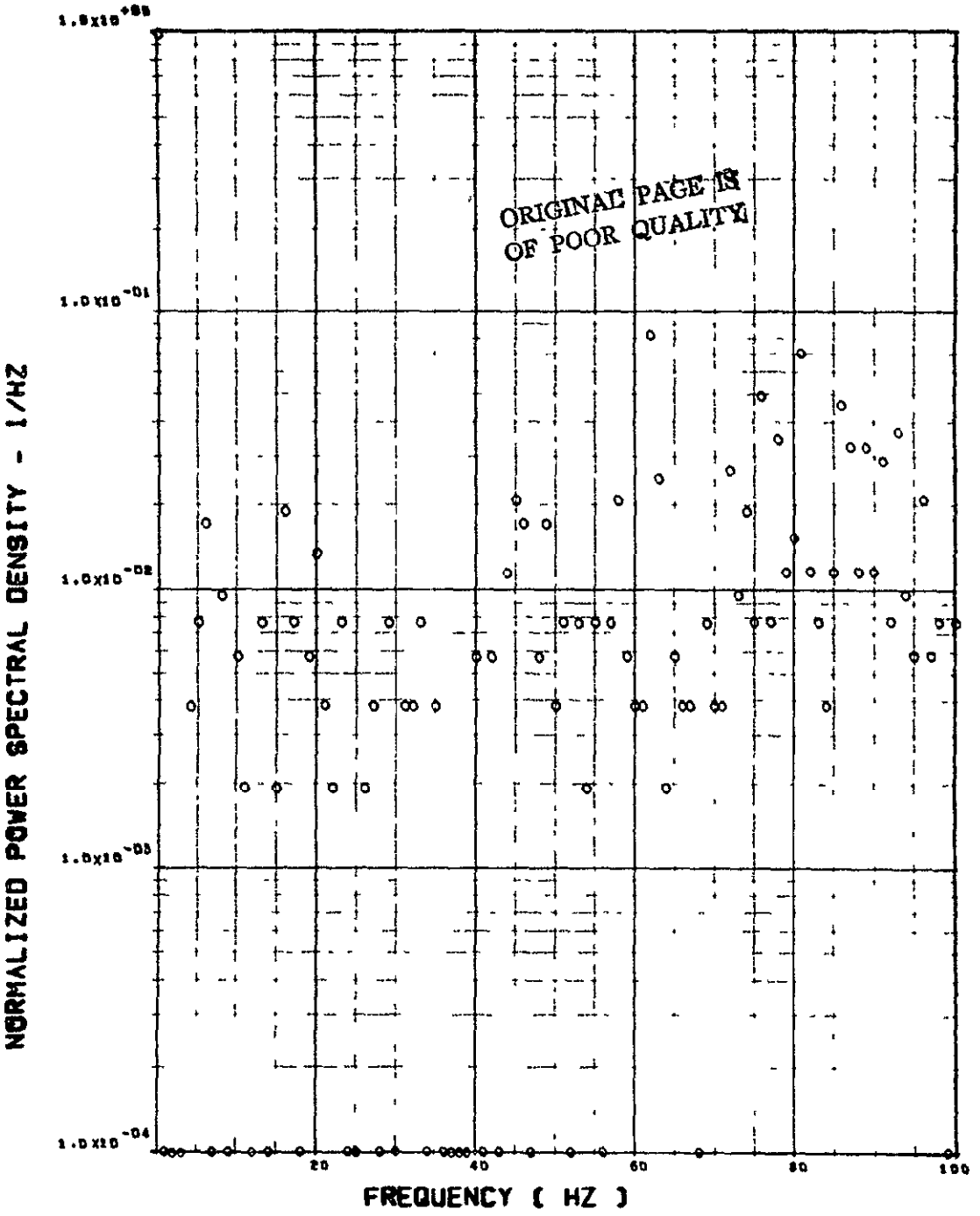

Figure 10. Power Spectra - Flight 61, Run 227, Point 3 T_1 = 110109.7, ΔT = 1 Sec, α_{Nom} = 10.42 deg, $\Delta\alpha$= 0.70 deg.

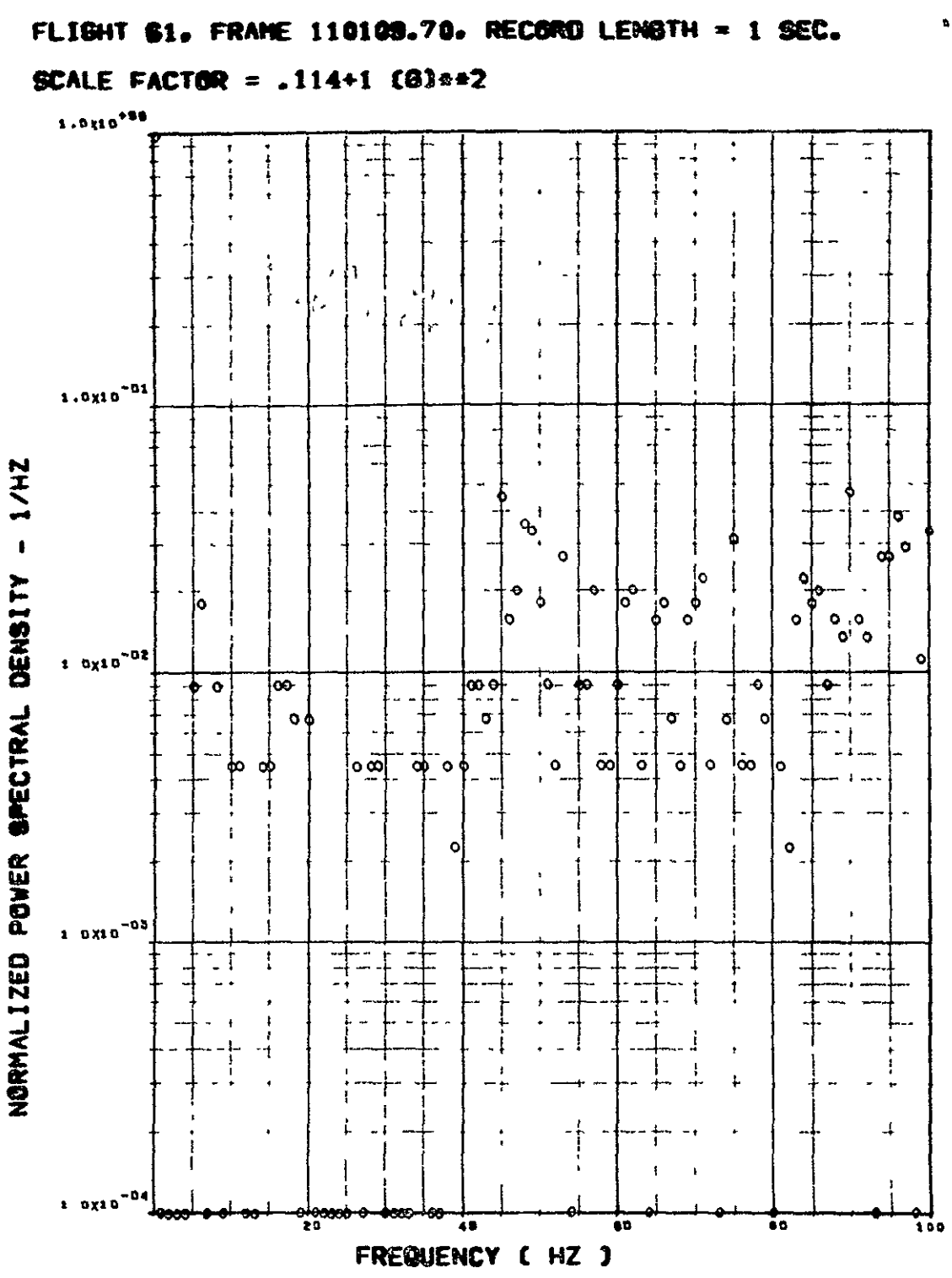

Figure 10. Continued

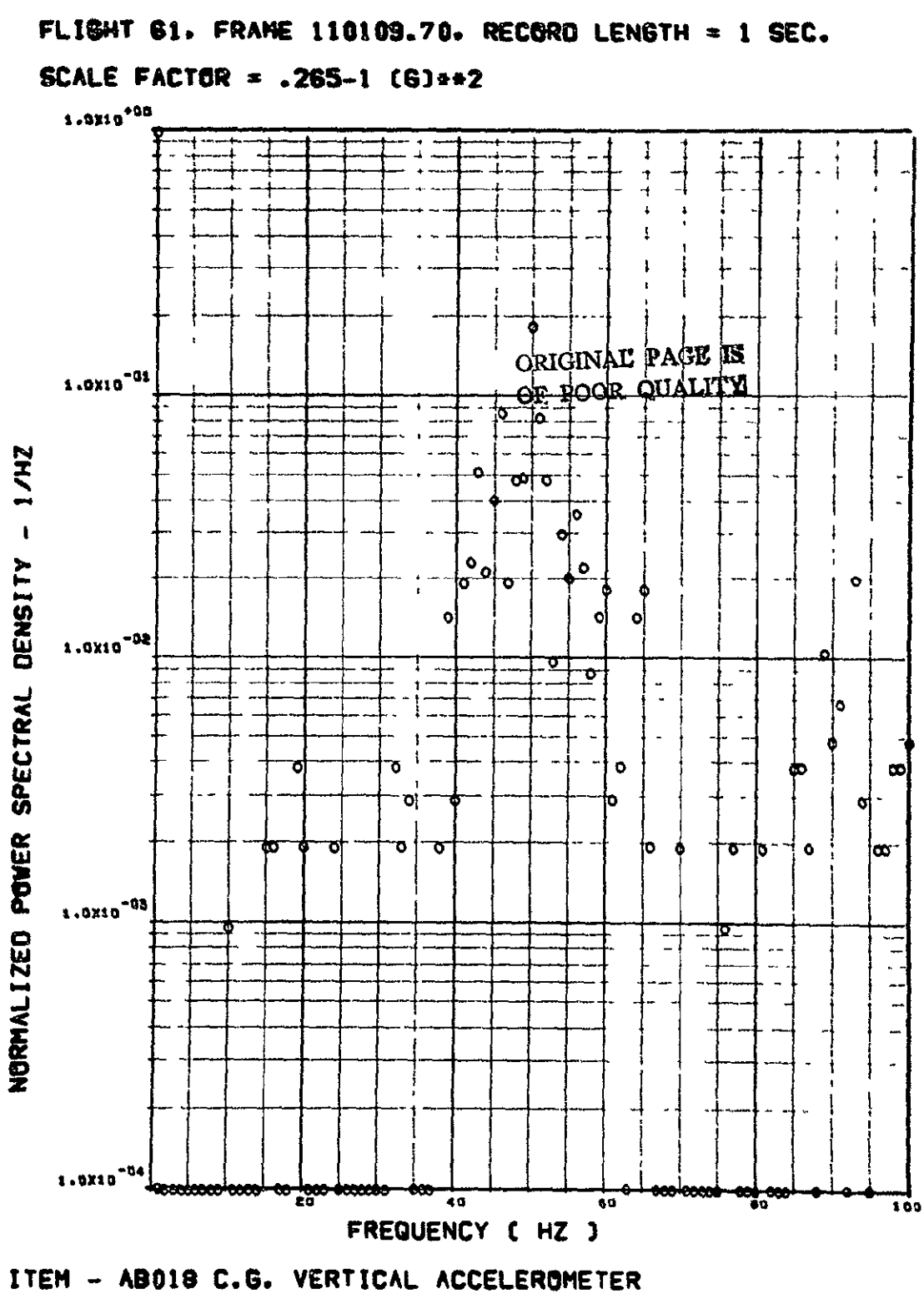

Figure 10. Continued

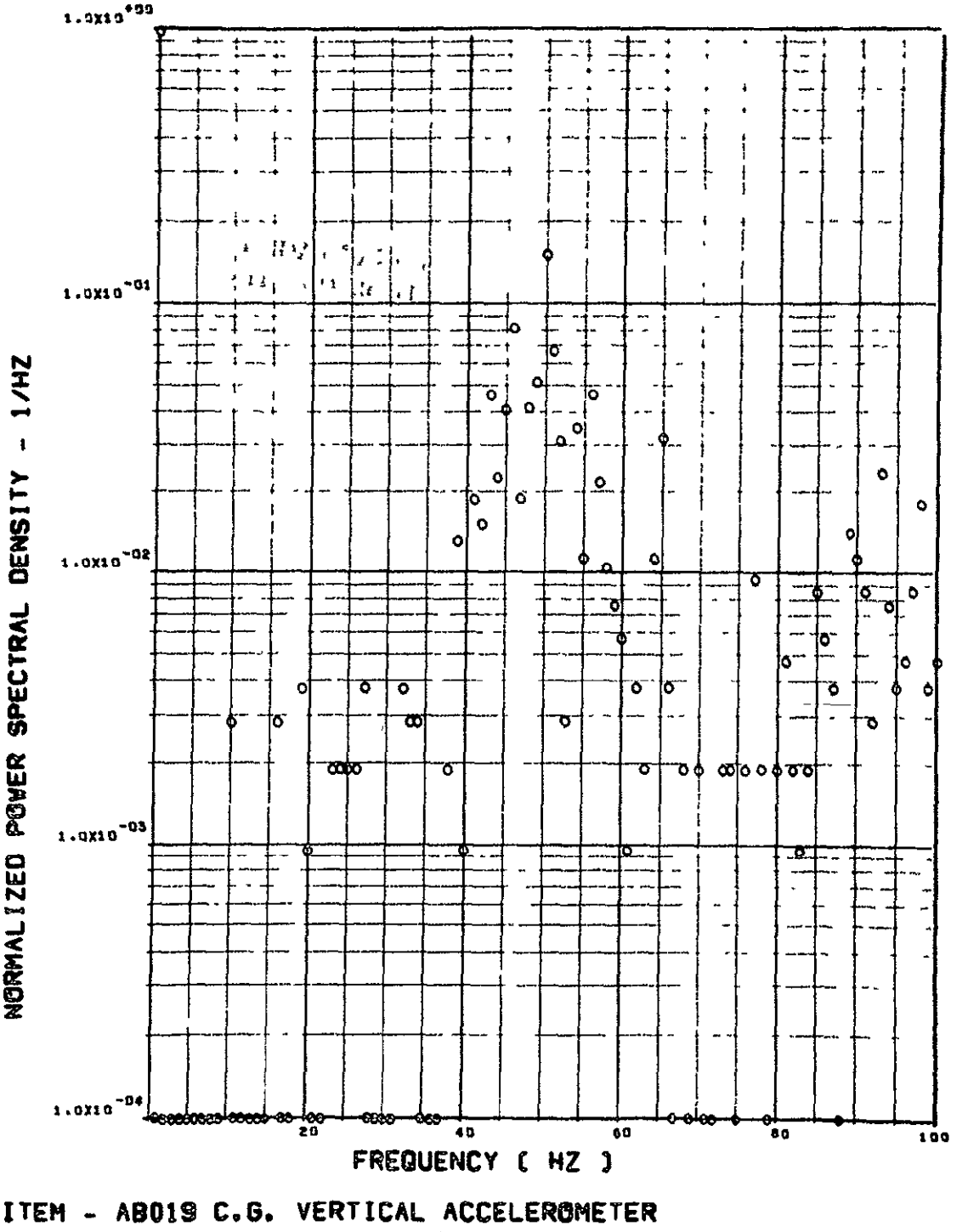

Figure 10. Continued

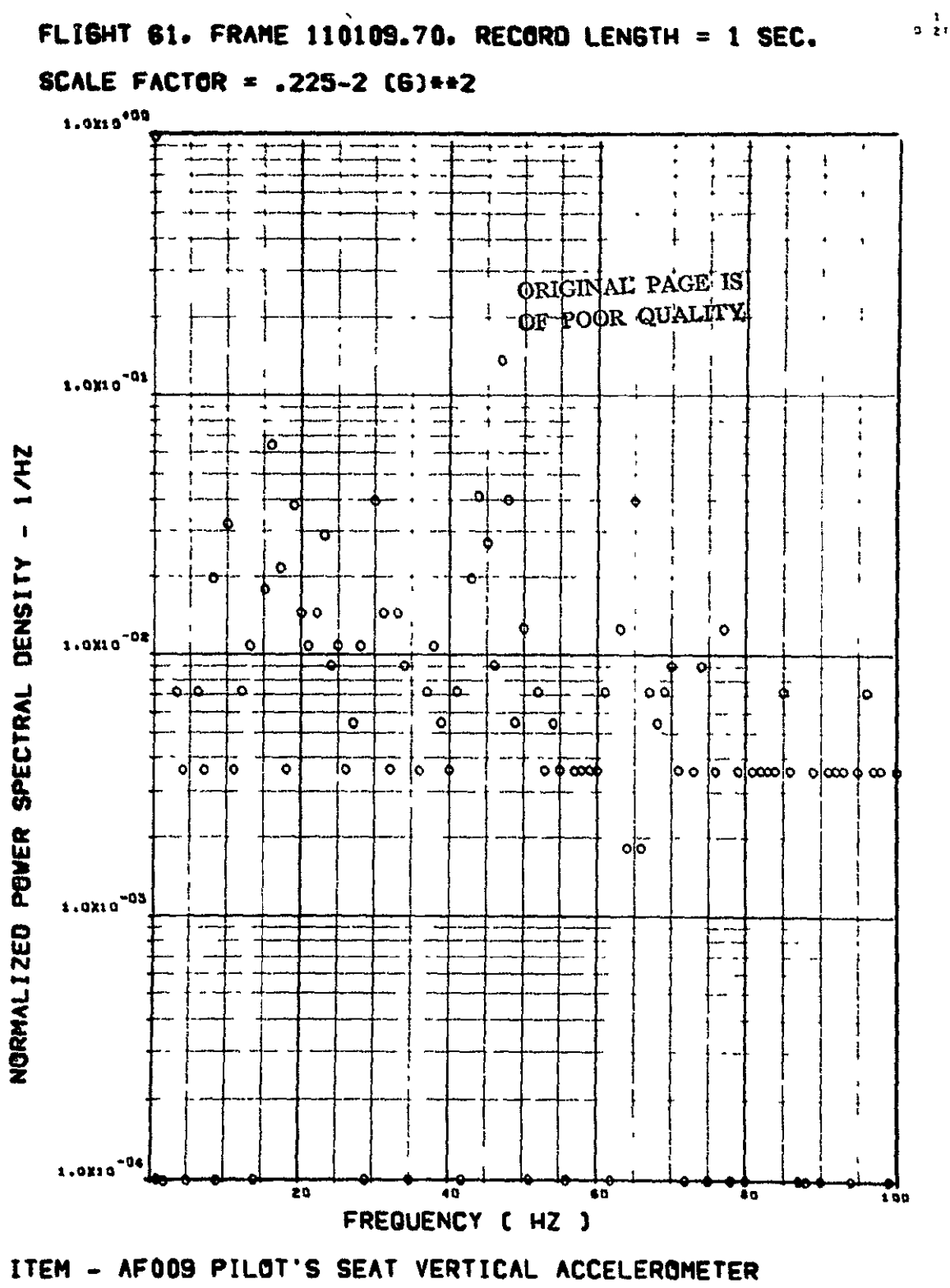

Figure 10. Continued

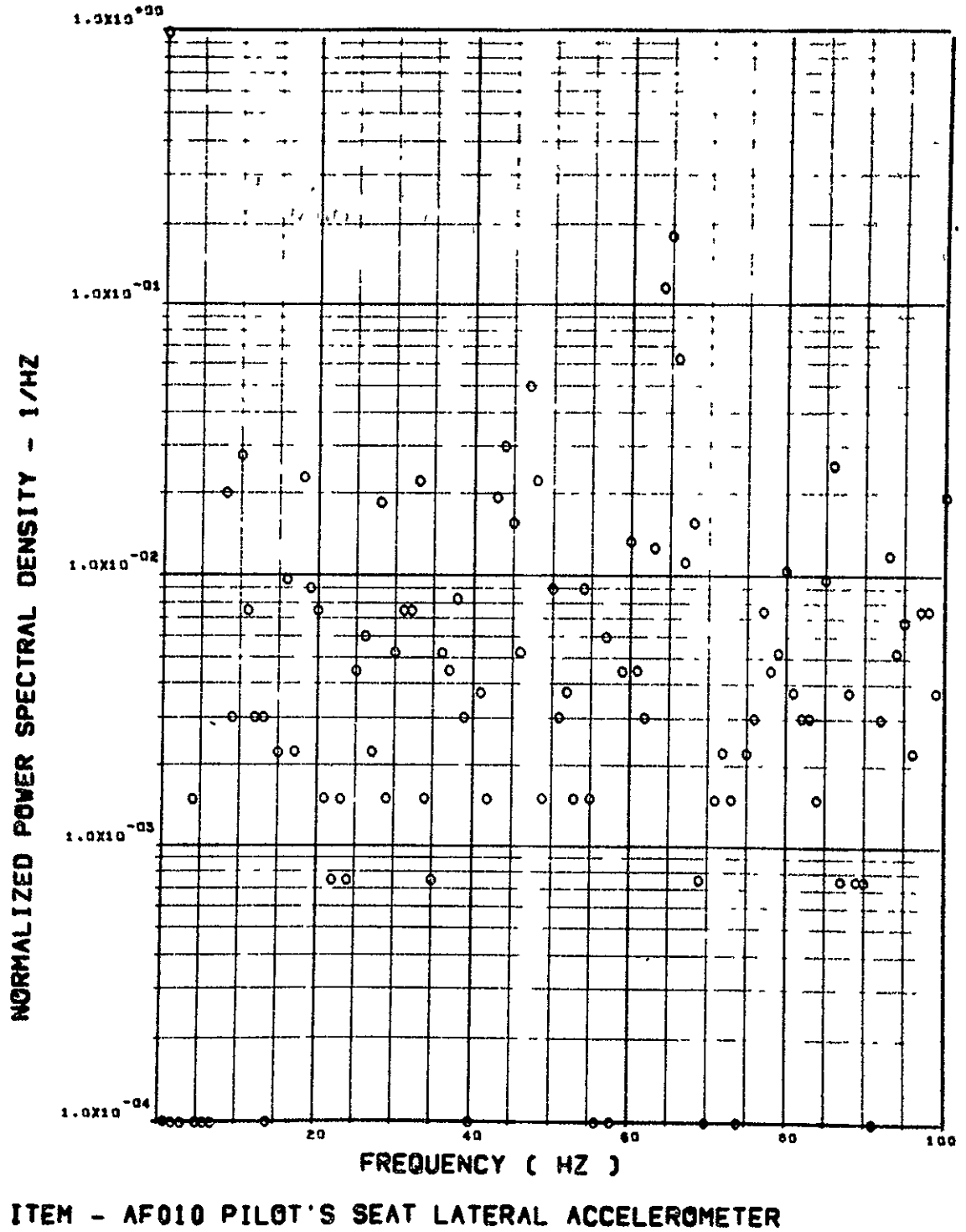

Figure 10. Continued

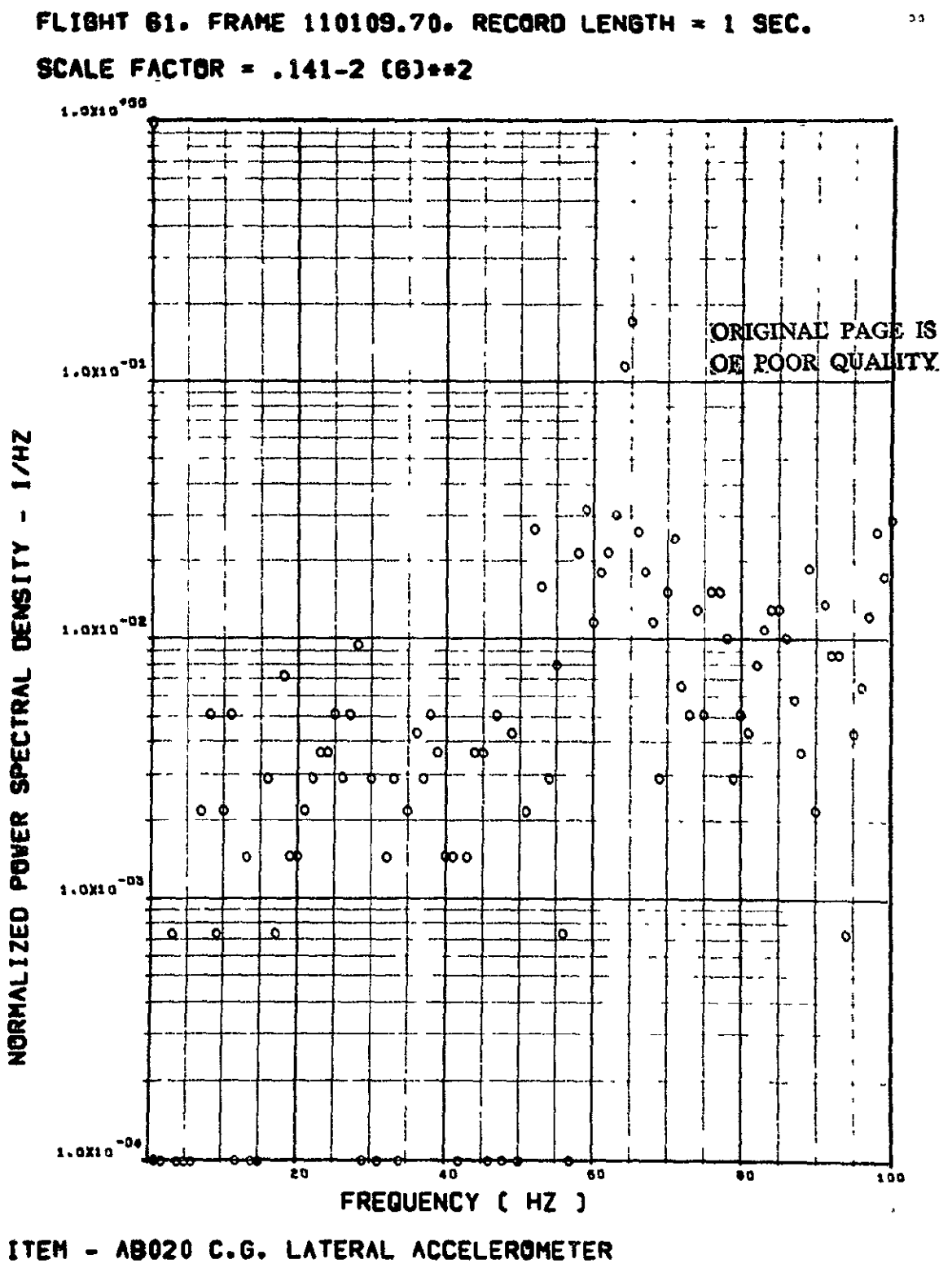

Figure 10. Continued

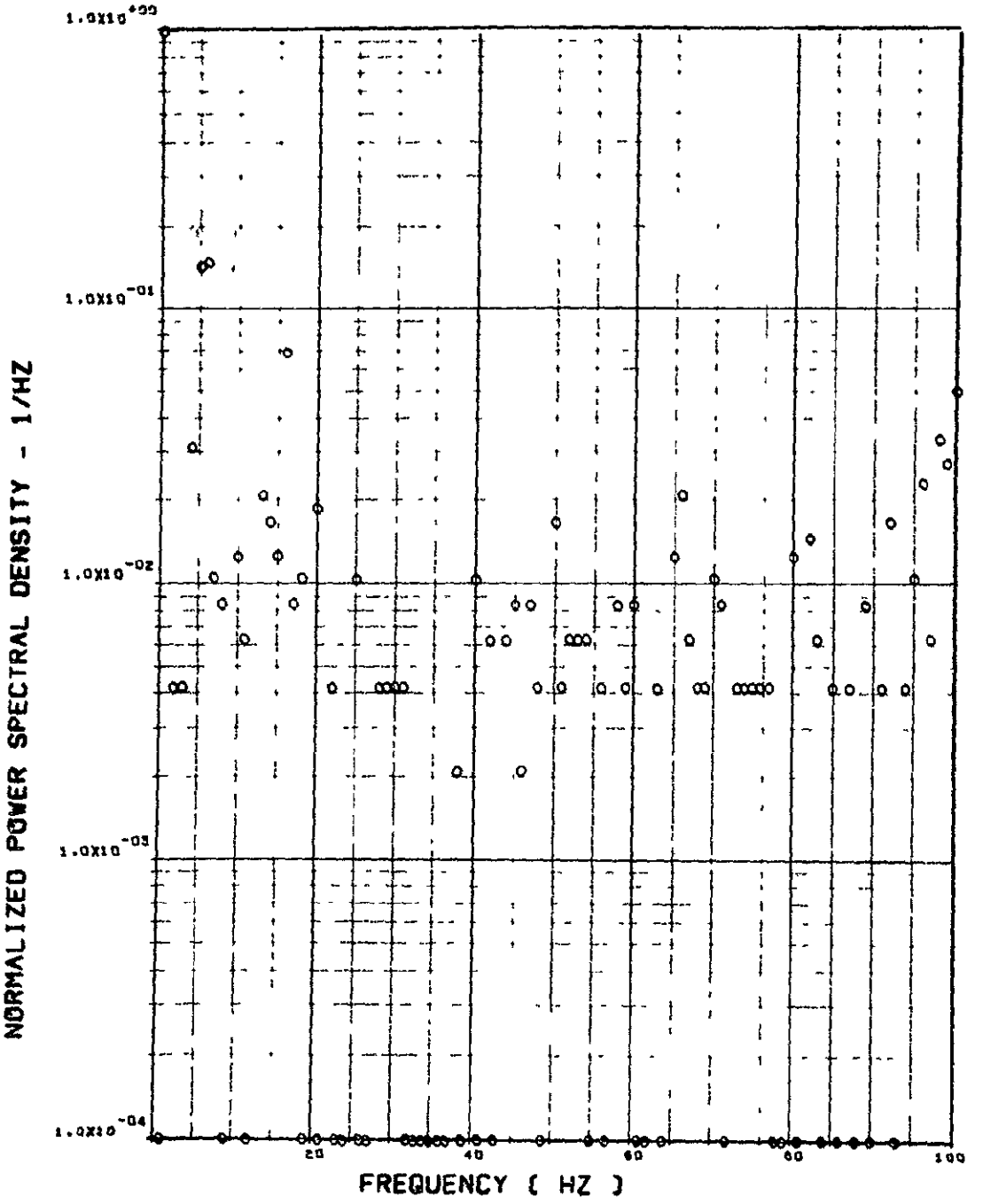

Figure 10. Continued

FLIGHT 61. FRAME 110109.70. RECORD LENGTH = 1 SEC.

SCALE FACTOR = .630+6 (N)**2 =.318+5 (LB)**2

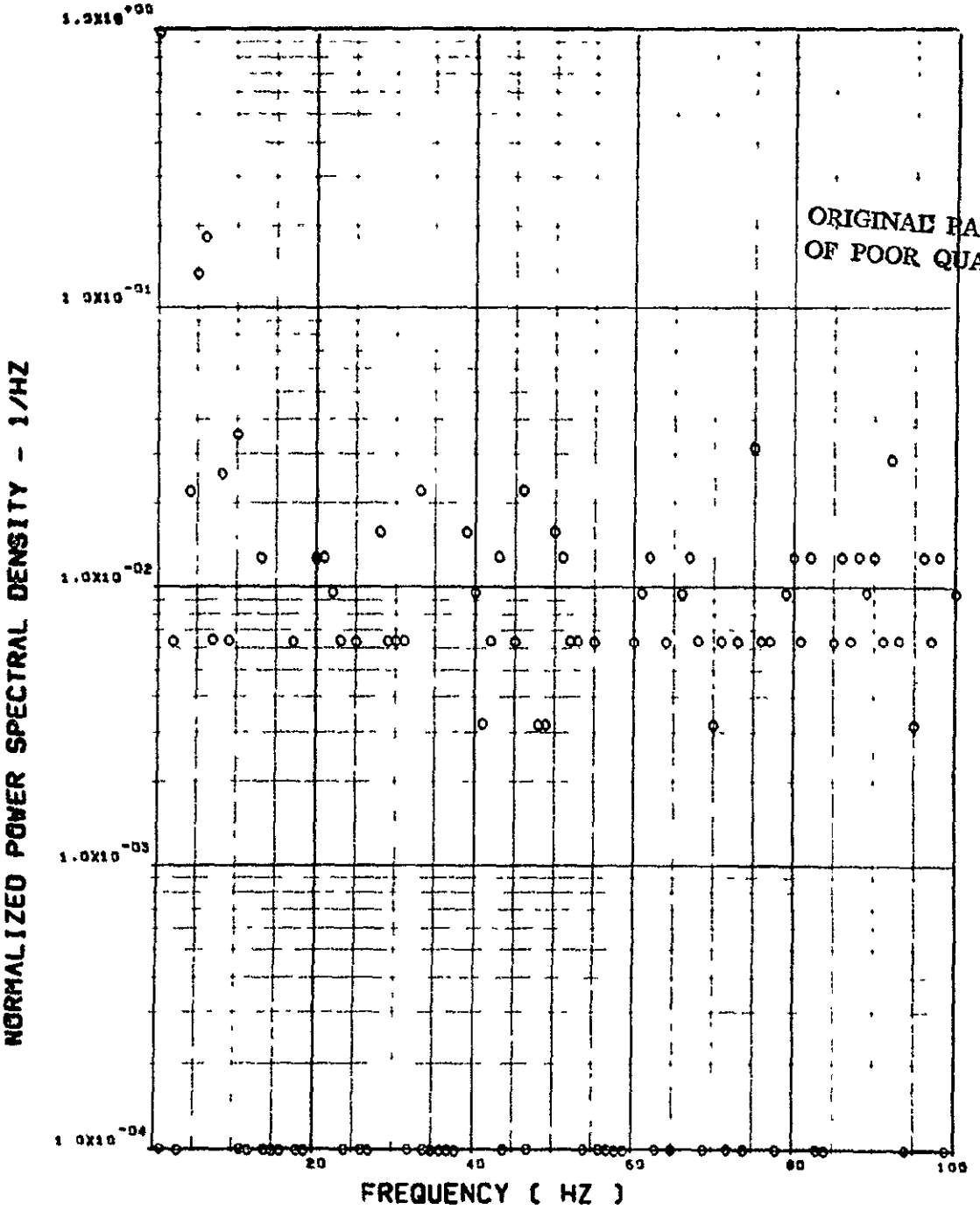

ITEM - SW126 SHEAR AT WING STATION 2

Figure 10. Continued

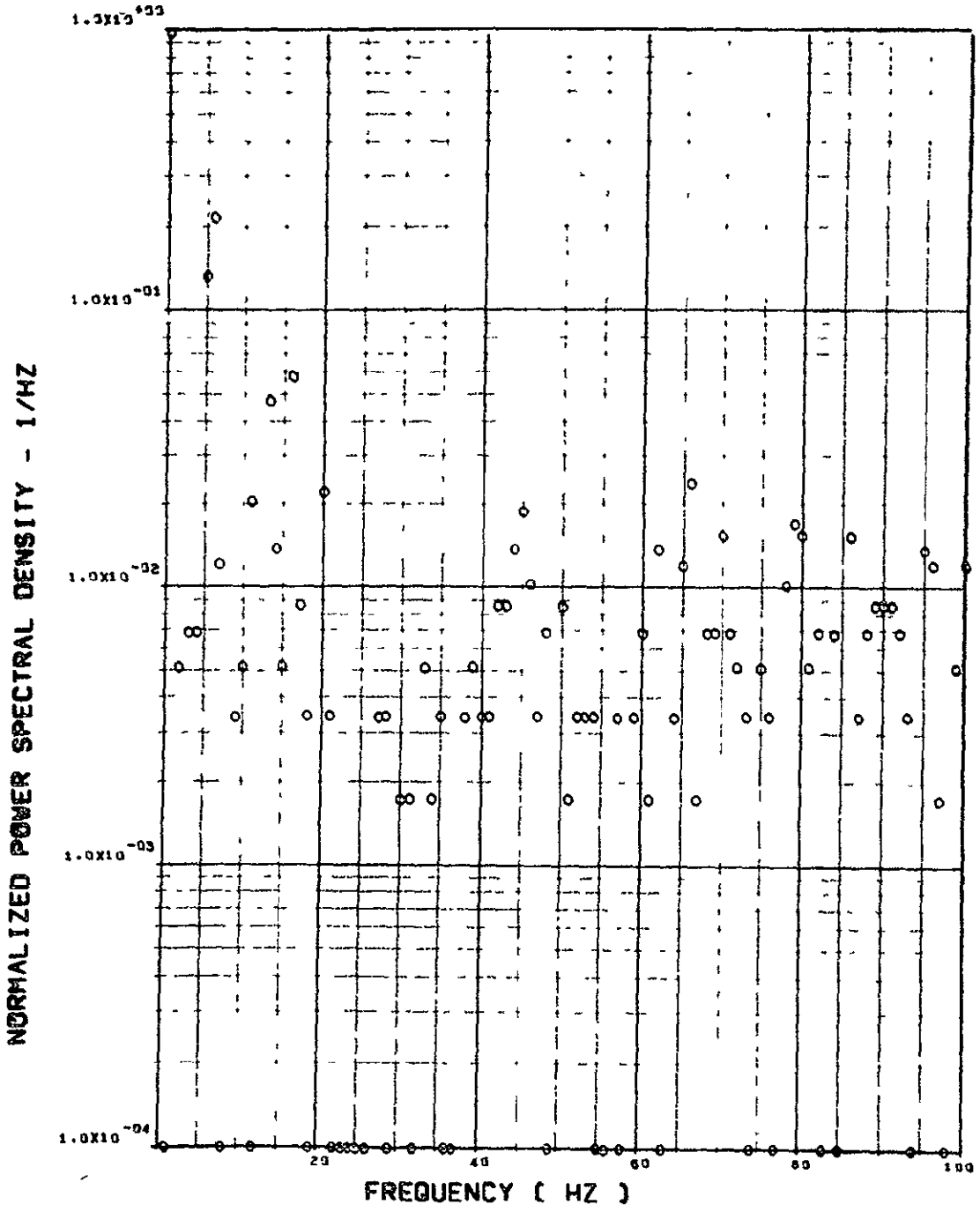

Figure 10. Continued

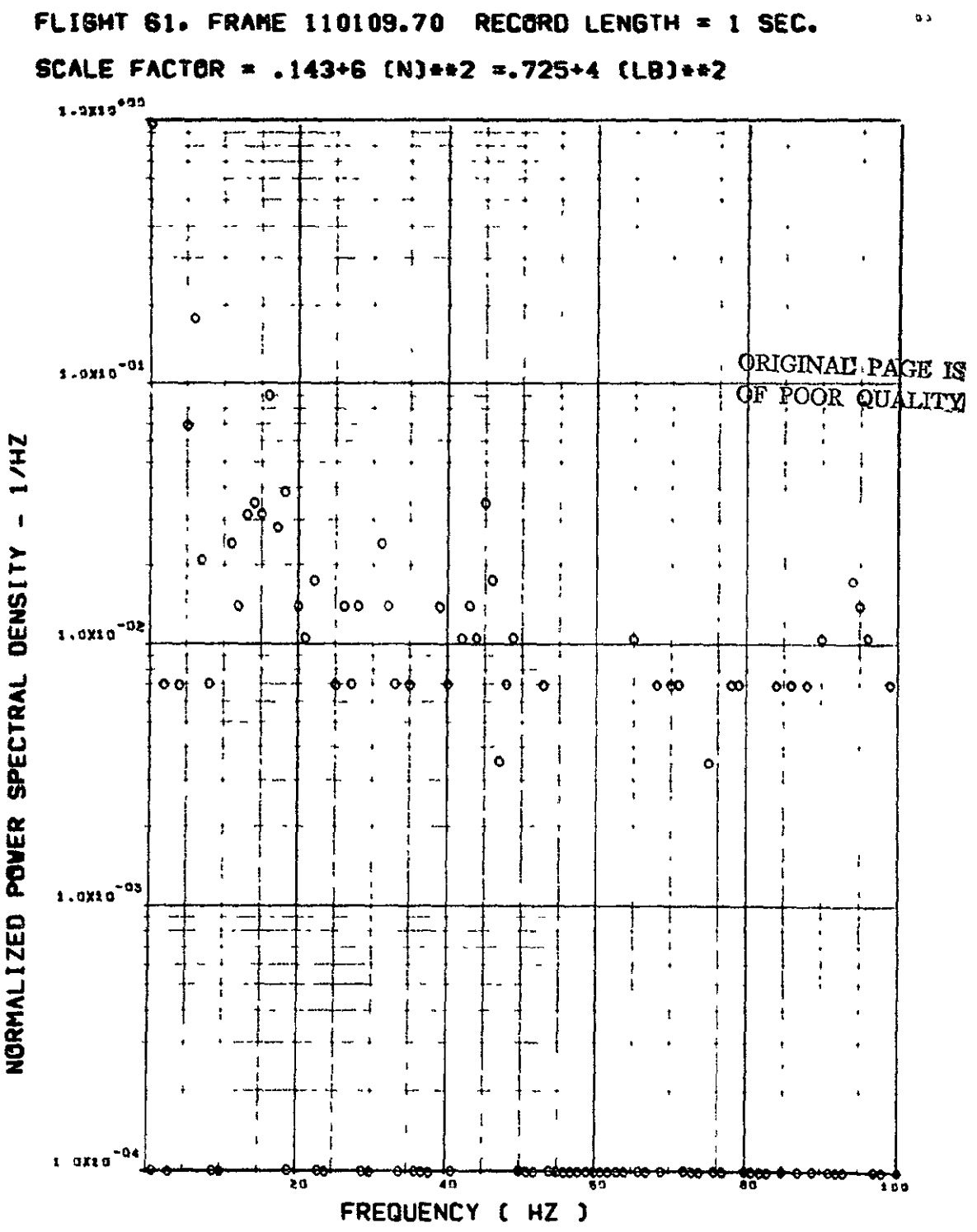

Figure 10. Continued

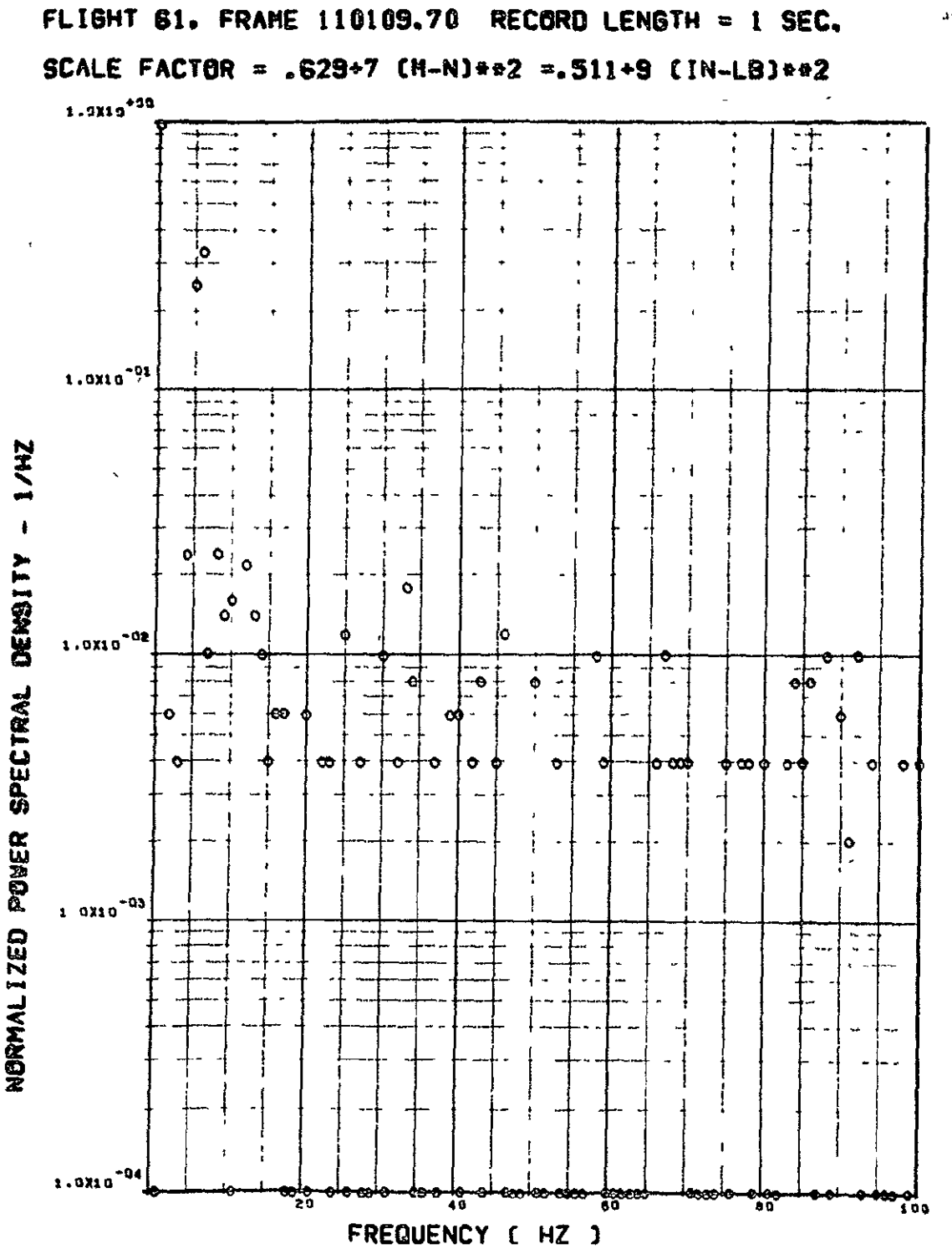

Figure 10. Continued

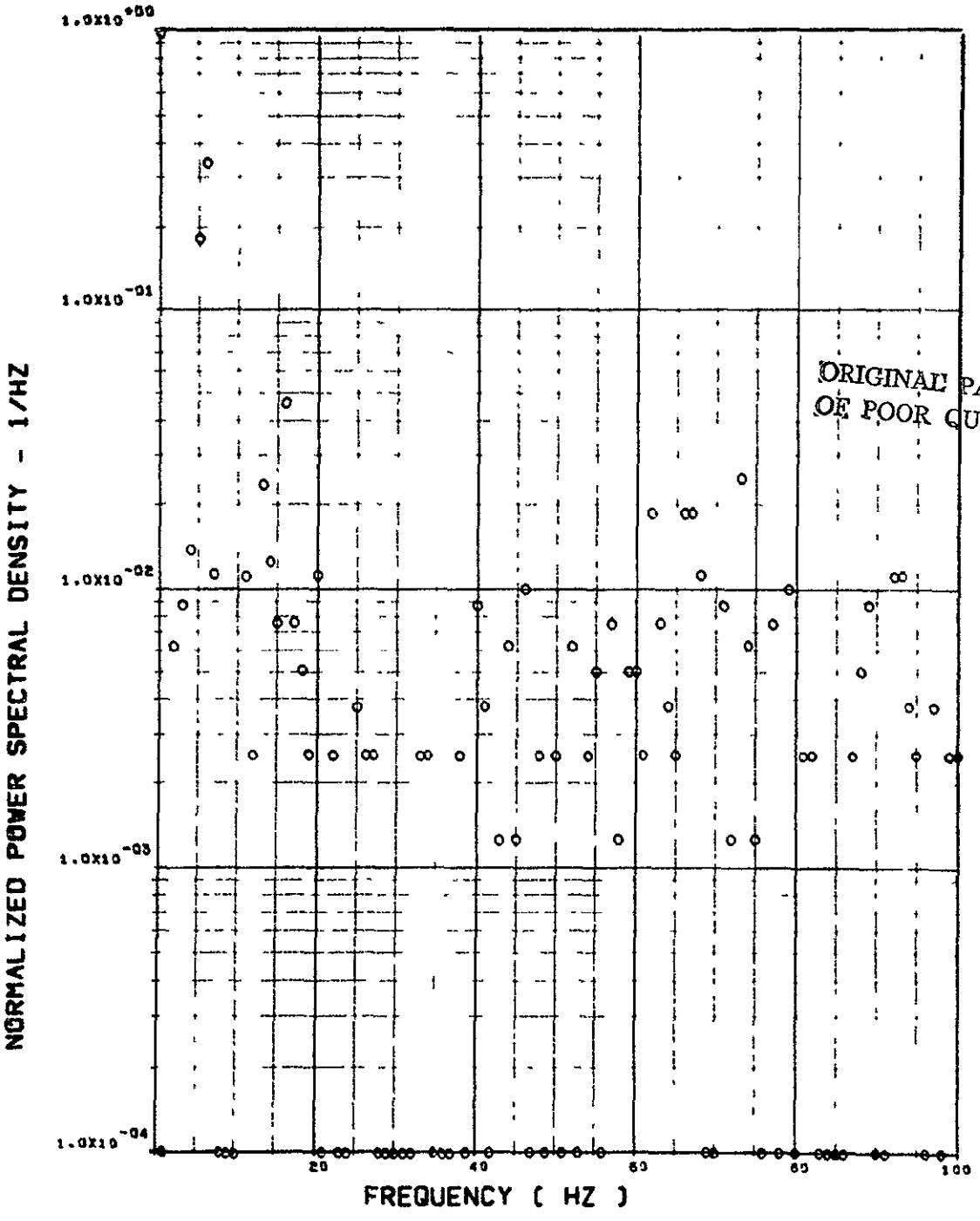

Figure 10. Continued

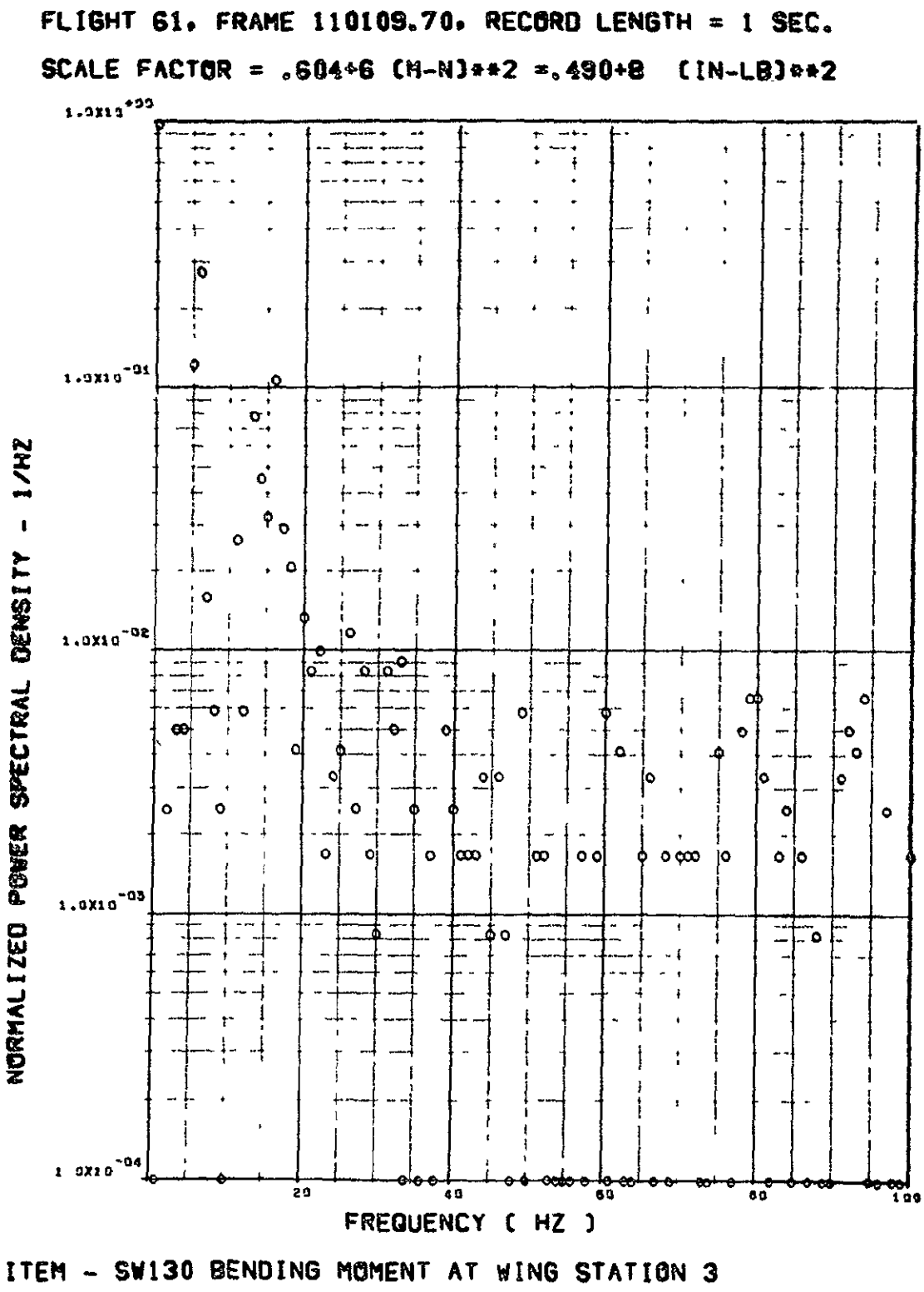

Figure 10. Continued

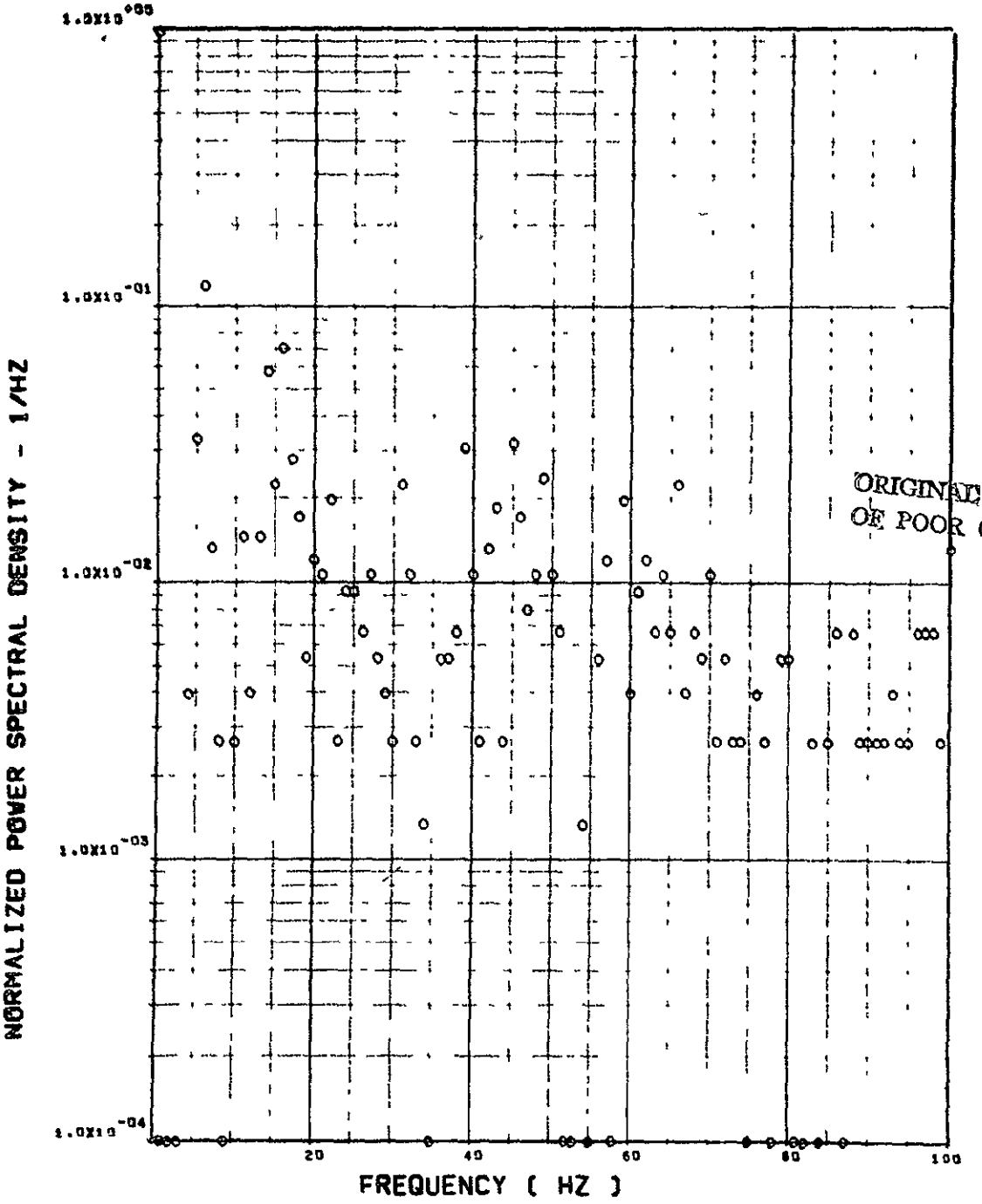

Figure 10. Continued

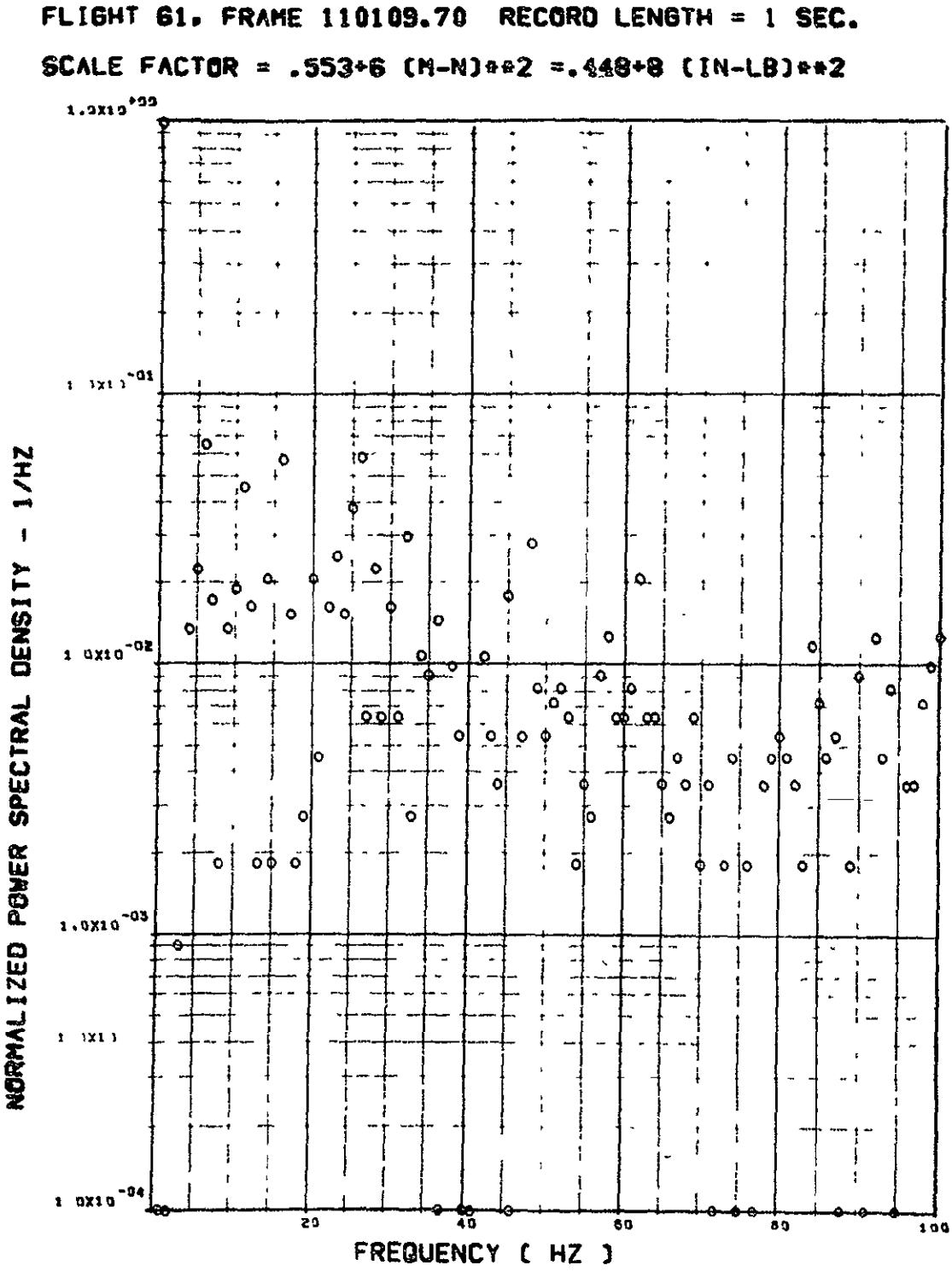

Figure 10. Continued

FLIGHT 61. FRAME 110109.70. RECORD LENGTH = 1 SEC.

SCALE FACTOR = .344+6 (M-N)**2 =.280+8 (IN-LB)**2

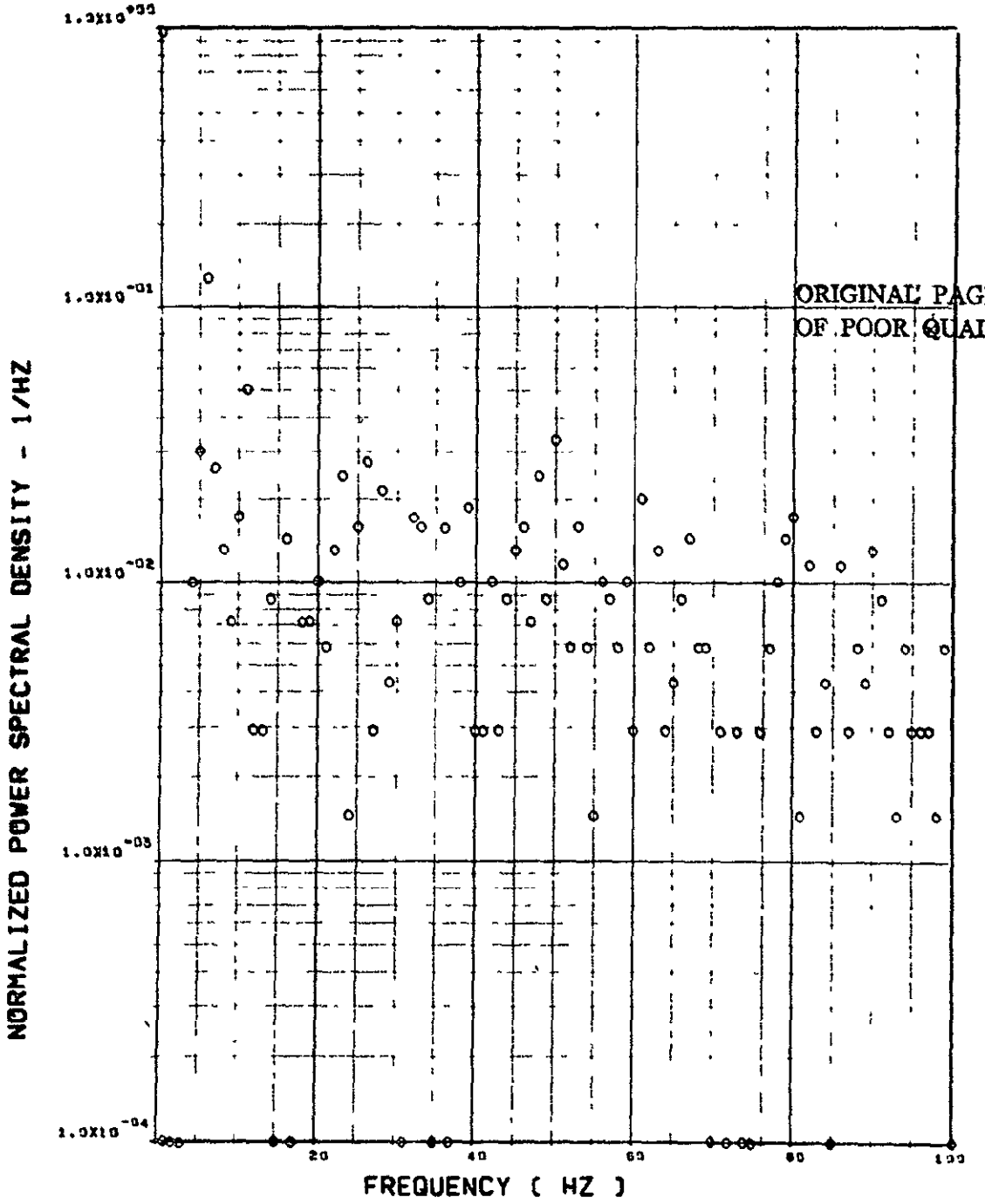

ITEM - SW128 TORSION AT WING STATION 2

Figure 10. Continued

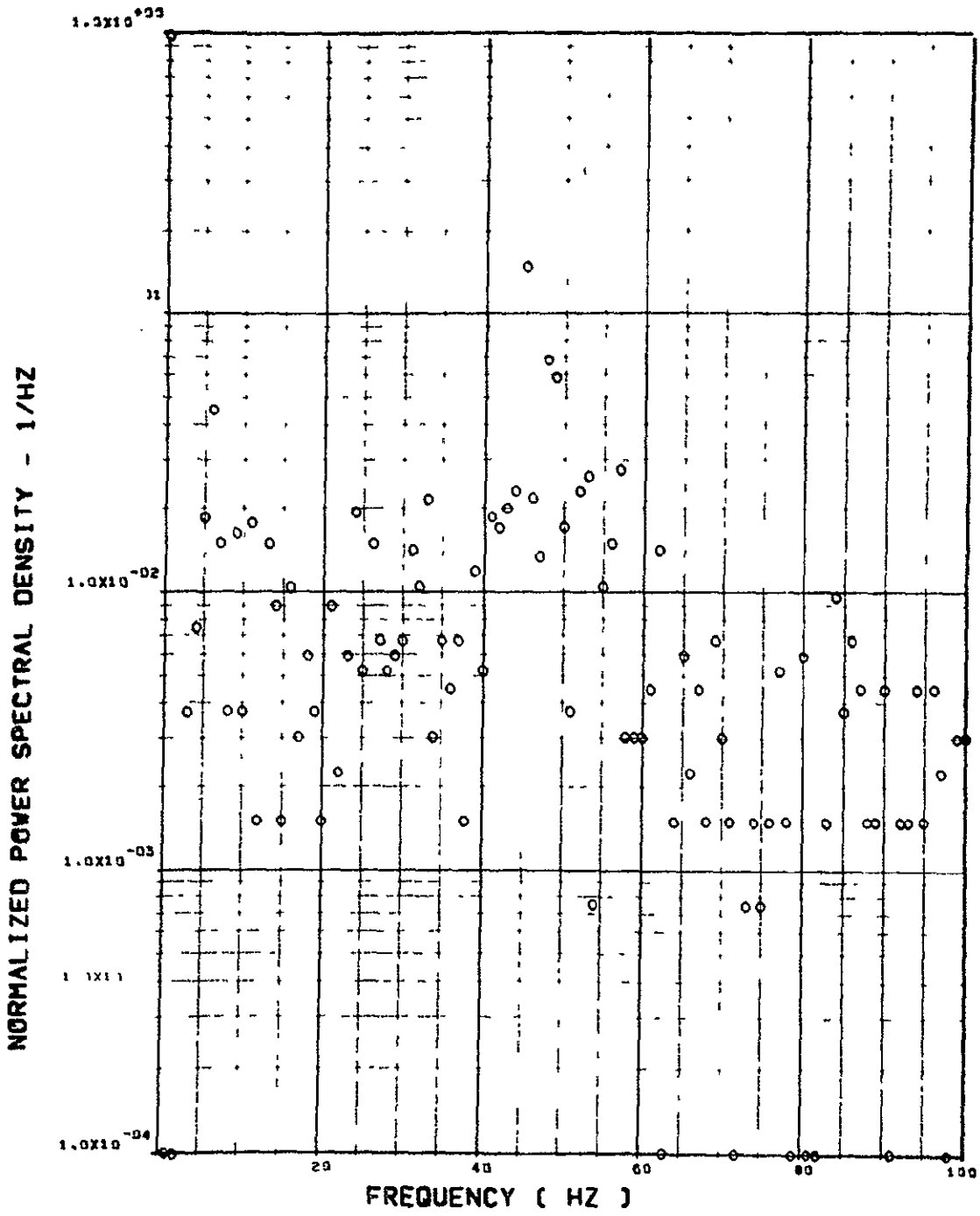

Figure 10. Continued

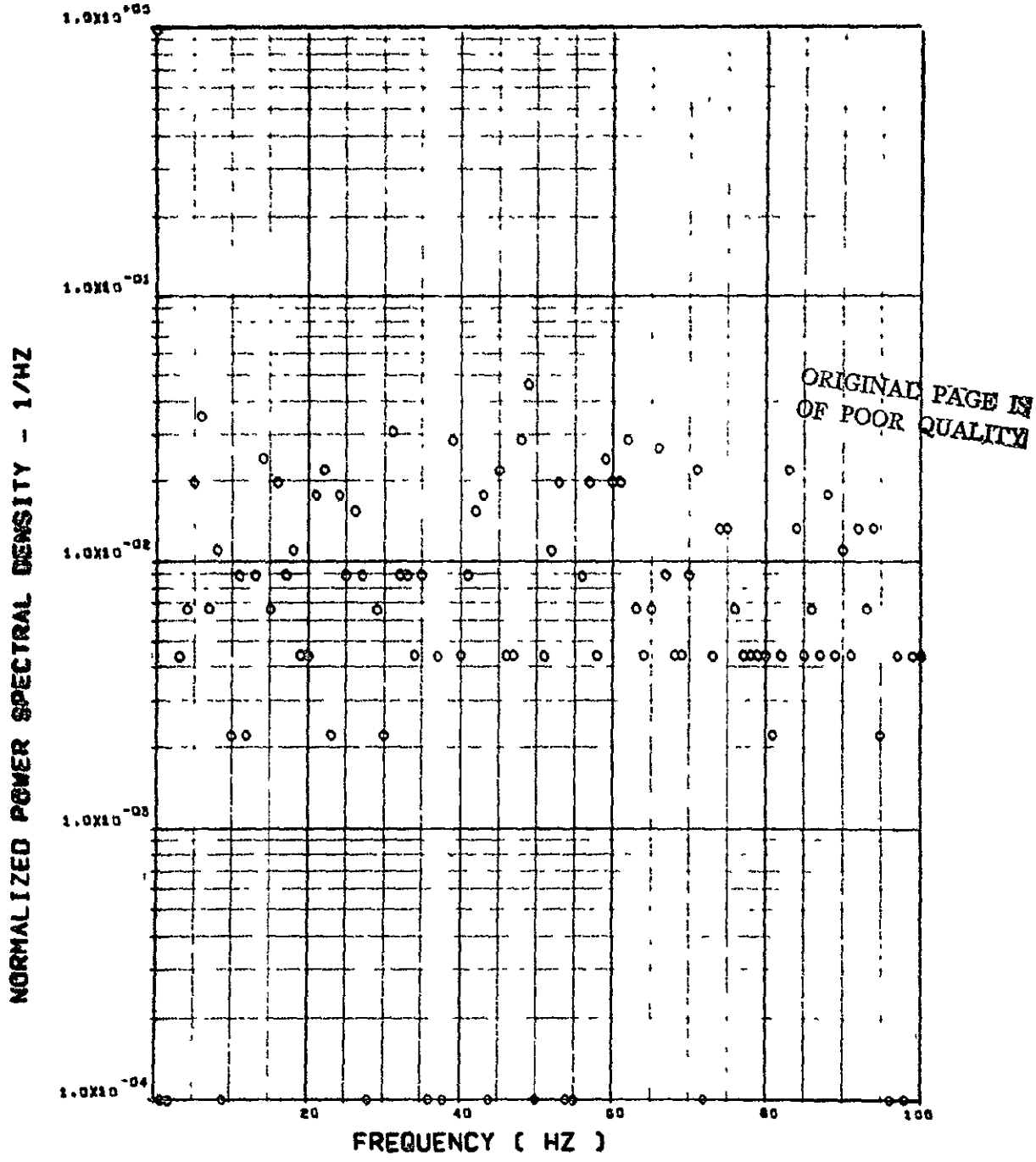

Figure 10. Continued

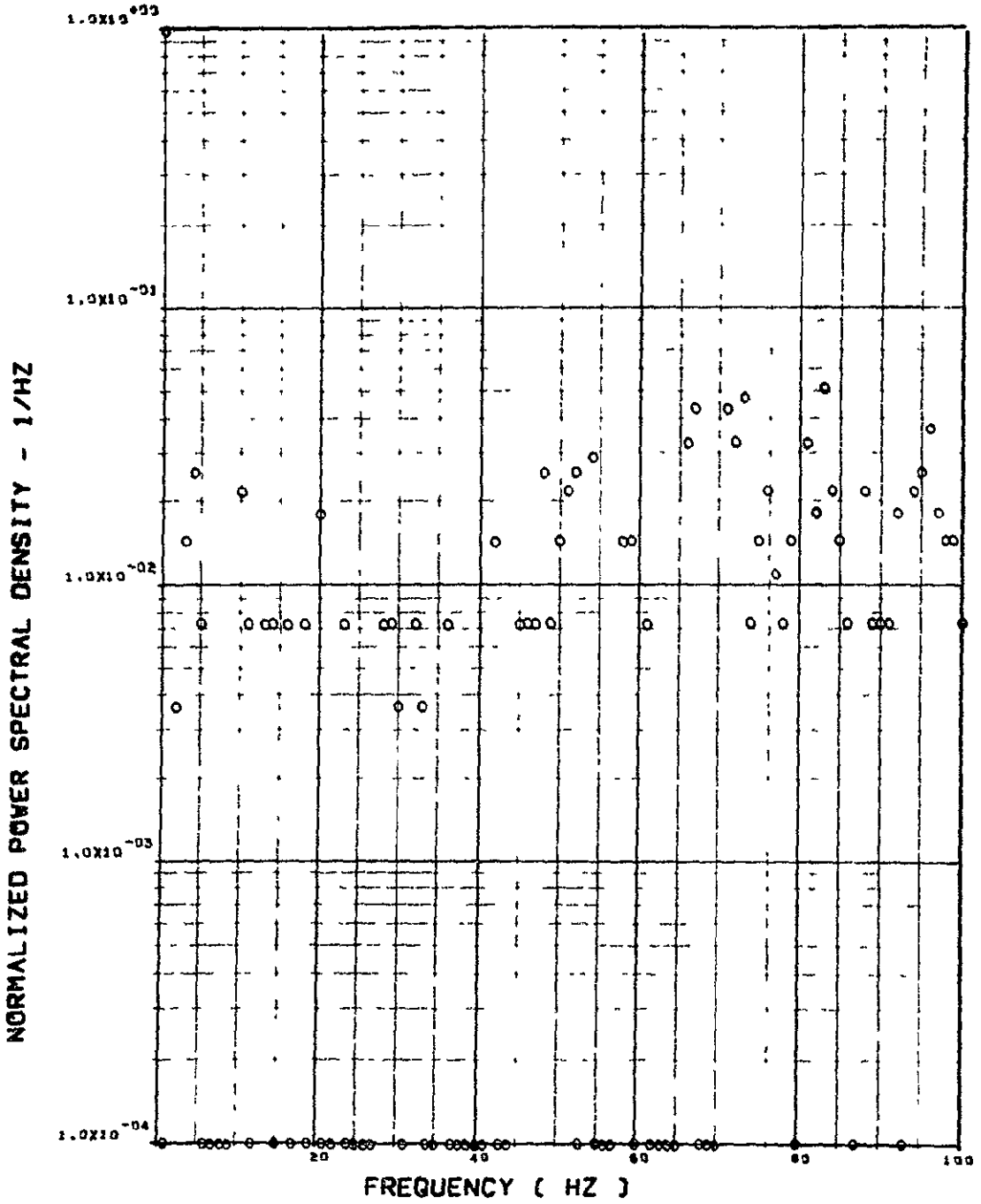

Figure 10. Continued

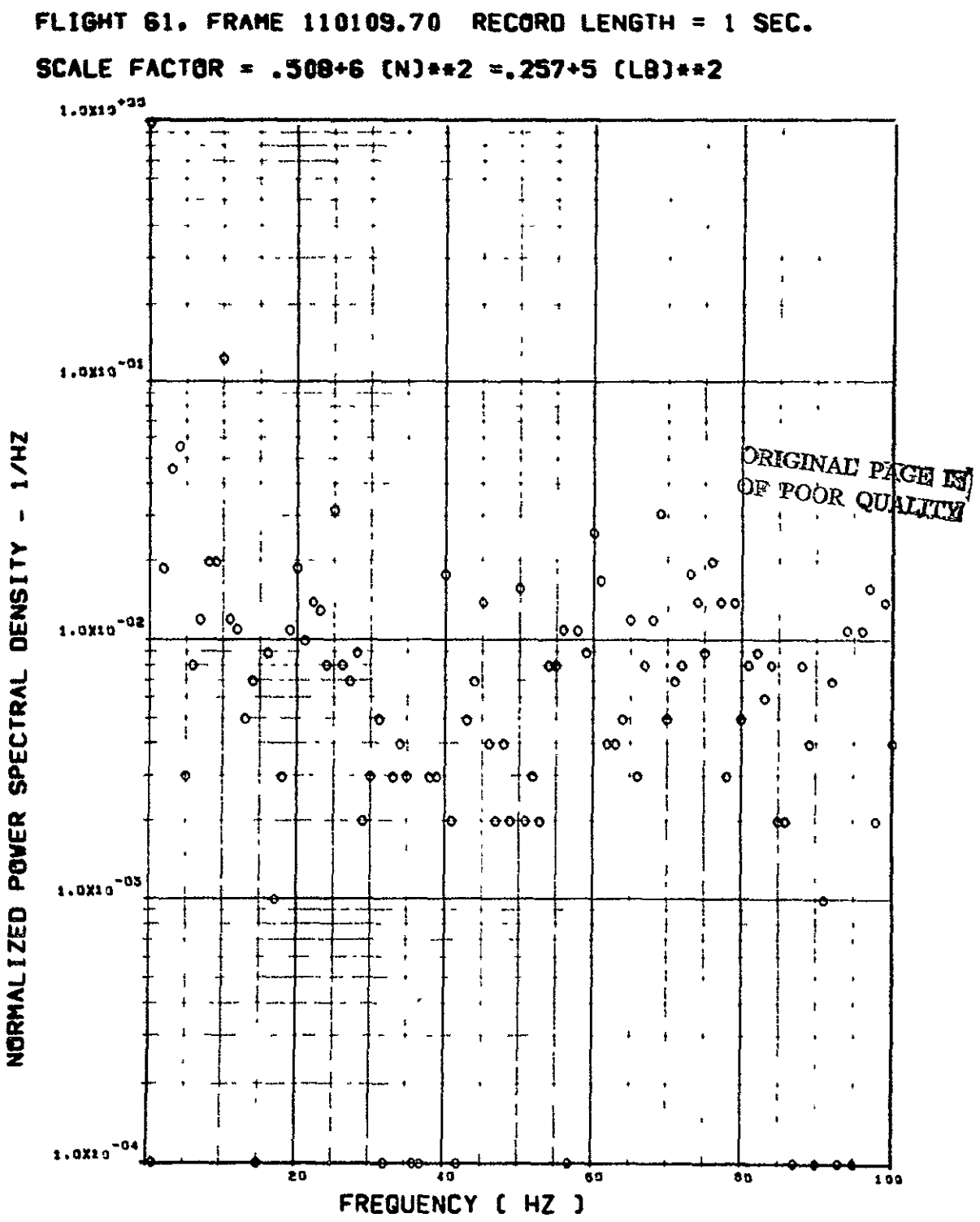

Figure 10. Continued

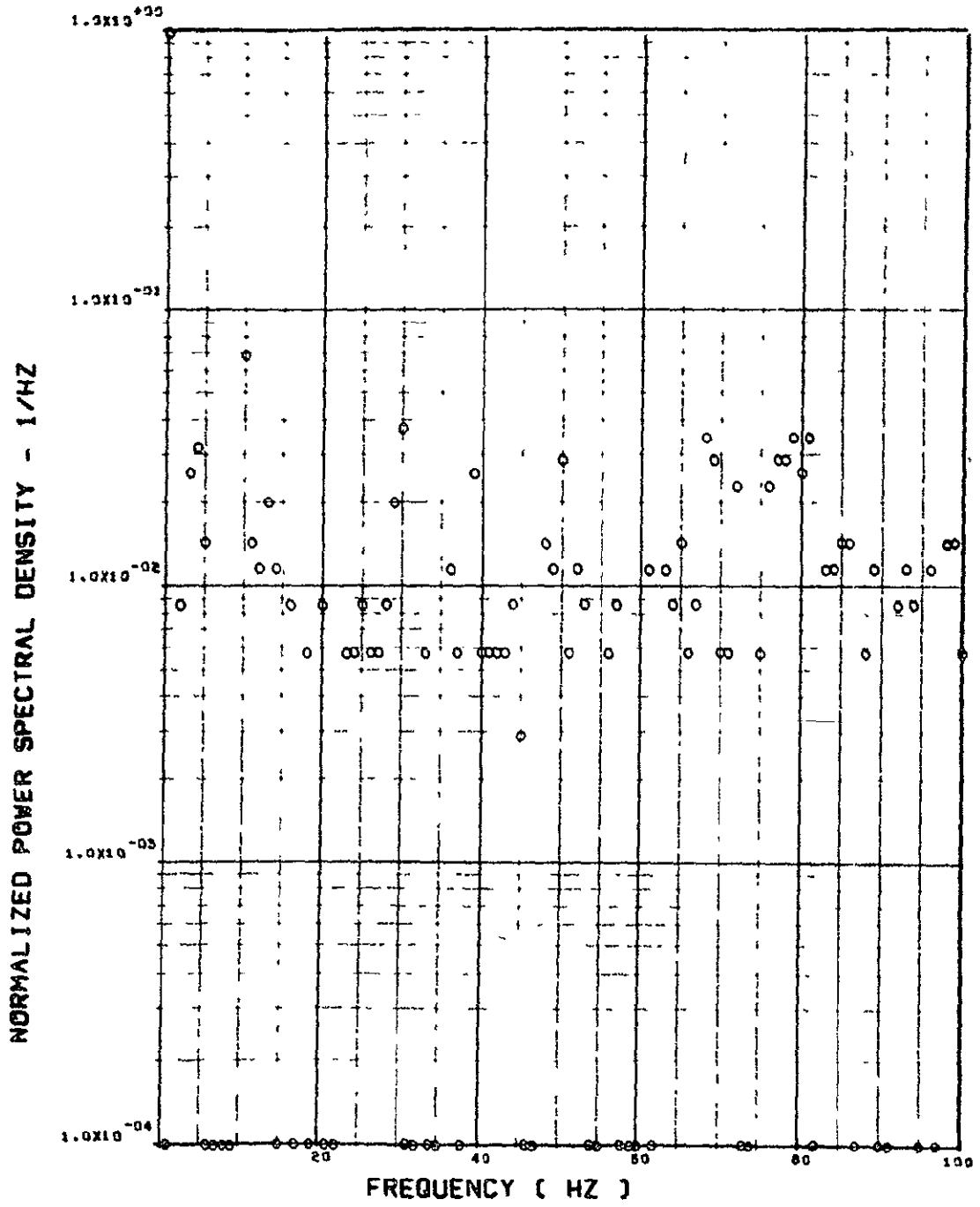

Figure 10. Continued

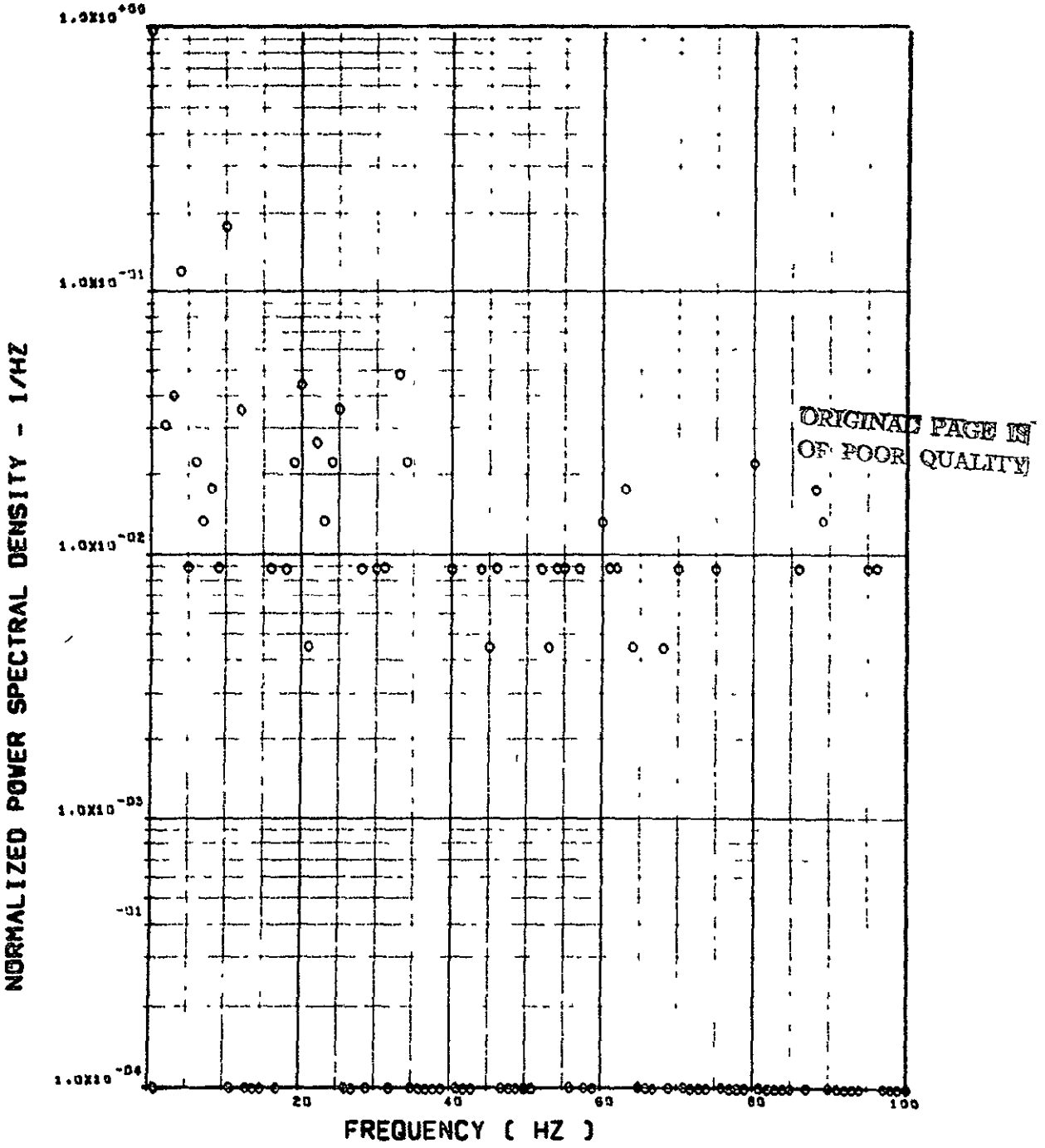

Figure 10. Continued

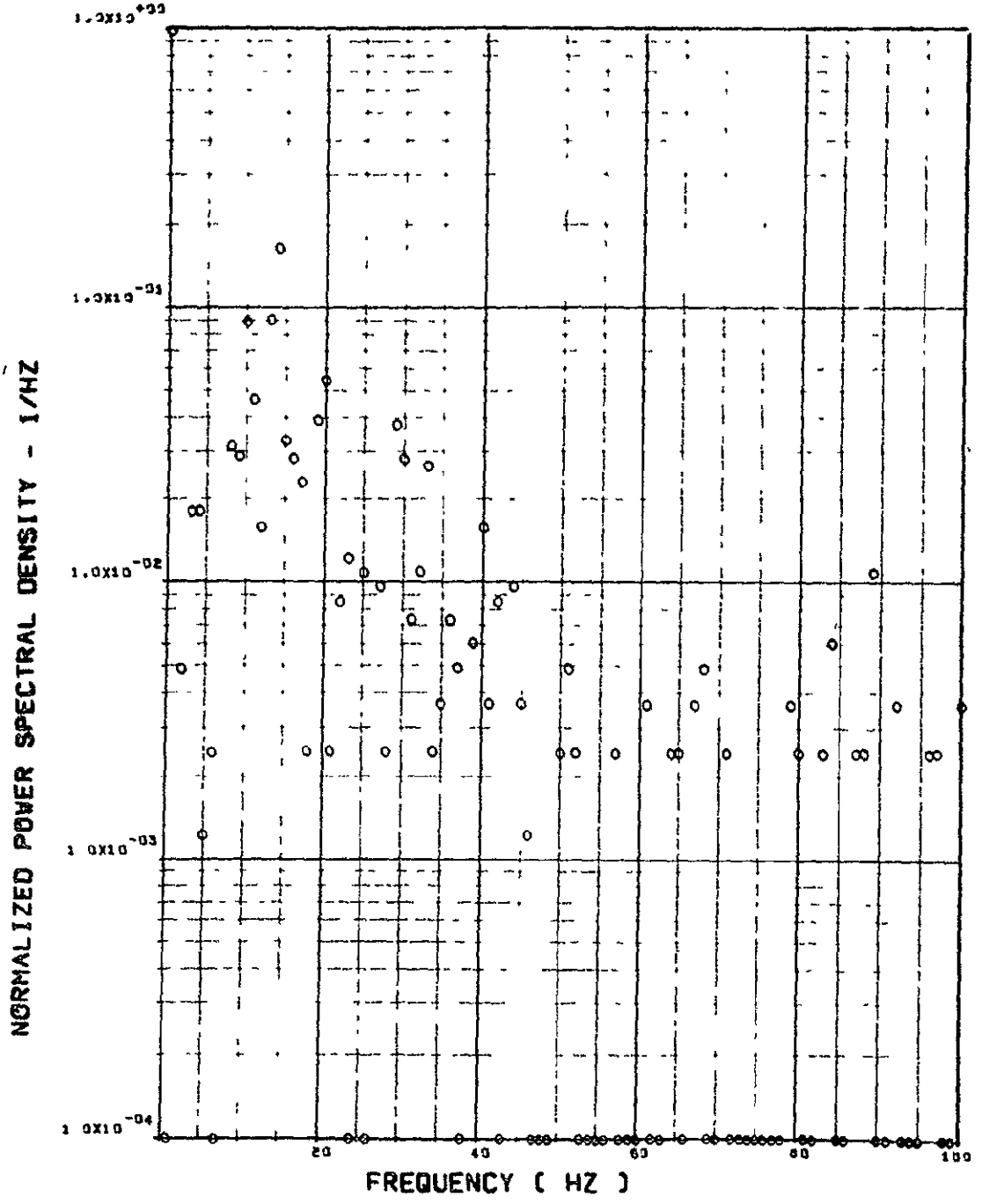

Figure 10. Continued

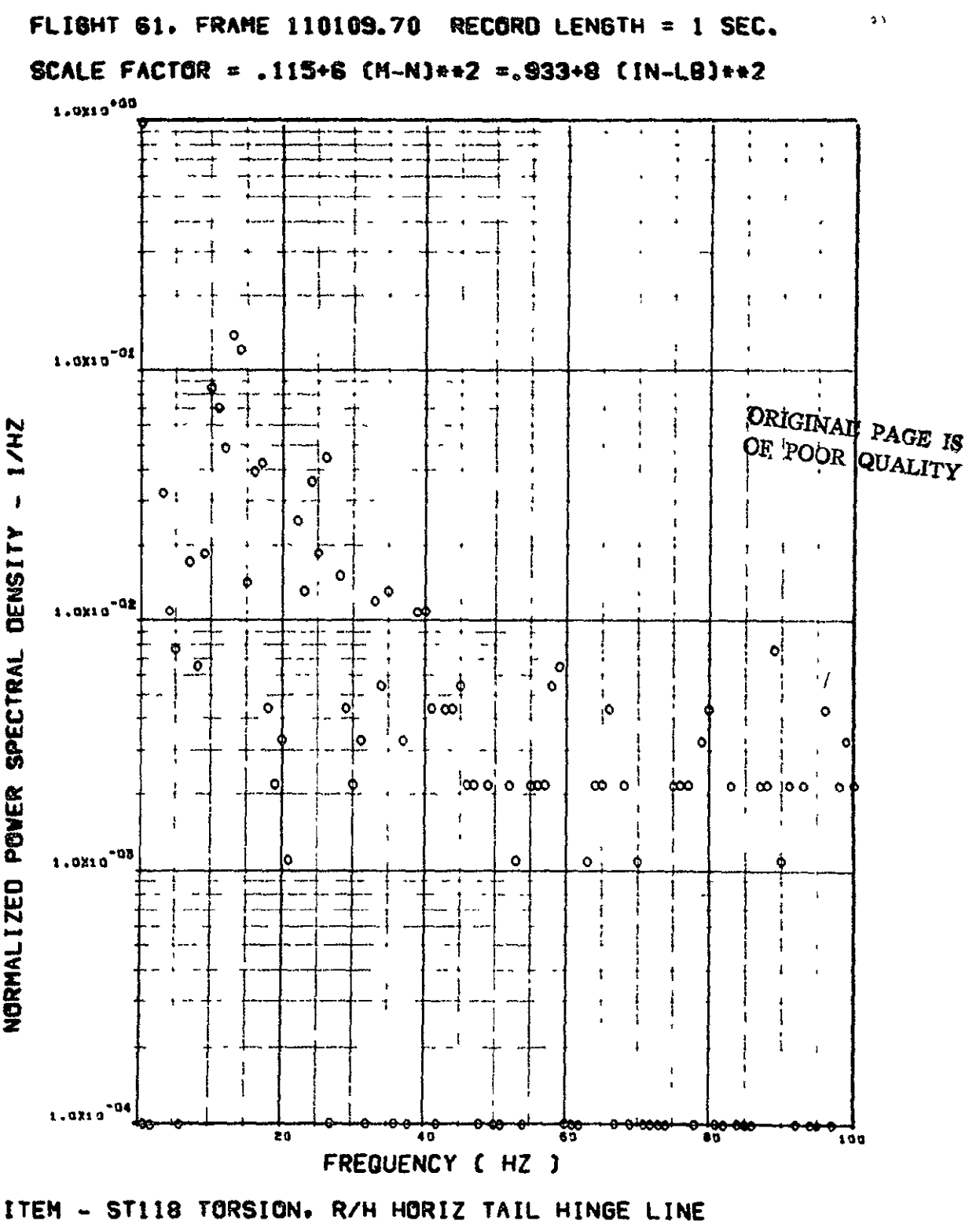

Figure 10. Concluded

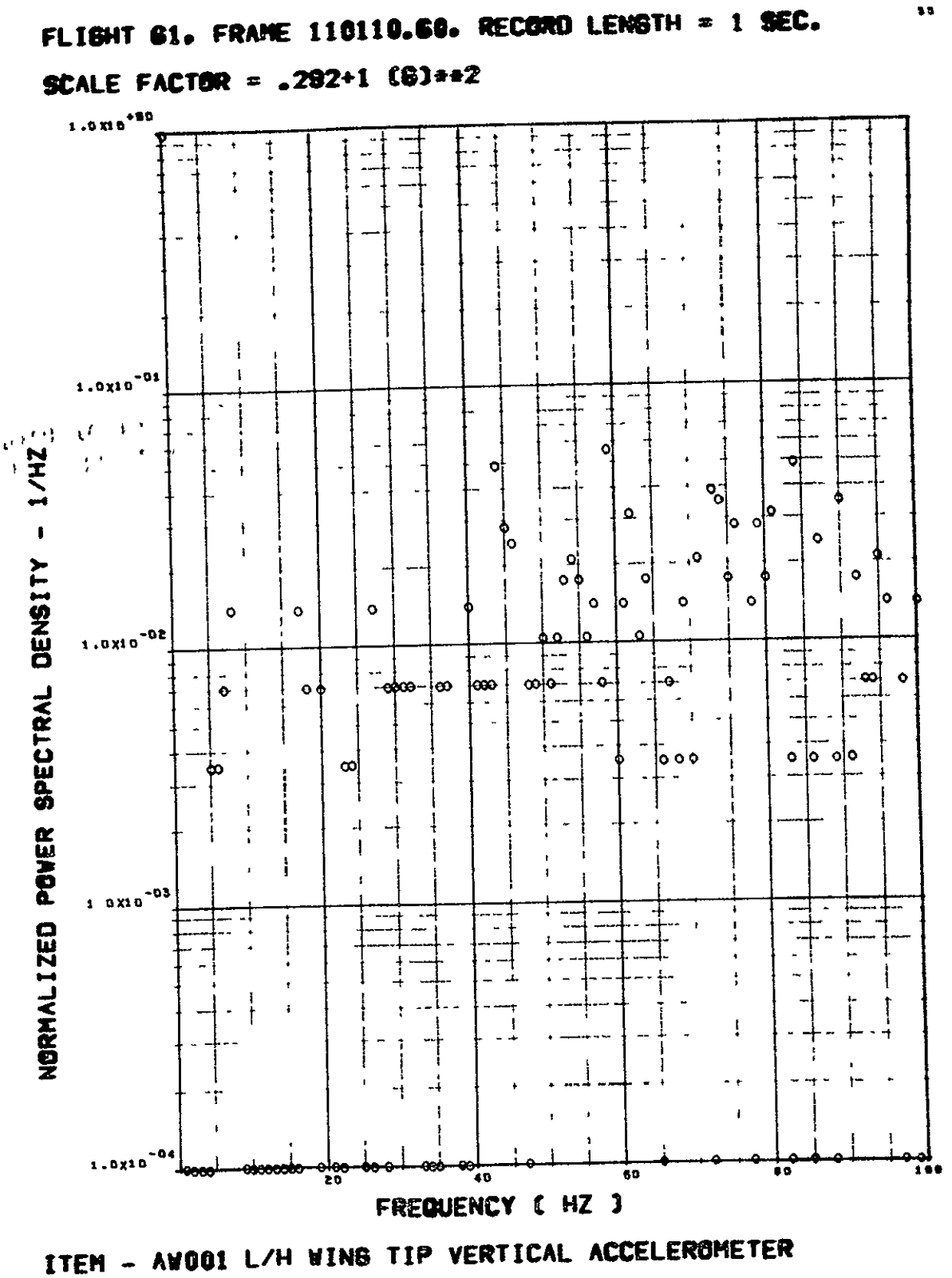

Figure 11. Power Spectra - Flight 61, Run 227, Point 4 T_1 = 110110.6, ΔT = 1 Sec, α_{Nom} = 11.65 deg, $\Delta\alpha$= 2.10 deg.

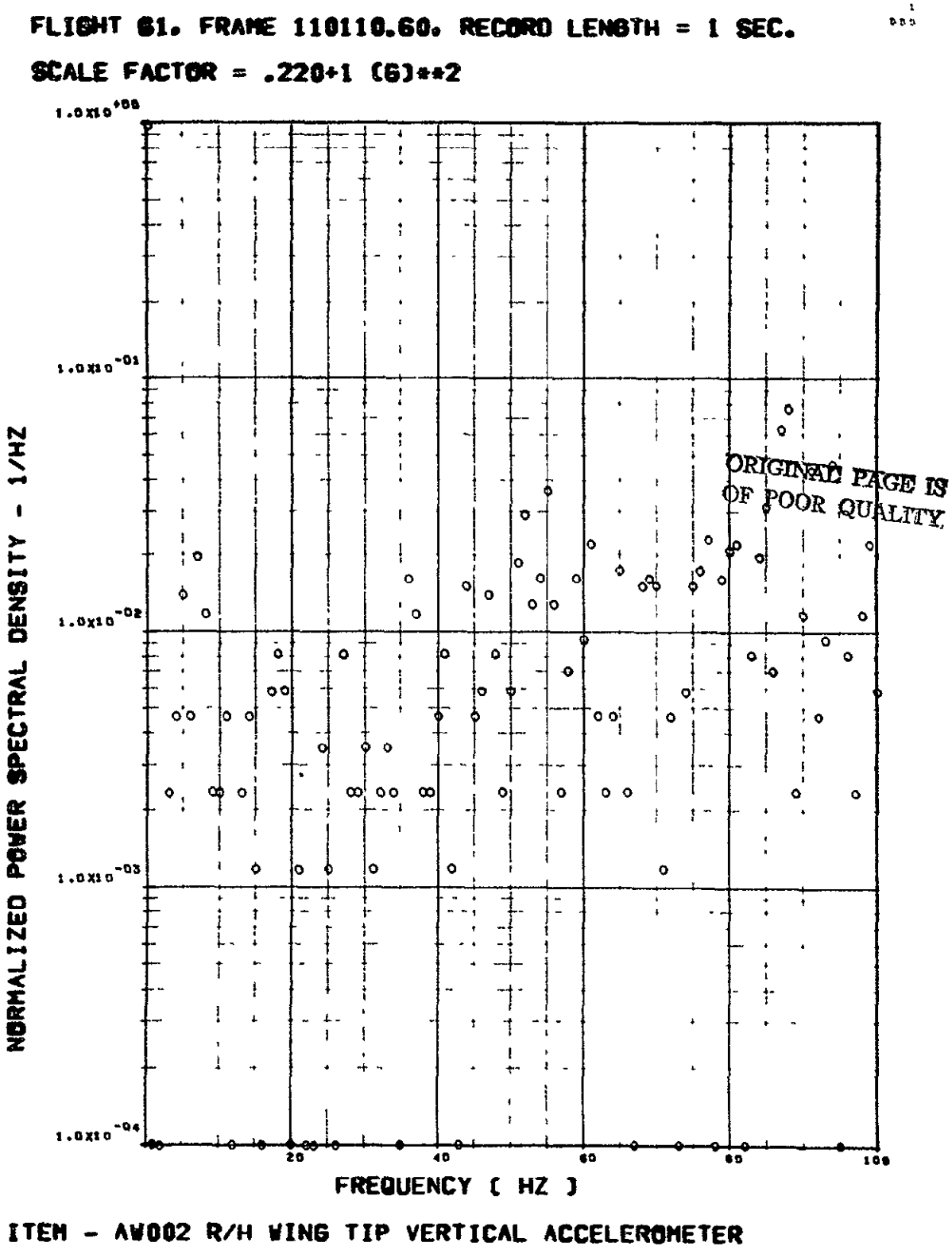

Figure 11. Continued

FLIGHT 61. FRAME 110110.60. RECORD LENGTH = 1 SEC.

SCALE FACTOR = .520-1 (G)**2

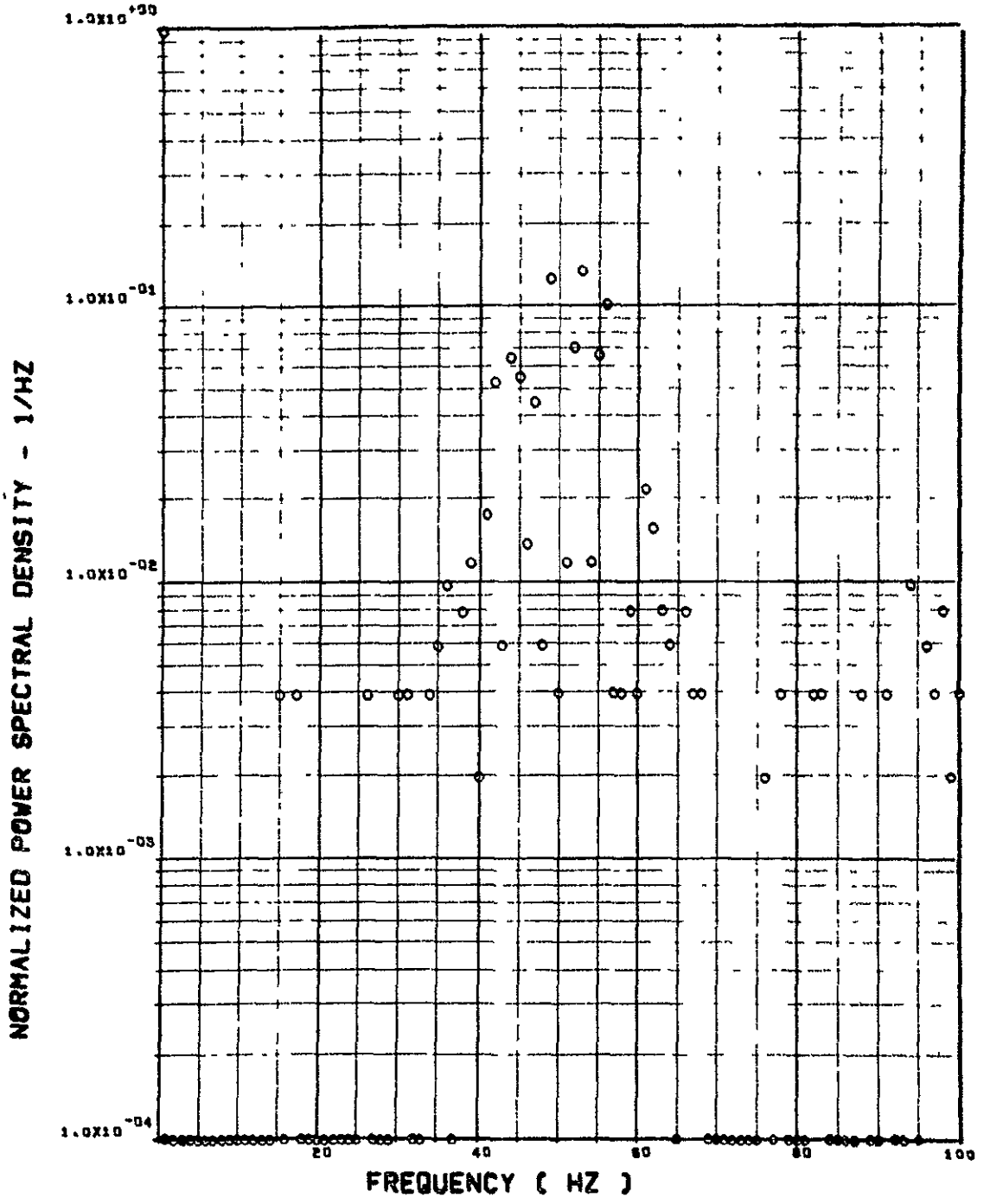

ITEM - AB018 C.G. VERTICAL ACCELEROMETER

Figure 11. Continued

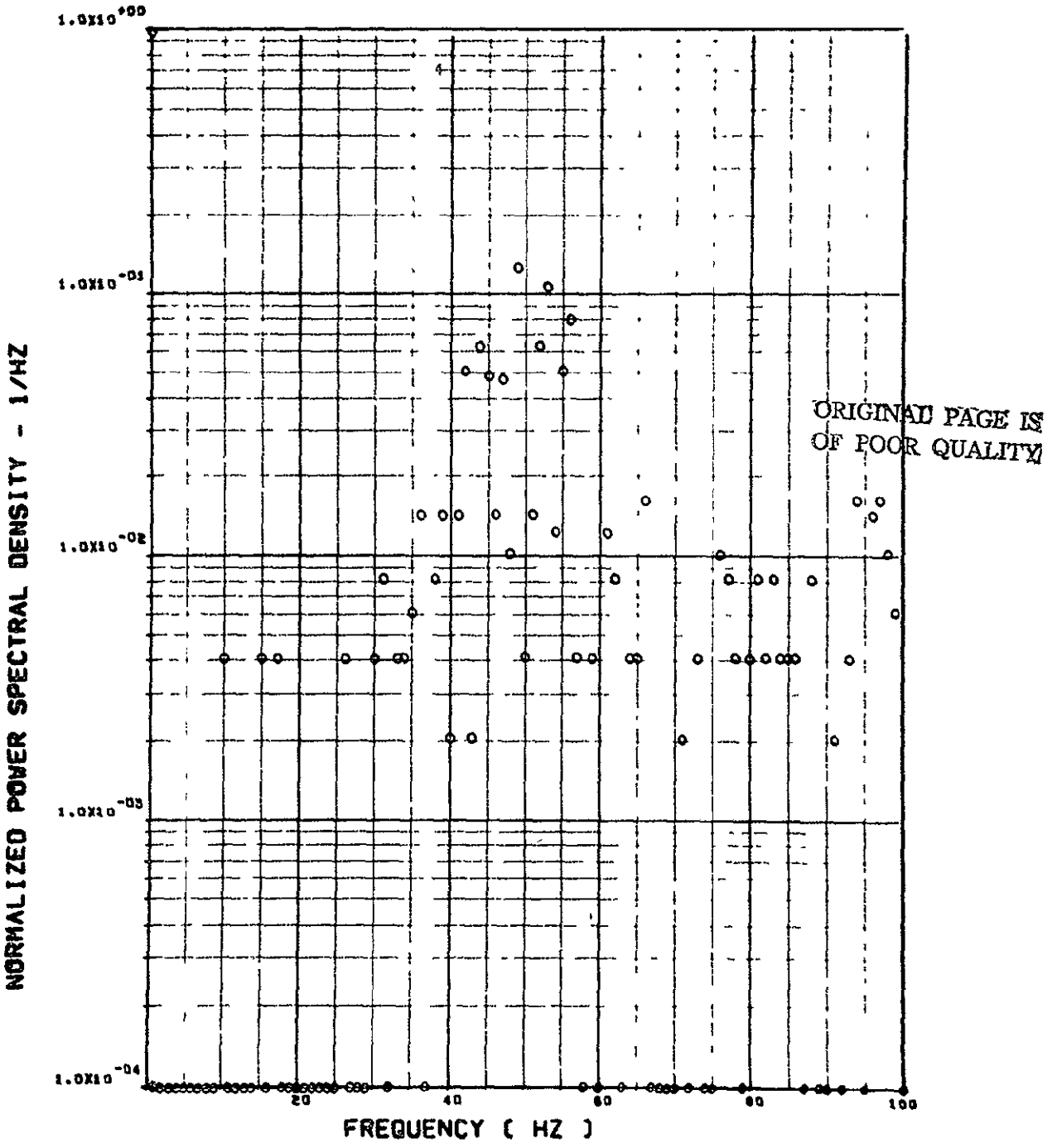

Figure 11. Continued

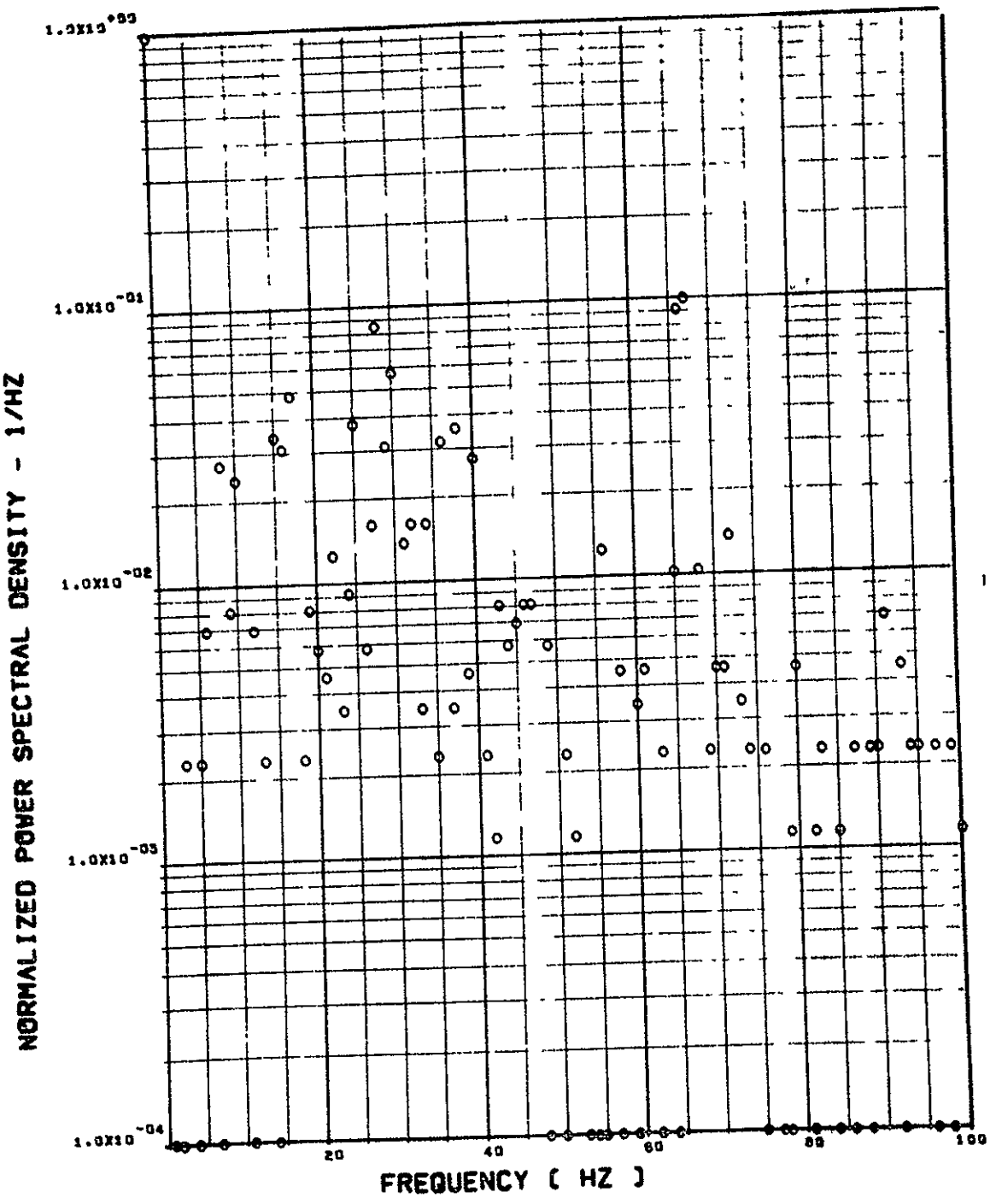

Figure 11. Continued

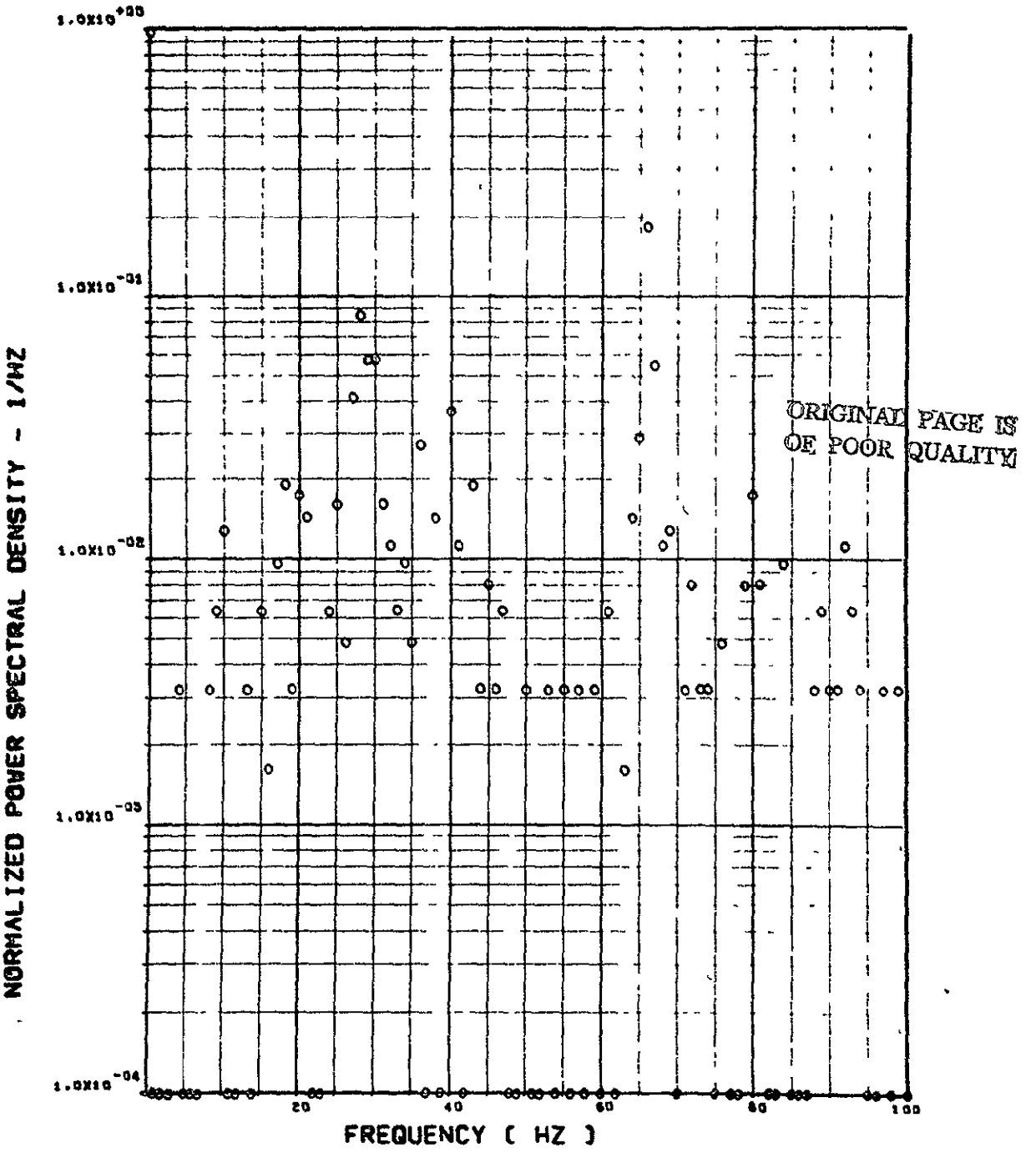

Figure 11. Continued

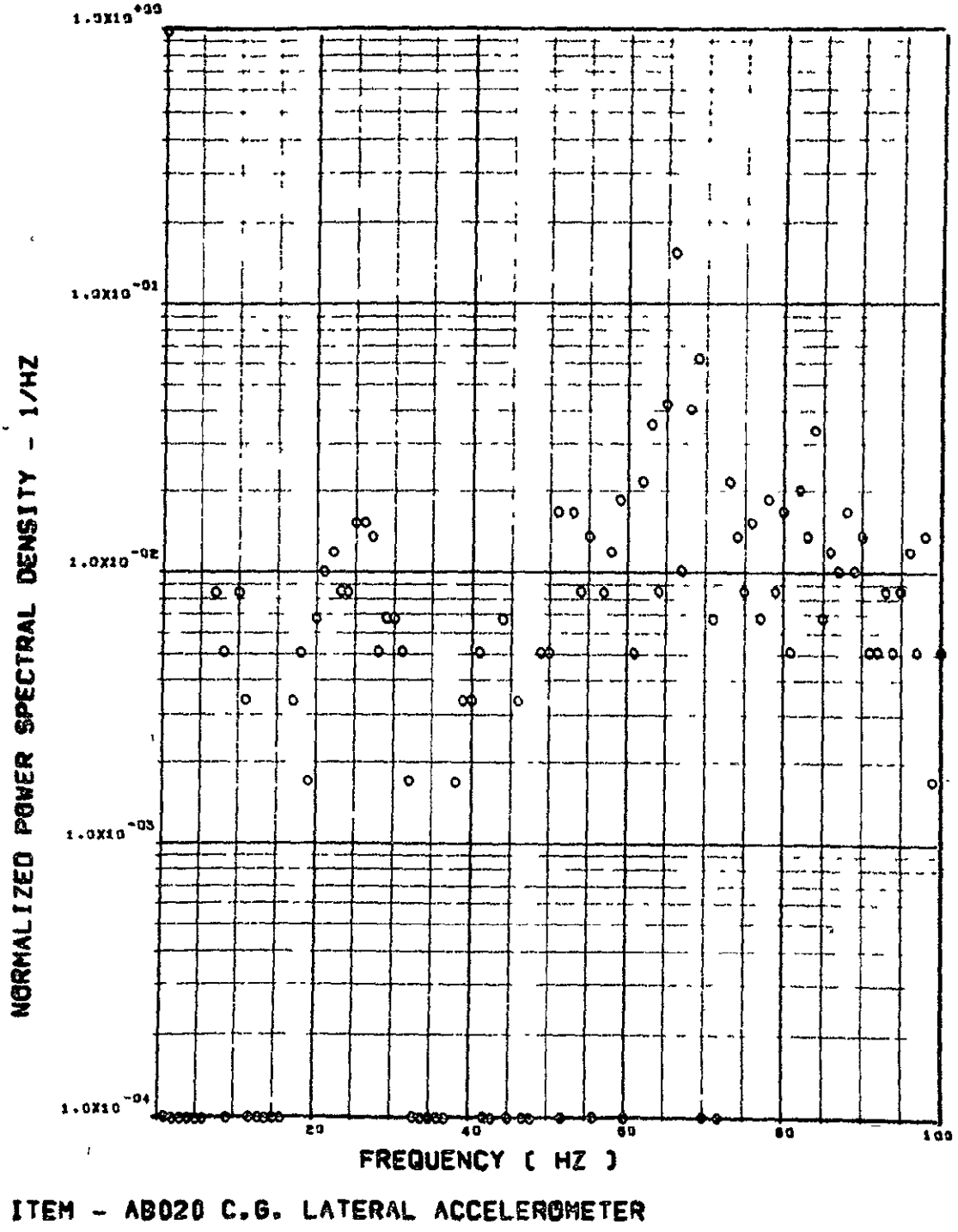

Figure 11. Continued

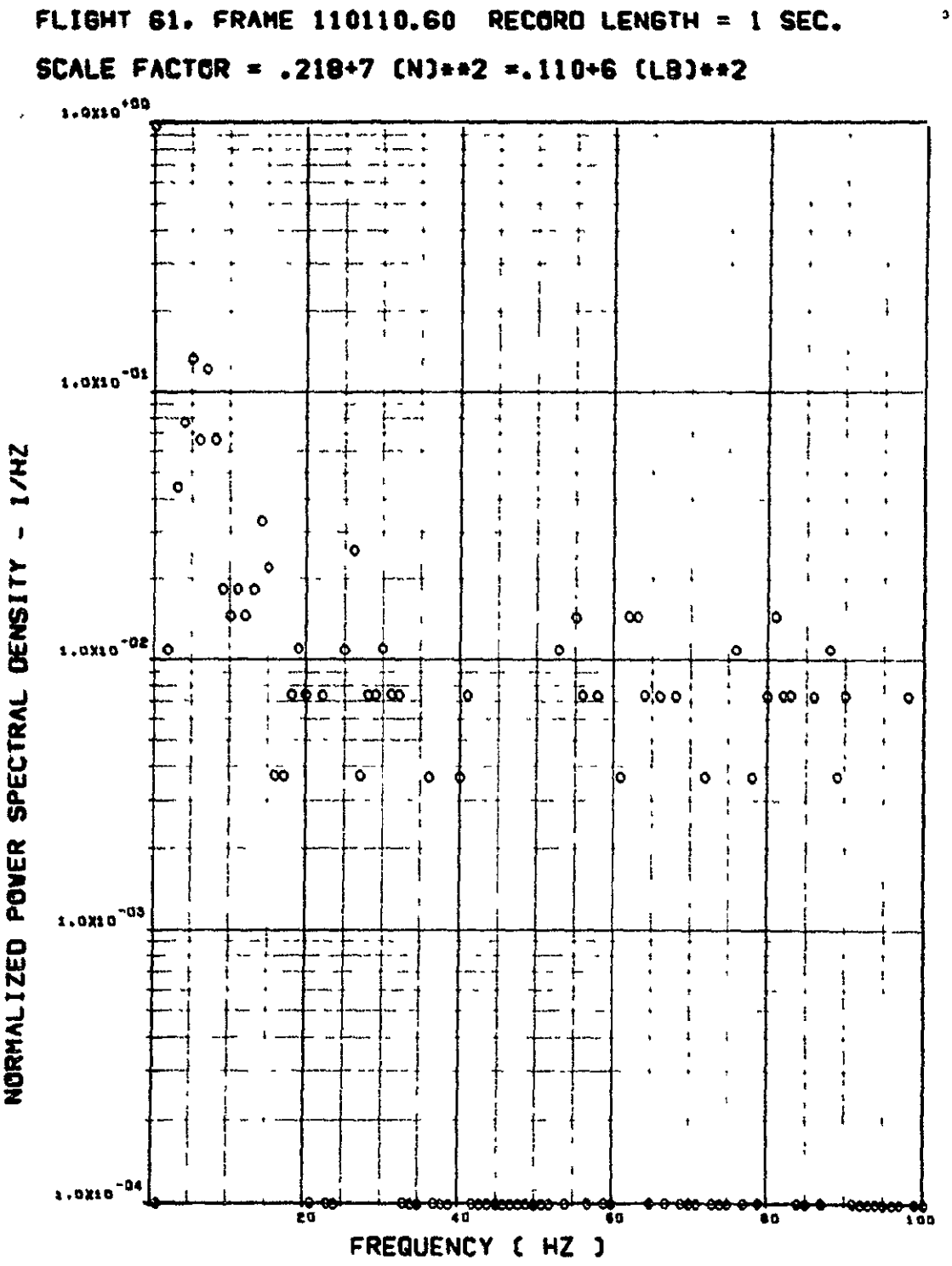

Figure 11. Continued

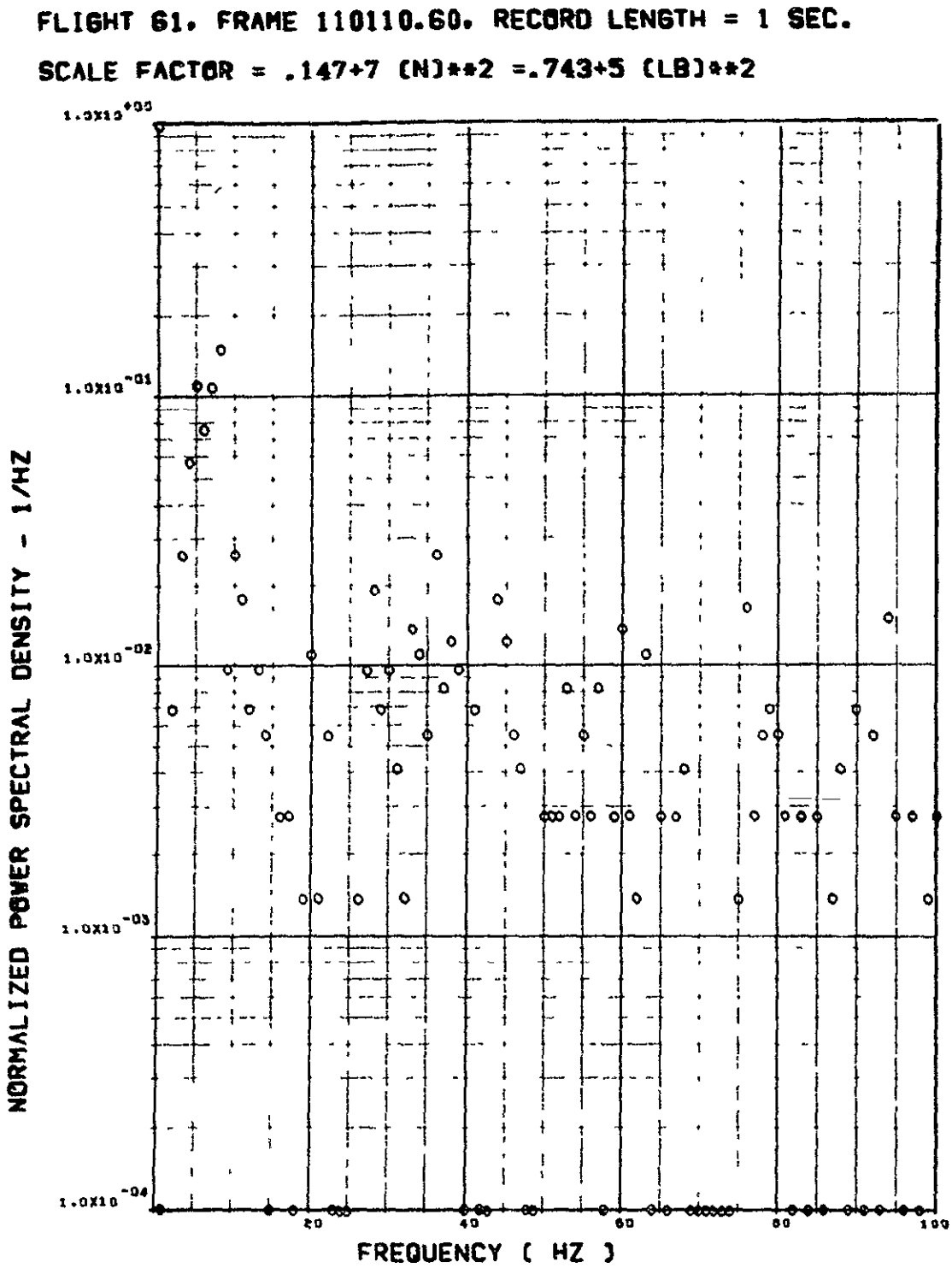

Figure 11. Continued

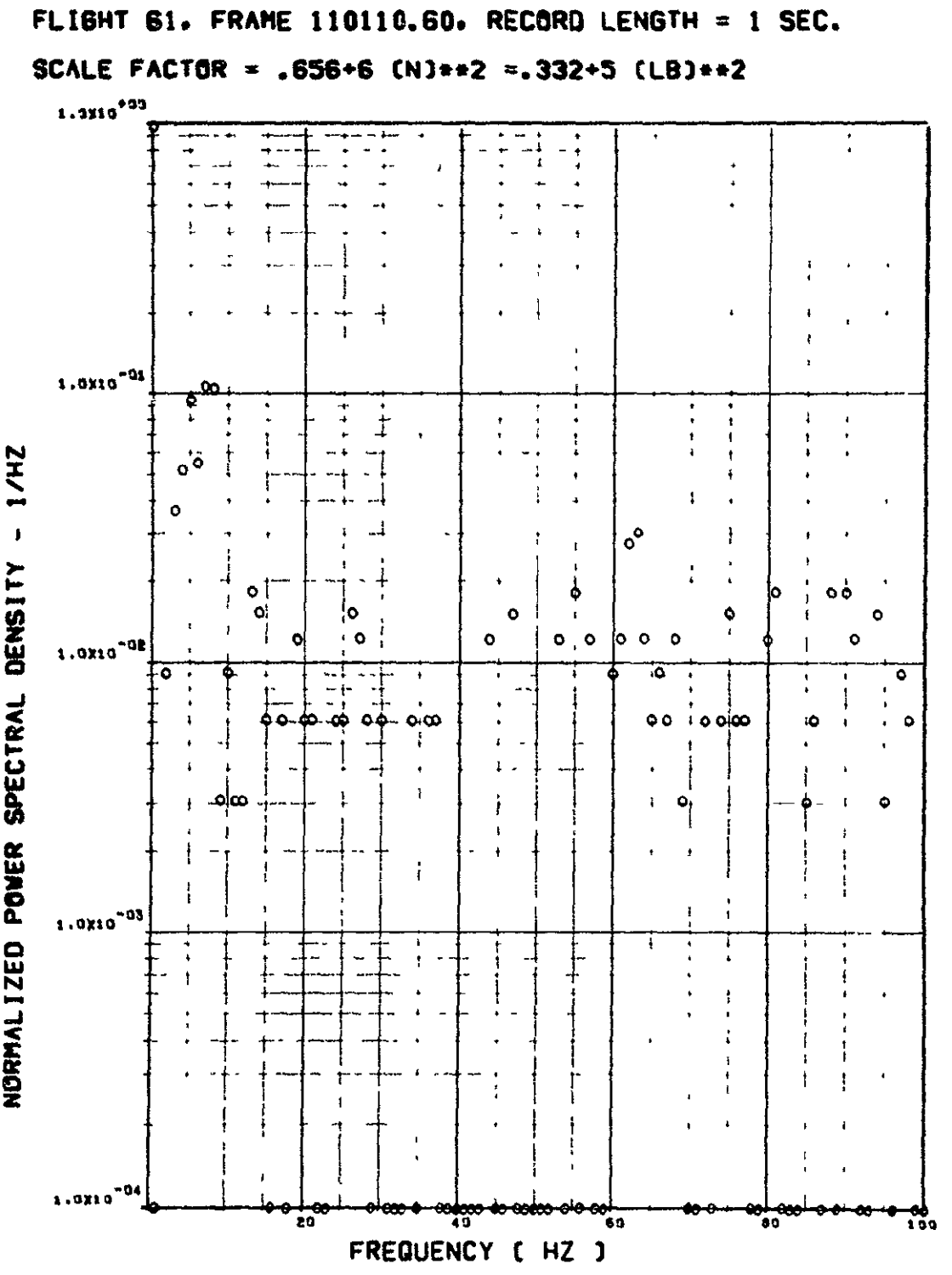

Figure 11. Continued

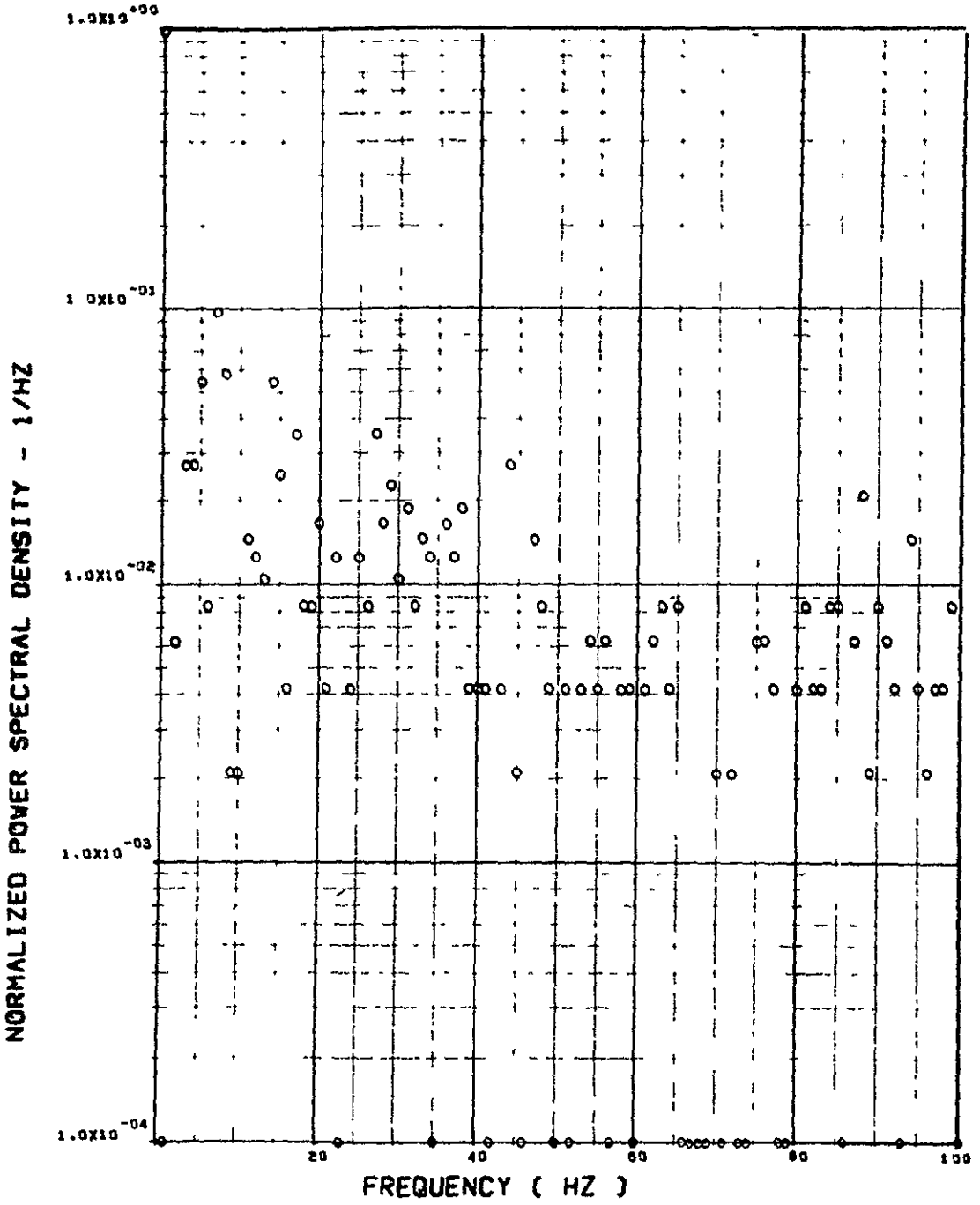

Figure 11. Continued

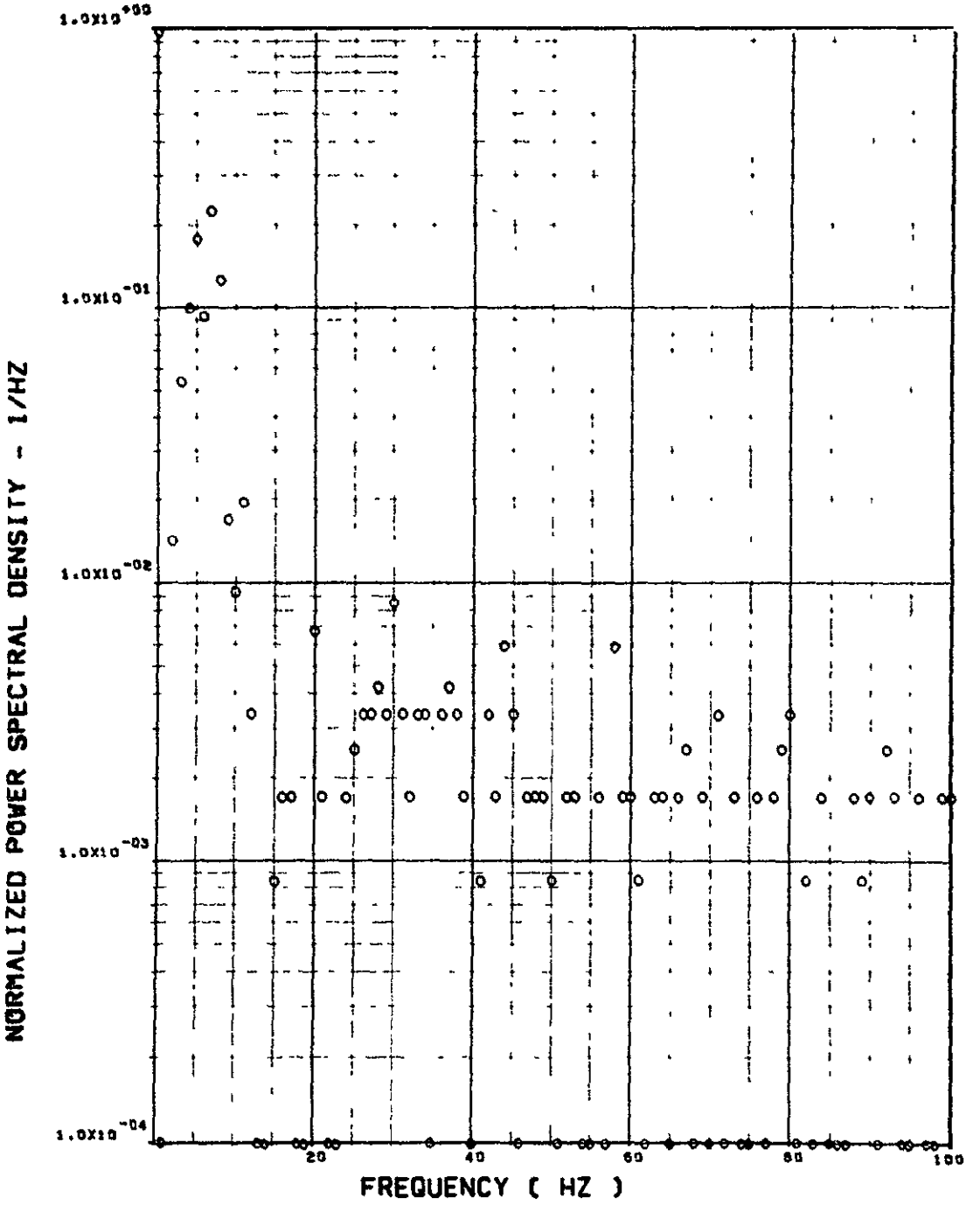

Figure 11. Continued

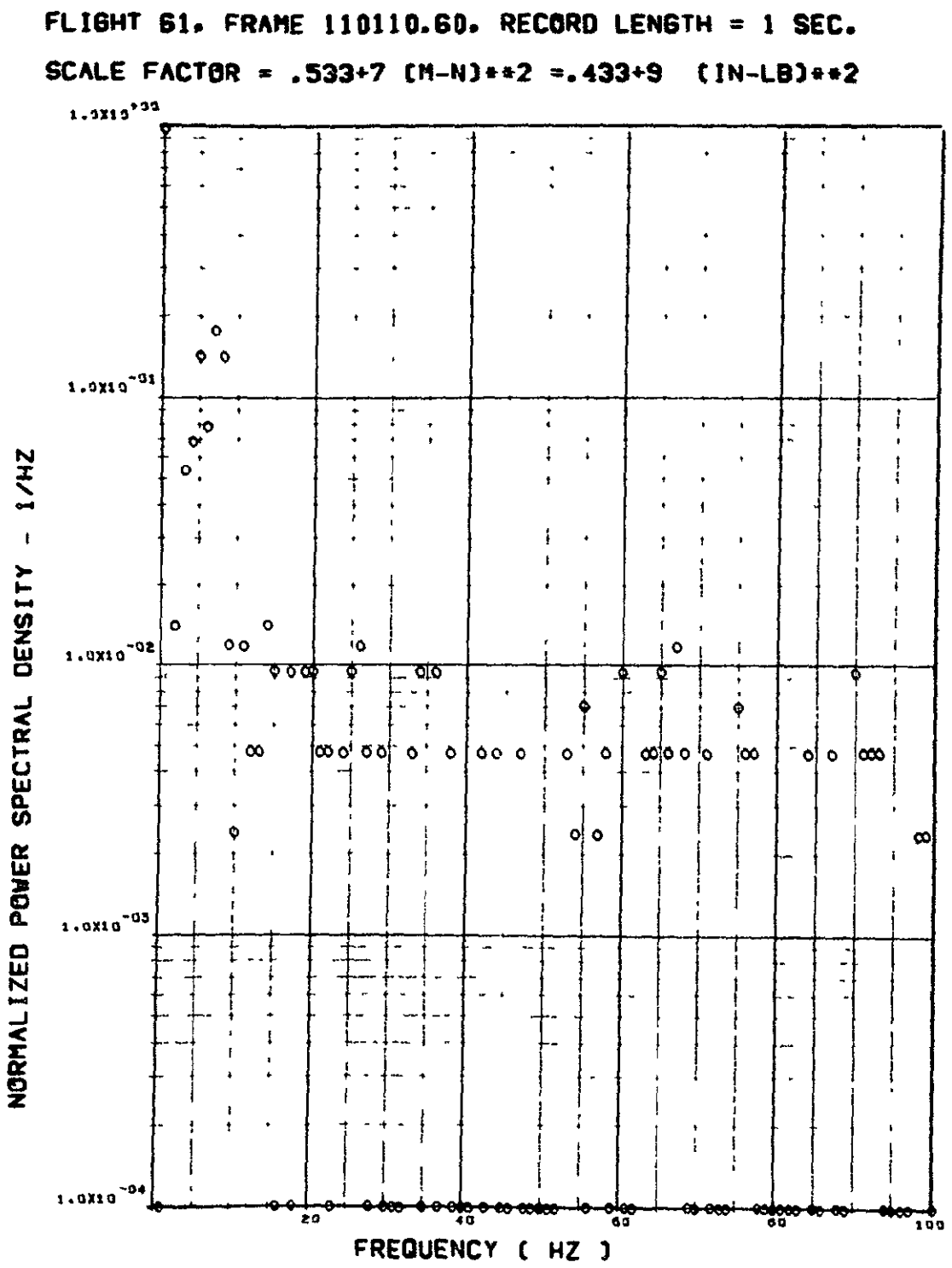

Figure 11. Continued

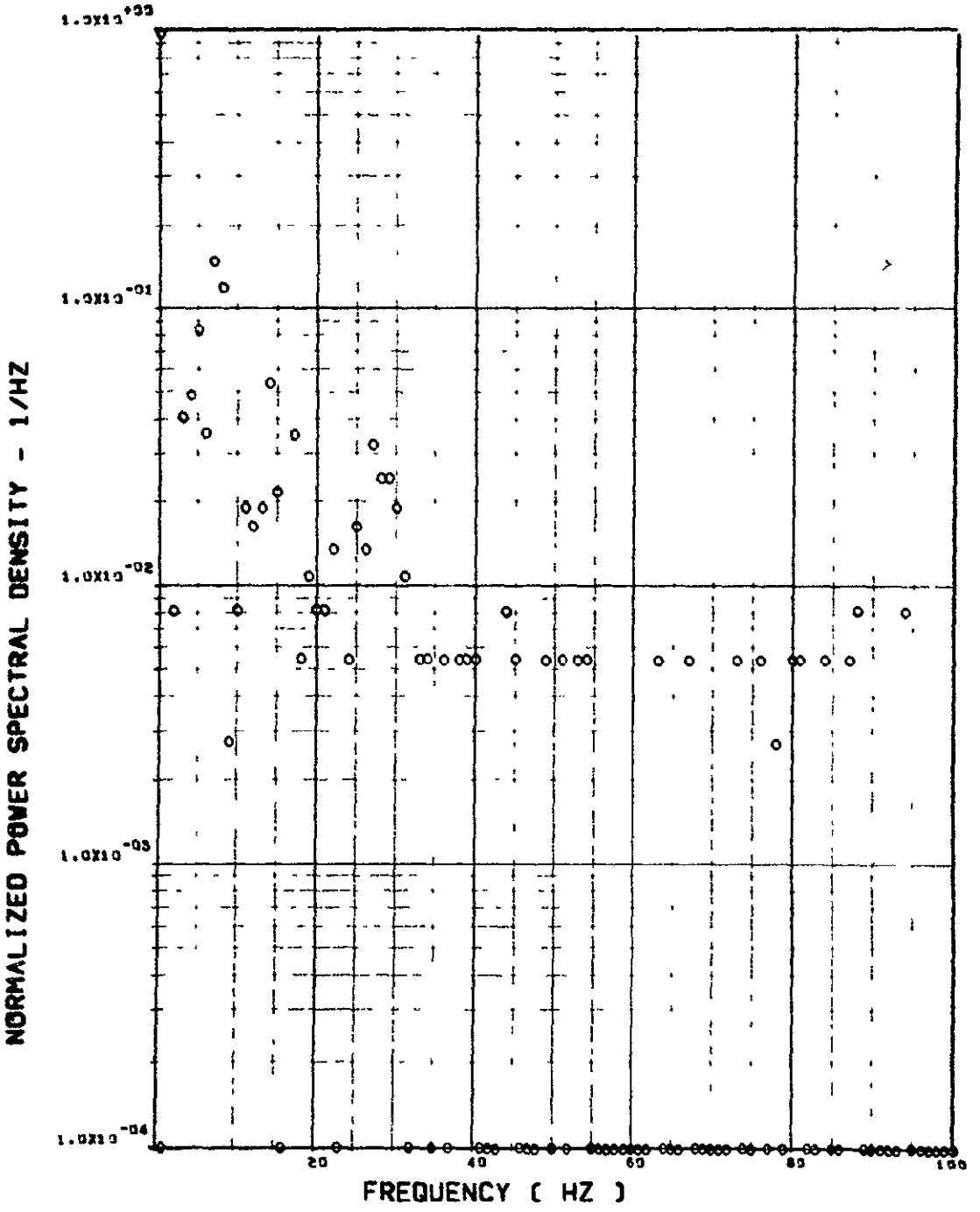

Figure 11. Continued

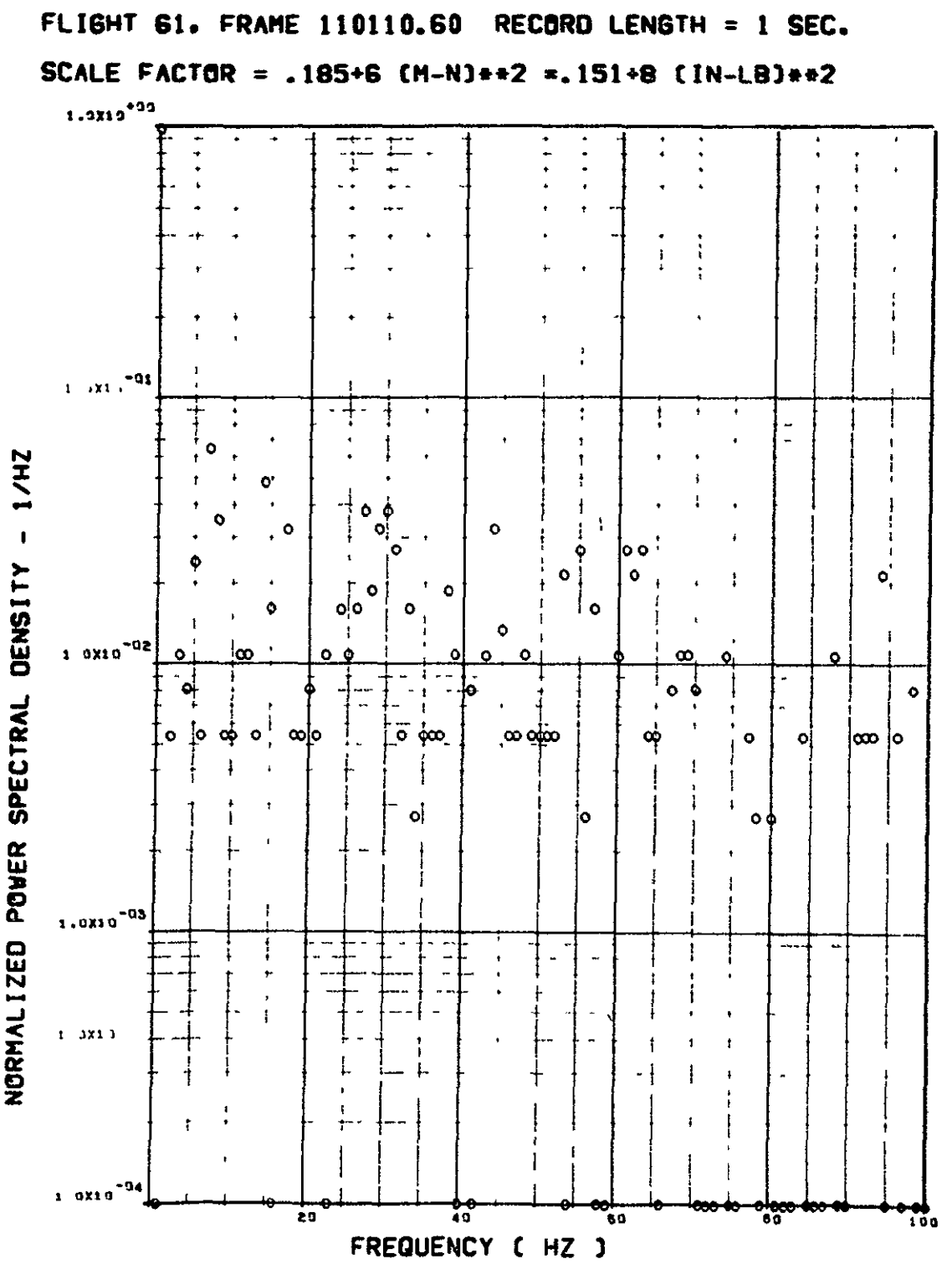

Figure 11. Continued

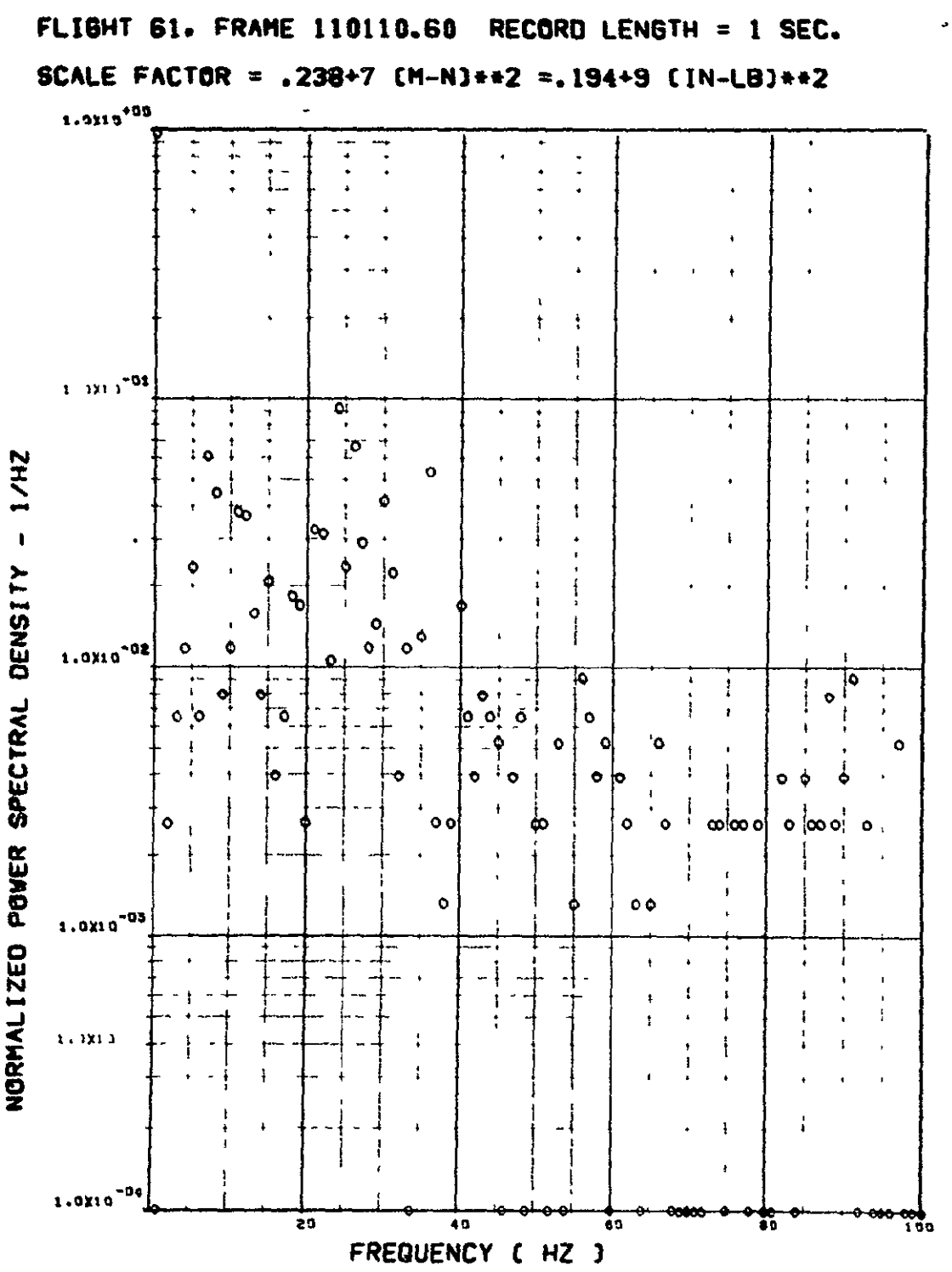

Figure 11. Continued

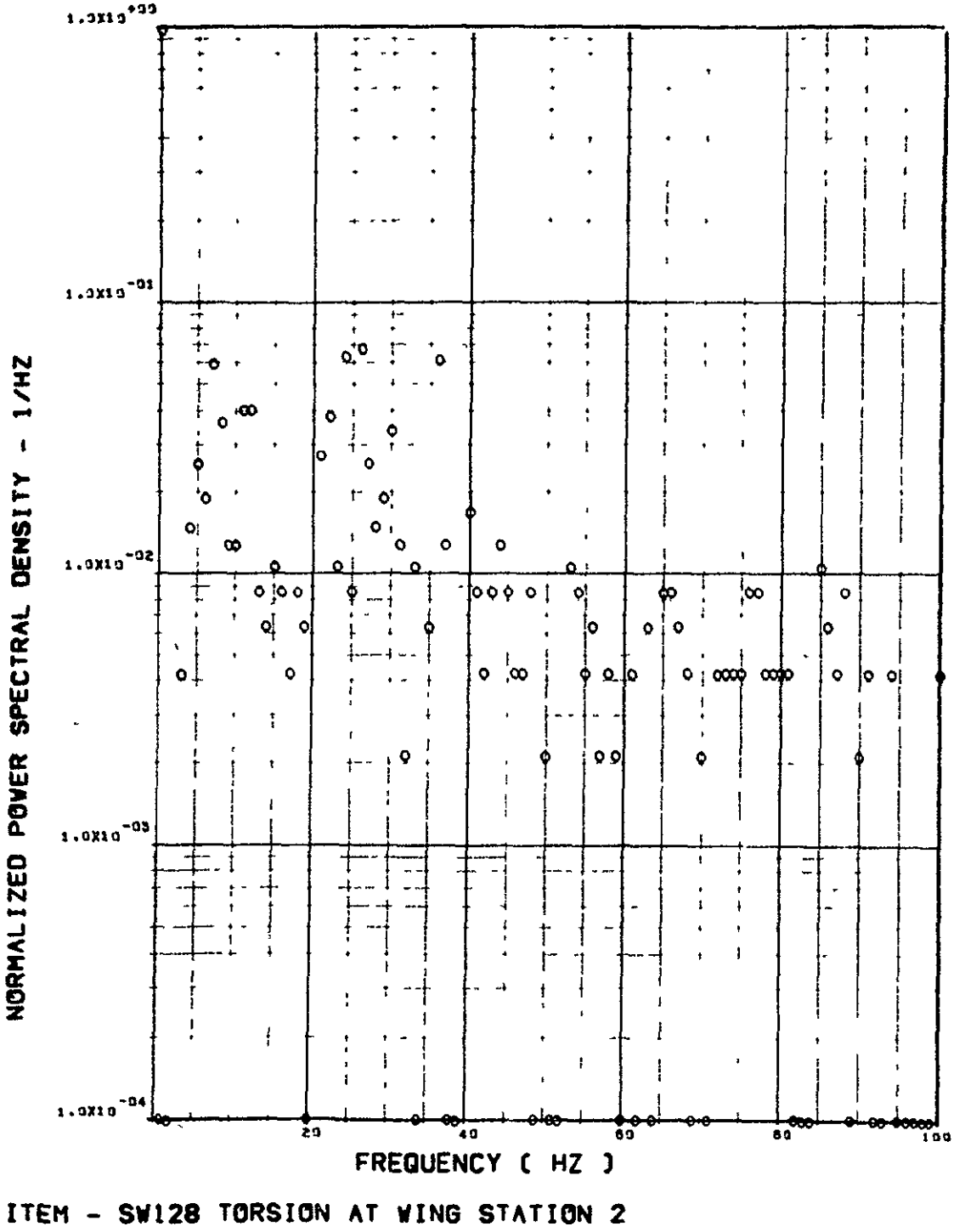

Figure 11. Continued

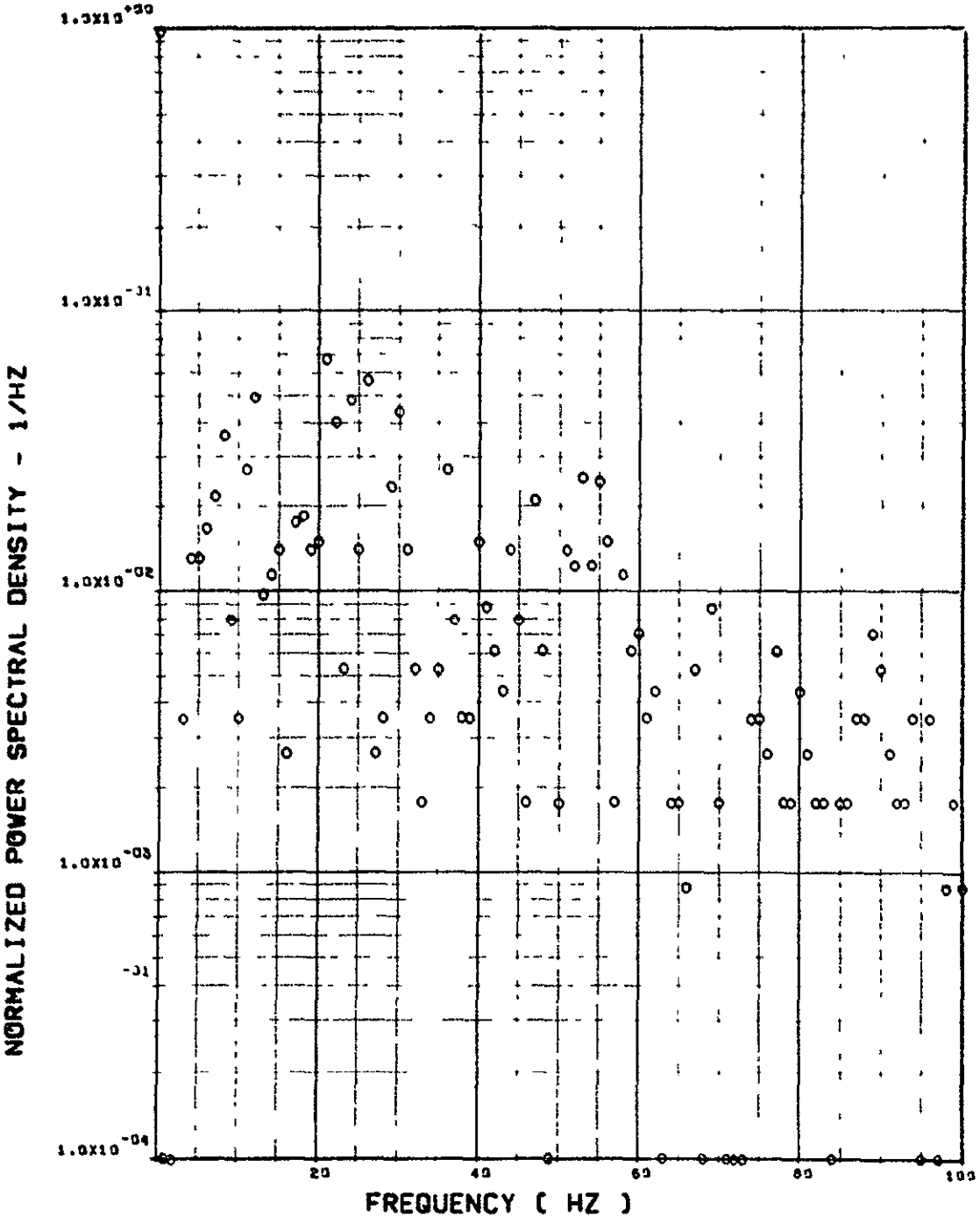

Figure 11. Continued

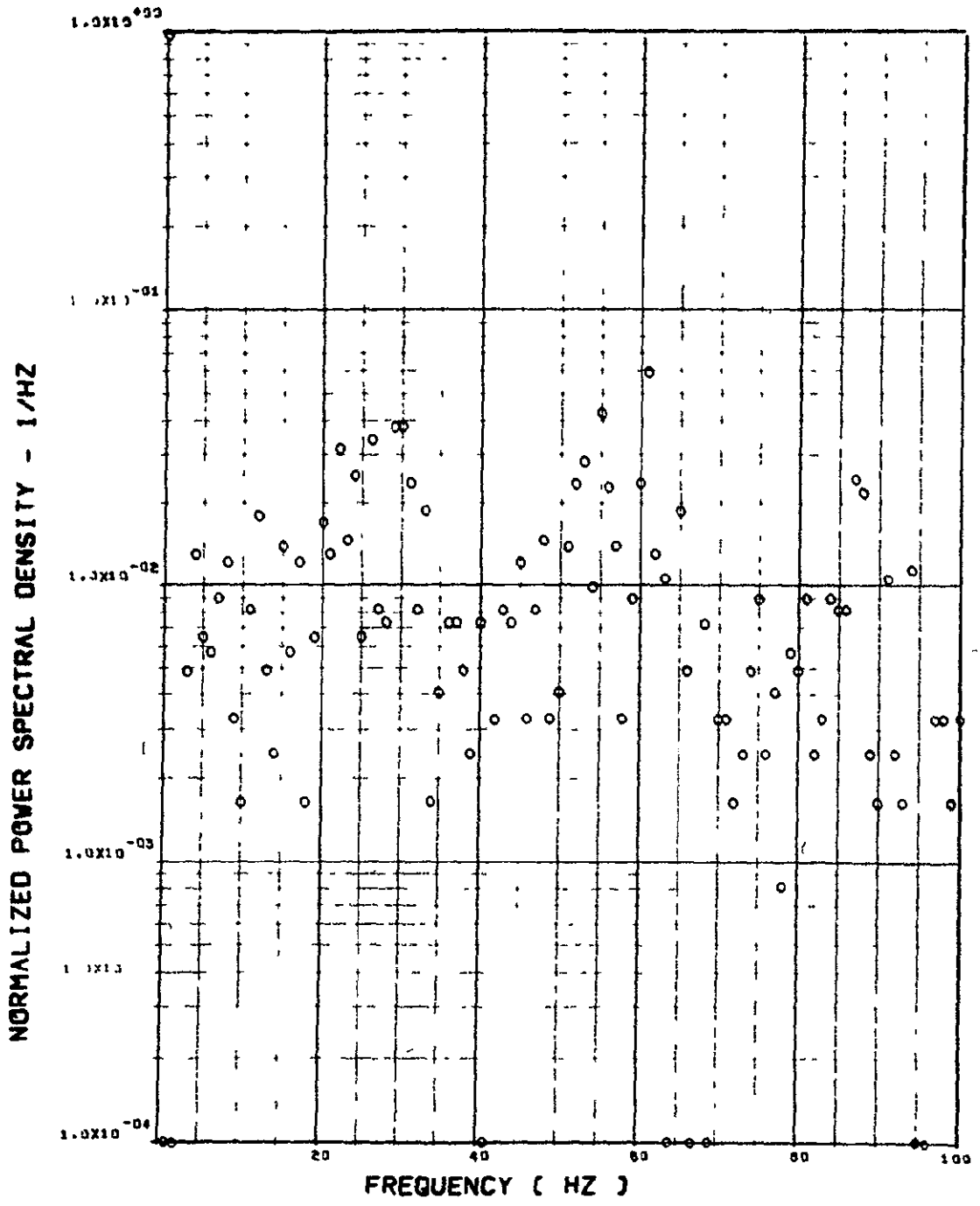

Figure 11. Continued

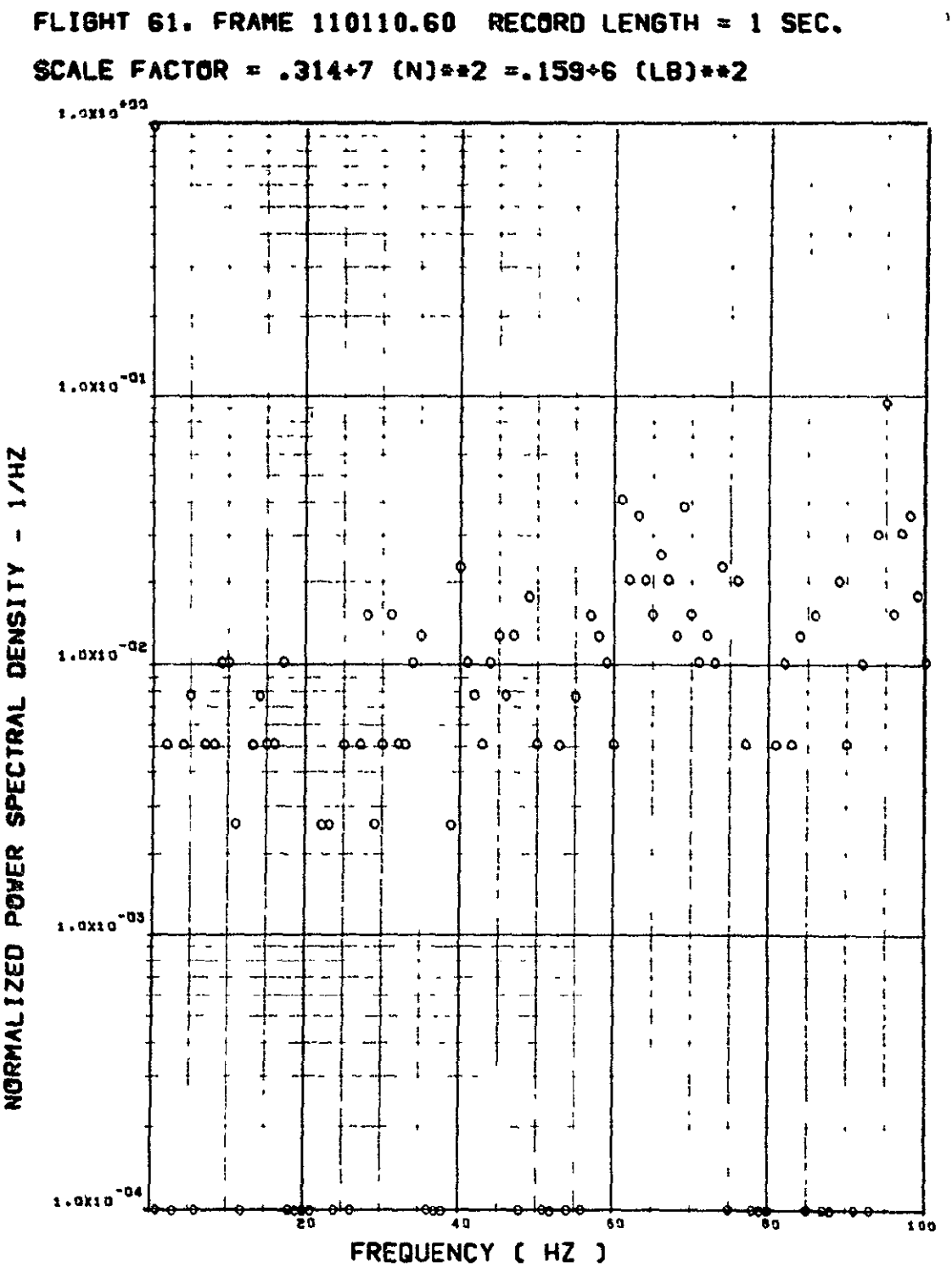

Figure 11. Continued

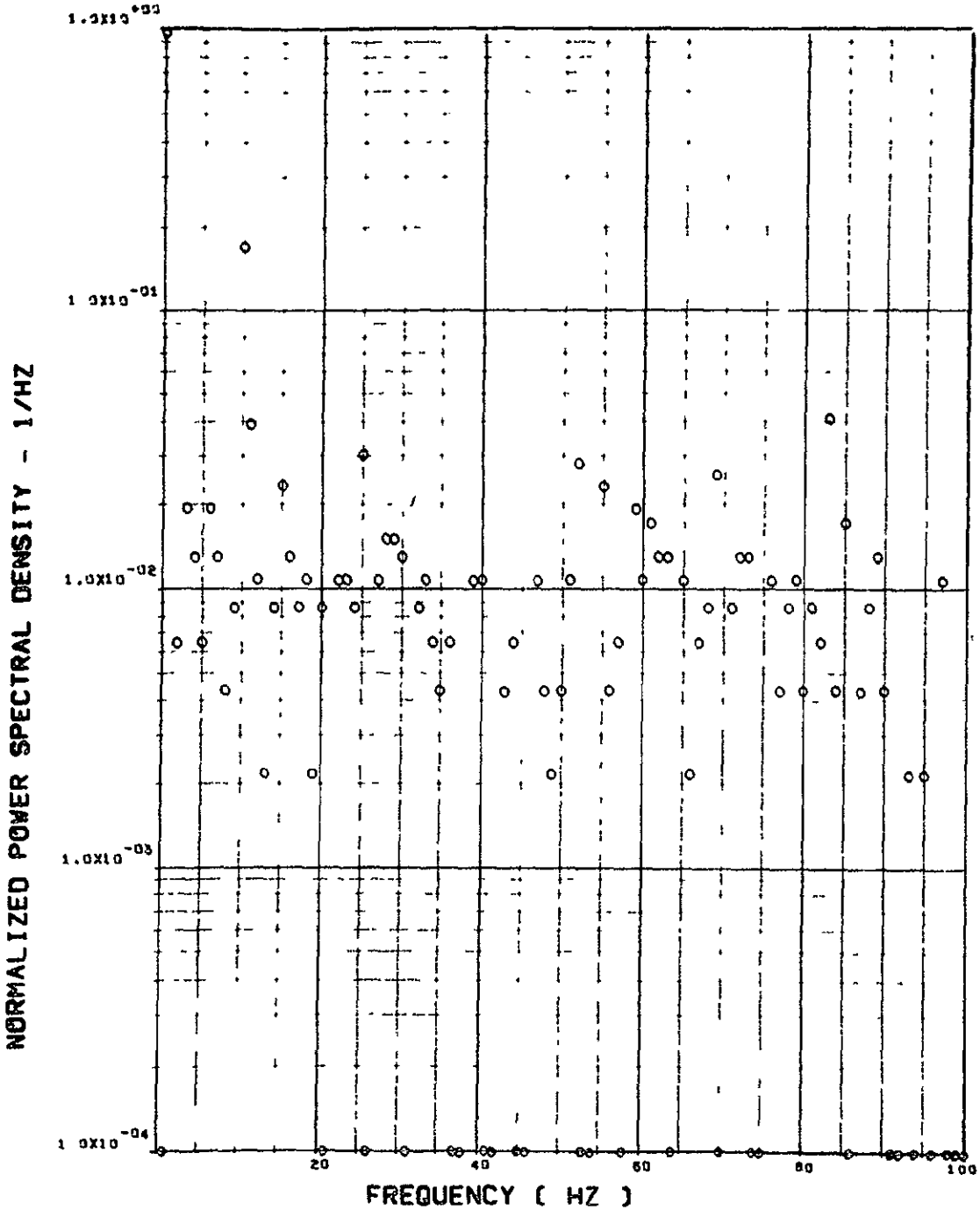

Figure 11. Continued

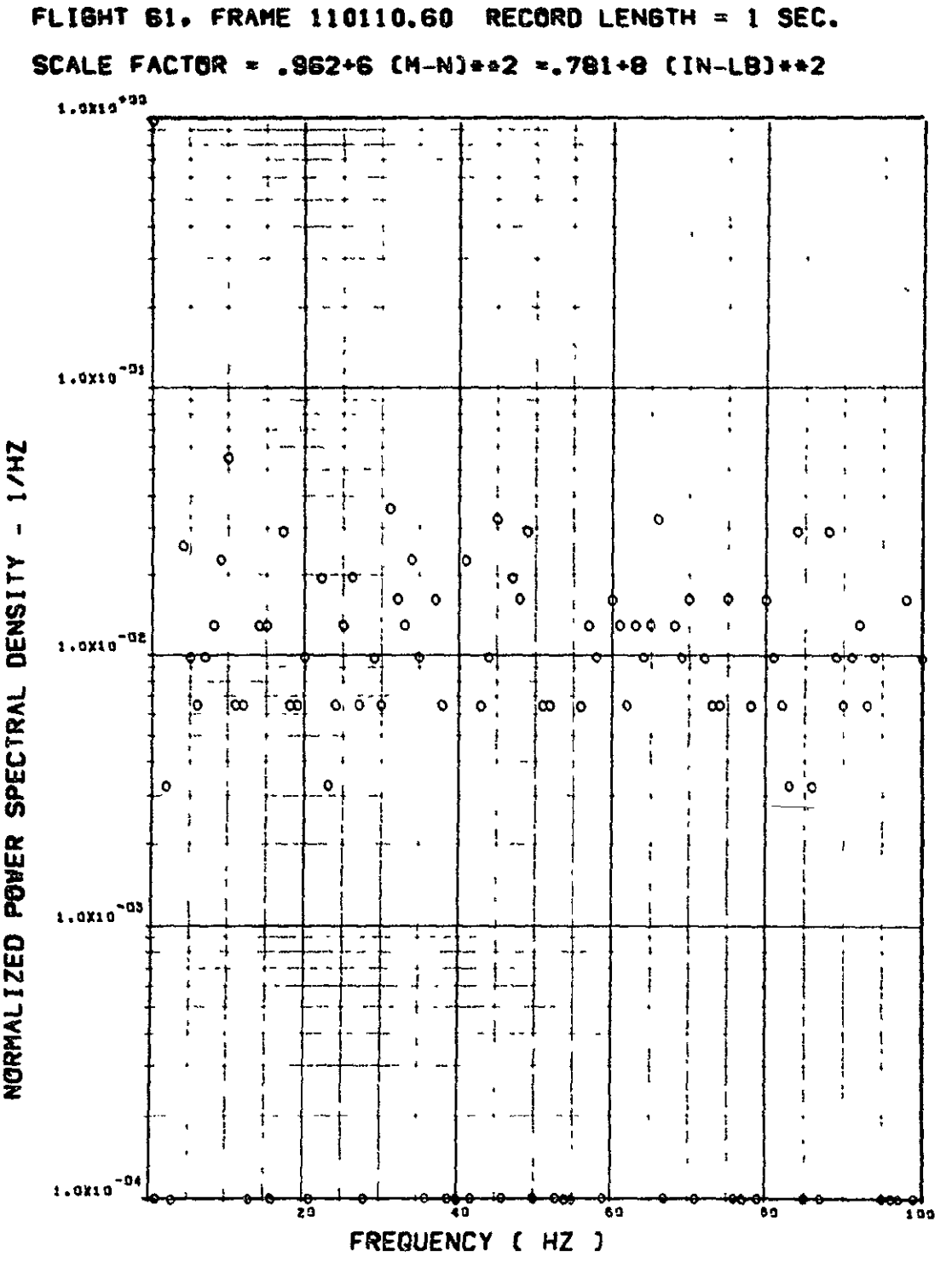

Figure 11. Continued

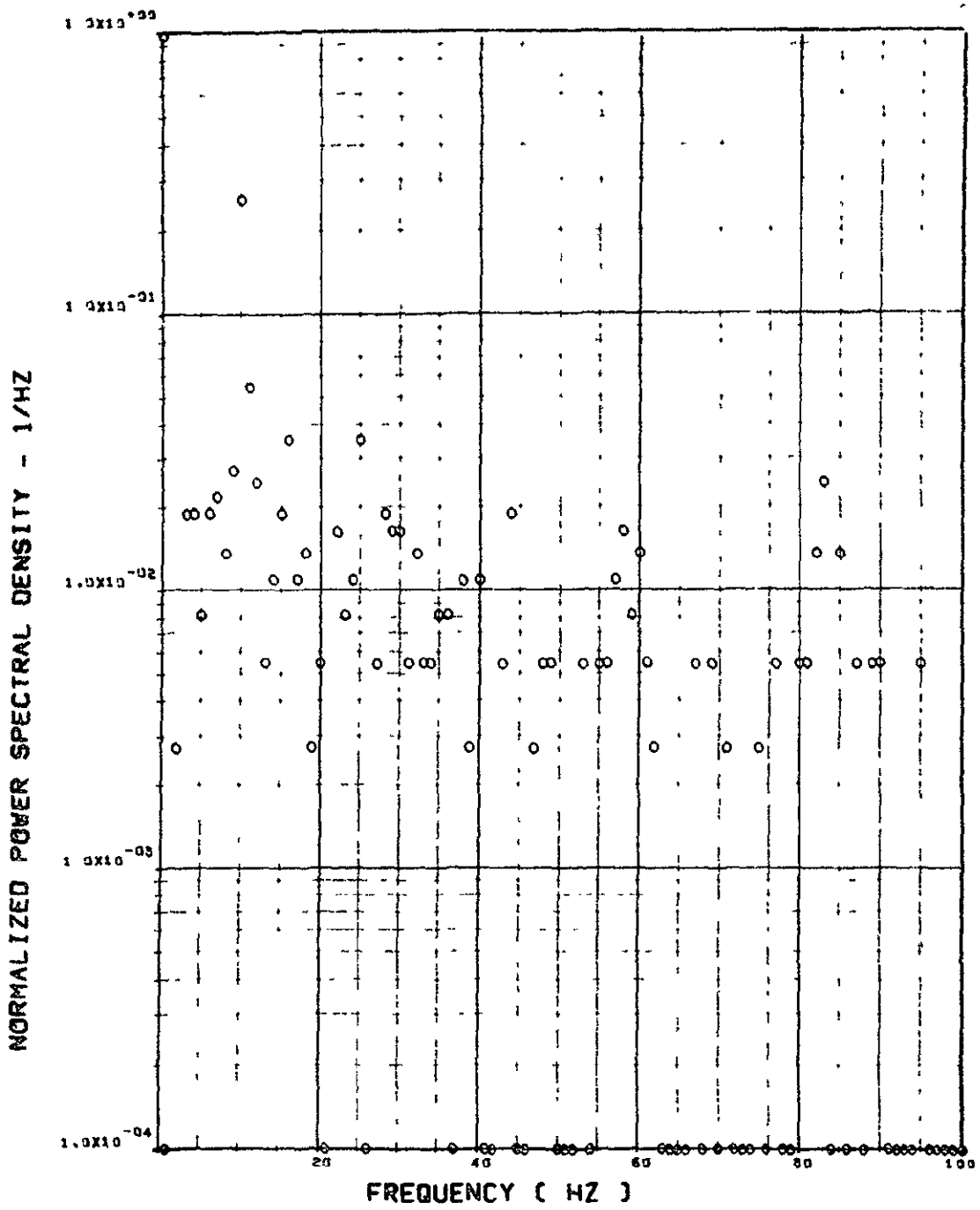

Figure 11. Continued

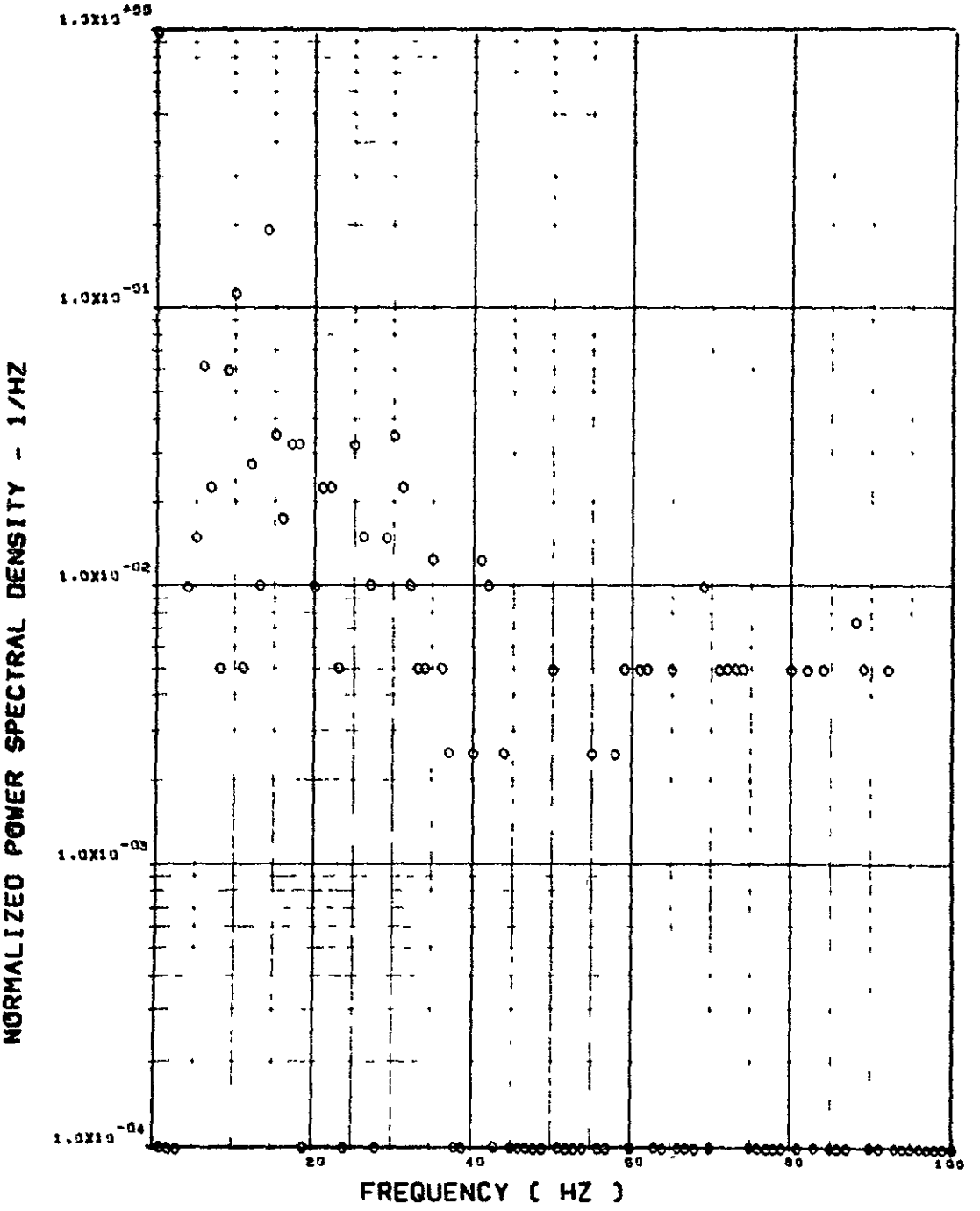

Figure 11. Continued

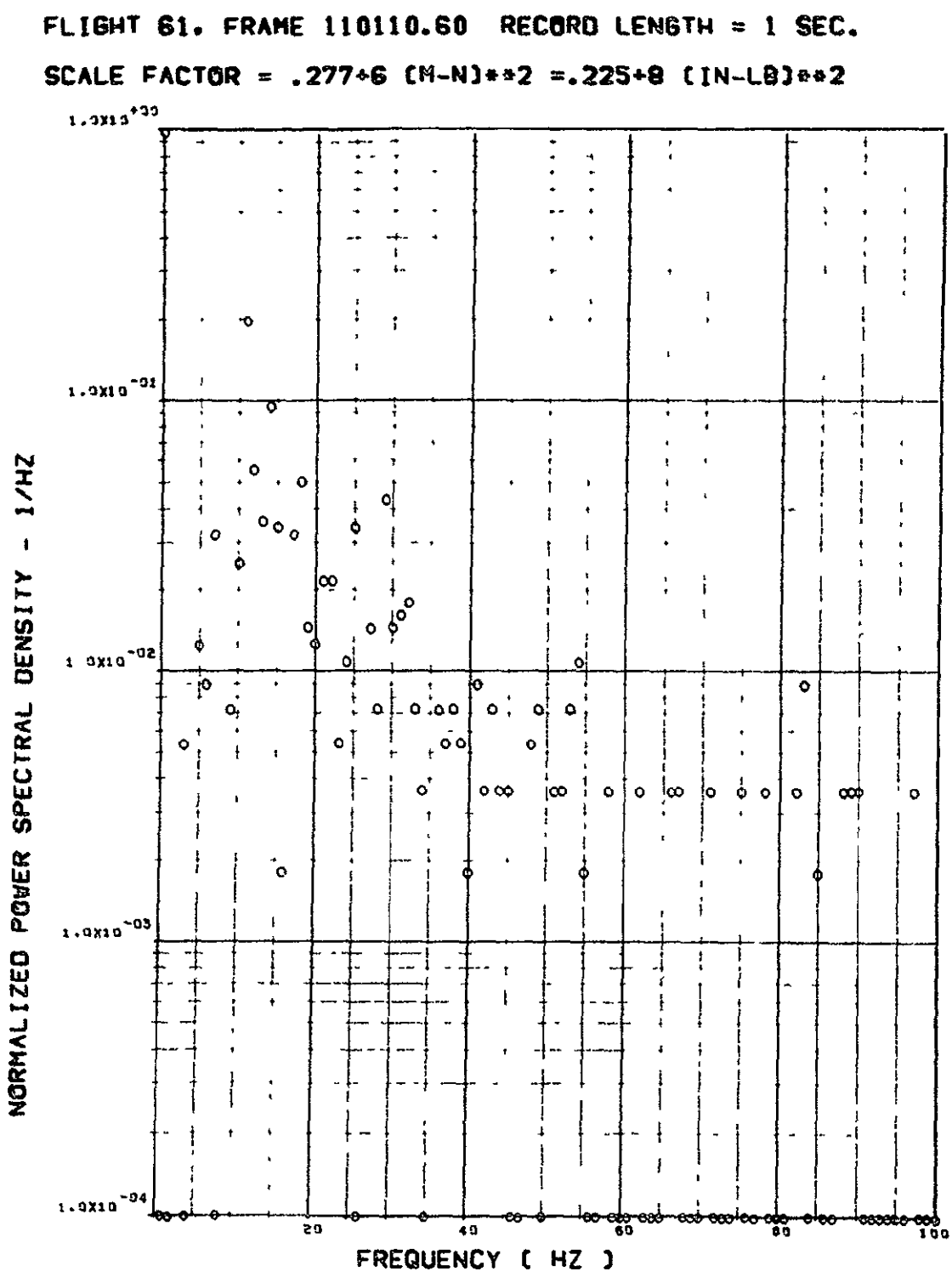

Figure 11. Concluded

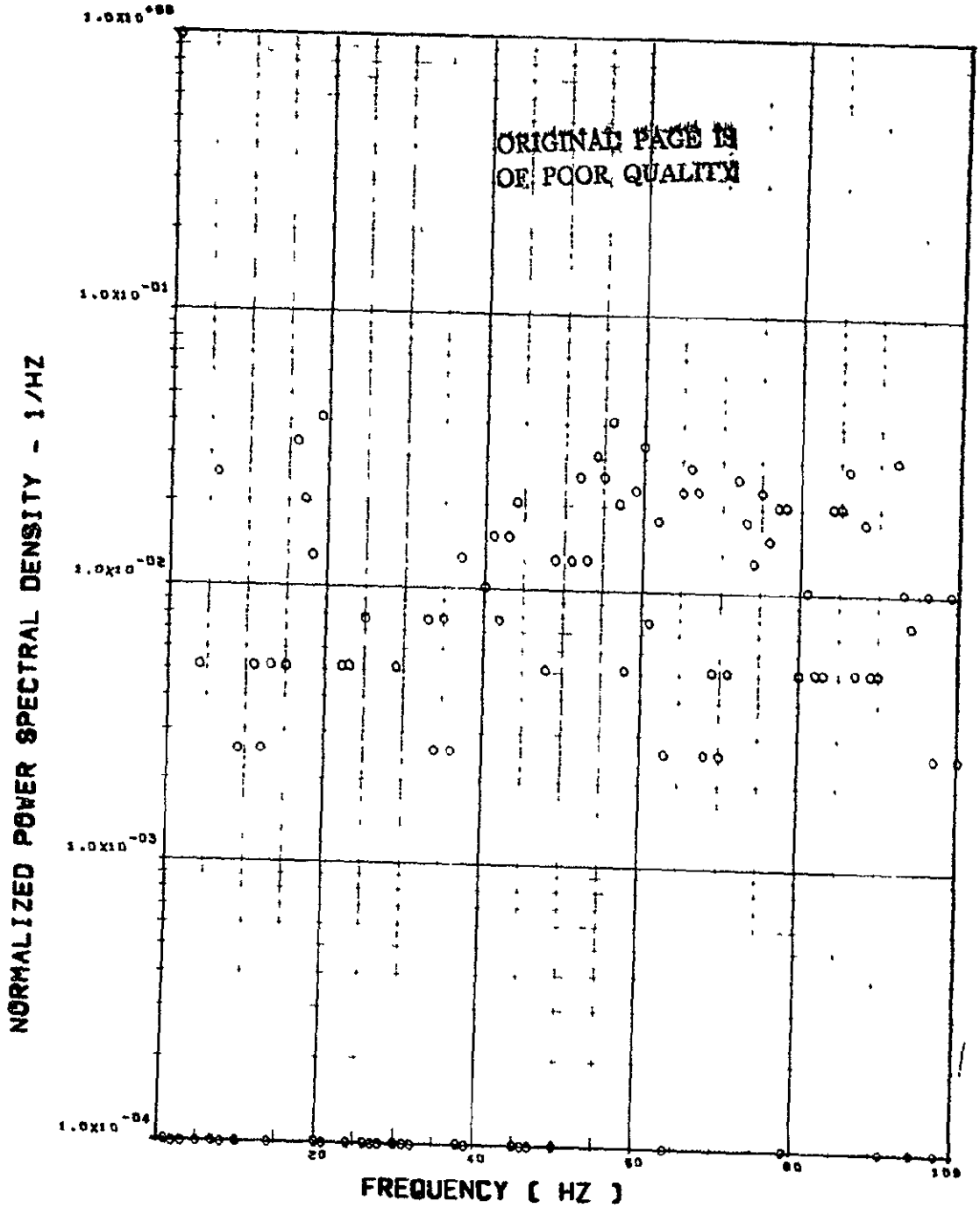

Figure 12. Power Spectra - Flight 61, Run 227, Point 5, T_1 = 110112.0, ΔT = 1 Sec, α_{Nom} = 13.75 deg, $\Delta\alpha$ = 1.70 deg.

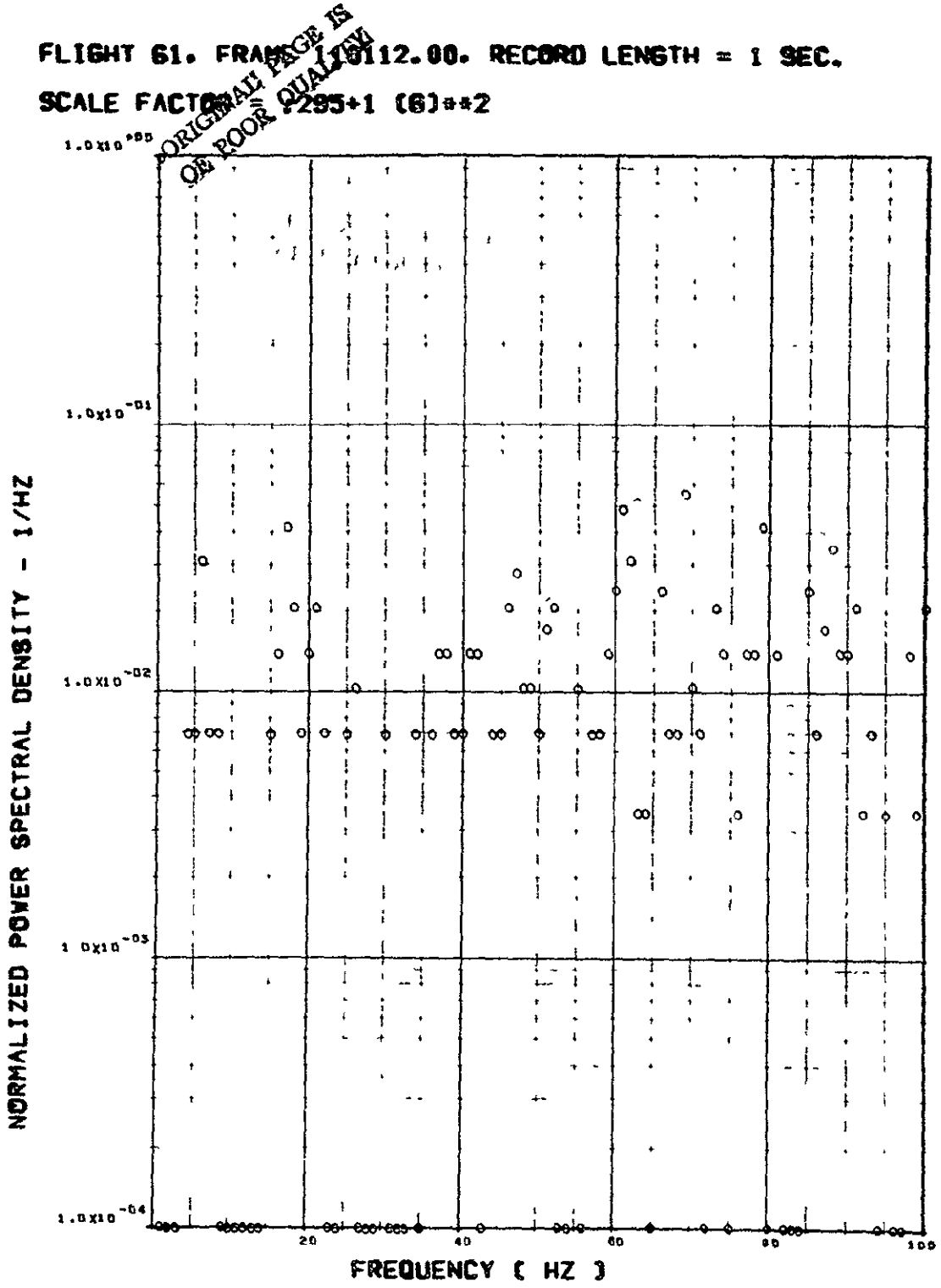

Figure 12. Continued

FLIGHT 61. FRAME 110112.00. RECORD LENGTH = 1 SEC.

SCALE FACTOR = .630-1 (G)**2

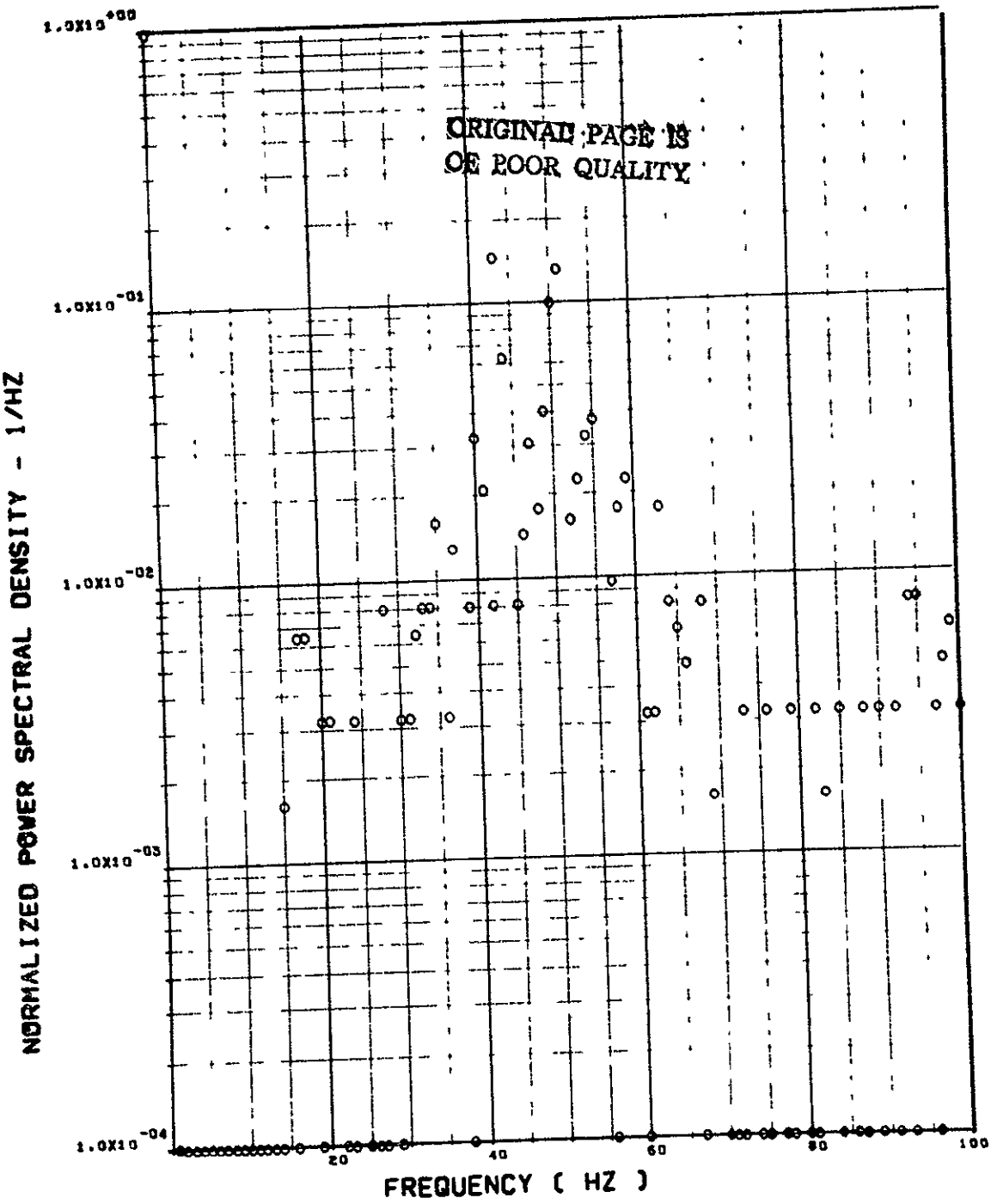

ITEM - AB018 C.G. VERTICAL ACCELEROMETER

Figure 12. Continued

FLIGHT 61. FRAME 110112.00. RECORD LENGTH = 1 SEC.

SCALE FACTOR = .613-1 (6)**2

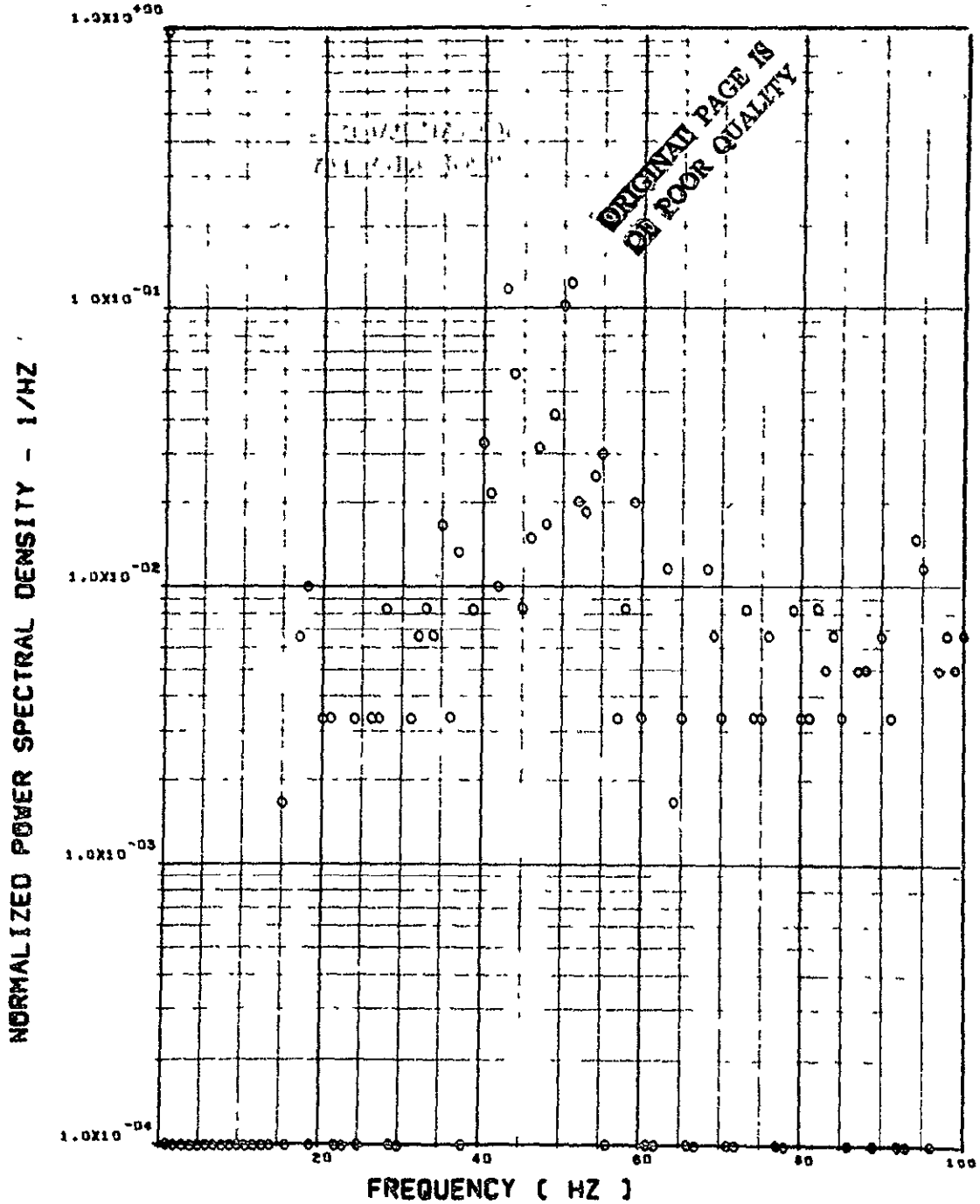

ITEM - AB019 C.G. VERTICAL ACCELEROMETER

Figure 12. Continued

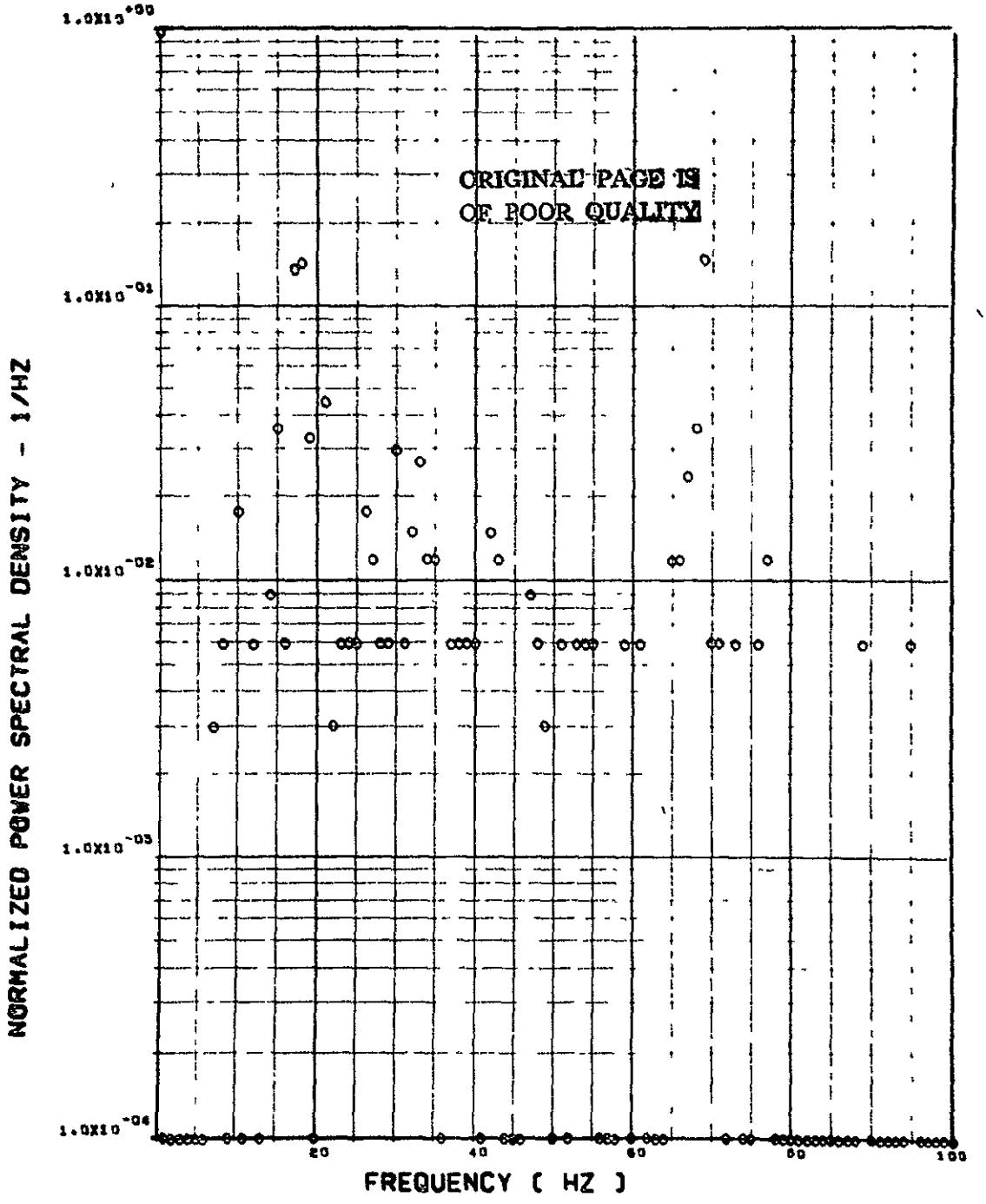

Figure 12. Continued

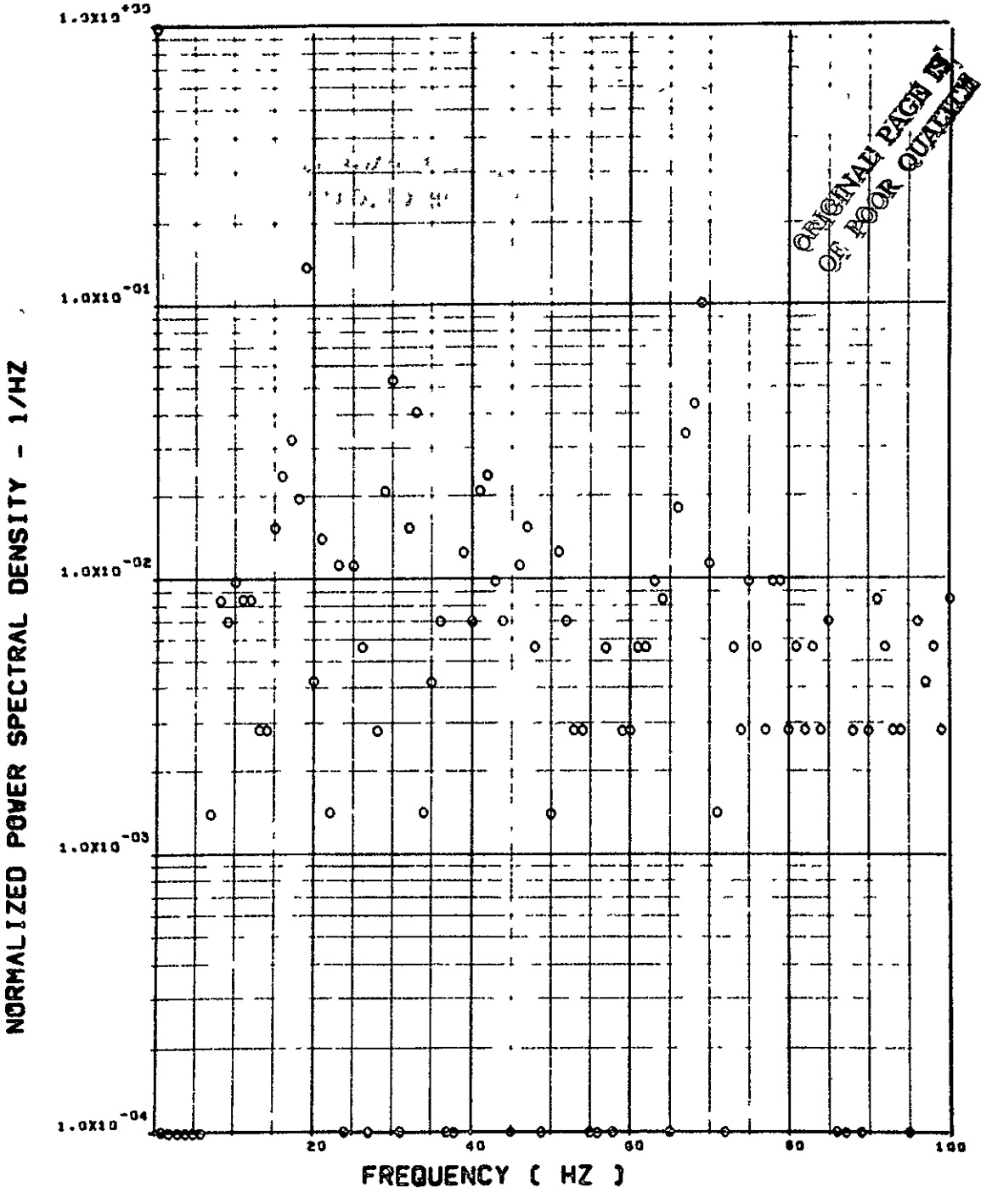

Figure 12. Continued

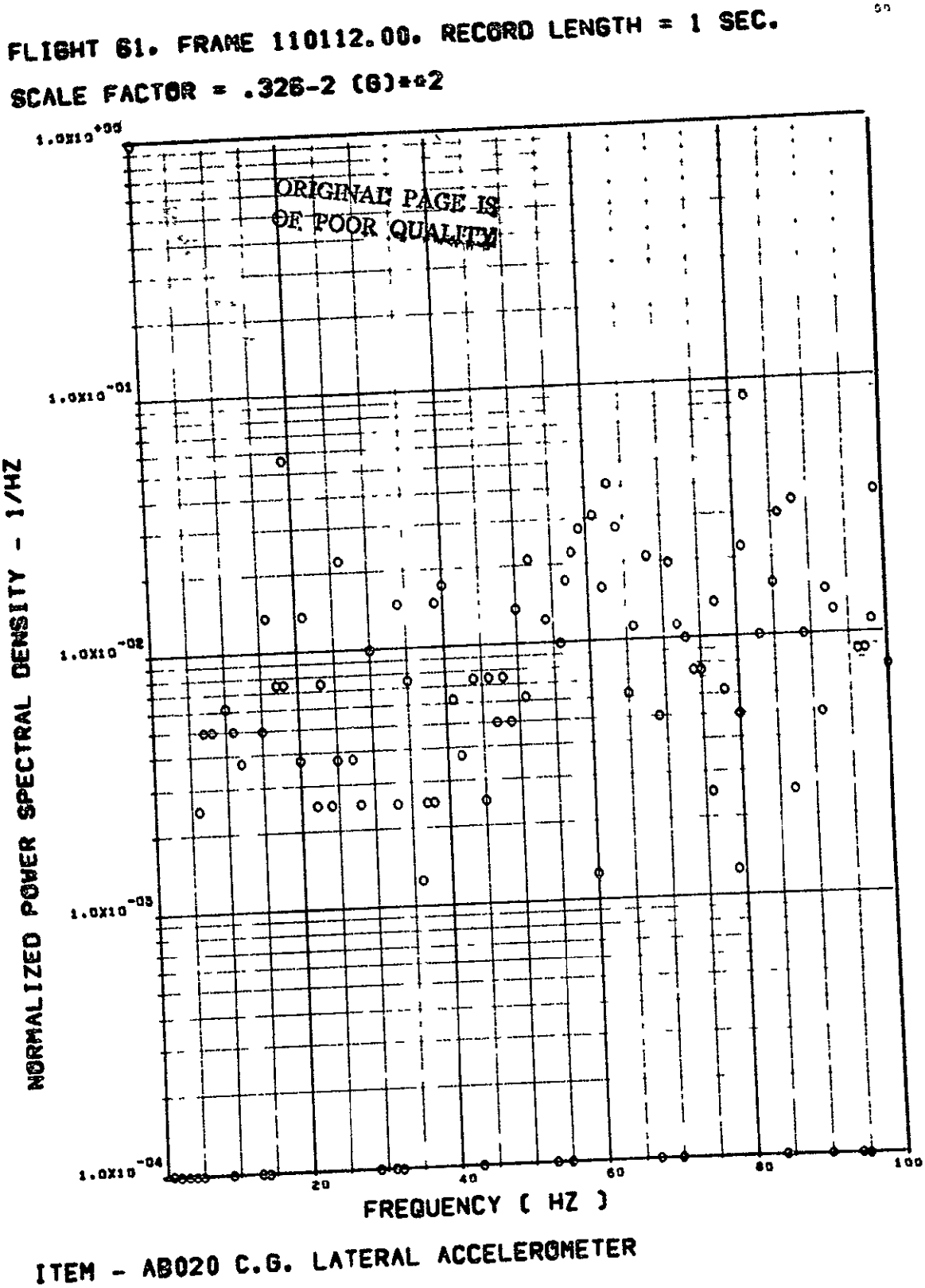

Figure 12. Continued

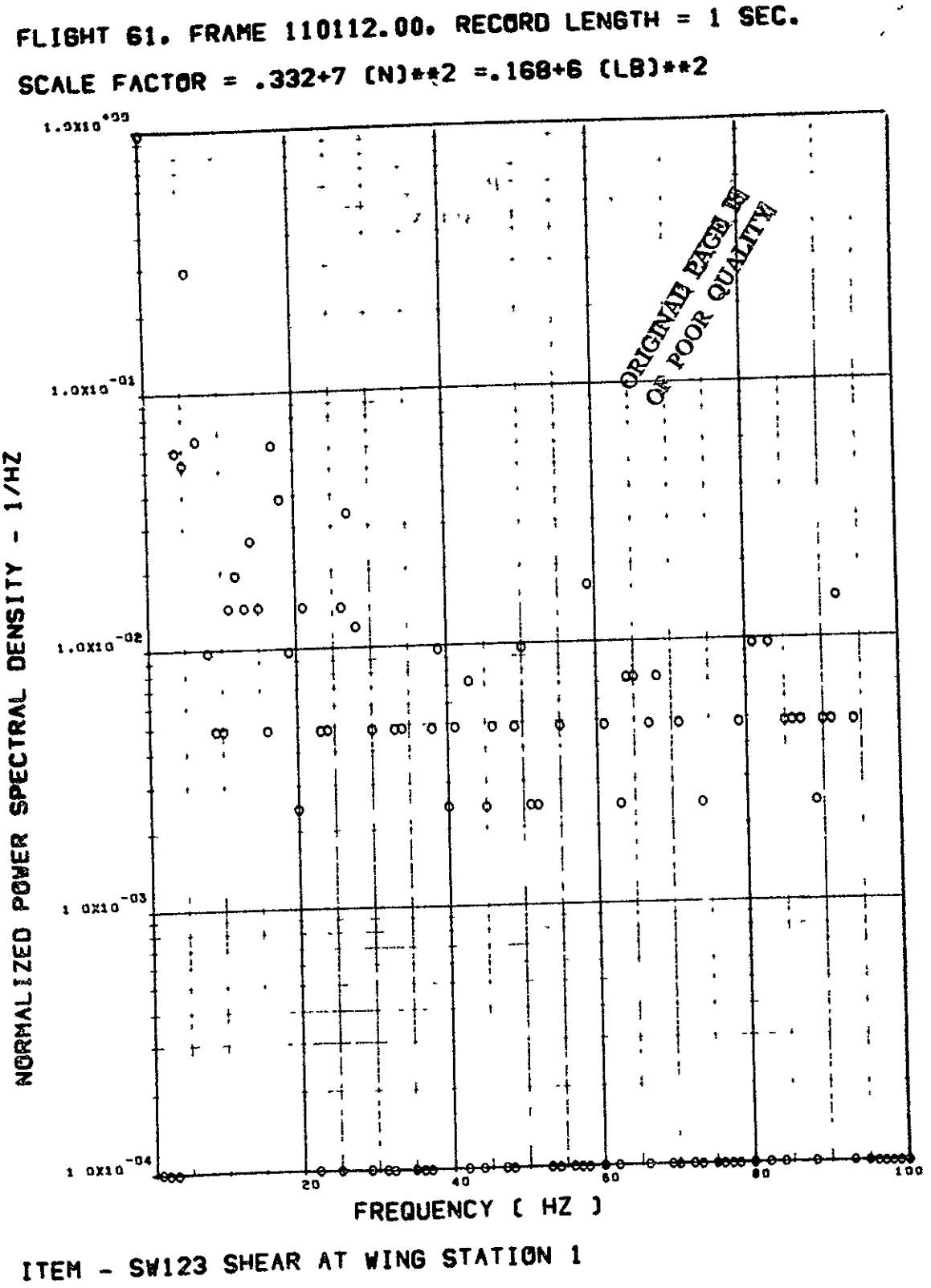

Figure 12. Continued

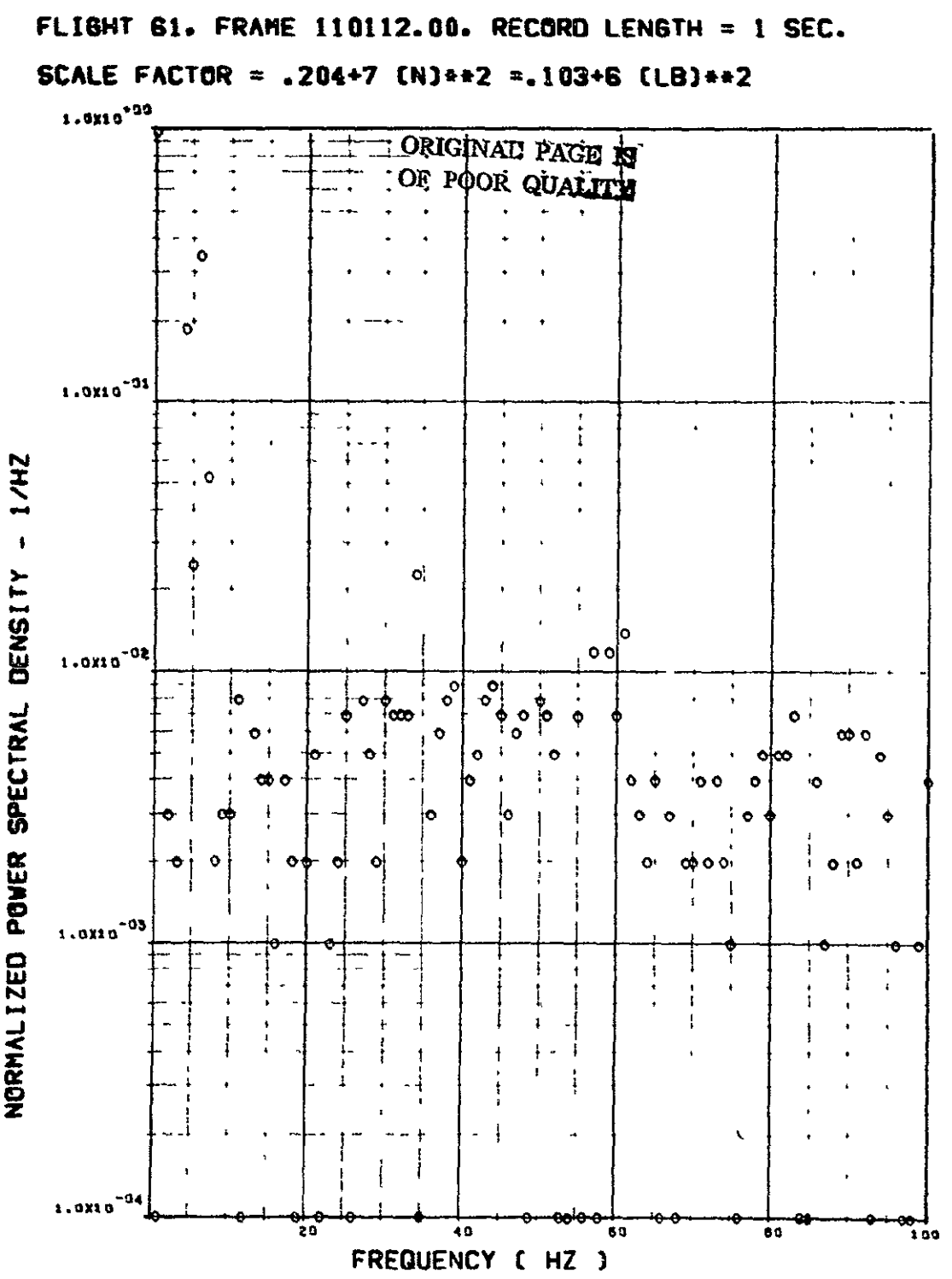

Figure 12. Continued

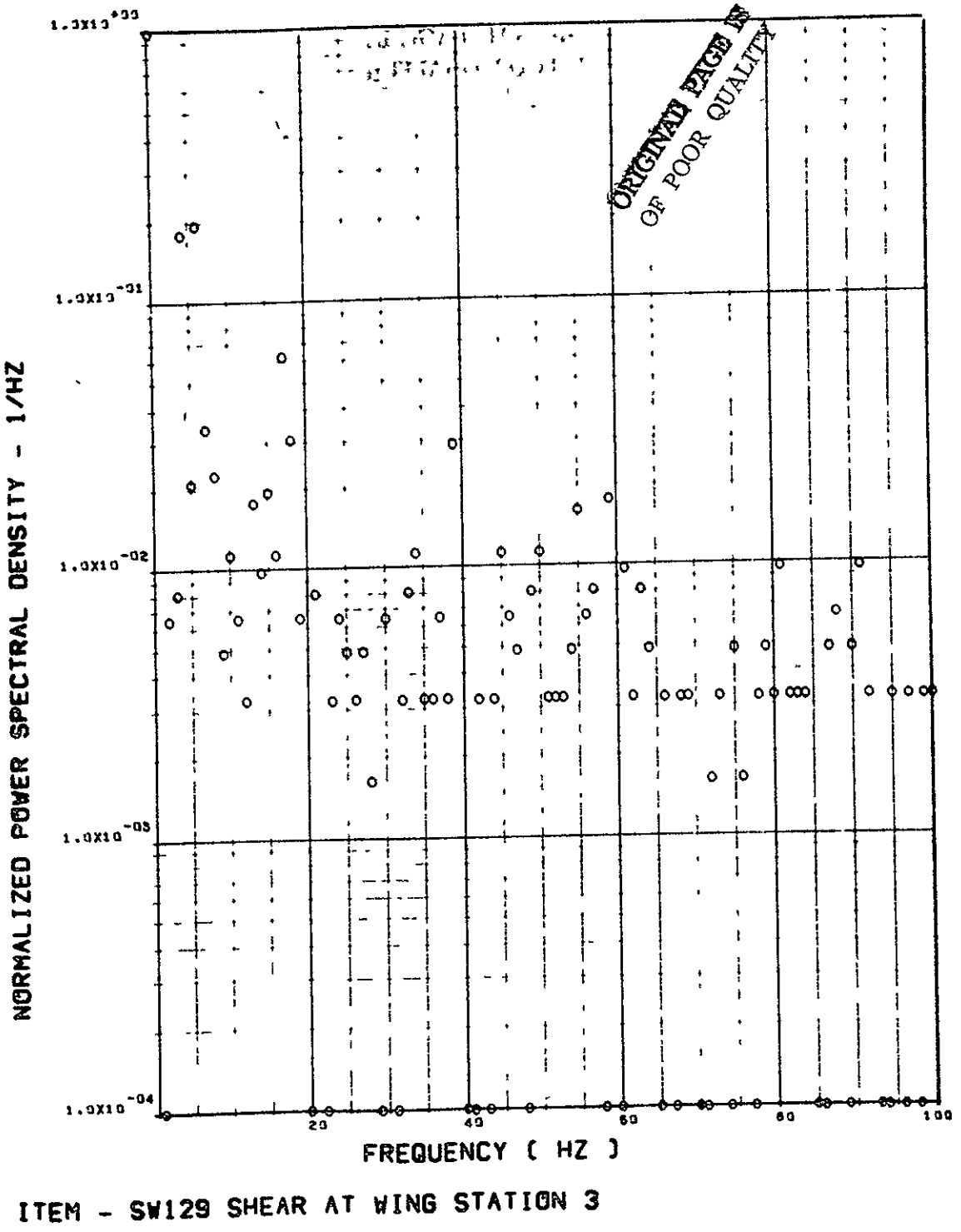

Figure 12. Continued

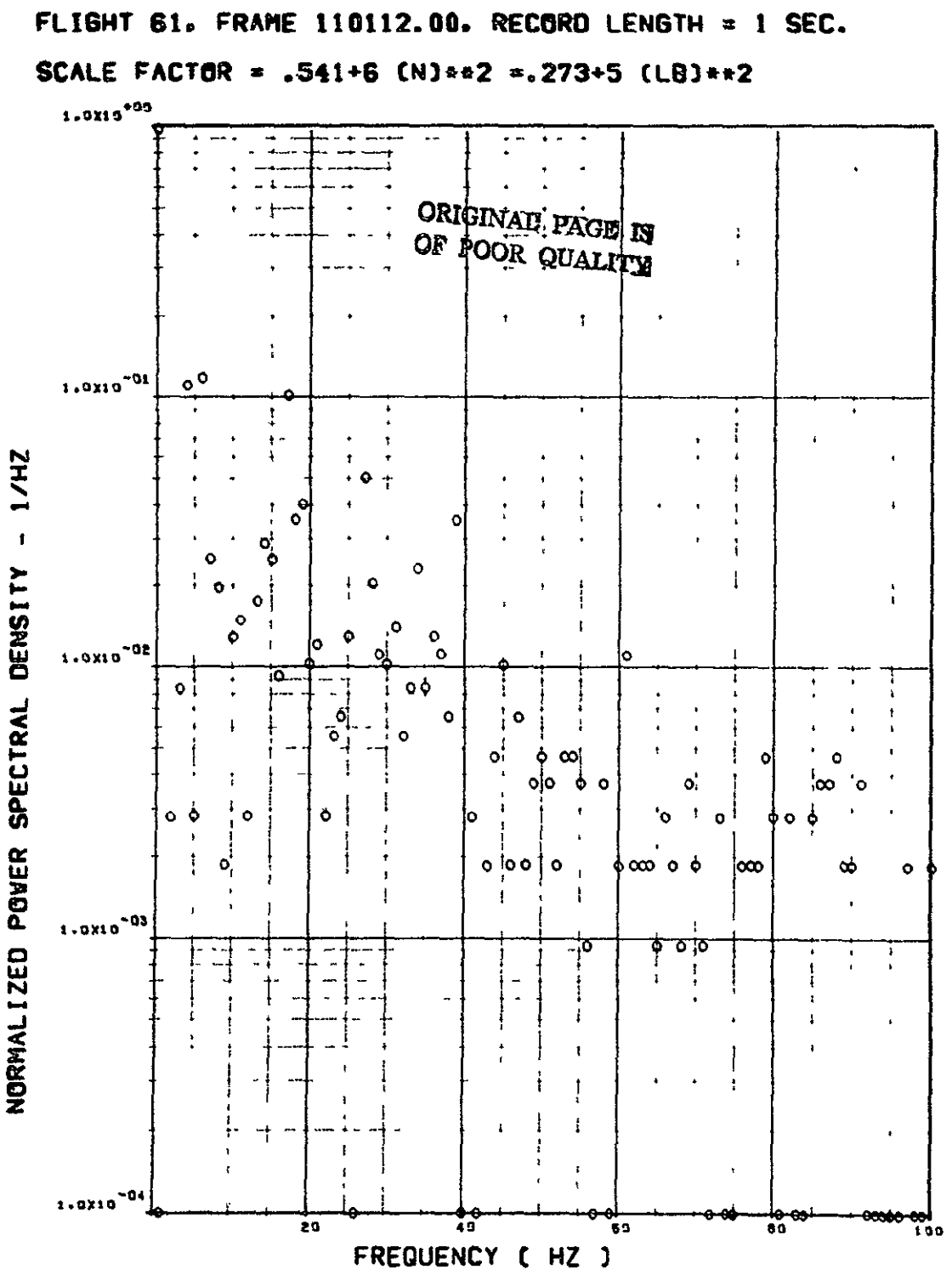

Figure 12. Continued

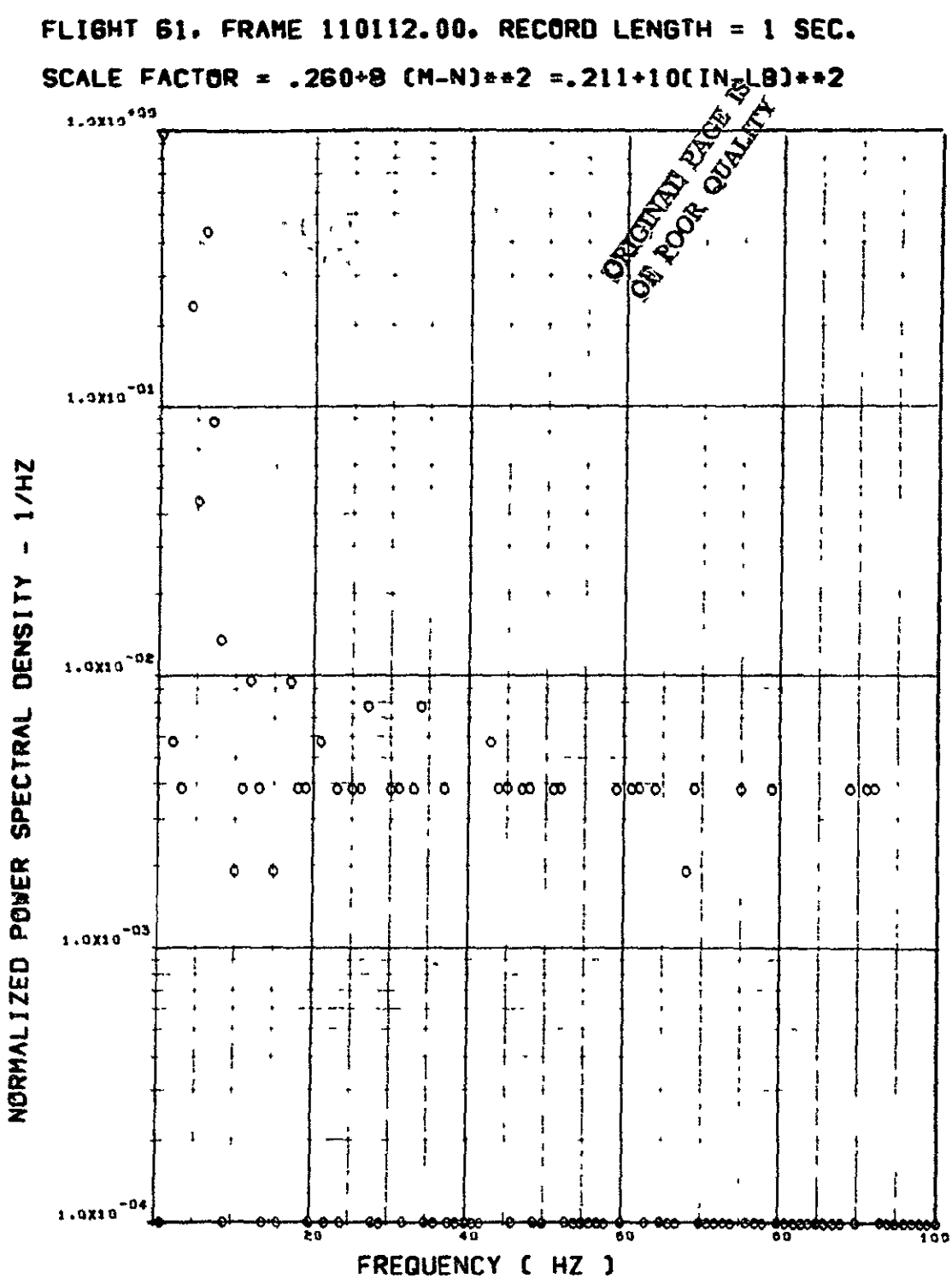

Figure 12. Continued

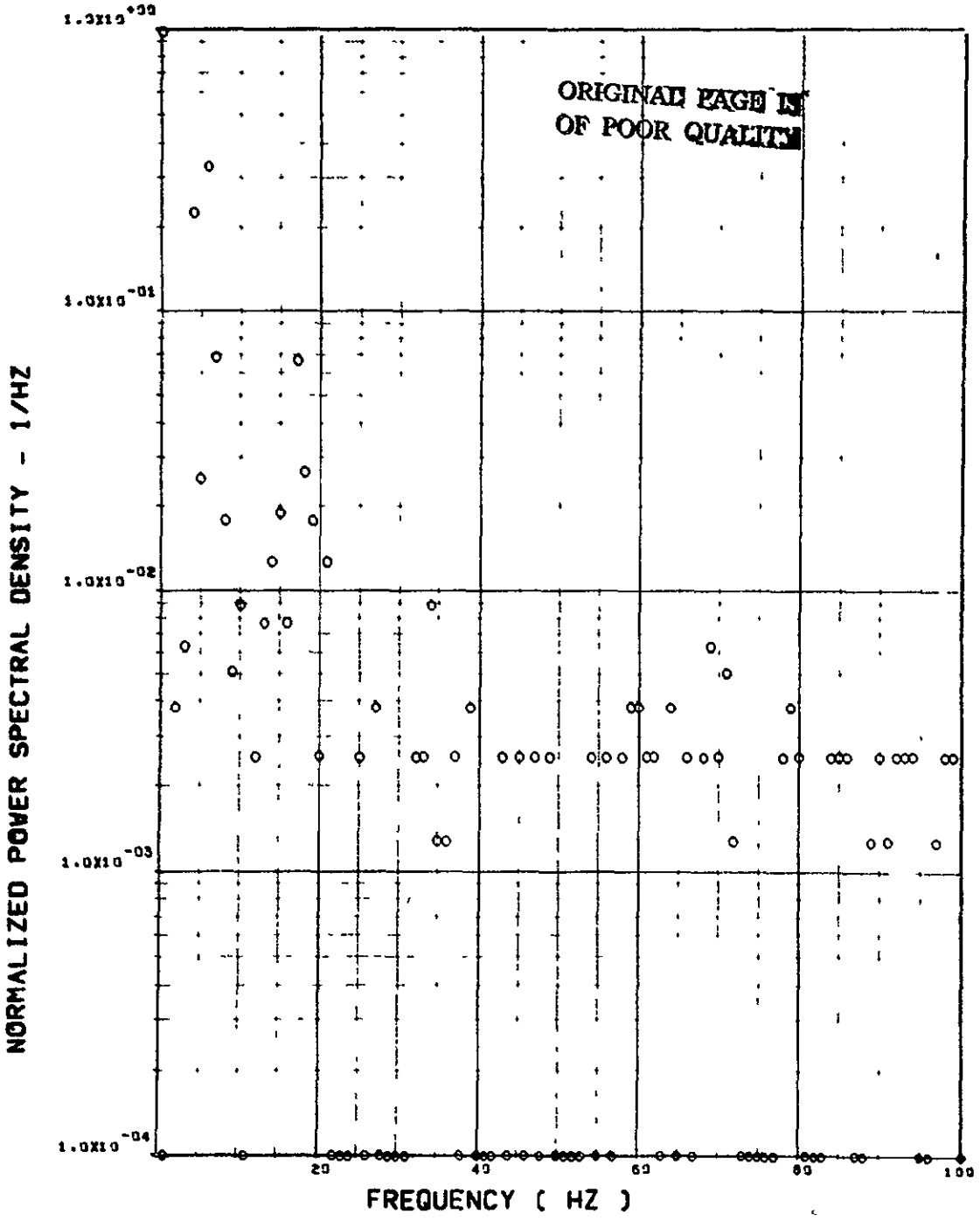

Figure 12. Continued

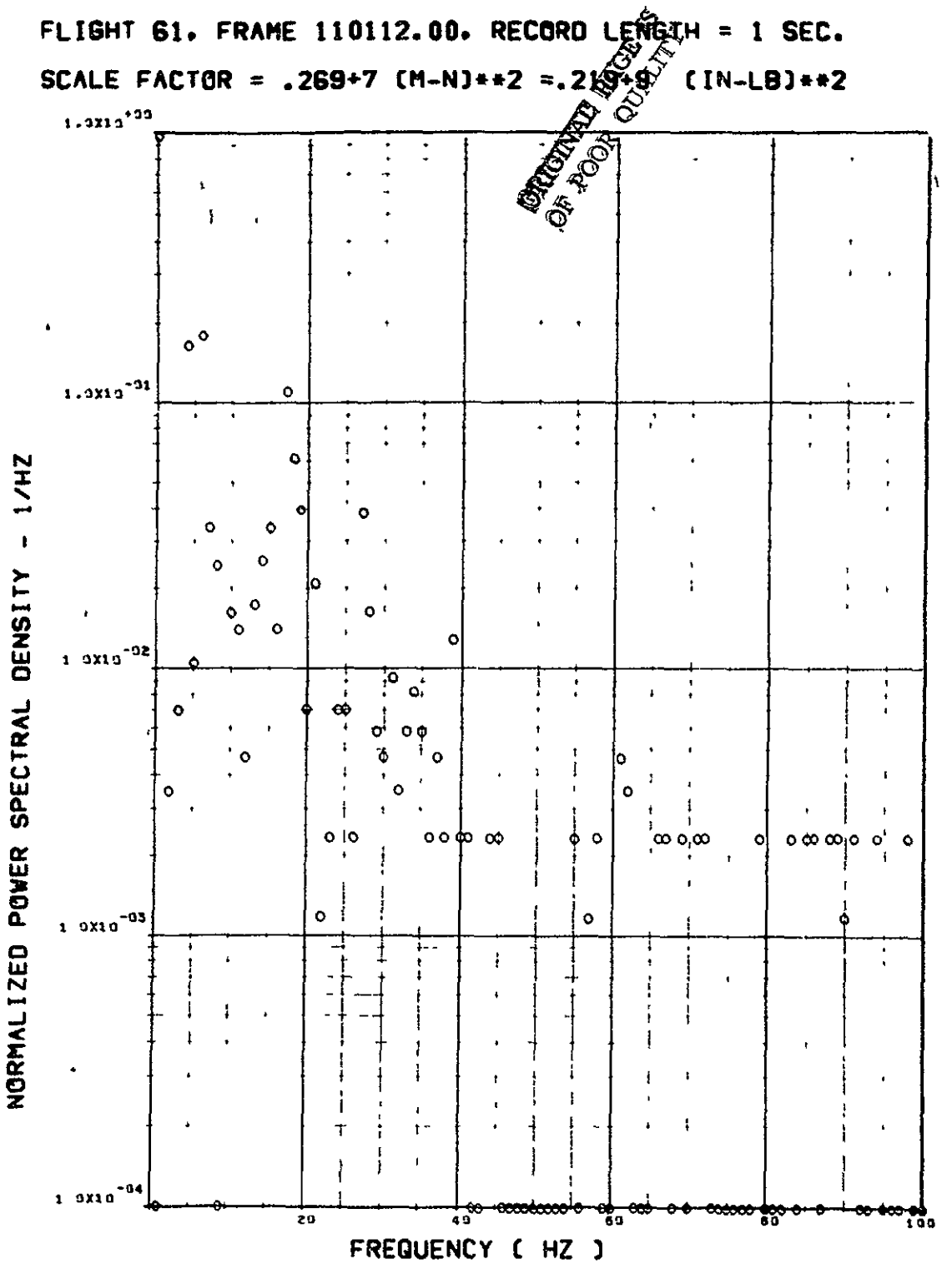

Figure 12. Continued

FLIGHT 61, FRAME 110112.00, RECORD LENGTH = 1 SEC.

SCALE FACTOR = .489+6 (M-N)**2 =.397+8 (IN-LB)**2

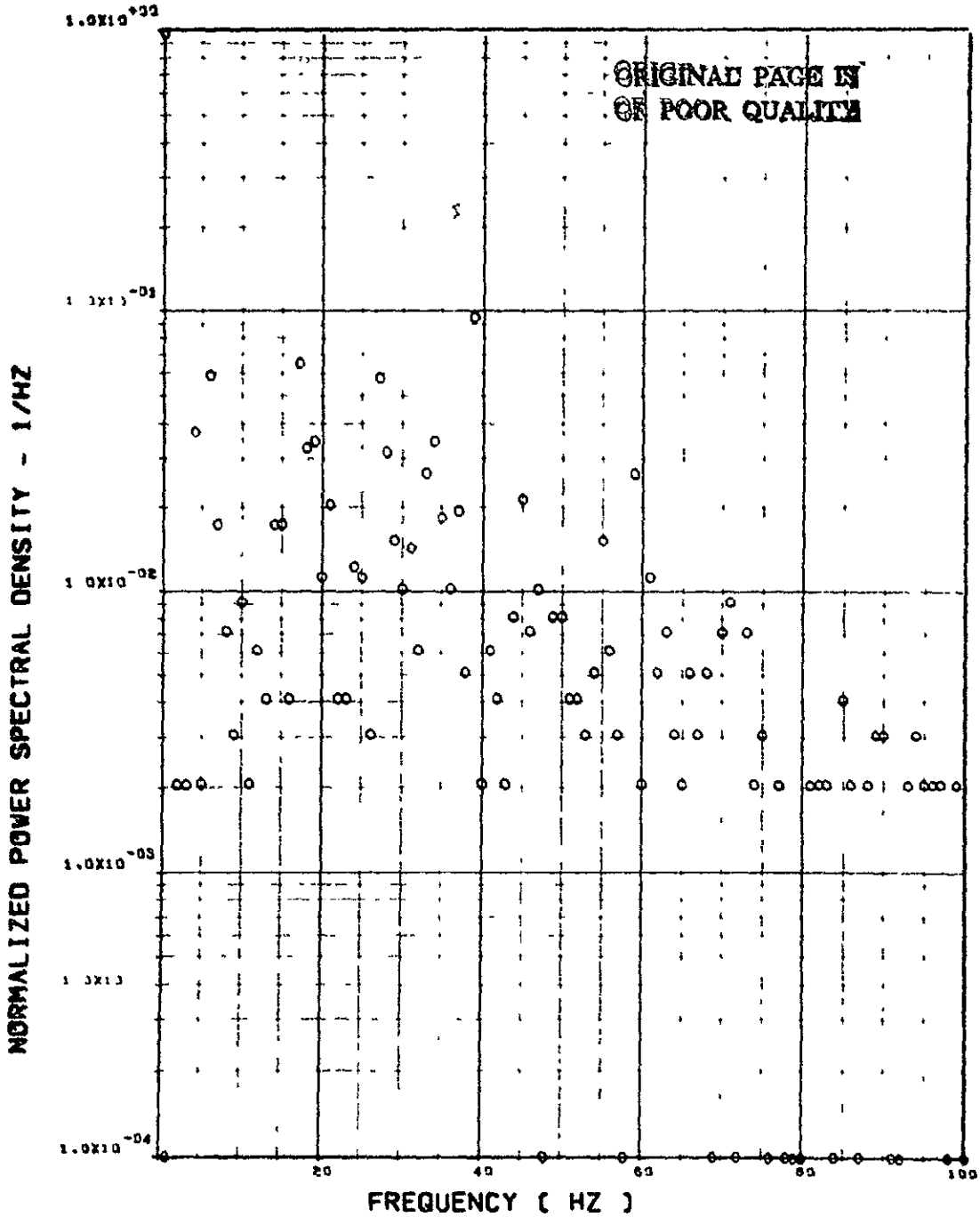

ITEM - SW133 BENDING MOMENT AT WING STATION 4

Figure 12. Continued

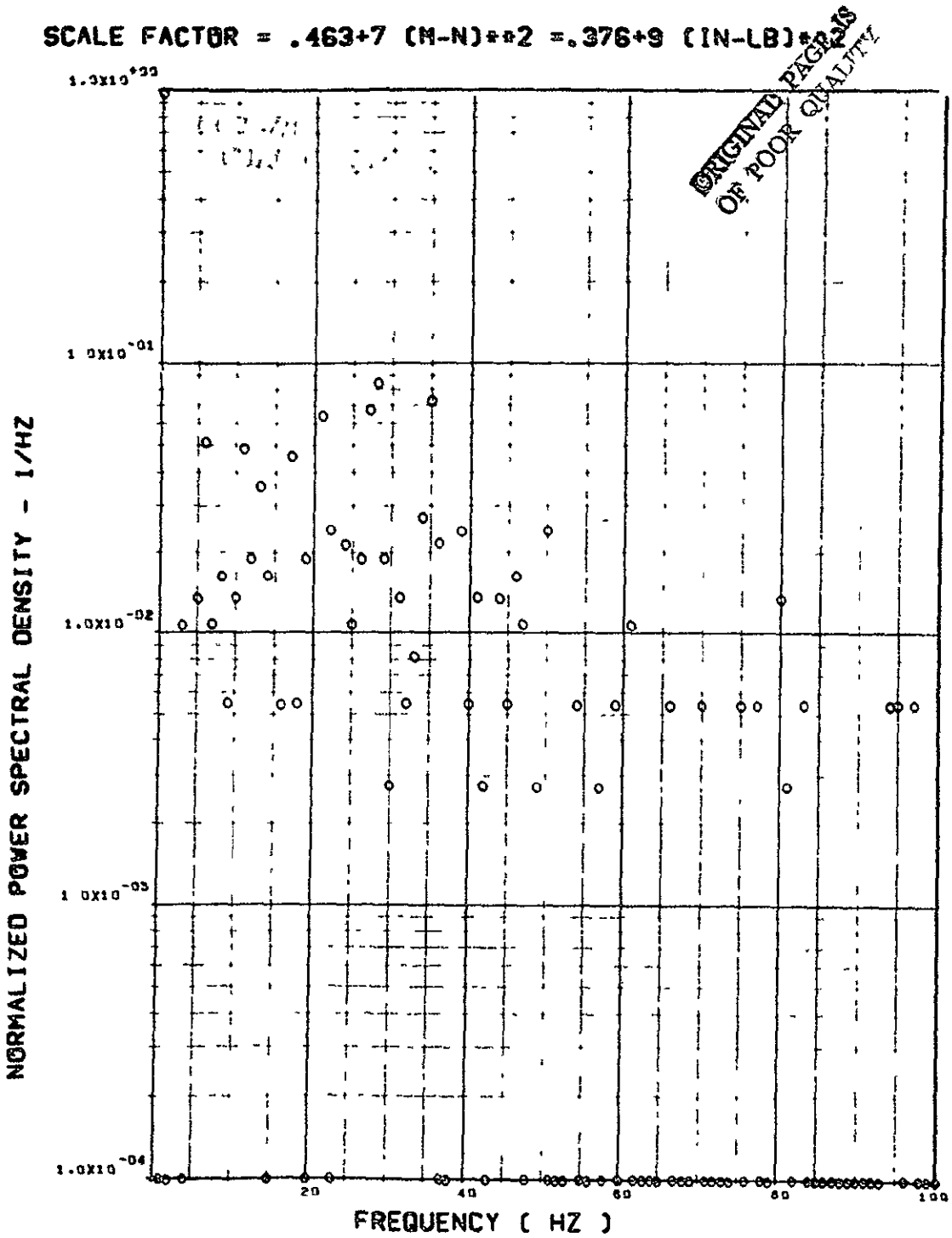

Figure 12. Continued

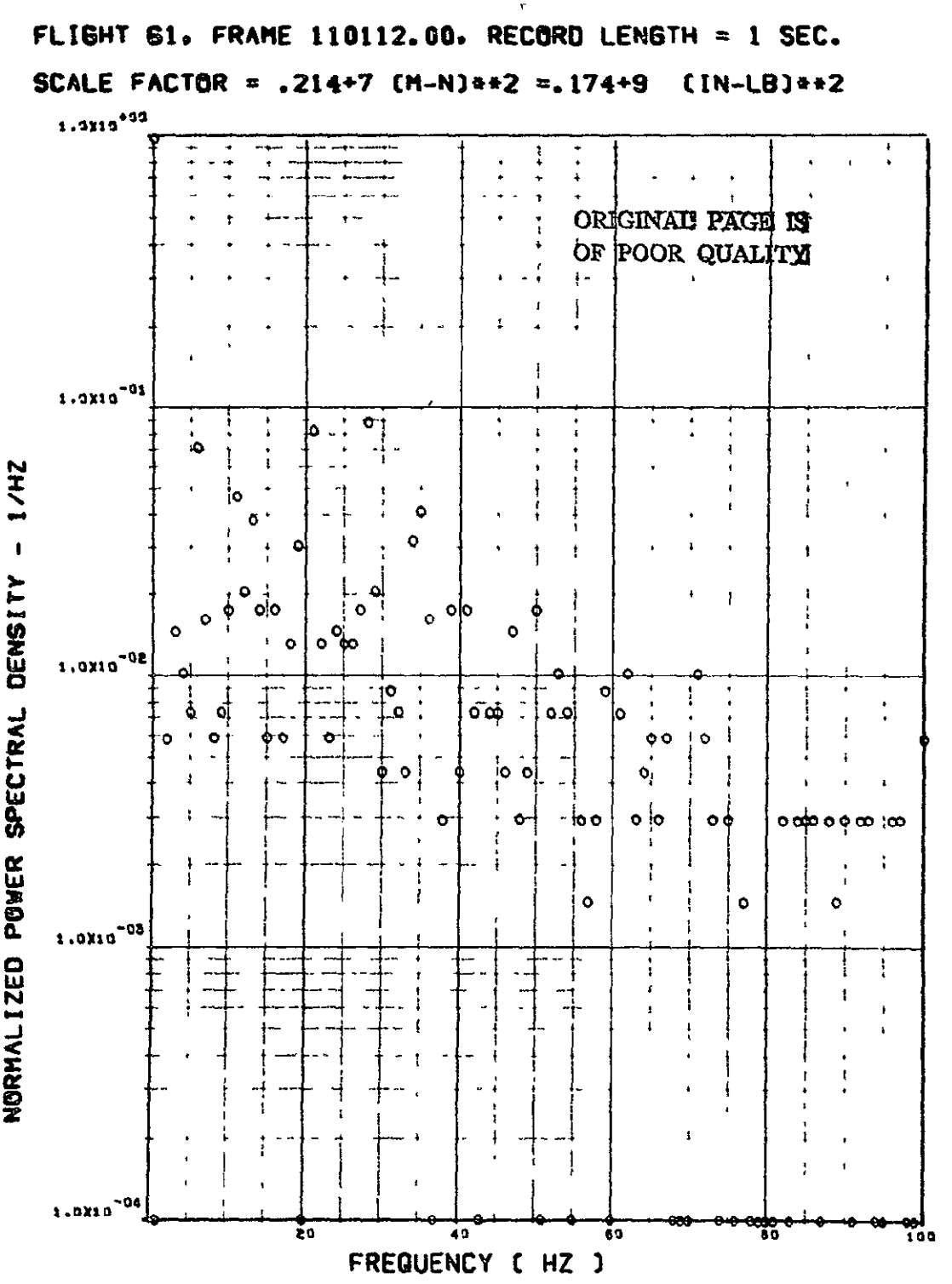

Figure 12. Continued

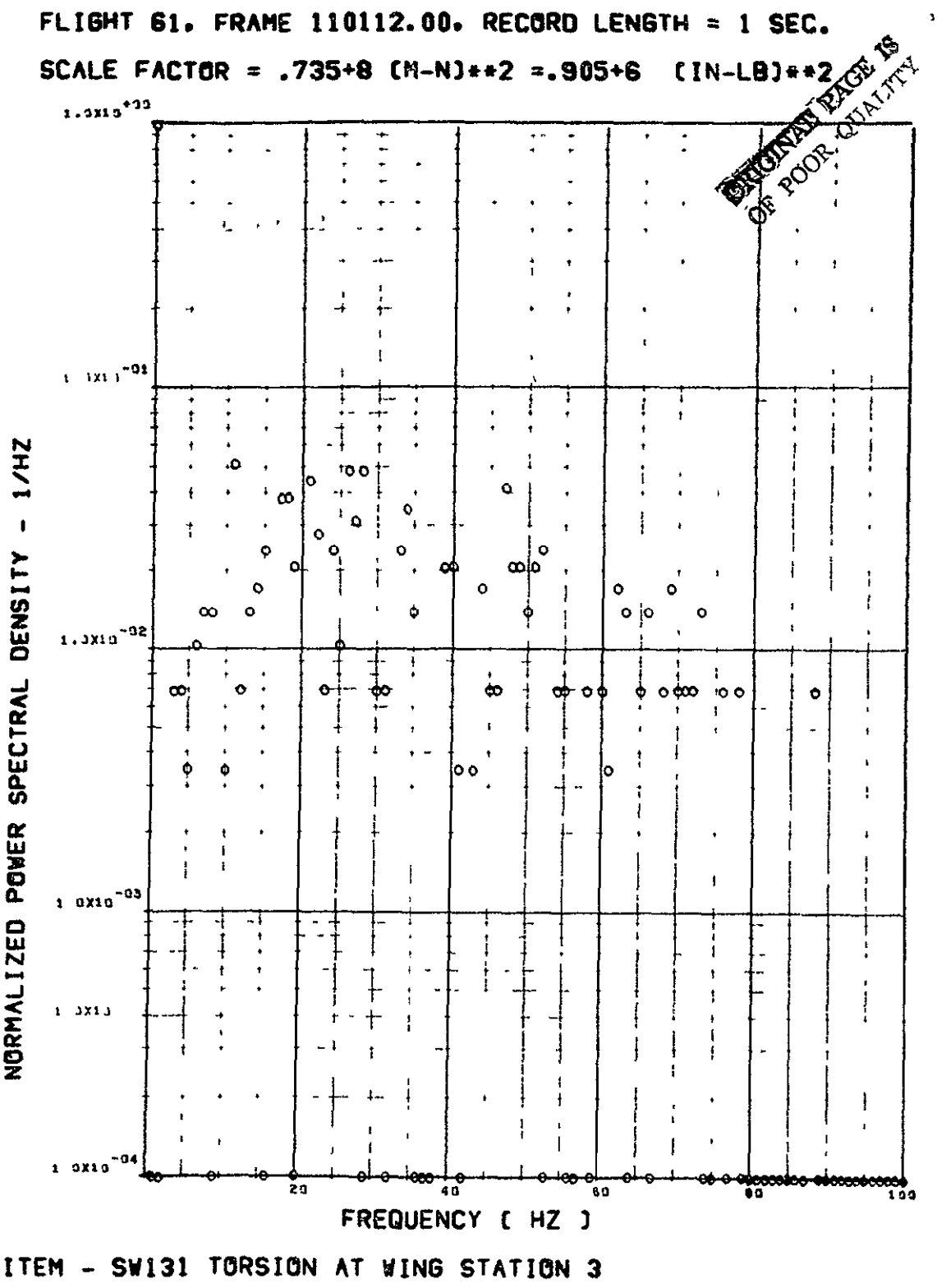

Figure 12. Continued

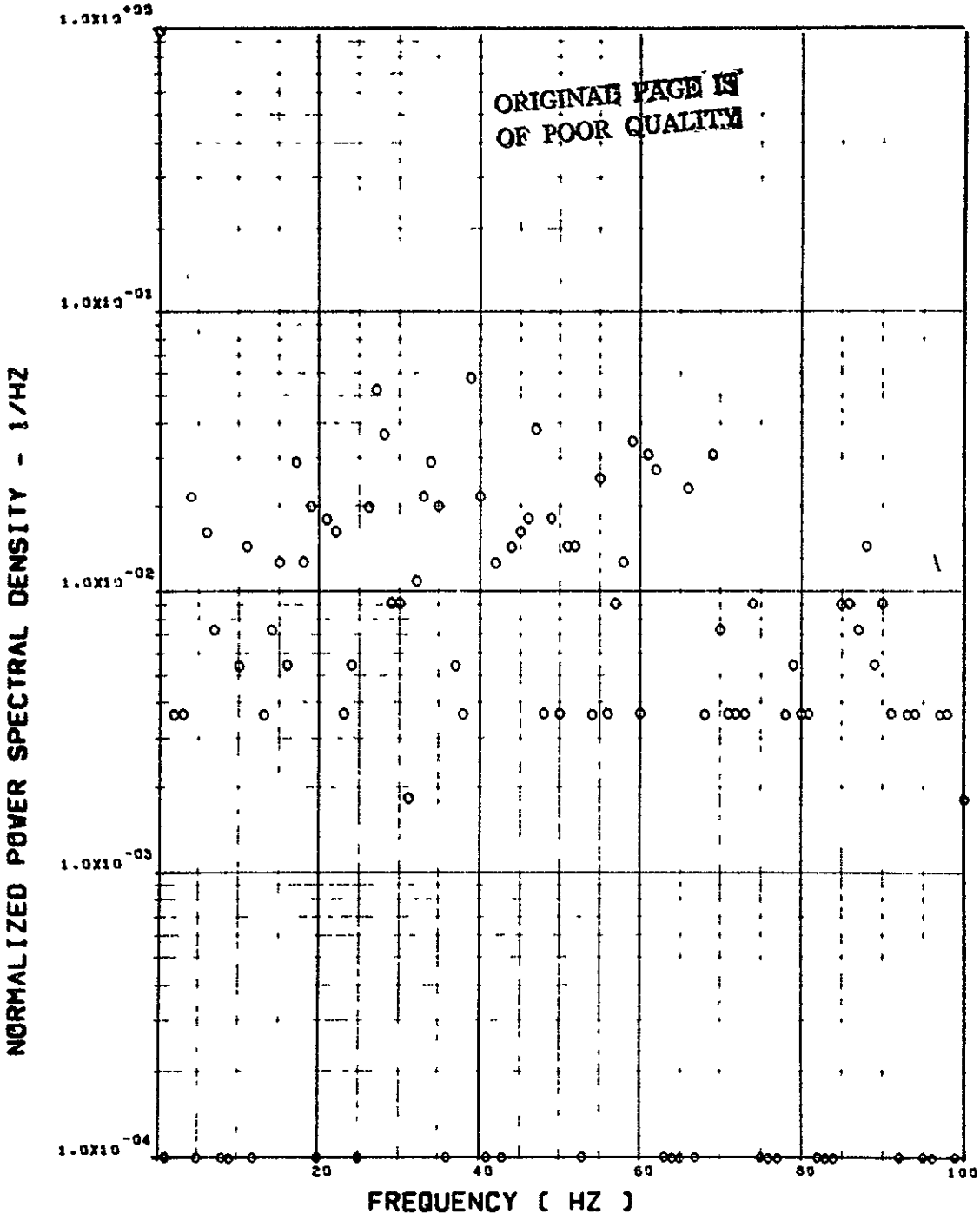

Figure 12. Continued

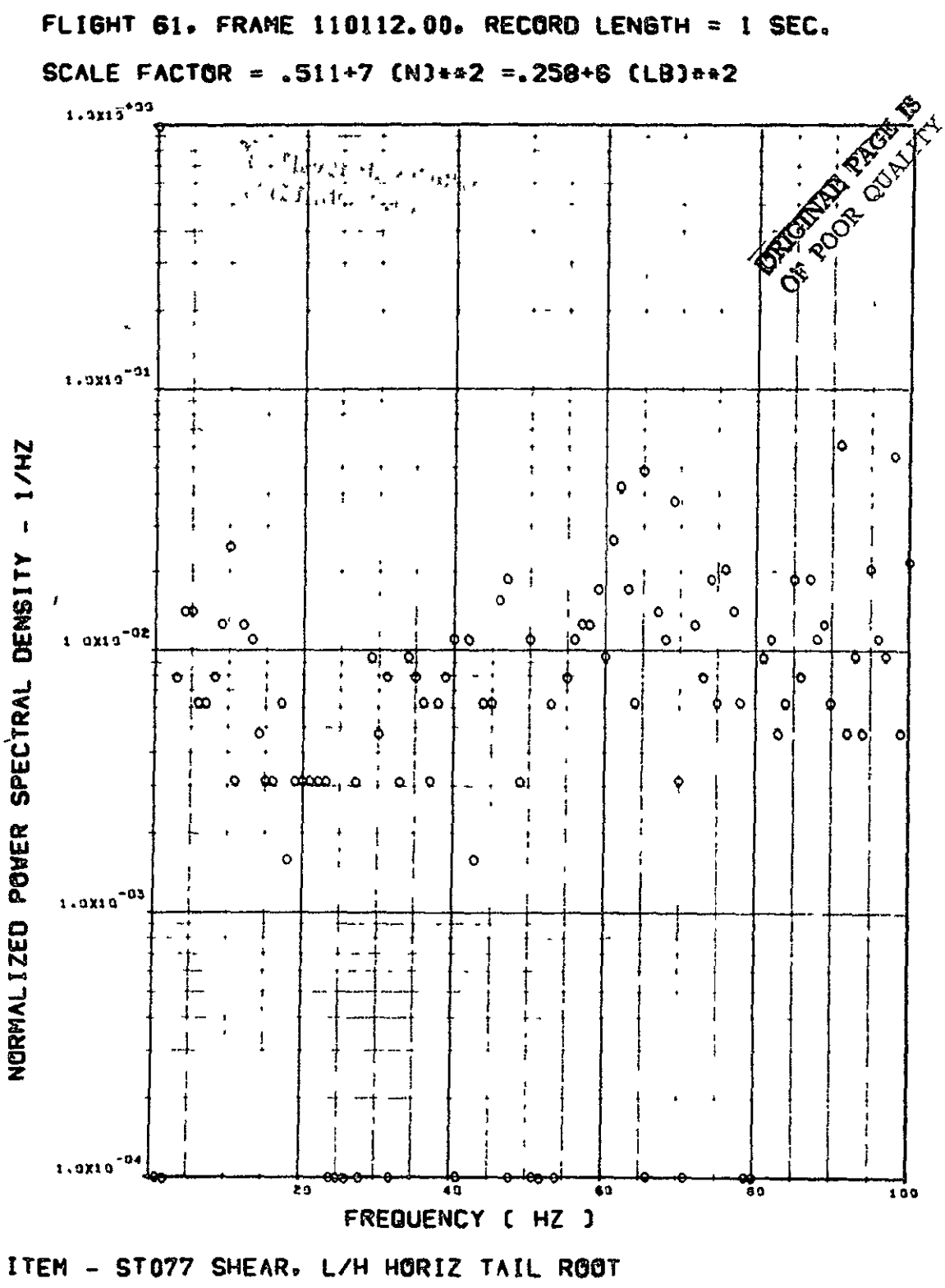

Figure 12. Continued

FLIGHT 61. FRAME 110112.00. RECORD LENGTH = 1 SEC.

SCALE FACTOR = .197+7 (N)**2 =.996+5 (LB)**2

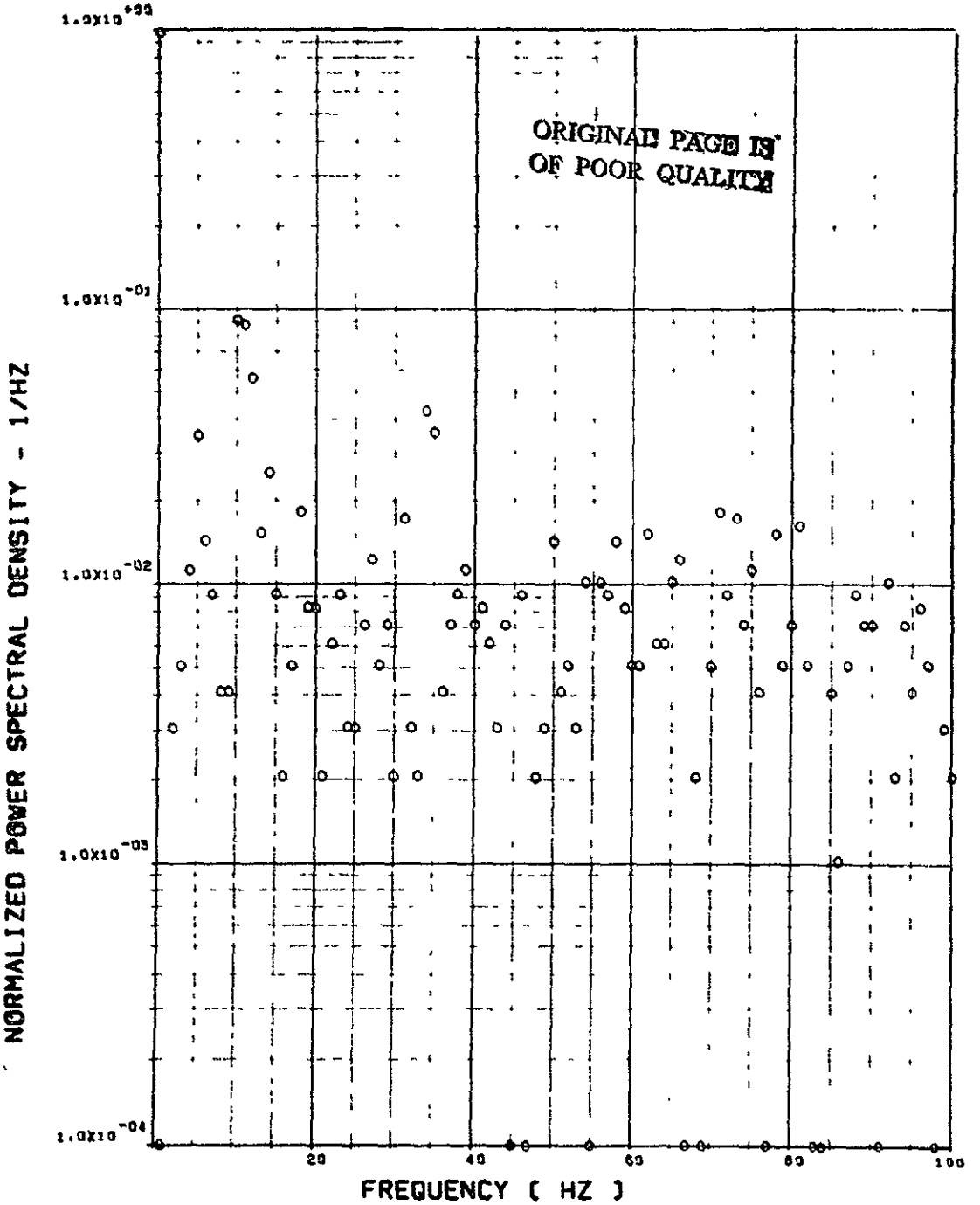

ITEM - ST072 SHEAR. R/H HORIZ TAIL ROOT

Figure 12. Continued

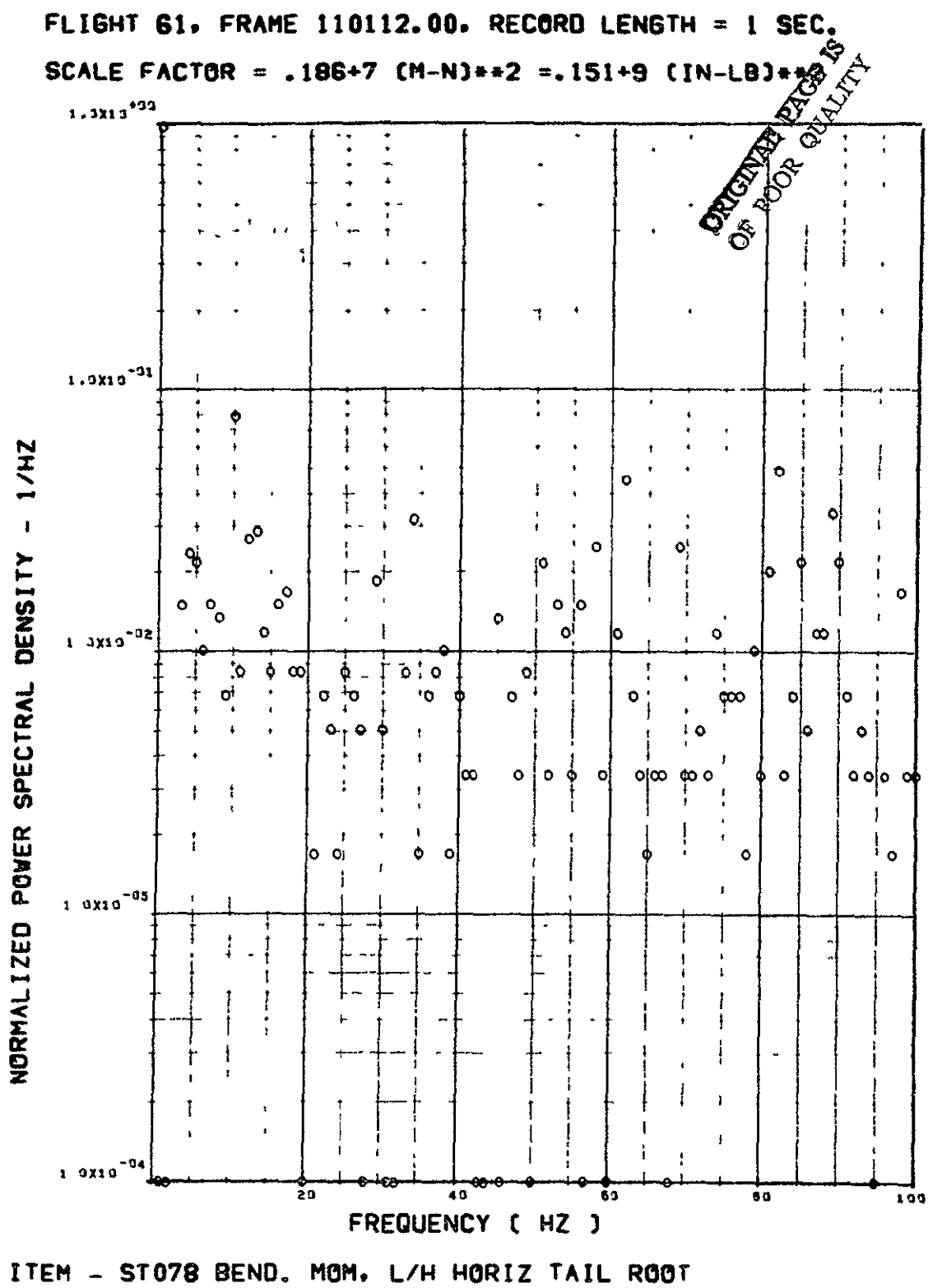

Figure 12. Continued

FLIGHT 61. FRAME 110112.00. RECORD LENGTH = 1 SEC.

SCALE FACTOR = .260+7 (M-N)**2 = 211+9 (IN-LB)**2

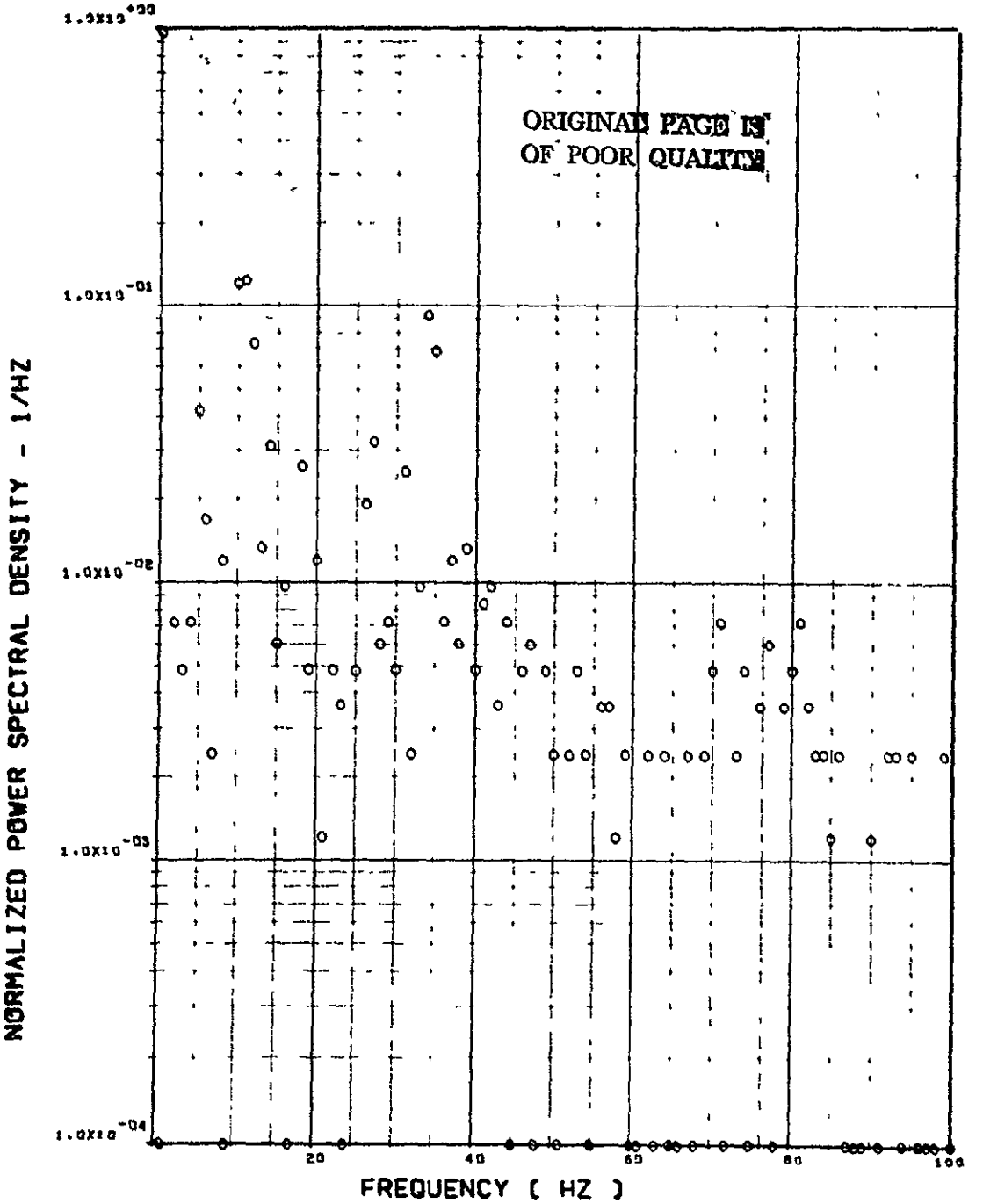

ITEM - ST073 BEND. MOM. R/H HORIZ TAIL ROOT

Figure 12. Continued

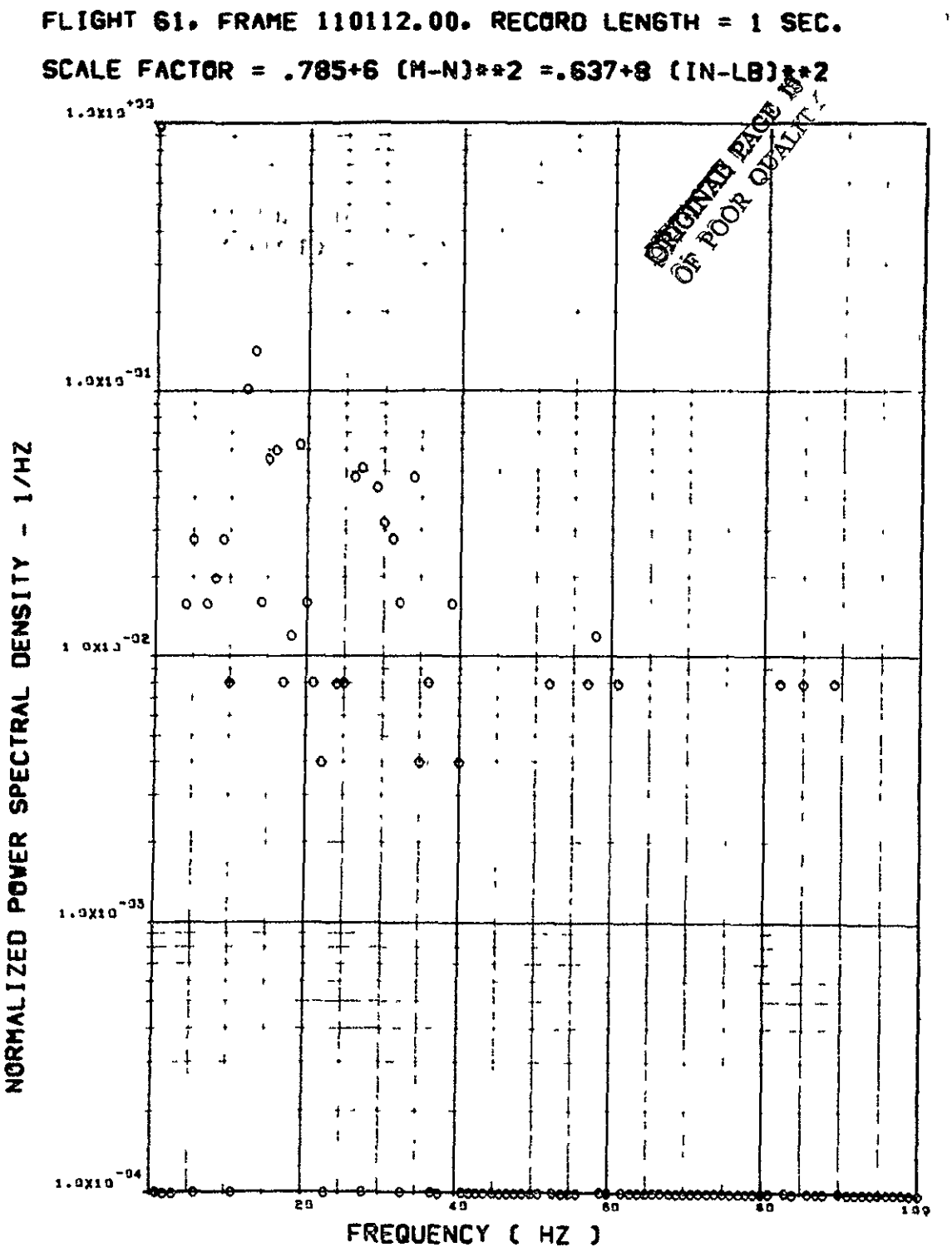

Figure 12. Continued

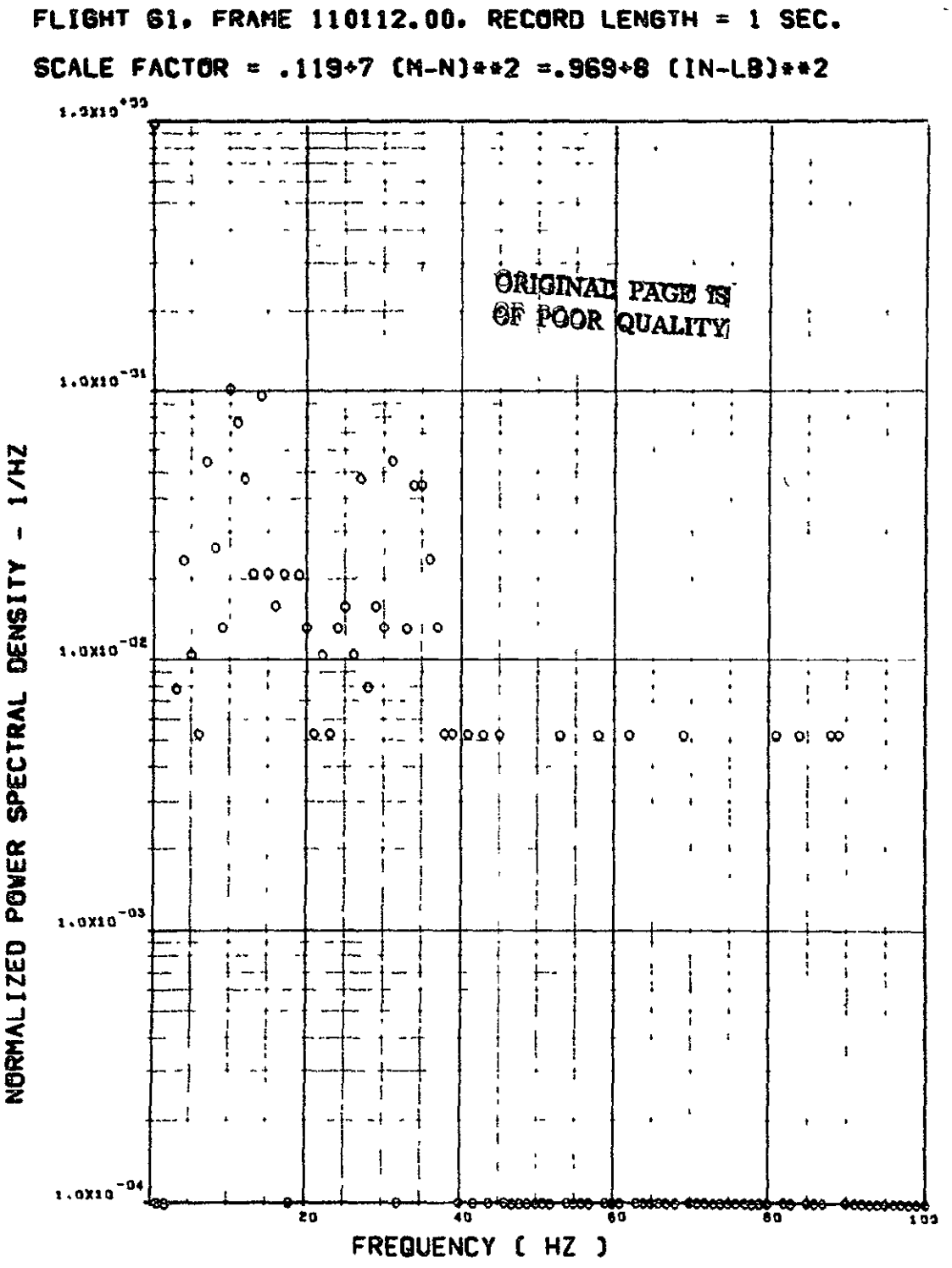

Figure 12. Concluded

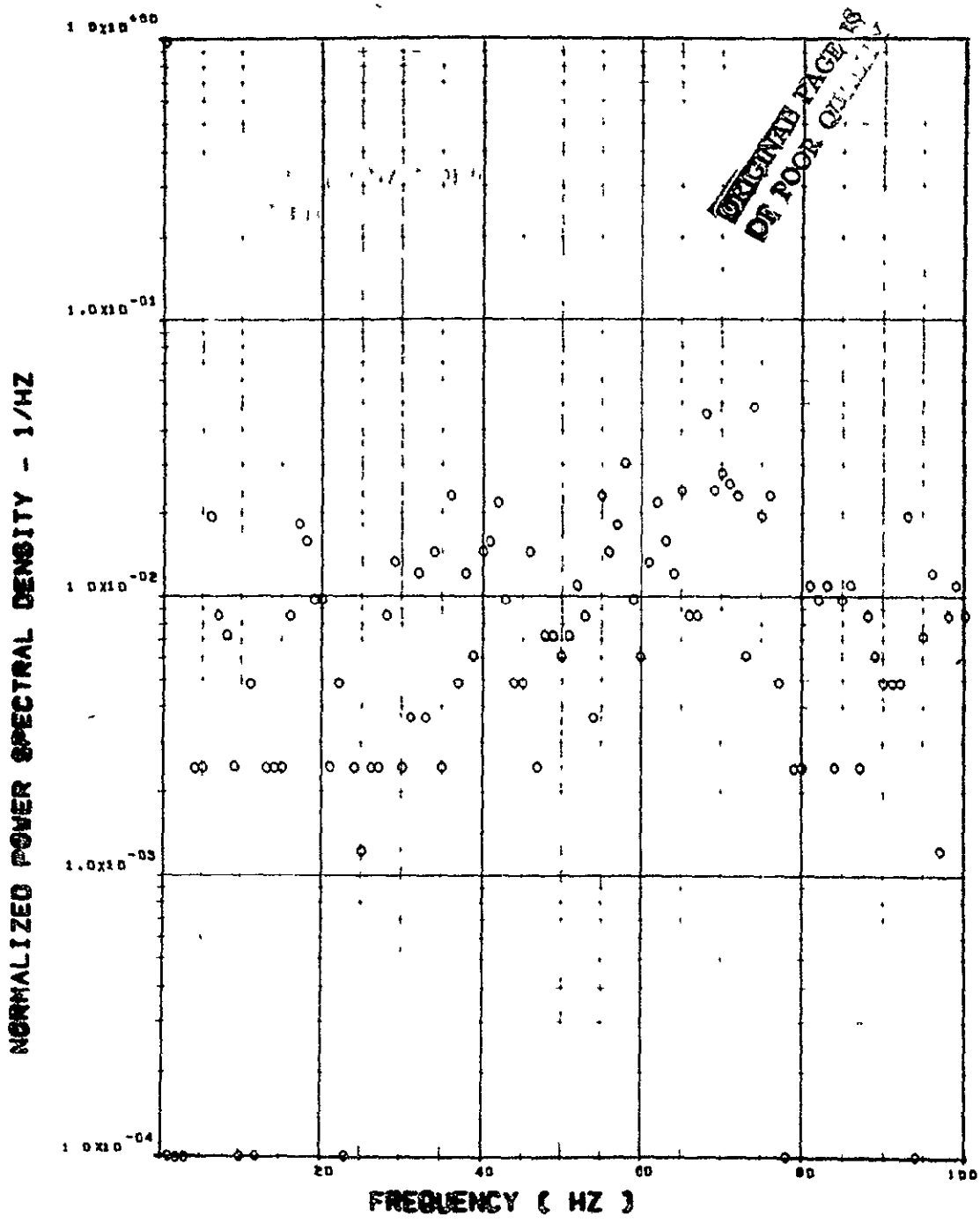

Figure 13. Power Spectra - Flight 51, Run S38/150, Point 1, T_1 = 95940.0, ΔT = 2 Sec, α_{Nom} = 14.85 deg, $\Delta\alpha$ = 0.75 deg.

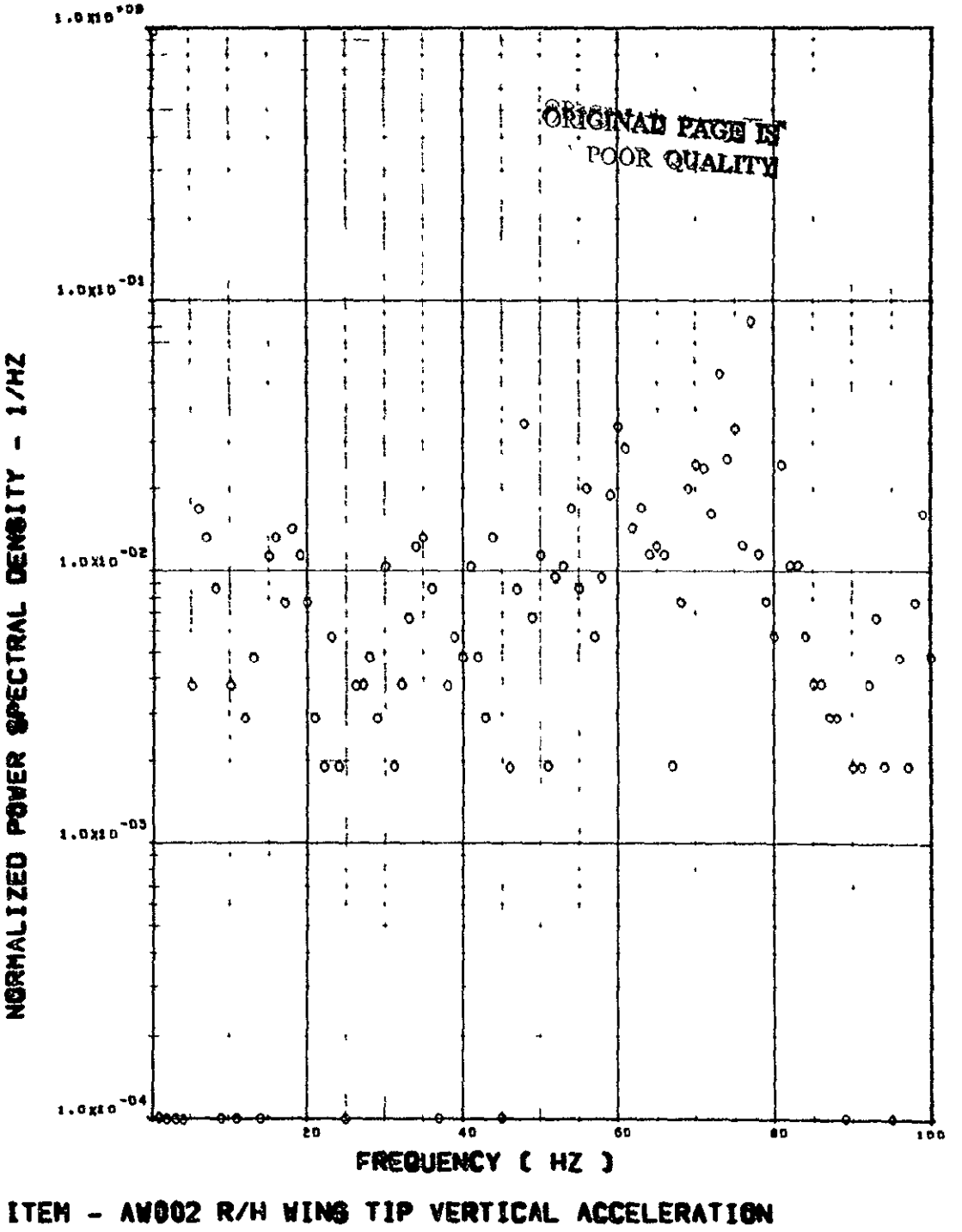

Figure 13. Continued

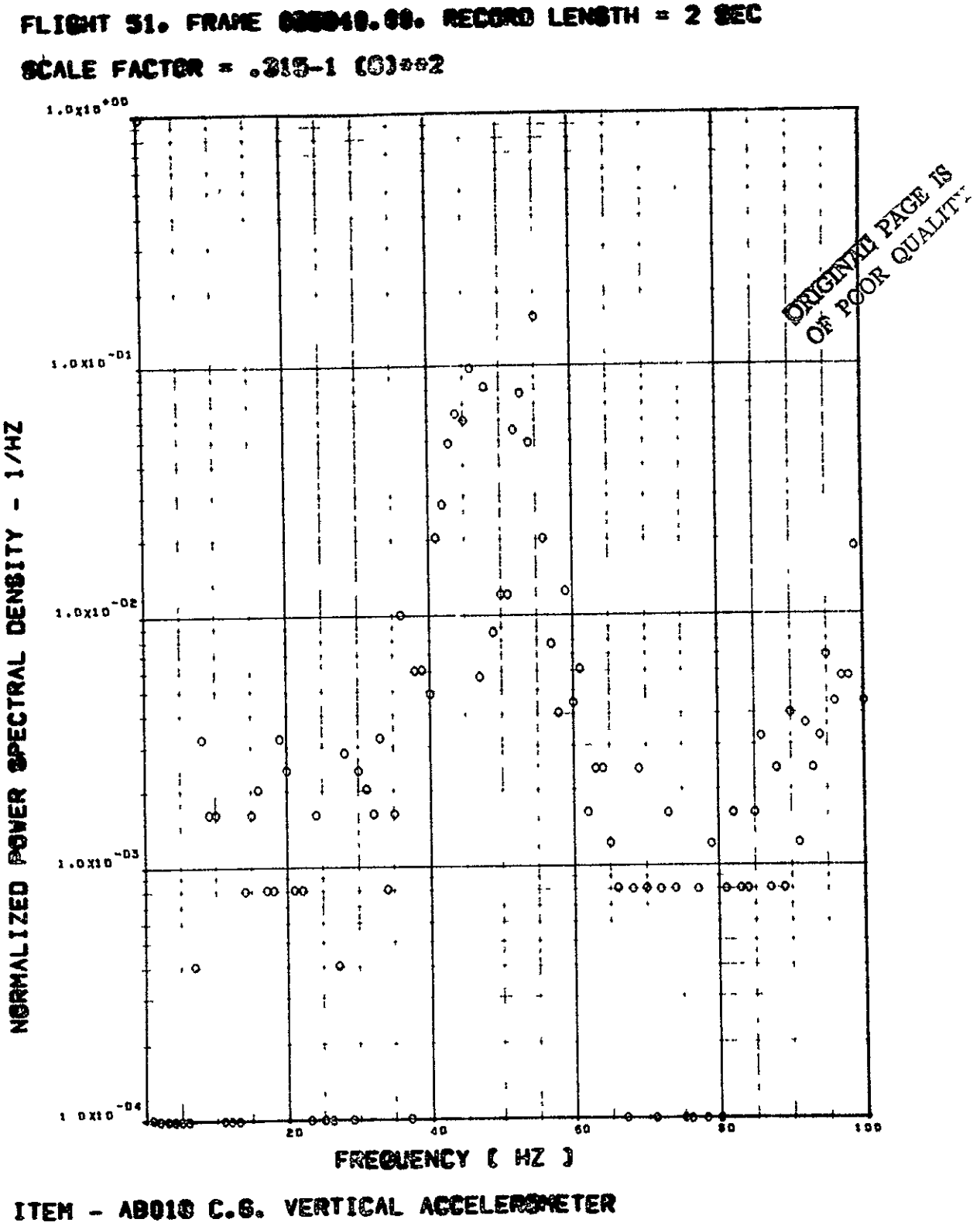

Figure 13. Continued

C-3

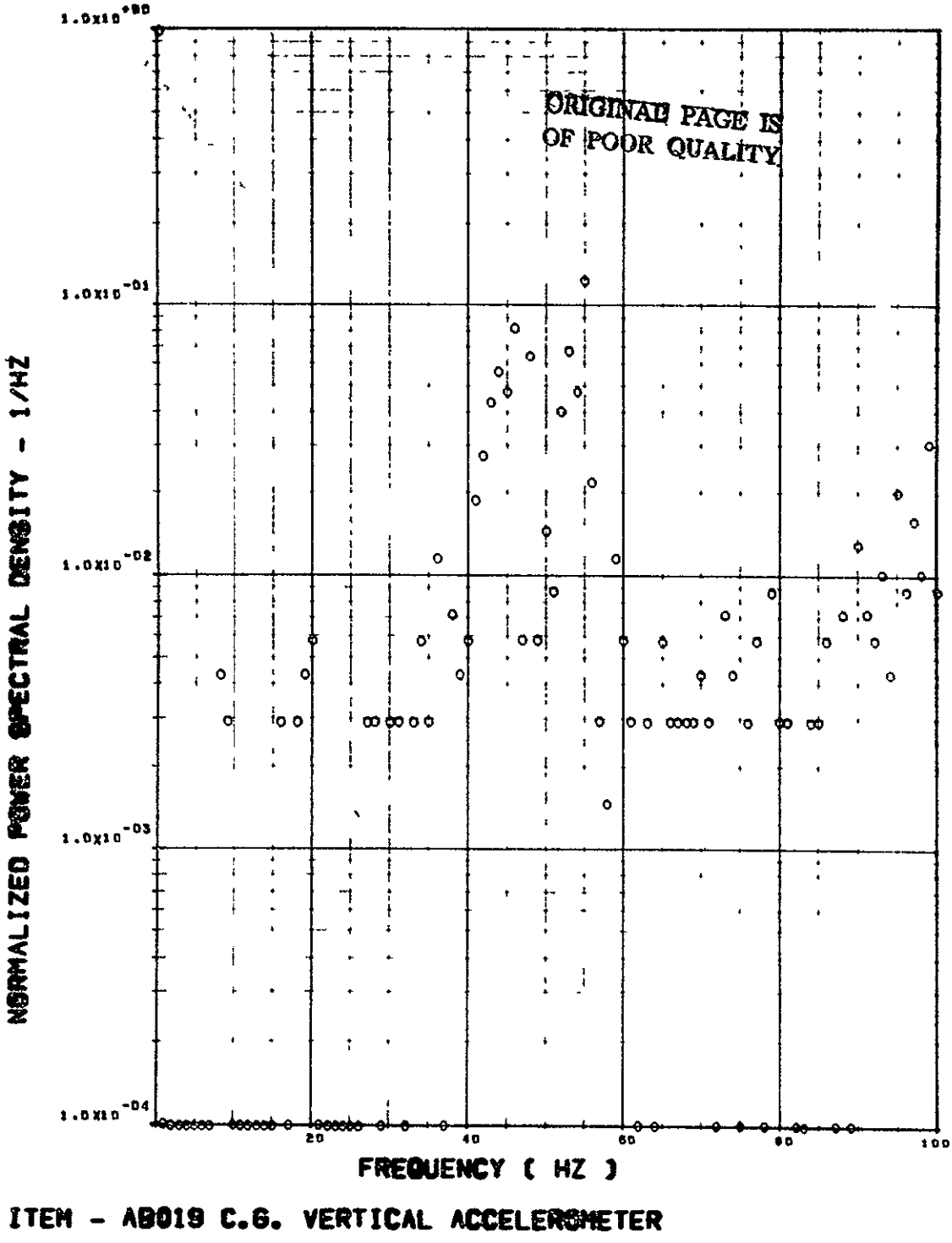

Figure 13. Continued

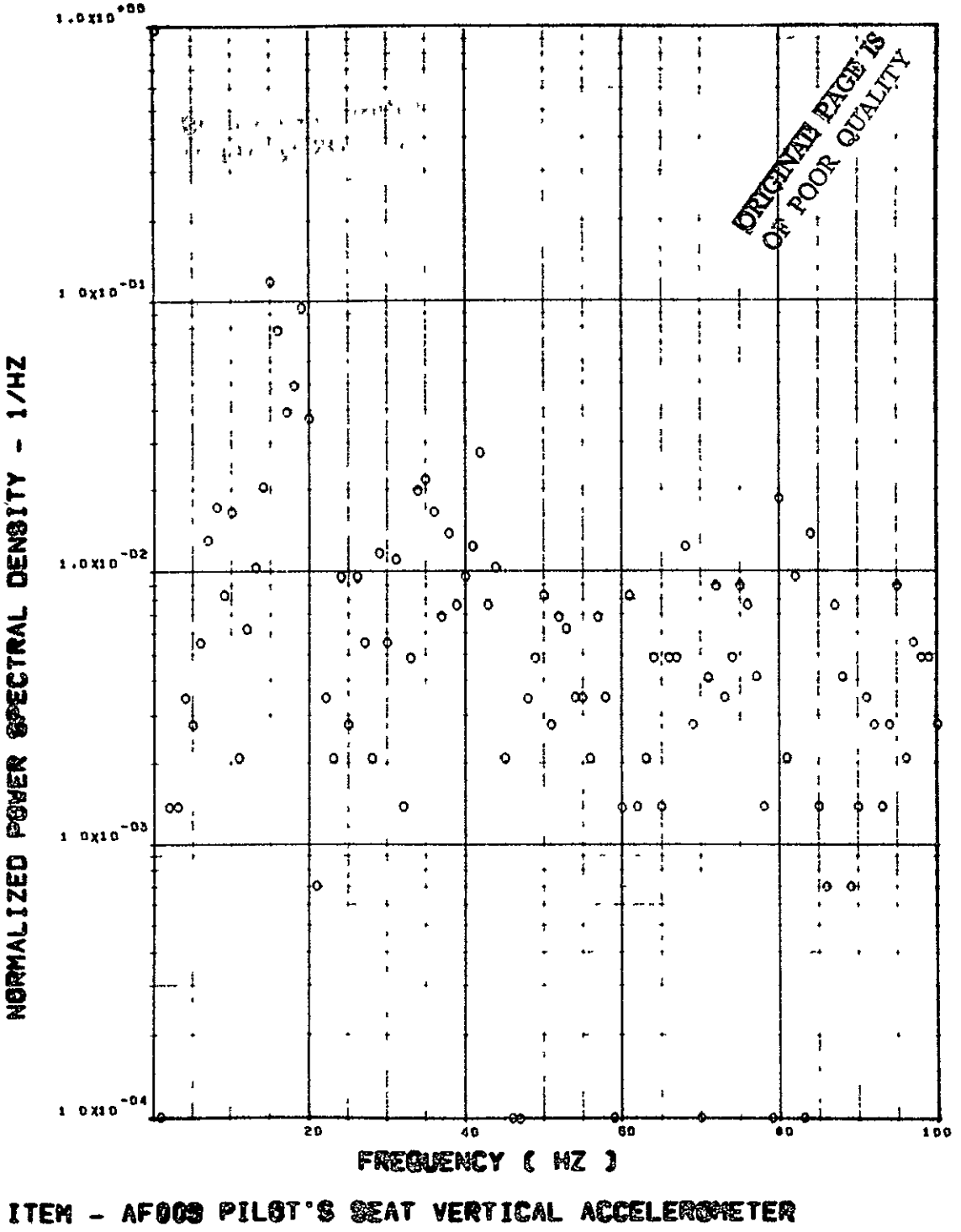

Figure 13. Continued

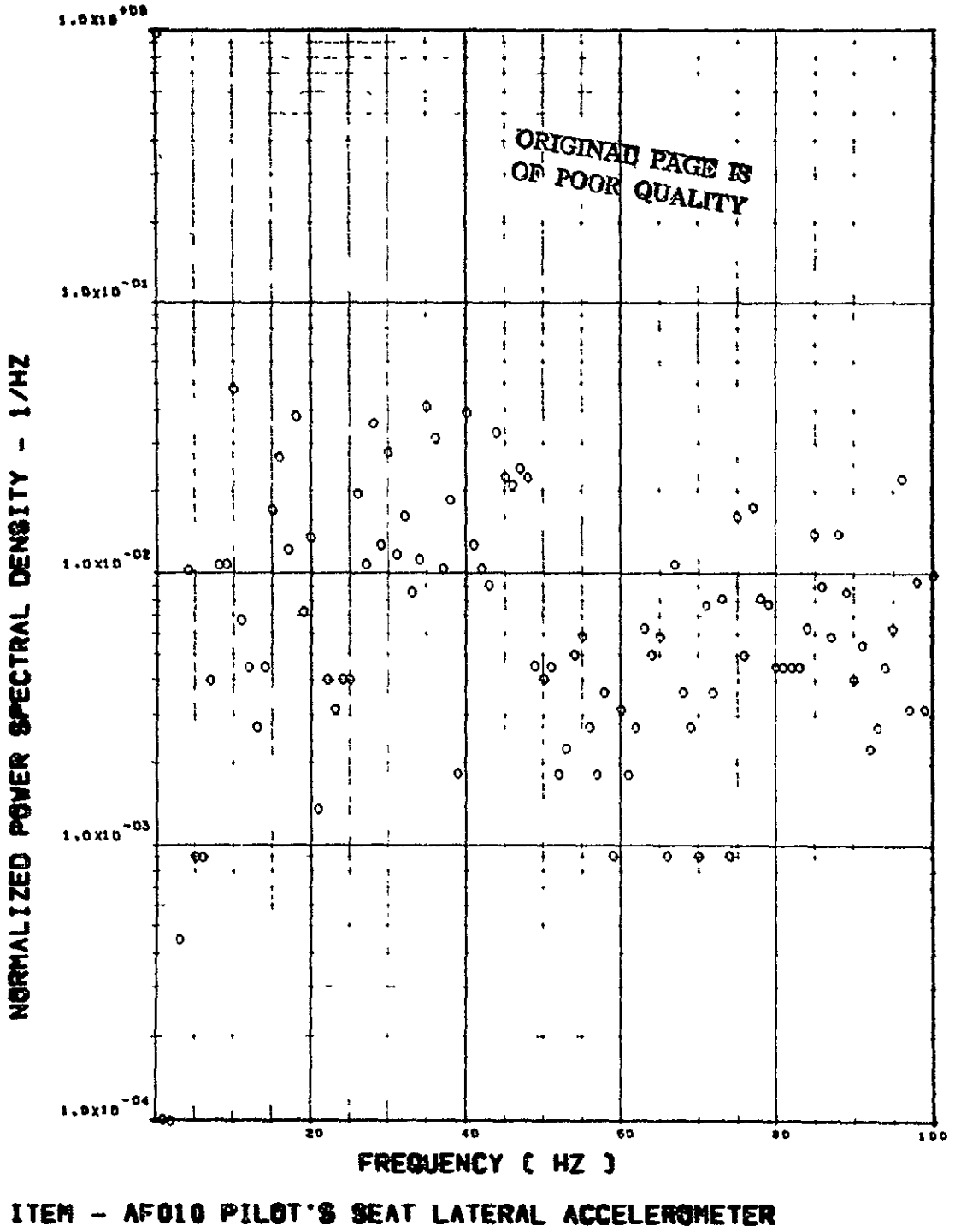

Figure 13. Continued

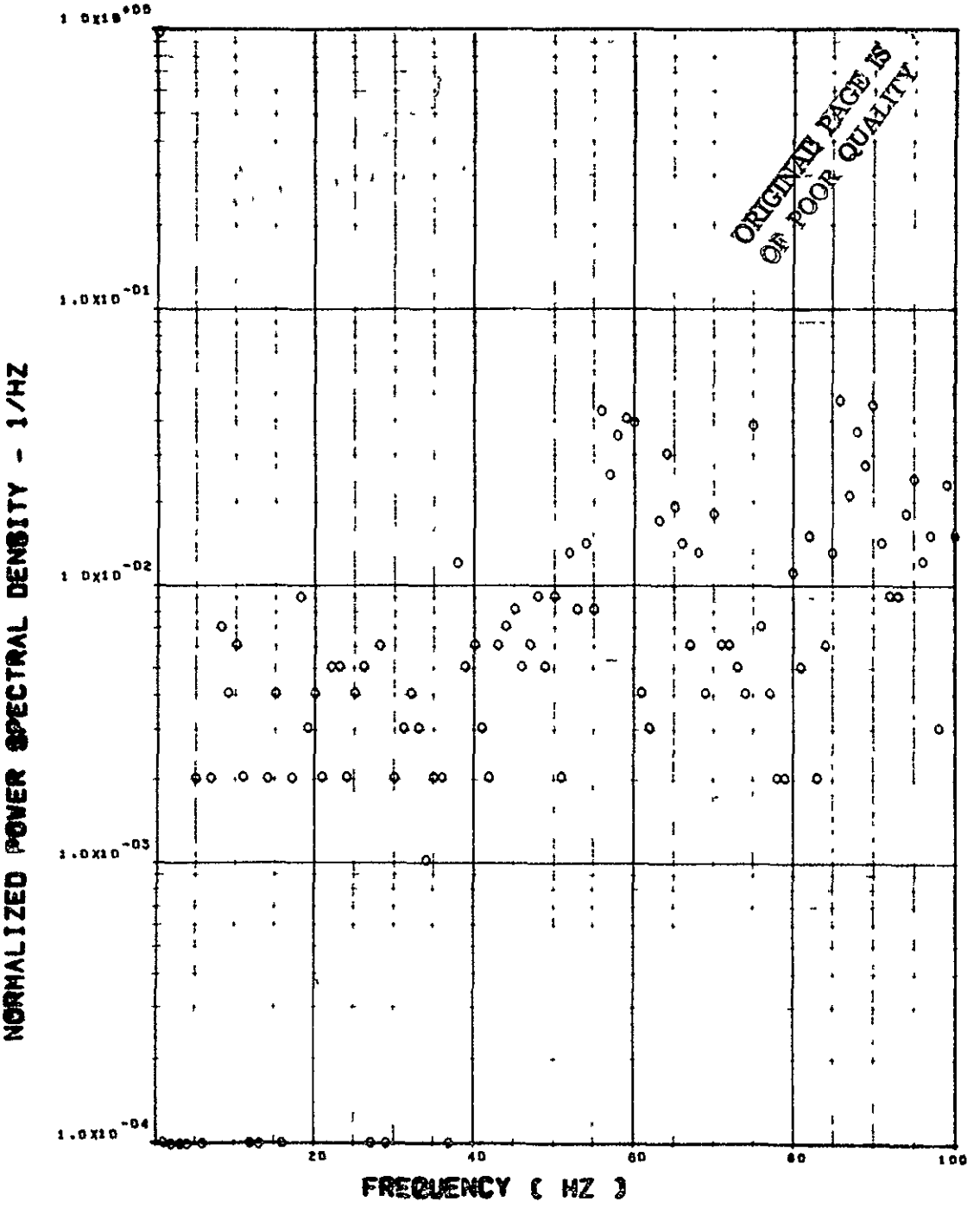

Figure 13. Continued

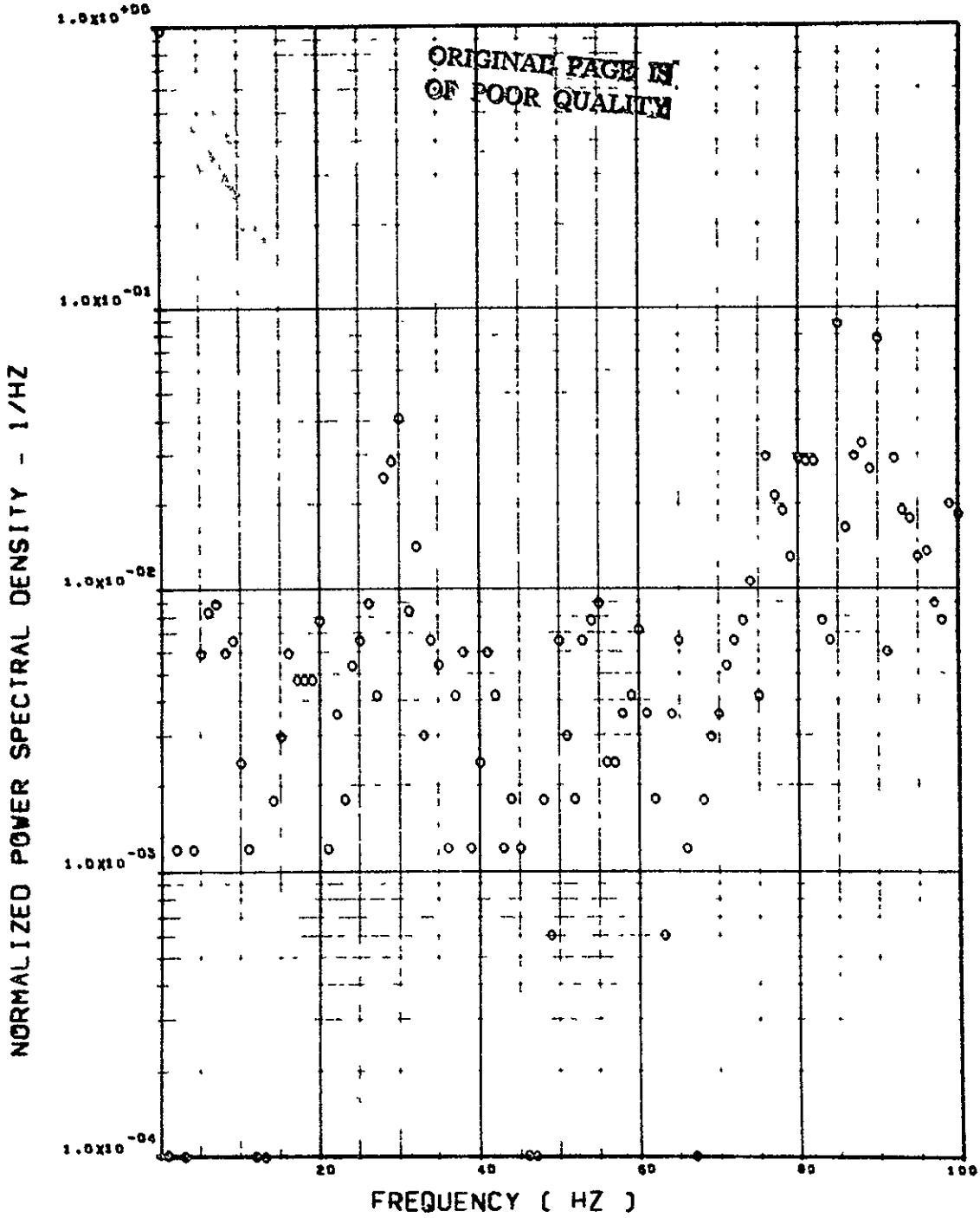

Figure 13. Continued

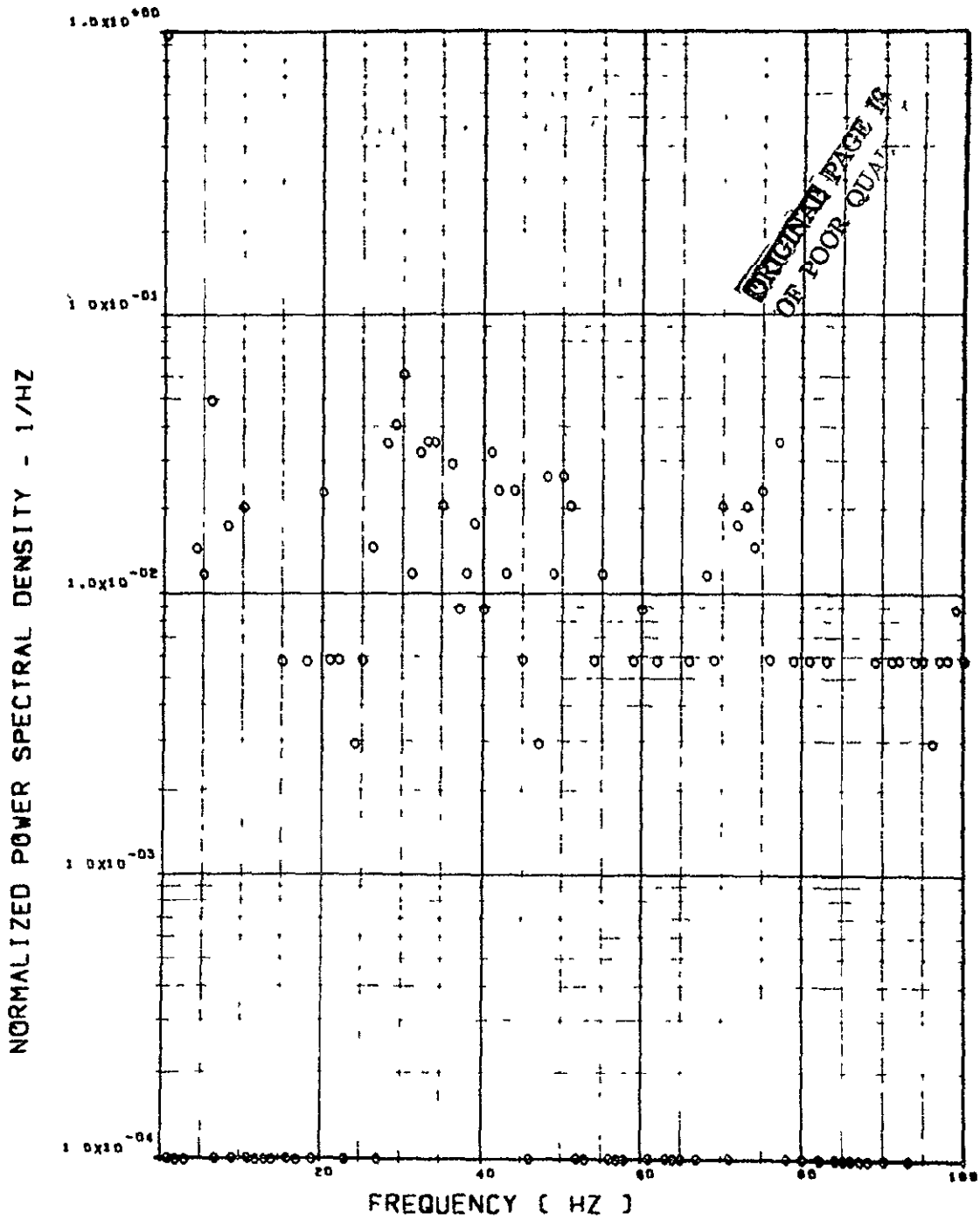

Figure 13. Continued

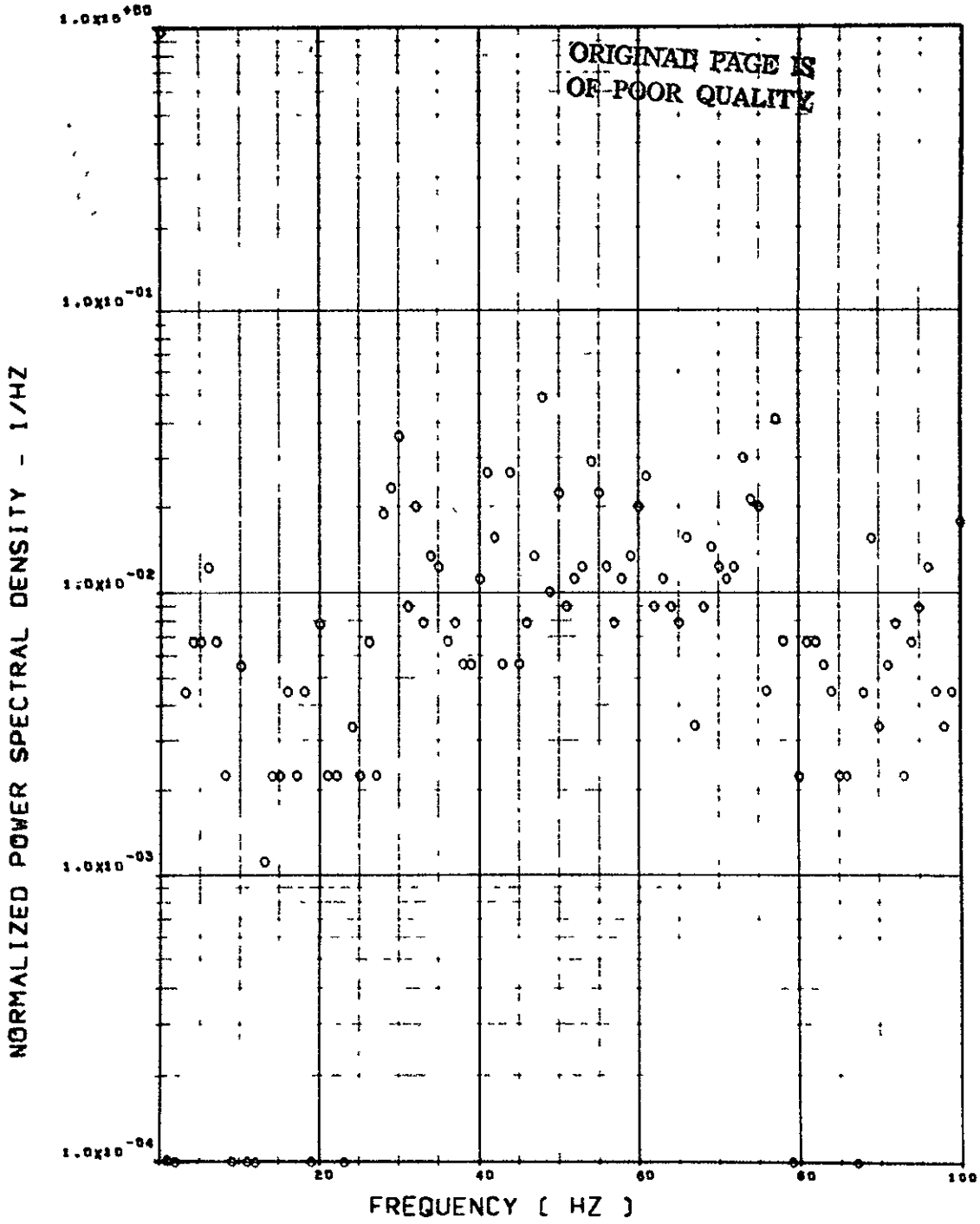

Figure 1). Continued

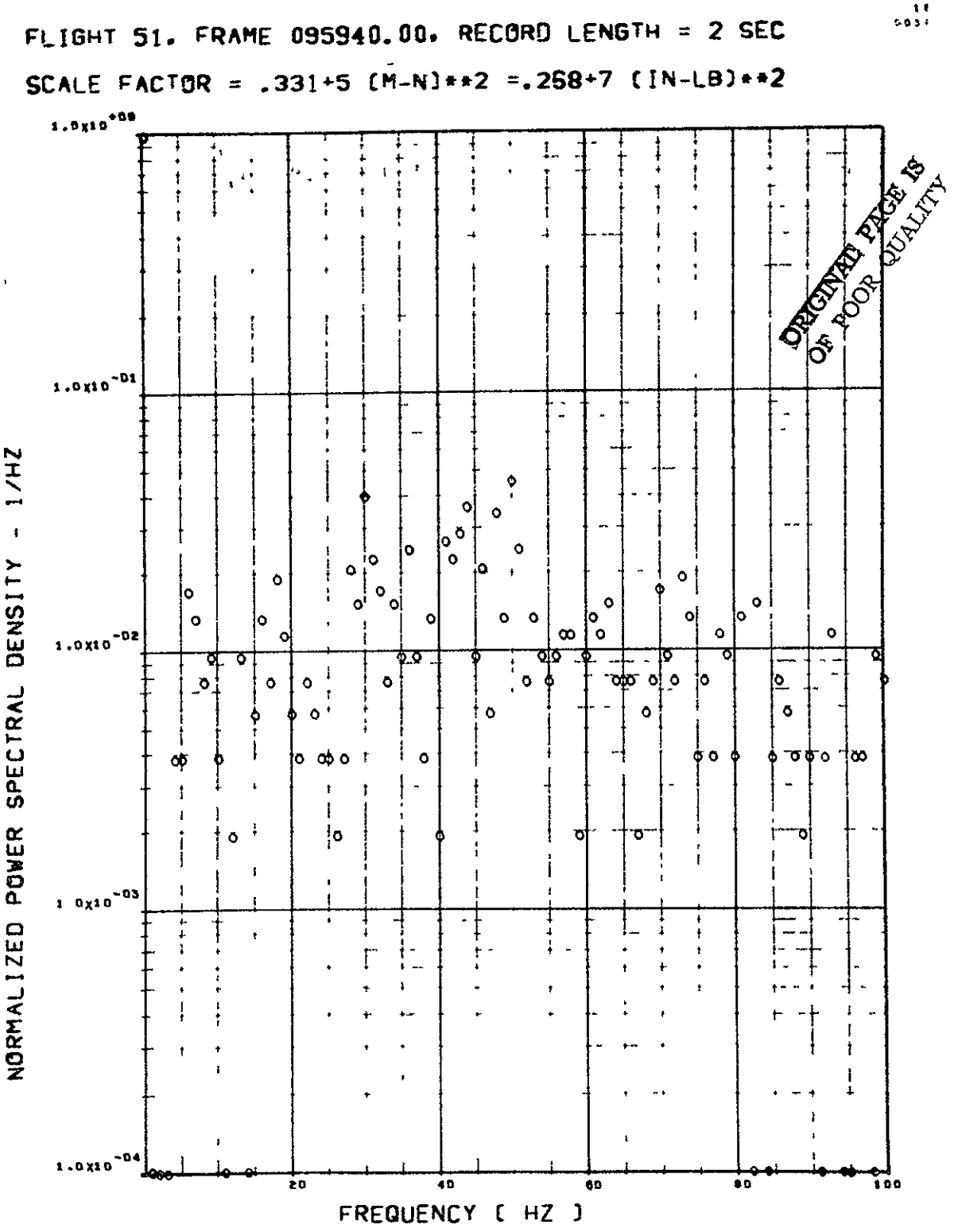

Figure 13. Continued

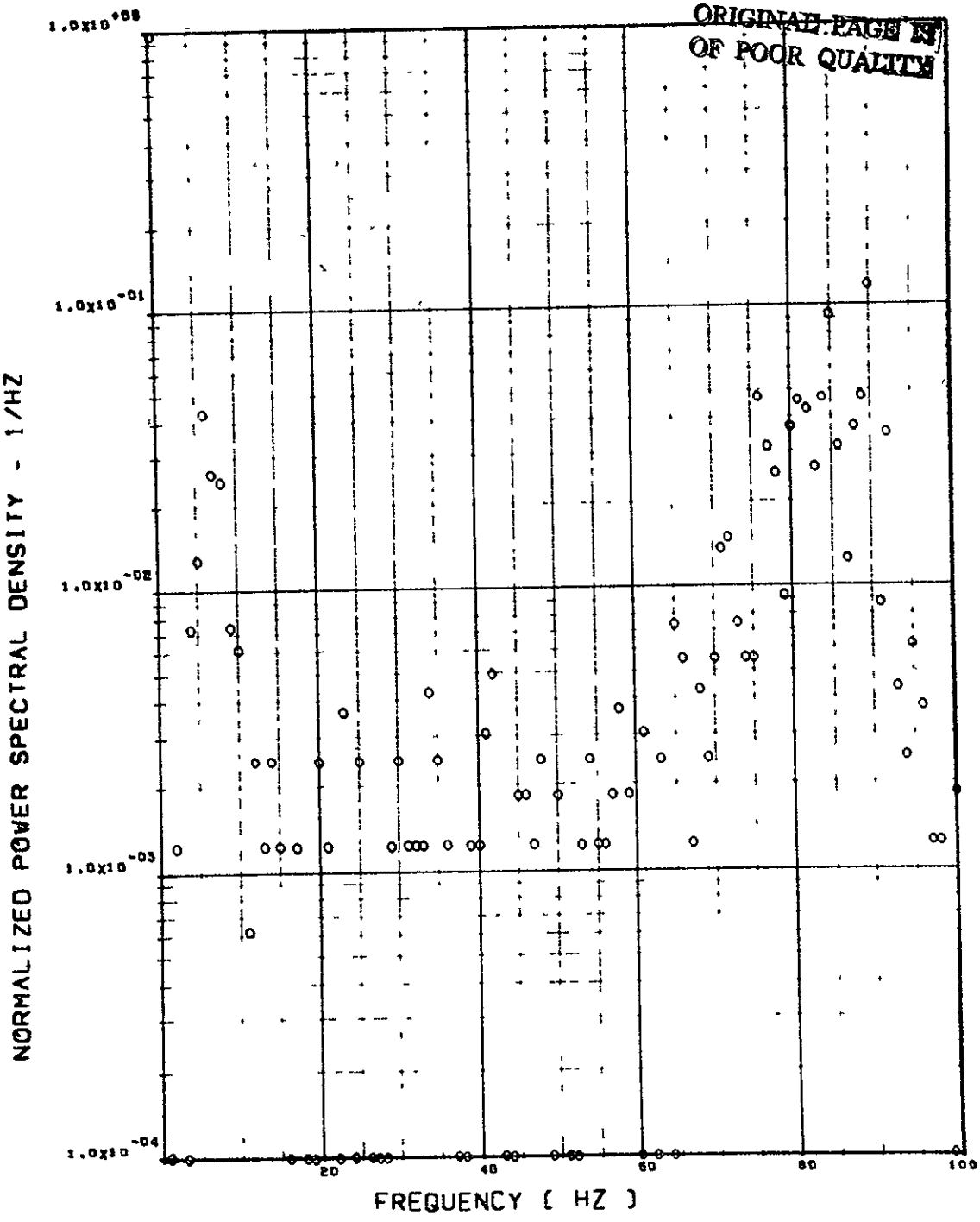

Figure 15. Continued

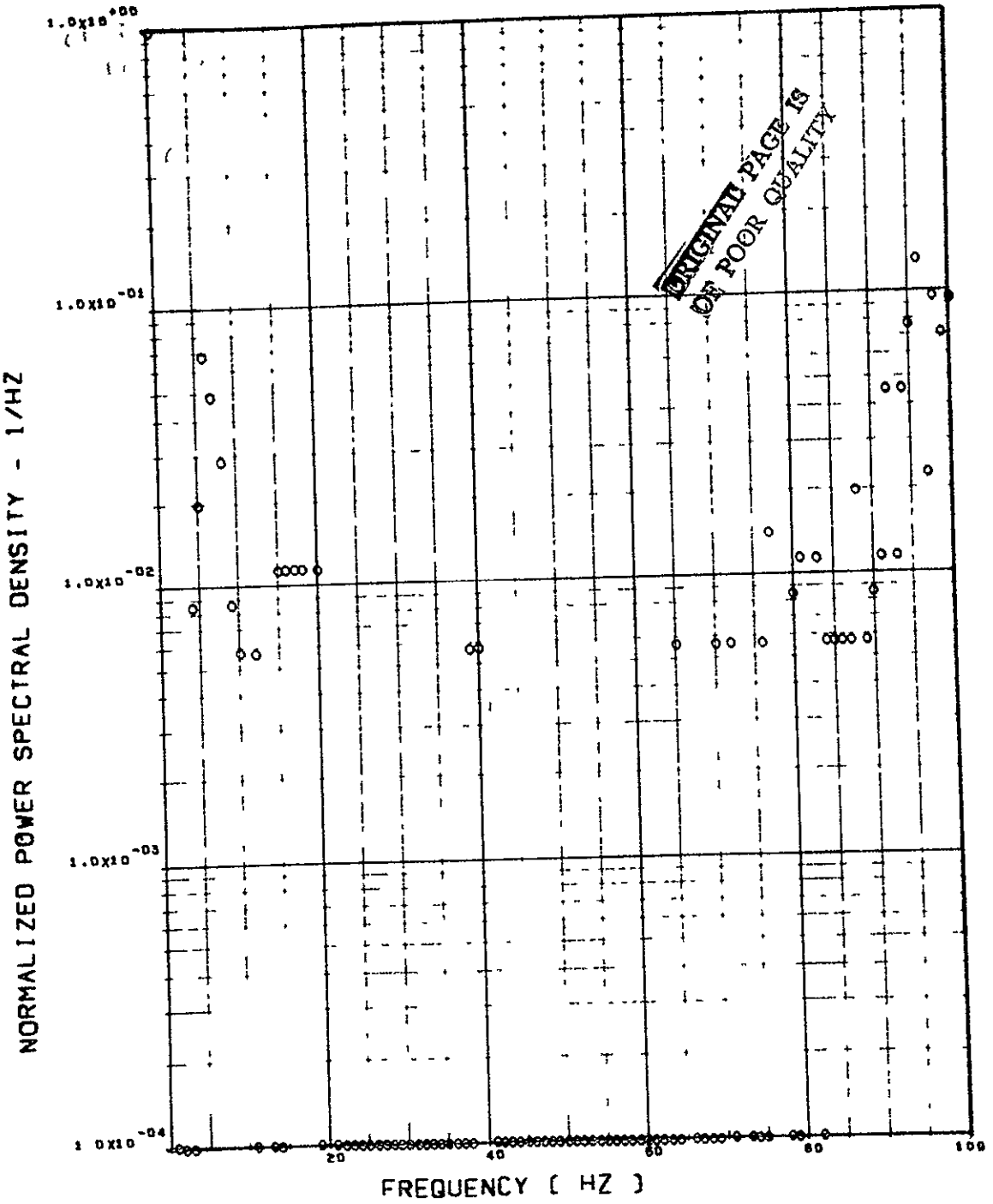

Figure 13. Continued

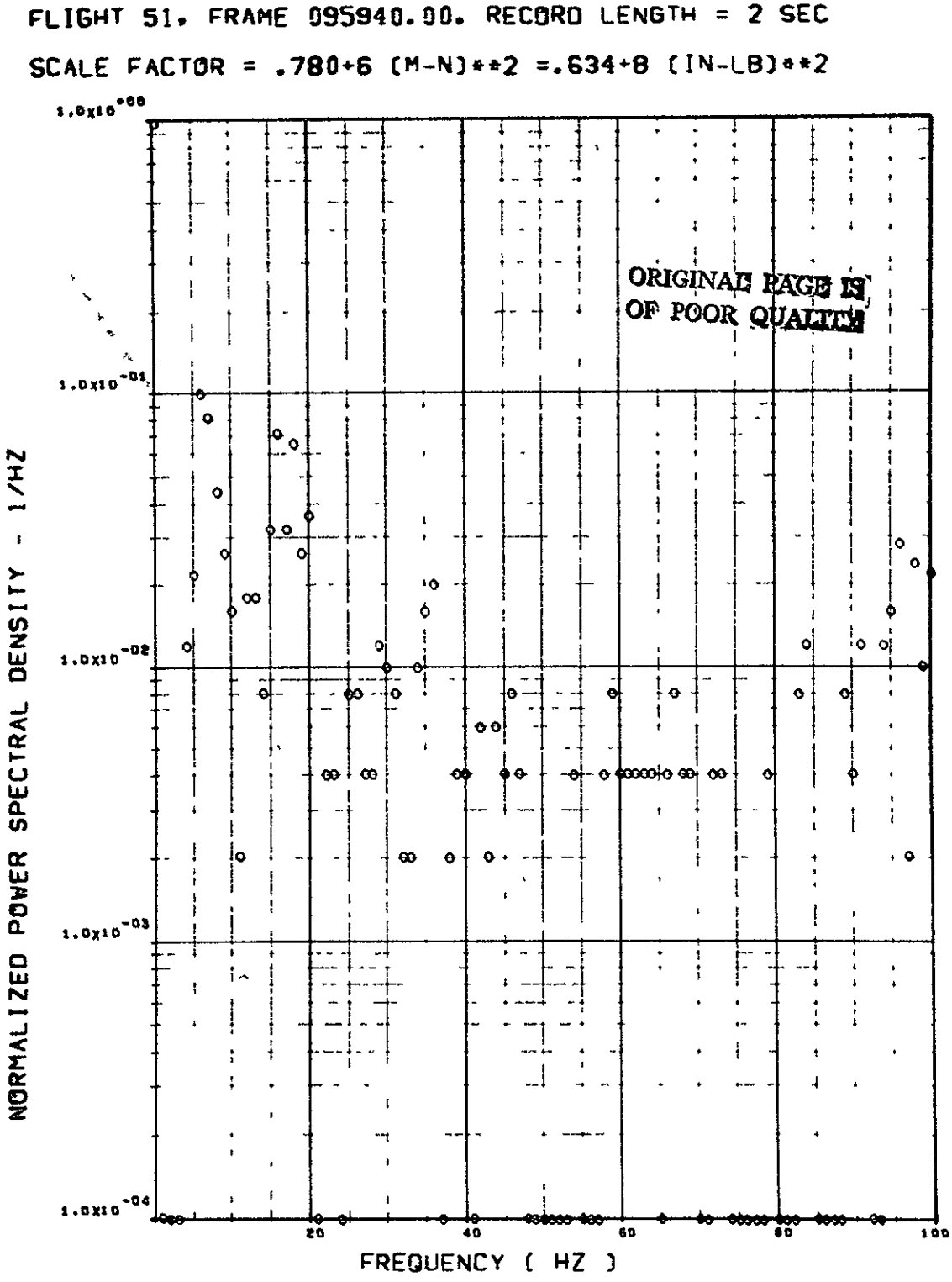

Figure 1b. Continued

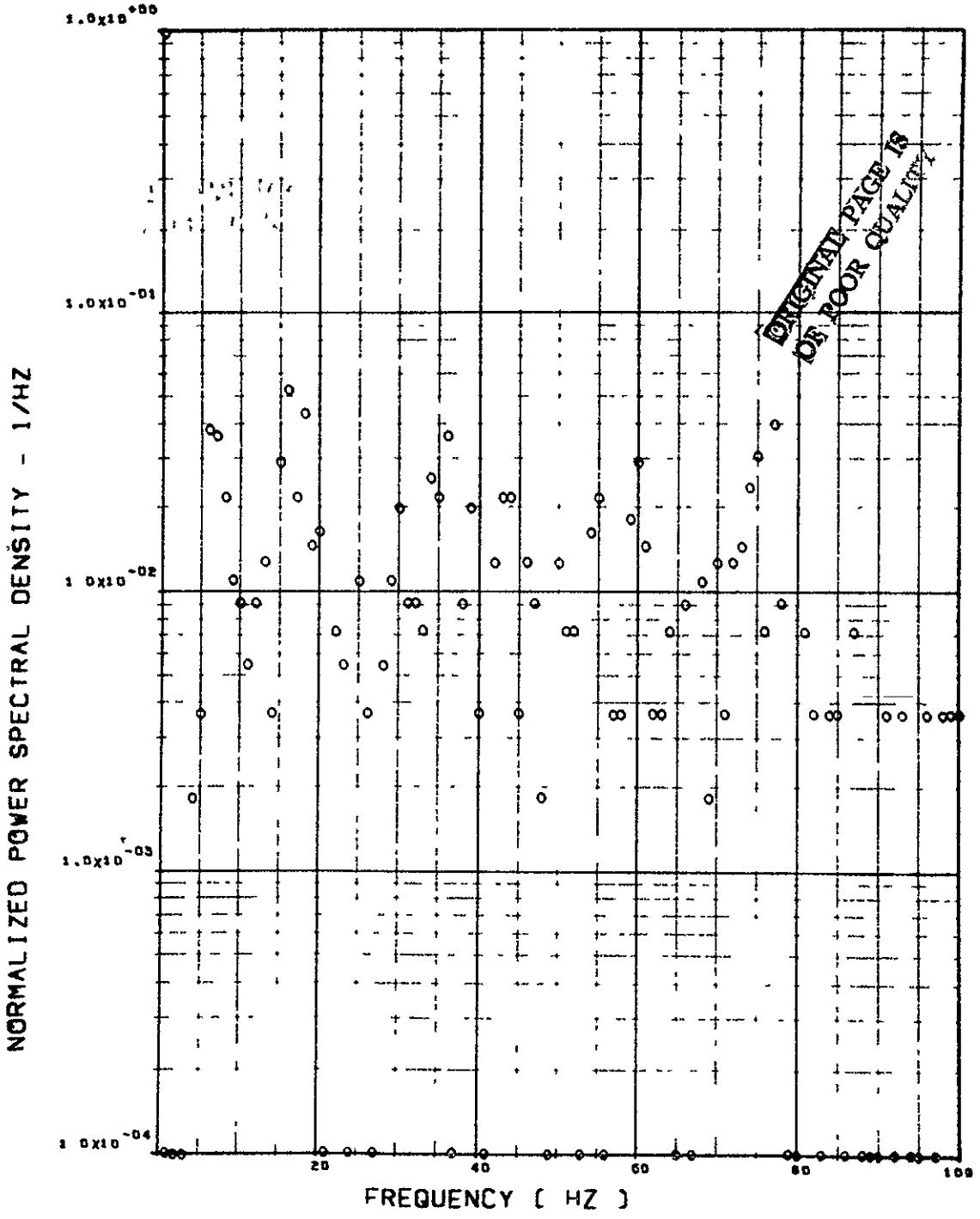

Figure 13. Continued

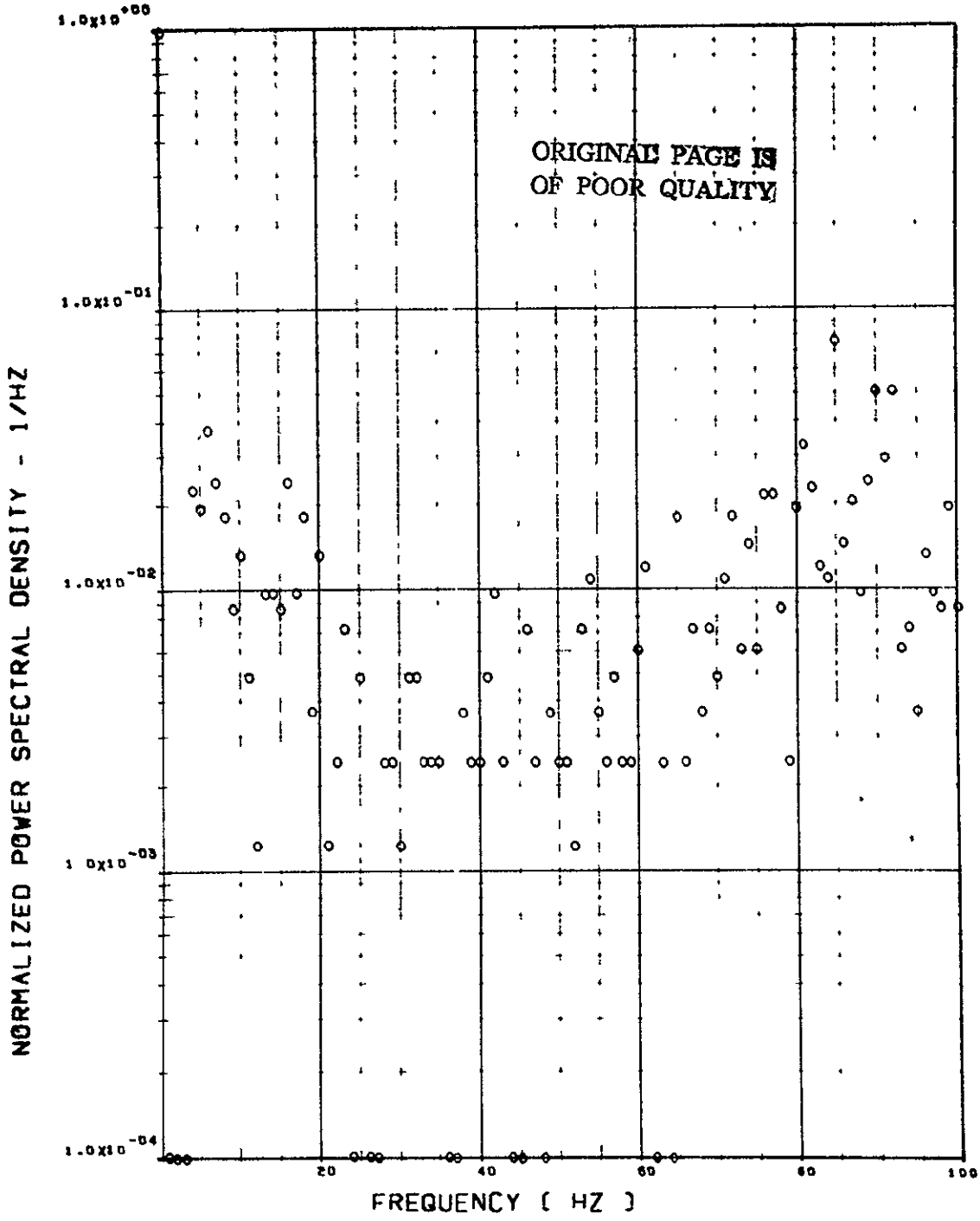

Figure 1>. Continued

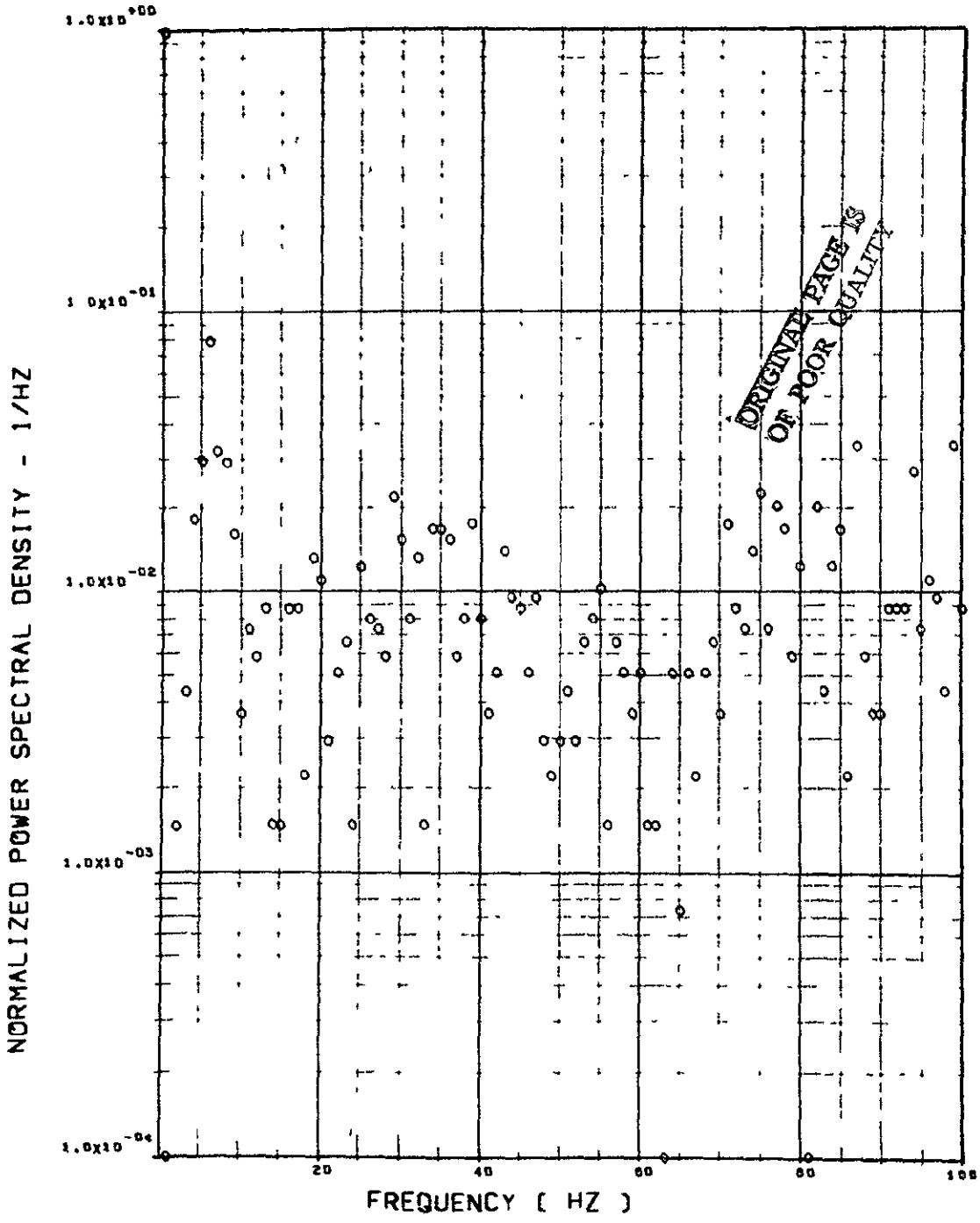

Figure 13. Continued

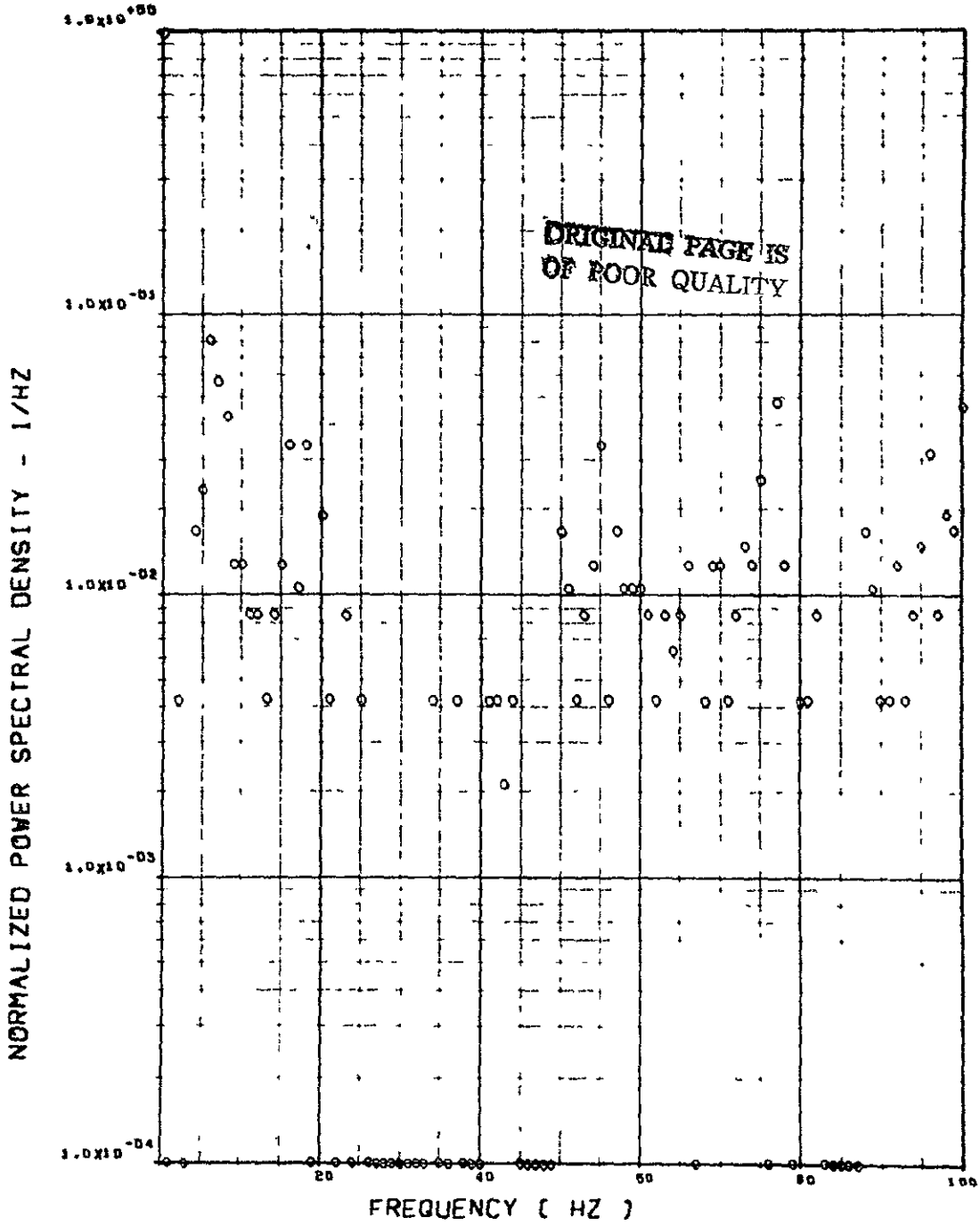

Figure 15. Continued

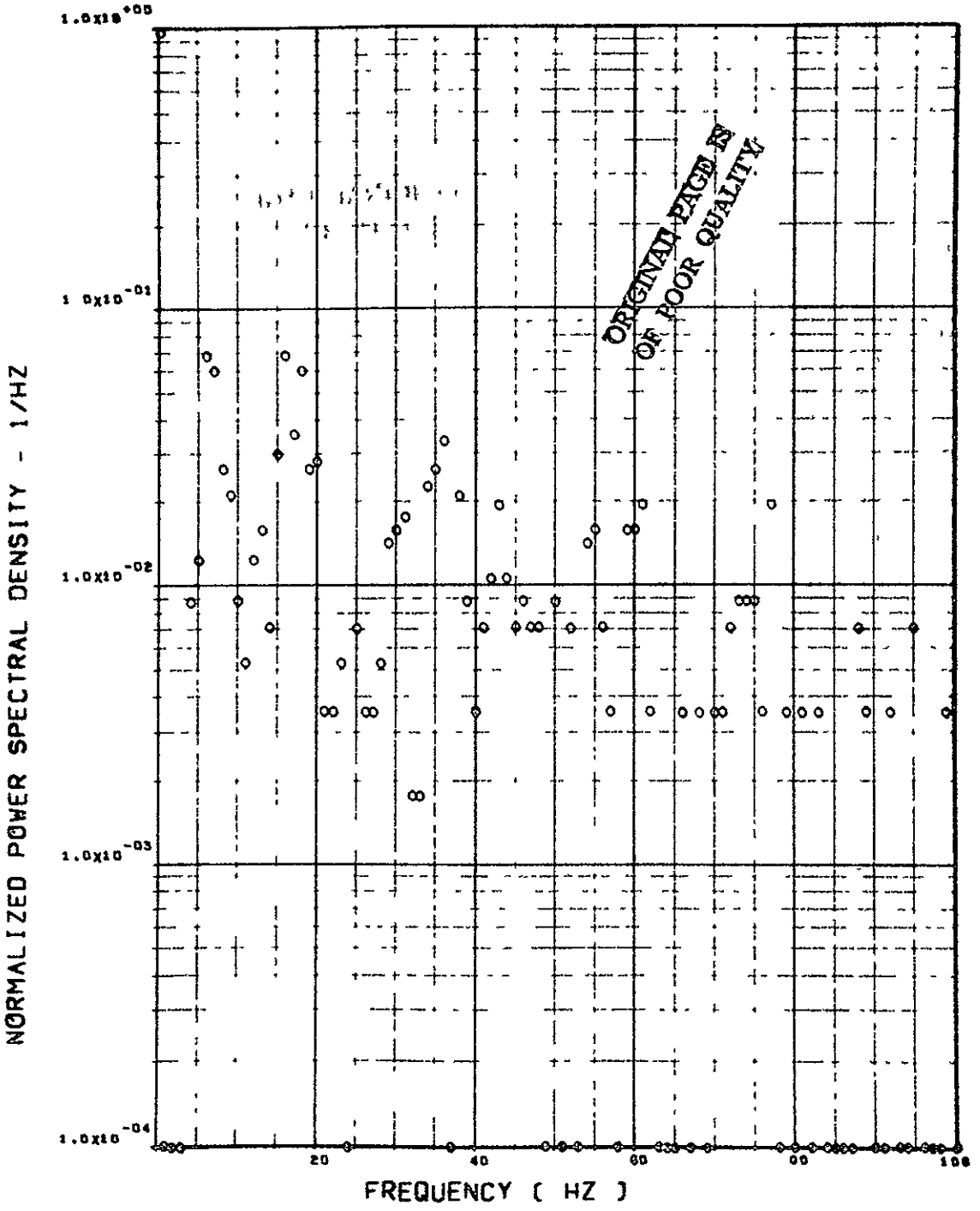

Figure 13. Continued

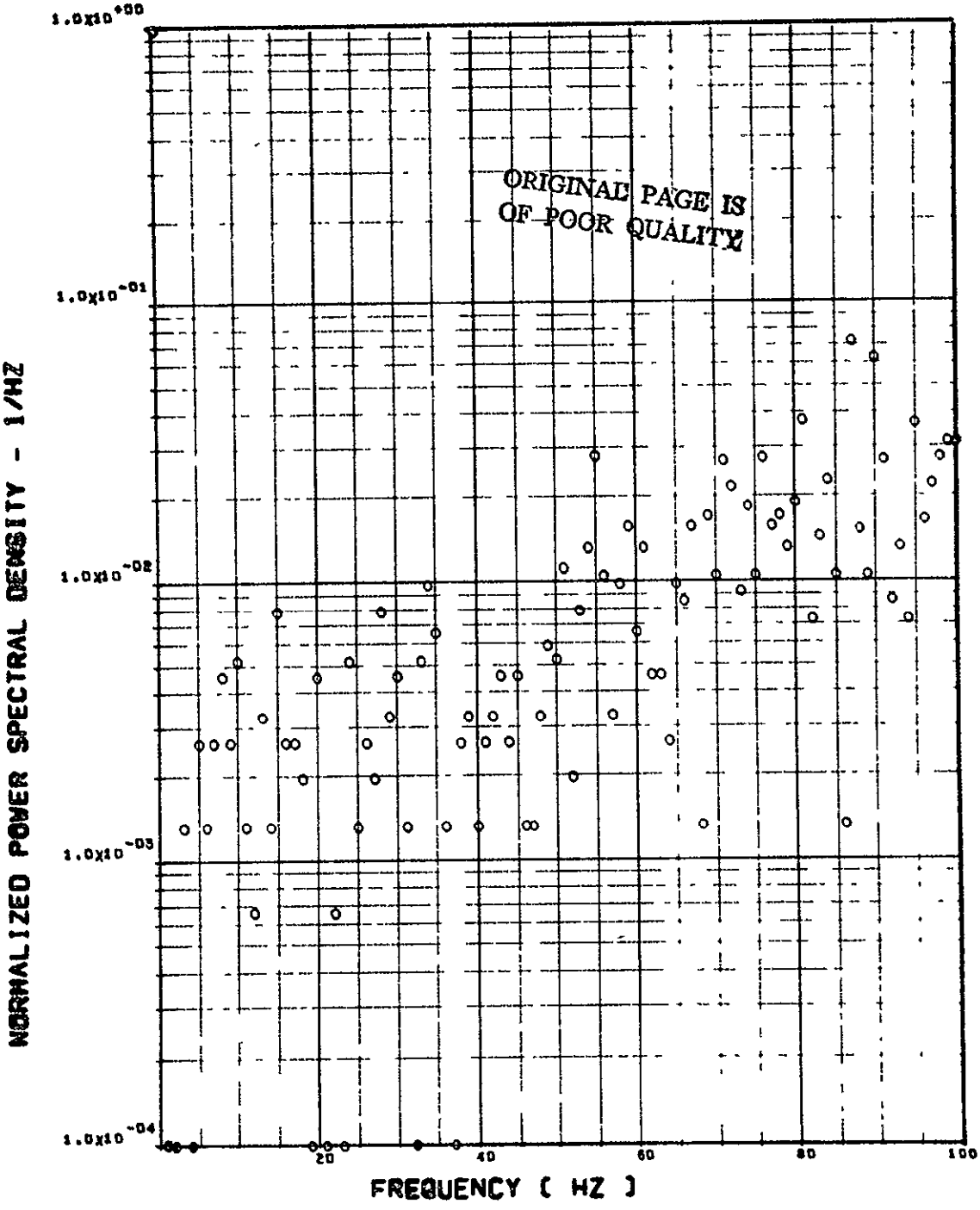

Figure 1). Continued

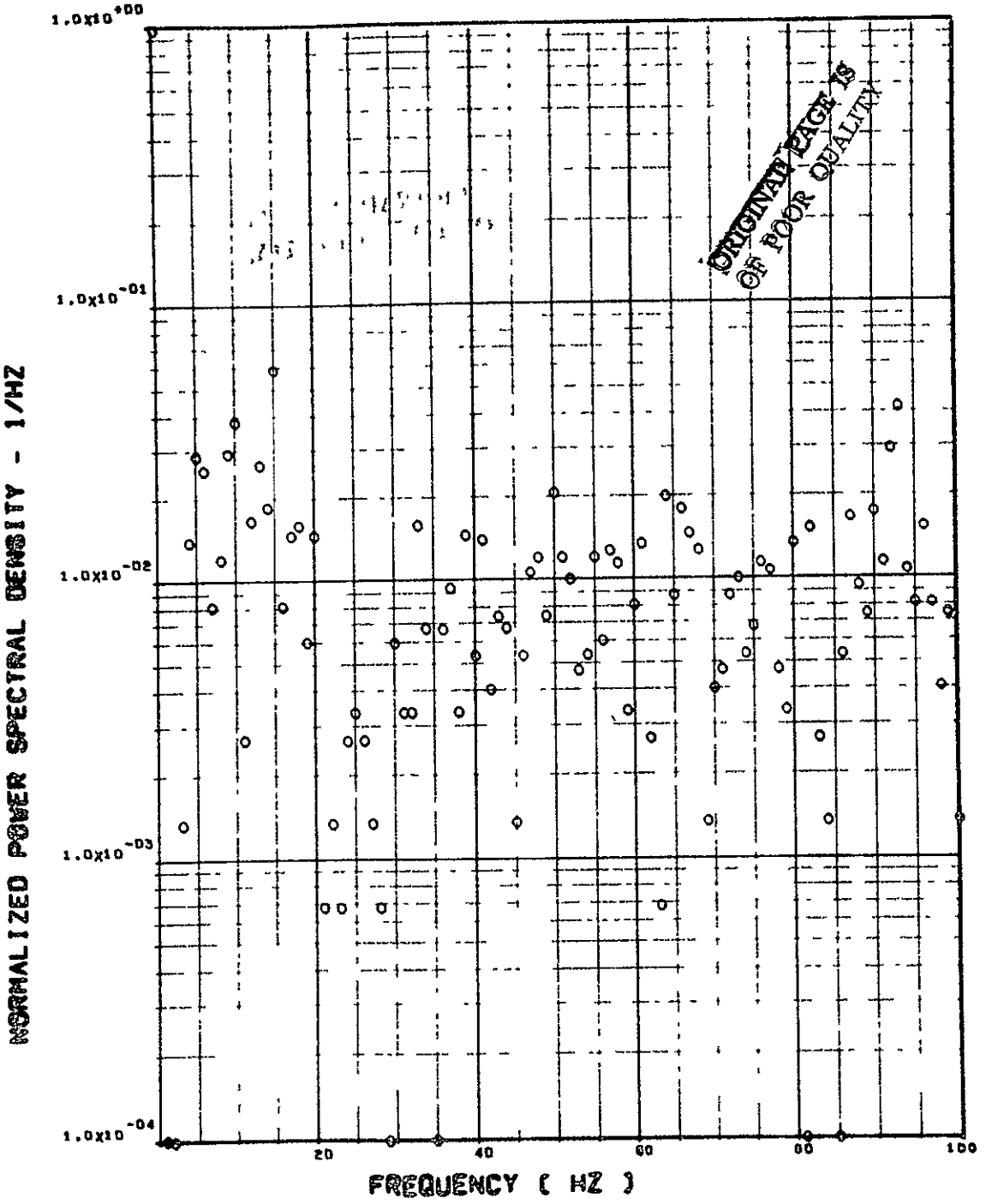

Figure 13. Continued

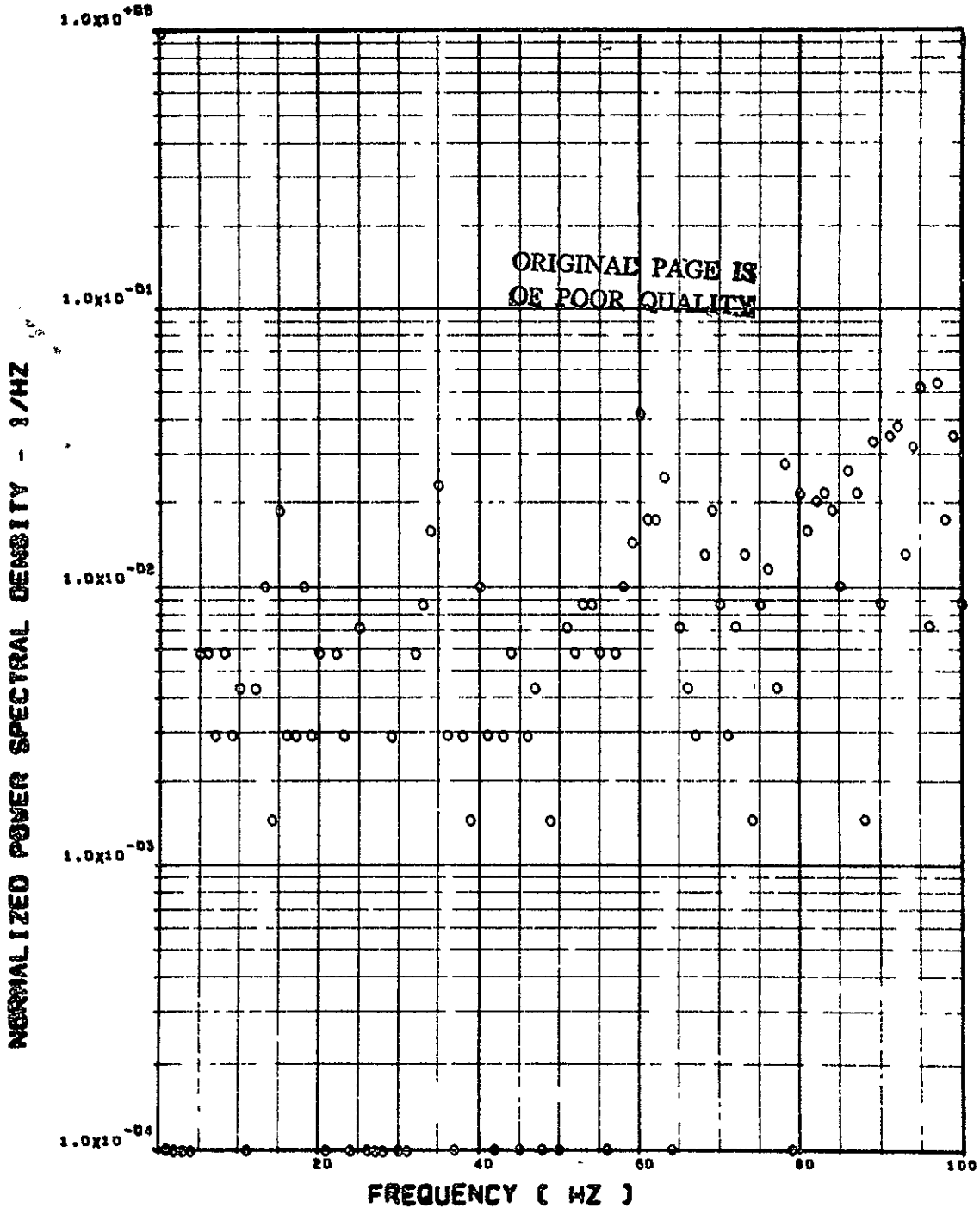

Figure 13. Continued

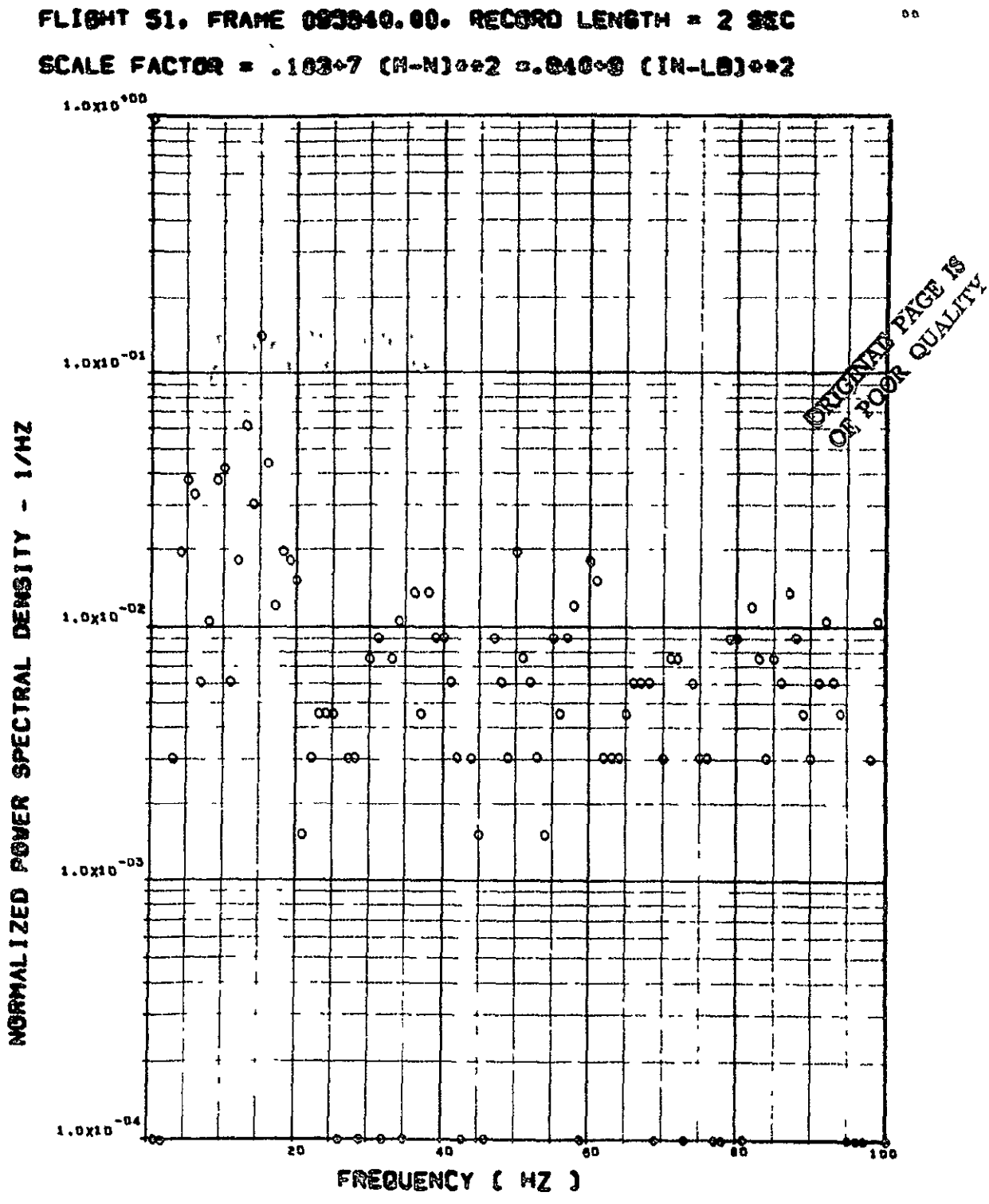

Figure 13. Continued

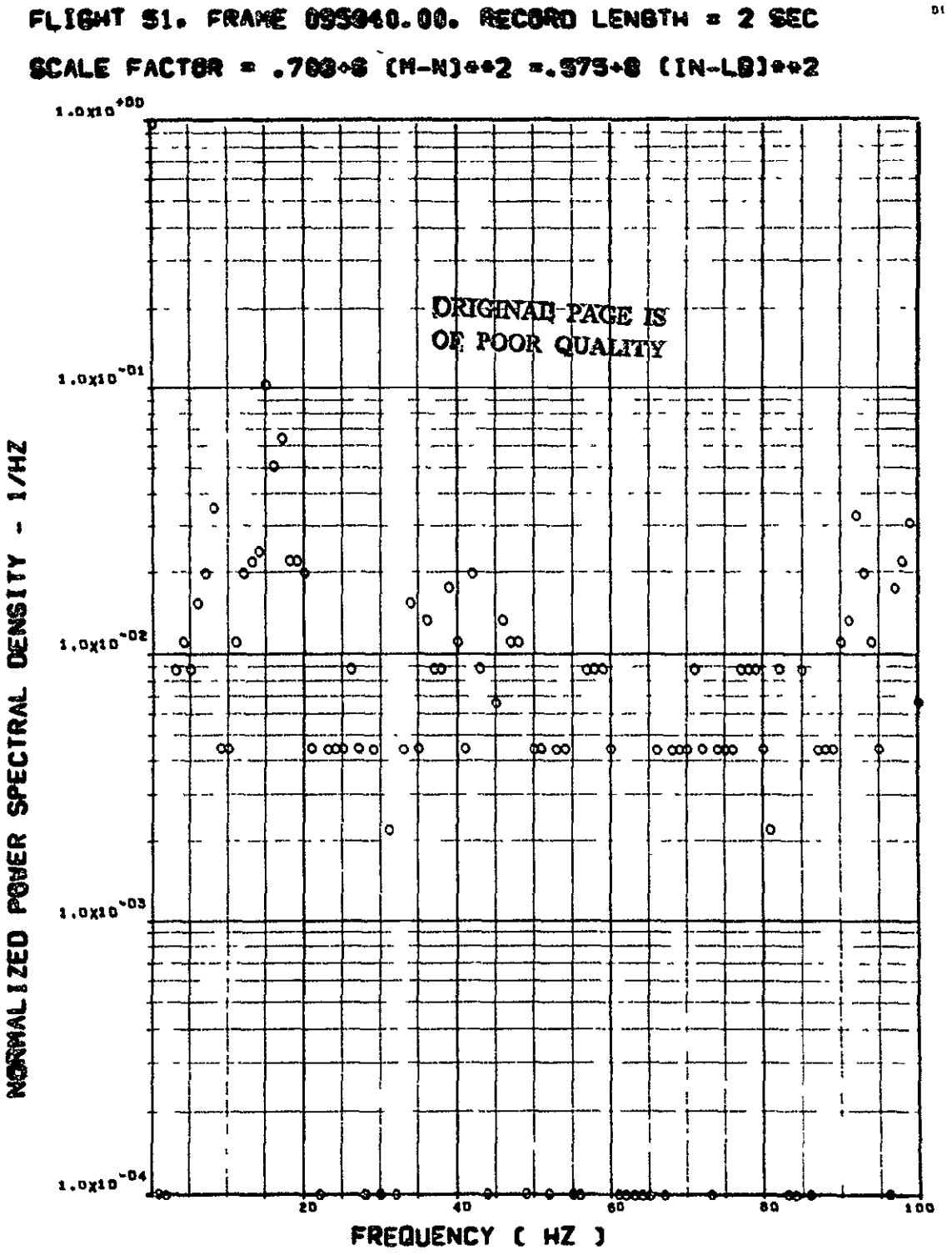

Figure 13. Continued

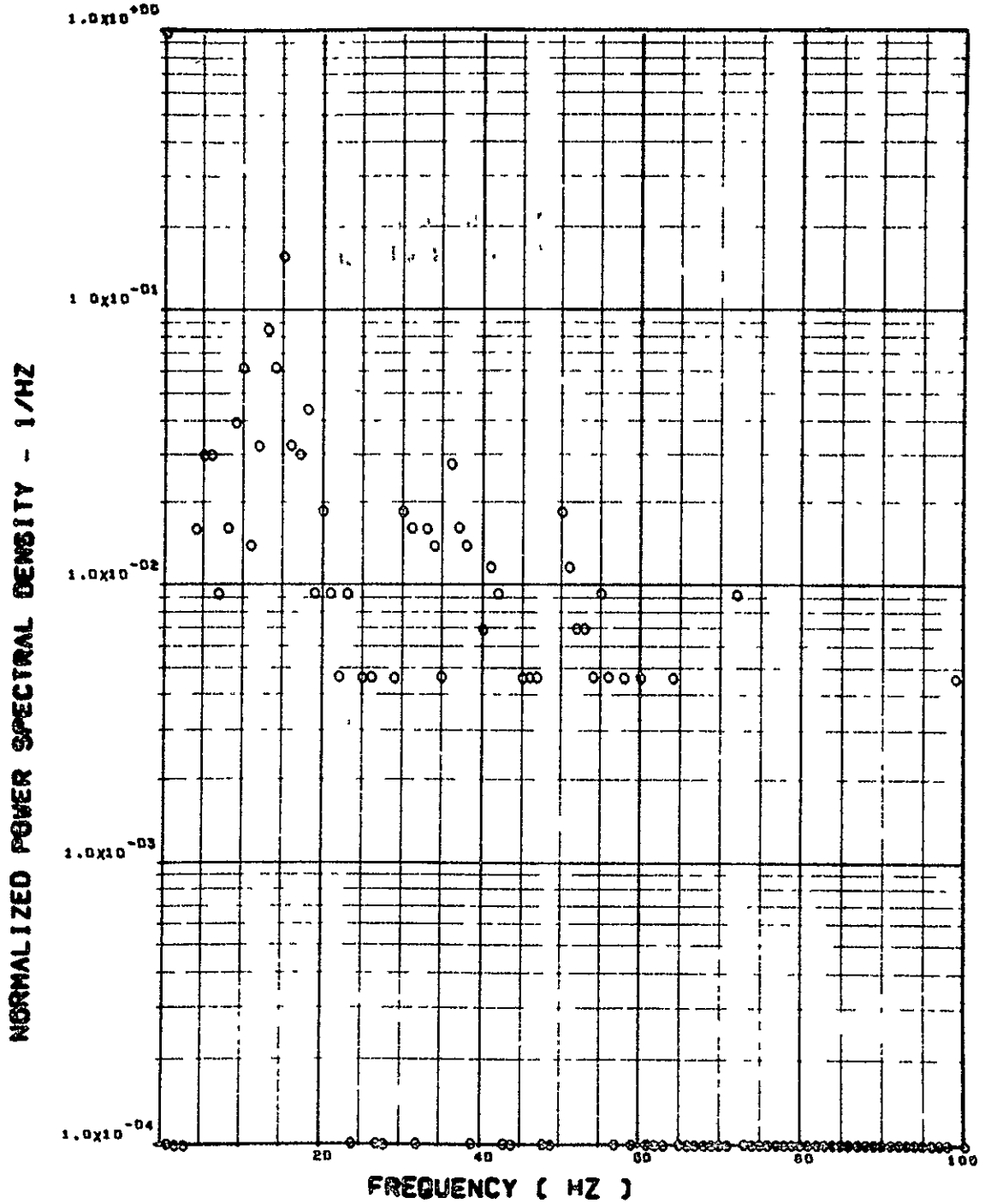

Figure 15. Concluded

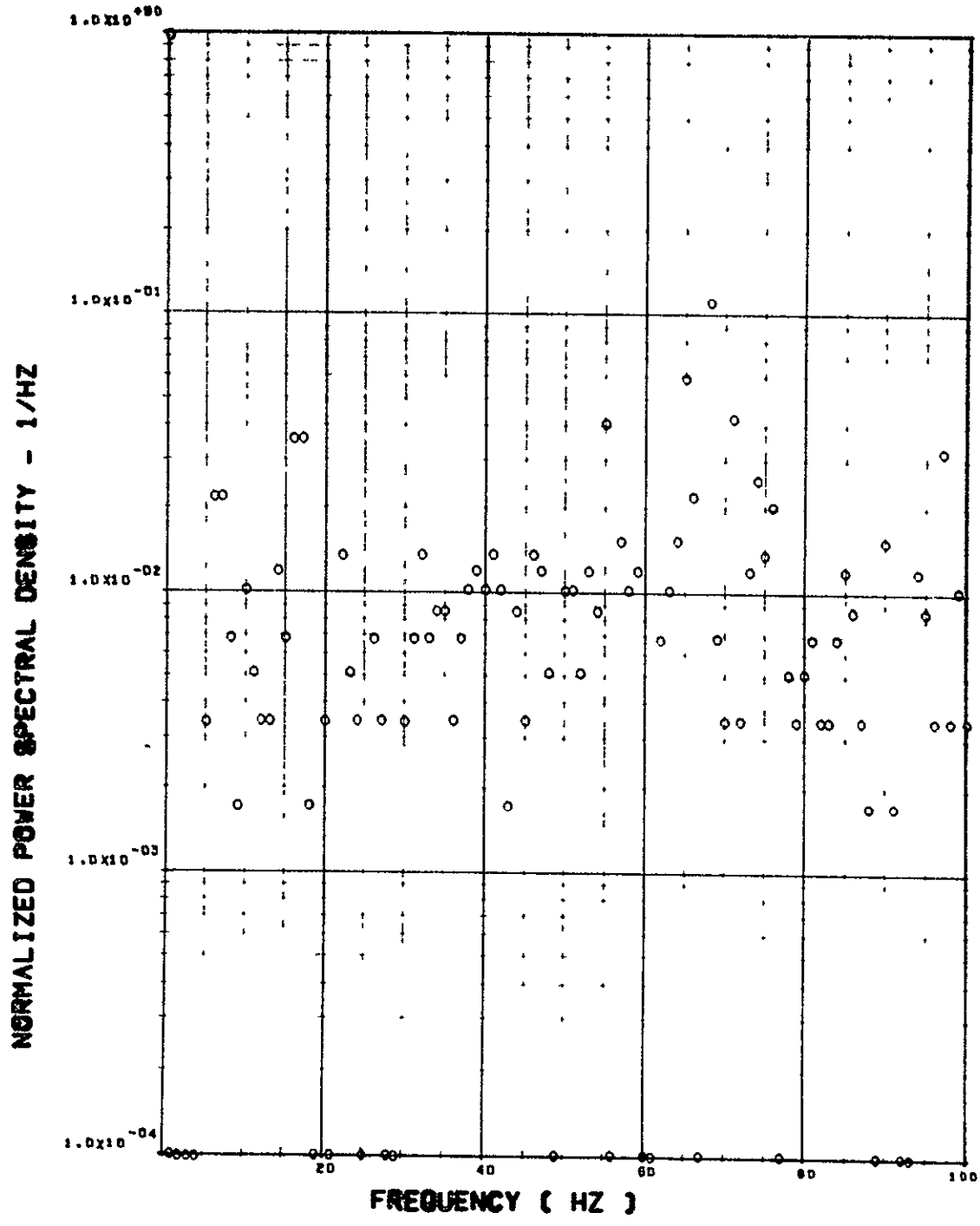

Figure 14. Power Spectra, Flight 51, Run S38/150, Point 2, T_1 = 95943.0, ΔT = 1 Sec, α_{Nom} = 16.25 deg, α = 0.50 deg

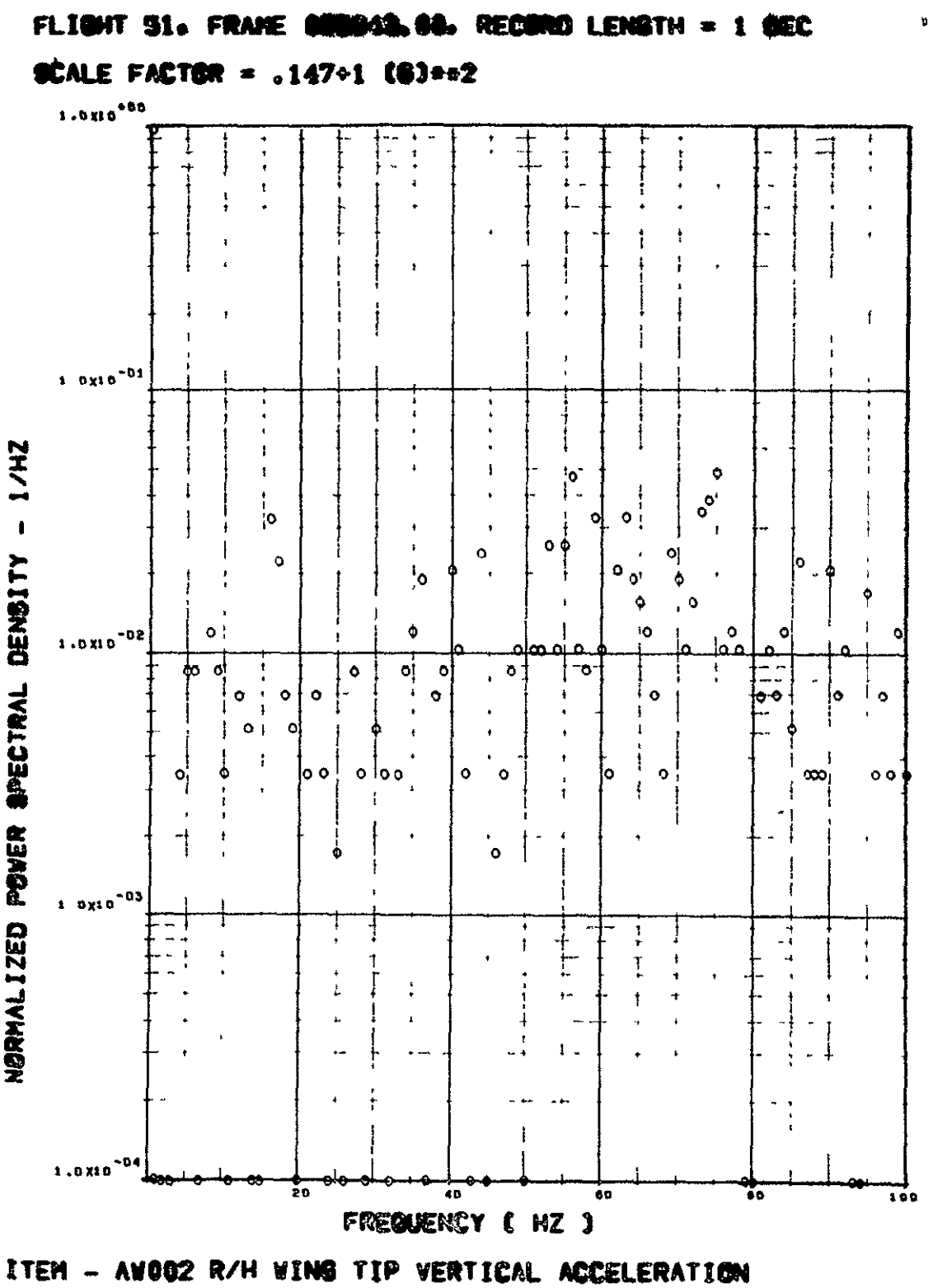

Figure 14. Continued

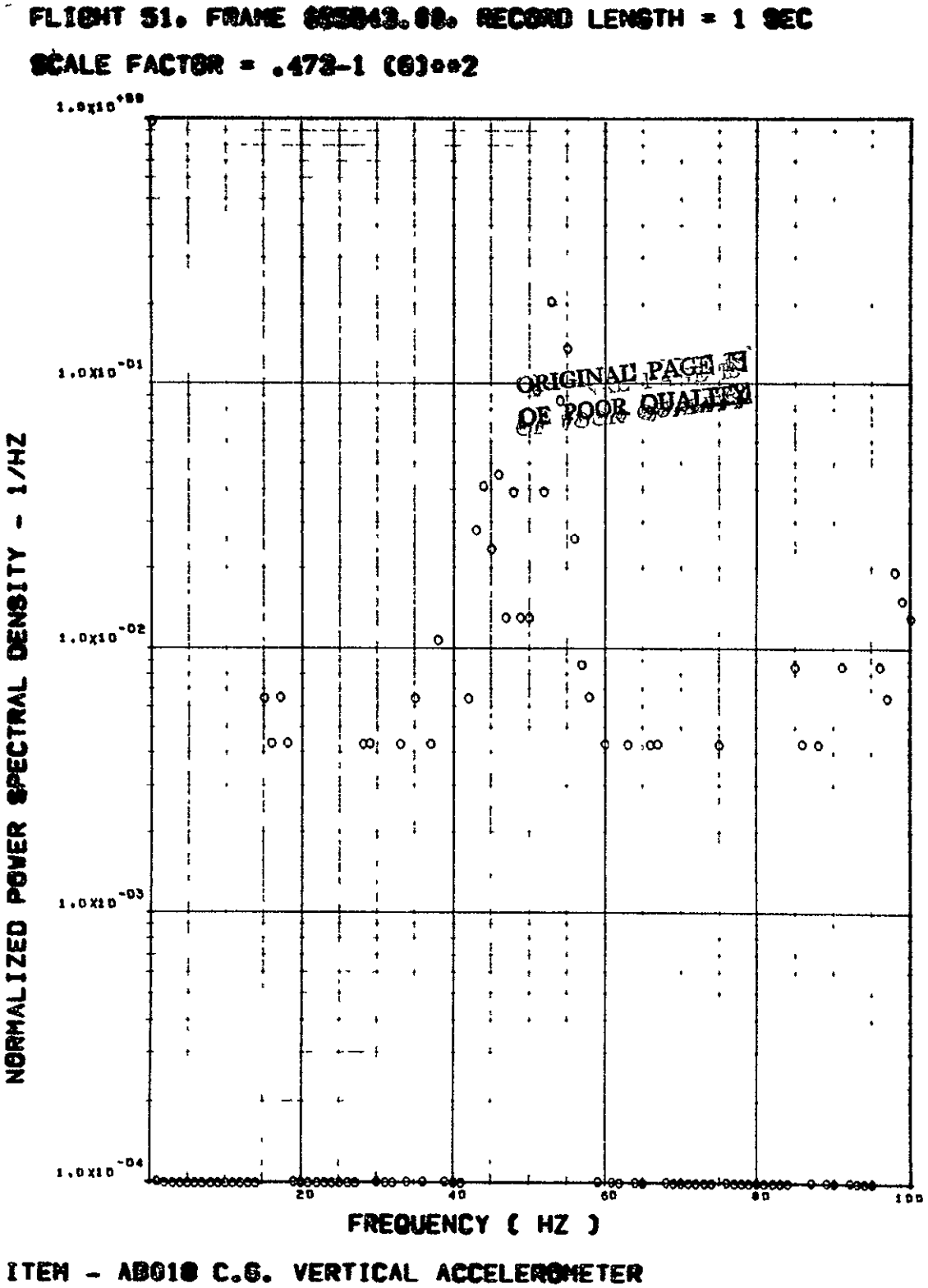

Figure 14. Continued

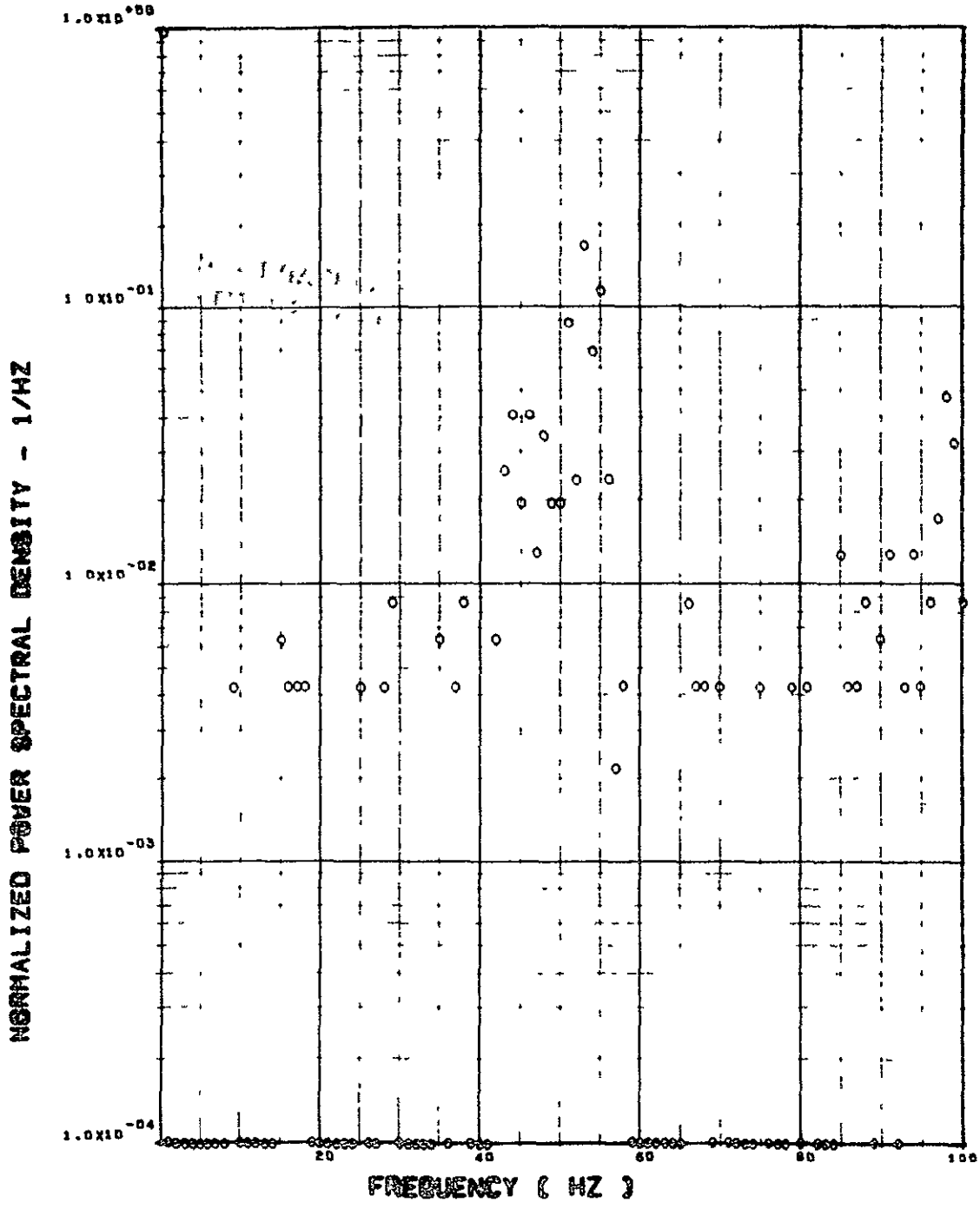

Figure 14. Continued

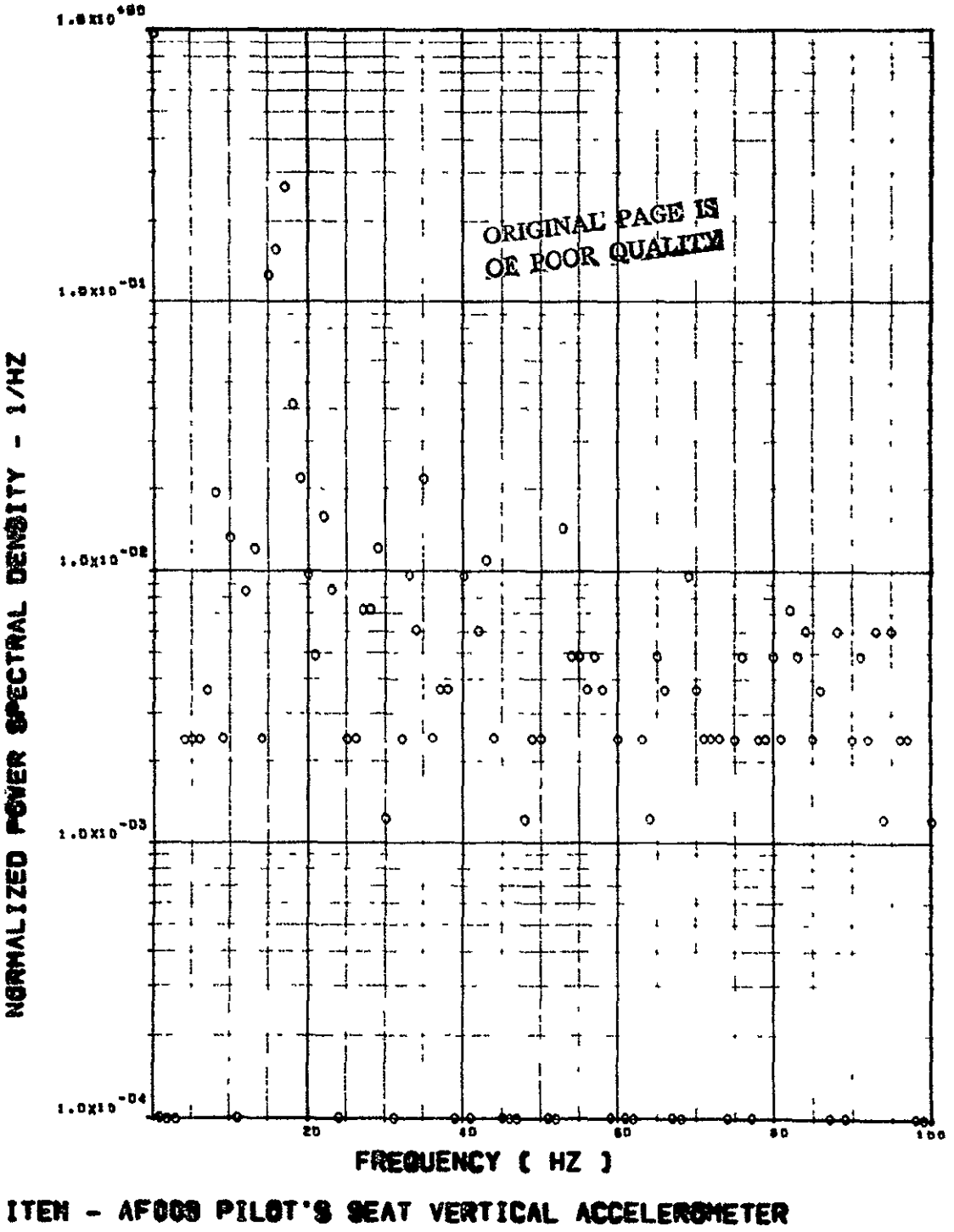

Figure 14. Continued

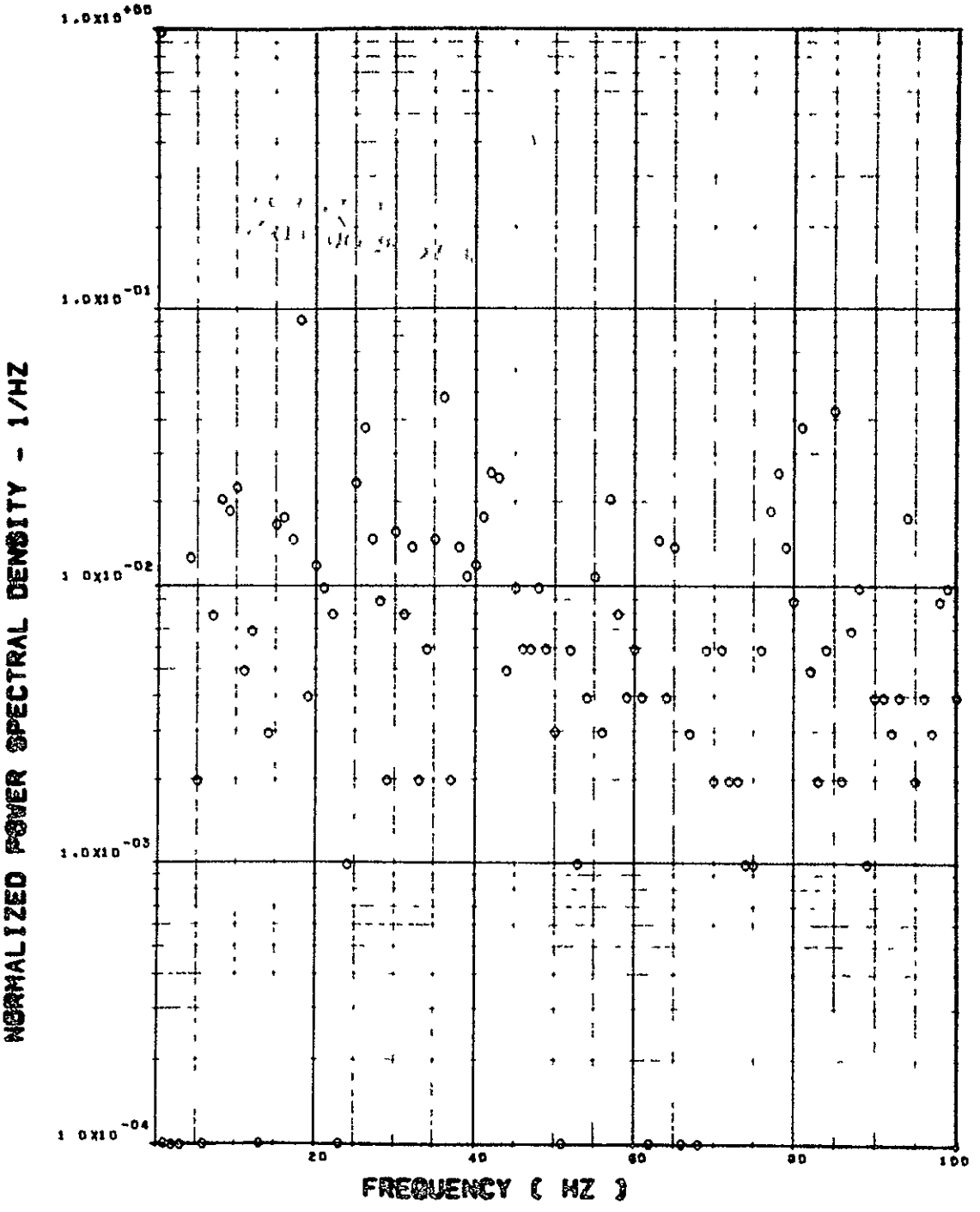

Figure 14. Continued

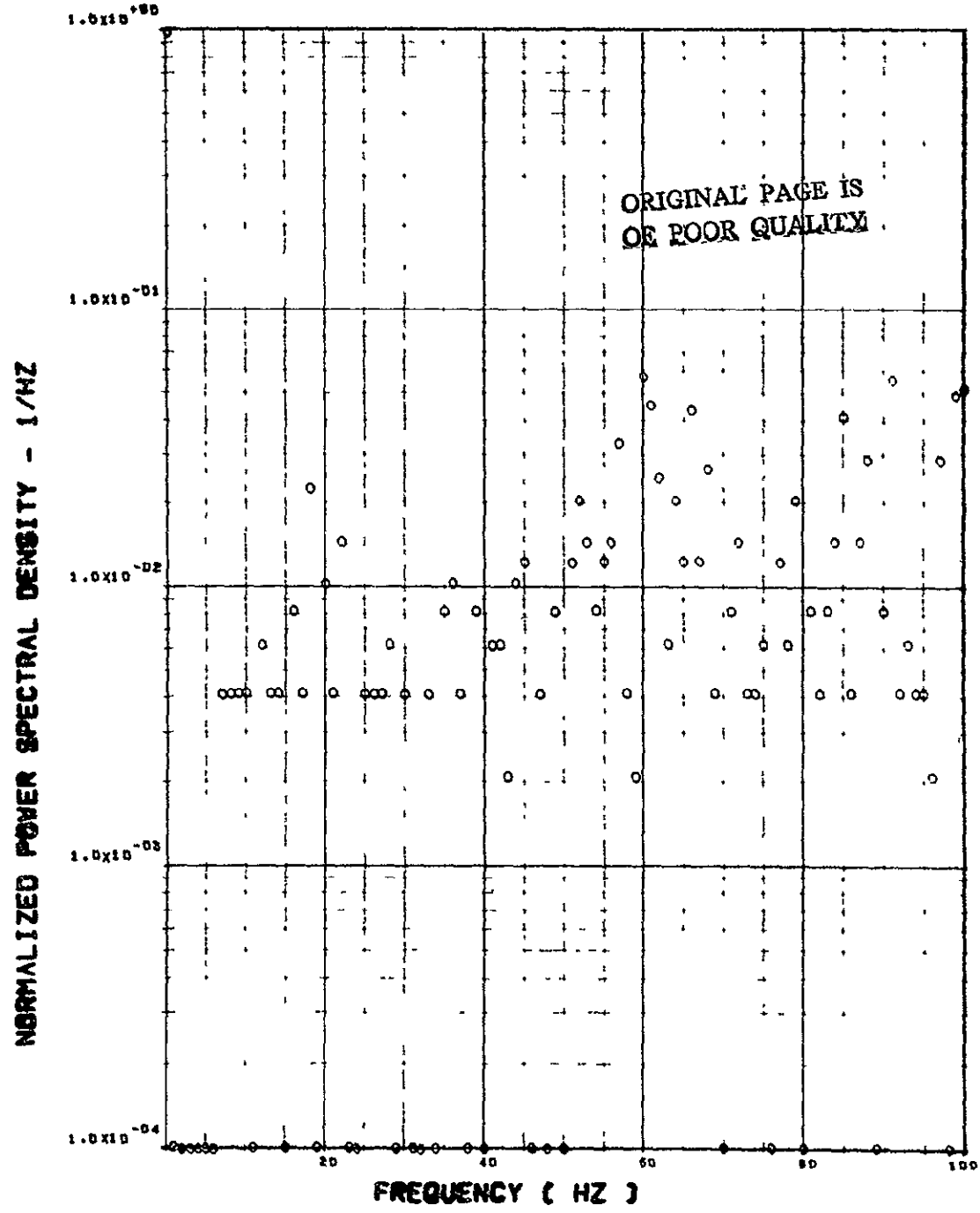

Figure 14. Continued

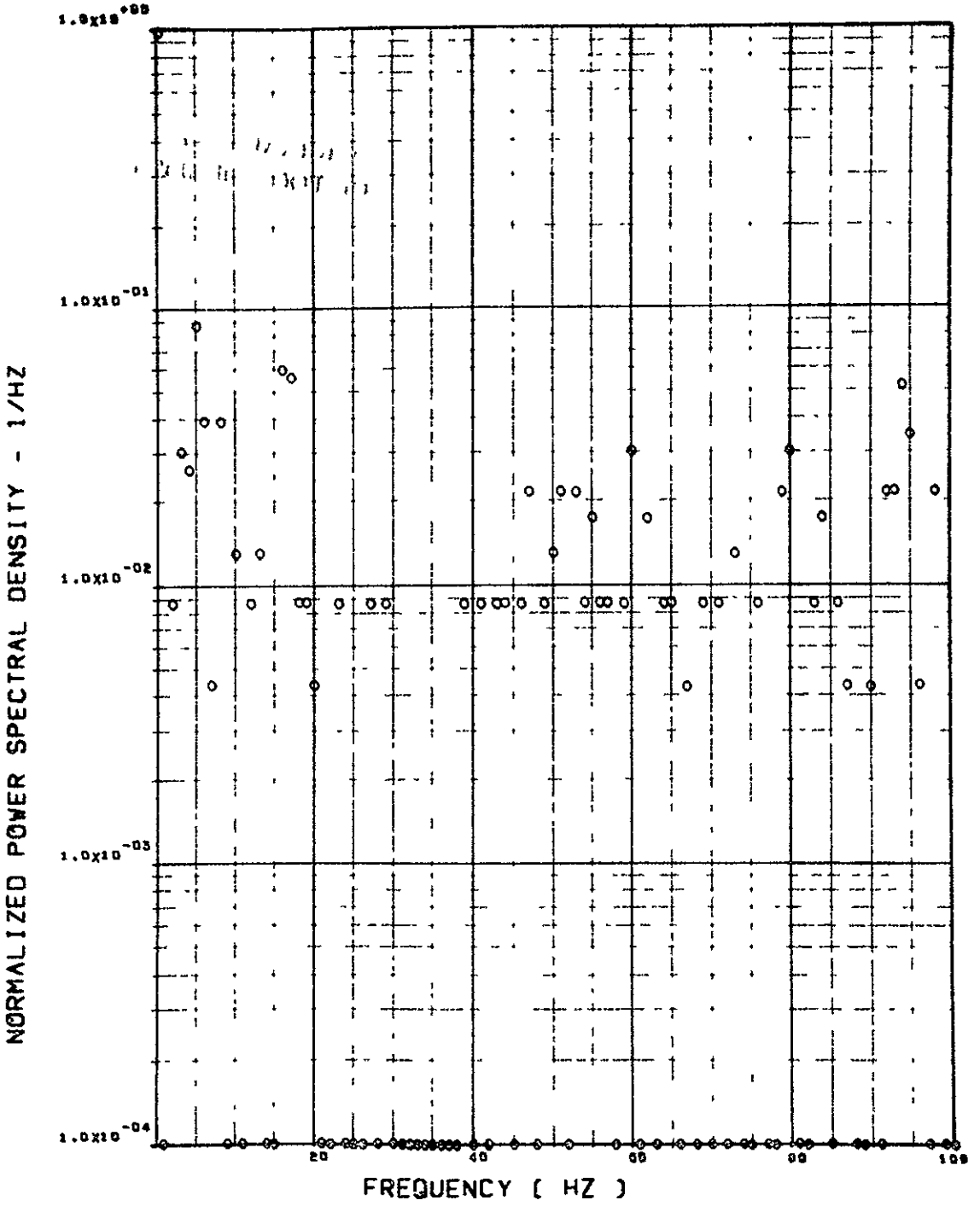

Figure 14. Continued

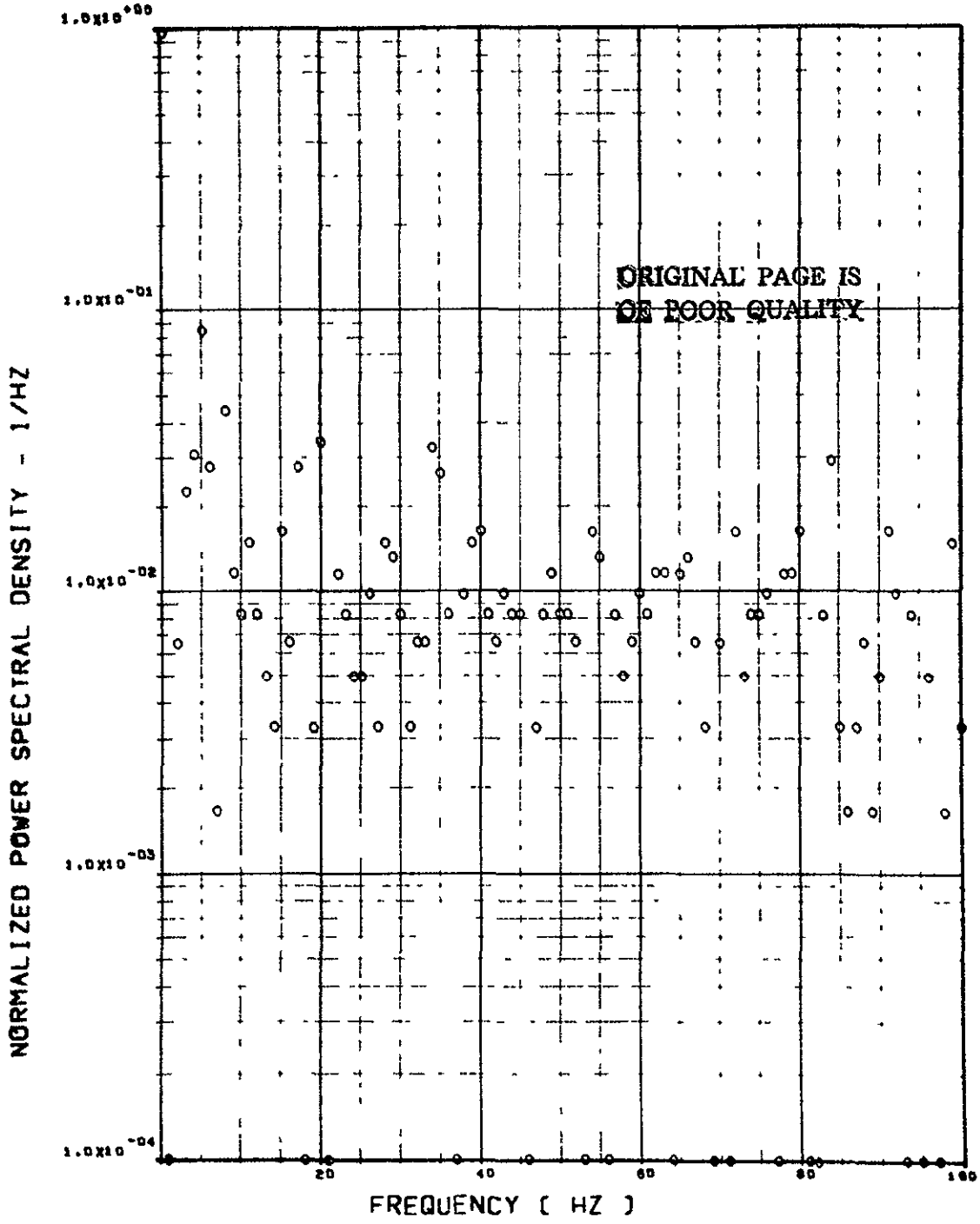

Figure 14. Continued

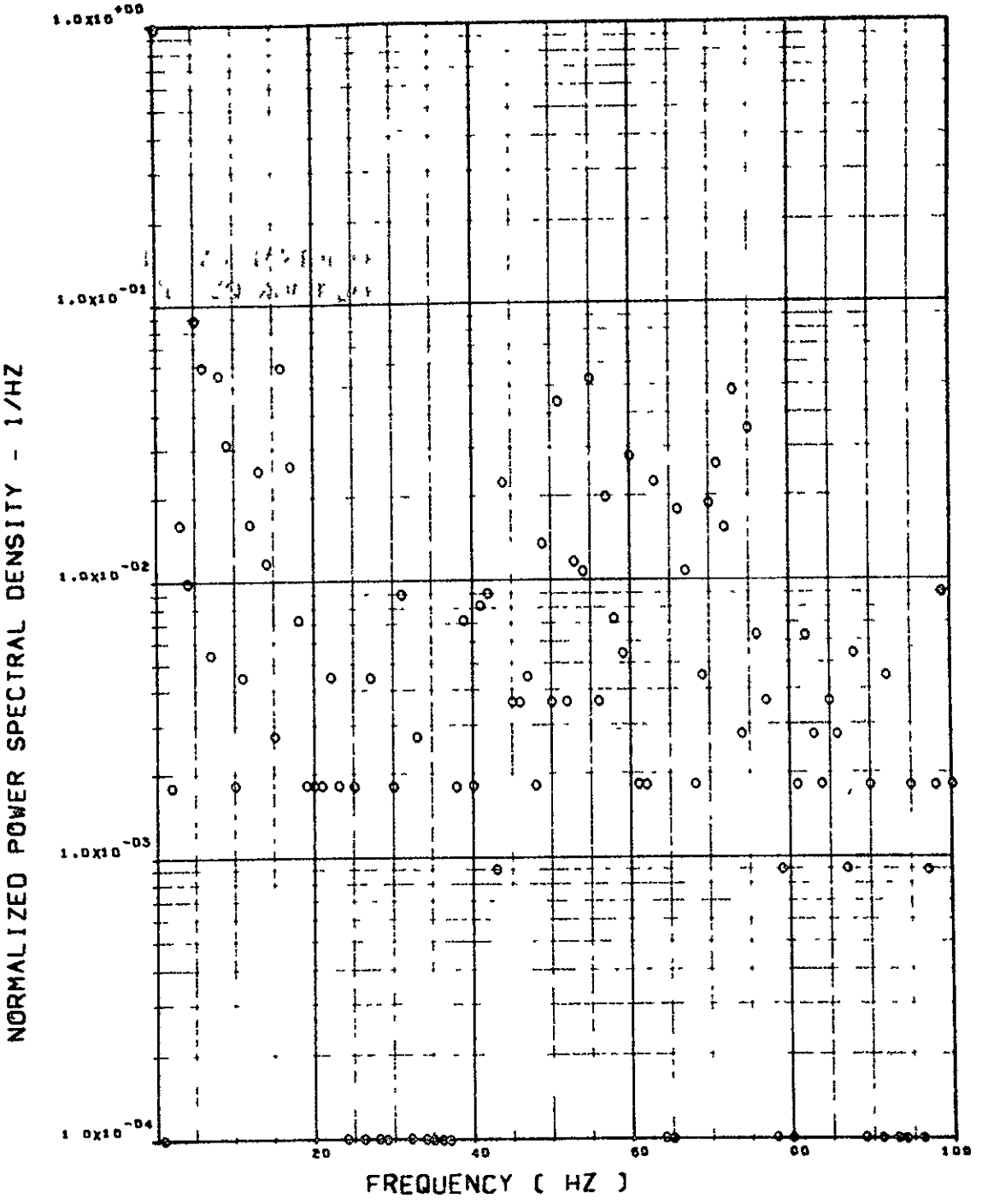

Figure 14. Continued

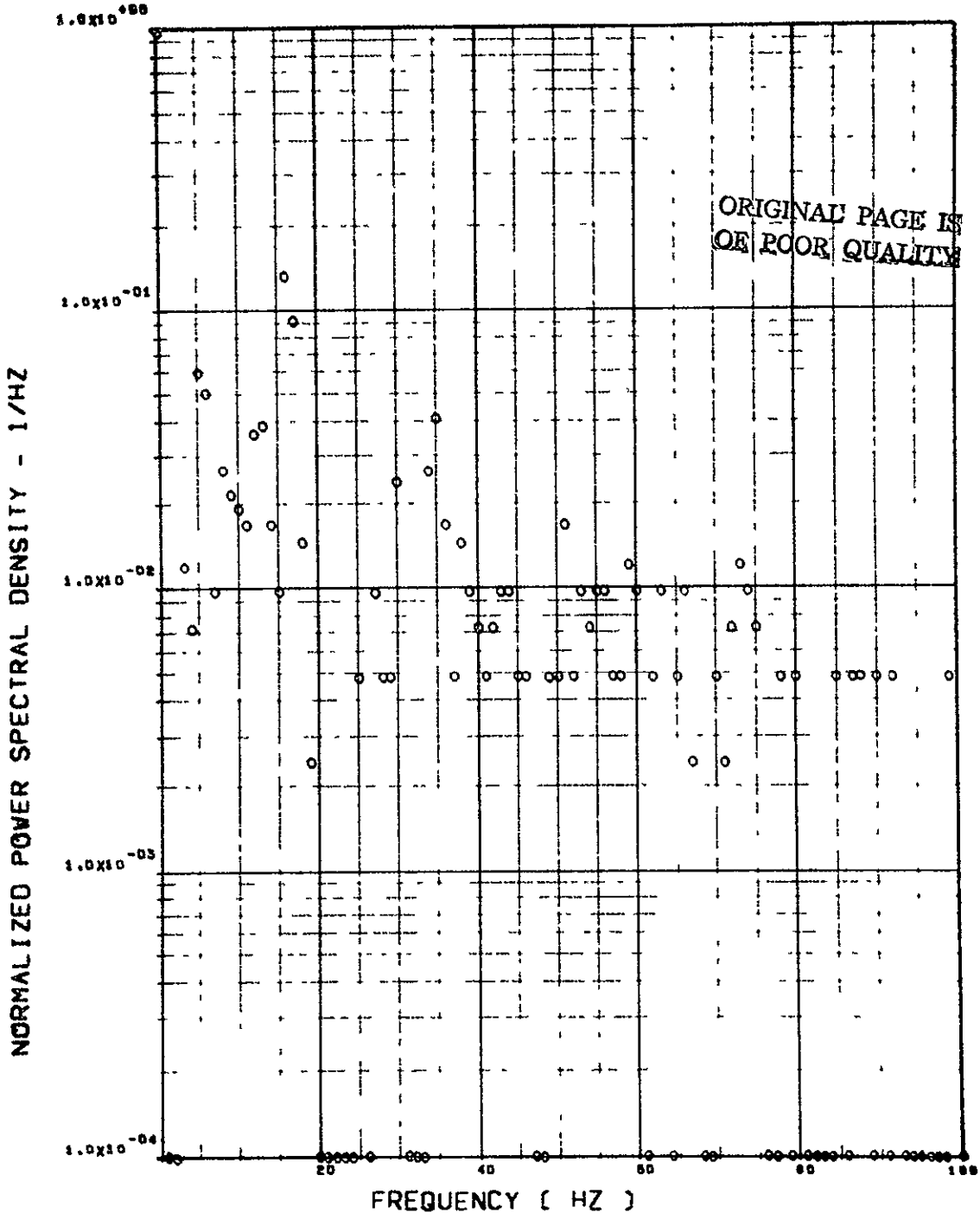

Figure 14. Continued

FLIGHT 51. FRAME 095943.00. RECORD LENGTH = 1 SEC

SCALE FACTOR = .213+8 (M-N)**2 =.173+10(IN-LB)**2

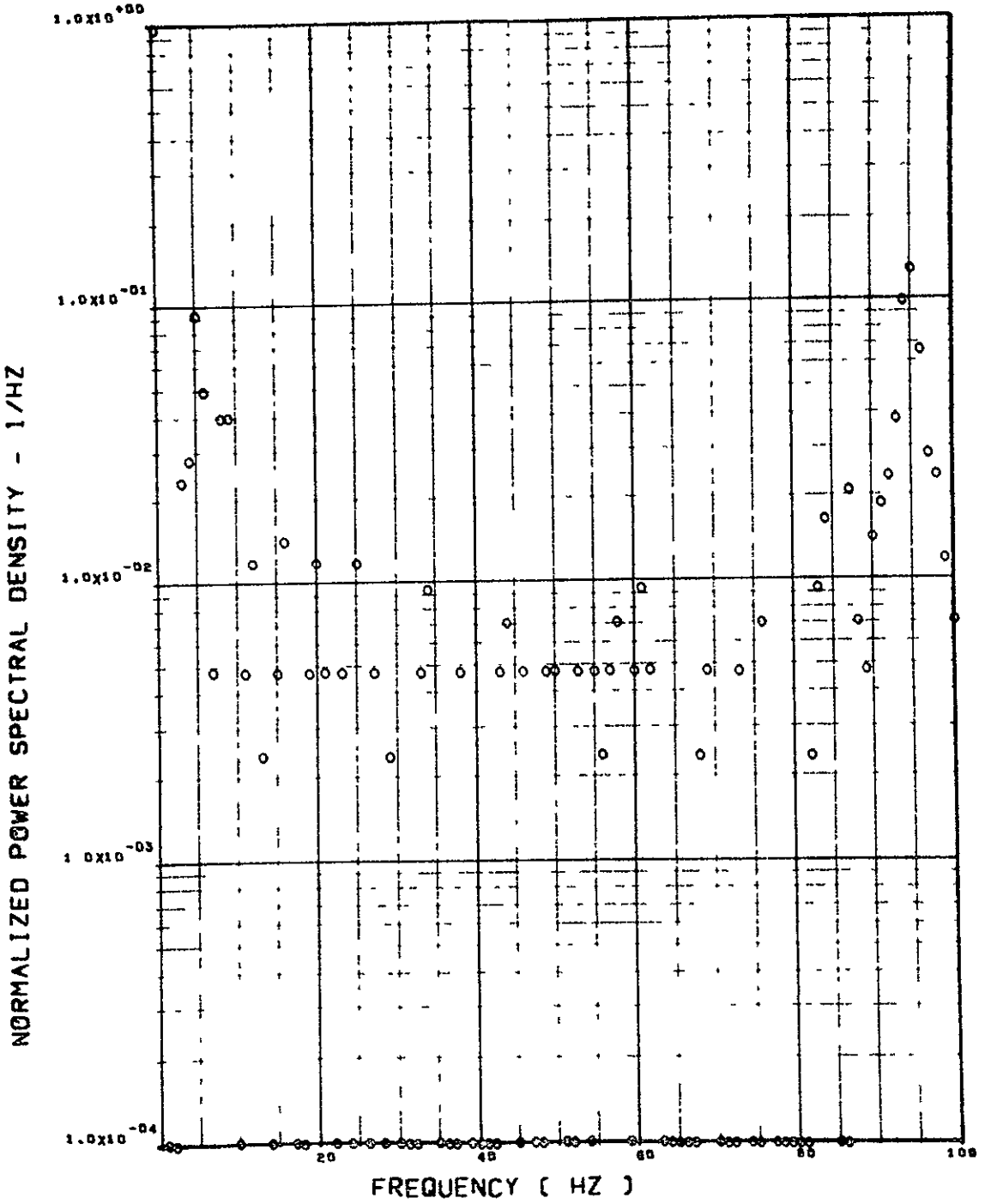

ITEM - SW124 BENDING MOMENT AT WING STATION 1

Figure 14. Continued

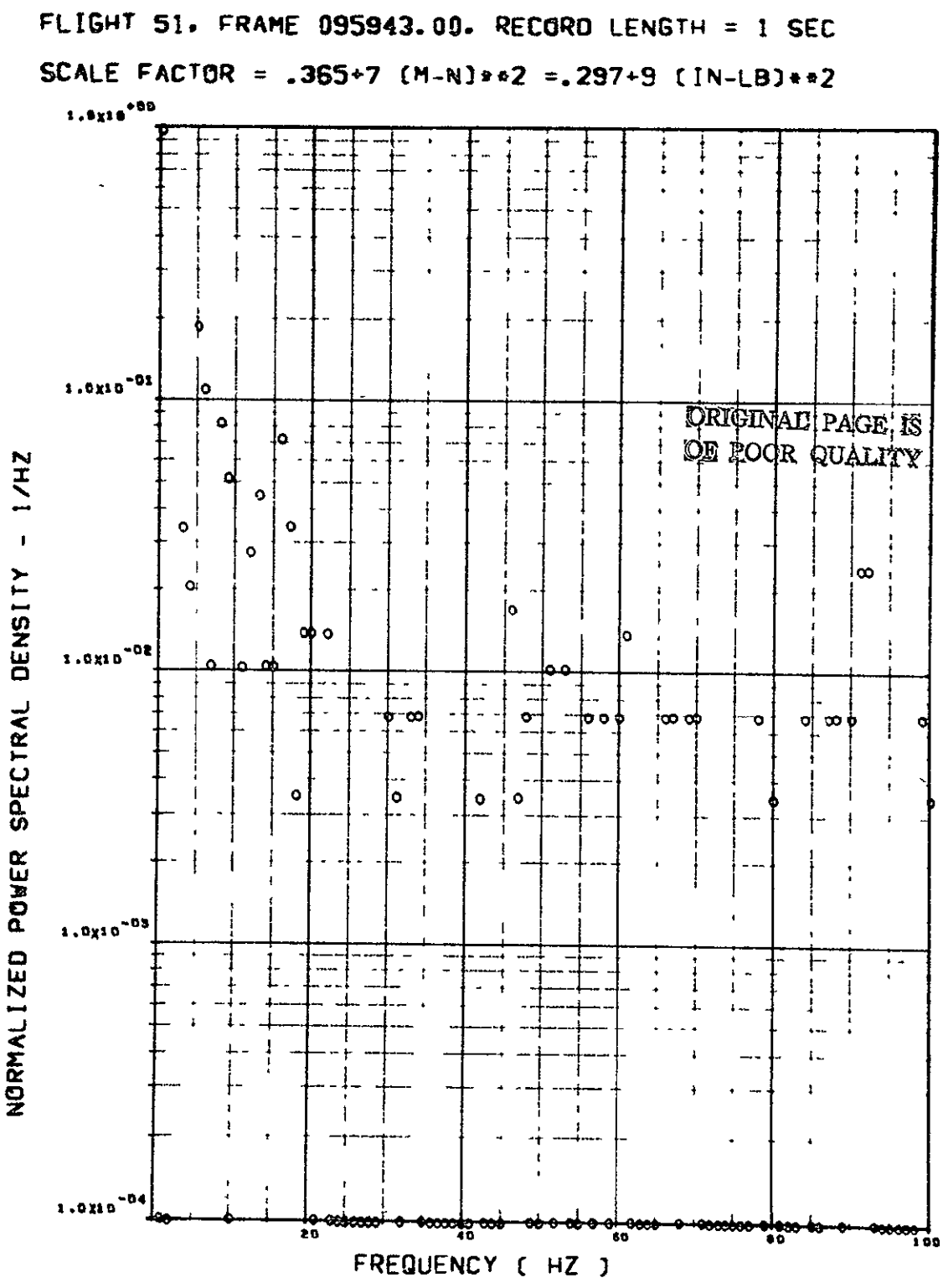

Figure 14. Continued

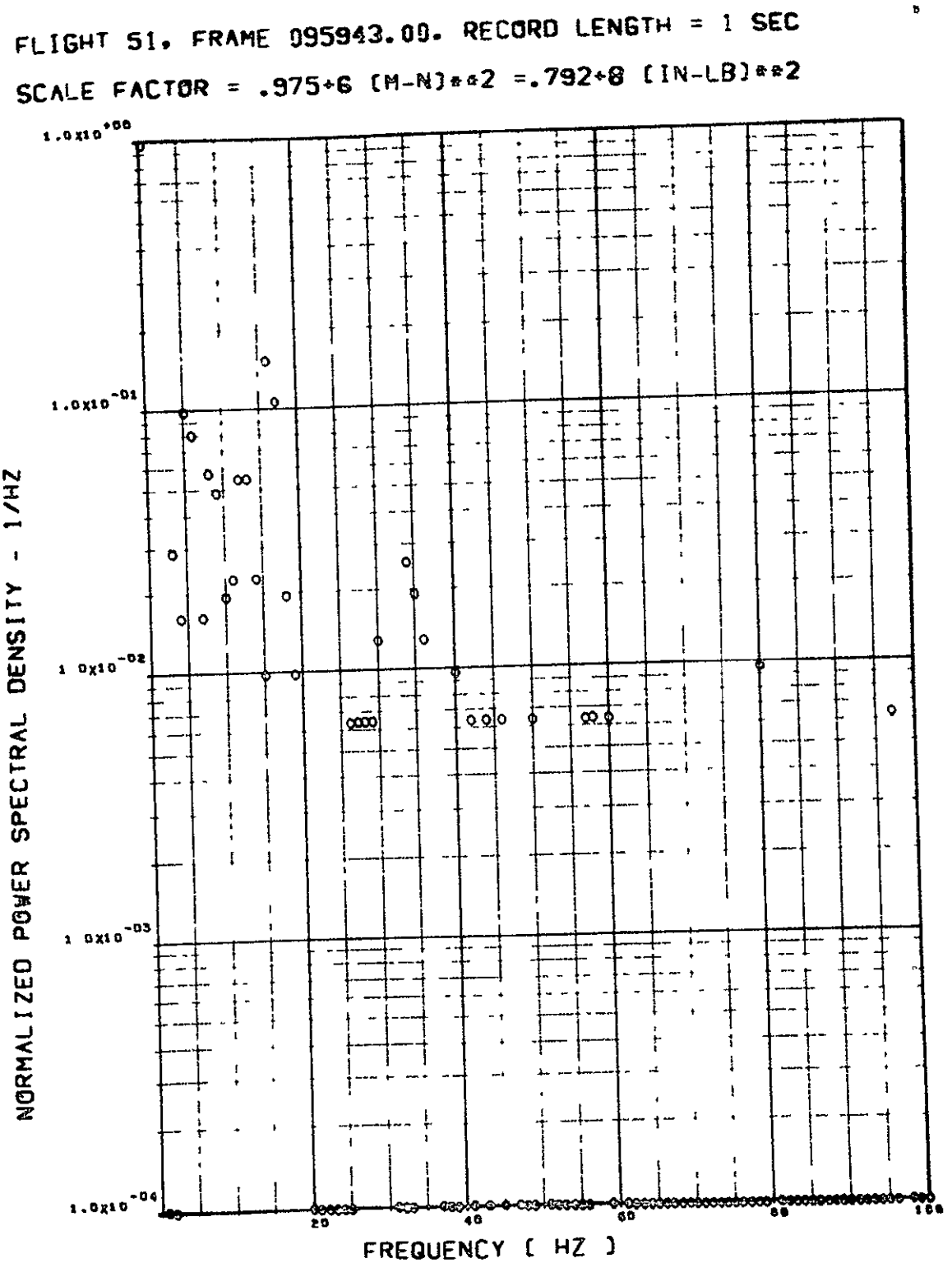

Figure 14. Continued

FLIGHT 51. FRAME 095943.00. RECORD LENGTH = 1 SEC

SCALE FACTOR = .187+6 (M-N)**2 =.152+8 (IN-LB)**2

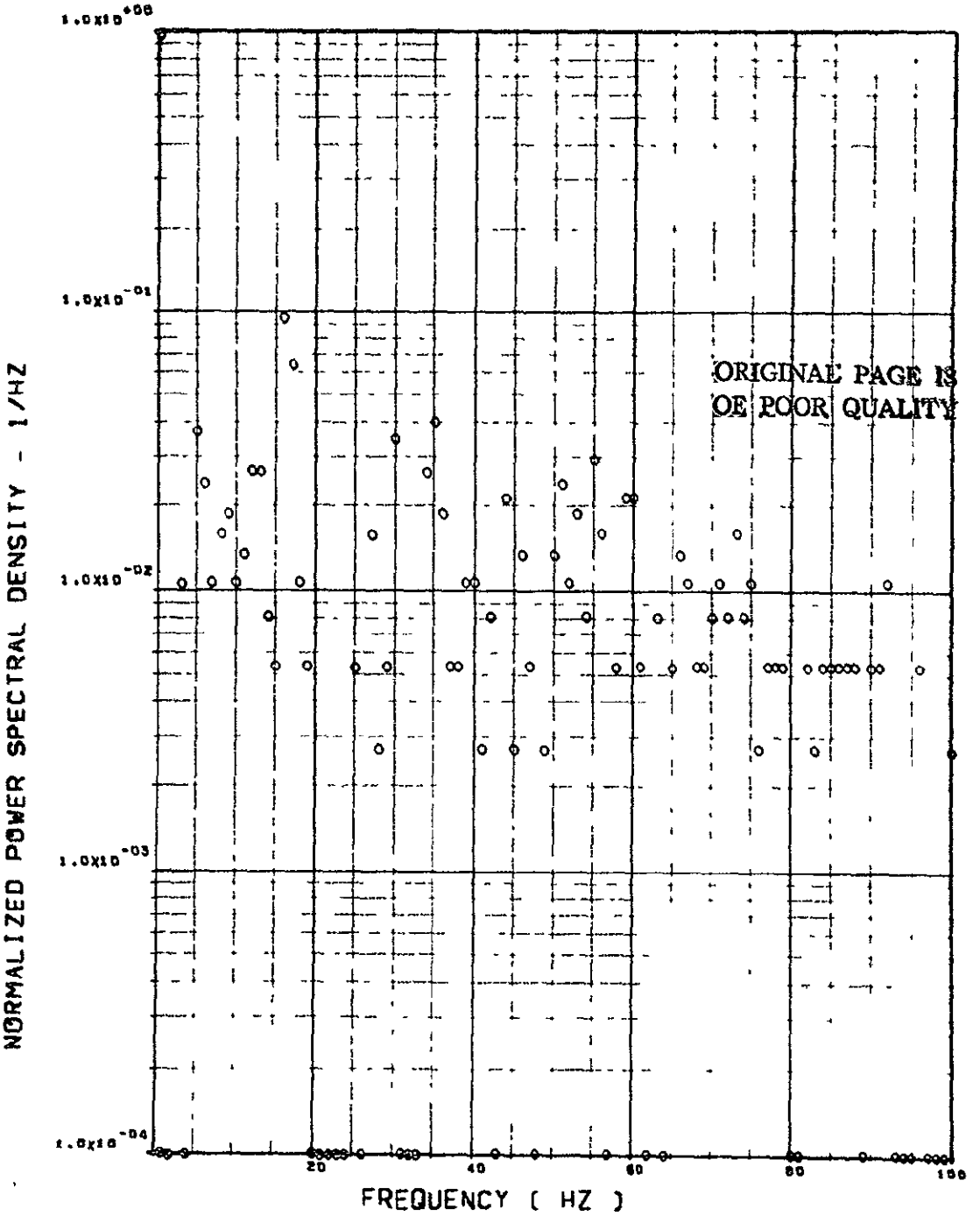

ITEM - SW133 BENDING MOMENT AT WING STATION 4

Figure 14. Continued

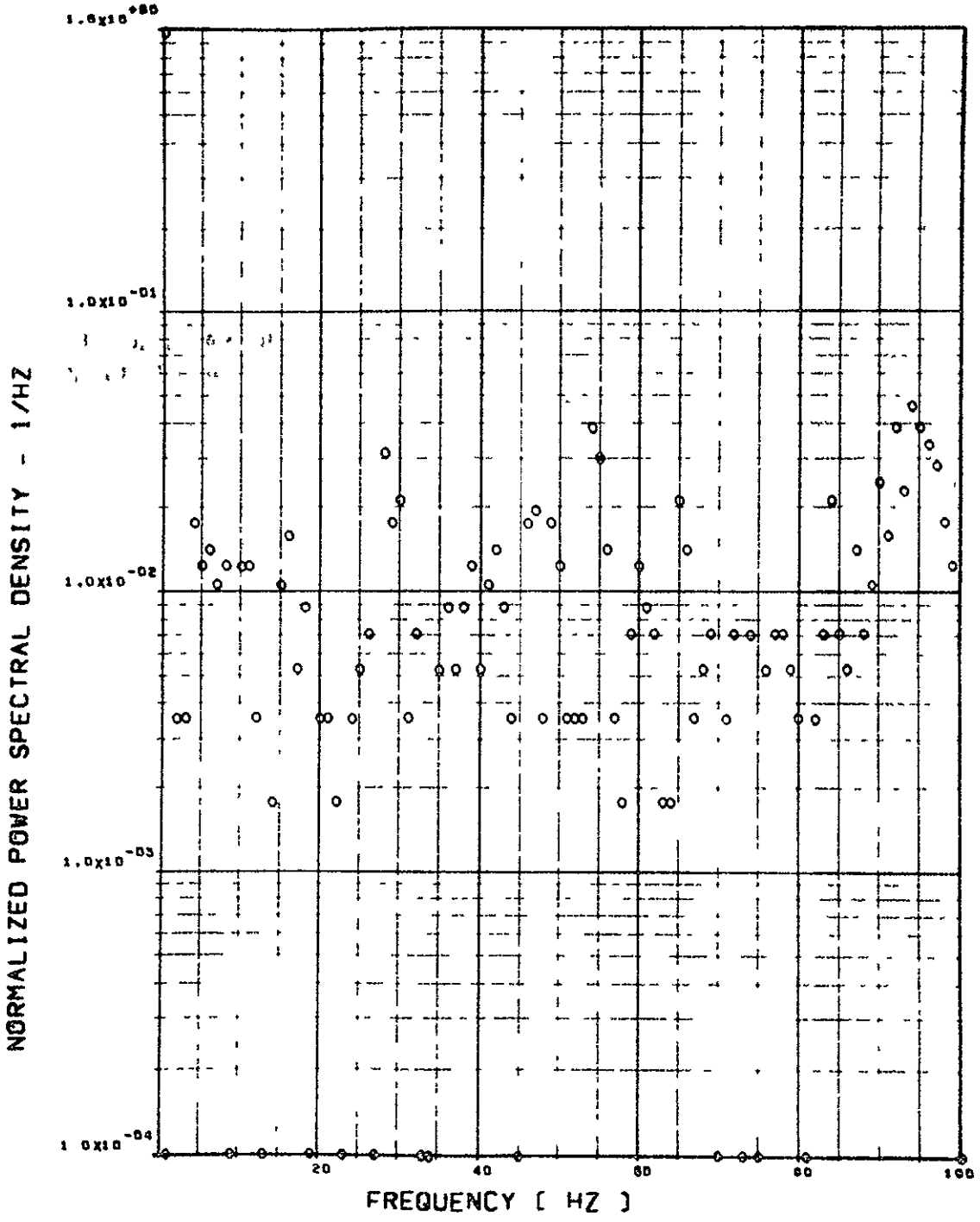

ITEM - SW125 TORSION AT WING STATION 1

Figure 14. Continued

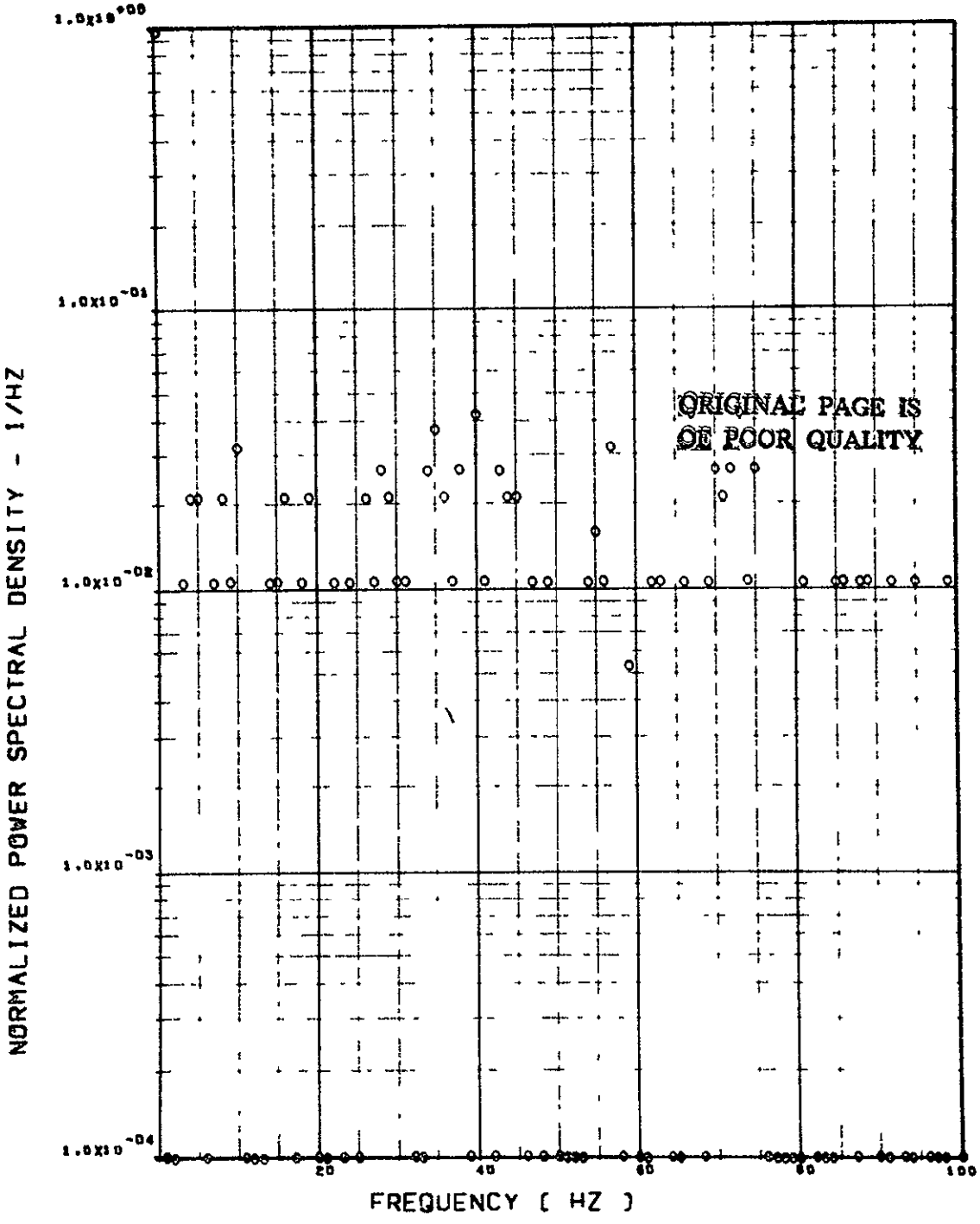

Figure 14. Continued

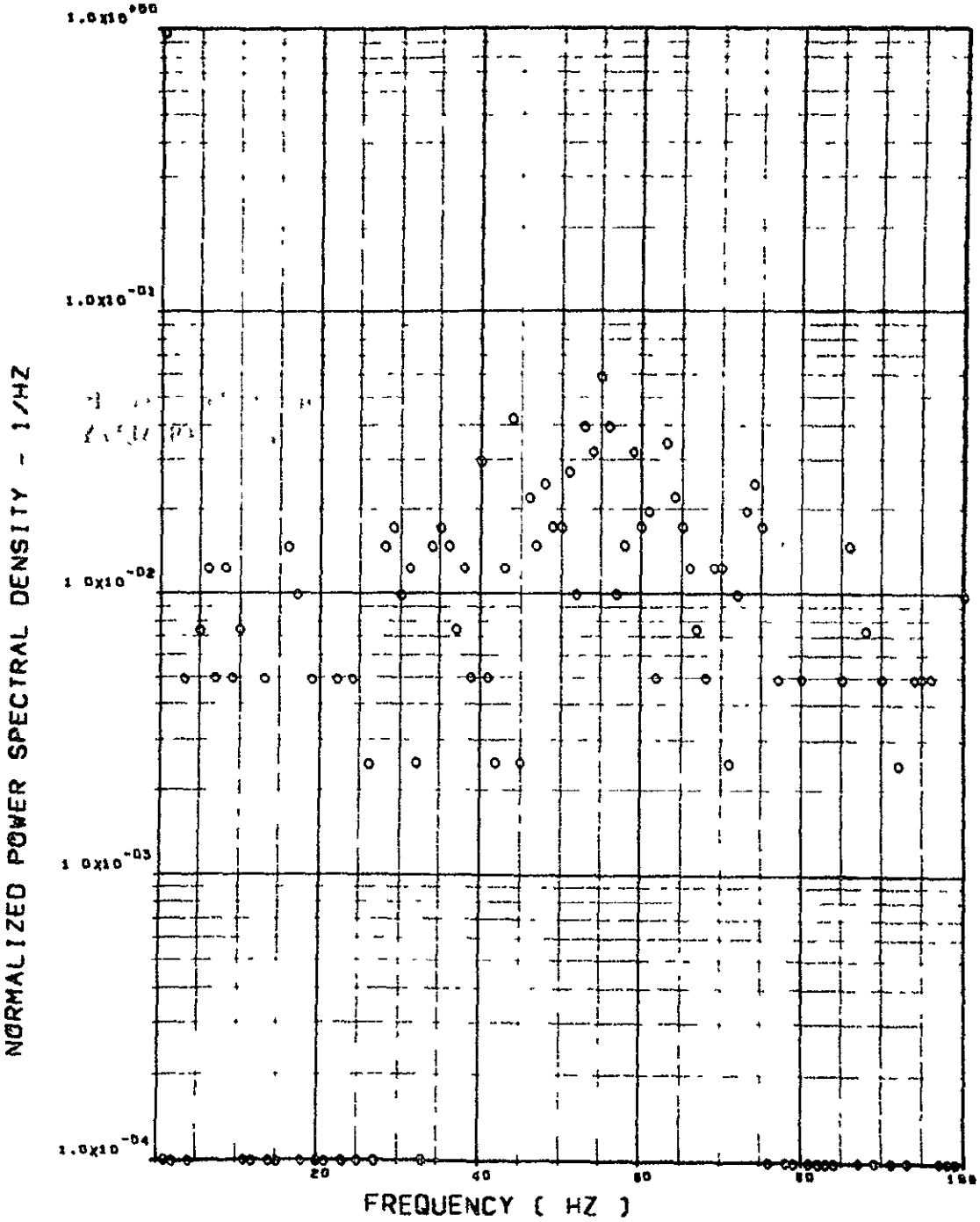

Figure 14. Continued

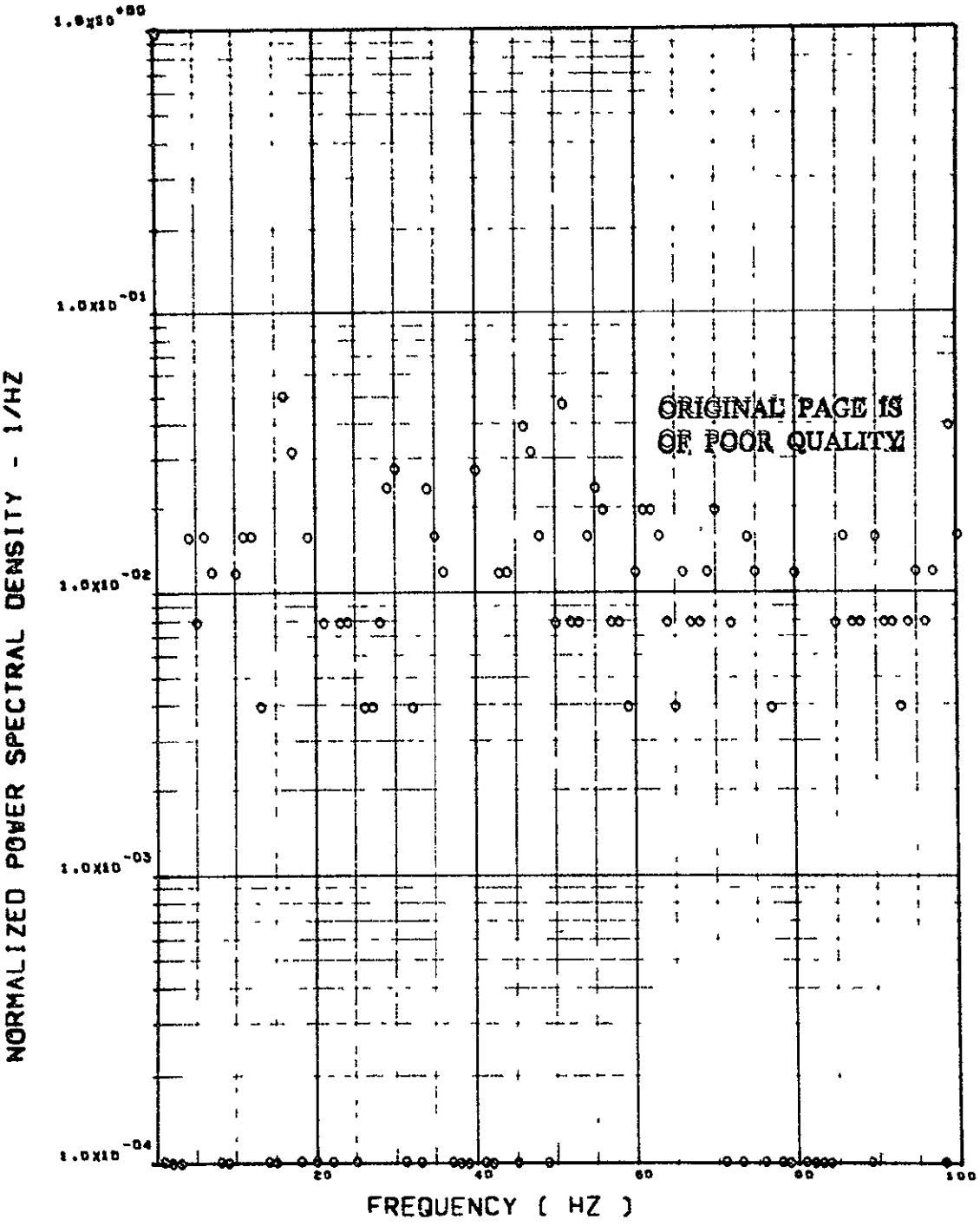

ITEM - SW134 TORSION AT WING STATION 4

Figure 11. Continued

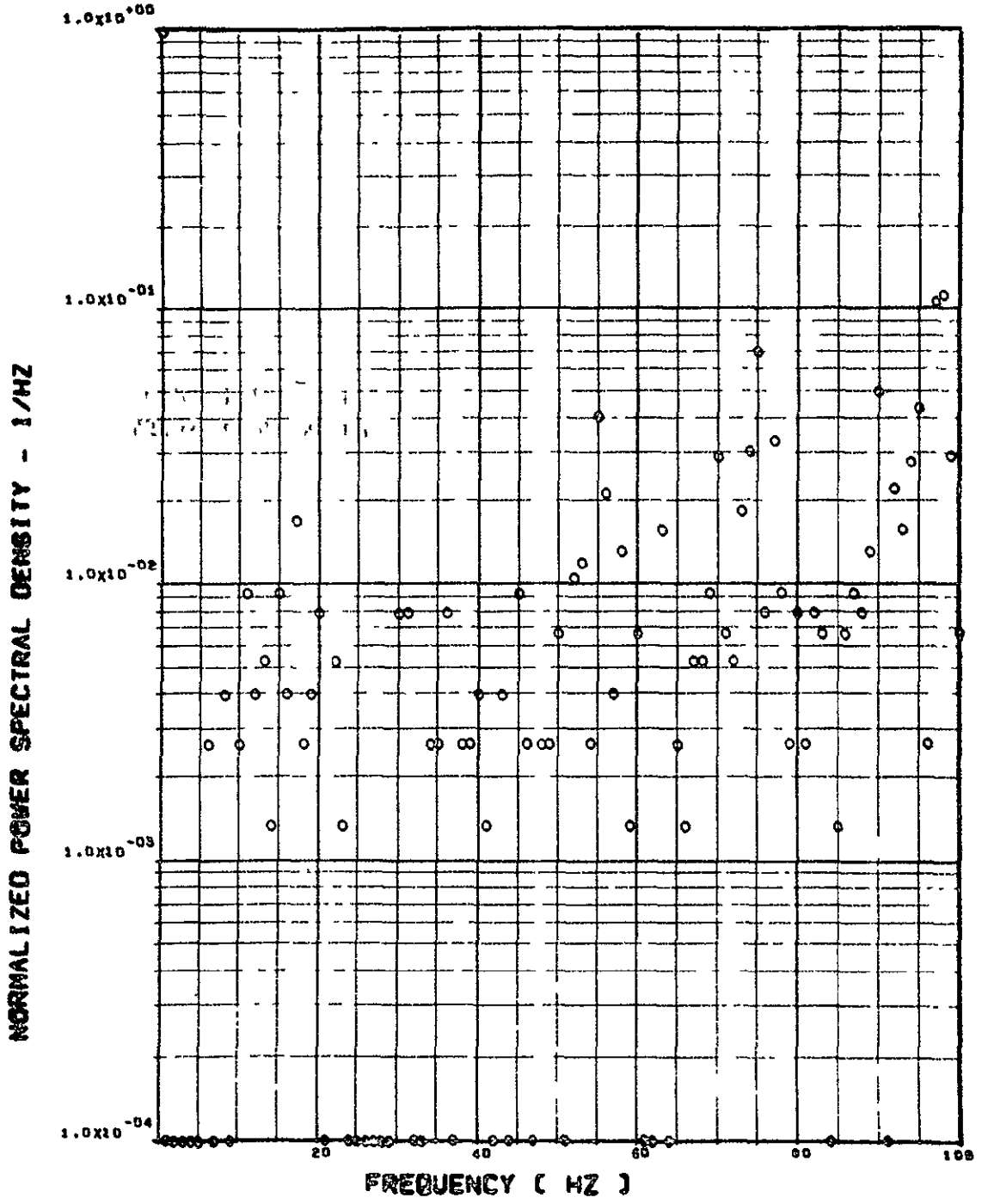

Figure 14. Continued

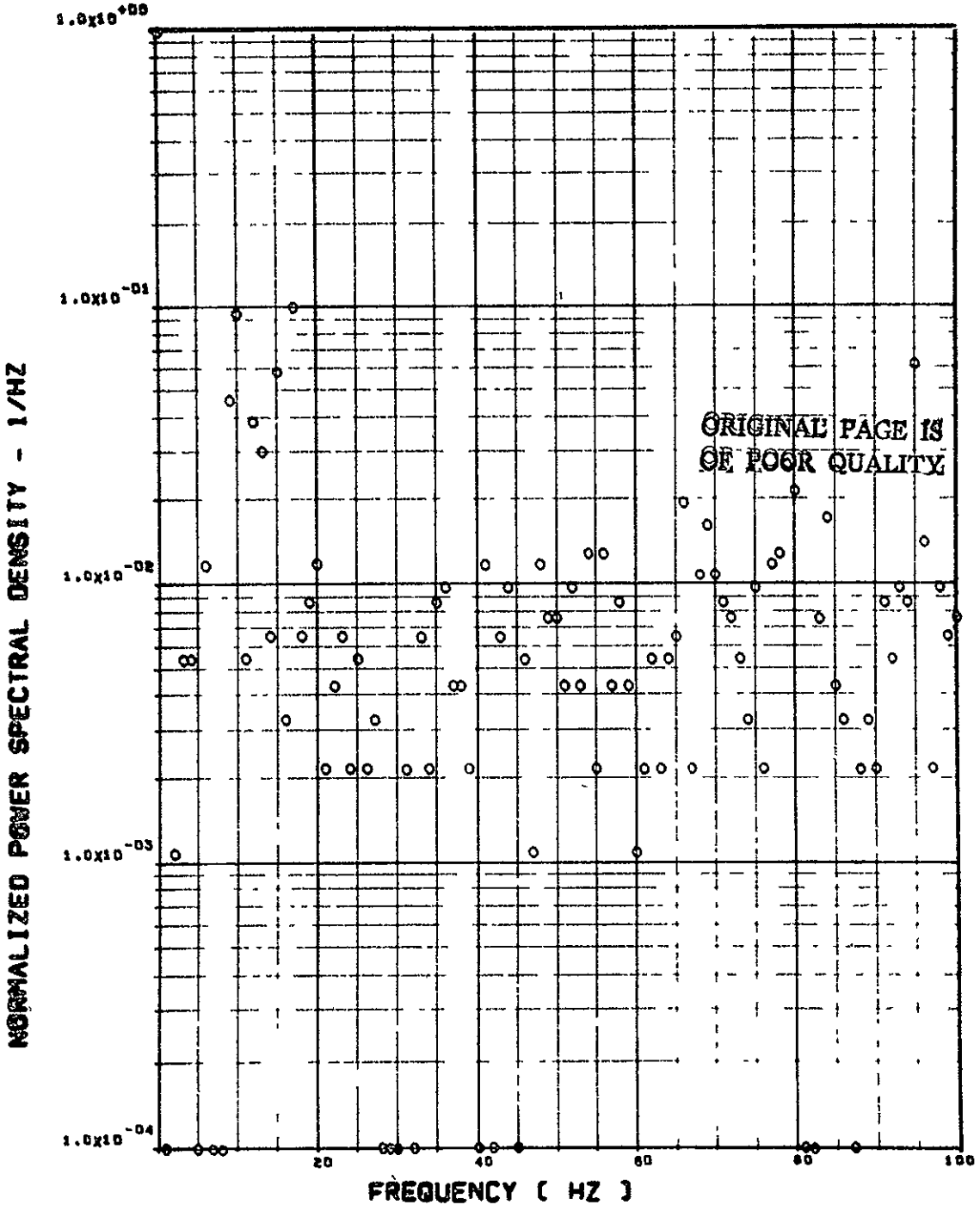

Figure 14. Continued

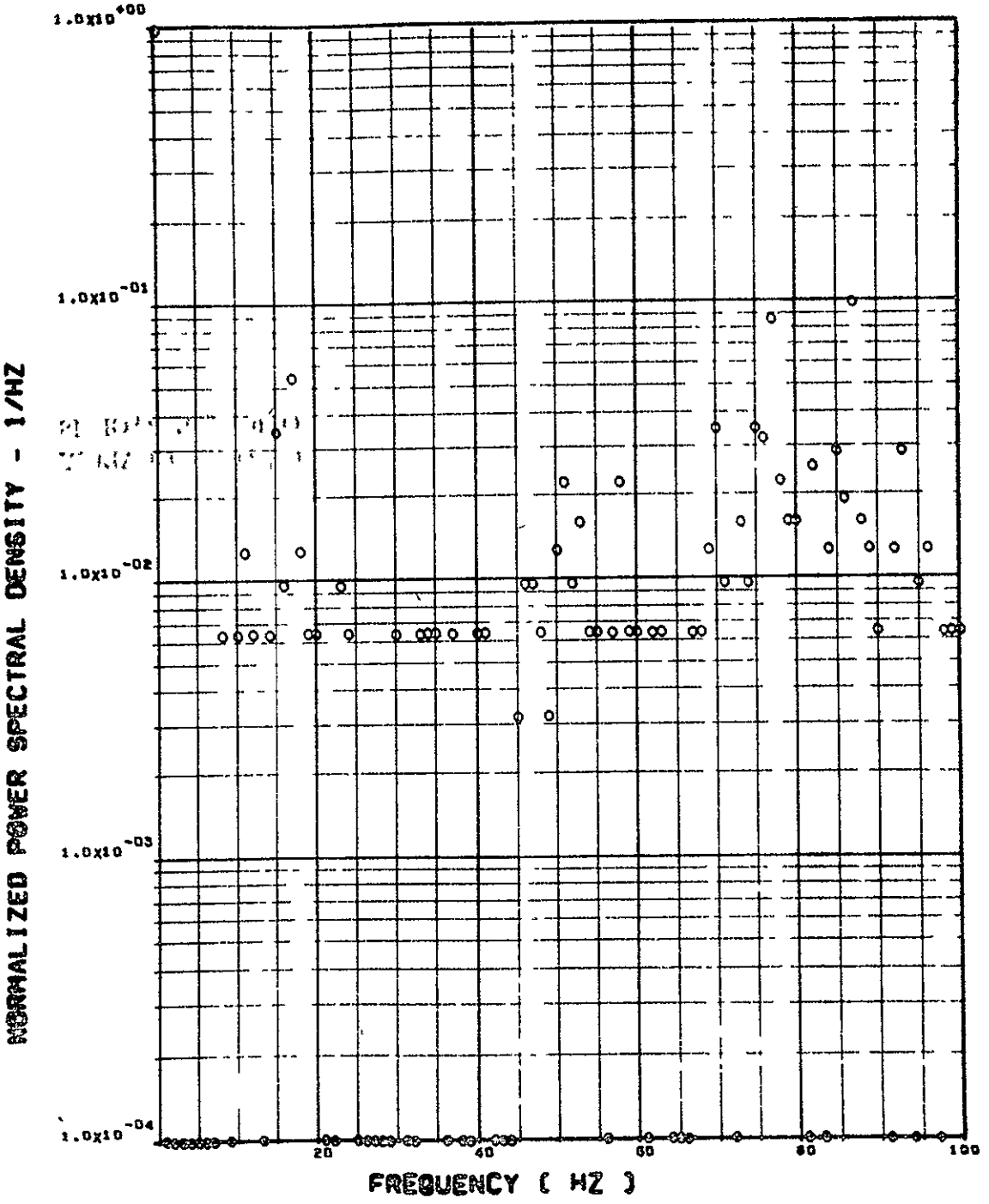

Figure 14. Continued

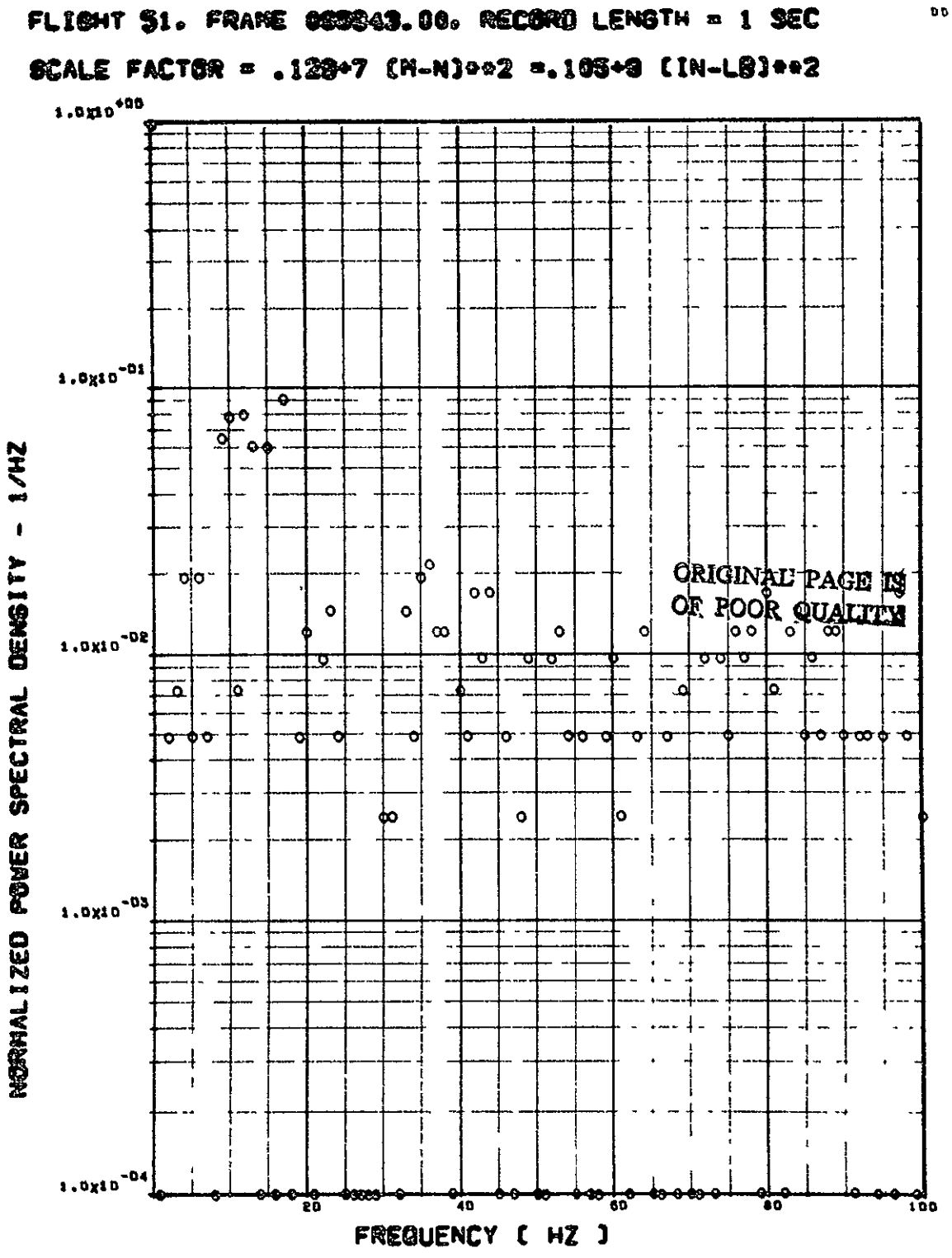

Figure 14. Continued

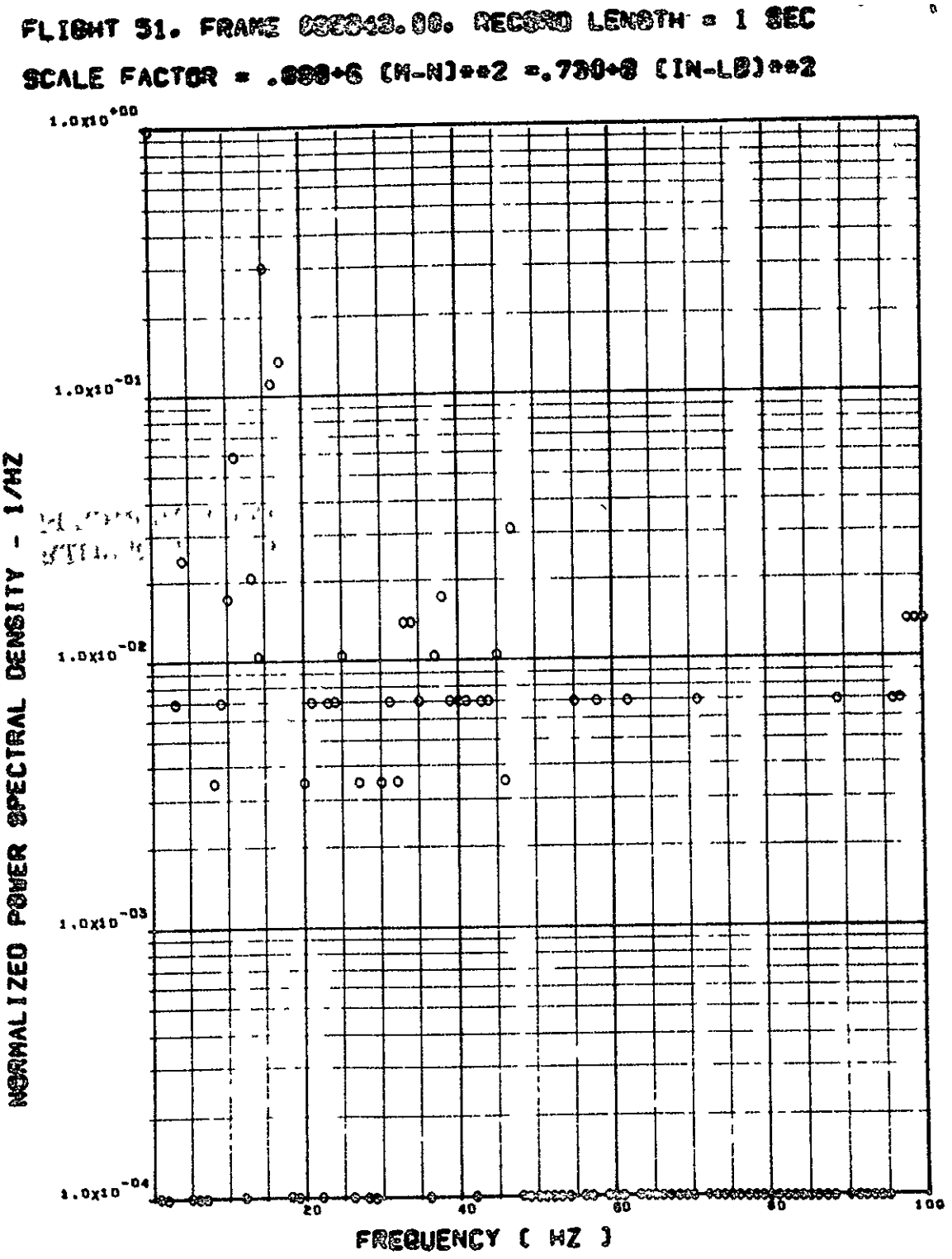

Figure 14. Continued

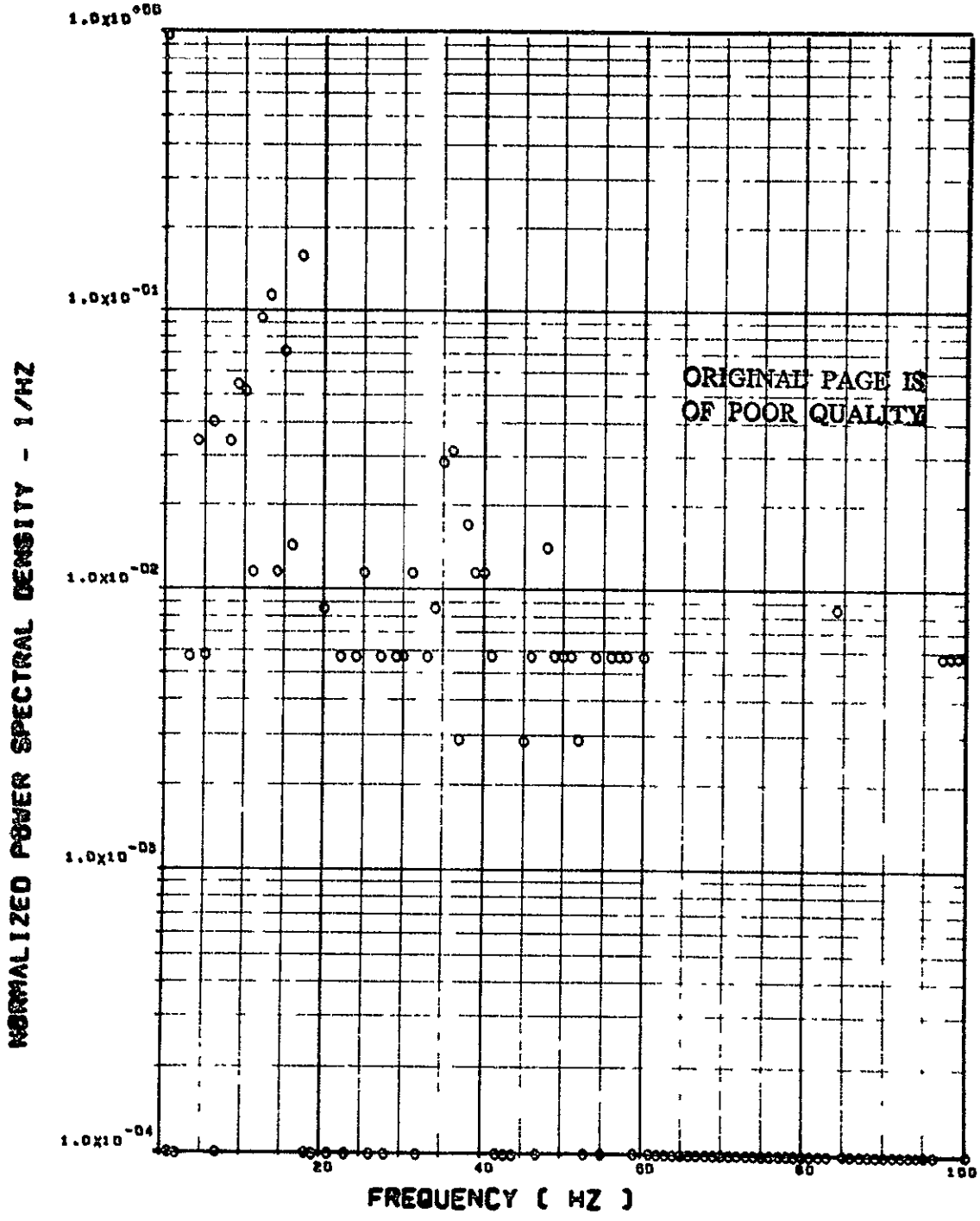

Figure 14. Concluded

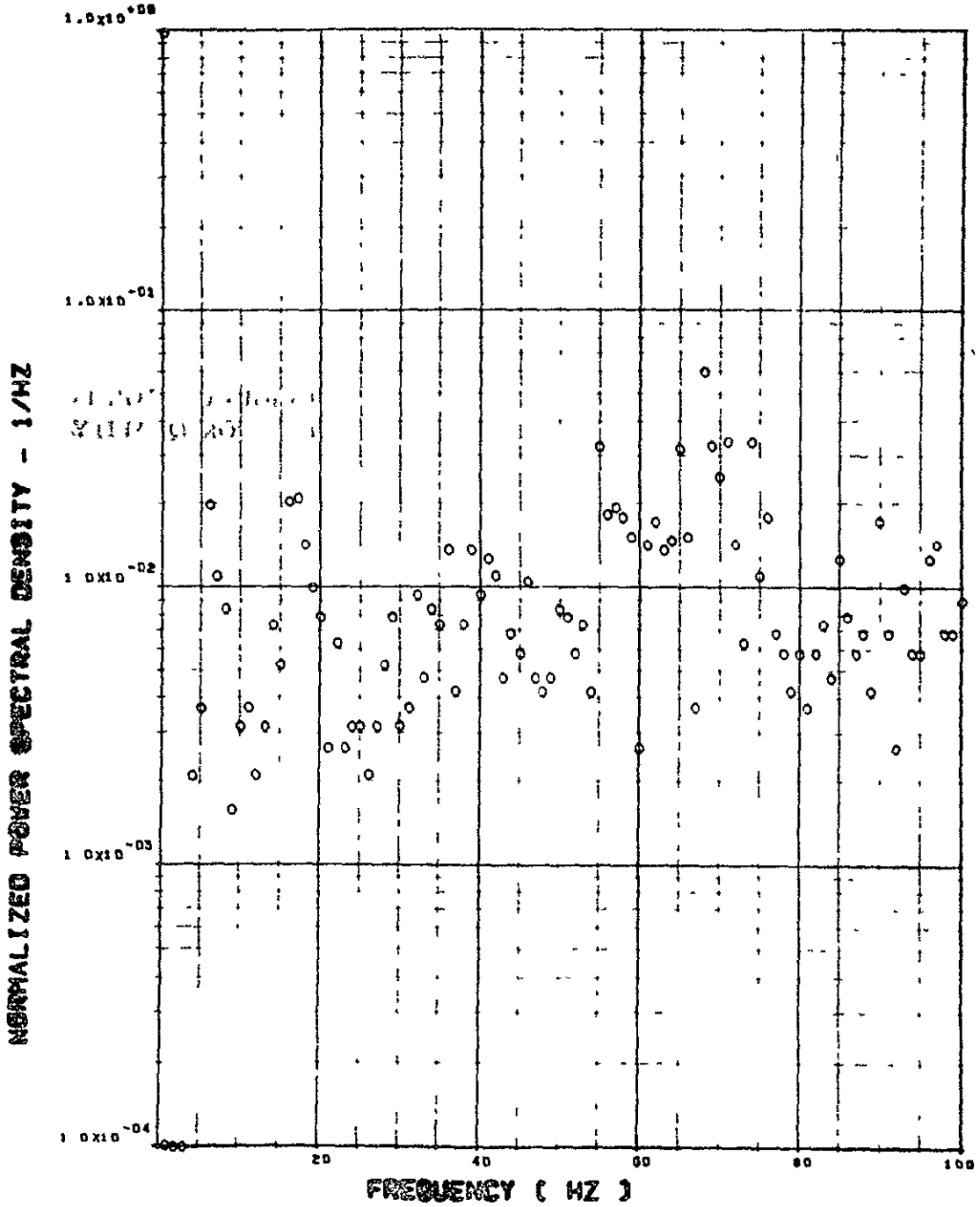

Figure 15. Power Spectra - Flight 51, Run S38/150, Point 3, T_1 = 95940.0, ΔT - 4 Sec, α_{Nom} = 15.12 deg, α= 1.90 deg.

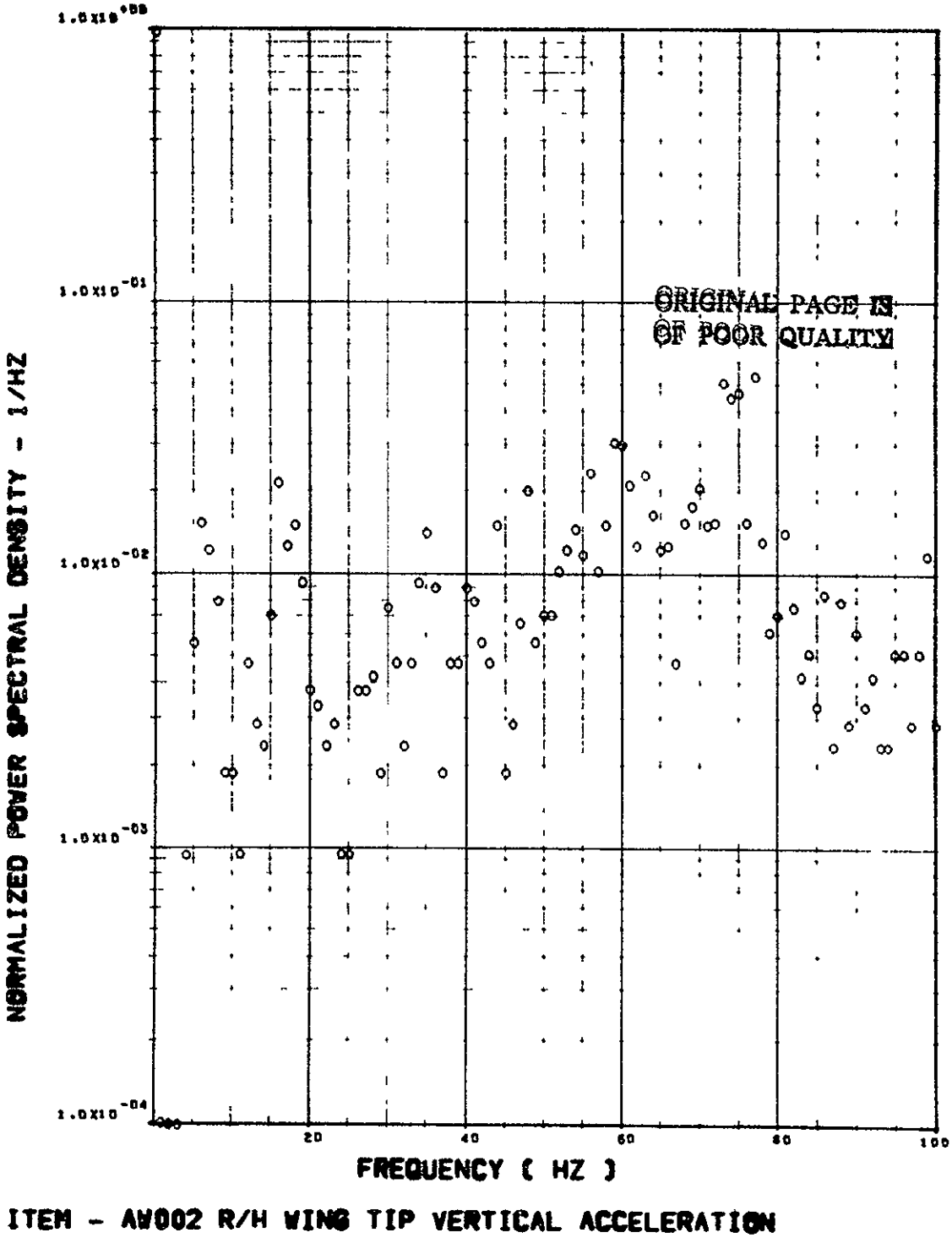

Figure 15. Continued

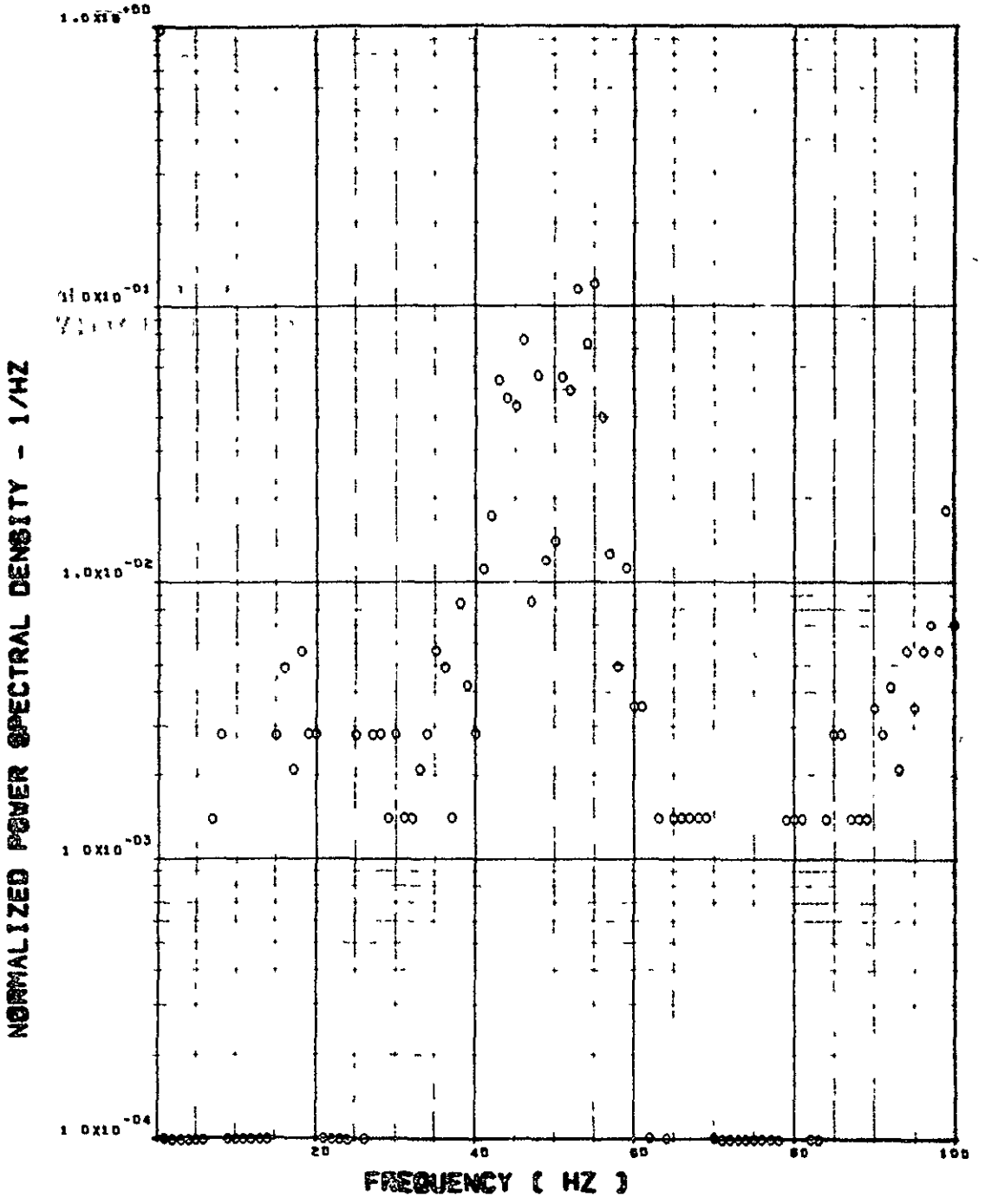

Figure 15. Continued

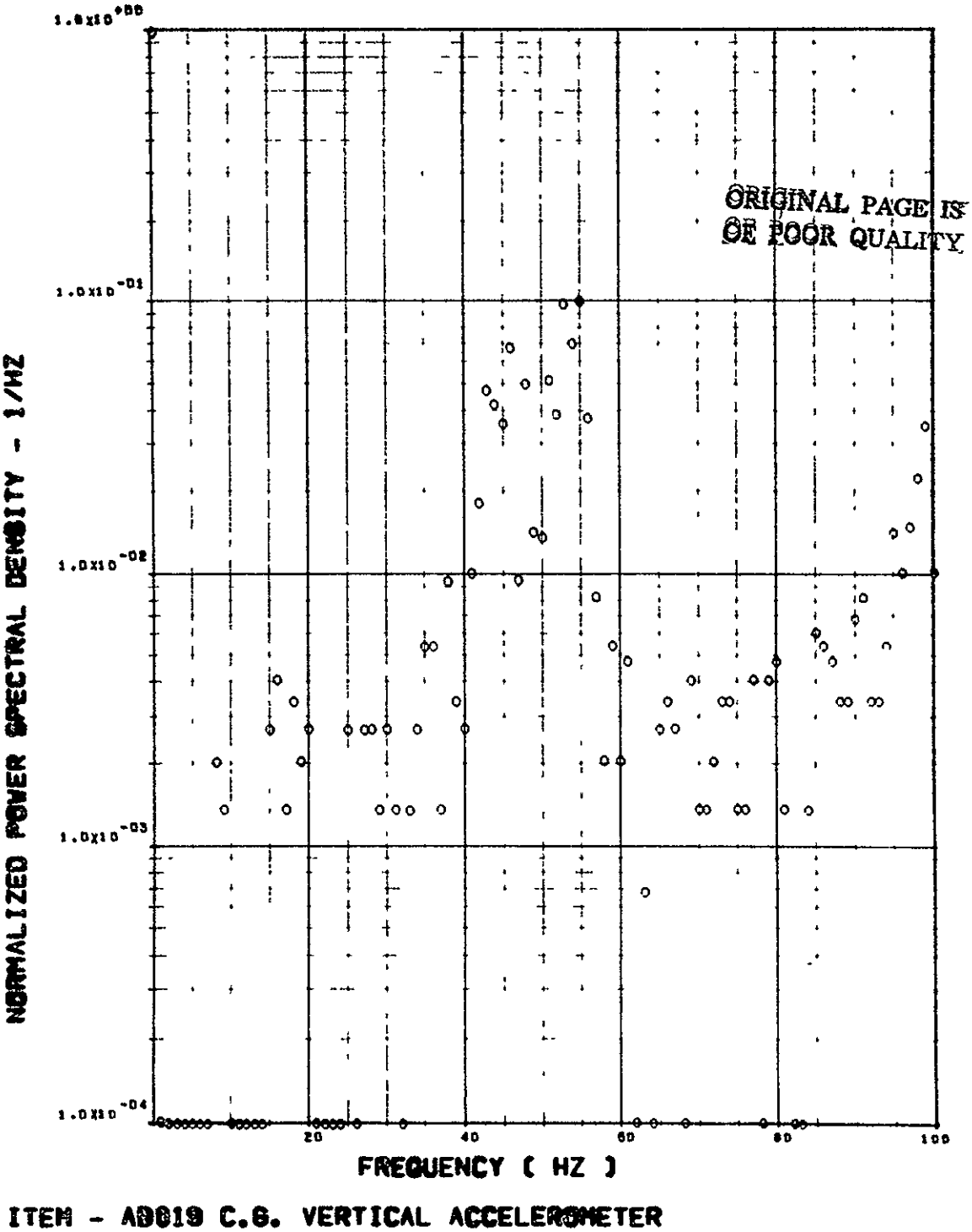

Figure 15. Continued

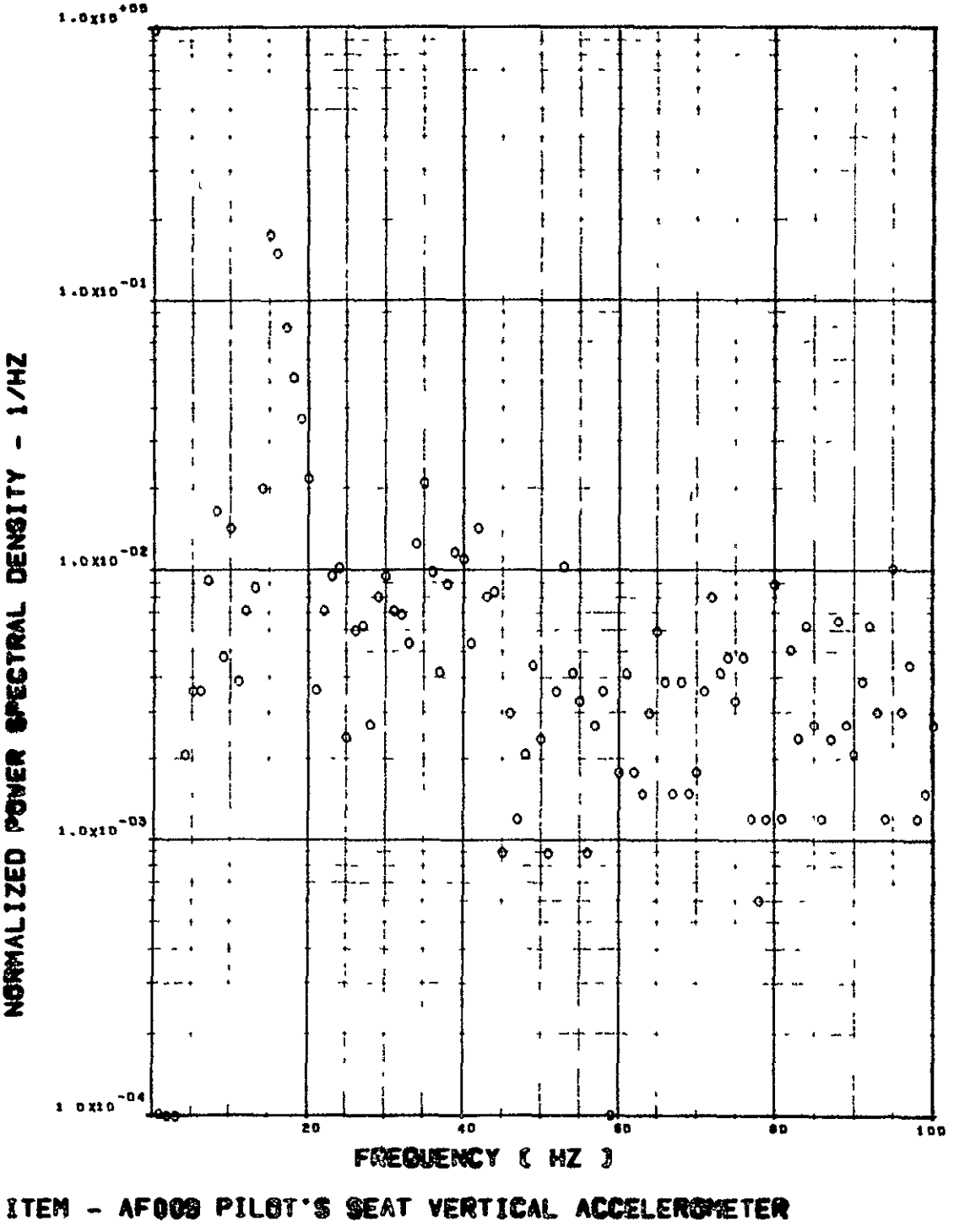

Figure 15. Continued

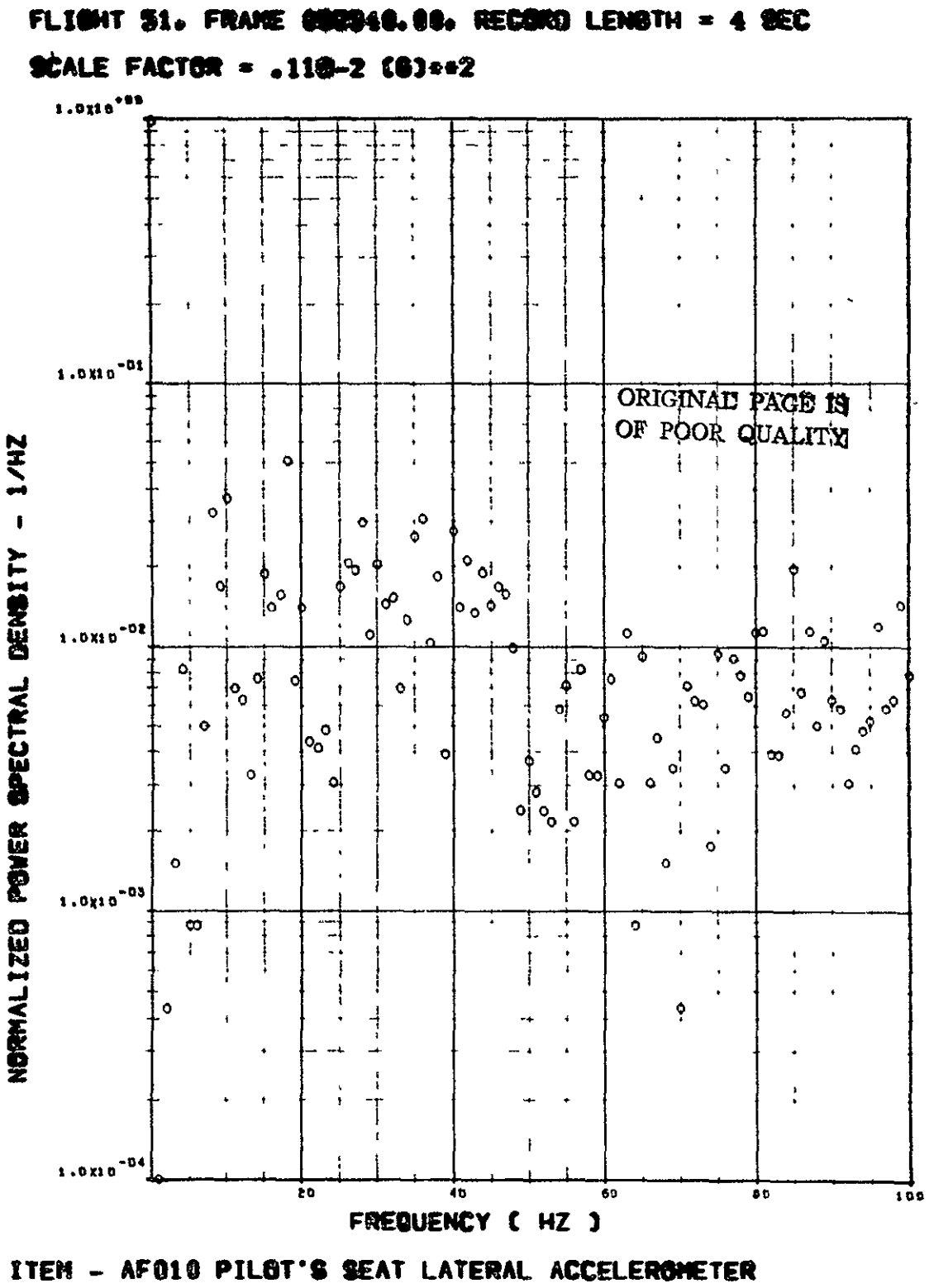

Figure 15. Continued

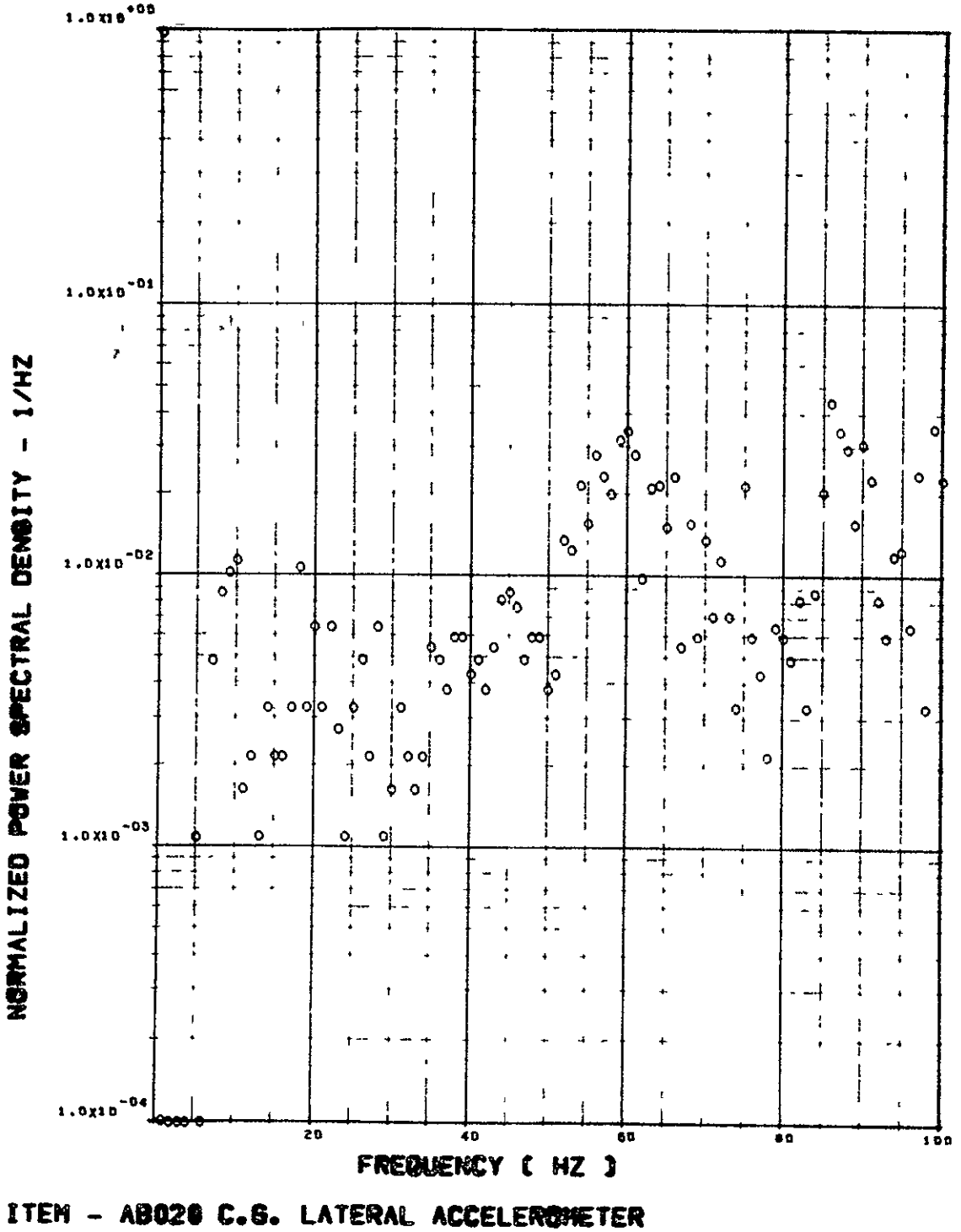

Figure 15. Continued

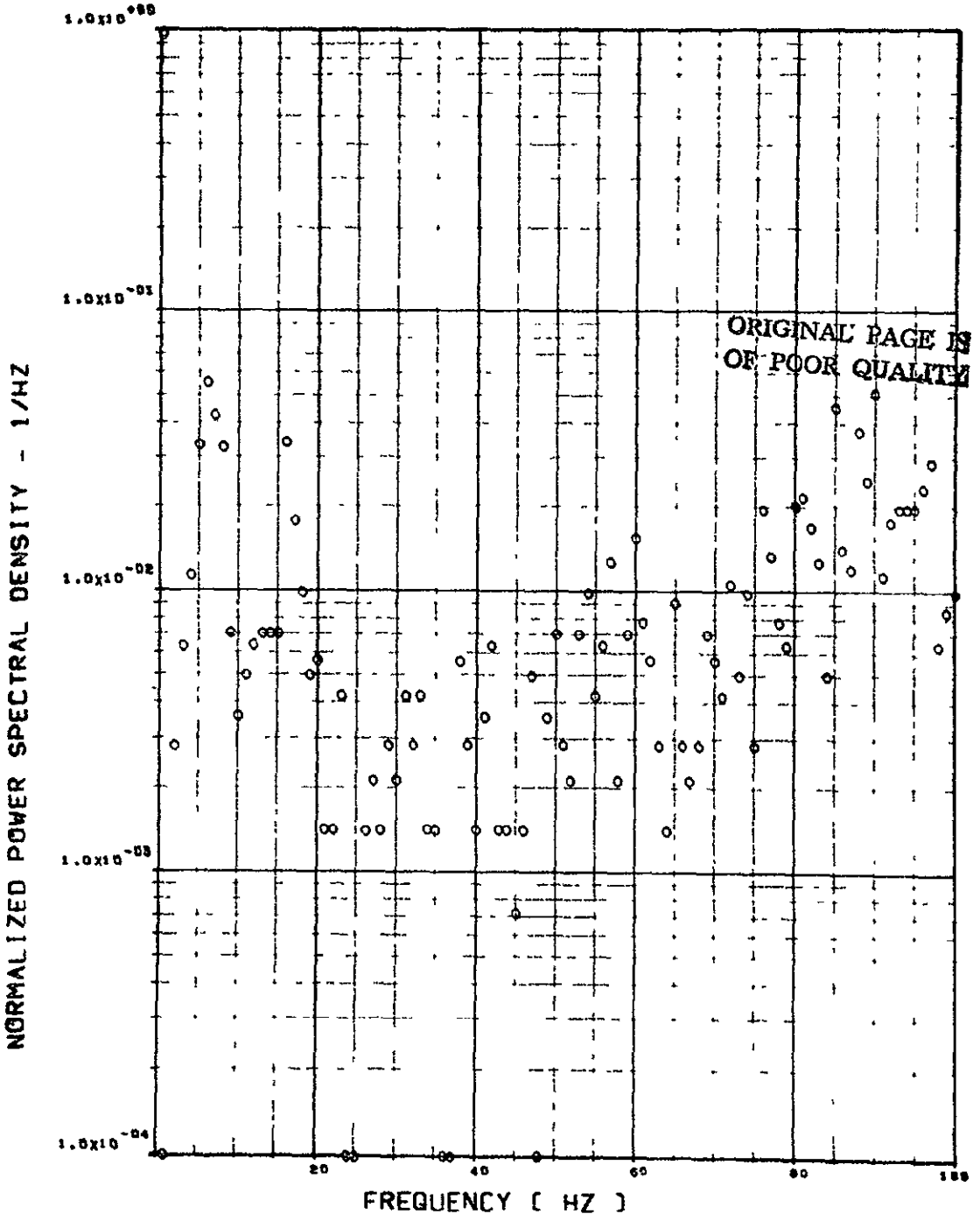

Figure 15. Continued

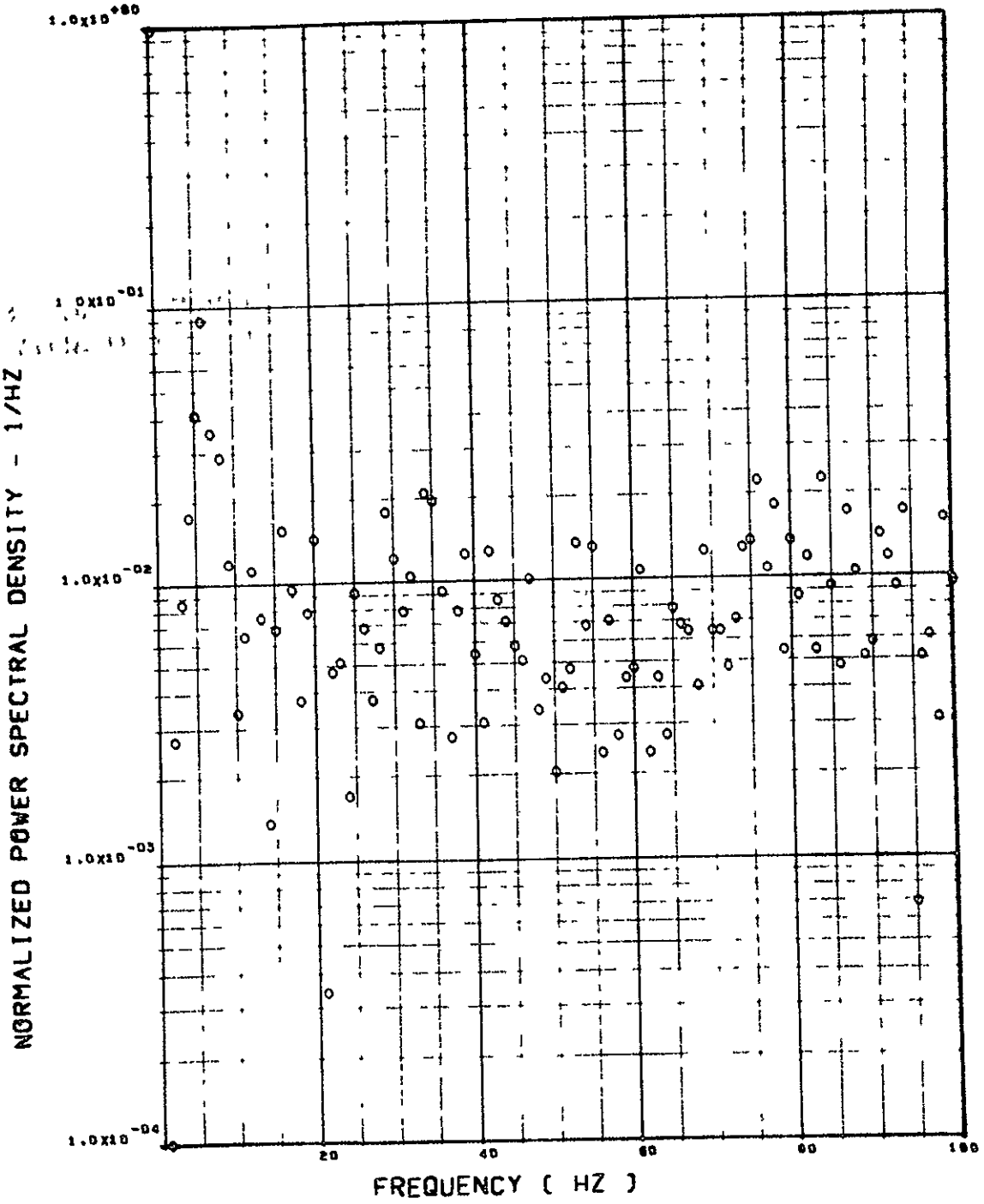

Figure 15. Continued

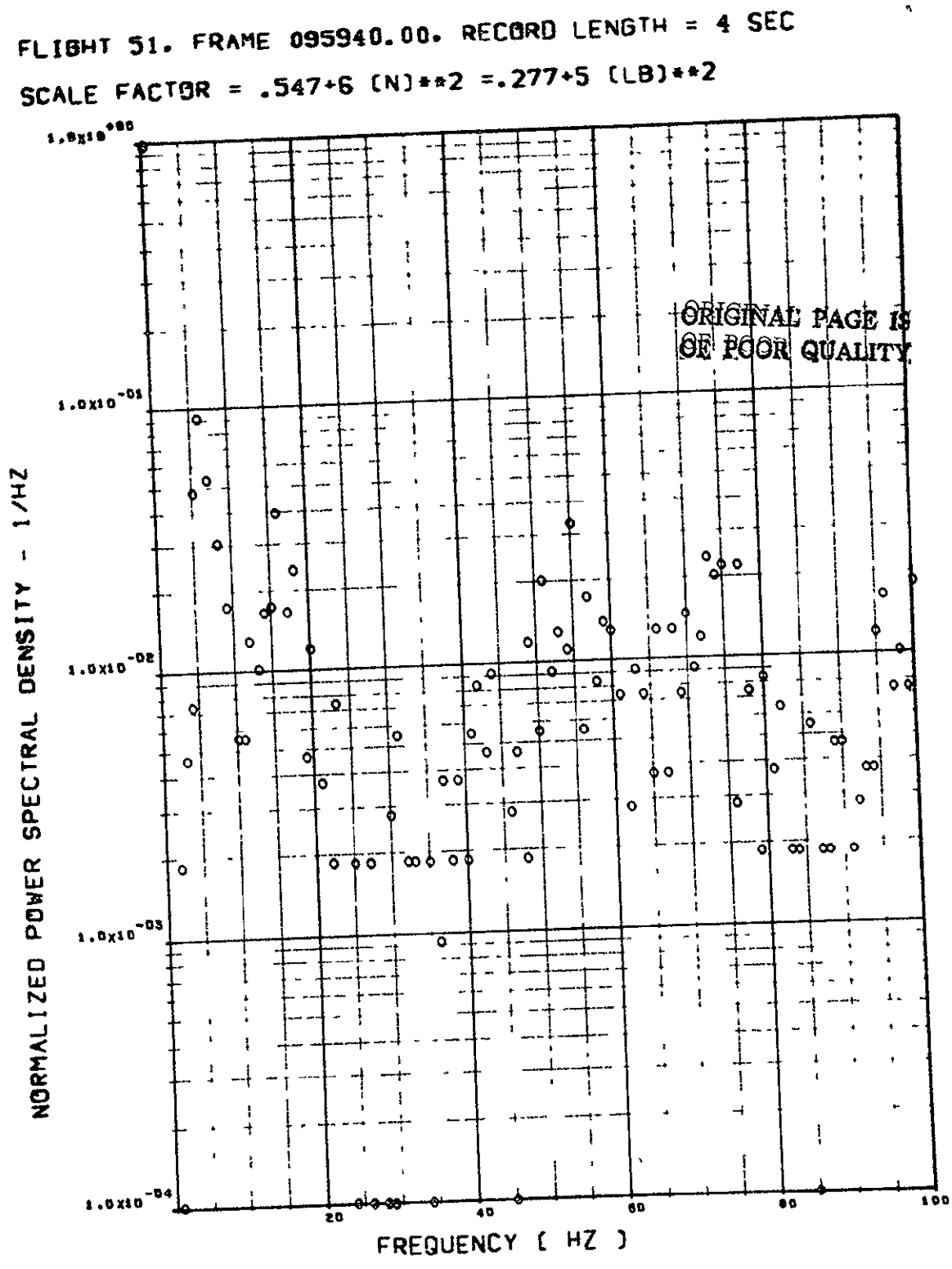

Figure 15. Continued

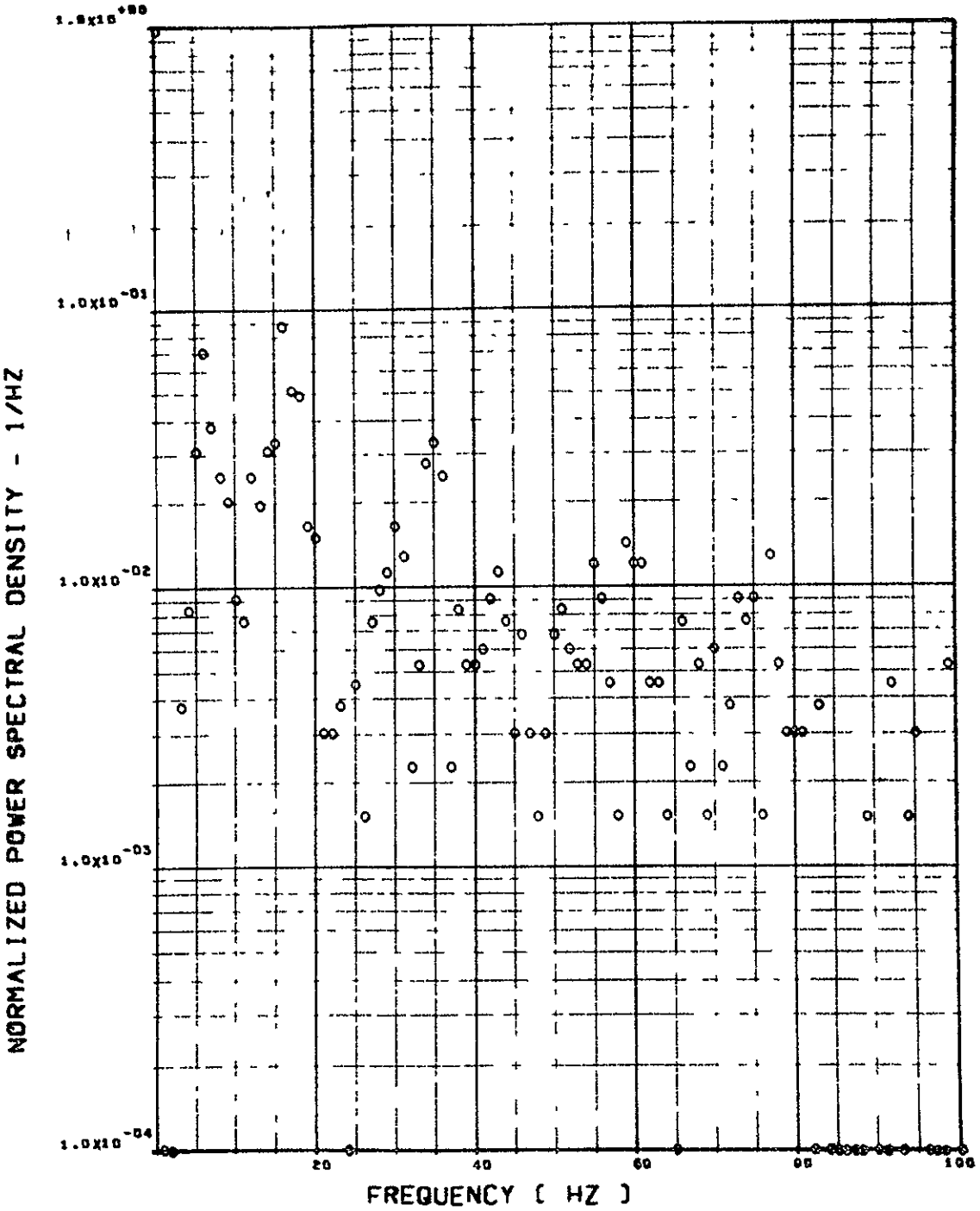

Figure 15. Continued

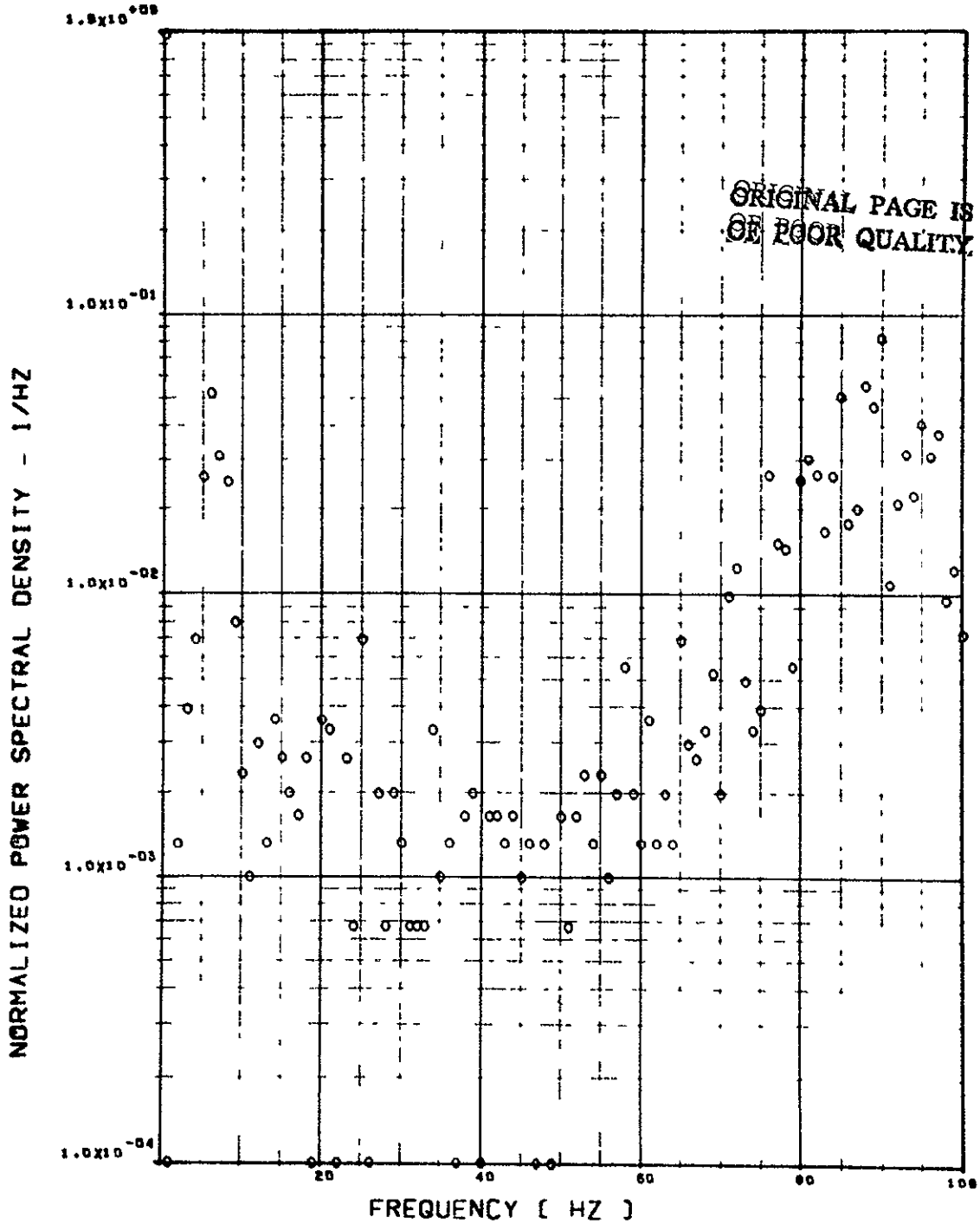

Figure 15. Continued

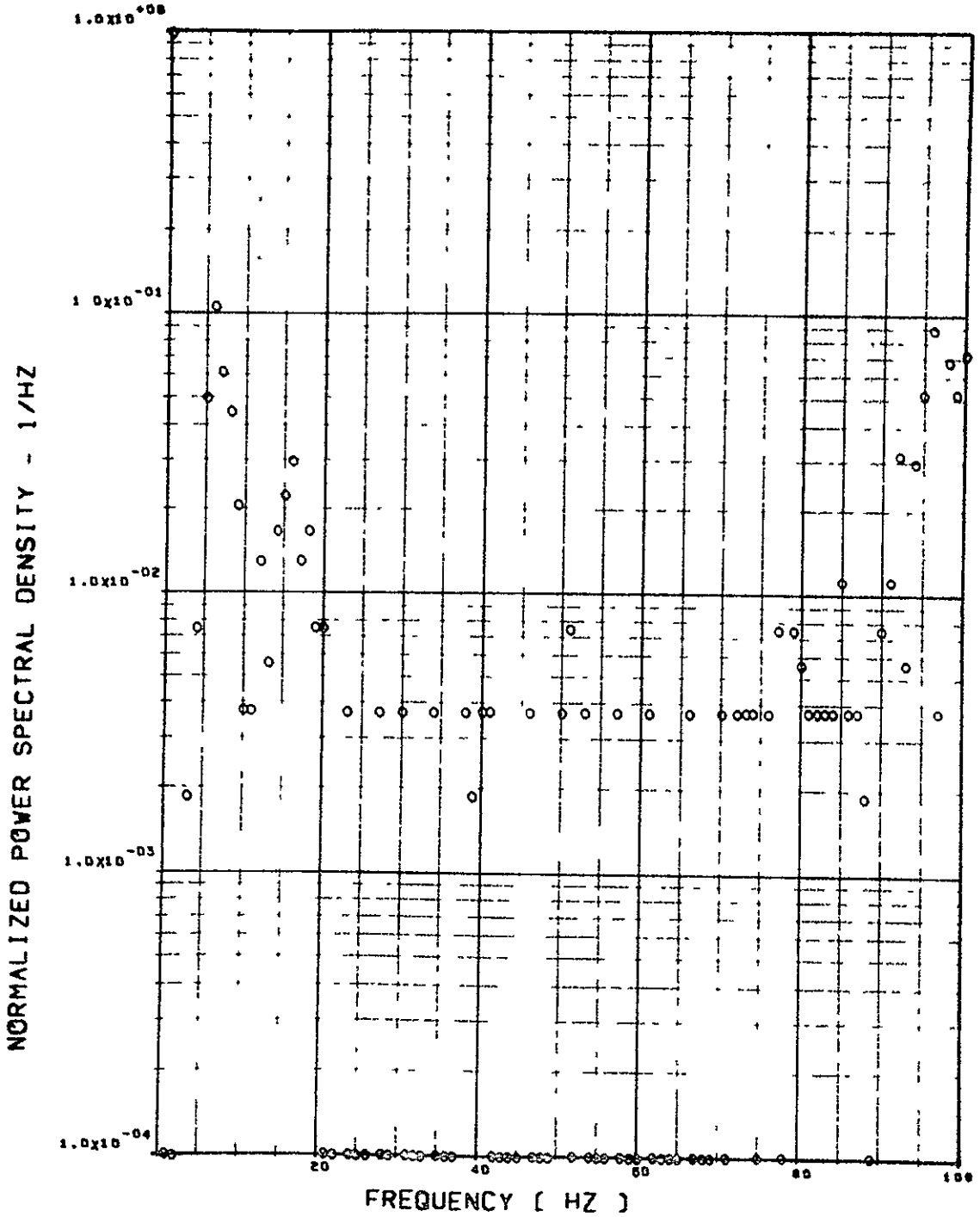

ITEM - SW127 BENDING MOMENT AT WING STATION 2

Figure 15. Continued

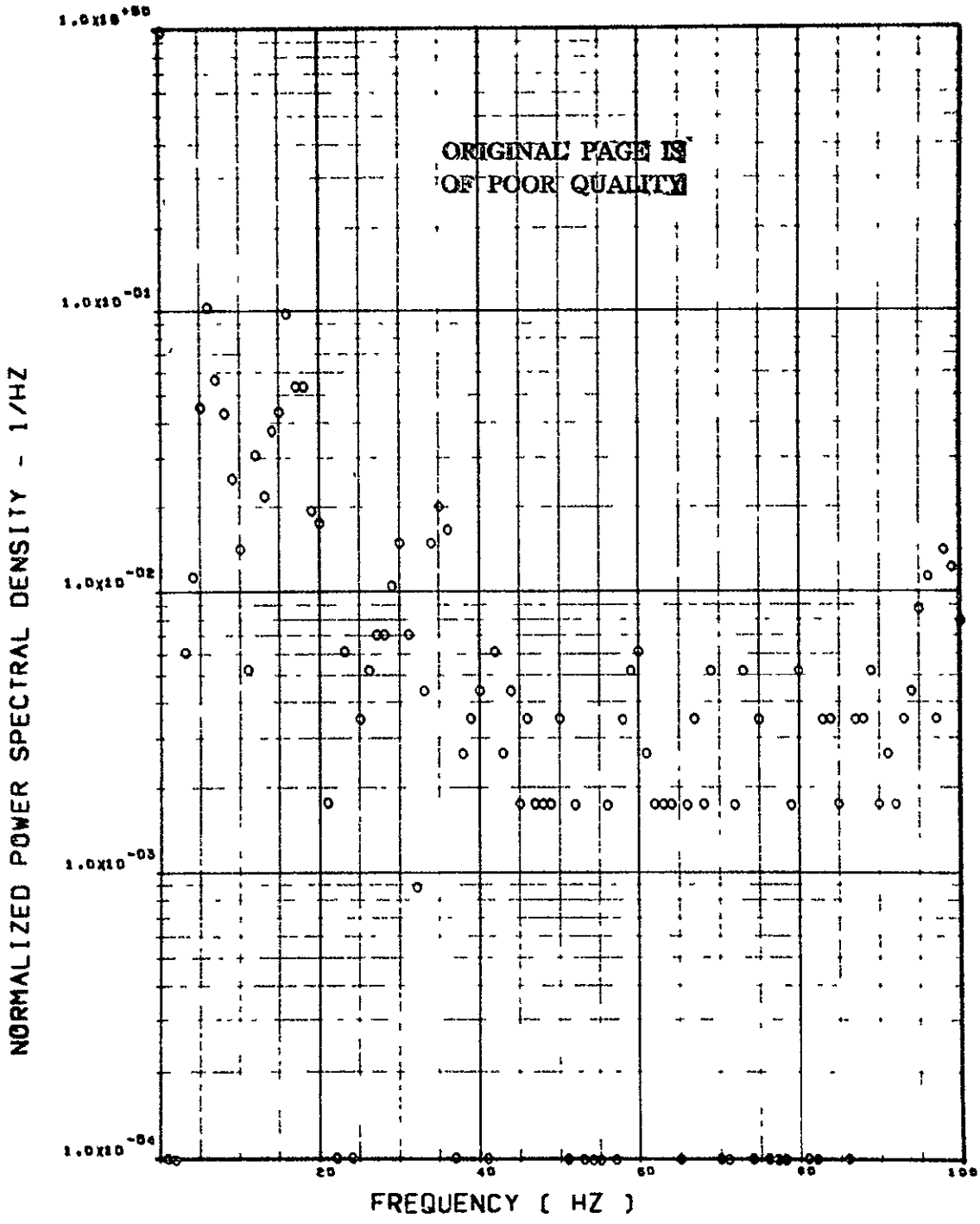

Figure 15. Continued

FLIGHT 51. FRAME 095940.00. RECORD LENGTH = 4 SEC

SCALE FACTOR = .164+6 (M-N)**2 =.133+8 (IN-LB)**2

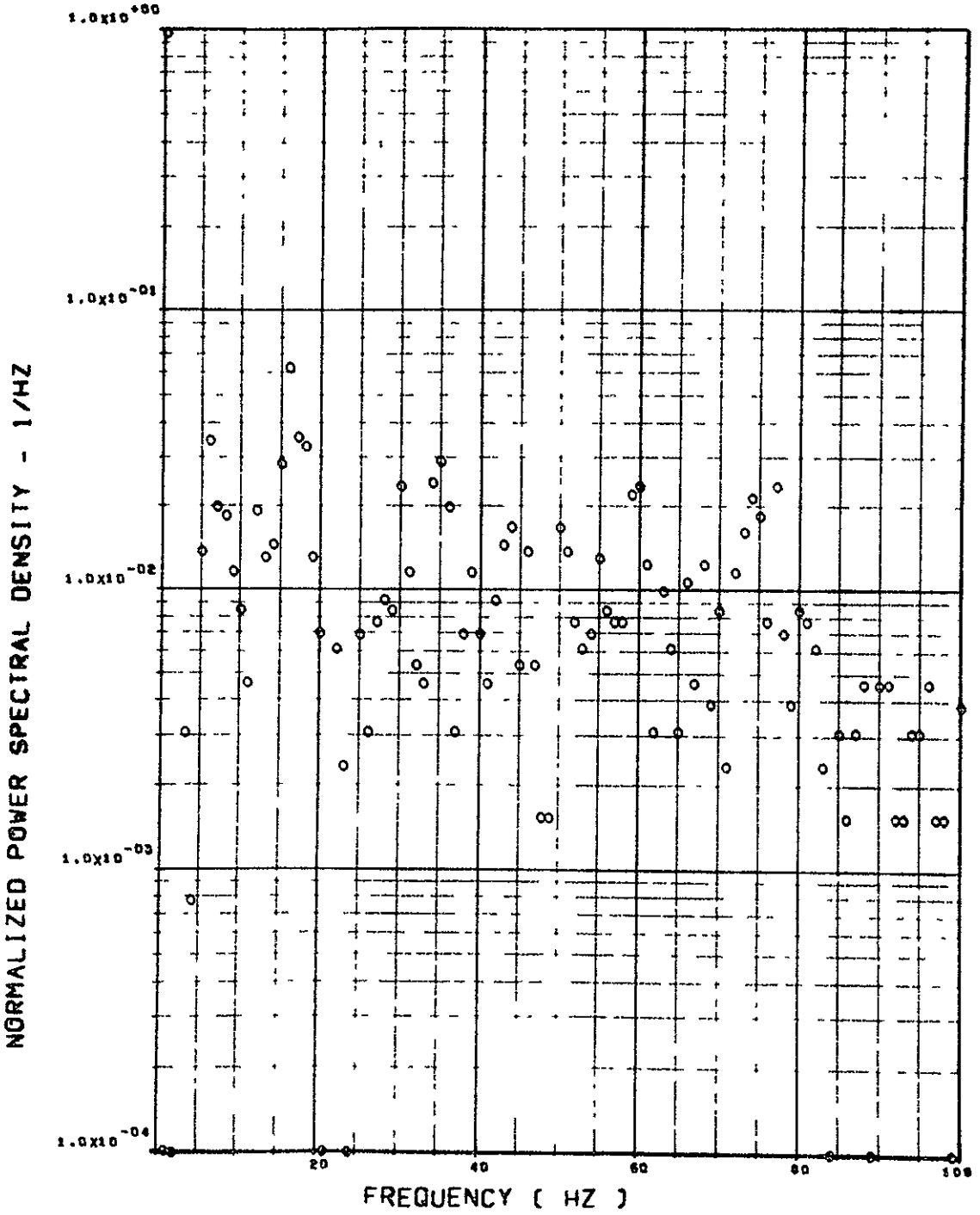

ITEM - SW133 BENDING MOMENT AT WING STATION 4

Figure 15. Continued

FLIGHT 51. FRAME 095940.00. RECORD LENGTH = 4 SEC

SCALE FACTOR = .234+7 (M-N)**2 =.190+9 (IN-LB)**2

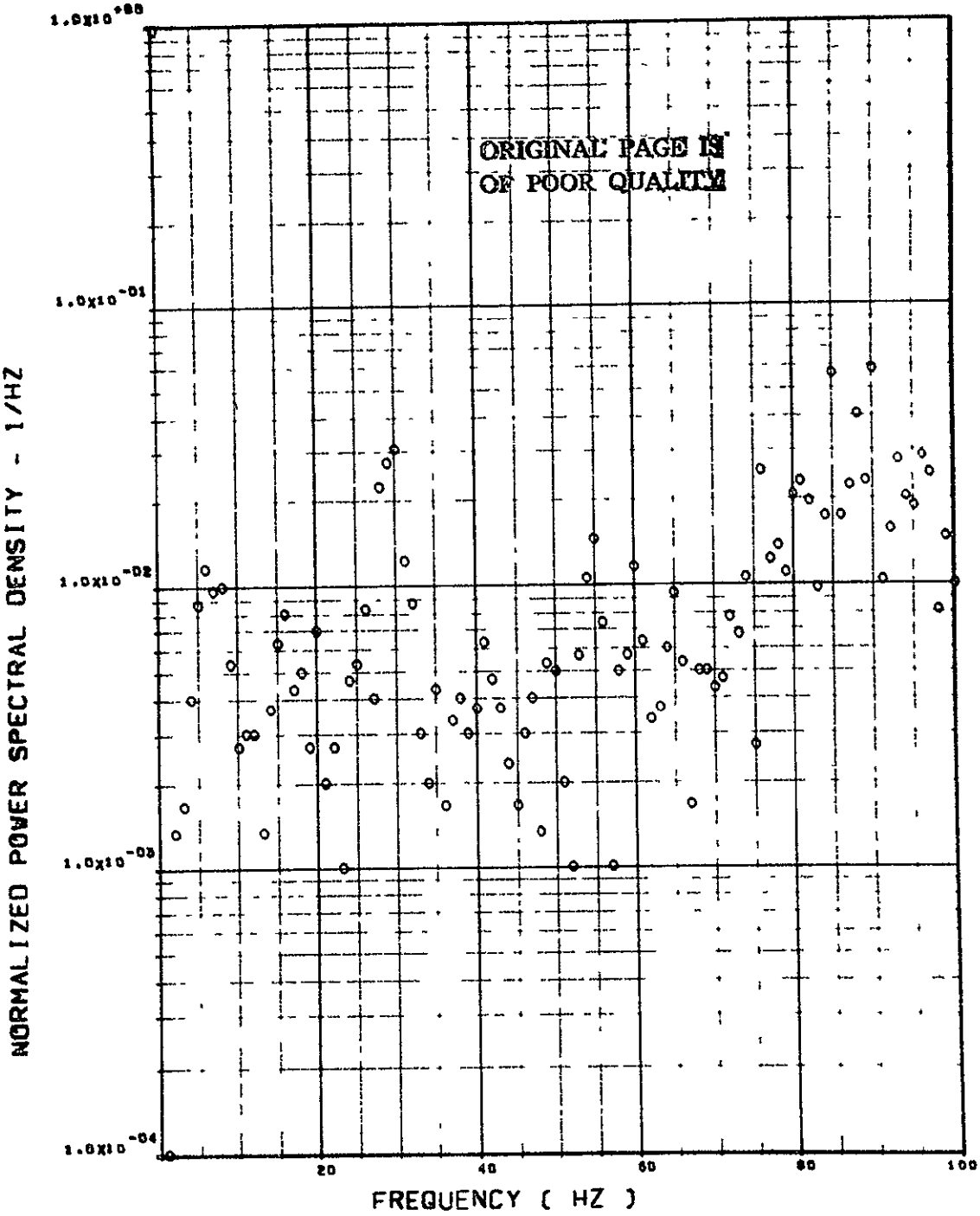

ITEM - SW125 TORSION AT WING STATION 1

Figure 15. Continued

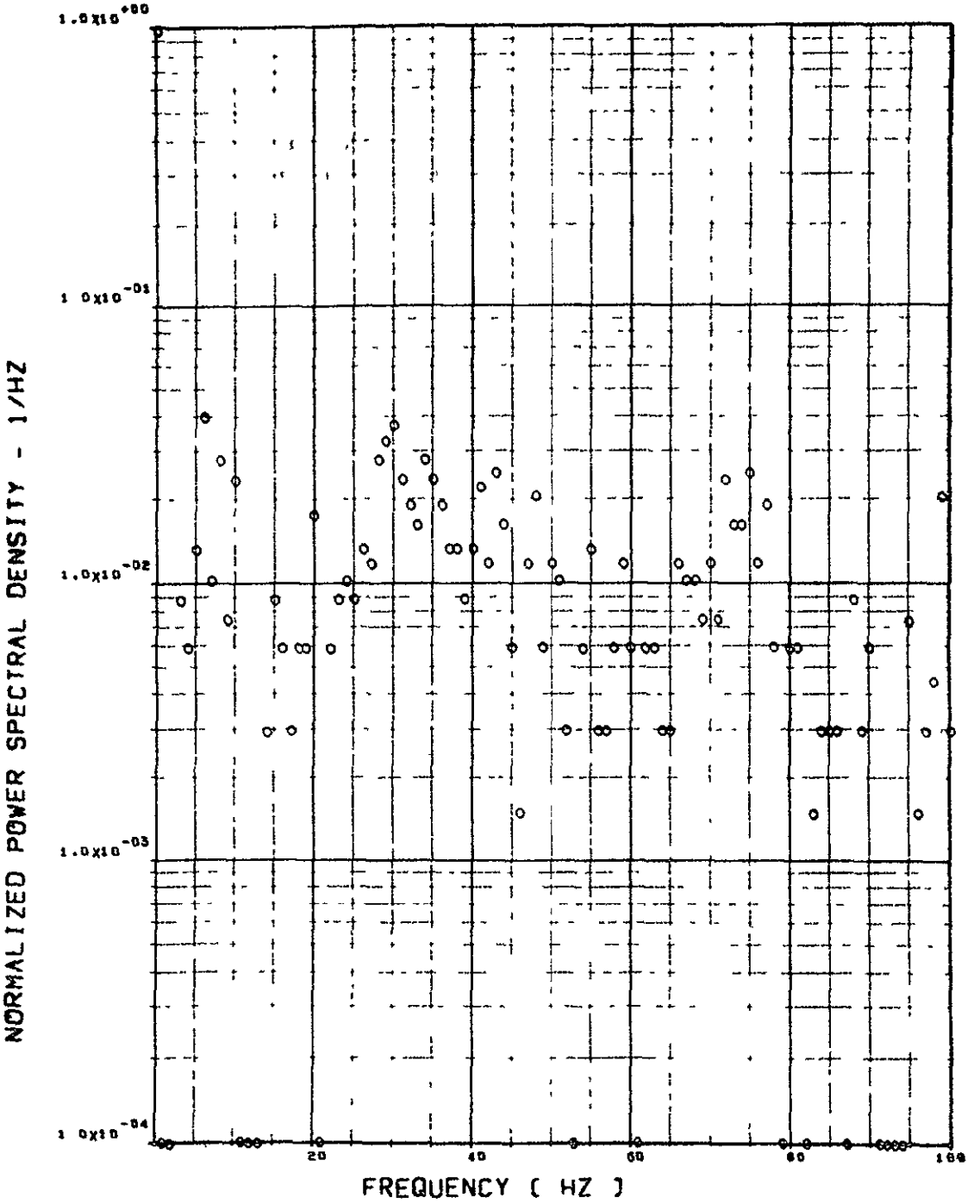

Figure 15. Continued

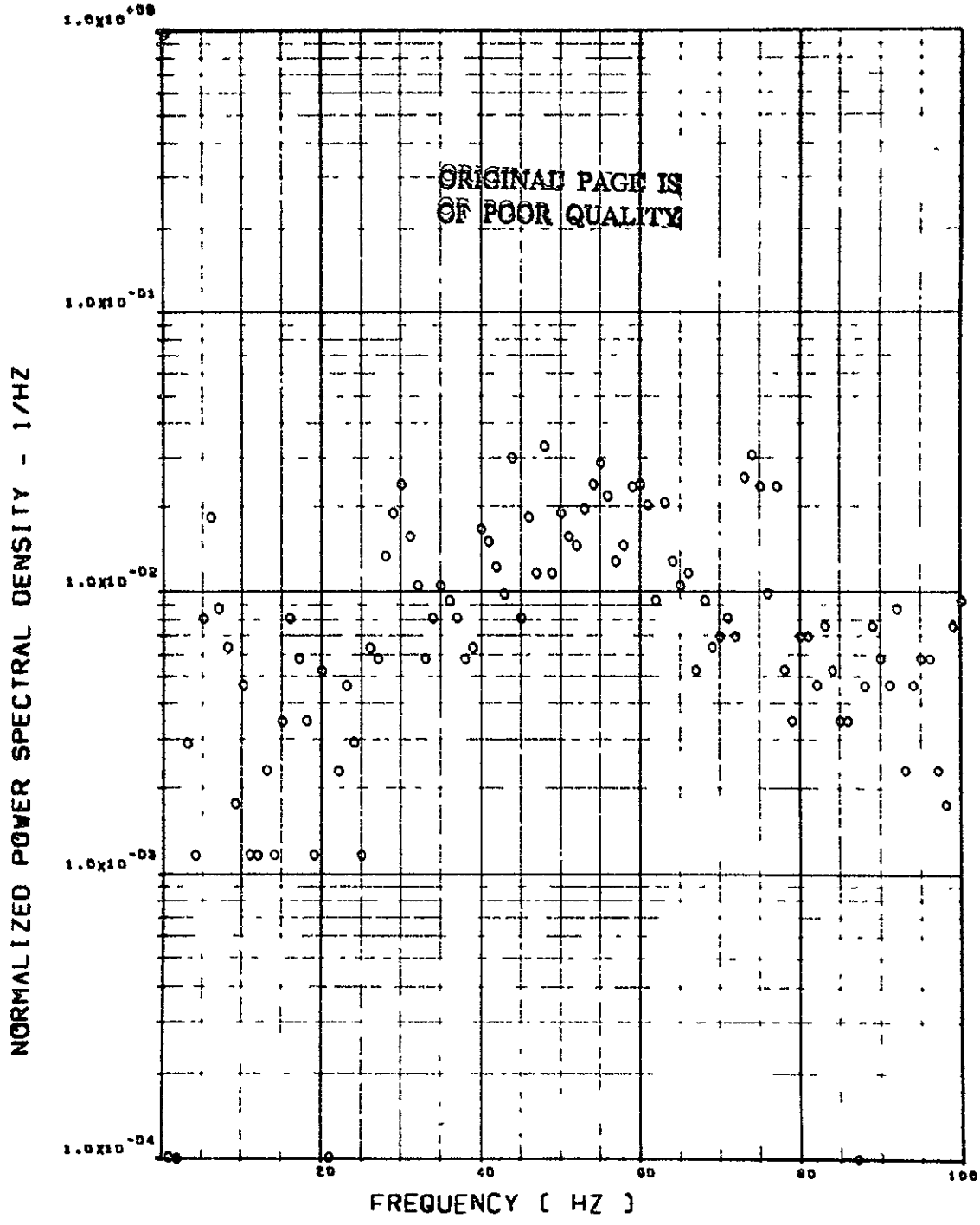

Figure 15. Continued

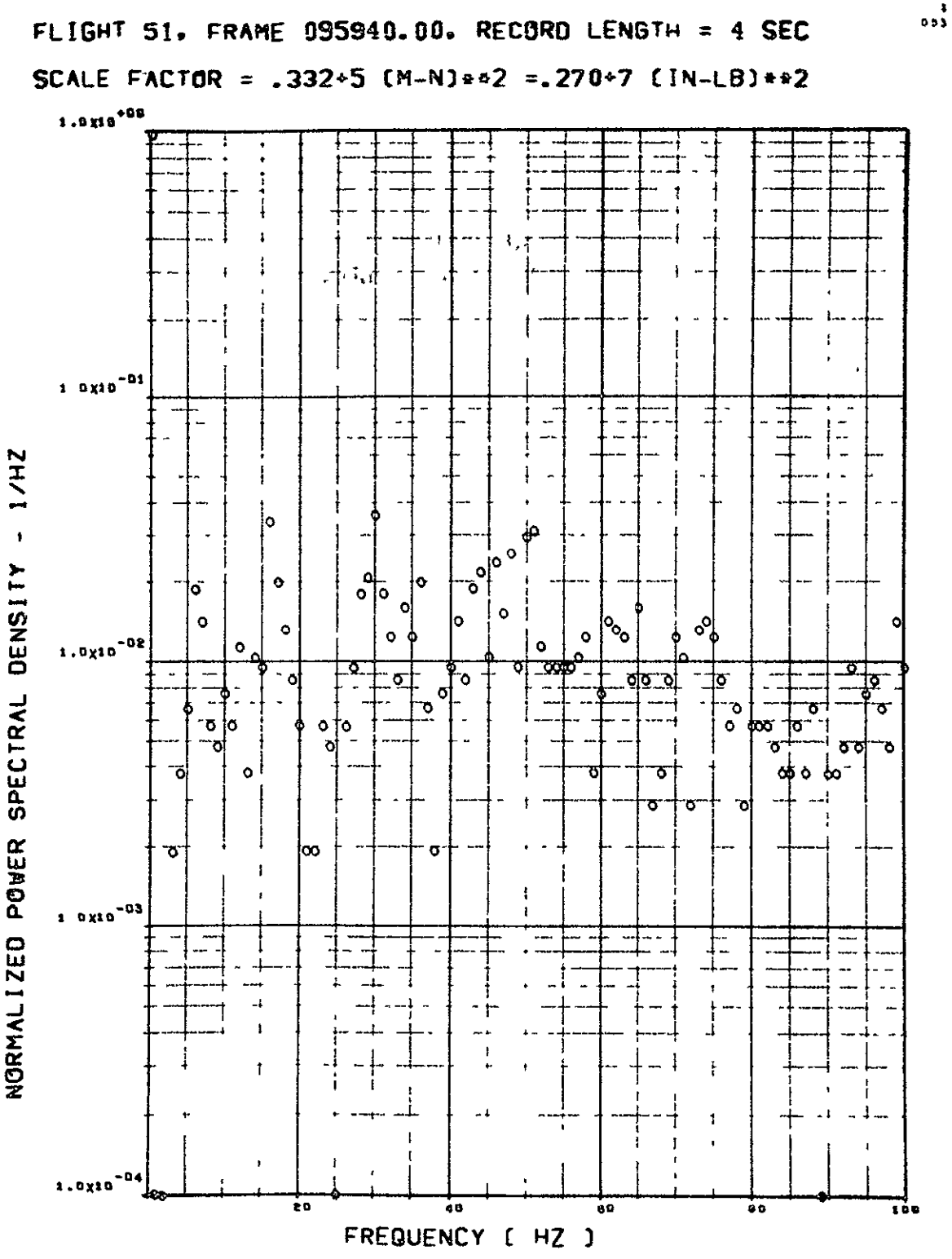

Figure 15. Continued

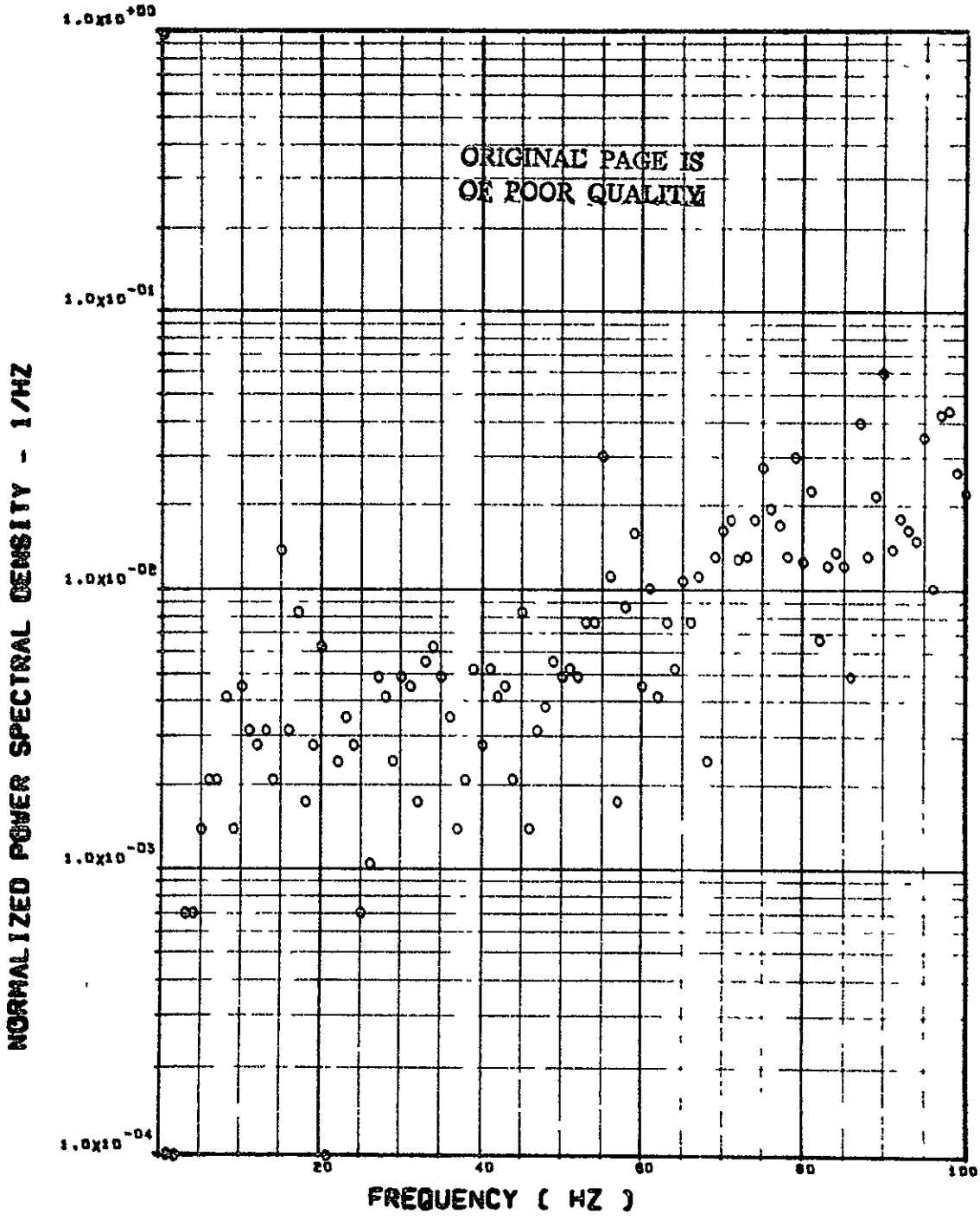

Figure 15. Continued

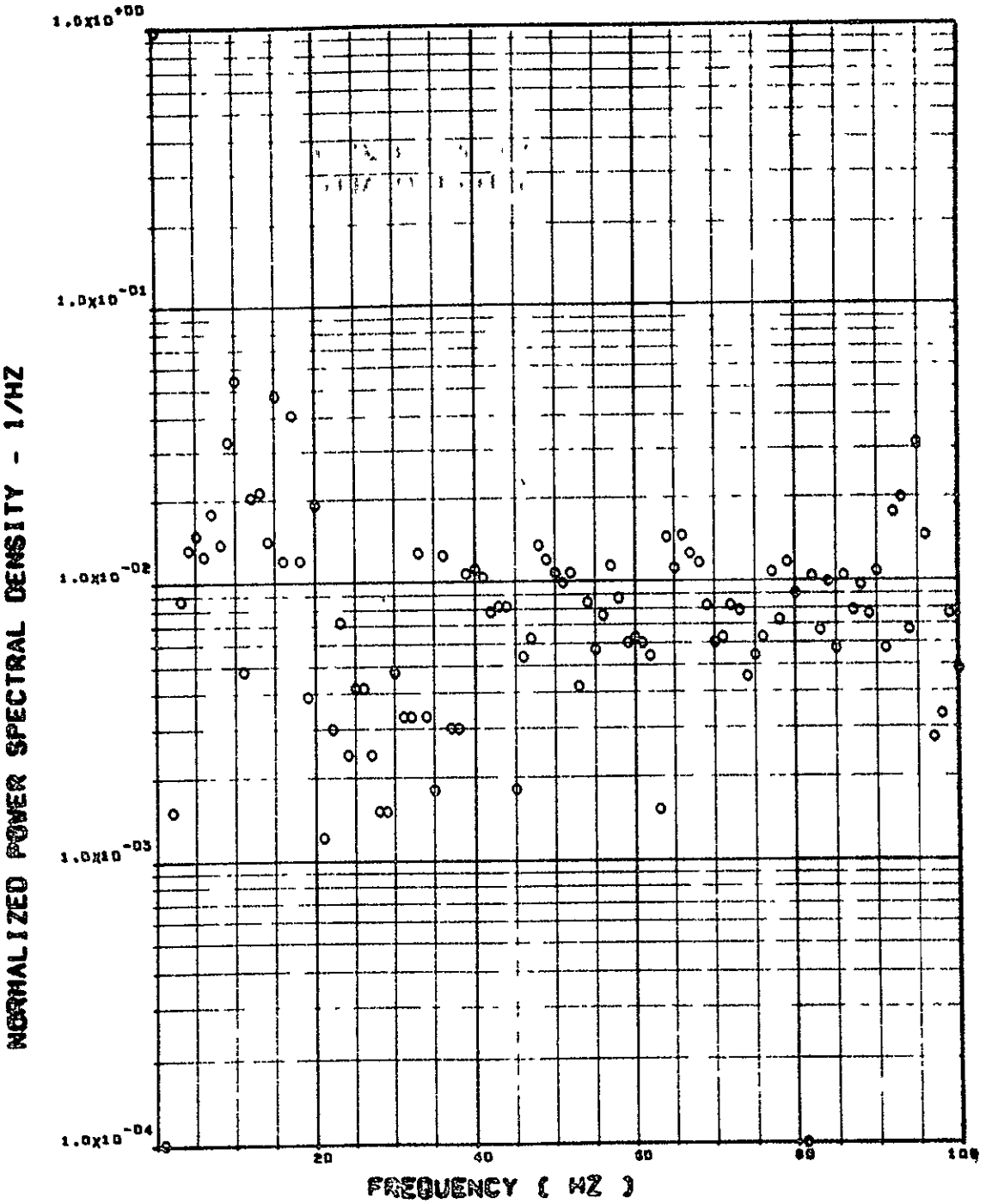

Figure 15. Continued

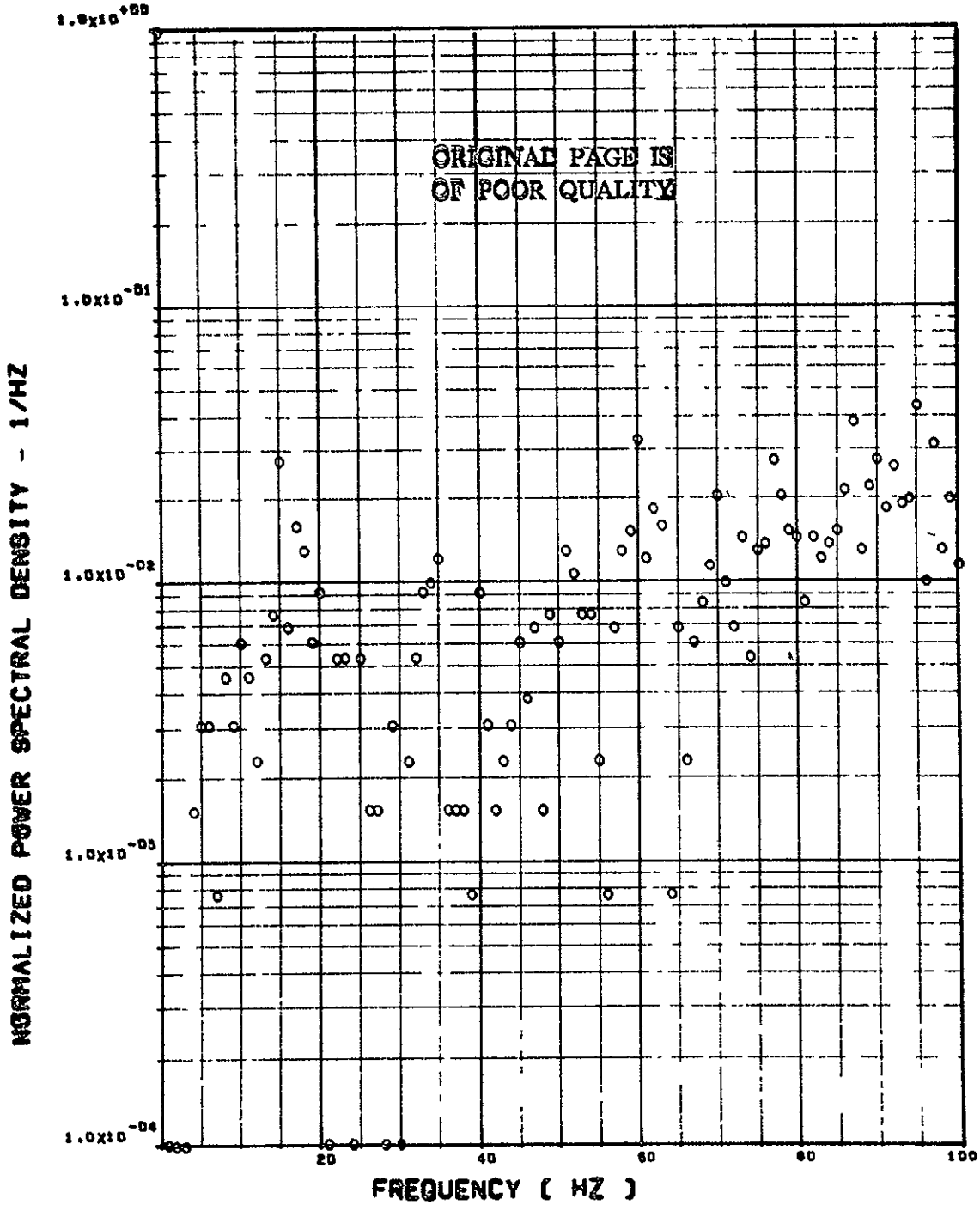

Figure 15. Continued

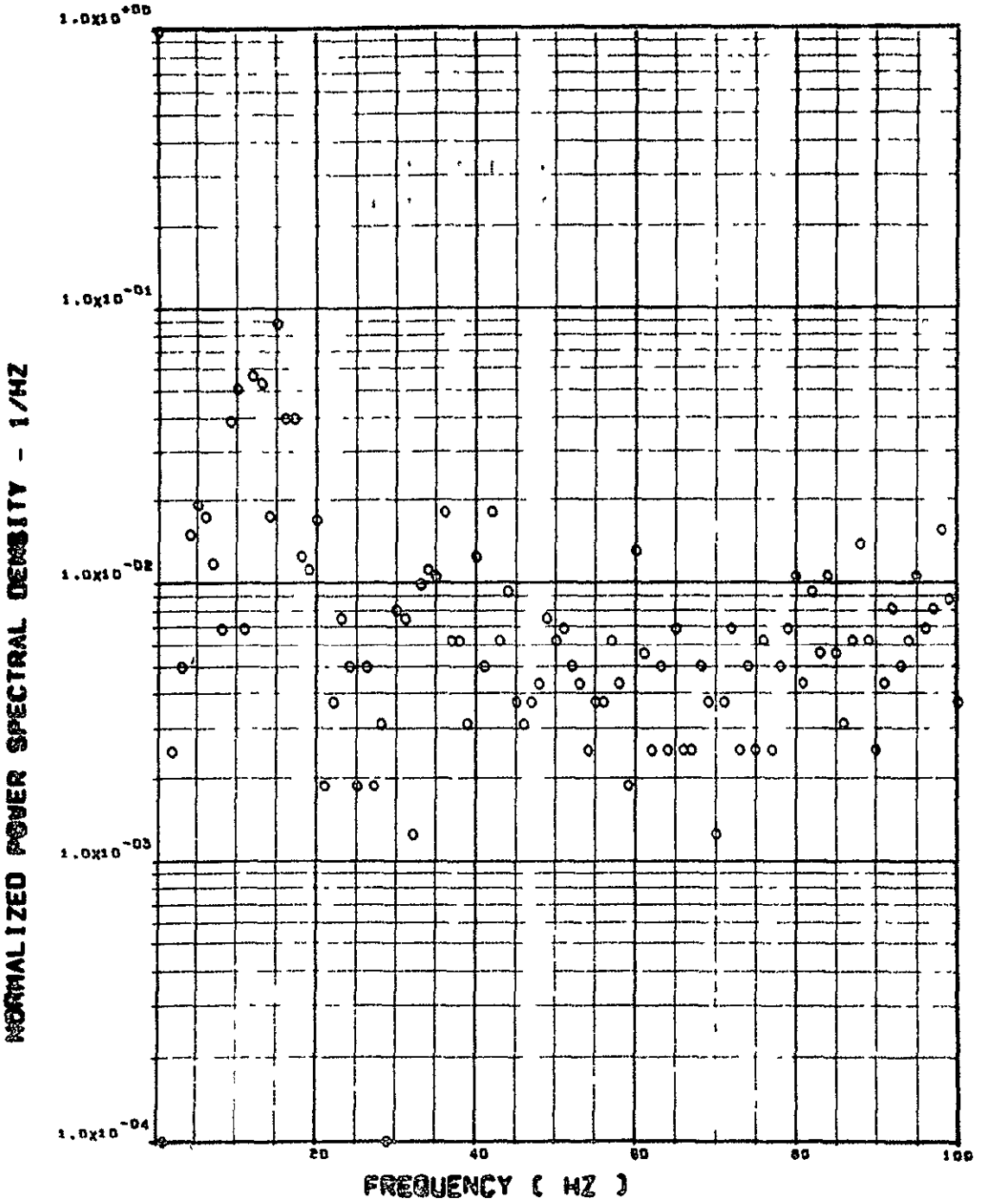

Figure 15. Continued

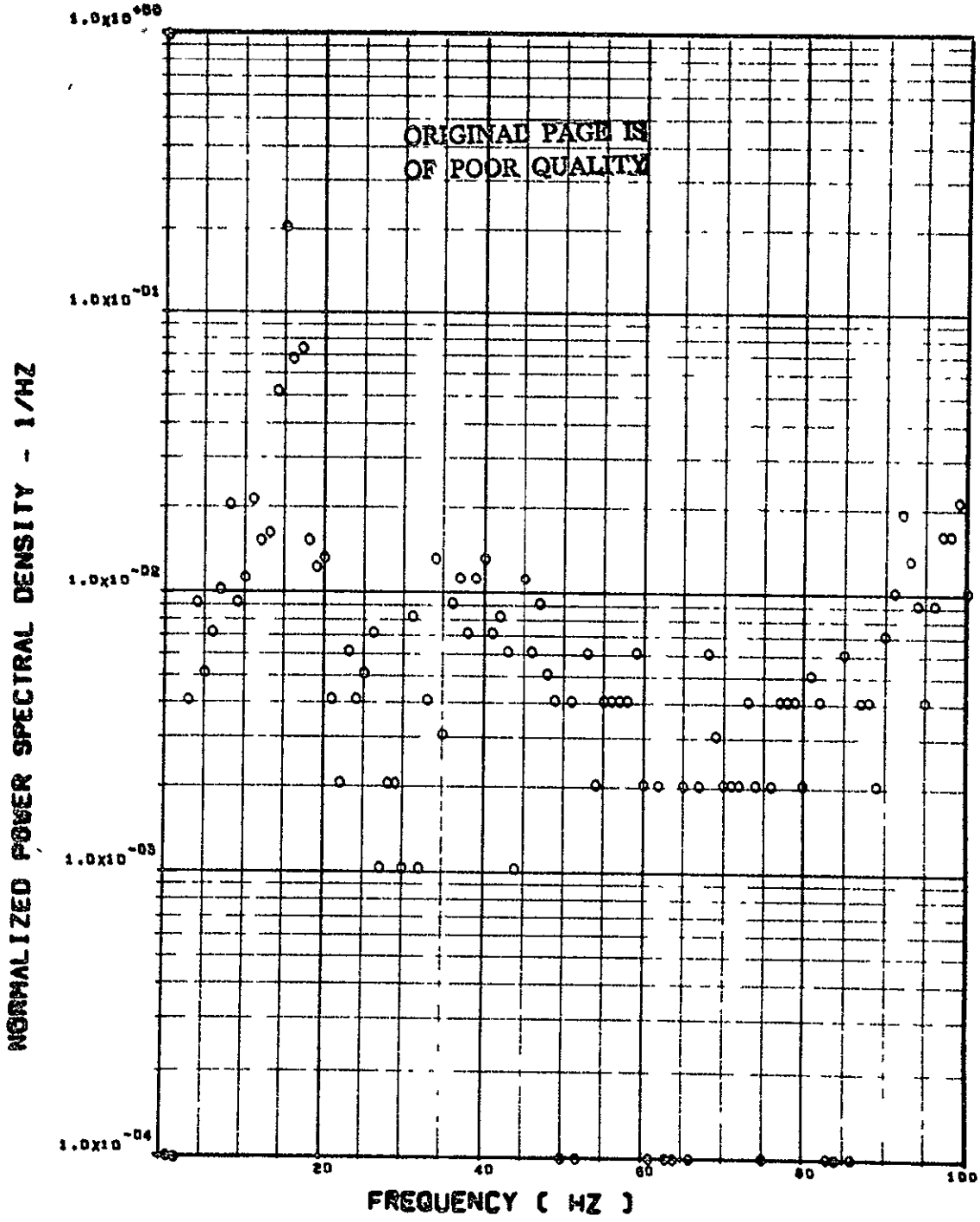

Figure 15. Continued

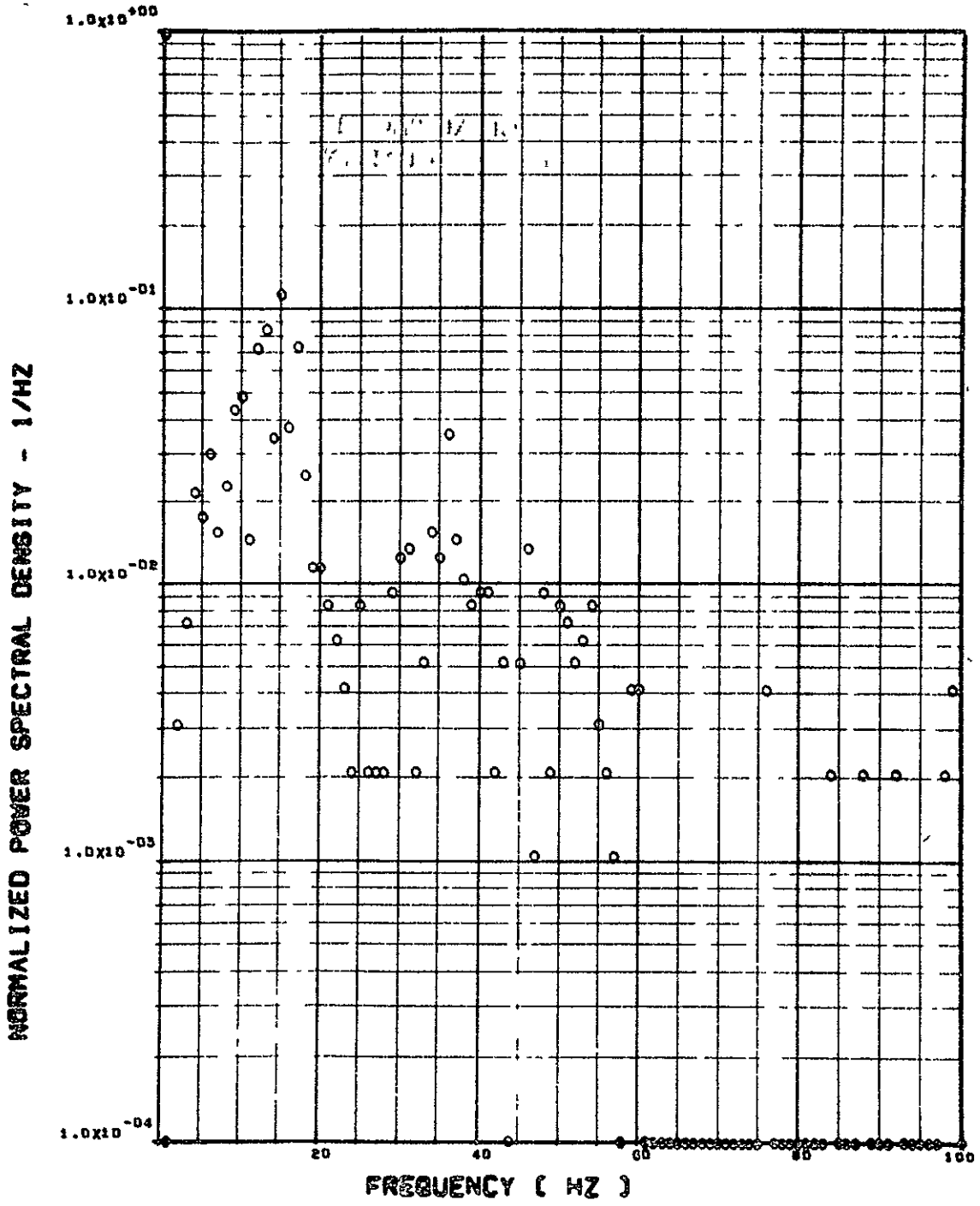

Figure 15. Concluded

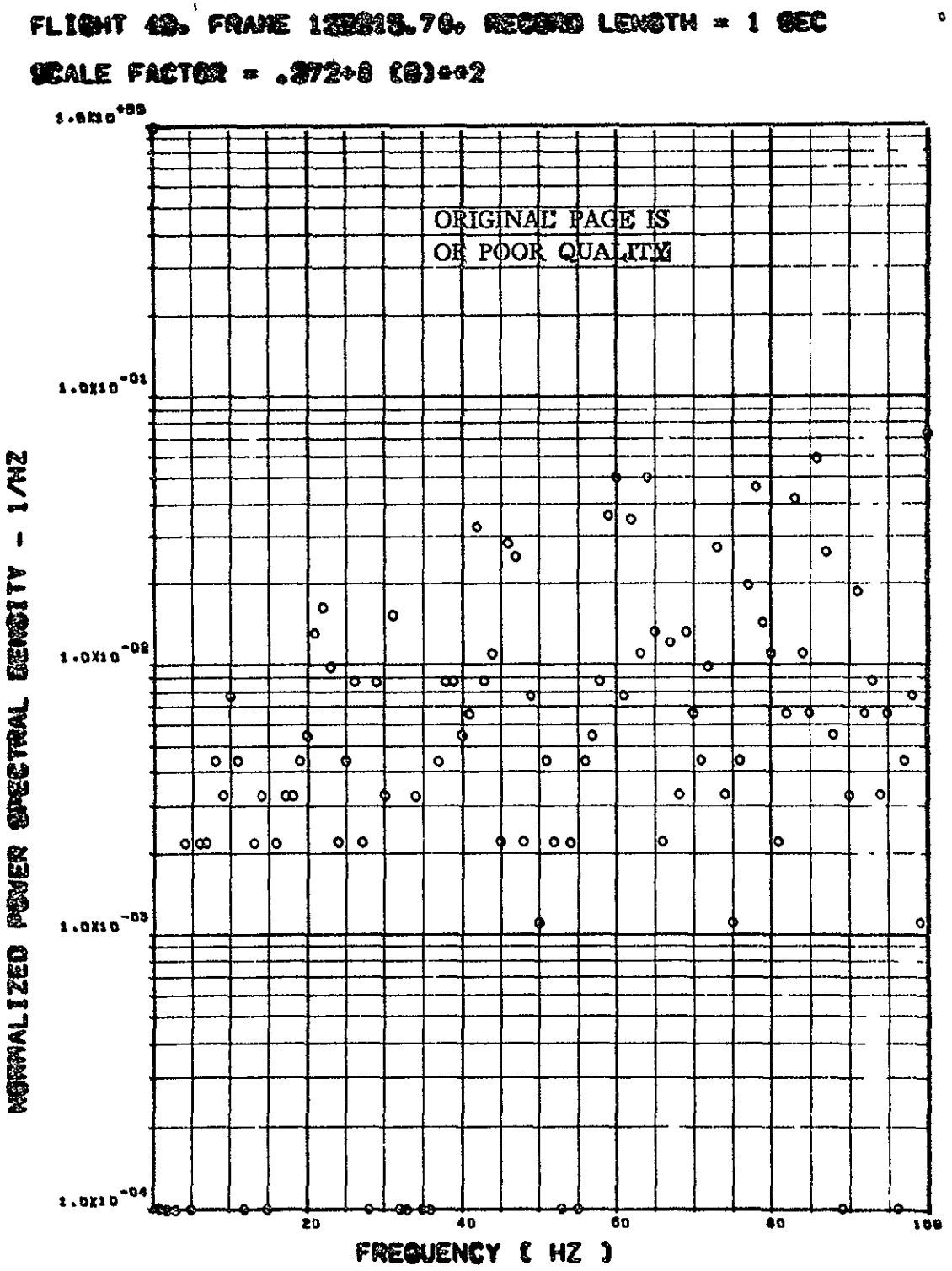

Figure 16. Power Spectra - Flight 48, Run 4, Point 1 T_1 = 135315.7, ΔT = 1 Sec, α_{Nom} = 4 95 deg, $\Delta\alpha$= 0.80 deg.

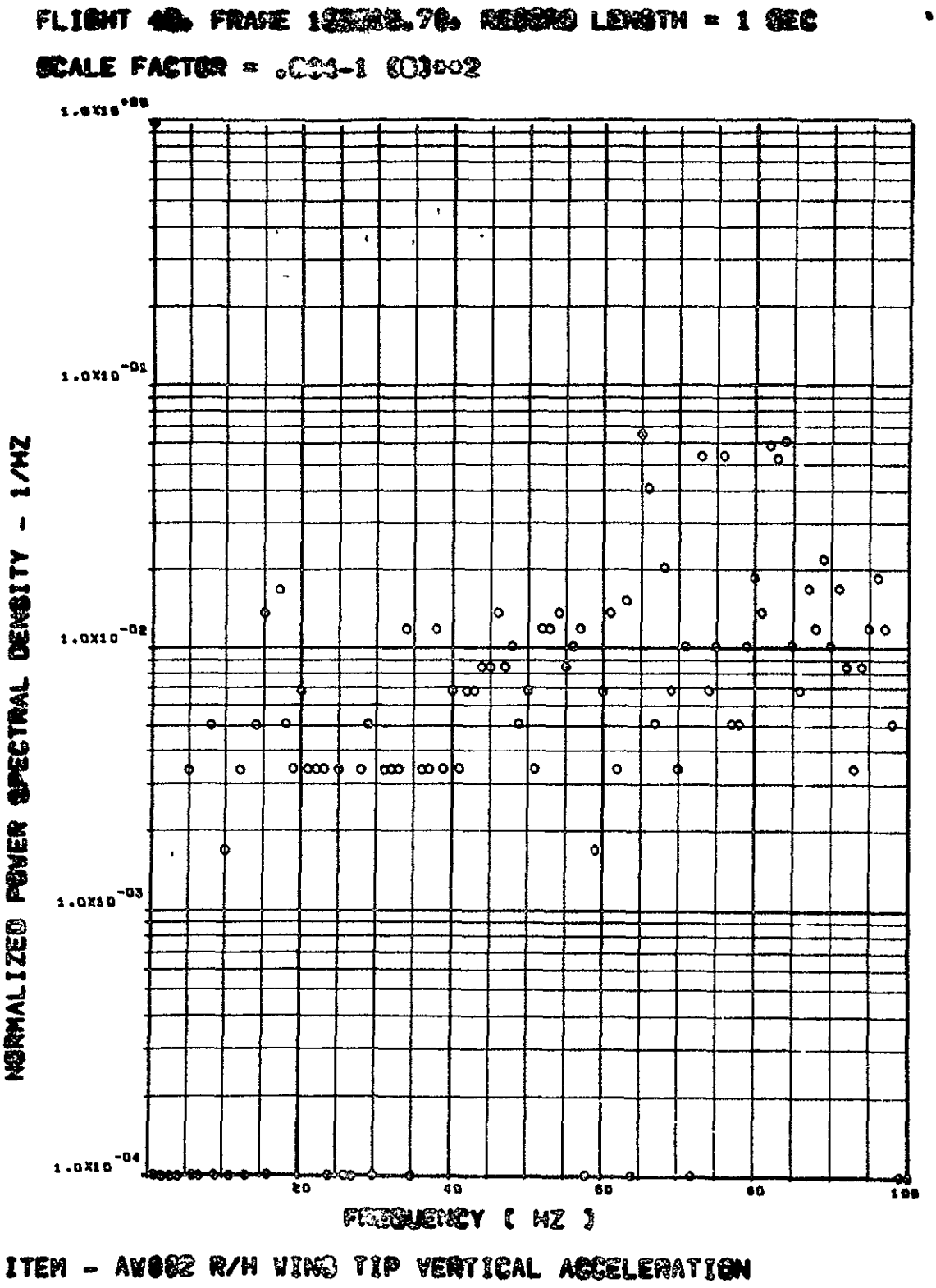

Figure 16. Continued

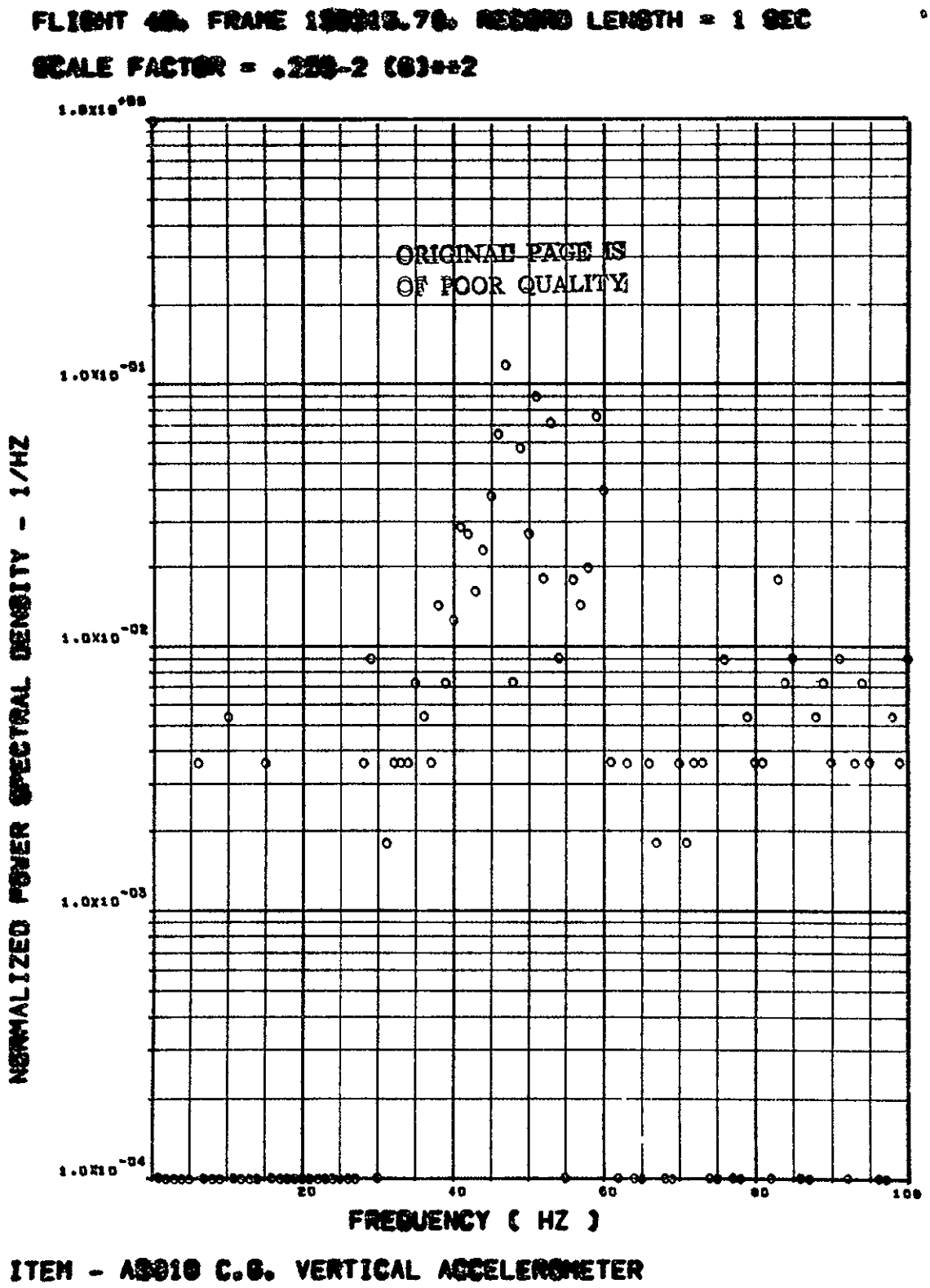

Figure 16. Continued

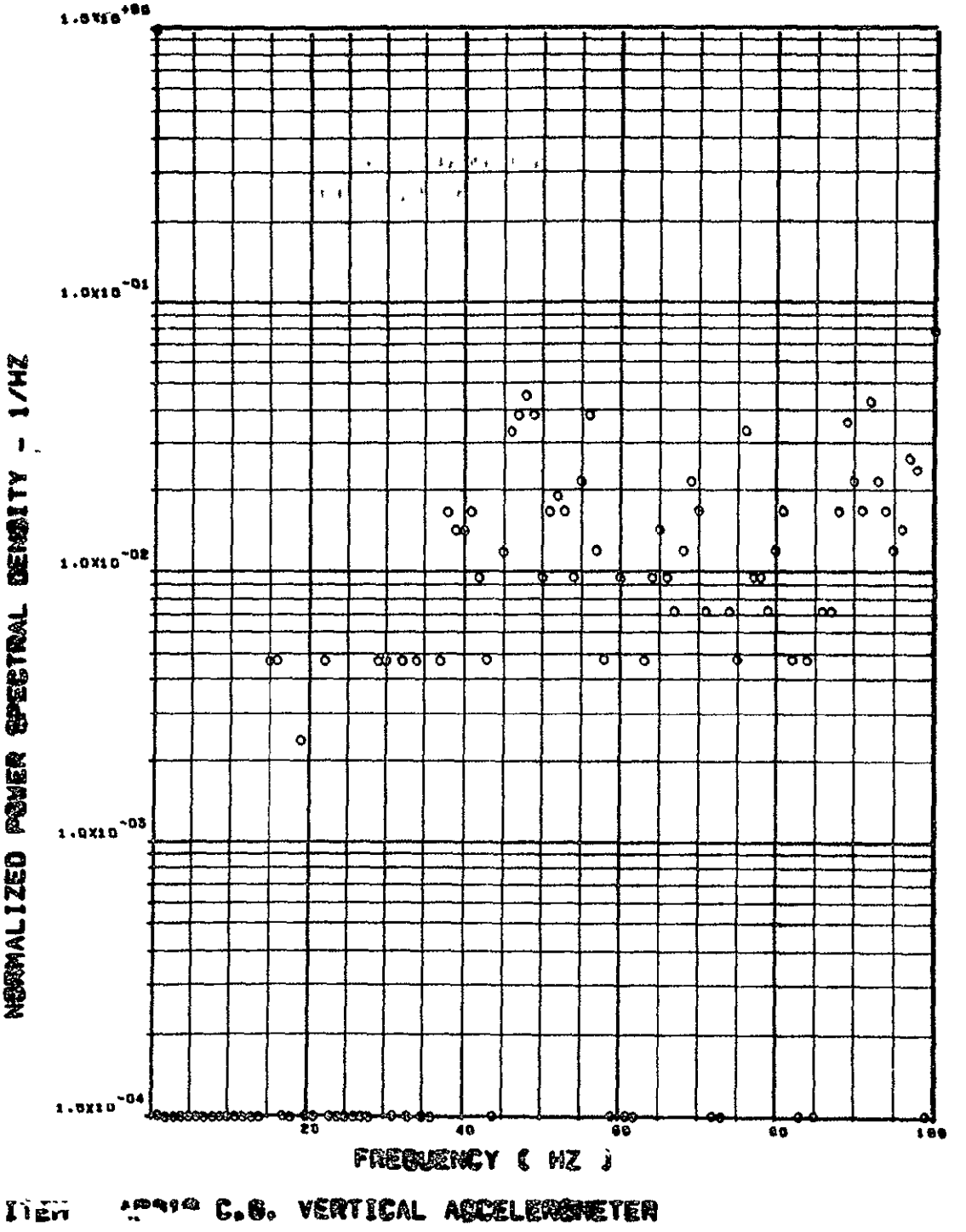

Figure 16. Continued

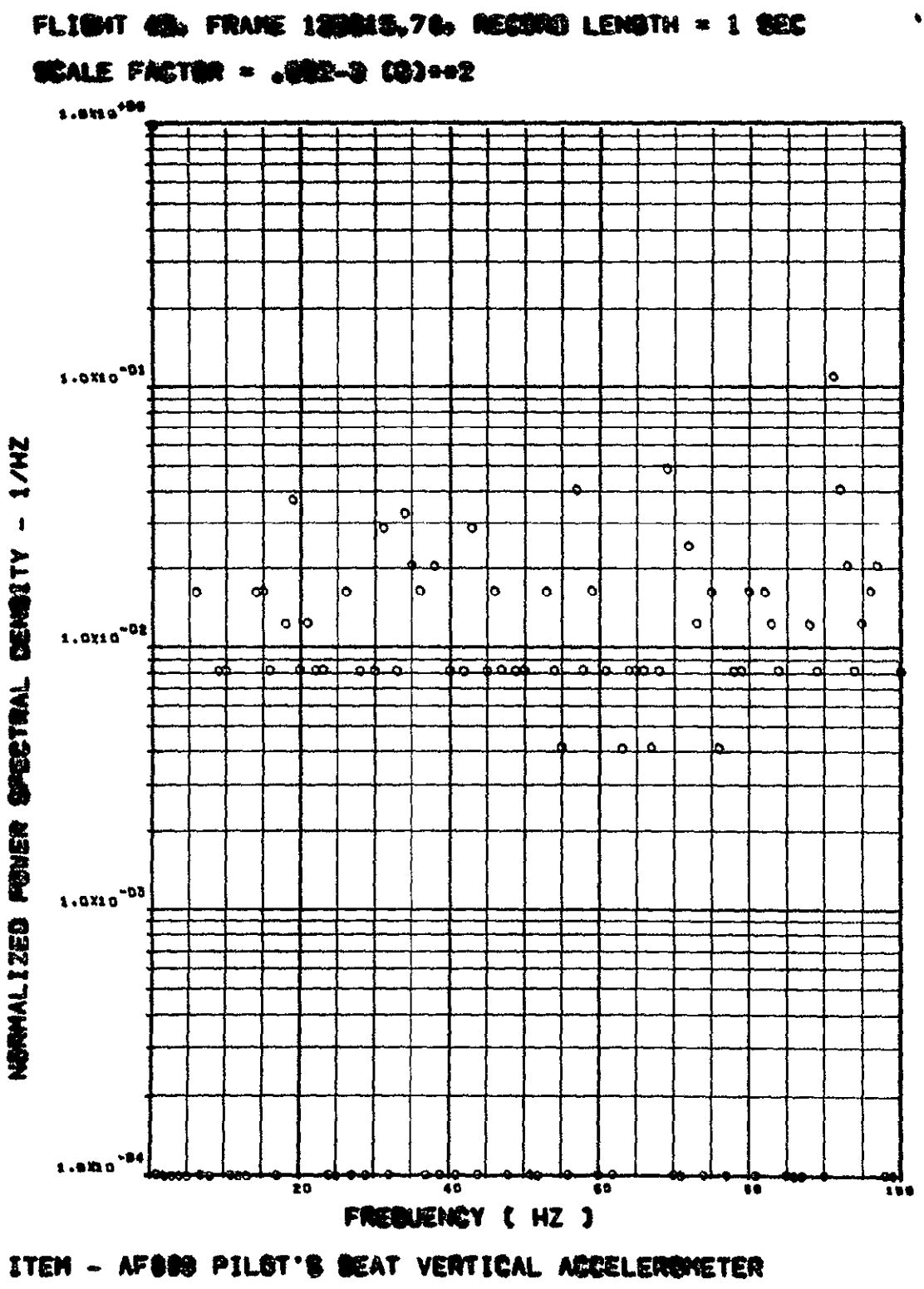

Figure 16. Continued

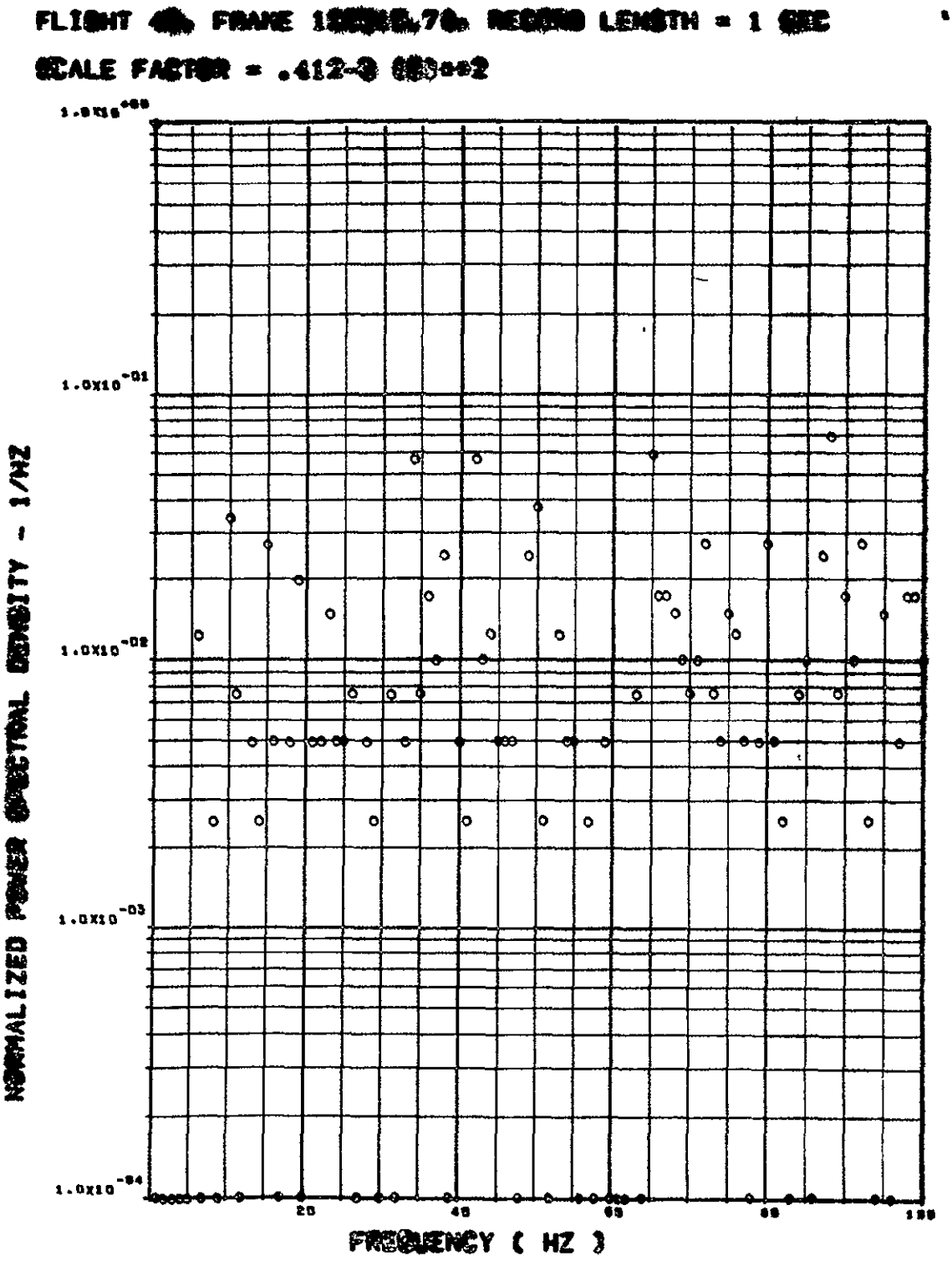

Figure 16. Continued

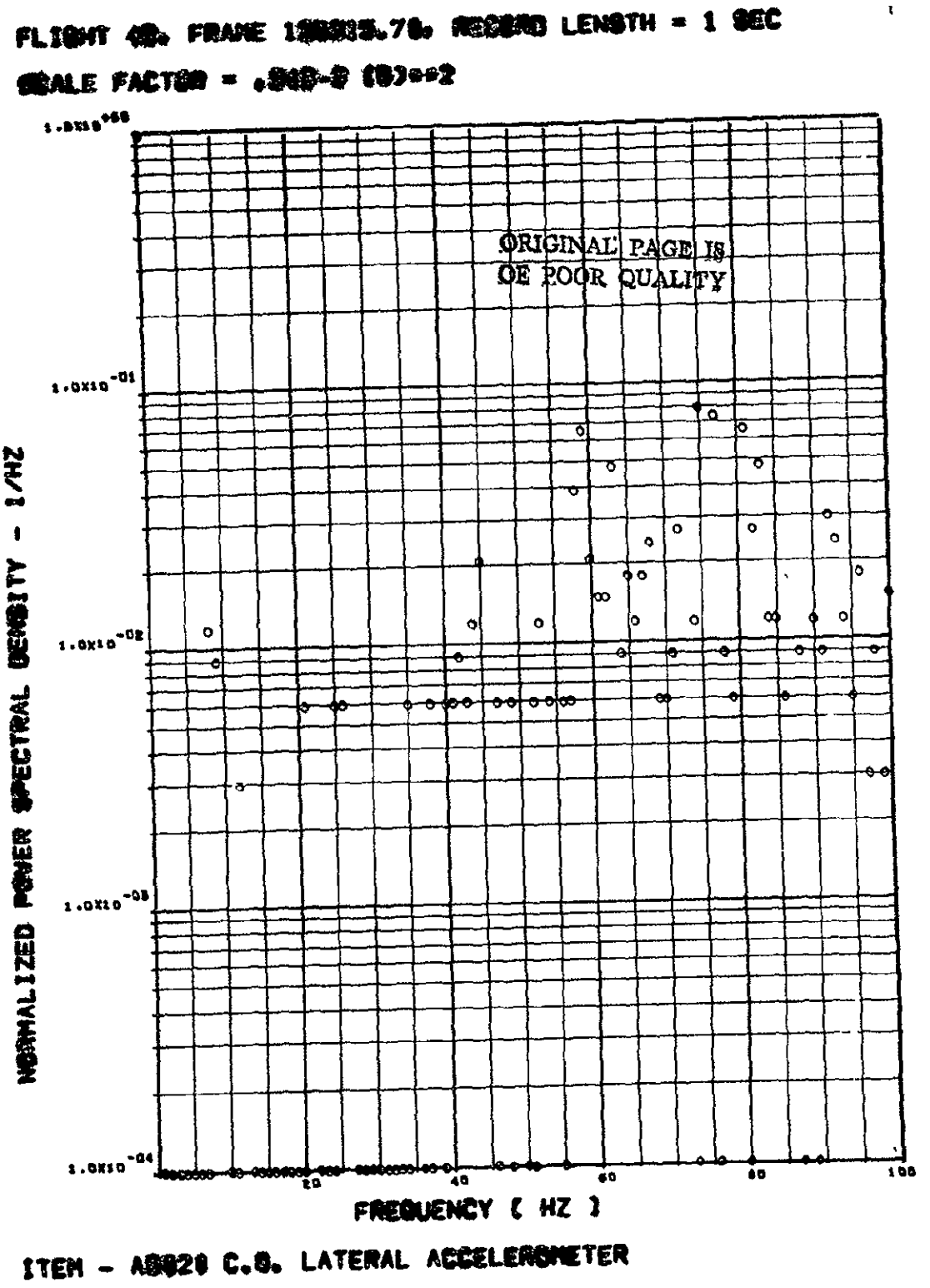

Figure 16. Continued

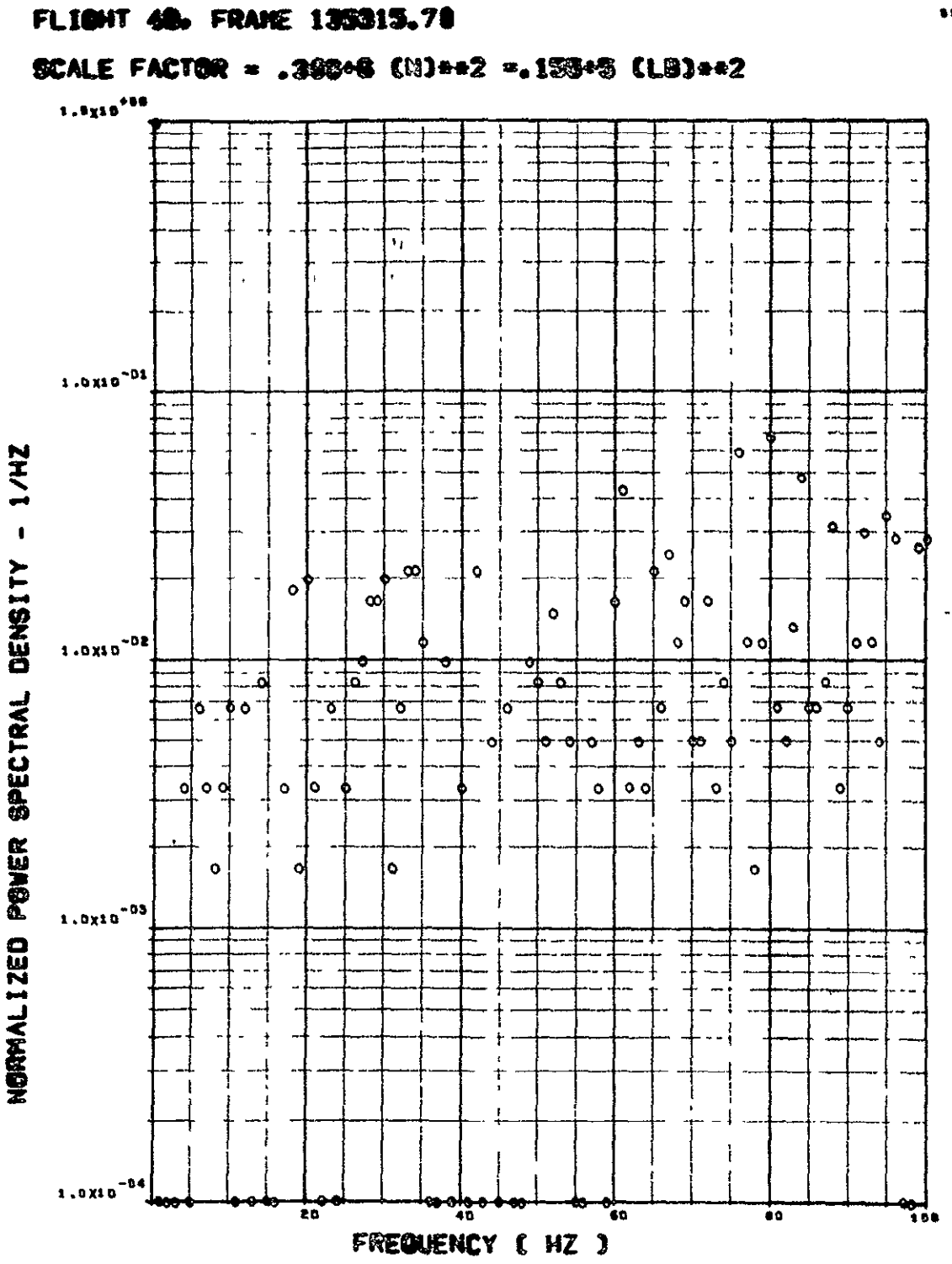

Figure 16. Continued

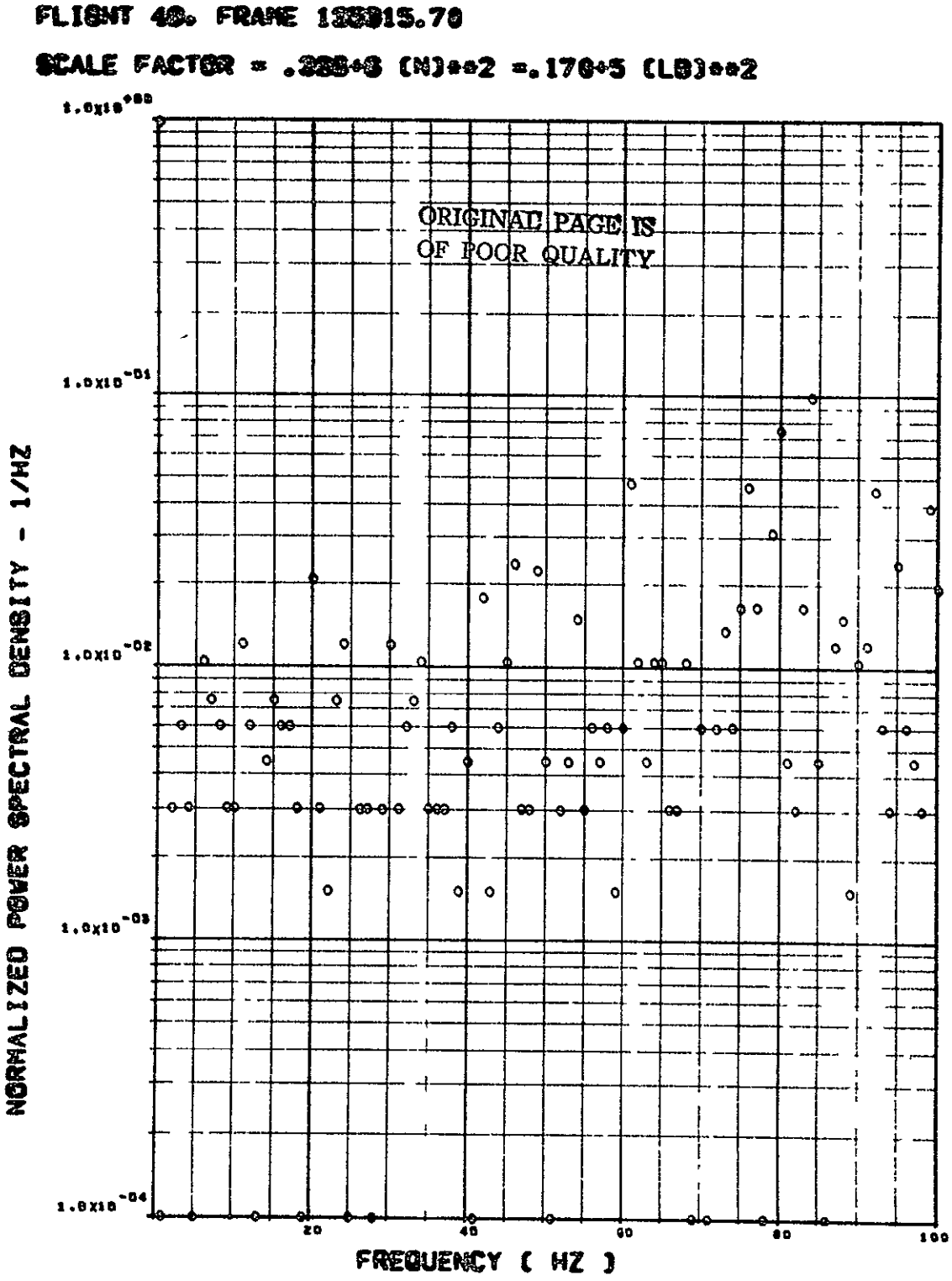

Figure 16. Continued

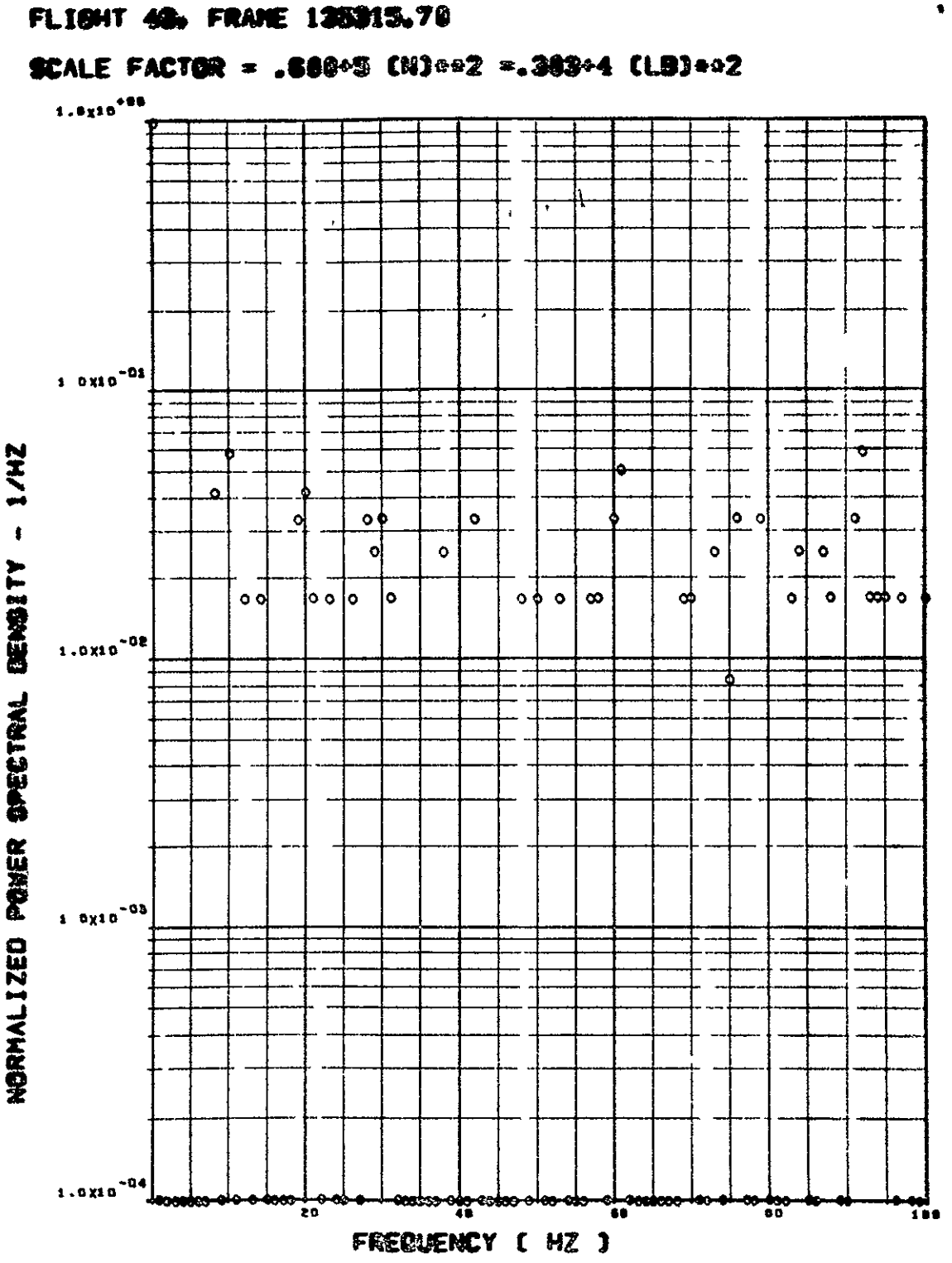

Figure 16. Continued

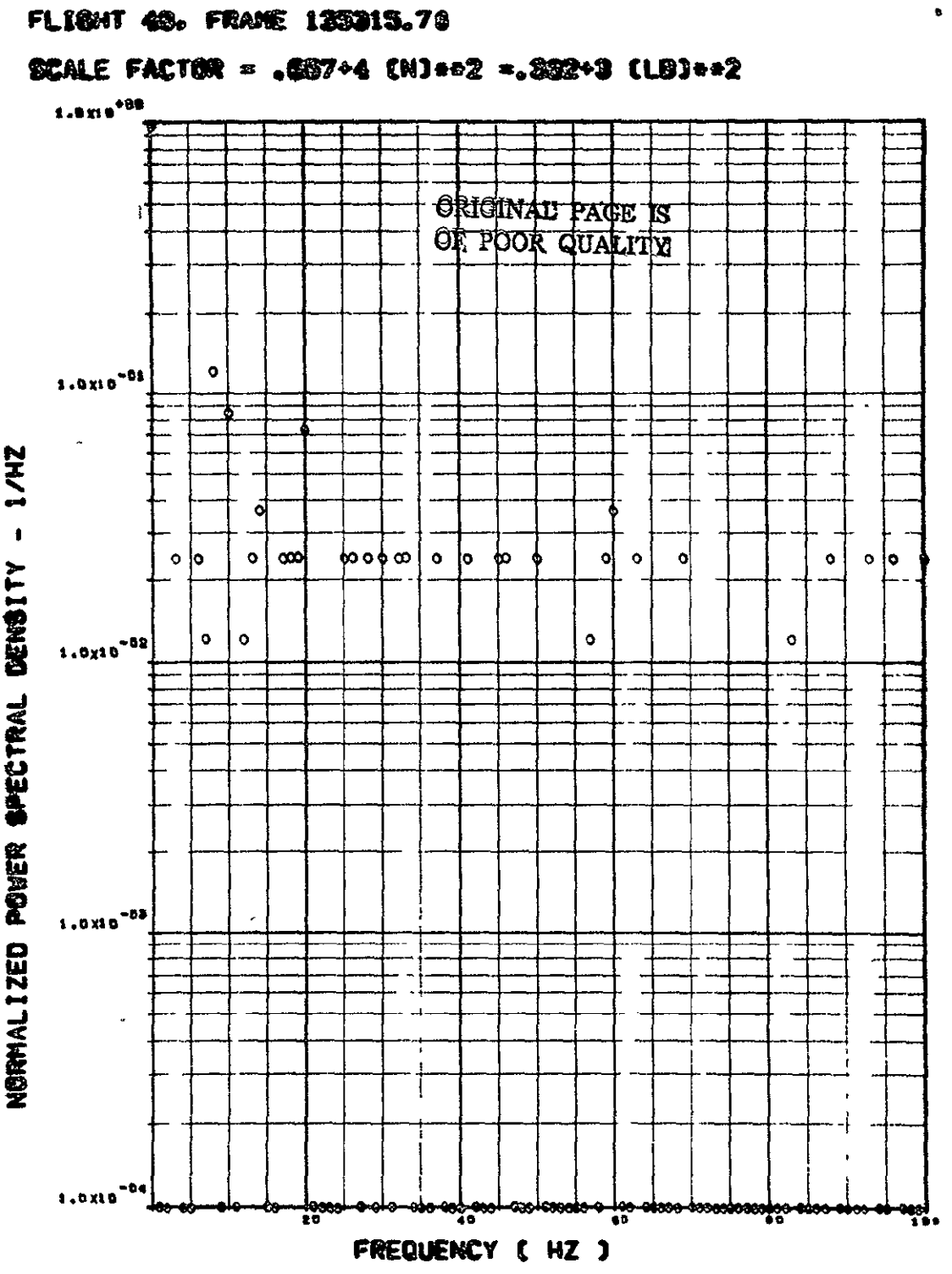

Figure 16. Continued

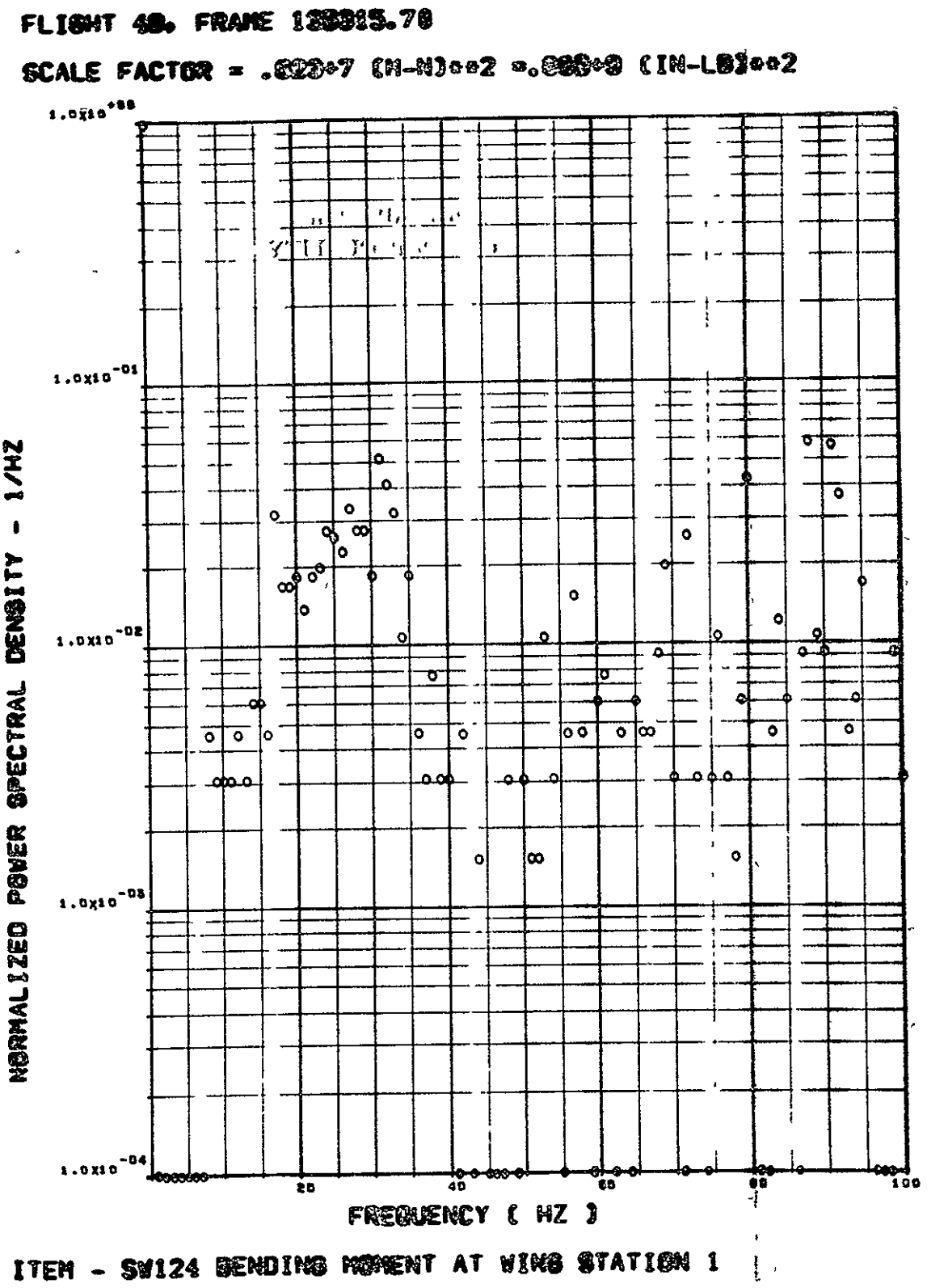

Figure 16. Continued

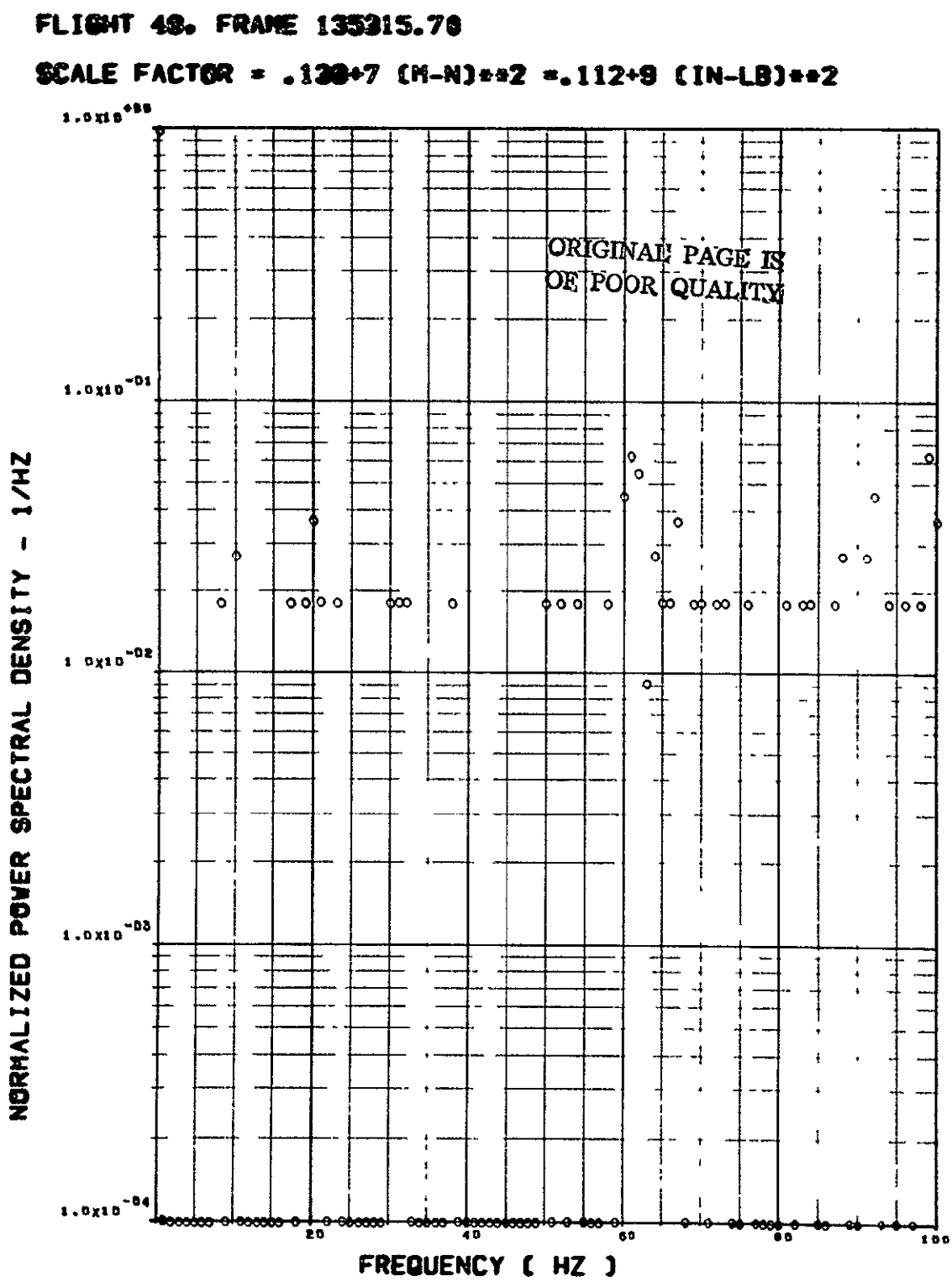

Figure 16. Continued

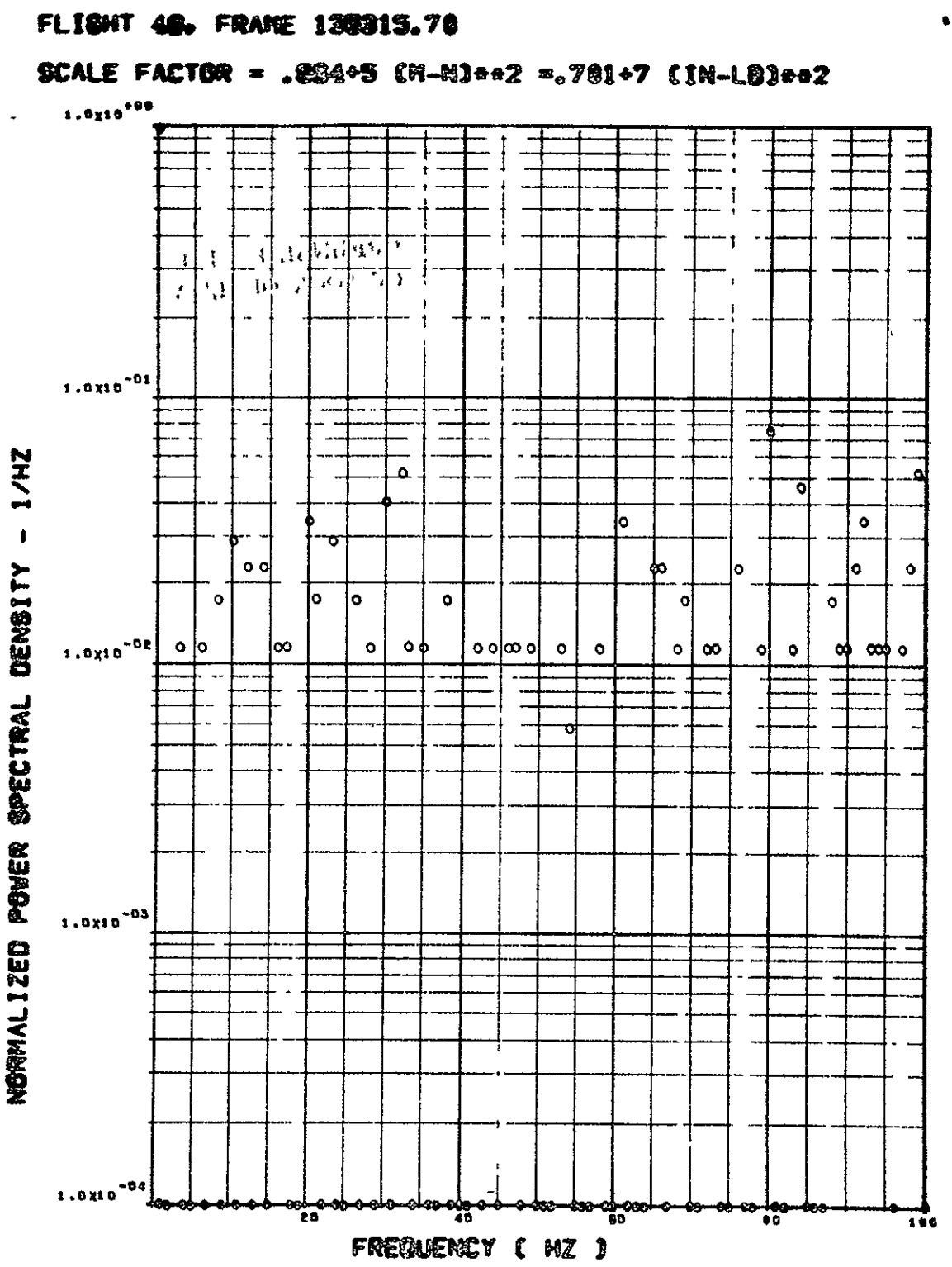

Figure 16. Continued

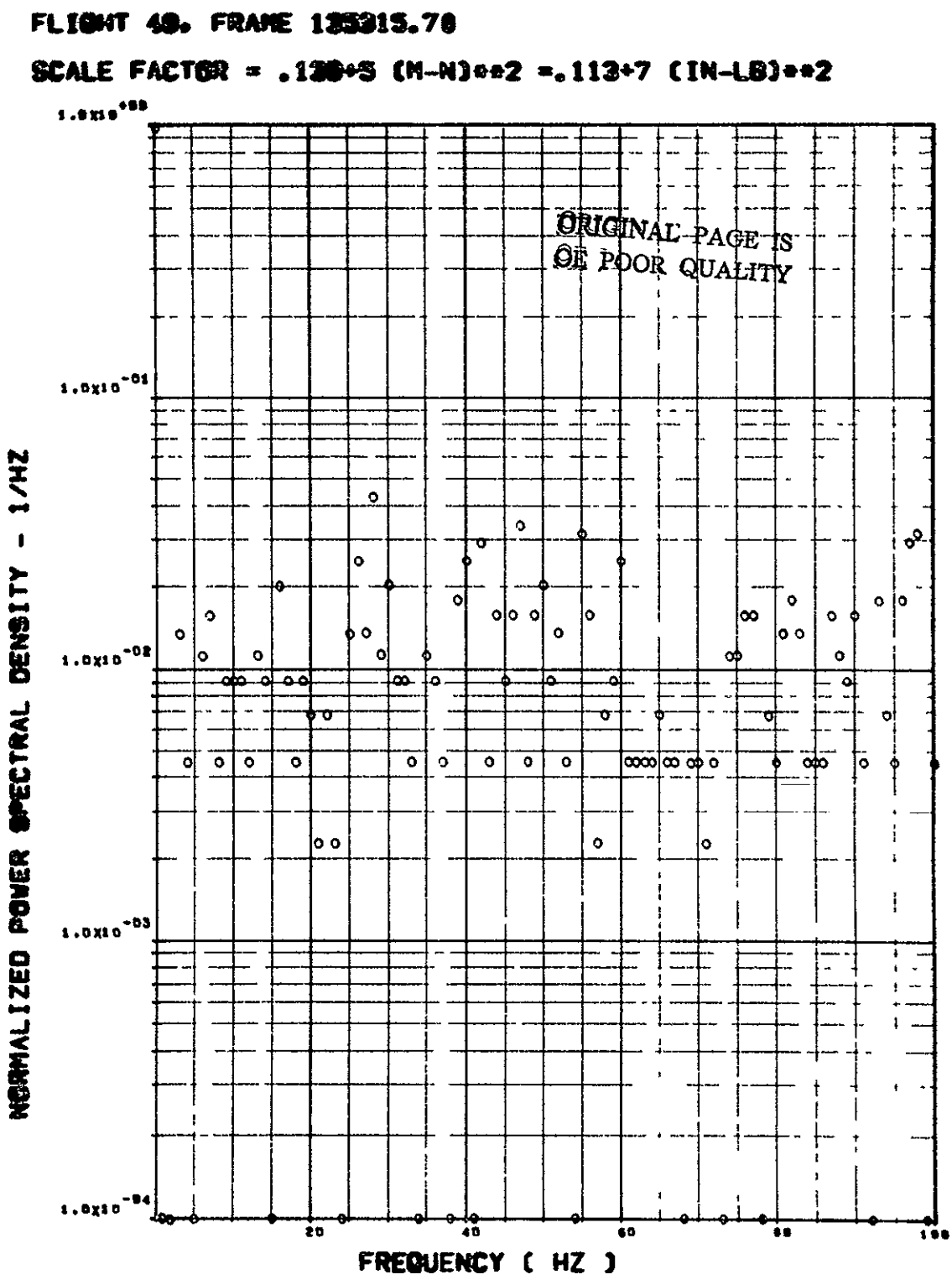

Figure 16. Continued

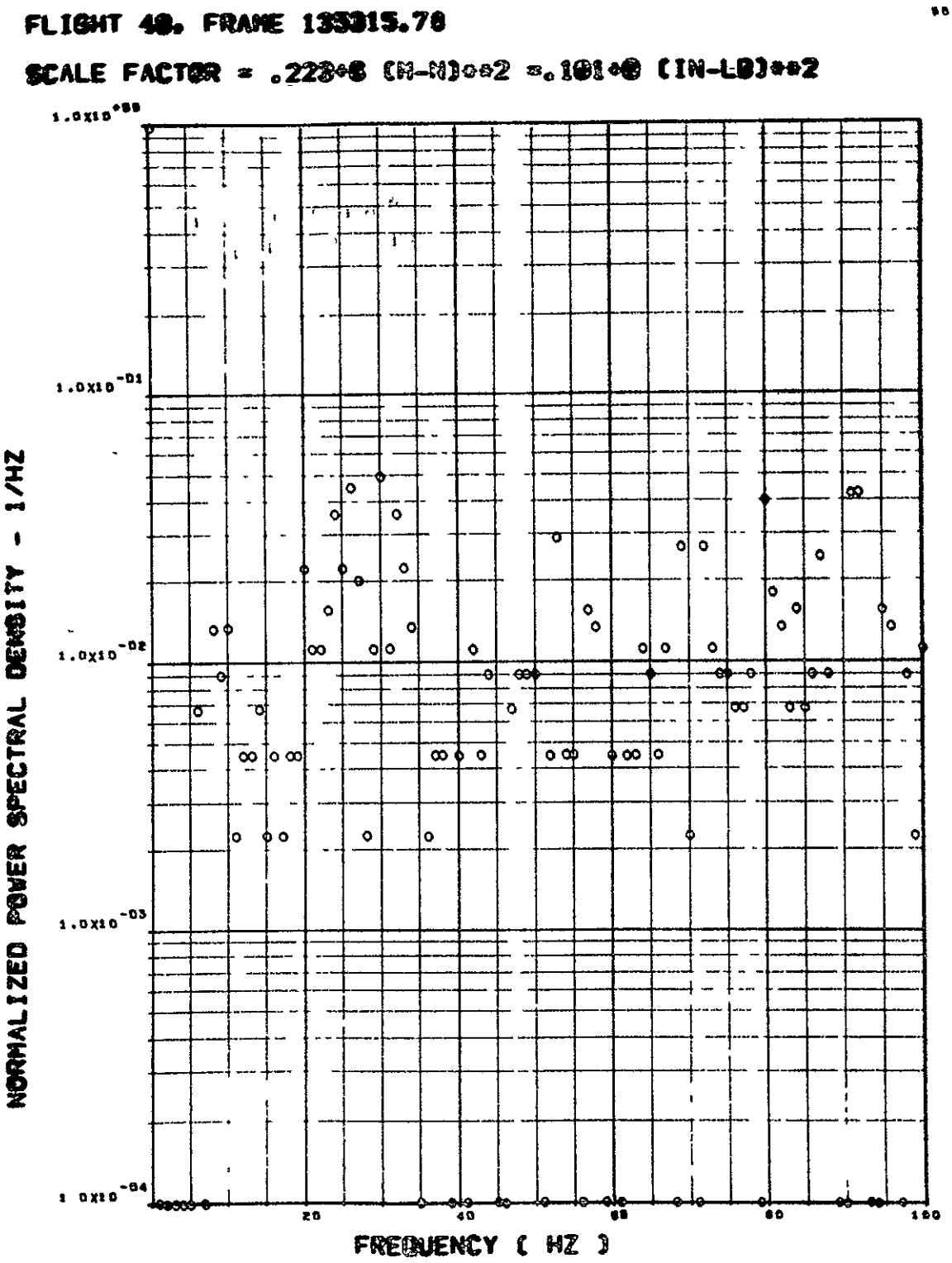

Figure 16. Continued

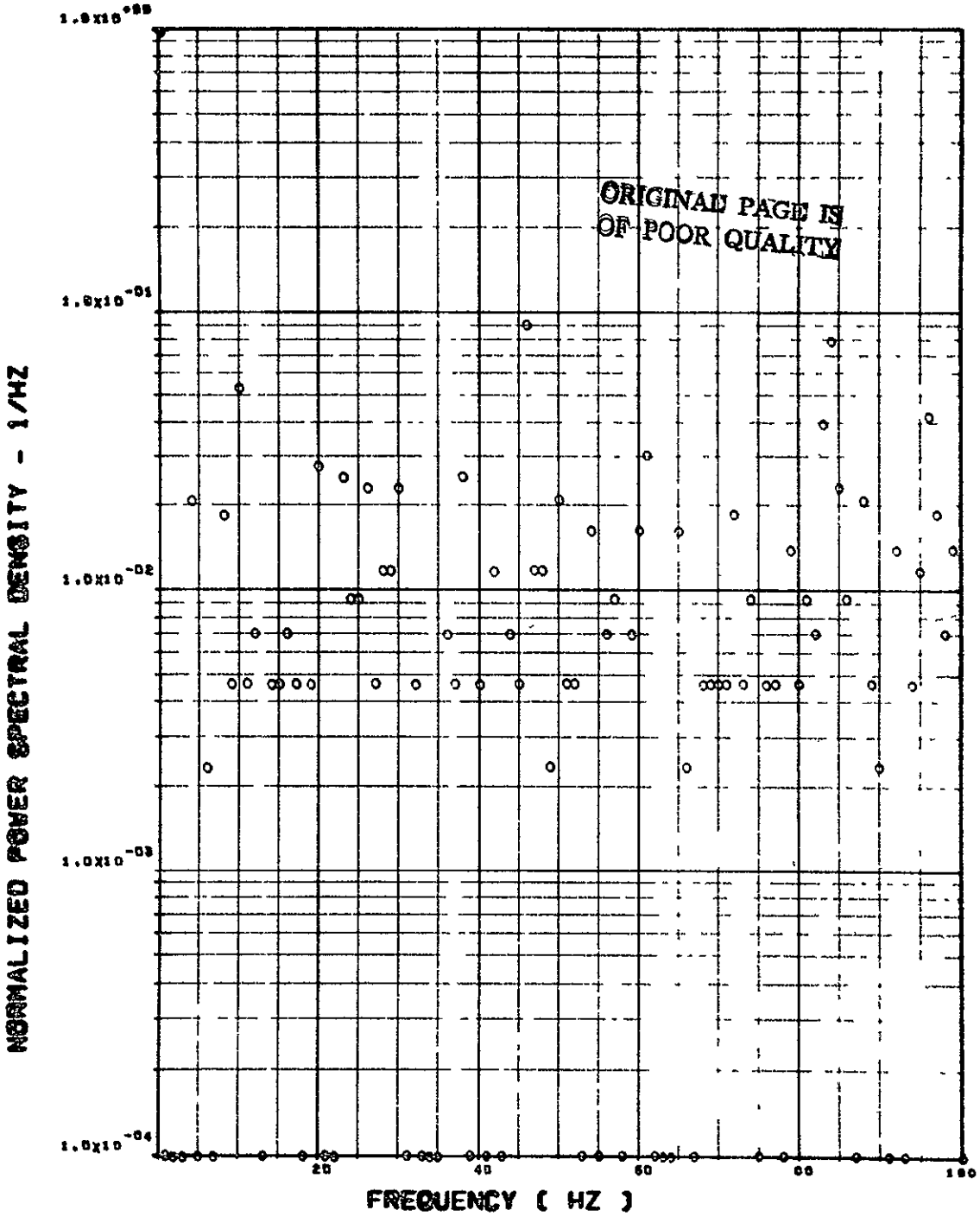

Figure 16. Continued

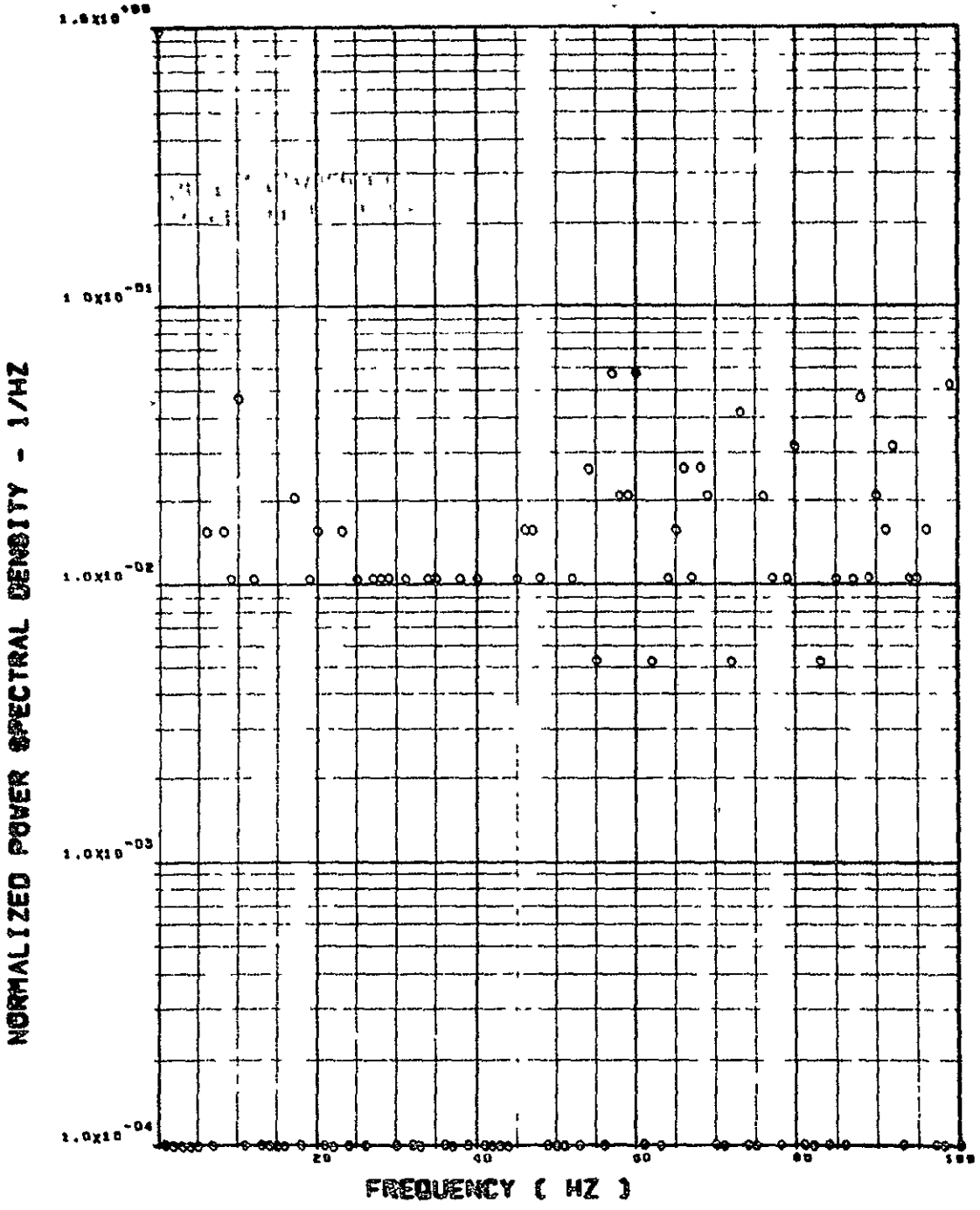

Figure 16. Continued

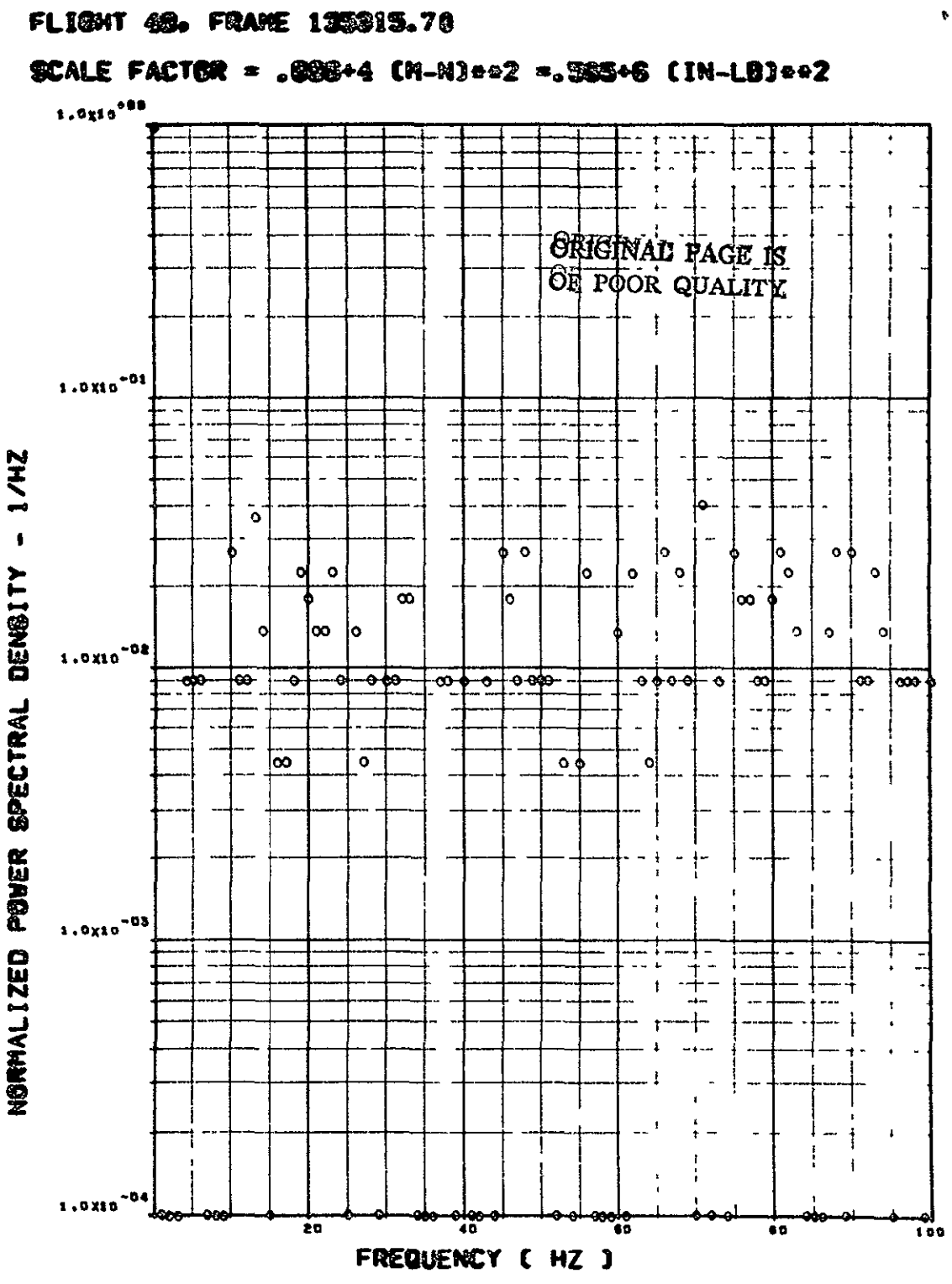

Figure 16. Continued

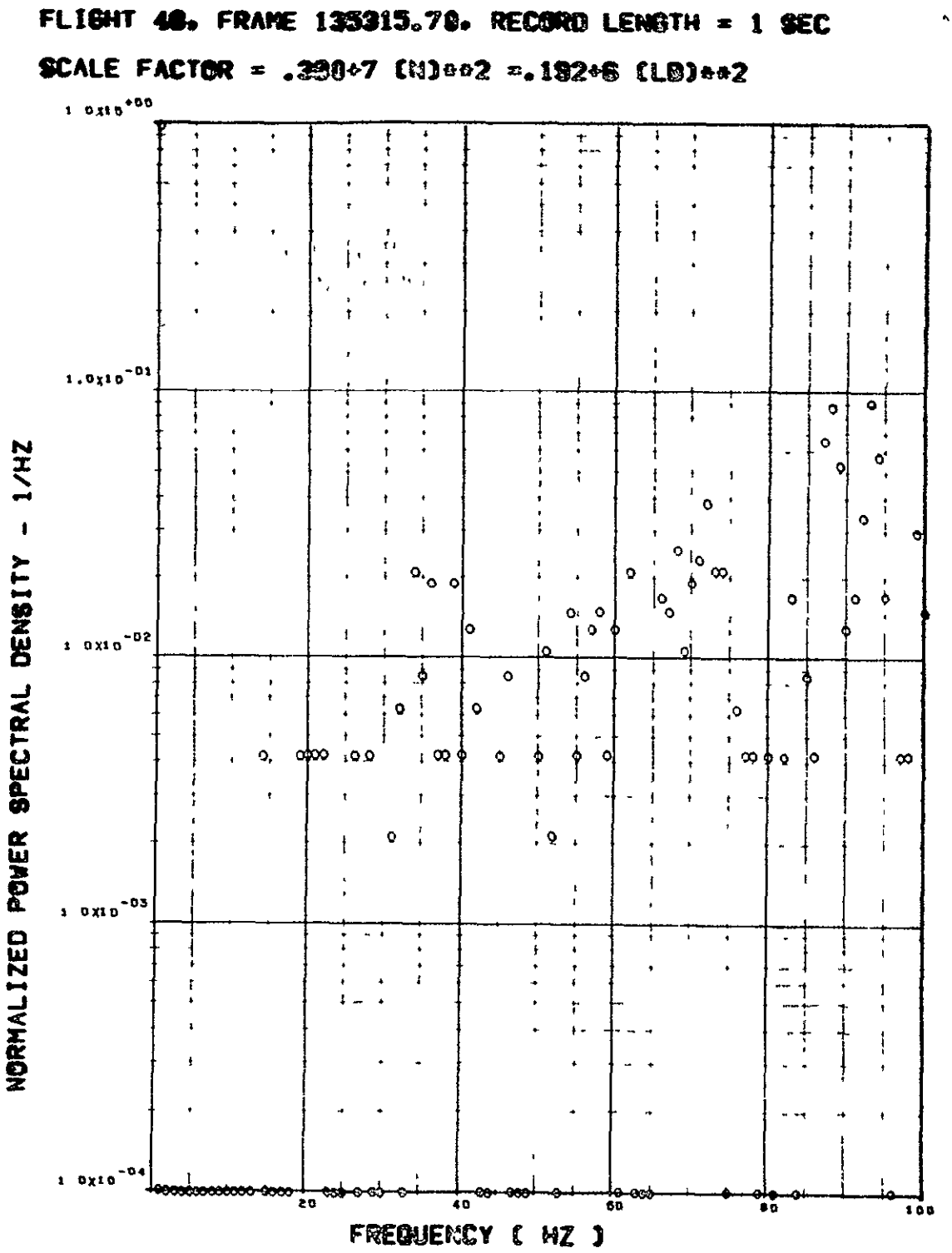

Figure 16. Continued

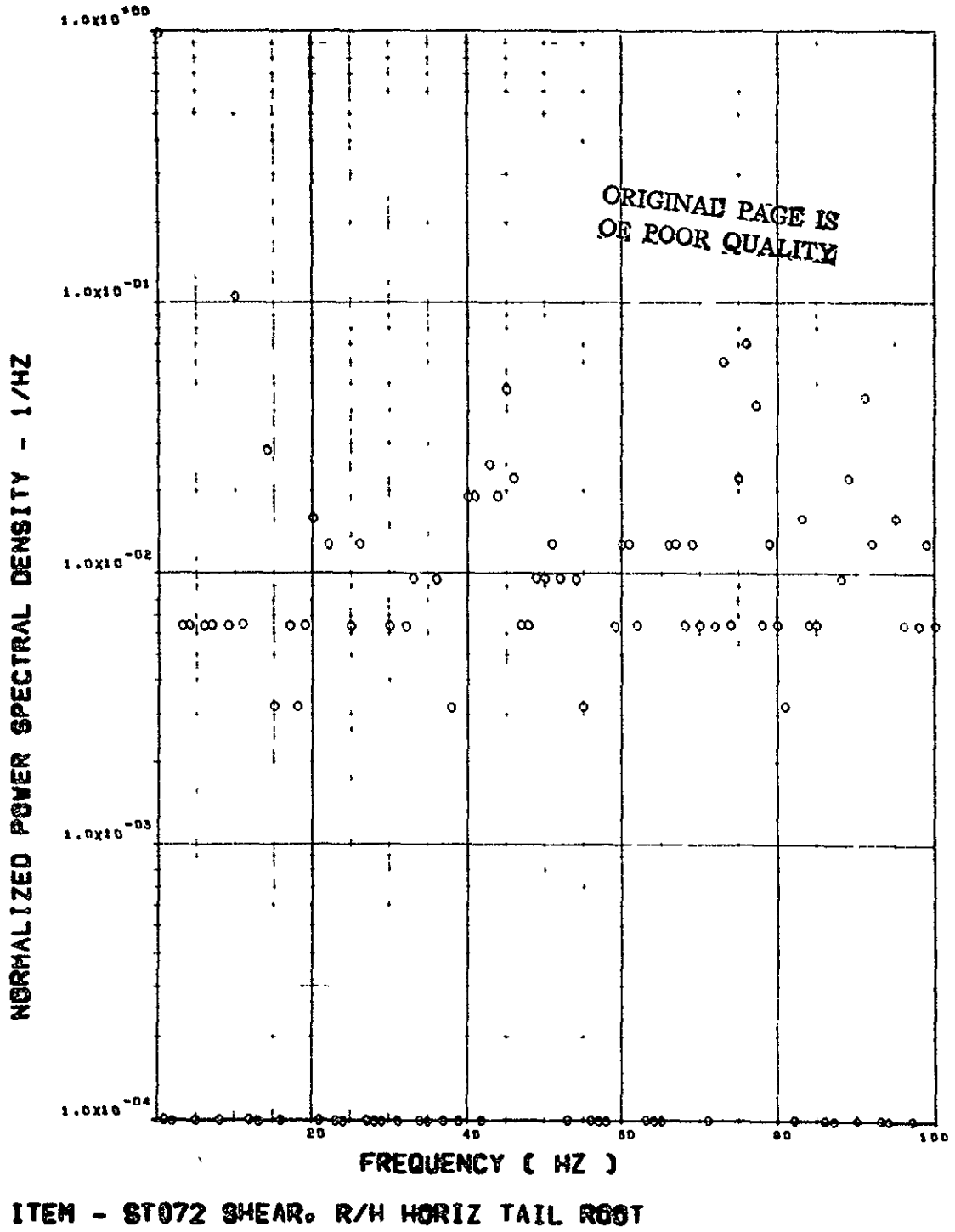

Figure 16. Continued

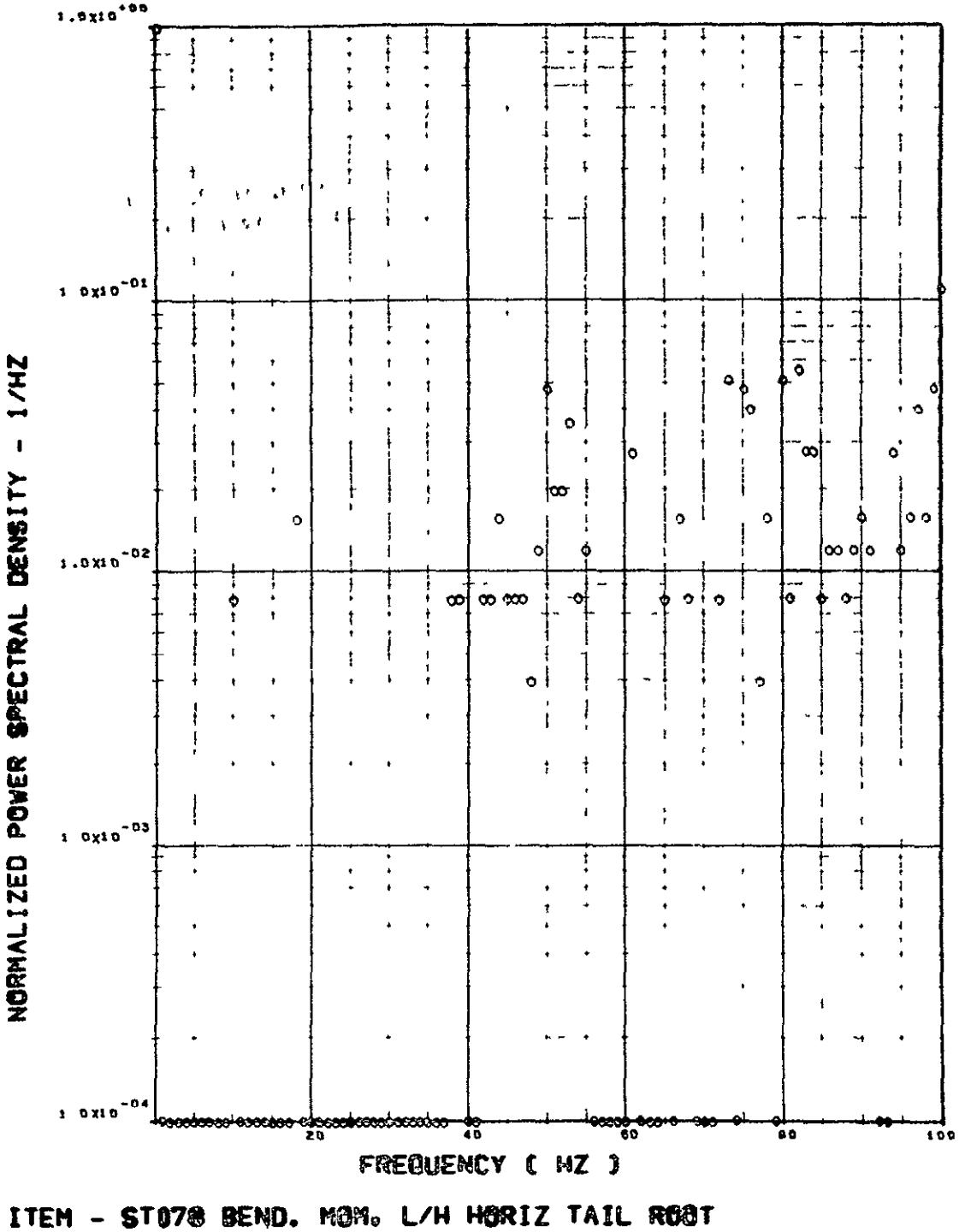

Figure 16. Continued

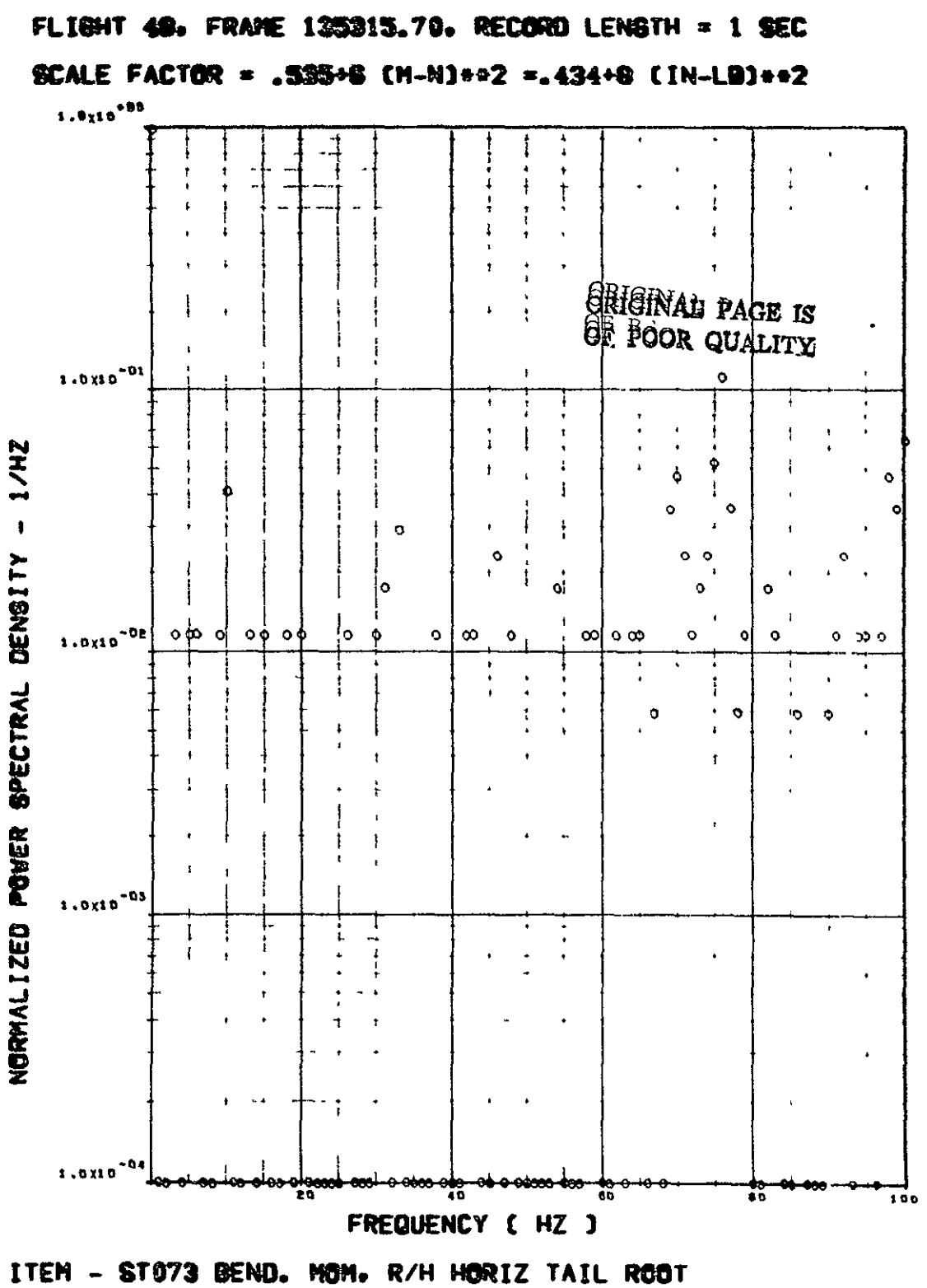

Figure 16. Continued

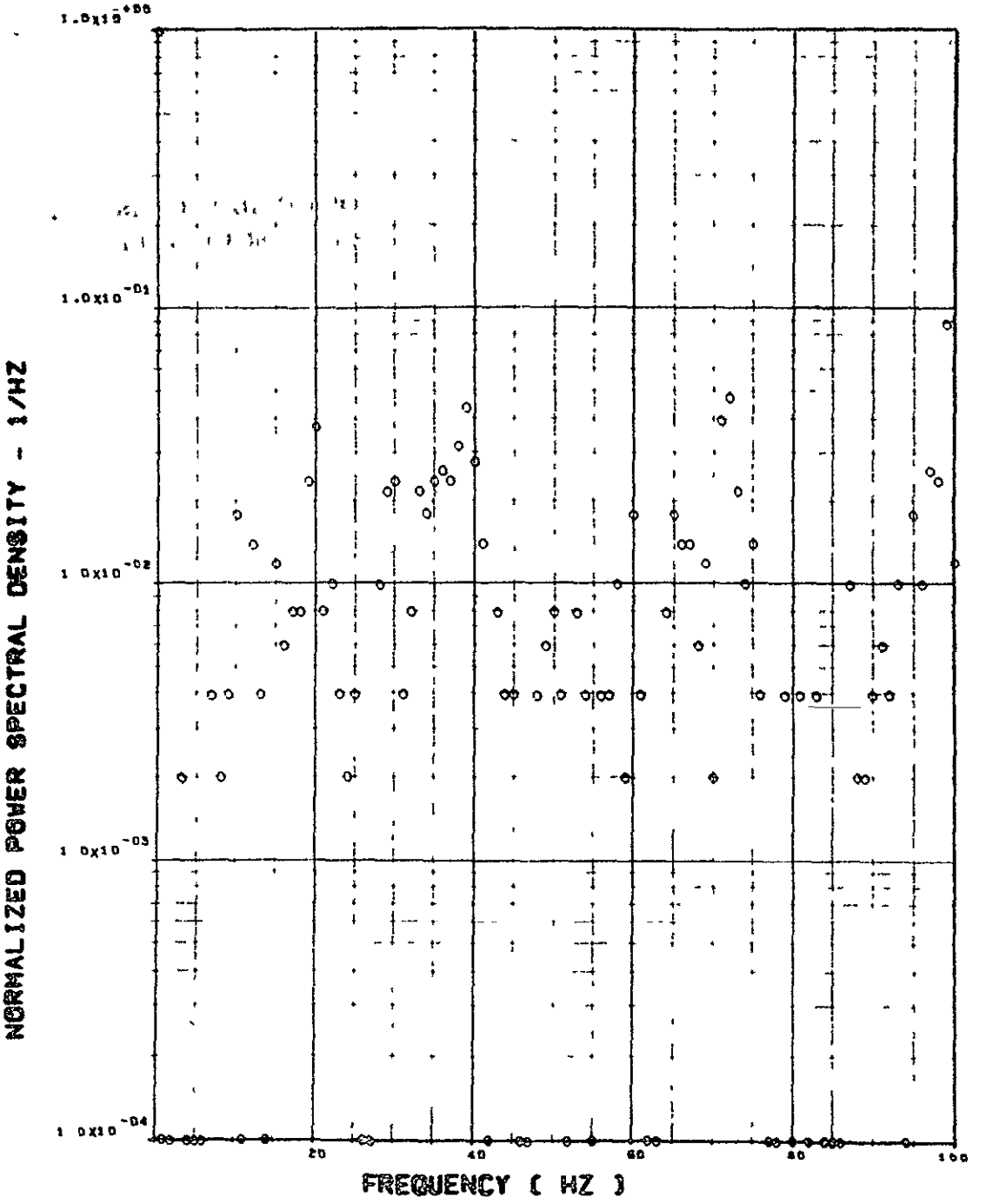

Figure 16. Continued

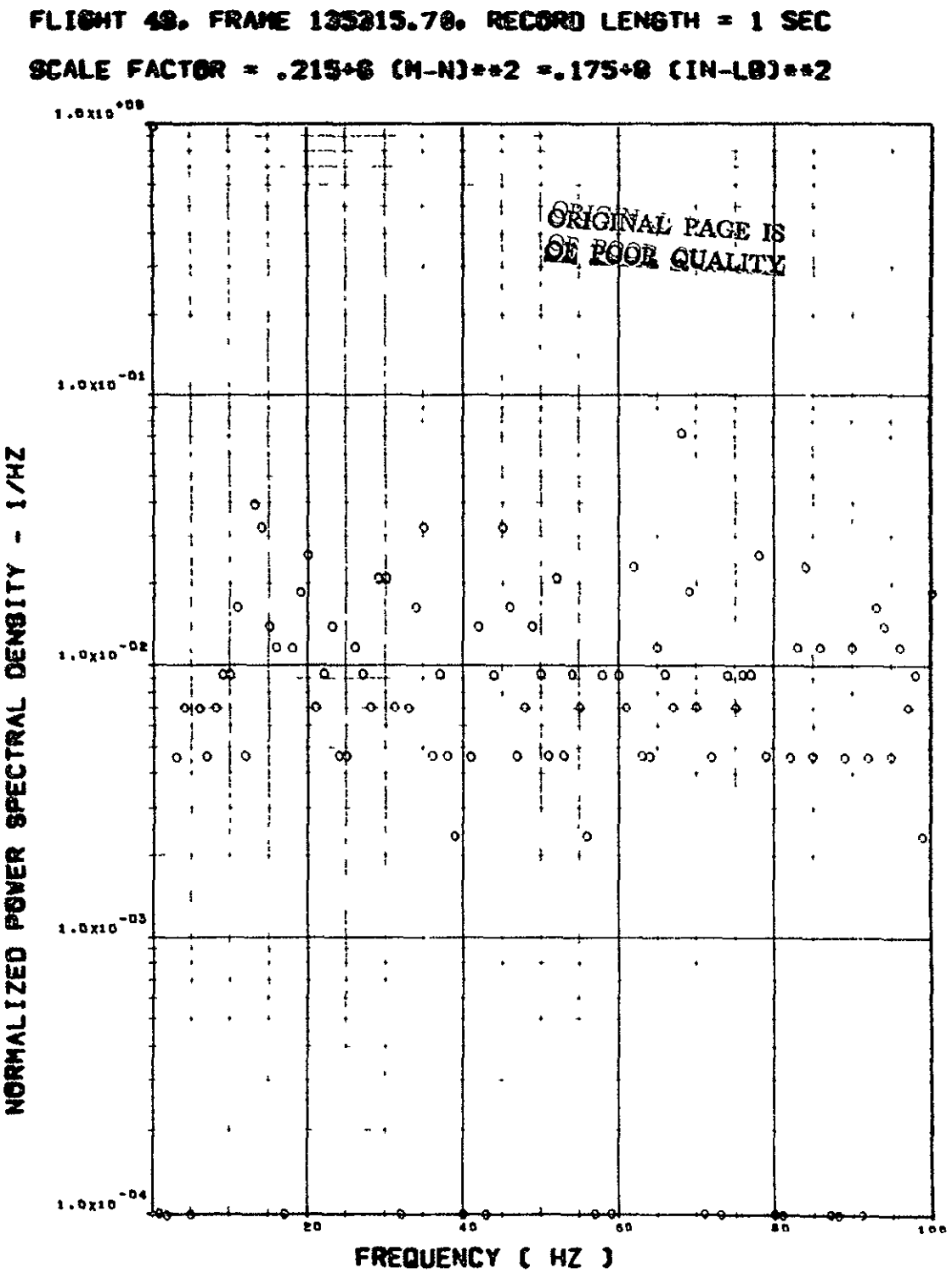

Figure 16. Concluded

C-4

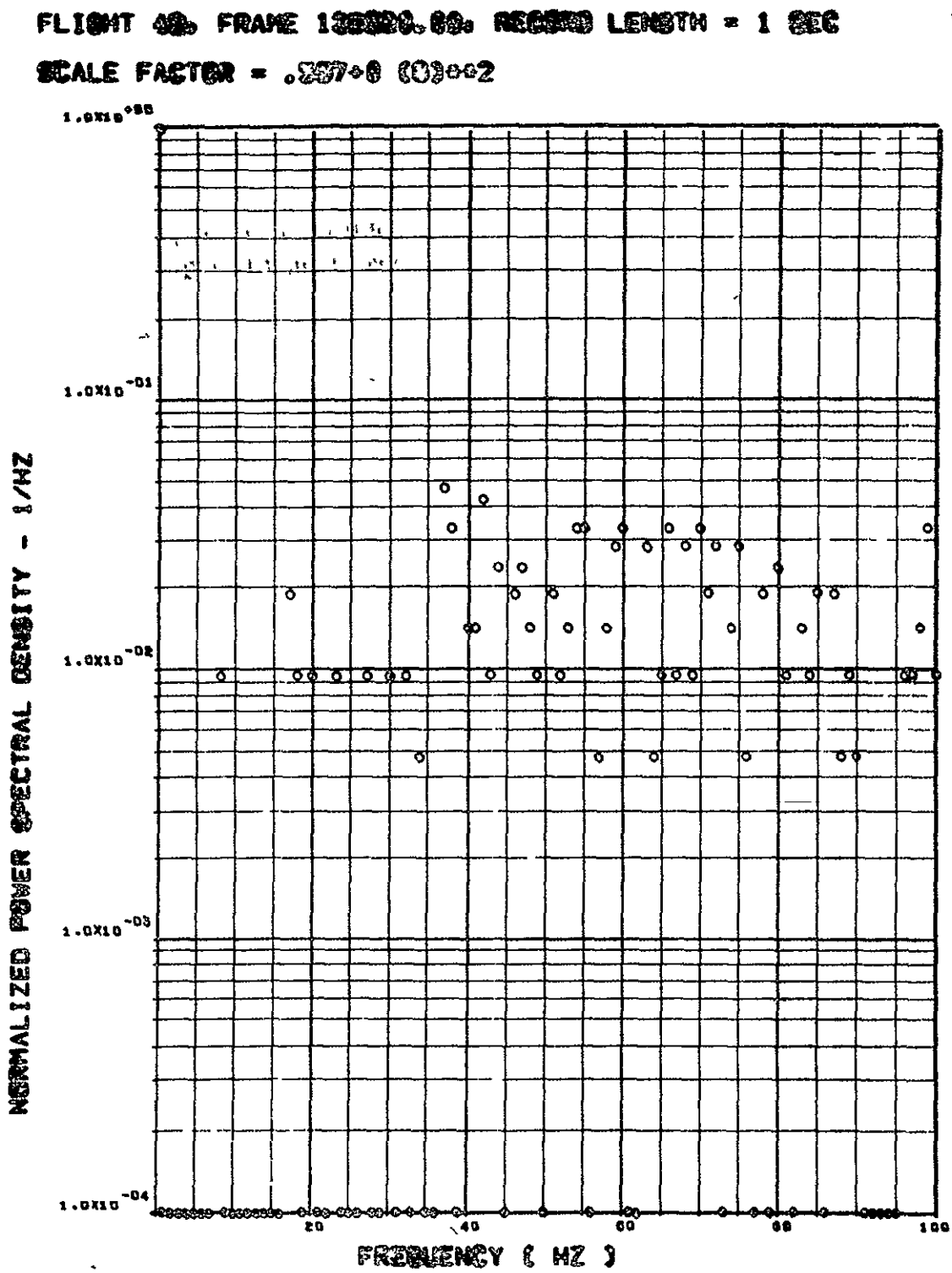

Figure 17. Power Spectra - Flight 48, Run 4, Point 2
T_1 = 135320.7, ΔT = 1 Sec, α_{Nom} = 8.90 deg,
$\Delta\alpha$ = 1.60 deg

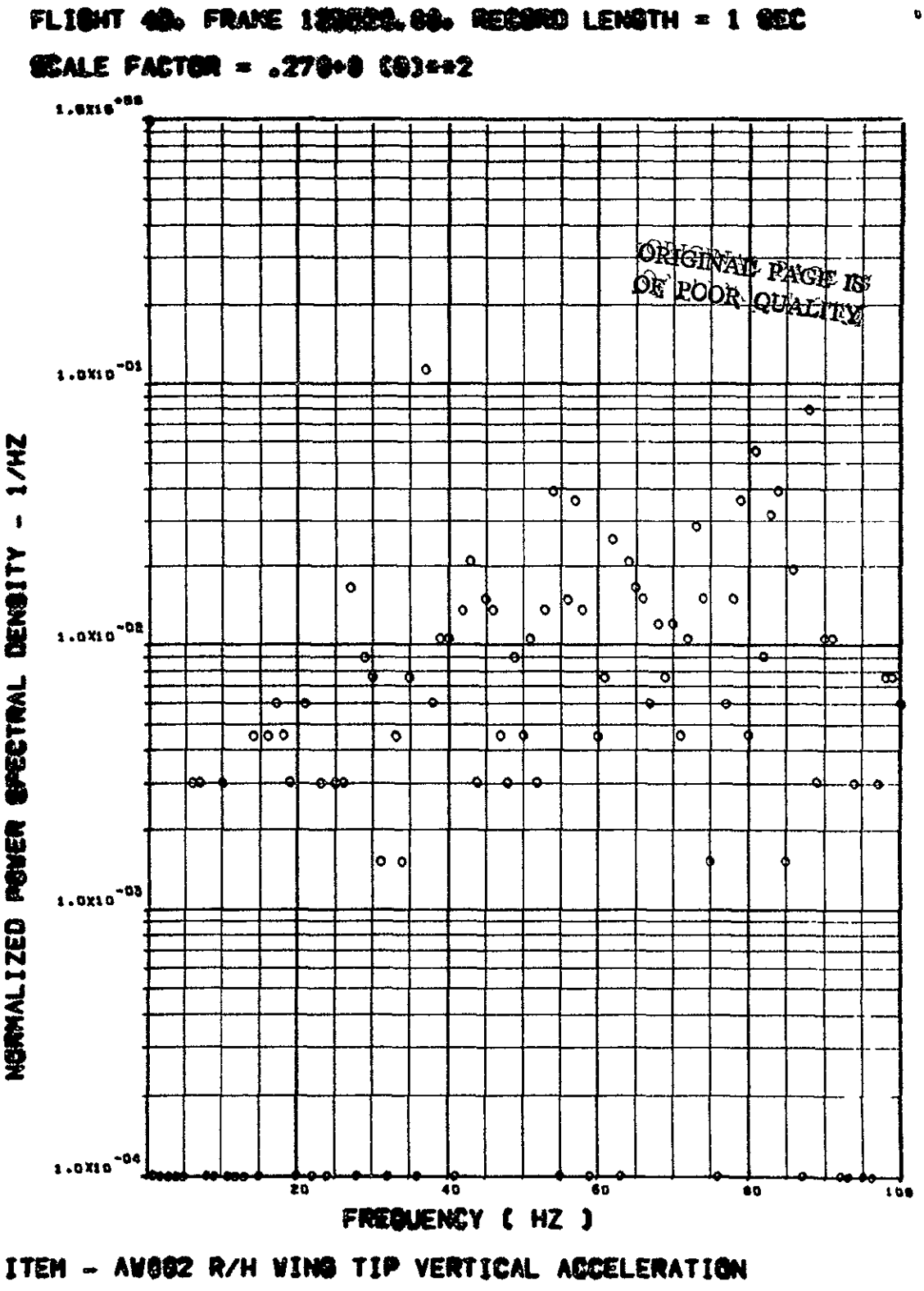

Figure 17. Continued

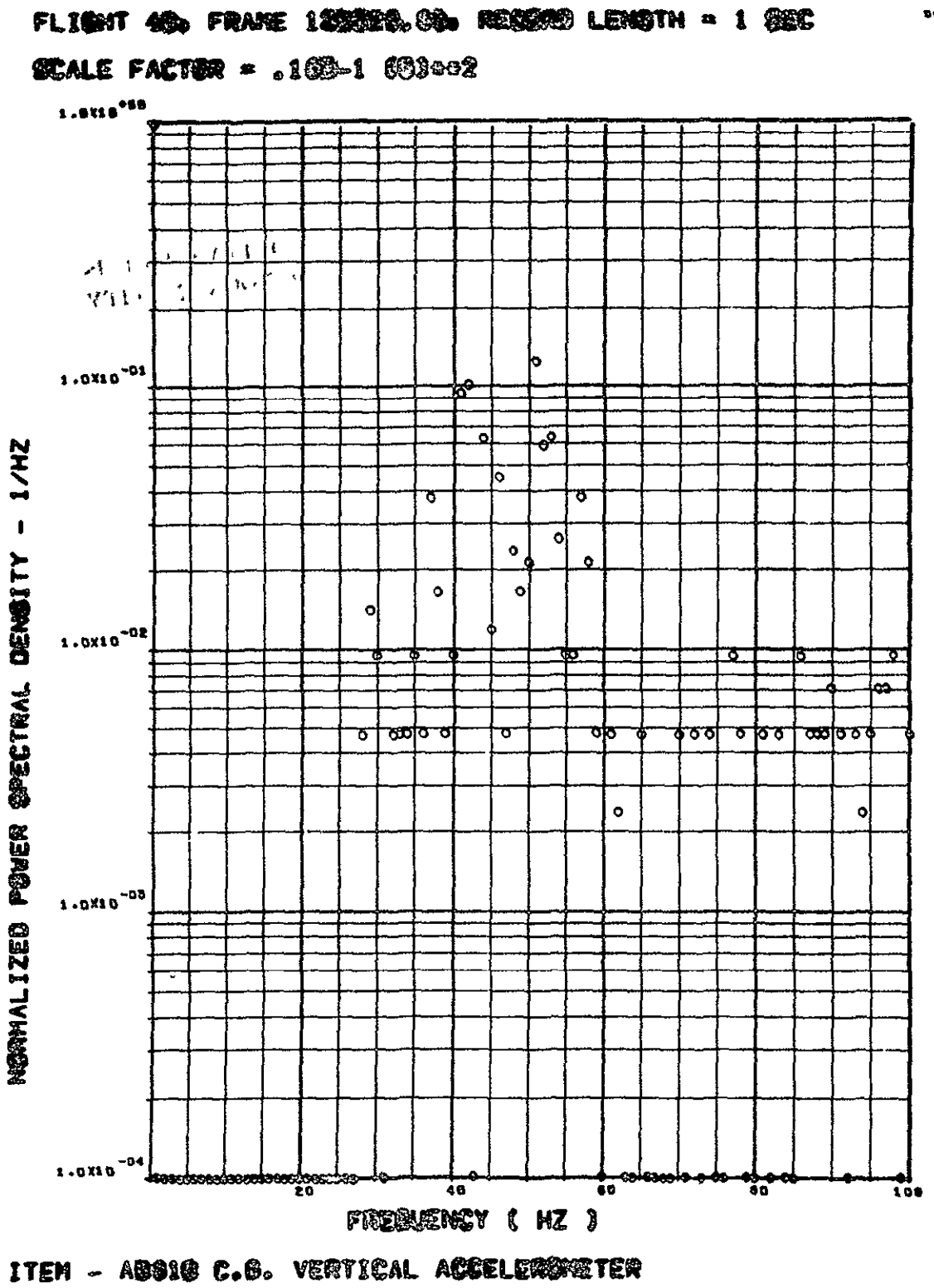

Figure 17. Continued

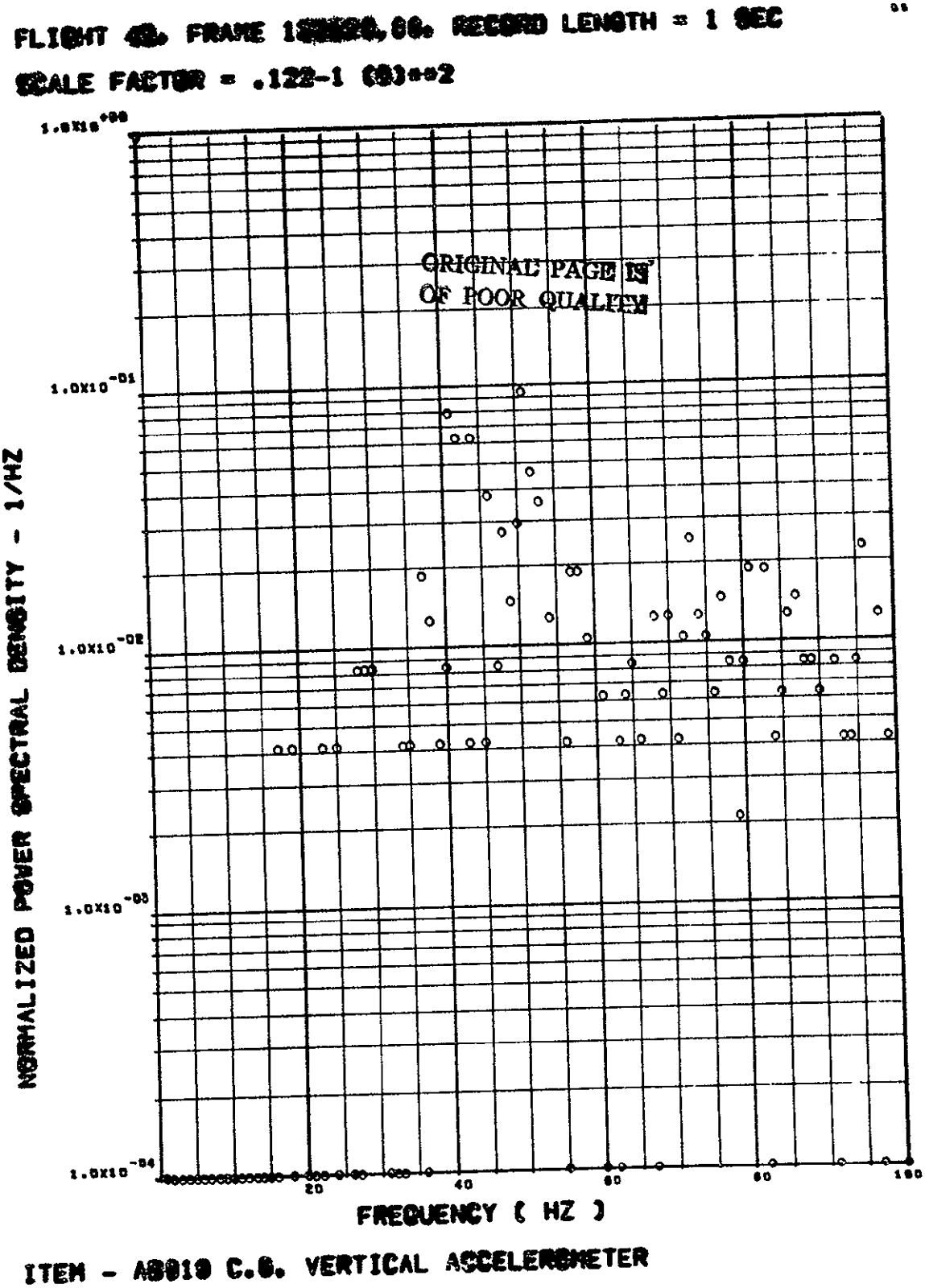

Figure 17. Continued

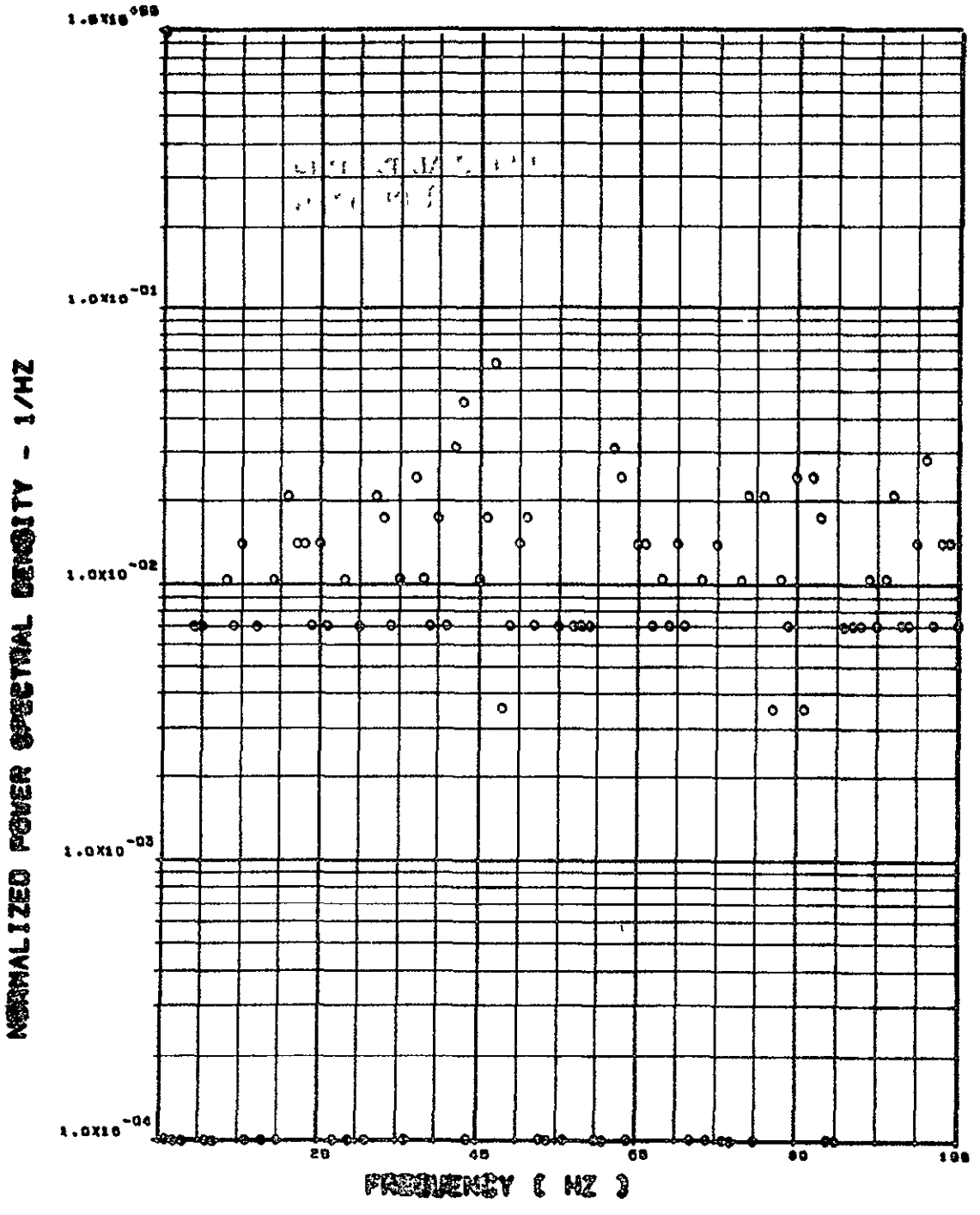

Figure 17. Continued

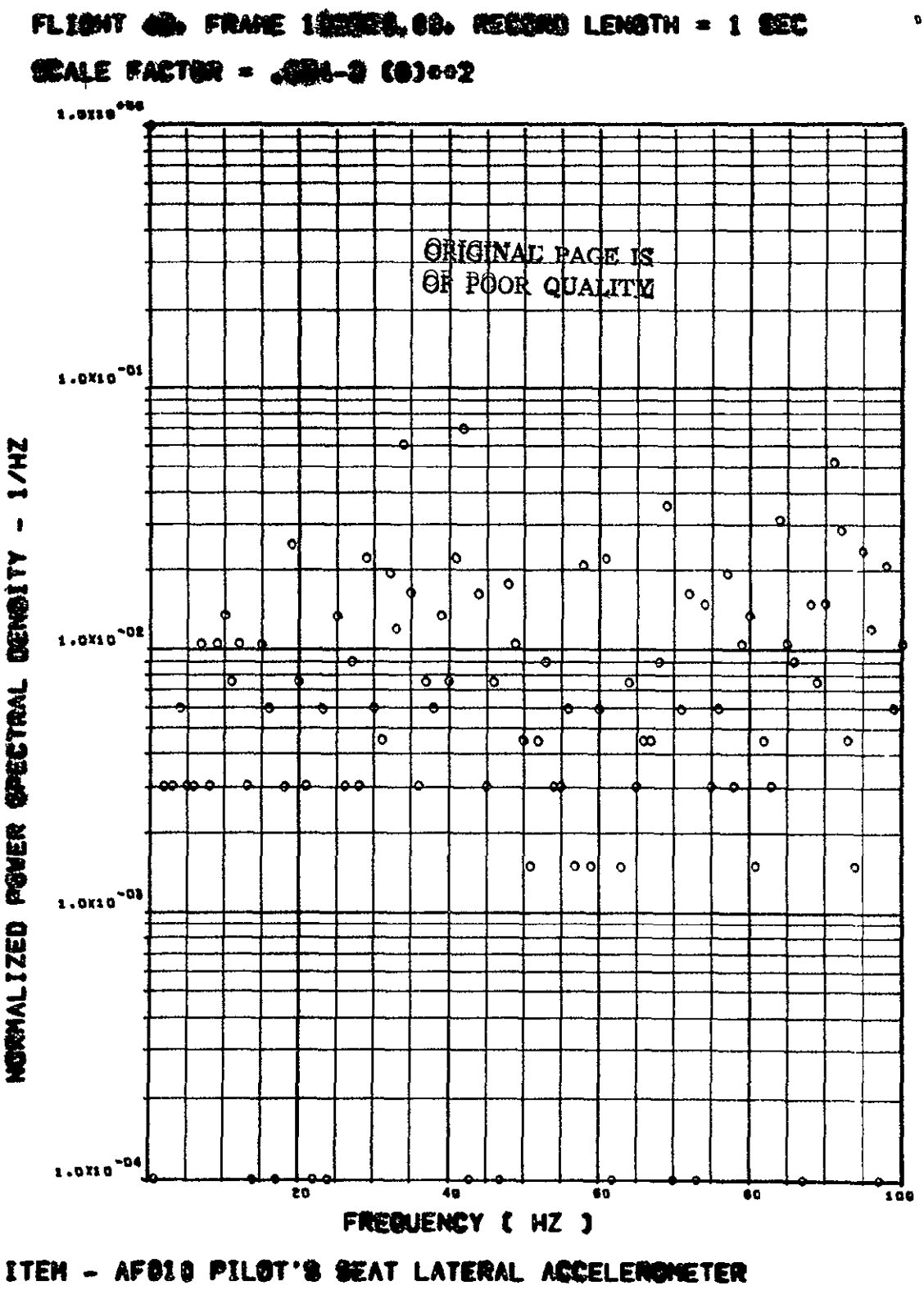

Figure 17. Continued

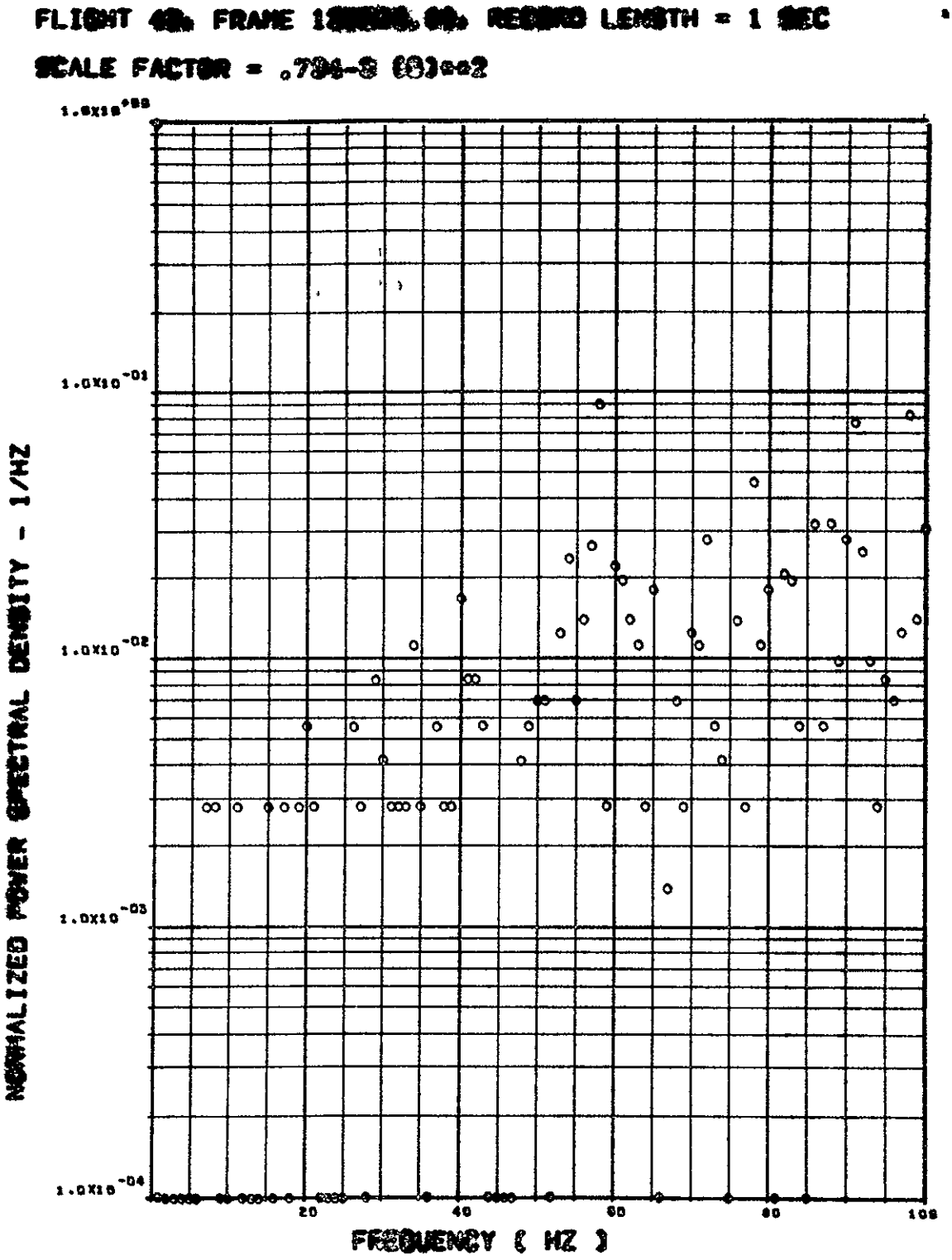

Figure 17. Continued

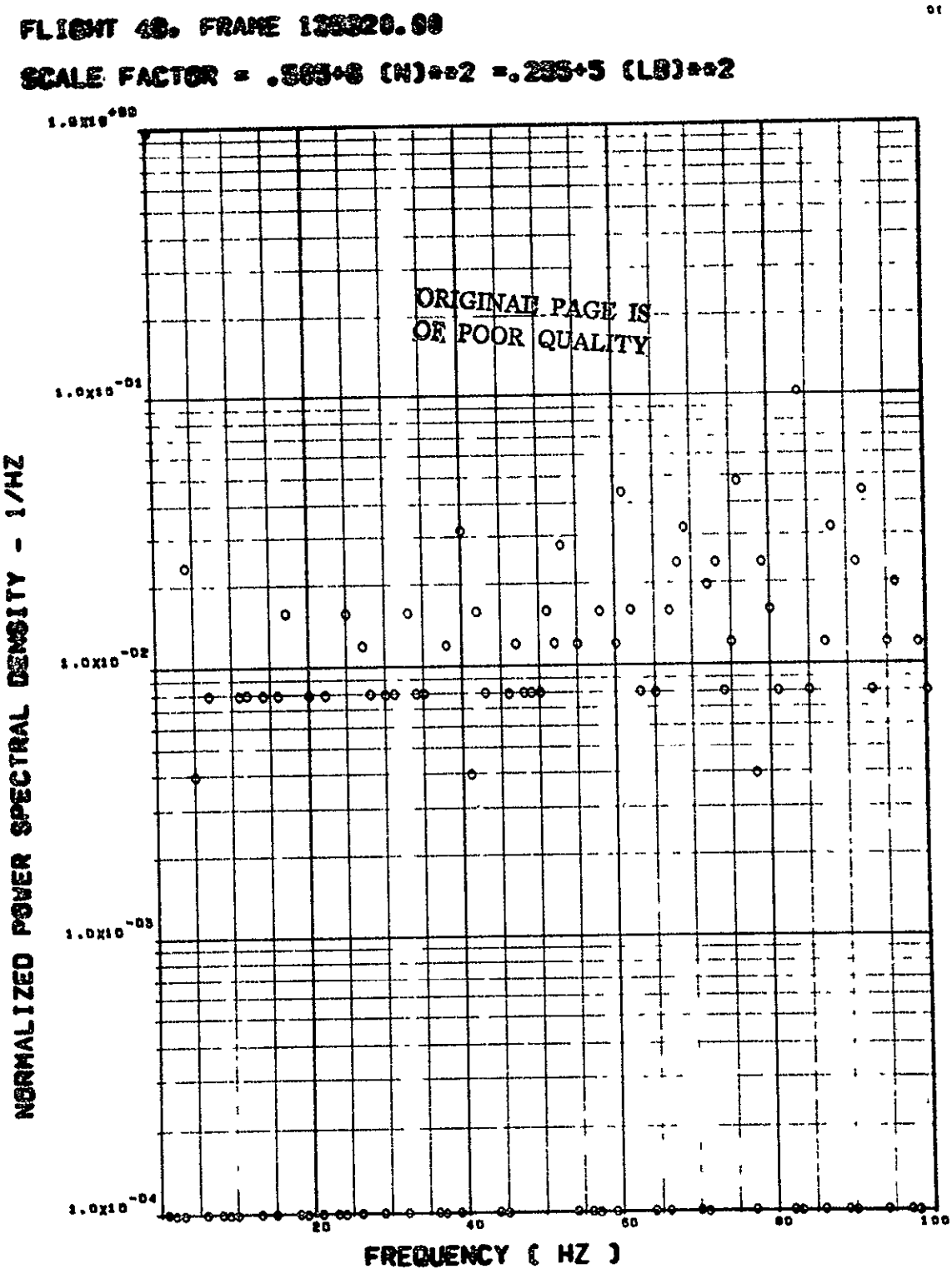

Figure 17. Continued

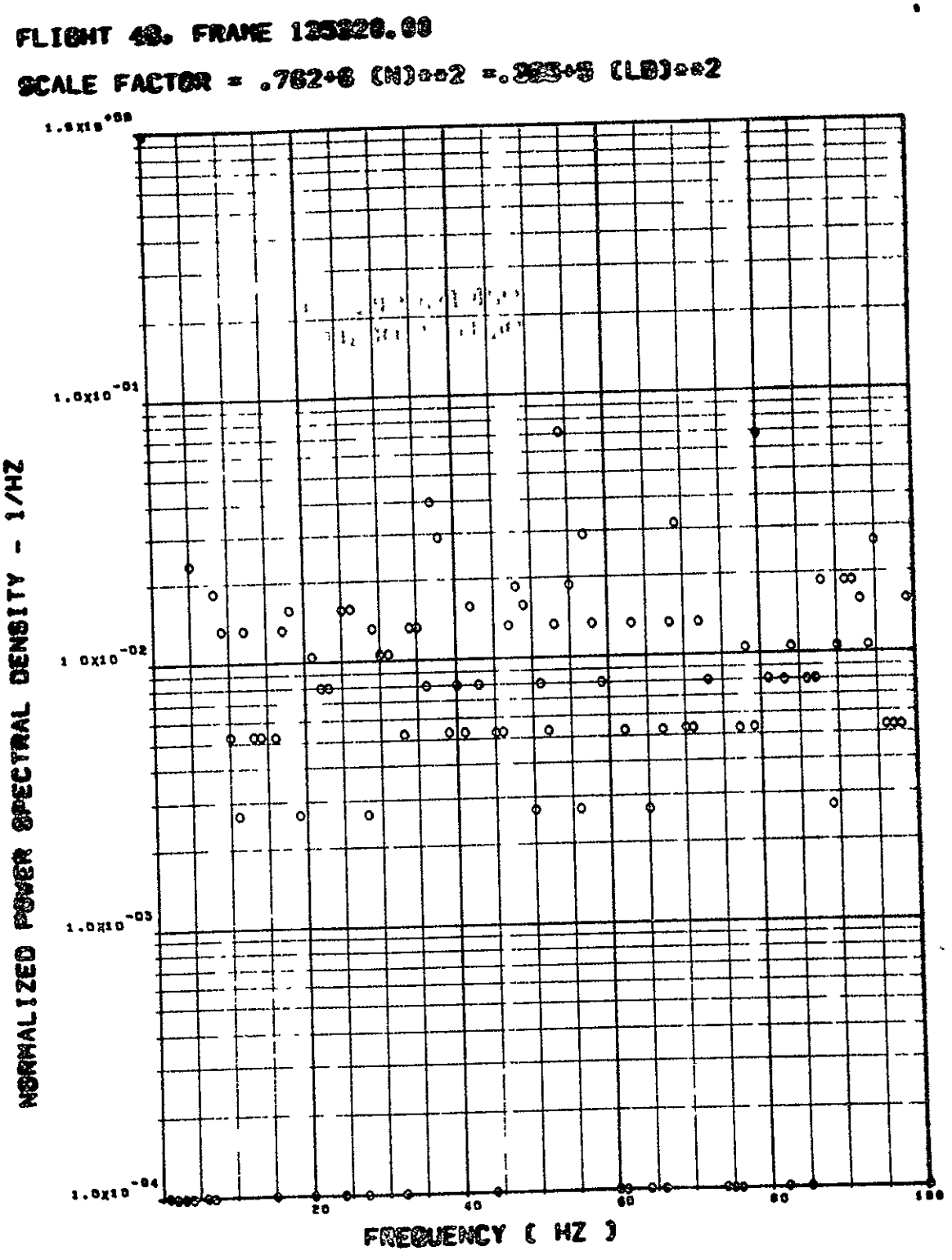

Figure 17. Continued

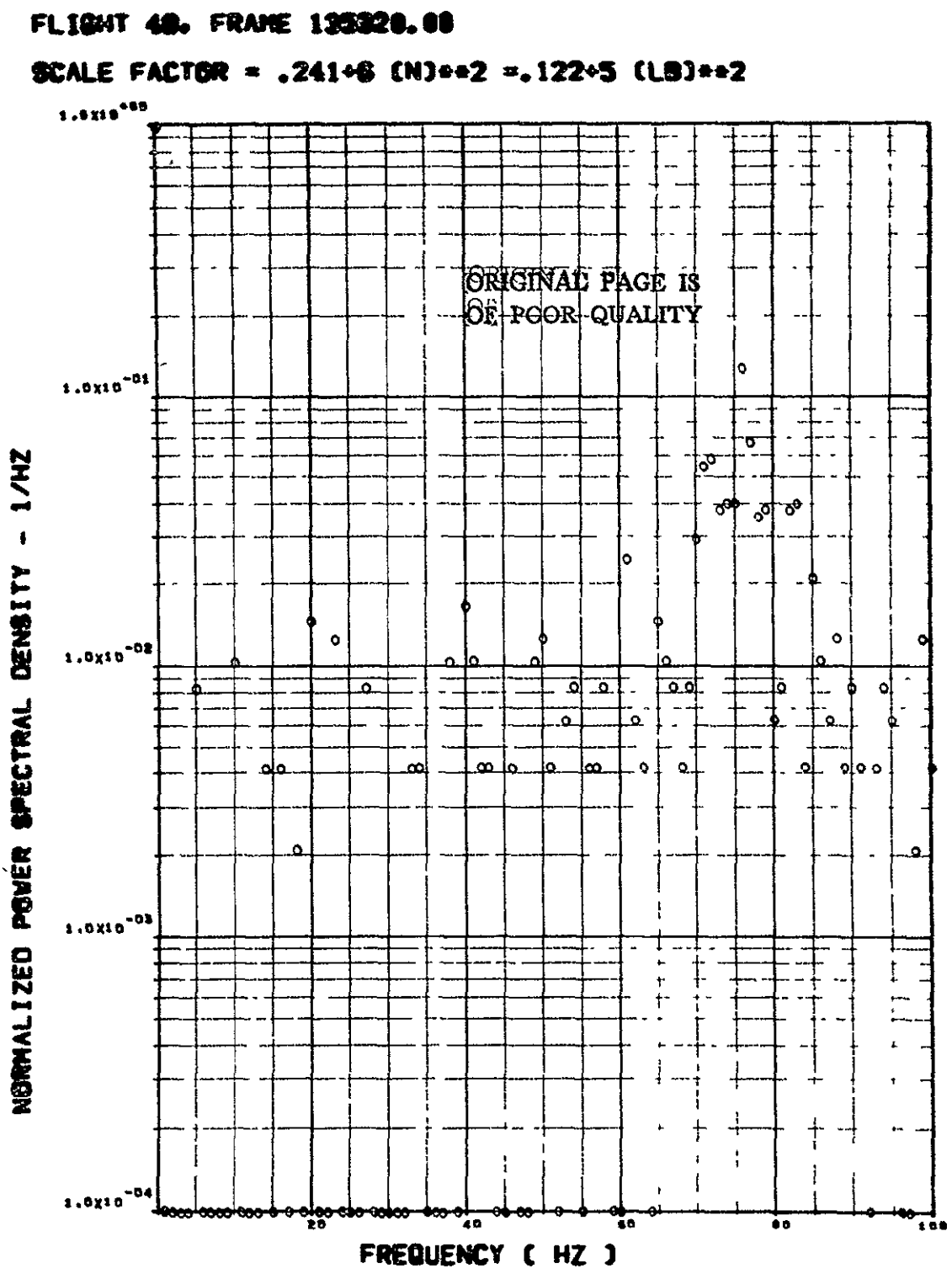

Figure 17. Continued

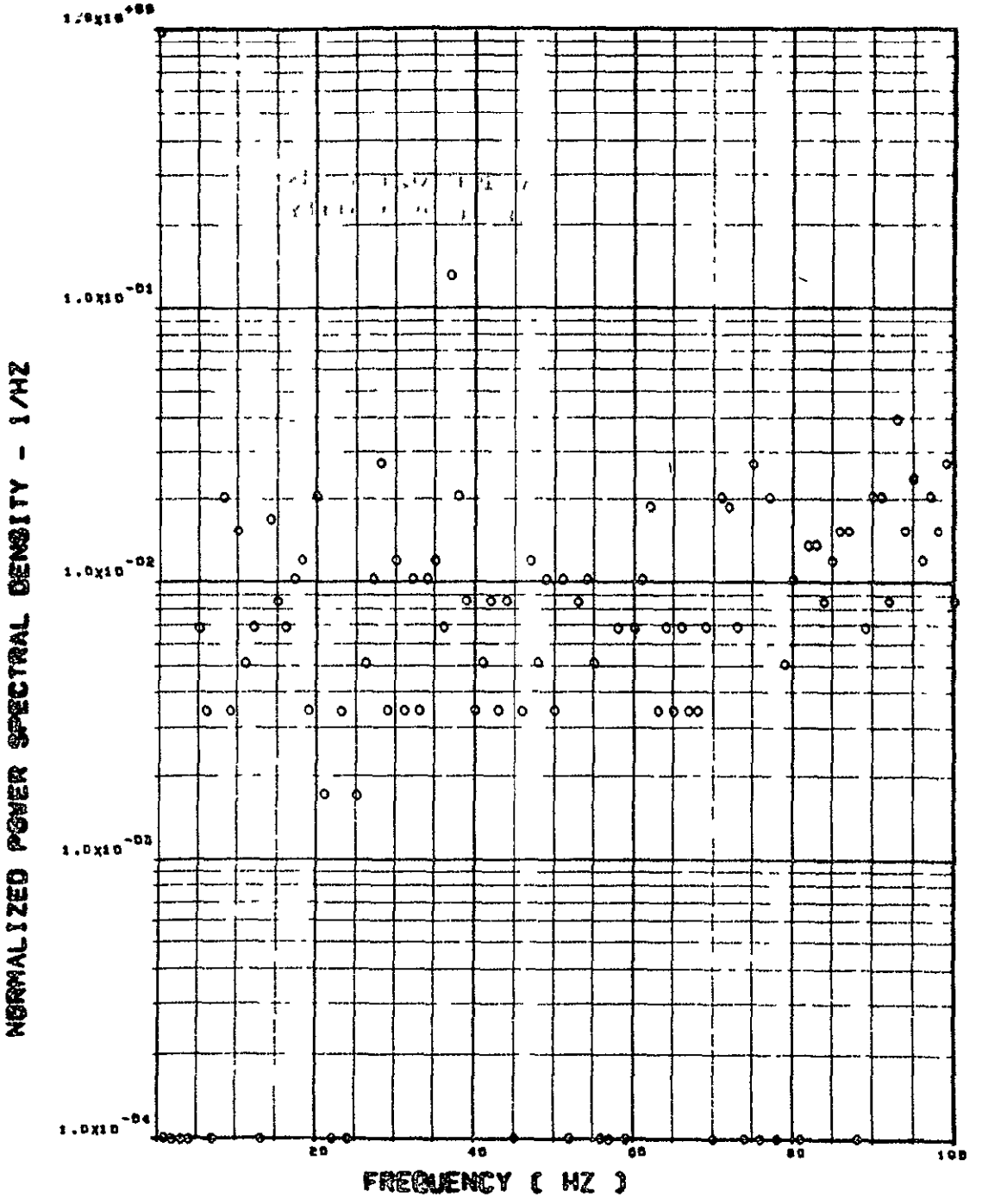

Figure 17. Continued

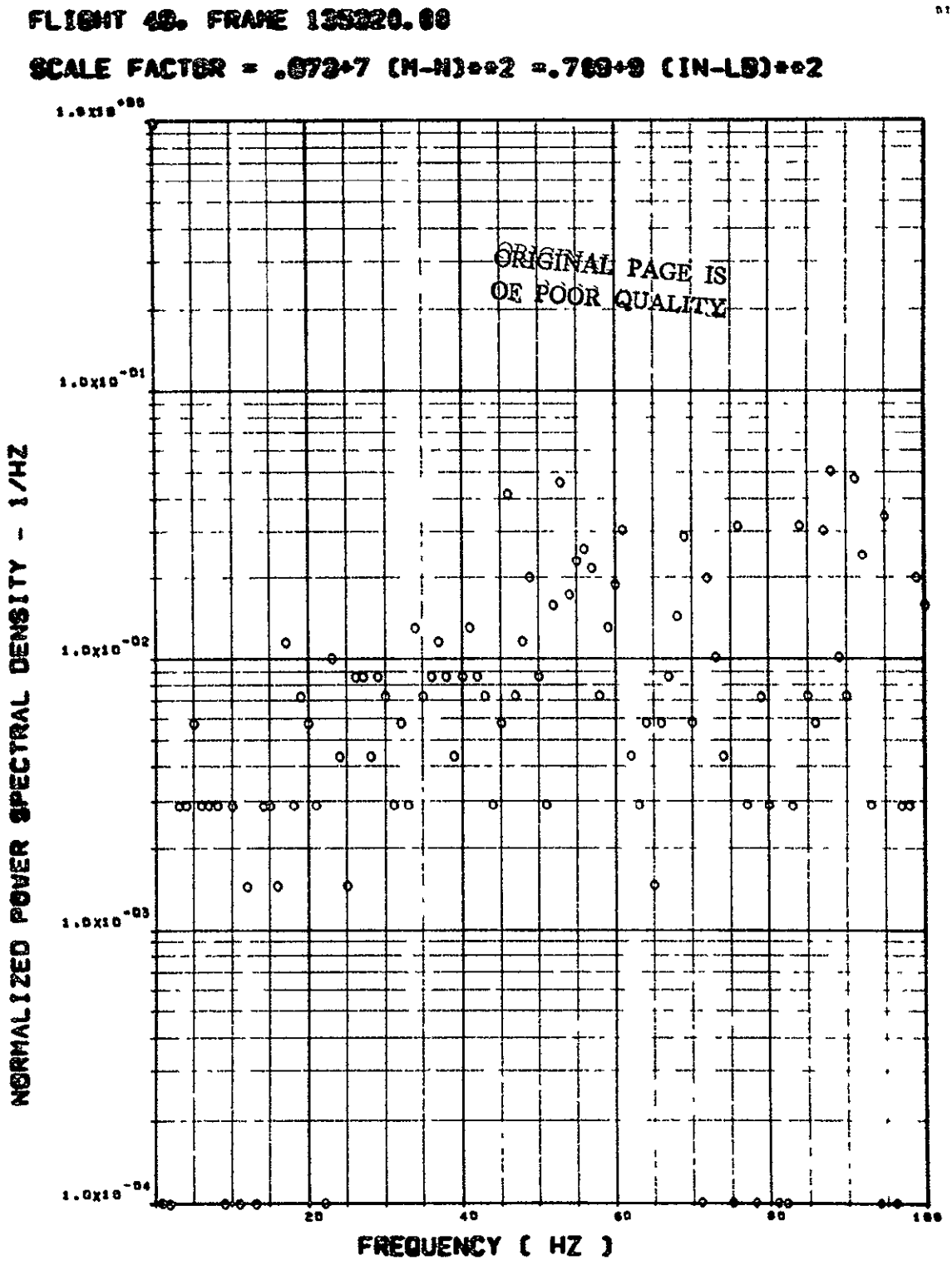

Figure 17. Continued

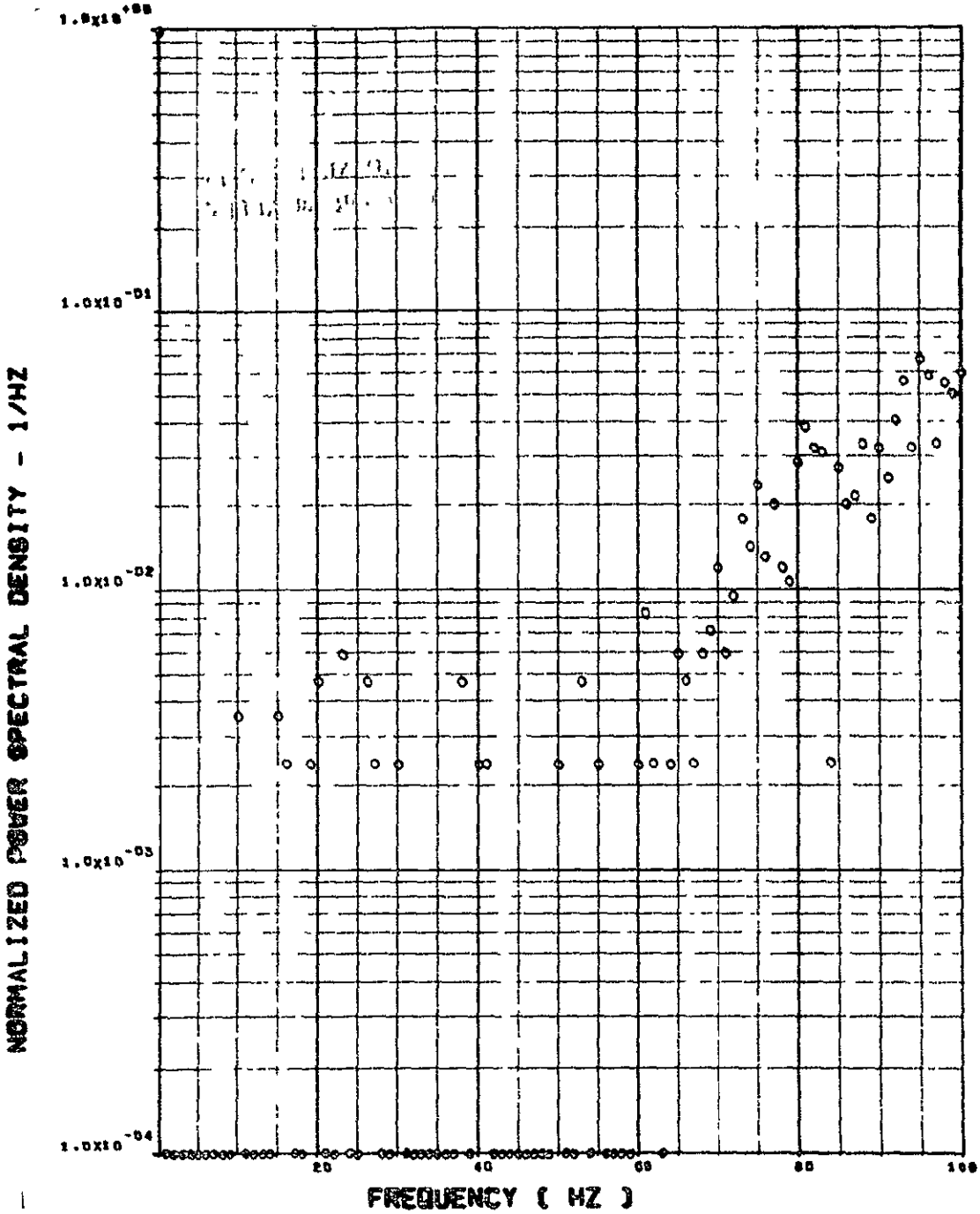

Figure 17. Continued

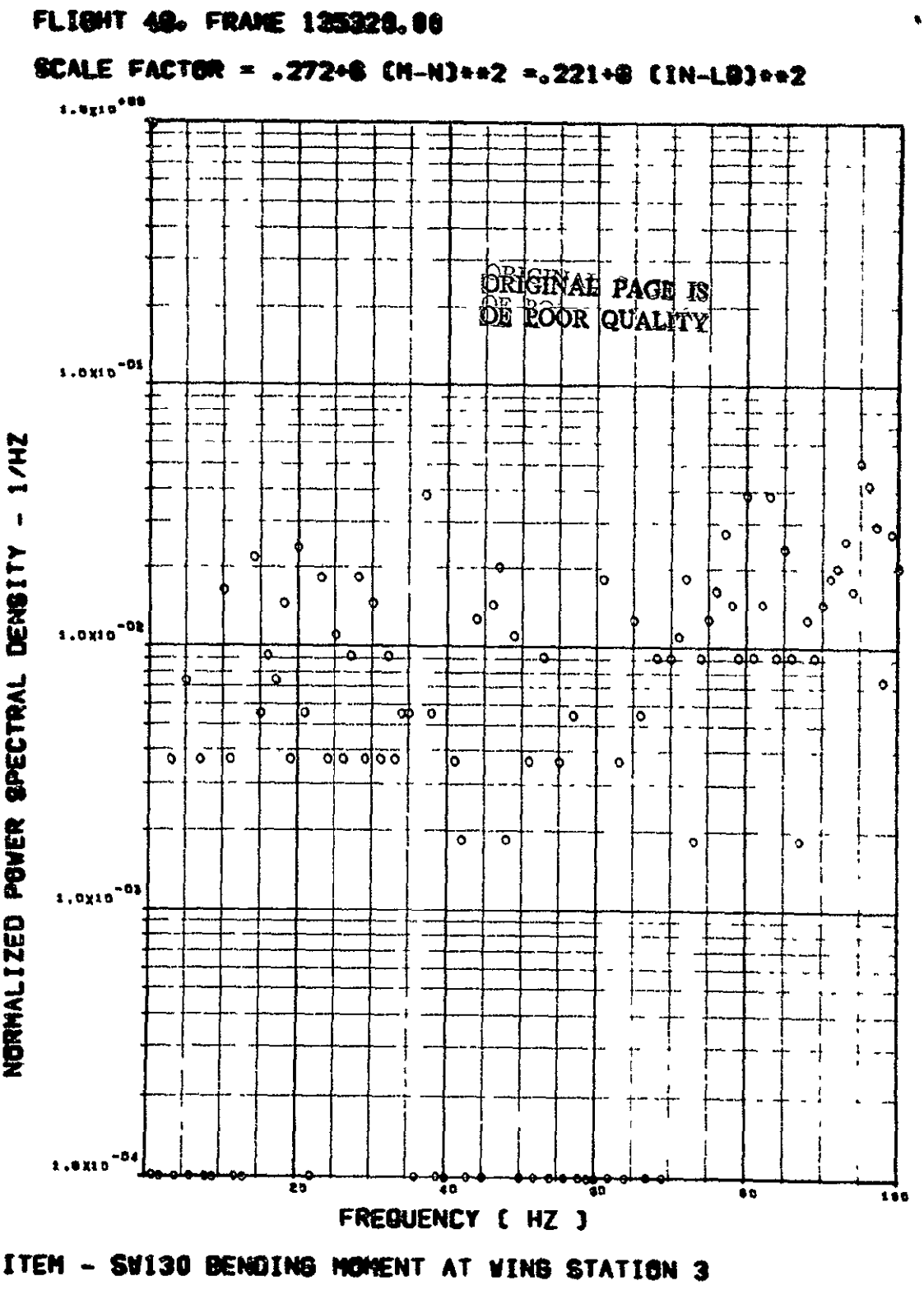

Figure 17. Continued

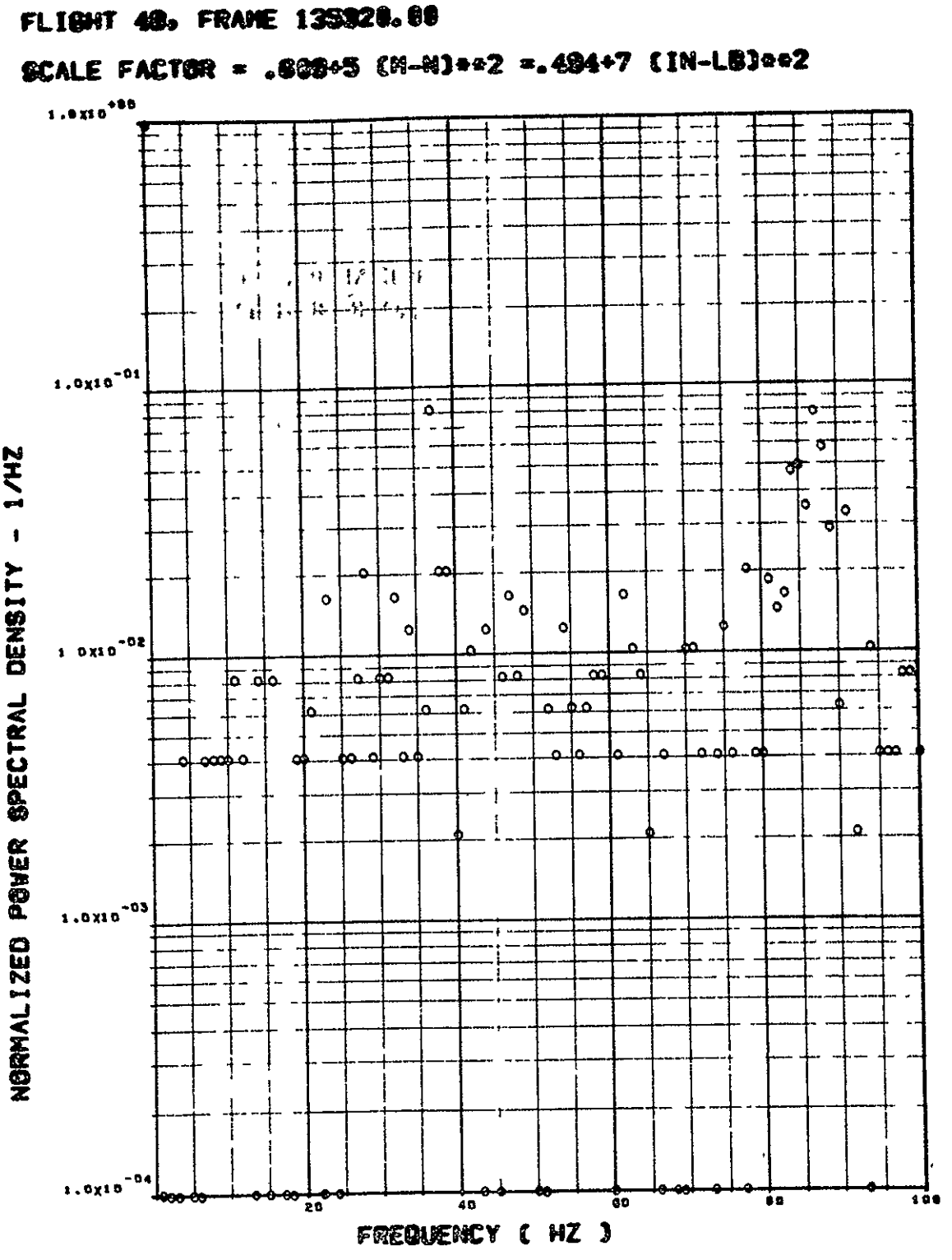

Figure 17. Continued

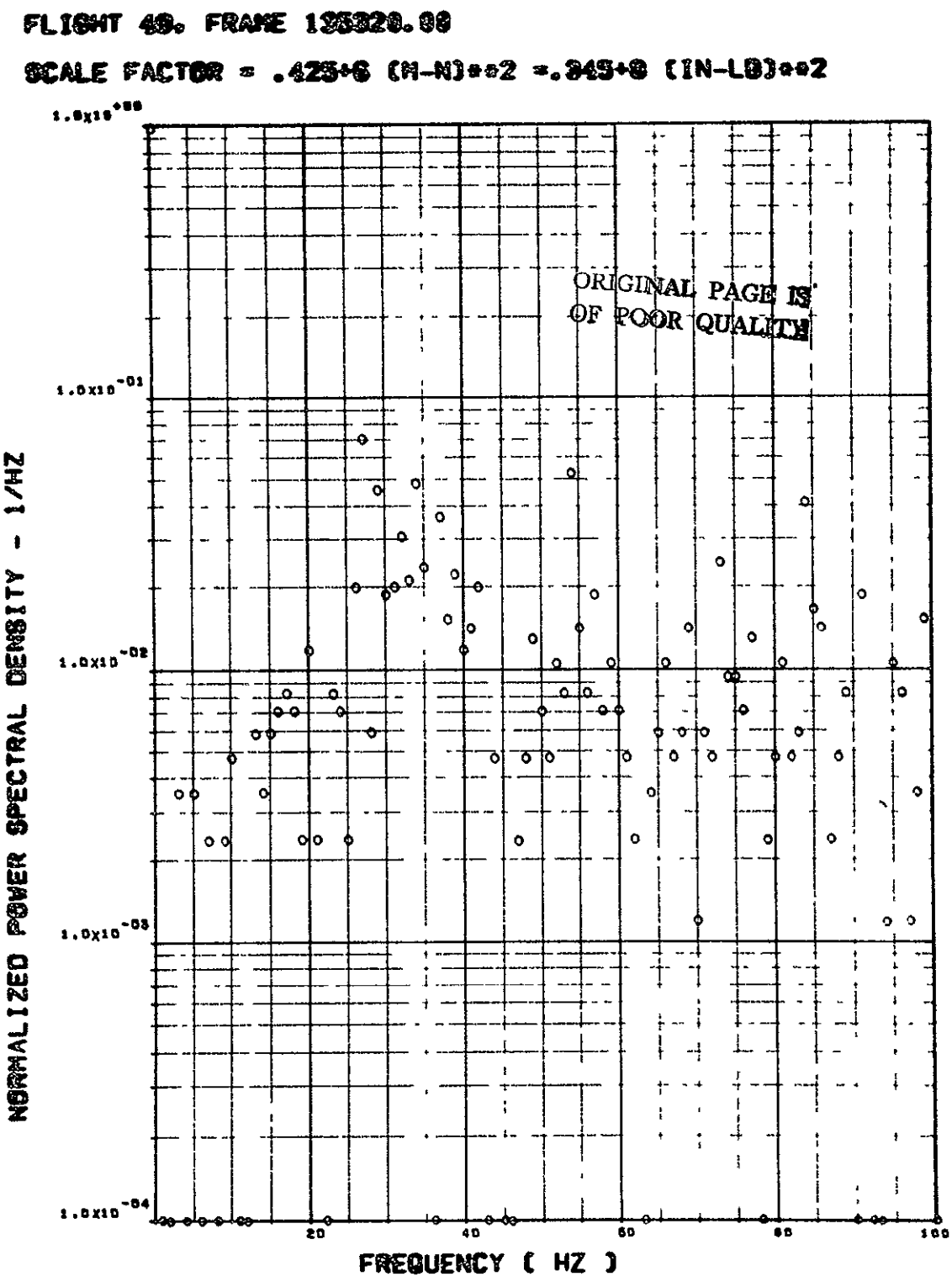

Figure 17. Continued

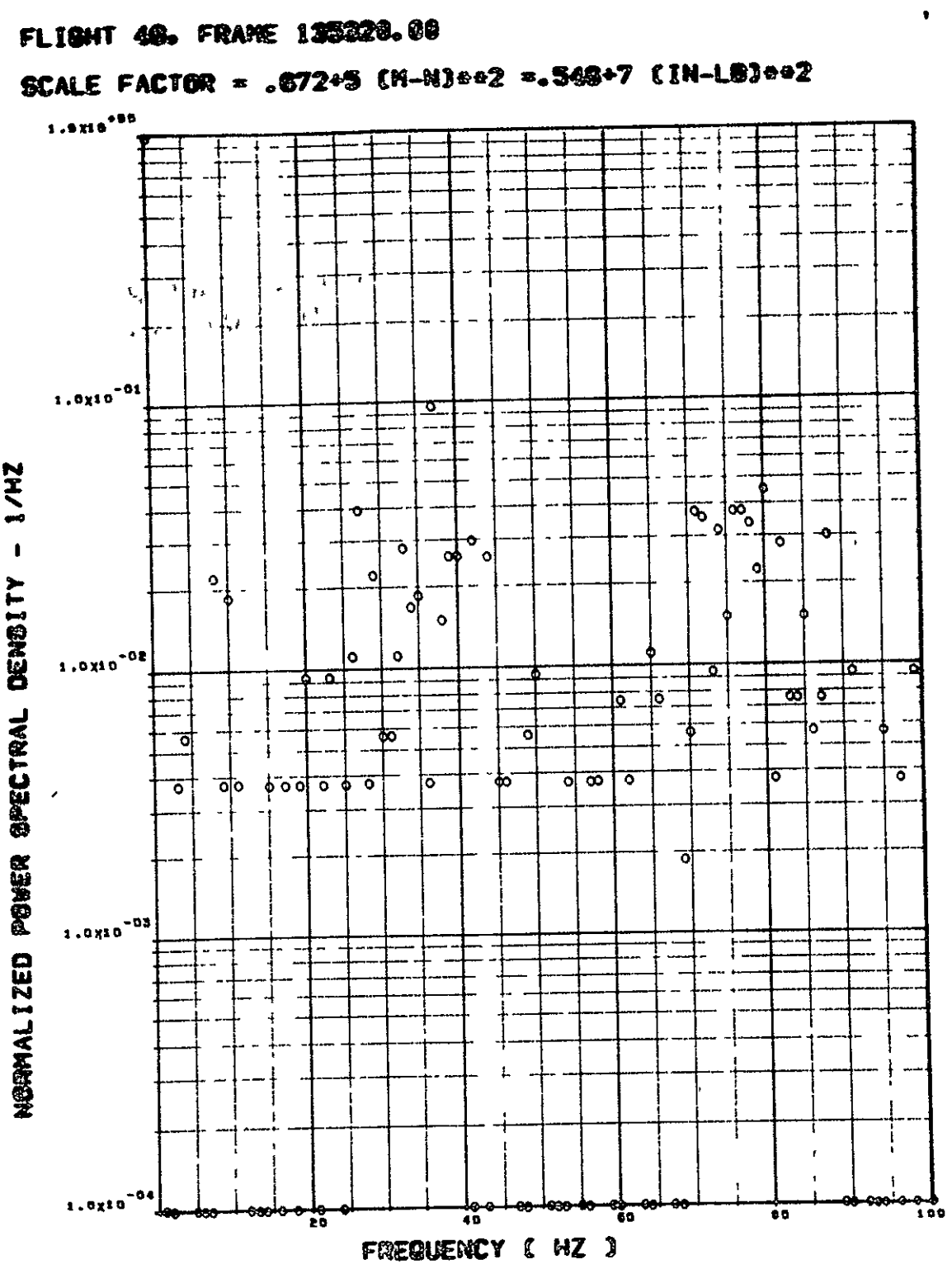

Figure 17. Continued

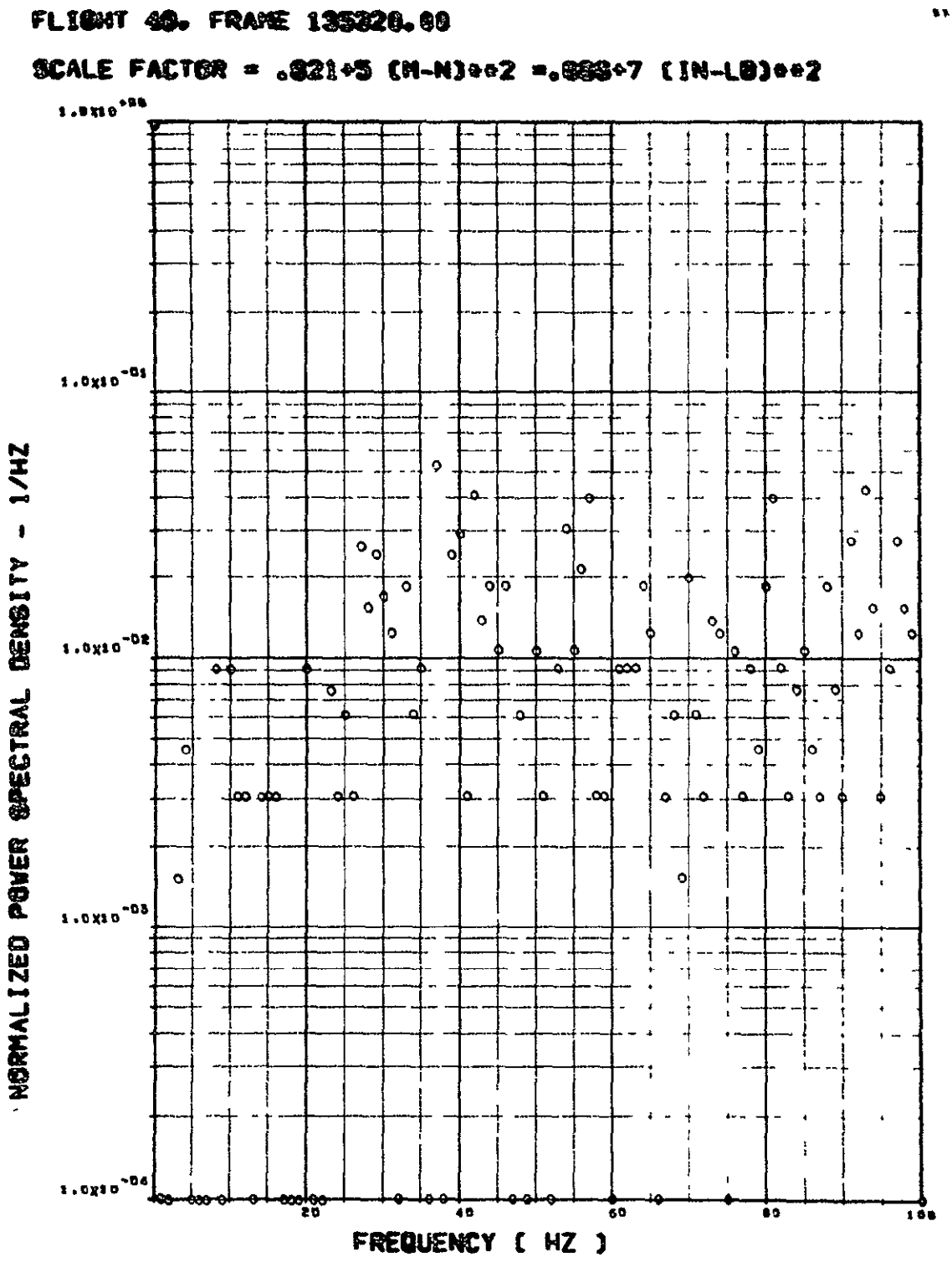

Figure 17. Continued

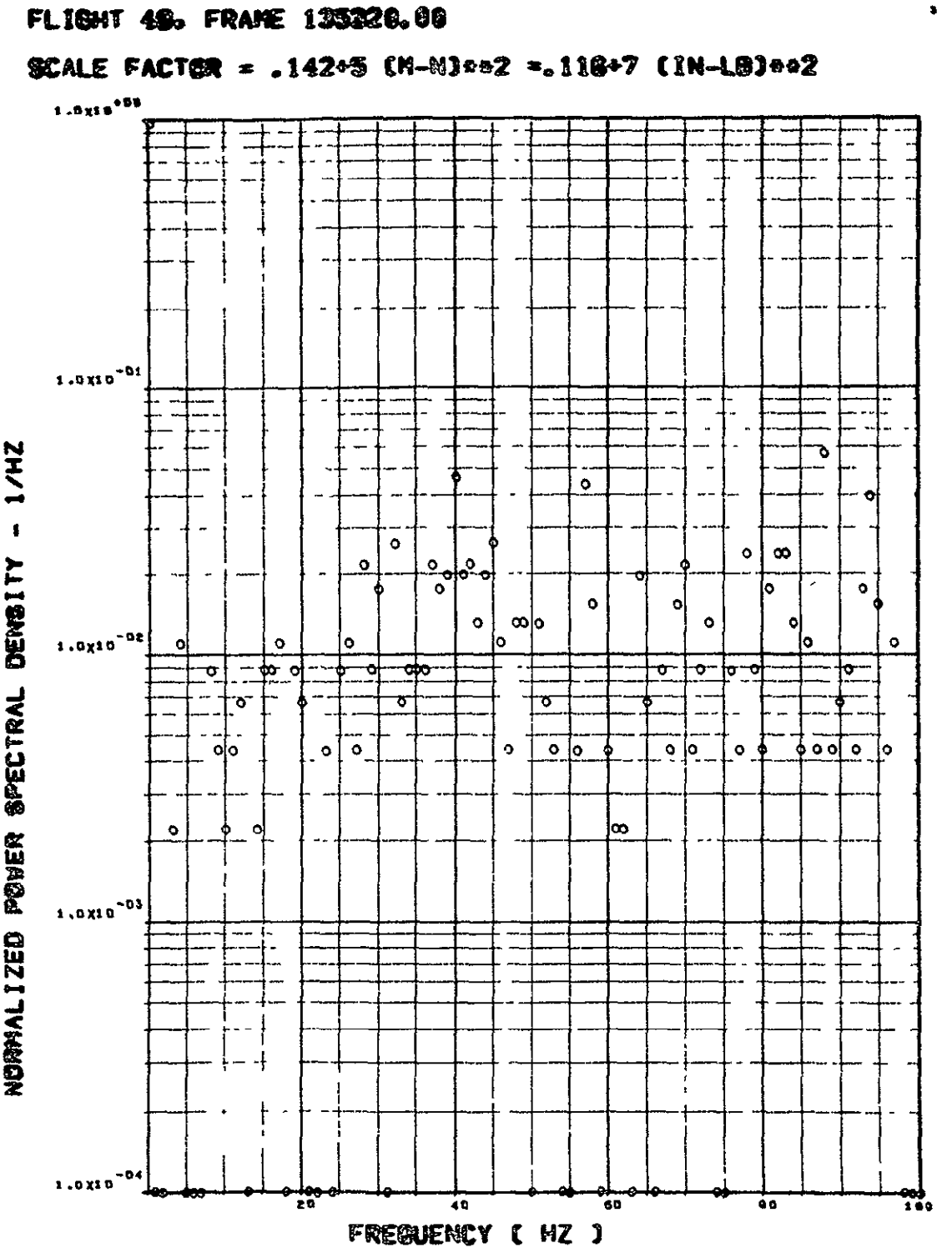

Figure 17. Continued

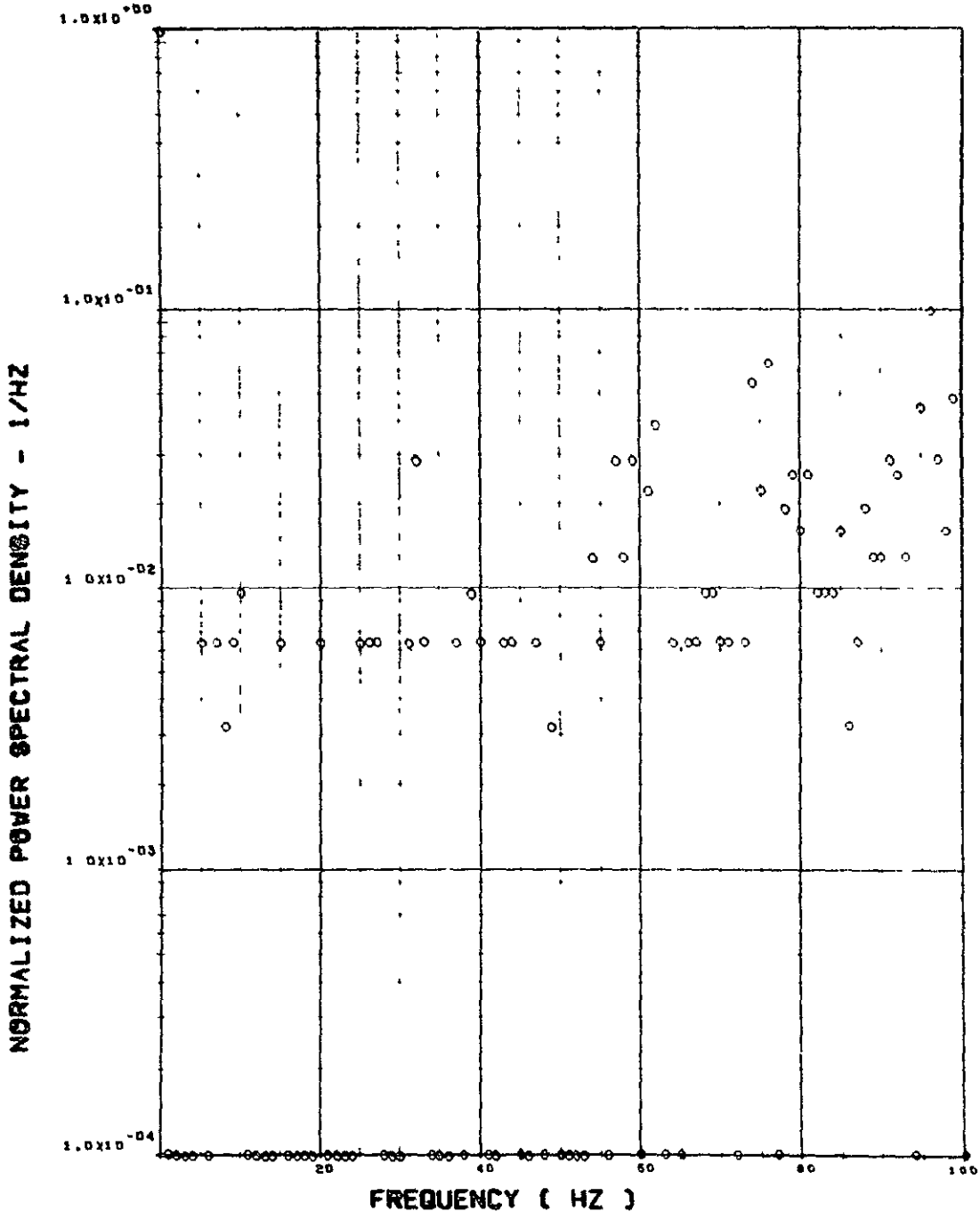

Figure 17. Continued

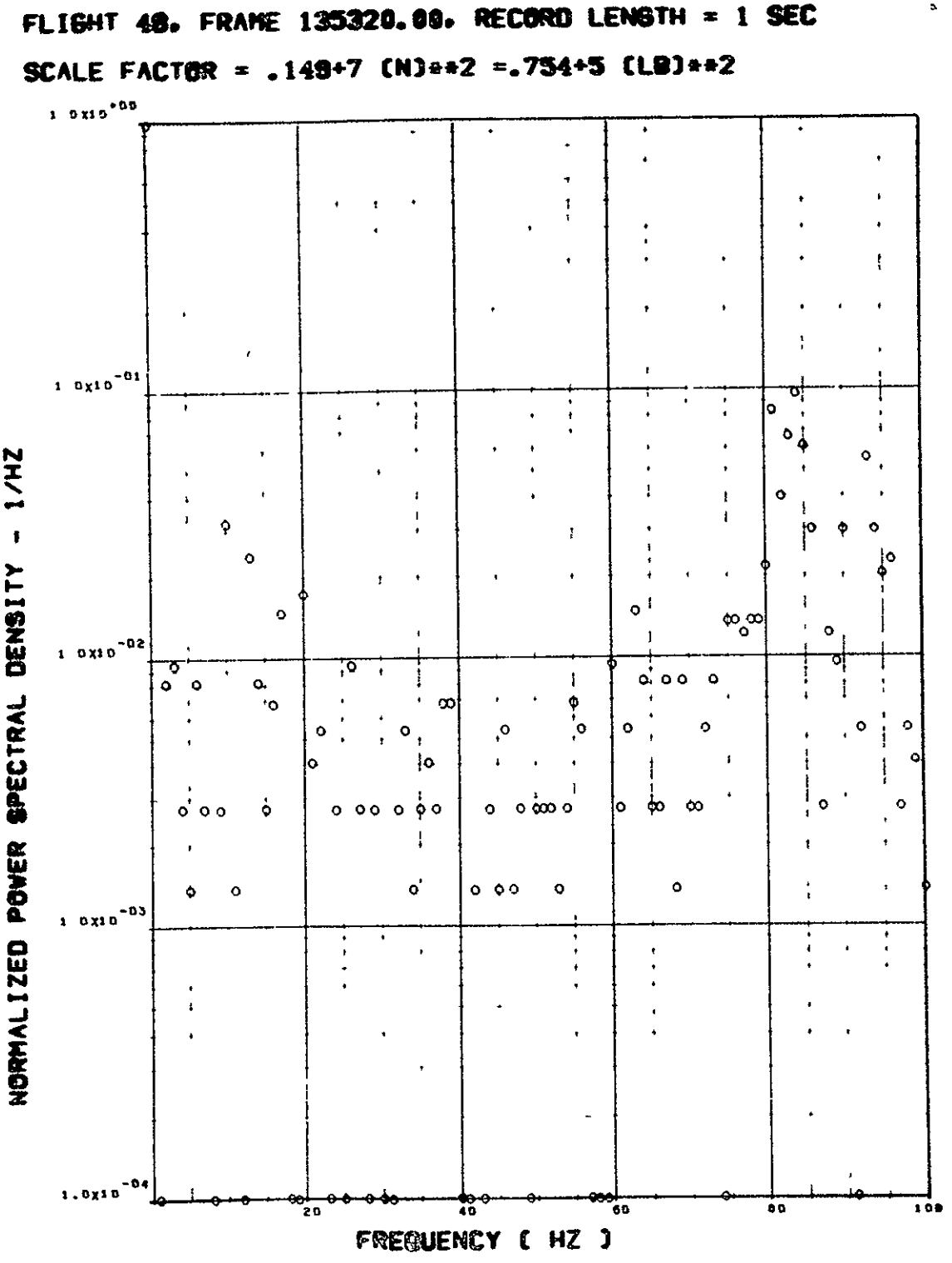

Figure 17. Continued

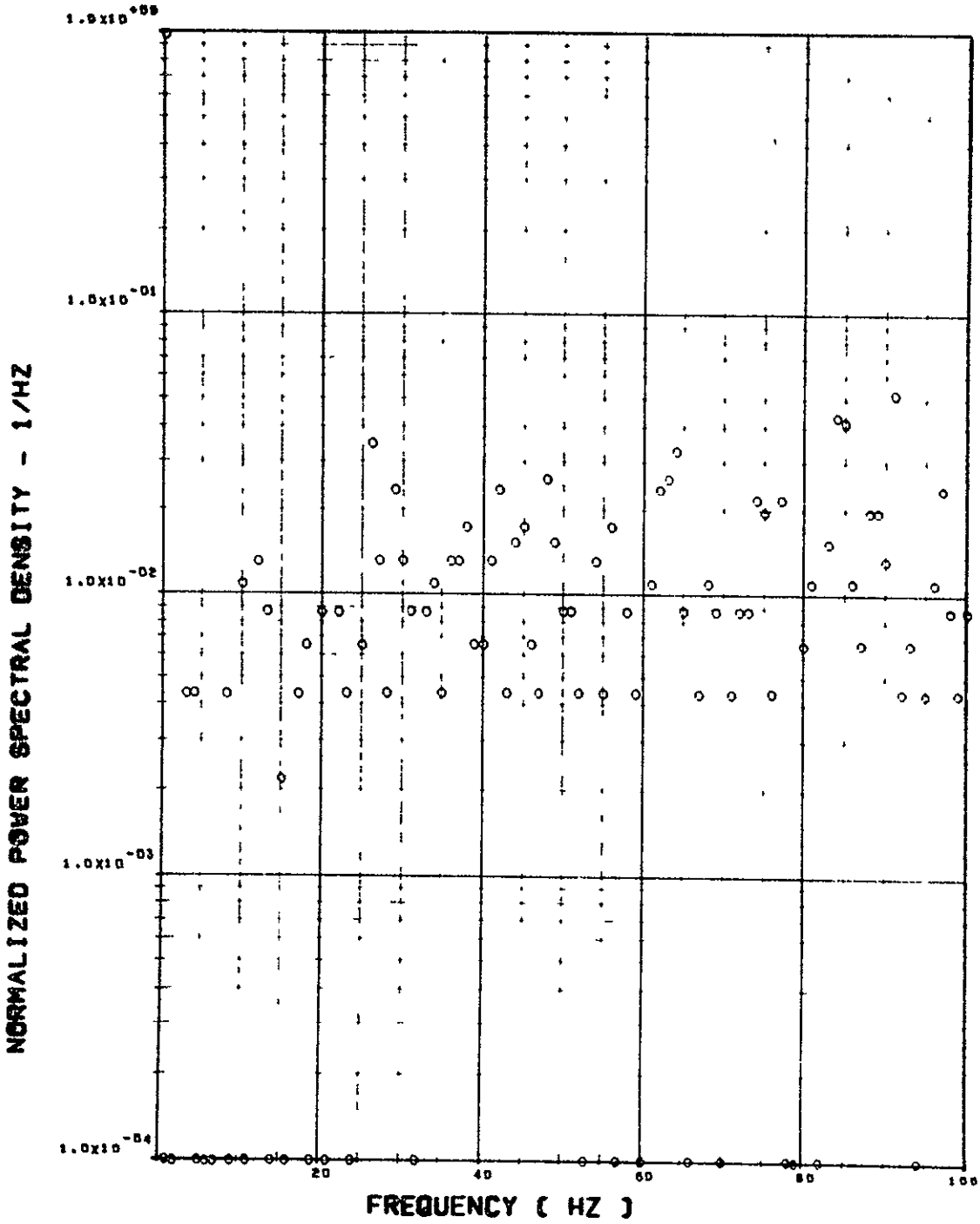

Figure 17. Continued

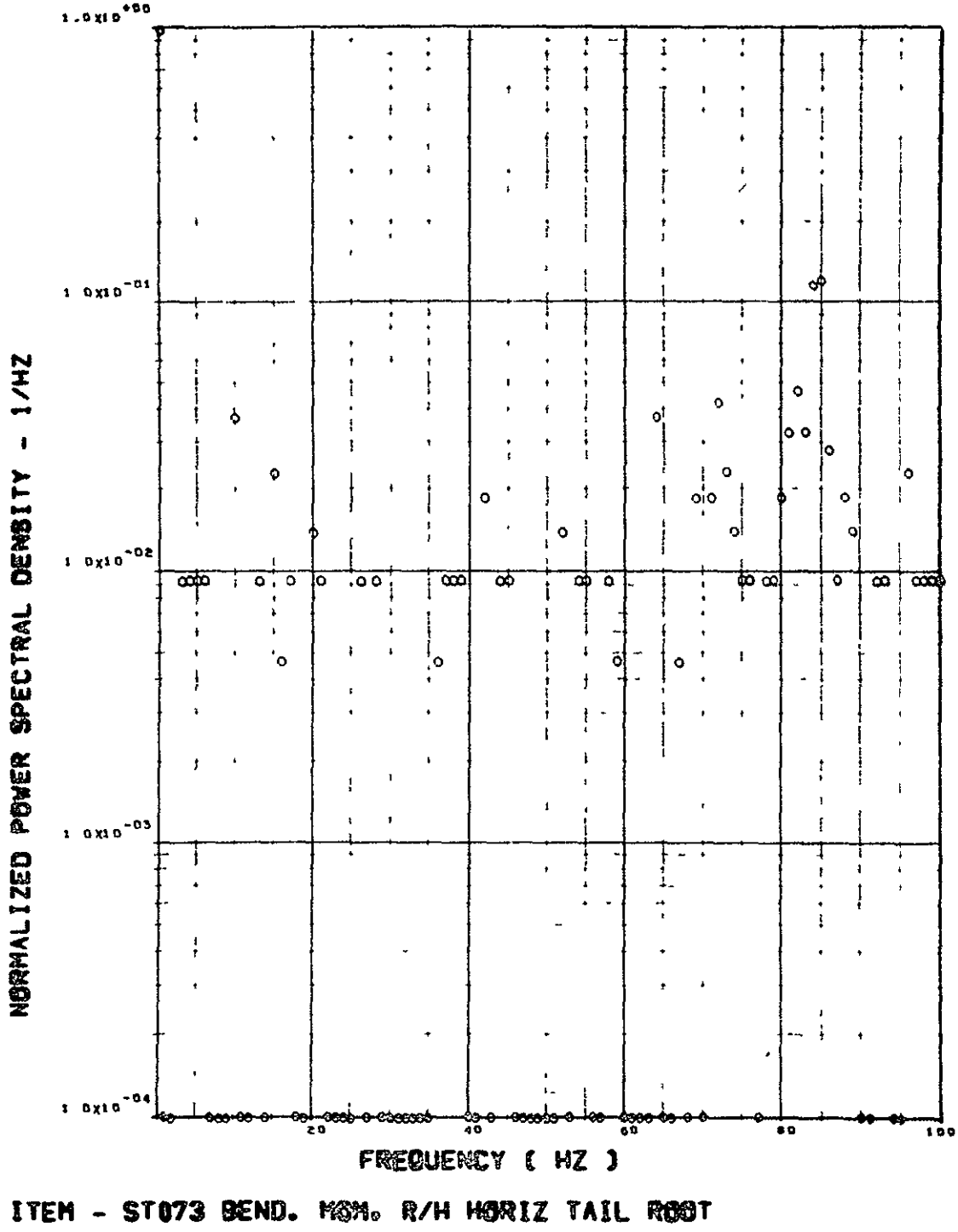

Figure 17. Continued

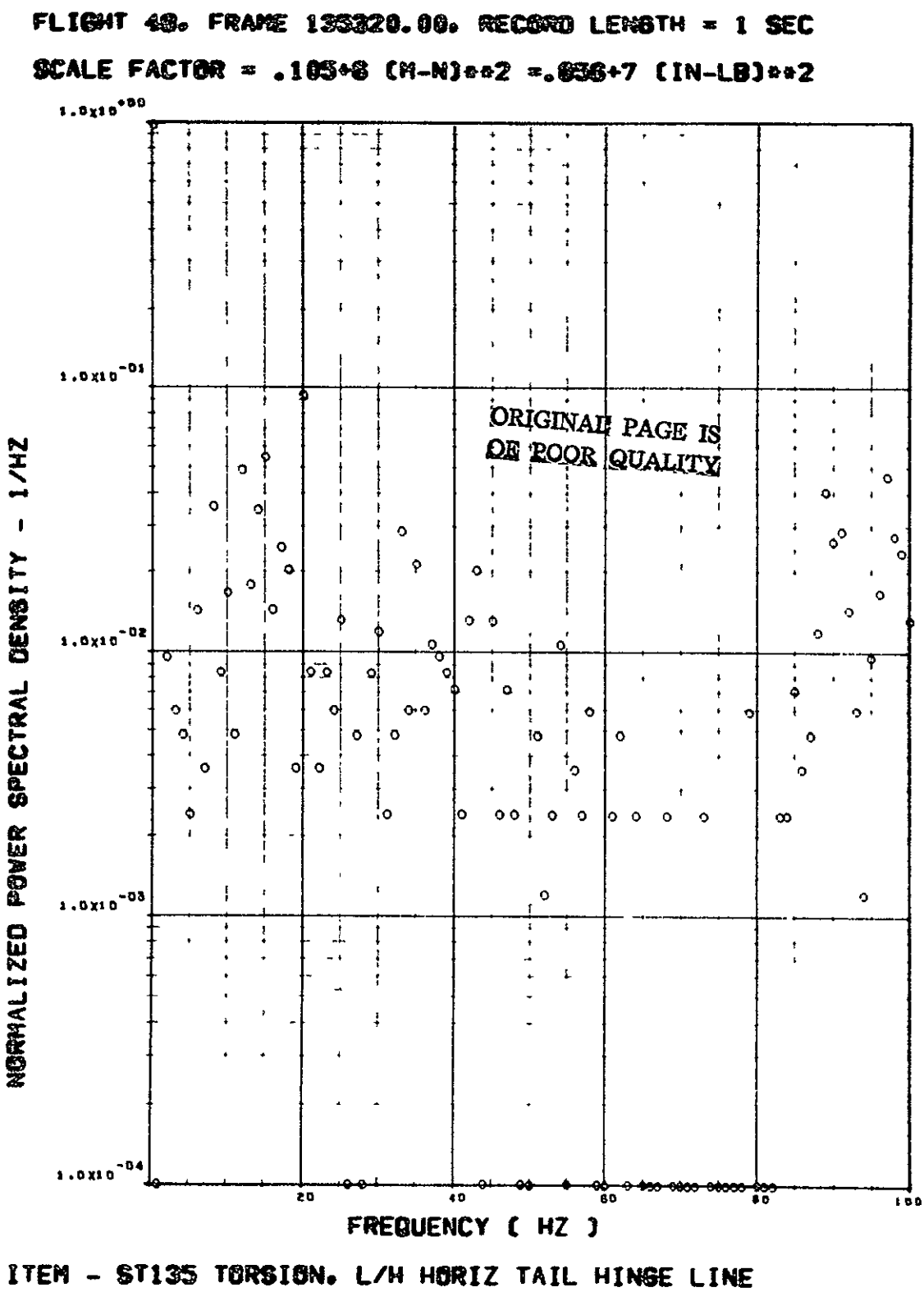

Figure 17. Continued

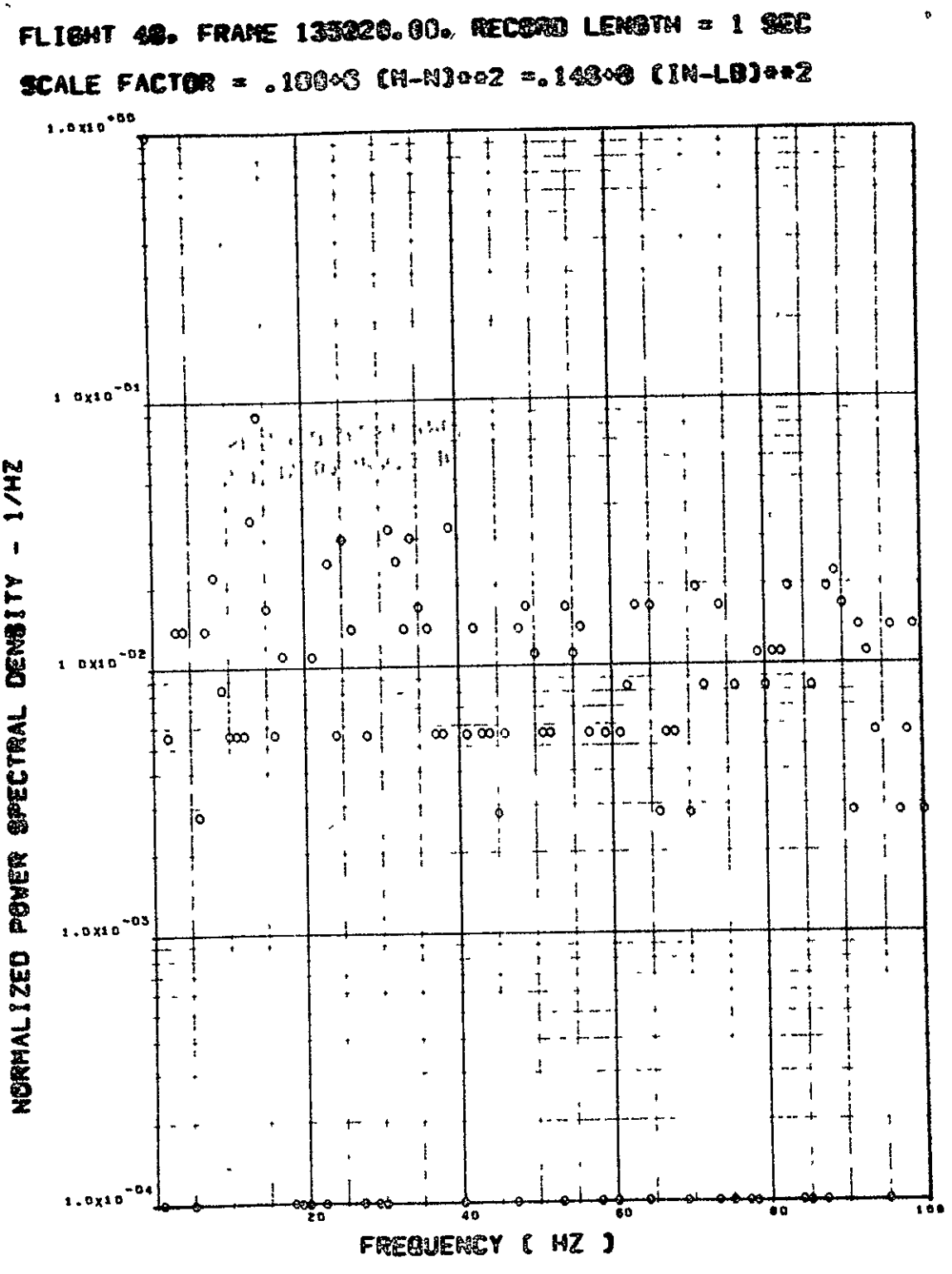

Figure 17. Concluded

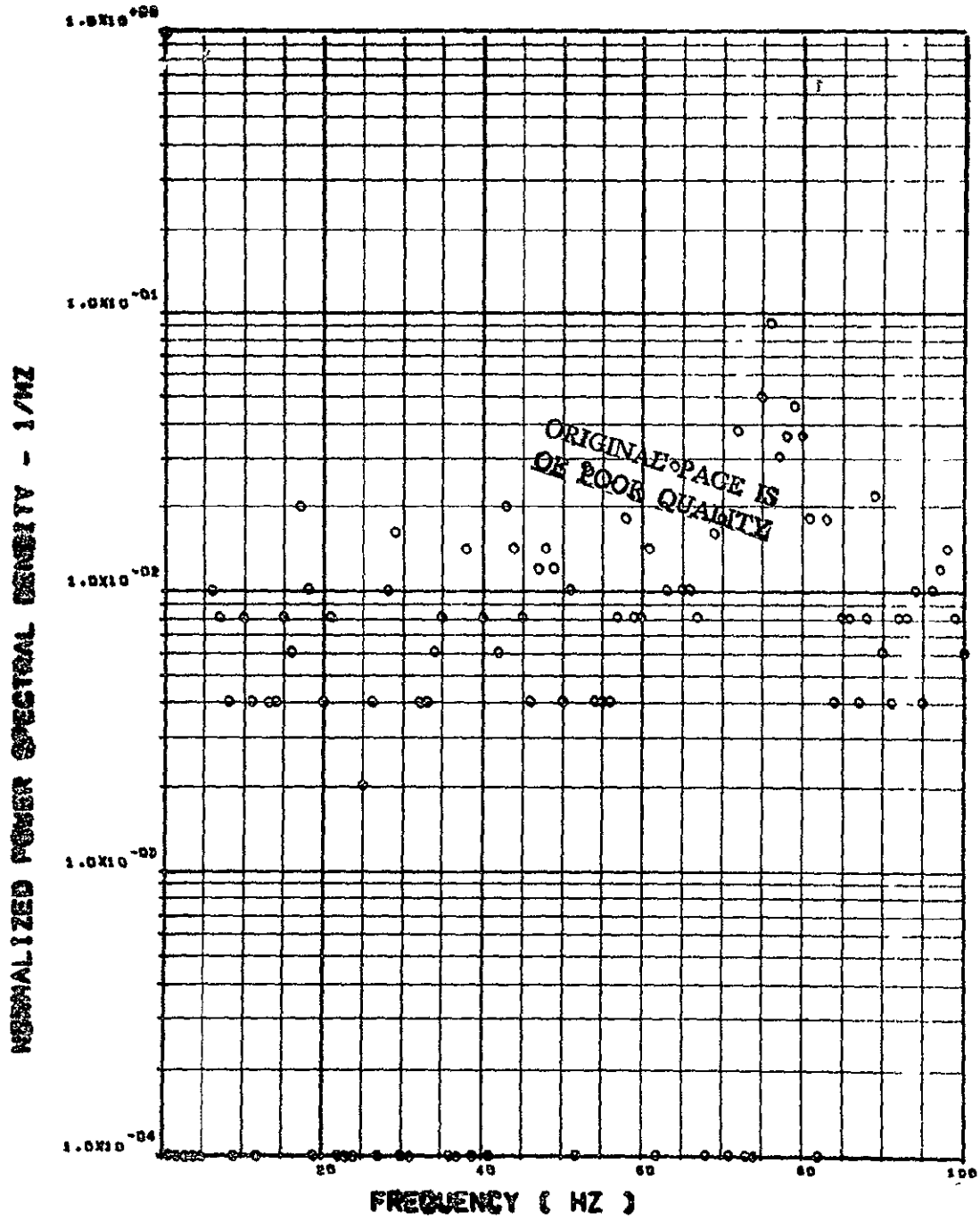

Figure 18. Power Spectra - Flight 48, Run 4, Point 3
T_1 = 135322.8, ΔT = 1 Sec, α_{Nom} = 12.95 deg,
$\Delta\alpha$ = 1.70 deg

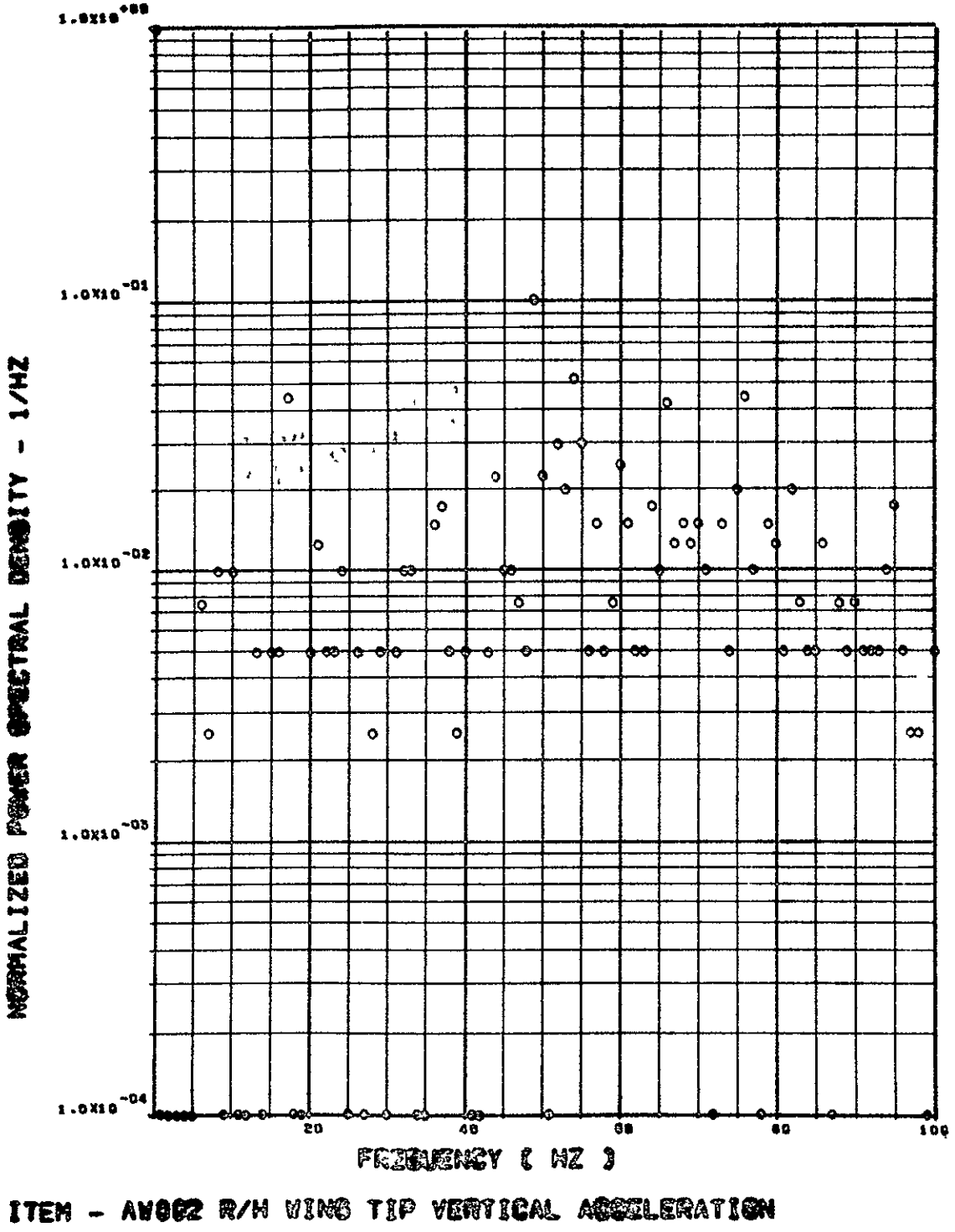

Figure 18. Continued

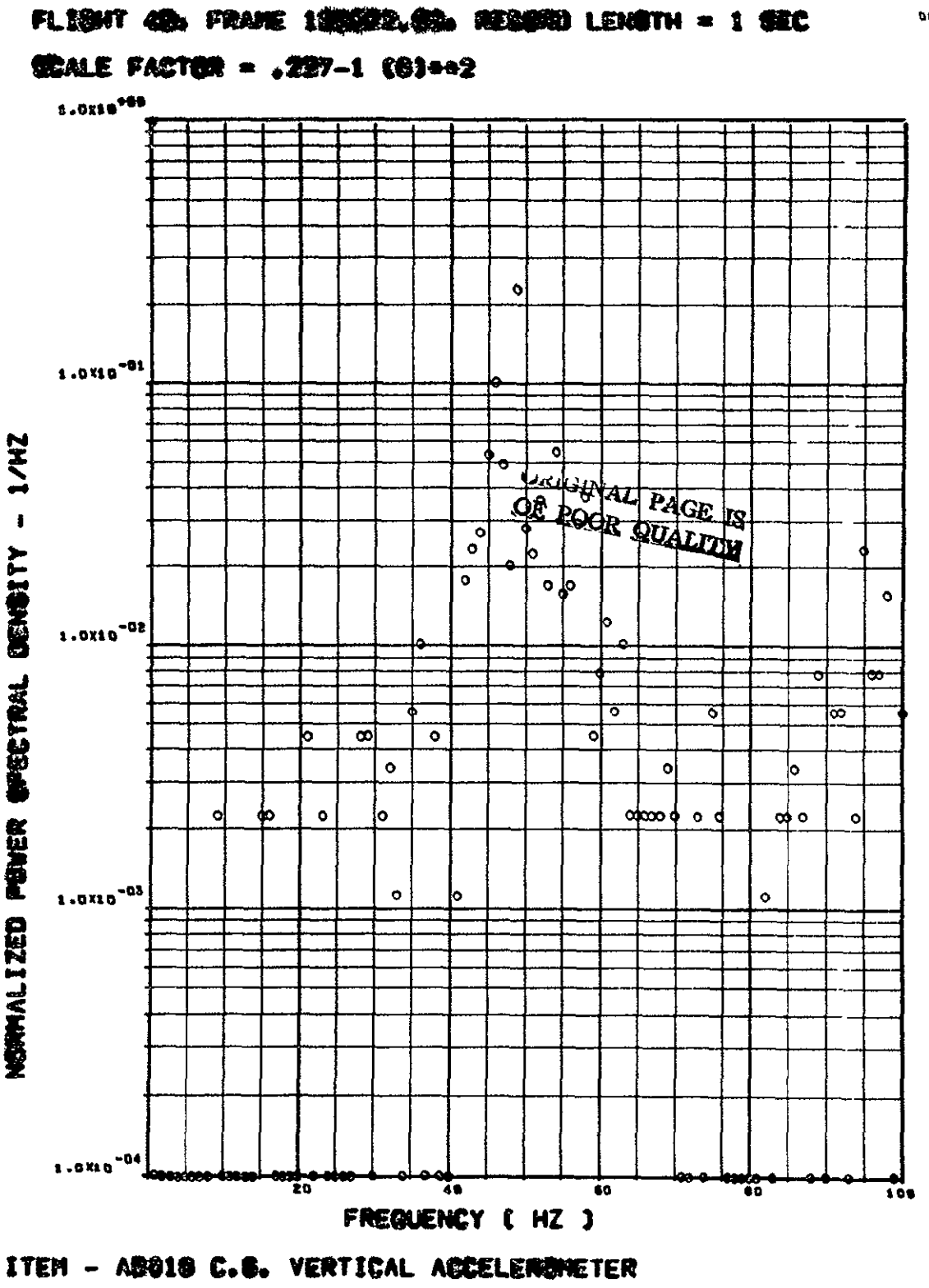

Figure 18. Continued

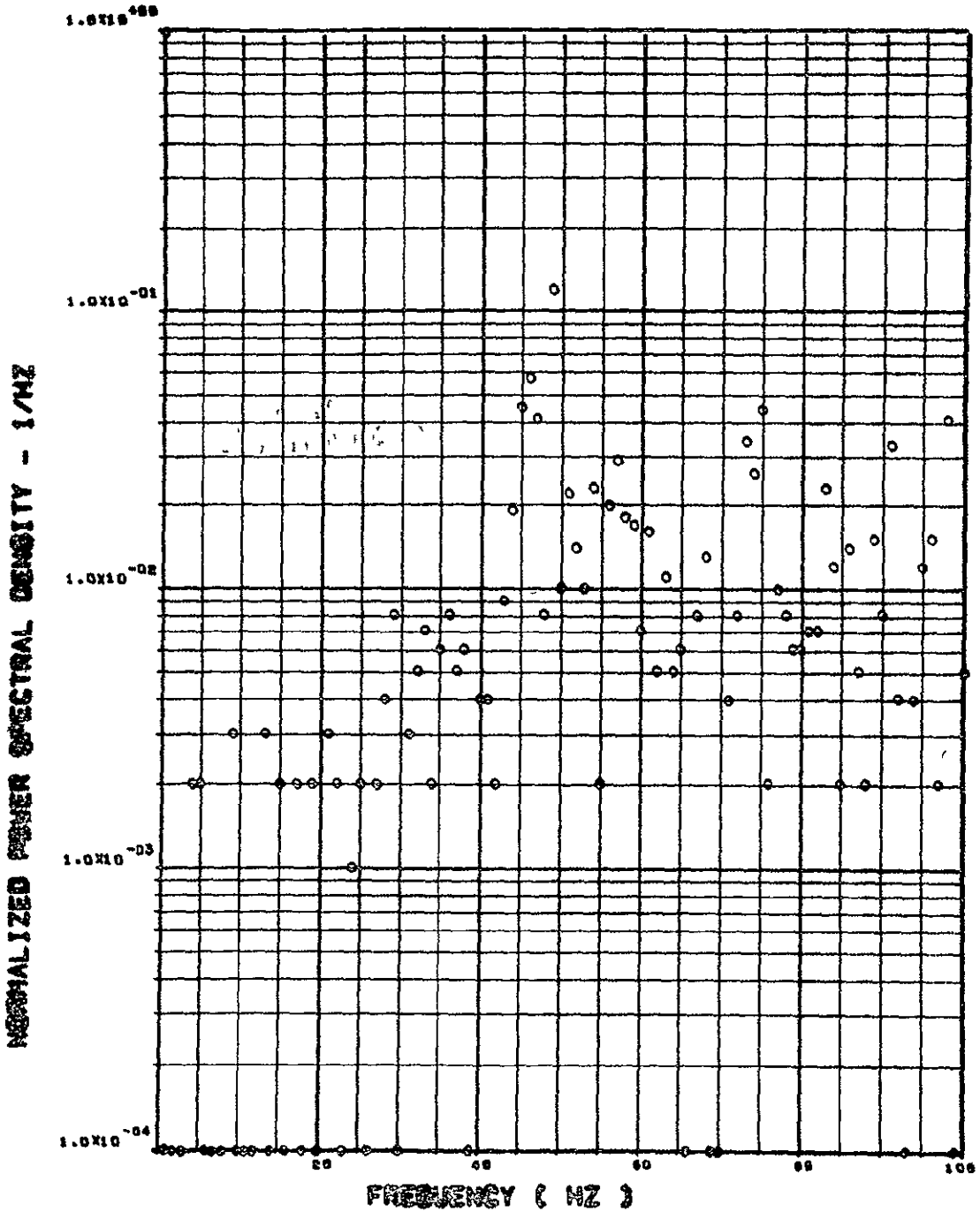

Figure 18. Continued

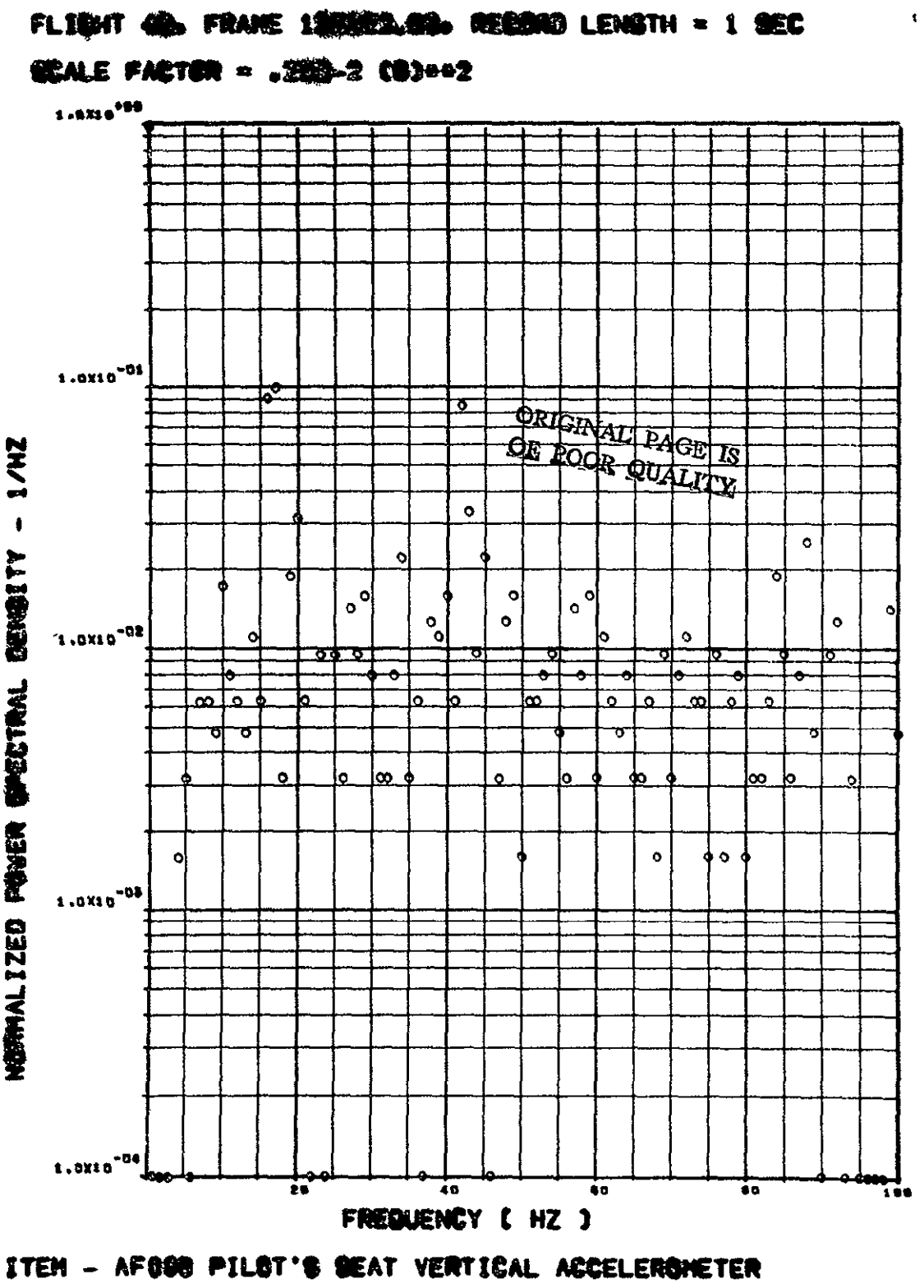

Figure 18. Continued

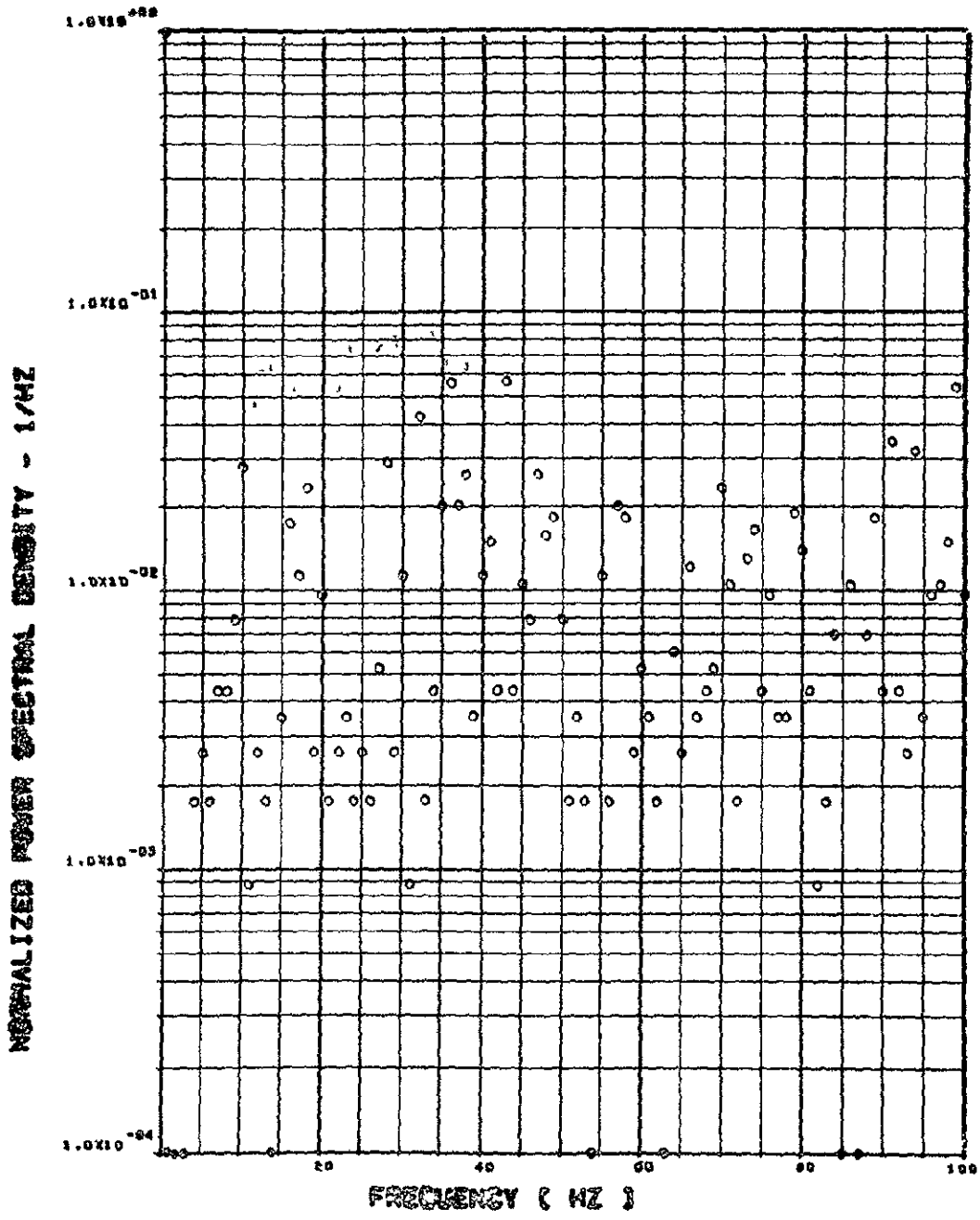

Figure 18. Continued

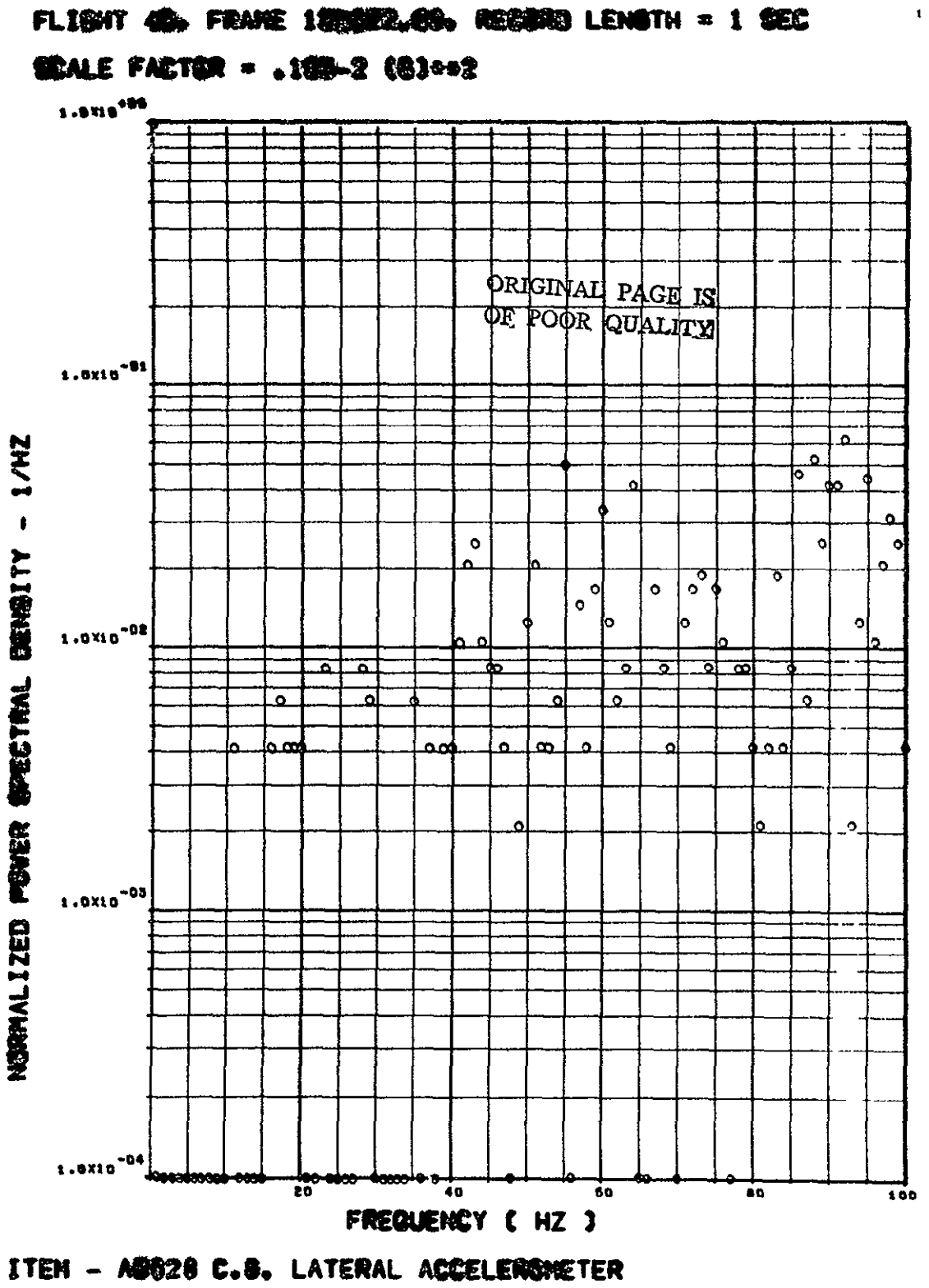

Figure 18. Continued

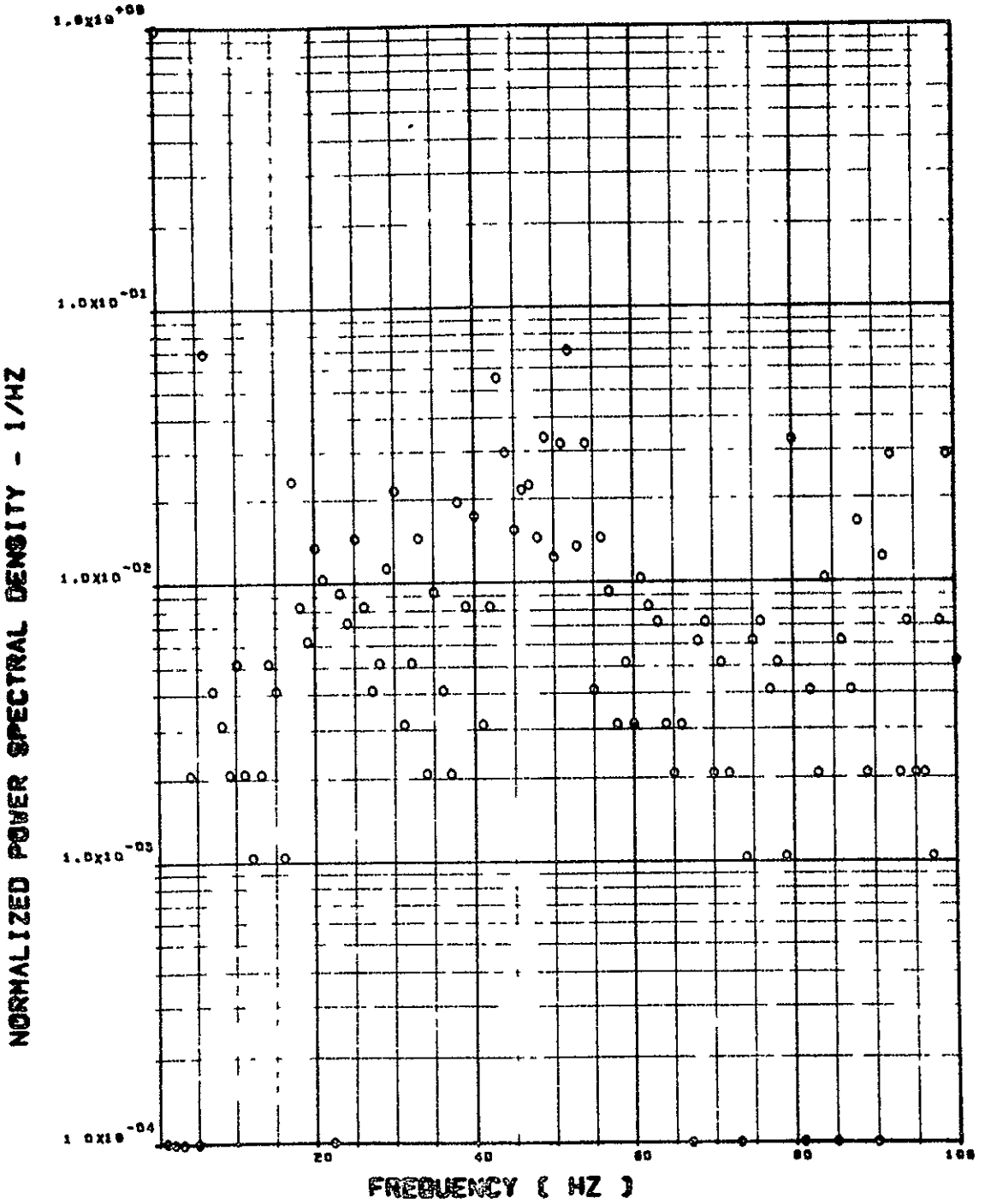

Figure 18. Continued

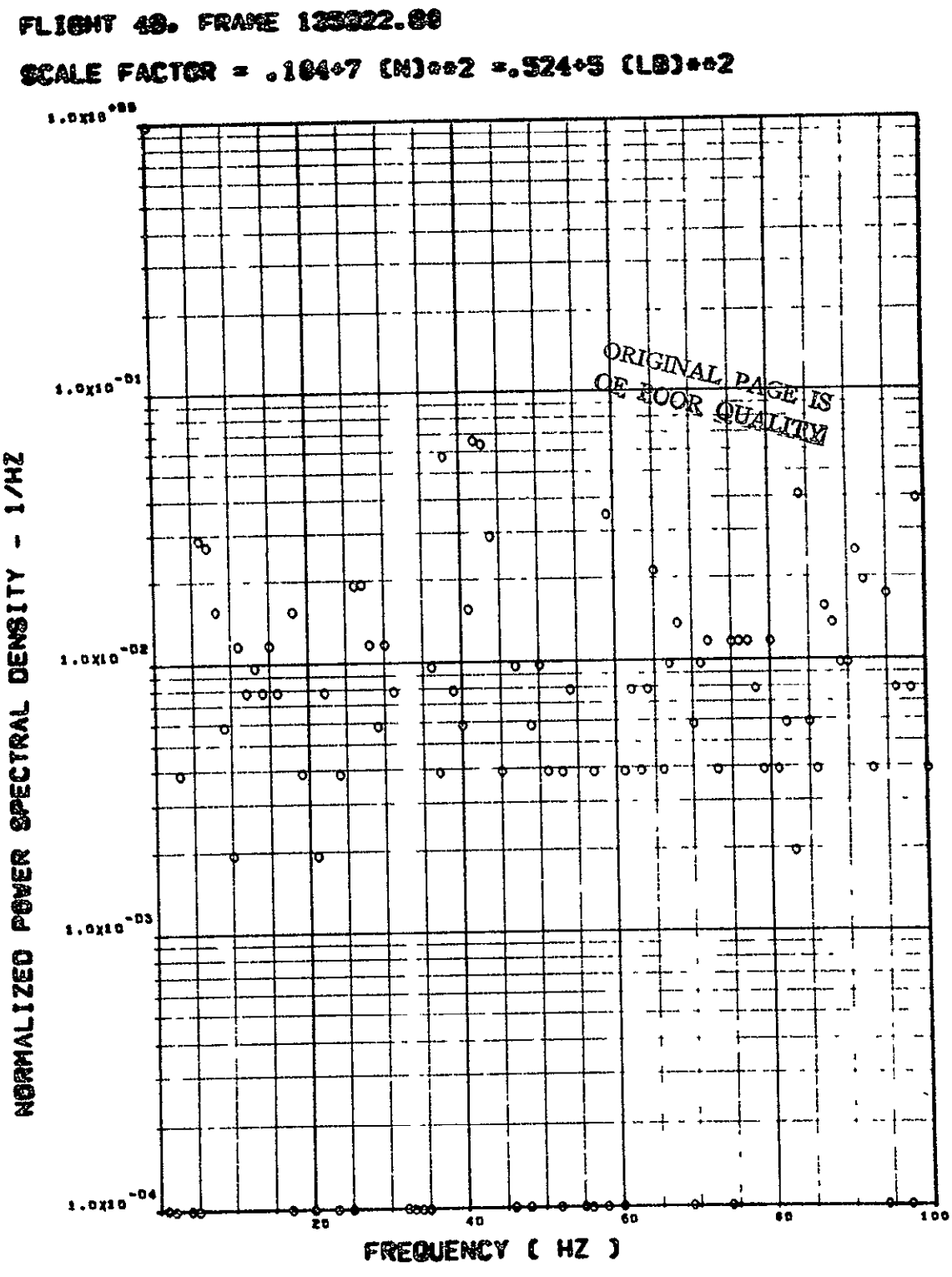

Figure 18. Continued

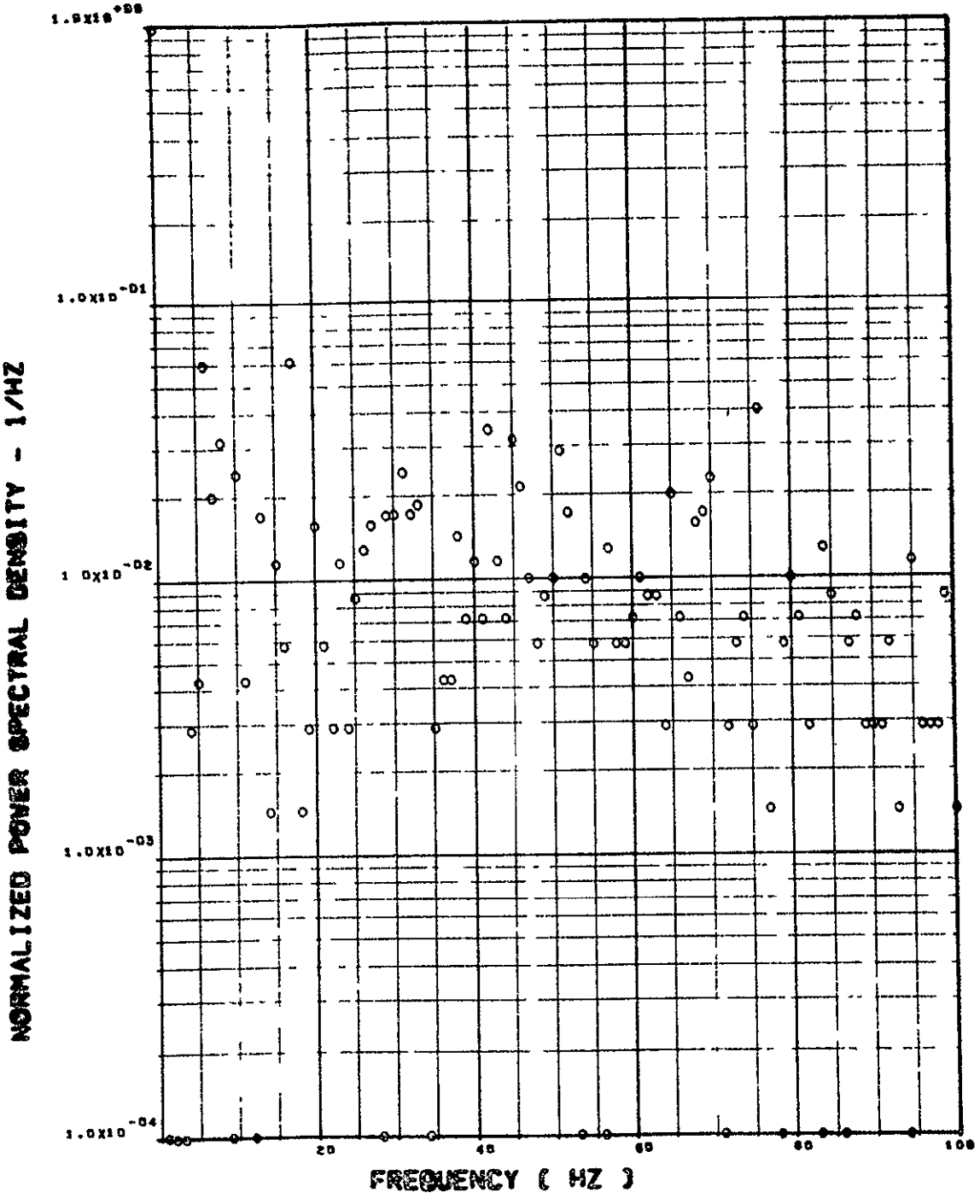

Figure 18. Continued

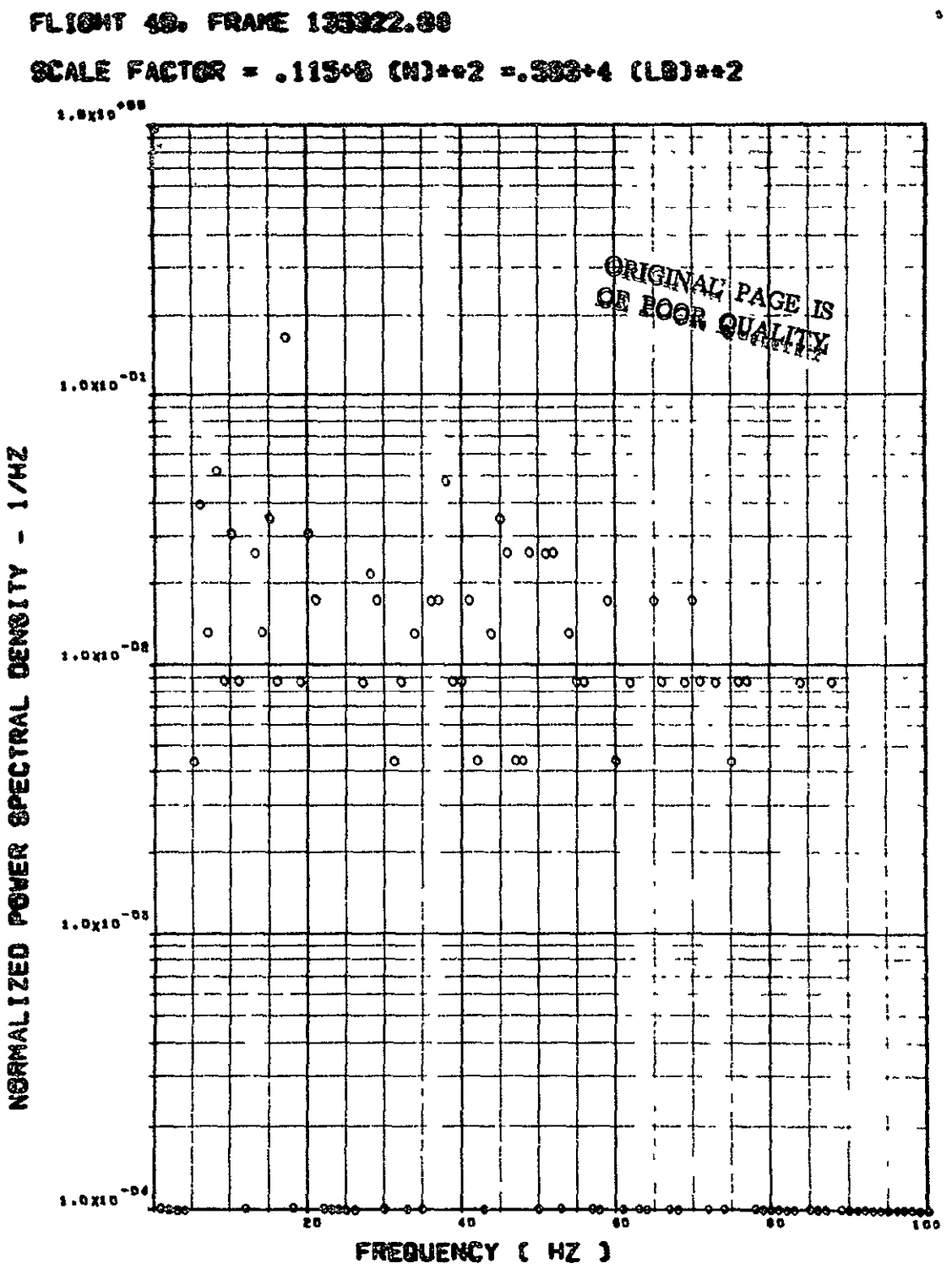

Figure 18. Continued

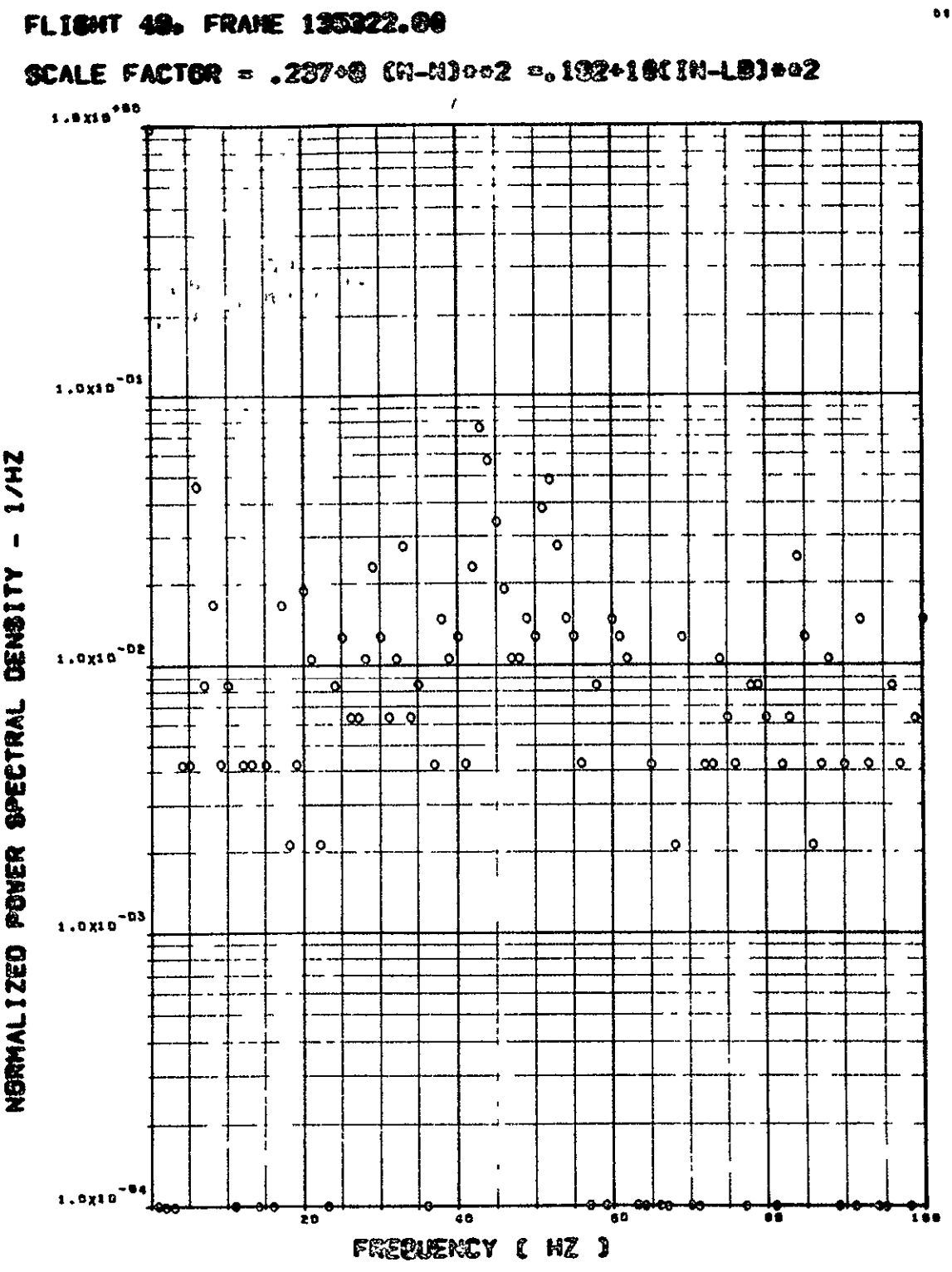

Figure 18. Continued

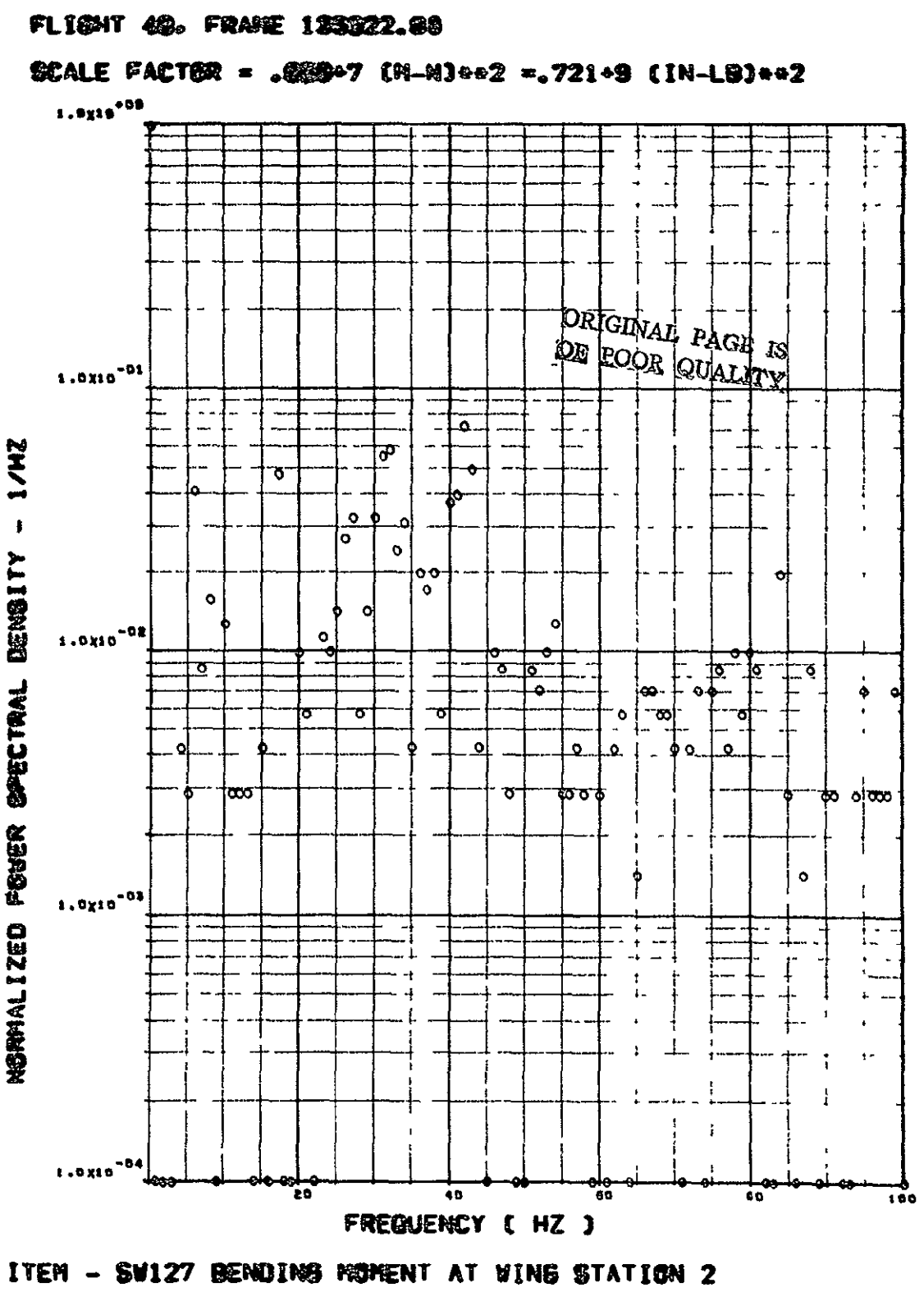

Figure 18. Continued

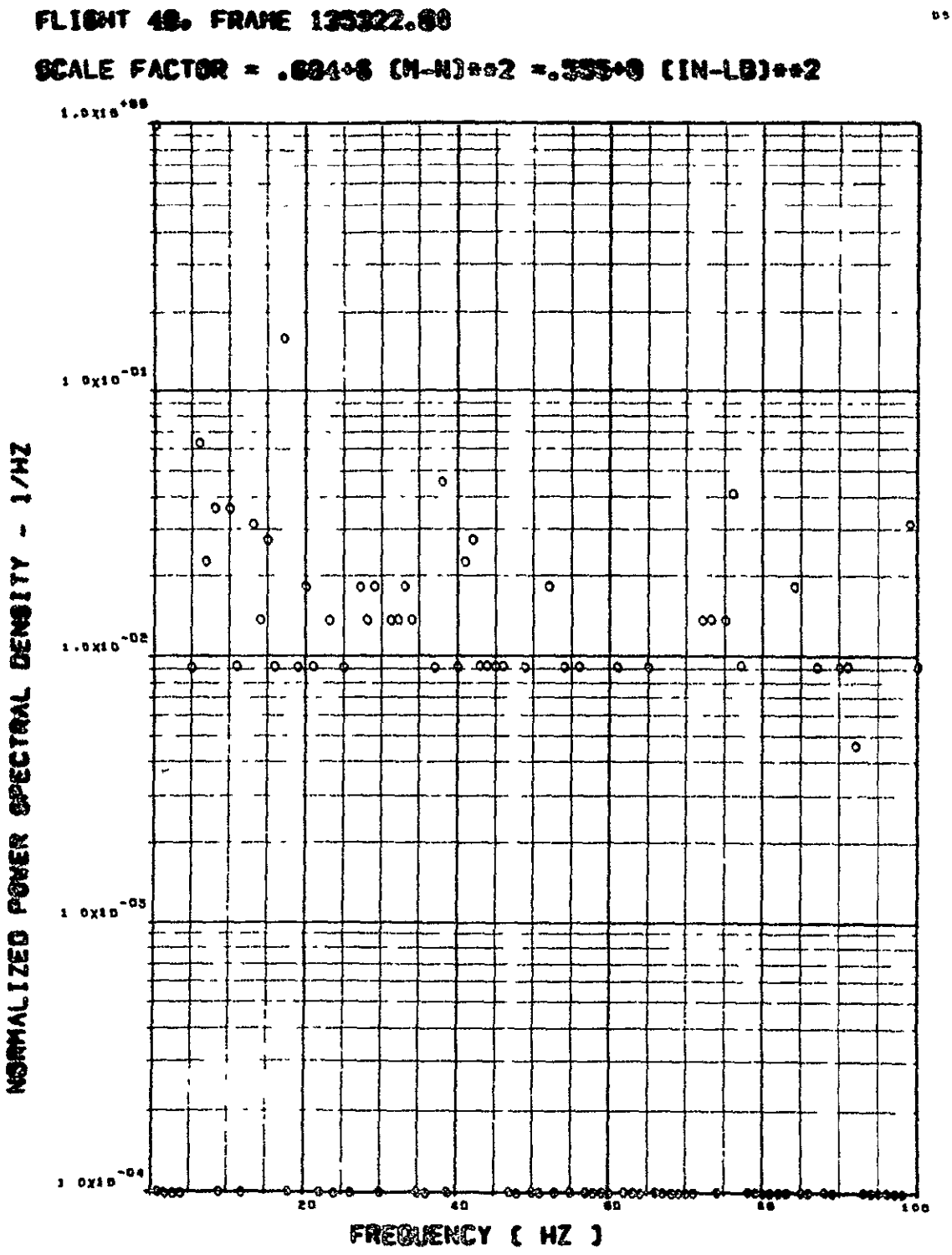

Figure 18. Continued

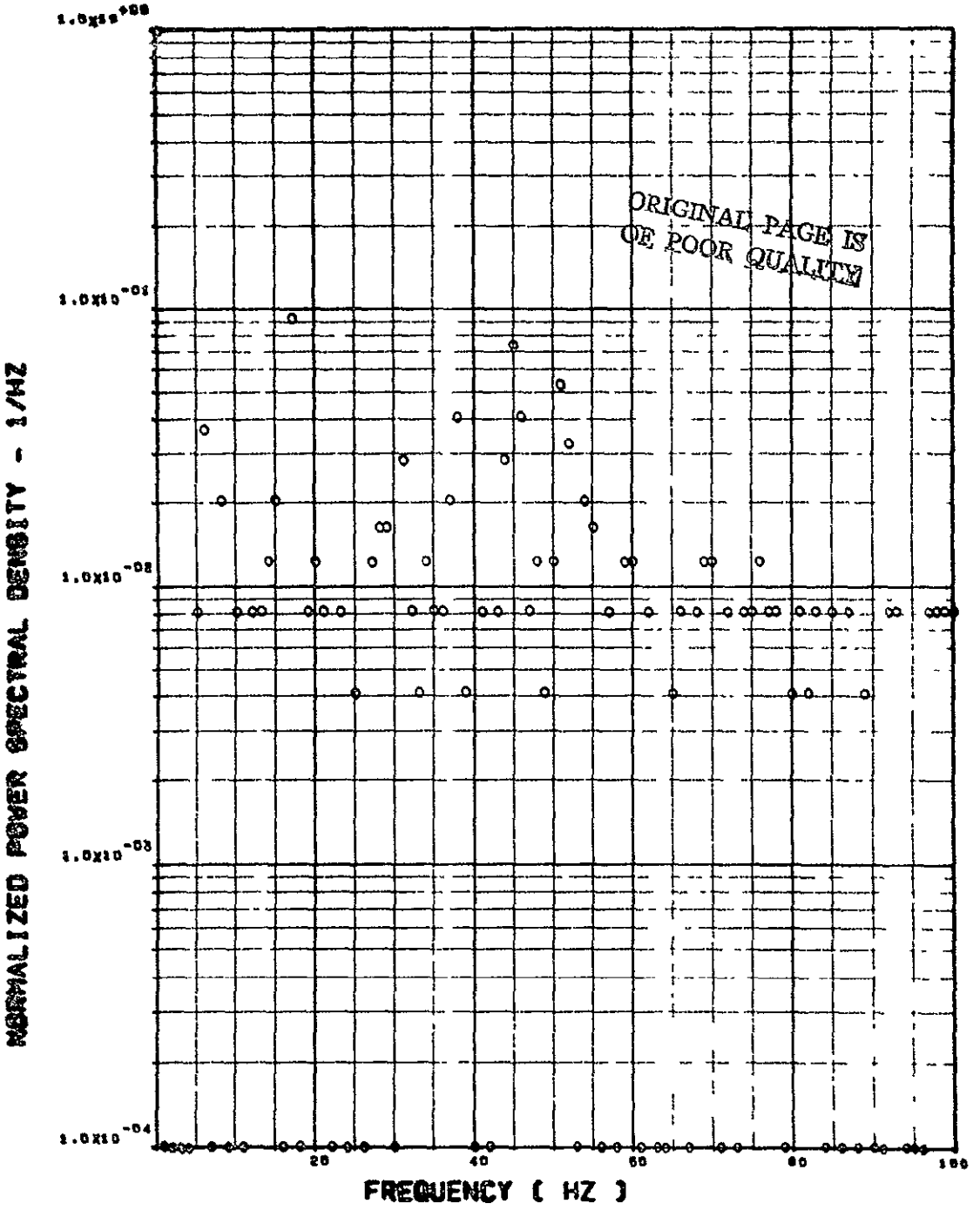

Figure 18. Continued

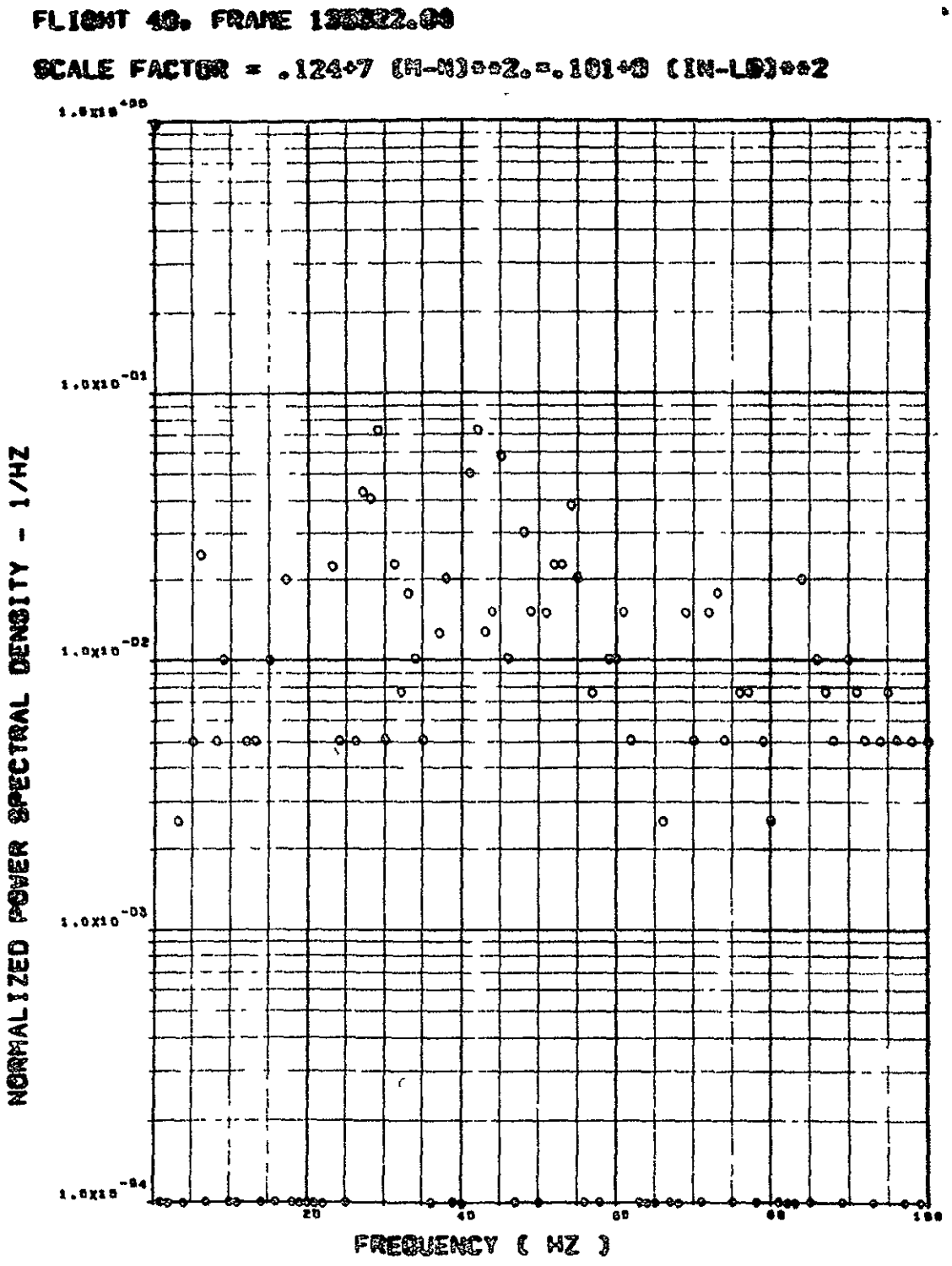

Figure 18. Continued

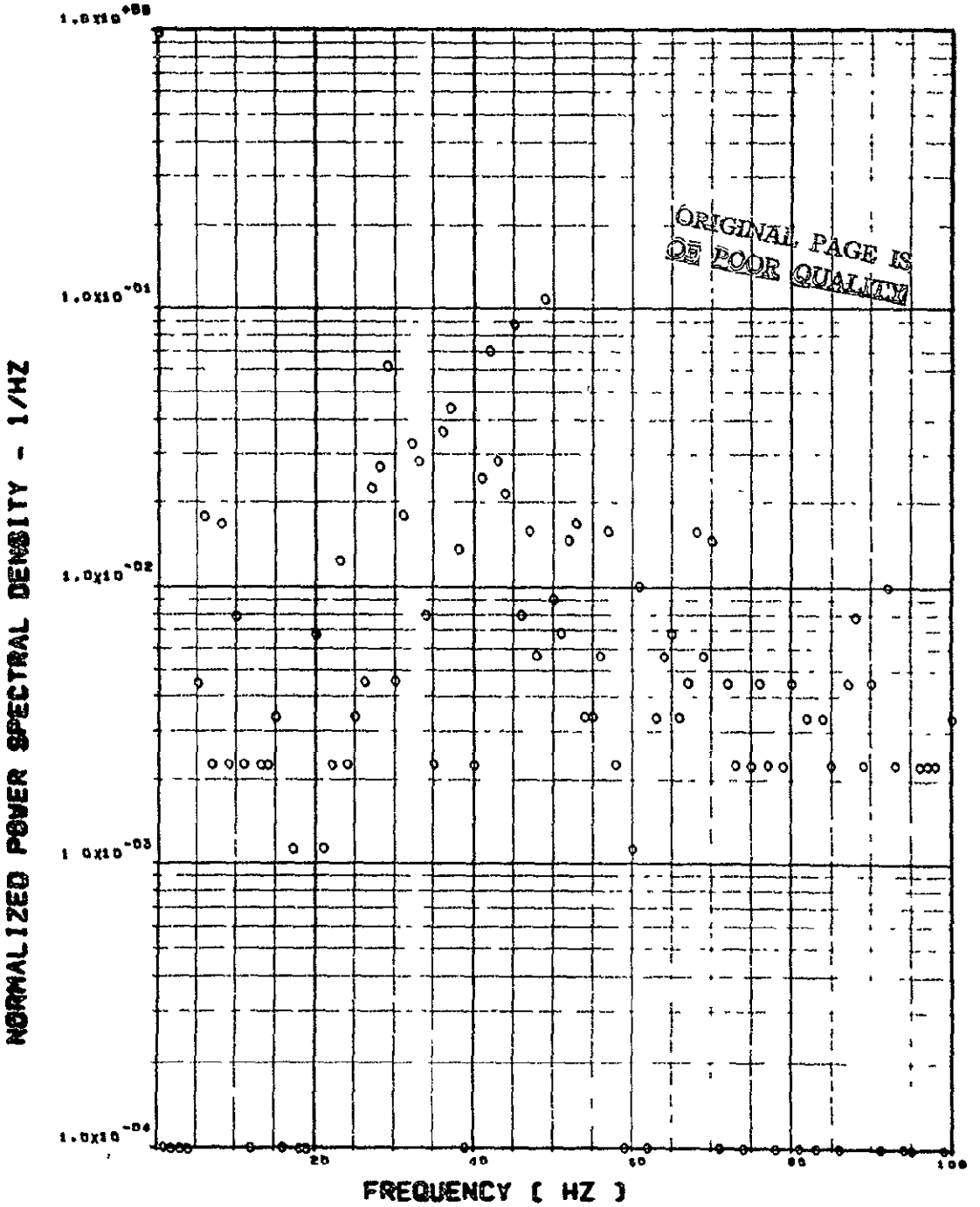

Figure 18. Continued

FLIGHT 48. FRAME 135822.00

SCALE FACTOR = .257+0 (N-N)**2 = .217+0 (IN-LB)**2

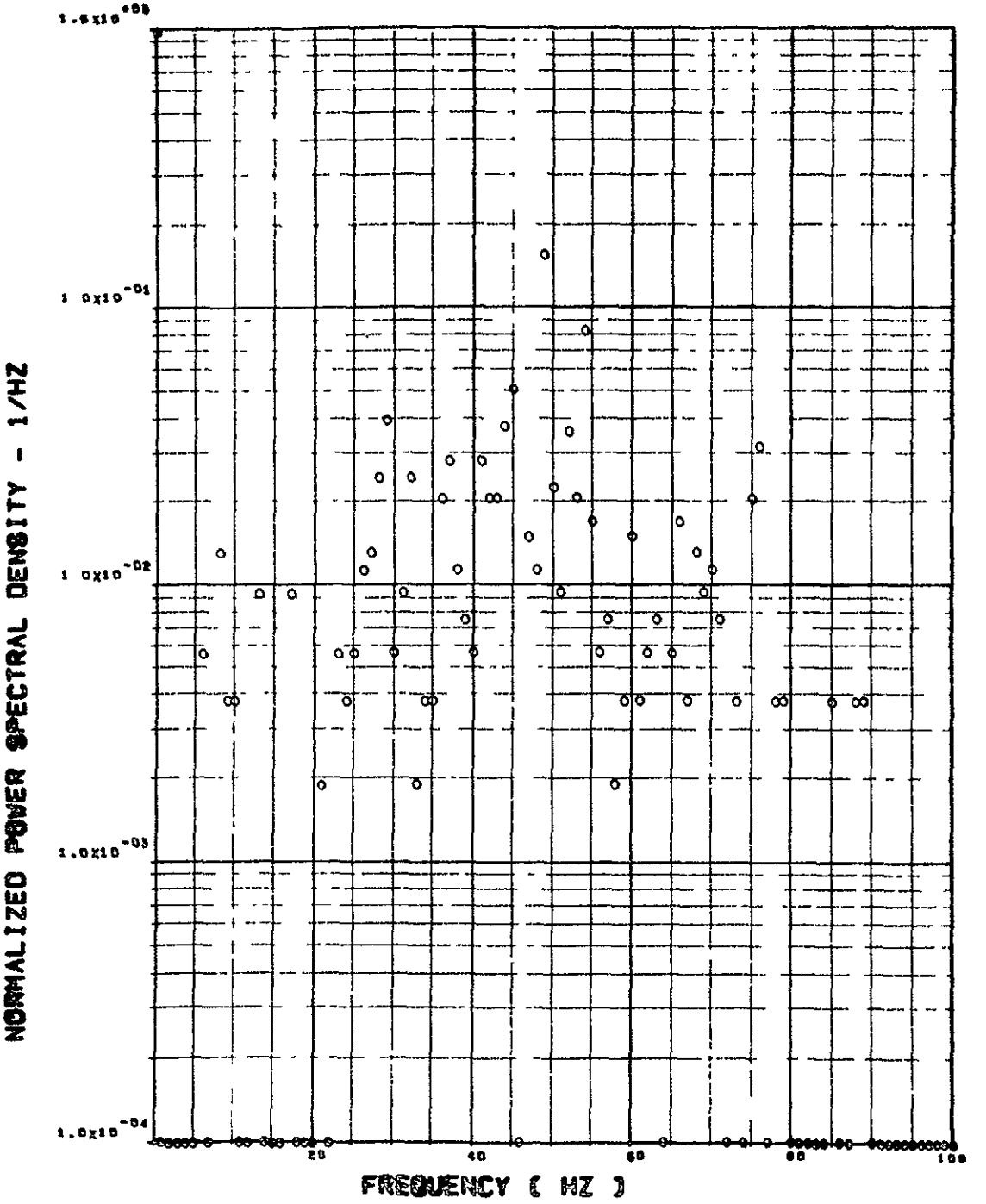

ITEM - SW131 TORSION AT WING STATION 3

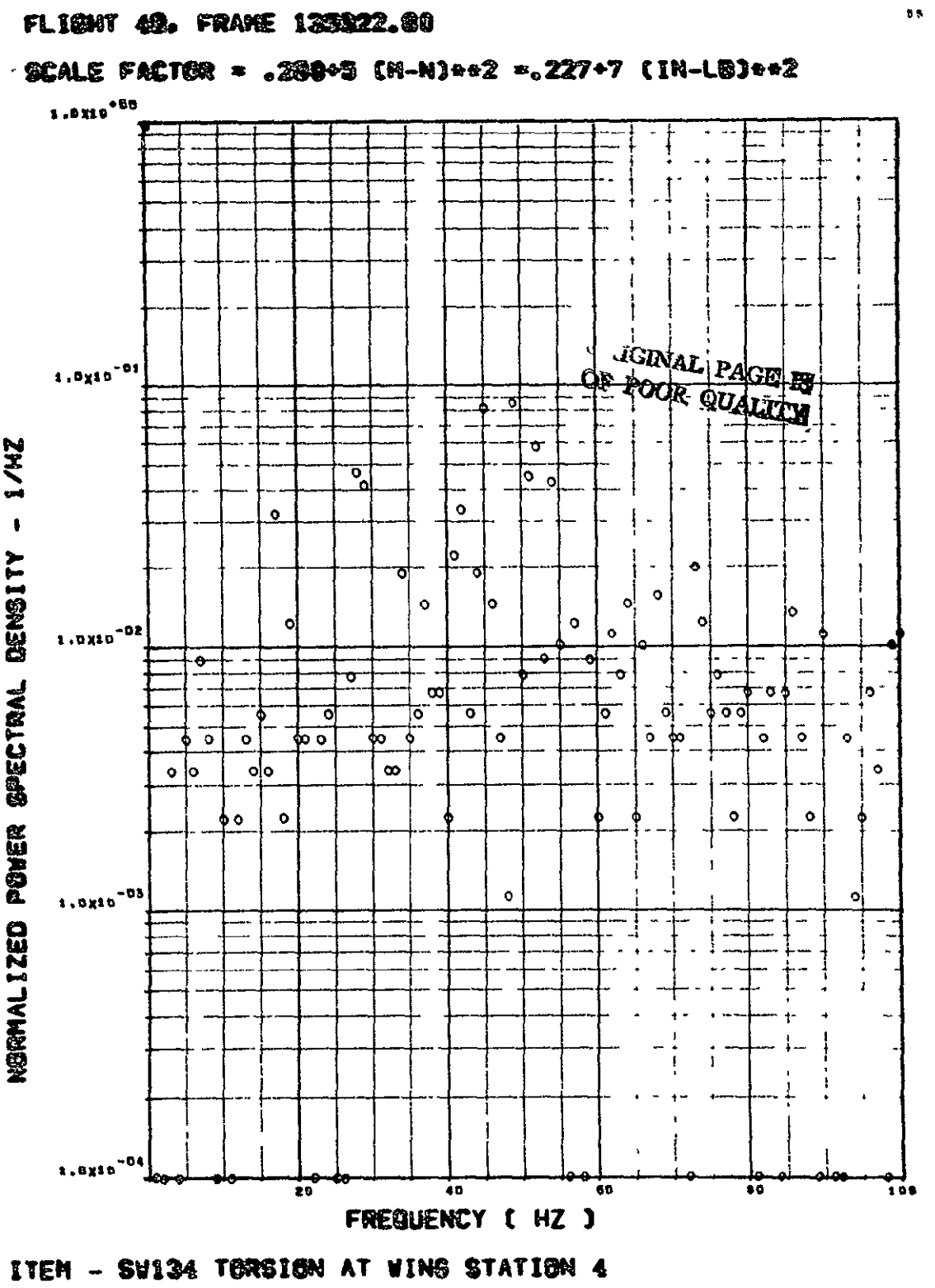

Figure 18. Continued

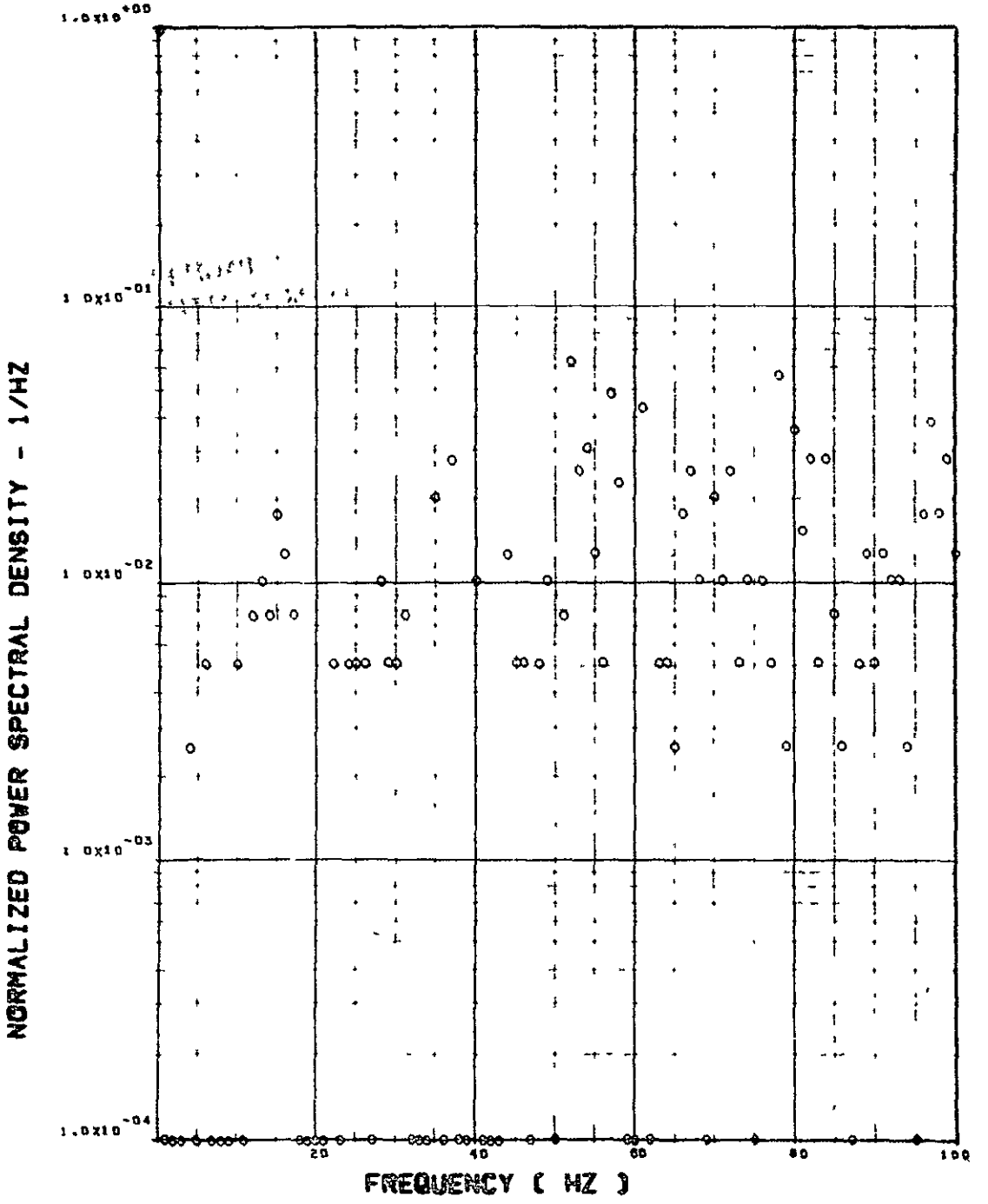

Figure 18. Continued

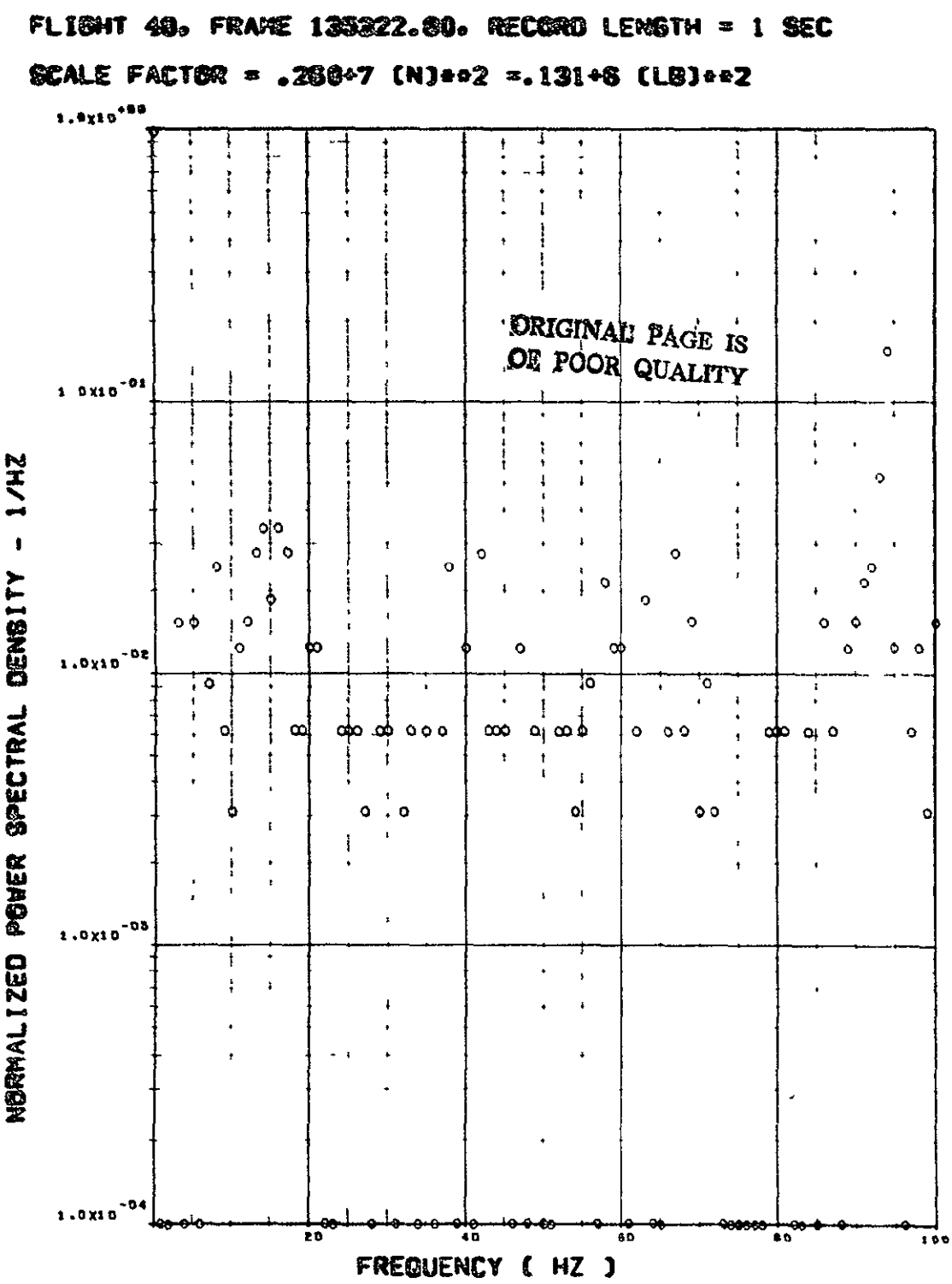

Figure 18. Continued

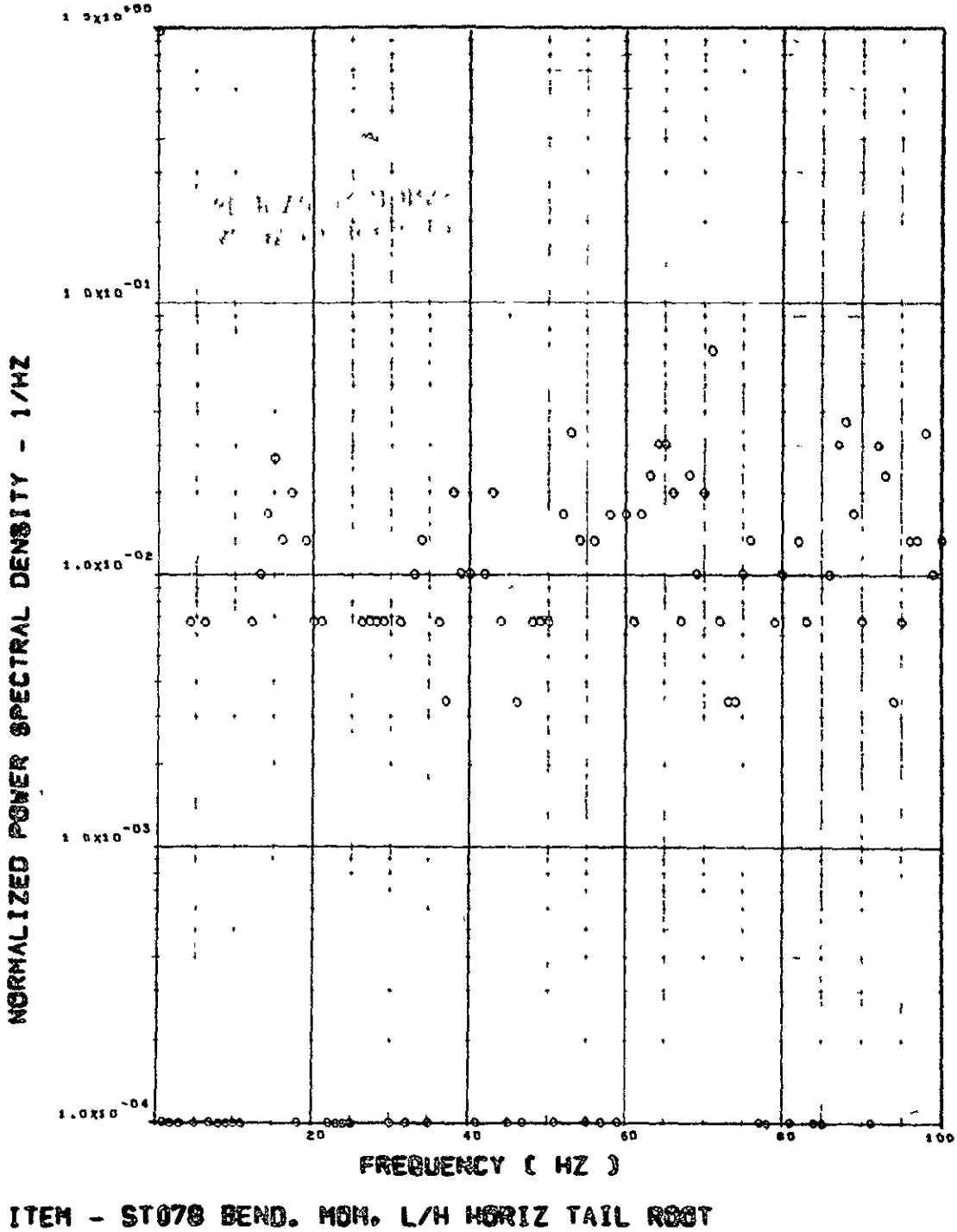

Figure 18. Continued

FLIGHT 48. FRAME 135322.00. RECORD LENGTH = 1 SEC

SCALE FACTOR = .107+7 (M-N)**2 =.666+8 (IN-LB)**2

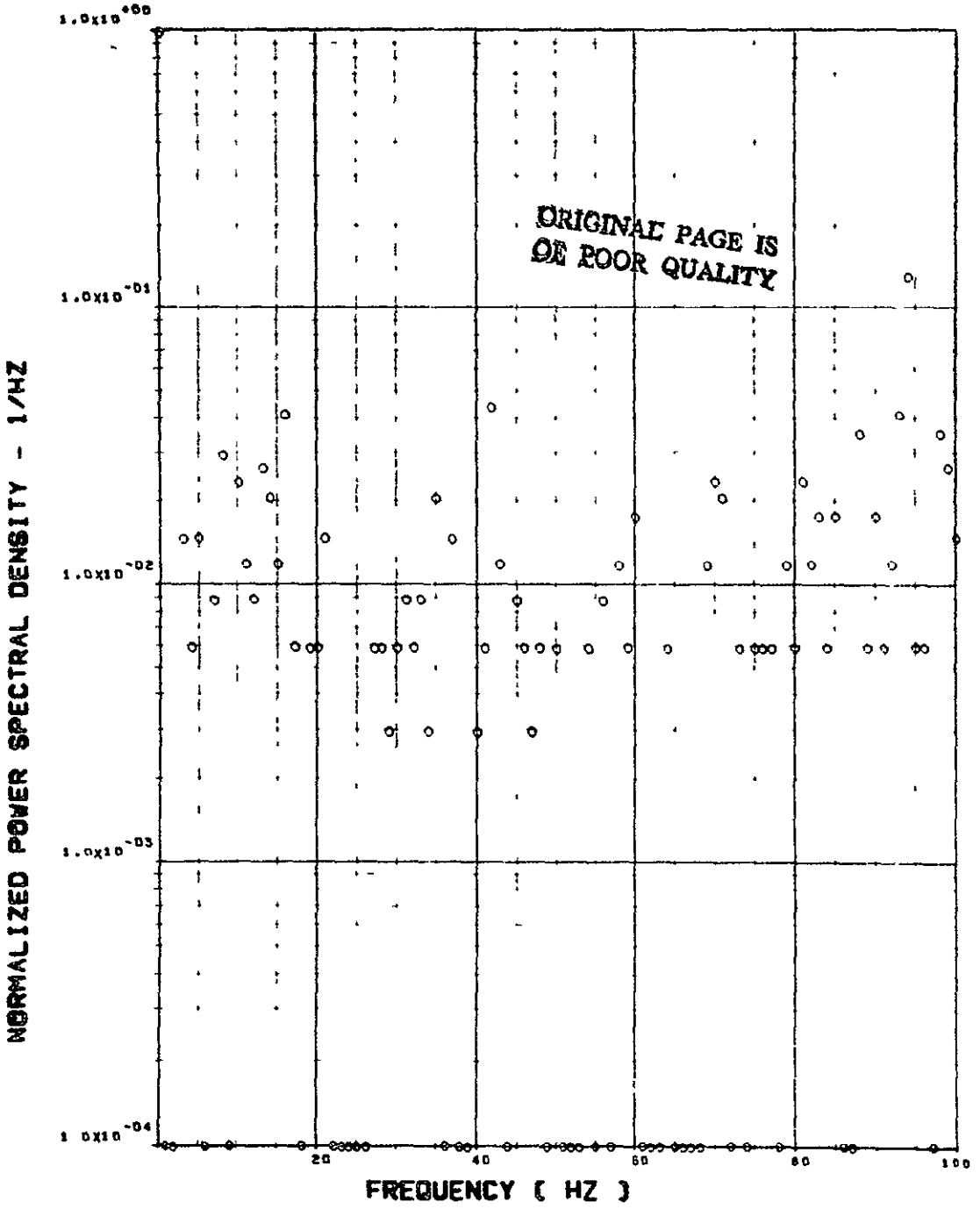

ITEM - ST073 BEND. MOM. R/H HORIZ TAIL ROOT

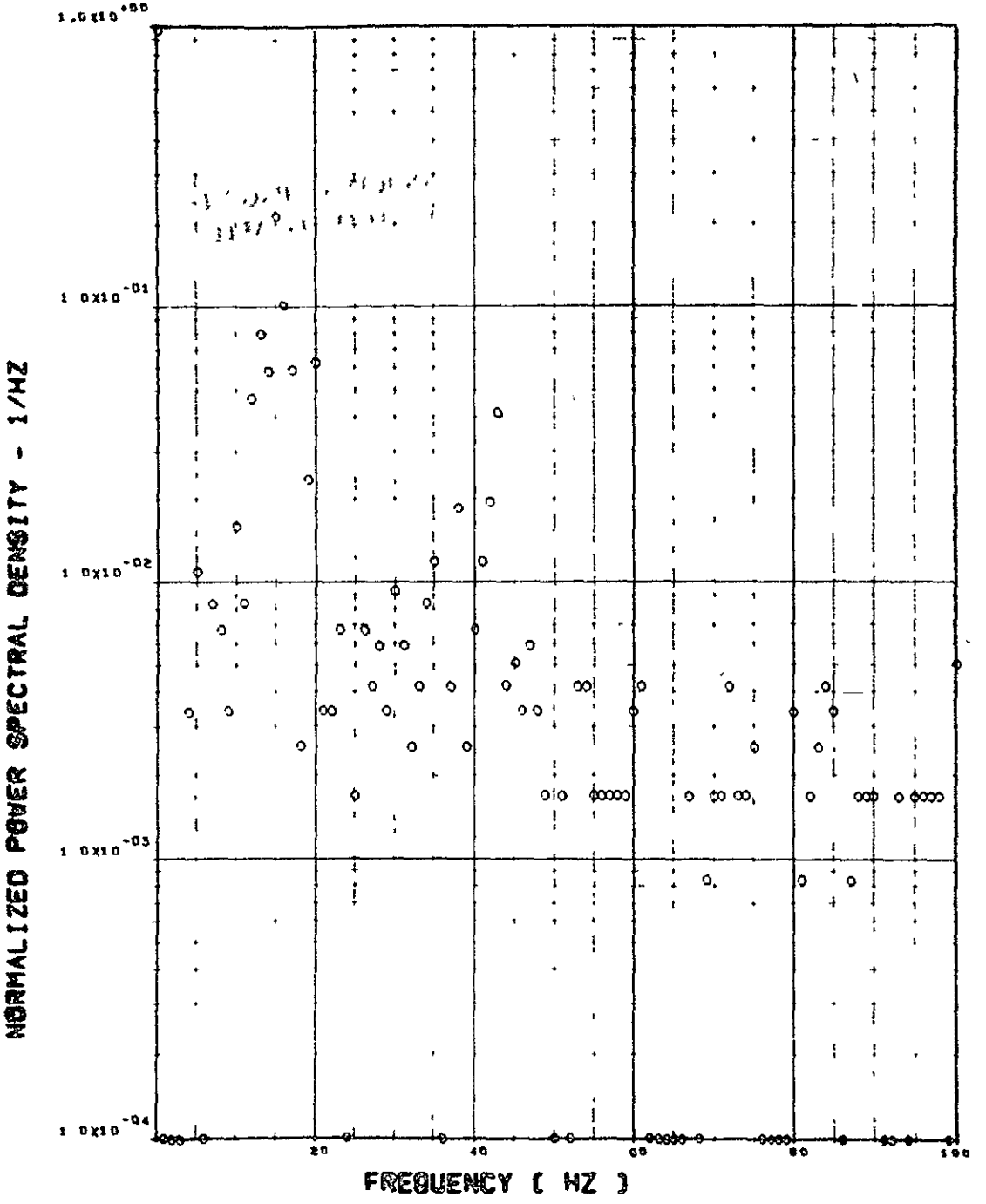

Figure 18. Continued

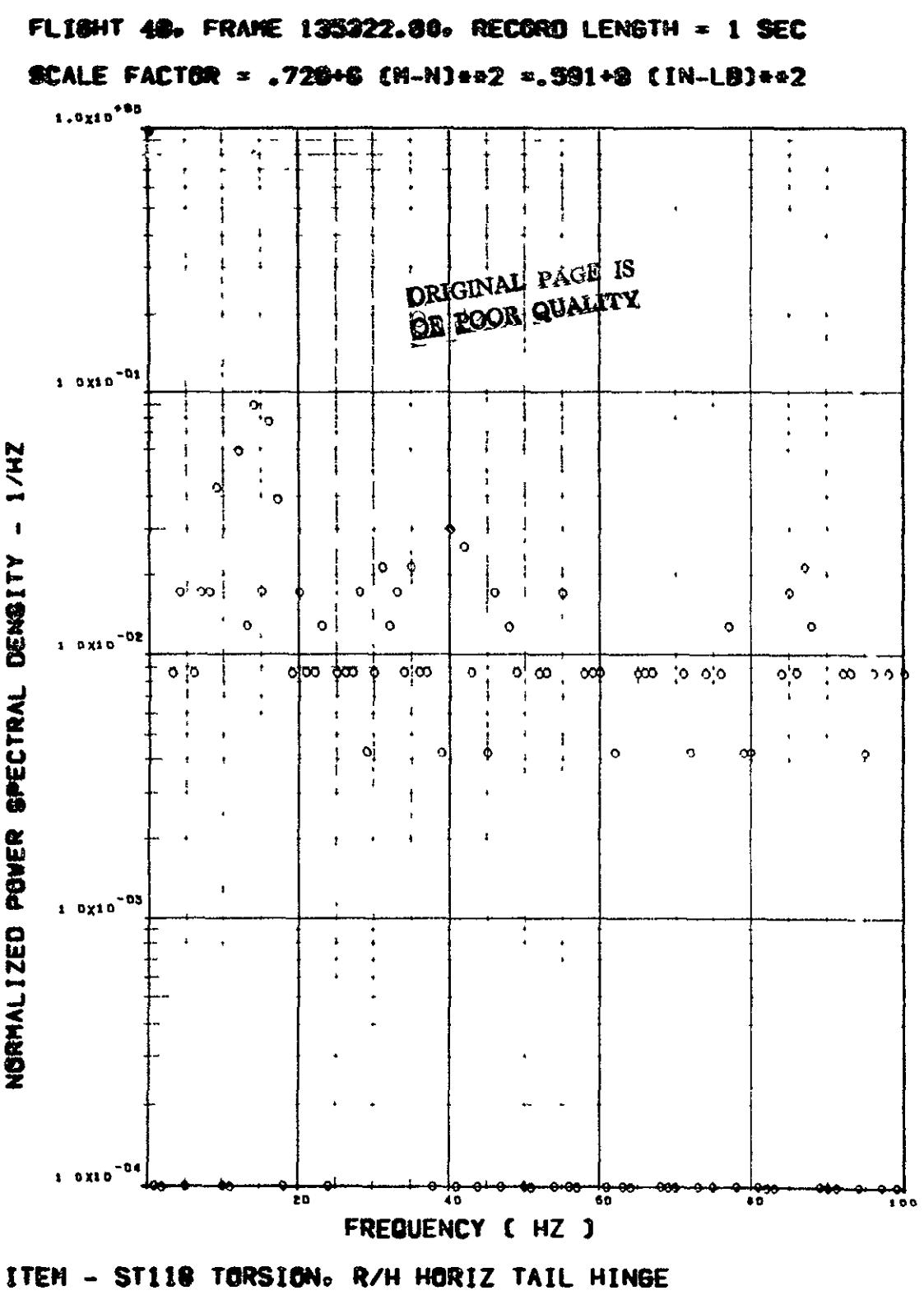

Figure 18. Concluded

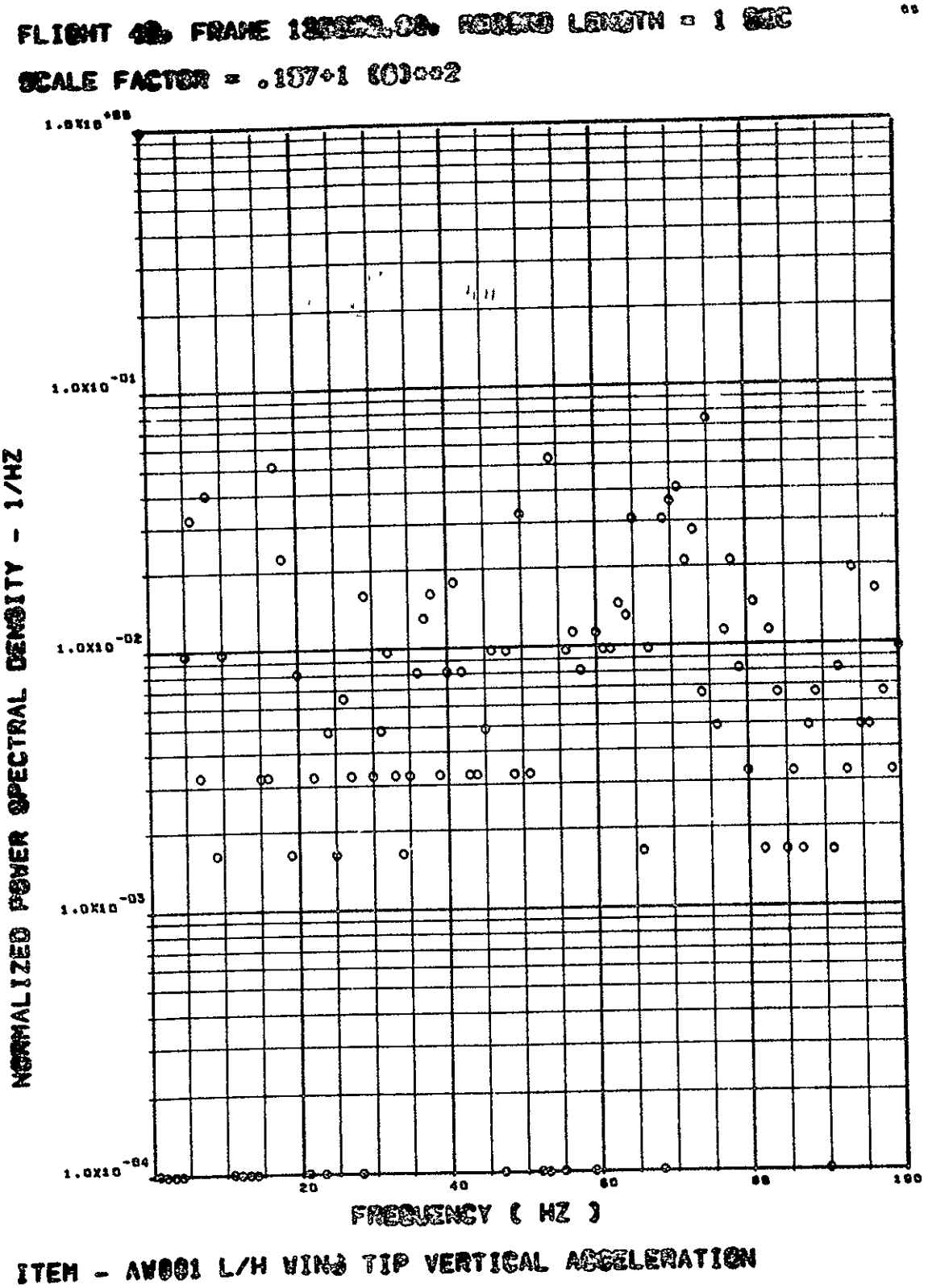

Figure 19. Power Spectra - Flight 48, Run 4, Point 4 T_1 = 135323.9, ΔT = 1 Sec, α_{Nom} = 14.3 deg, $\Delta\alpha$= 1 30 deg.

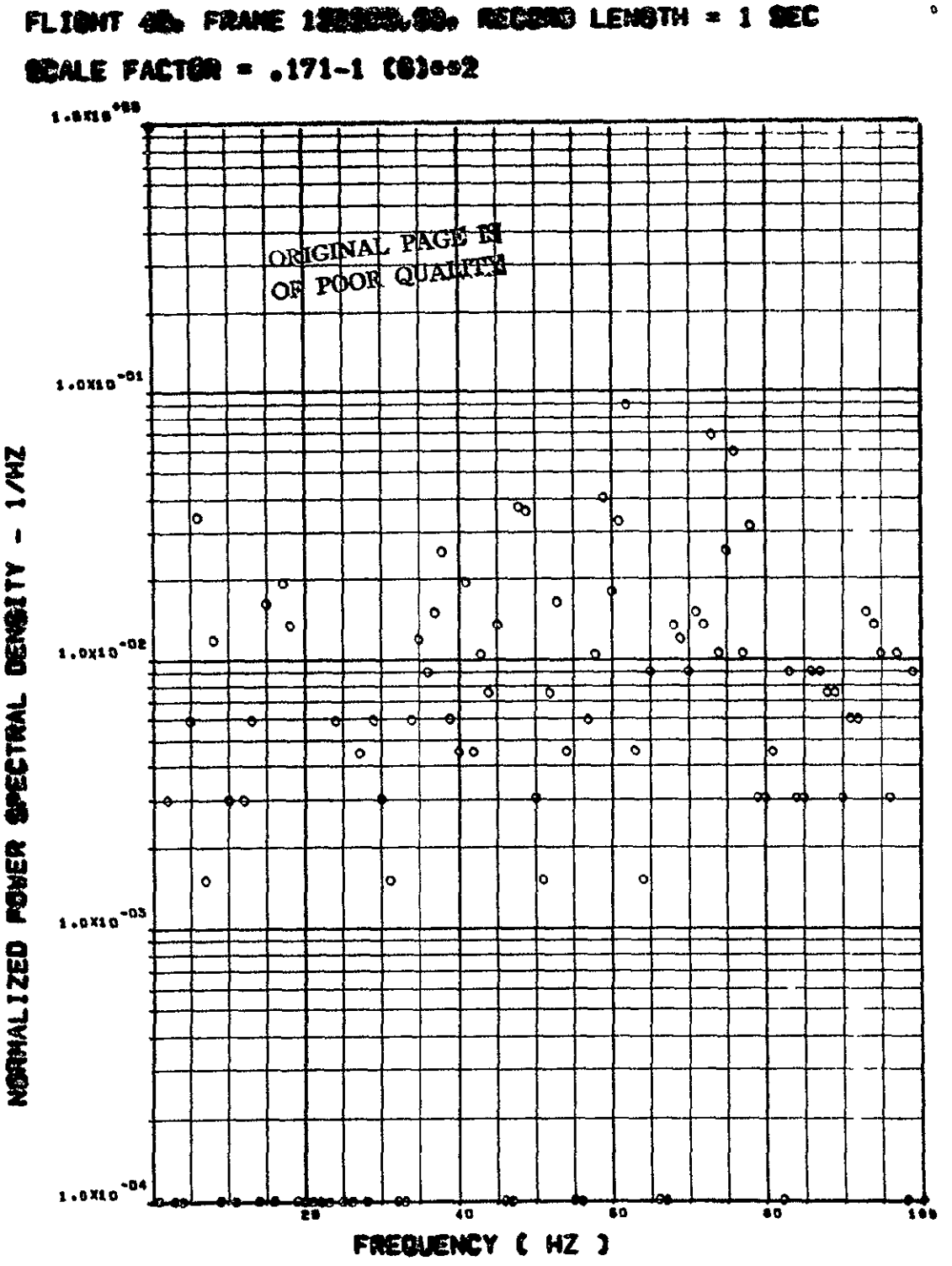

Figure 19. Continued

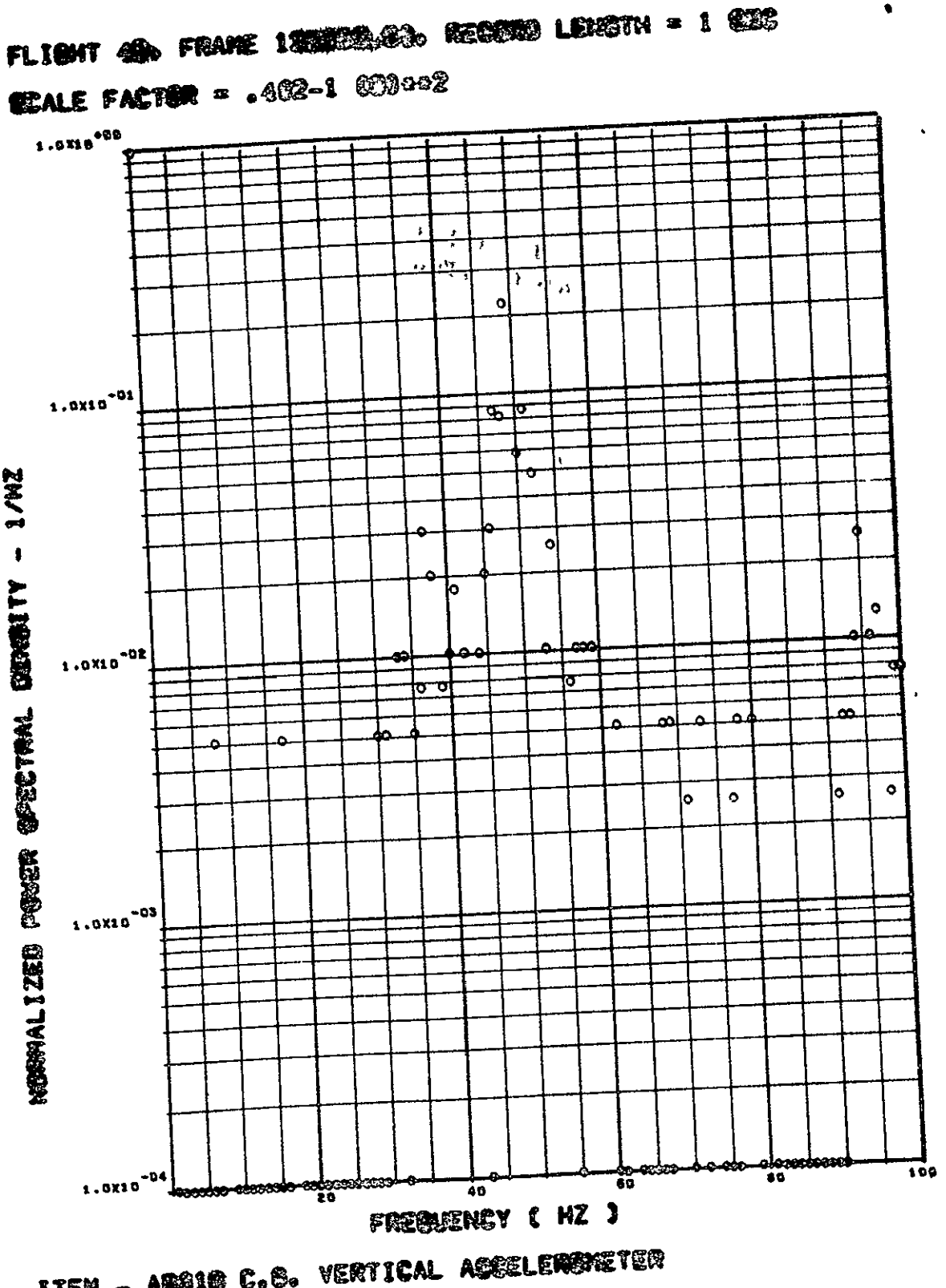

Figure 19. Continued

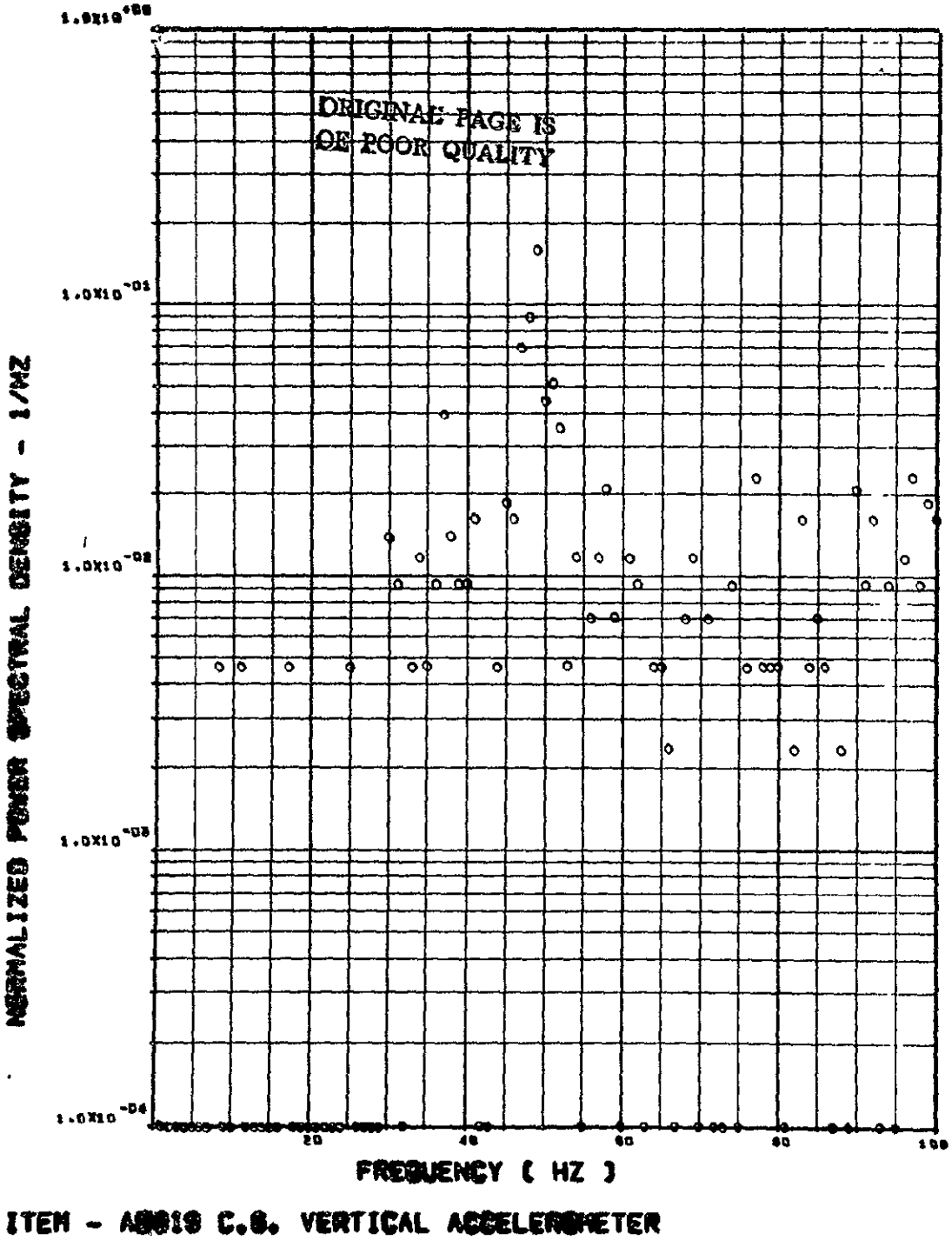

Figure 19. Continued

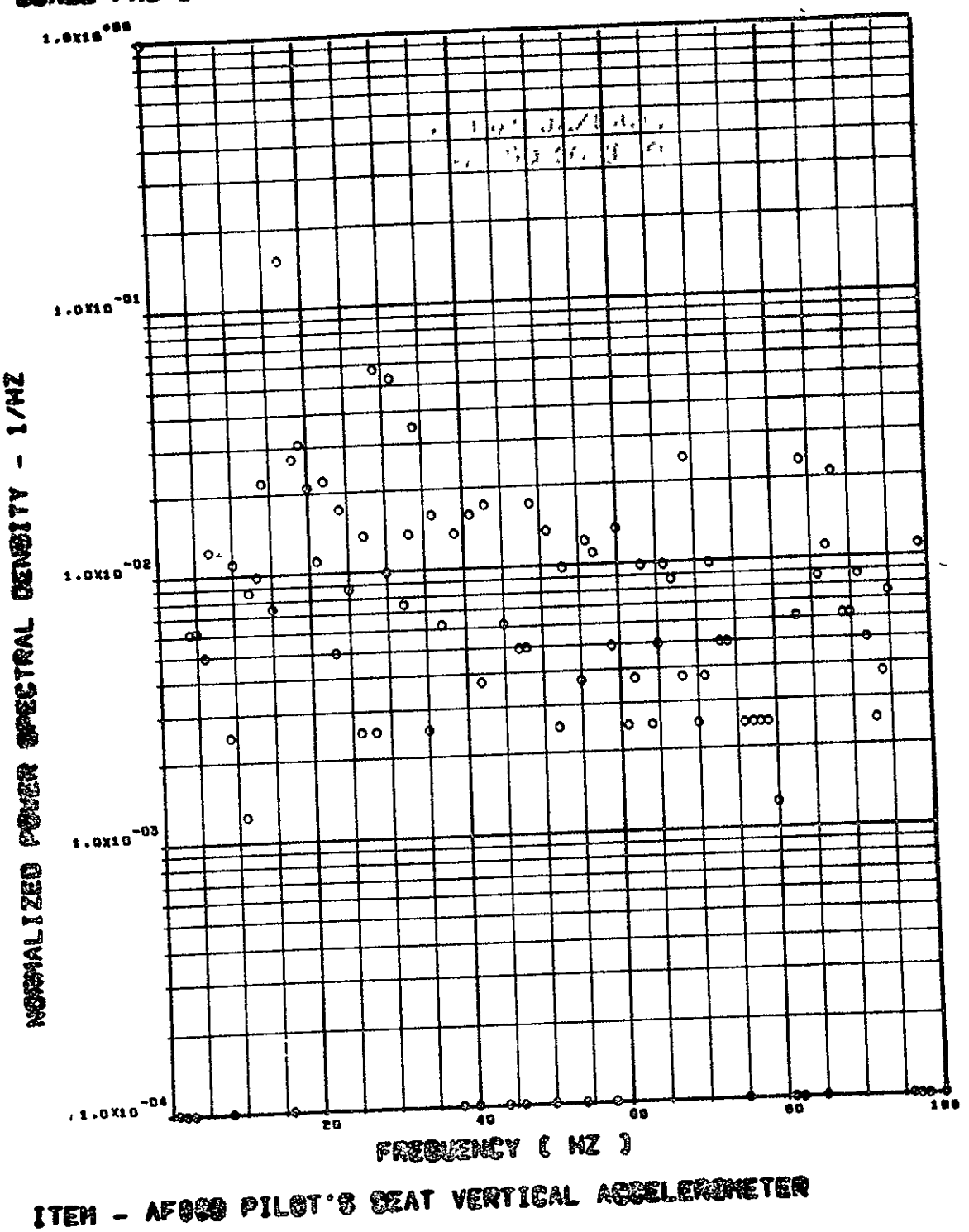

Figure 19. Continued

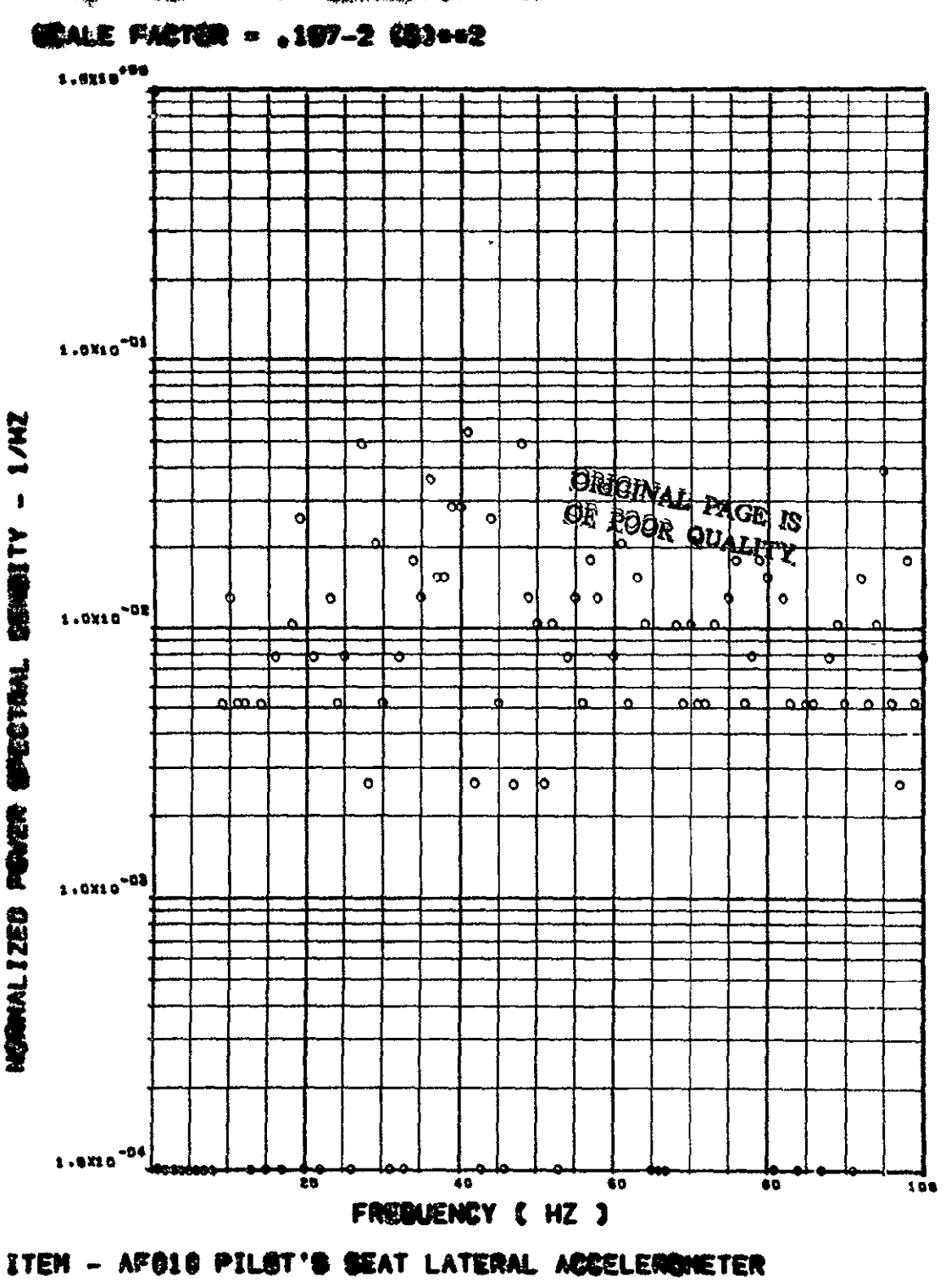

Figure 19. Continued

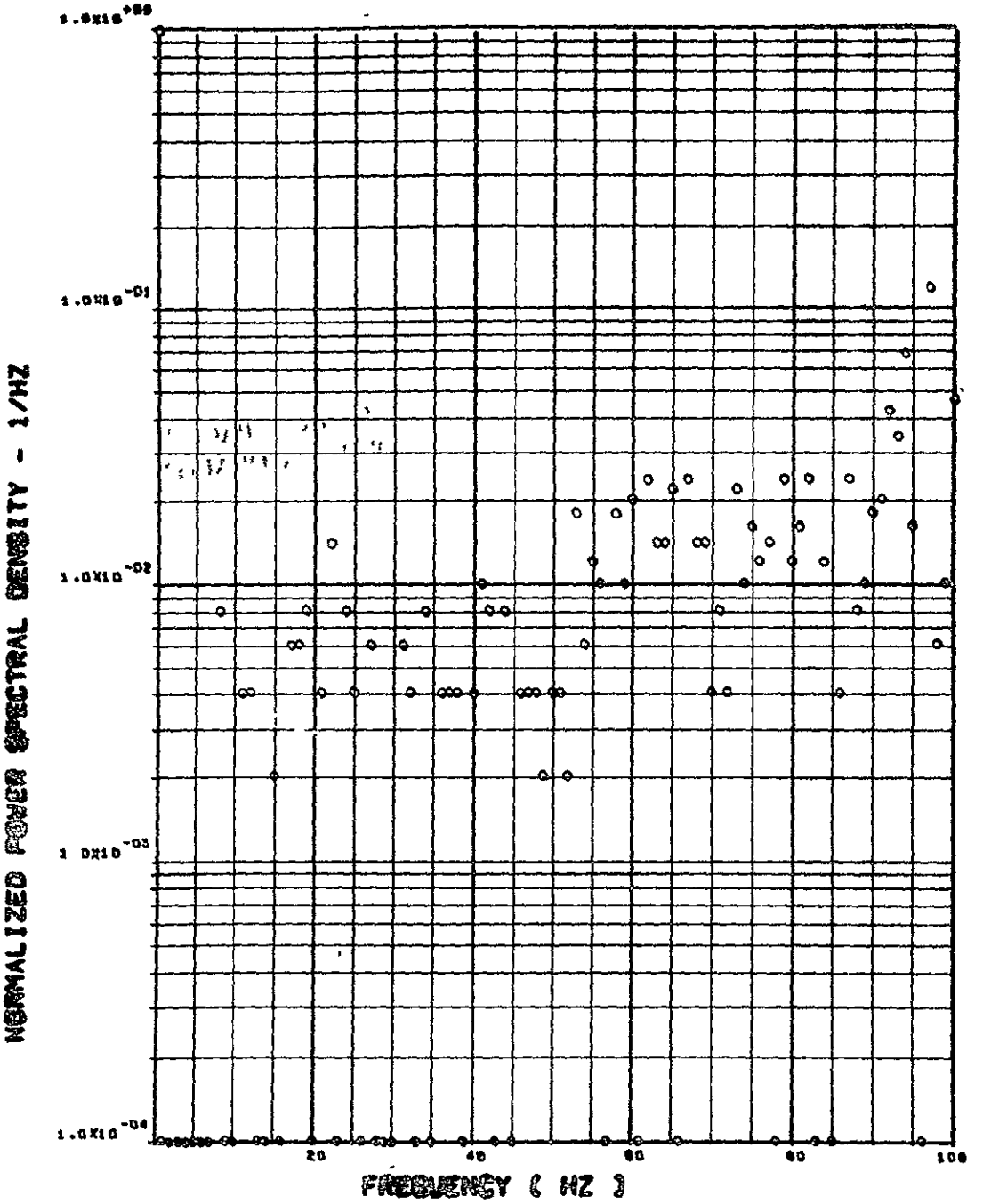

Figure 19. Continued

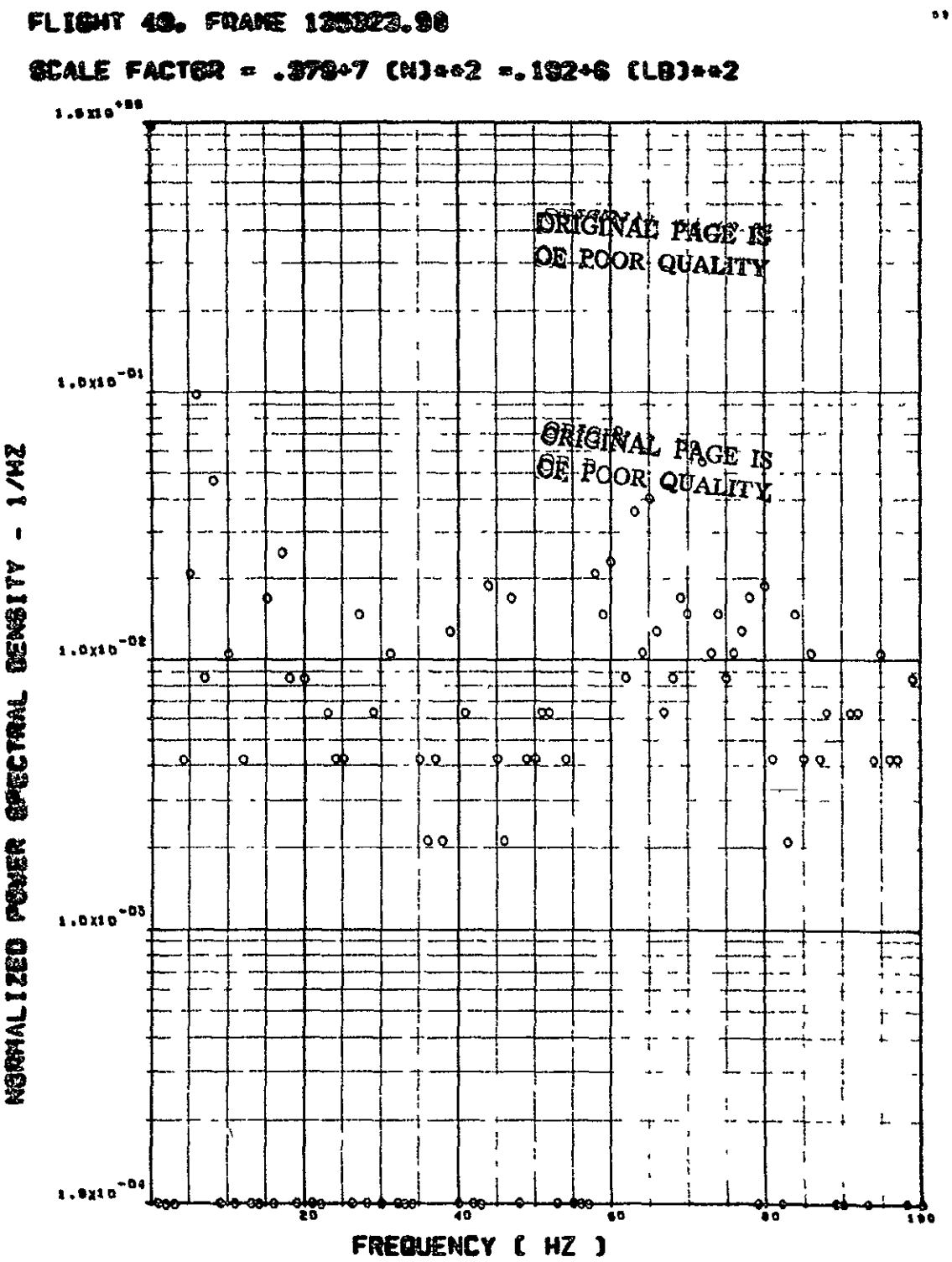

Figure 19. Continued

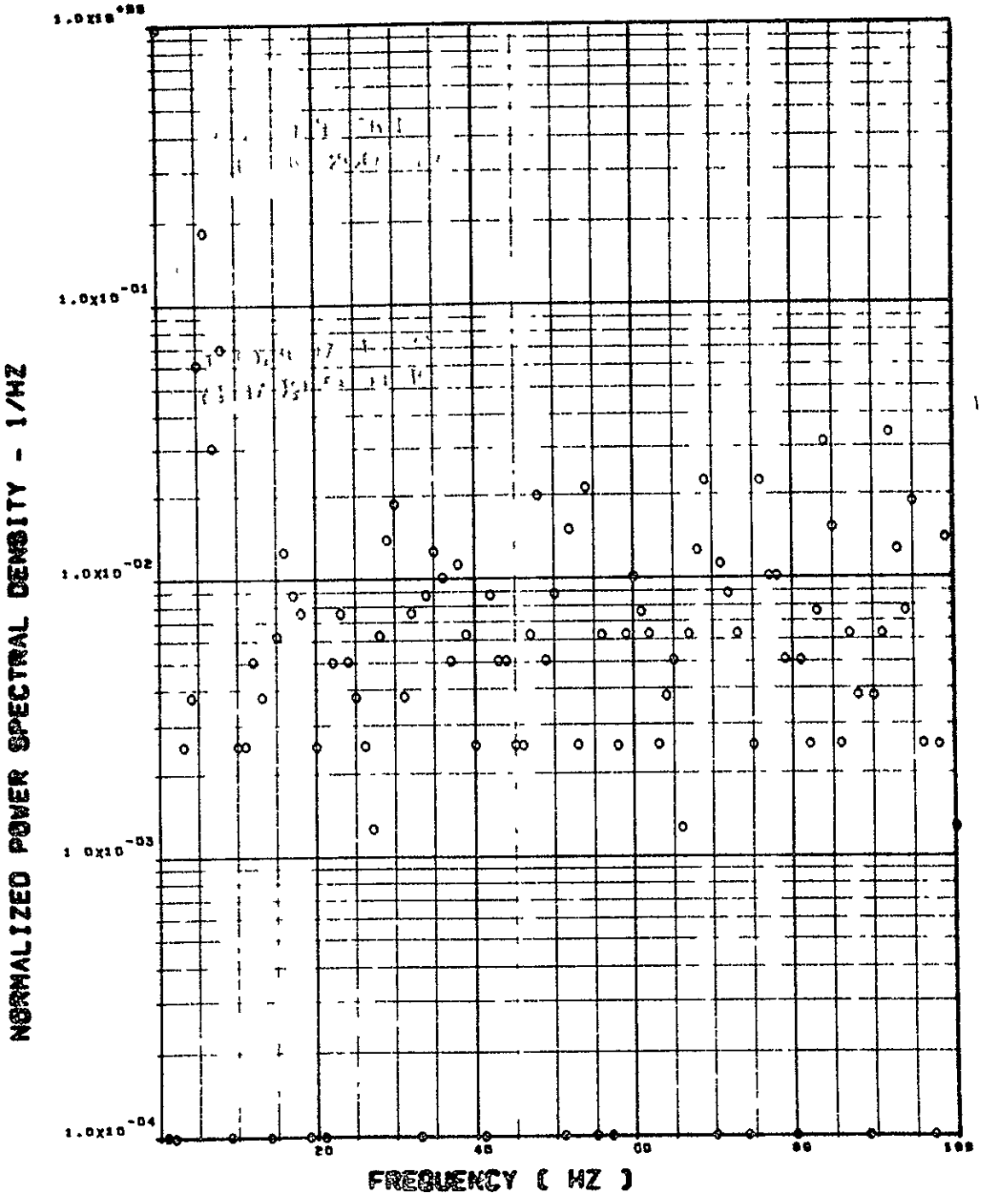

Figure 19. Continued

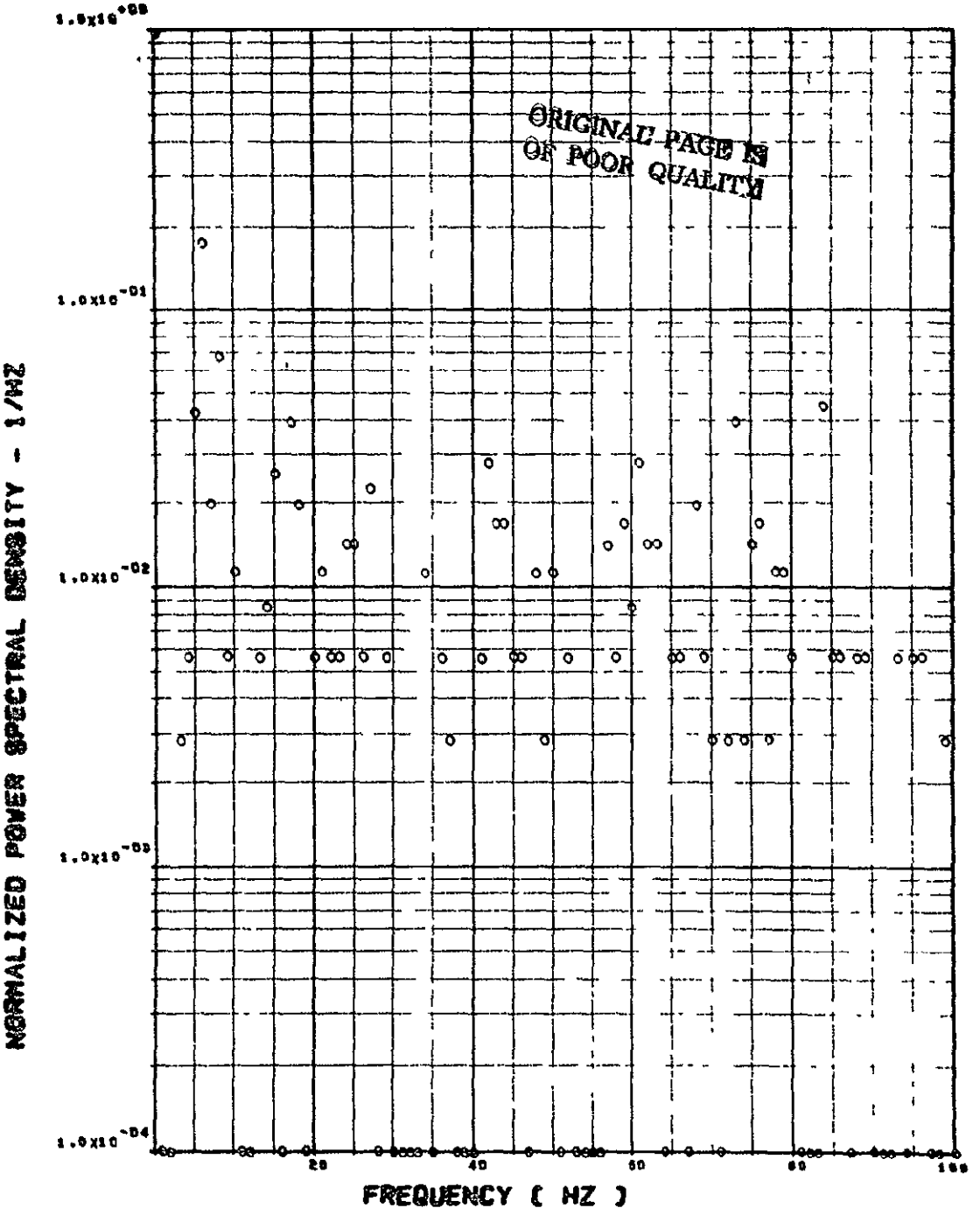

Figure 19. Continued

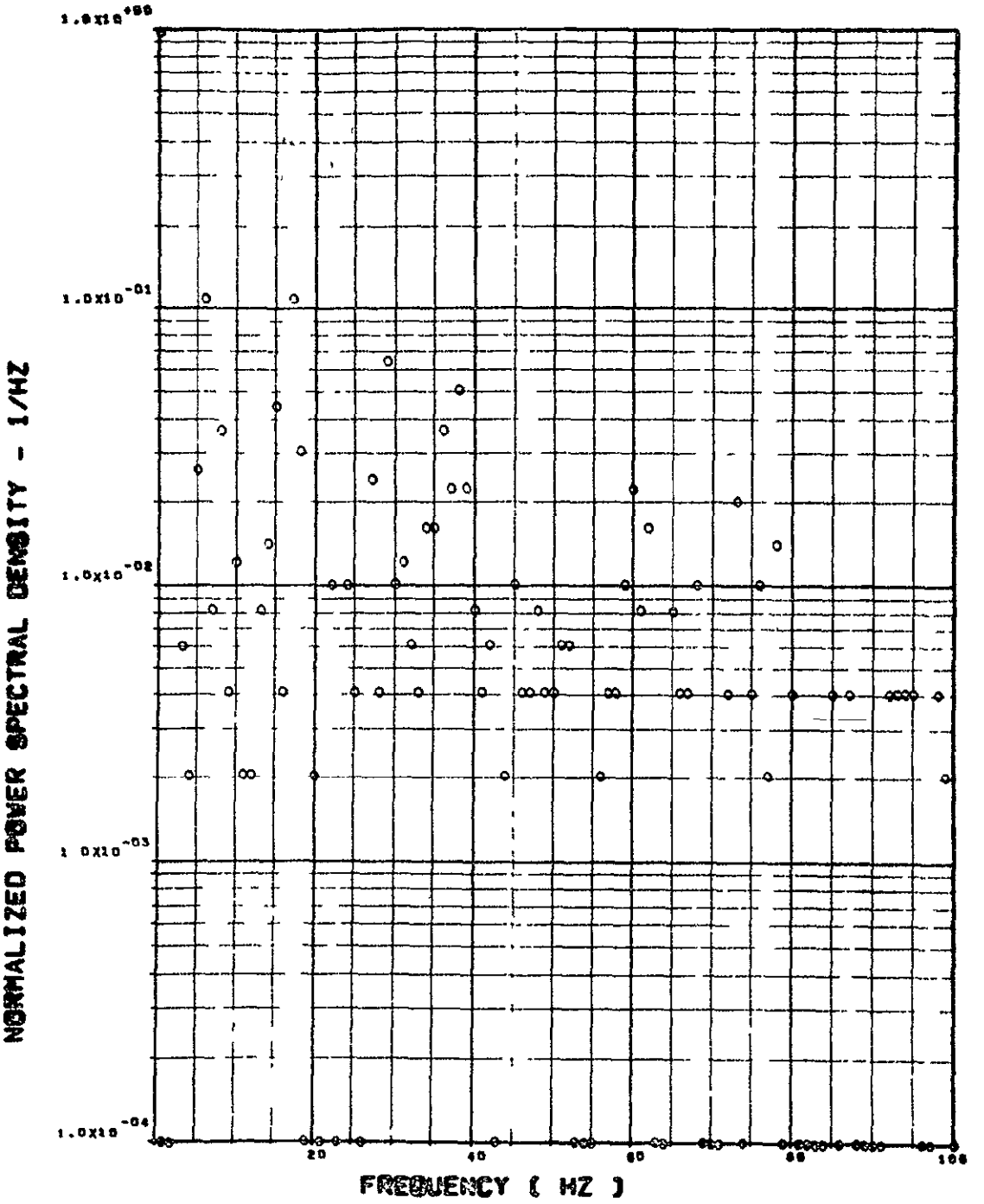

Figure 19. Continued

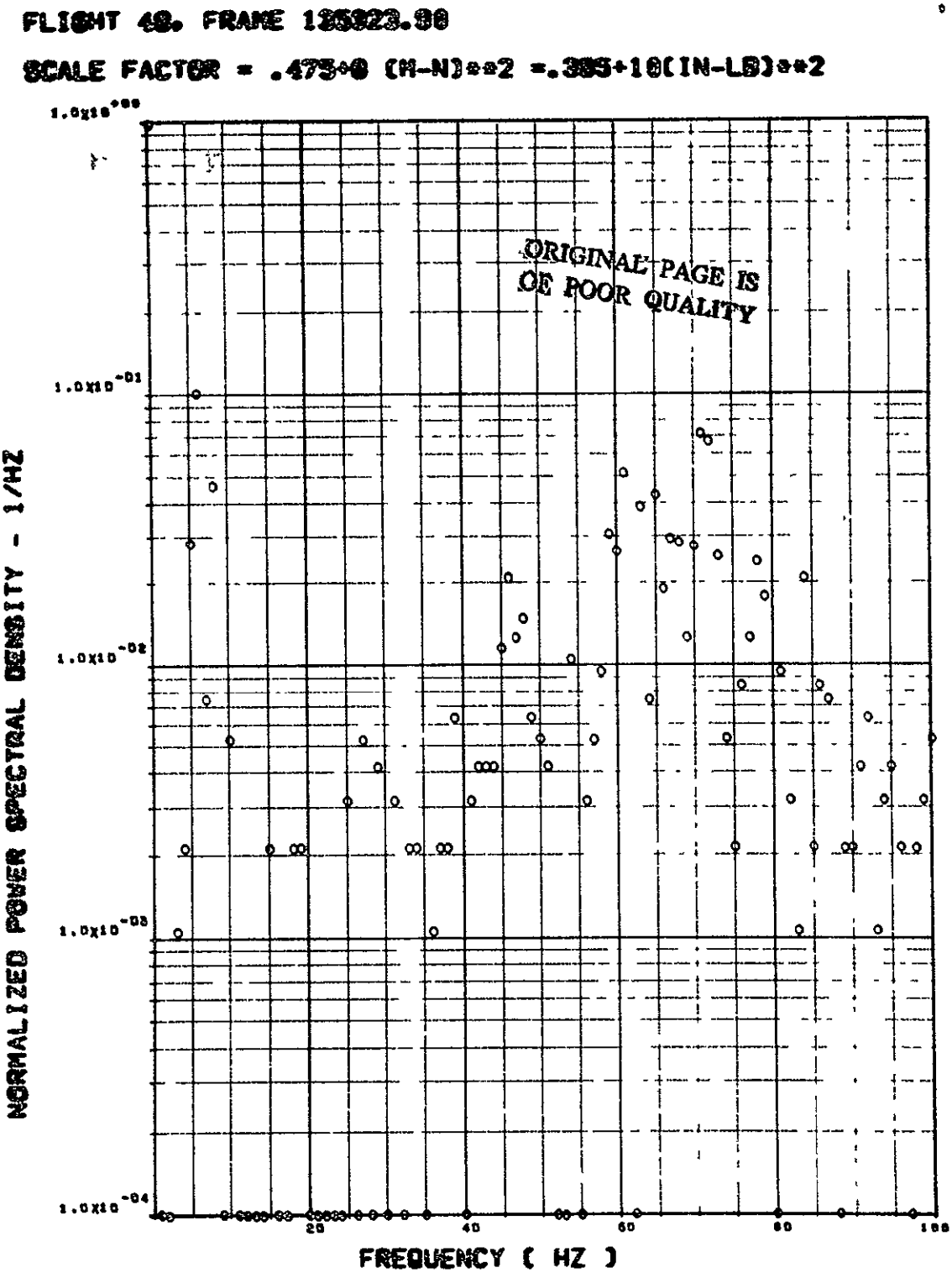

Figure 19. Continued

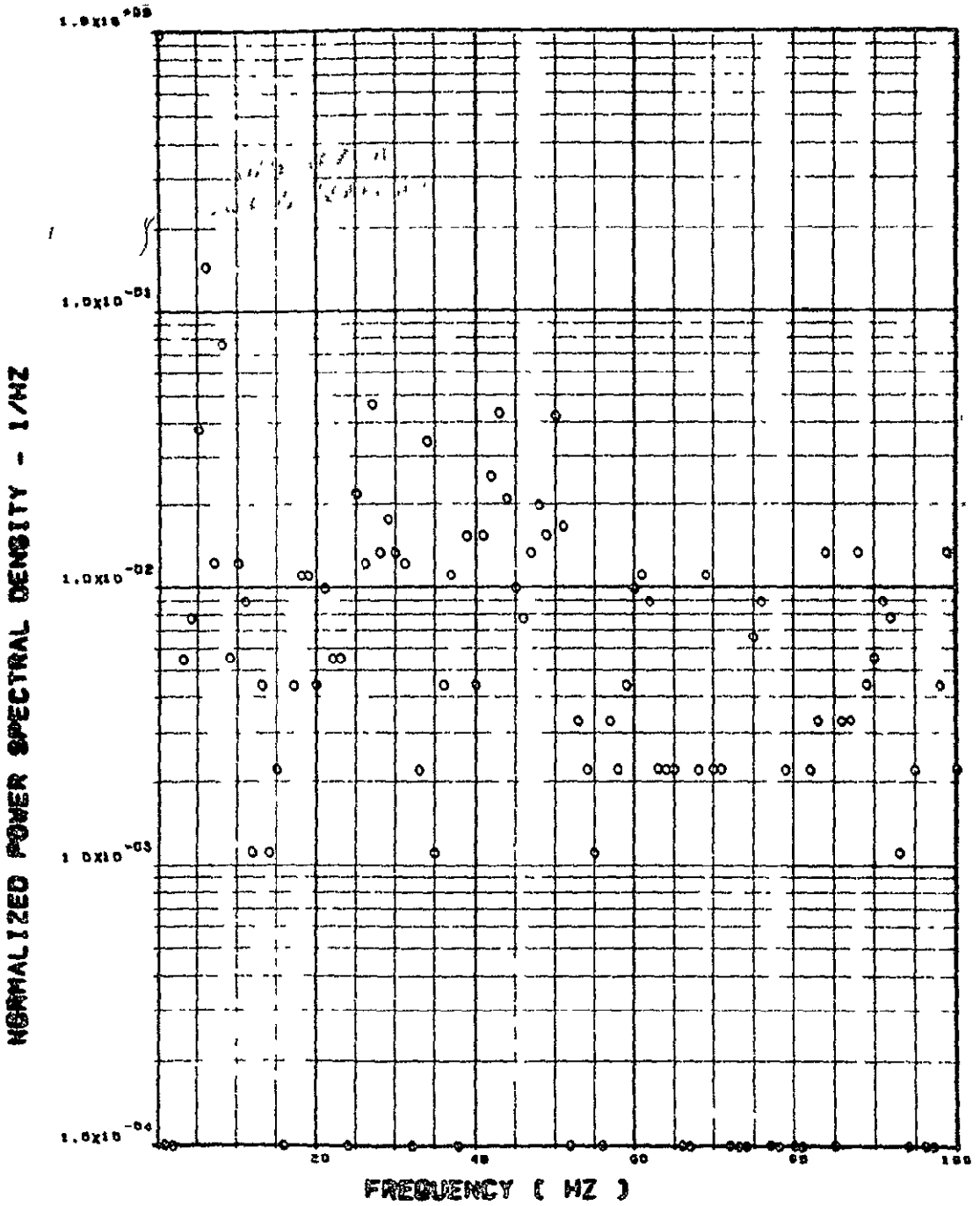

Figure 19. Continued

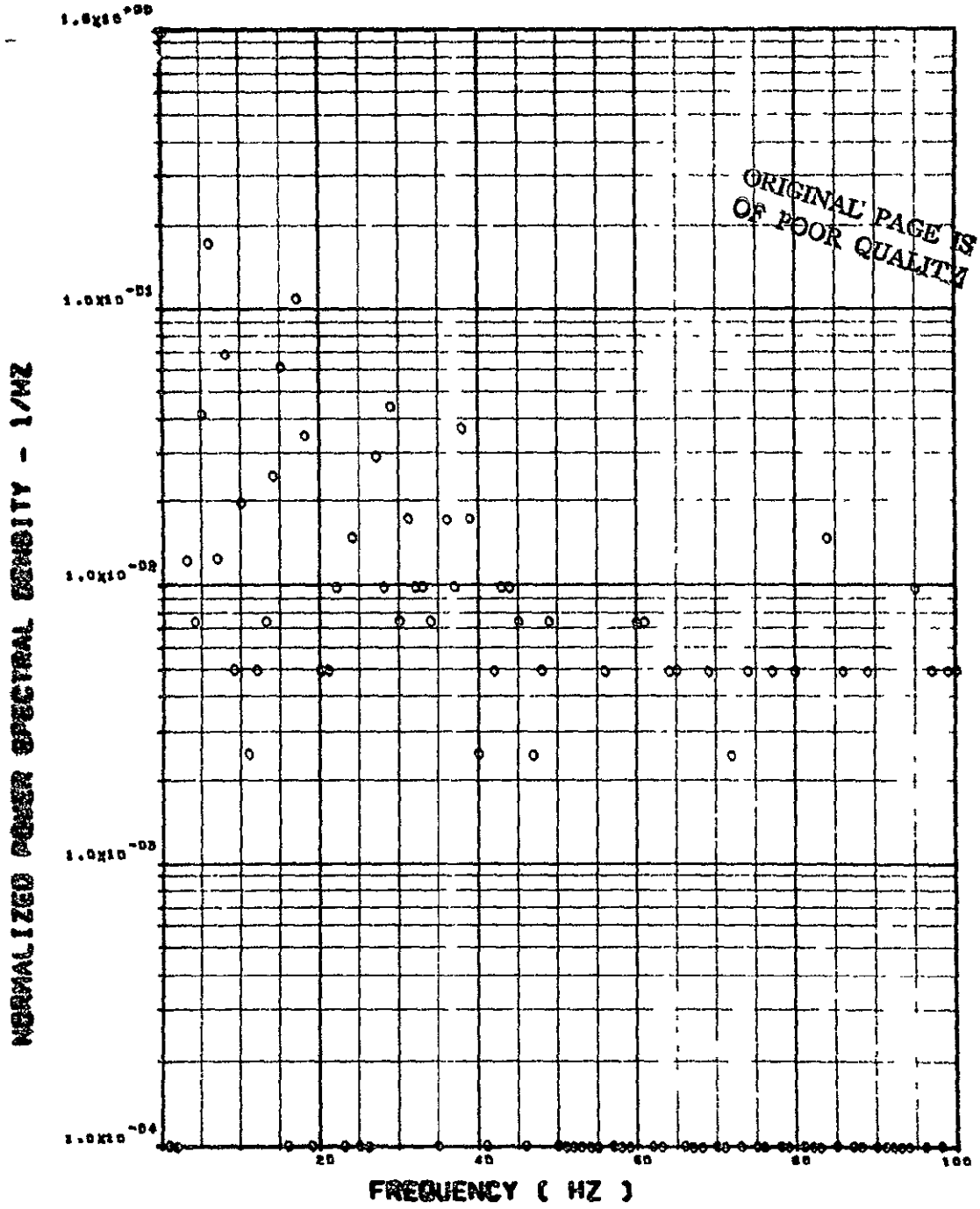

Figure 19. Continued

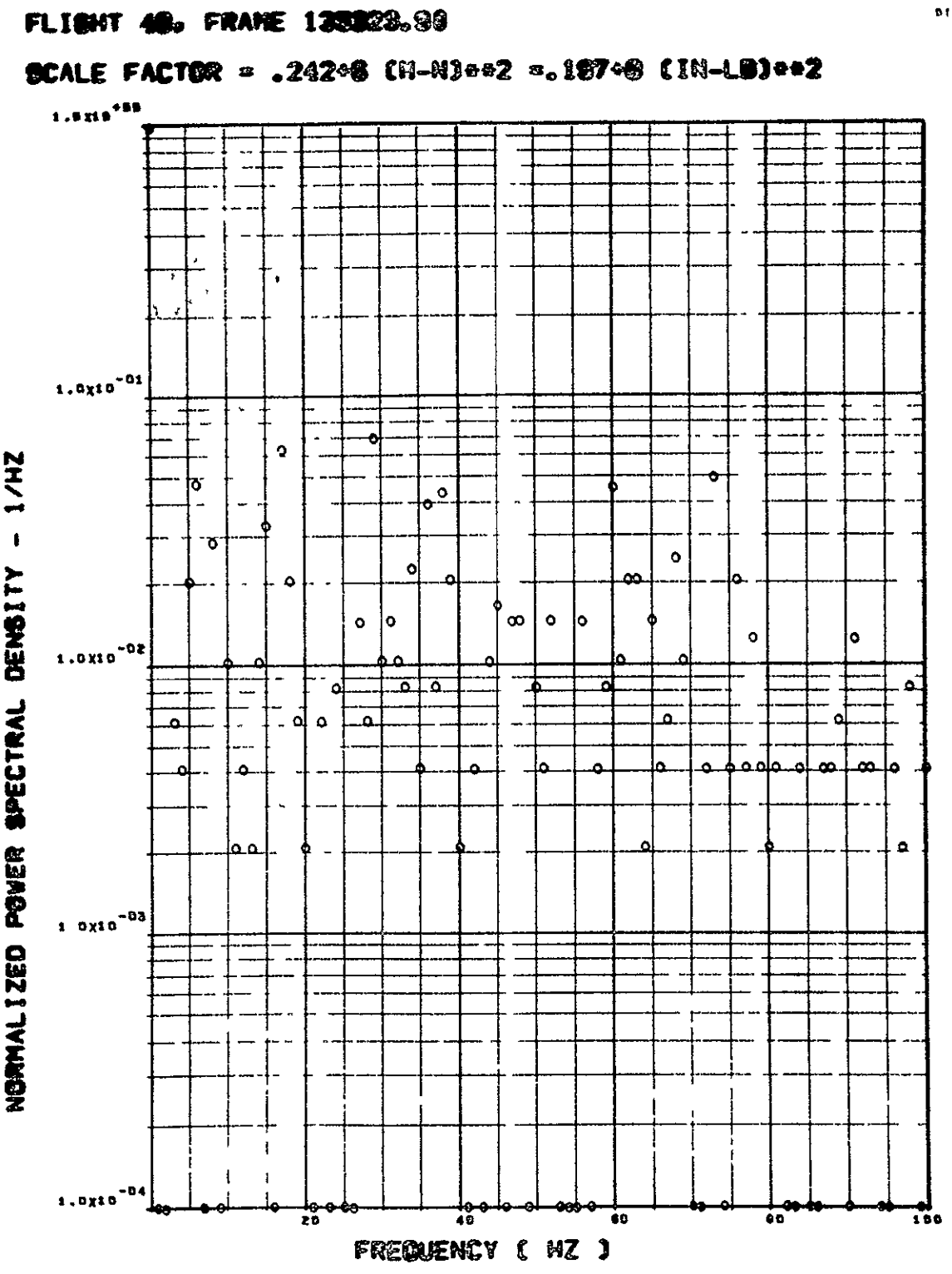

Figure 19. Continued

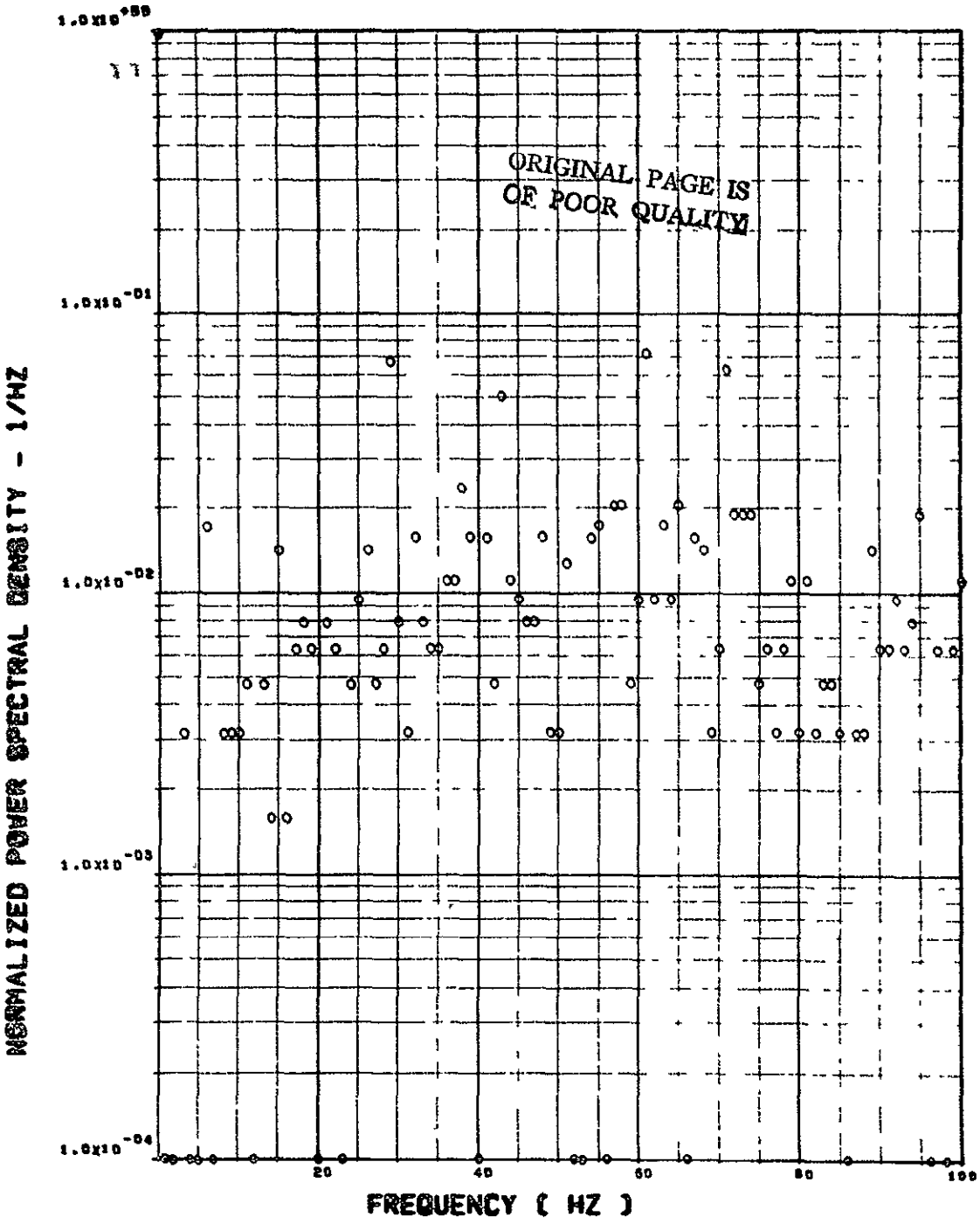

Figure 19. Continued

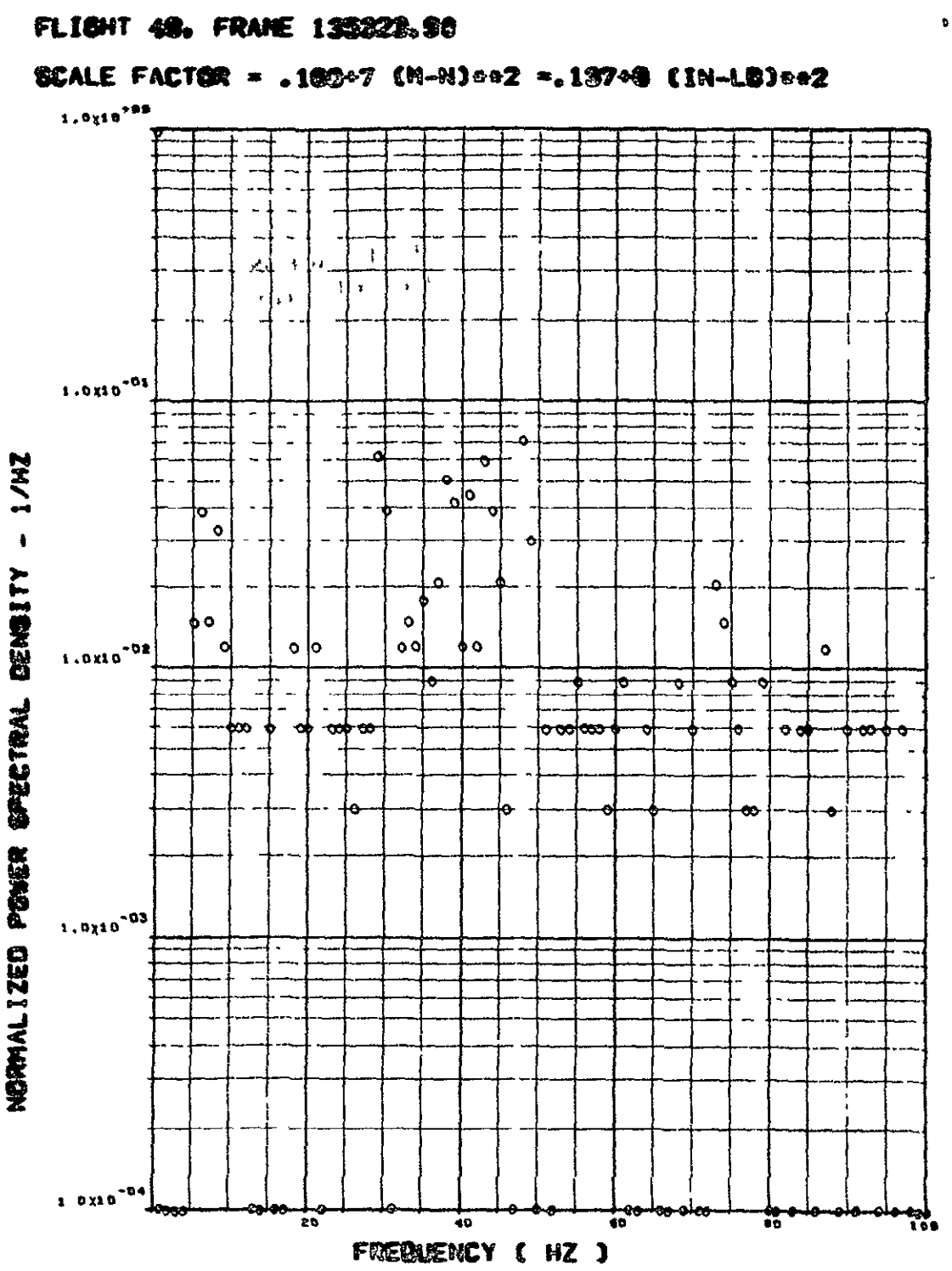

Figure 19. Continued

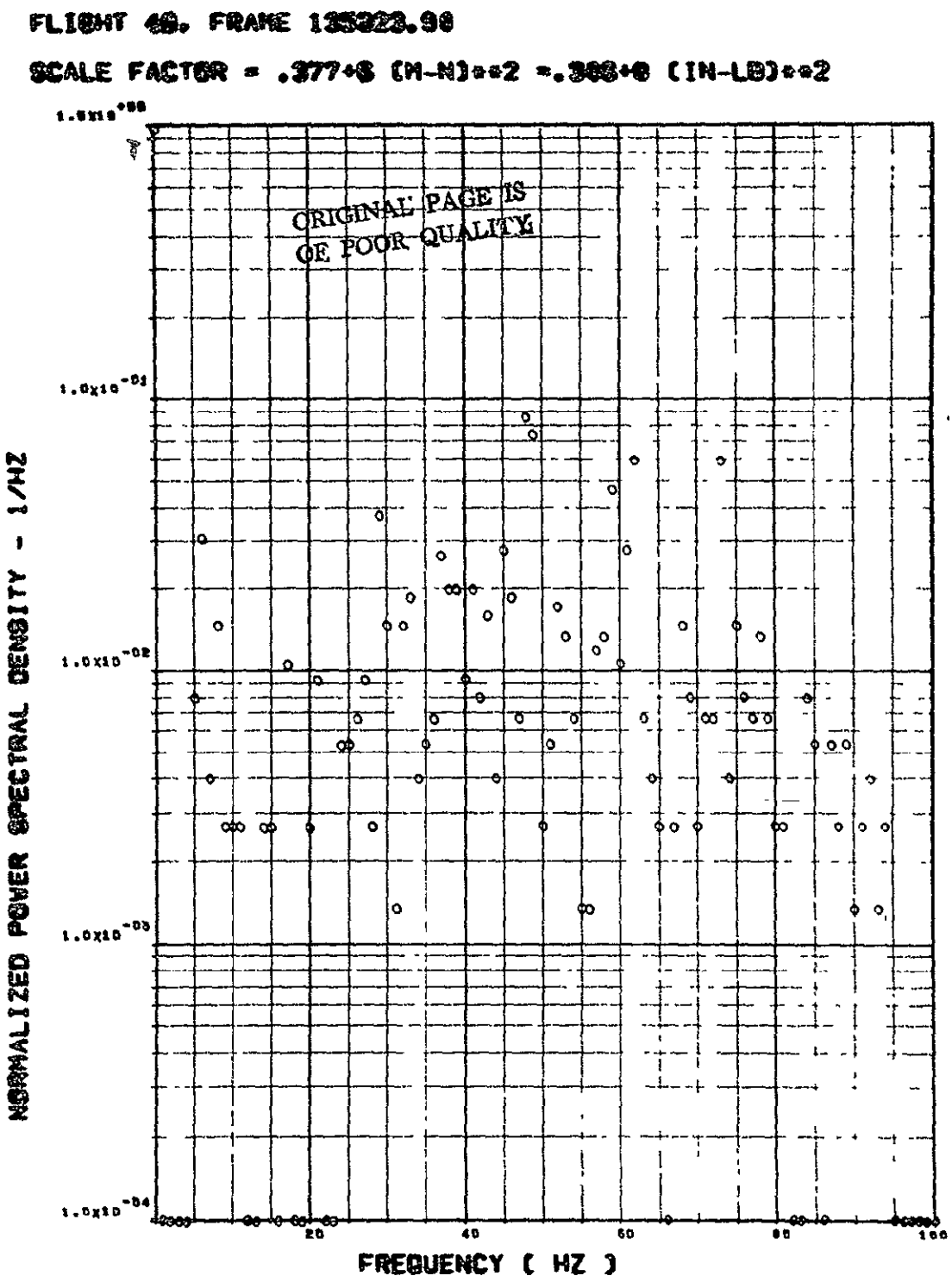

Figure 19. Continued

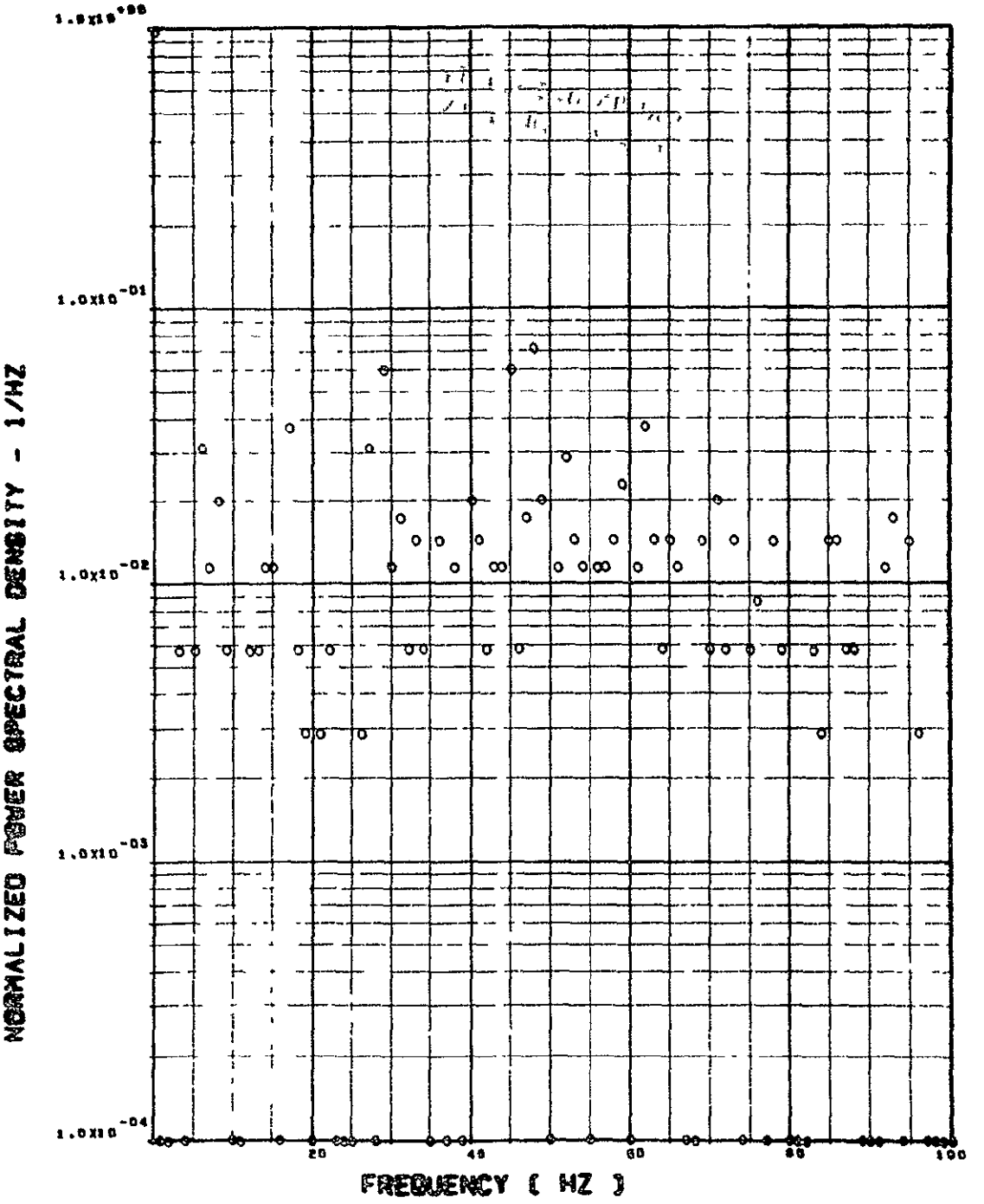

Figure 19. Continued

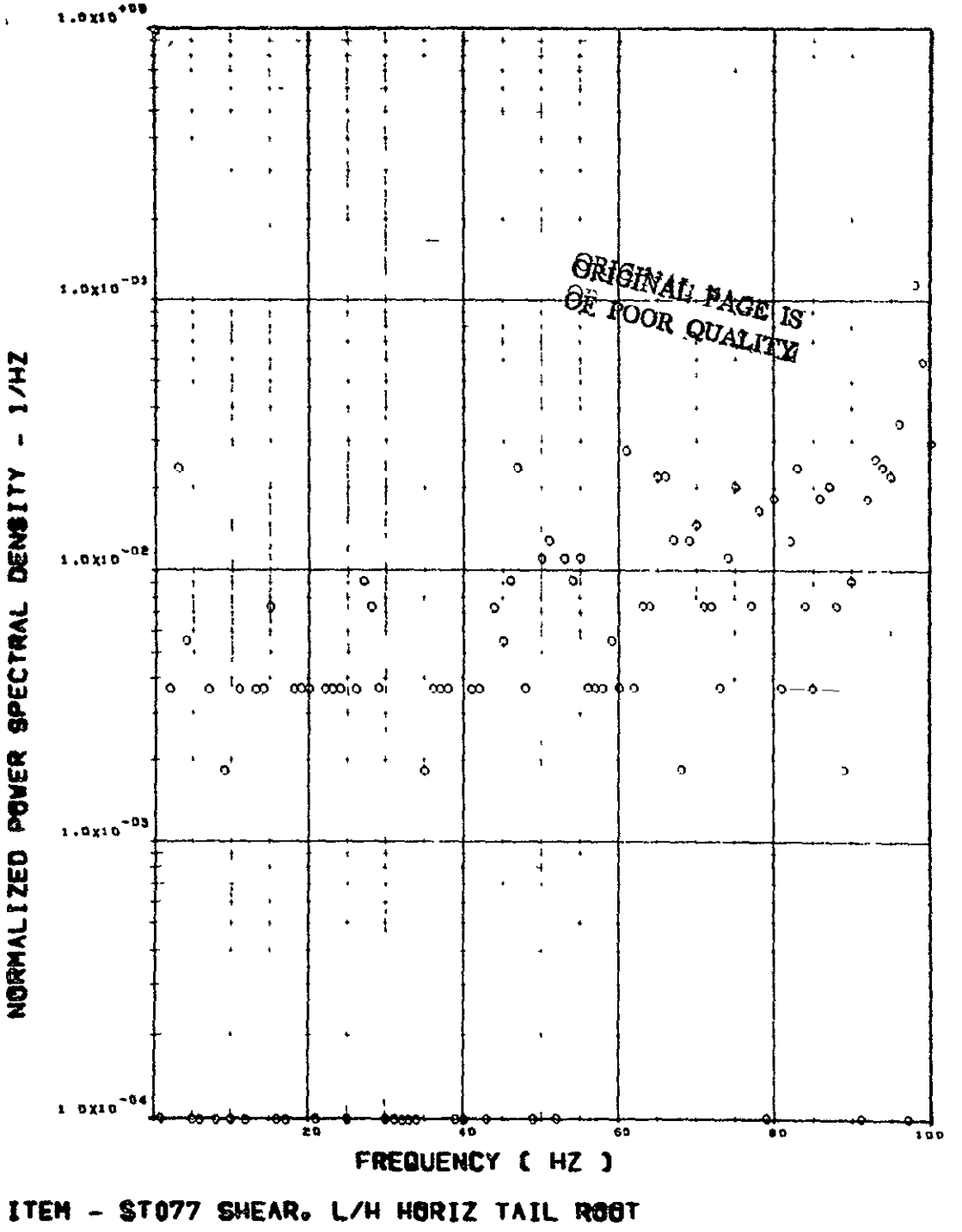

Figure 19. Continued

FLIGHT 48. FRAME 135323.98. RECORD LENGTH = 1 SEC

SCALE FACTOR = .201+7 (N)**2 =.142+8 (LB)**2

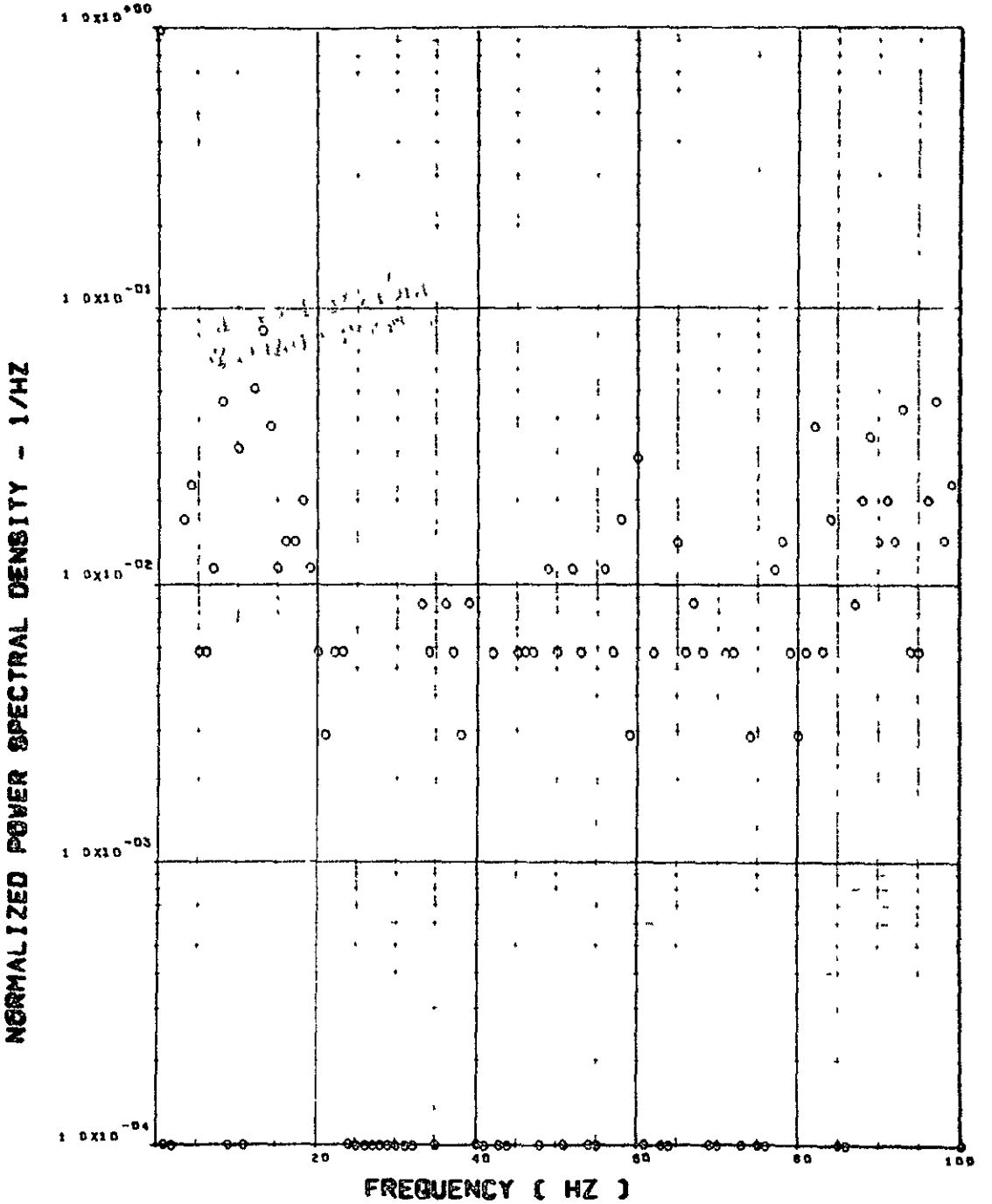

ITEM - ST072 SHEAR. R/H HORIZ TAIL ROOT

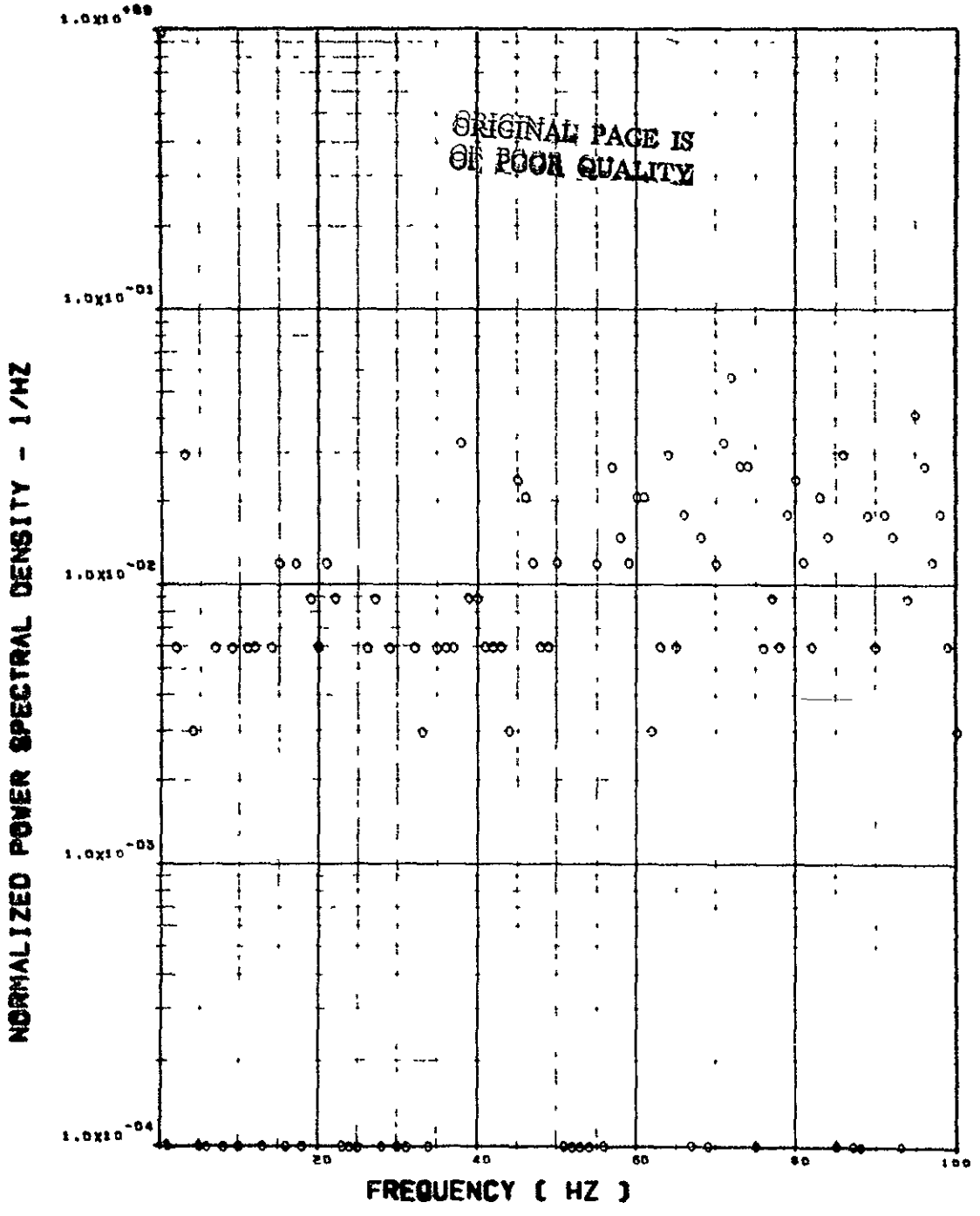

Figure 19. Continued

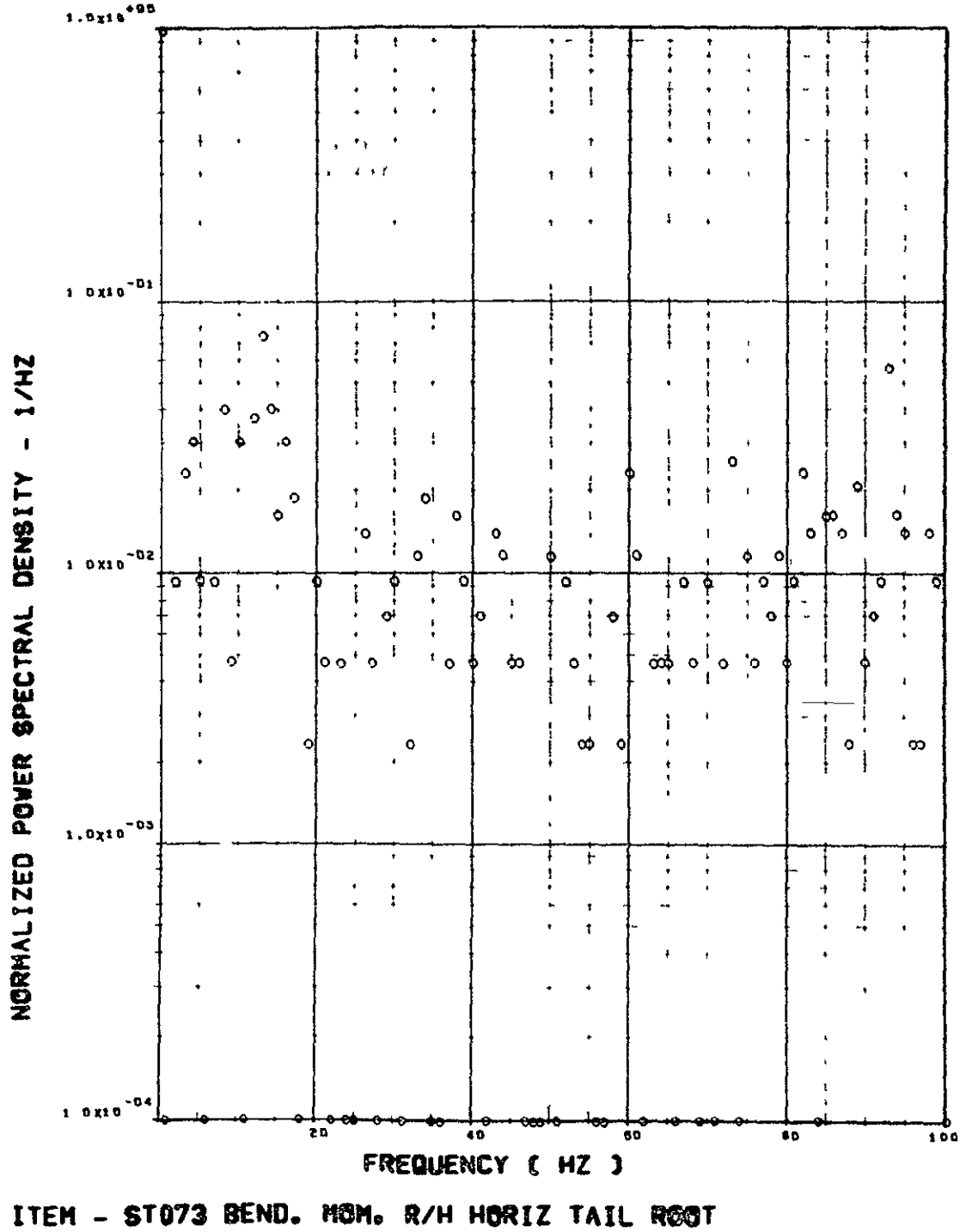

Figure 19. Continued

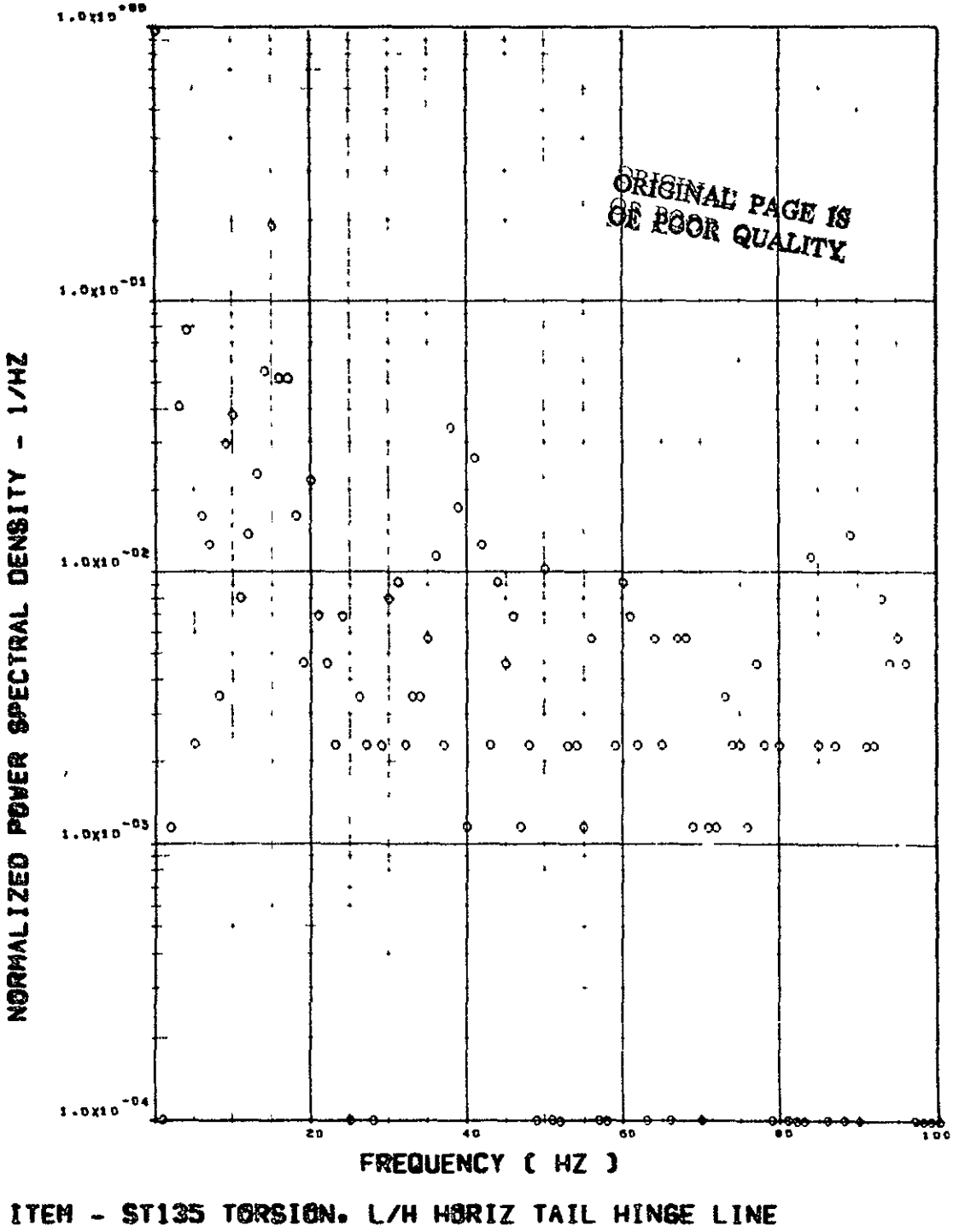

Figure 19. Continued

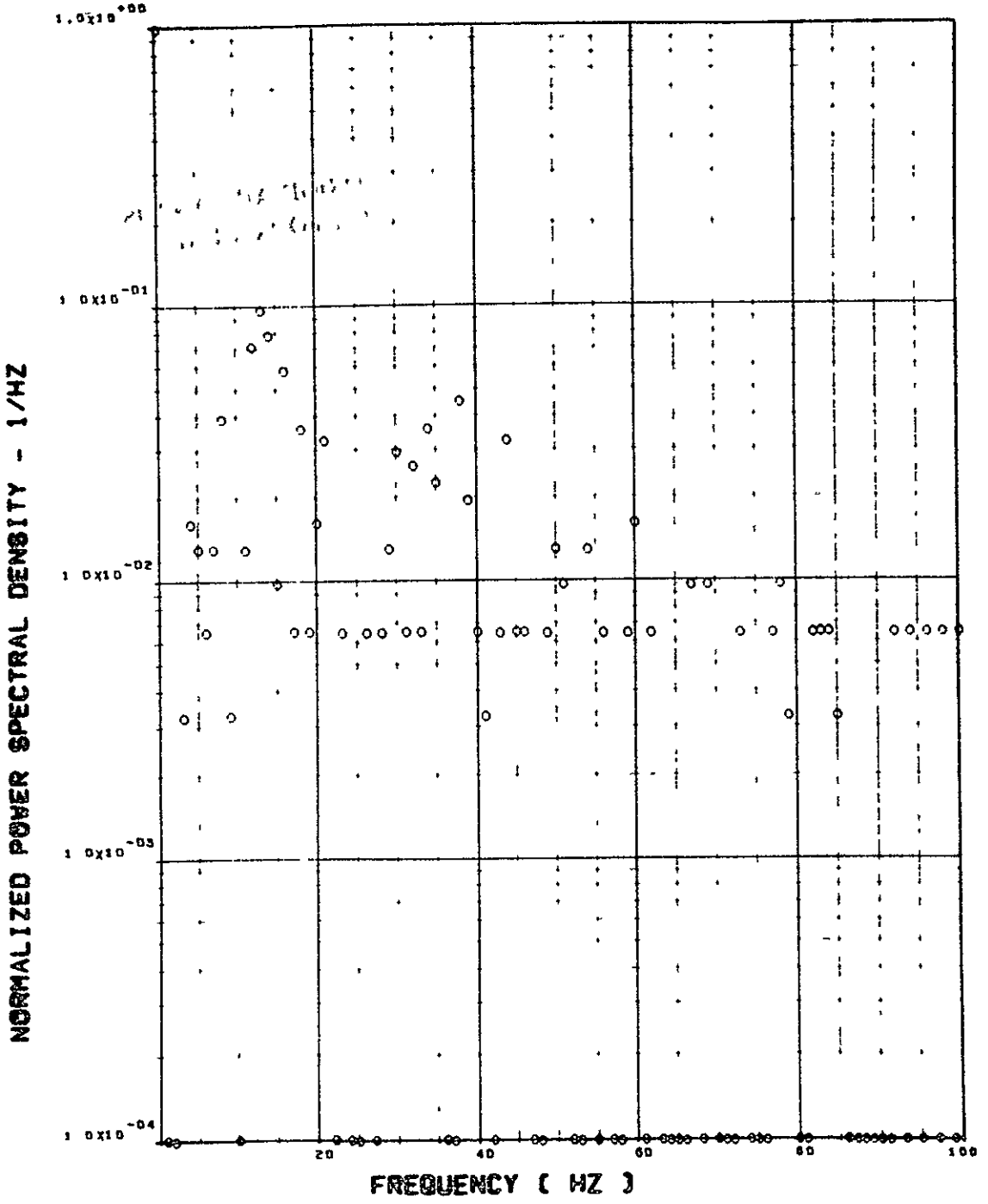

Figure 19. Concluded

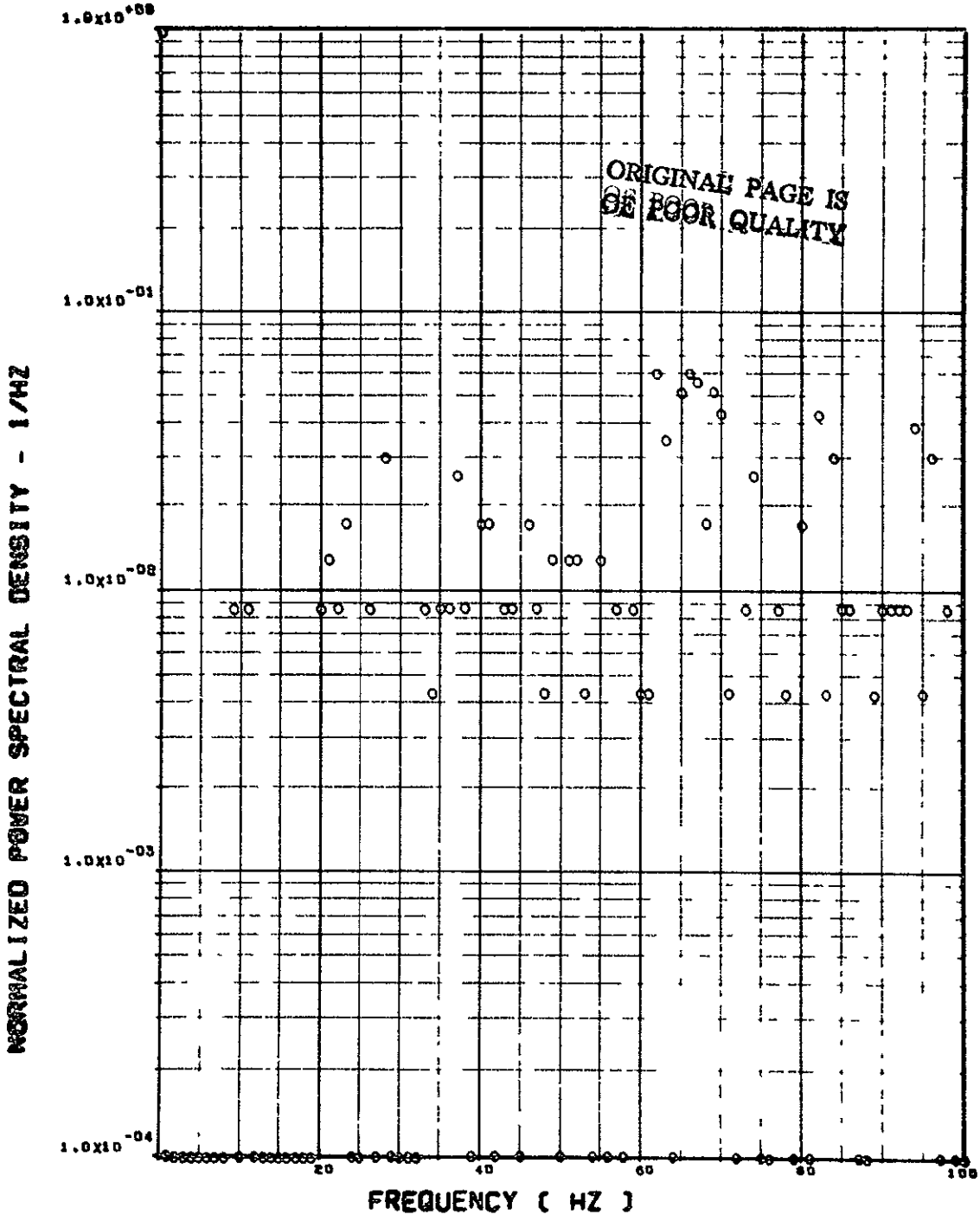

Figure 20. Power Spectra - Flight 48, Run 7R1, Point 1 T_1 = 135951.7, ΔT = 1 Sec, α_{Nom} = 8.00 deg, $\Delta\alpha$= 1.50 deg

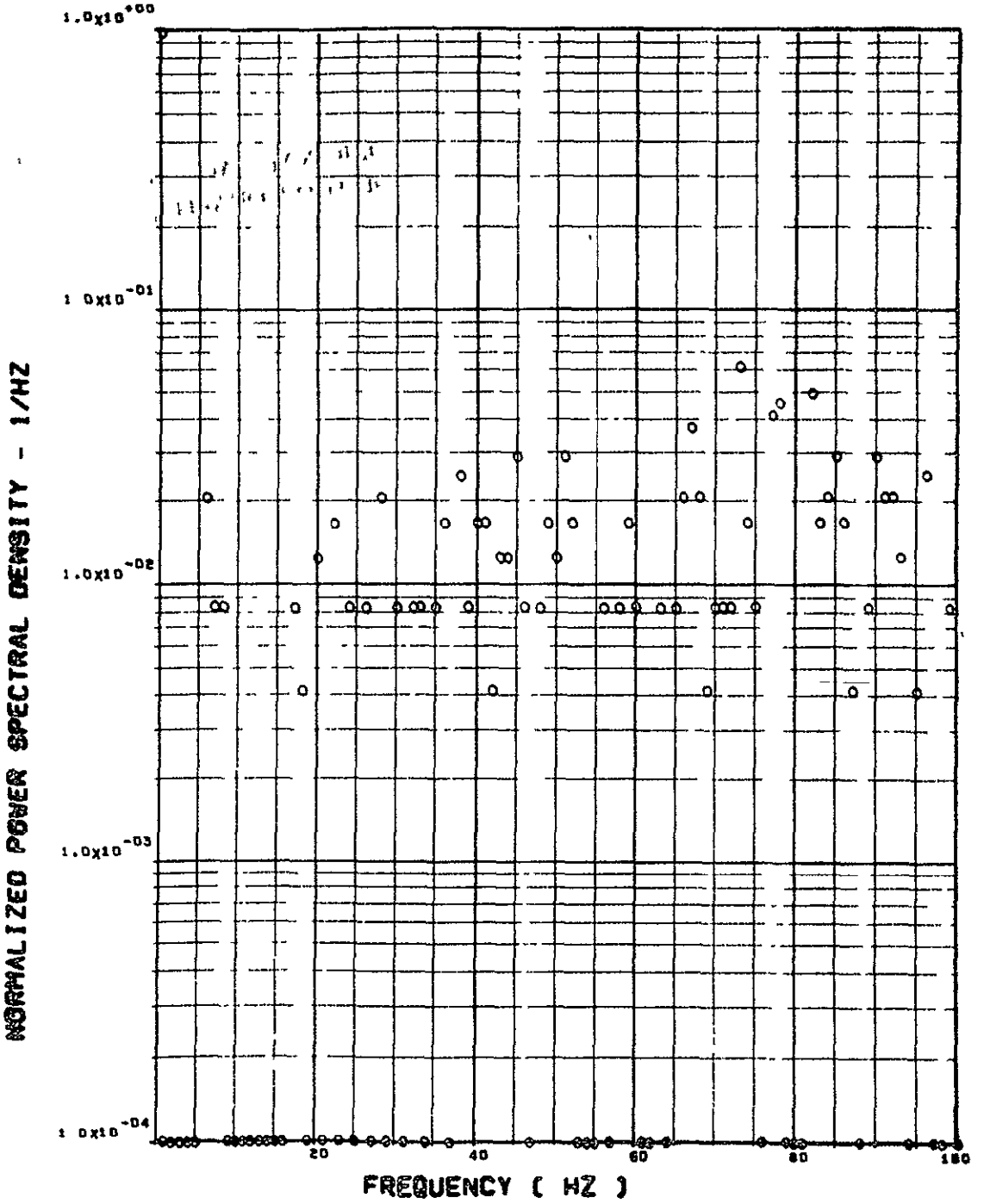

Figure 20. Continued

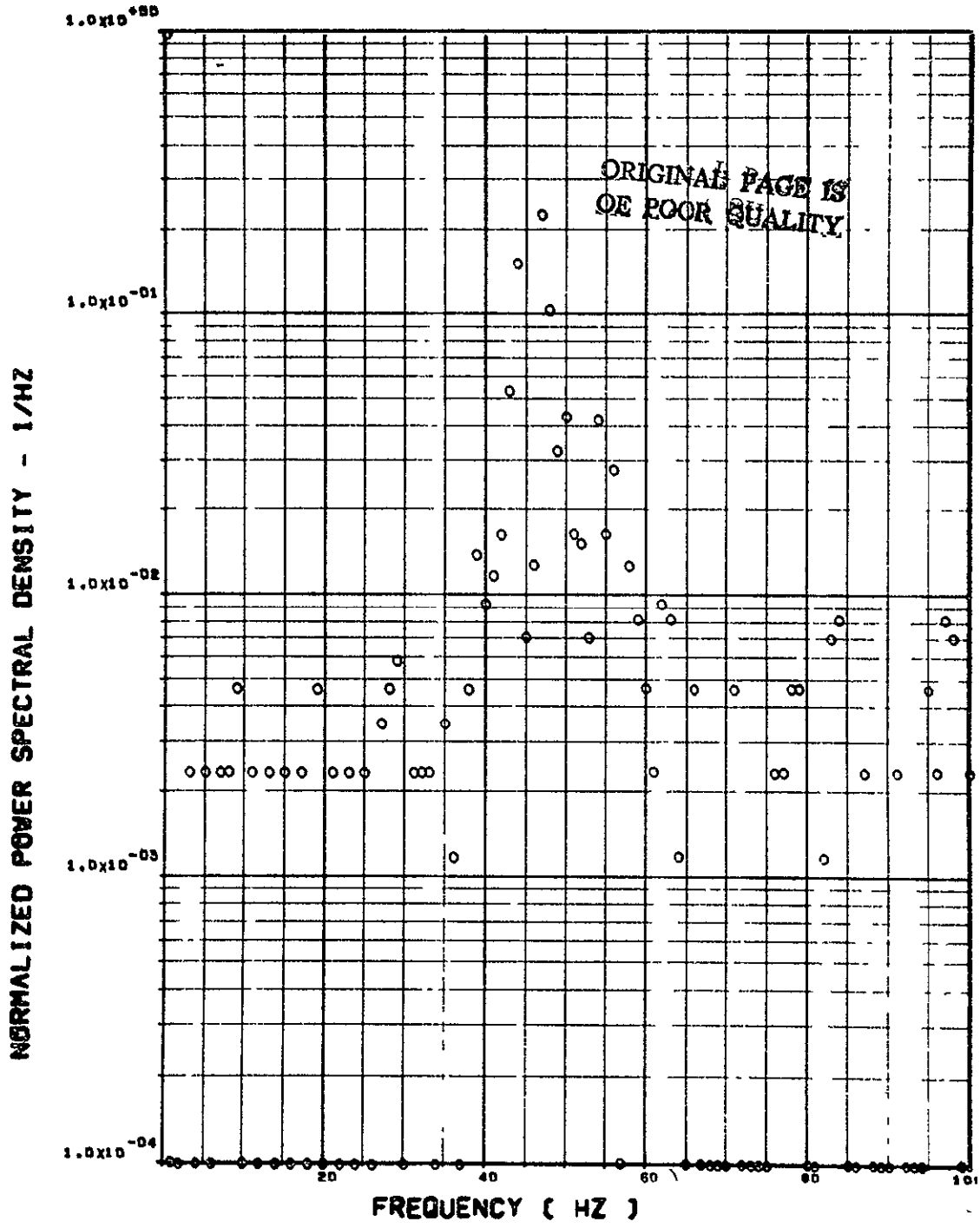

Figure 20. Continued

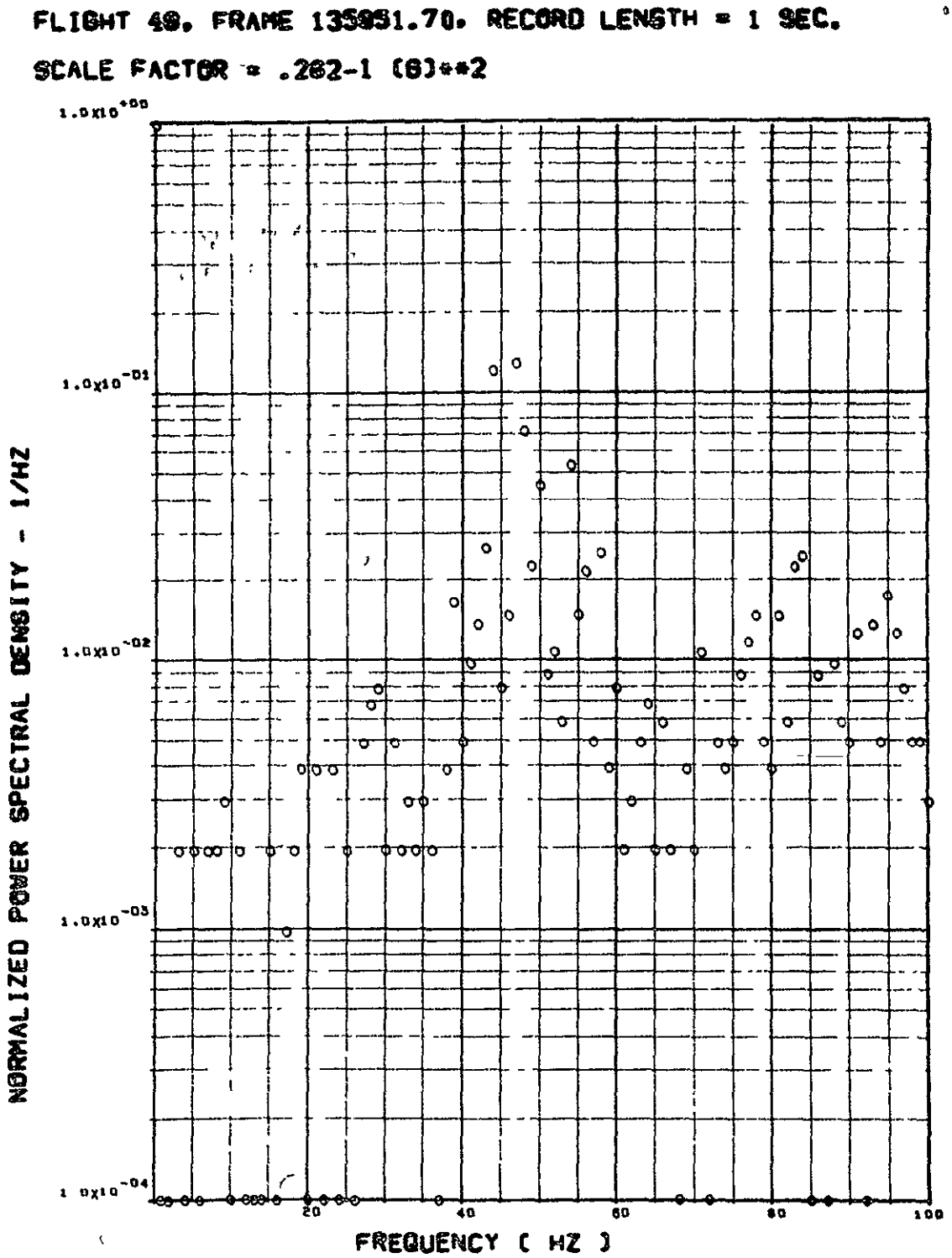

Figure 20. Continued

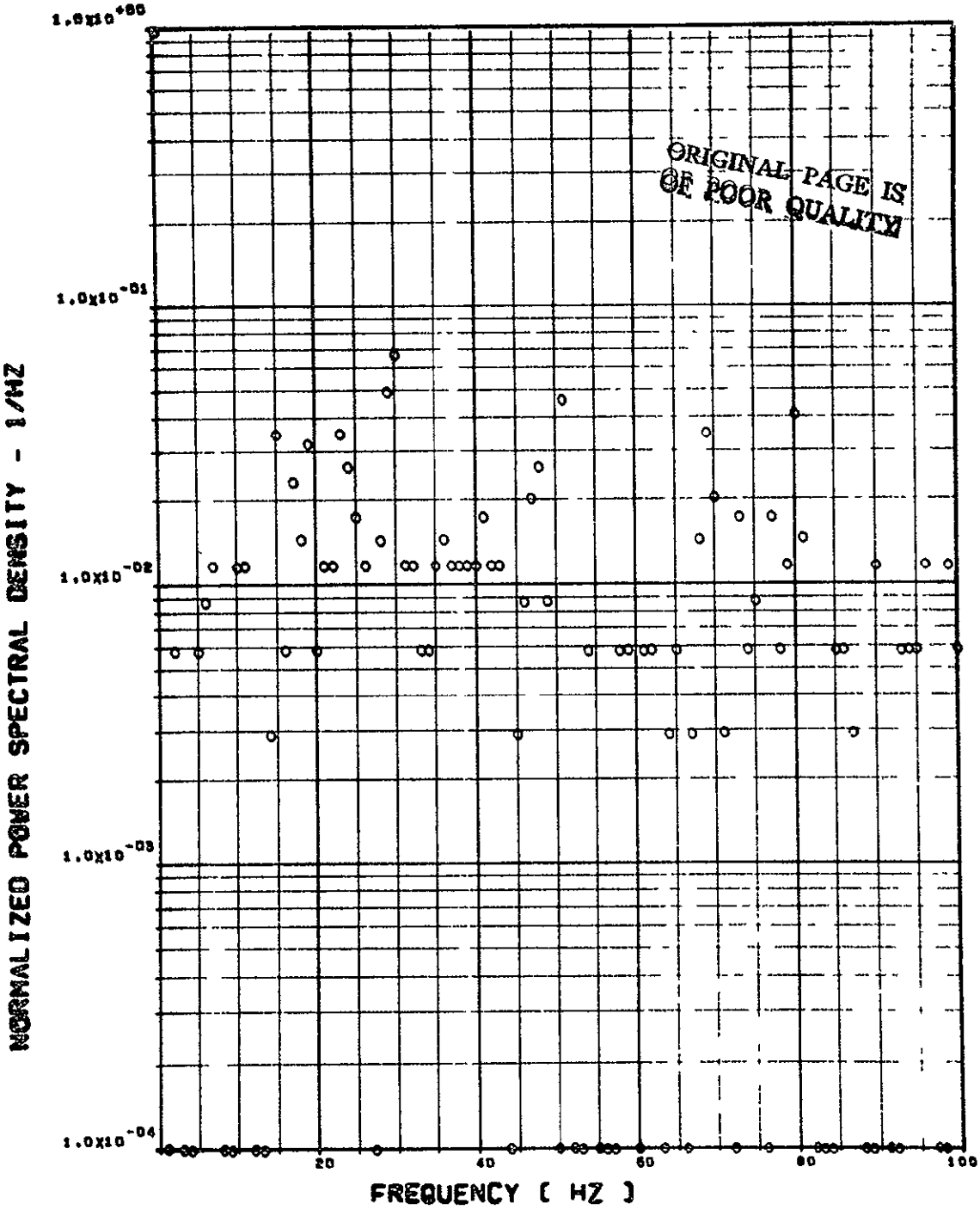

Figure 20. Continued

FLIGHT 48. FRAME 135851.70. RECORD LENGTH = 1 SEC.

SCALE FACTOR = .733-3 (G)**2

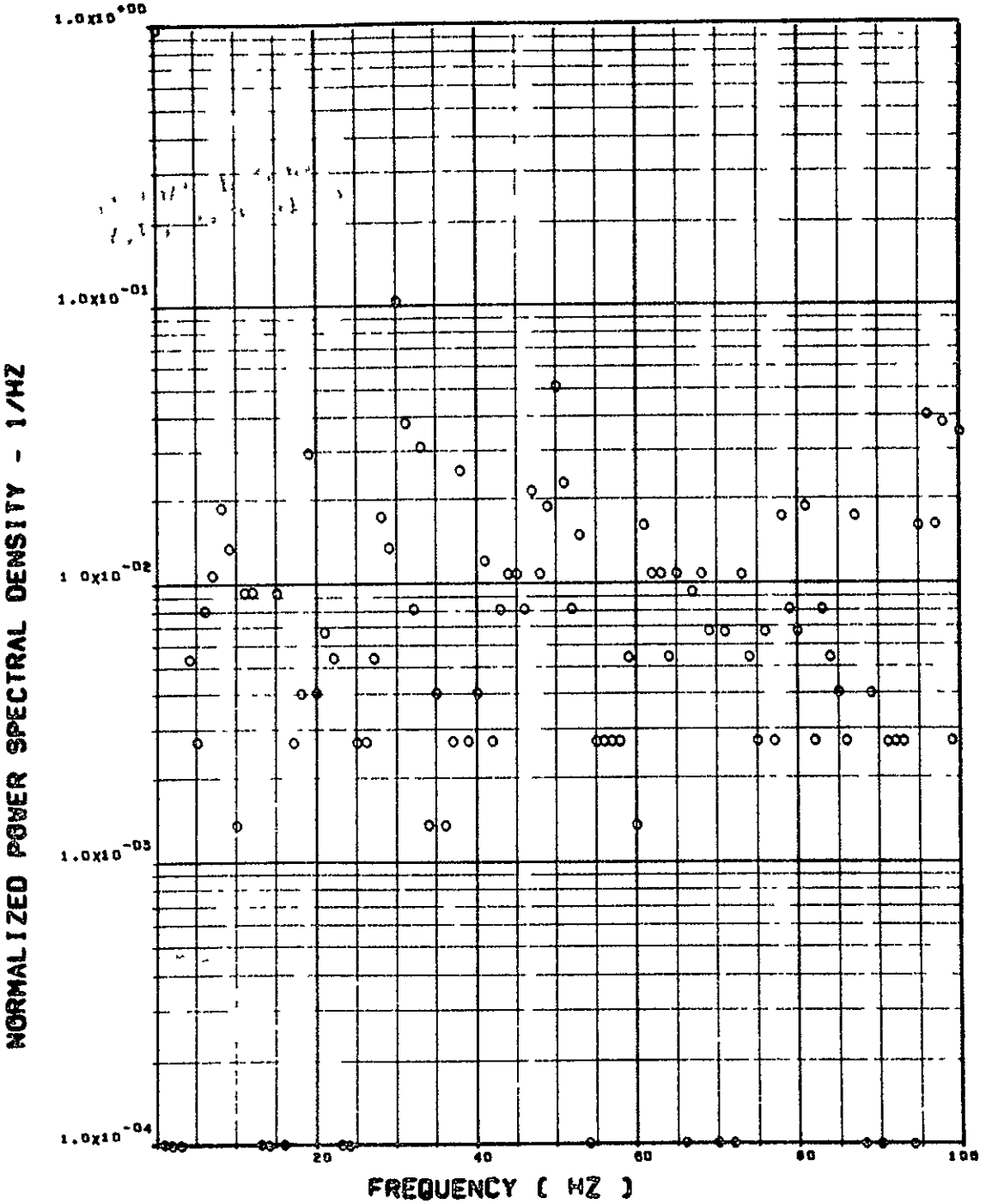

ITEM - AF010 PILOT'S SEAT LATERAL ACCELEROMETER

Figure 20. Continued

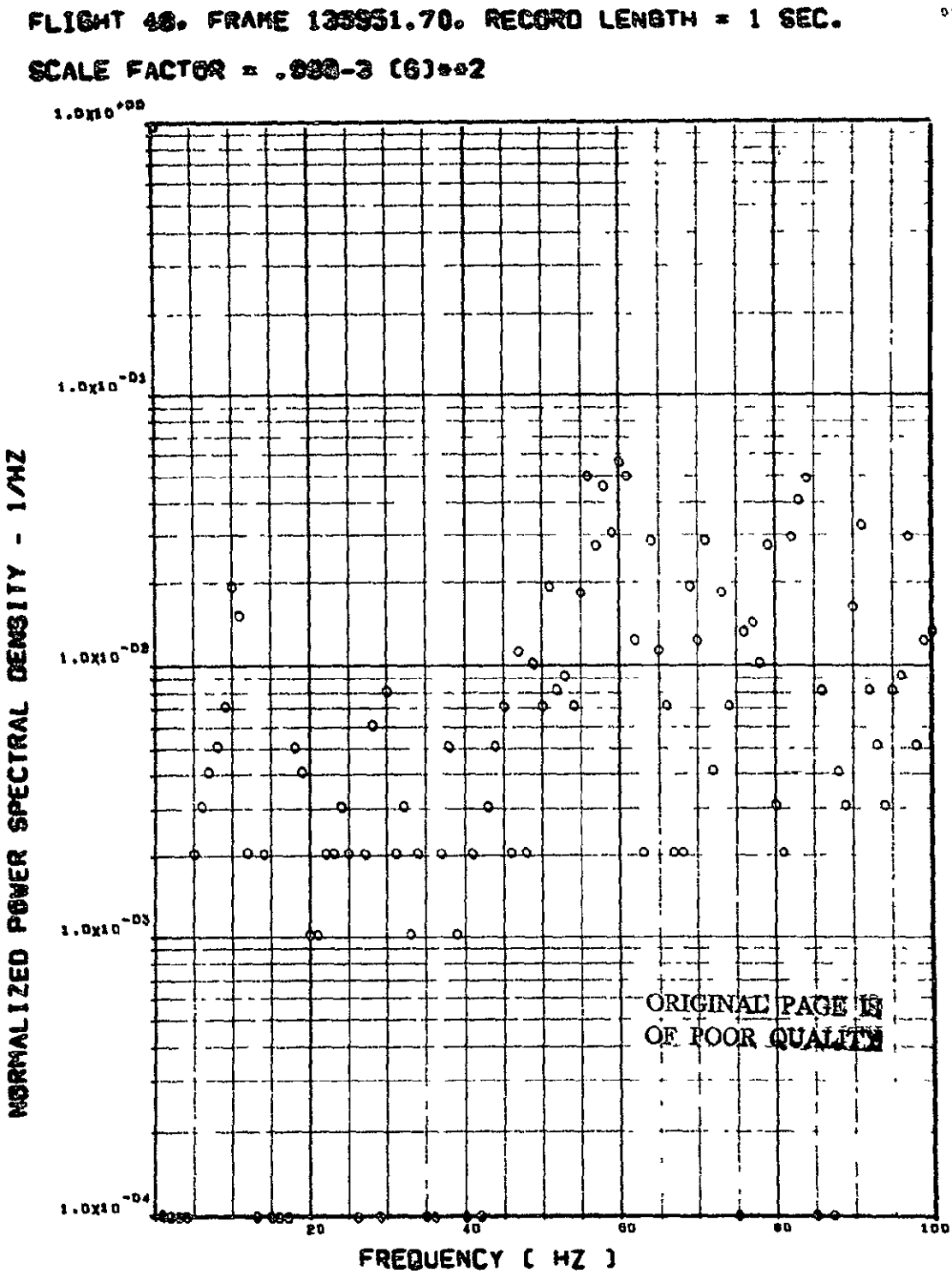

Figure 20. Continued

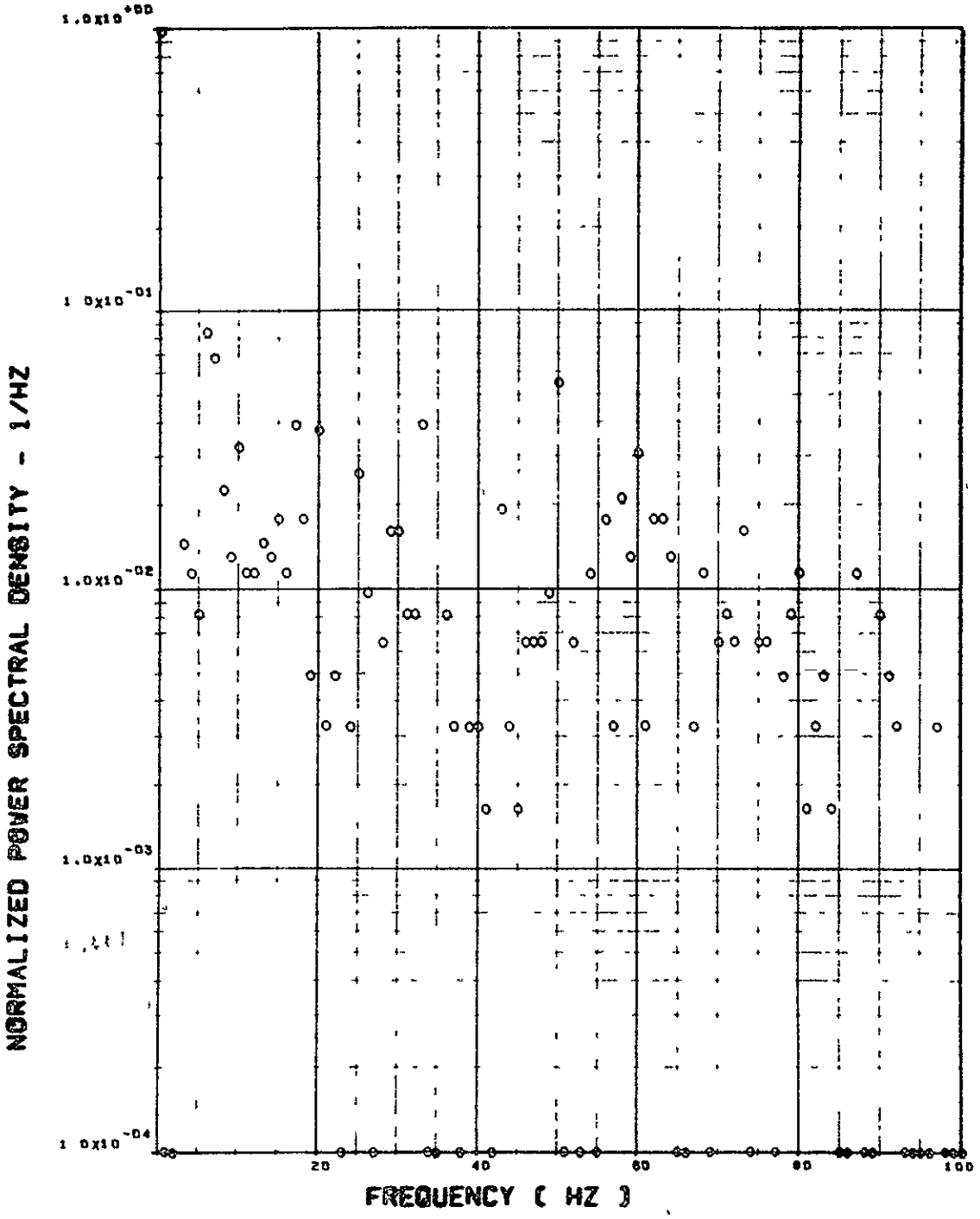

Figure 20. Continued

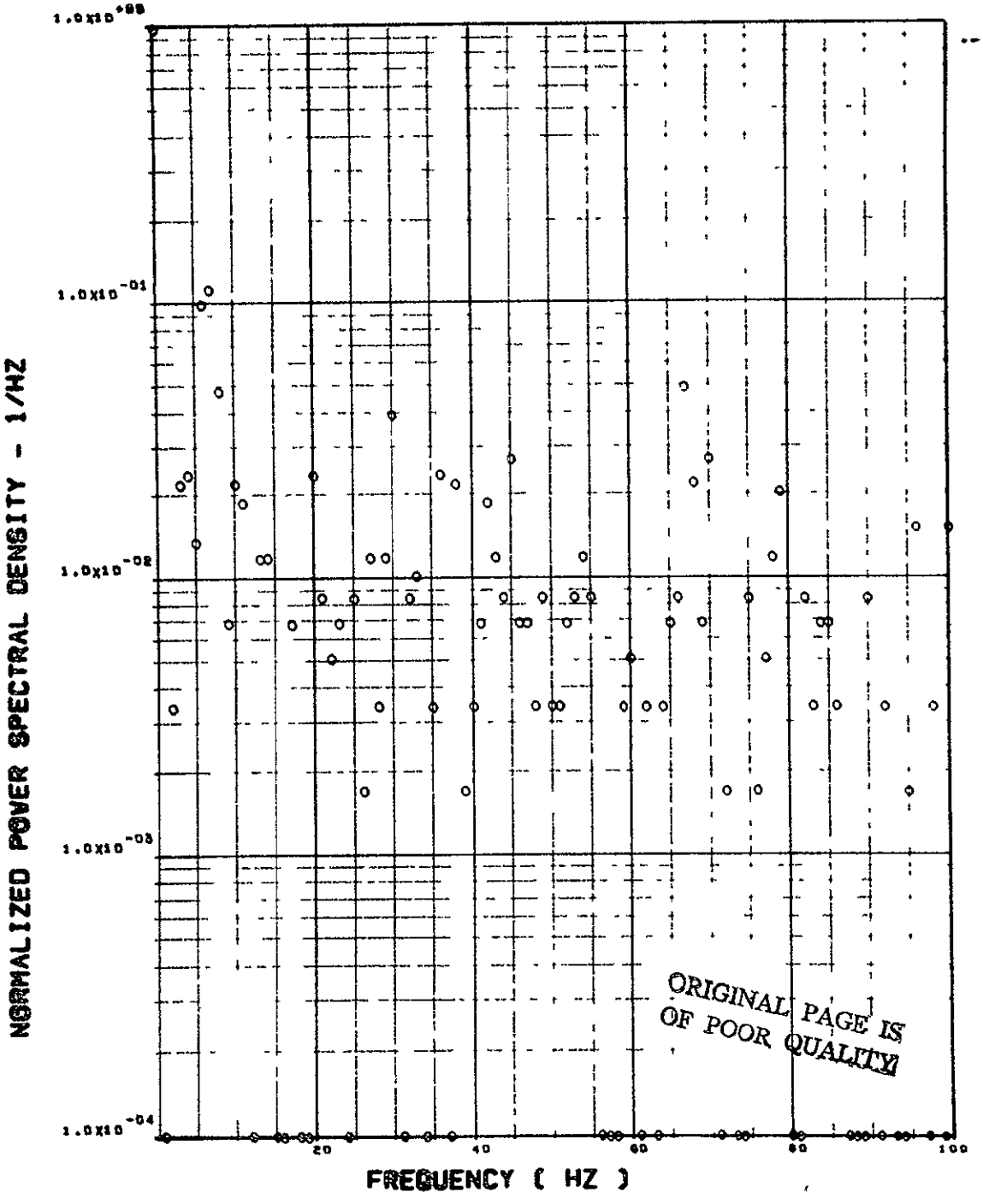

Figure 20. Continued

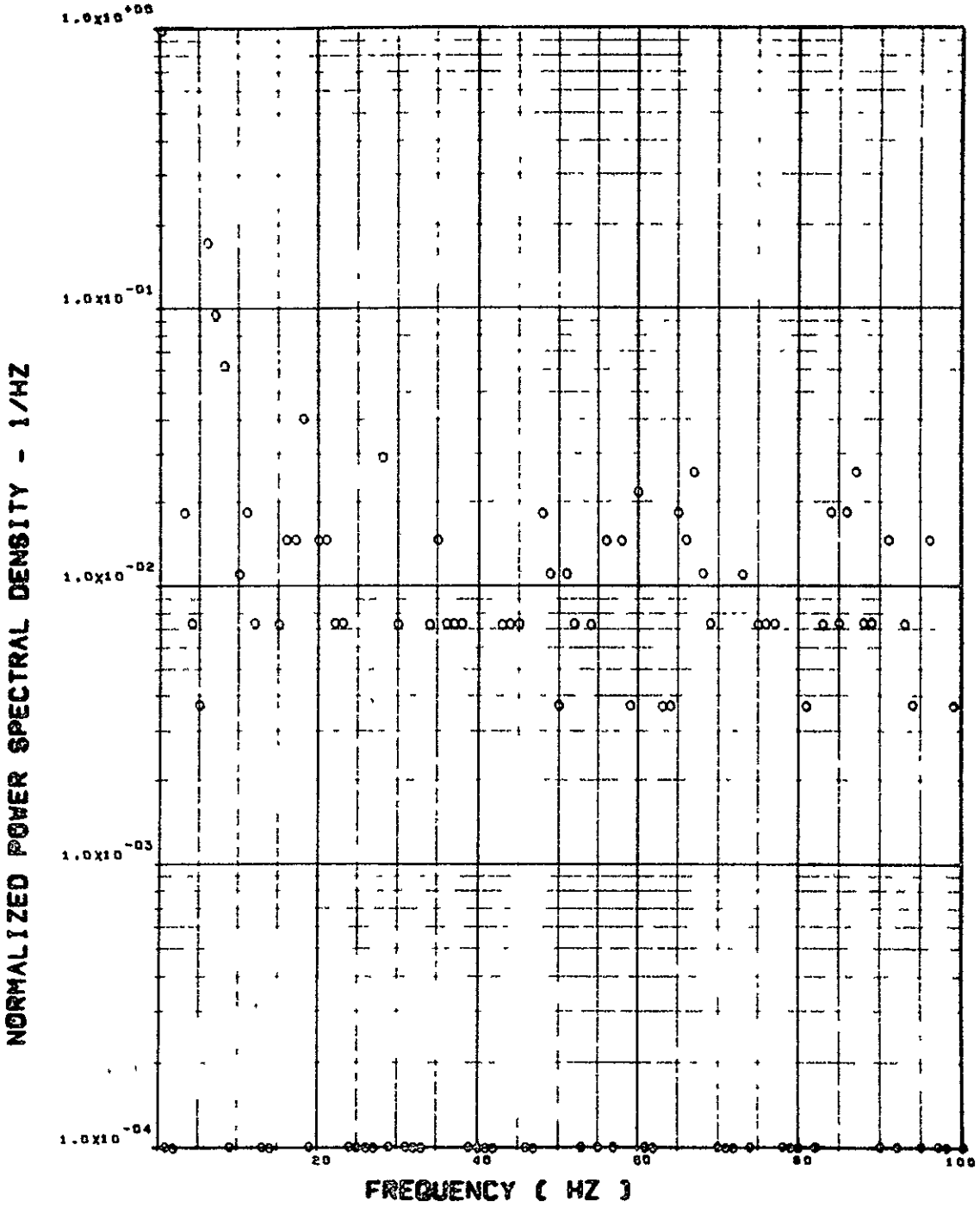

Figure 20. Continued

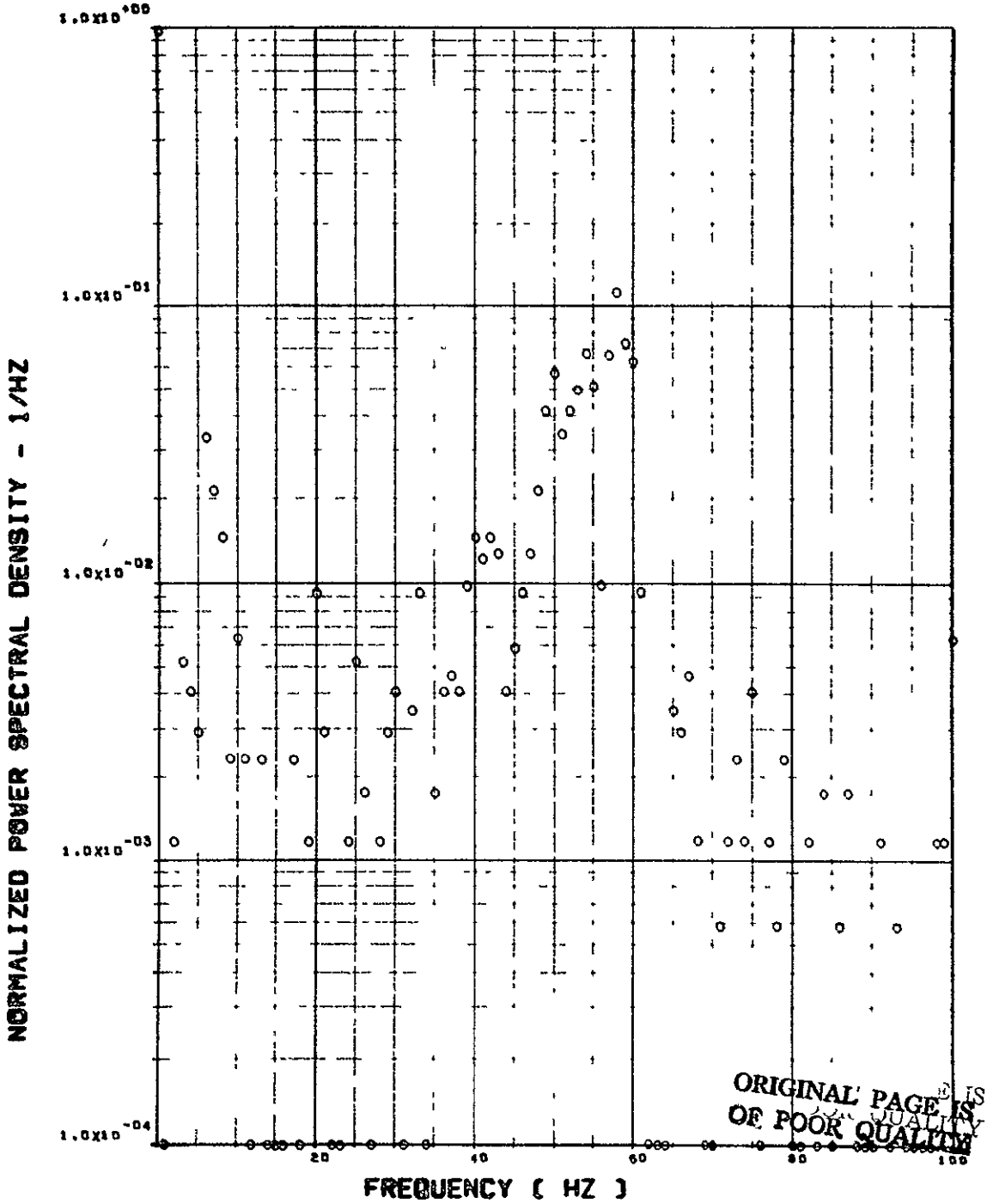

Figure 20. Continued

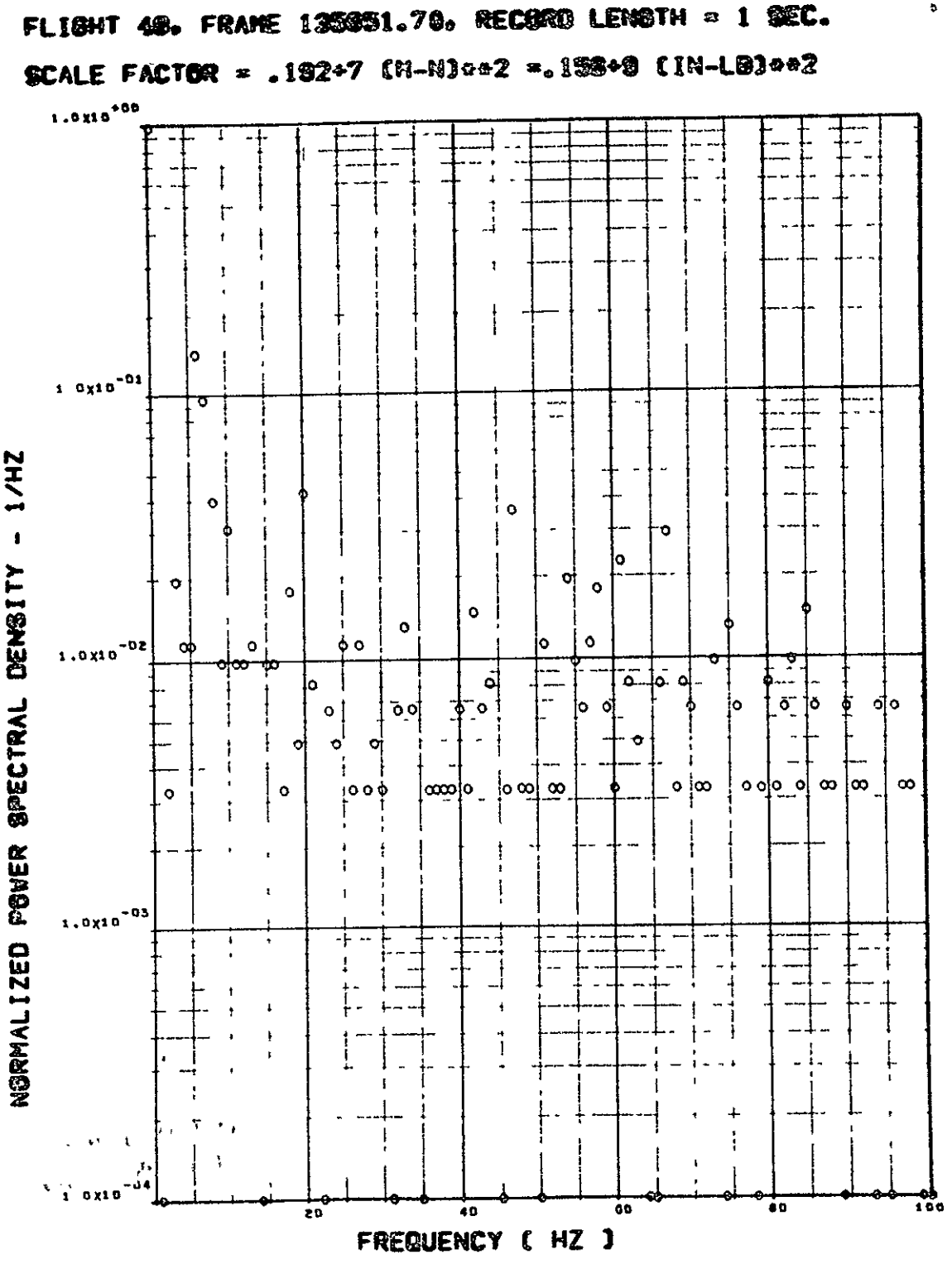

Figure 20. Continued

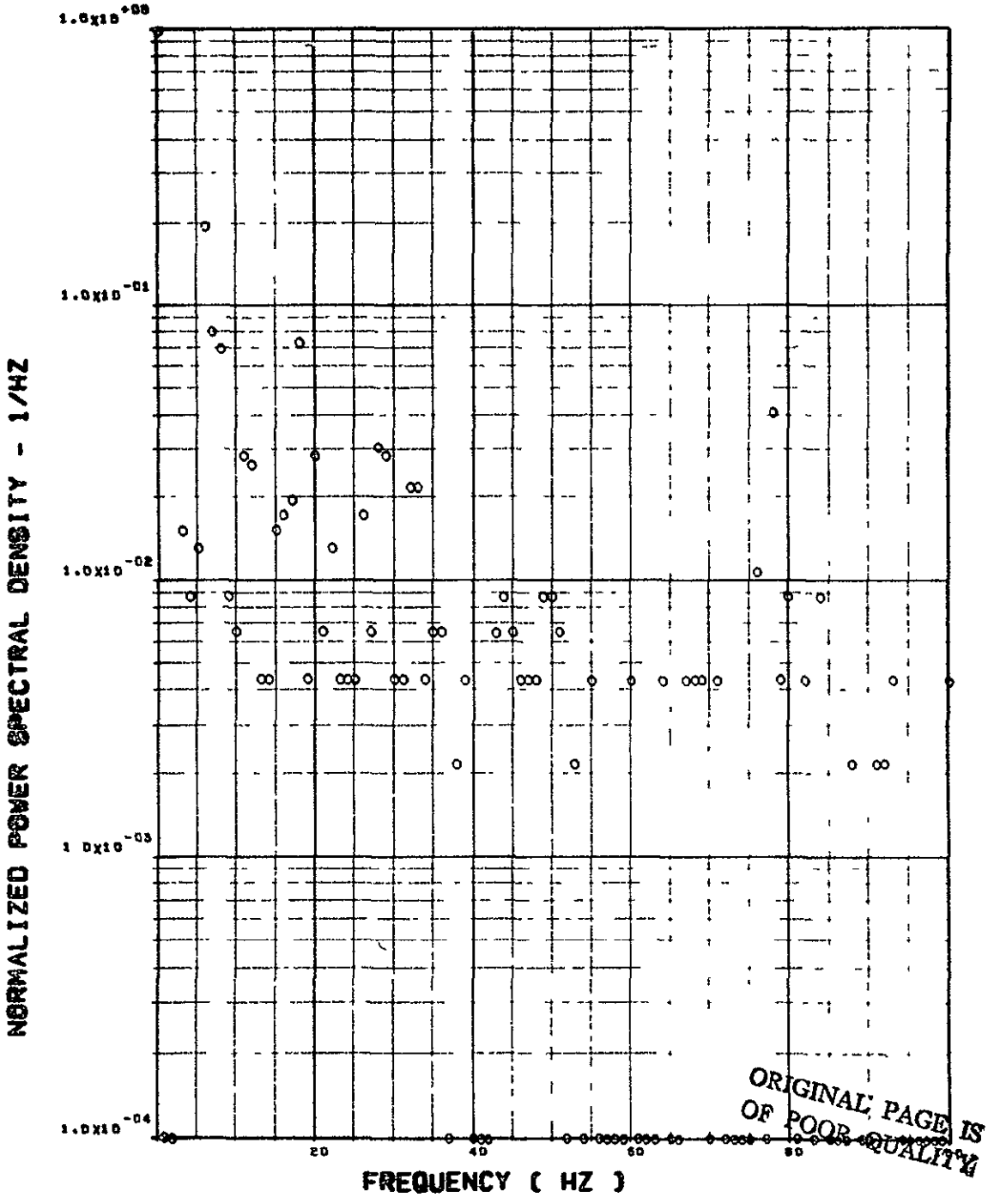

Figure 20. Continued

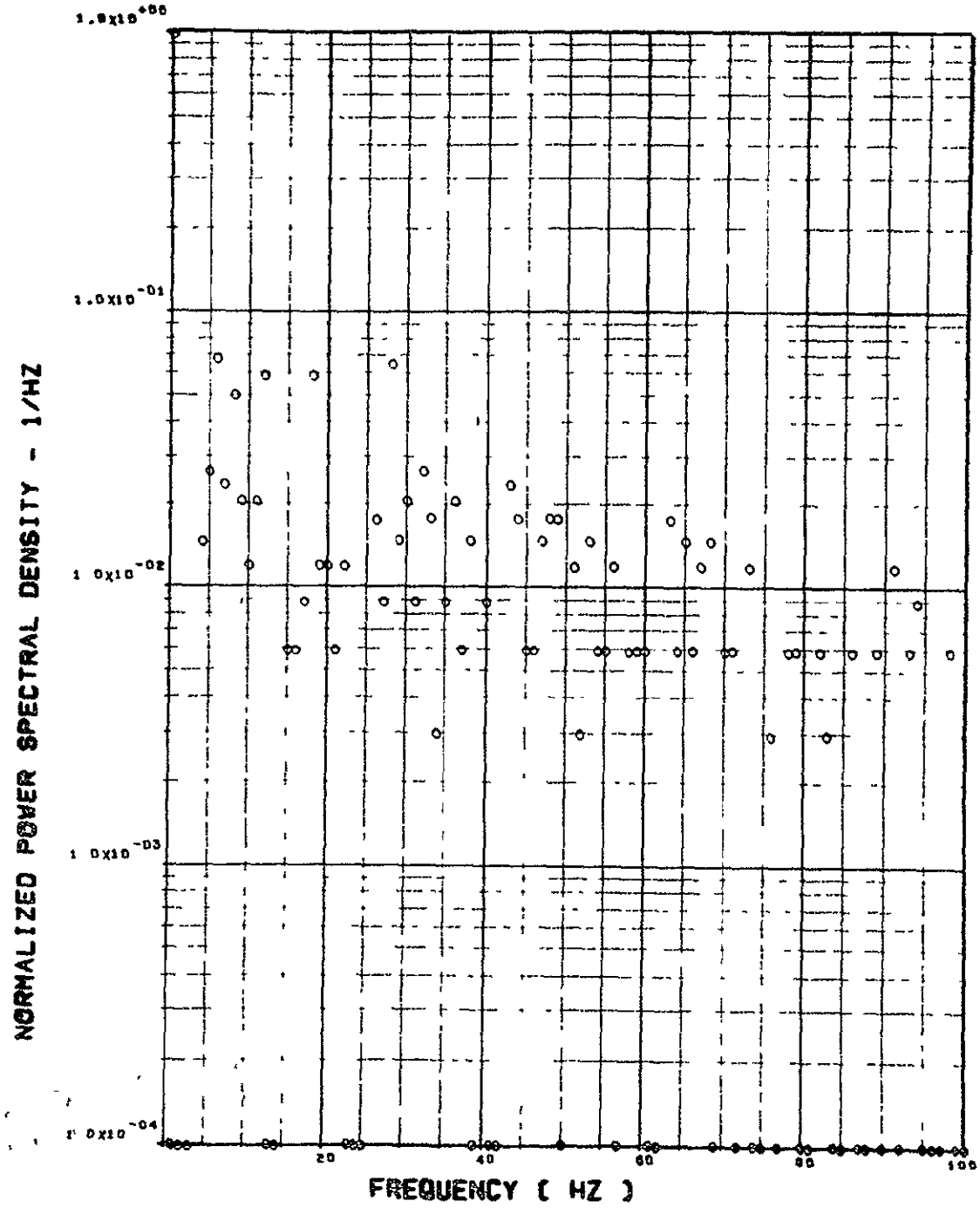

Figure 20. Continued

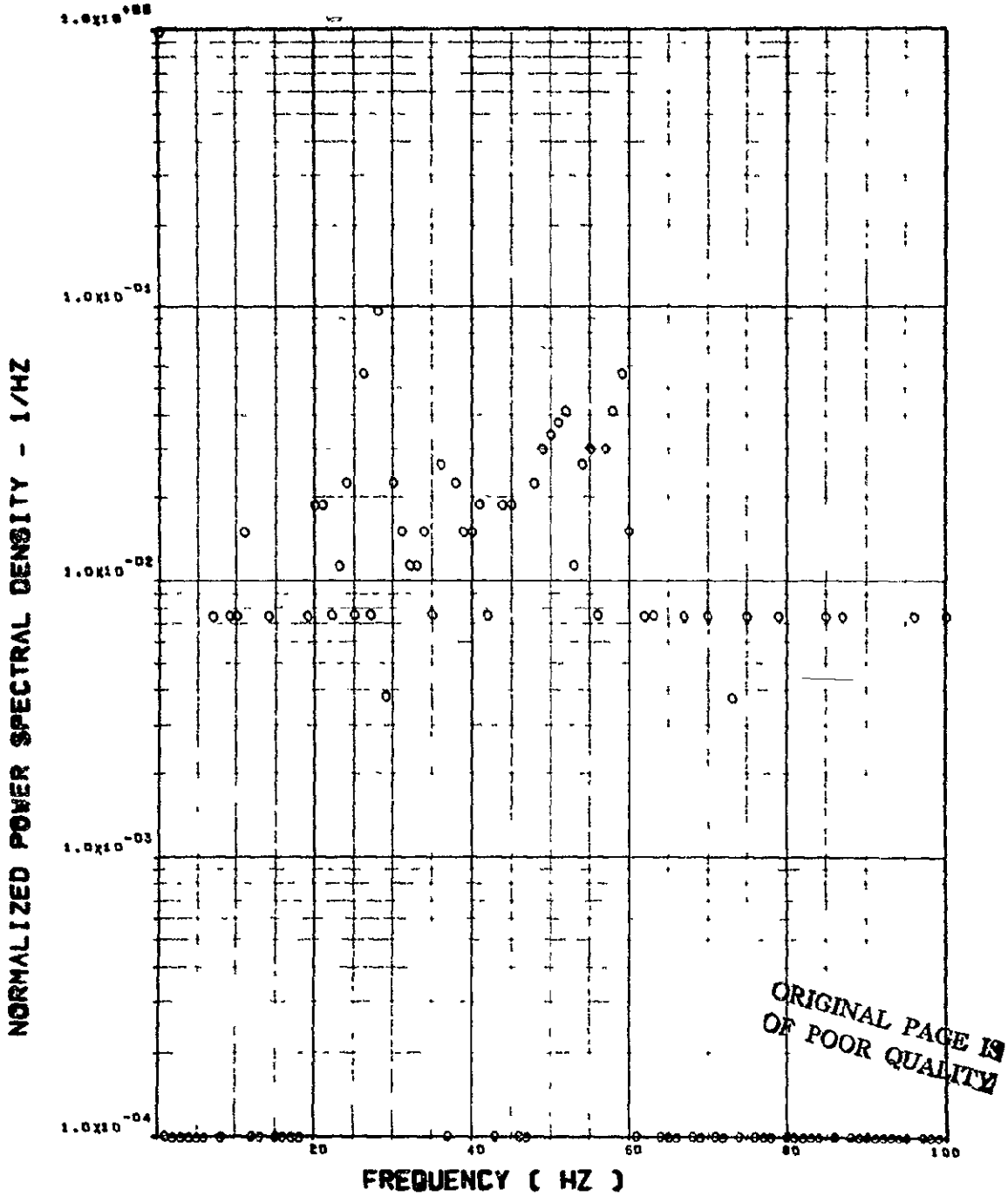

Figure 20. Continued

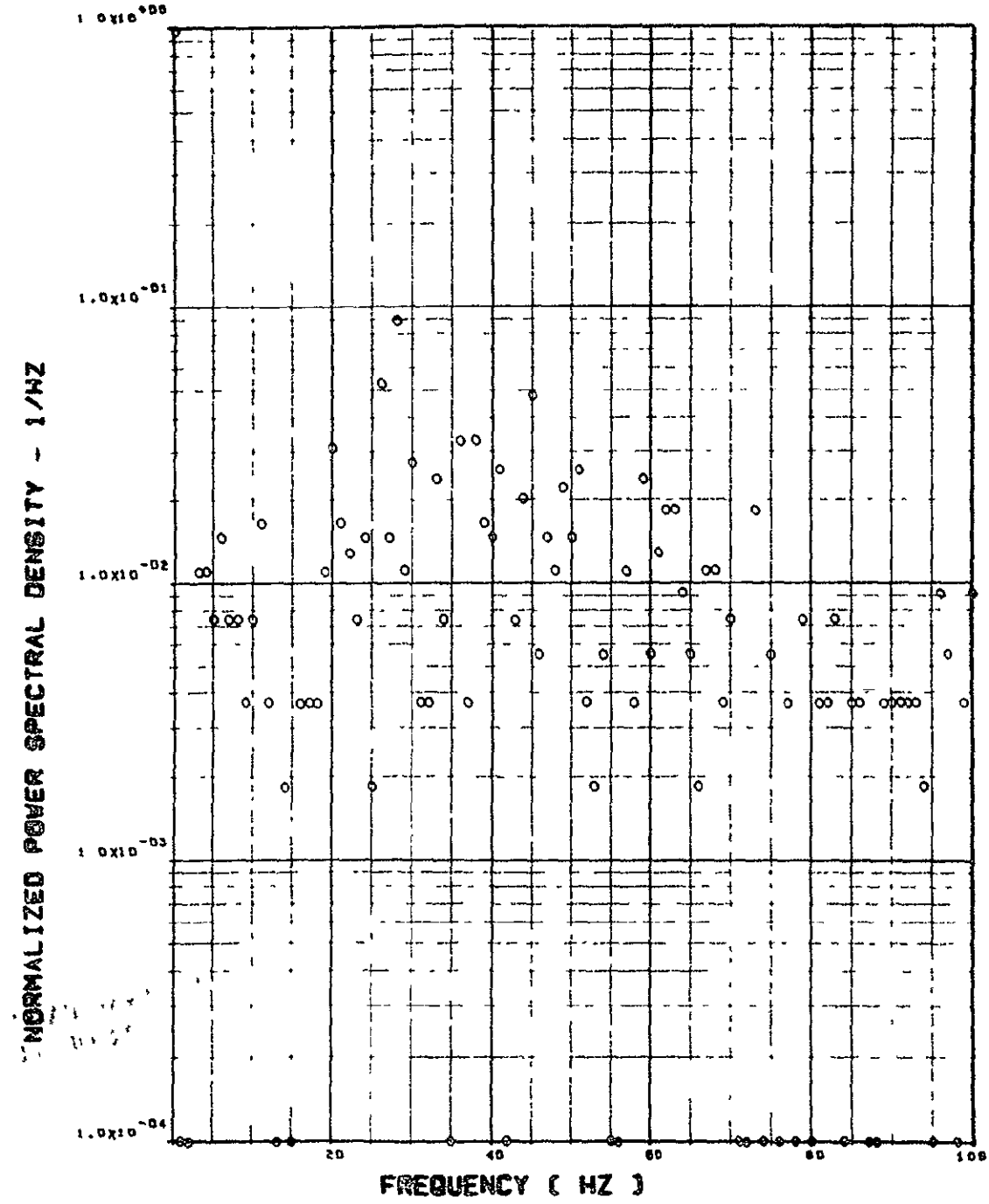

Figure 20. Continued

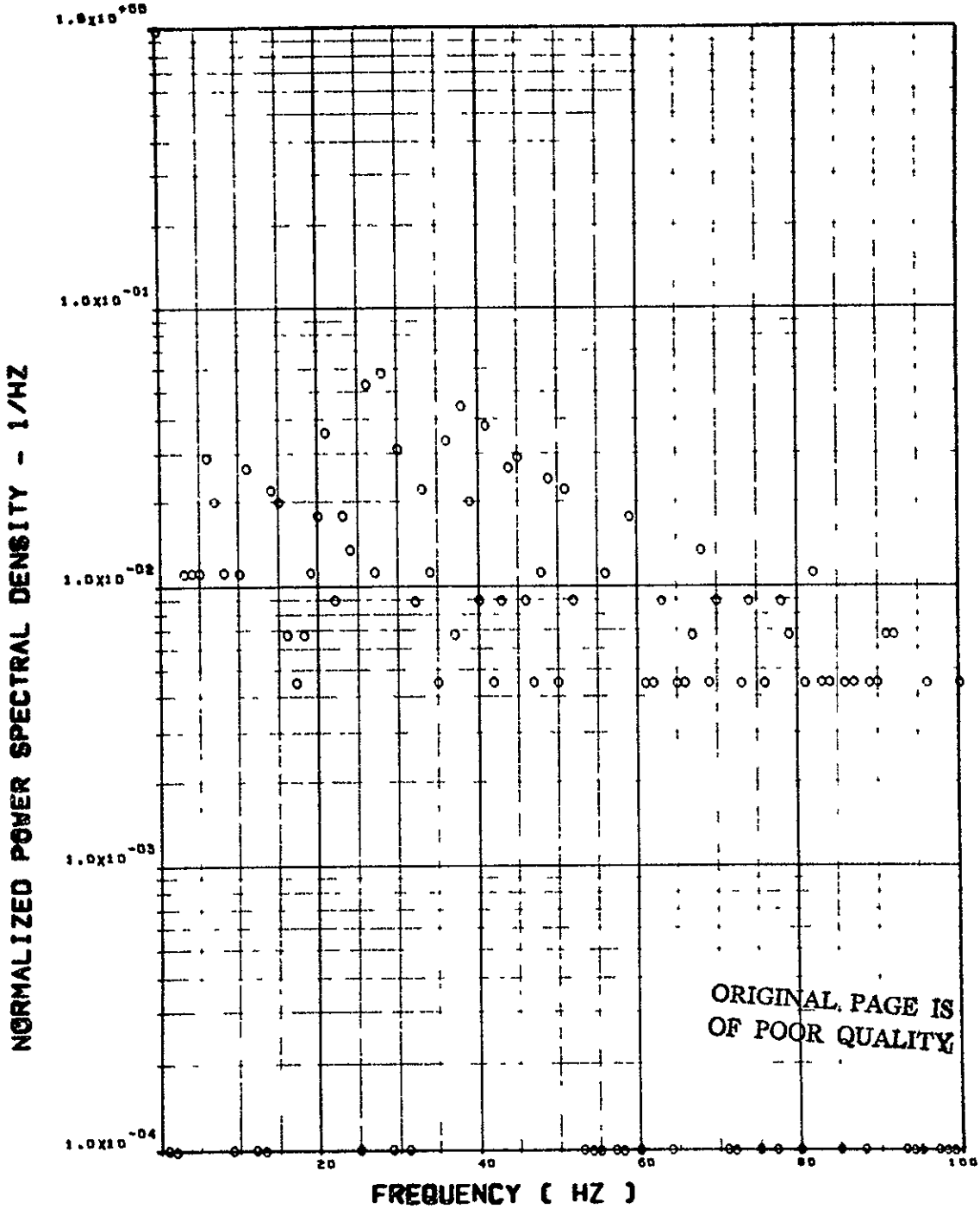

Figure 20. Continued

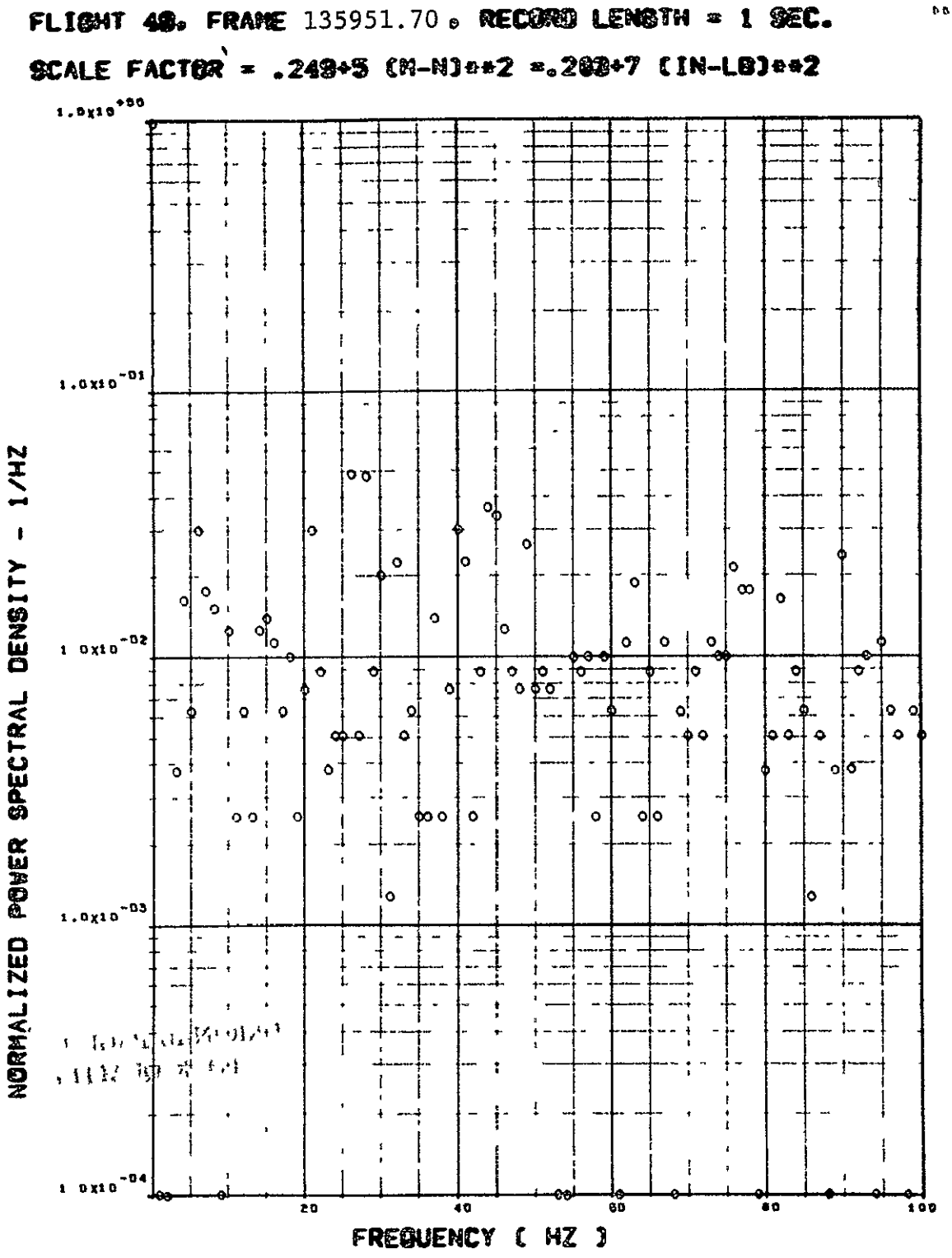

ITEM - SW134 TORSION AT WING STATION 4

Figure 20. Continued

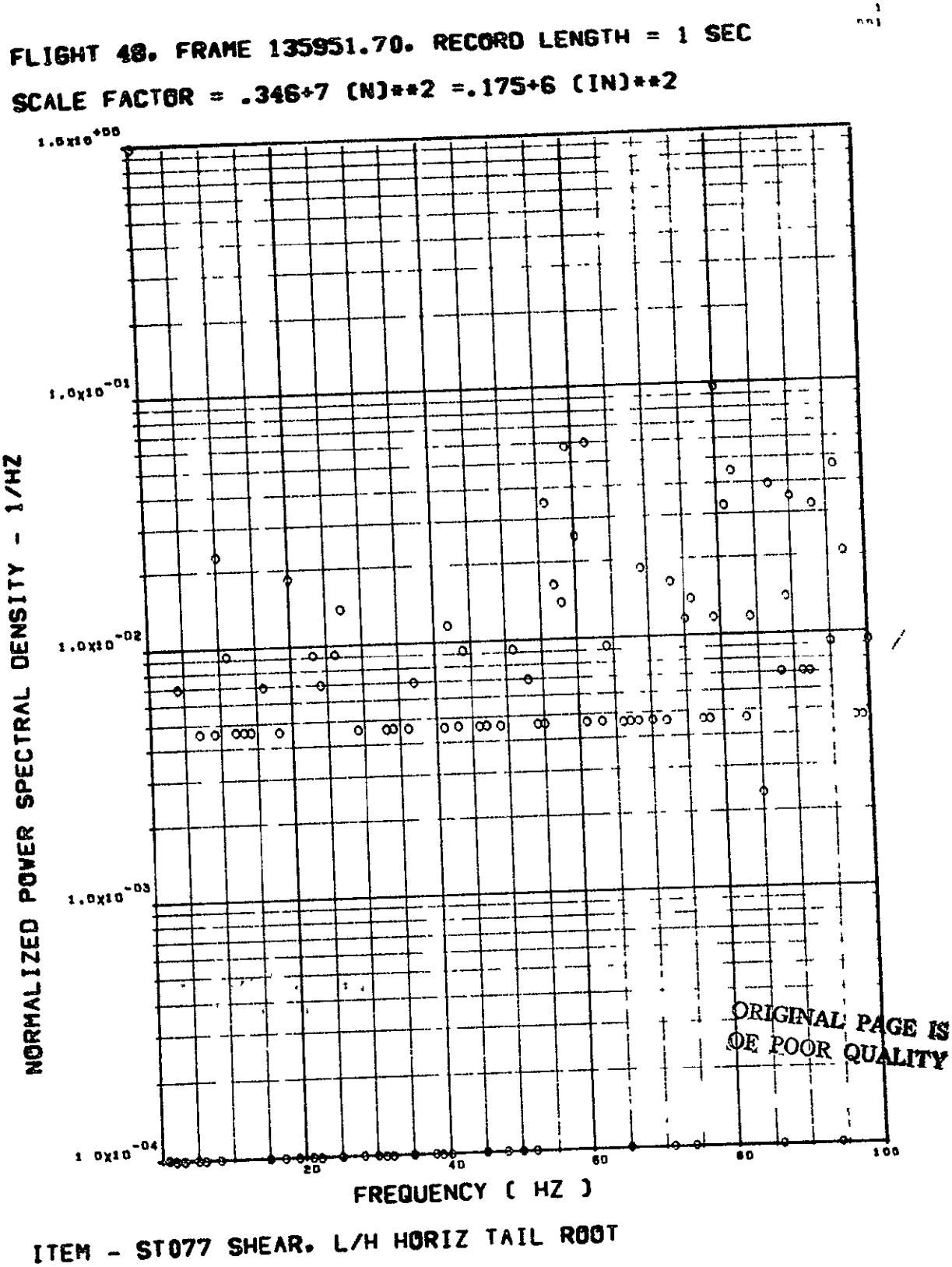

Figure 20. Continued

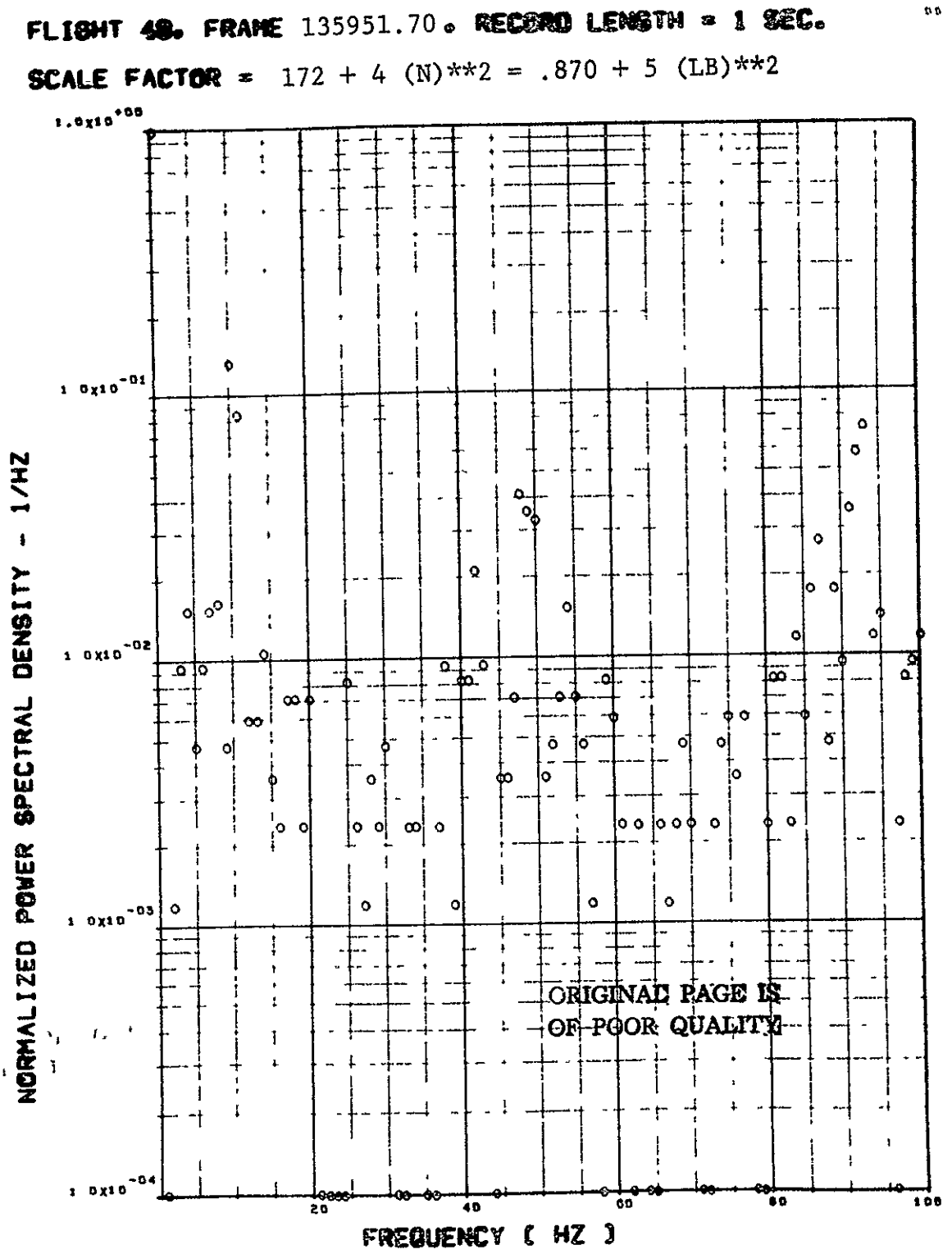

Figure 20. Continued

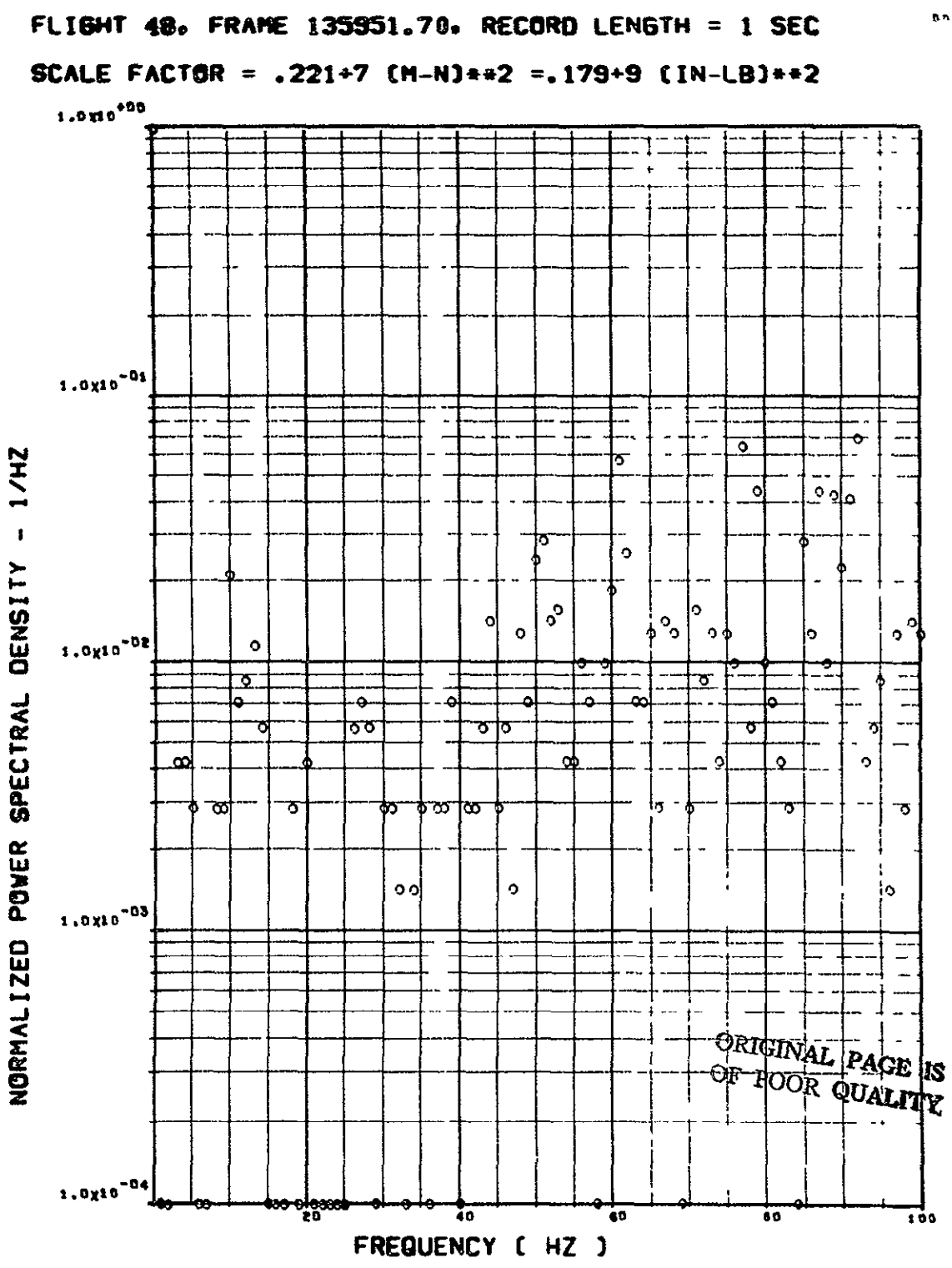

Figure 20. Continued

FLIGHT 48. FRAME 135951.70. RECORD LENGTH = 1 SEC

SCALE FACTOR = .576+2 (M-N)**2 =.469+4 (IN-LB)**2

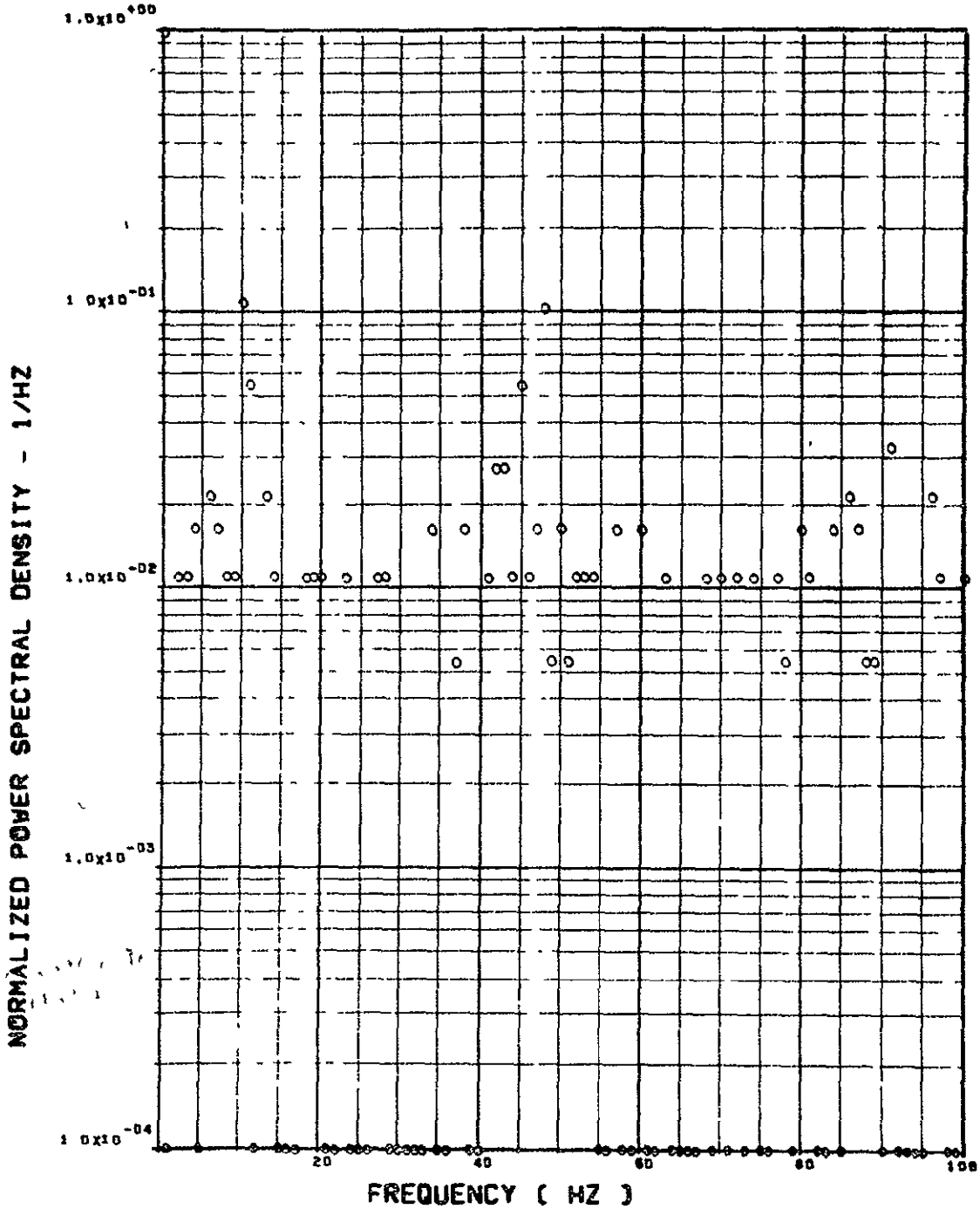

ITEM - ST073 BEND. MOM. R/H HORIZ TAIL ROOT

Figure 20. Continued

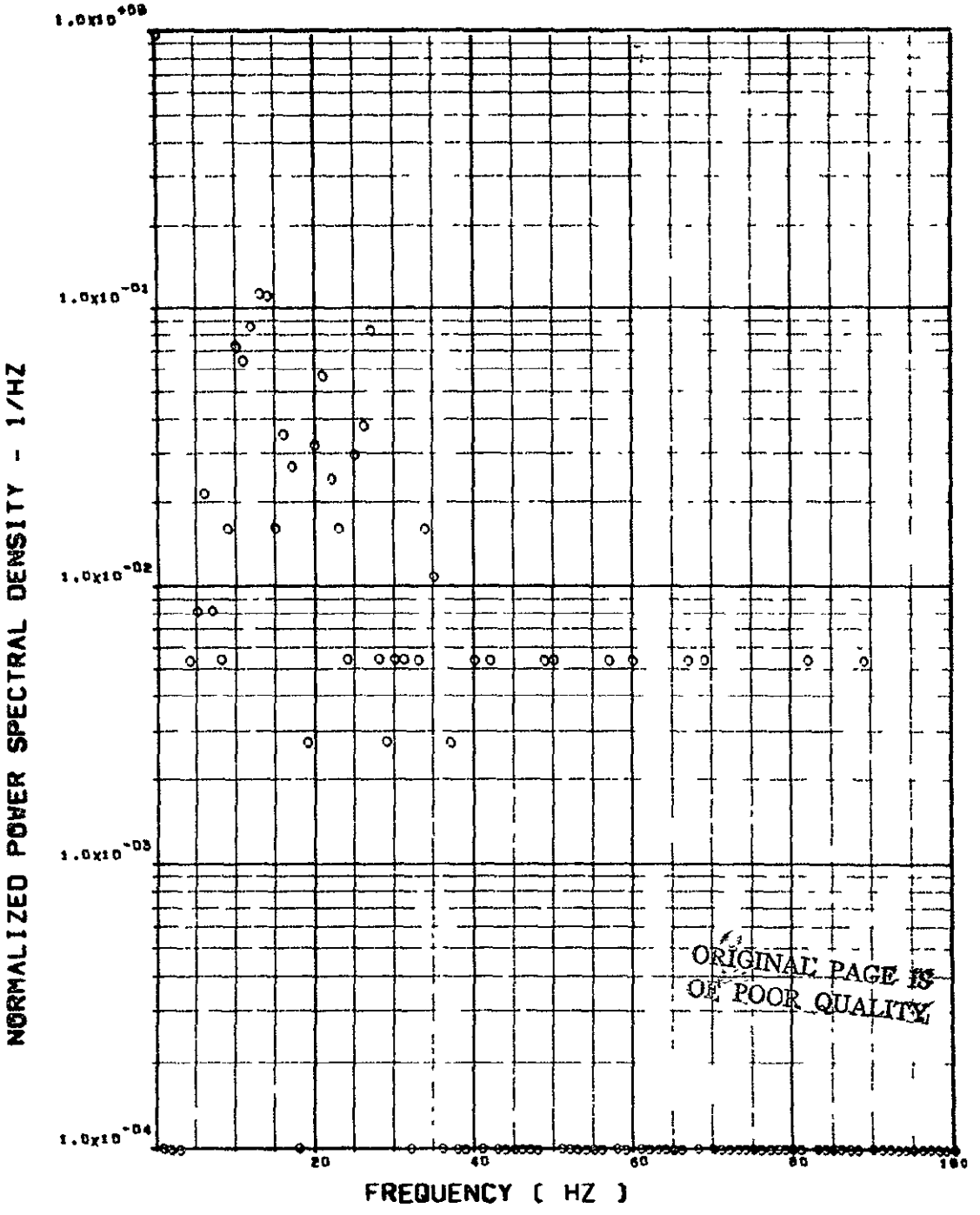

Figure 20. Continued

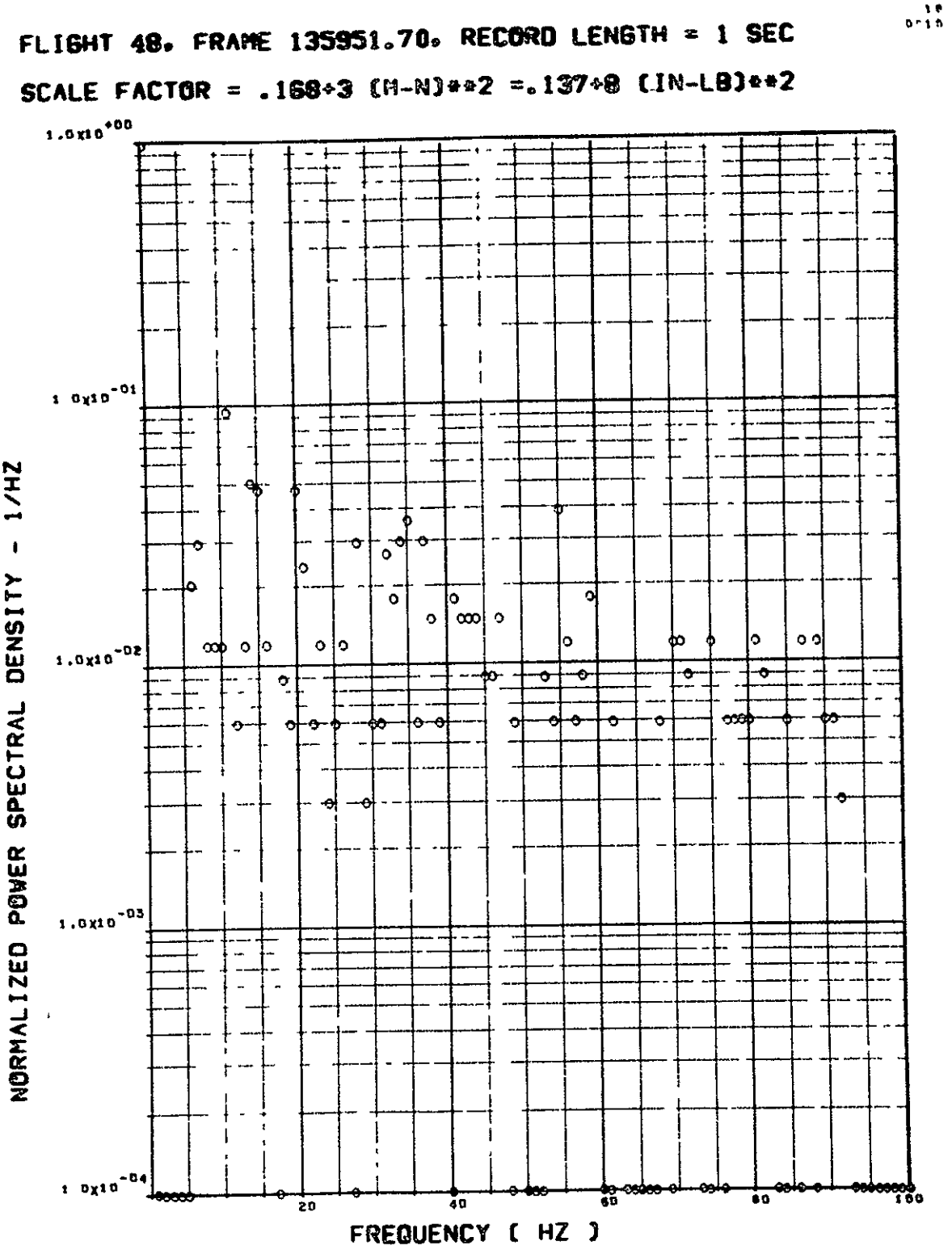

Figure 20. Concluded

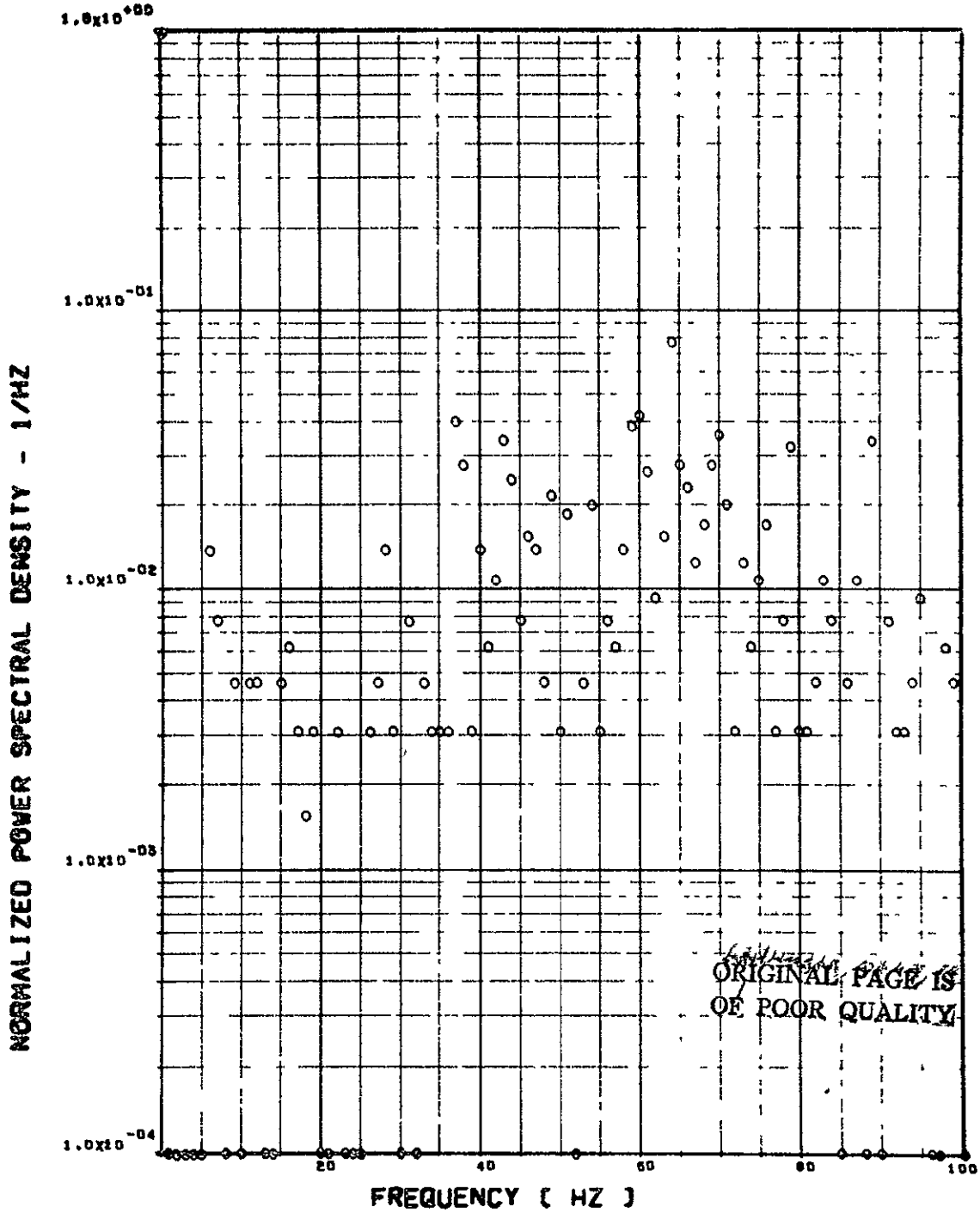

Figure 21. Power Spectra - Flight 48, Run 7R1, Point 2 T_1 = 135952.7, ΔT = 1 Sec, α_{Nom} = 1.35 deg, $\Delta\alpha$= 1.35 deg.

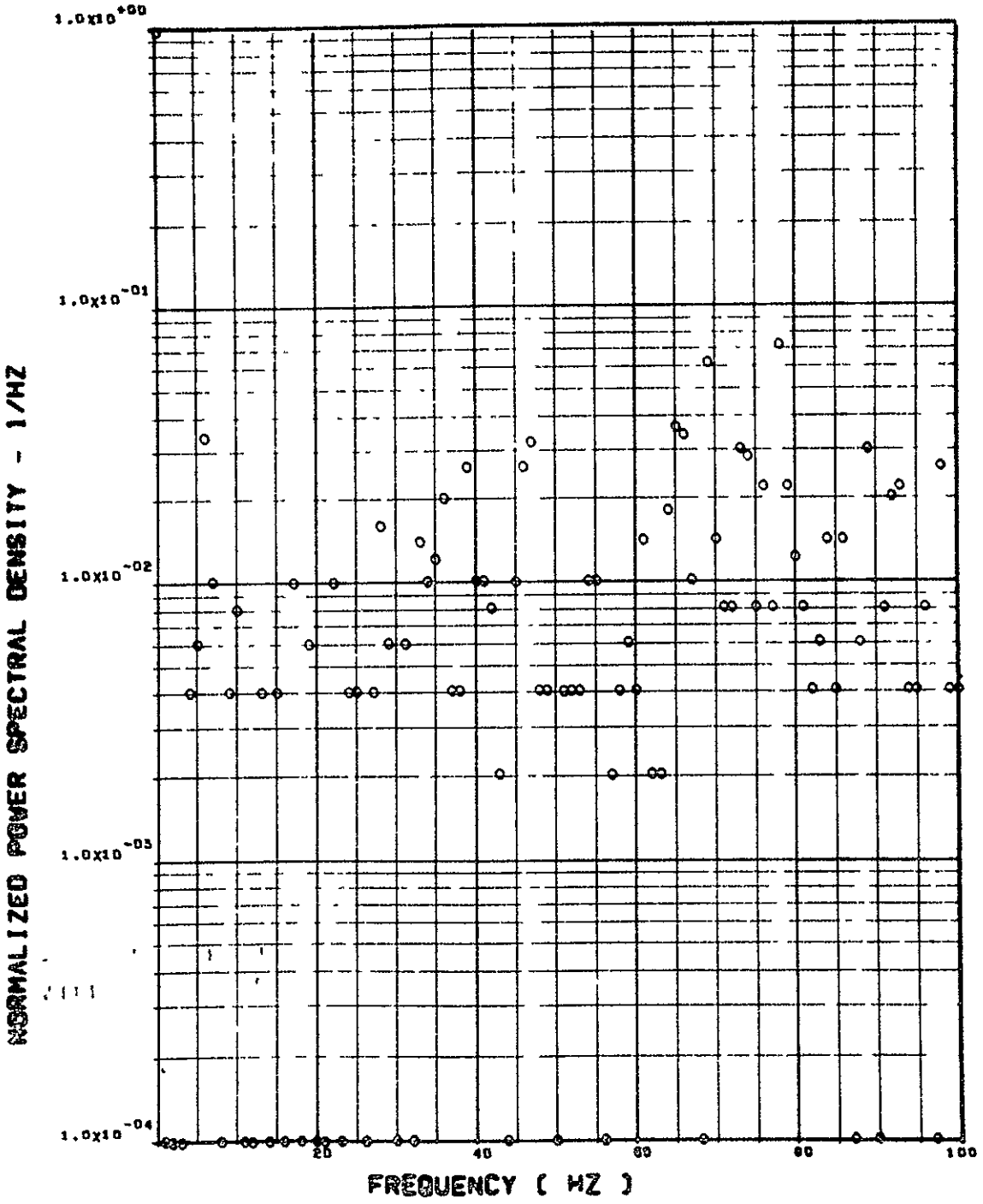

Figure 21. Continued

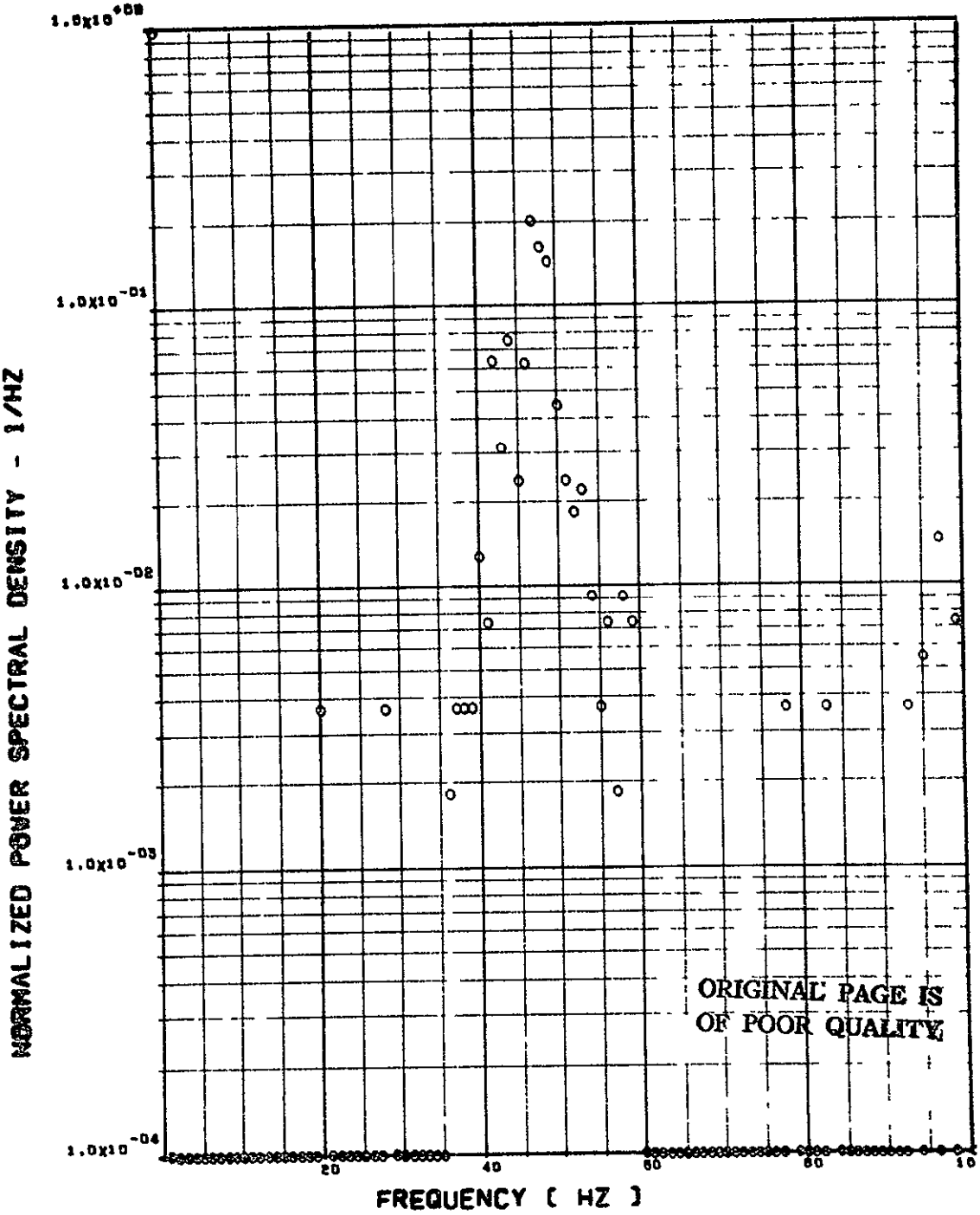

Figure 21. Continued

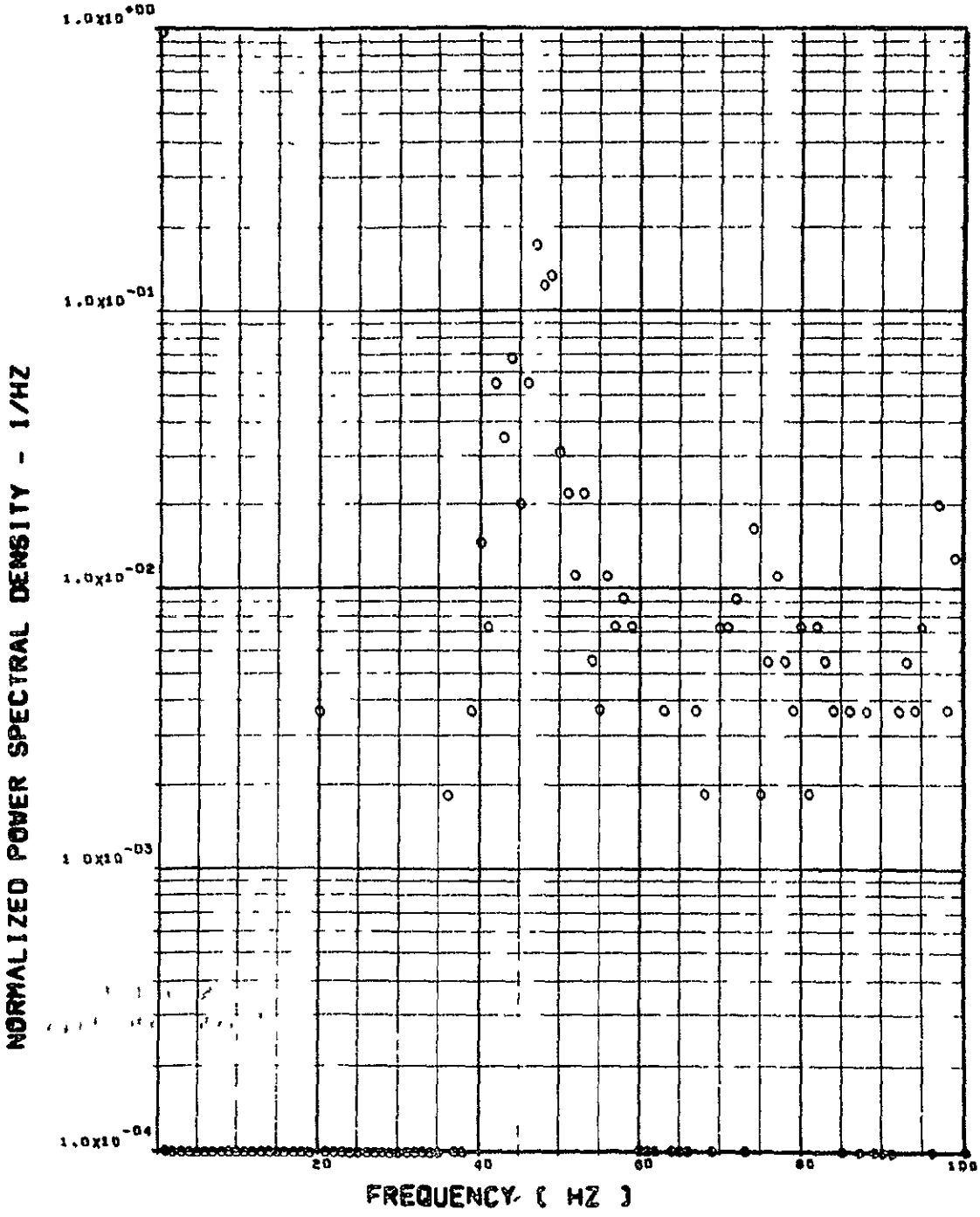

Figure 21. Continued

FLIGHT 48. FRAME 135852.70. RECORD LENGTH = 1 SEC.

SCALE FACTOR = .177-2 (6)**2

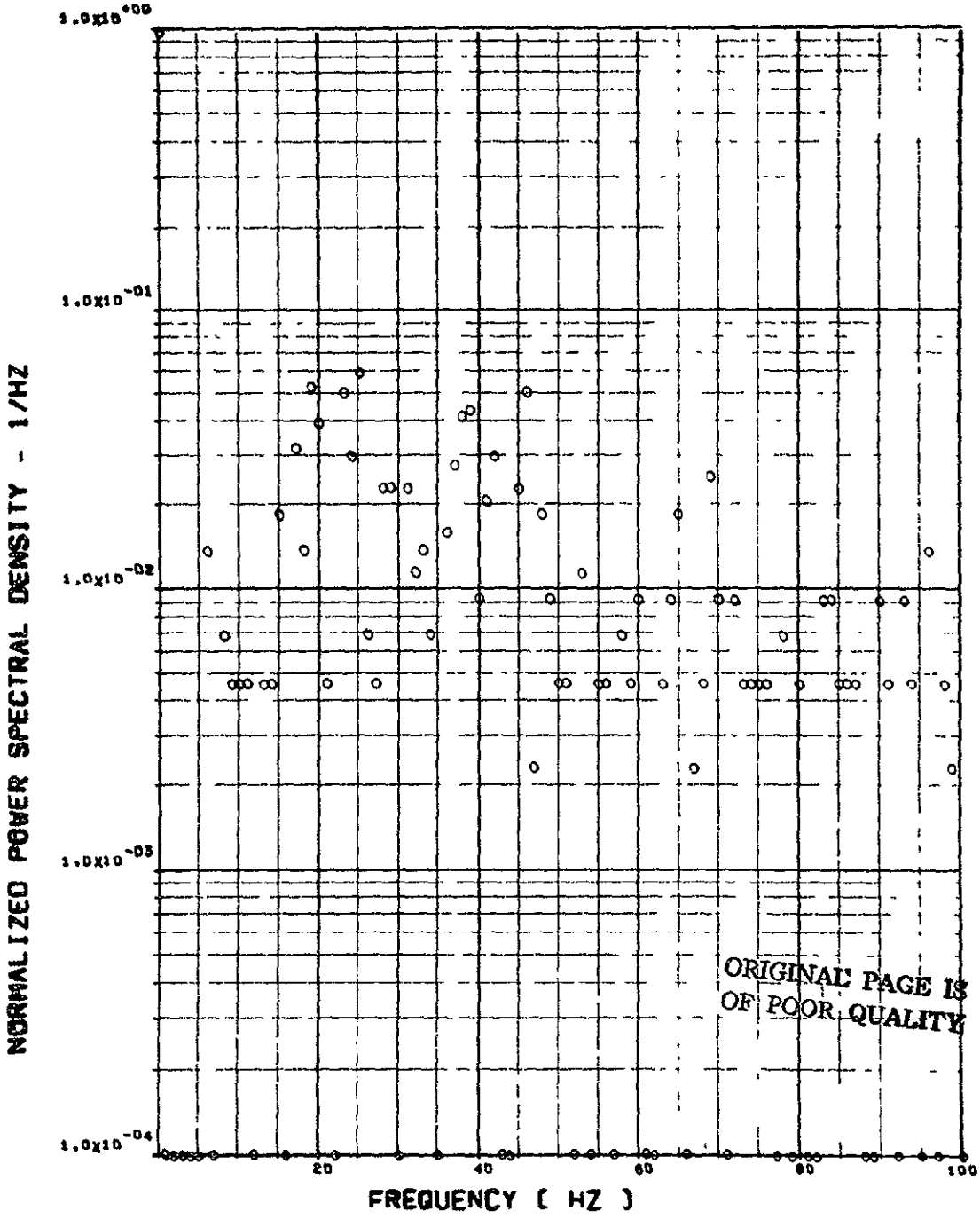

ITEM - AF009 PILOT'S SEAT VERTICAL ACCELERGMETER

Figure 21. Continued

FLIGHT 40. FRAME 135952.70. RECORD LENGTH = 1 SEC.

SCALE FACTOR = .871-3 (6)**2

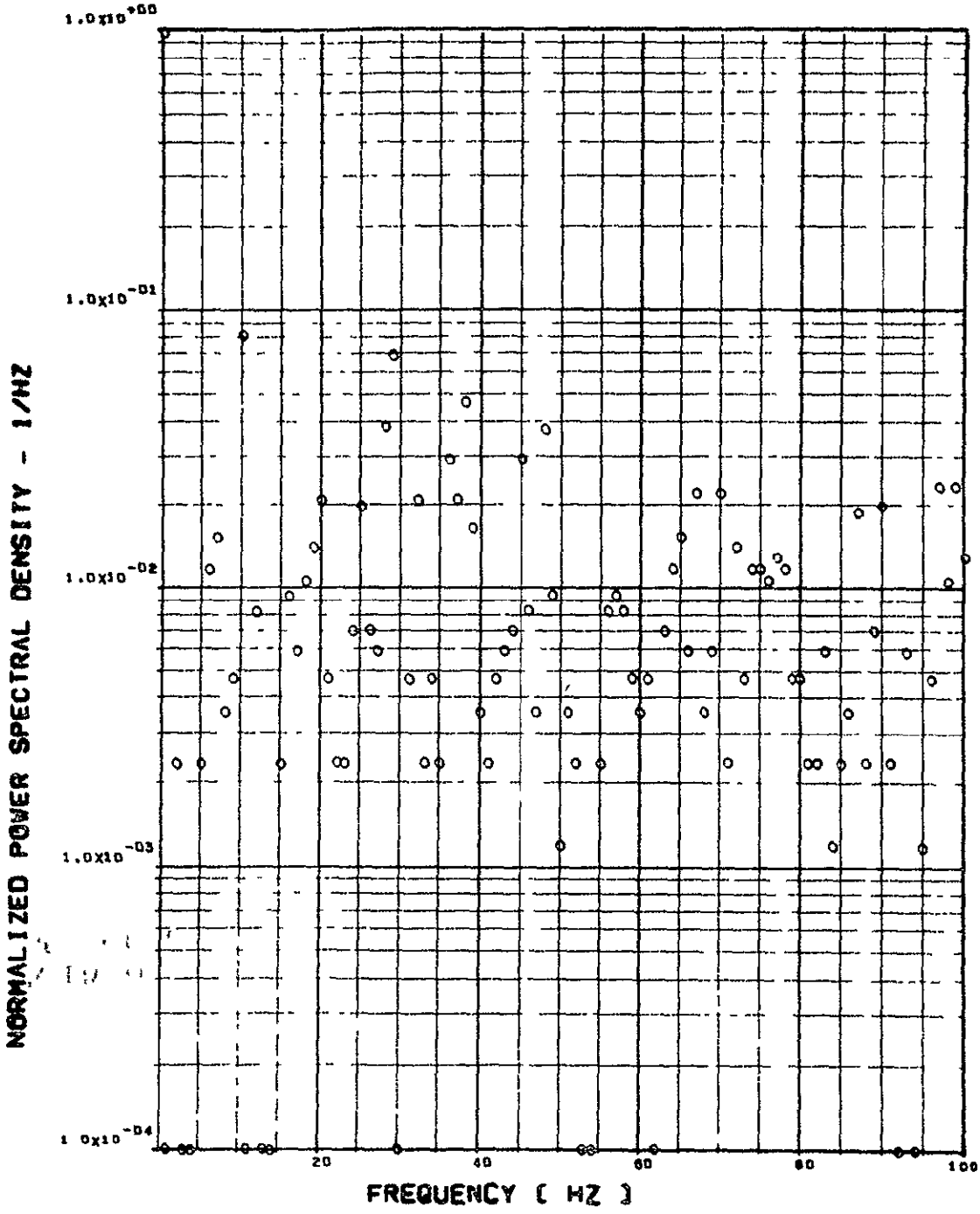

ITEM - AF010 PILOT'S SEAT LATERAL ACCELEROMETER

Figure 21. Continued

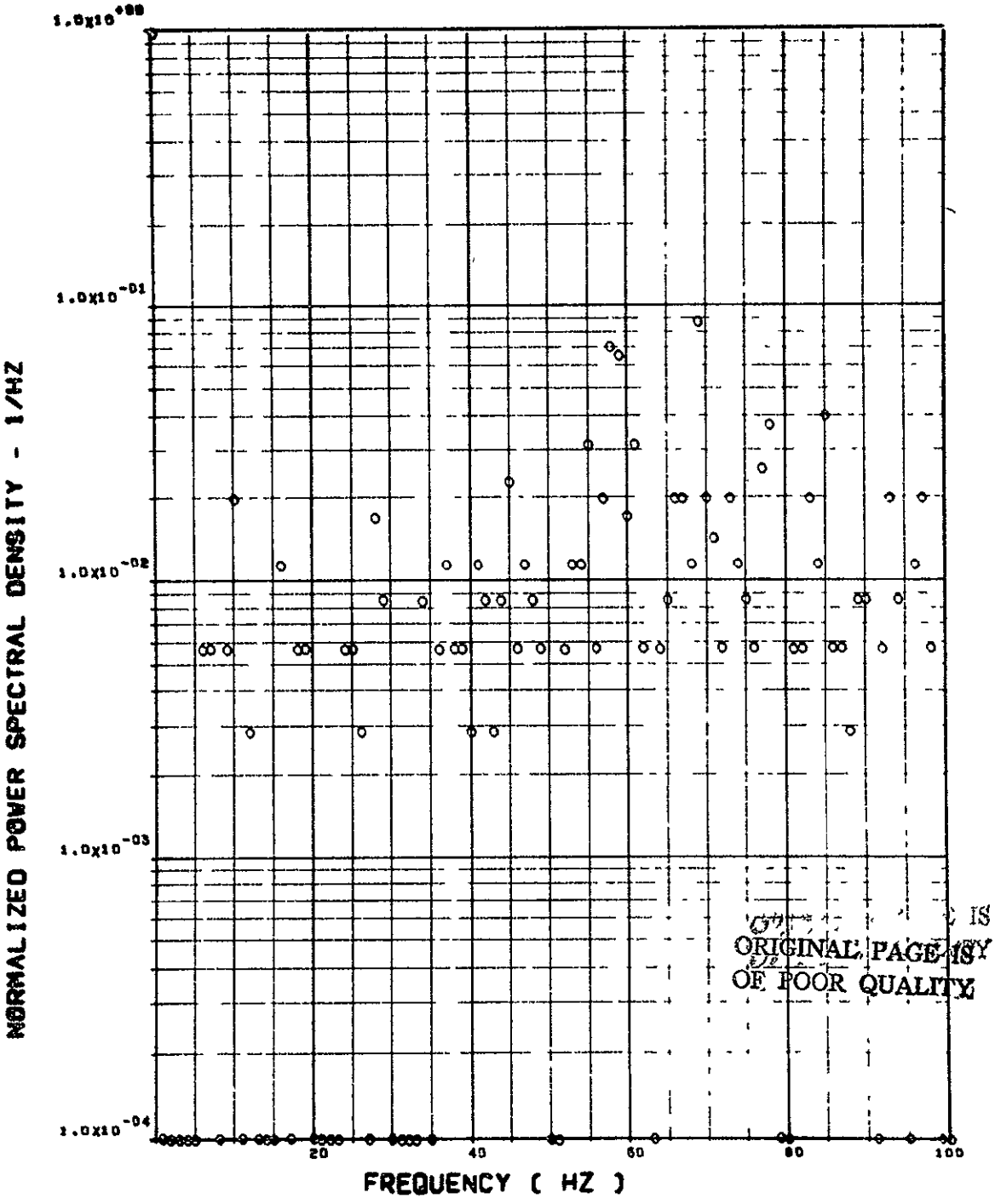

Figure 21. Continued

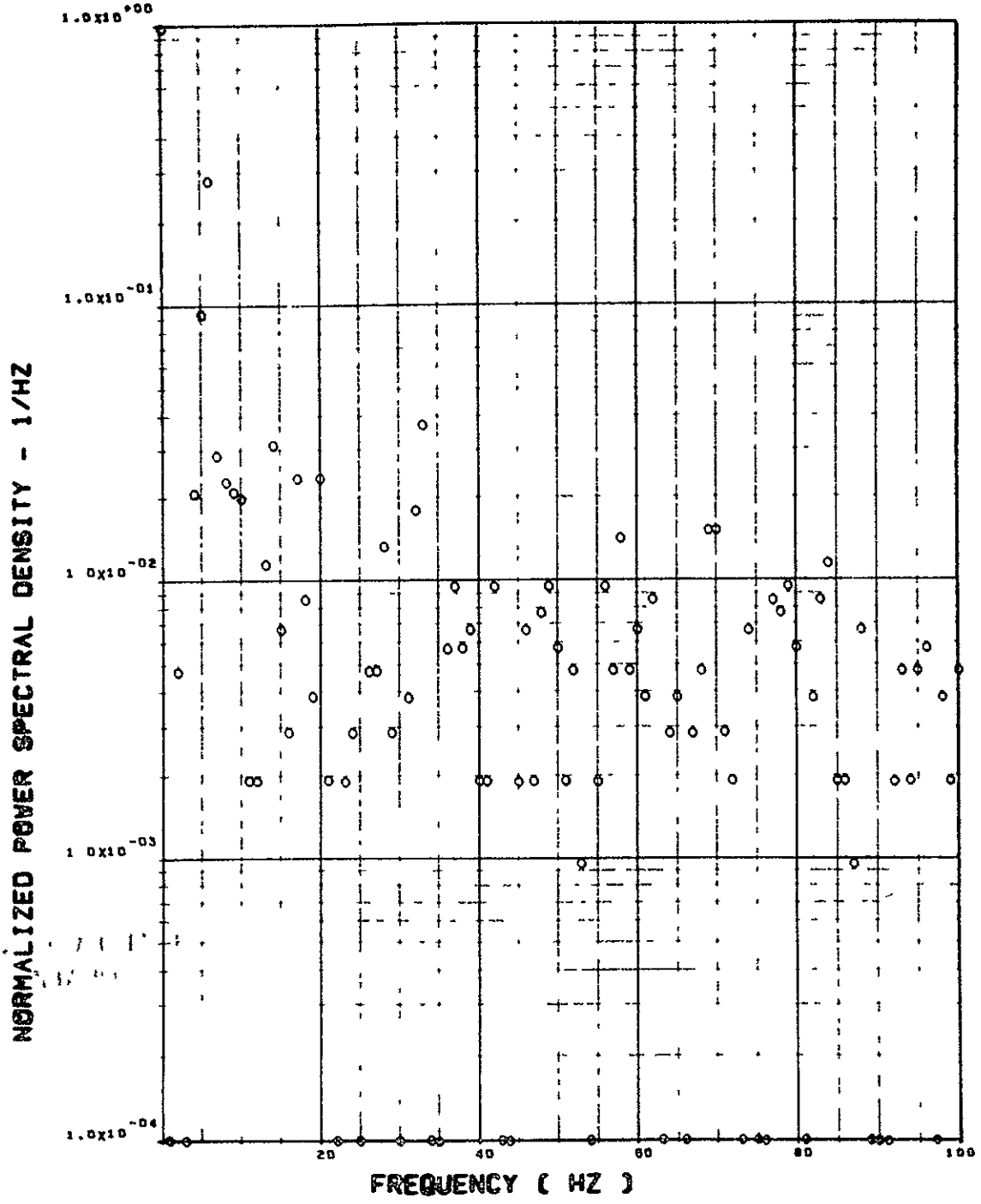

Figure 21. Continued

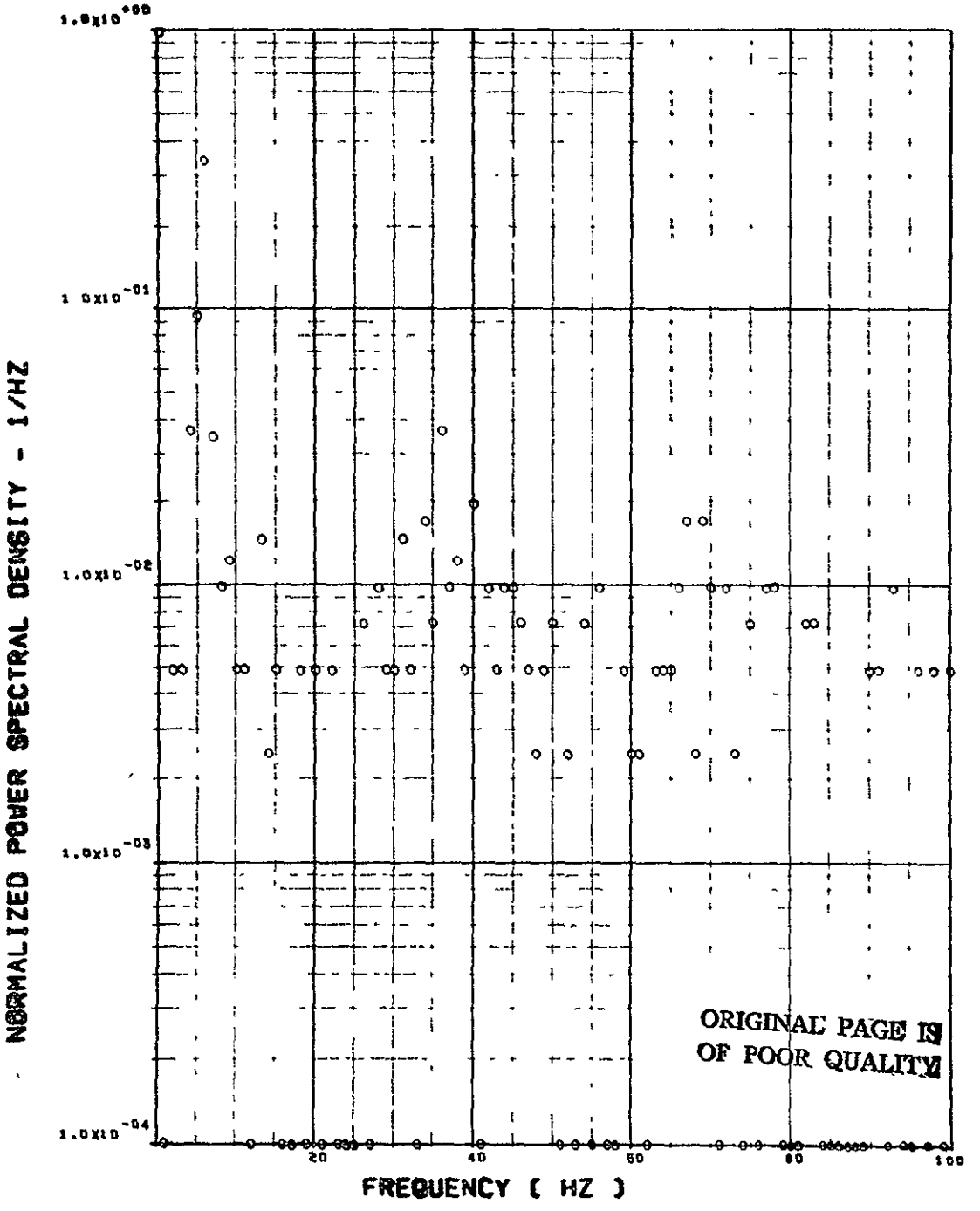

Figure 21. Continued

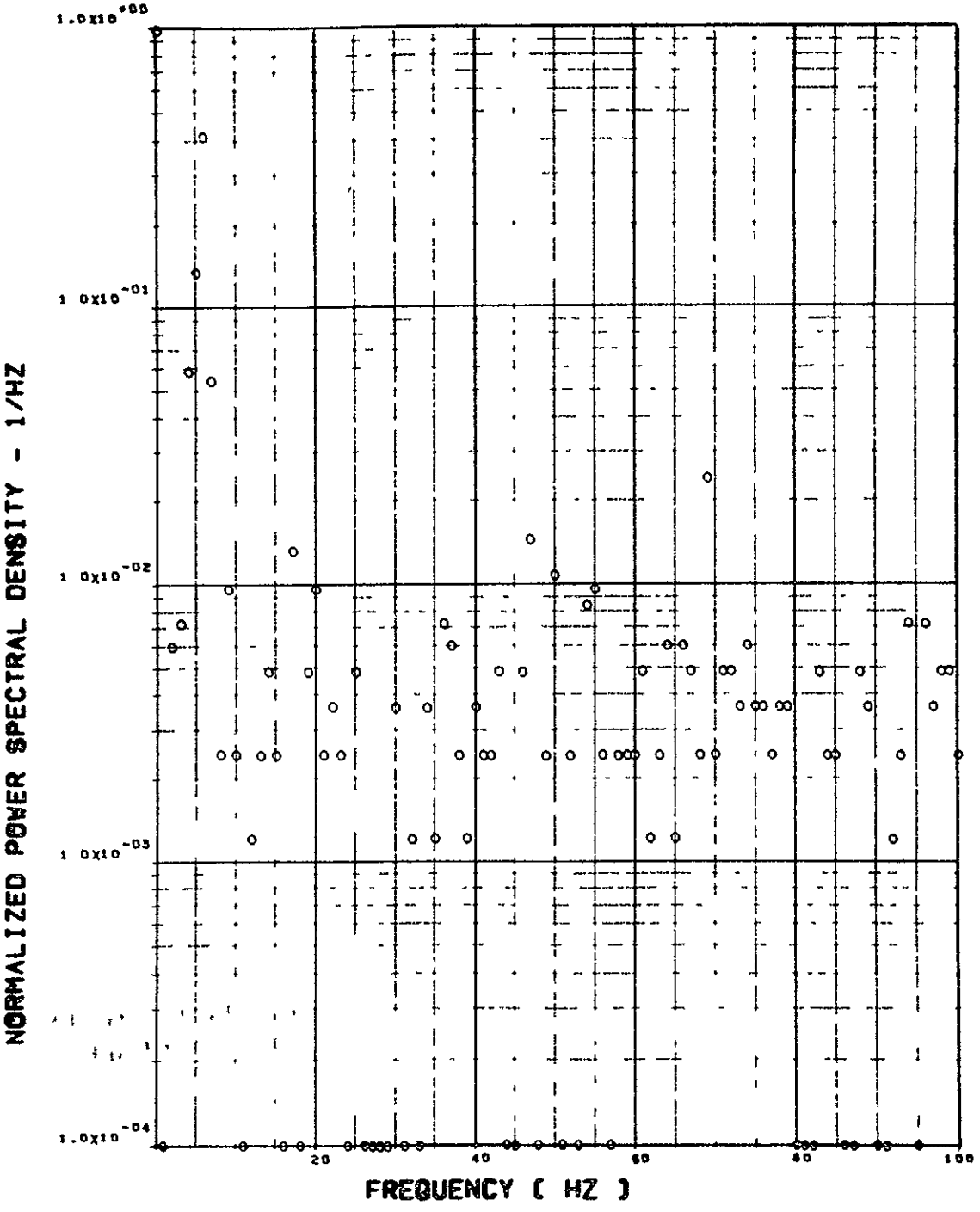

Figure 21. Continued

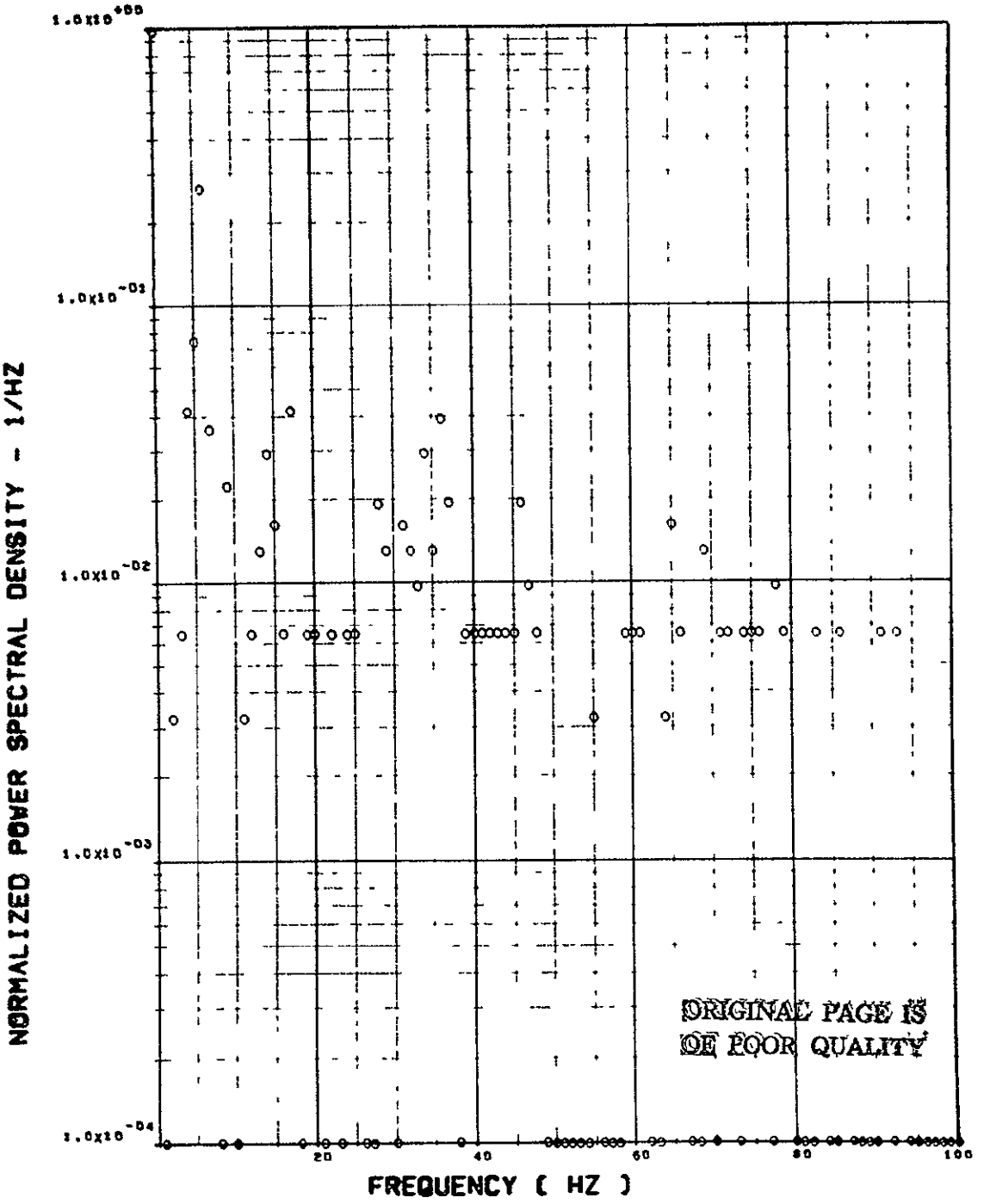

Figure 21. Continued

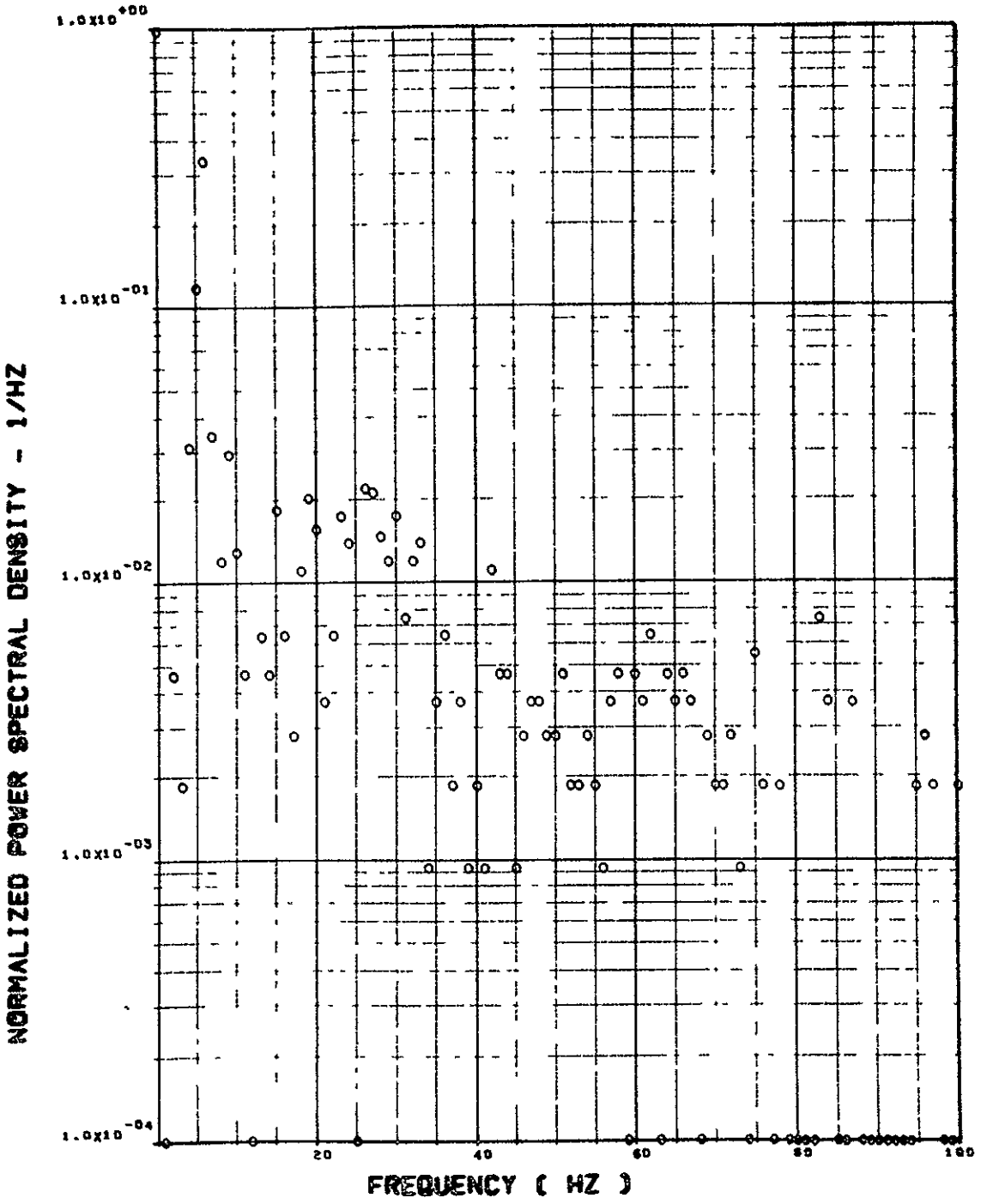

Figure 21. Continued

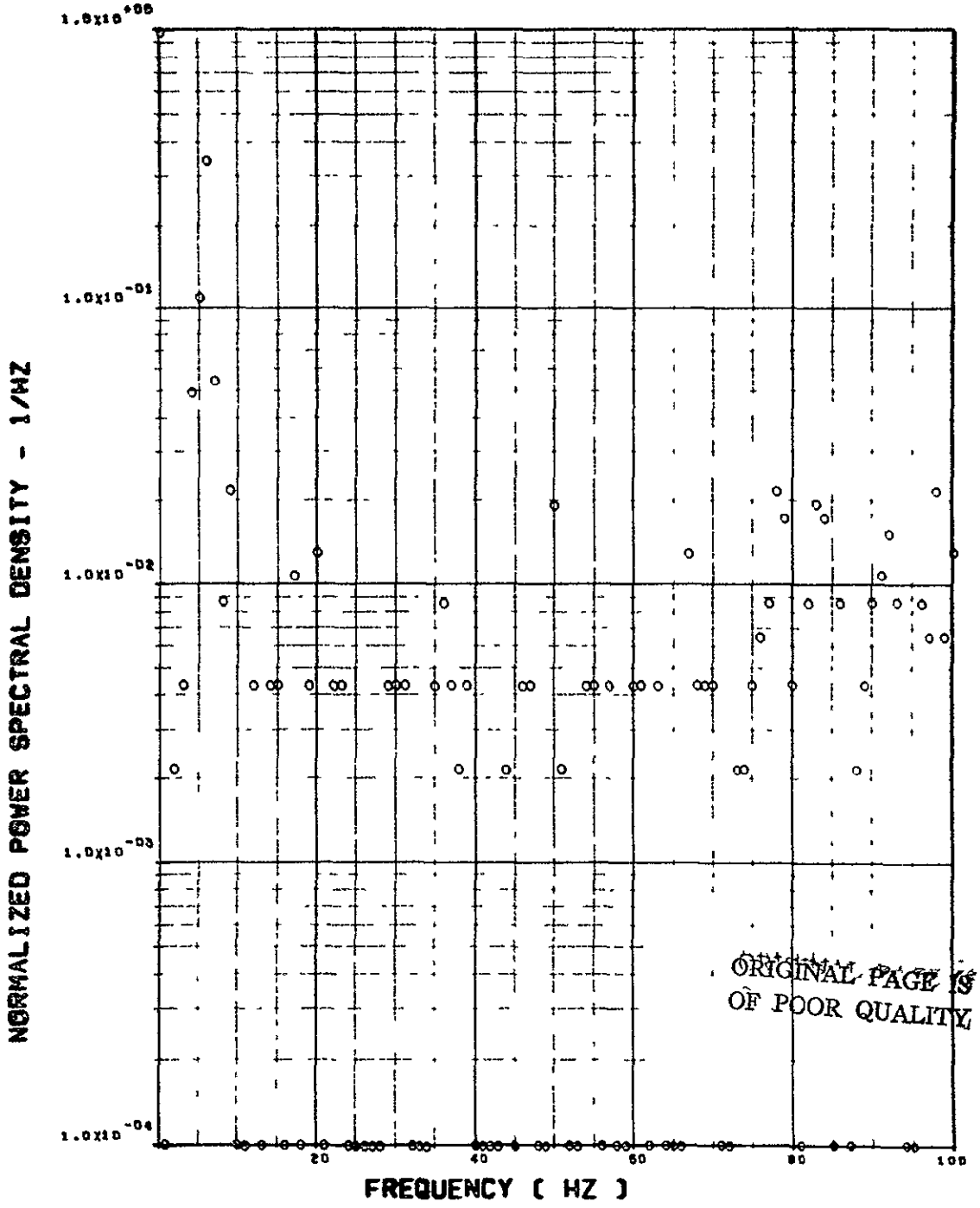

Figure 21. Continued

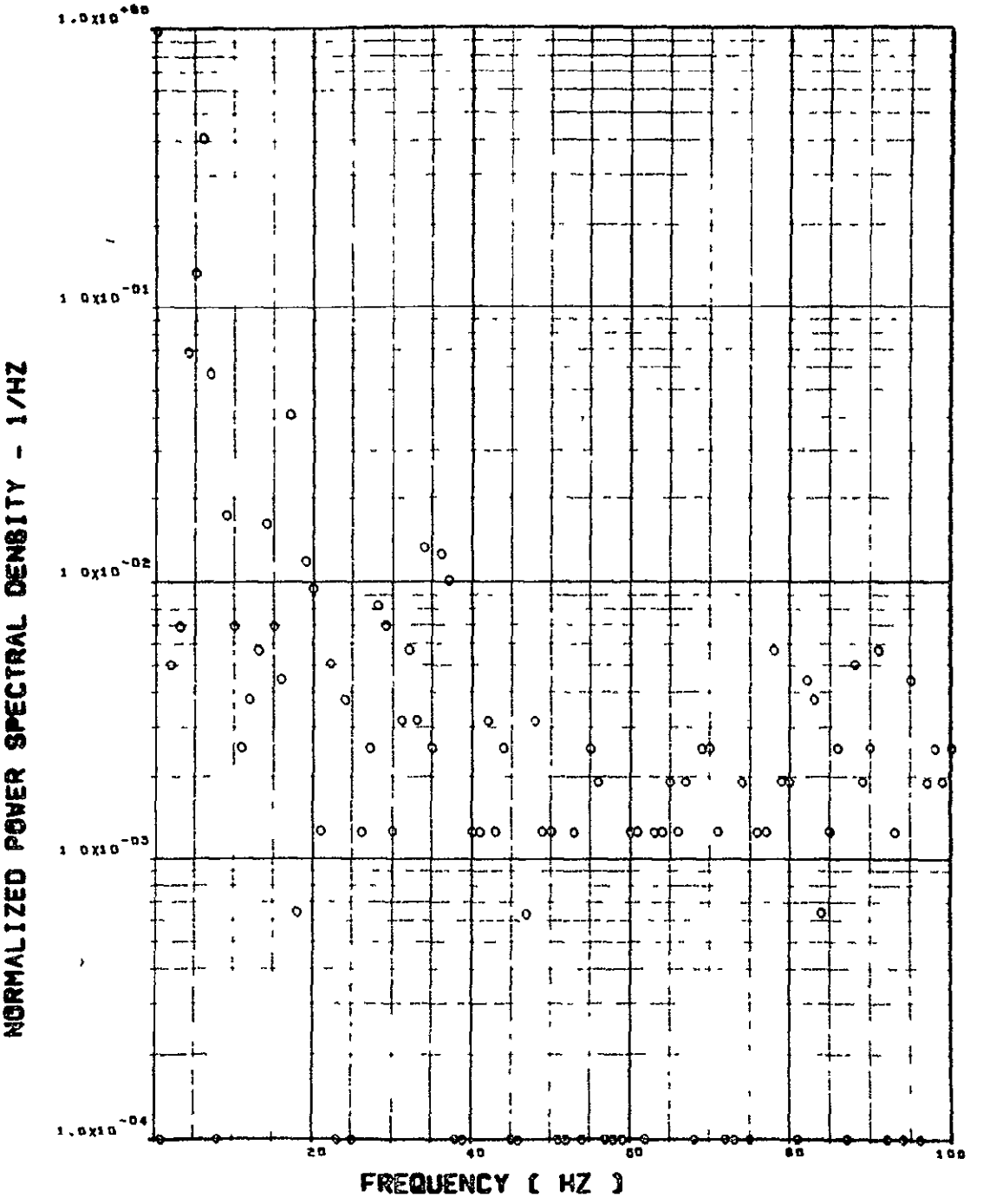

Figure 21. Continued

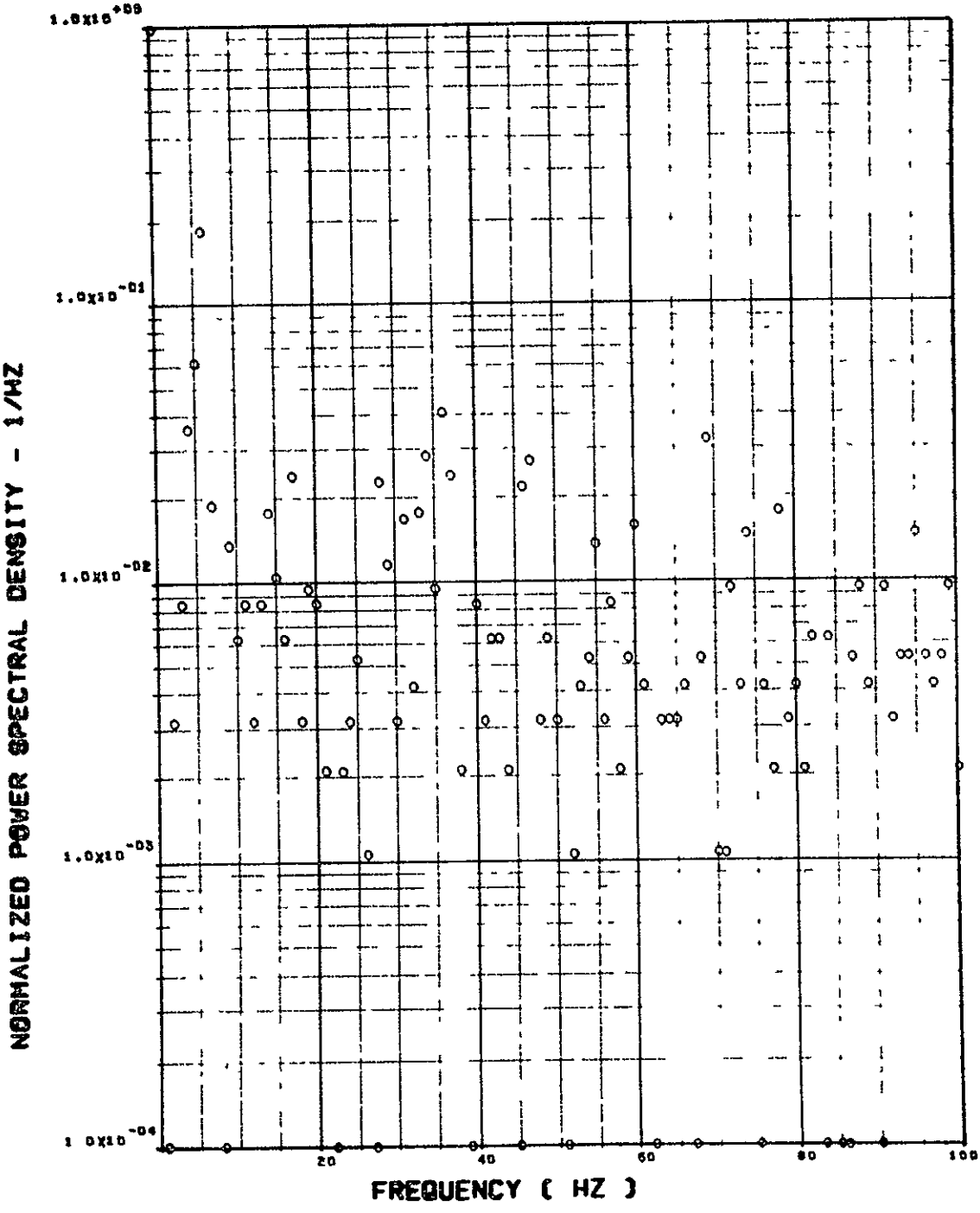

Figure 21. Continued

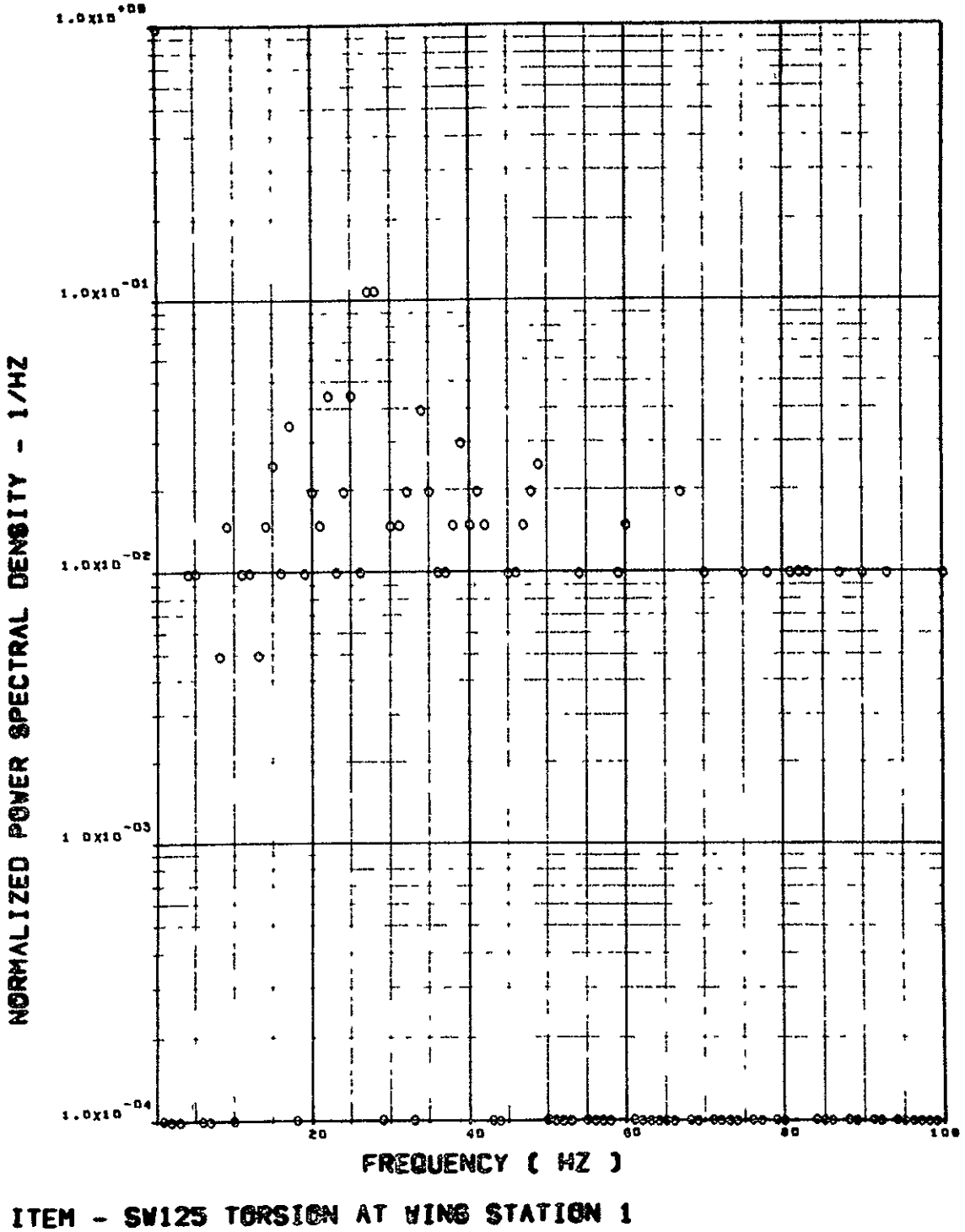

Figure 21. Continued

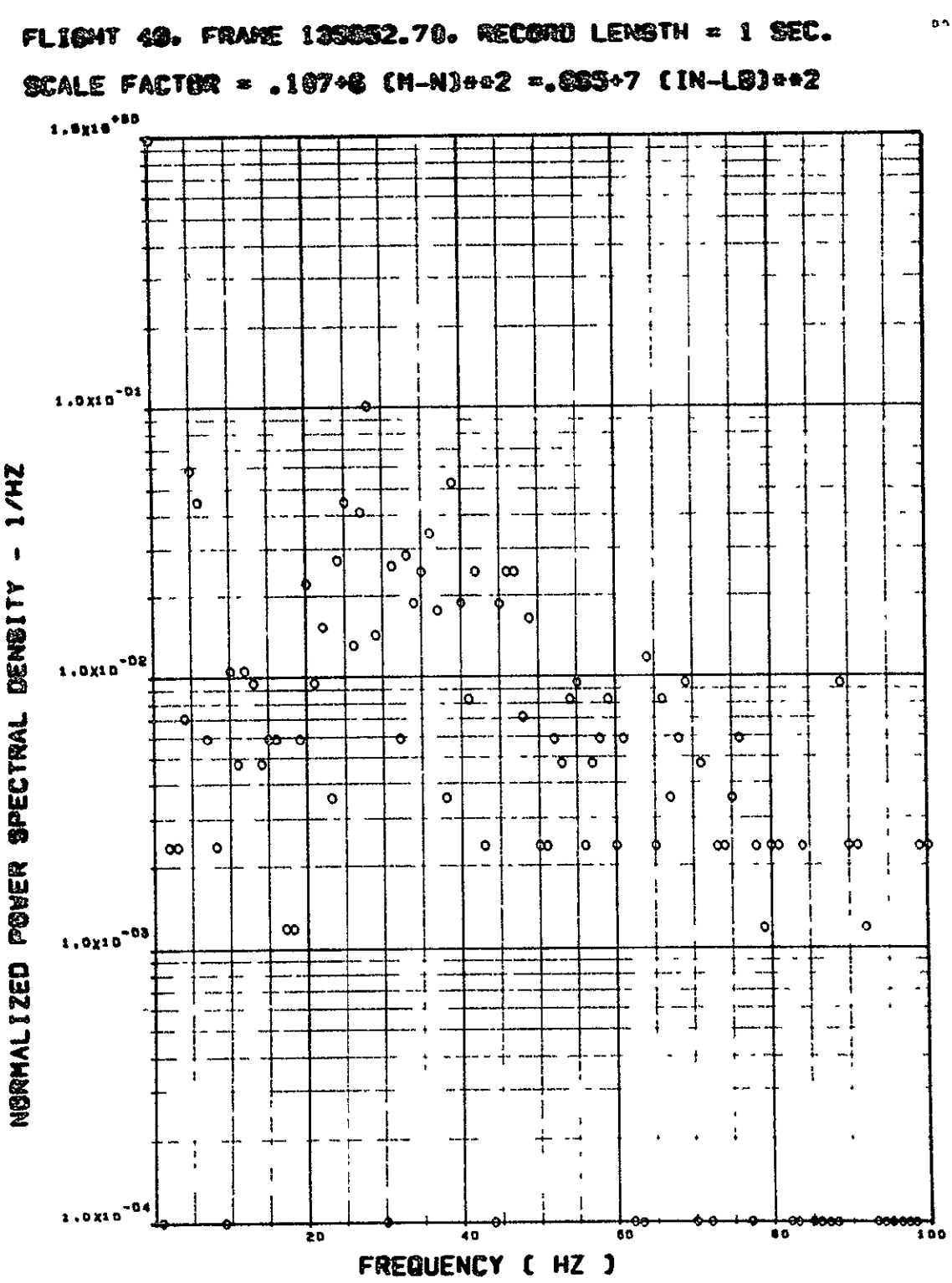

Figure 21. Continued

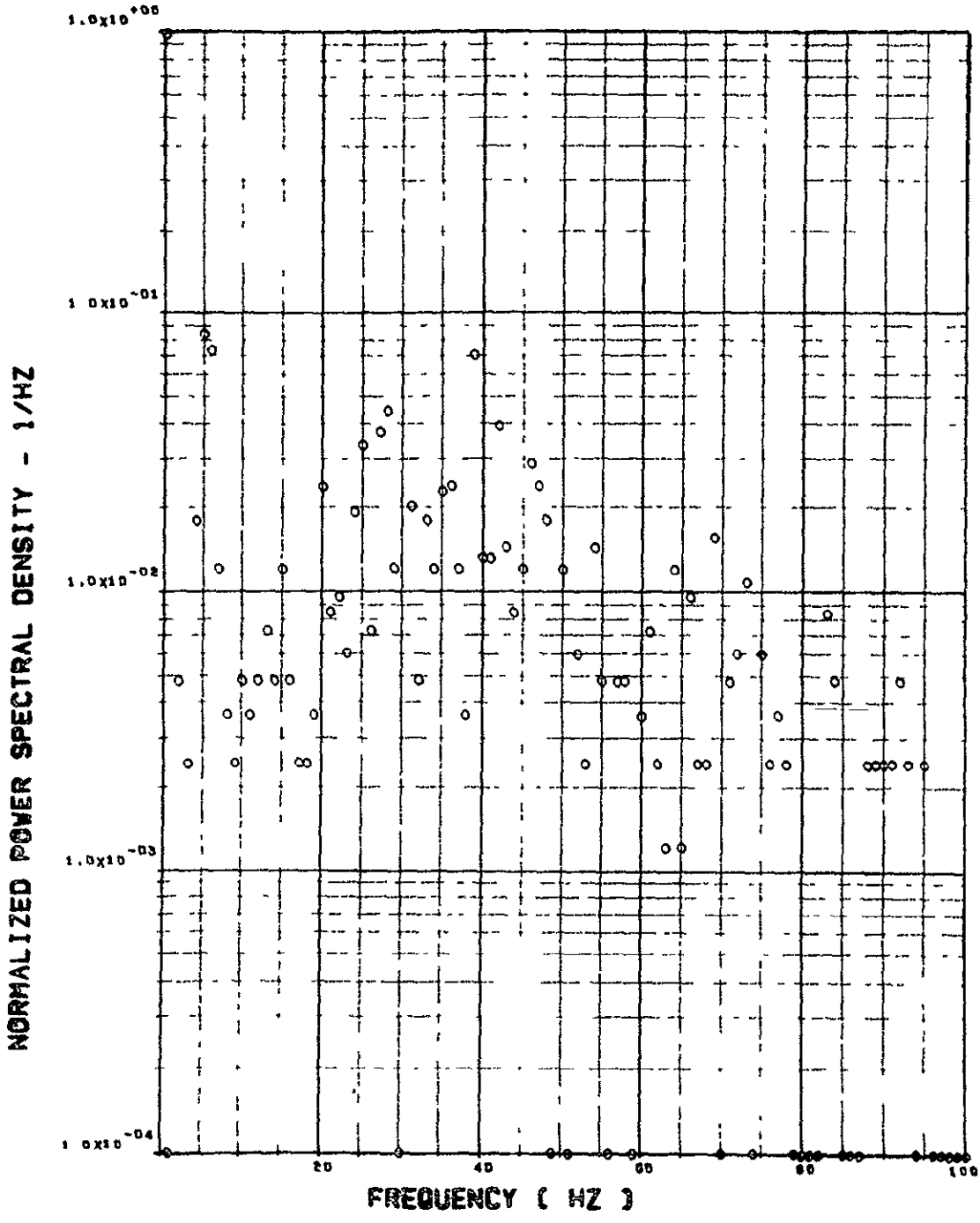

Figure 21. Continued

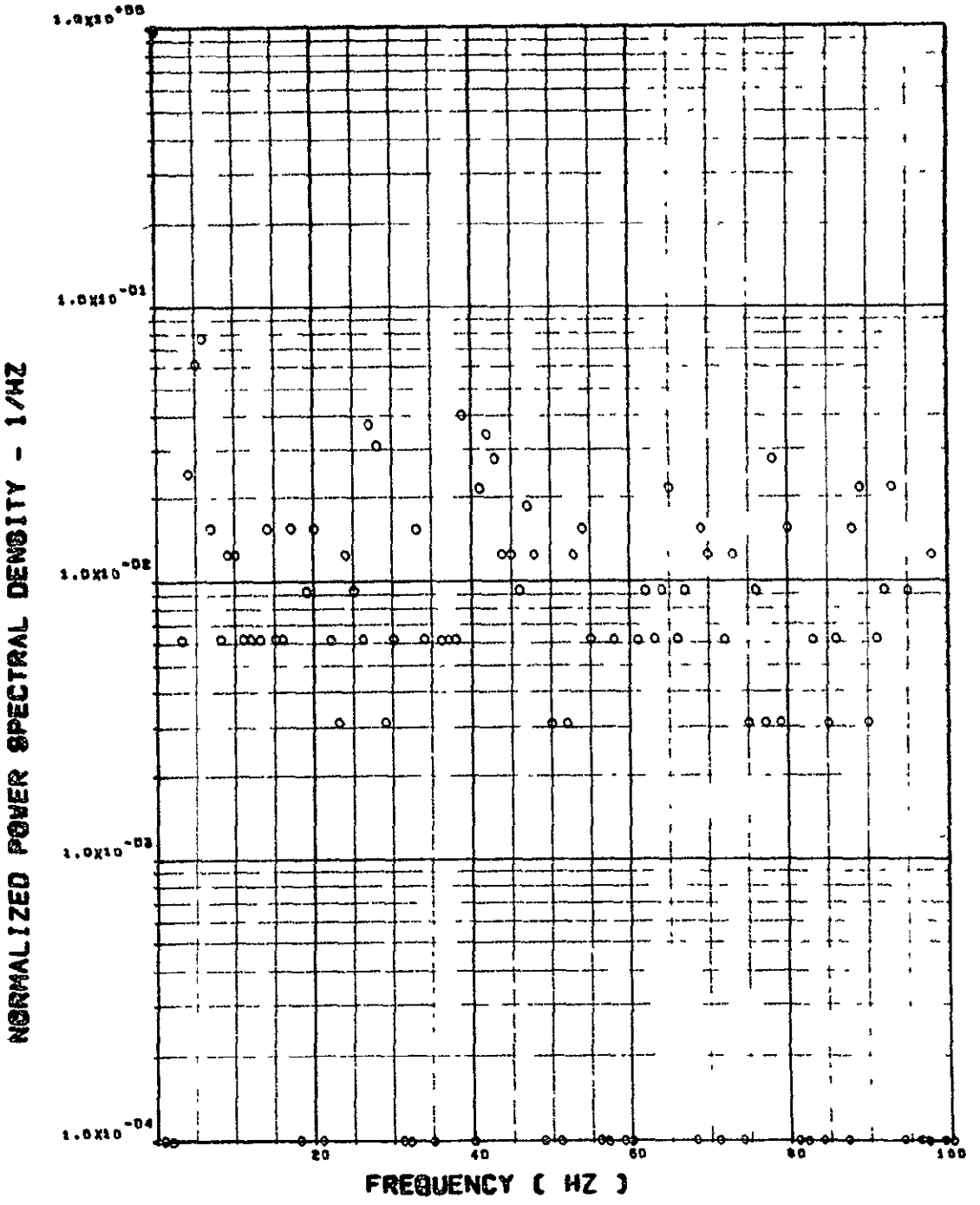

Figure 21. Continued

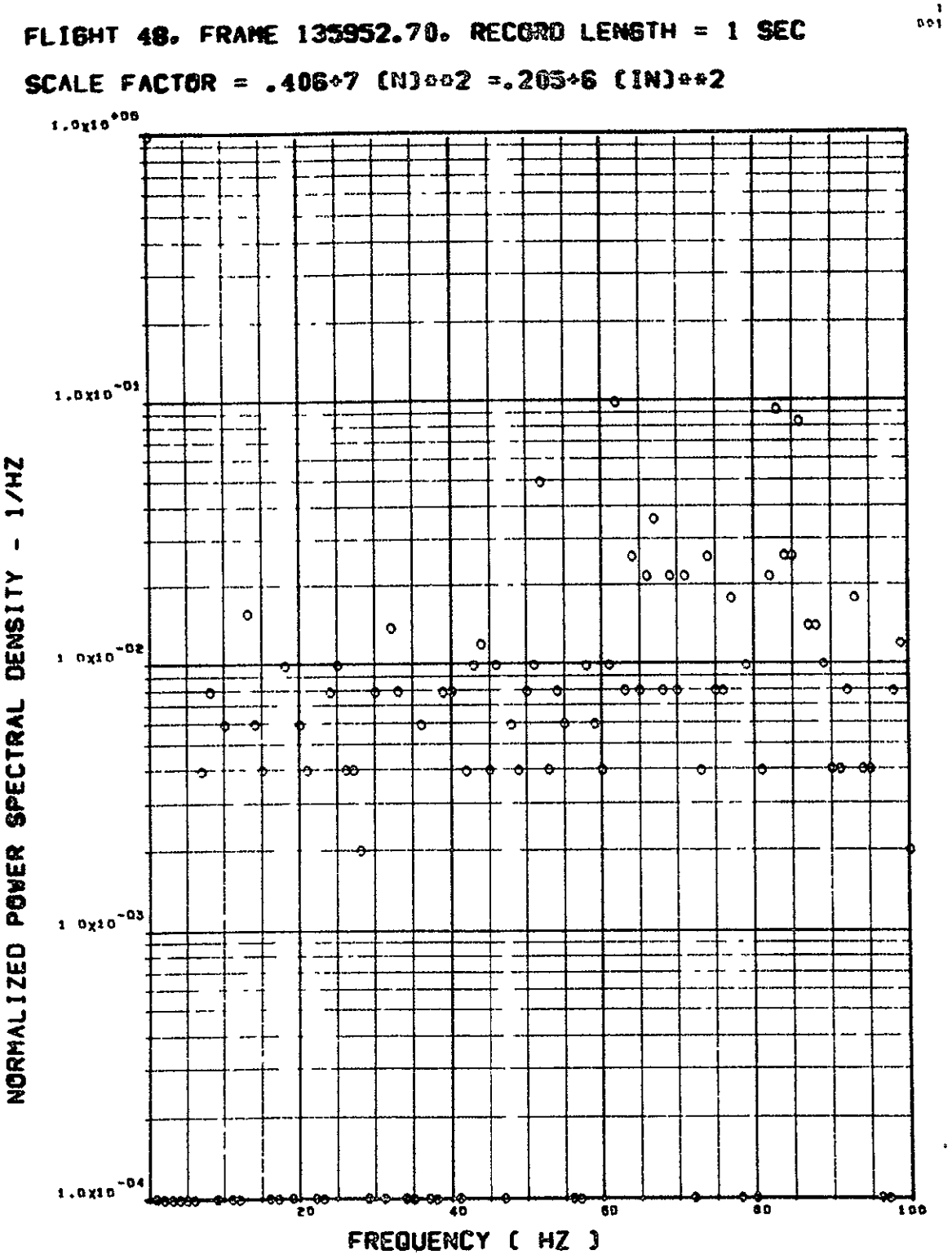

Figure 21. Continued

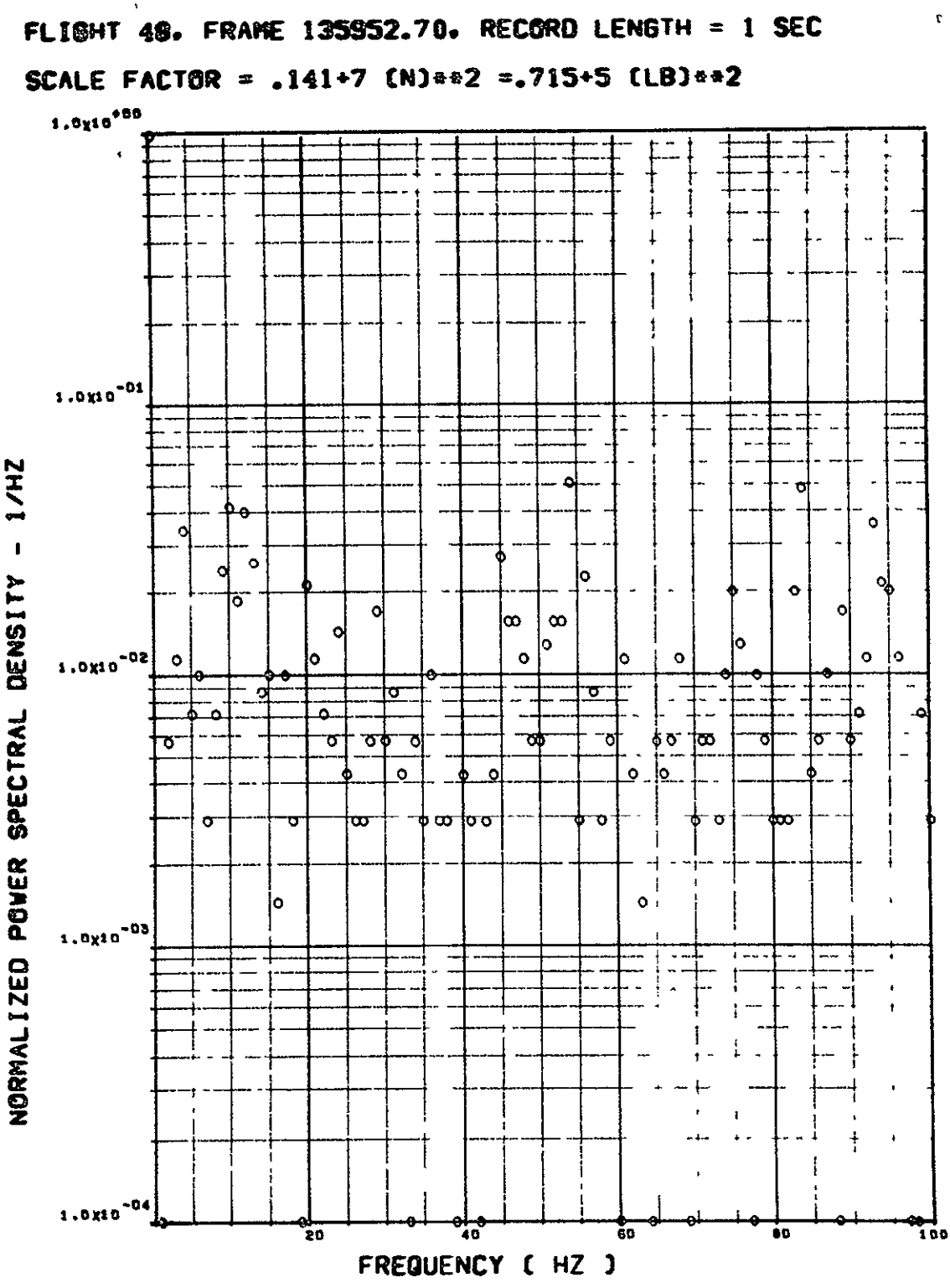

Figure 21. Continued

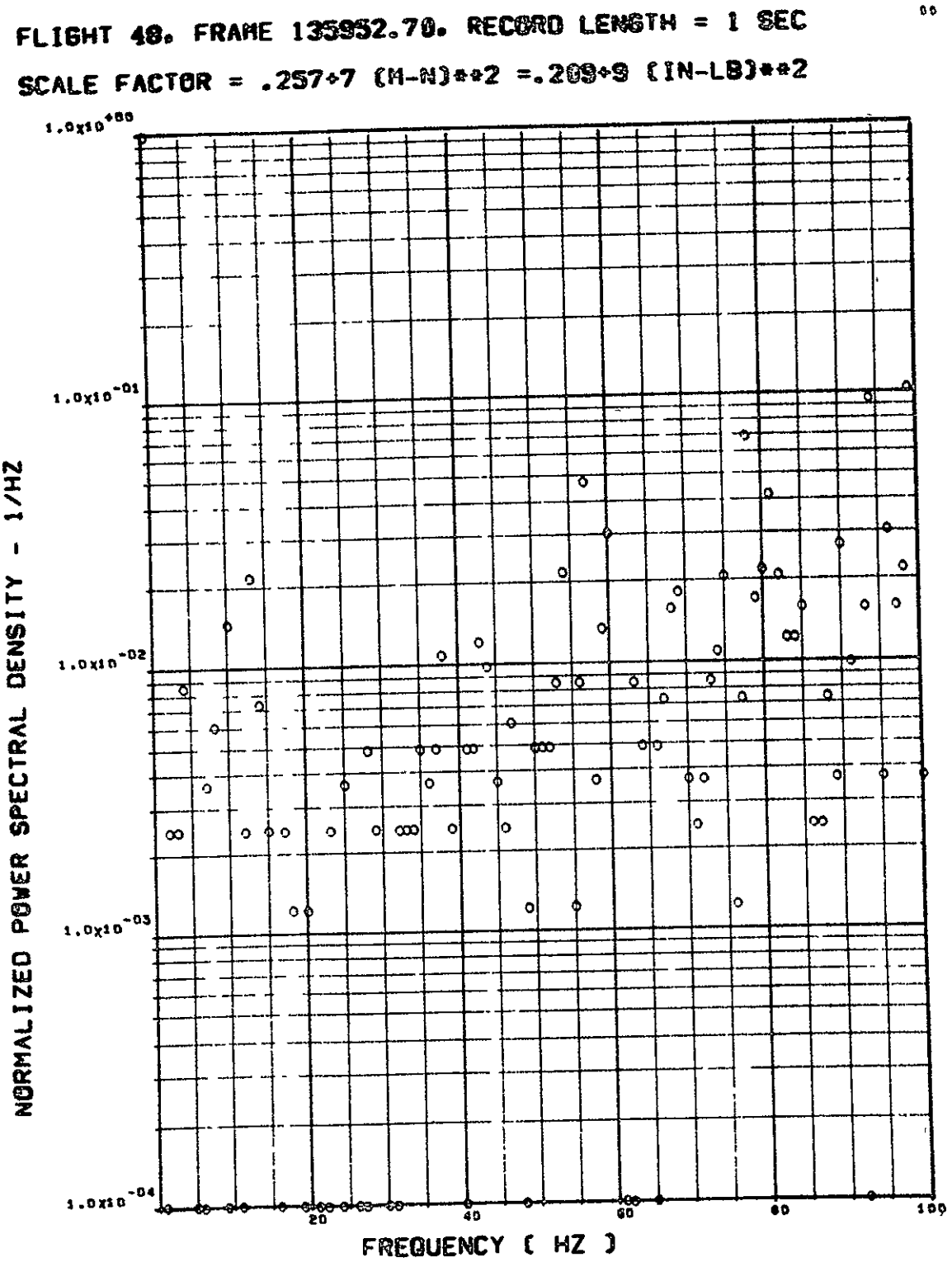

Figure 21. Continued

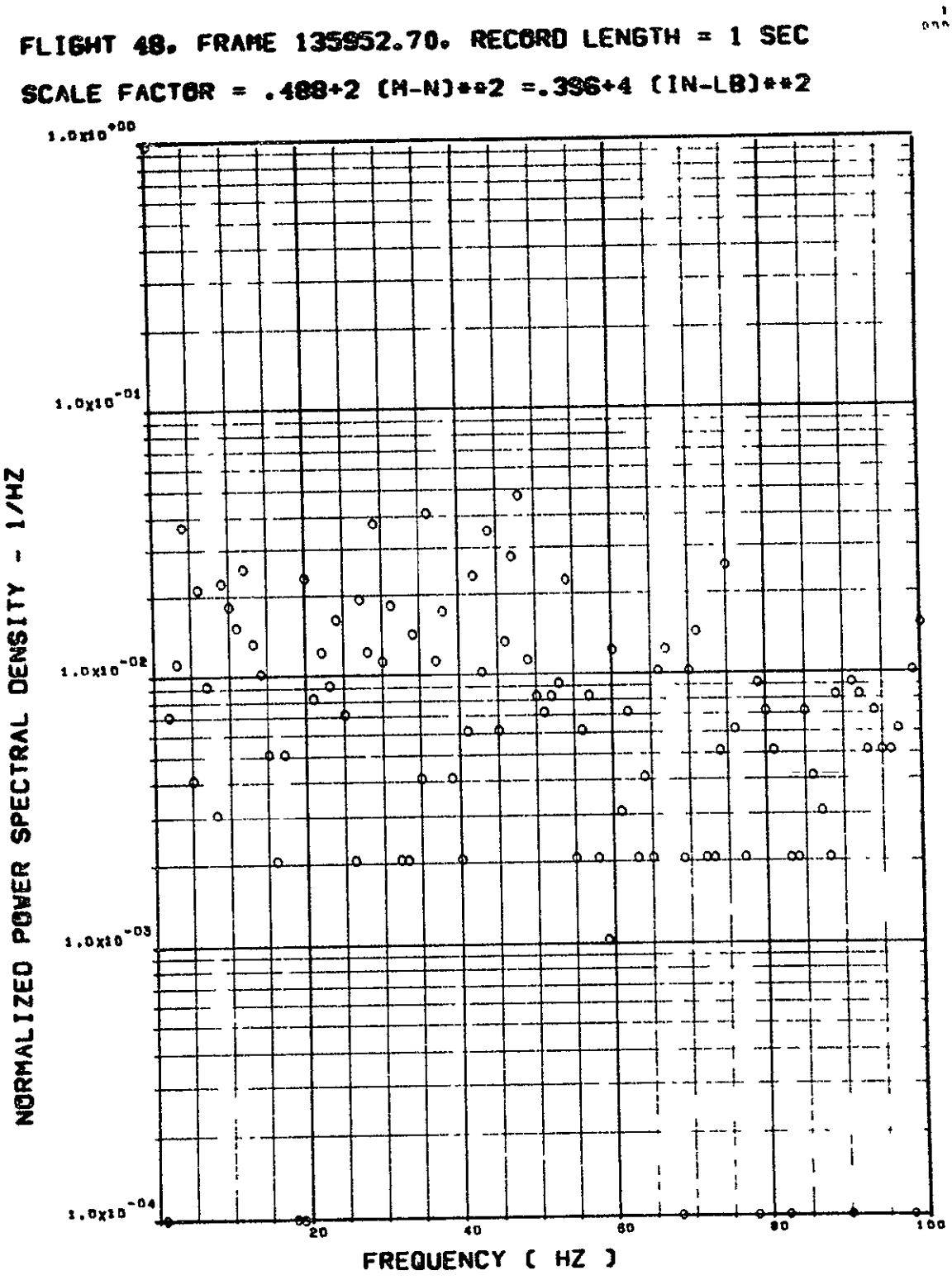

Figure 21. Continued

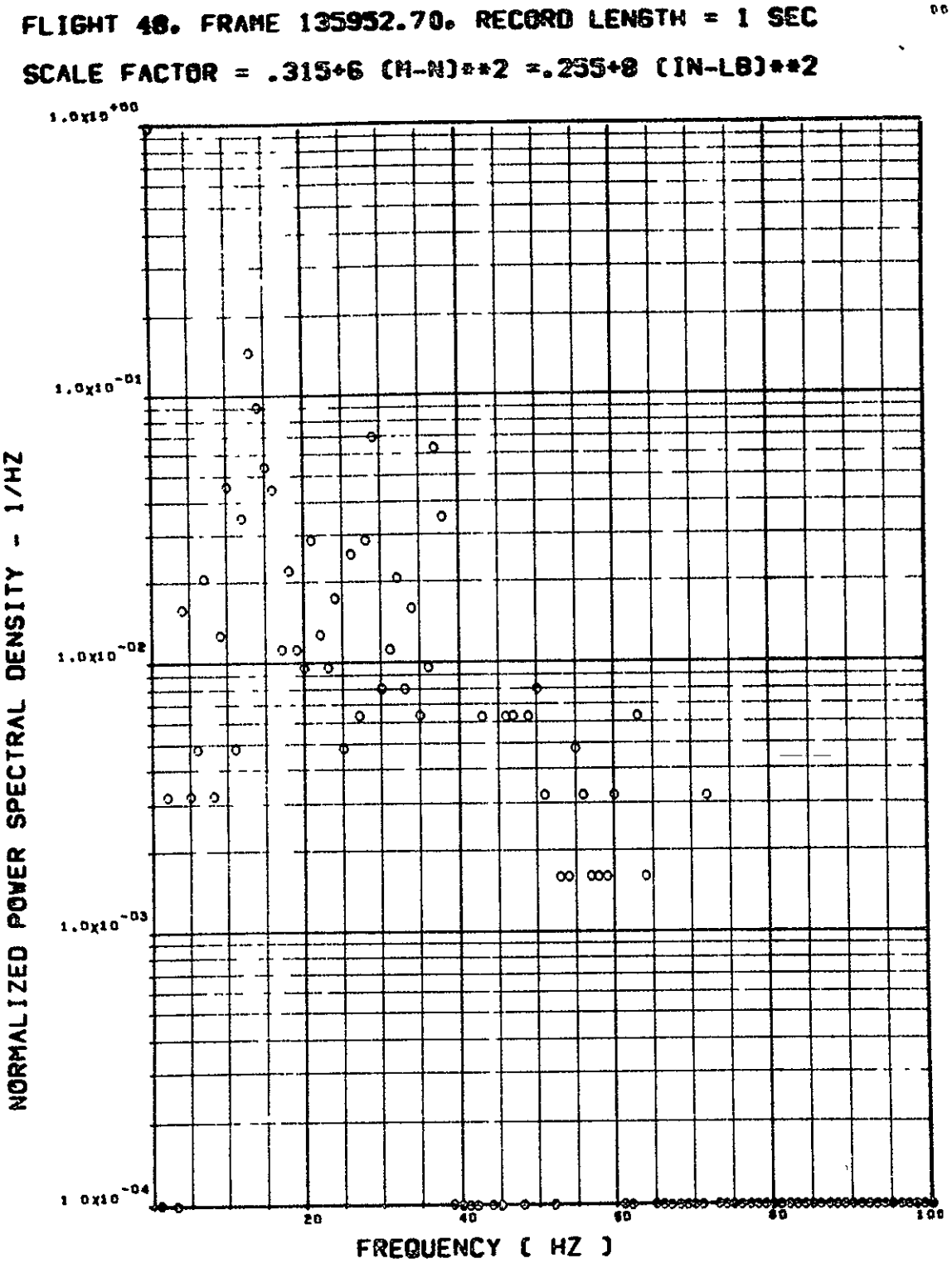

Figure 21. Continued

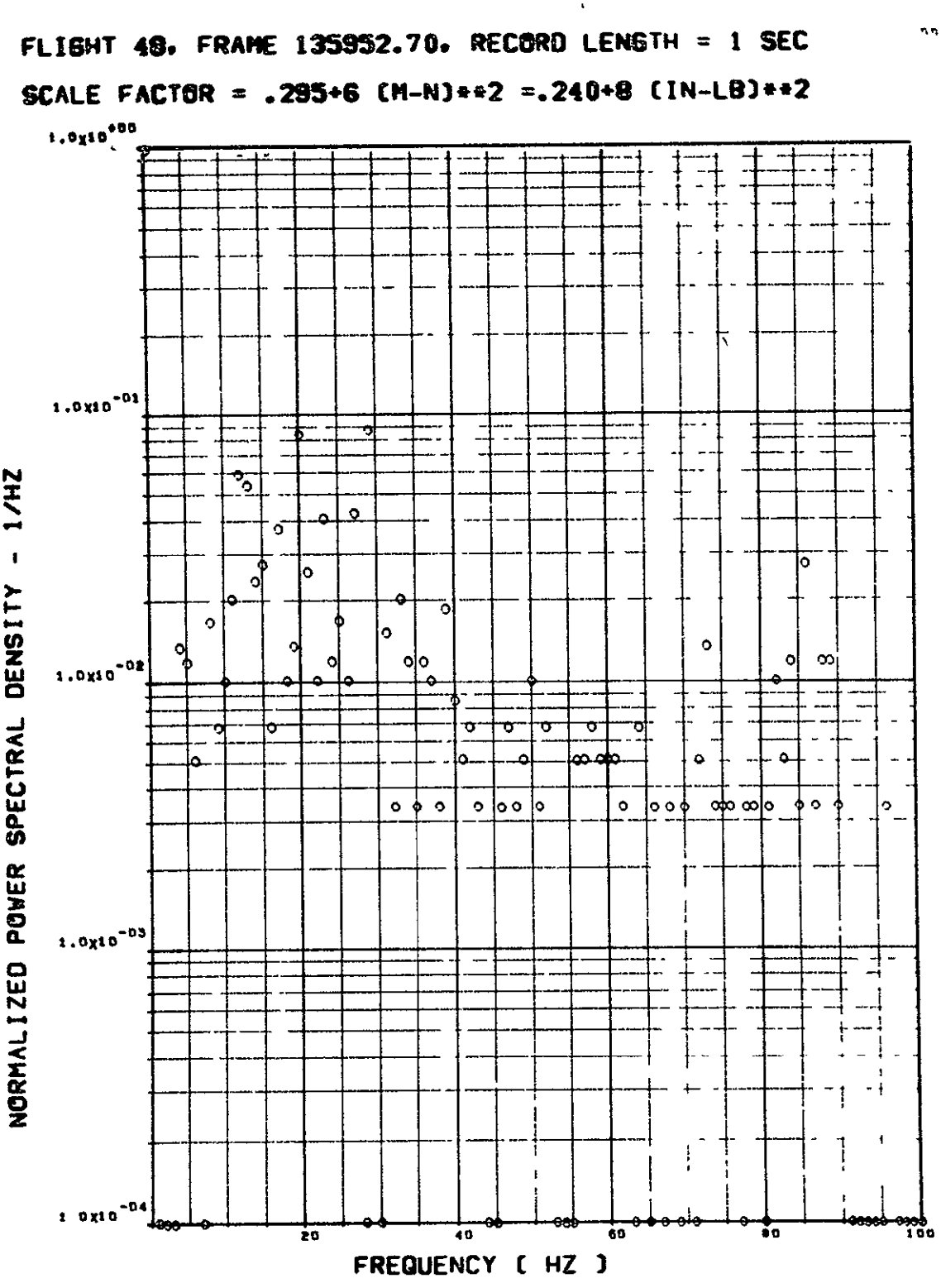

Figure 21. Concluded

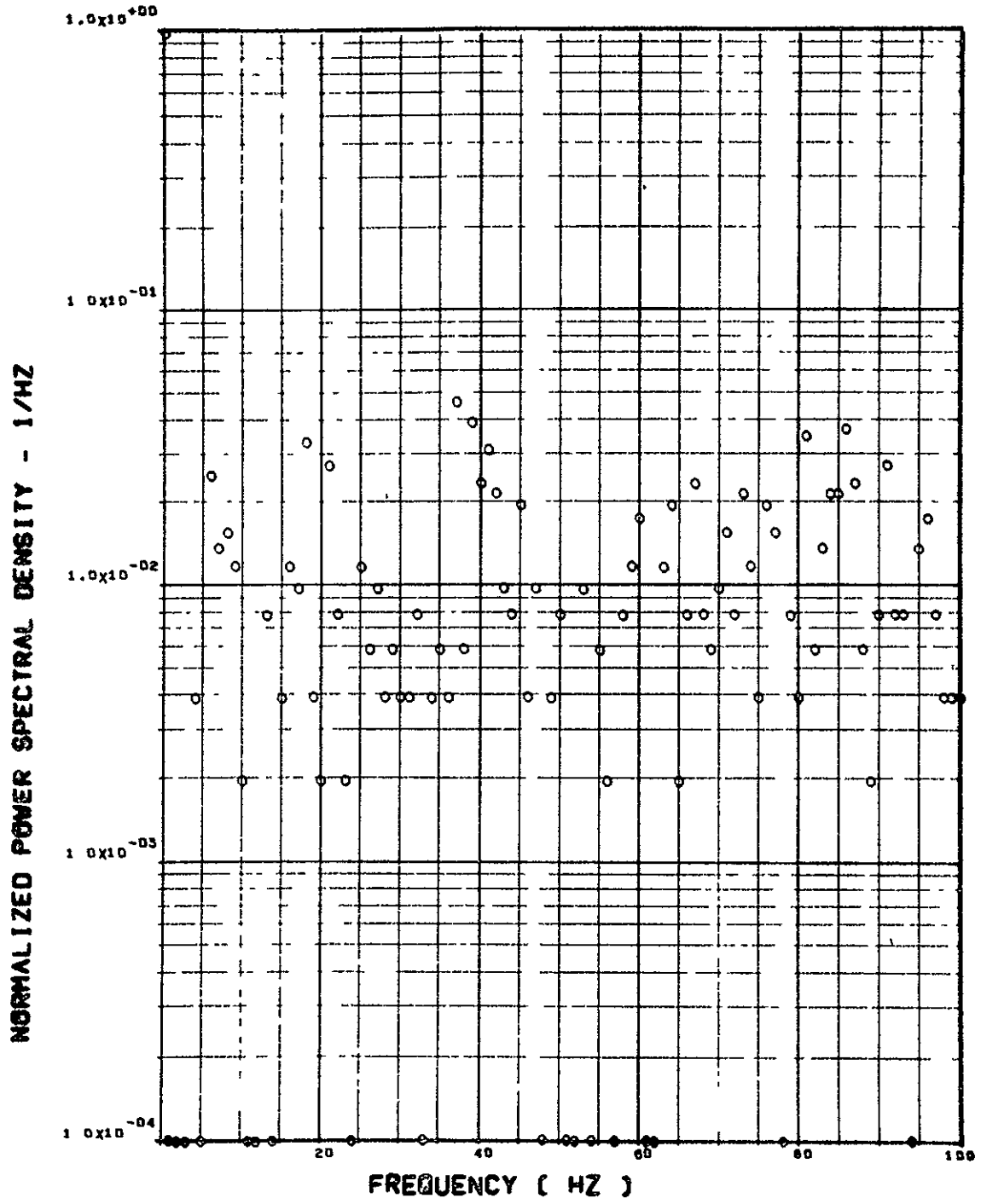

Figure 22. Power Spectra - Flight 48, Run 7R1, Point 3 T_1 = 135954.3, ΔT = 1 Sec, α_{Nom} = 11.62 deg, $\Delta\alpha$ = 1.45 deg.

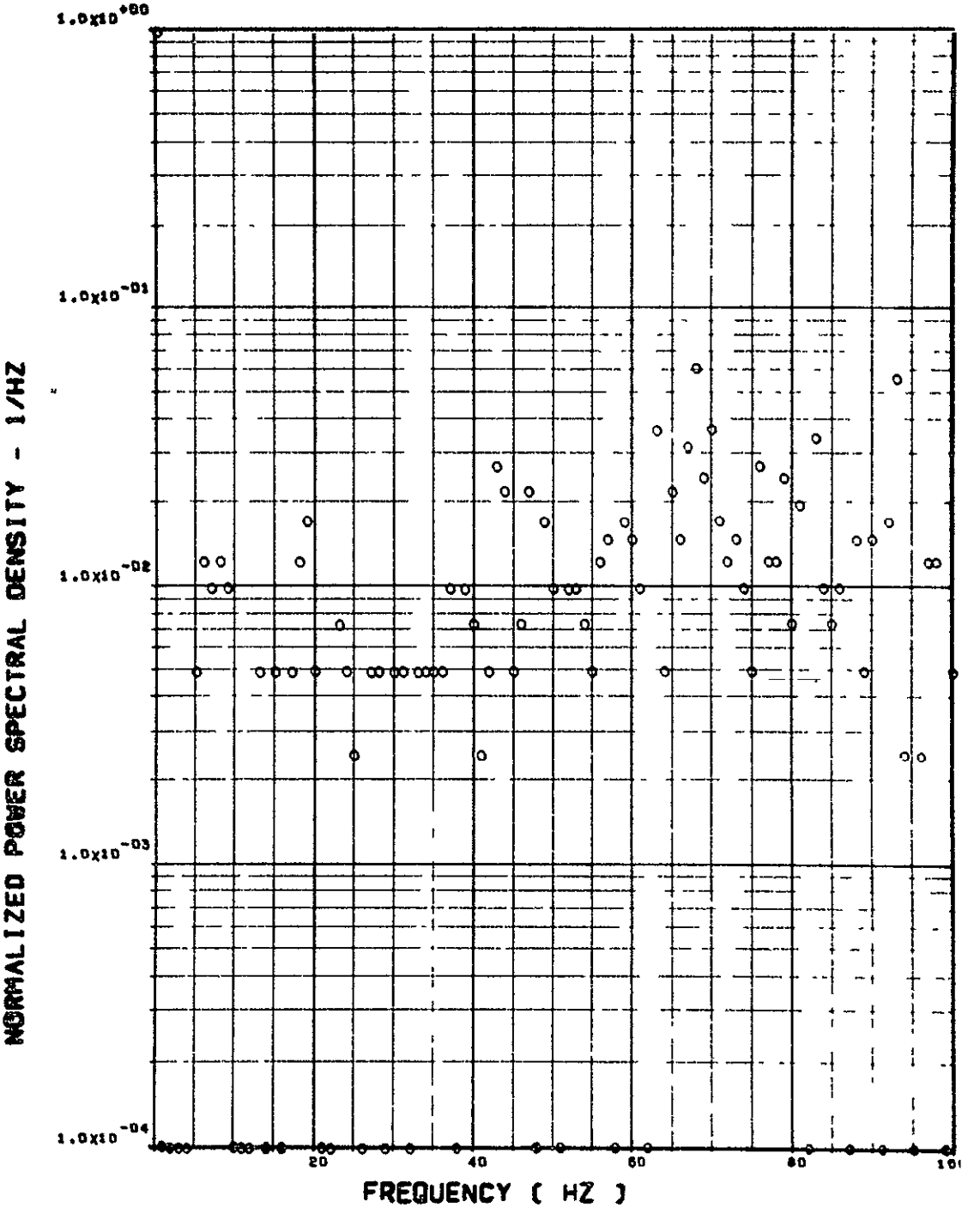

Figure 22. Continued

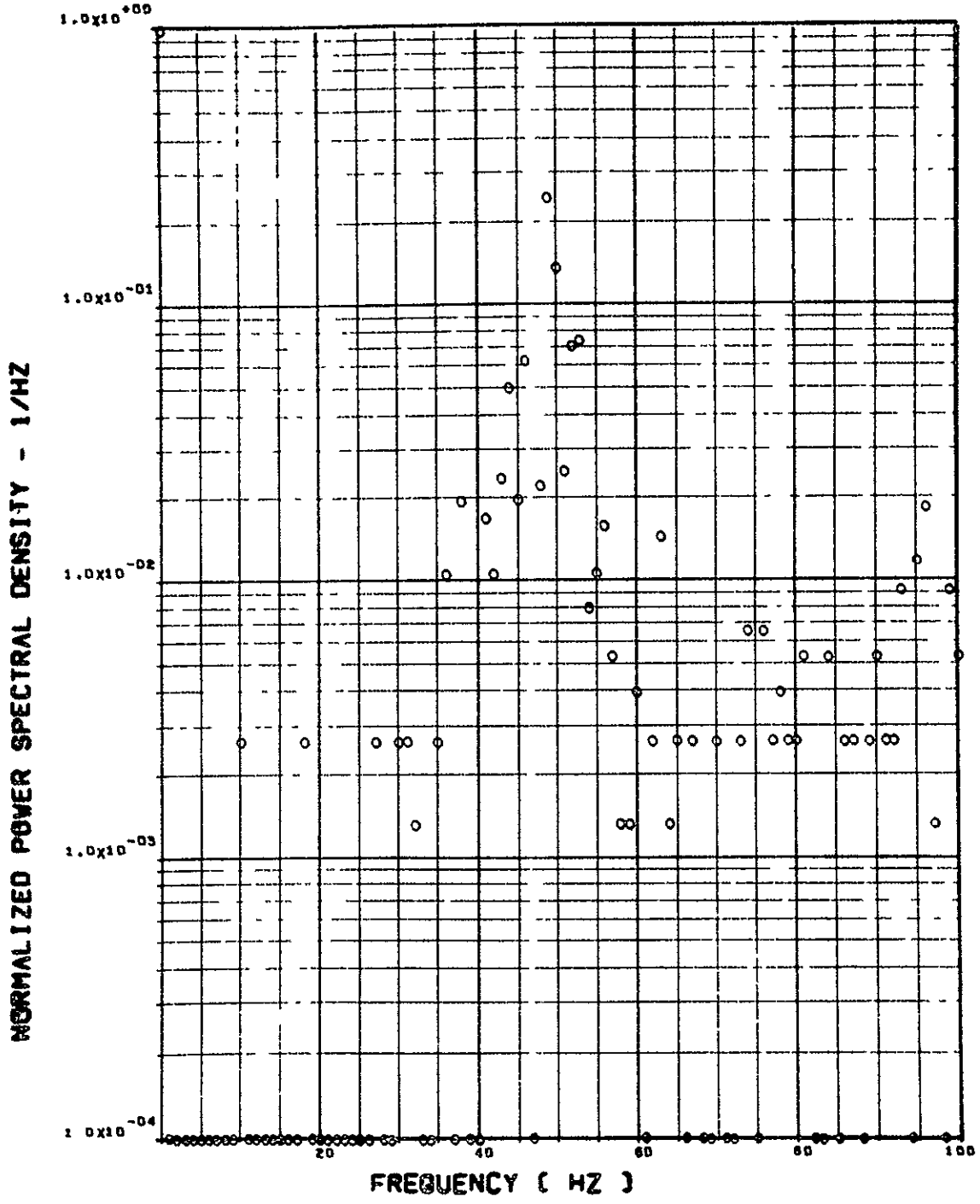

Figure 22. Continued

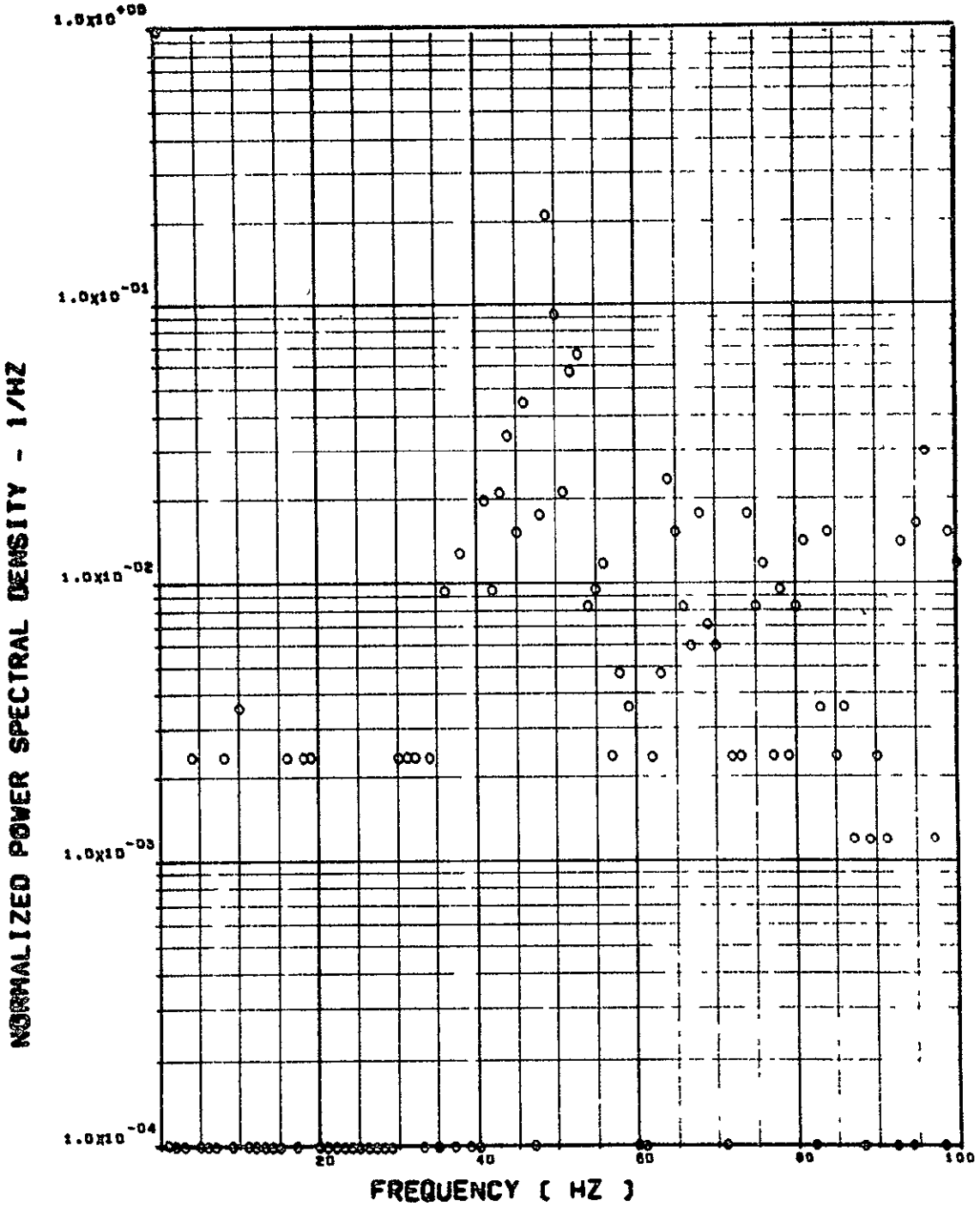

Figure 22. Continued

FLIGHT 48. FRAME 135854.30. RECORD LENGTH = 1 SEC.

SCALE FACTOR = .134-2 (6)**2

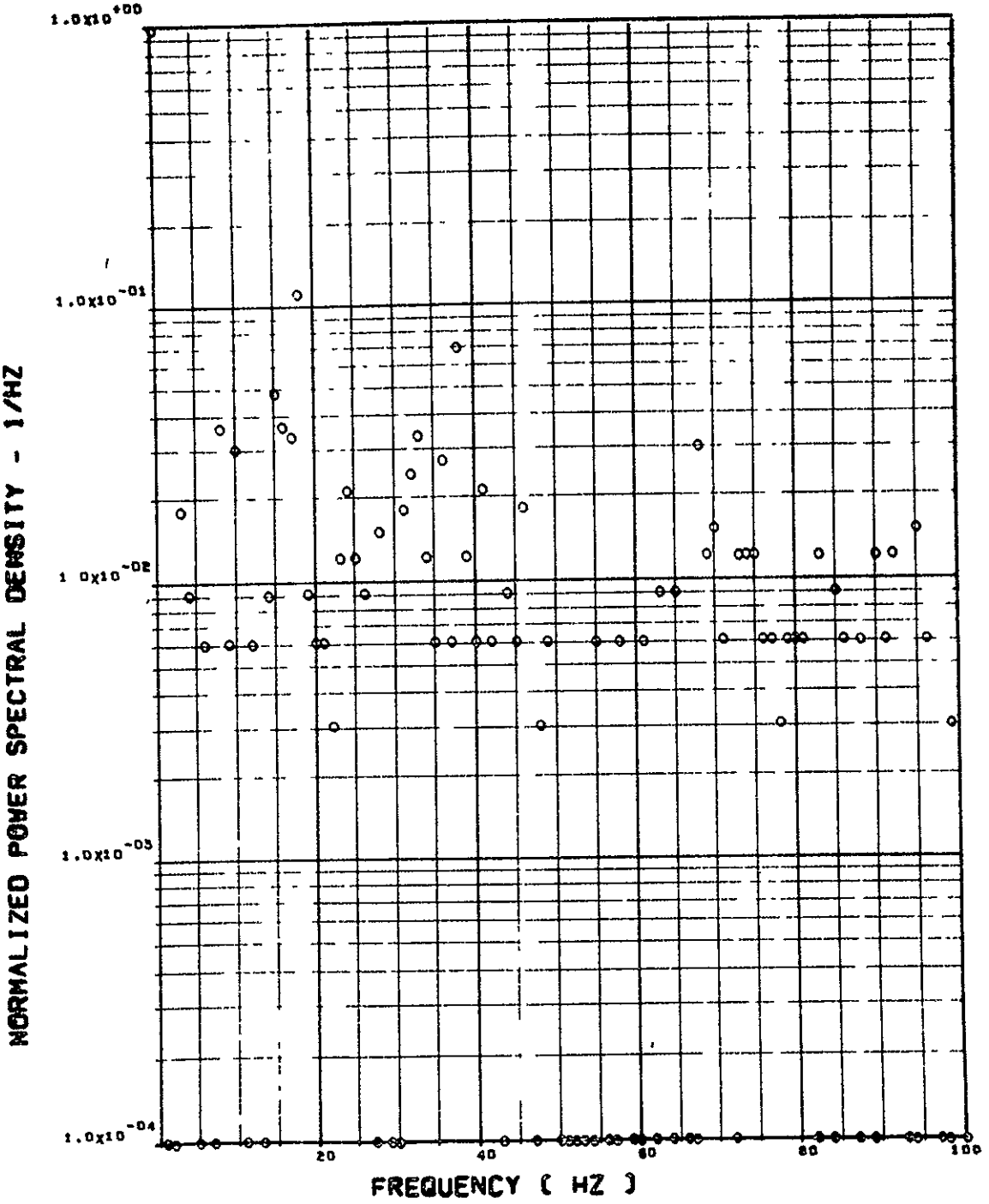

ITEM - AF008 PILOT'S SEAT VERTICAL ACCELEROMETER

Figure 22. Continued

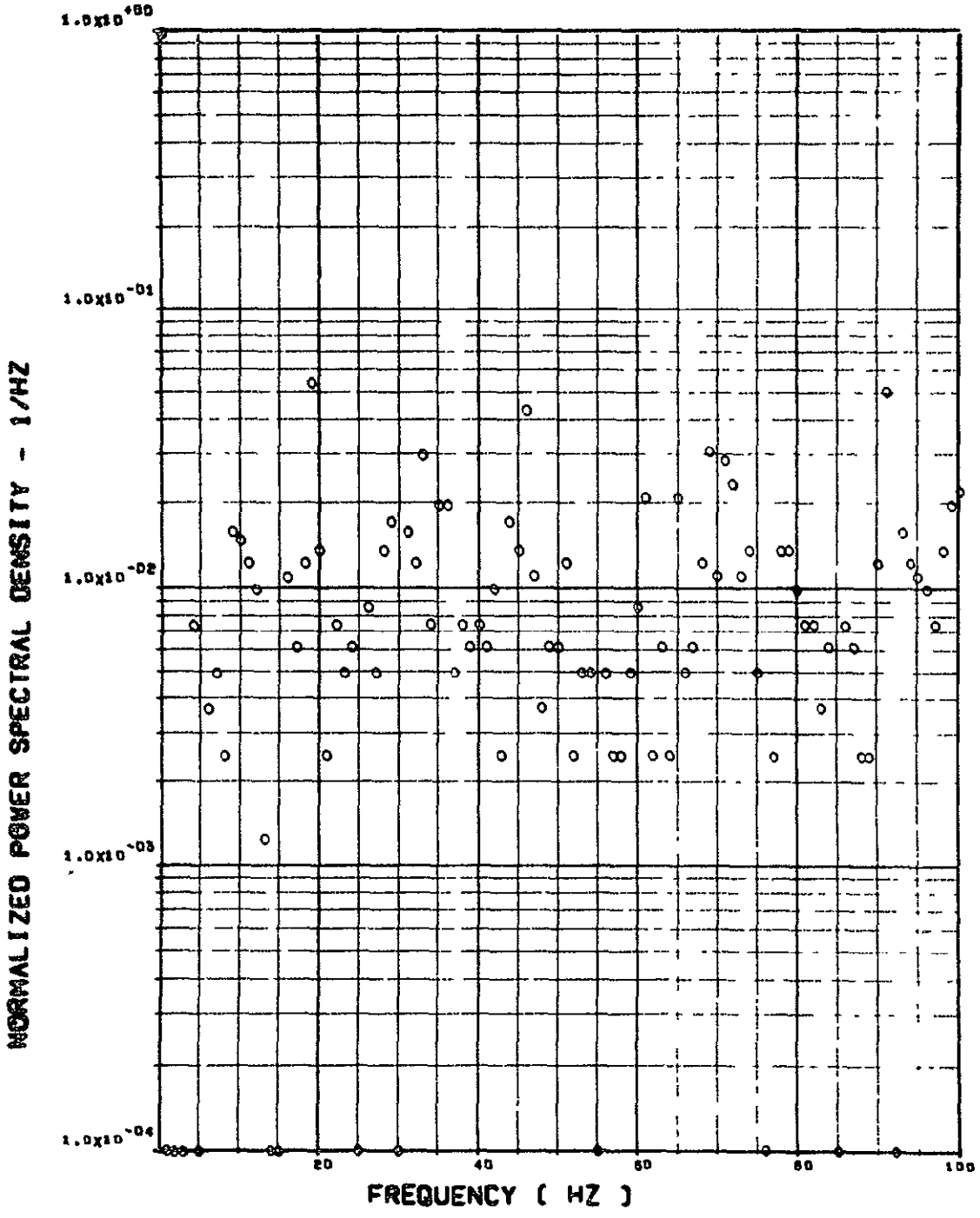

Figure 22. Continued

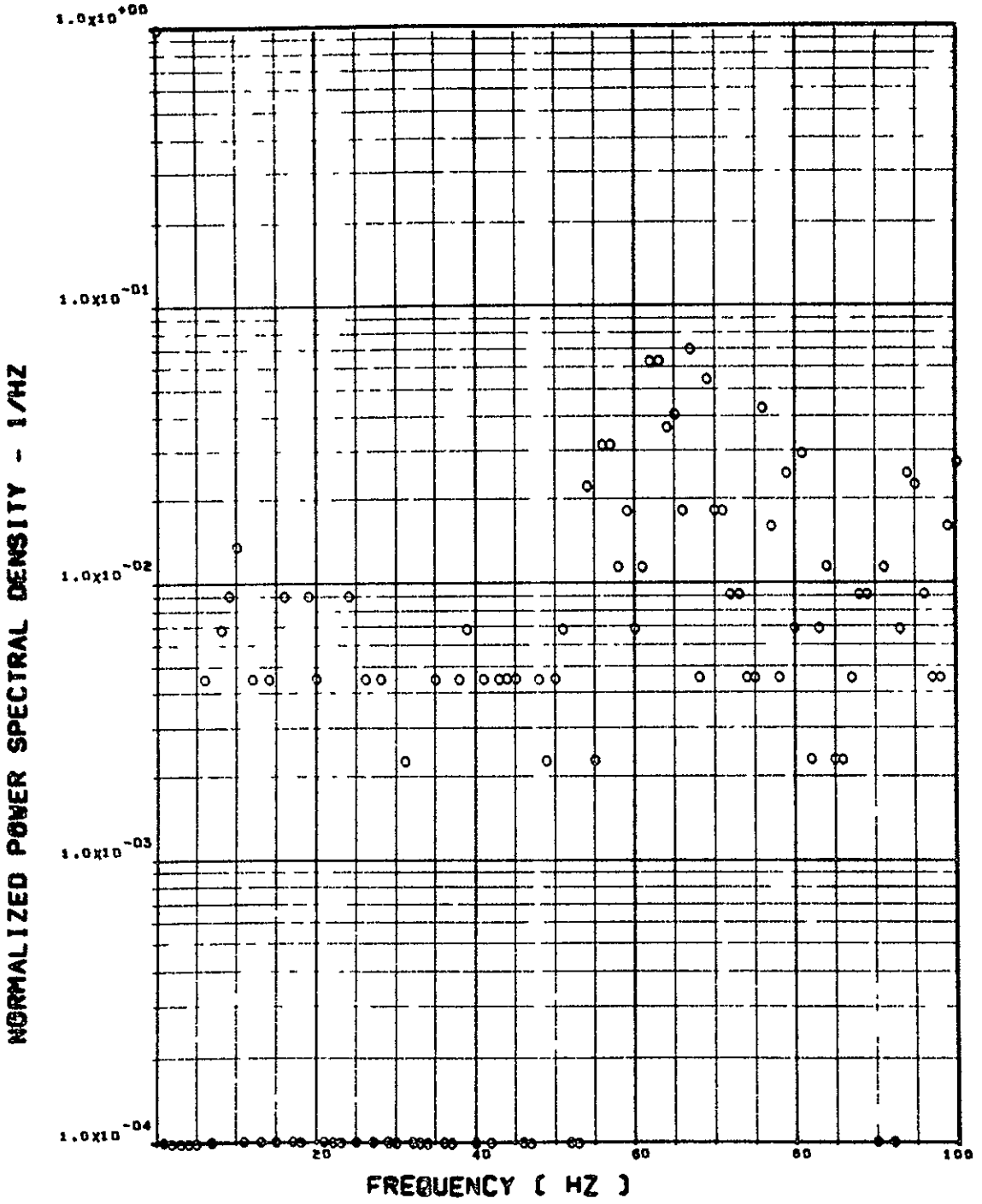

Figure 22. Continued

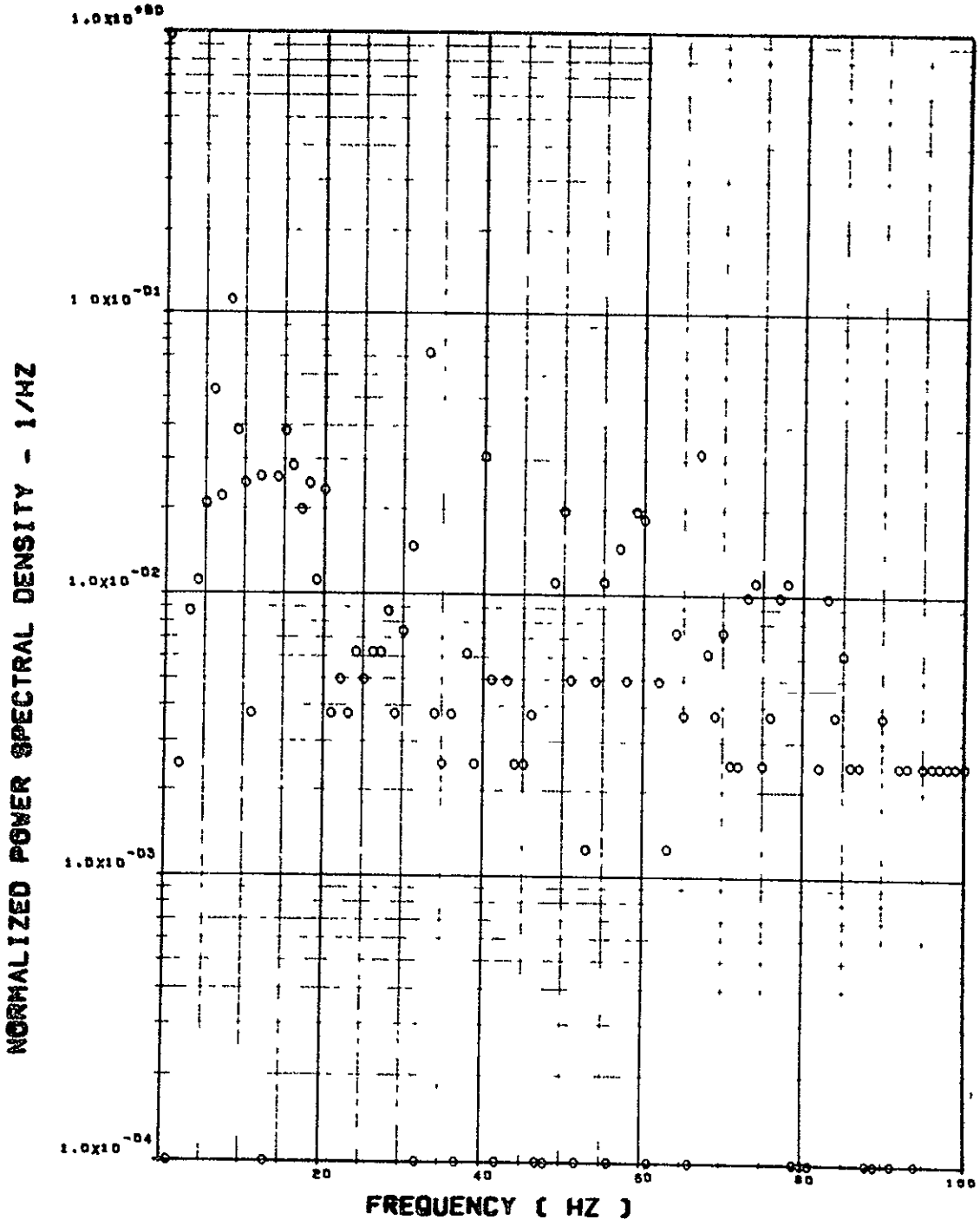

Figure 22. Continued

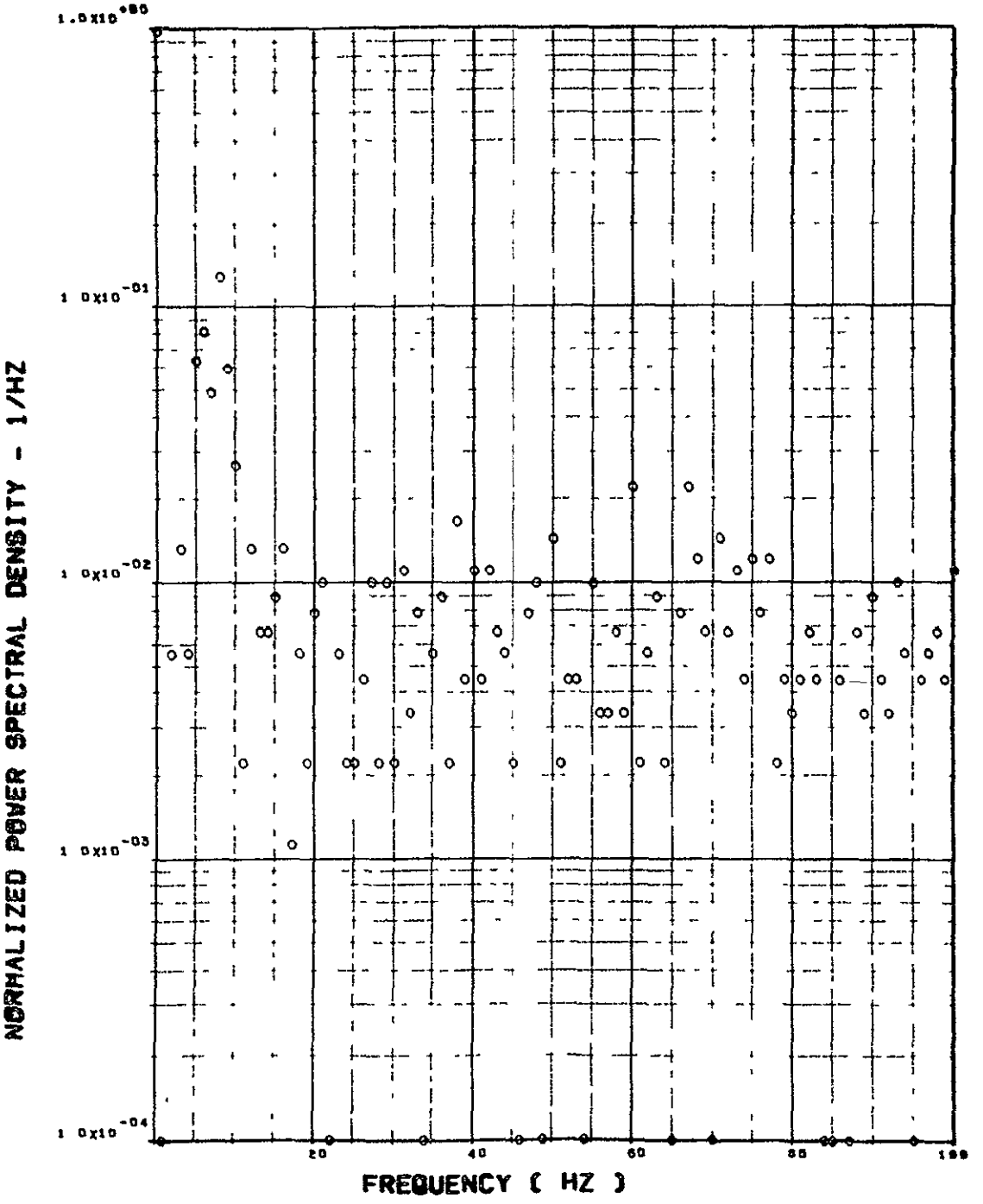

Figure 22. Continued

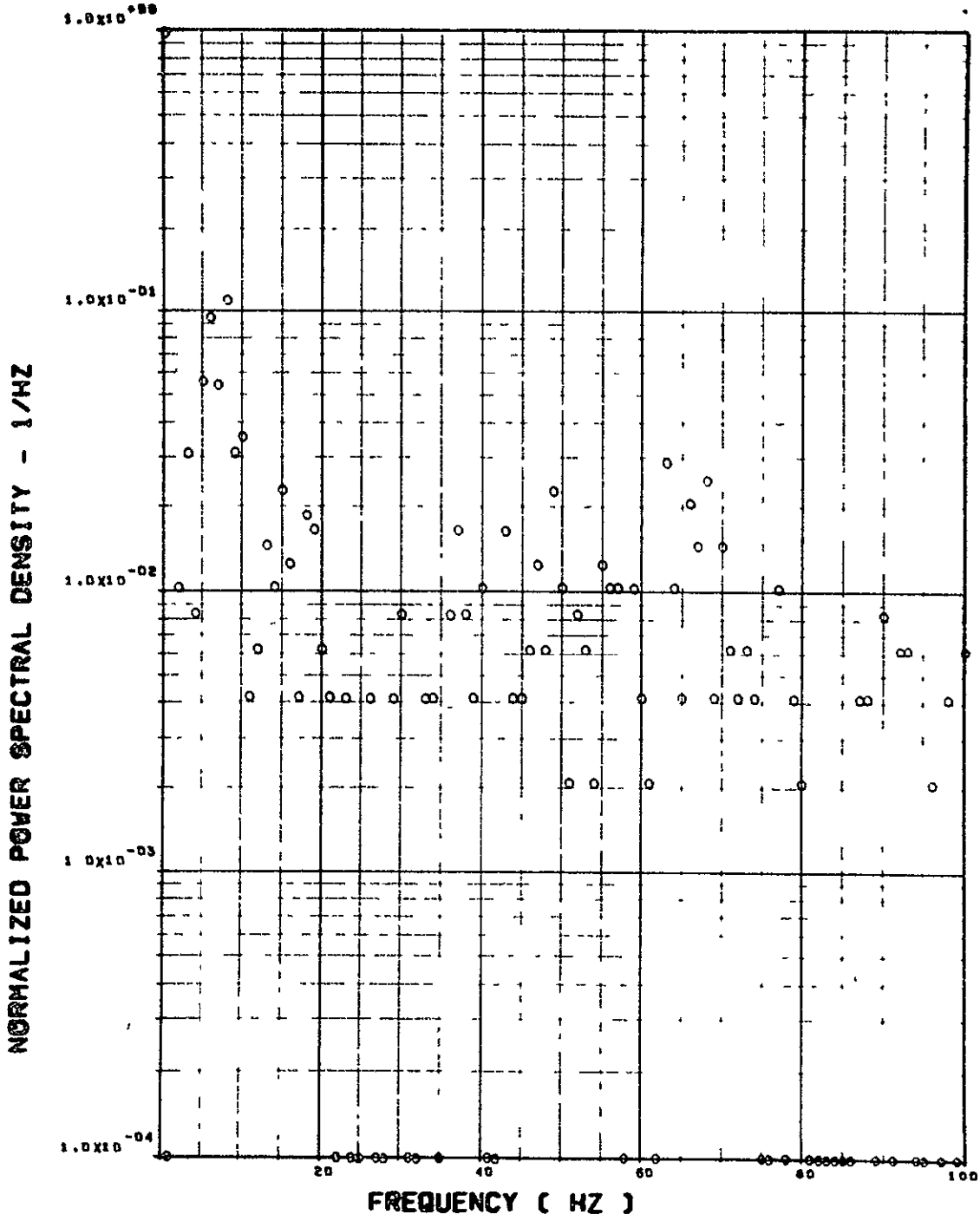

Figure 22. Continued

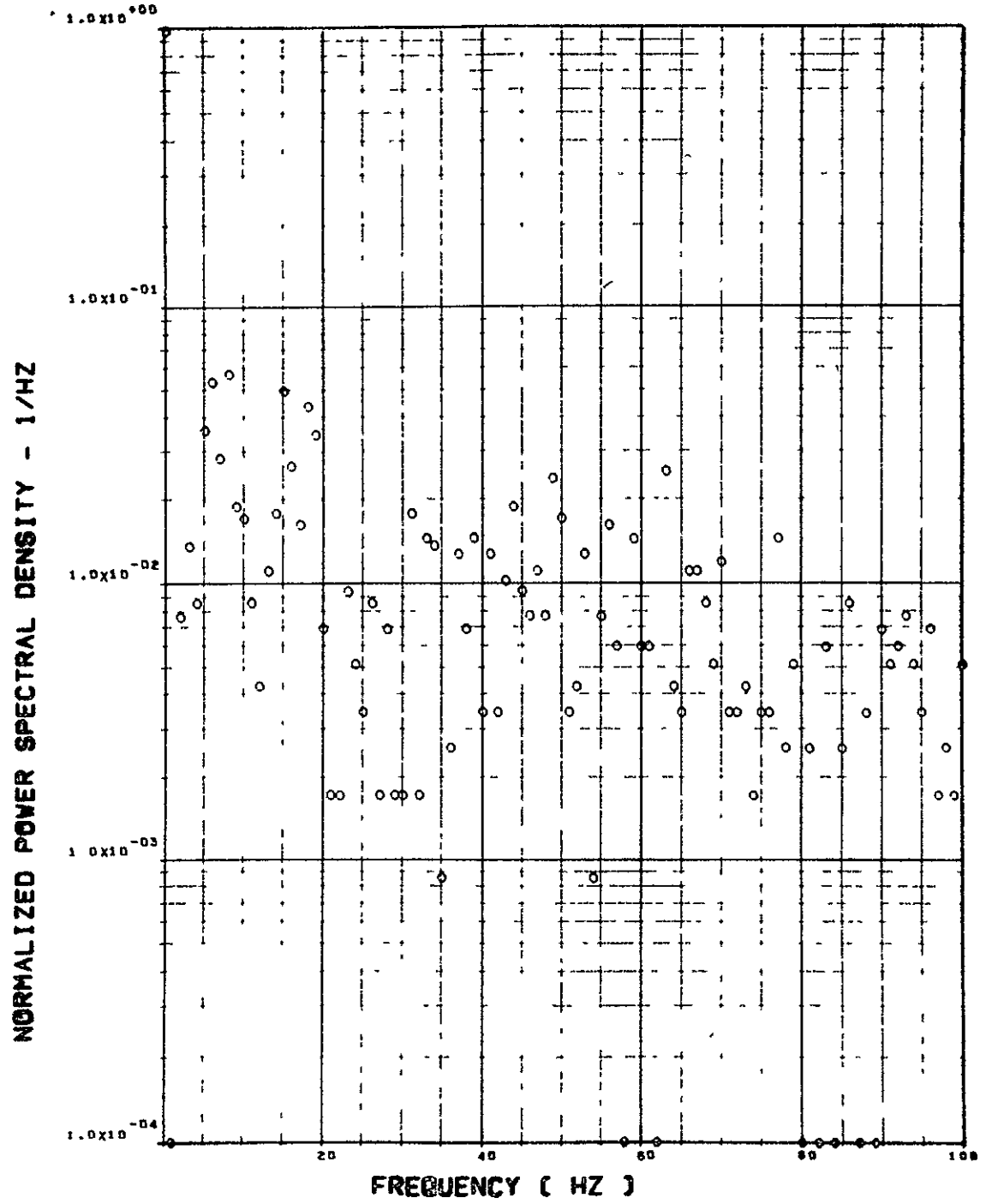

Figure 22. Continued

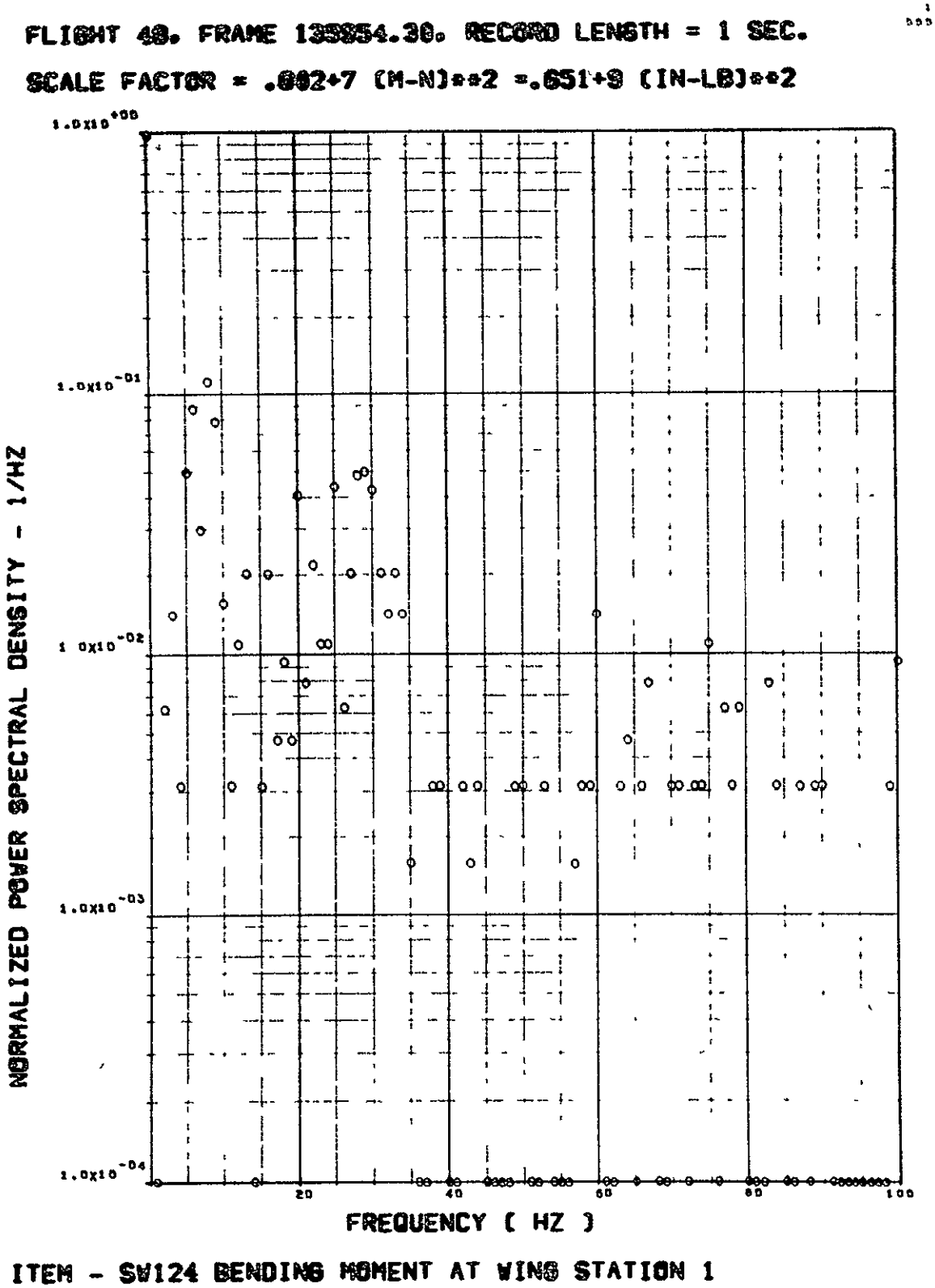

Figure 22. Continued

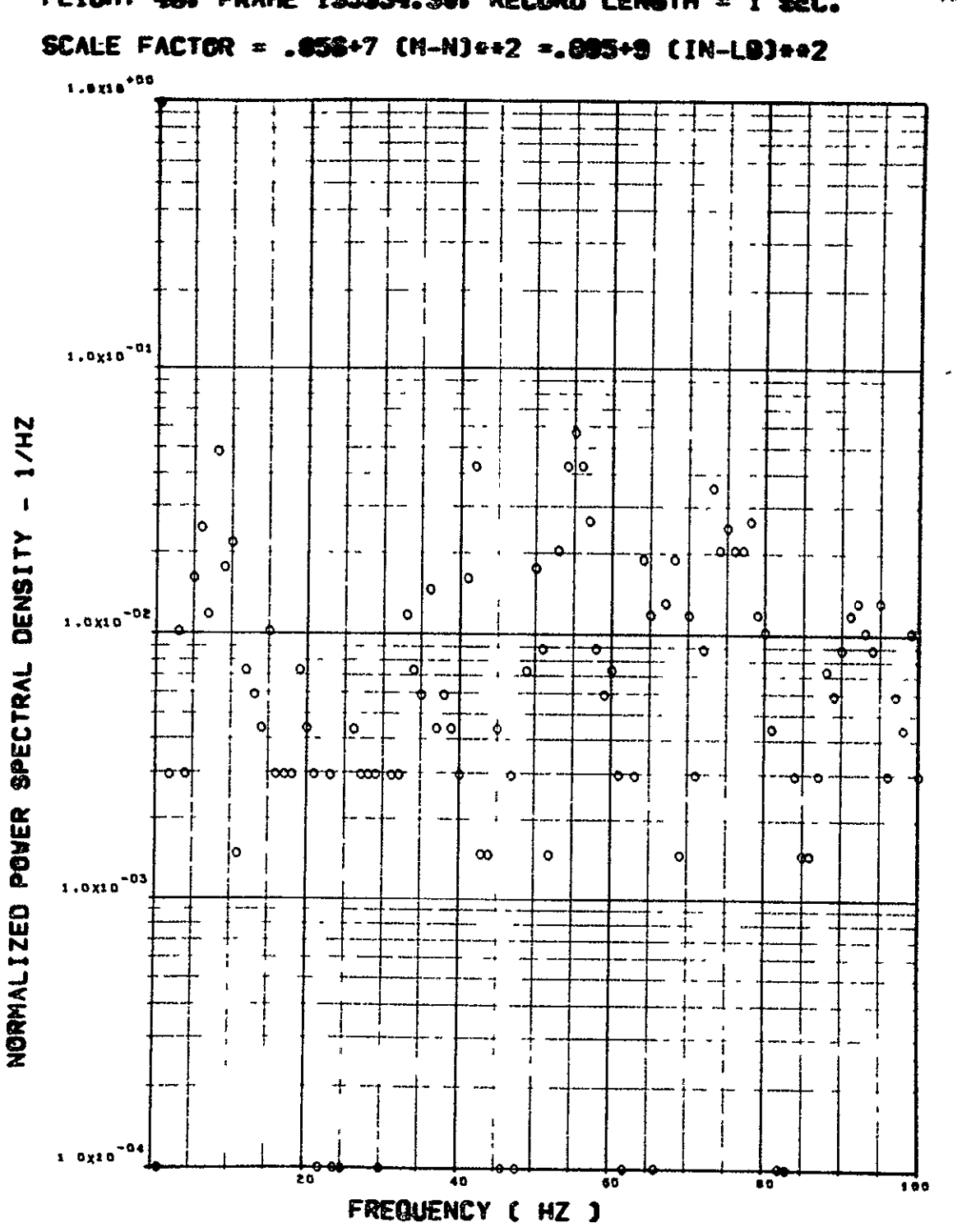

Figure 22. Continued

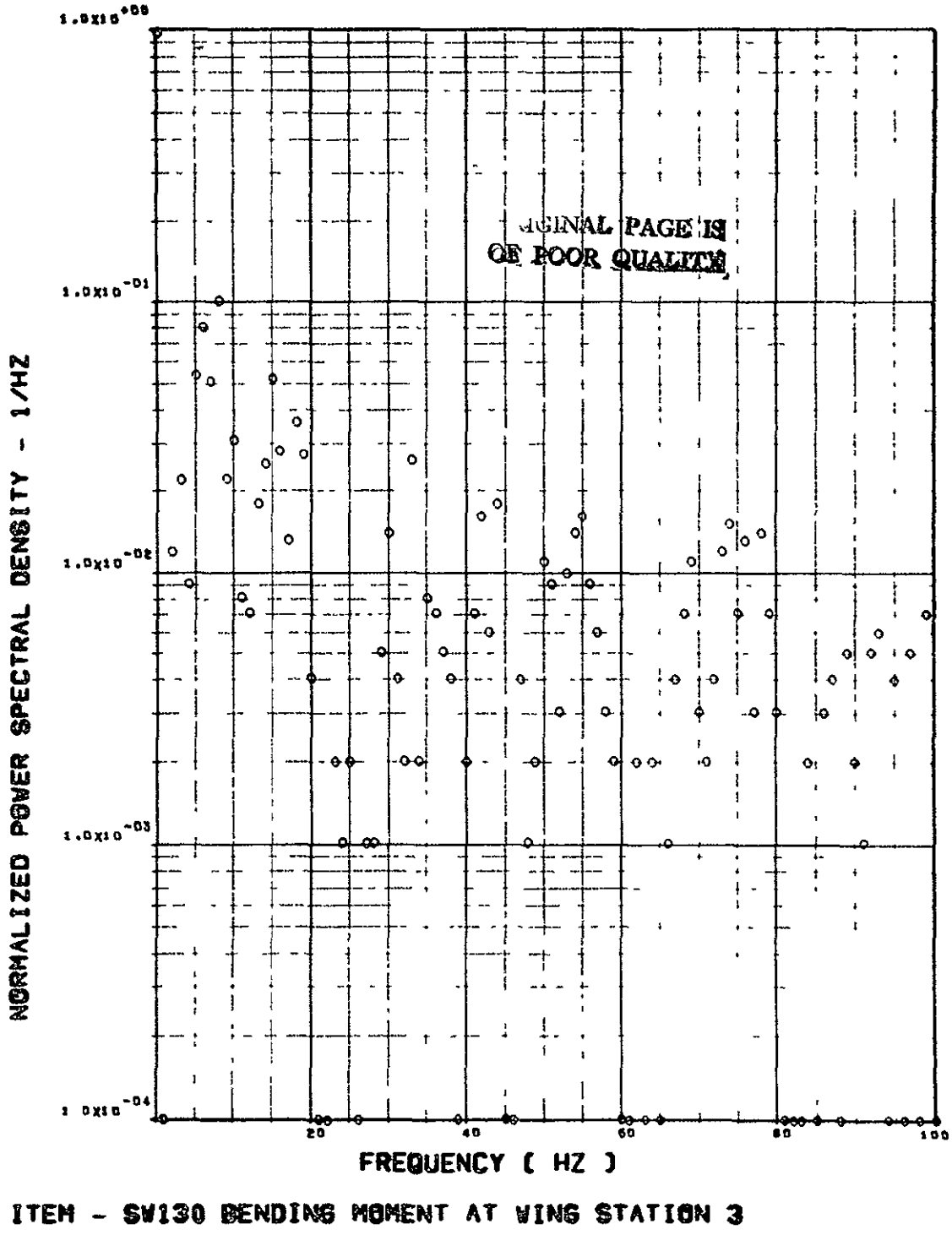

Figure 22. Continued

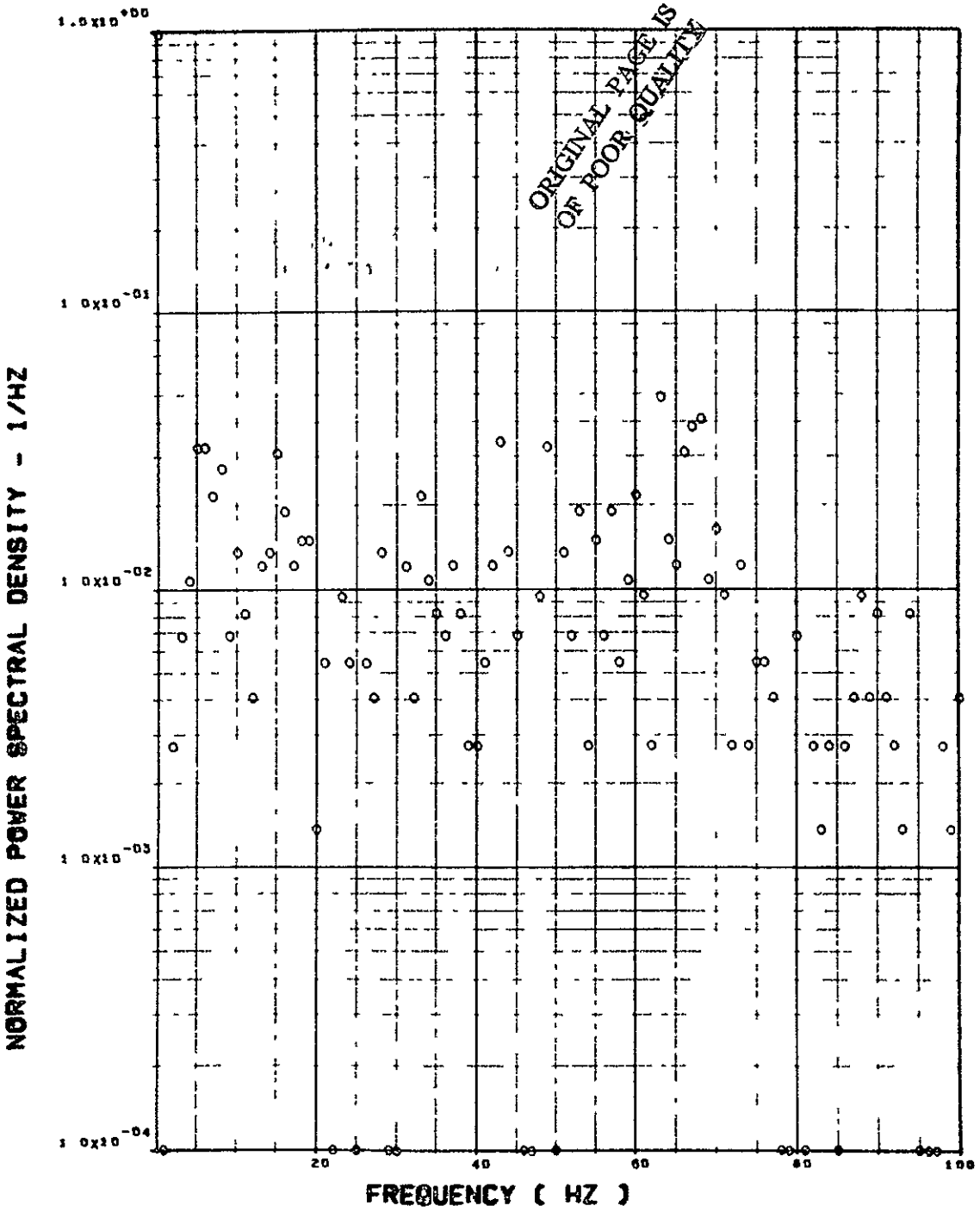

Figure 22. Continued

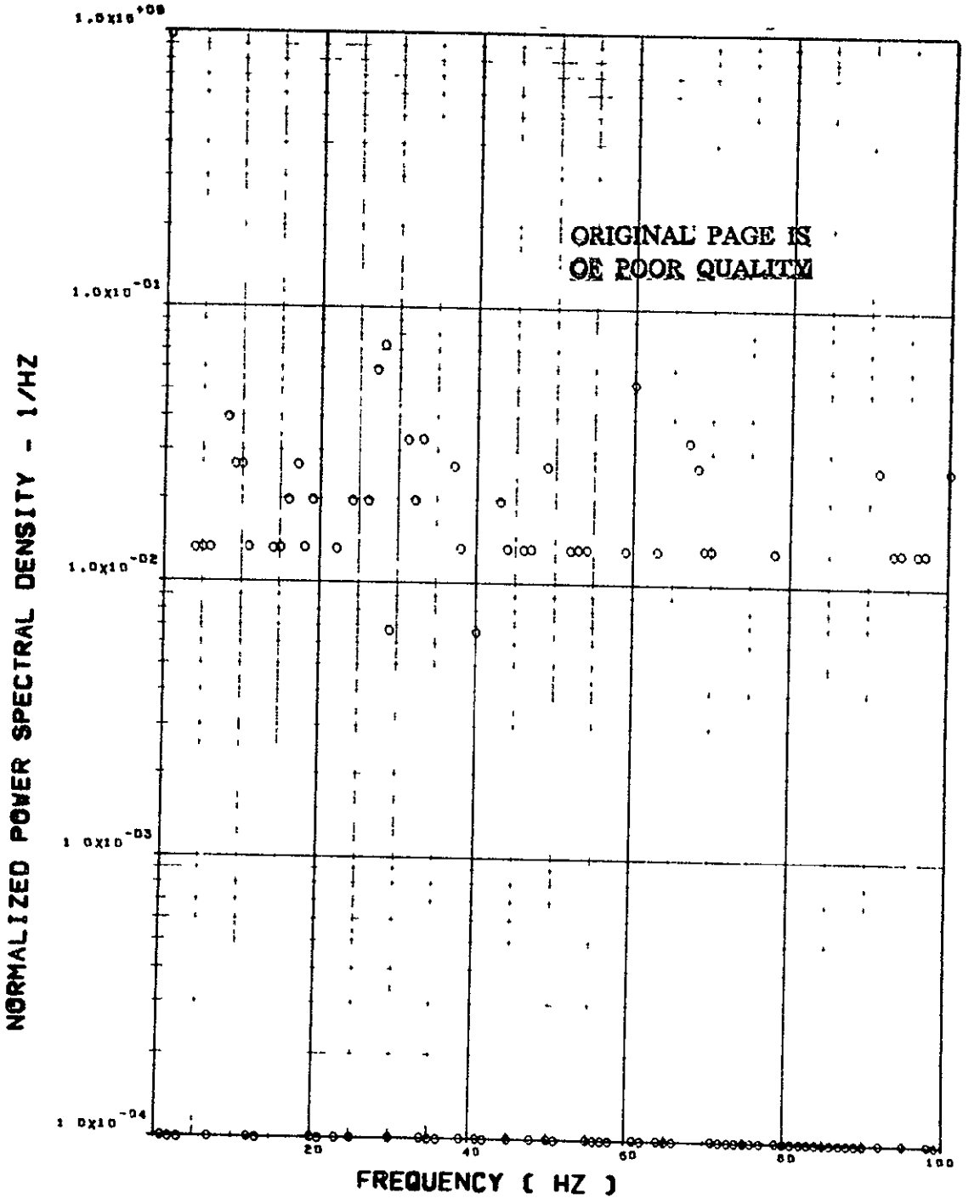

Figure 2. Continued

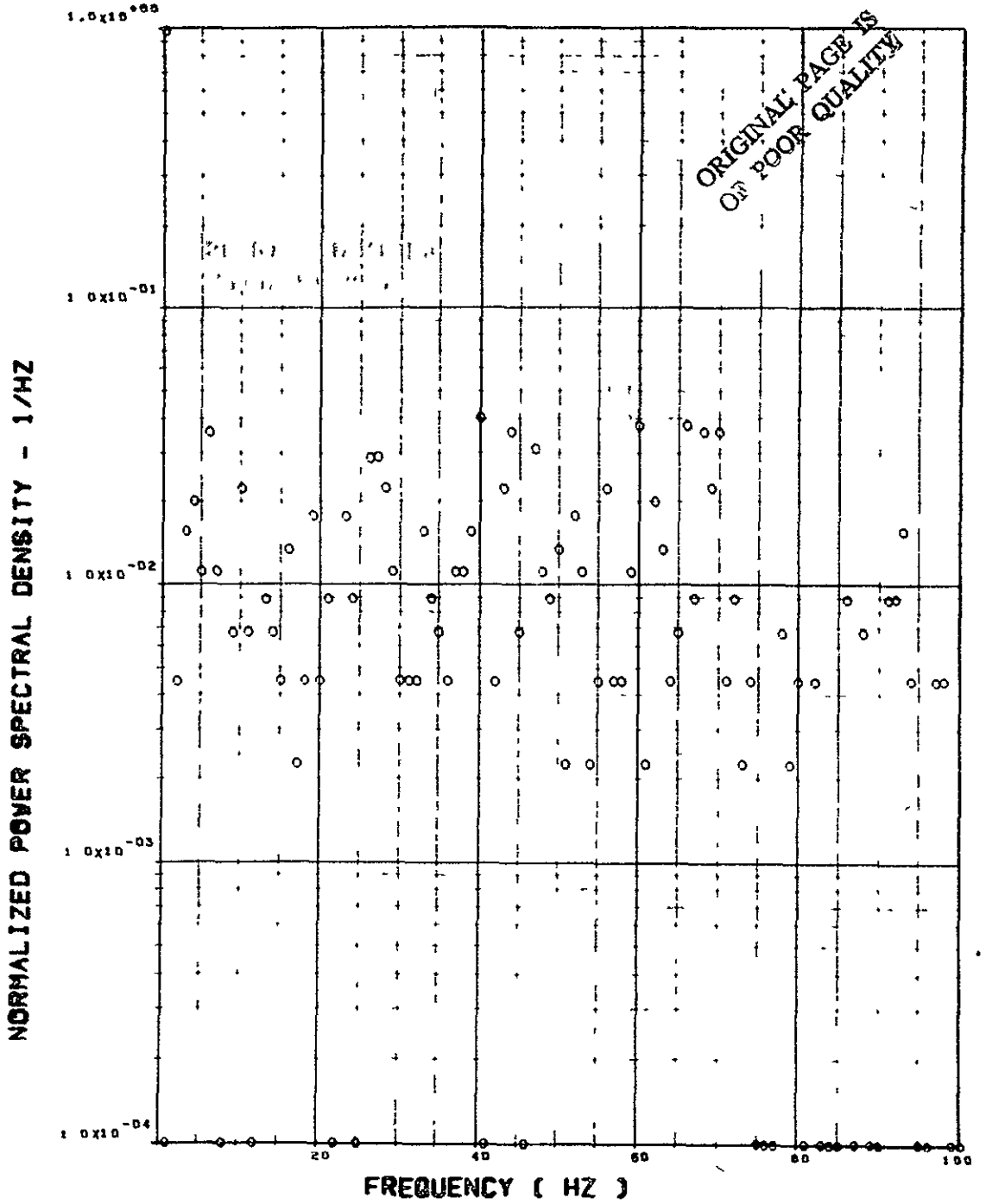

Figure 22. Continued

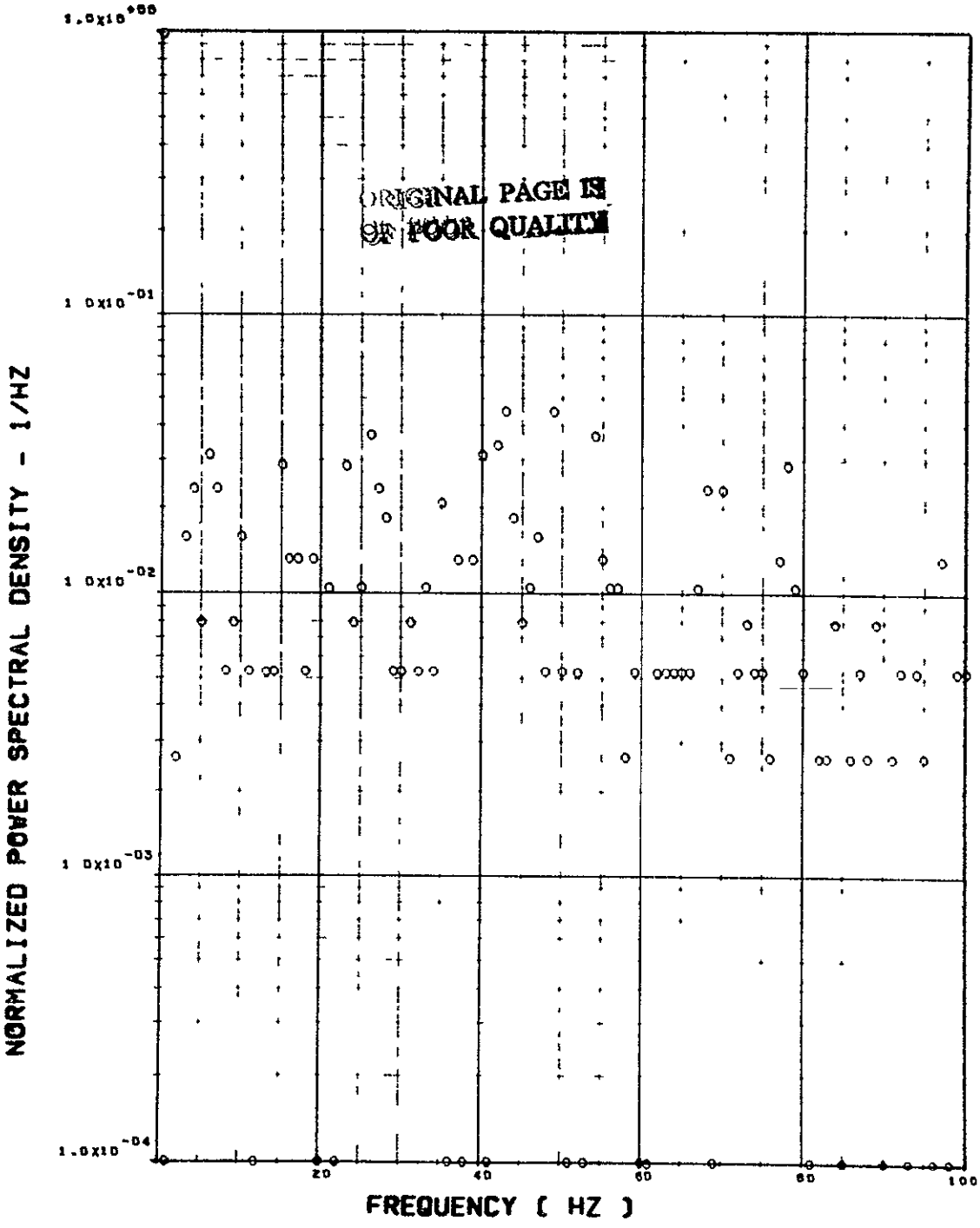

Figure 22. Continued

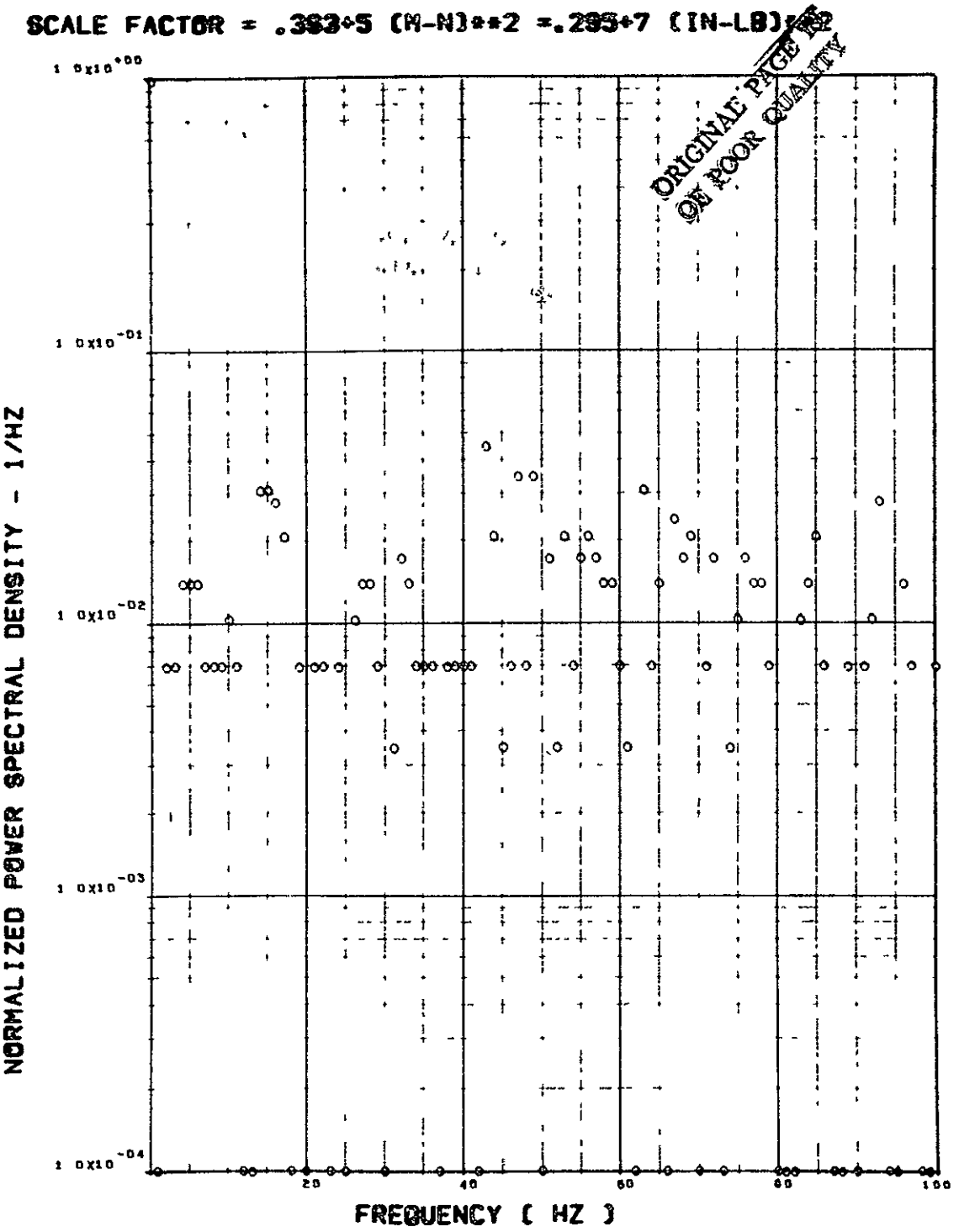

Figure 22. Continued

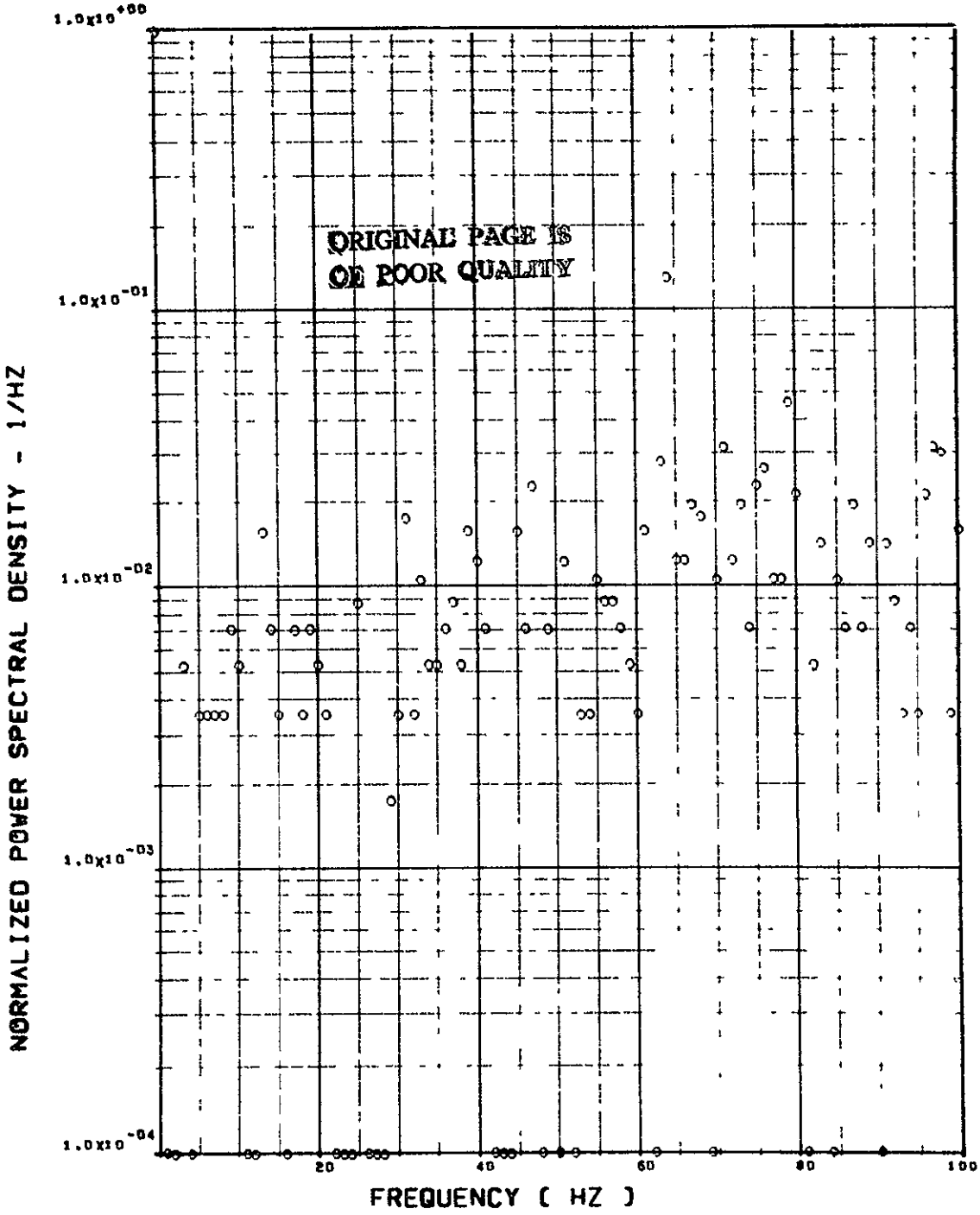

Figure 2. Continued

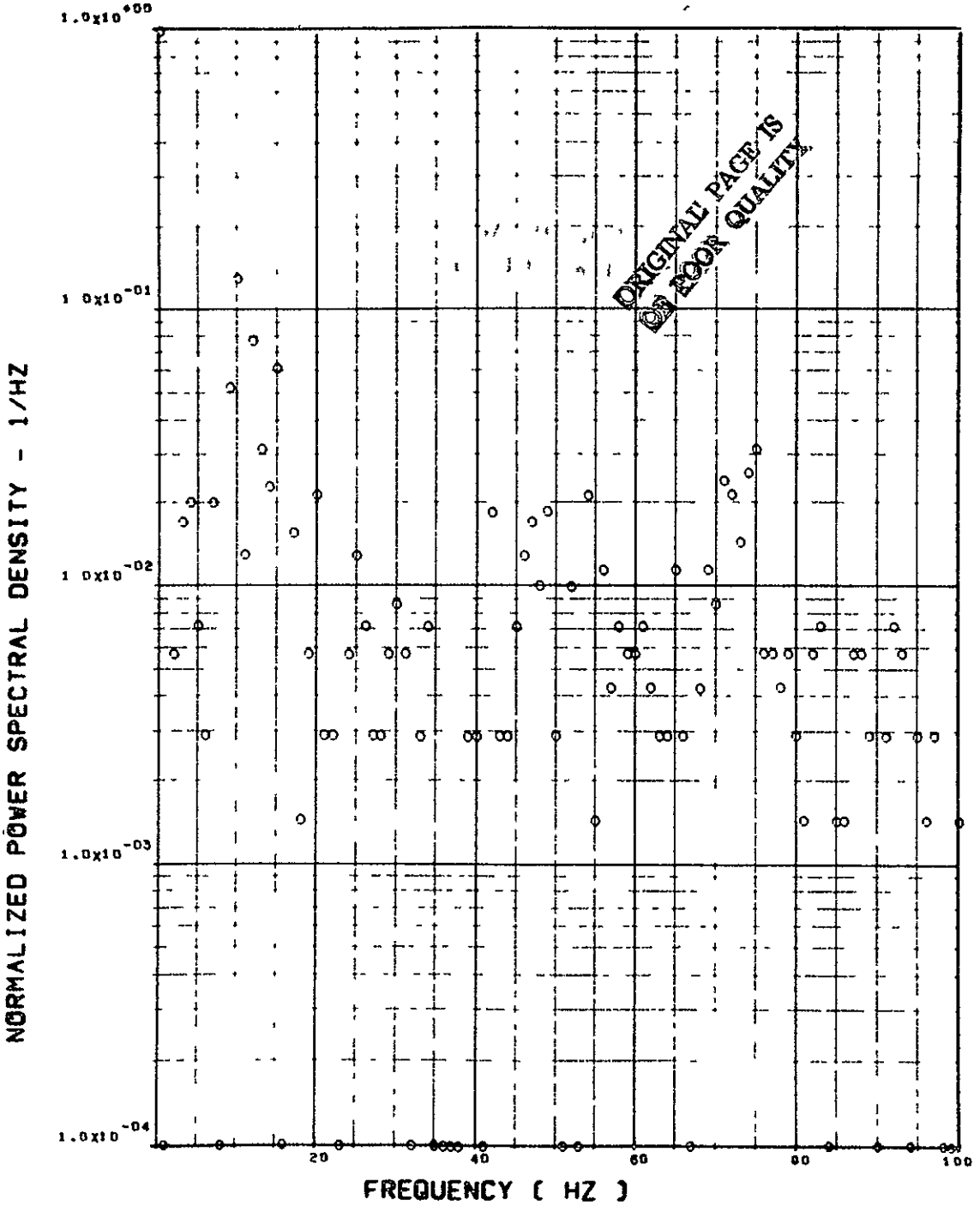

Figure 22. Continued

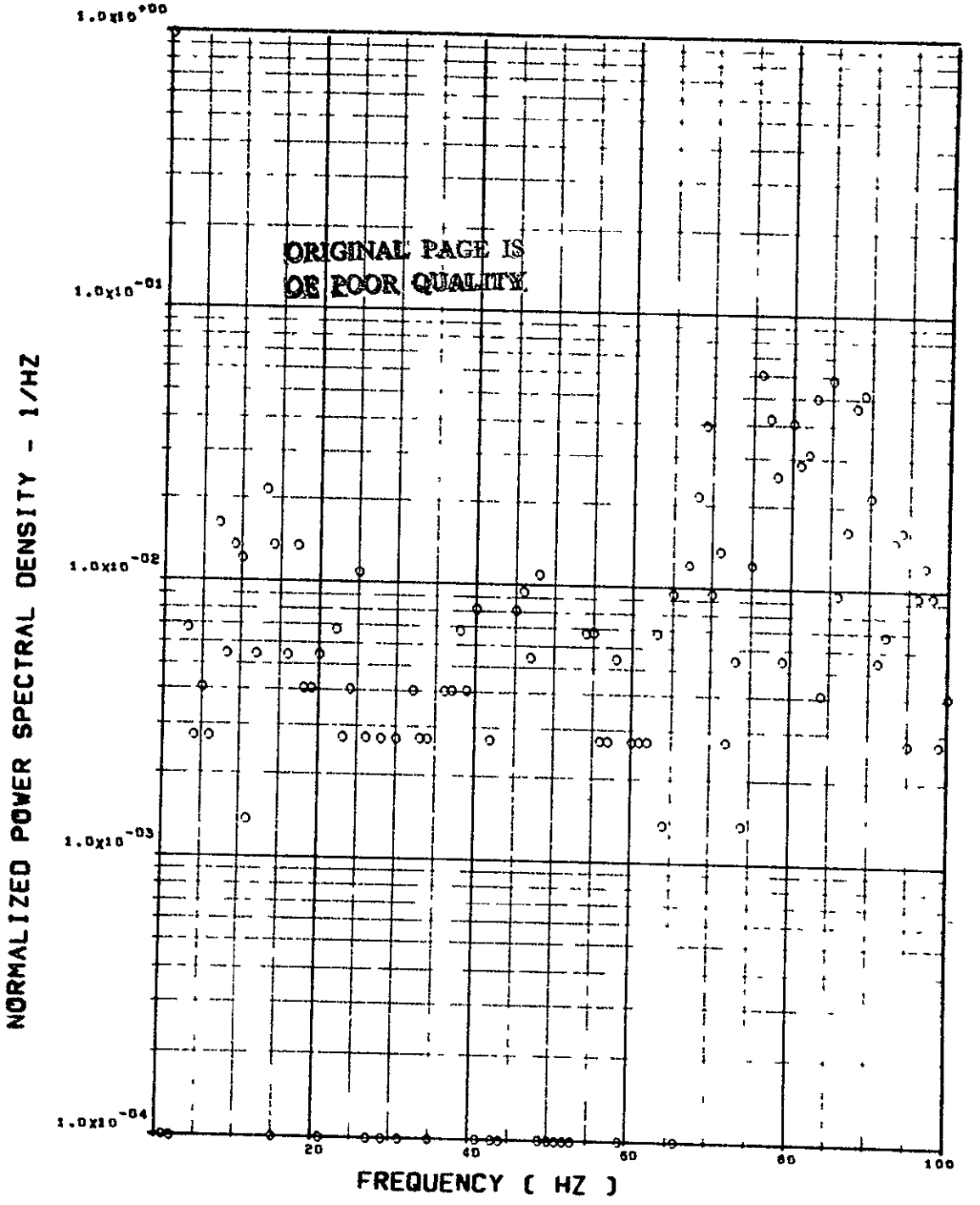

Figure 2.. Continued

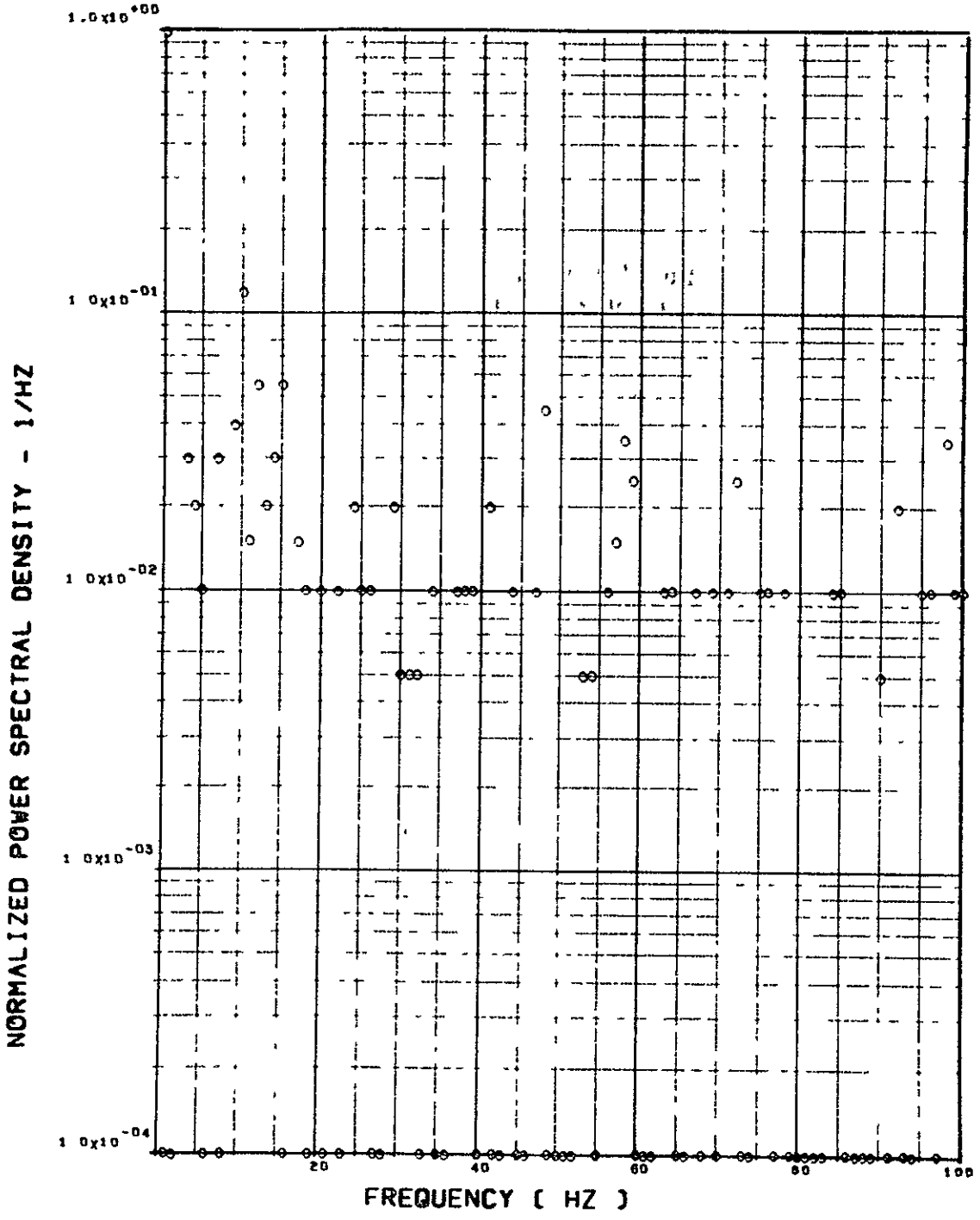

Figure 22. Continued

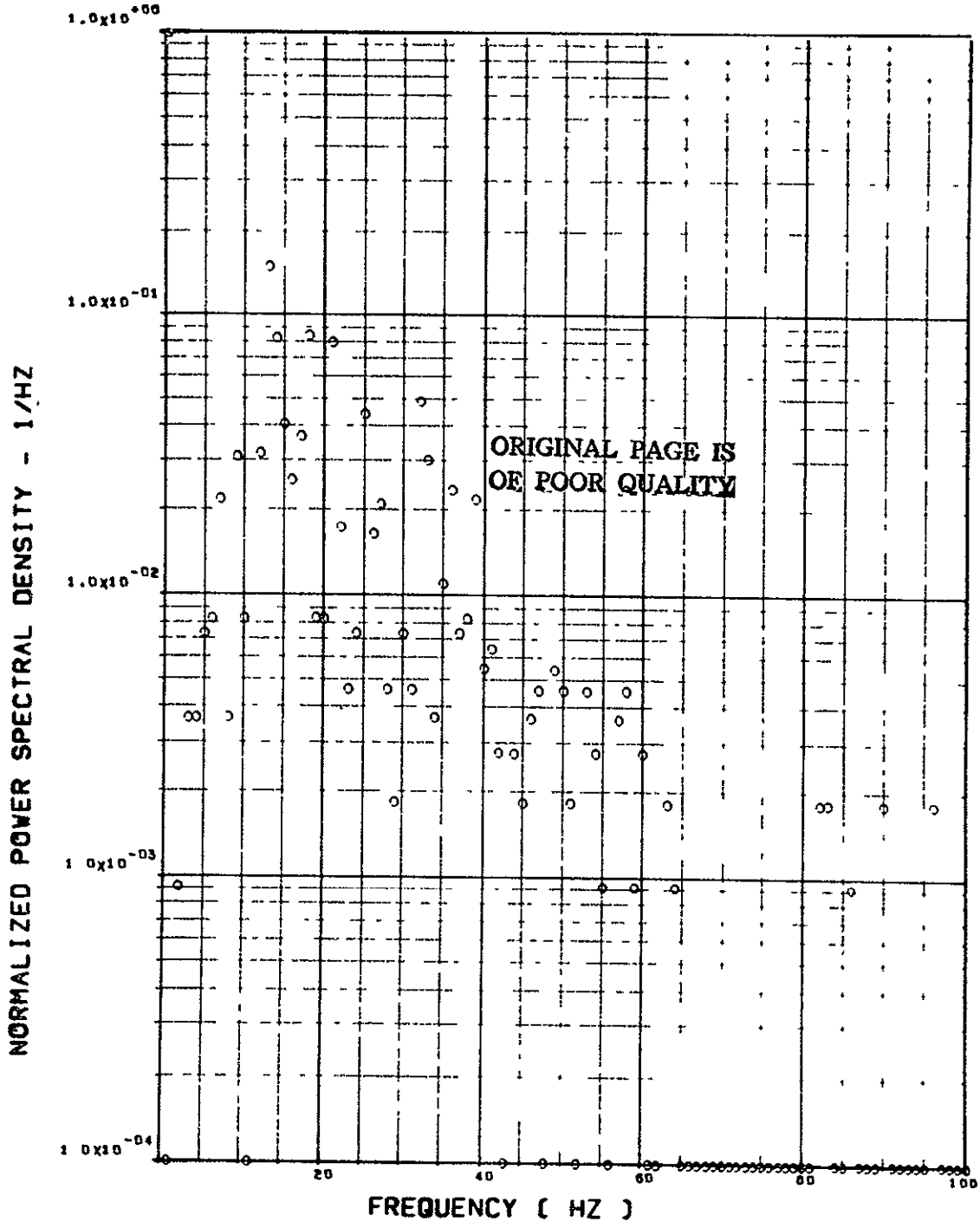

Figure 22. Continued

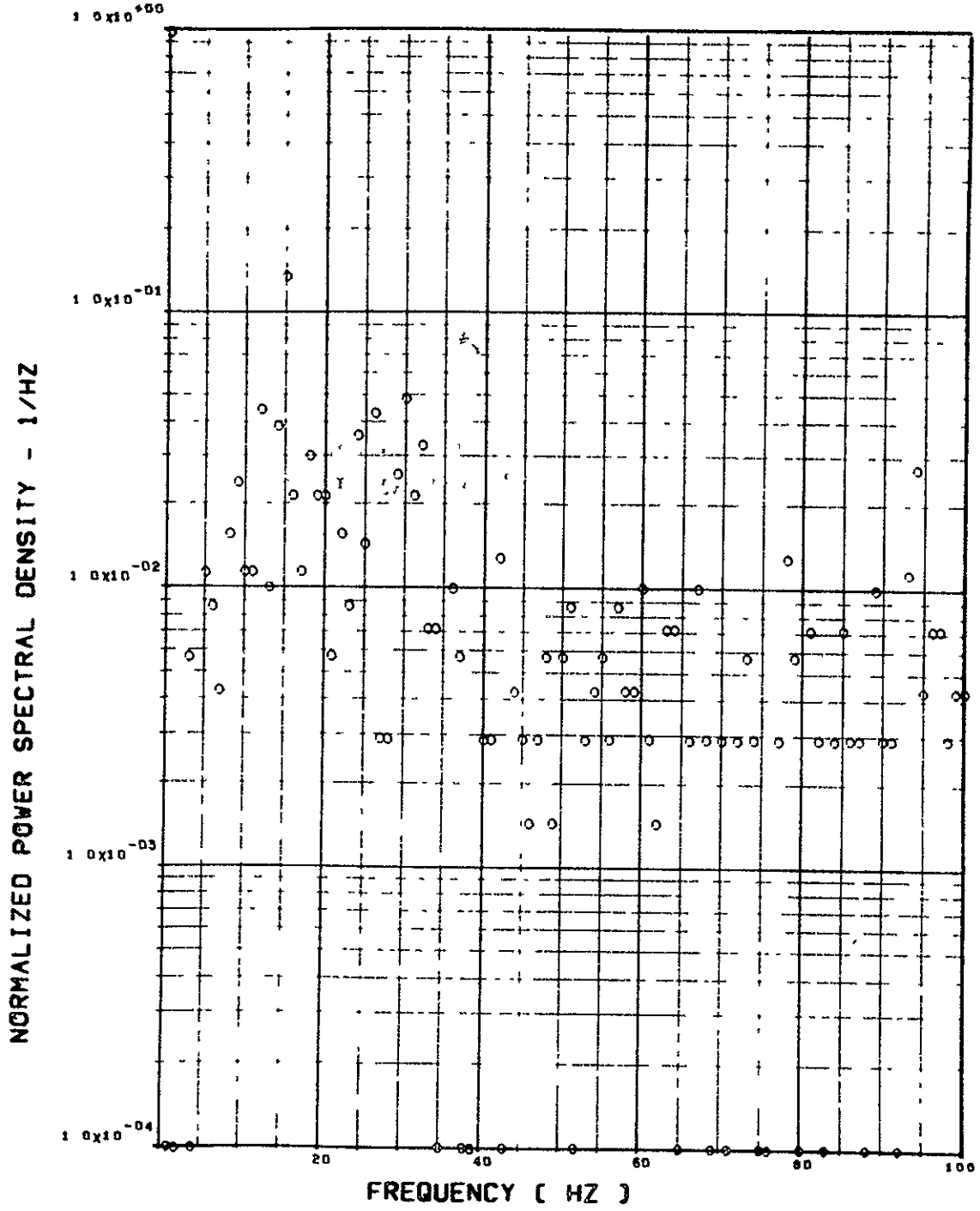

Figure 22. Concluded

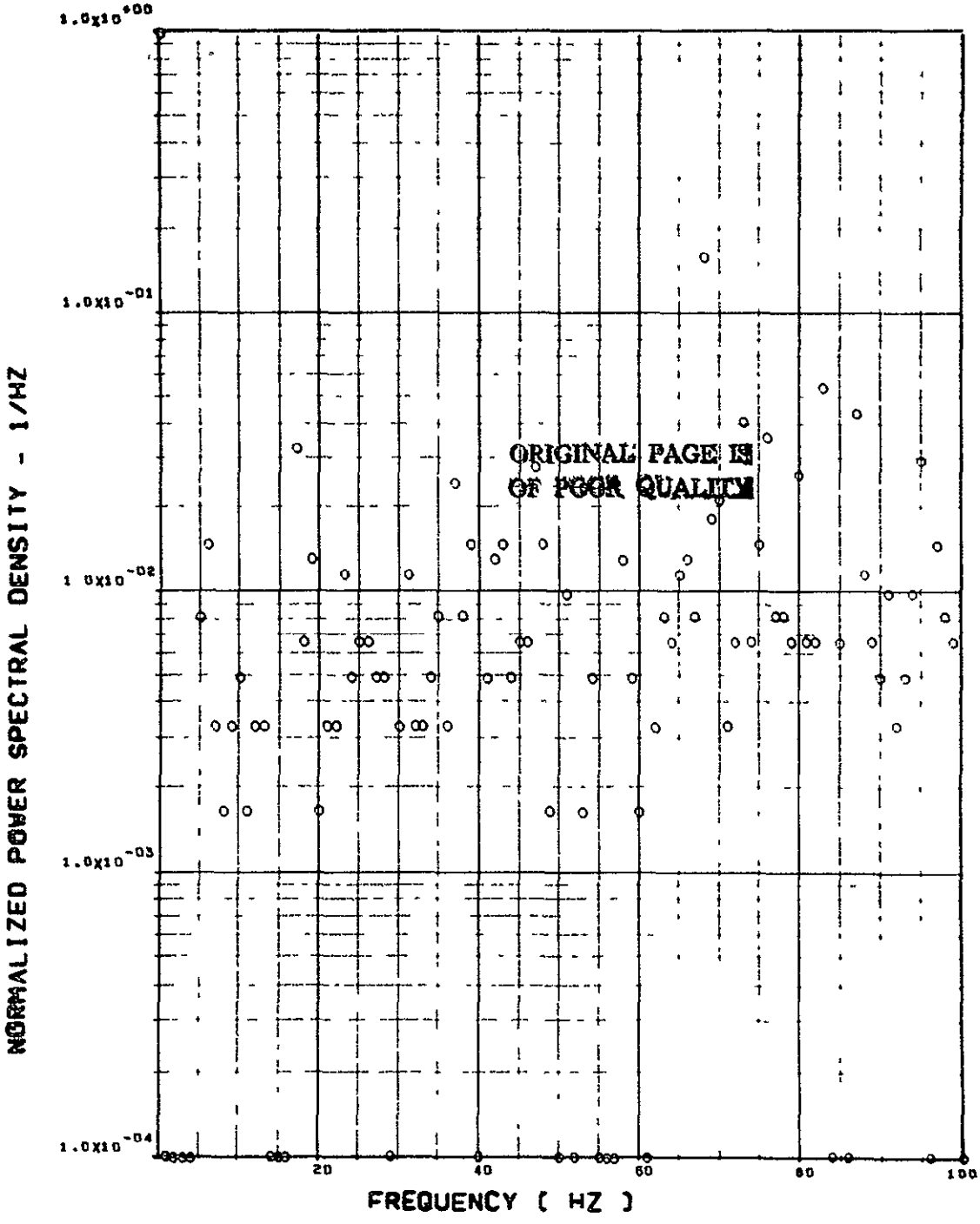

Figure 23. Power Spectra - Flight 48, Run 7R1, Point 4 T_1 = 135956.8, ΔT = 1 Sec, α_{Nom} = 15 15 deg, α= 2.00 deg.

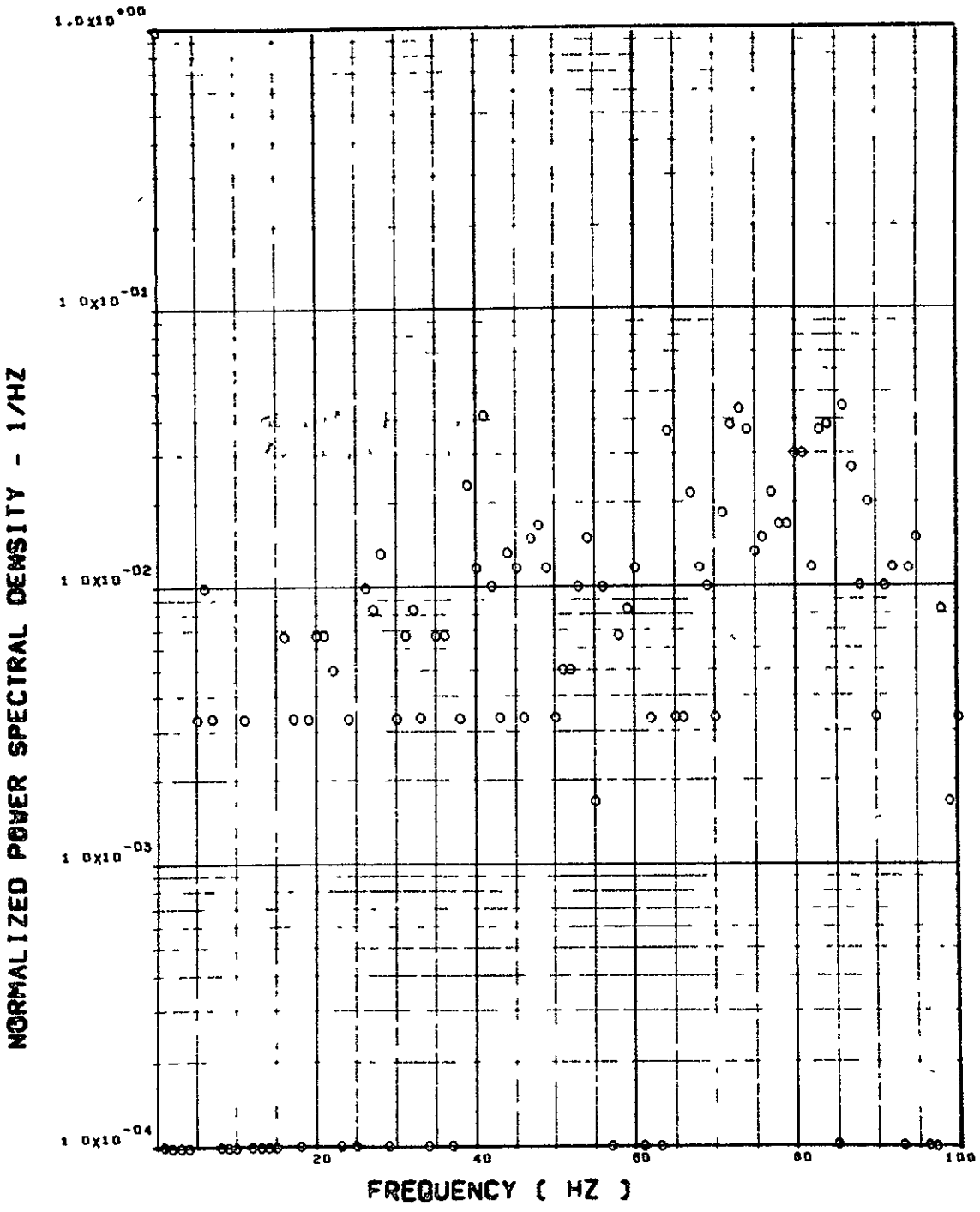

Figure 25. Continued

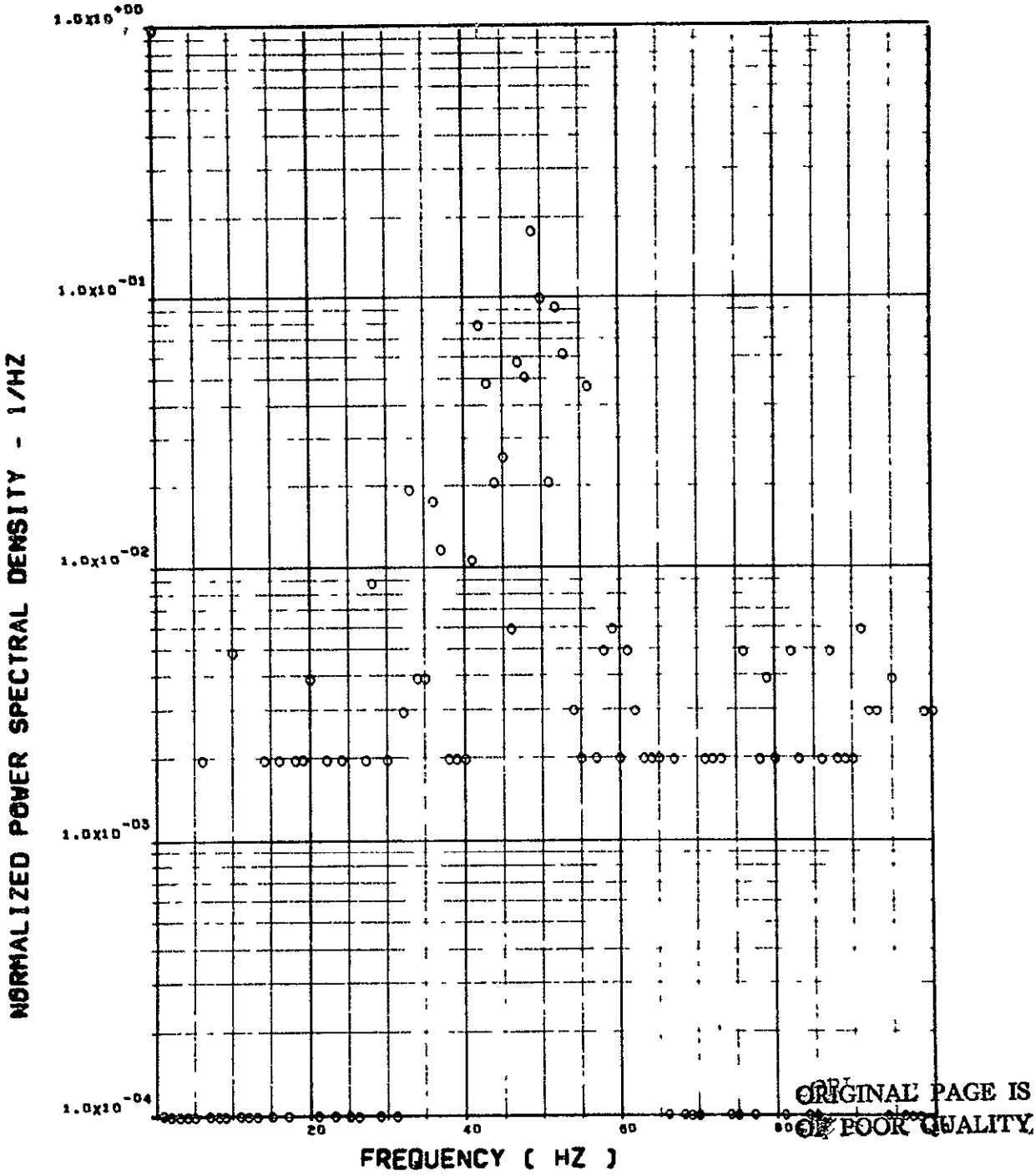

Figure 23. Continued

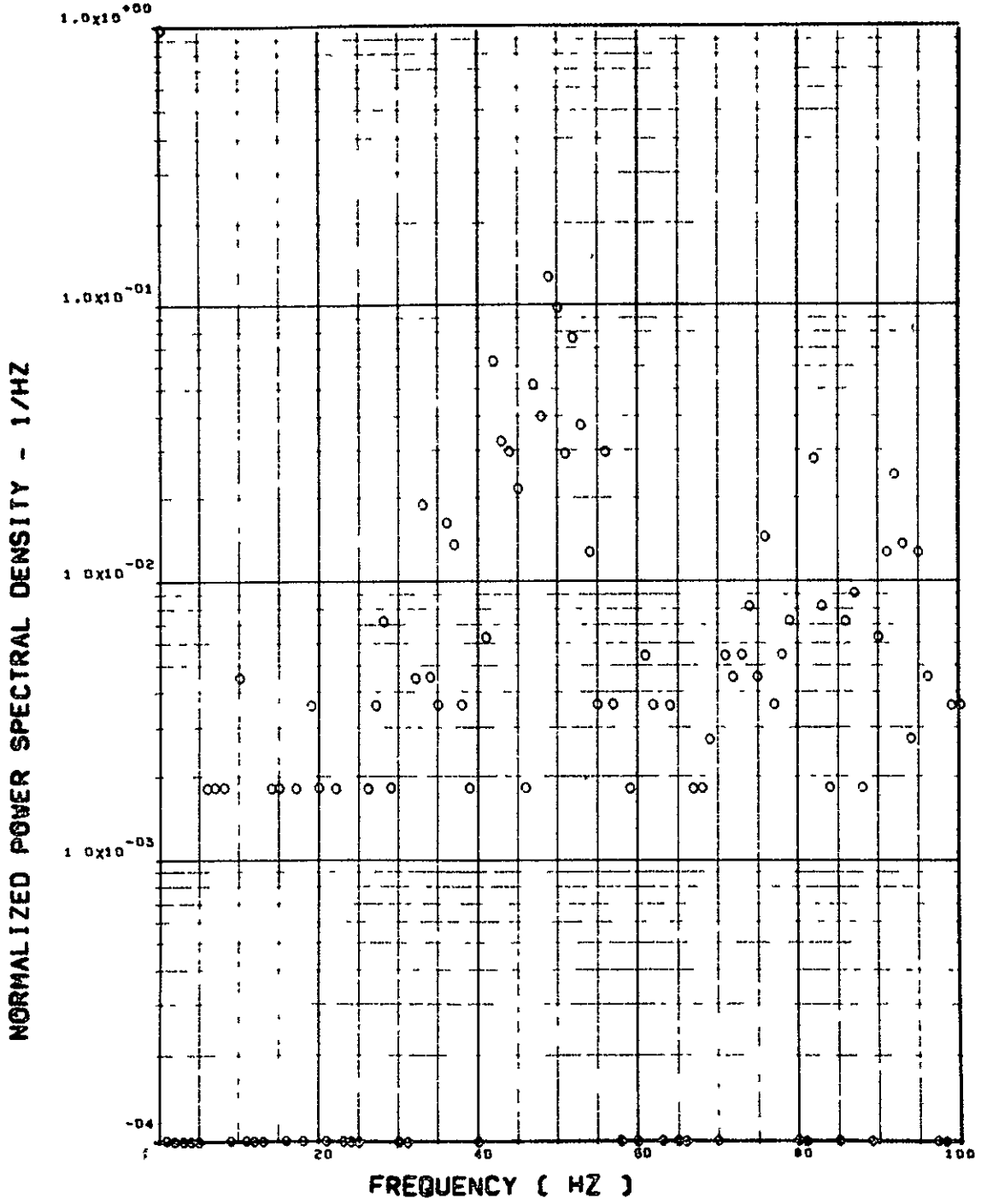

Figure 23. Continued

FLIGHT 40. FRAME 135956.00. RECORD LENGTH = 1 SEC.

SCALE FACTOR = .166-2 (G)**2

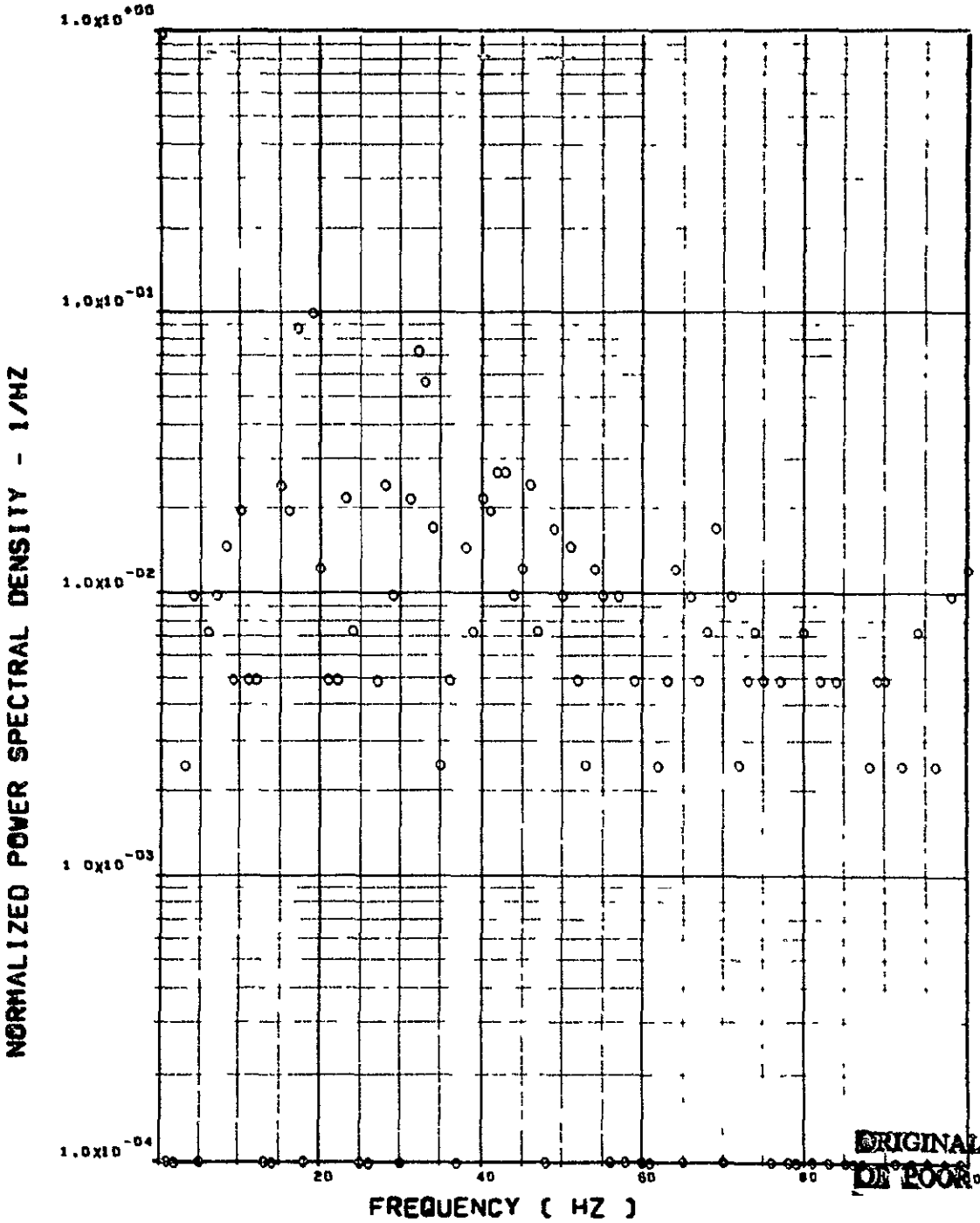

ITEM - AF009 PILOT'S SEAT VERTICAL ACCELEROMETER

Figure 23. Continued

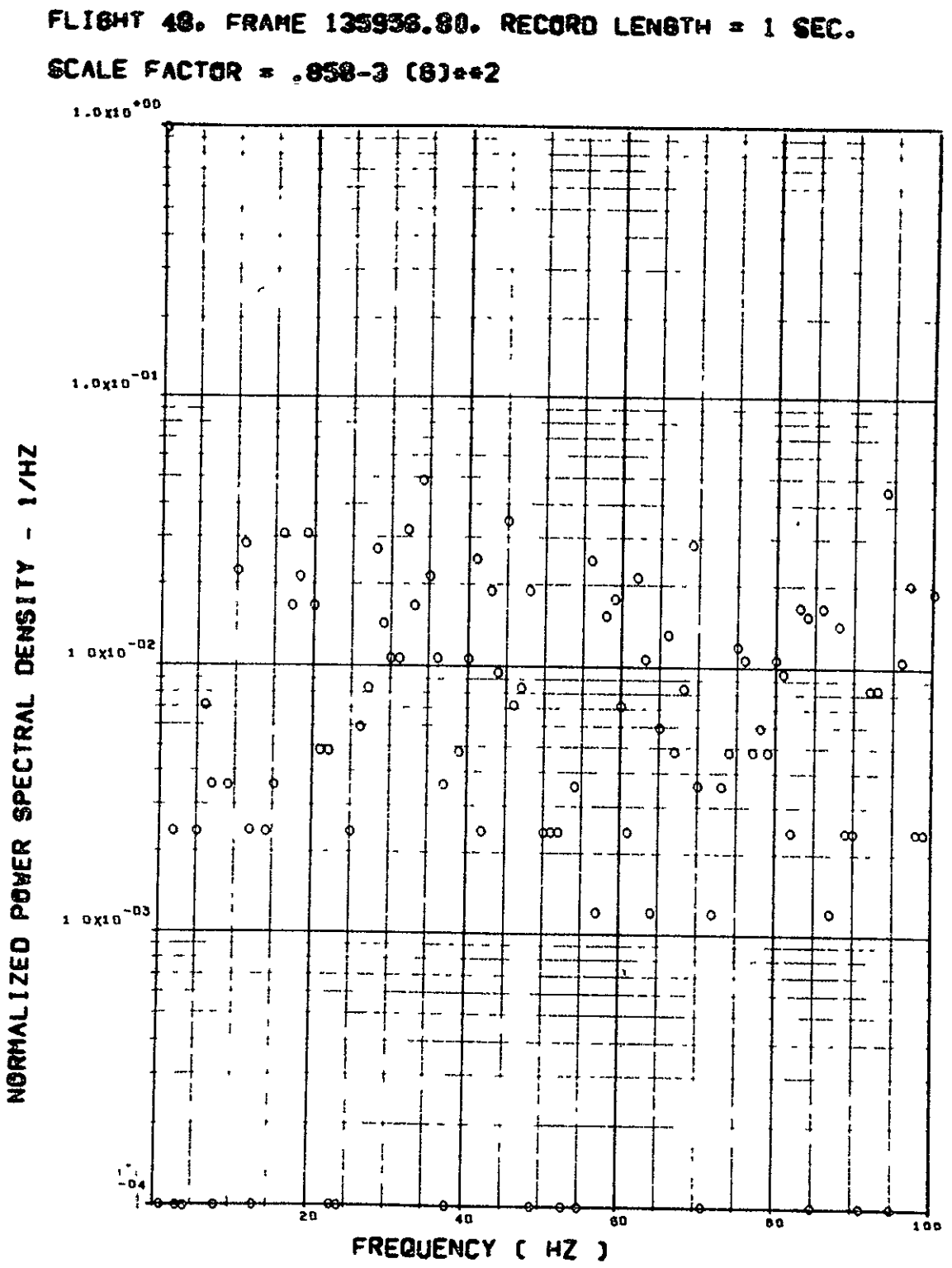

Figure 23. Continued

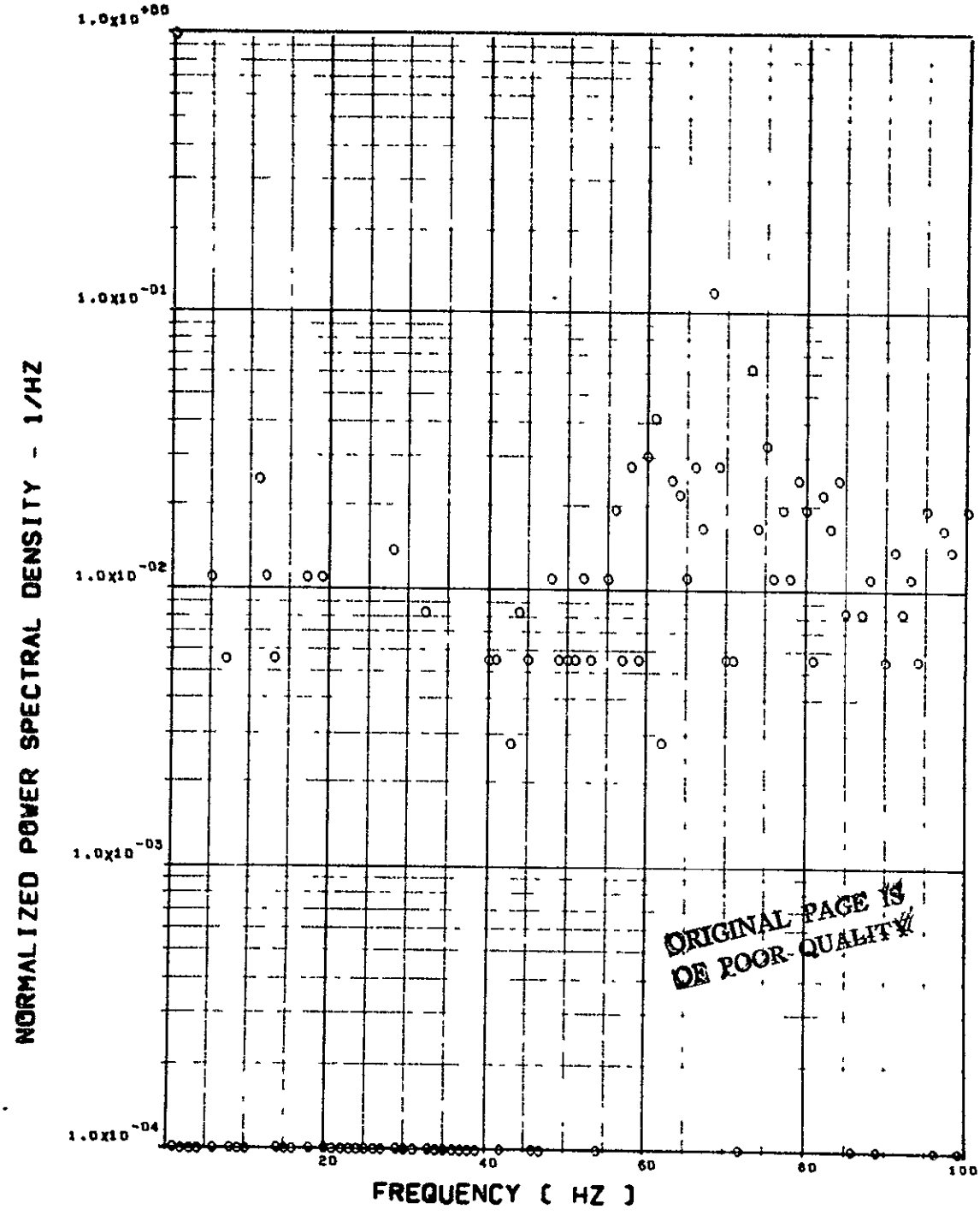

Figure 2). Continued

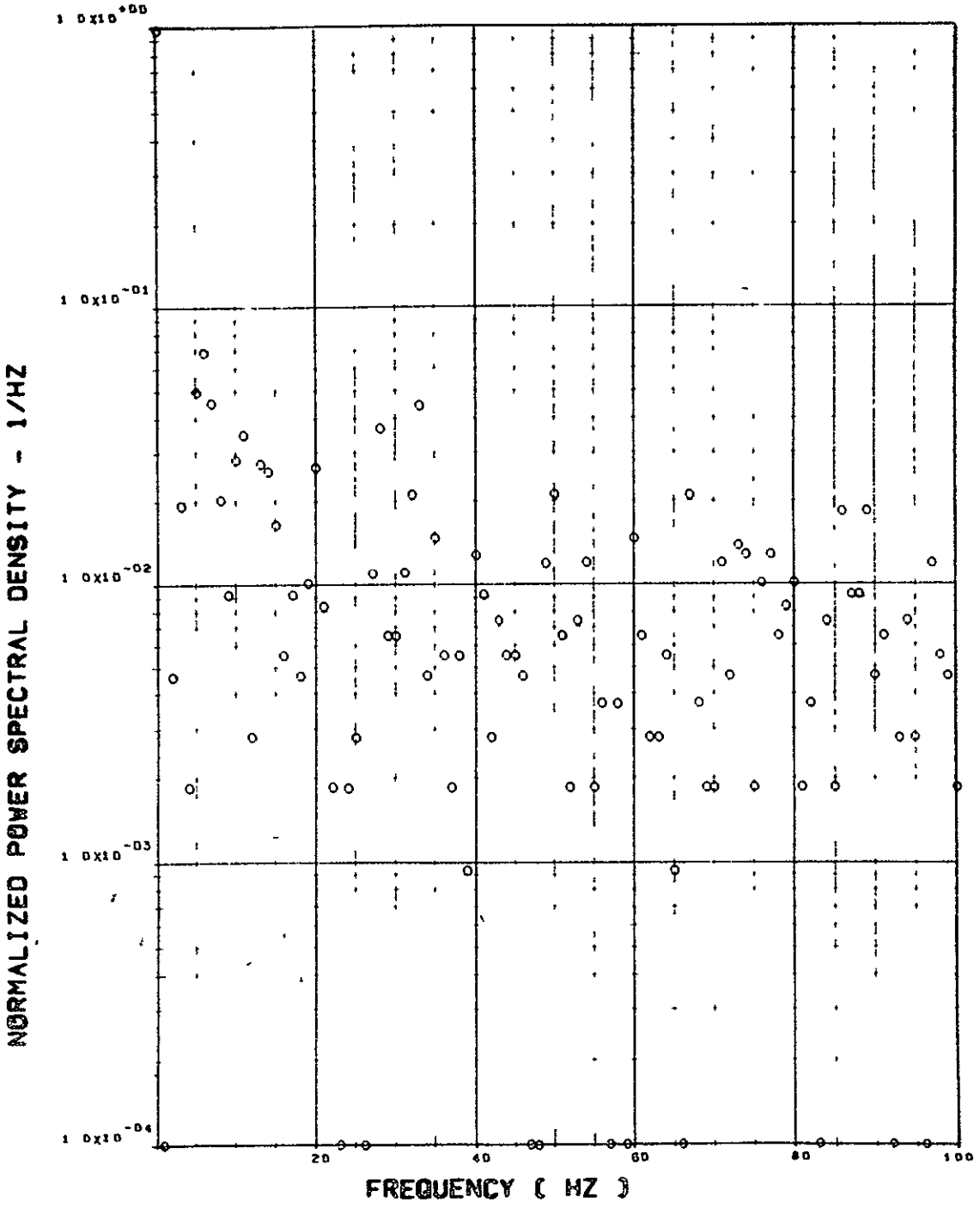

Figure 23. Continued

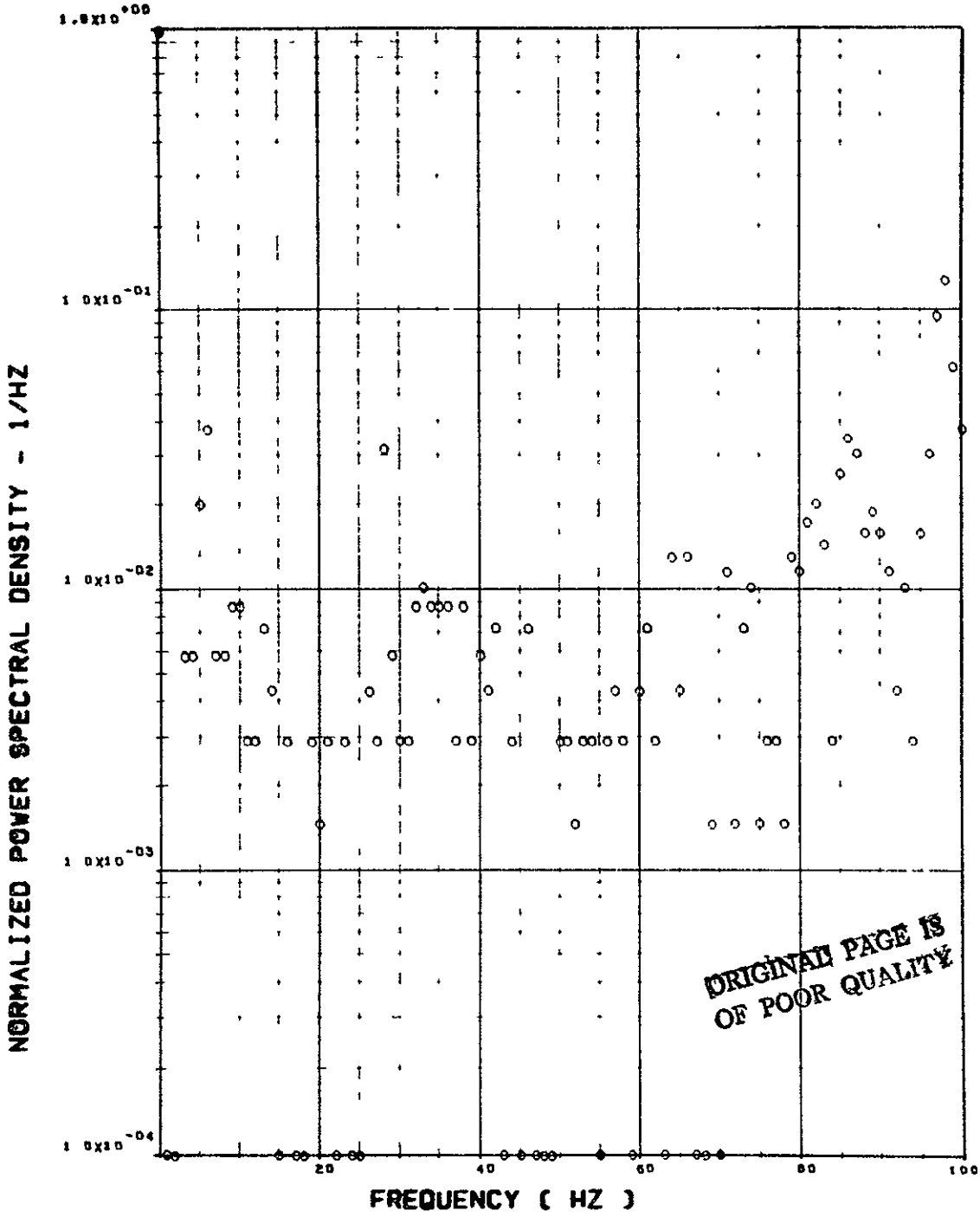

Figure 23. Continued

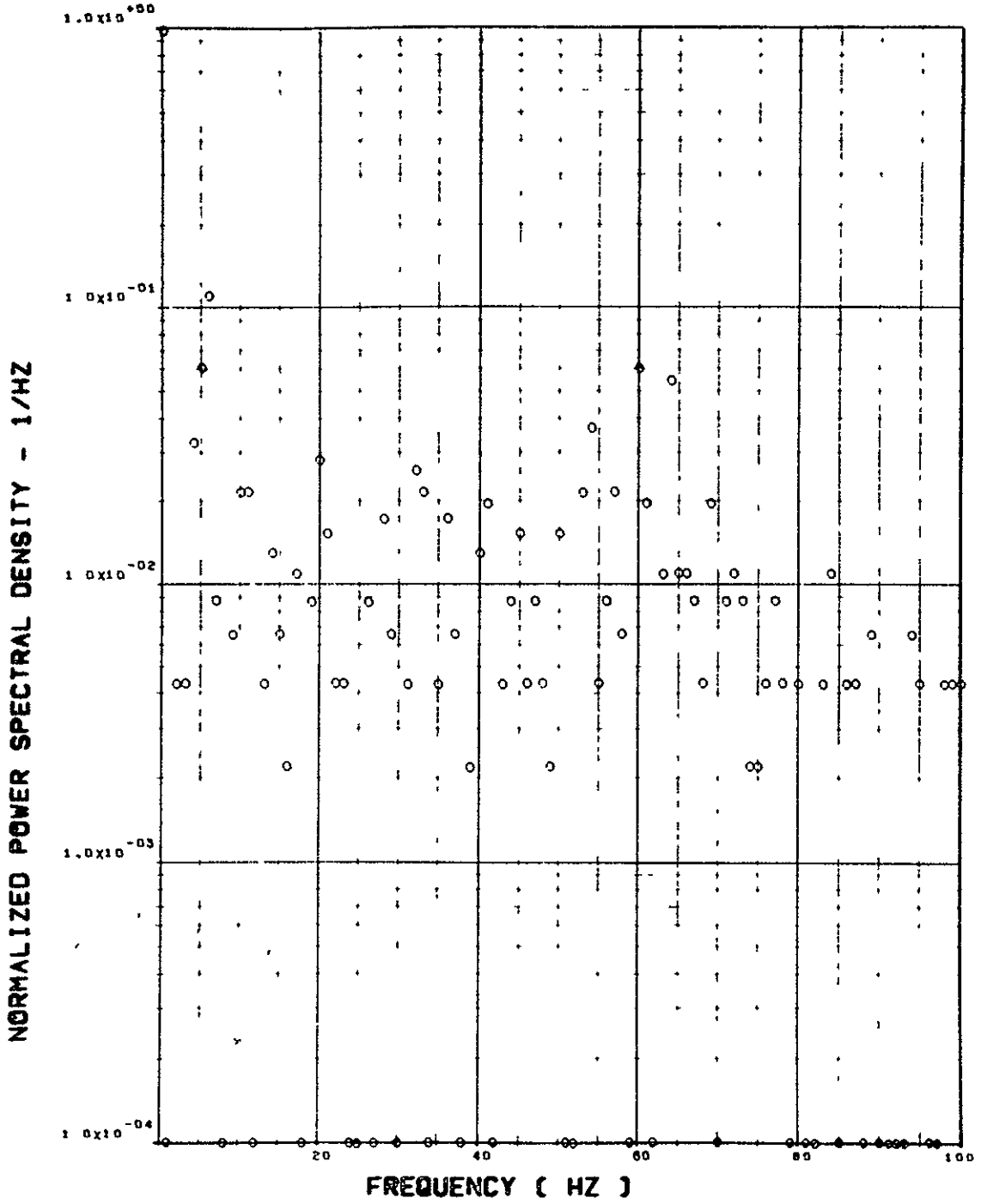

Figure 23. Continued

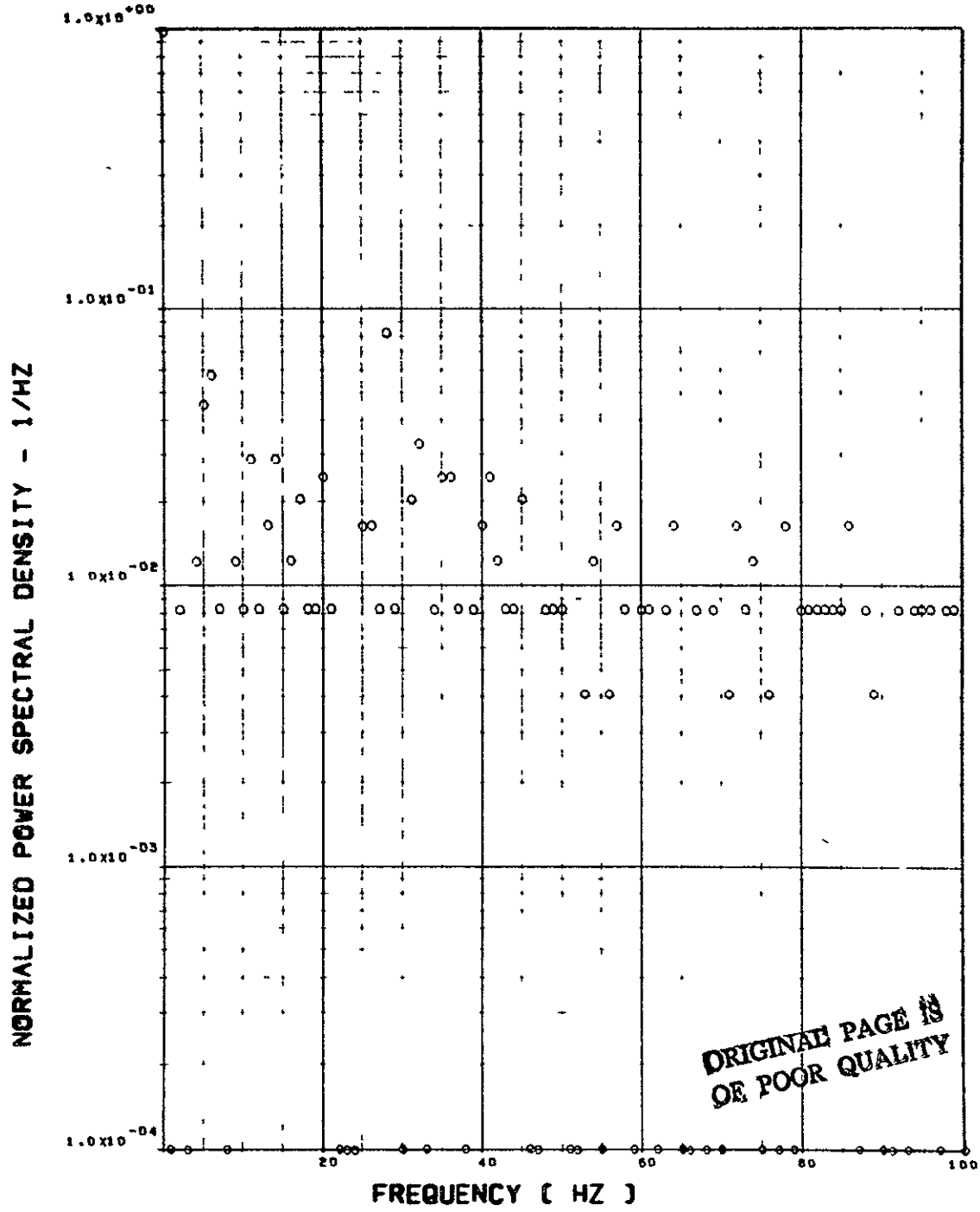

Figure 23. Continued

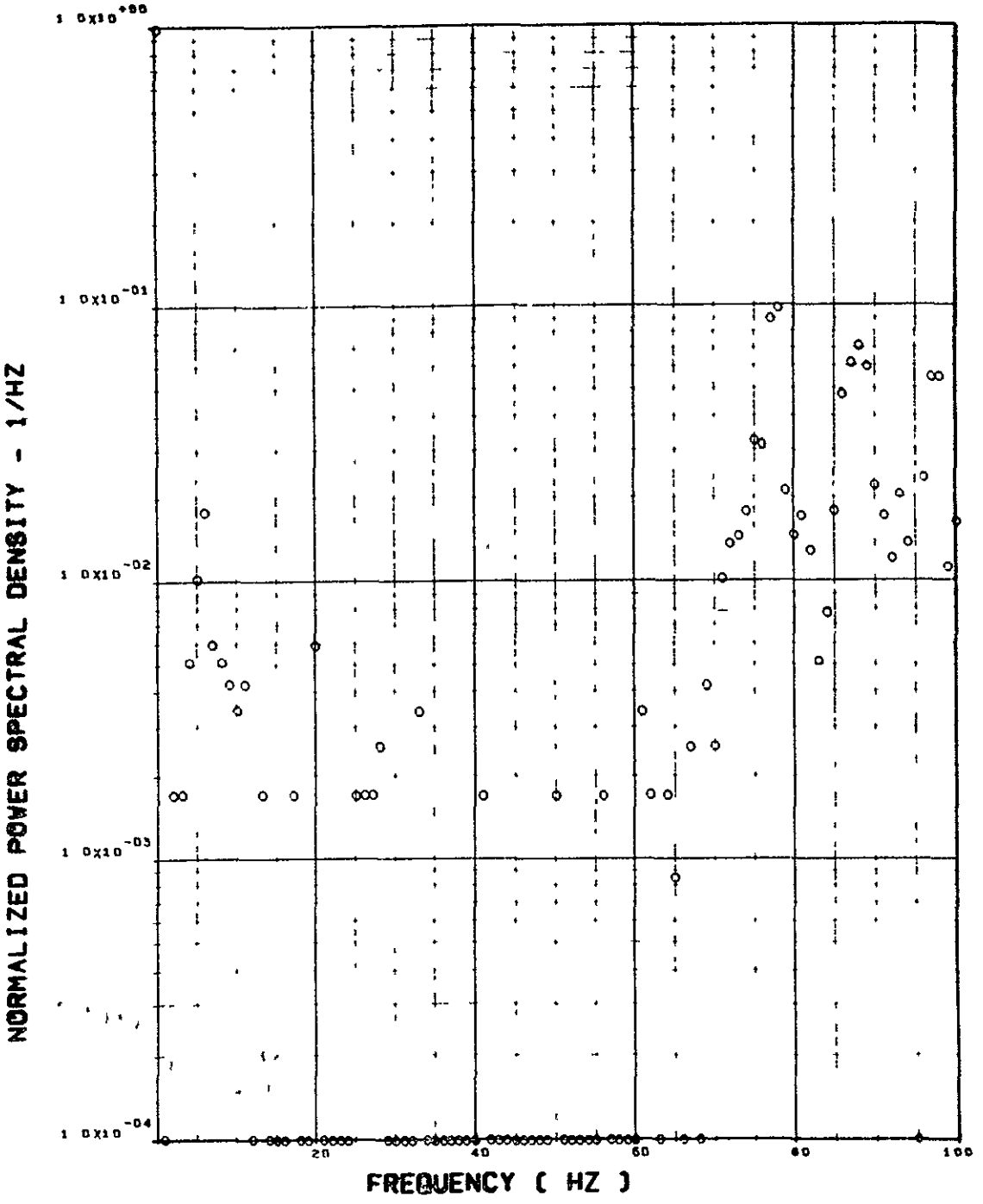

Figure 23. Continued

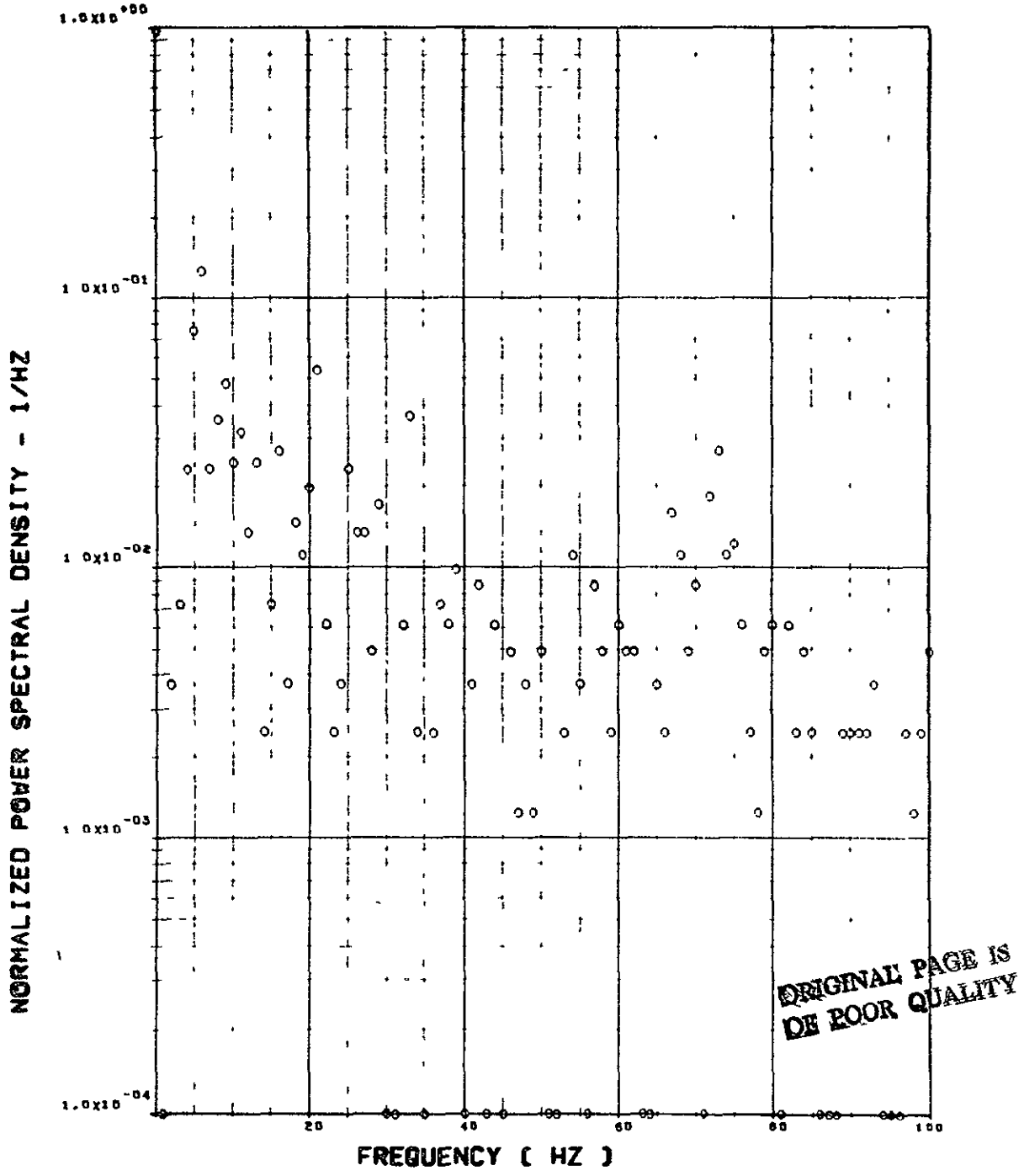

Figure 23. Continued

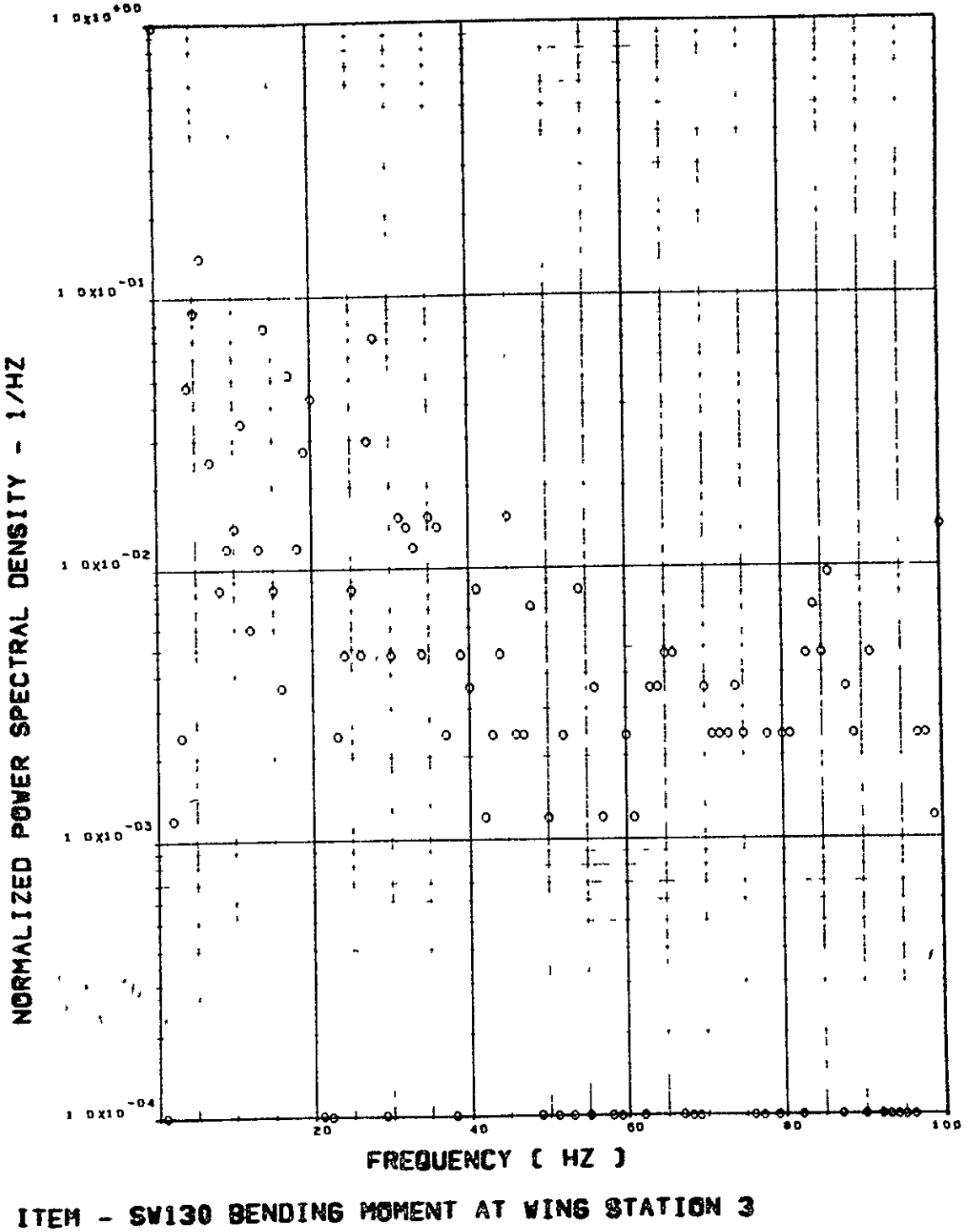

Figure 23. Continued

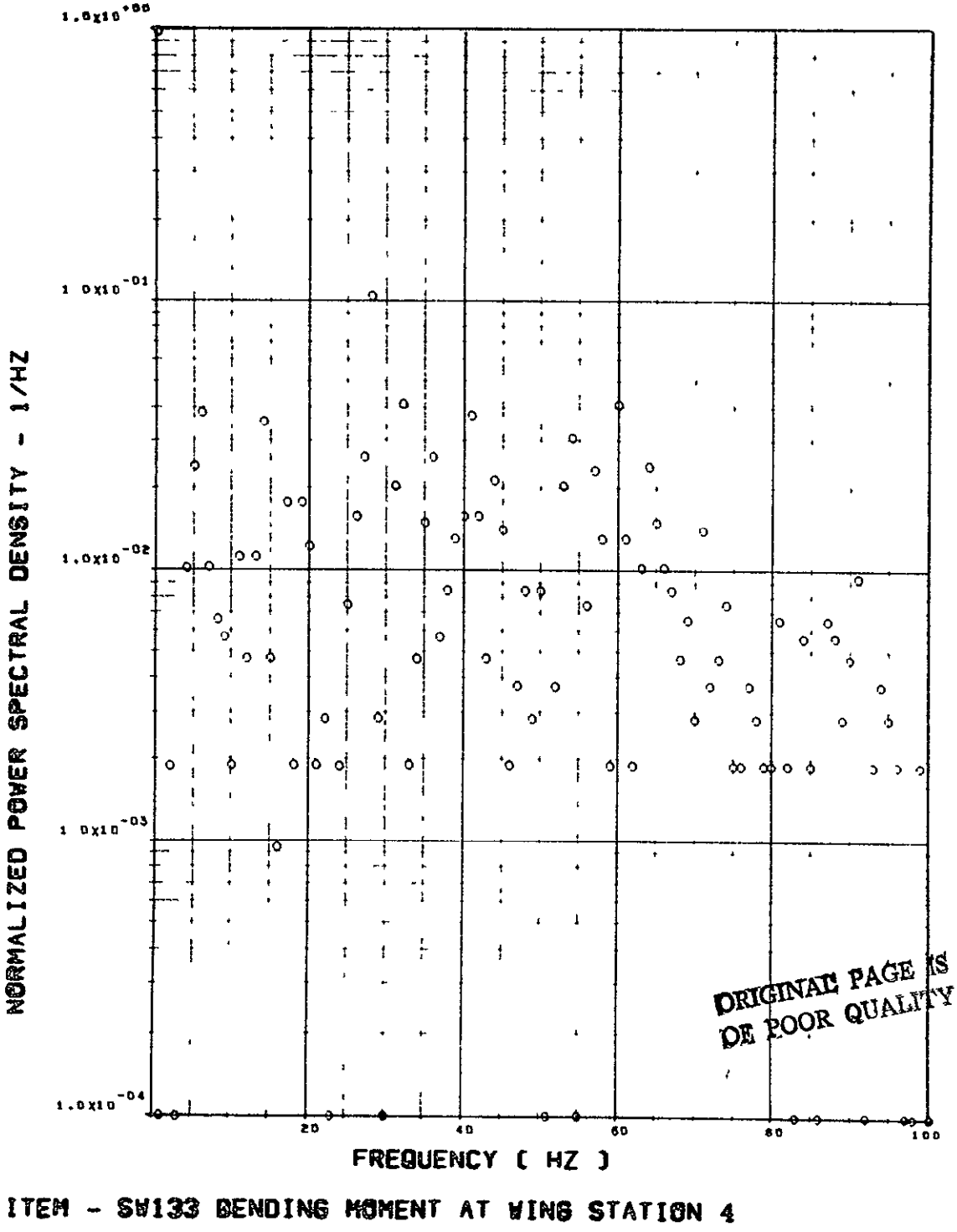

Figure 23. Continued

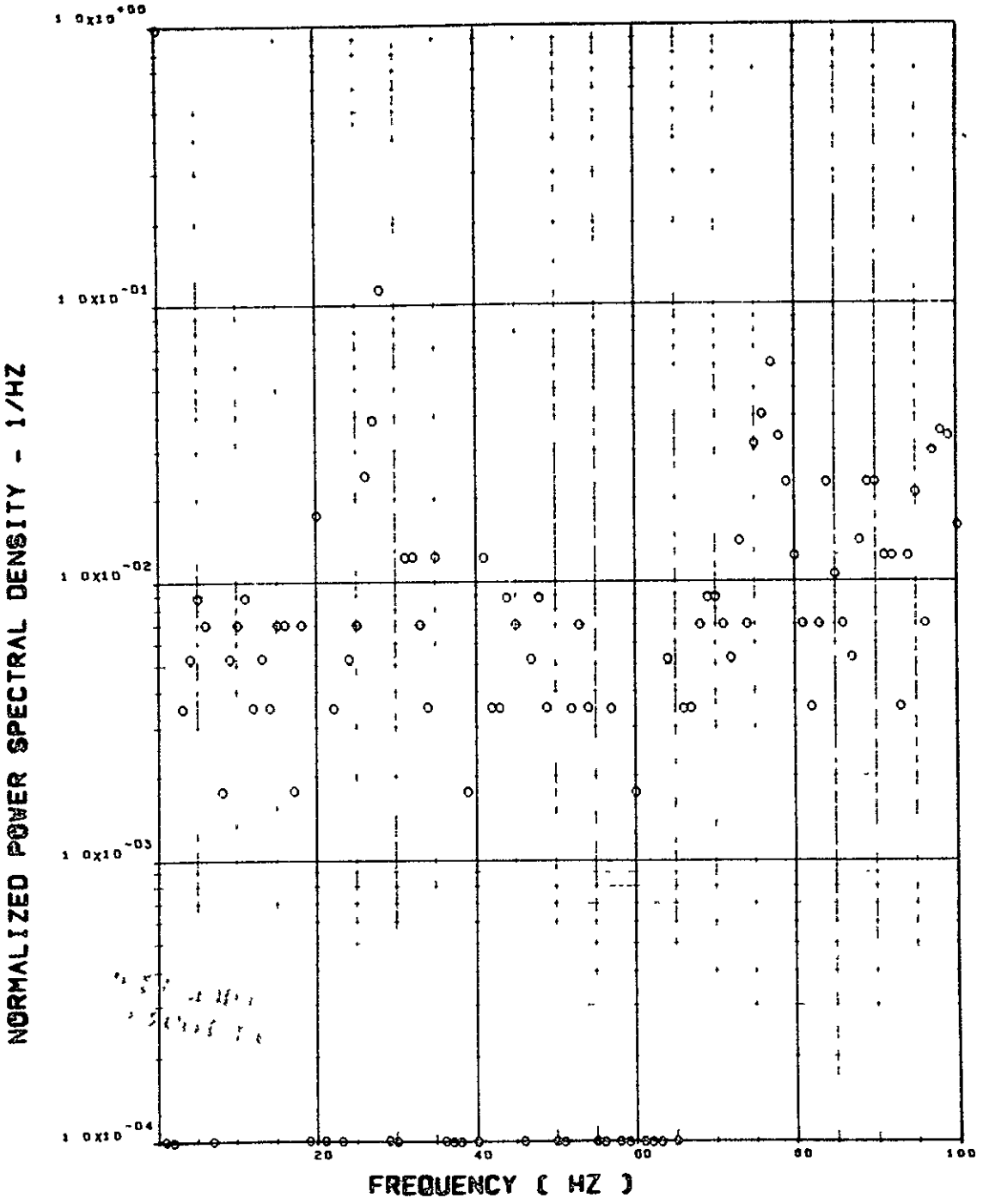

Figure 2). Continued

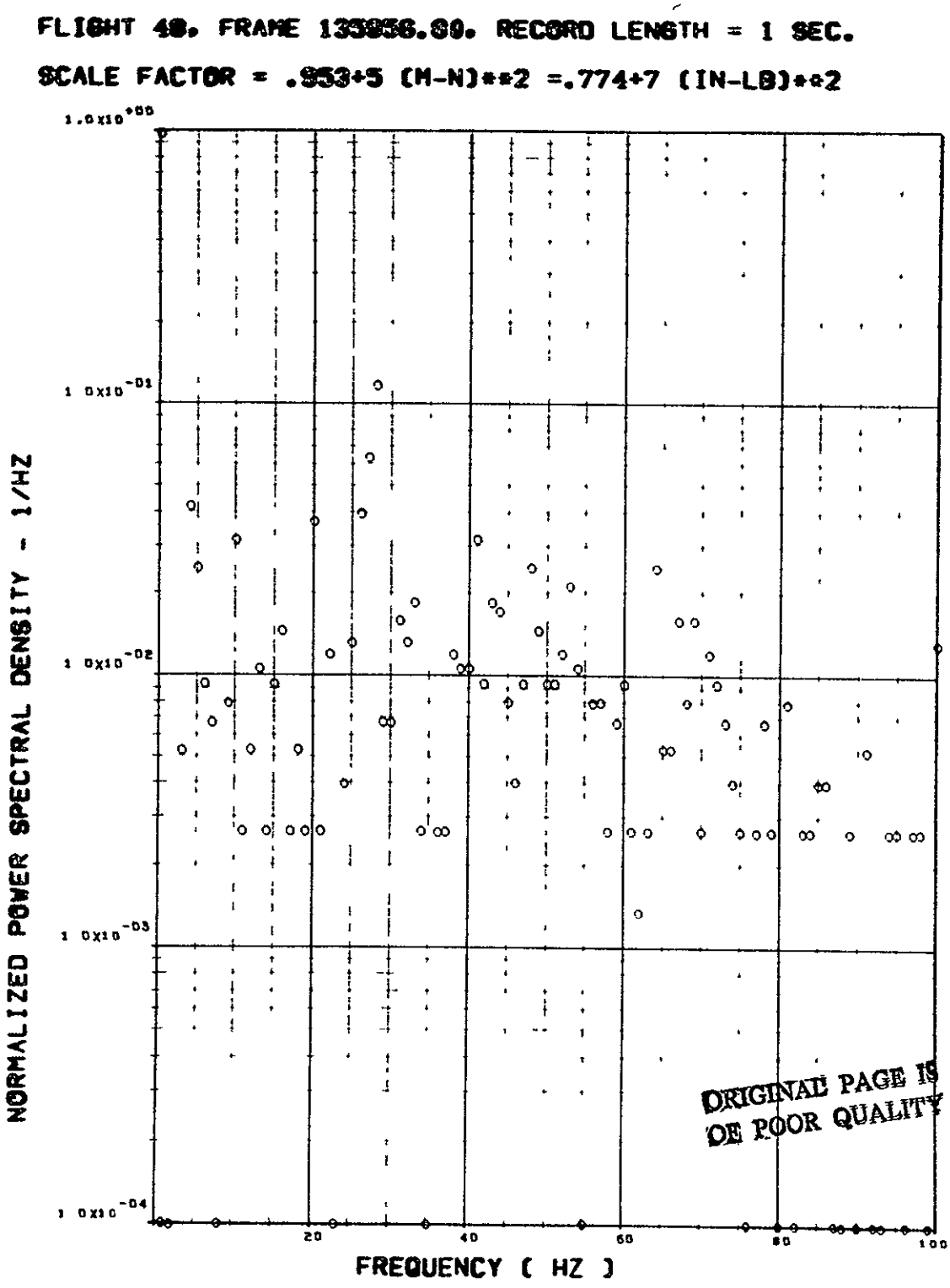

Figure 29. Continued

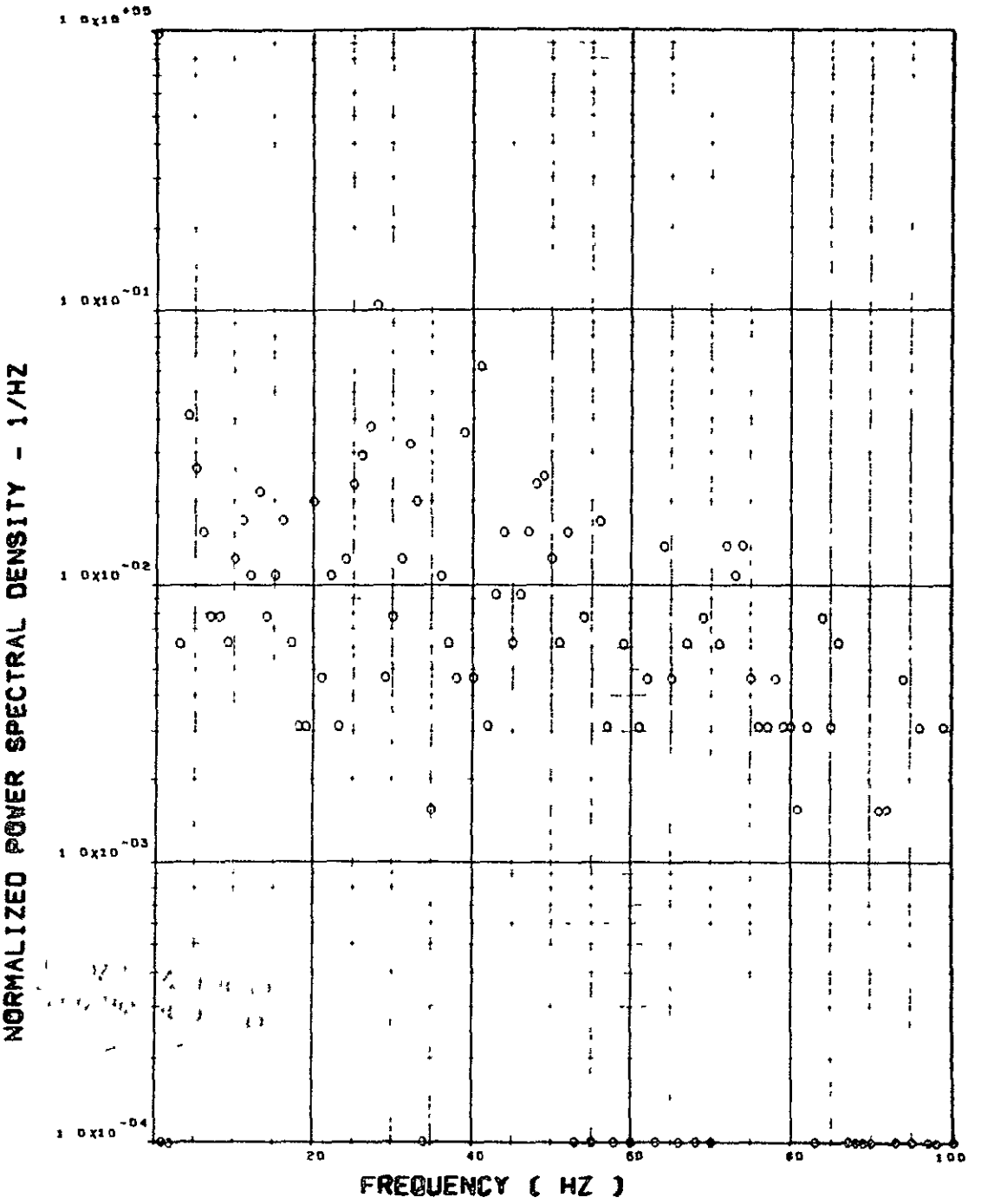

Figure 23. Continued

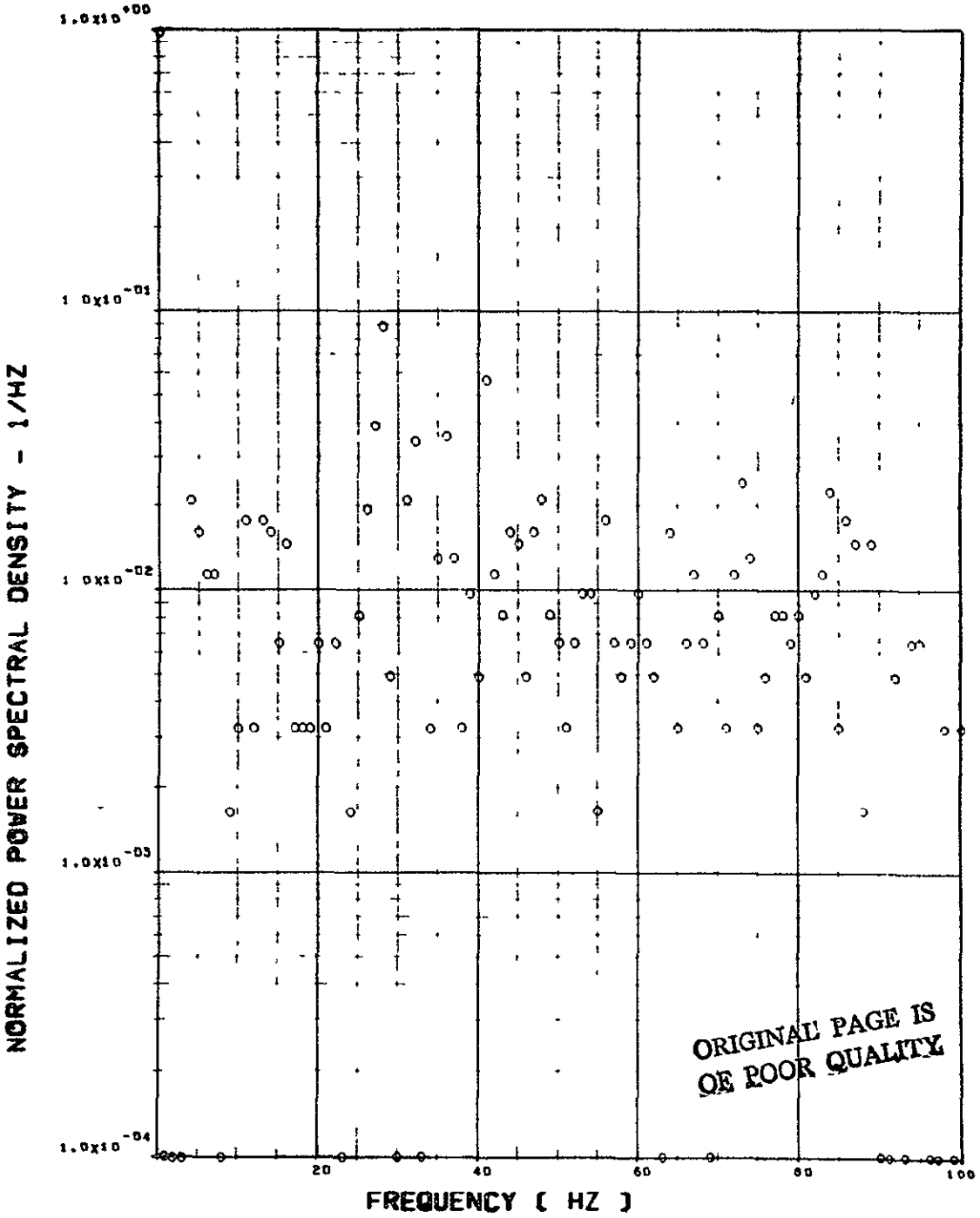

Figure 23. Continued

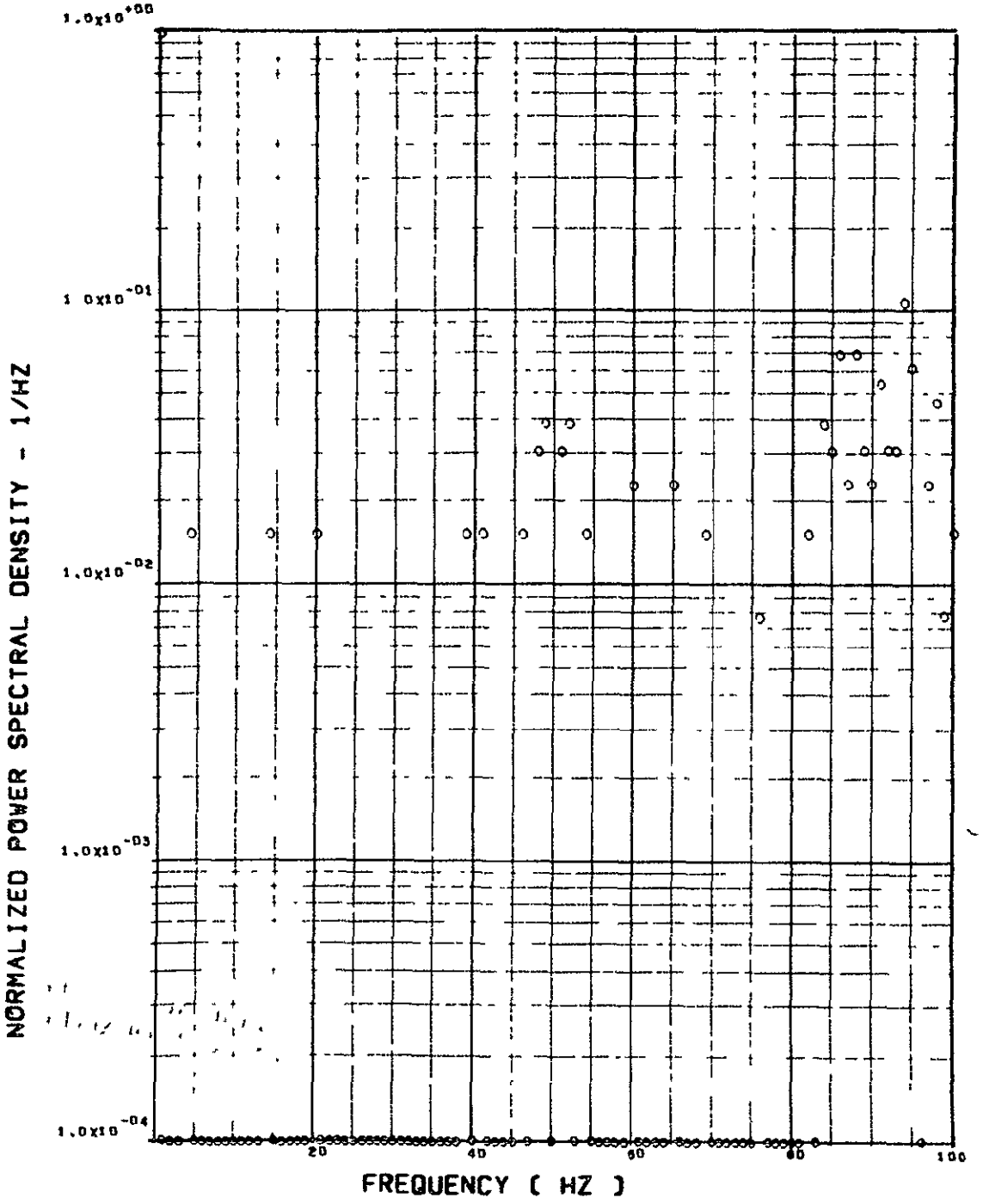

Figure 23. Continued

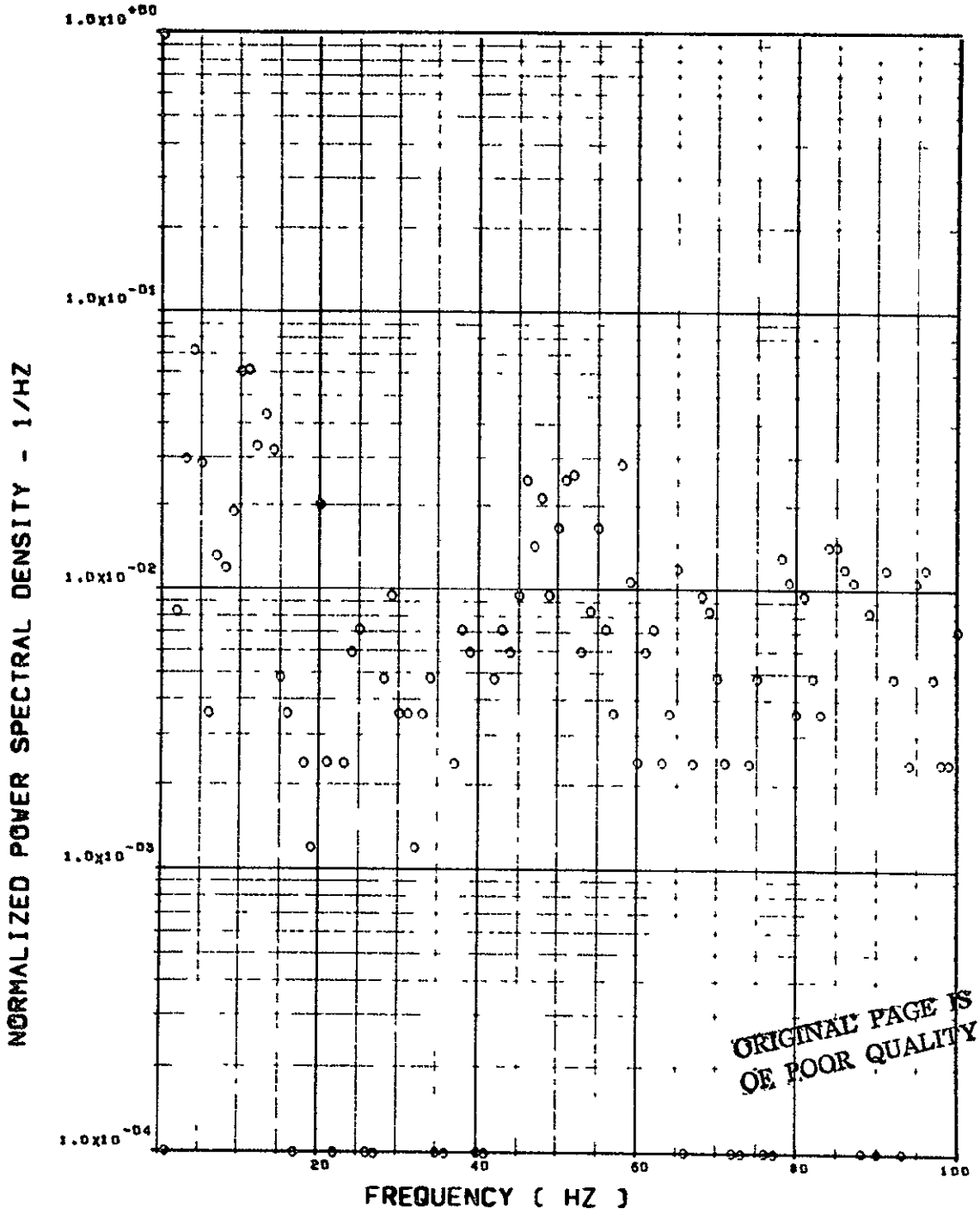

Figure 23. Continued

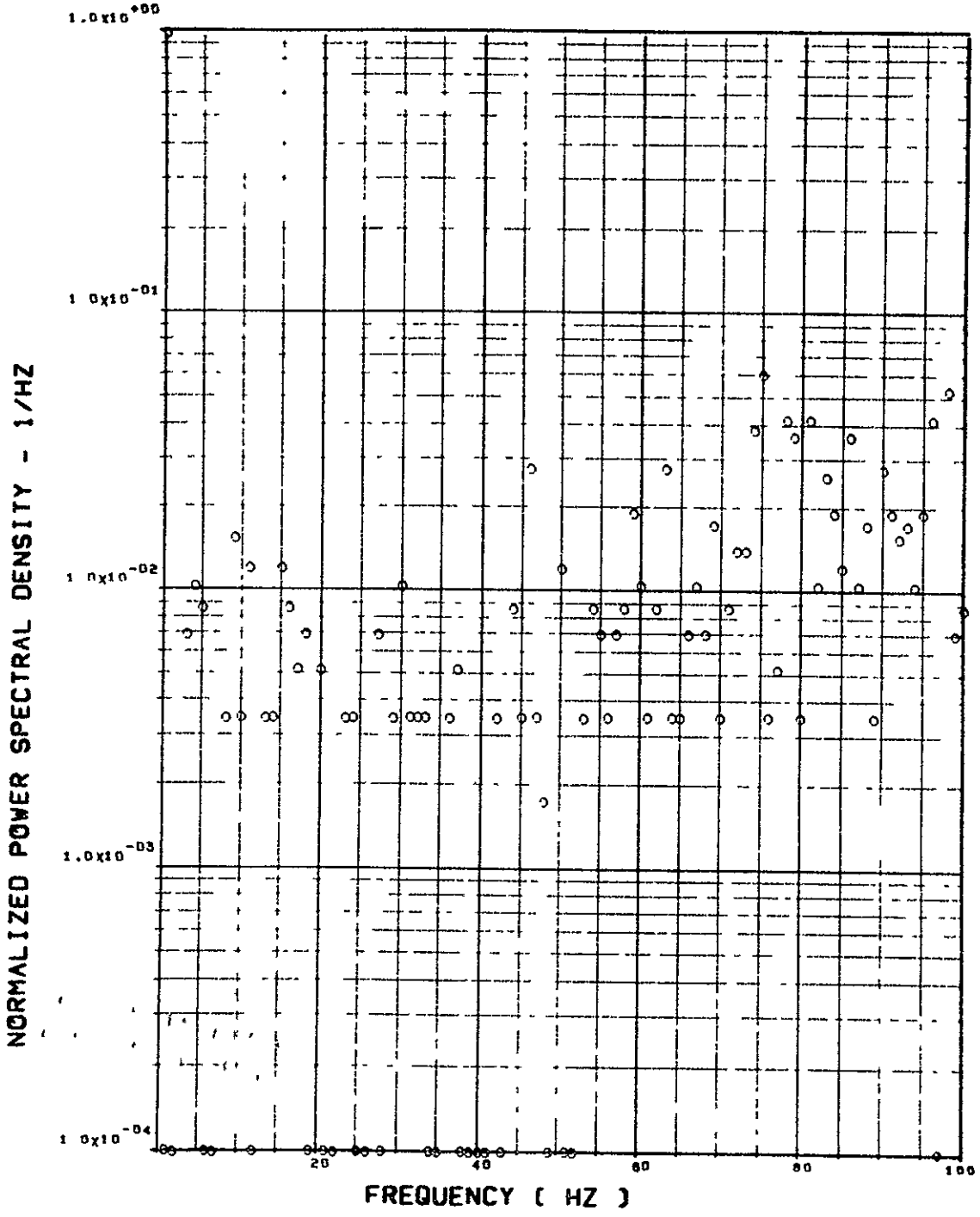

Figure 23. Continued

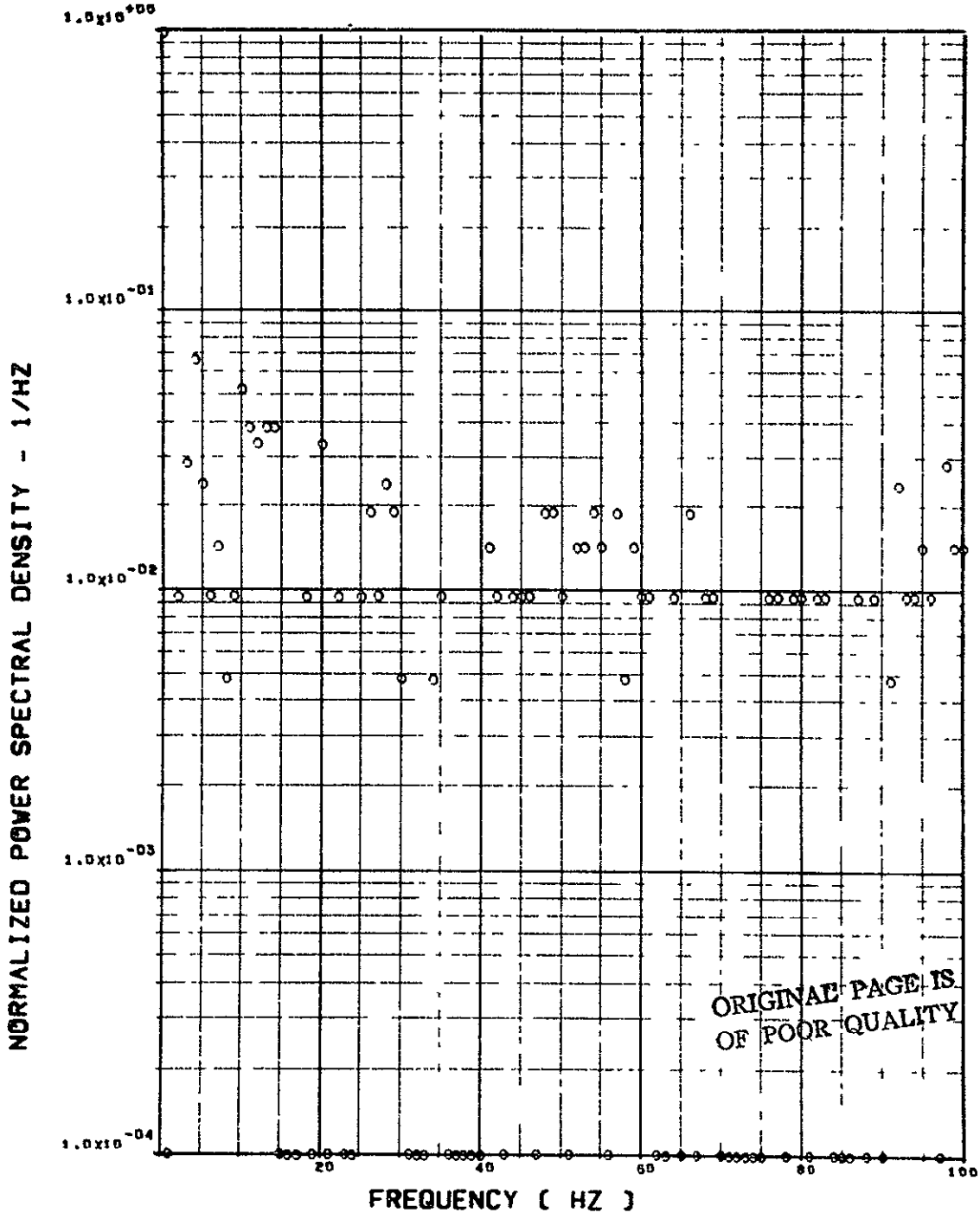

Figure 23. Continued

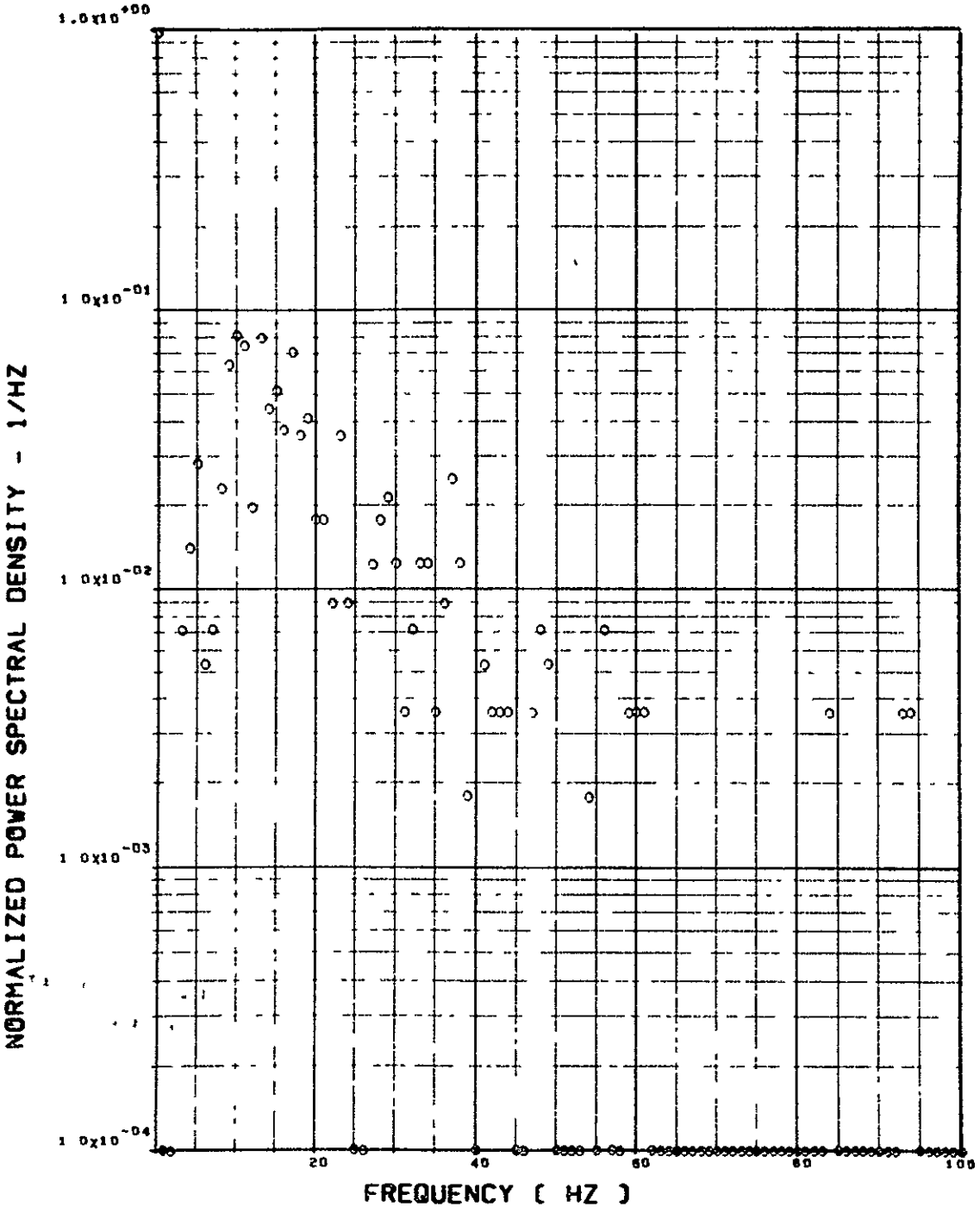

Figure 23. Continued

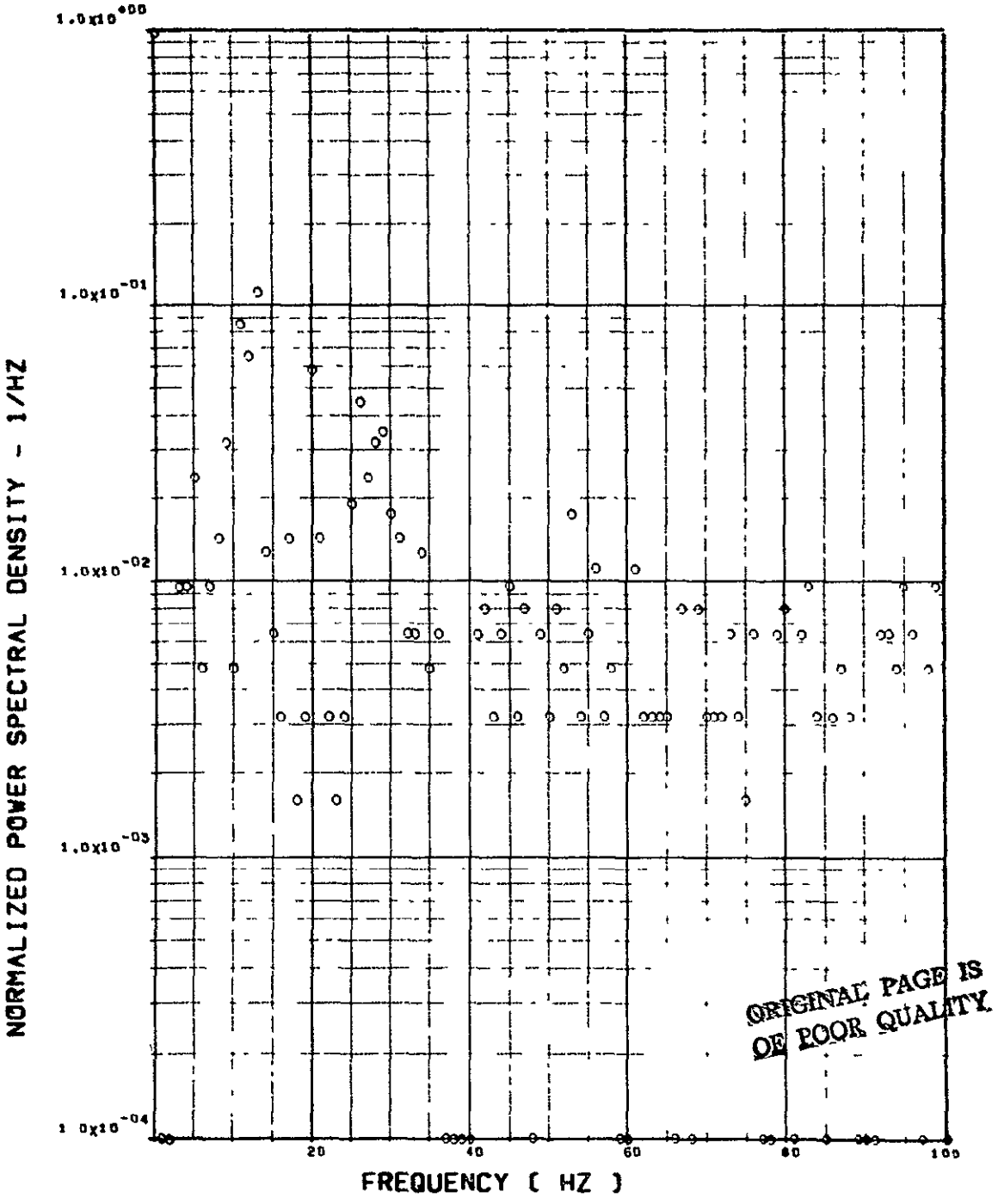

Figure 2). Concluded

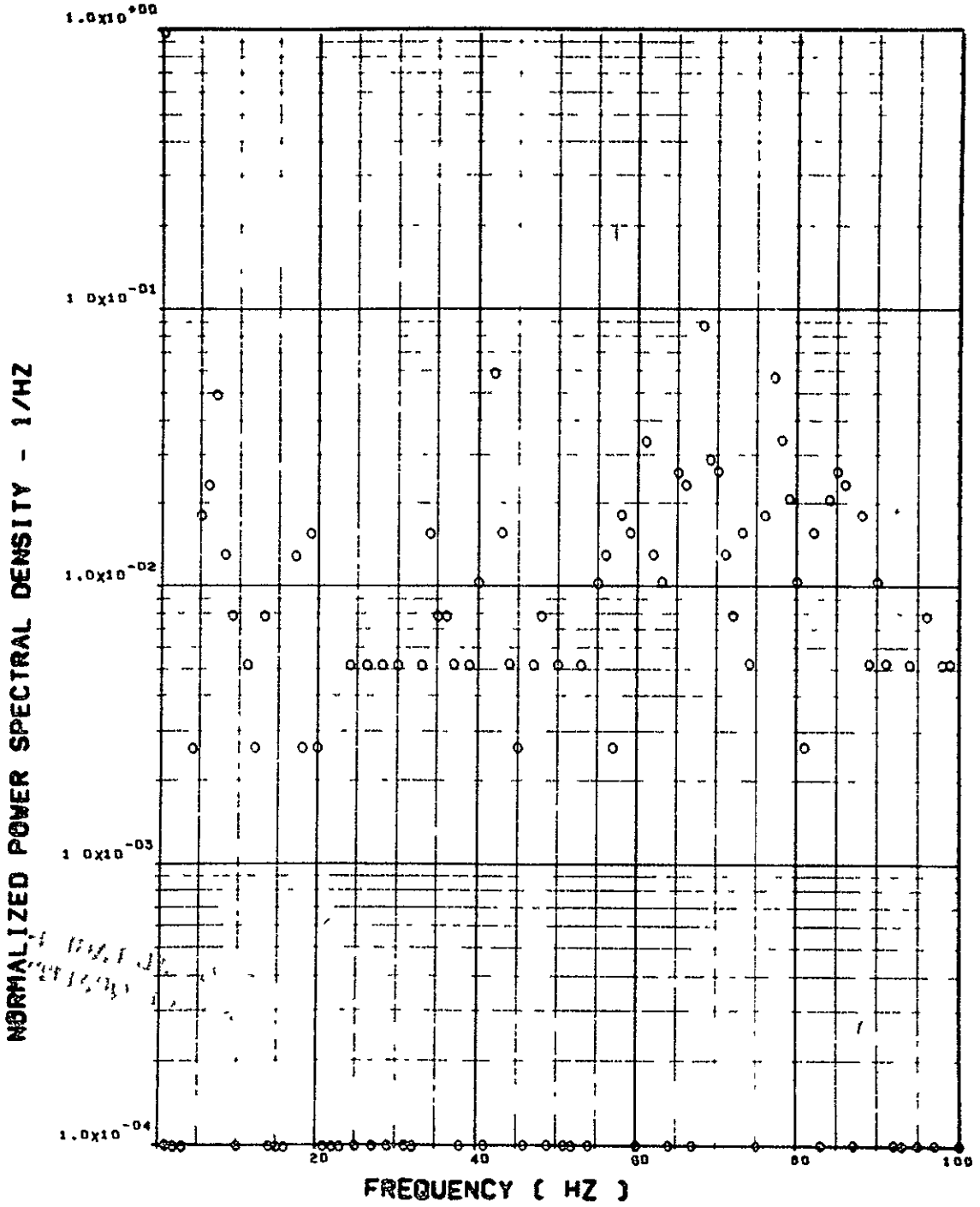

Figure 24. Power Spectra - Flight 48, Run 7R1, Point 5
T_1 = 135958.55, ΔT = 1 Sec, α_{Nom} = 18.70 deg,
$\Delta\alpha$= 1 45 deg.

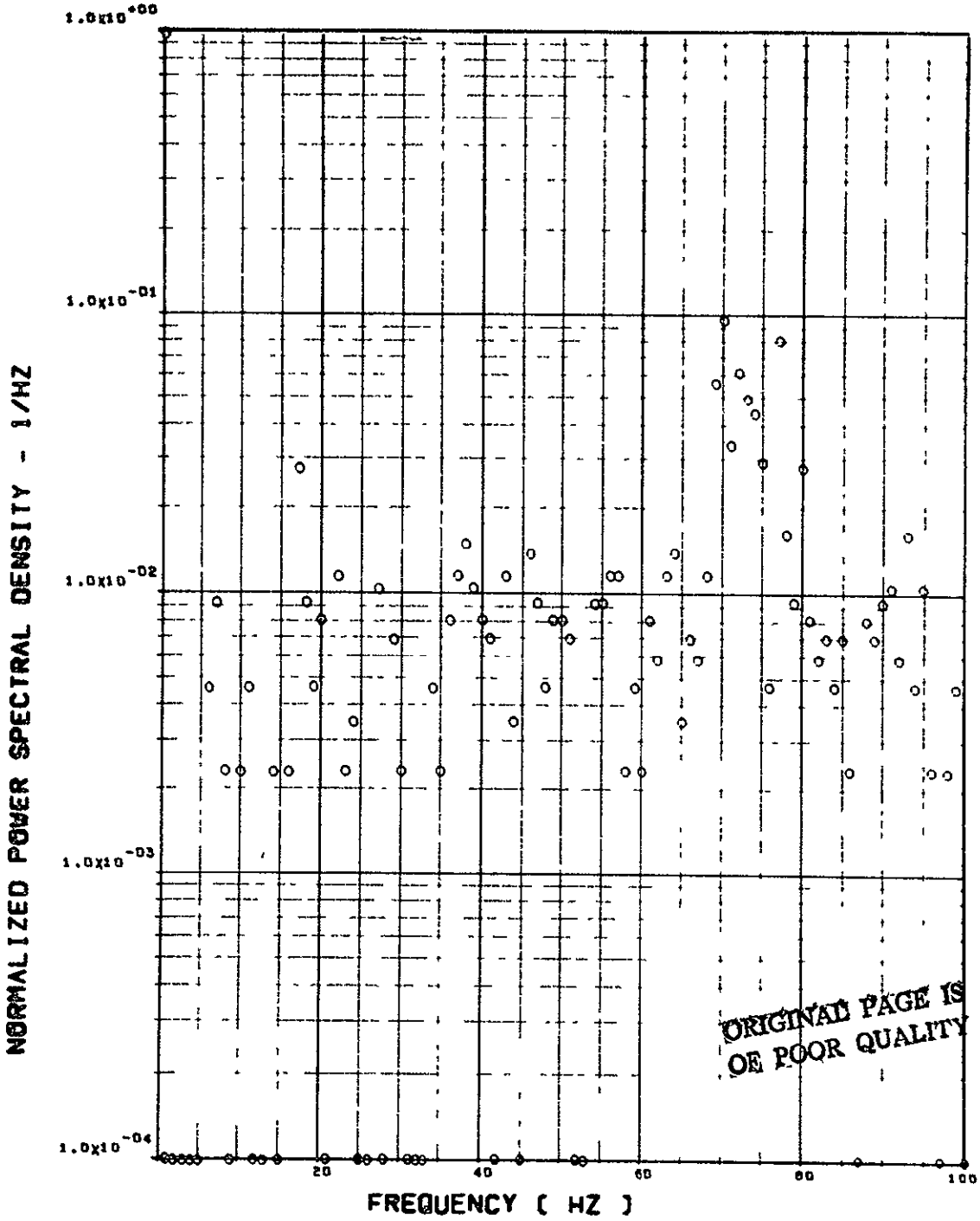

Figure 74. Continued

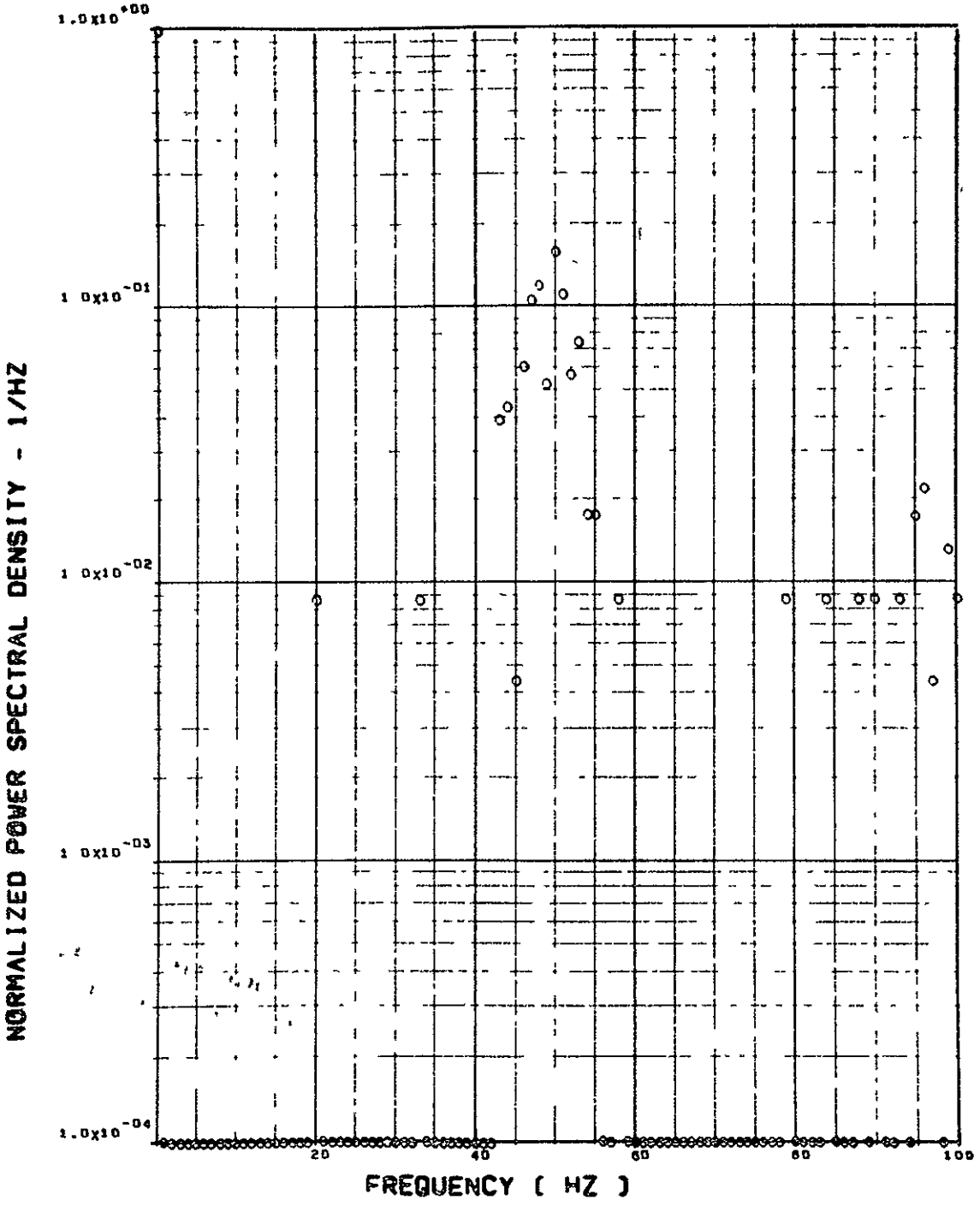

Figure 24. Continued

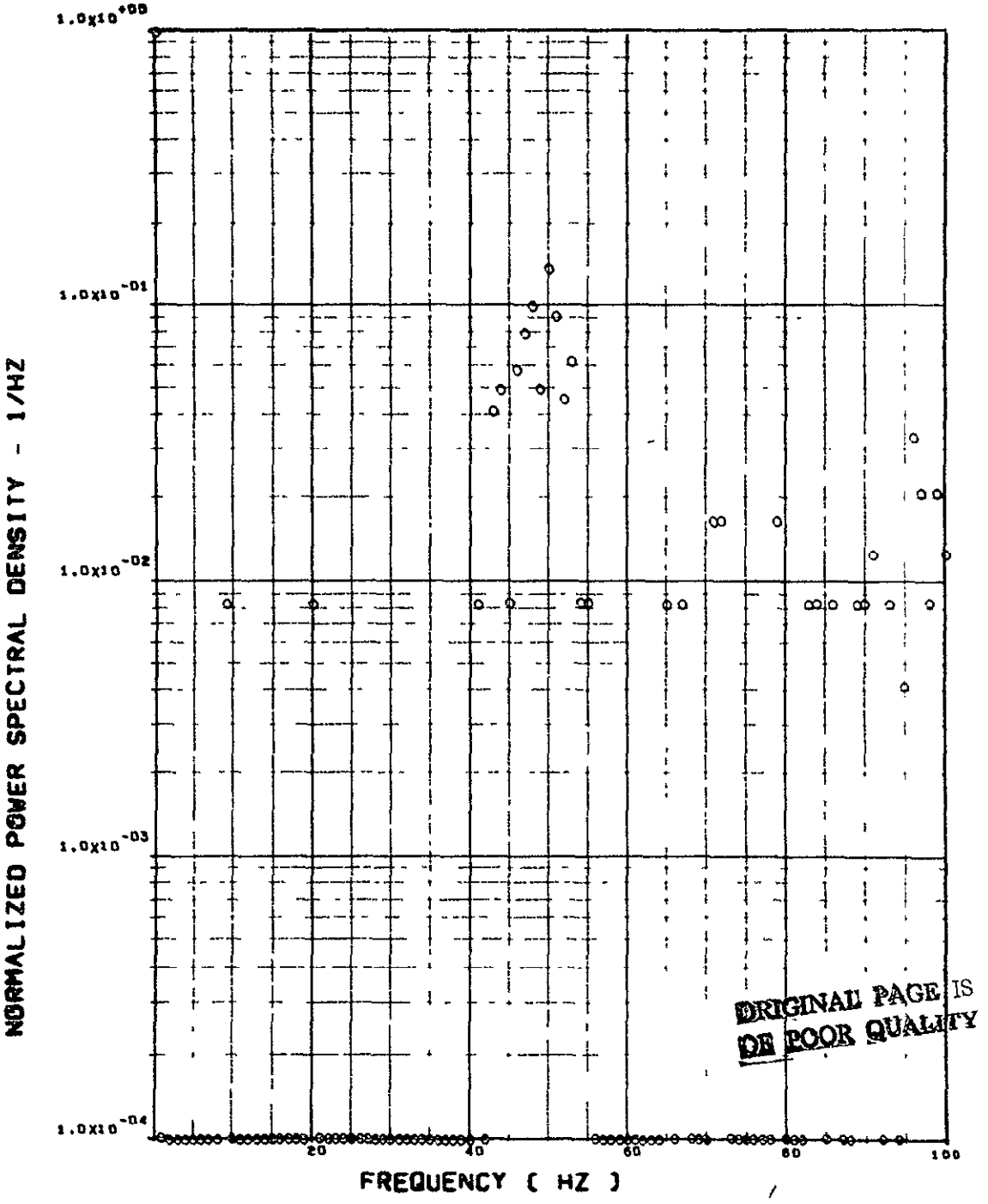

Figure 24. Continued

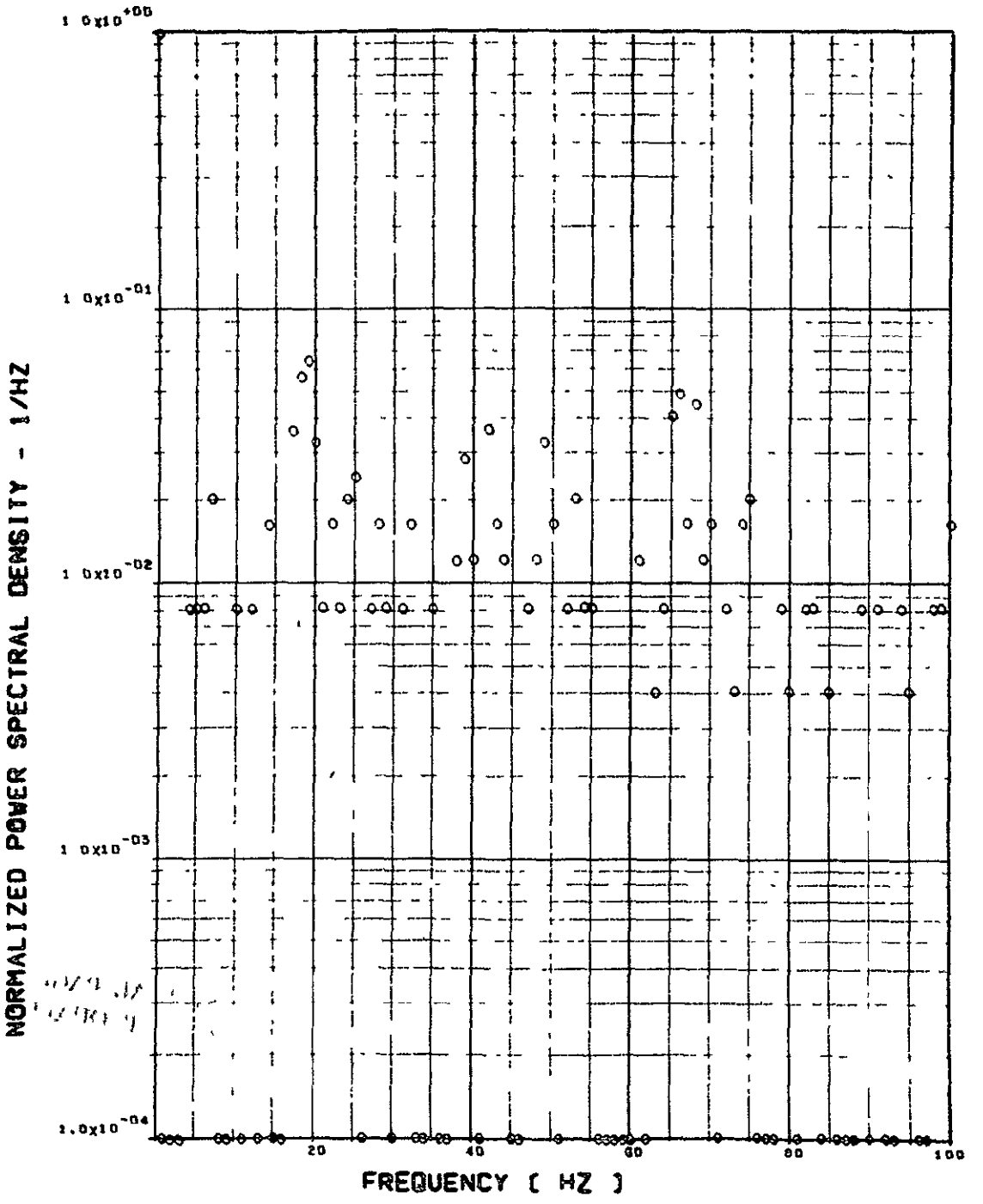

Figure 24. Continued

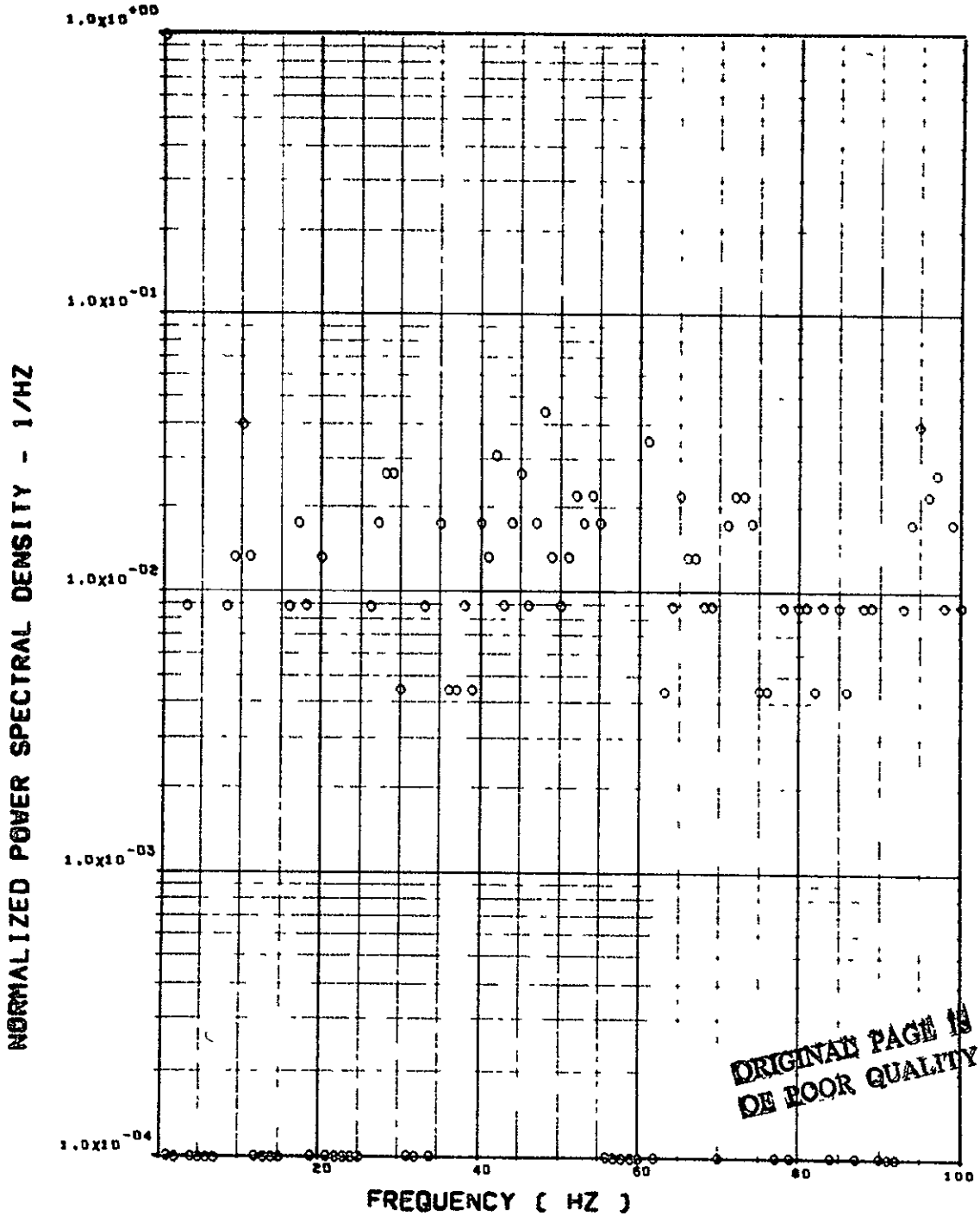

Figure 24. Continued

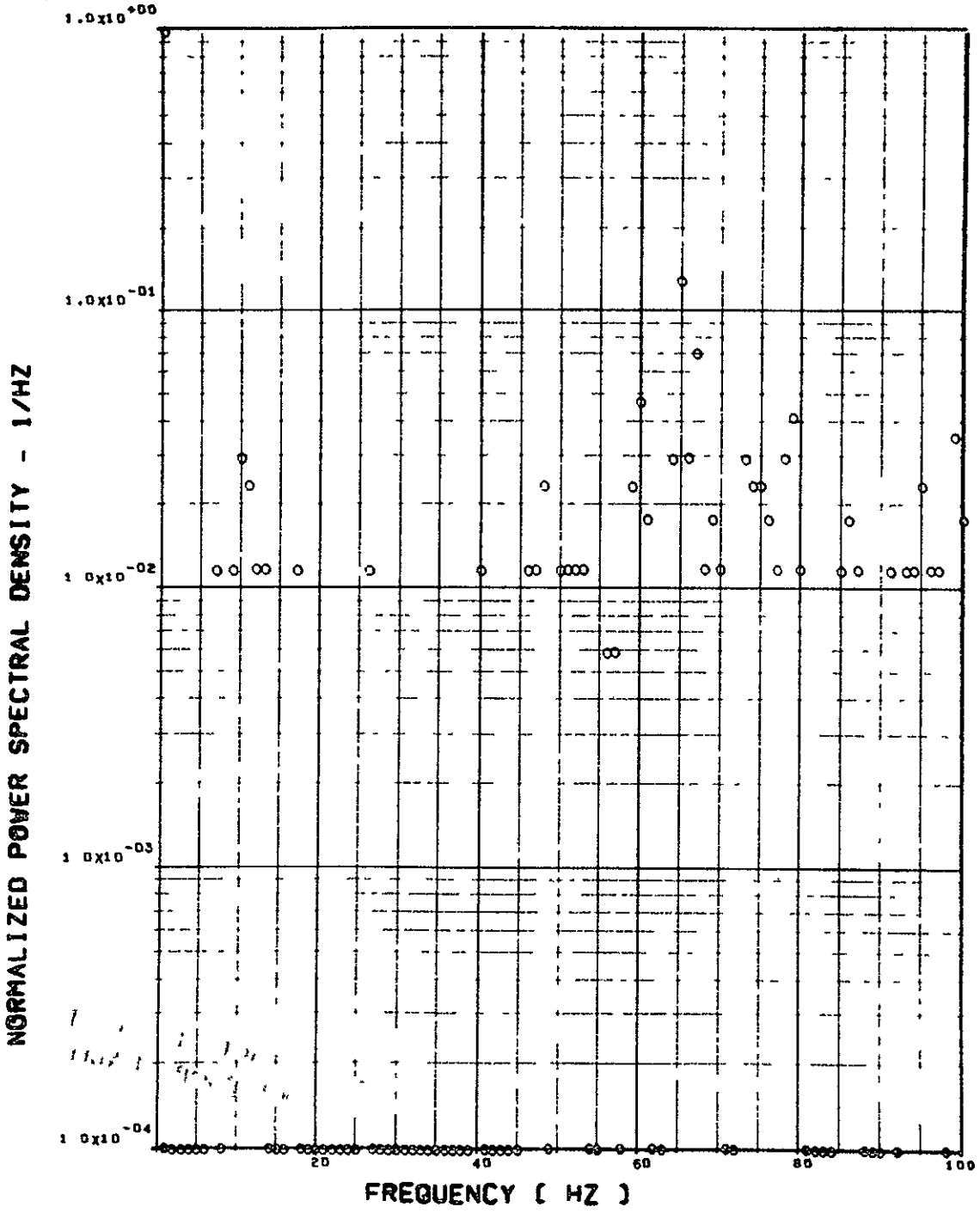

Figure 24. Continued

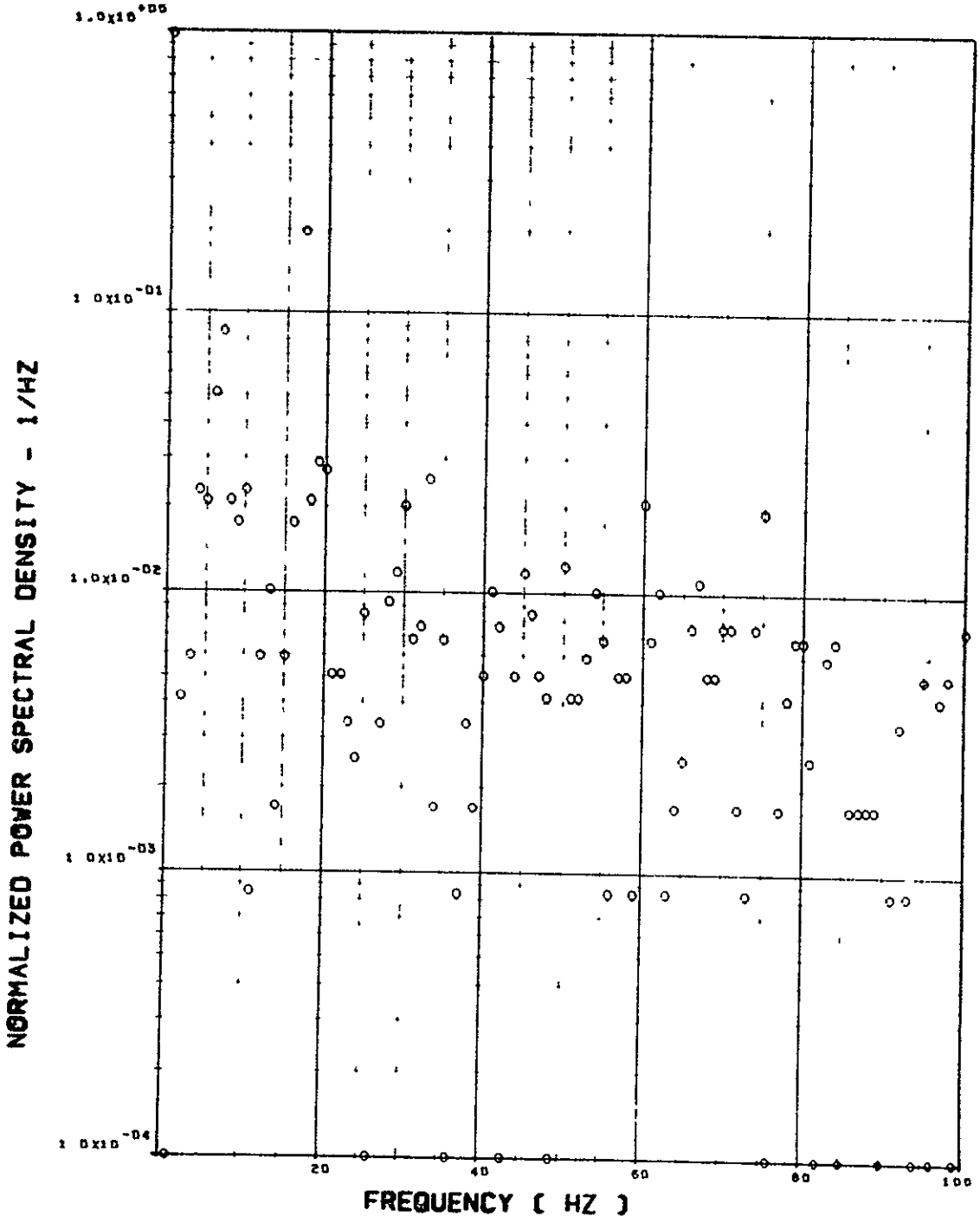

Figure 24. Continued

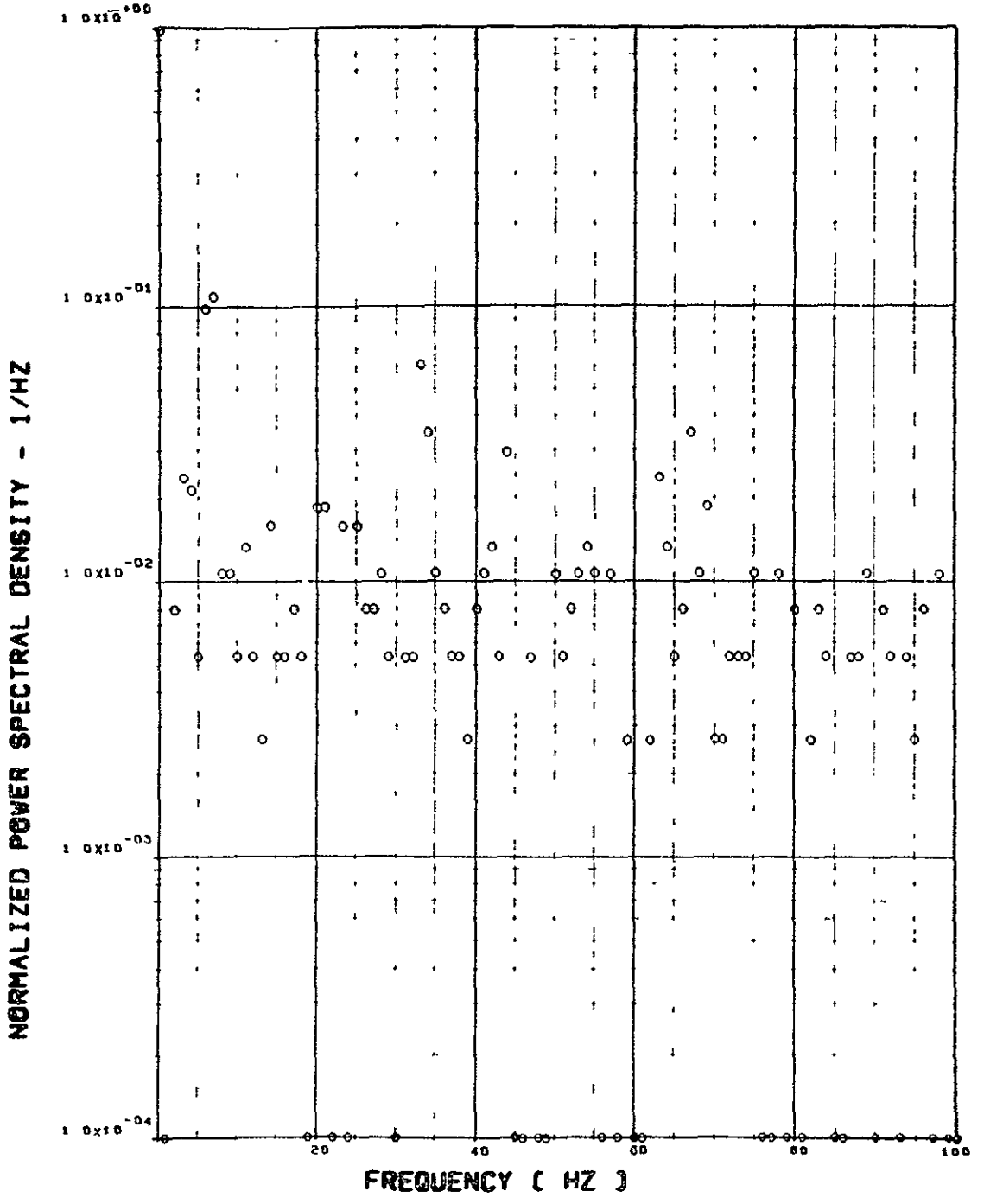

Figure 24. Continued

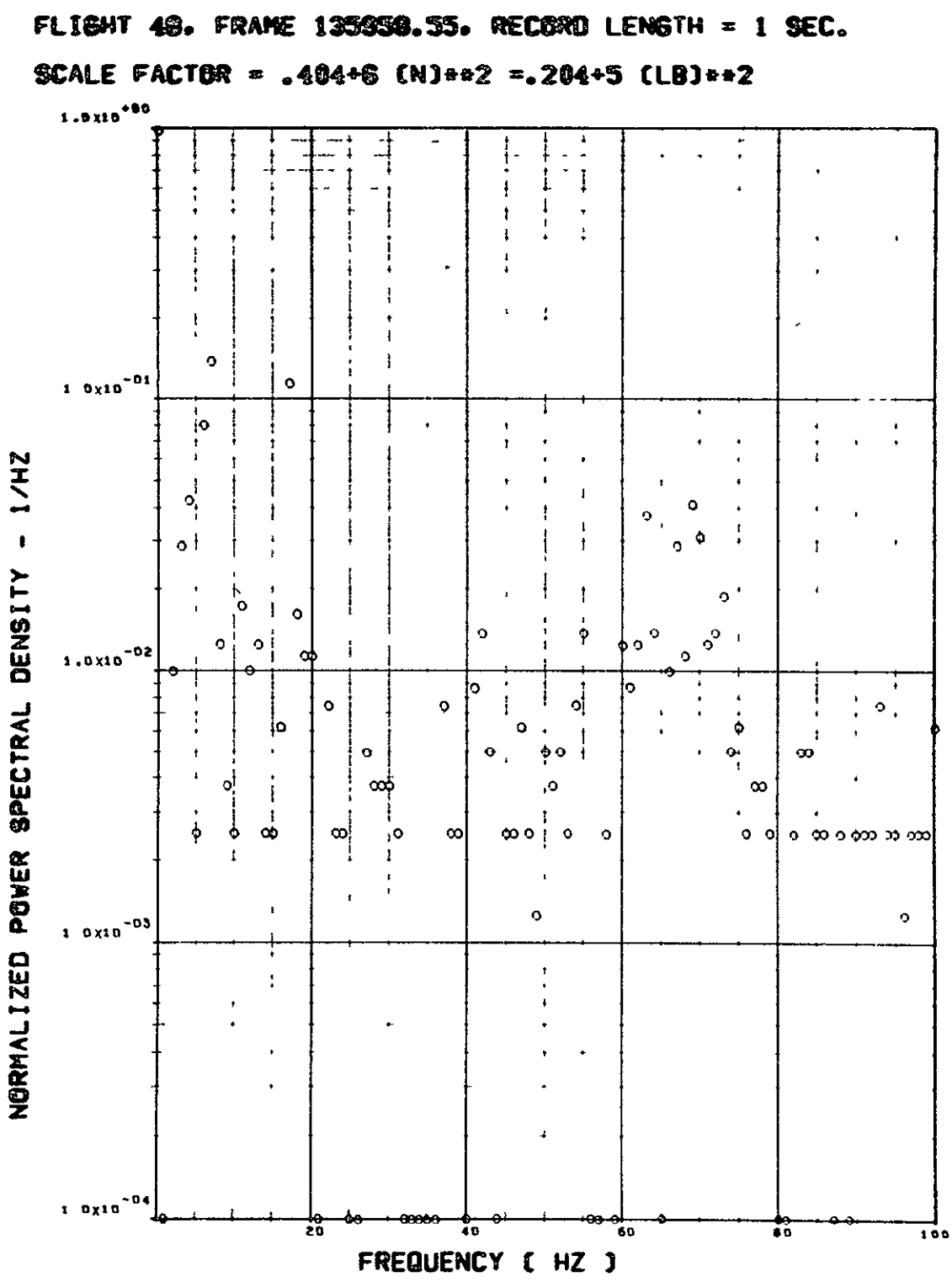

Figure 24. Continued

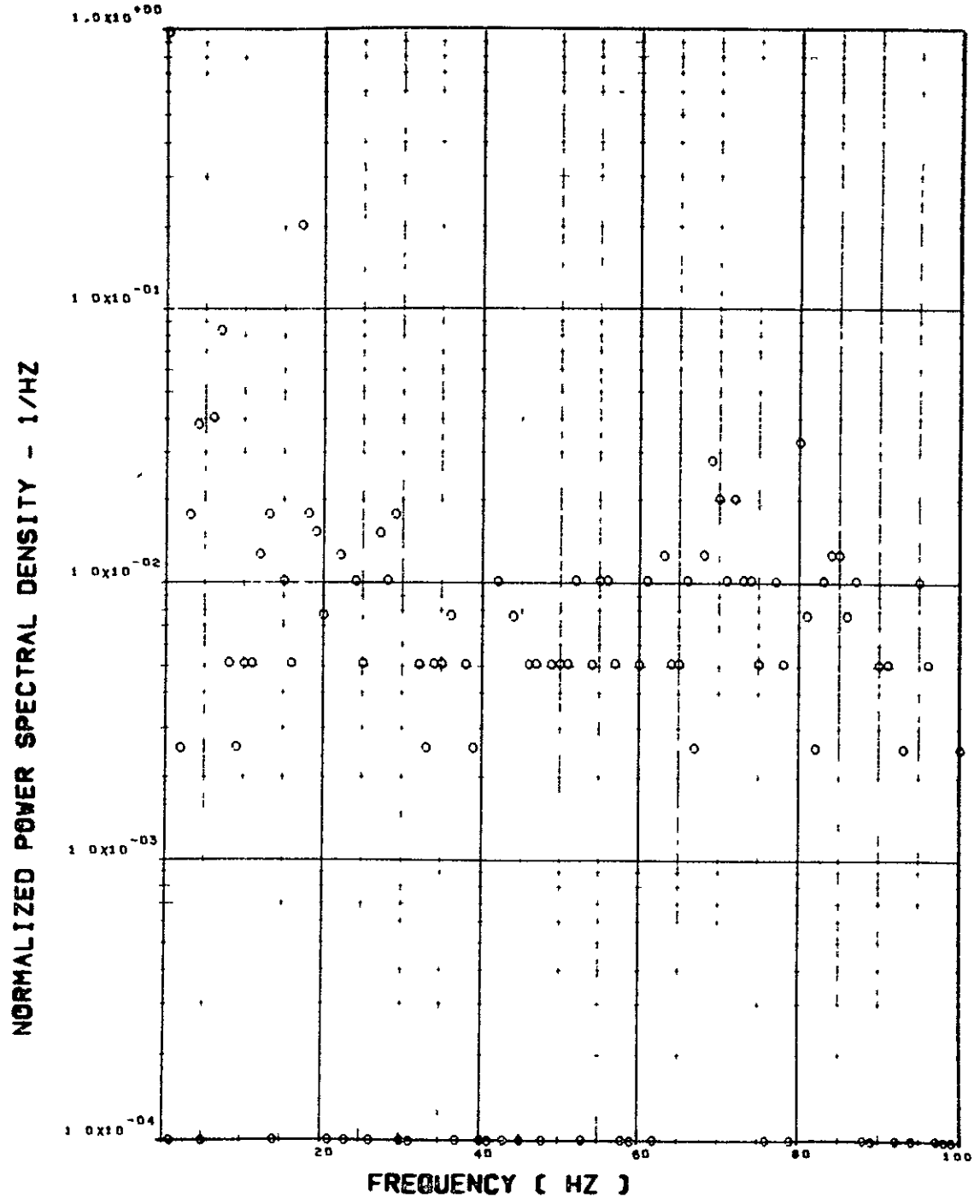

Figure 24. Continued

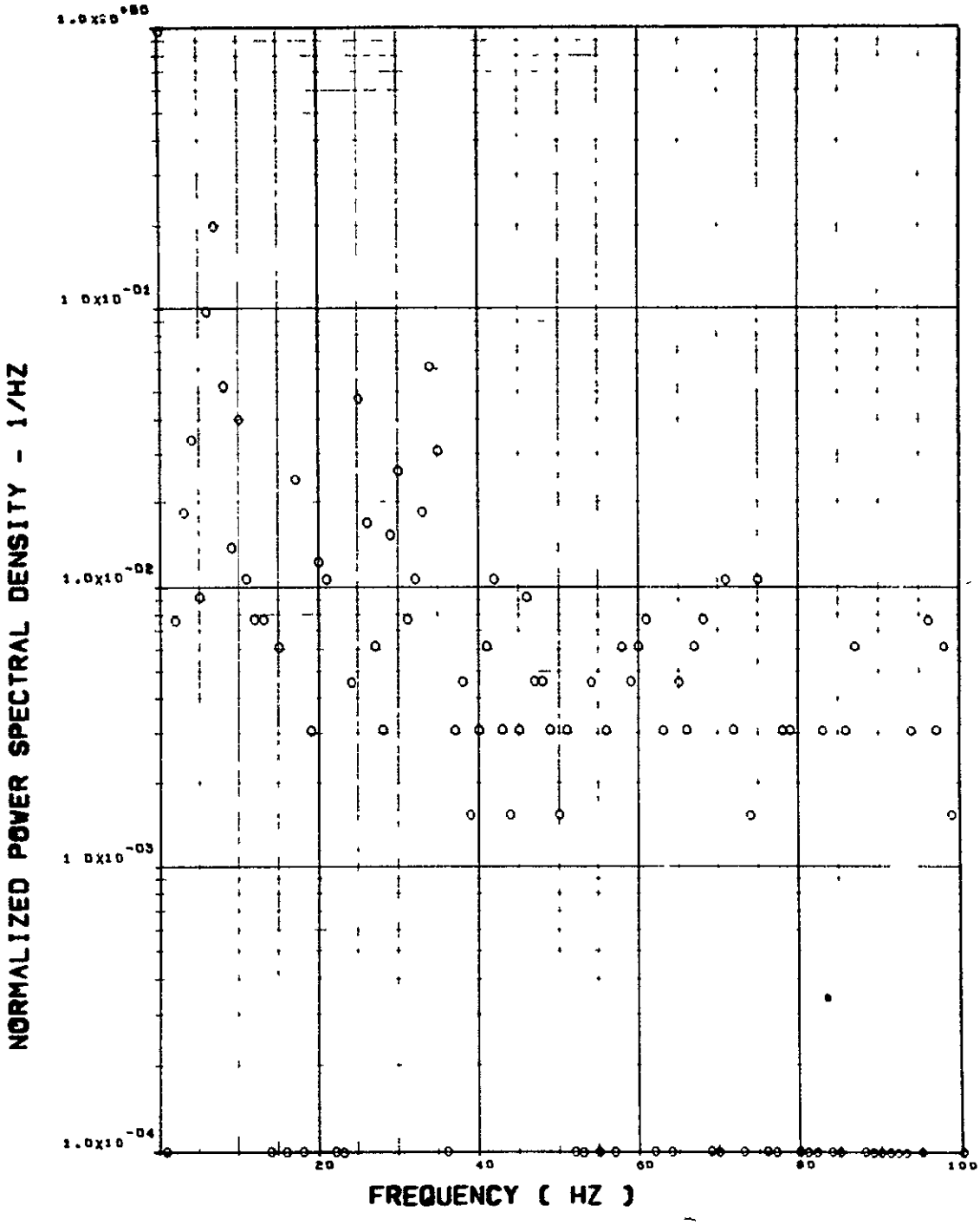

Figure 74. Continued

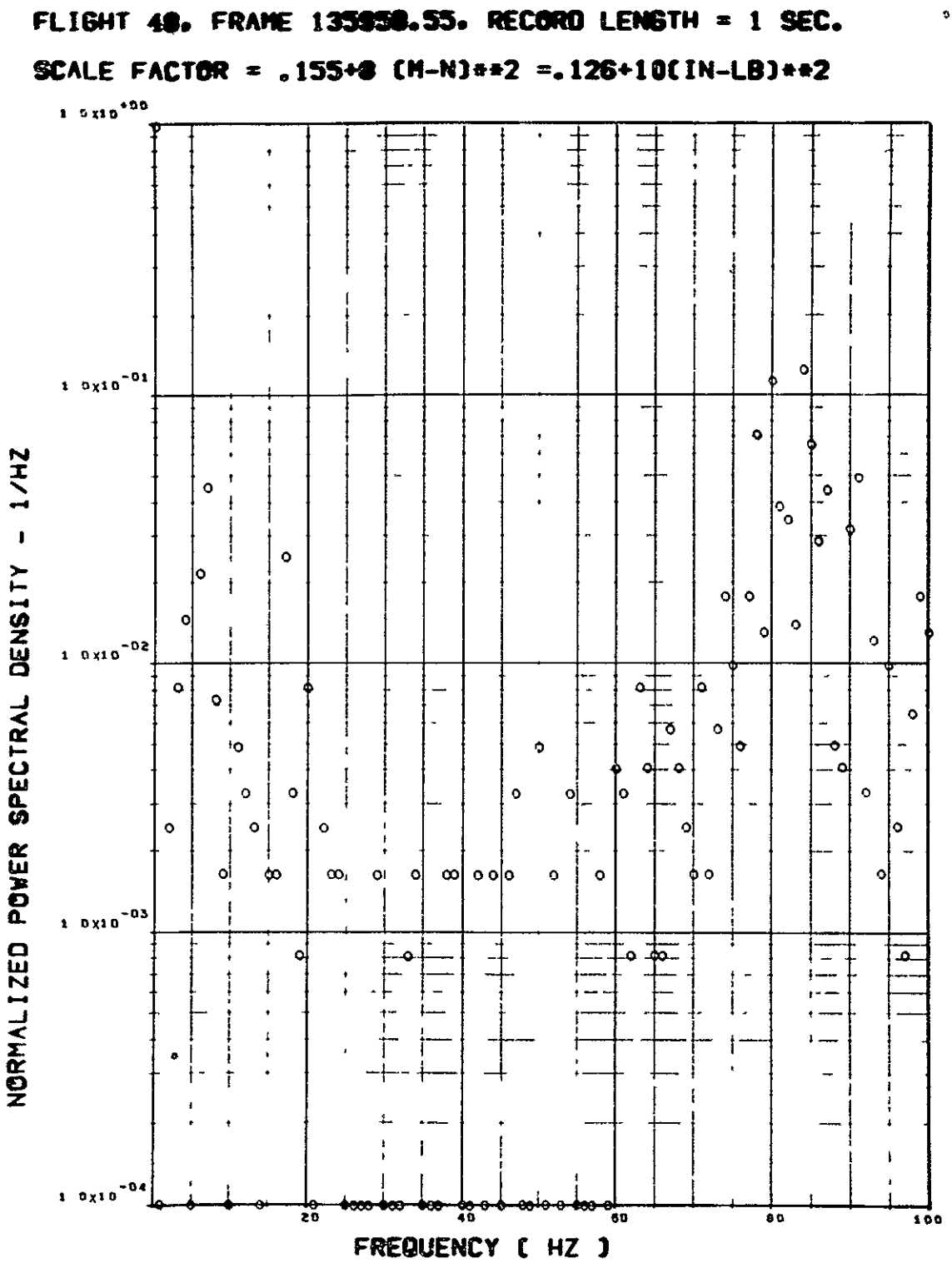

Figure 24. Continued

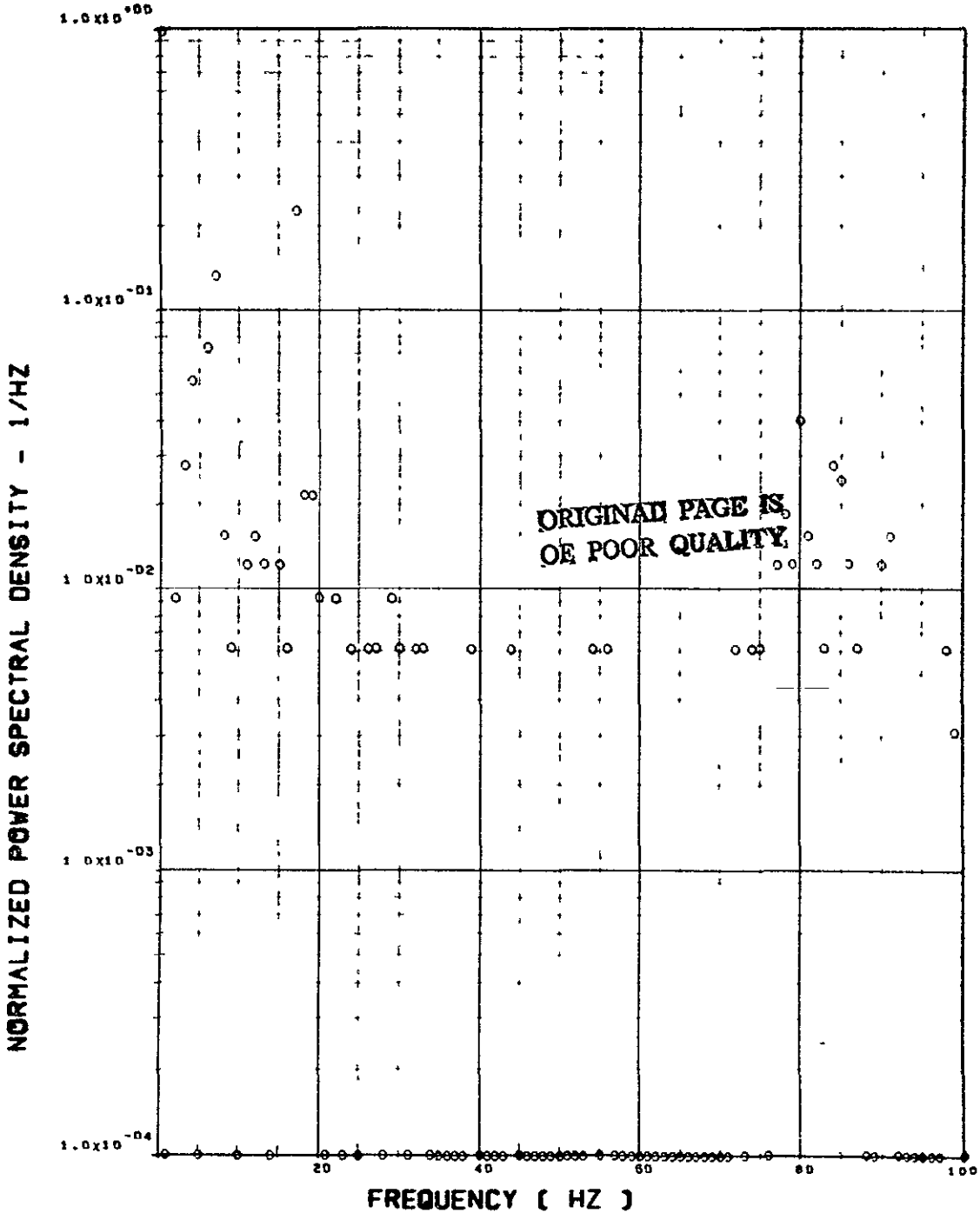

Figure 24. Continued

FLIGHT 48. FRAME 135958 55 . RECORD LENGTH [illegible] SEC.

SCALE FACTOR = .169+6 (M-N)**2 =.137+8 (IN-LB)**2

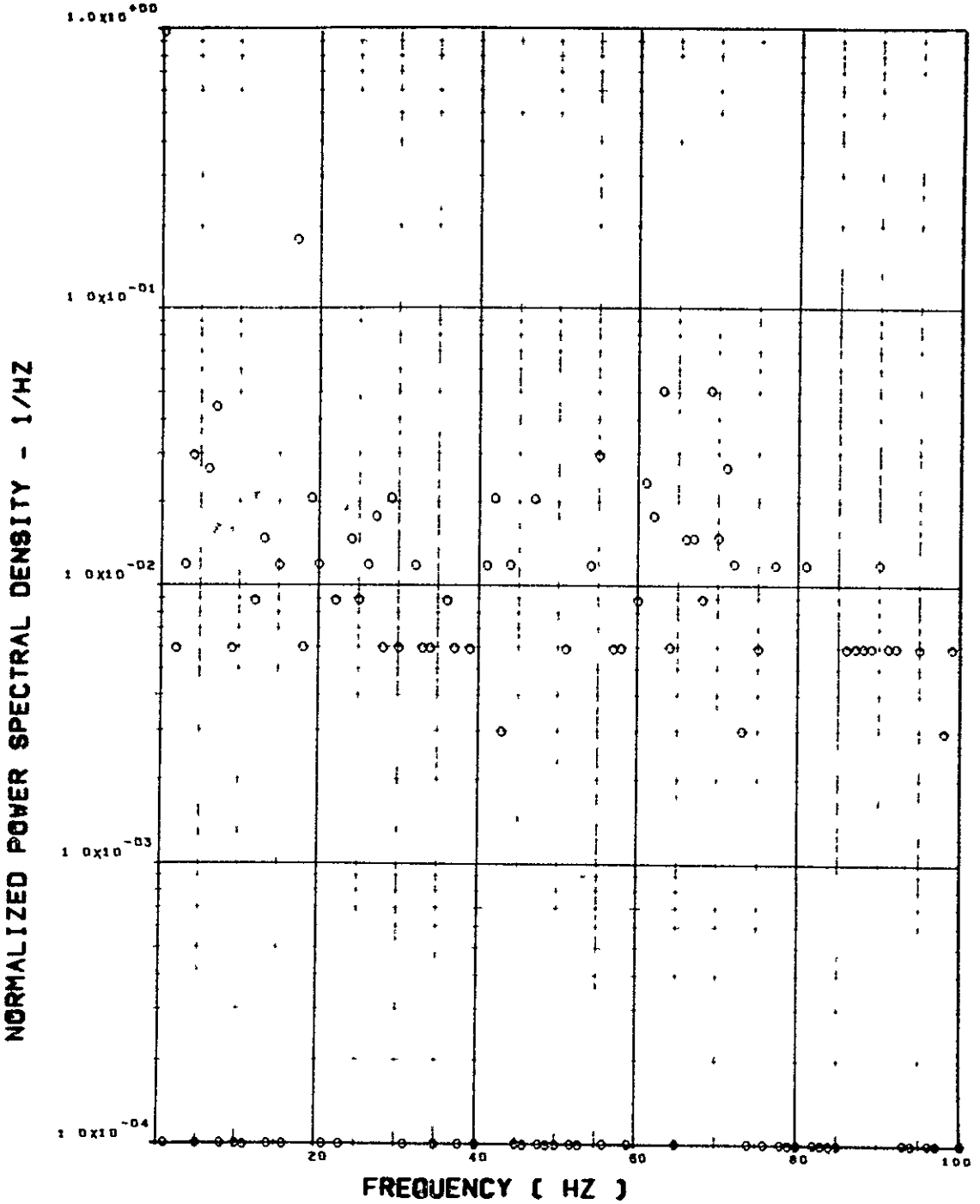

ITEM - SW133 BENDING MOMENT AT WING STATION 4

Figure 24. Continued

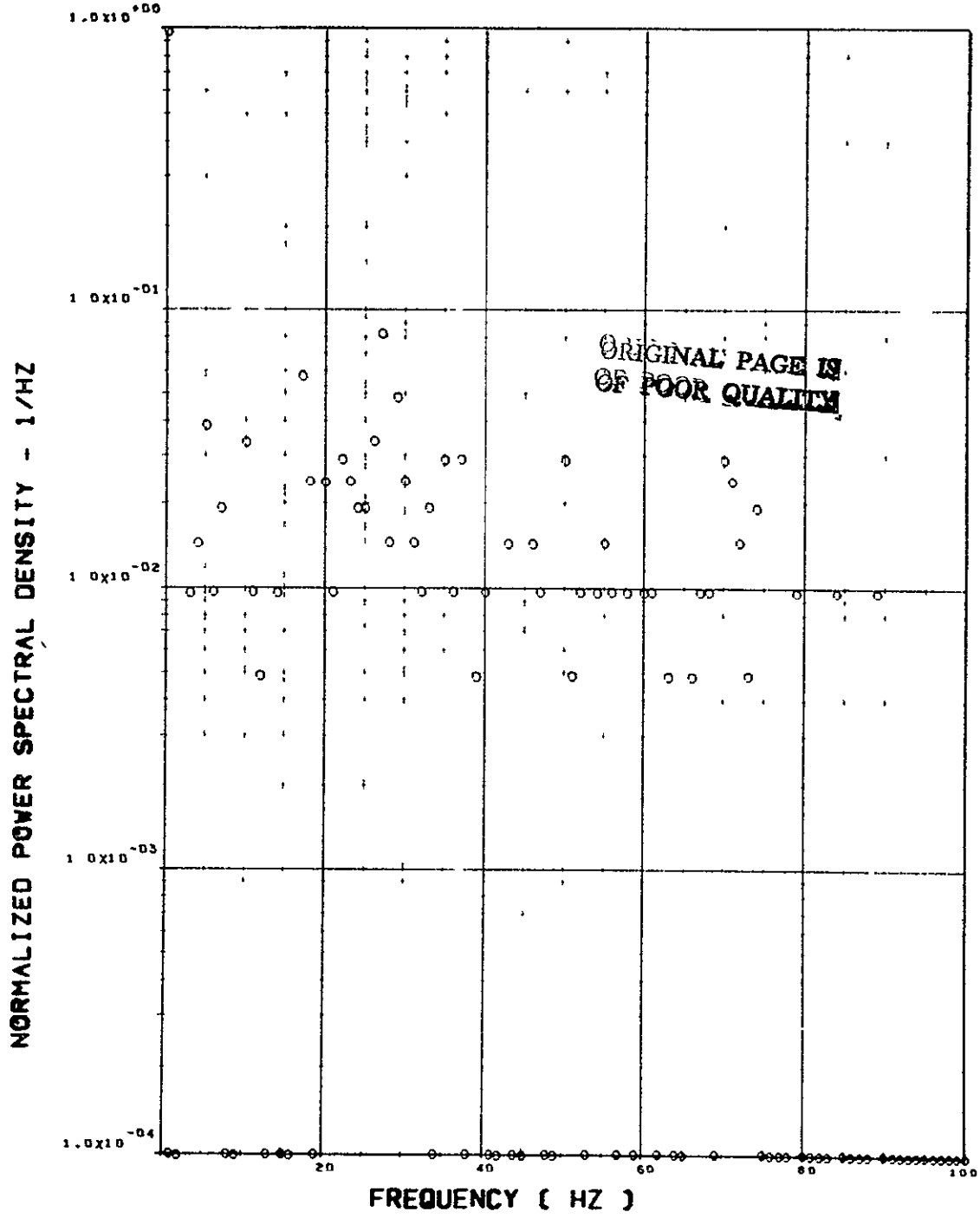

Figure 21. Continued

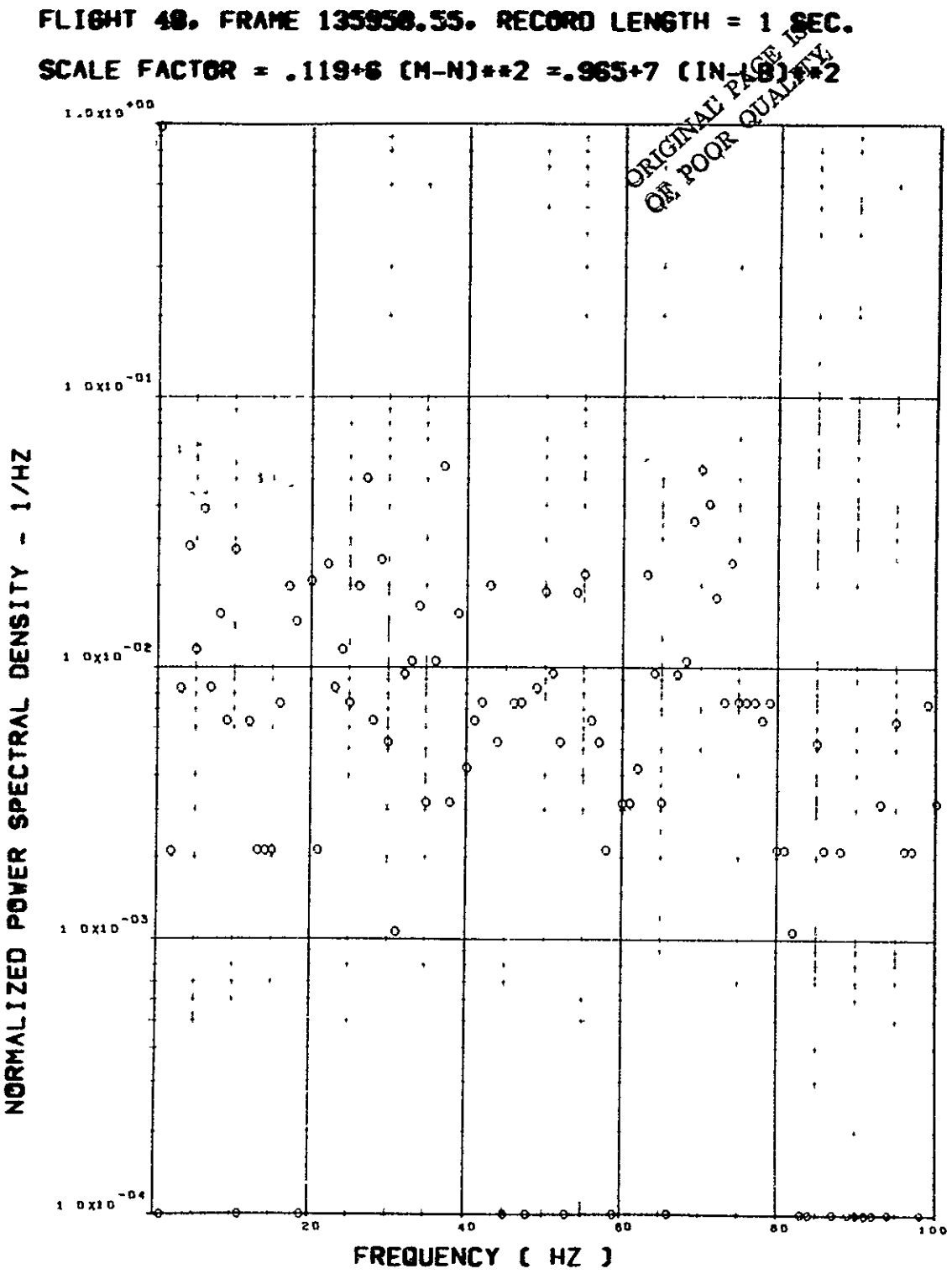

Figure 24. Continued

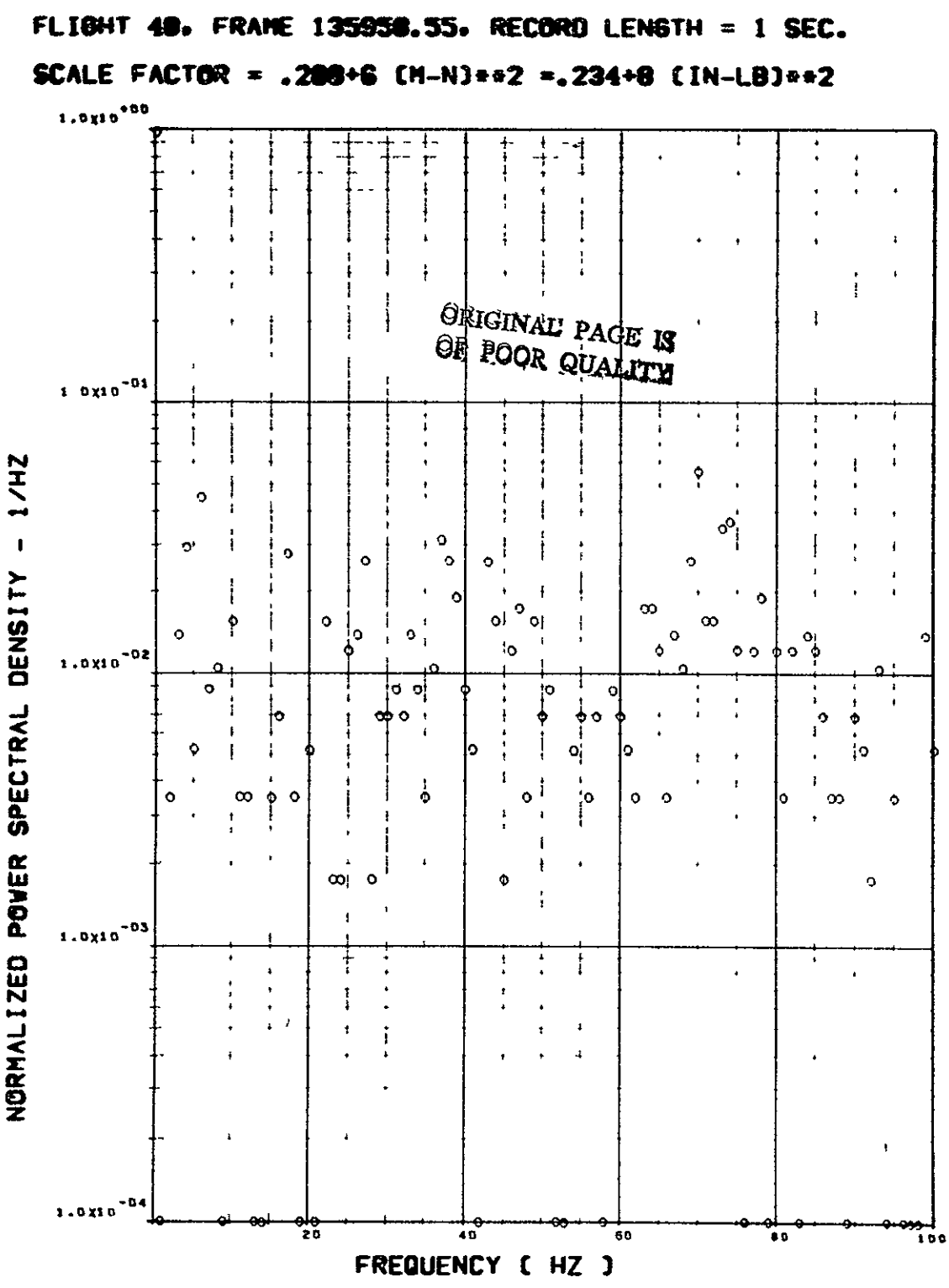

Figure 24. Continued

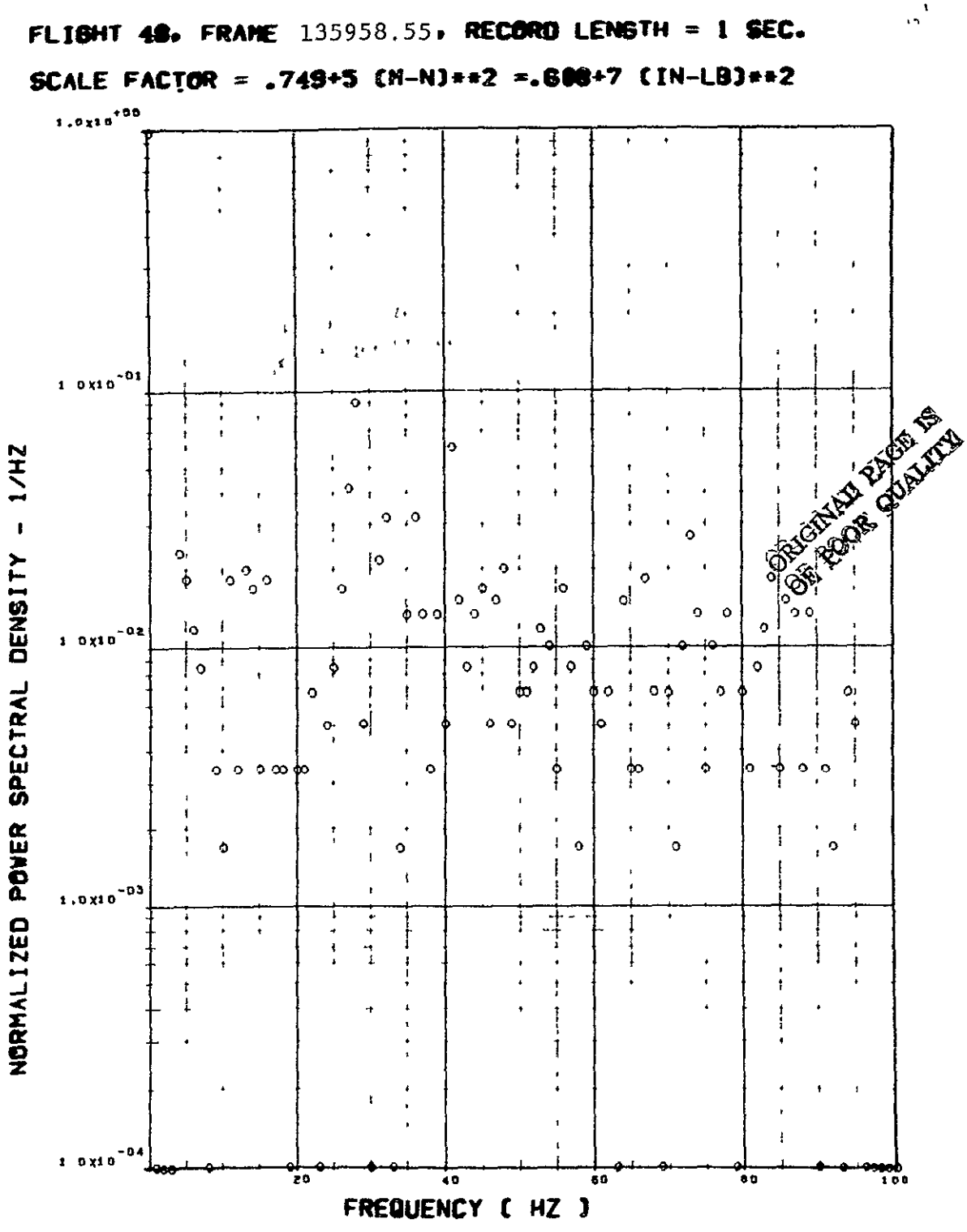

Figure 24. Continued

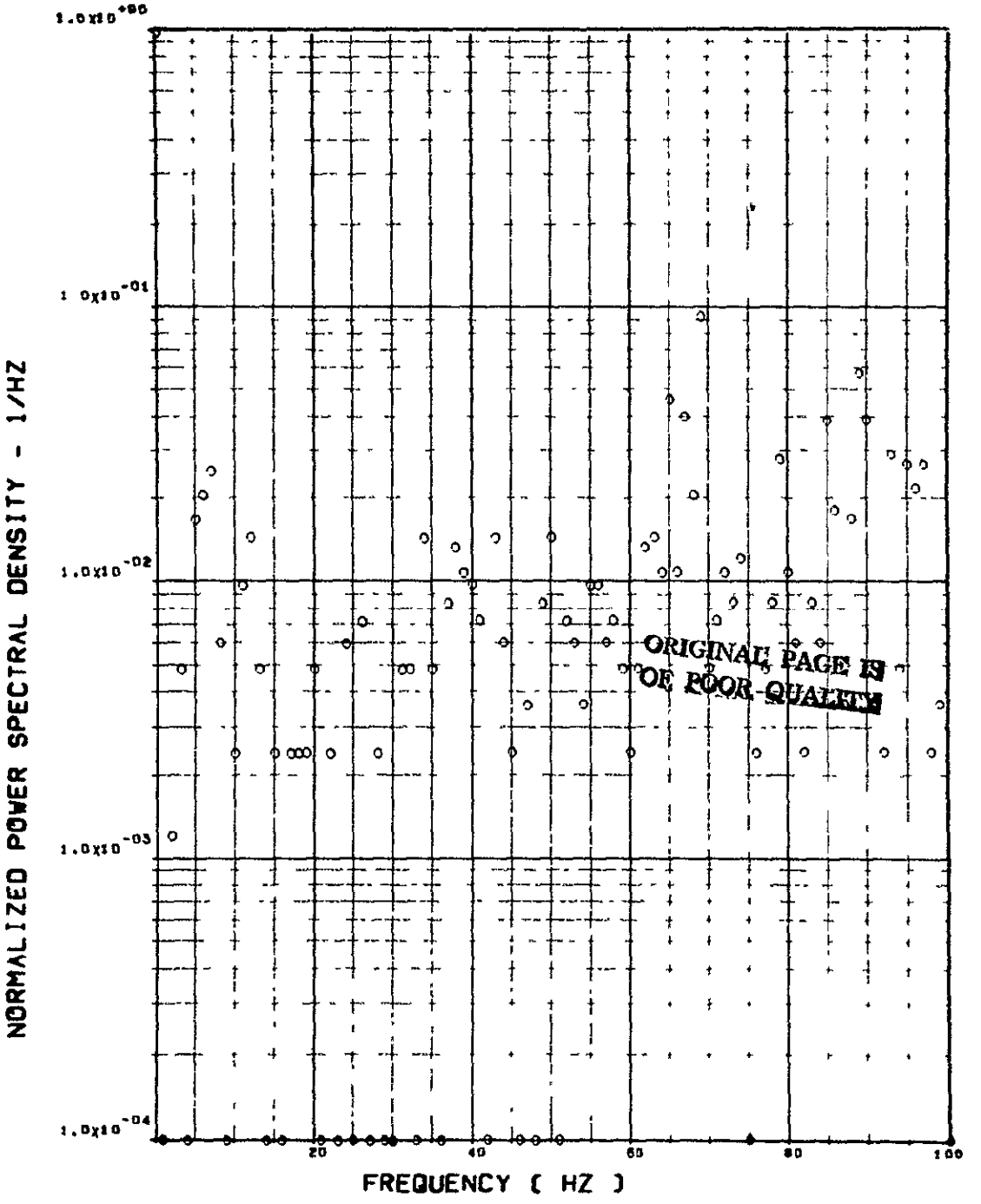

Figure 24. Continued

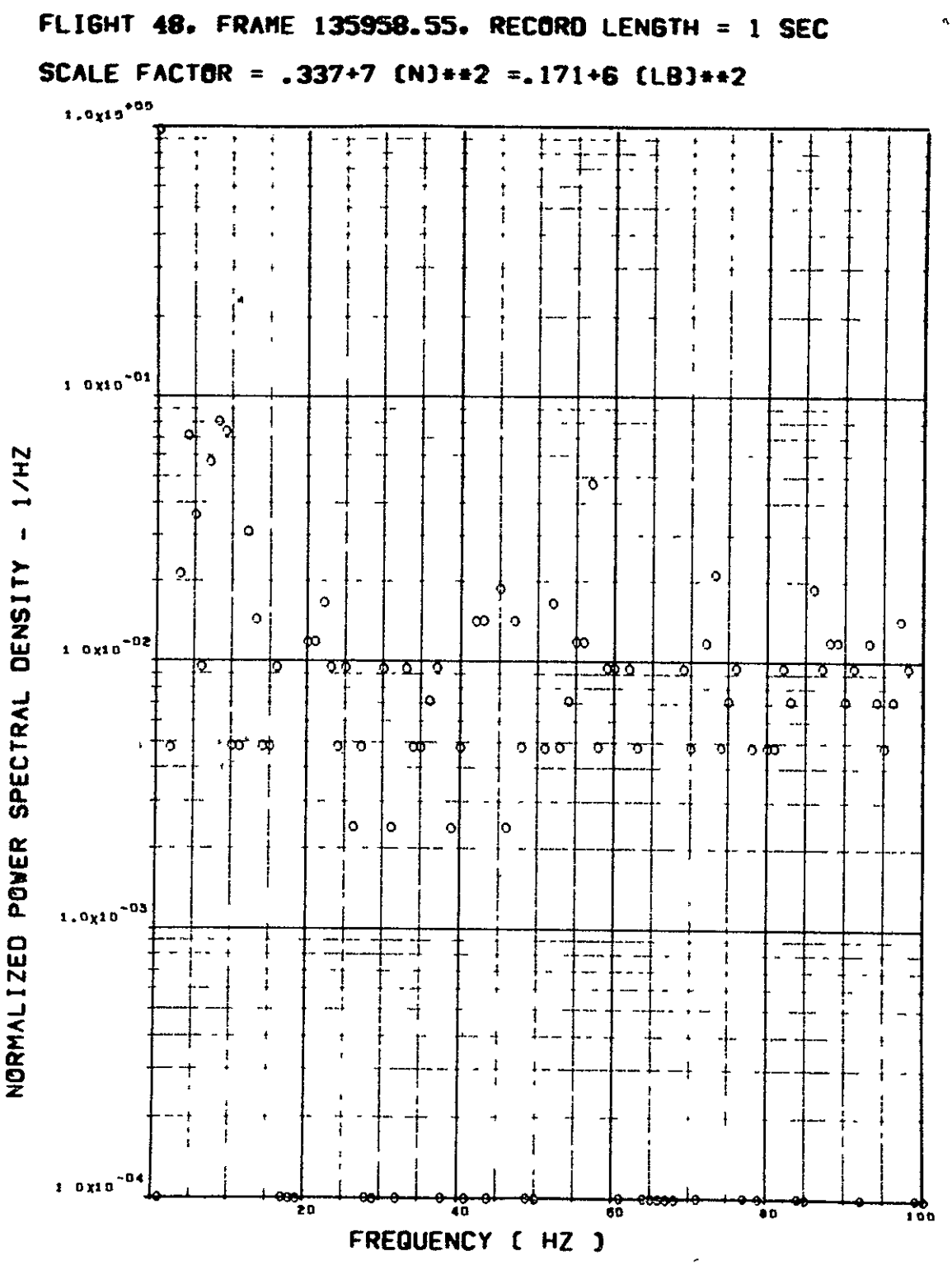

Figure 24. Continued

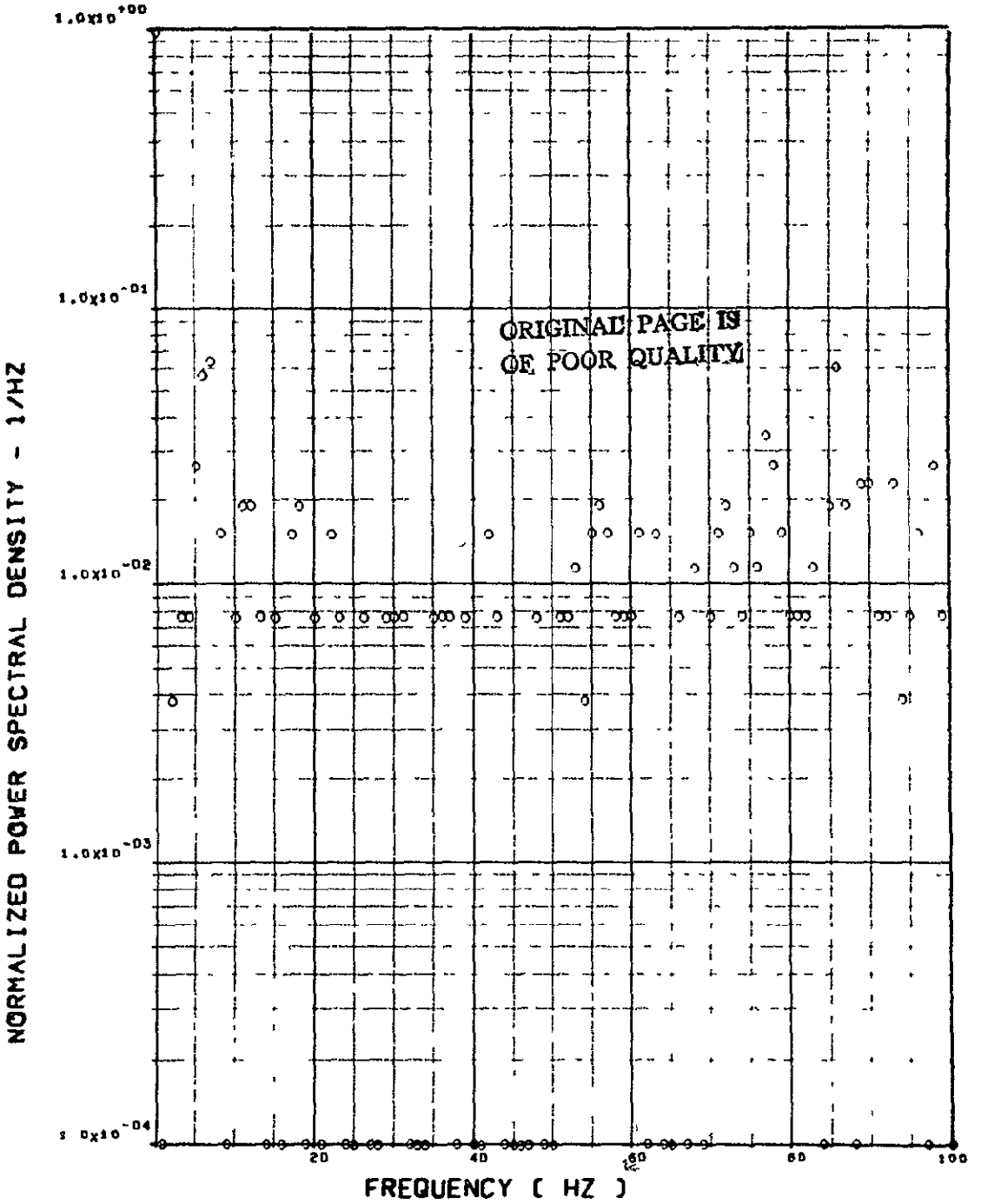

Figure 24. Continued

FLIGHT 48. FRAME 135958.55. RECORD LENGTH = 1 SEC

SCALE FACTOR = .969+2 (M-N)**2 =.786+4 (IN-LB)**2

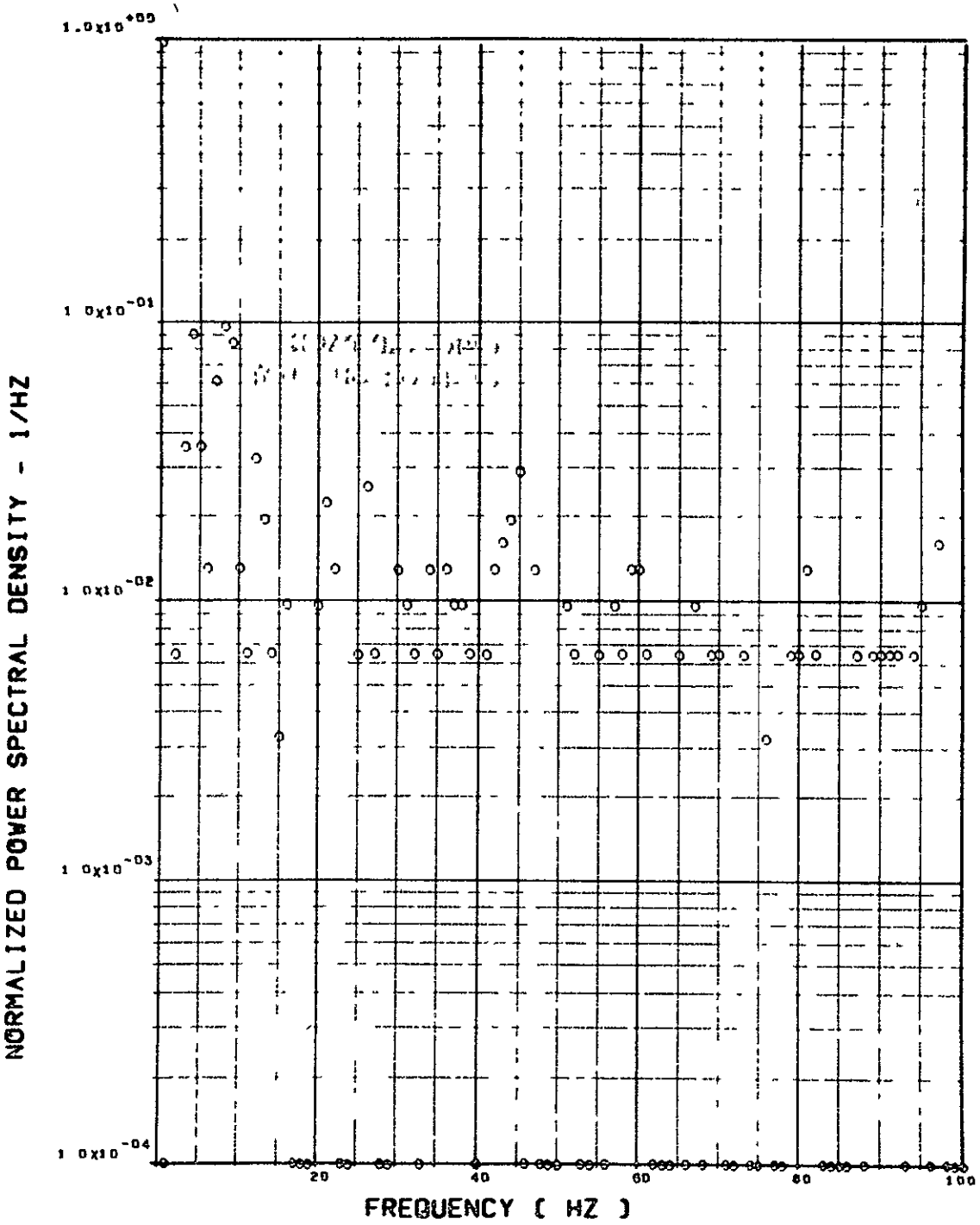

ITEM - ST073 BEND. MOM. R/H HORIZ TAIL ROOT

Figure 24. Continued

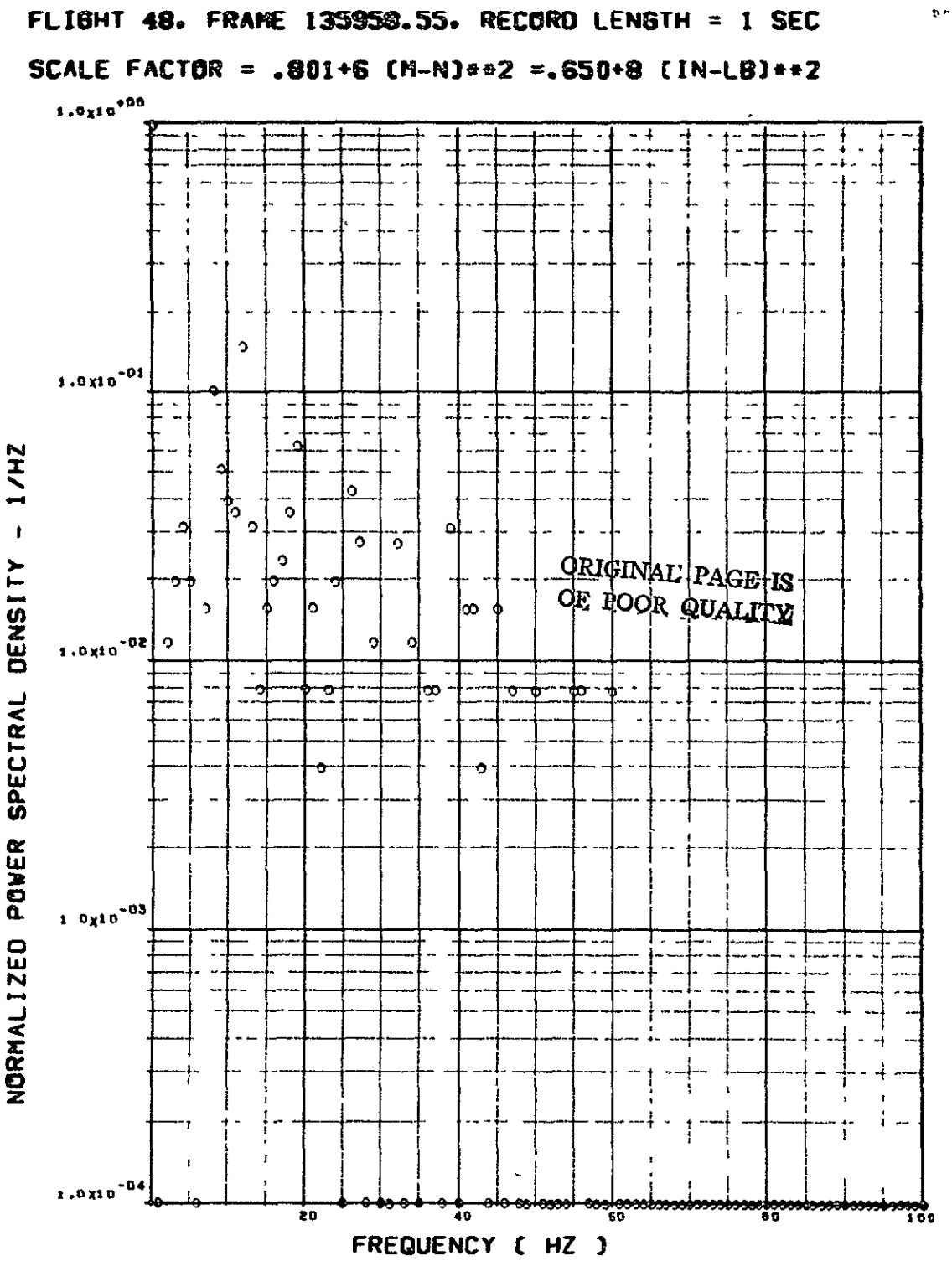

Figure 24. Continued

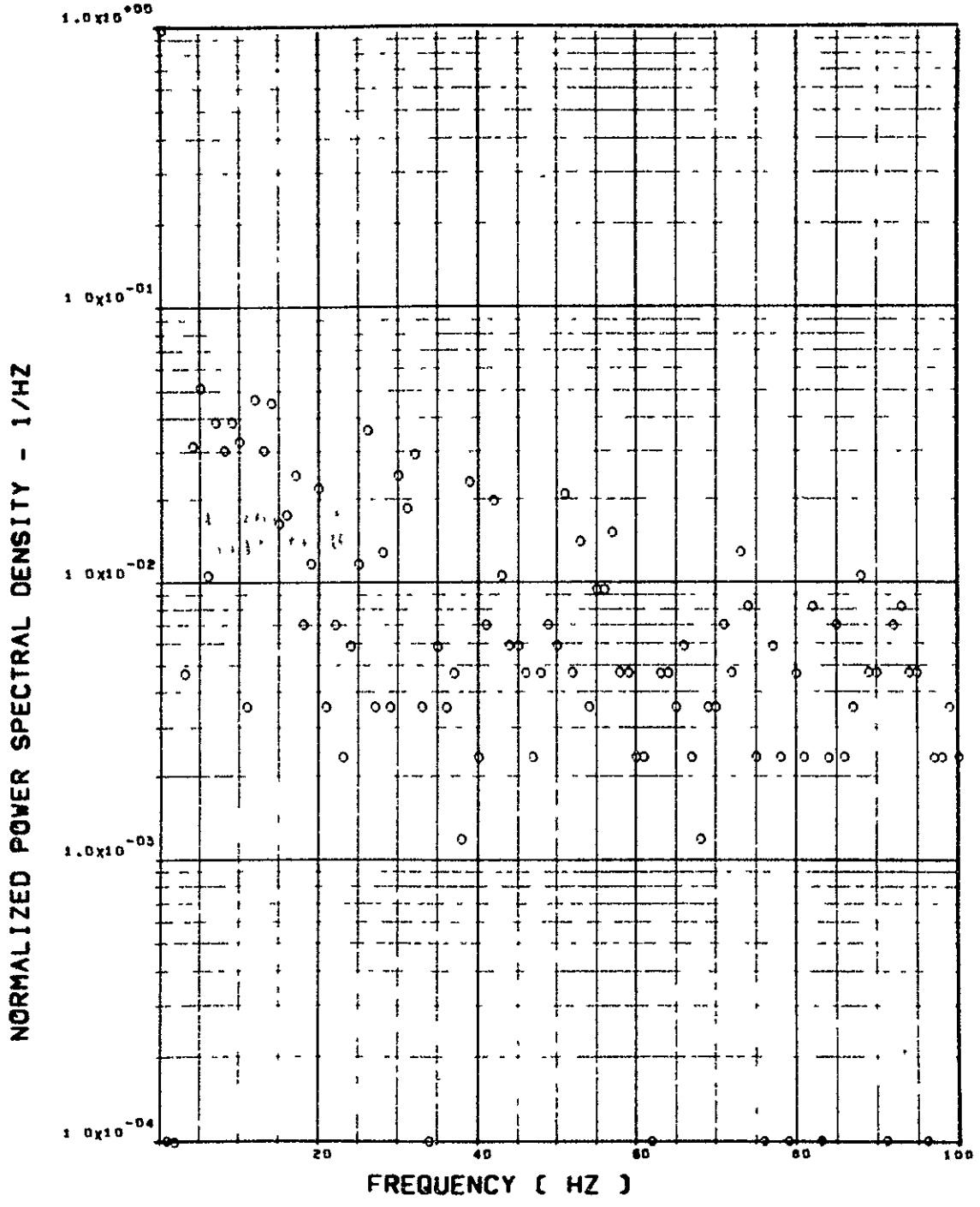

Figure 24. Concluded

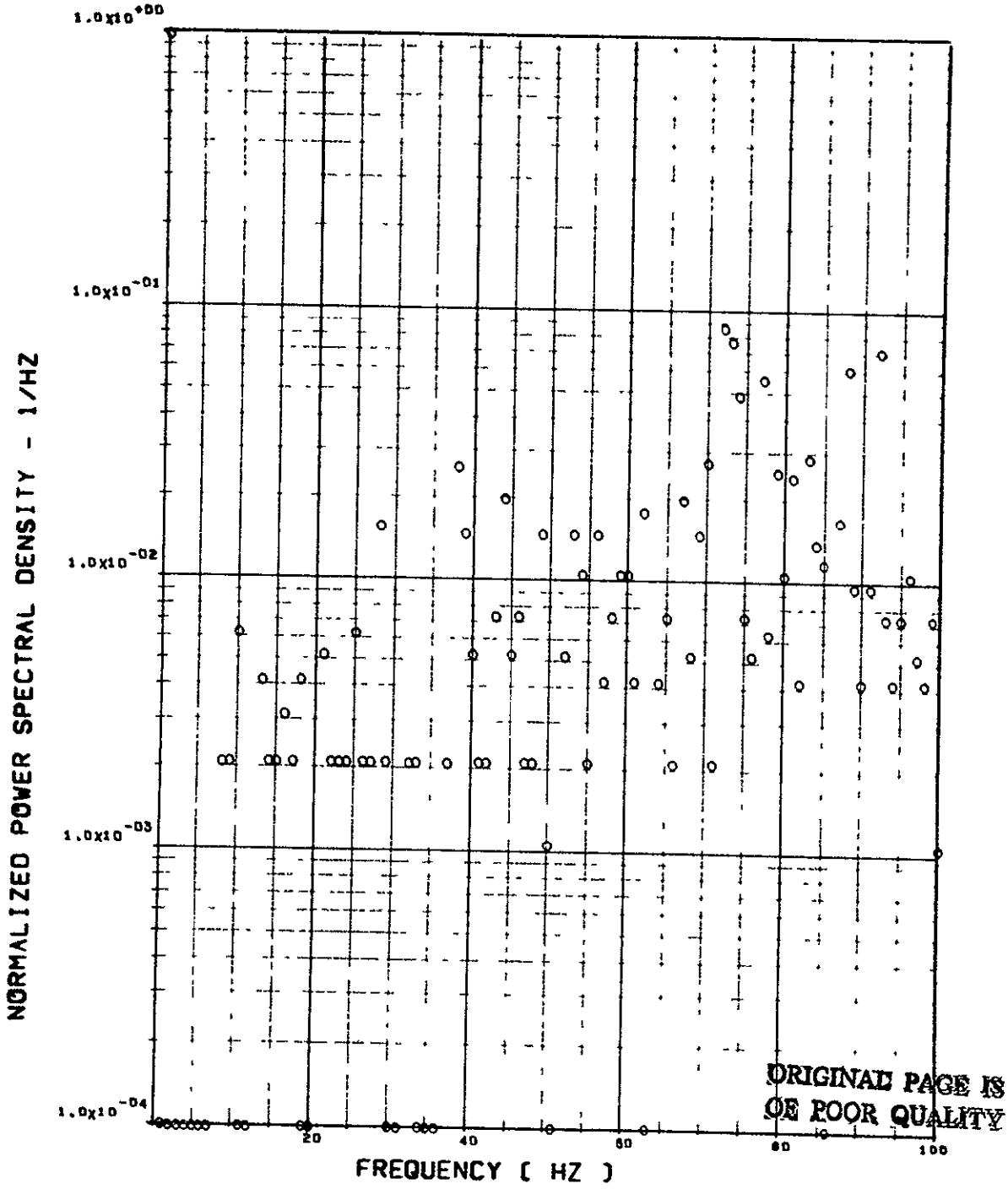

Figure 25. Power Spectra - Flight 48, Run 5, Point 1 T_1 = 134426.2, ΔT - 1 Sec, α_{Nom} = 4 80 deg, $\Delta\alpha$= $\pm$ 0.1 deg.

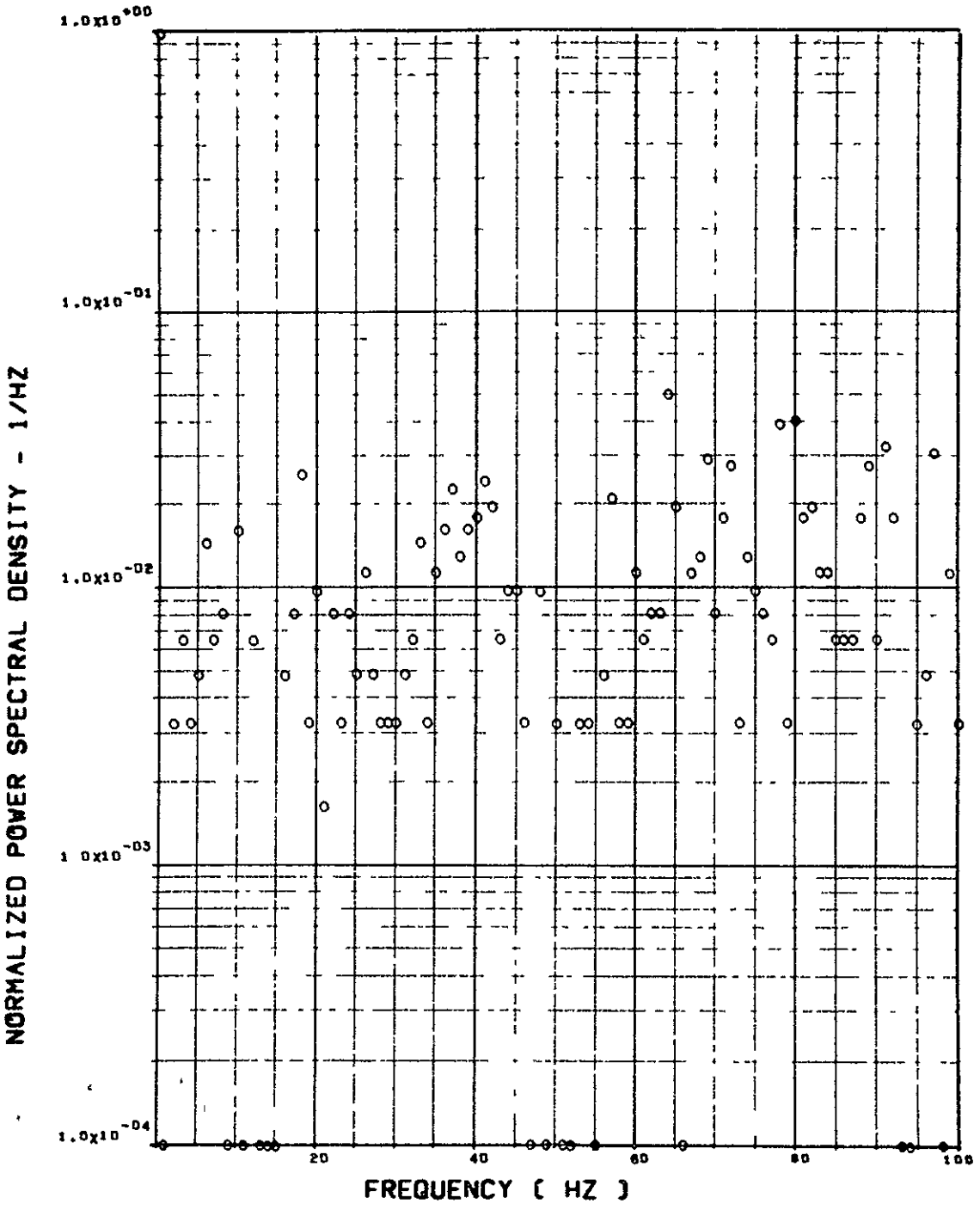

Figure 25. Continued

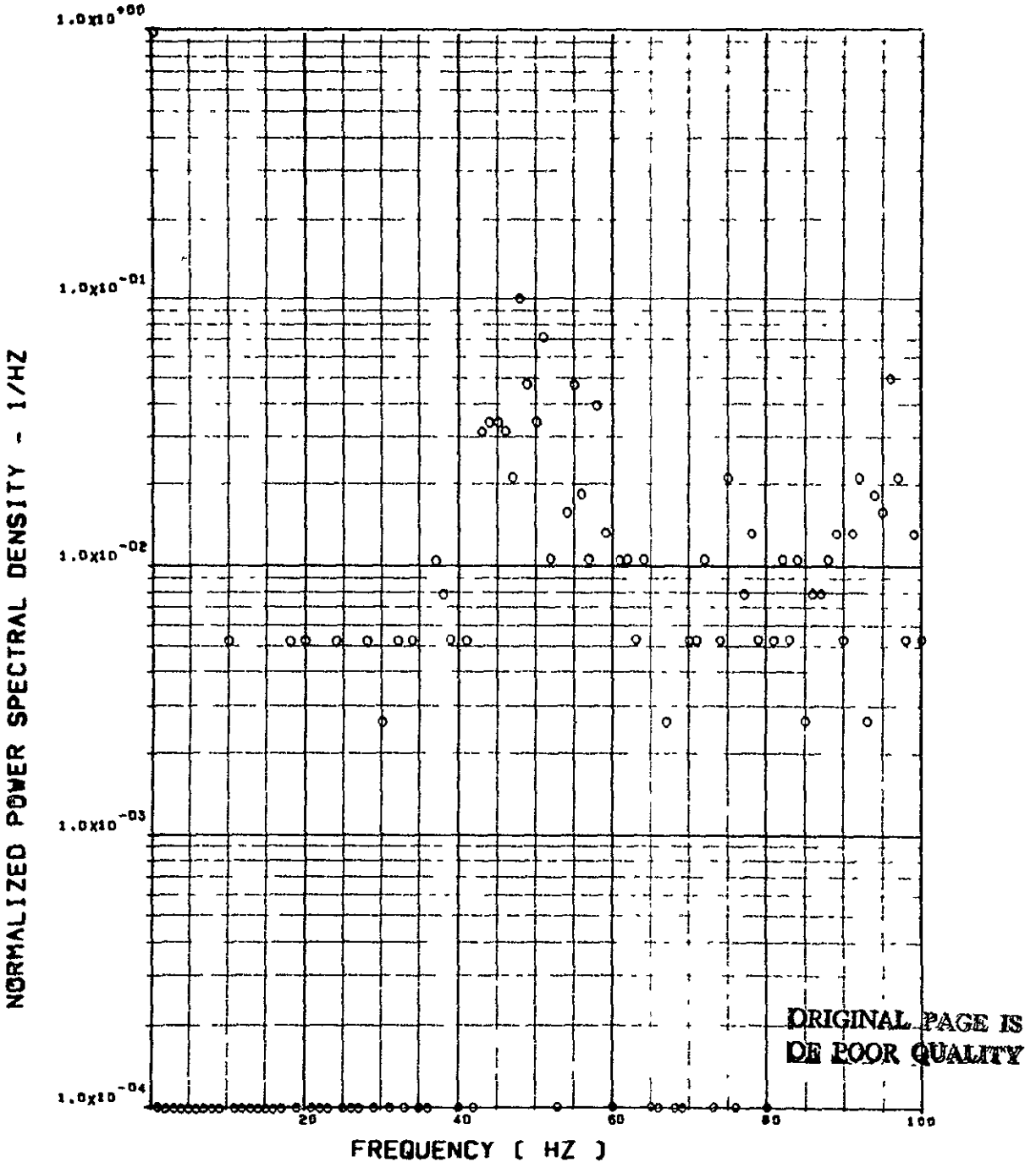

Figure 25. Continued

FLIGHT 48. FRAME 134426.20. RECORD LENGTH = 1 SEC

SCALE FACTOR = .307-2 (6)**2

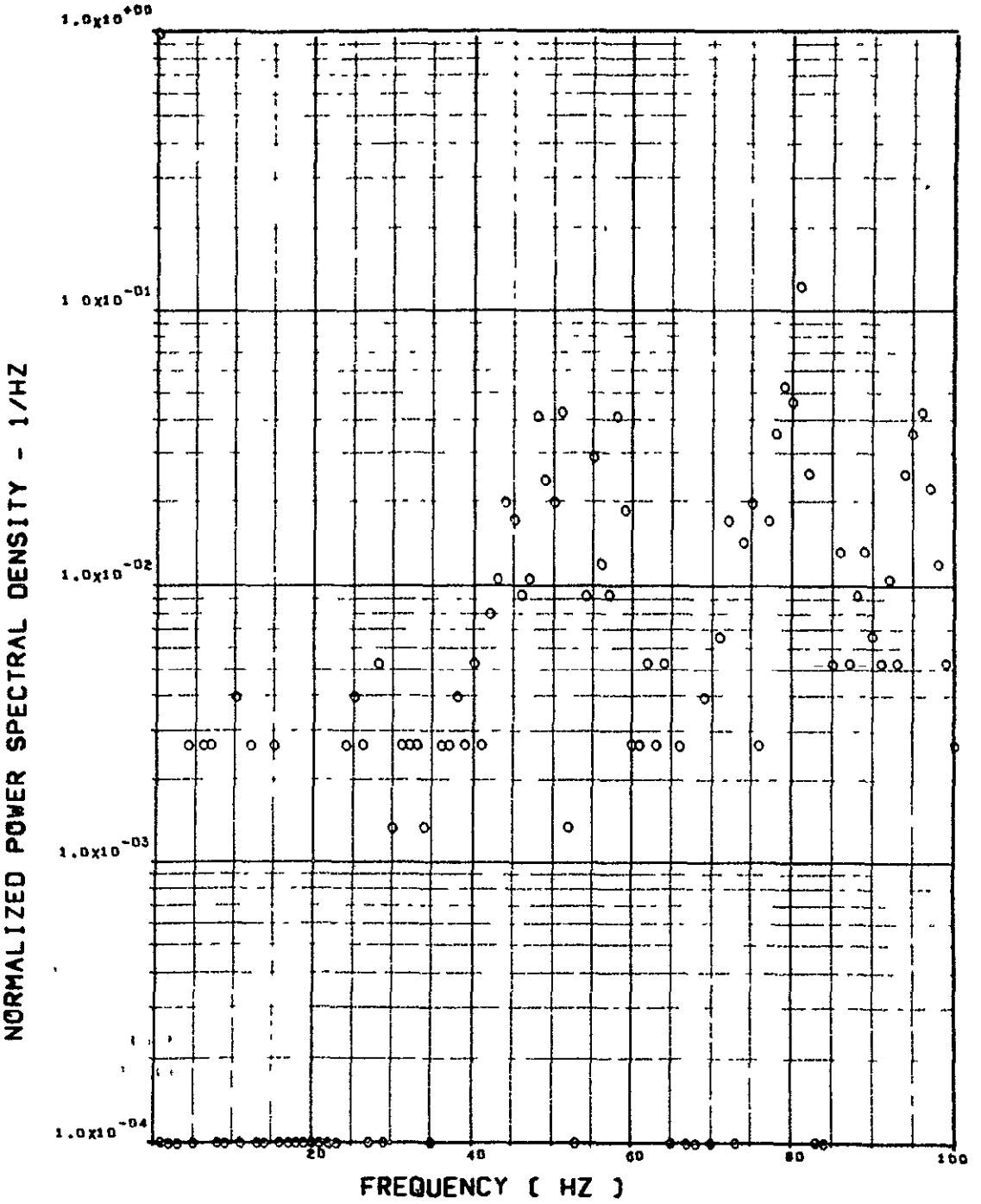

ITEM - AB019 C.G. VERTICAL ACCELEROMETER

Figure 25. Continued

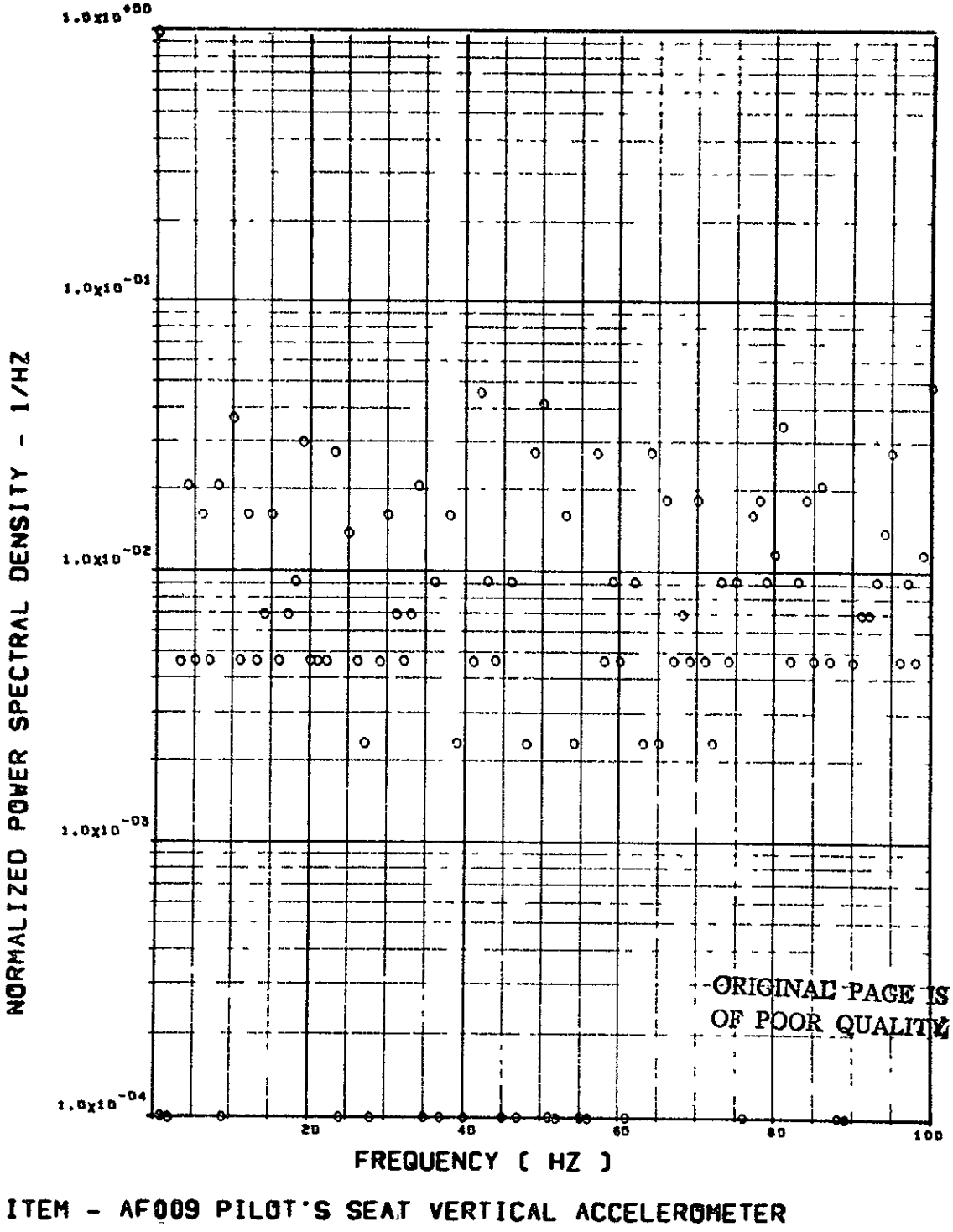

Figure 25. Continued

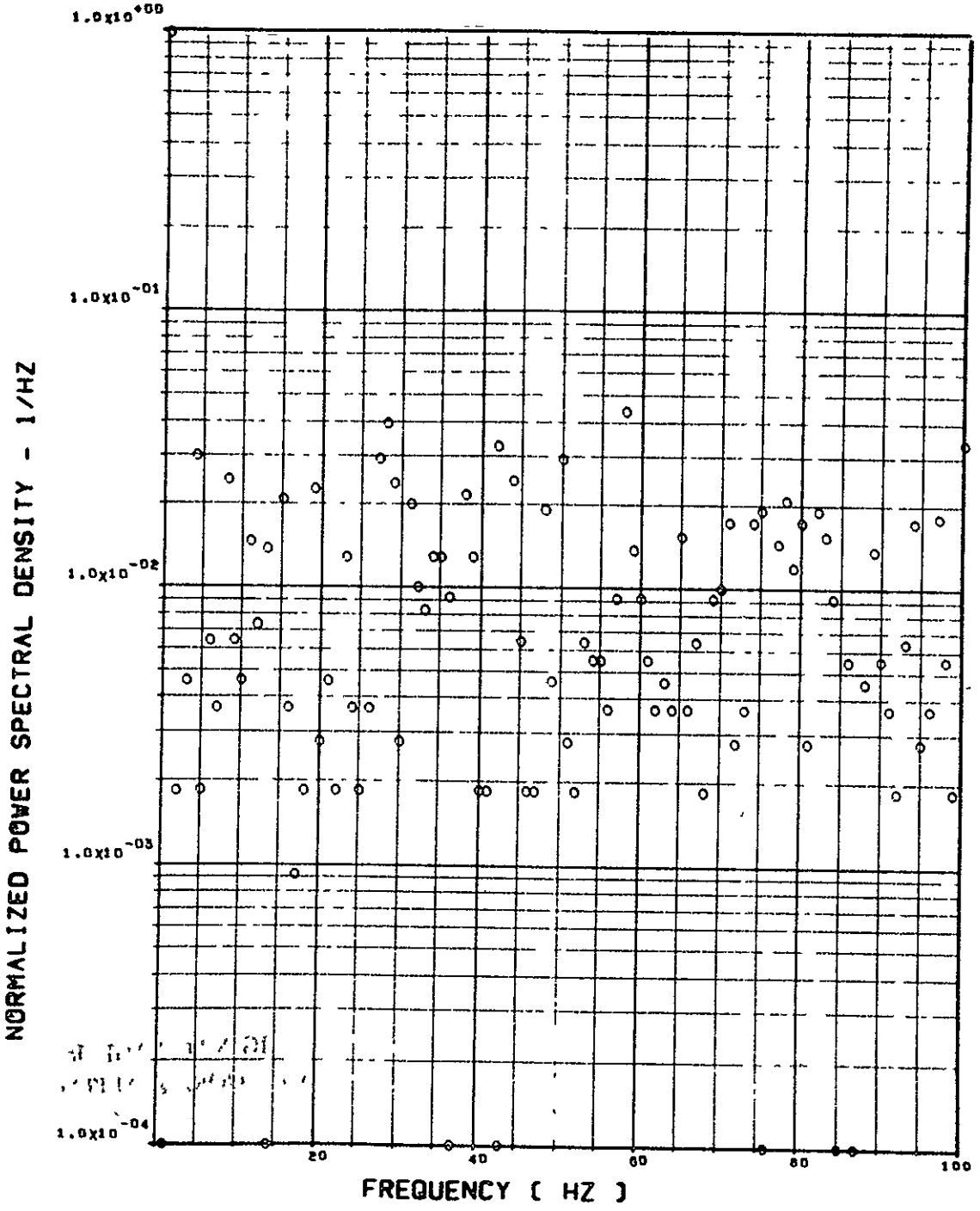

Figure 25. Continued

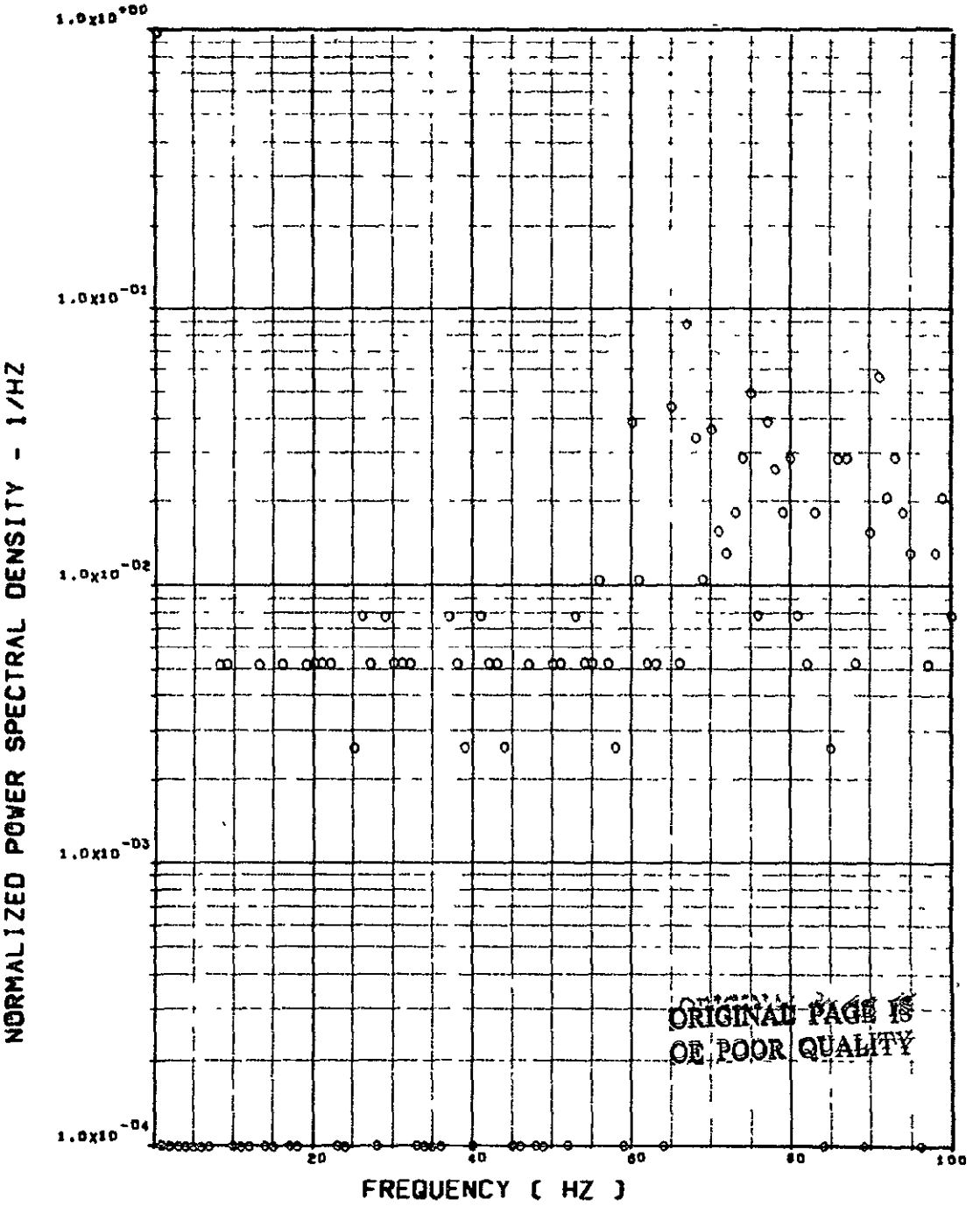

Figure 25. Continued

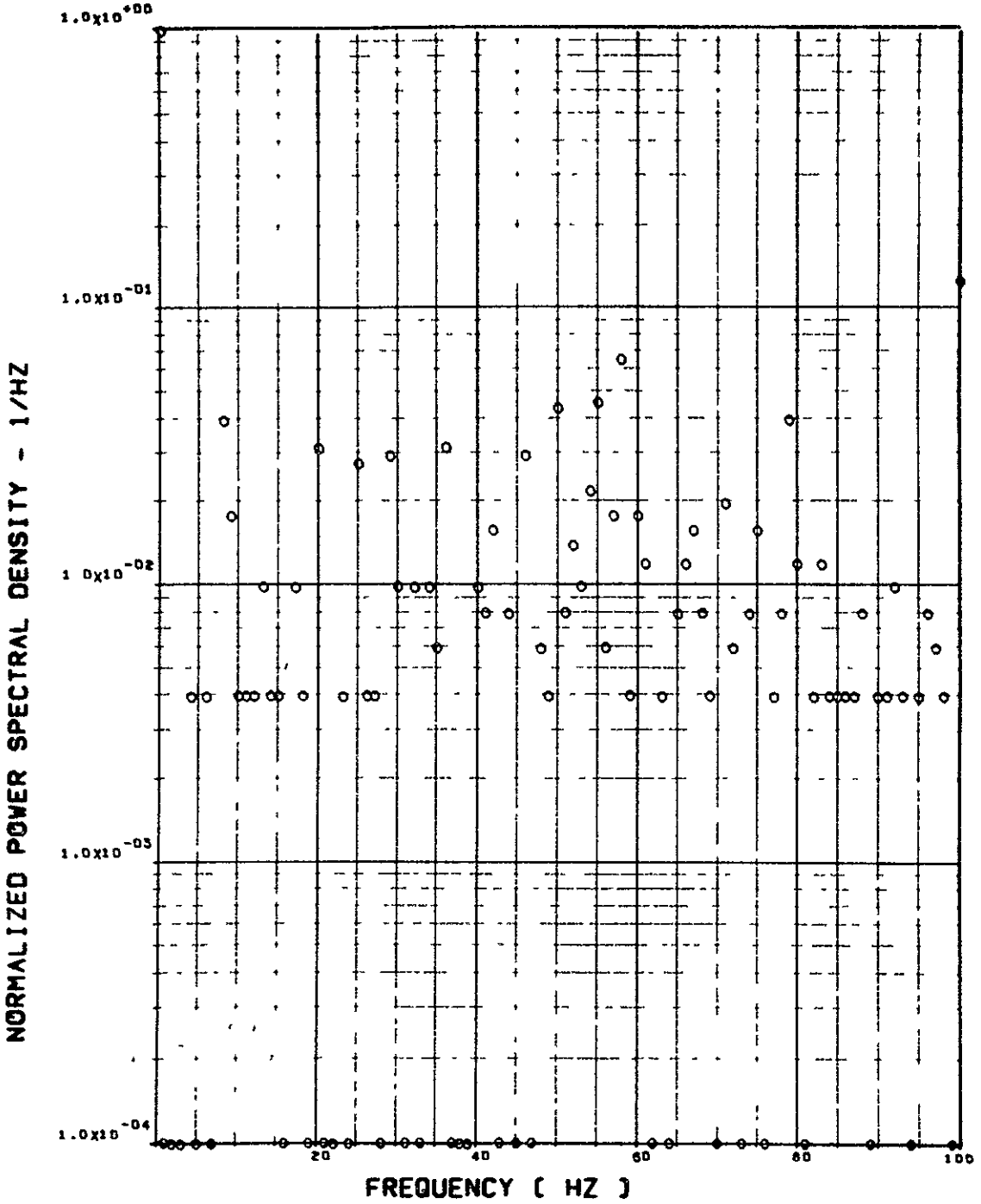

Figure 25. Continued

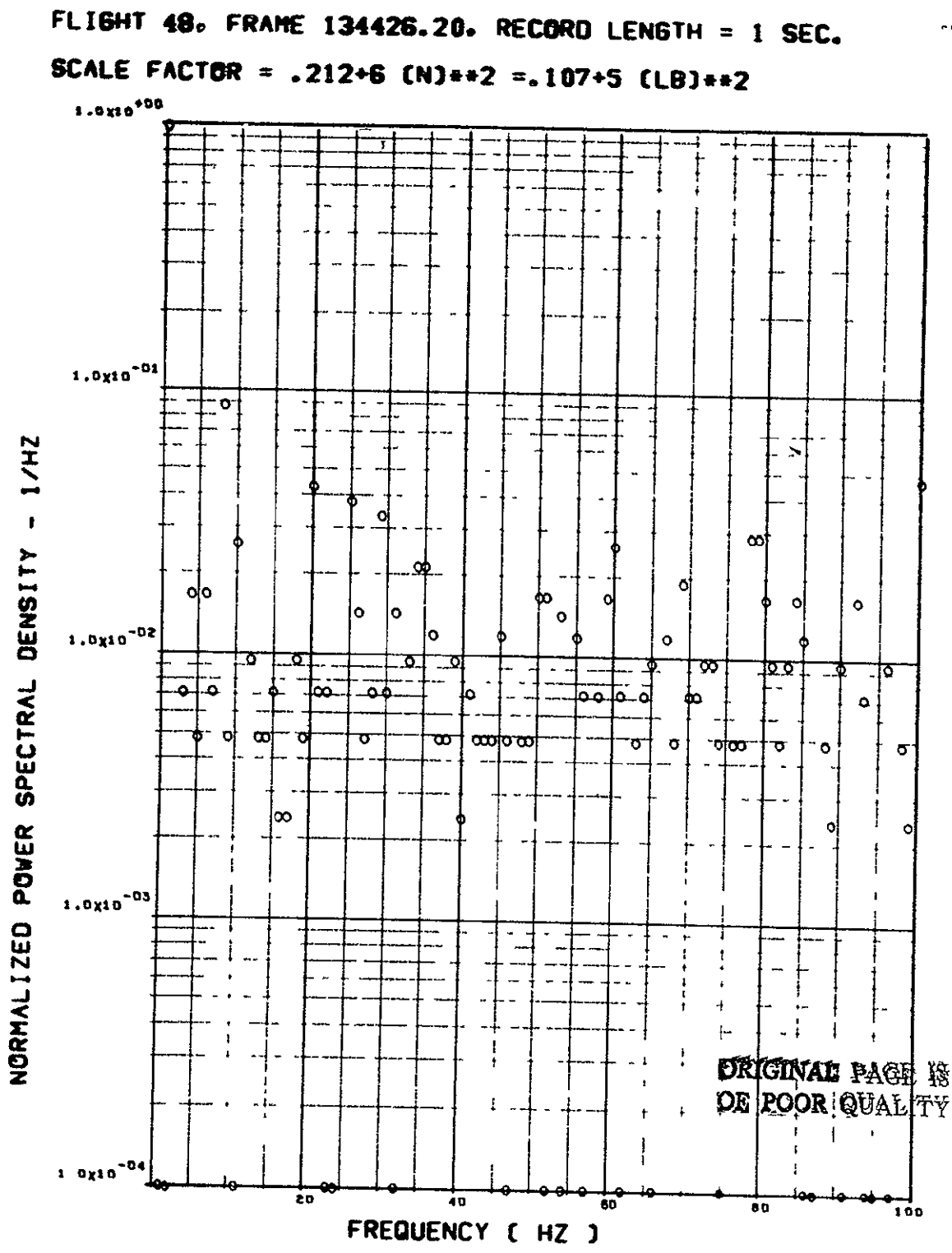

Figure 25. Continued

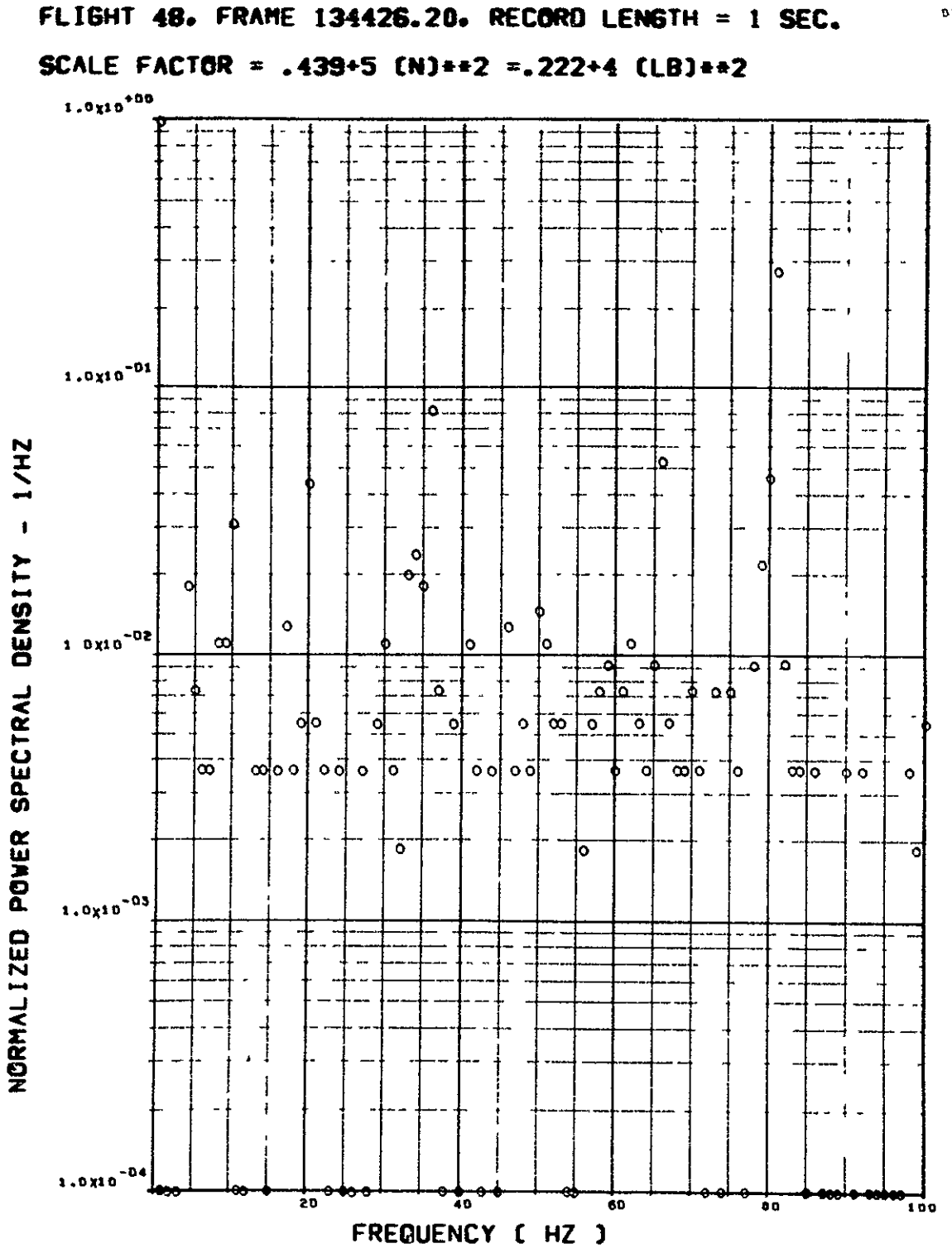

Figure 25. Continued

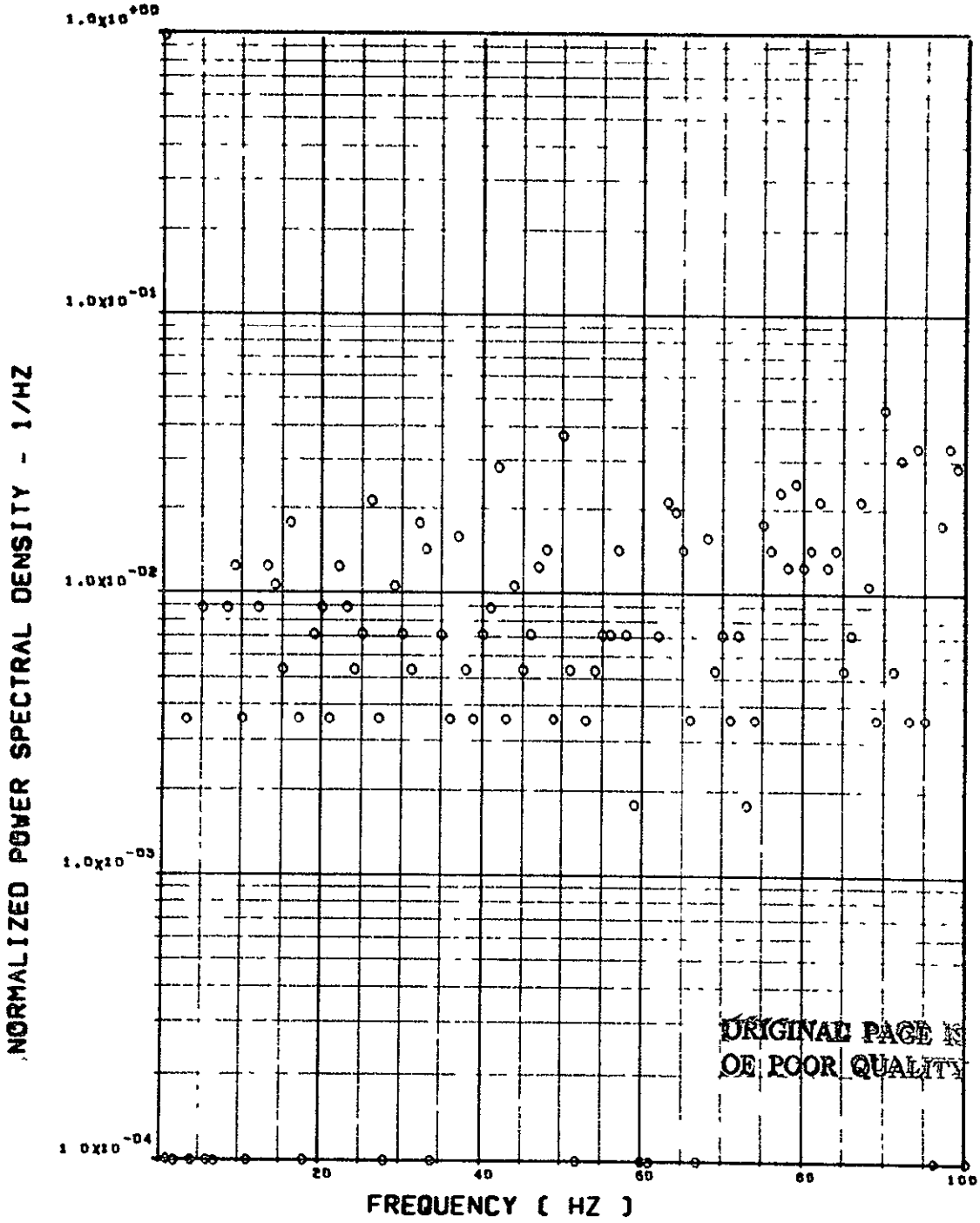

Figure 25. Continued

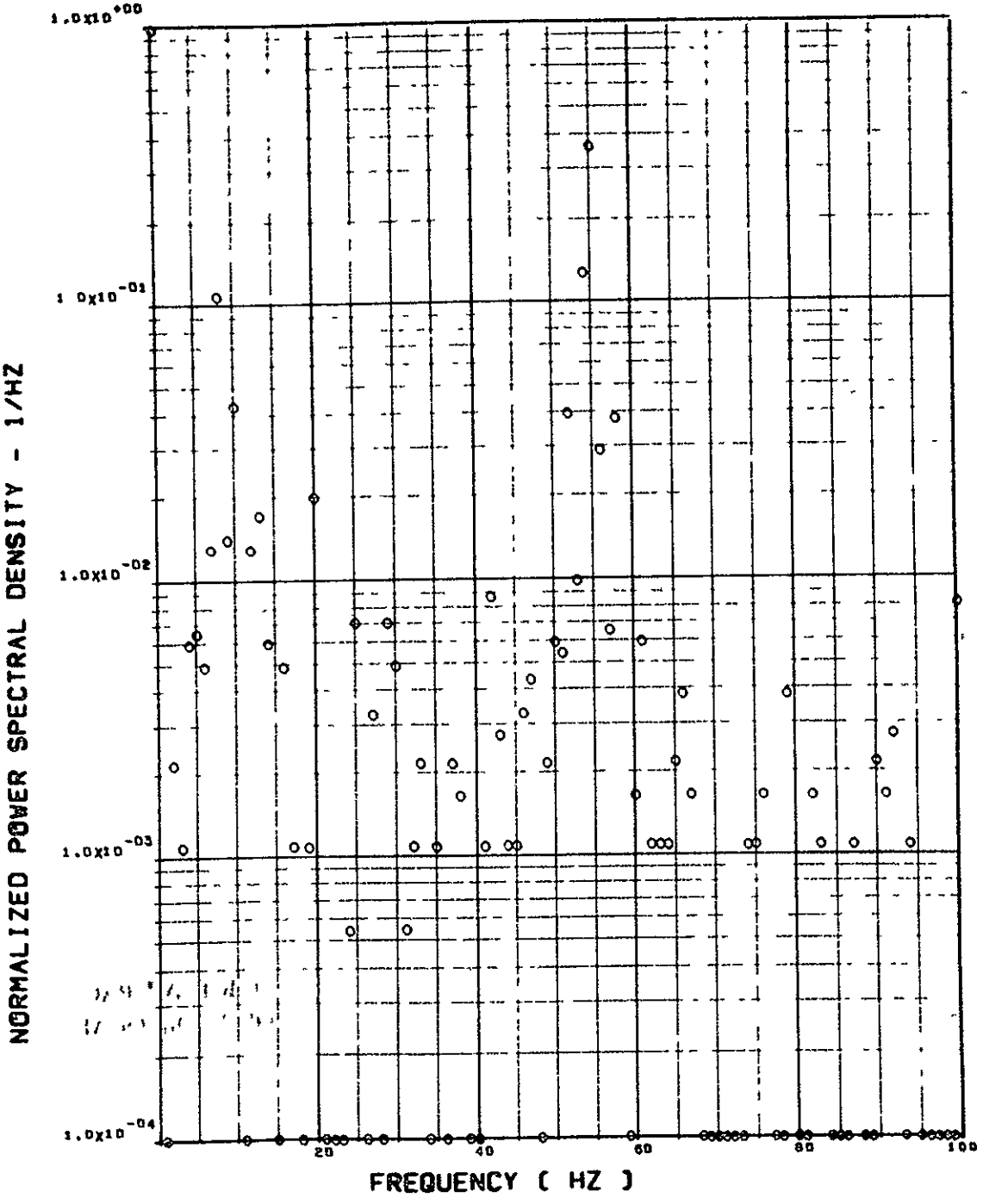

Figure 25. Continued

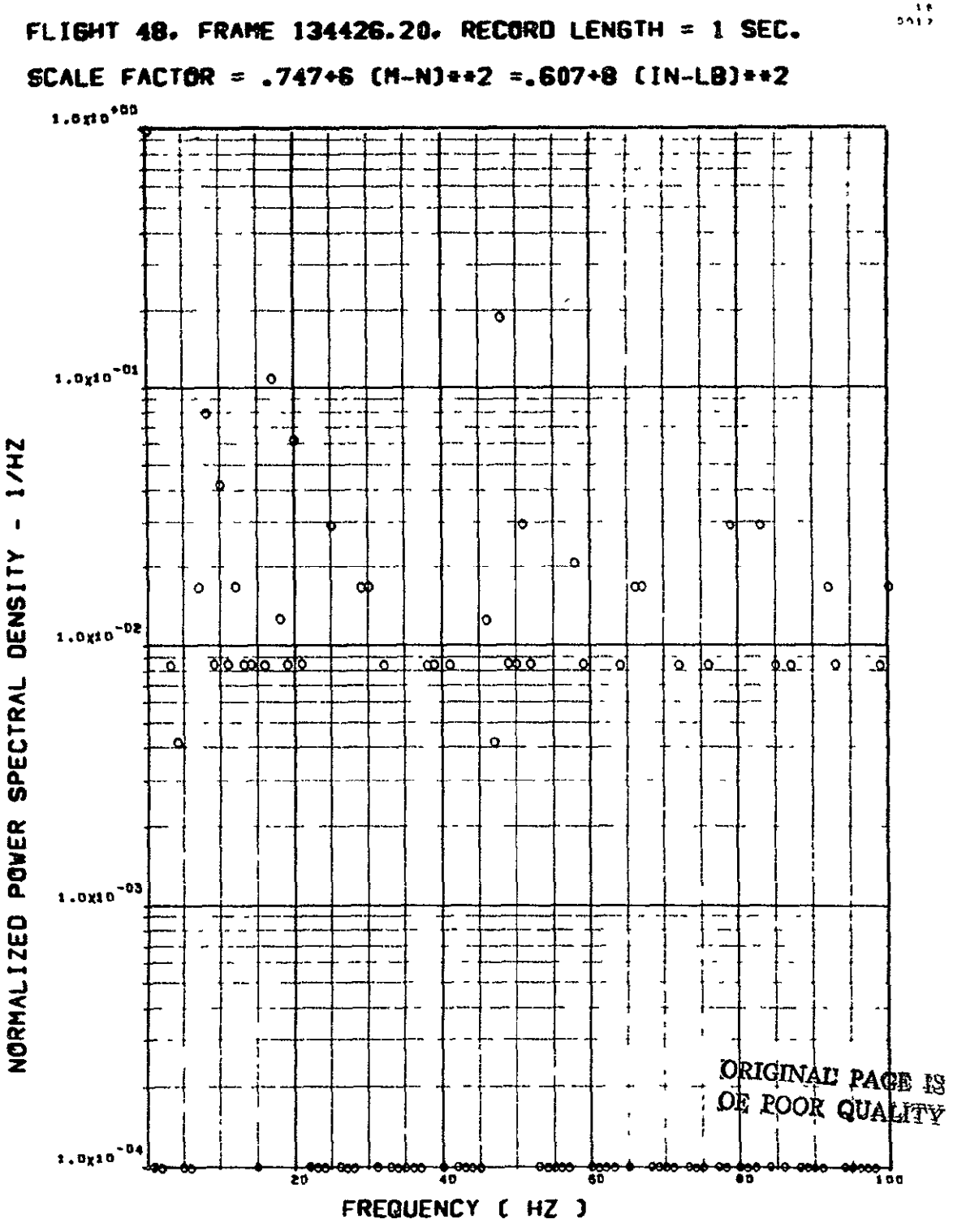

Figure 25. Continued

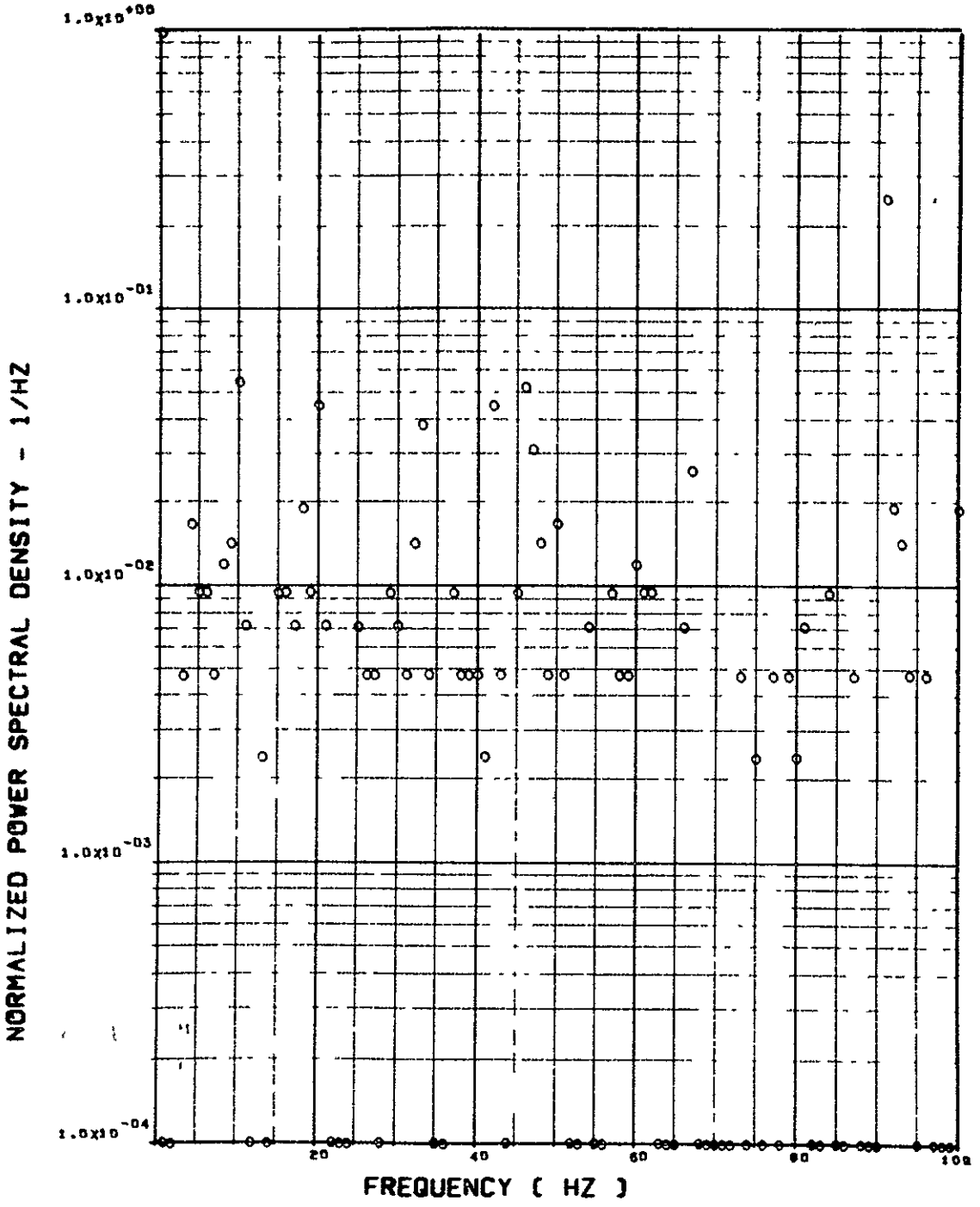

Figure 25. Continued

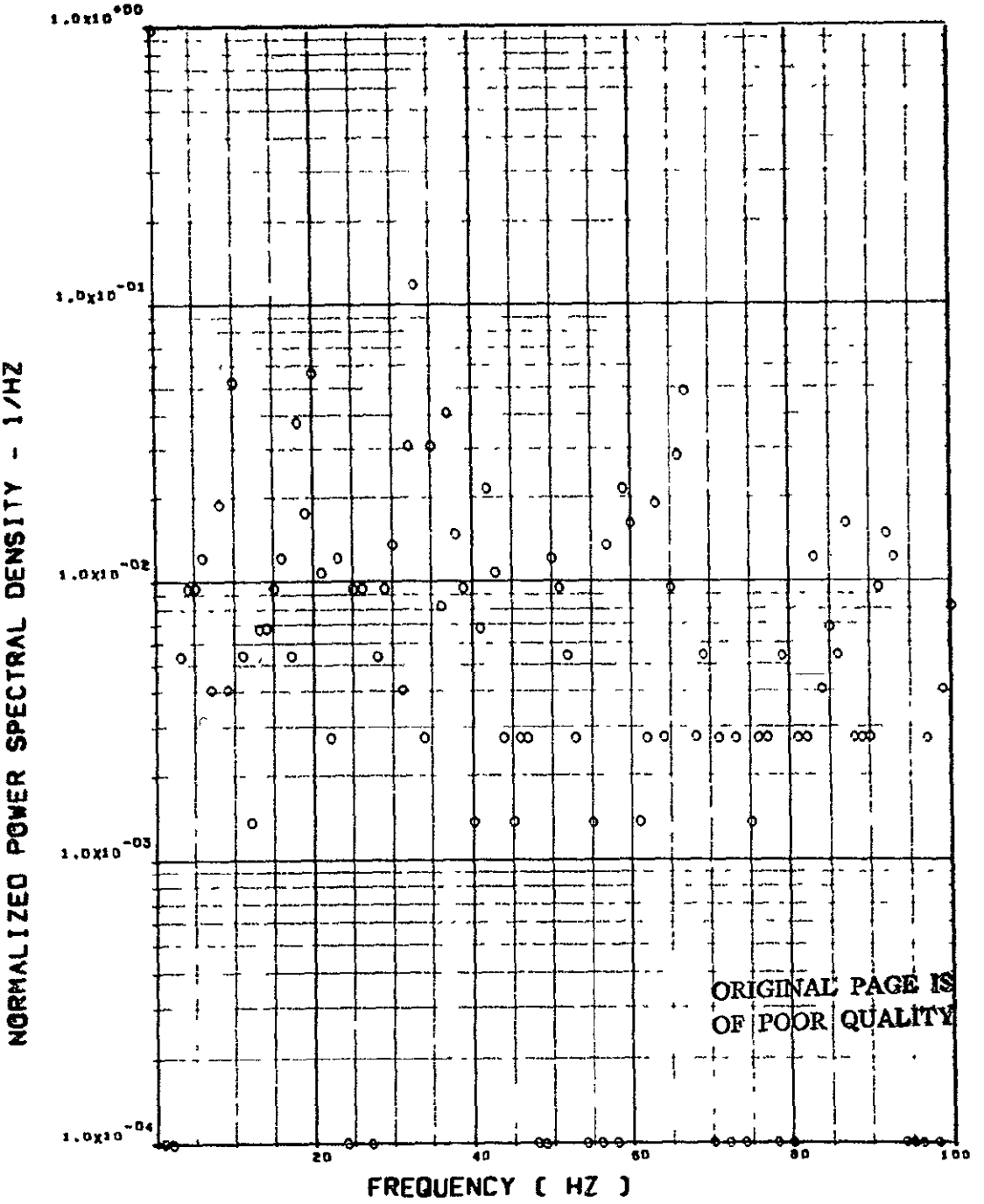

Figure 25. Continued

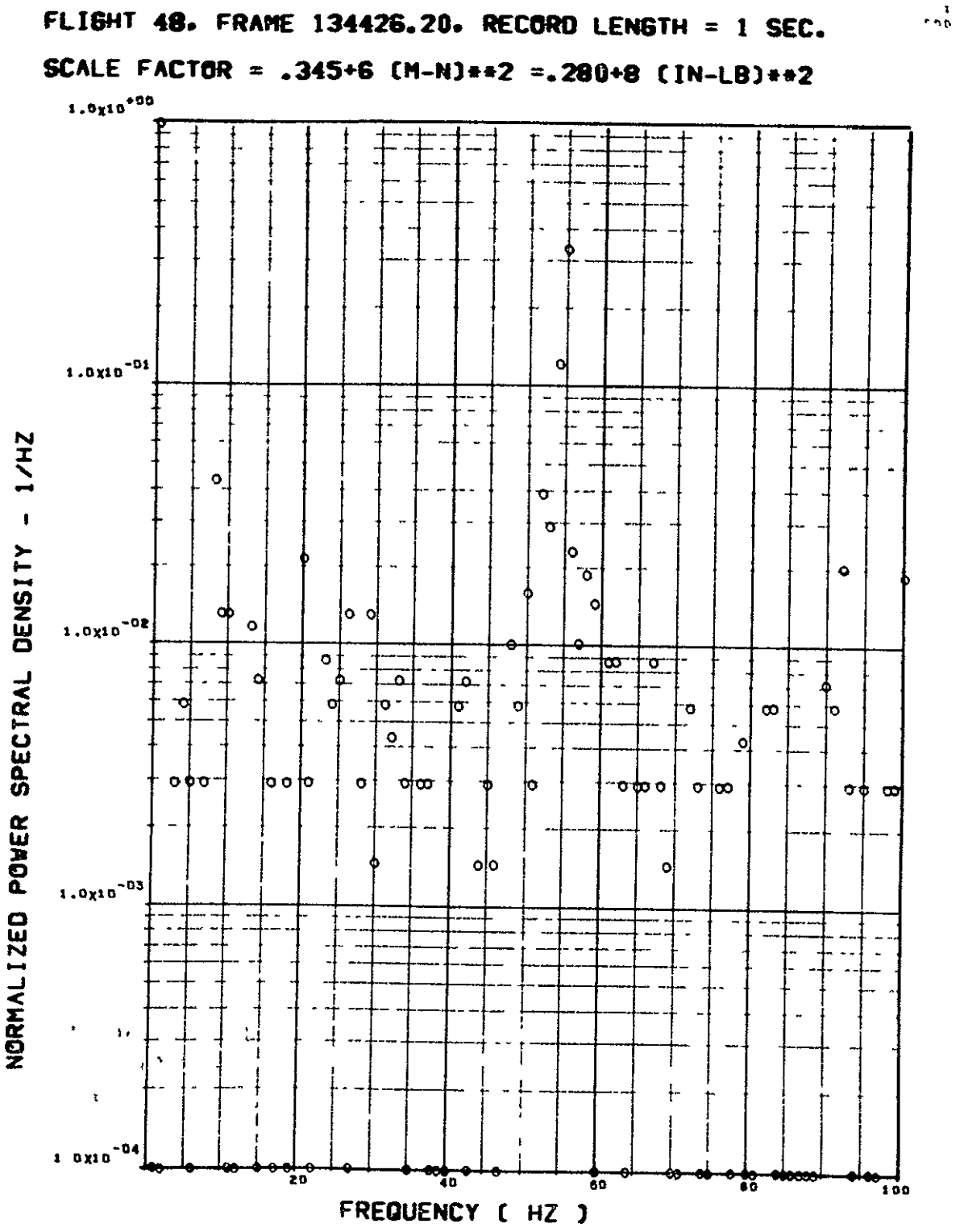

Figure 25. Continued

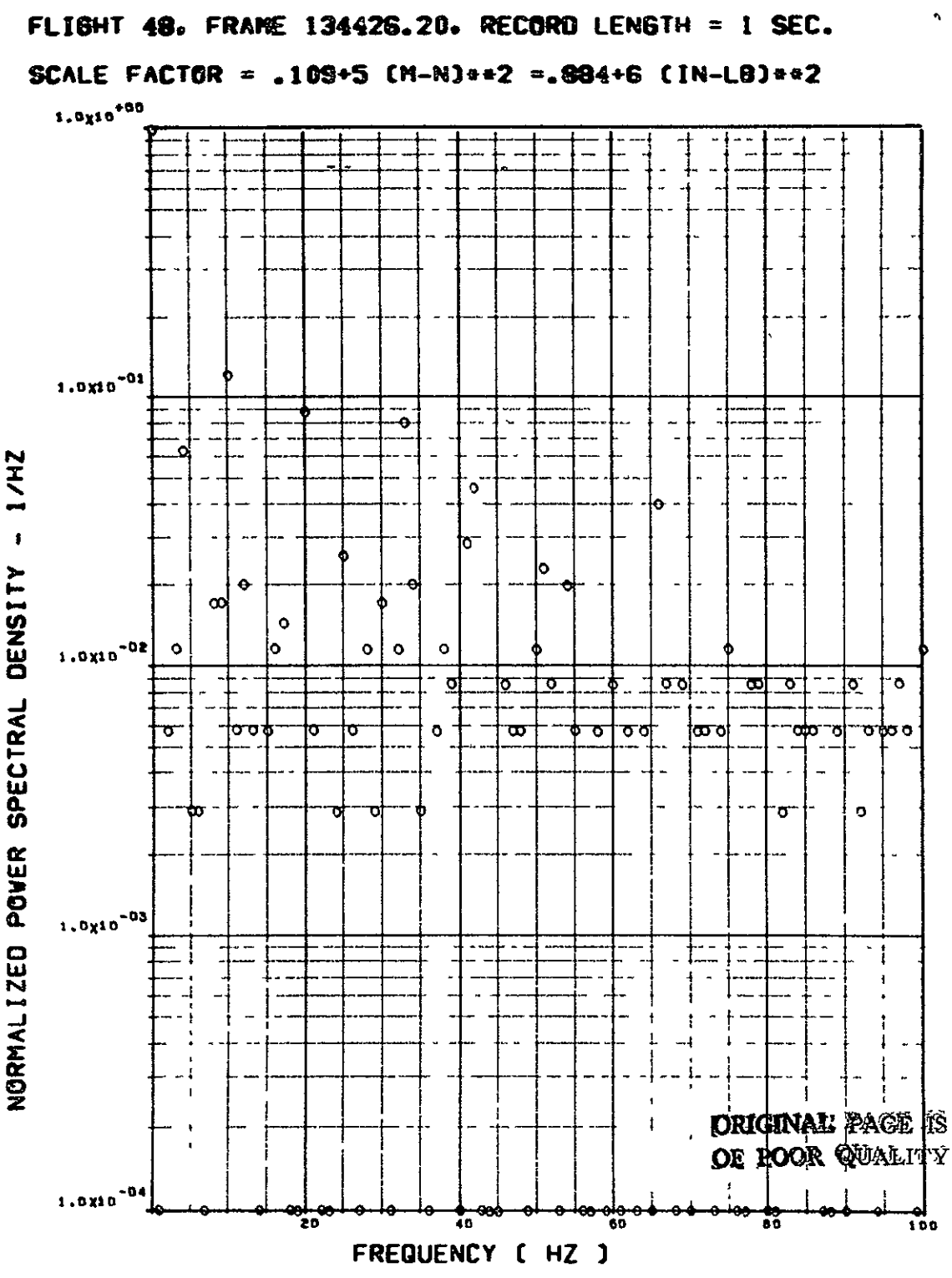

Figure 25. Continued

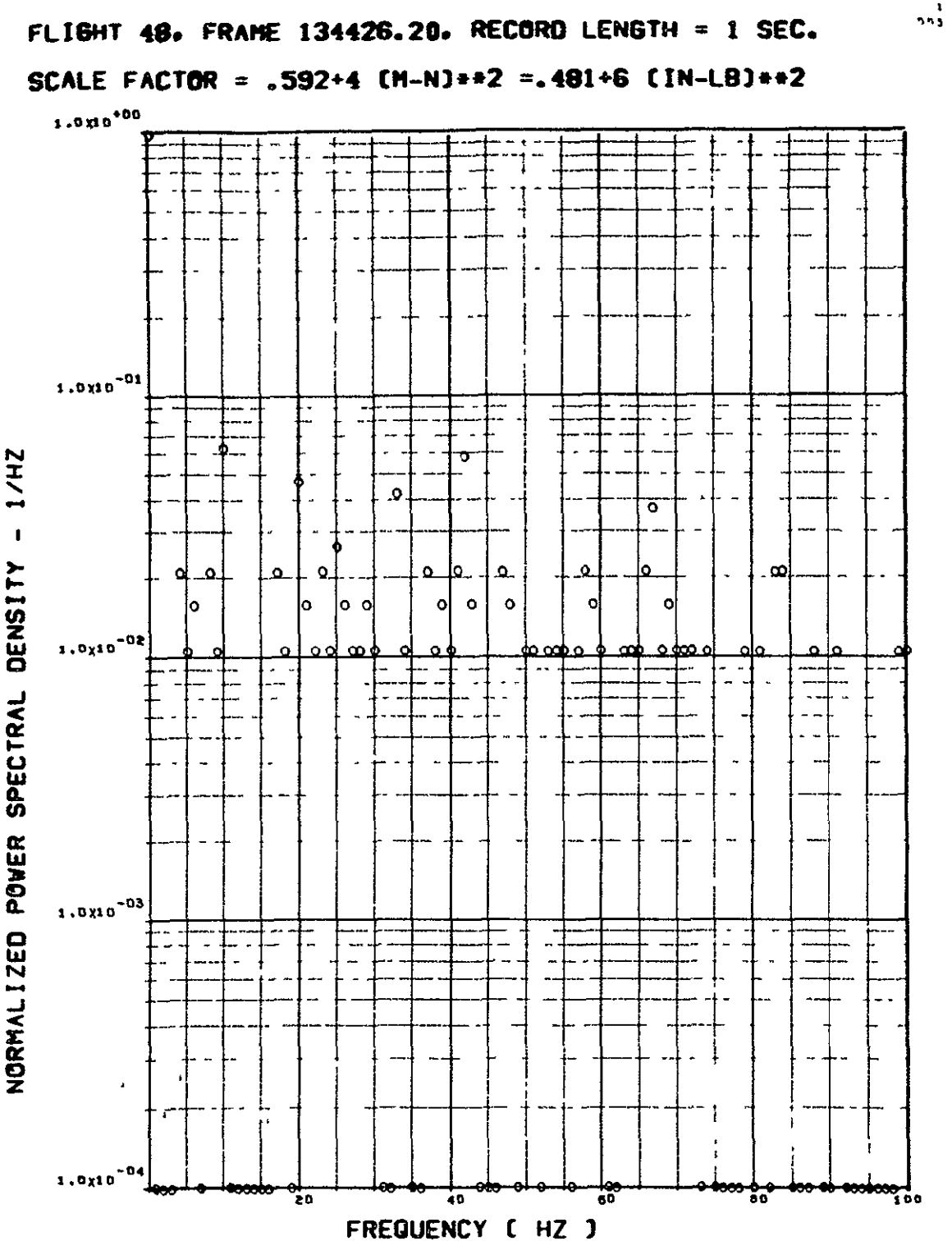

Figure 25. Continued

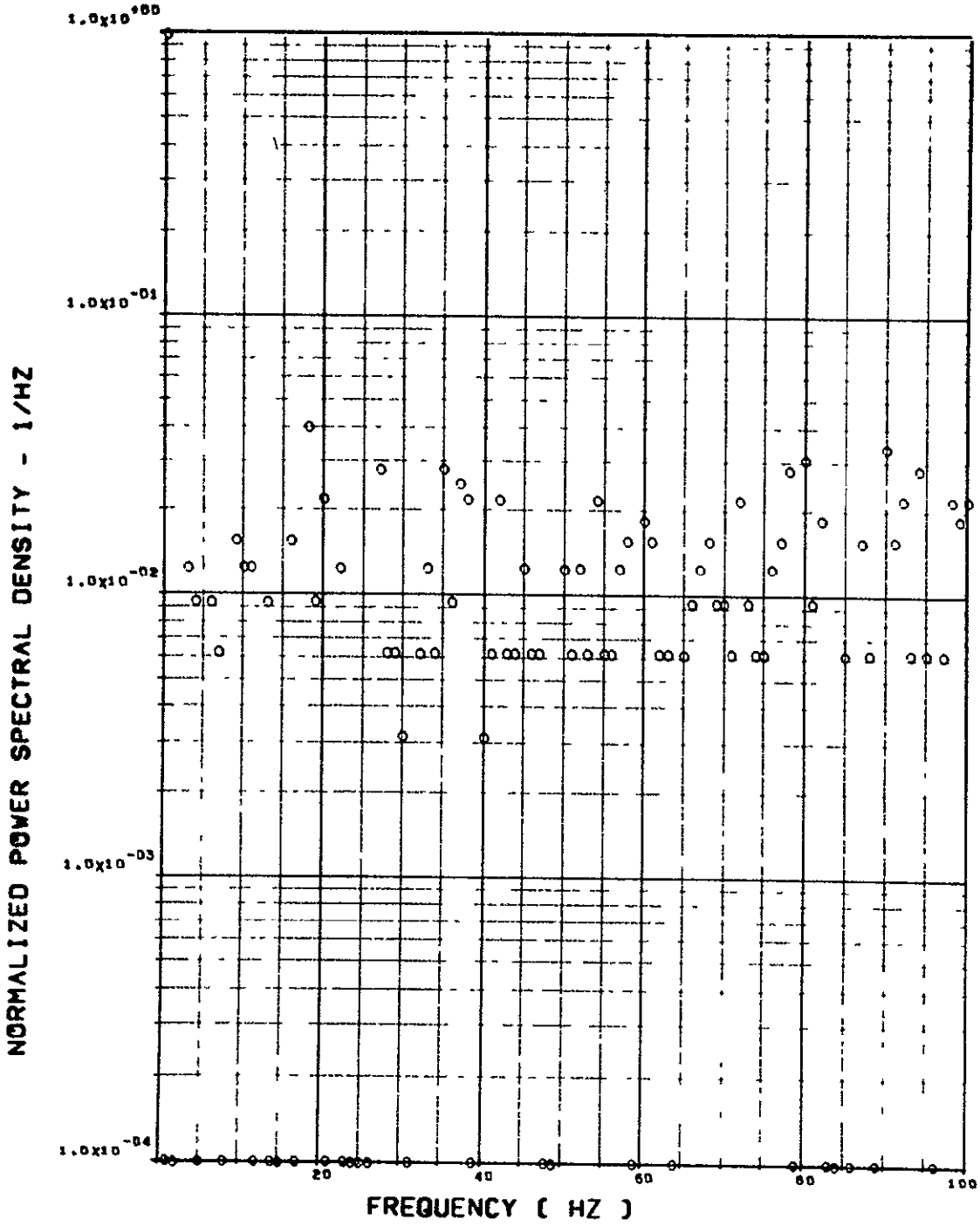

Figure 25. Continued

FLIGHT 48. FRAME 134426.20. RECORD LENGTH = 1 SEC

SCALE FACTOR = .337+7 (N)**2 =.170+6 (LB)**2

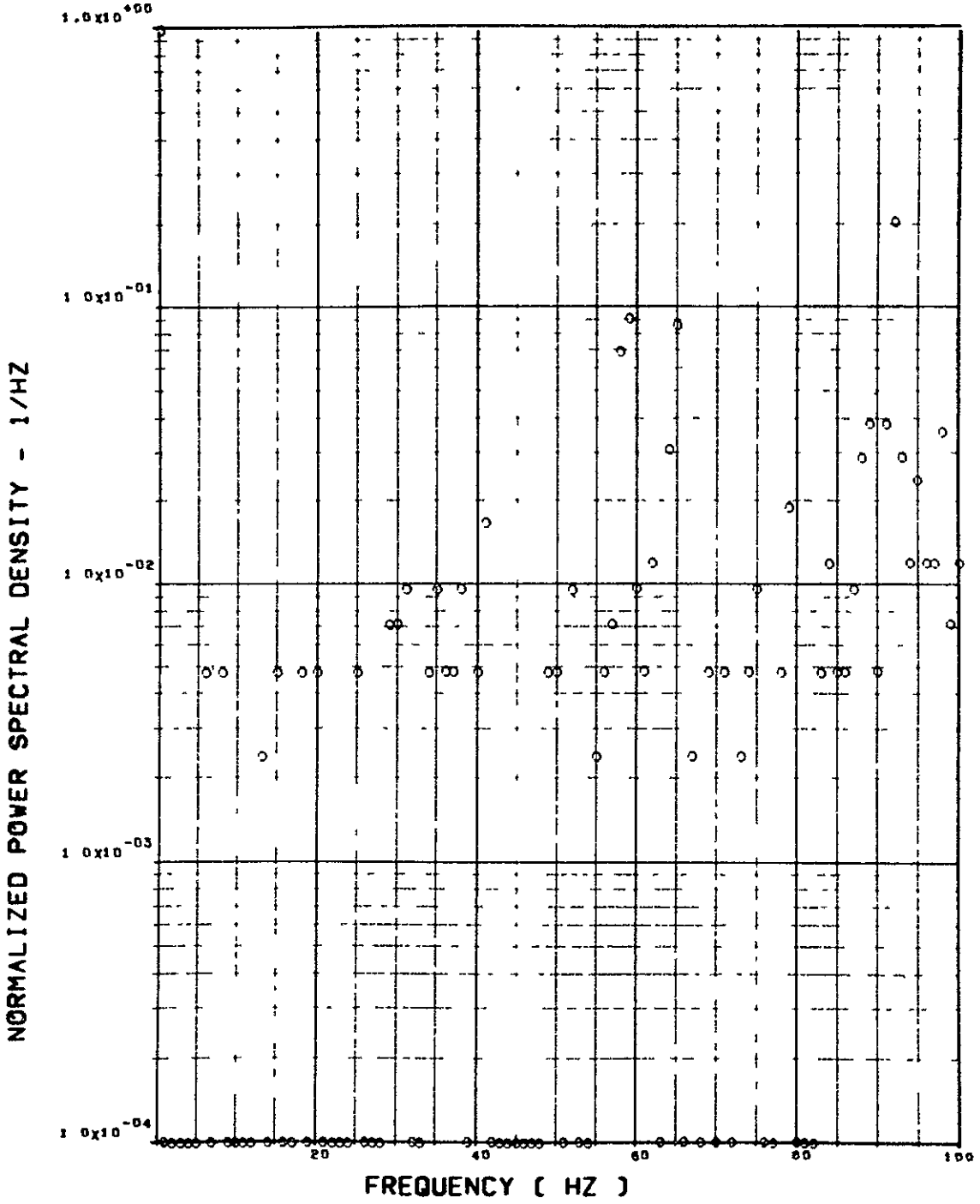

ITEM - ST077 SHEAR. L/H HORIZ TAIL ROOT

Figure 25. Continued

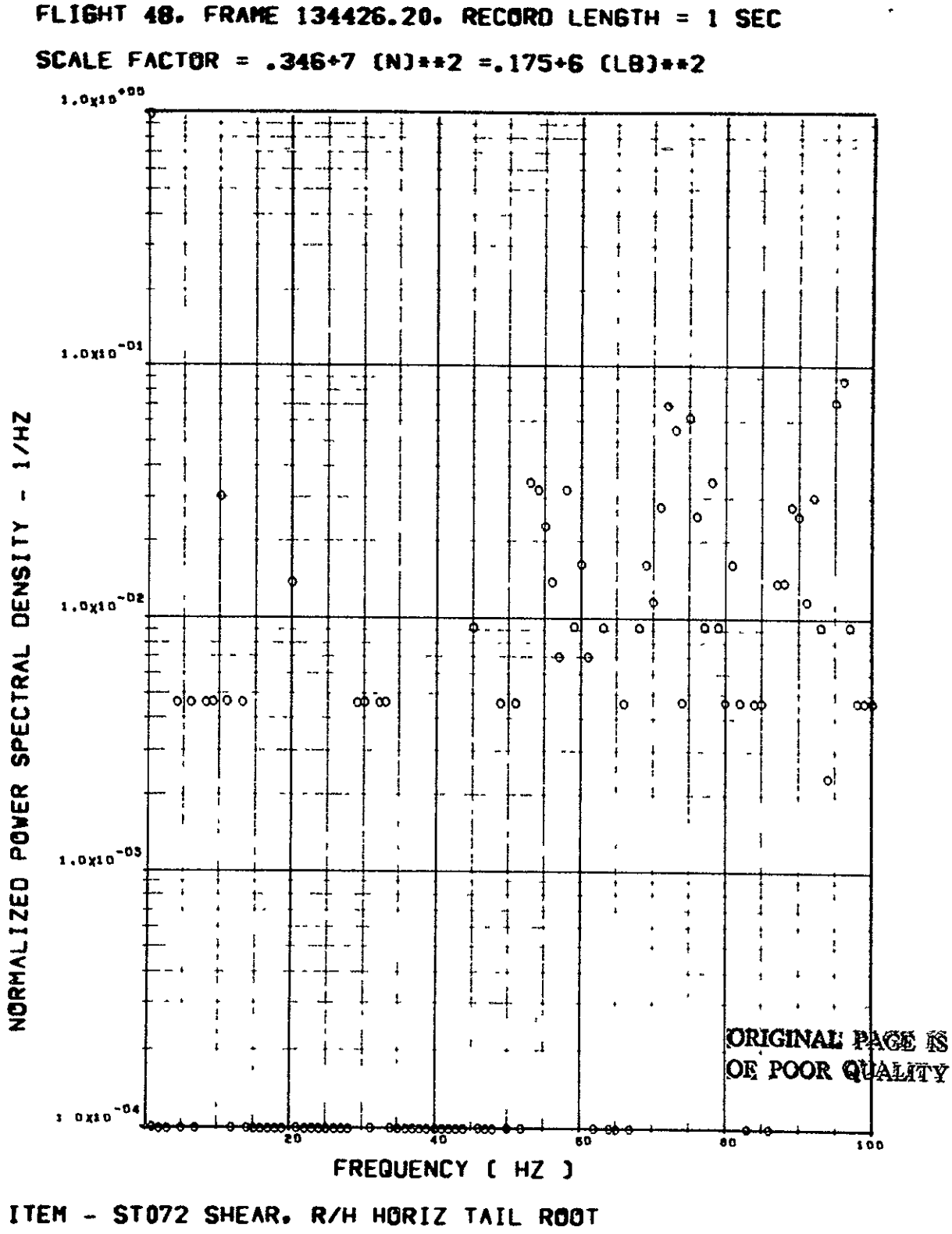

Figure 25. Continued

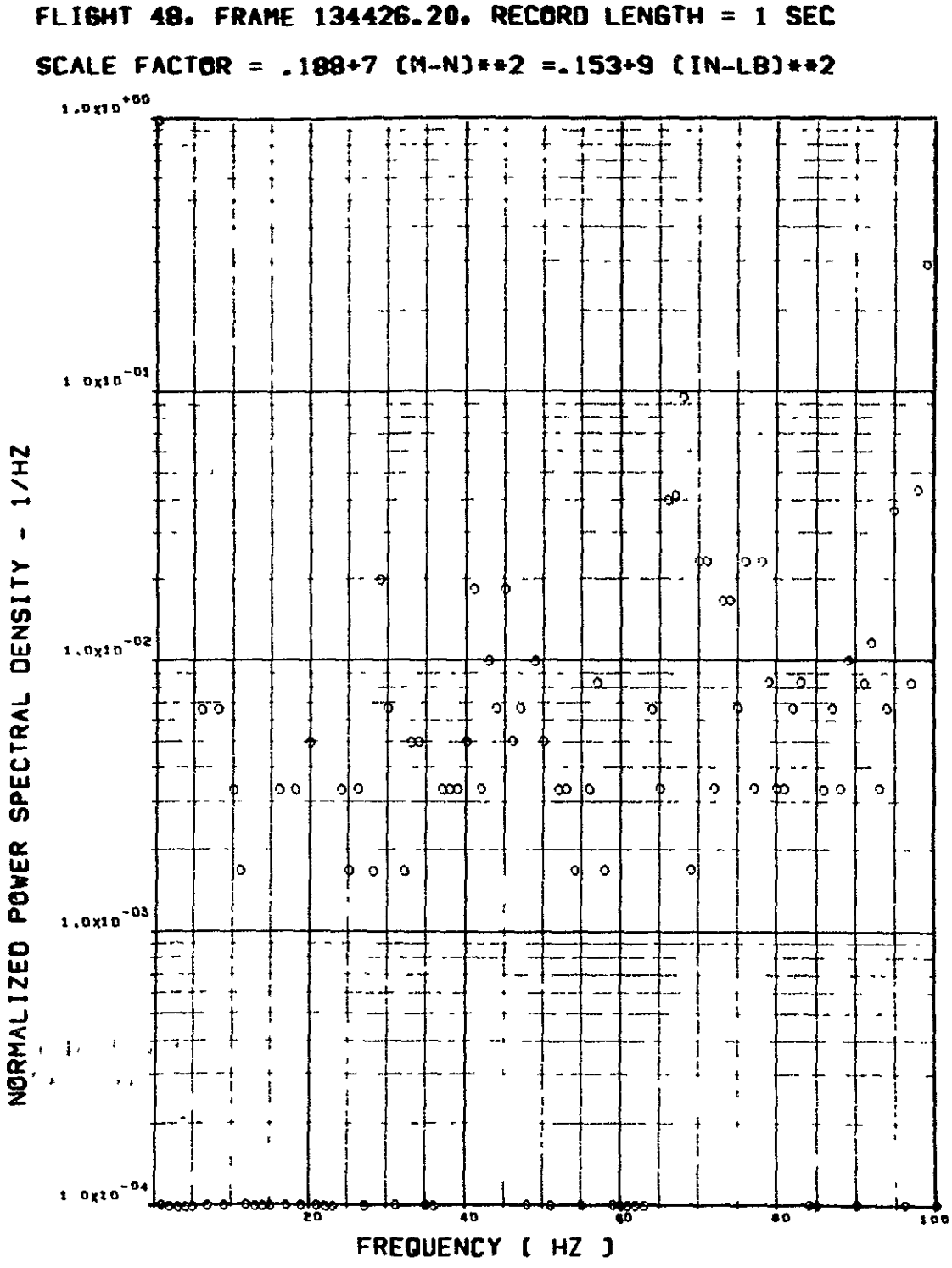

Figure 25. Continued

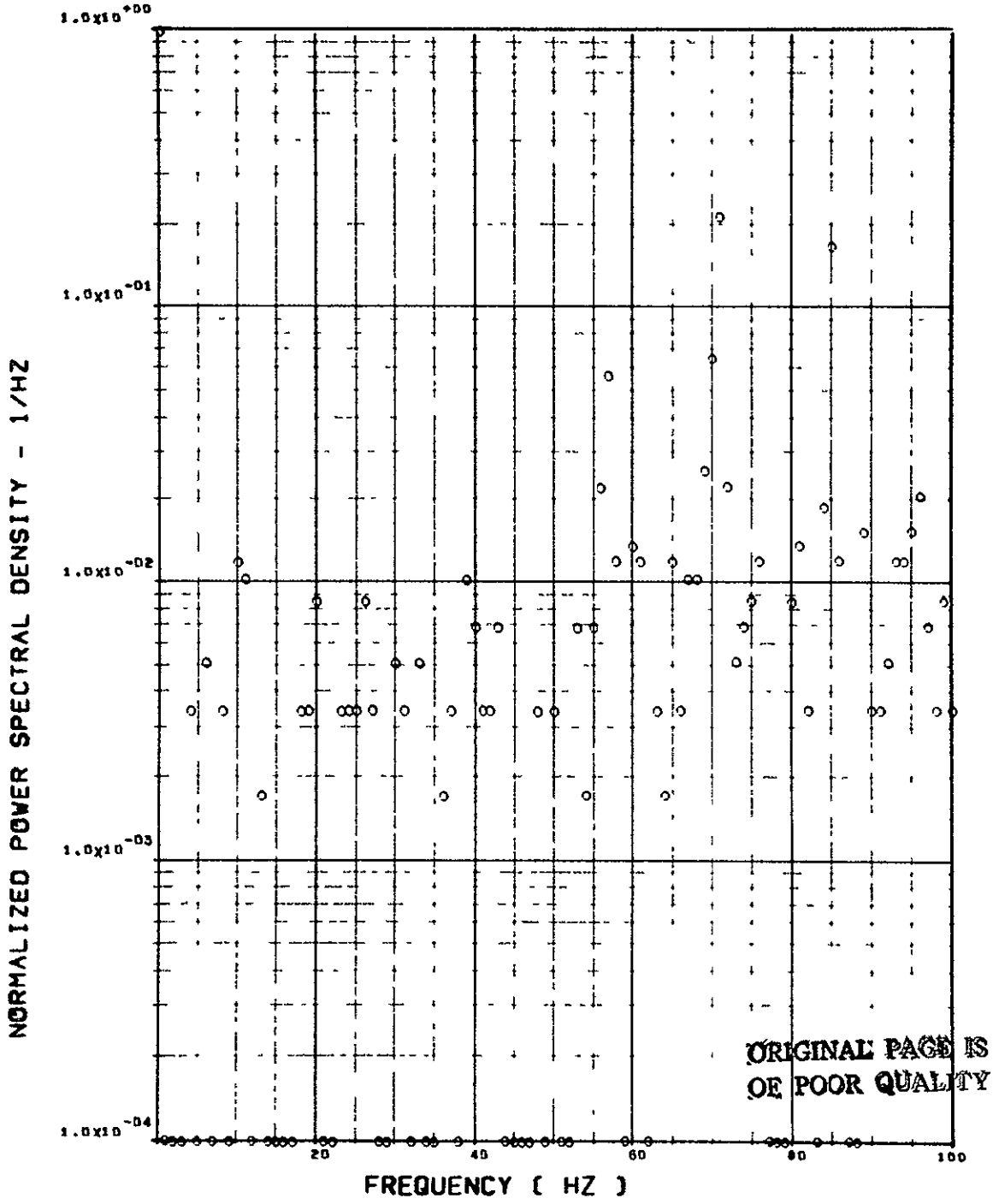

Figure 25. Continued

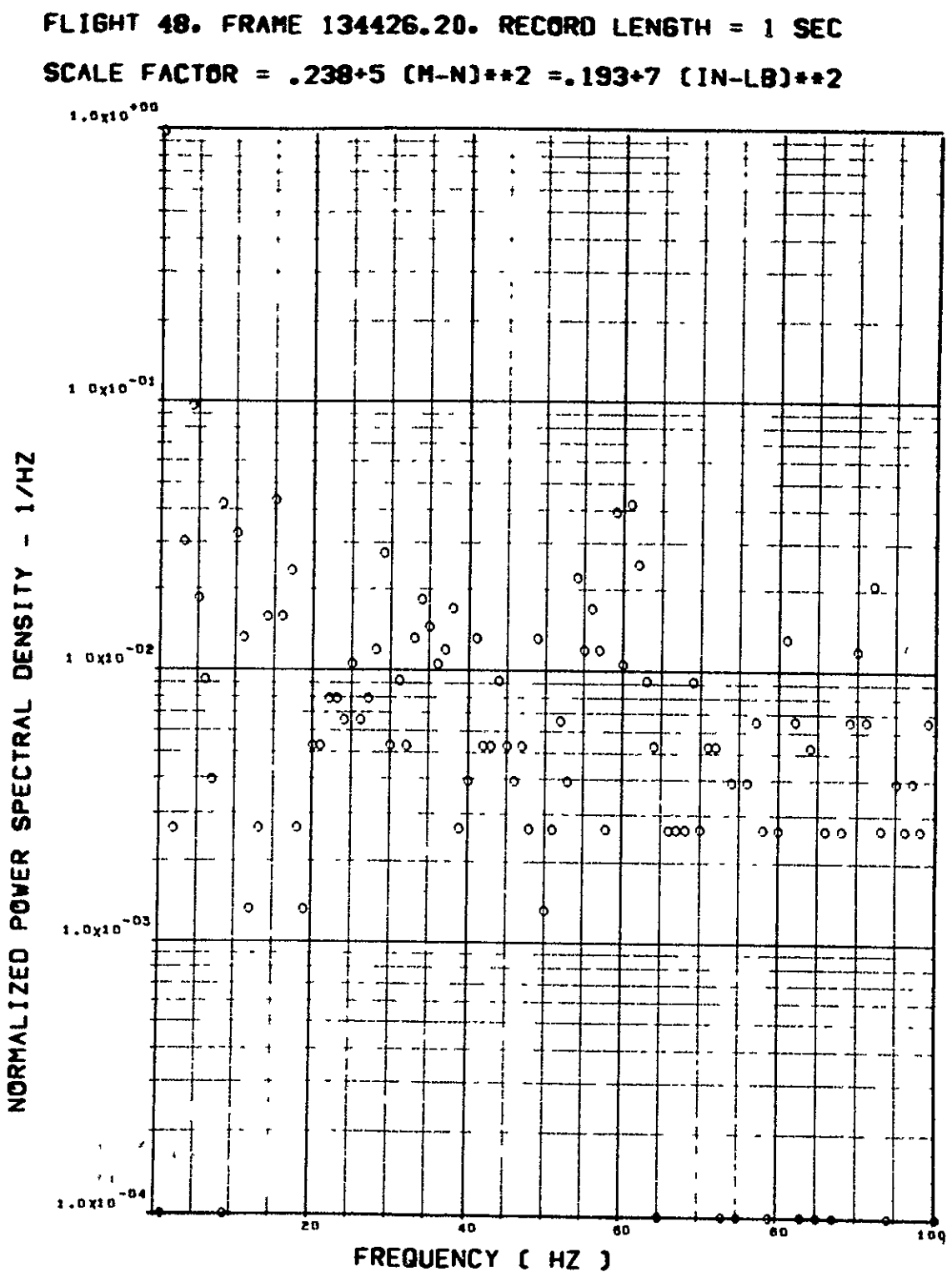

Figure 25. Continued

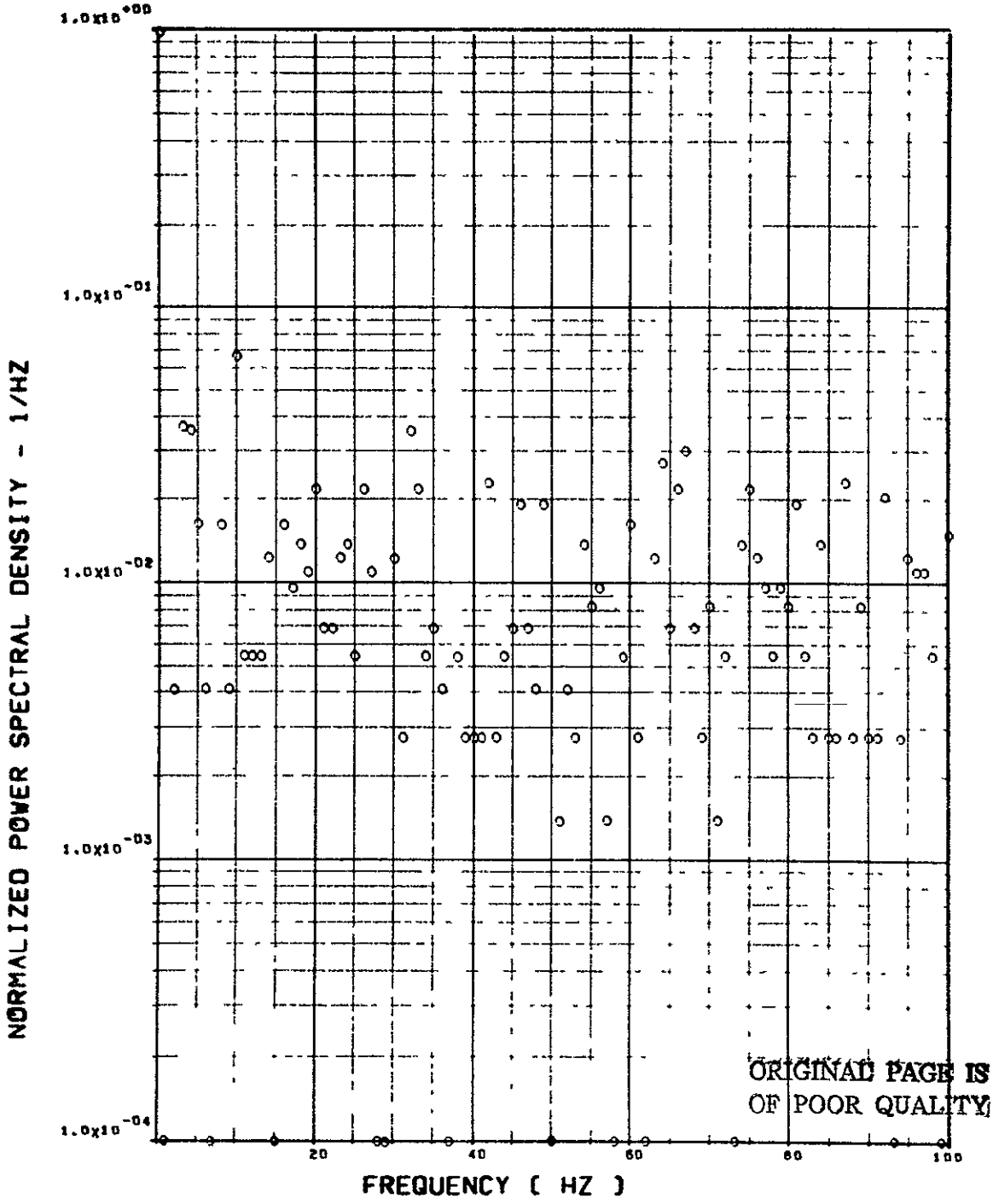

Figure 2). Concluded

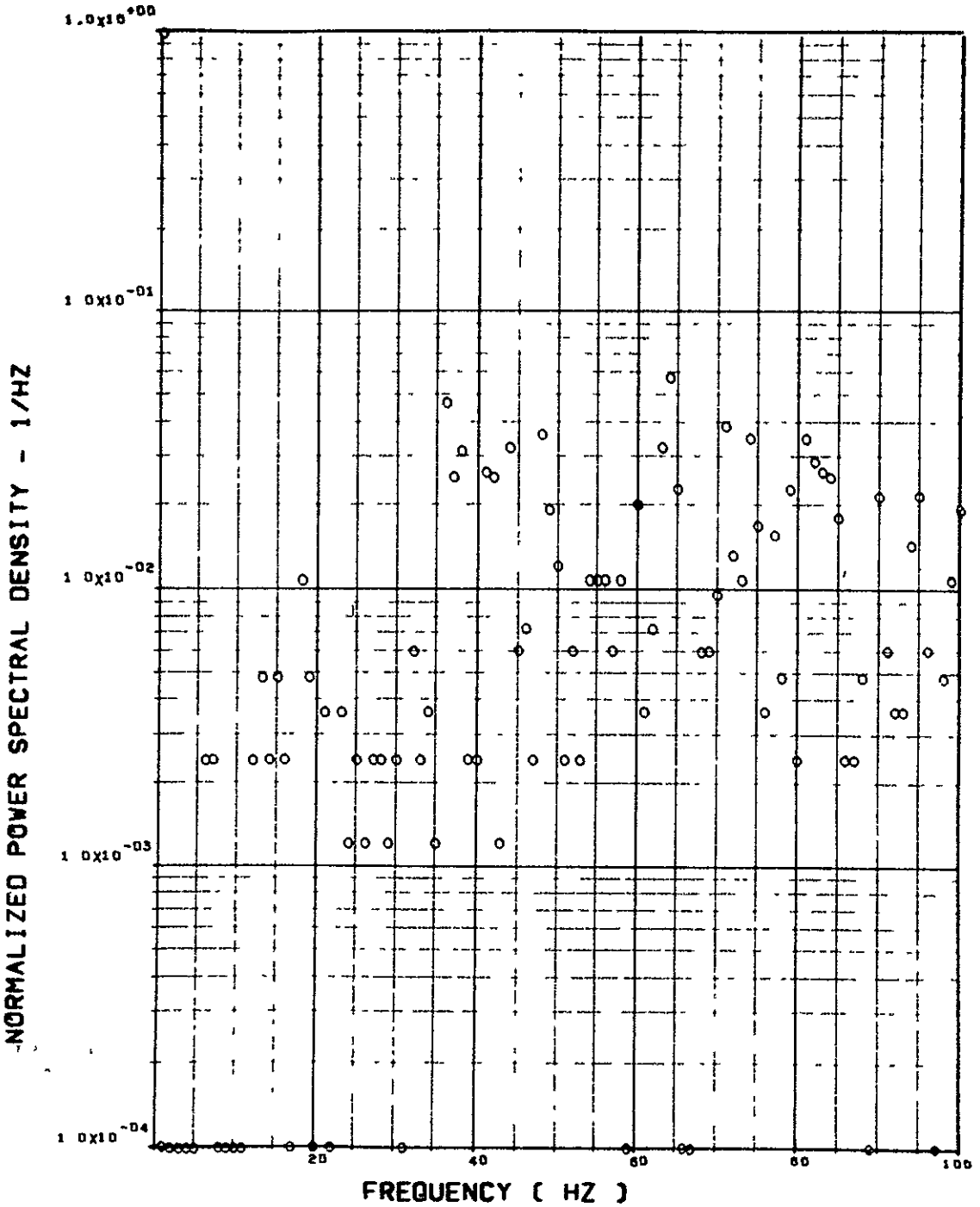

Figure 26. Power Spectra - Flight 48, Run 5, Point 2 T_1 = 134432 3, ΔT = 1 Sec, α_{Nom} = 8.41 deg, $\Delta\alpha$= 0 80 deg.

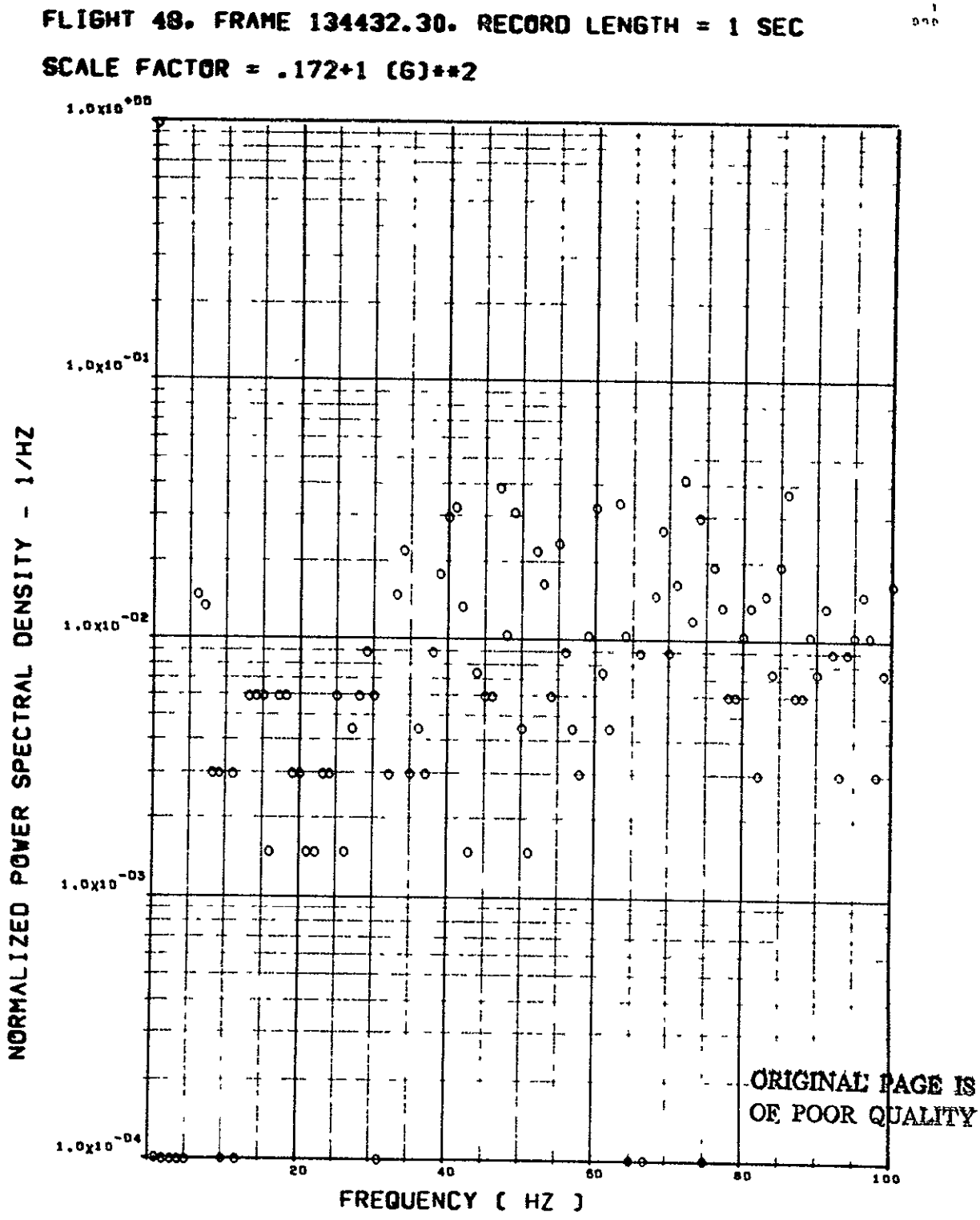

Figure 26. Continued

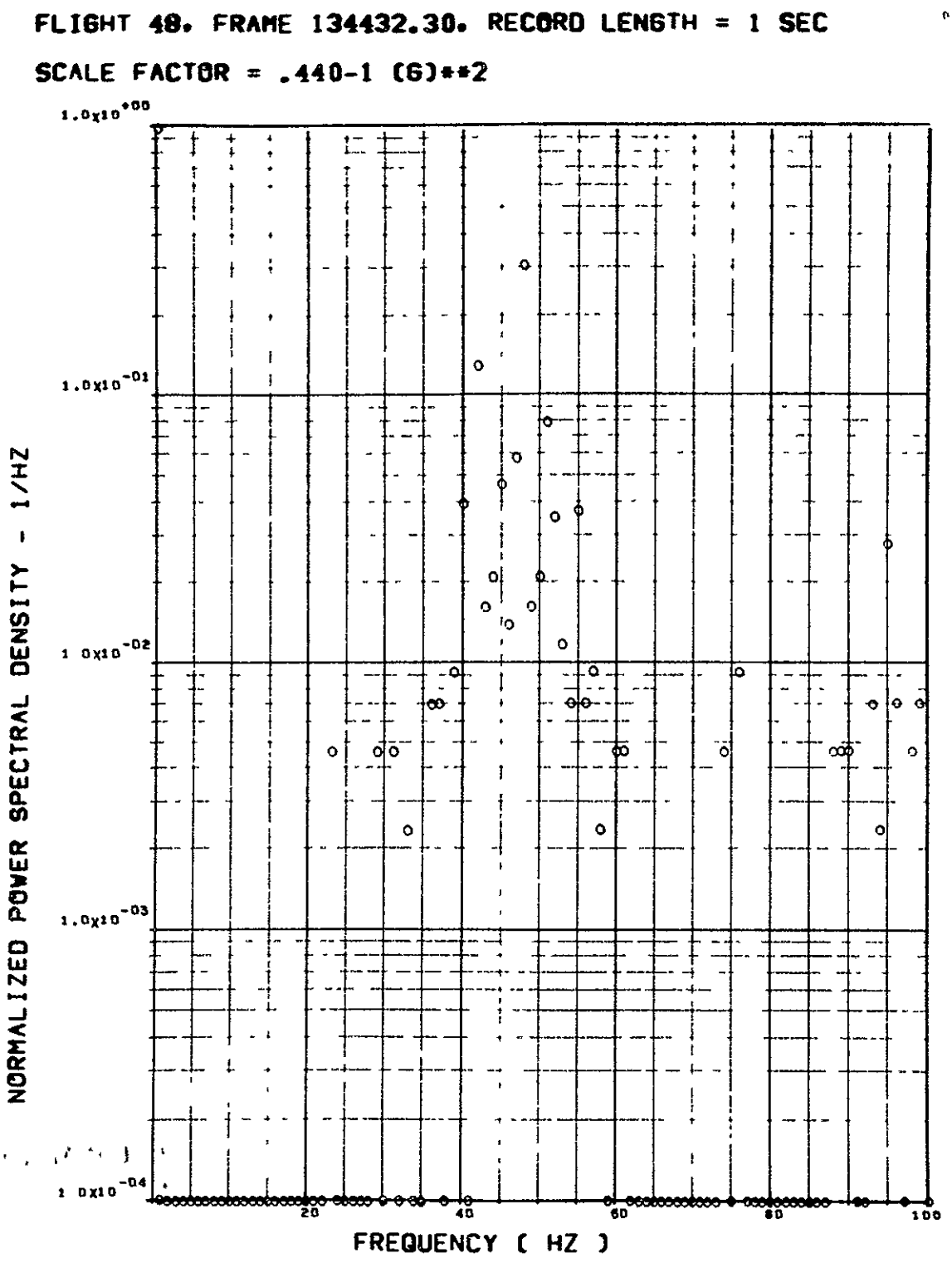

Figure 26. Continued

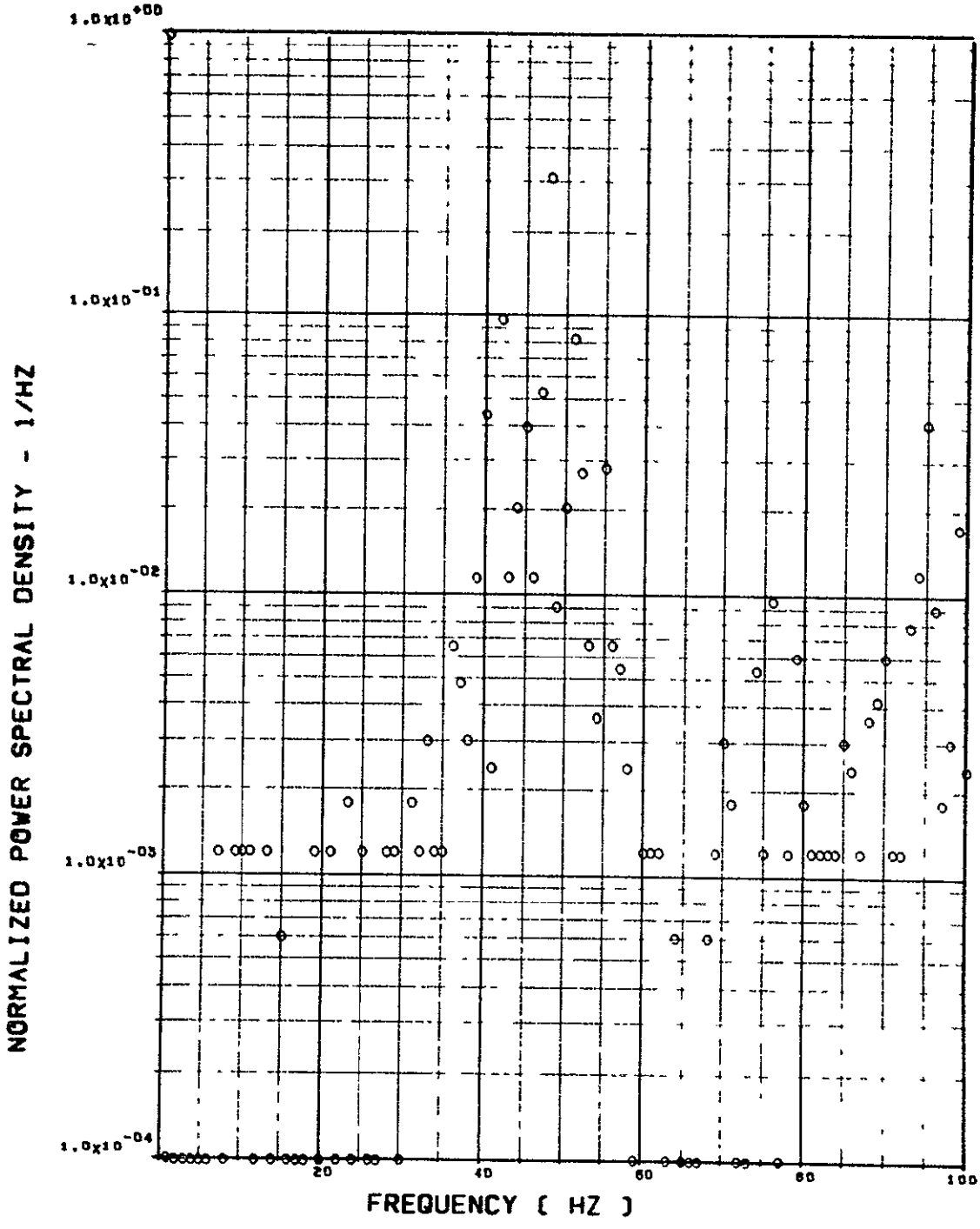

Figure 26. Continued

FLIGHT 48. FRAME 134432.30. RECORD LENGTH = 1 SEC

SCALE FACTOR = .197-2 (G)**2

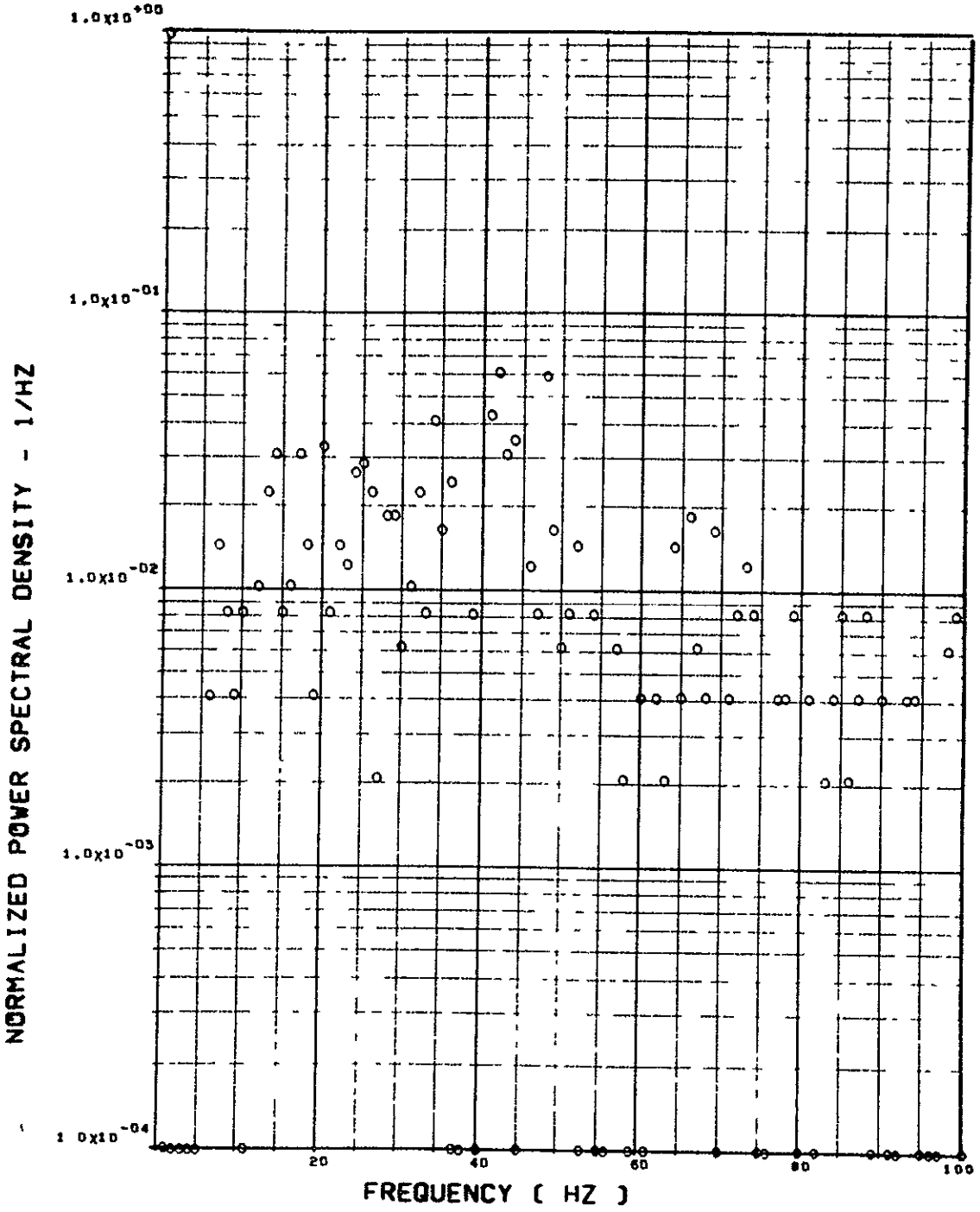

ITEM - AF009 PILOT'S SEAT VERTICAL ACCELEROMETER

Figure 26. Continued

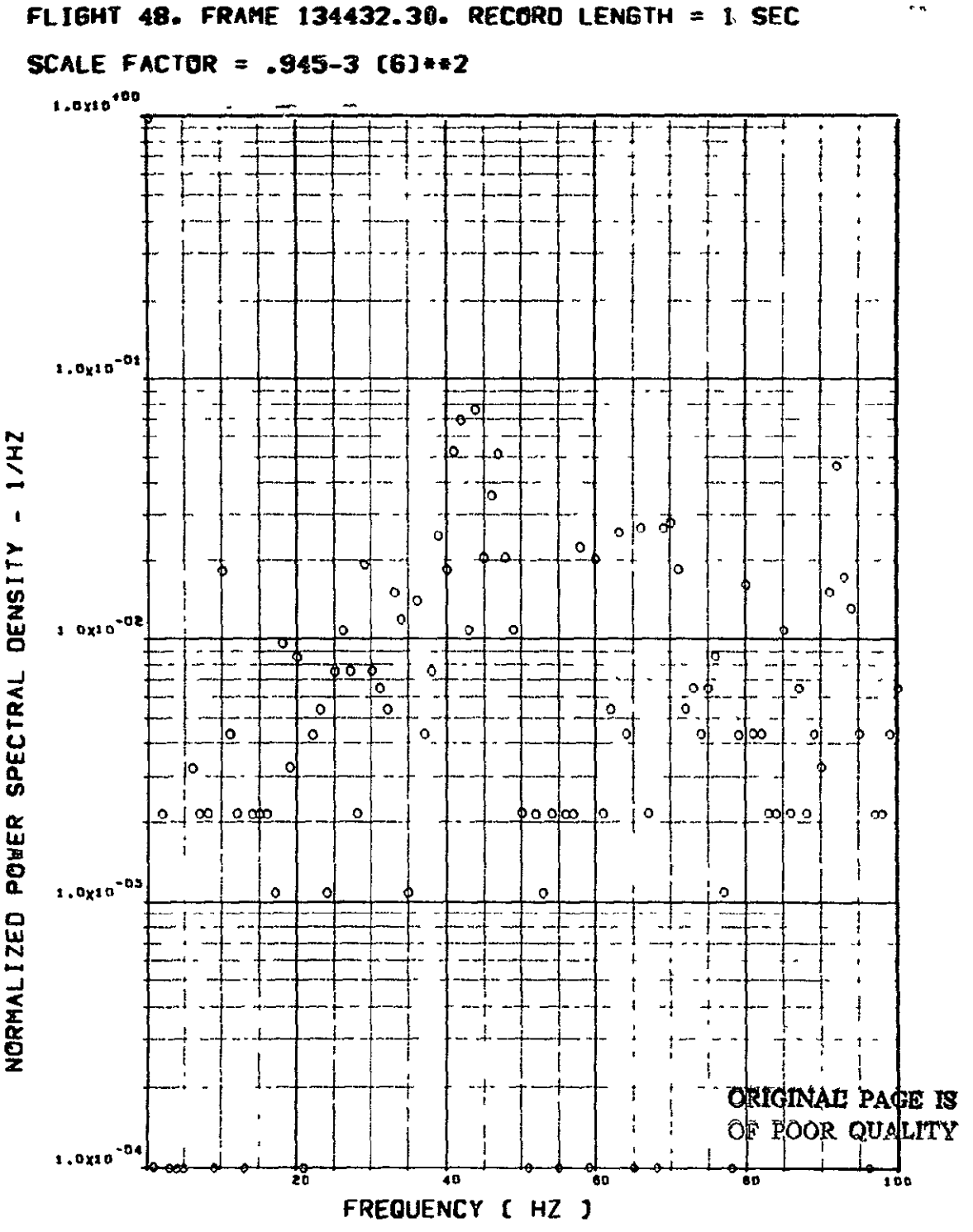

Figure 26. Continued

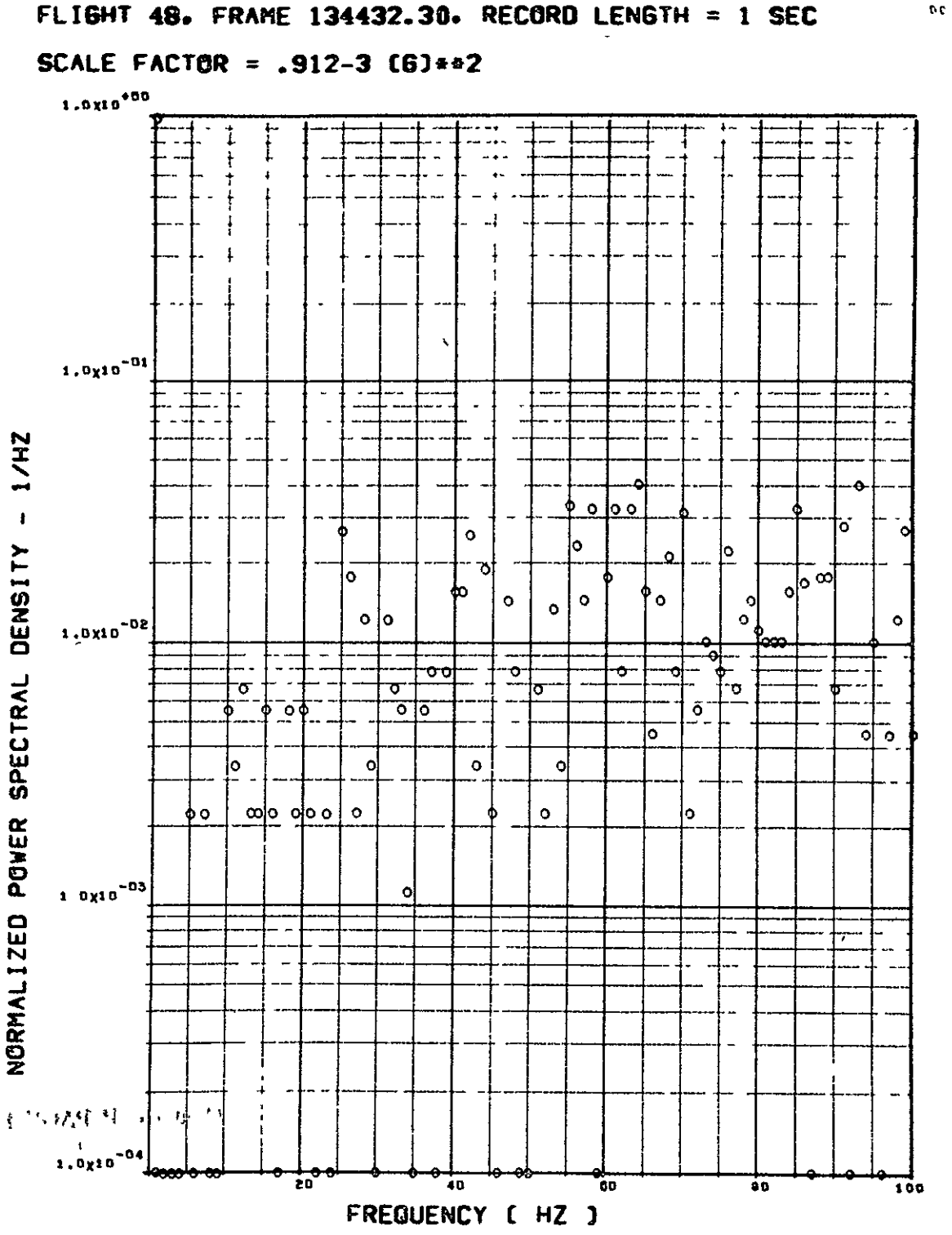

Figure 26. Continued

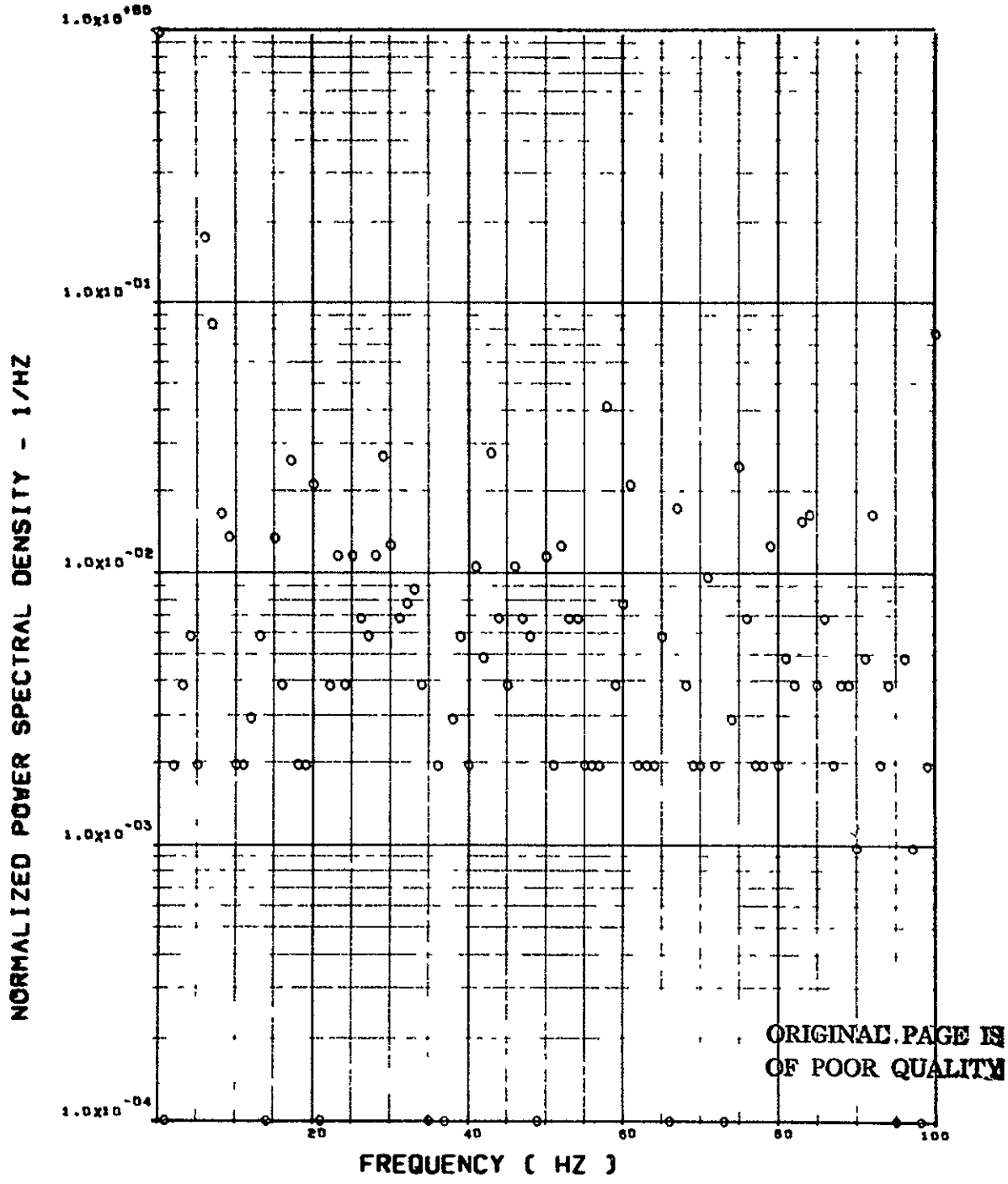

Figure 26. Continued

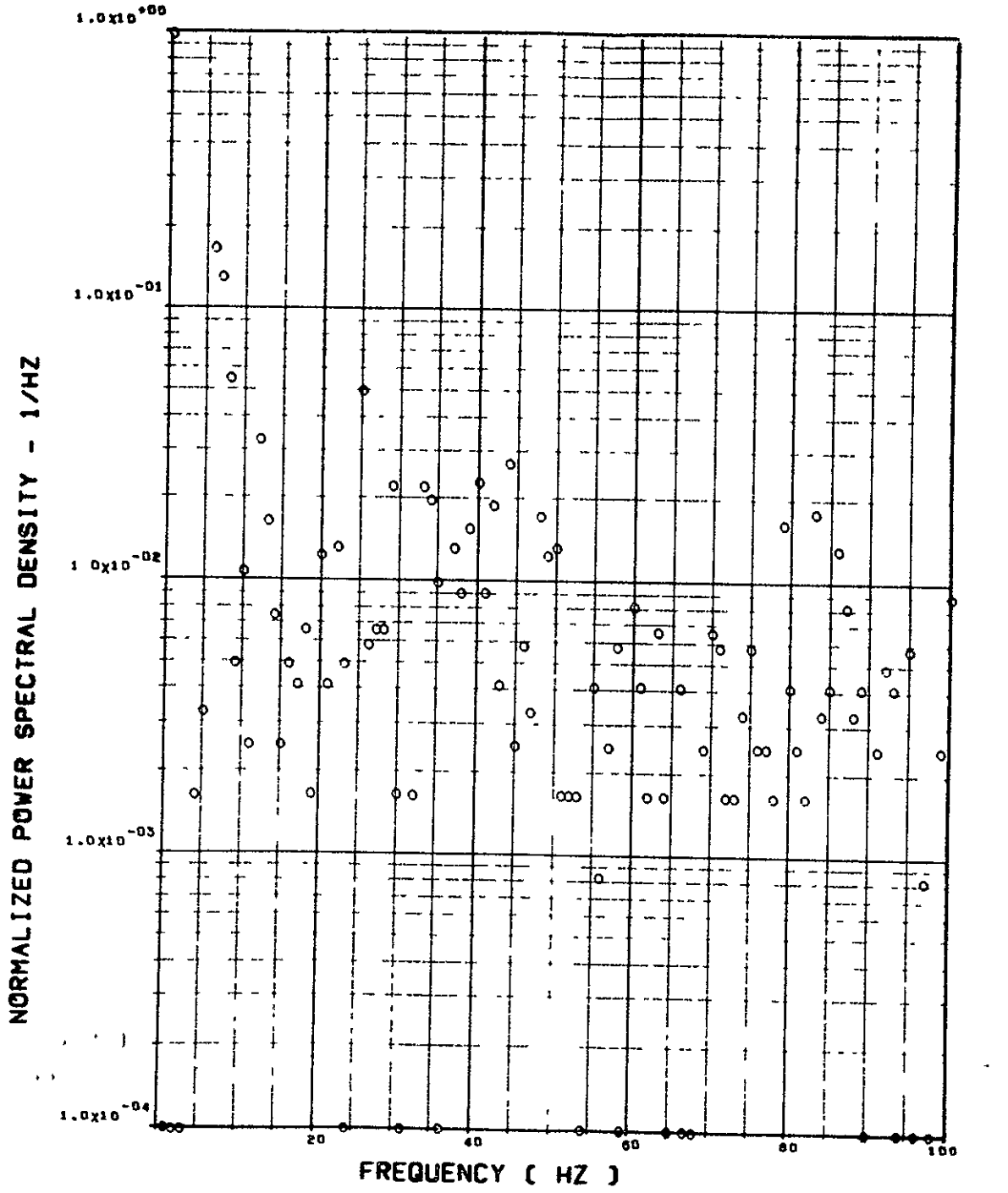

Figure 26. Continued

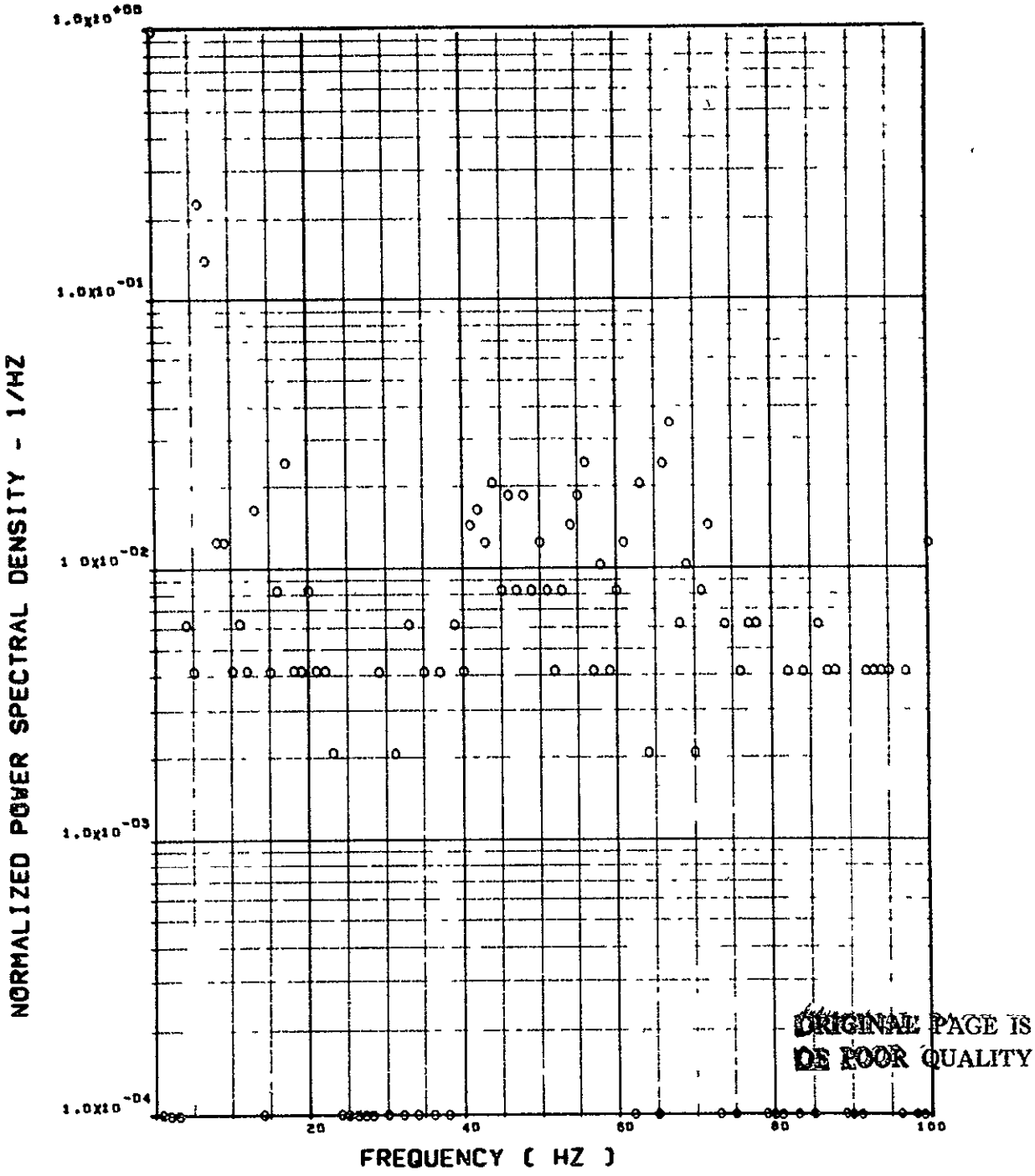

Figure 26. Continued

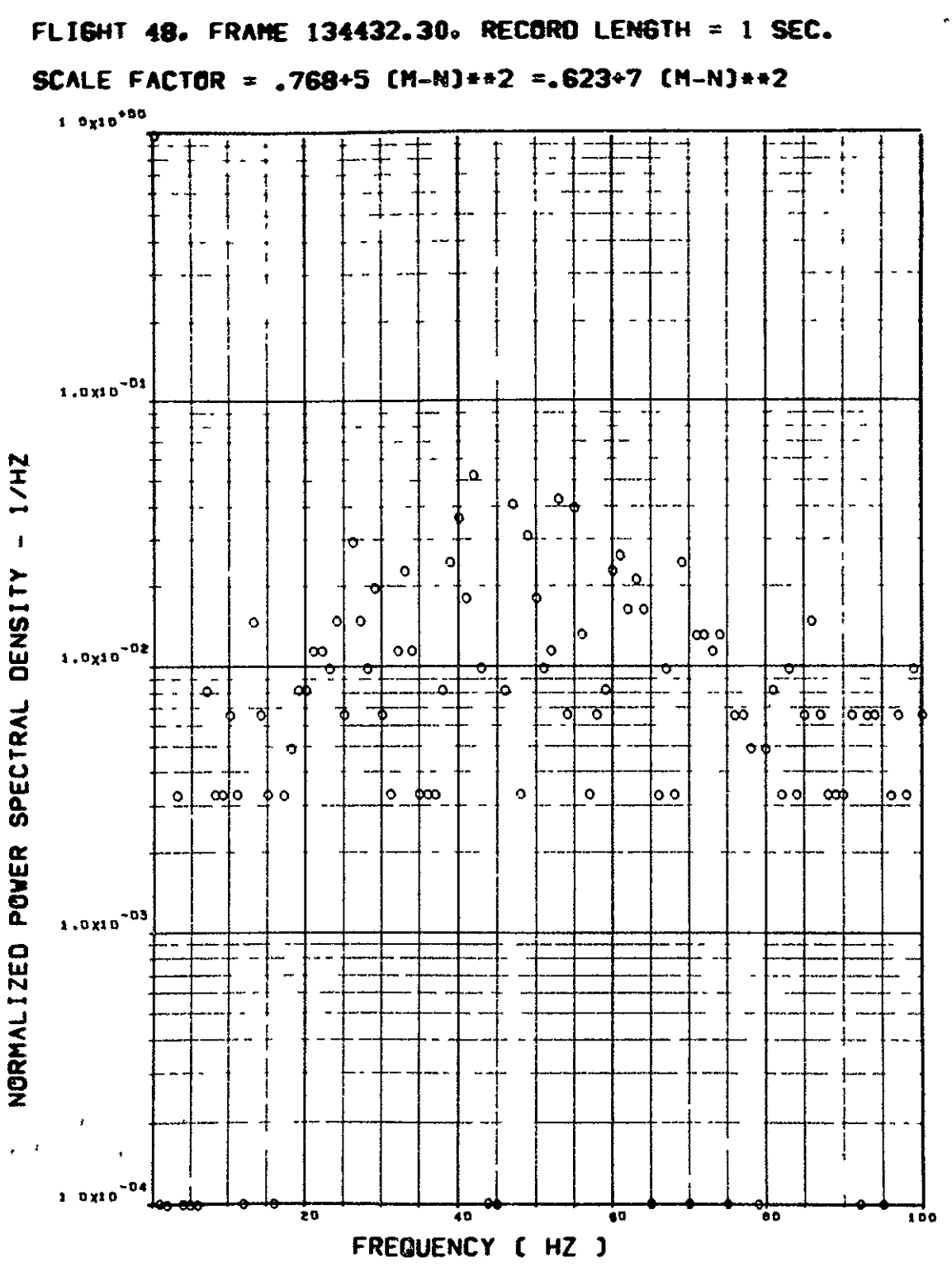

Figure 26. Continued

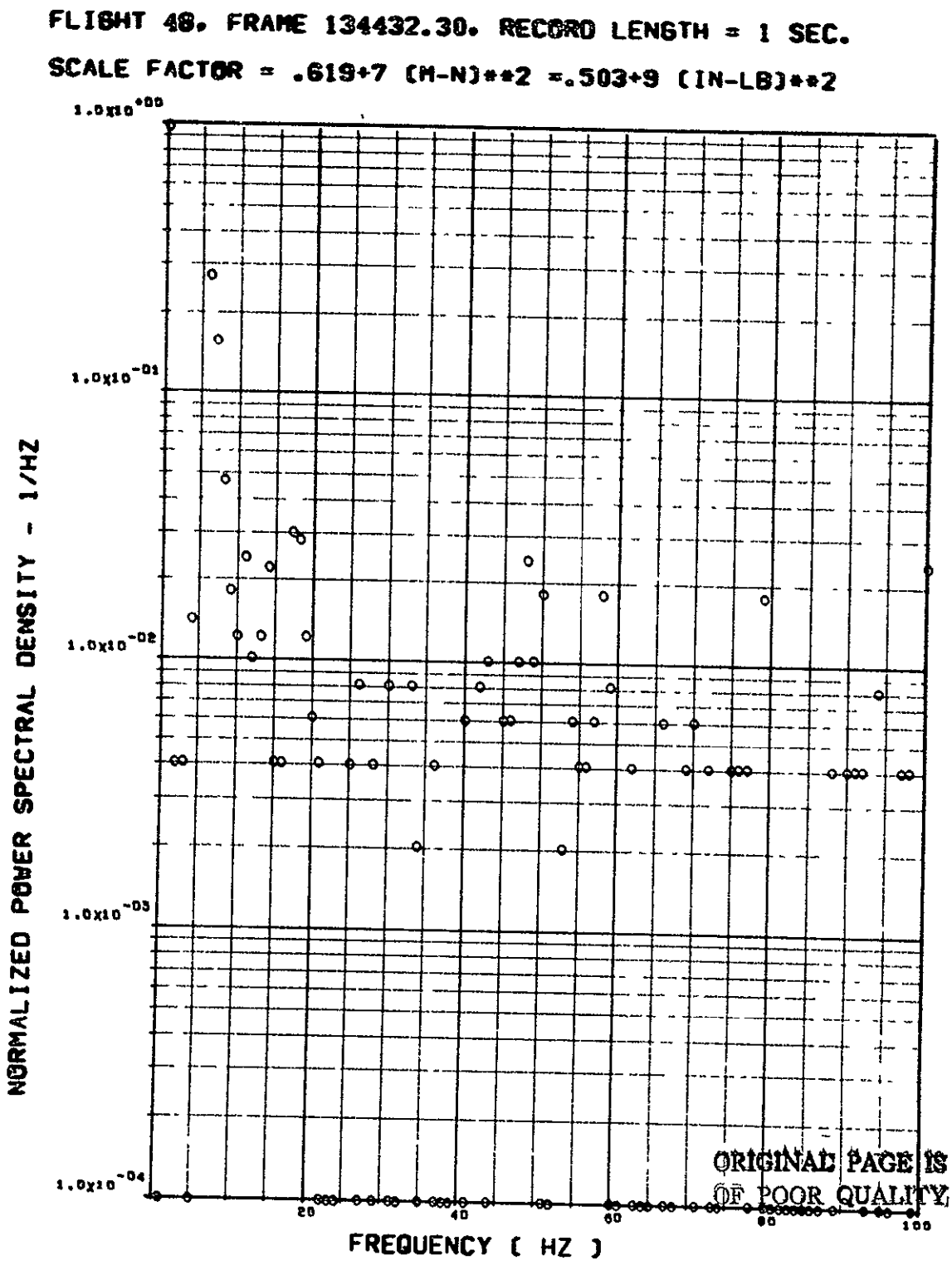

Figure 26. Continued

FLIGHT 48. FRAME 134432.30. RECORD LENGTH = 1 SEC.

SCALE FACTOR = .823+7 (M-N)**2 =.669+9 (IN-LB)**2

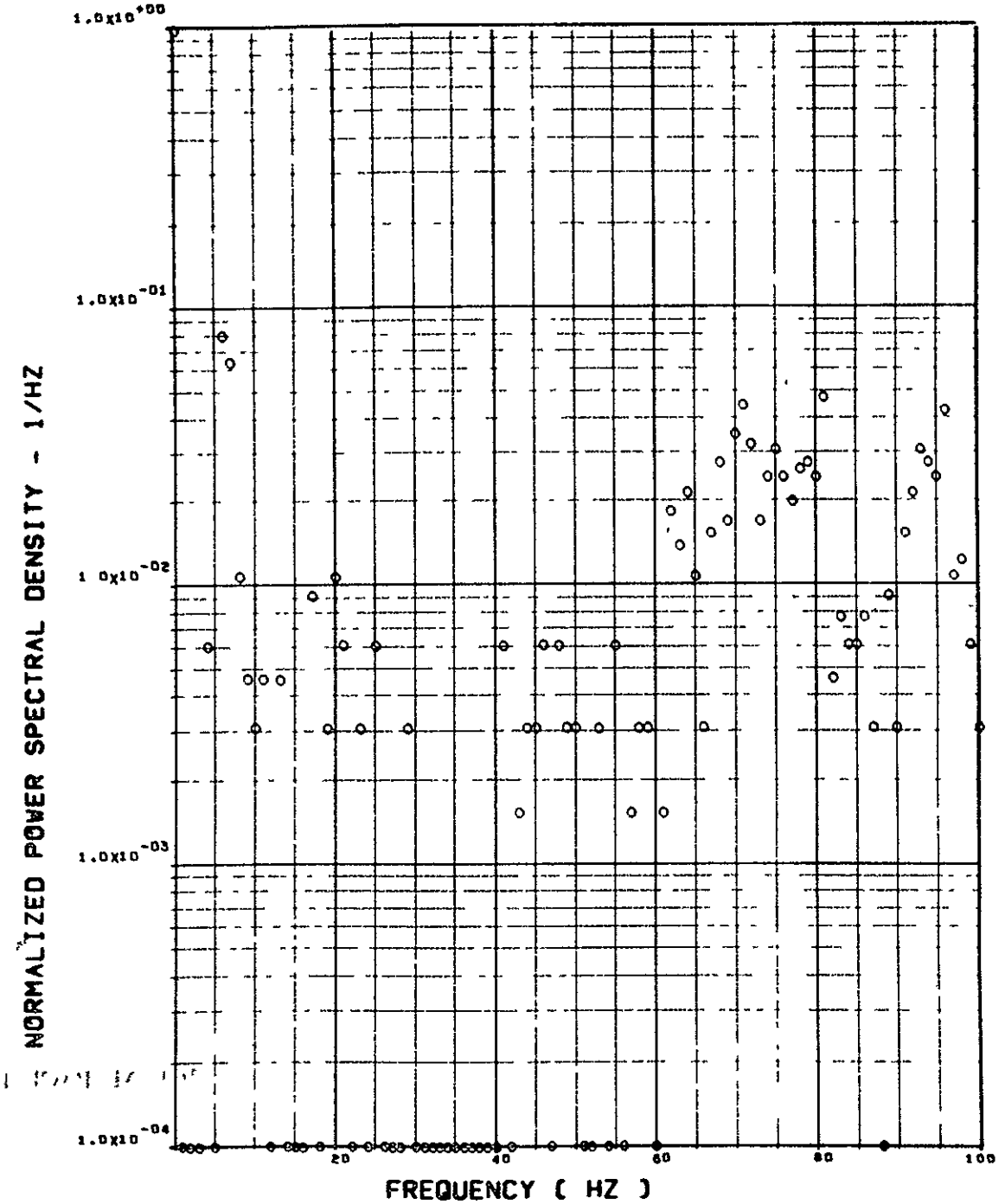

ITEM - SW127 BENDING MOMENT AT WING STATION 2

Figure 26. Continued

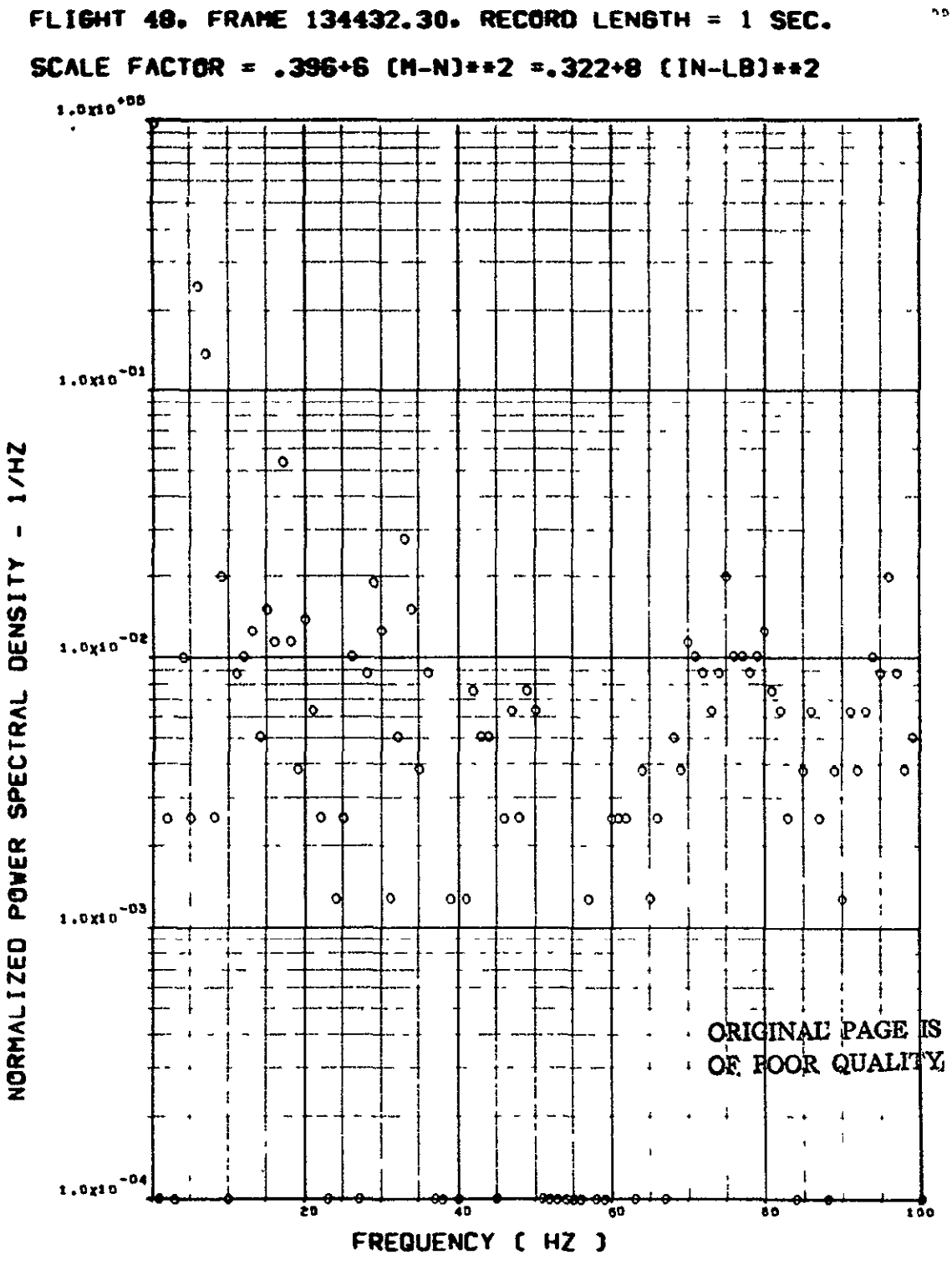

Figure 26. Continued

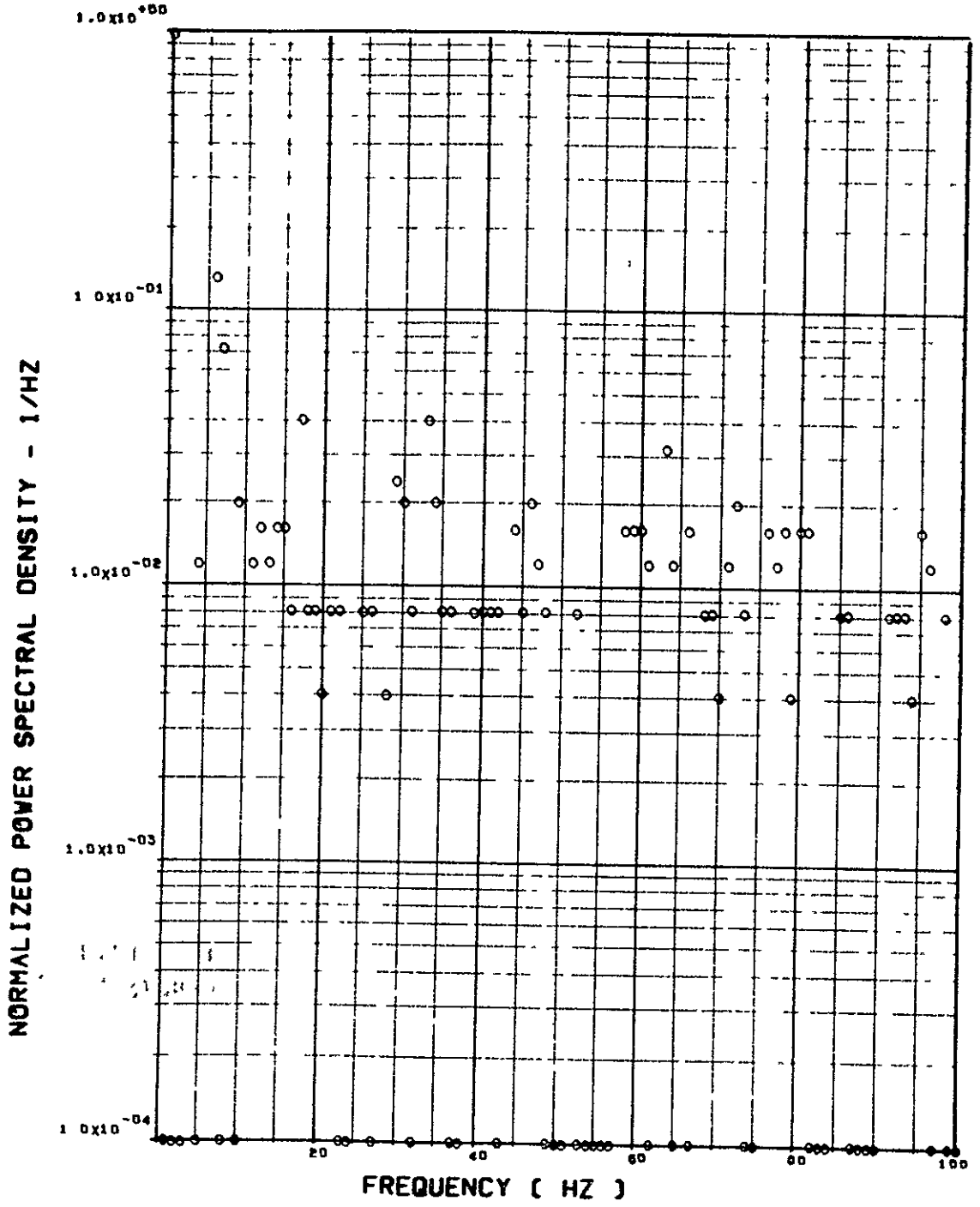

Figure 26. Continued

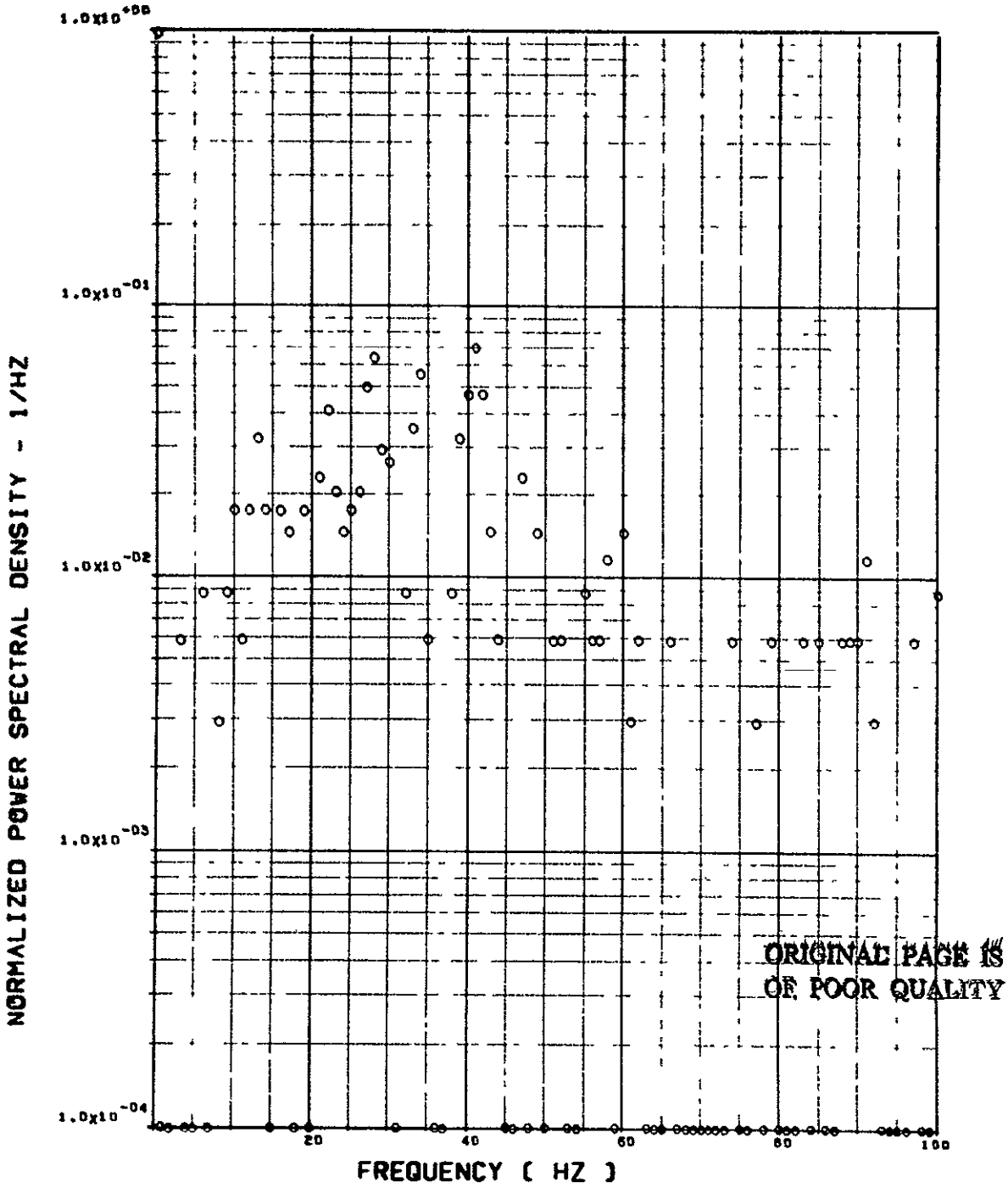

Figure 26. Continued

FLIGHT 48. FRAME 134432.30. RECORD LENGTH = 1 SEC.

SCALE FACTOR = .239+6 (M-N)**2 =.194+8 (IN-LB)**2

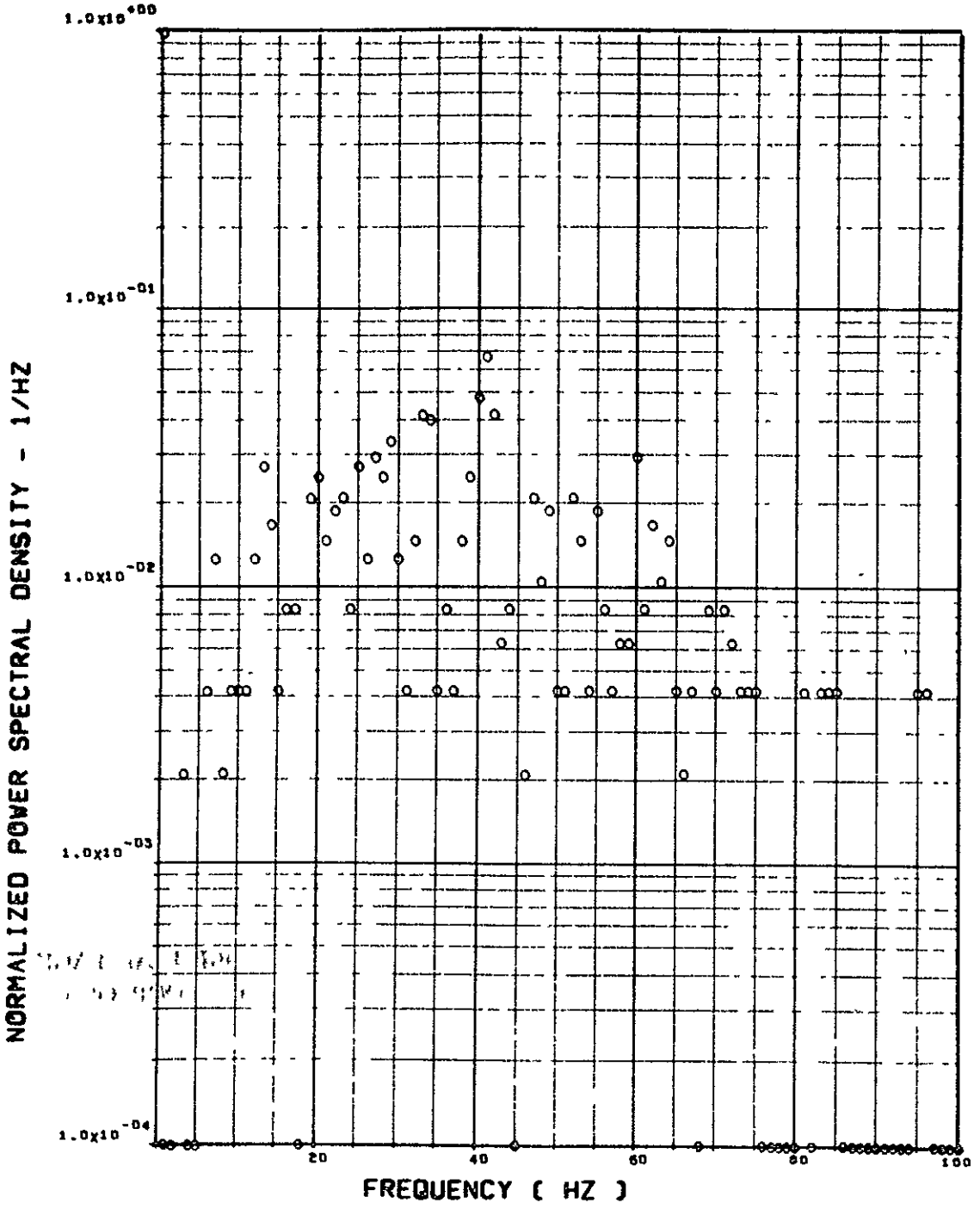

ITEM - SW128 TORSION AT WING STATION 2

Figure 26. Continued

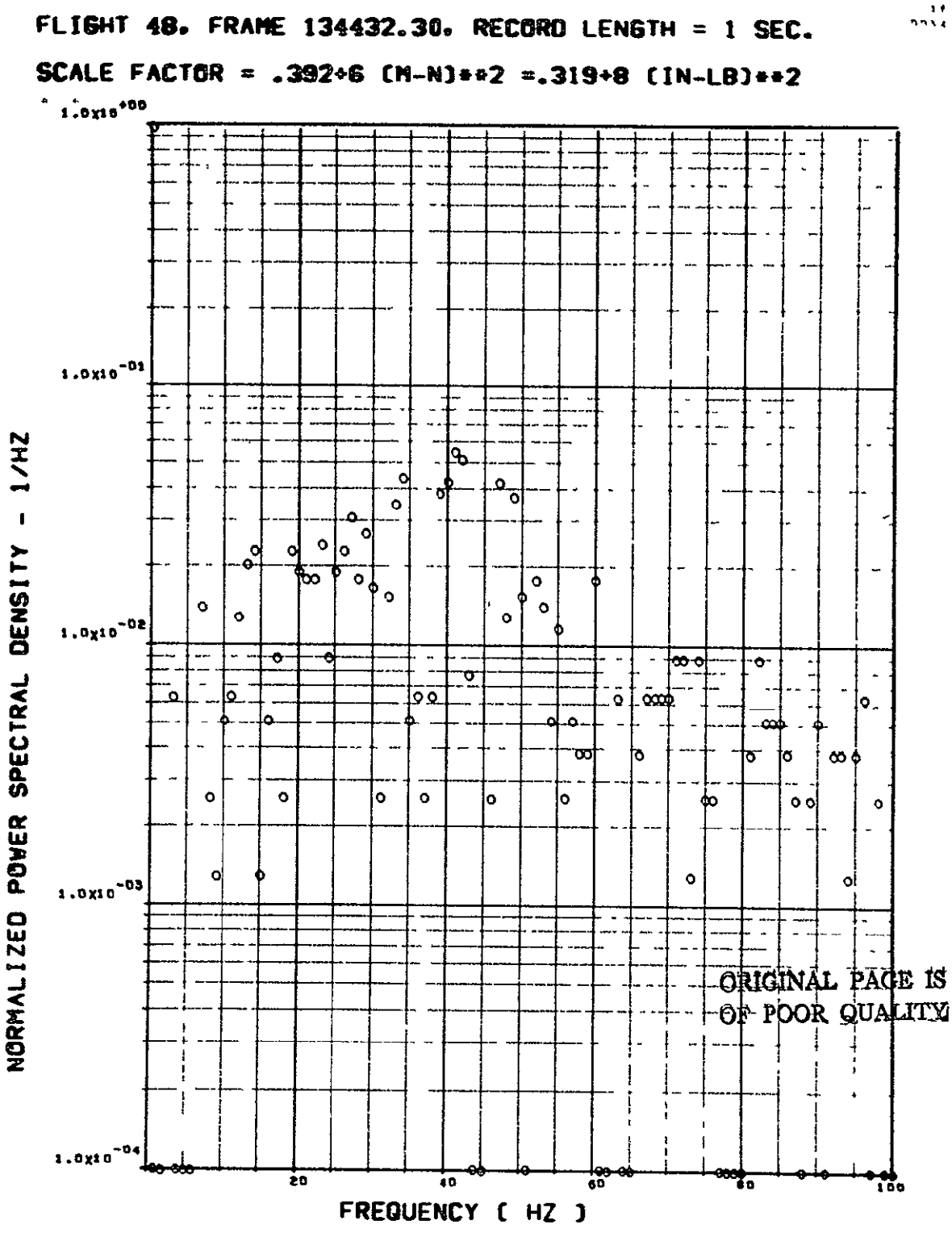

Figure 26. Continued

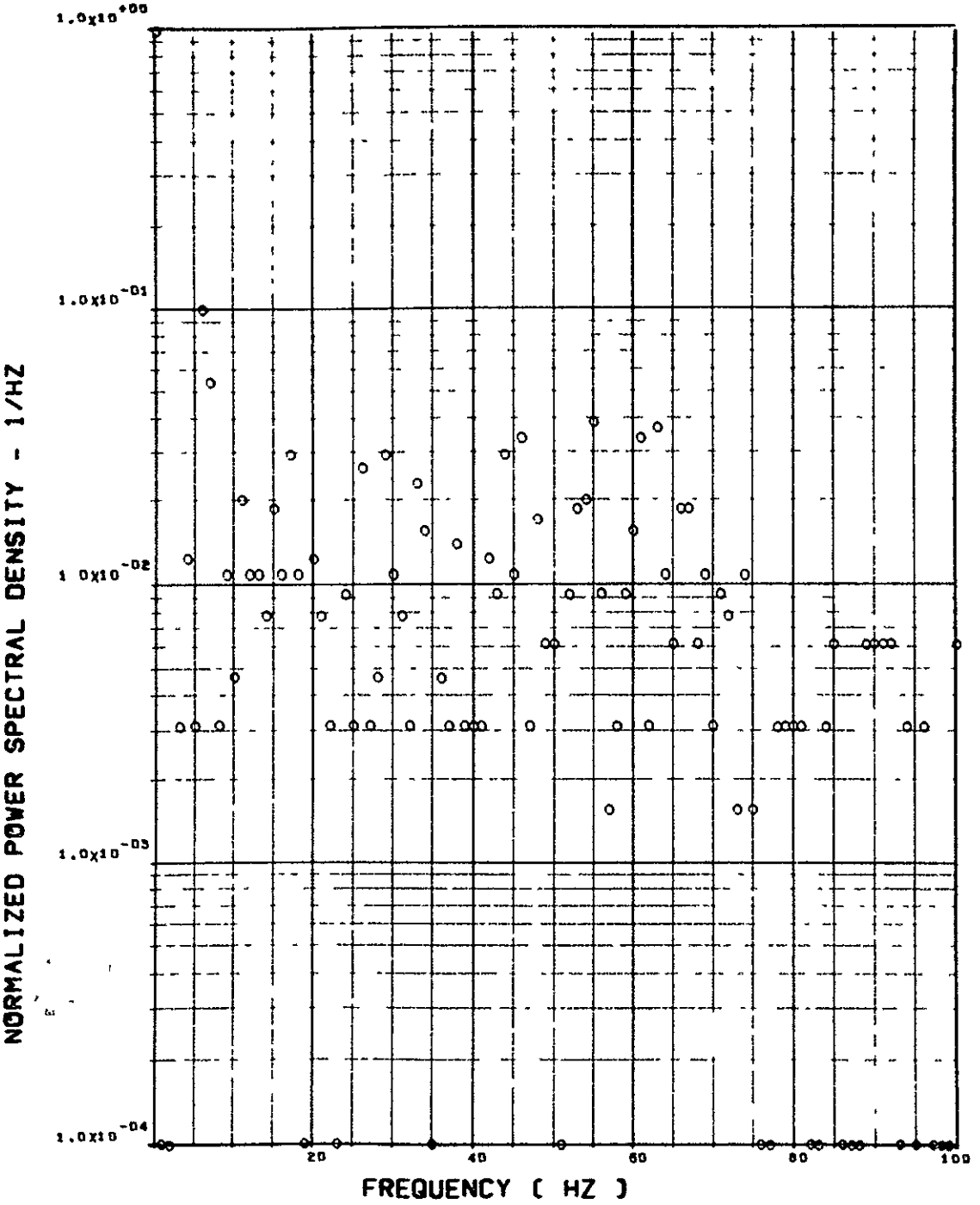

Figure 26. Continued

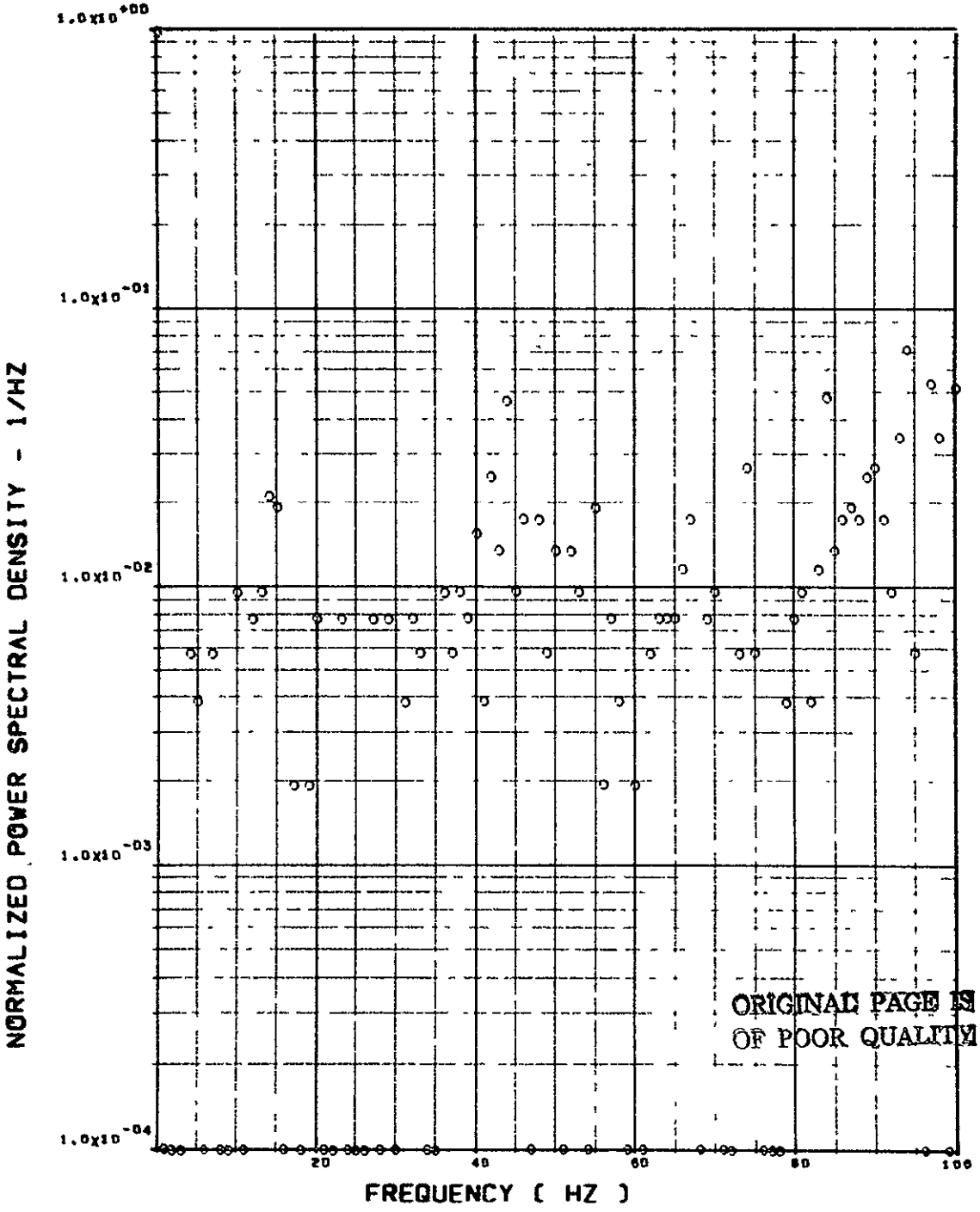

Figure 26. Continued

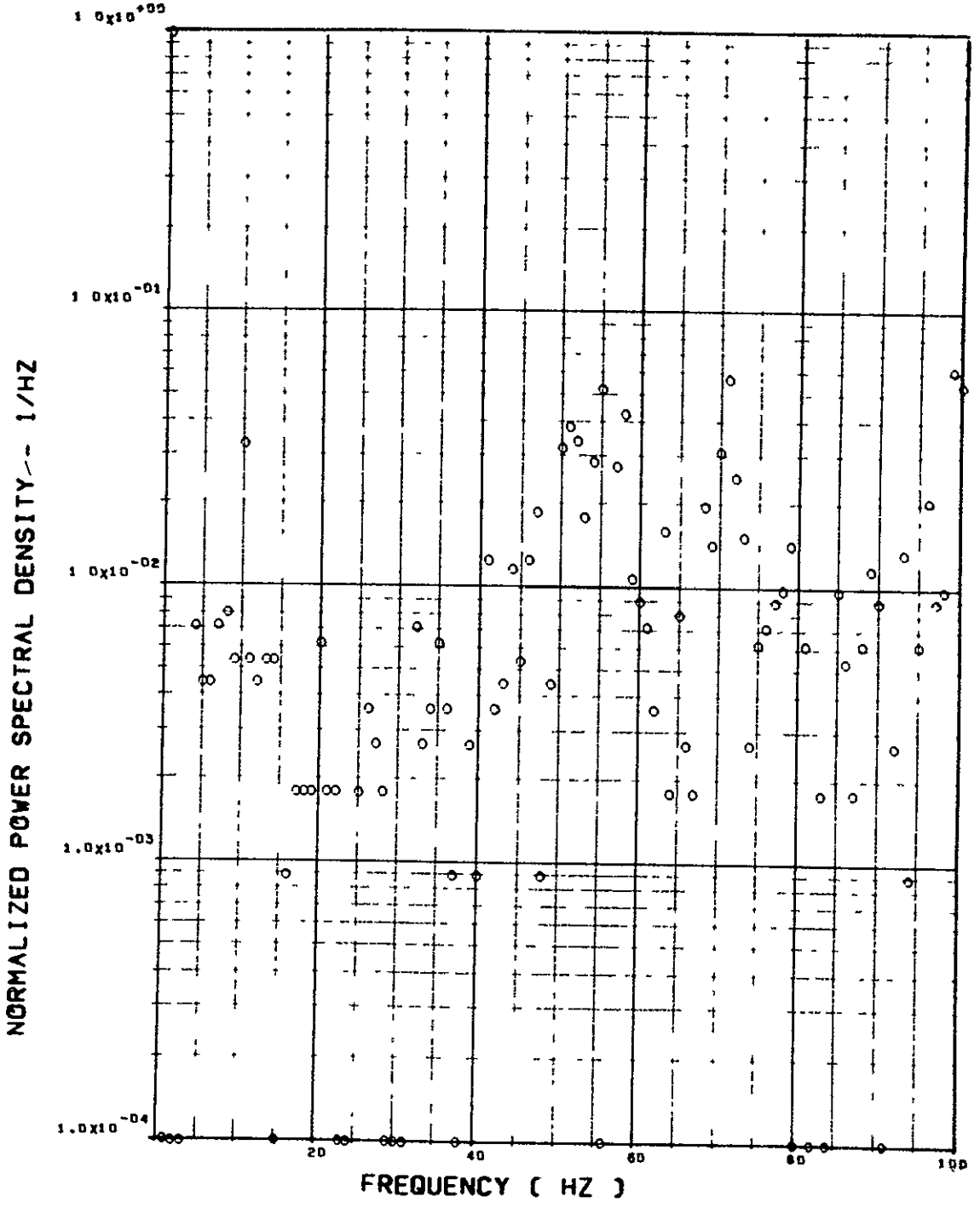

Figure 26. Continued

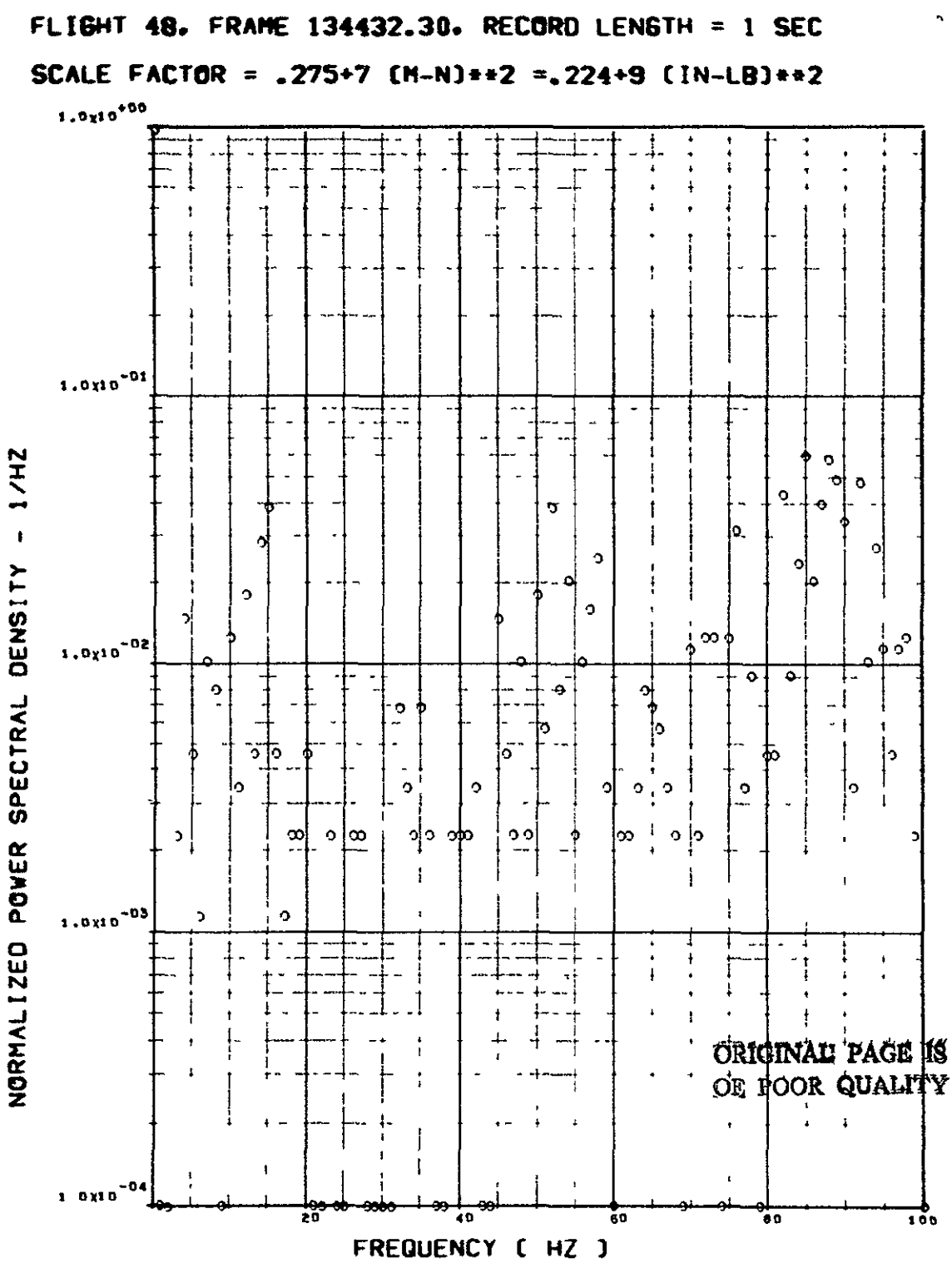

Figure 26. Continued

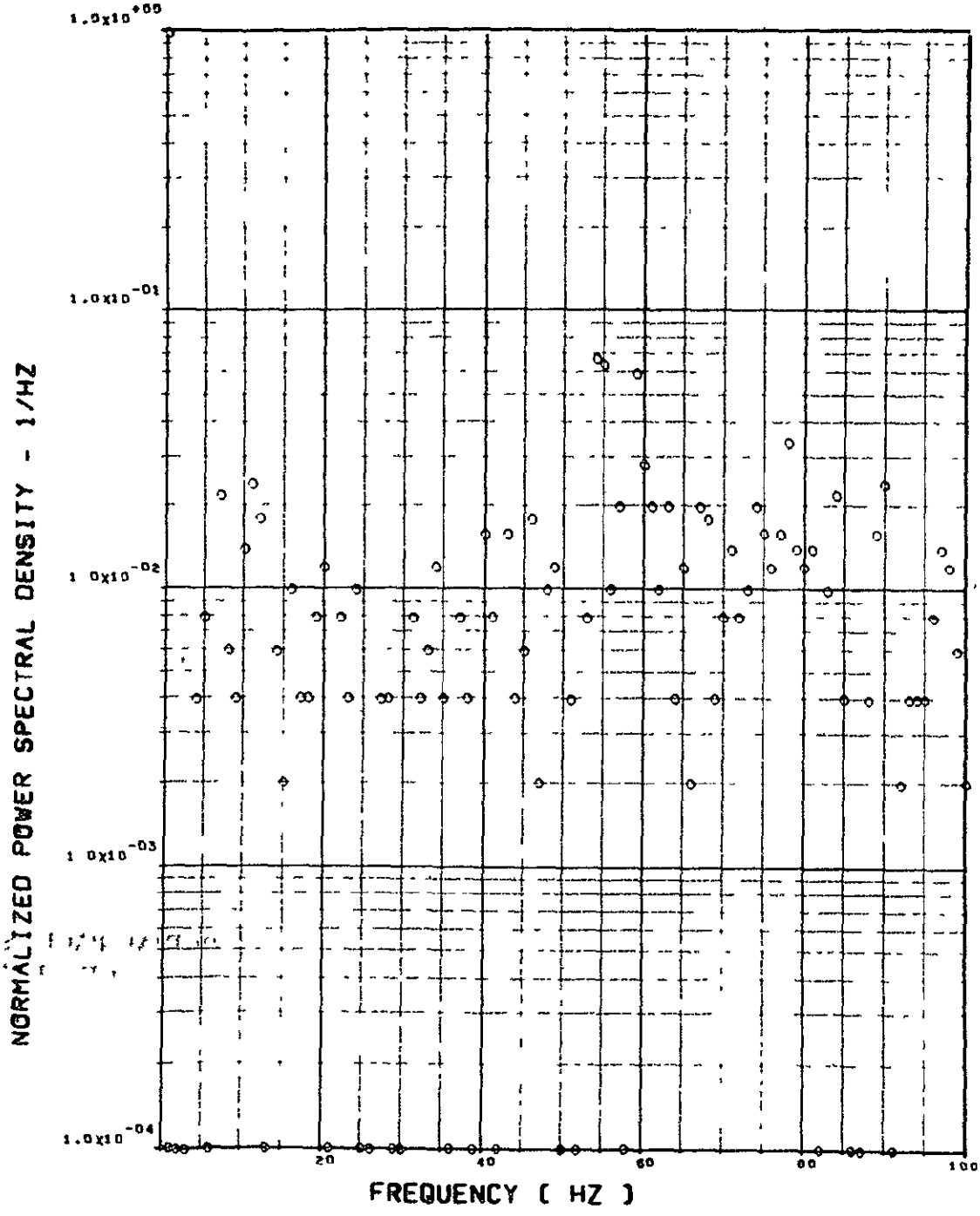

Figure 26. Continued

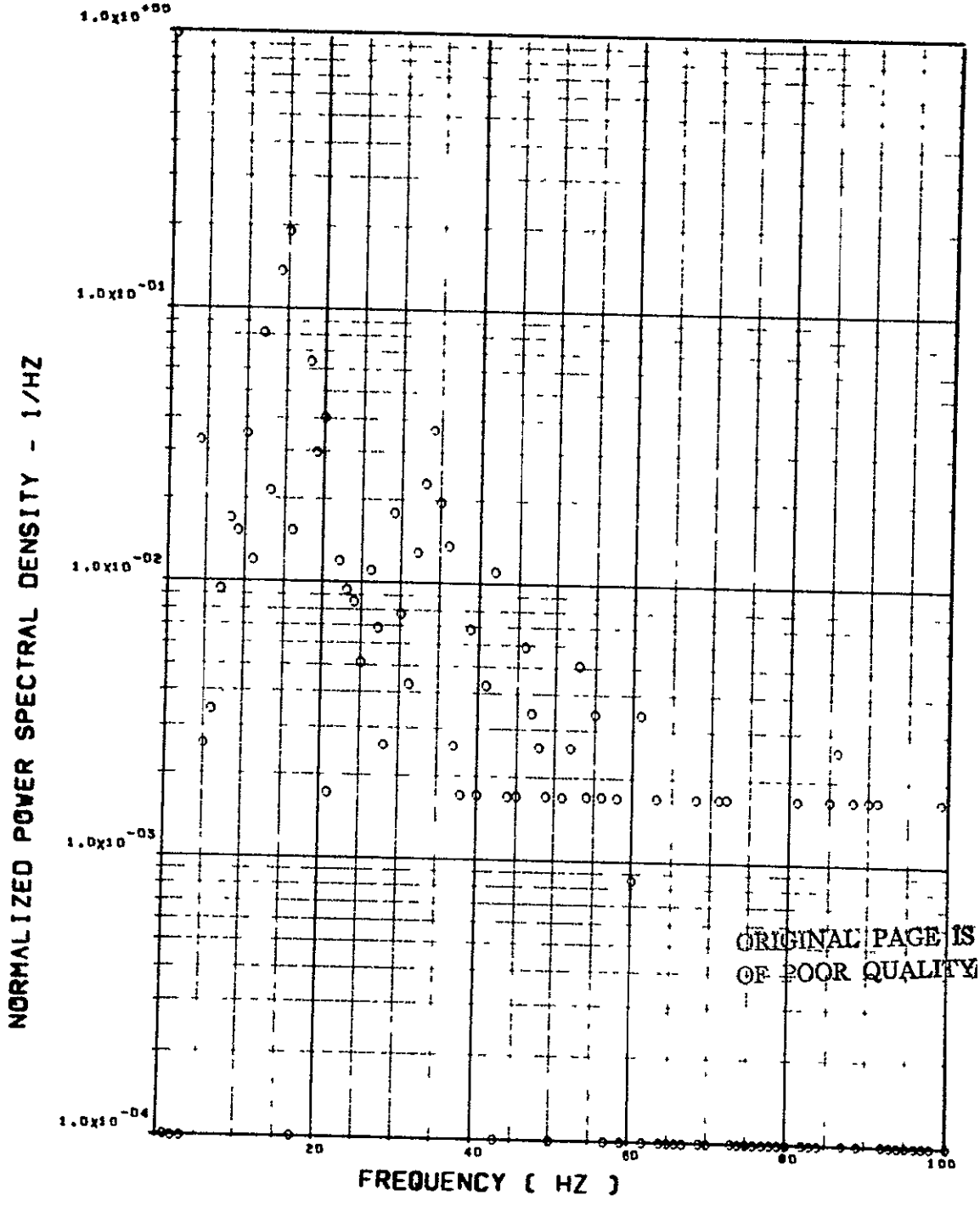

Figure 26. Continued

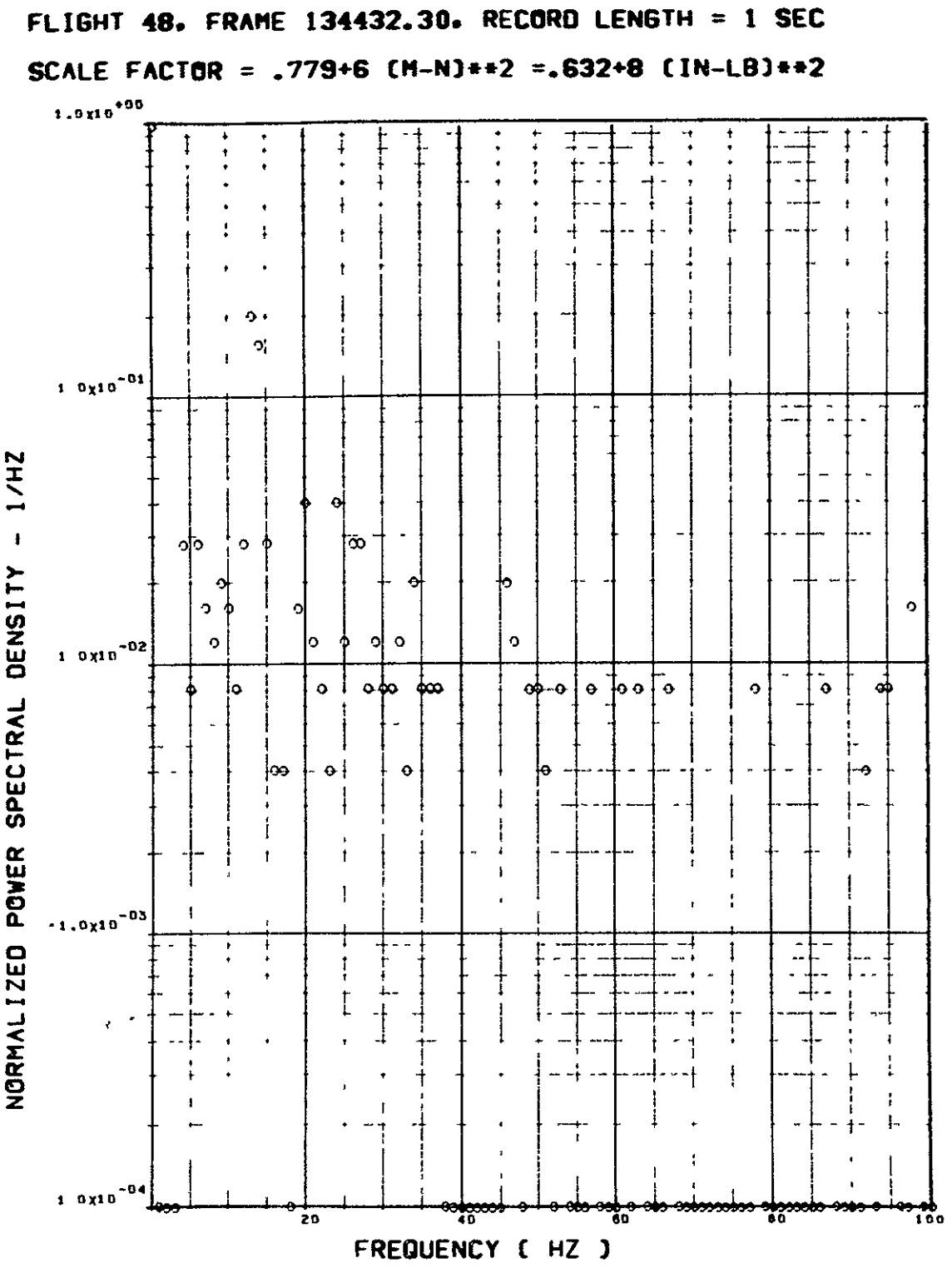

Figure 26. Concluded

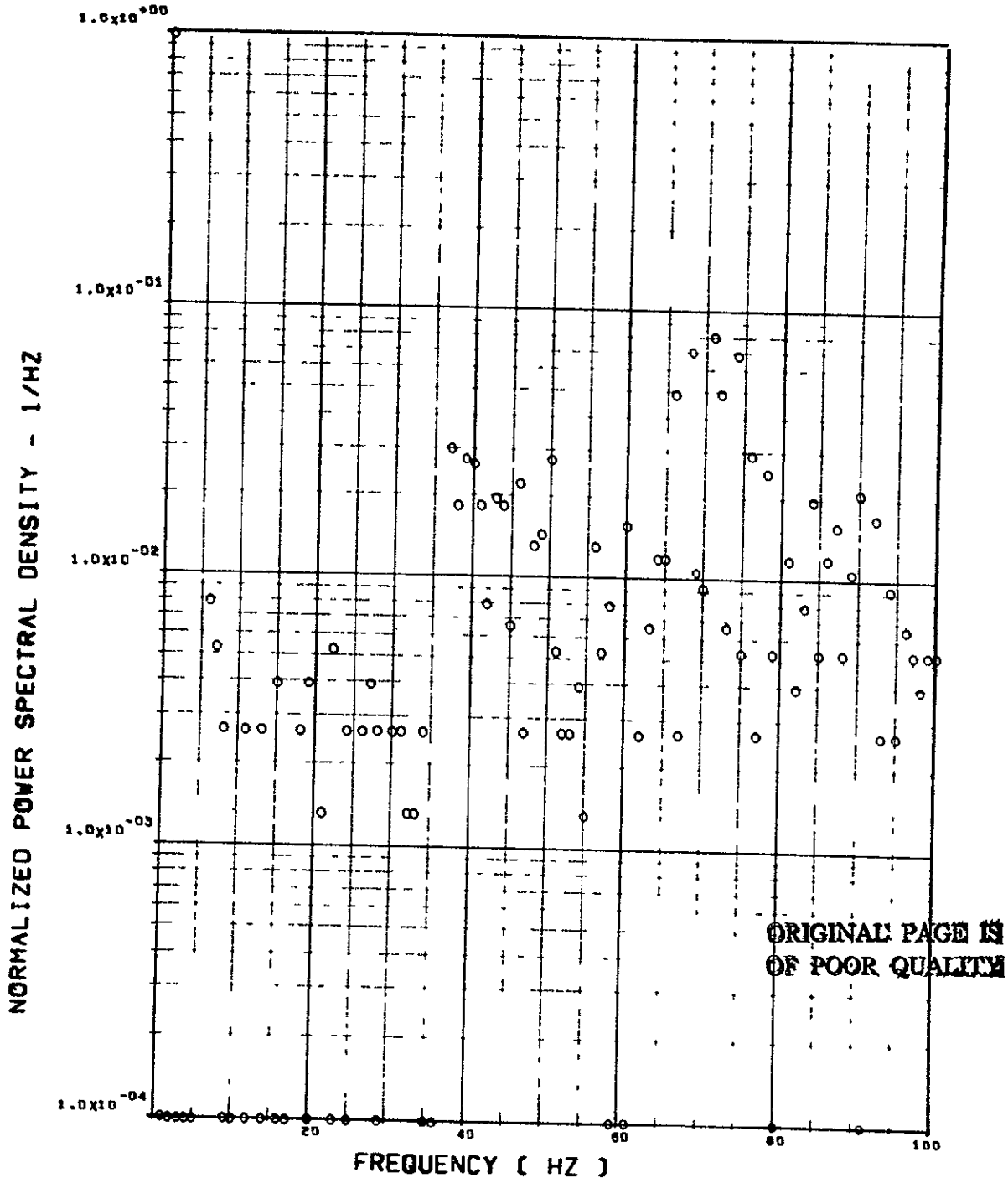

Figure 21. Power Spectra - Flight 48, Run 5, Point 3
T_1 = 134436 2, ΔT = 1 Sec, α_{Nom} = 12 10 deg,
$\Delta\alpha$= 1.40 deg.

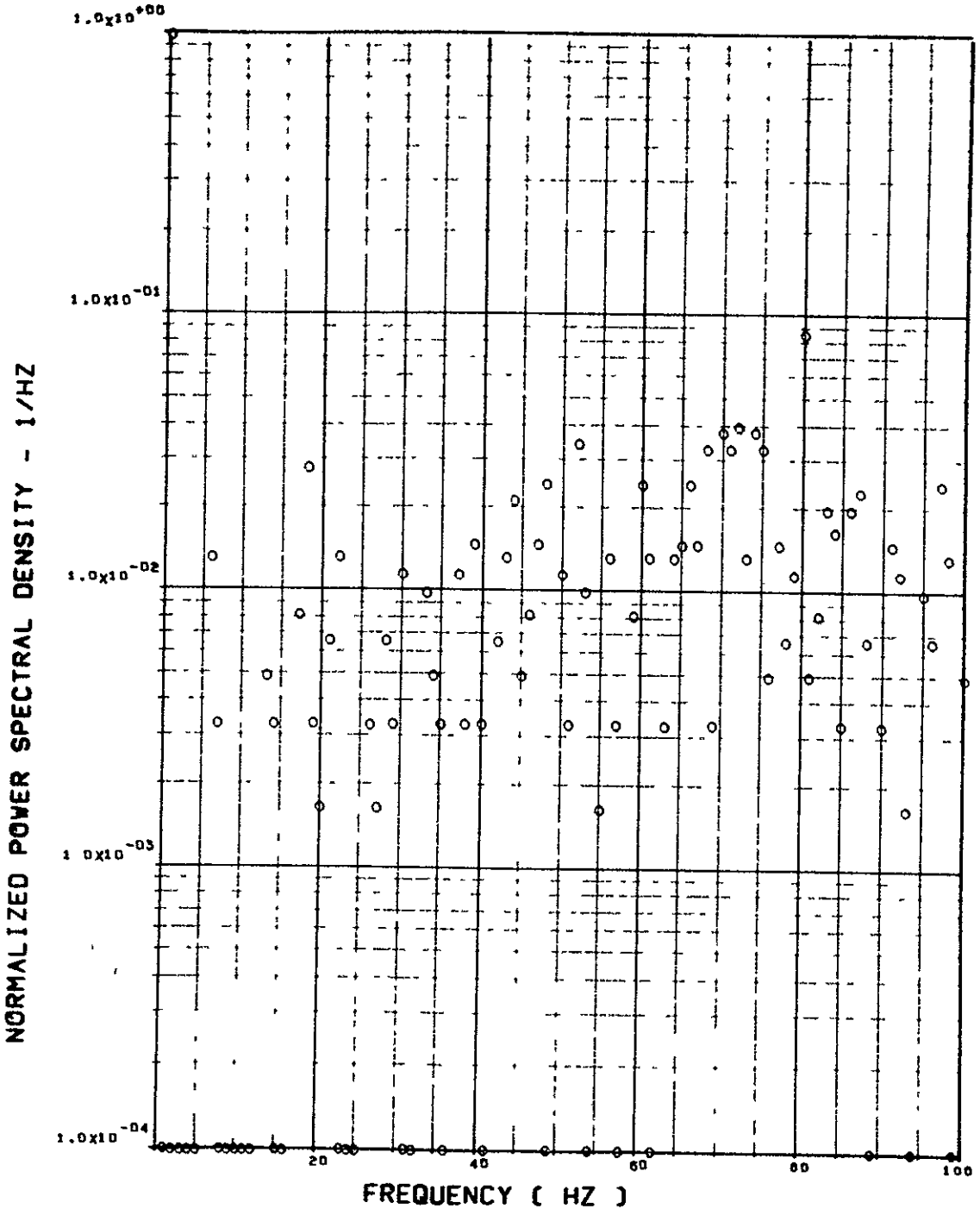

Figure 27. Continued

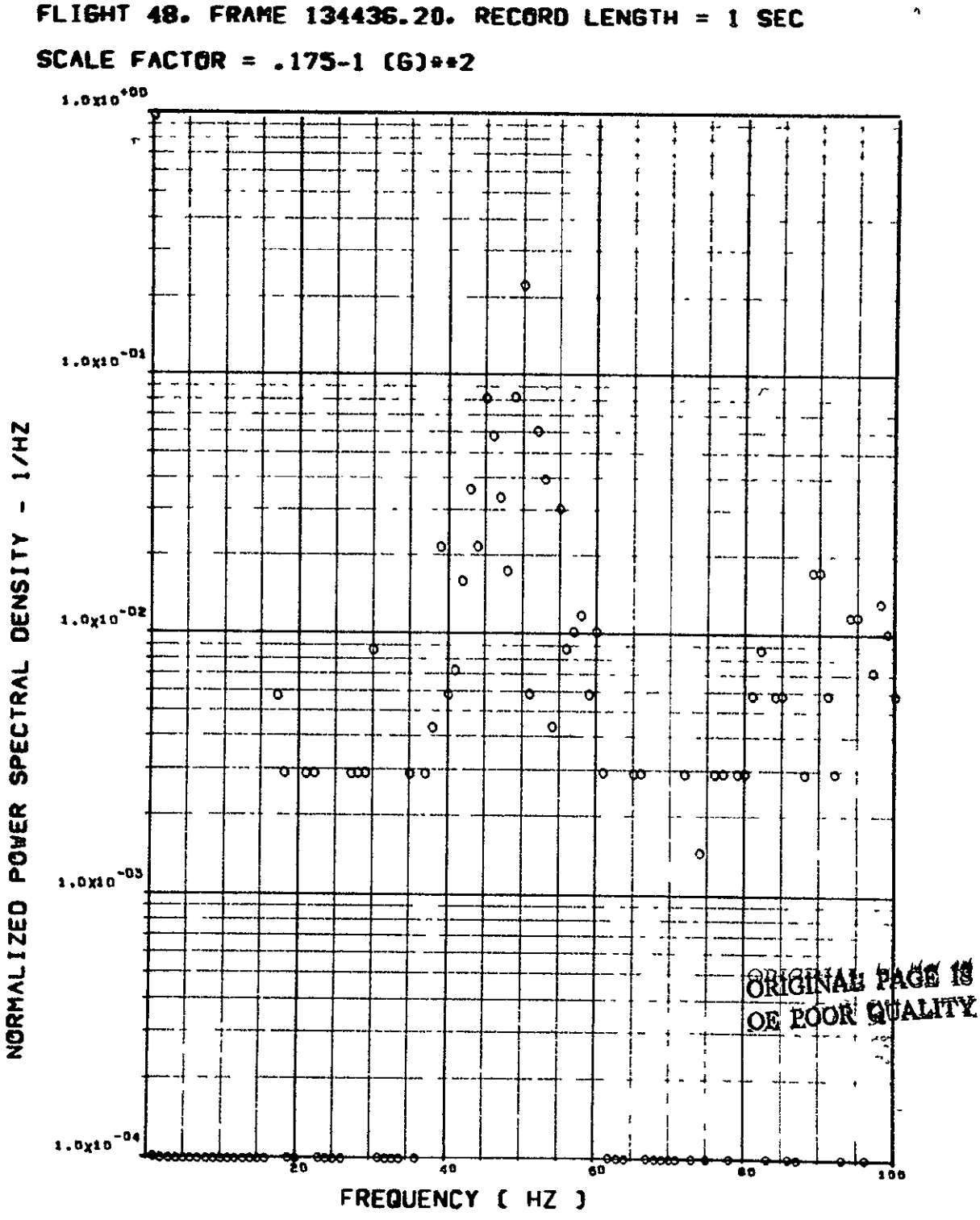

Figure 2/. Continued

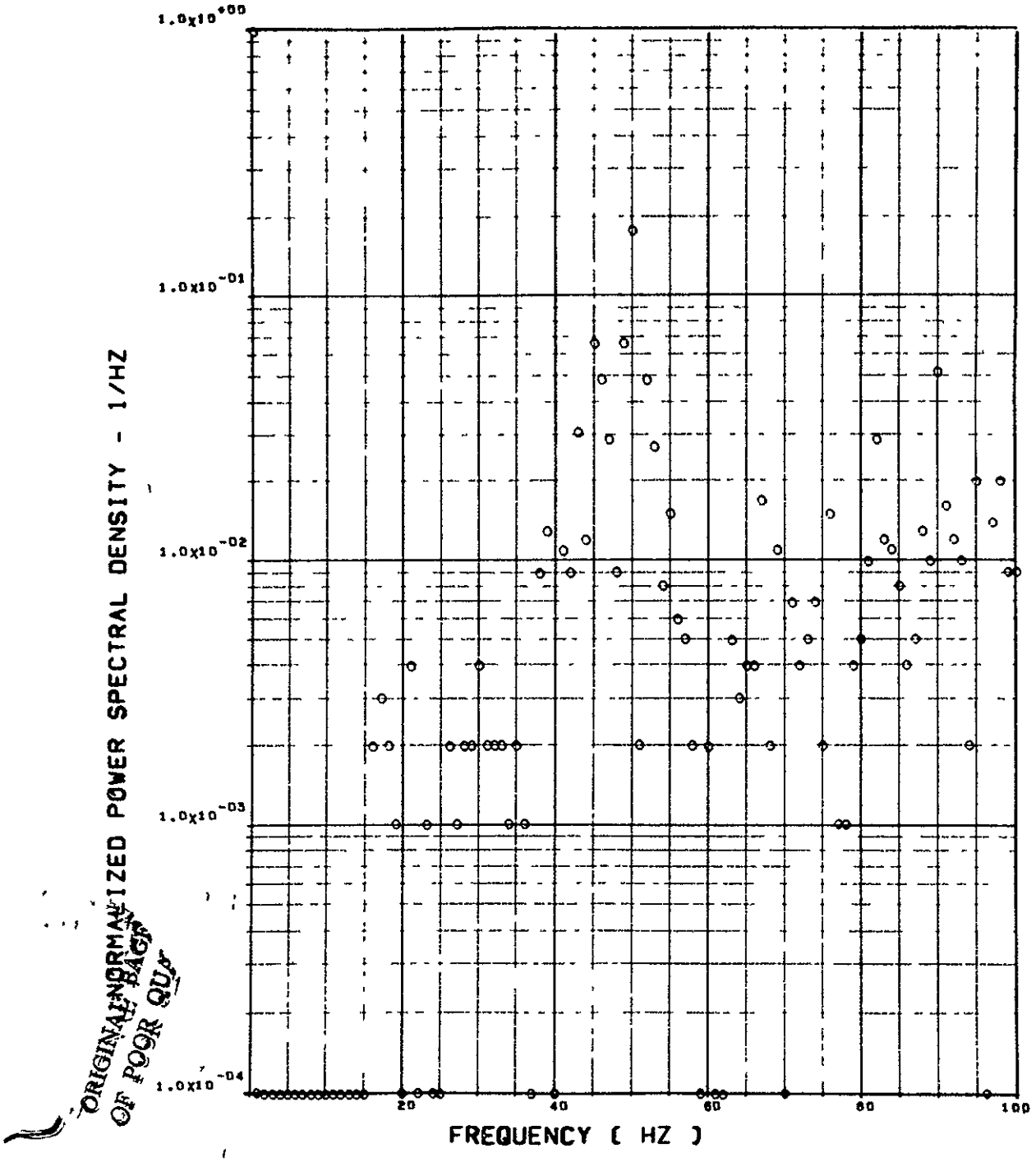

Figure 27. Continued

FLIGHT 48. FRAME 134436.20. RECORD LENGTH = 1 SEC

SCALE FACTOR = .222-2 (G)**2

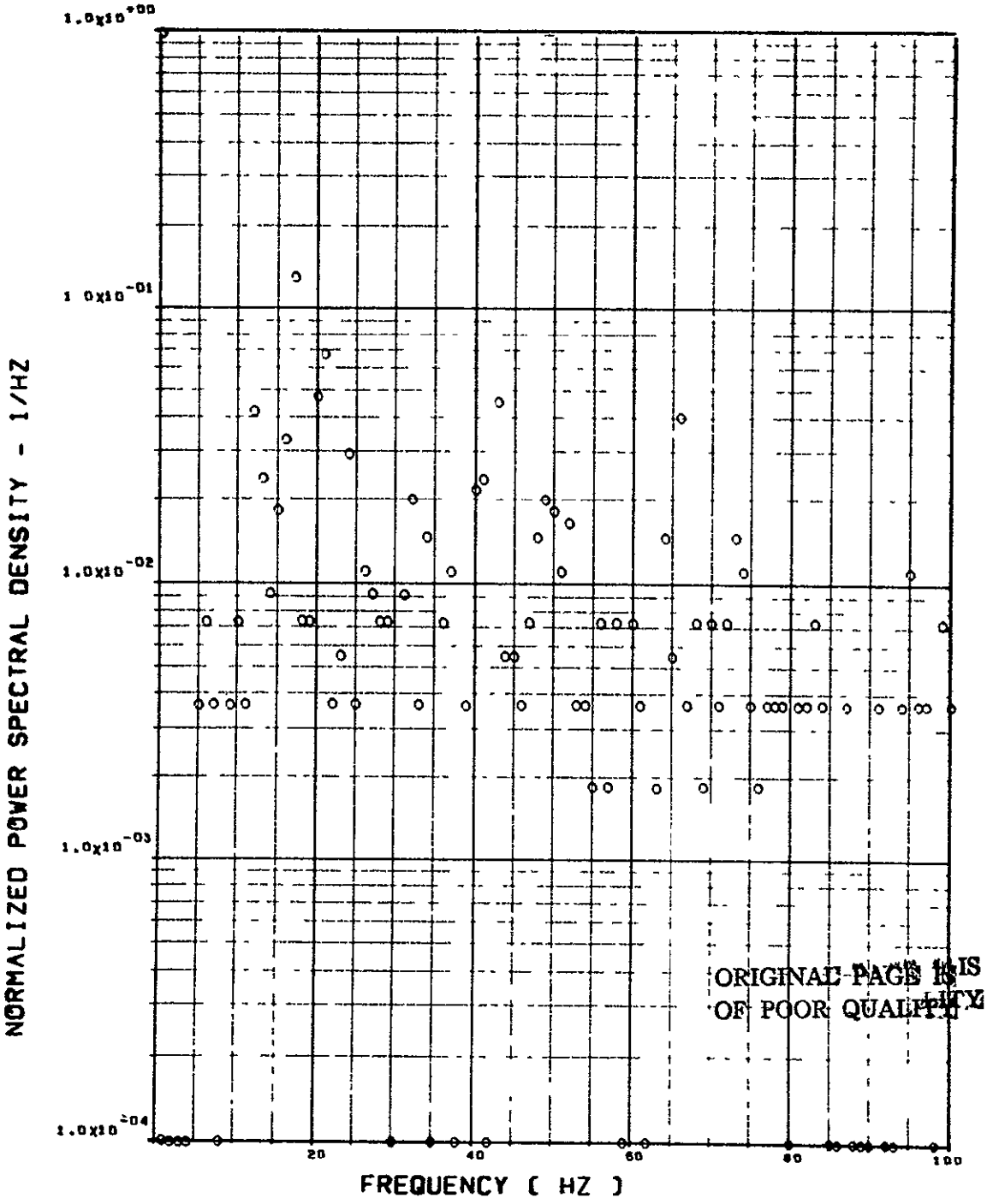

ITEM - AF009 PILOT'S SEAT VERTICAL ACCELEROMETER

Figure 2/. Continued

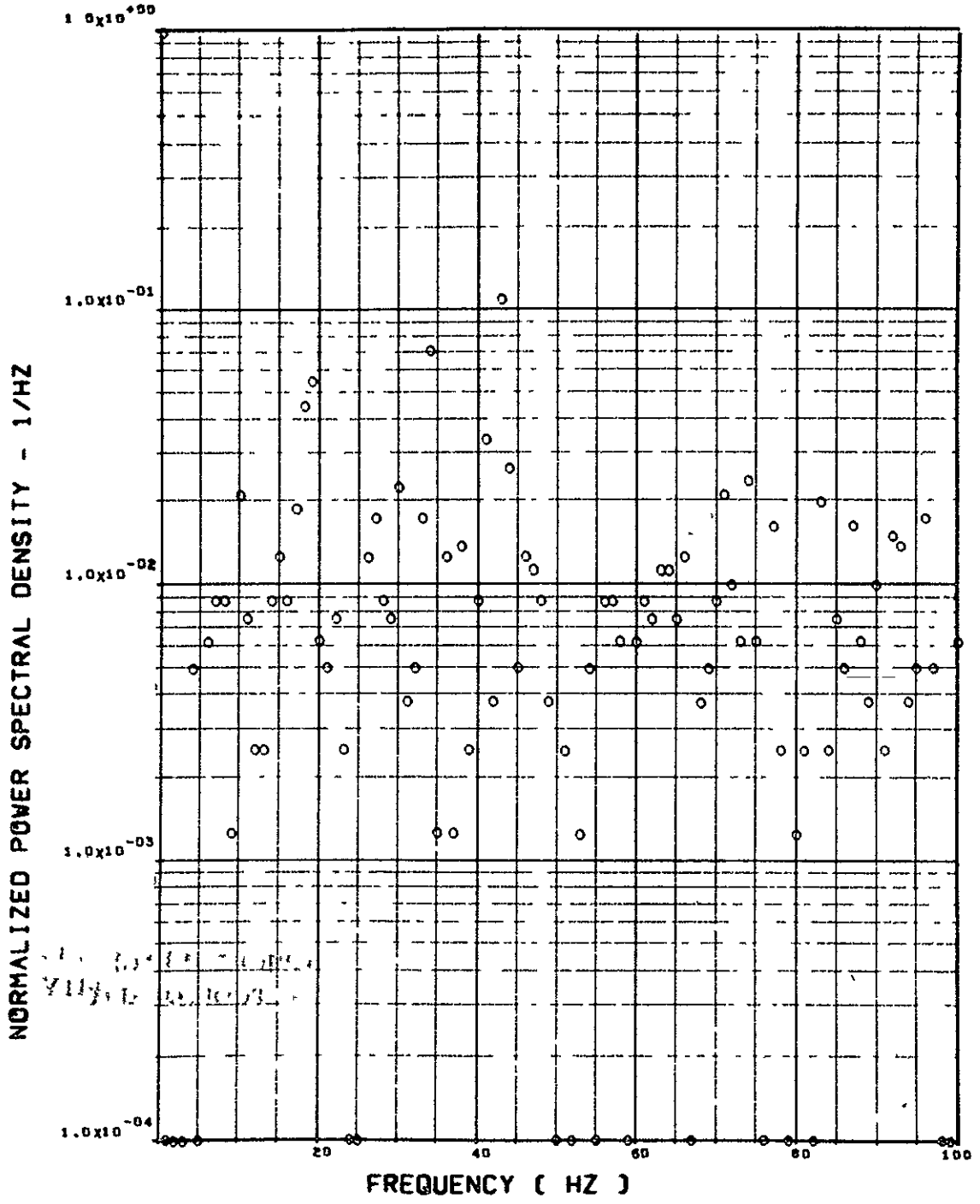

Figure 27. Continued

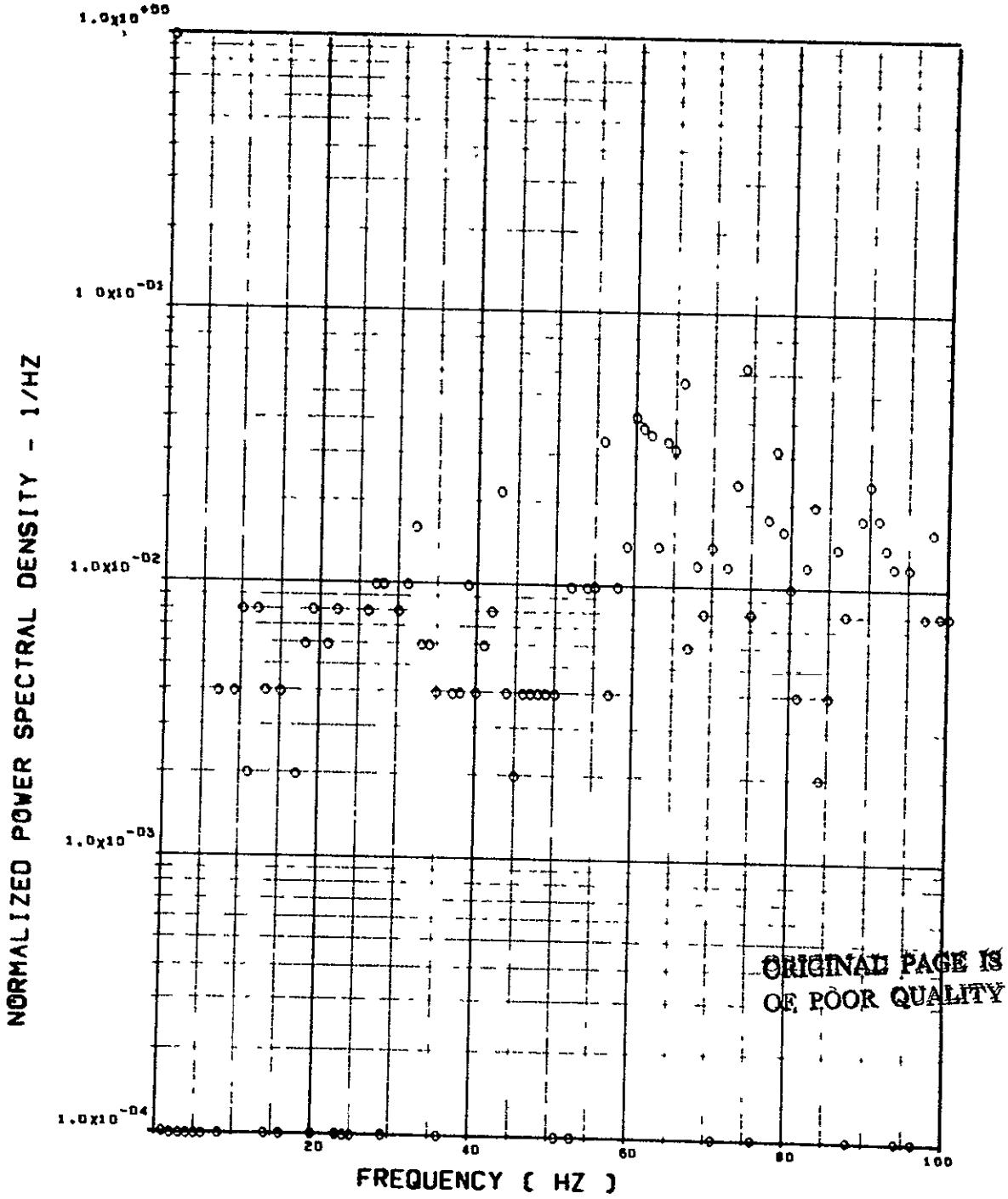

Figure 27. Continued

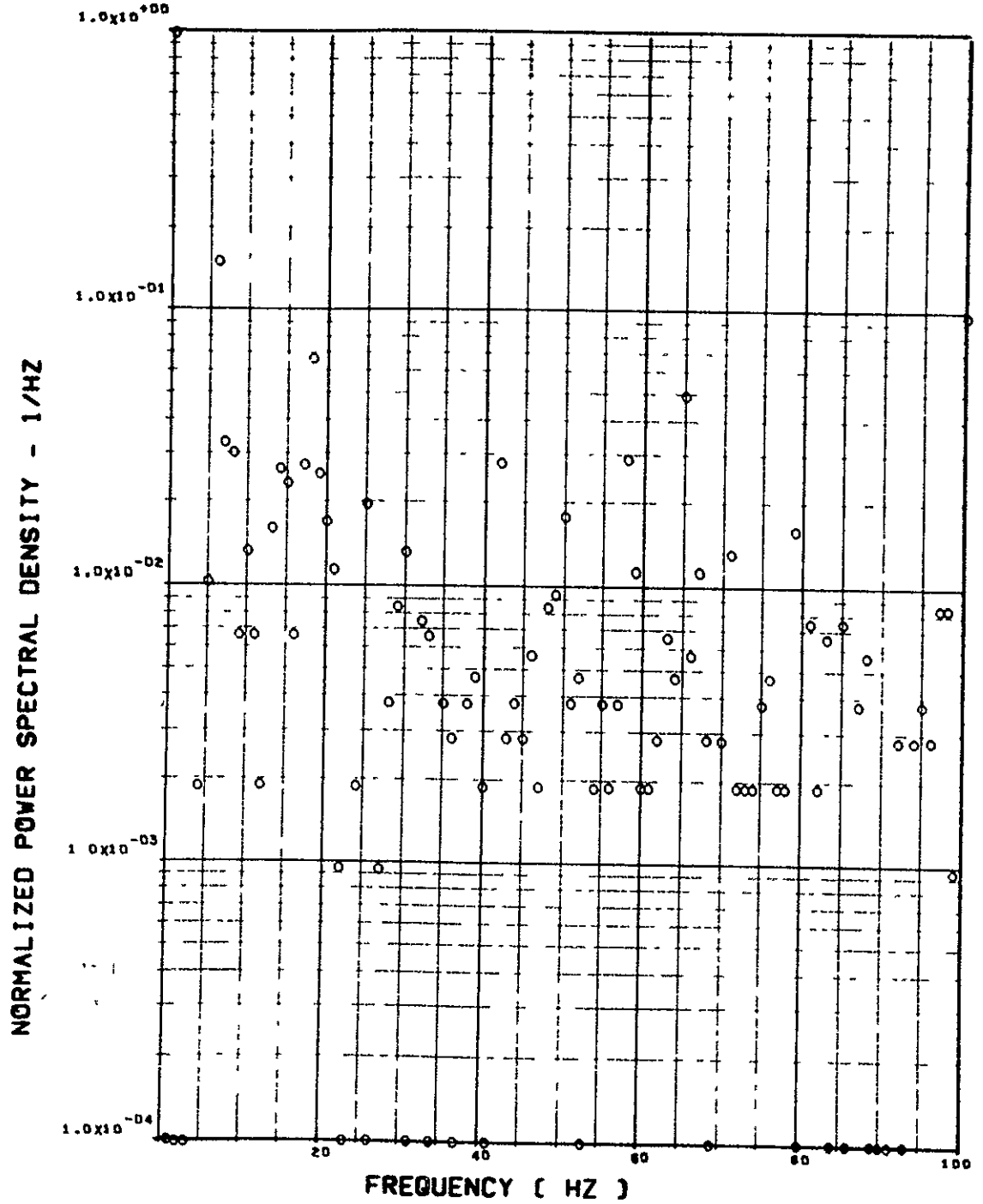

Figure 27. Continued

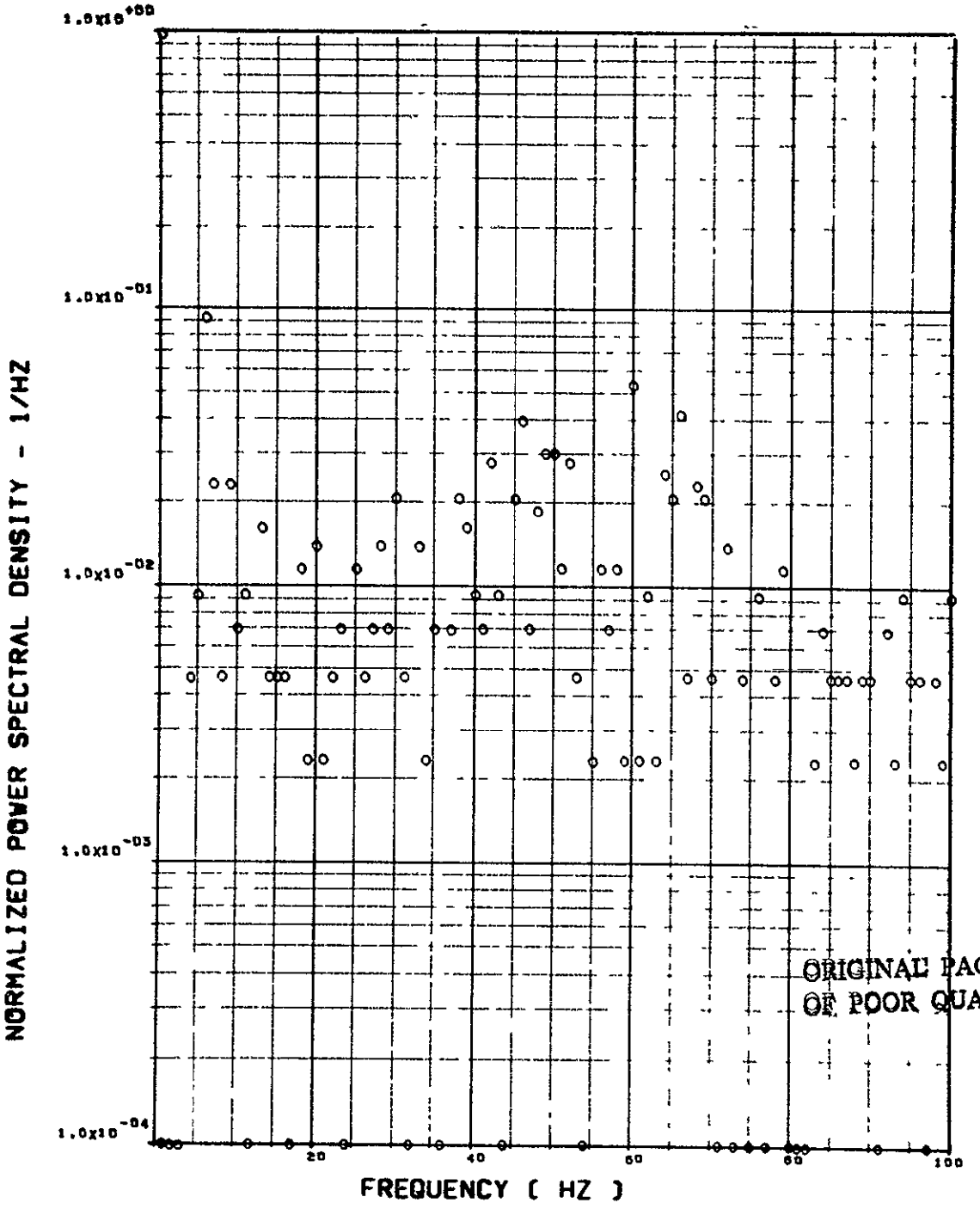

Figure 27. Continued

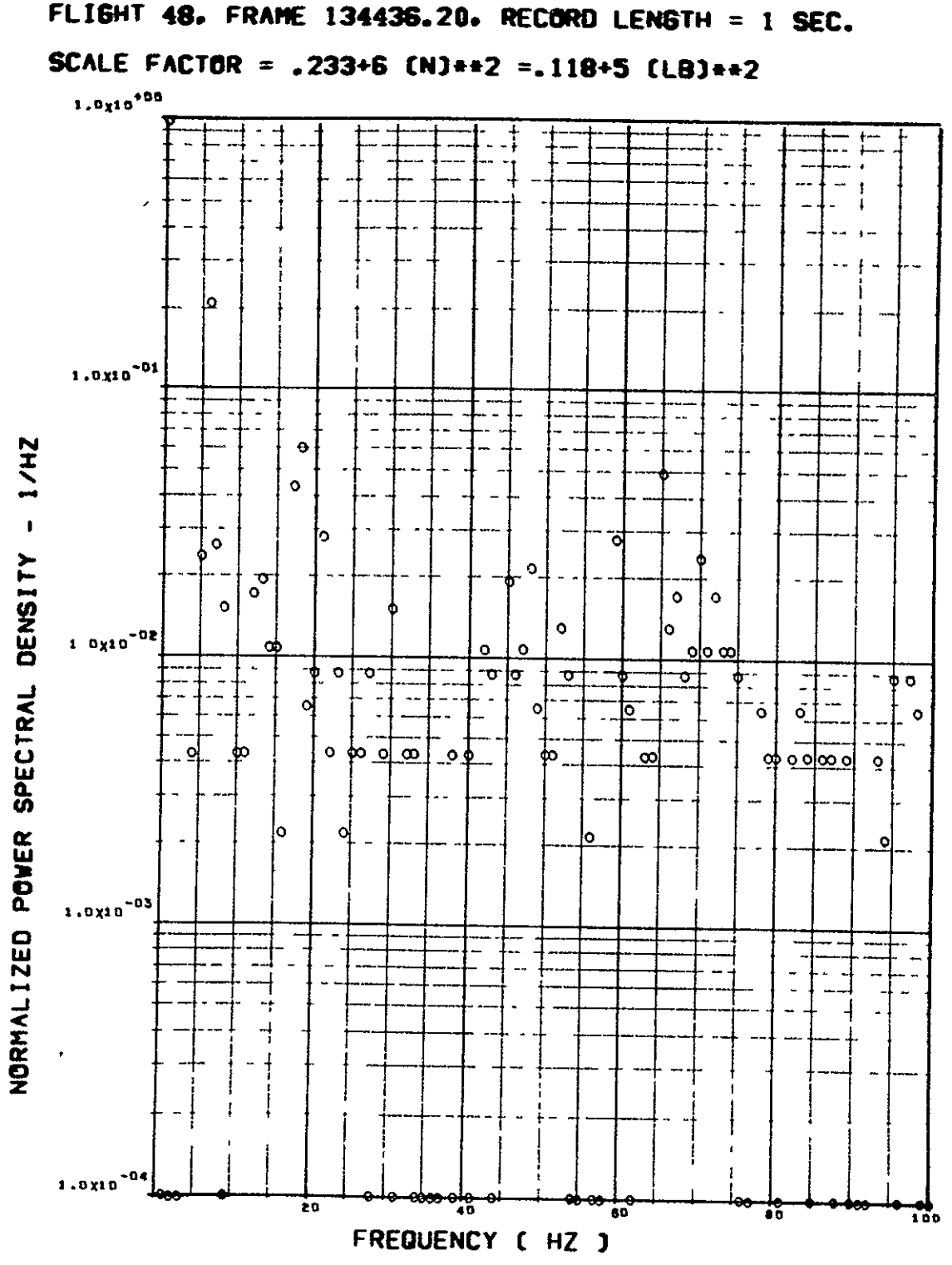

Figure 27. Continued

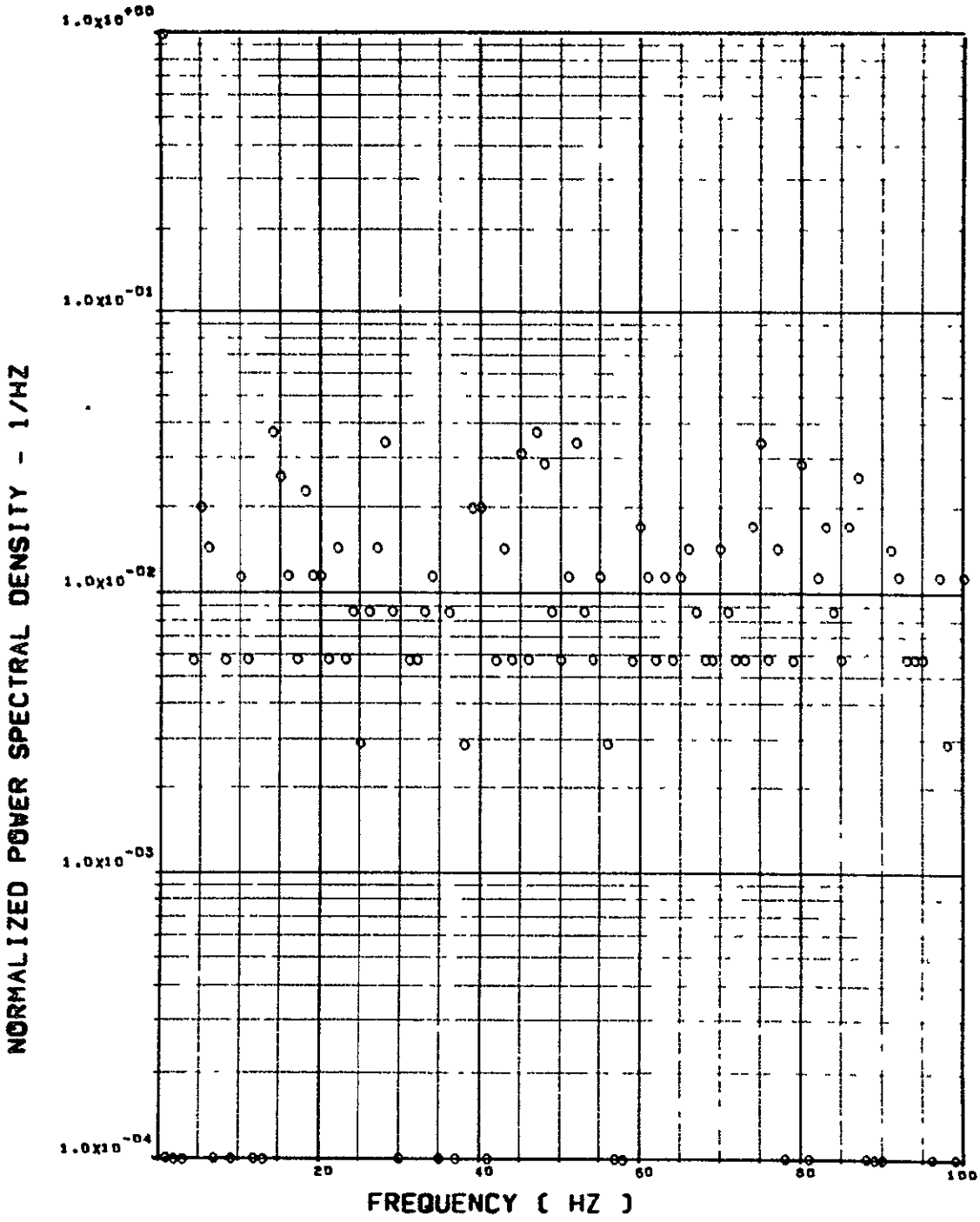

Figure 27. Continued

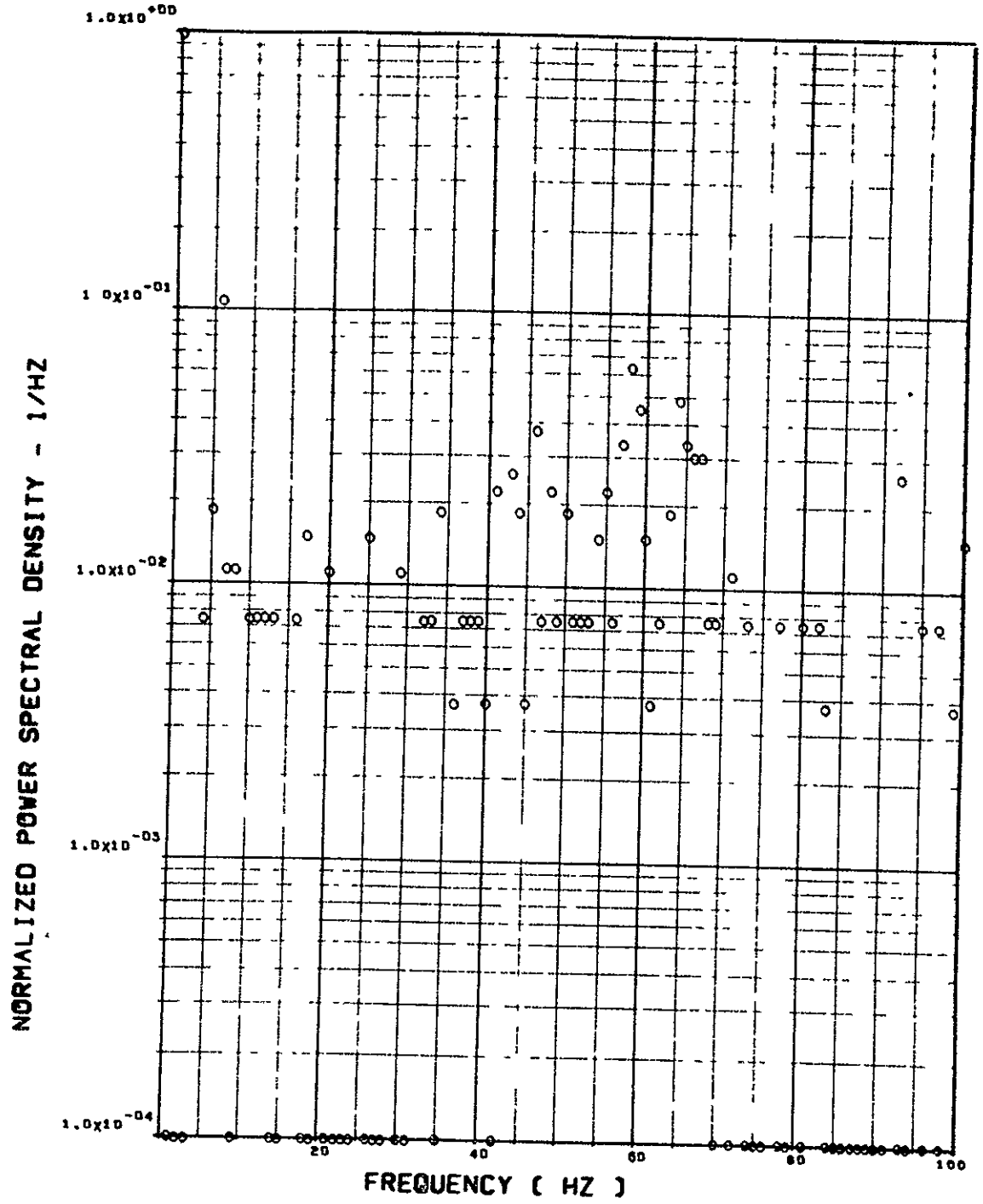

Figure 27. Continued

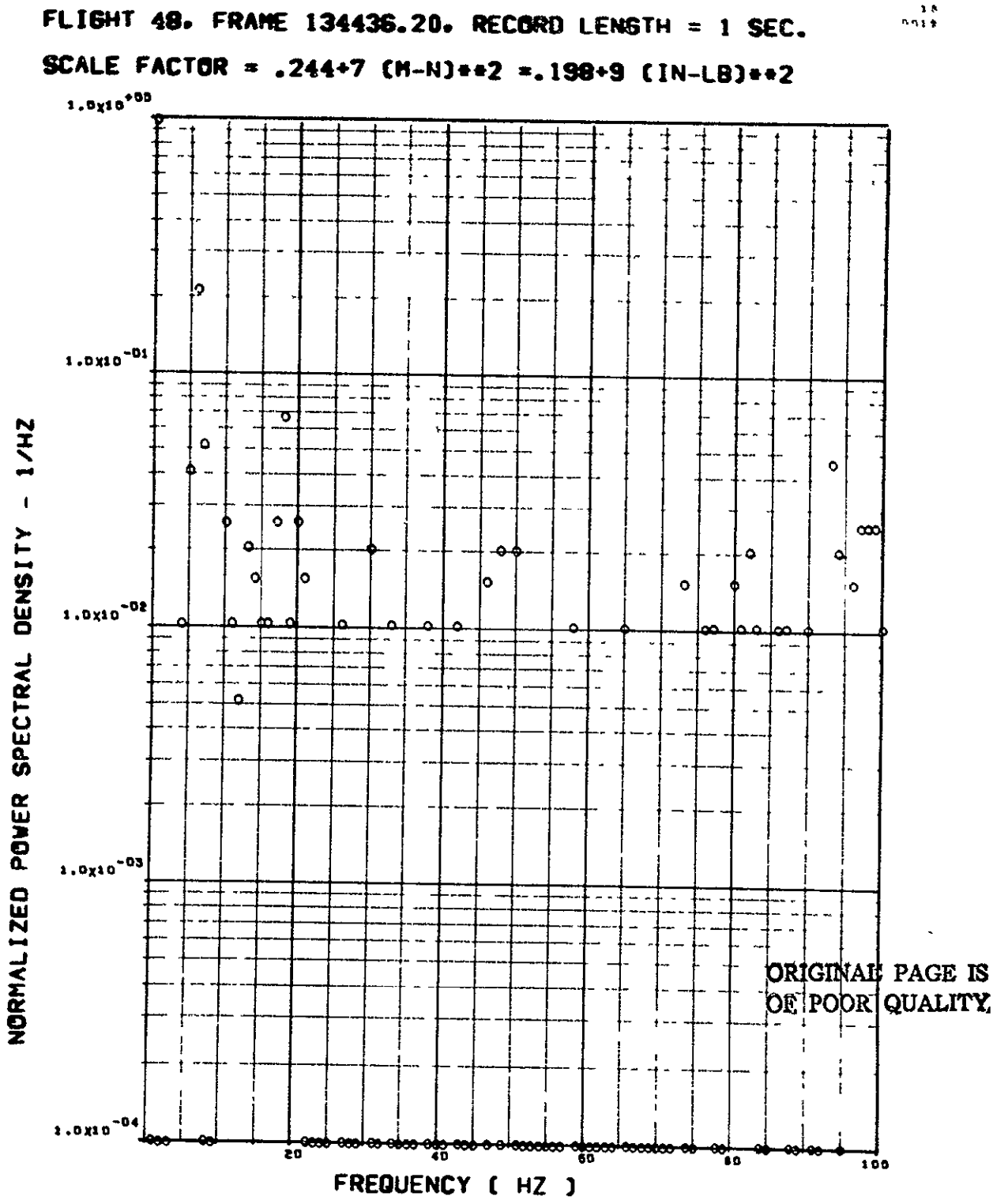

Figure 27. Continued

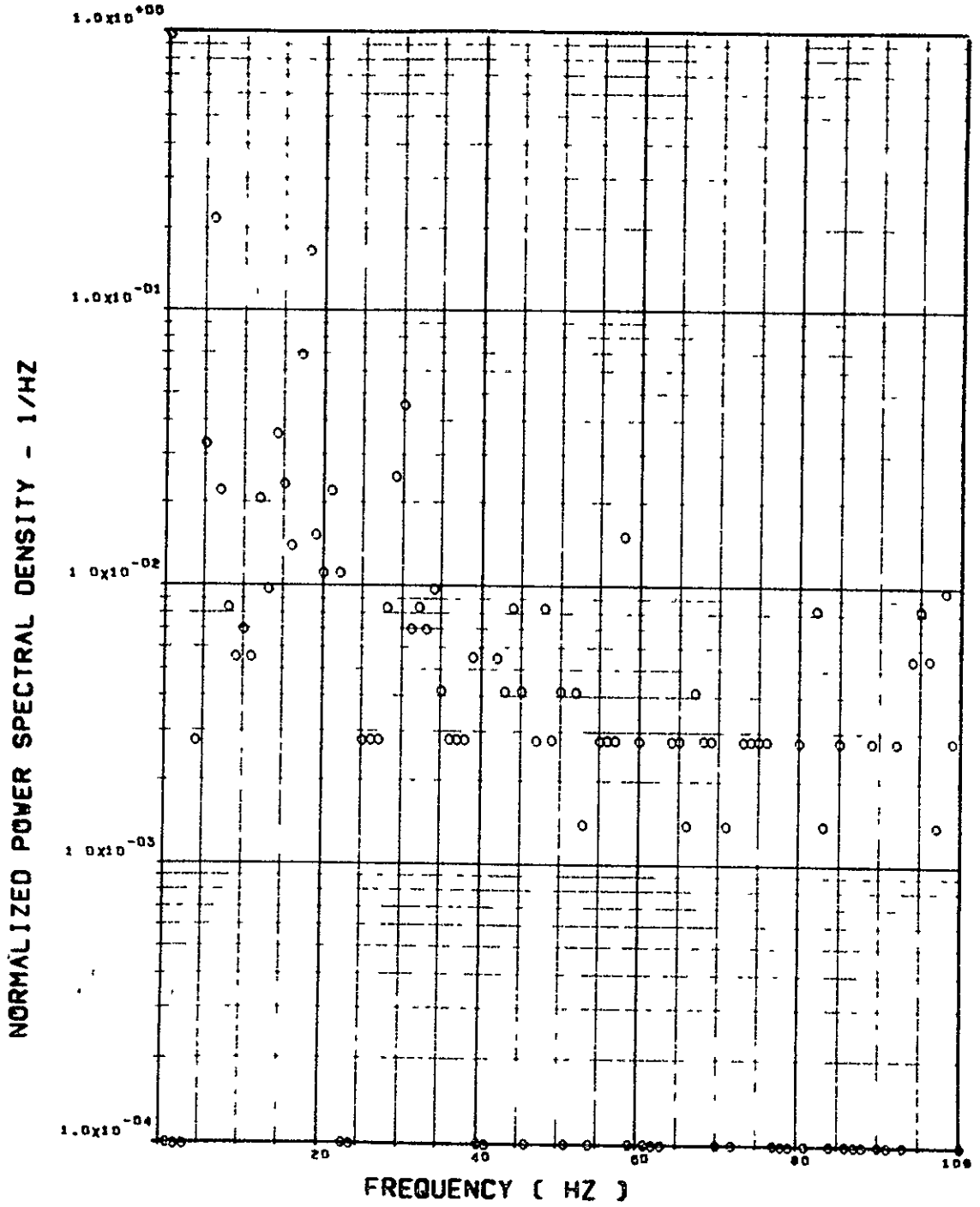

Figure 27. Continued

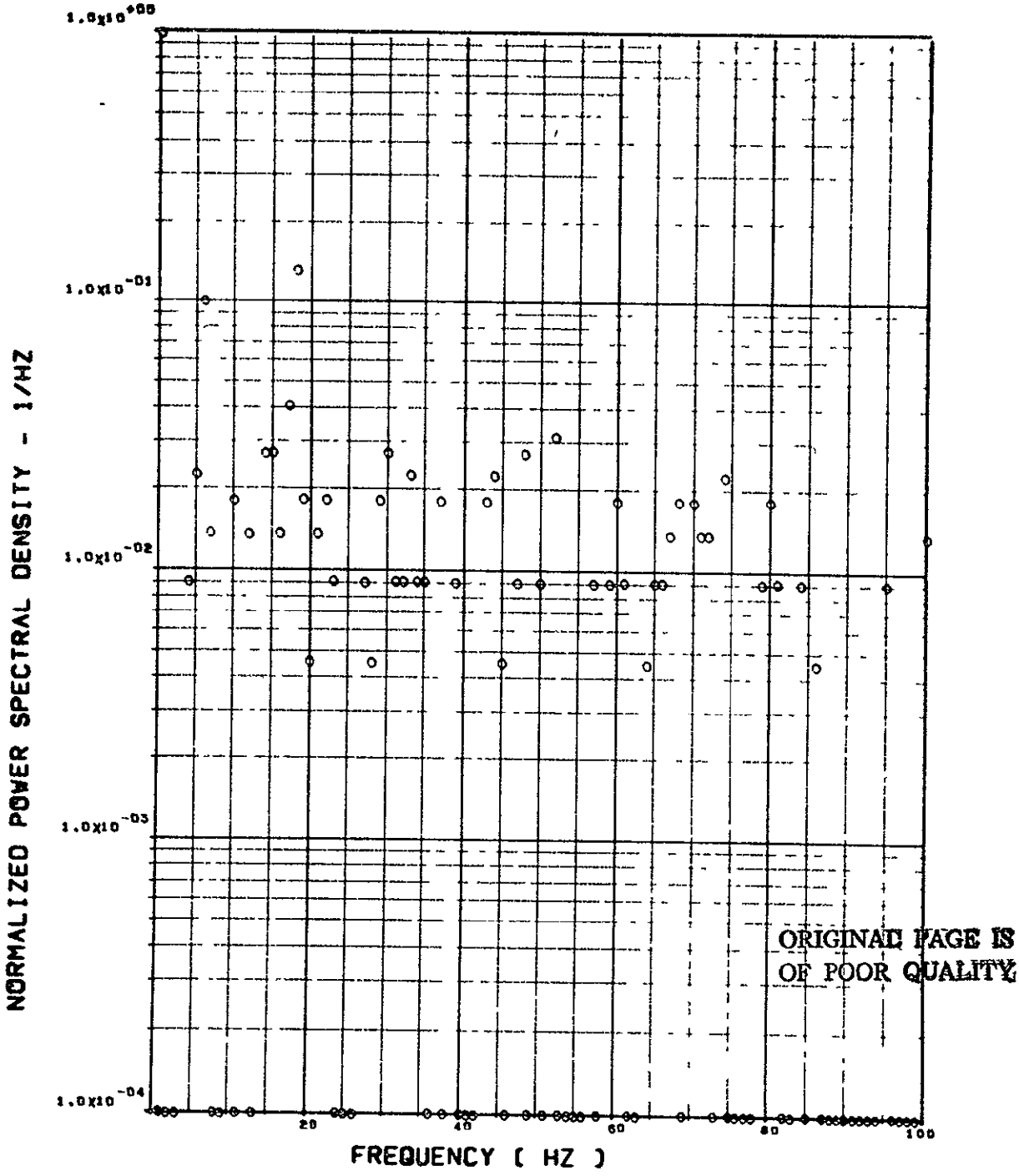

Figure 27. Continued

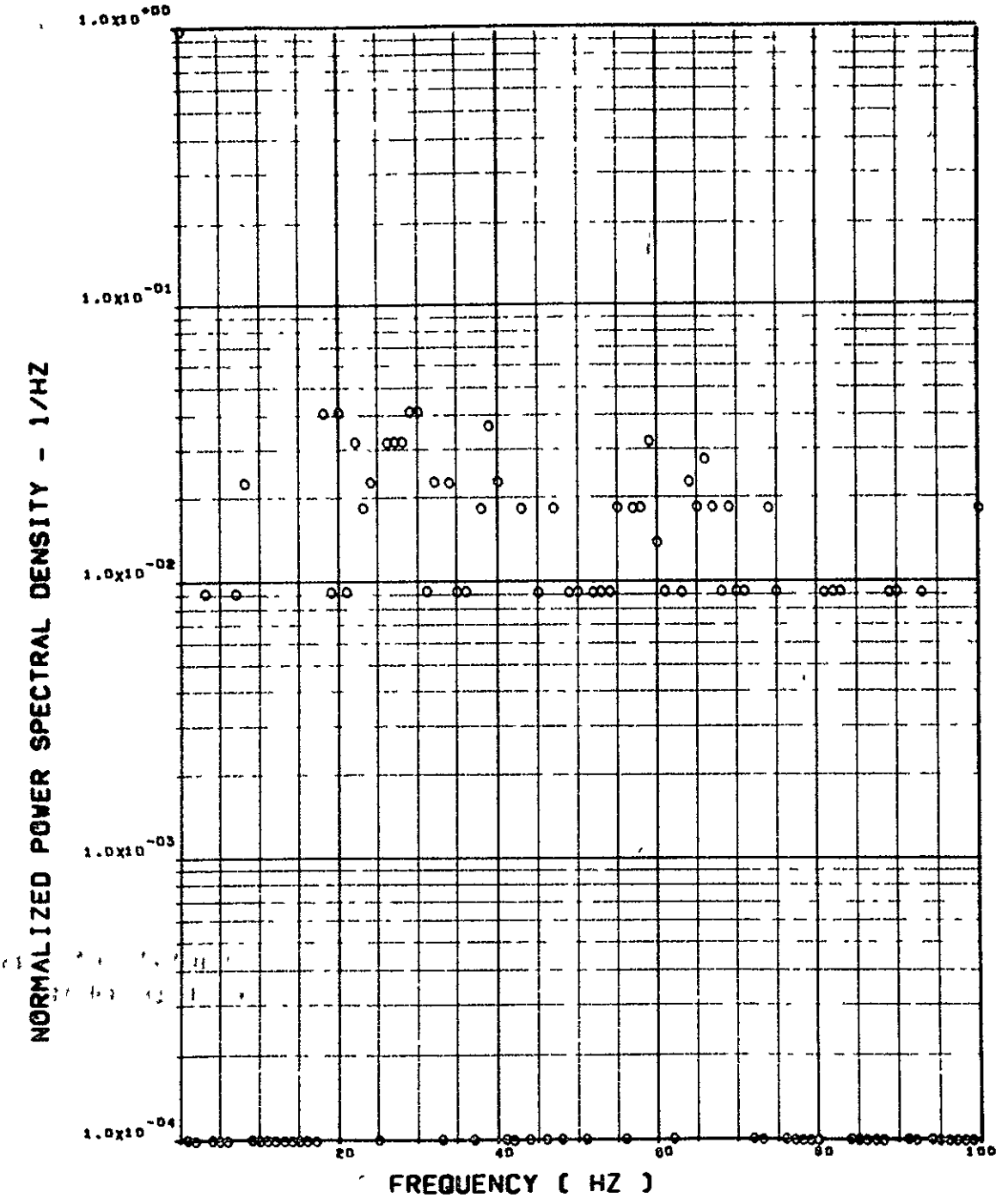

Figure 27. Continued

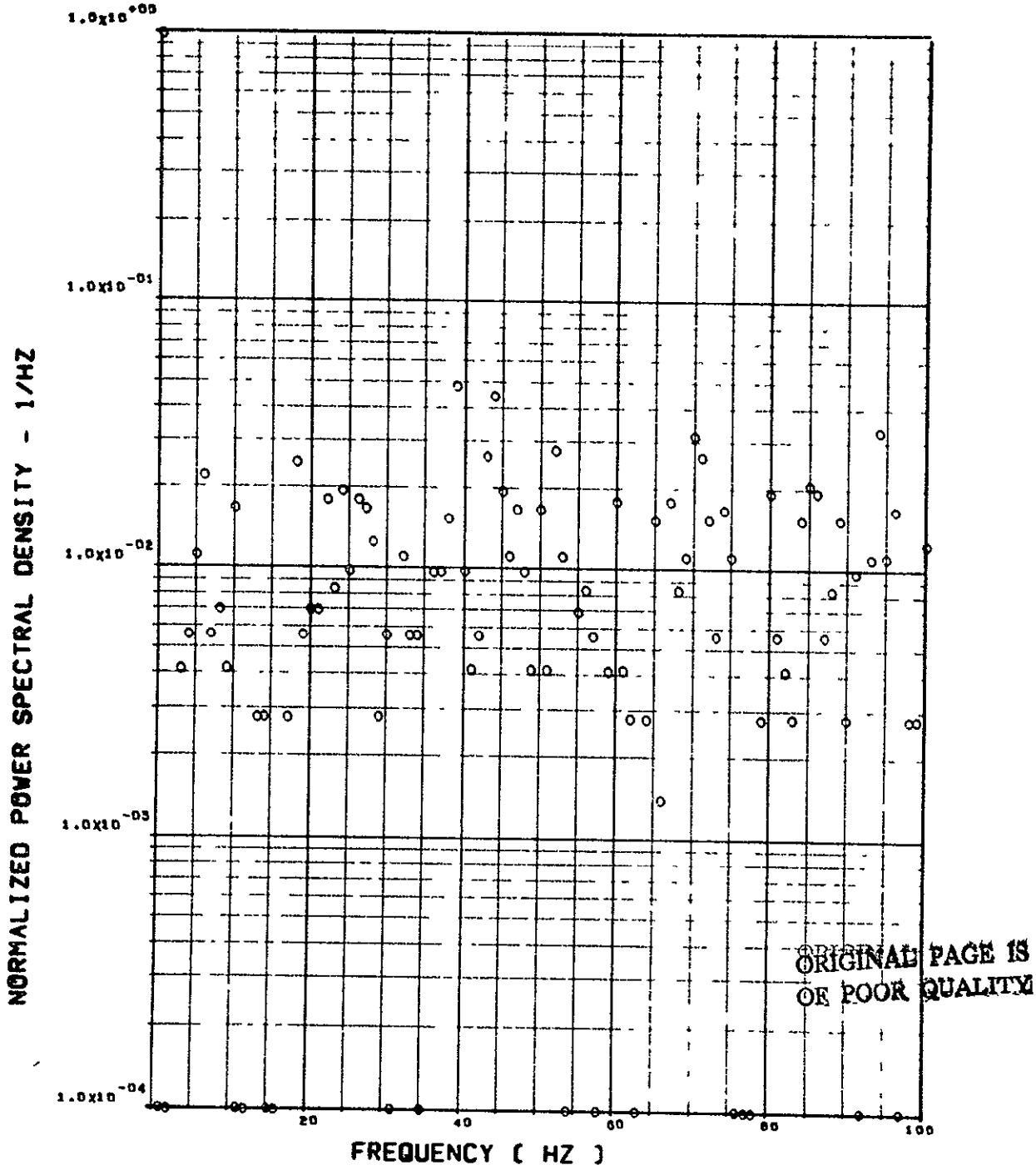

Figure 27. Continued

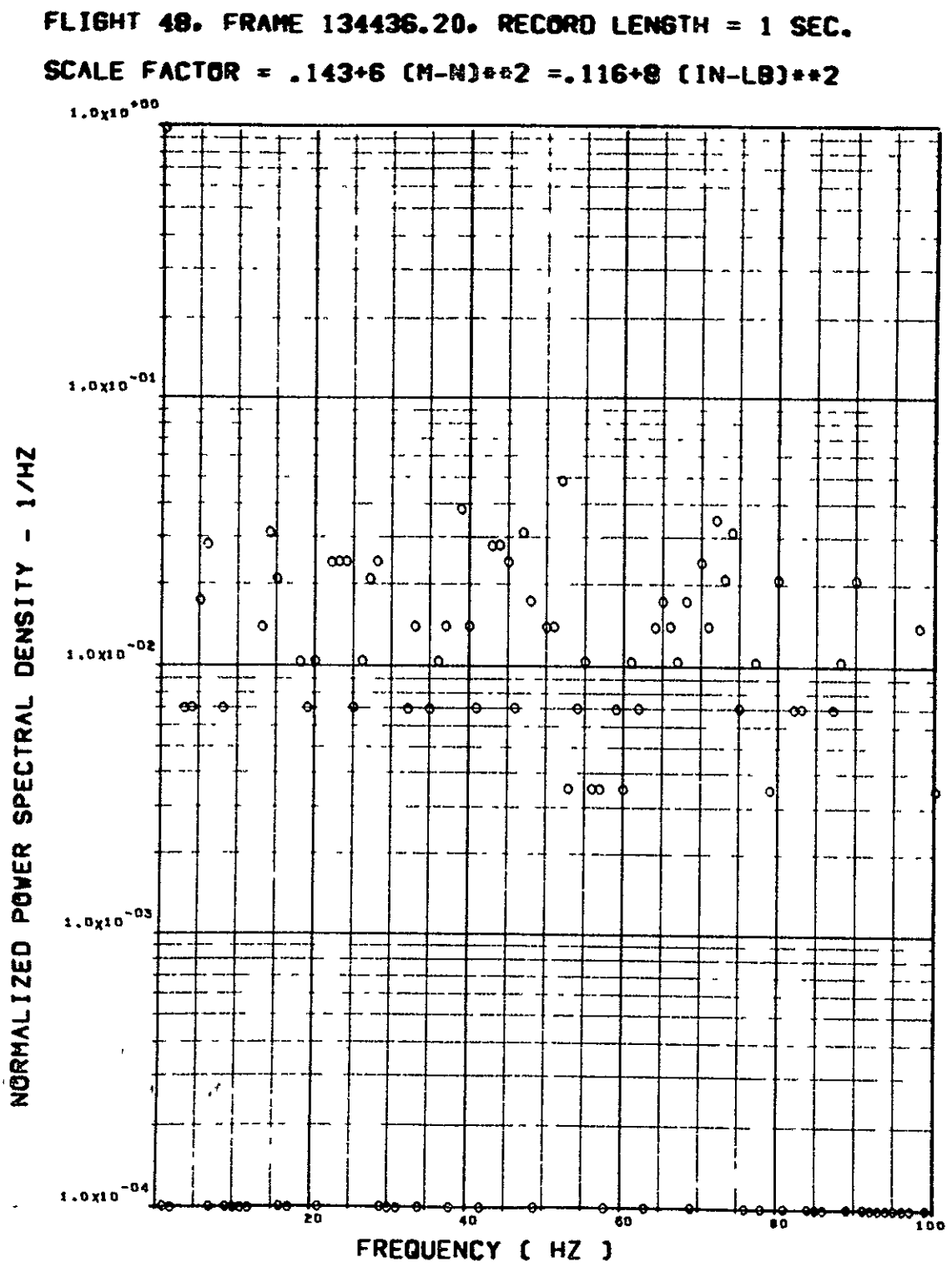

Figure 27. Continued

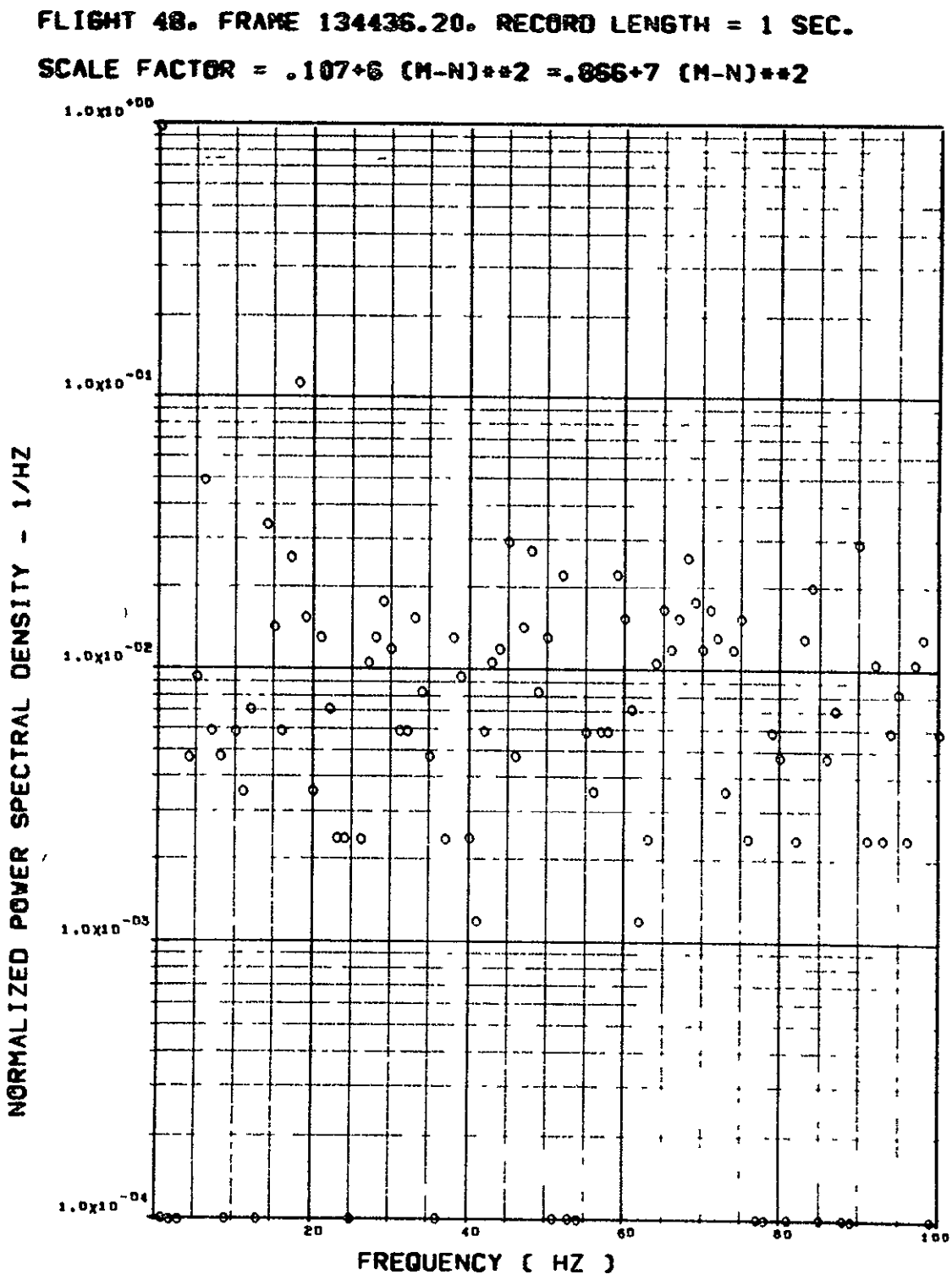

Figure 27. Continued

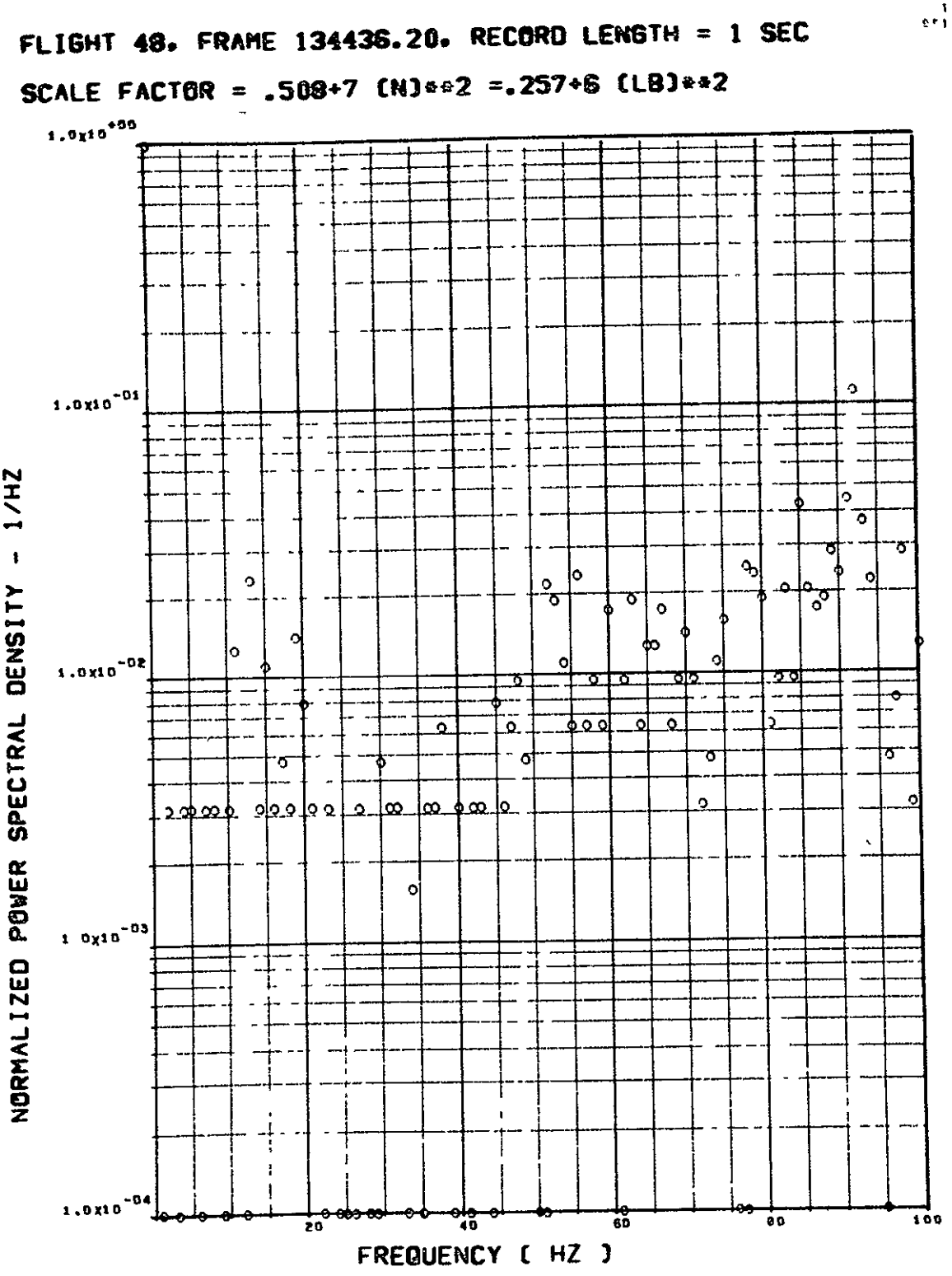

Figure 27. Continued

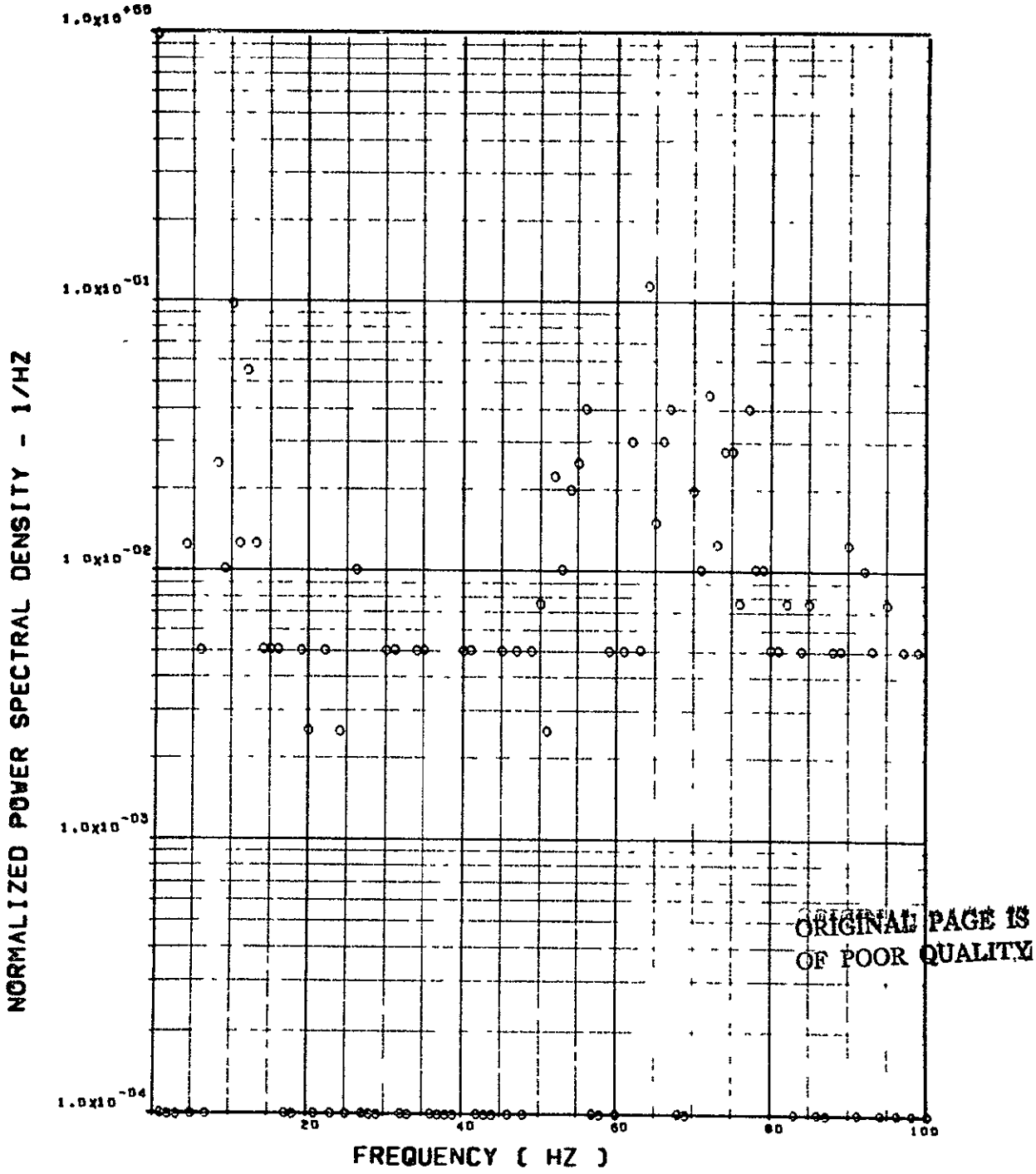

Figure 27. Continued

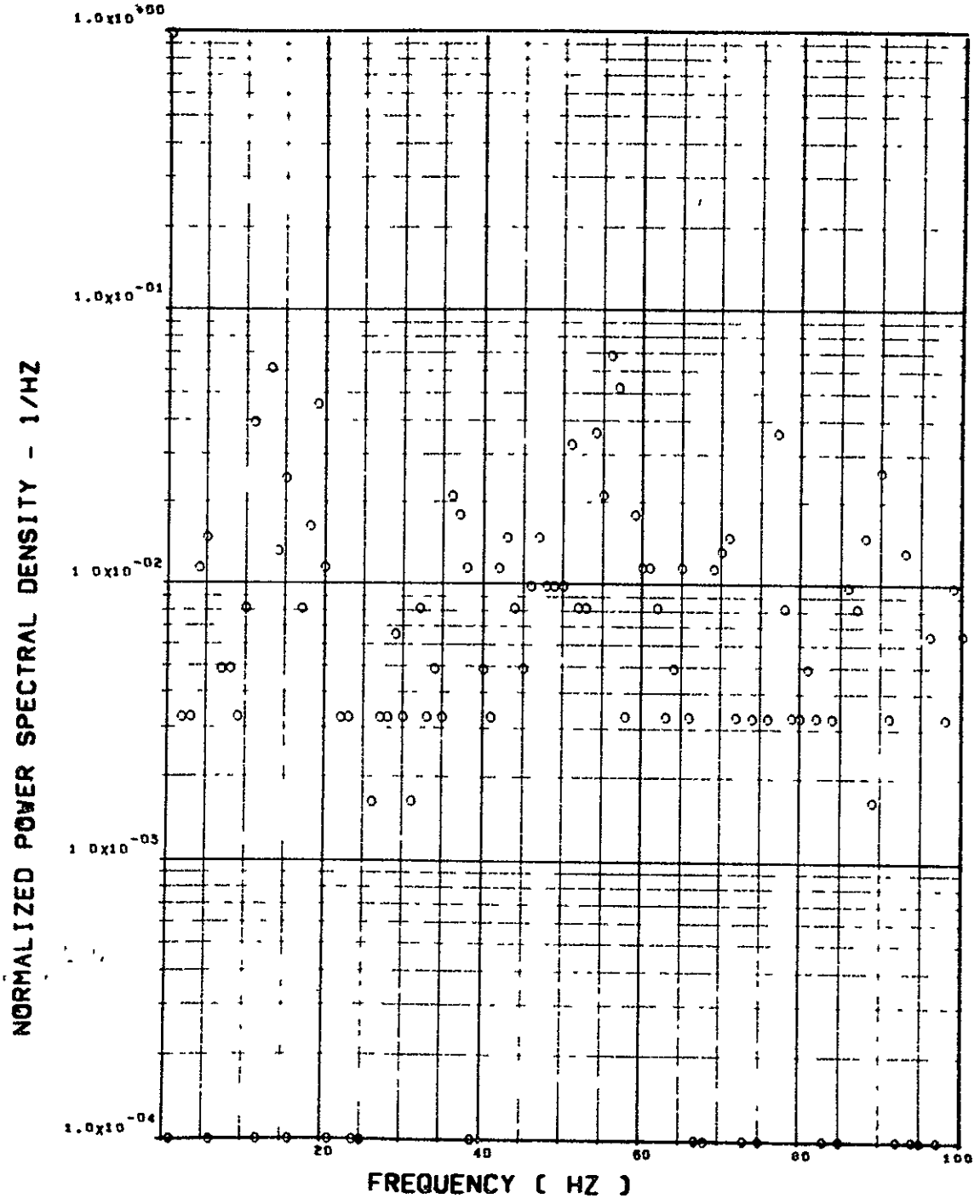

Figure 27. Continued

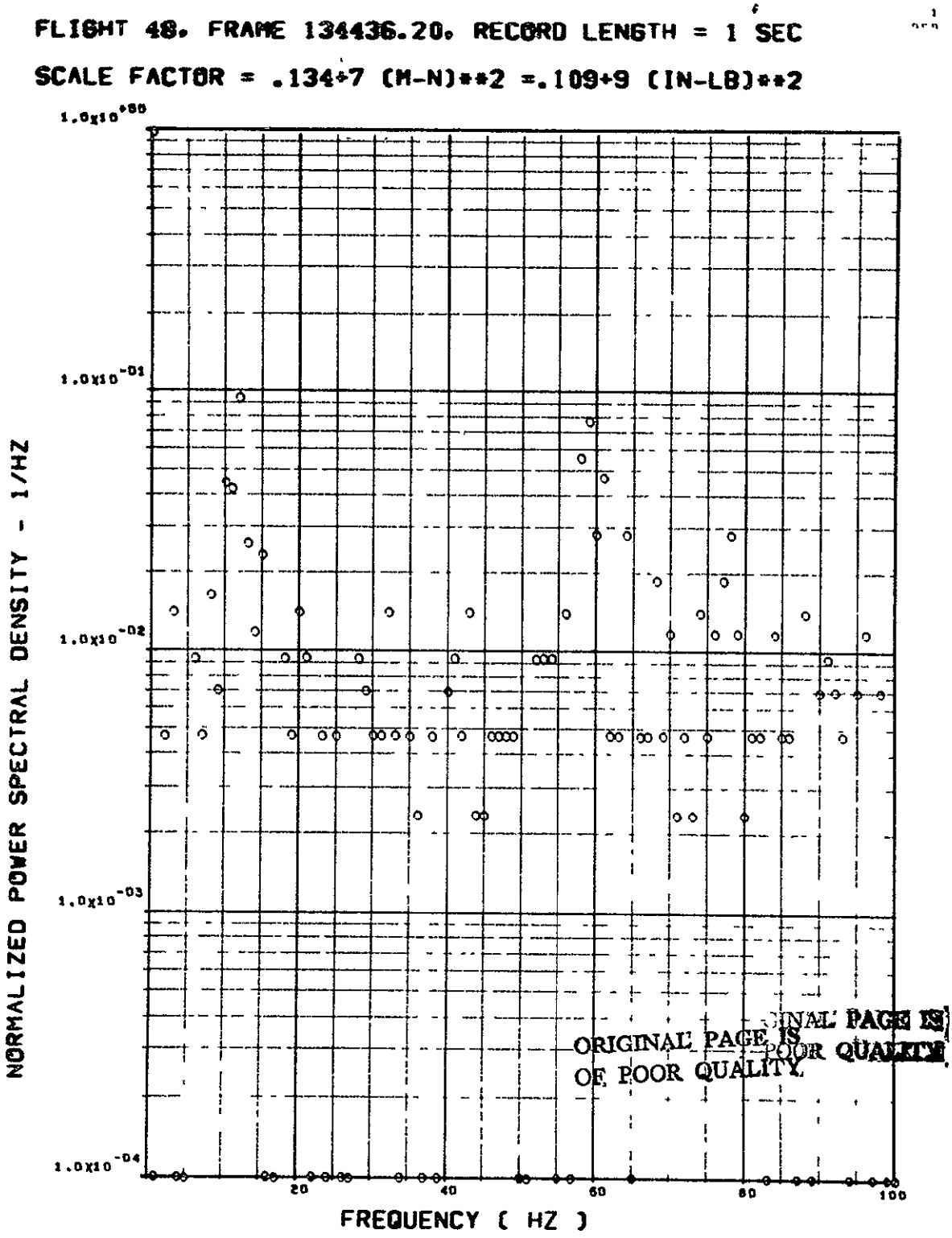

Figure 27. Continued

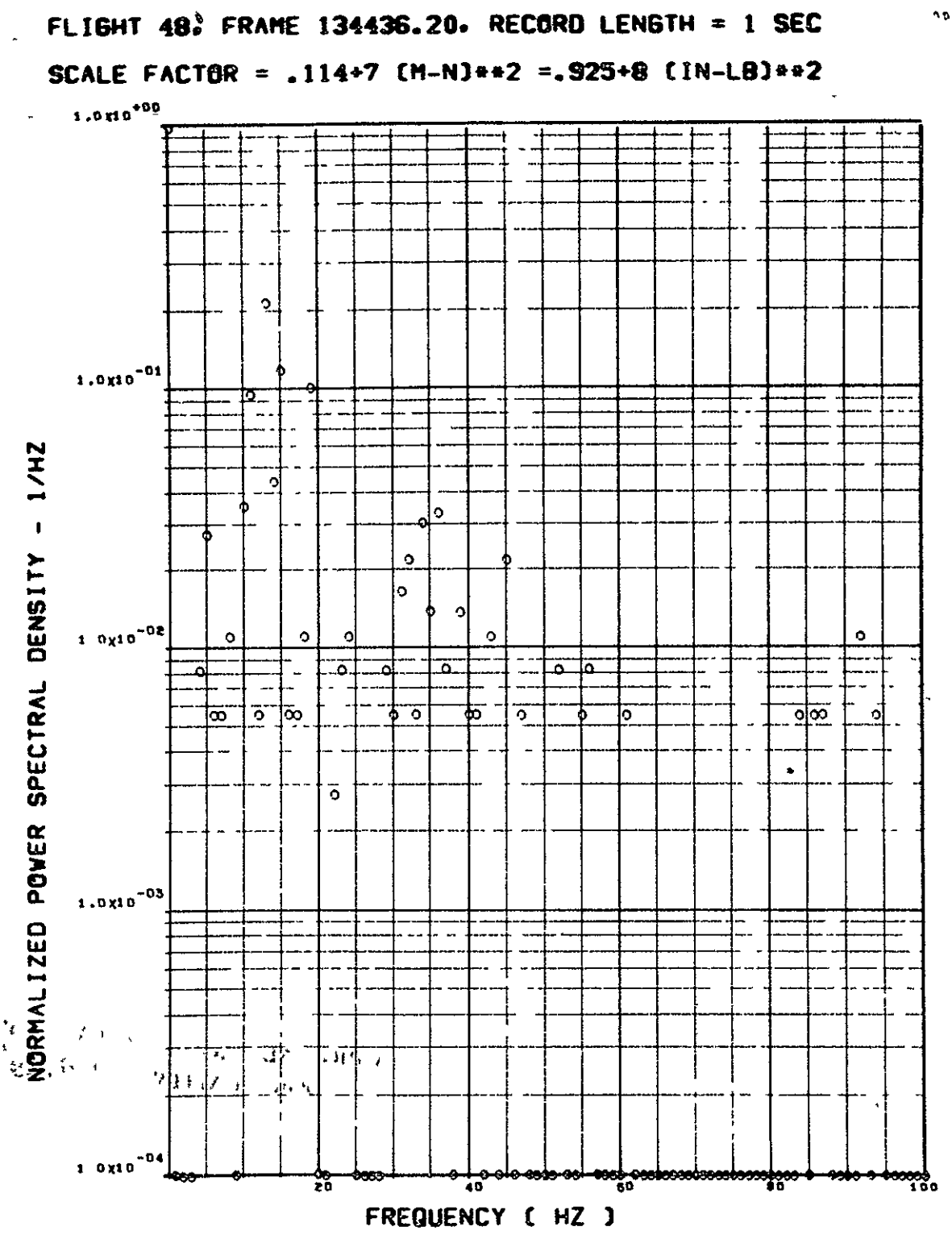

Figure 27. Continued

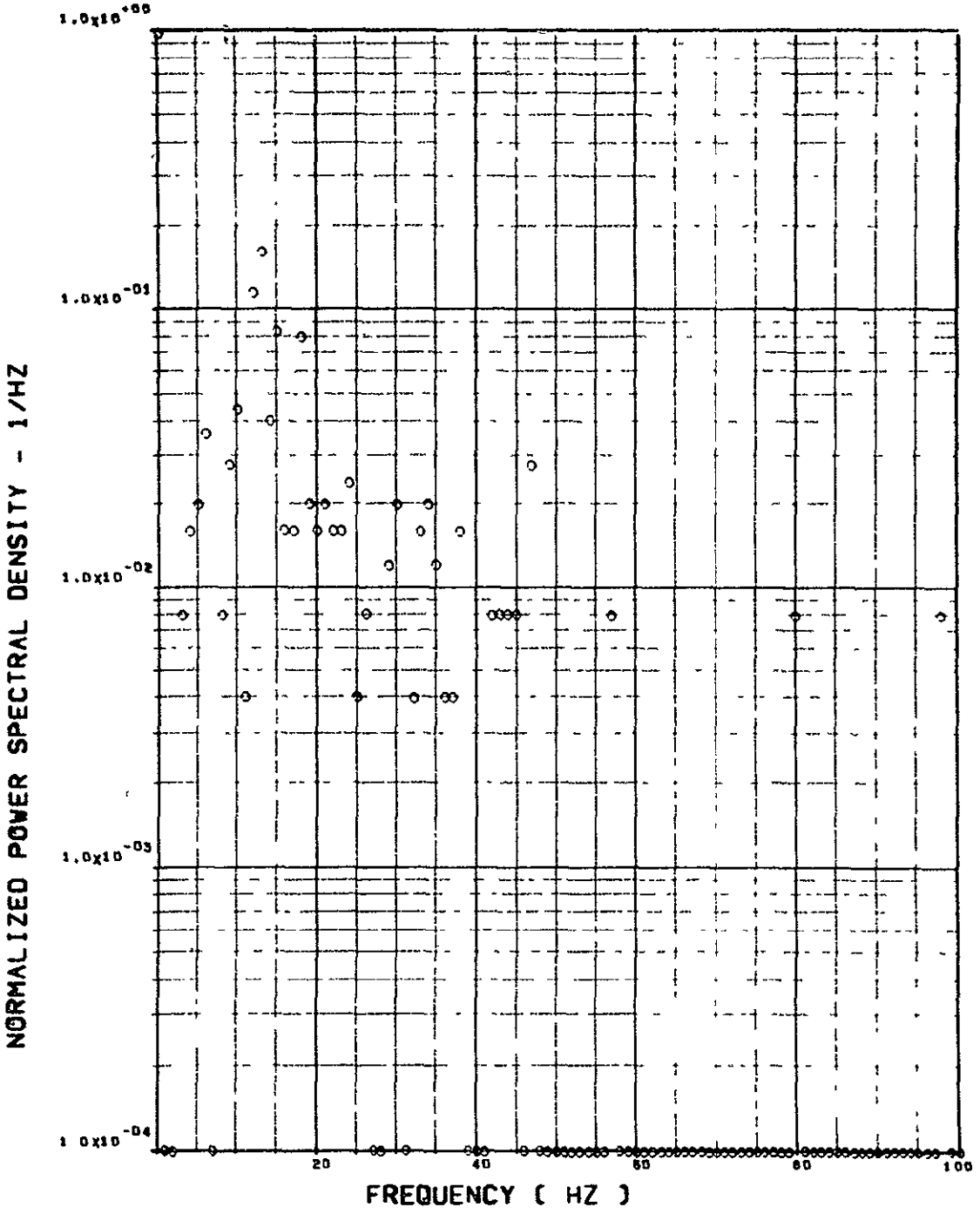

Figure 27. Concluded

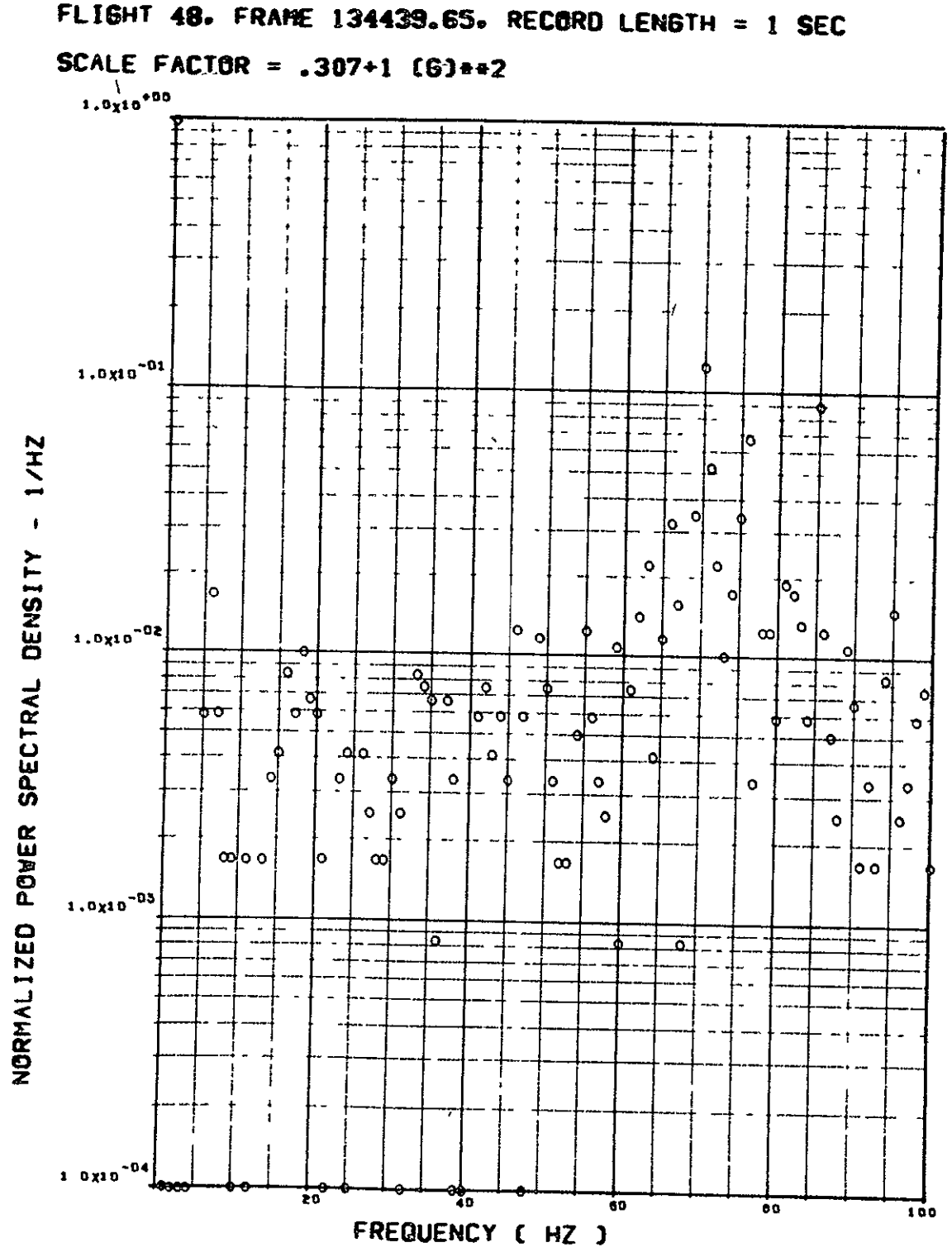

Figure 28. Power Spectra - Flight 48, Run 5, Point 4
T_1 = 134439.65, ΔT = 1 Sec, α_{Nom} = 15.95 deg,
$\Delta\alpha$= 1.80 deg.

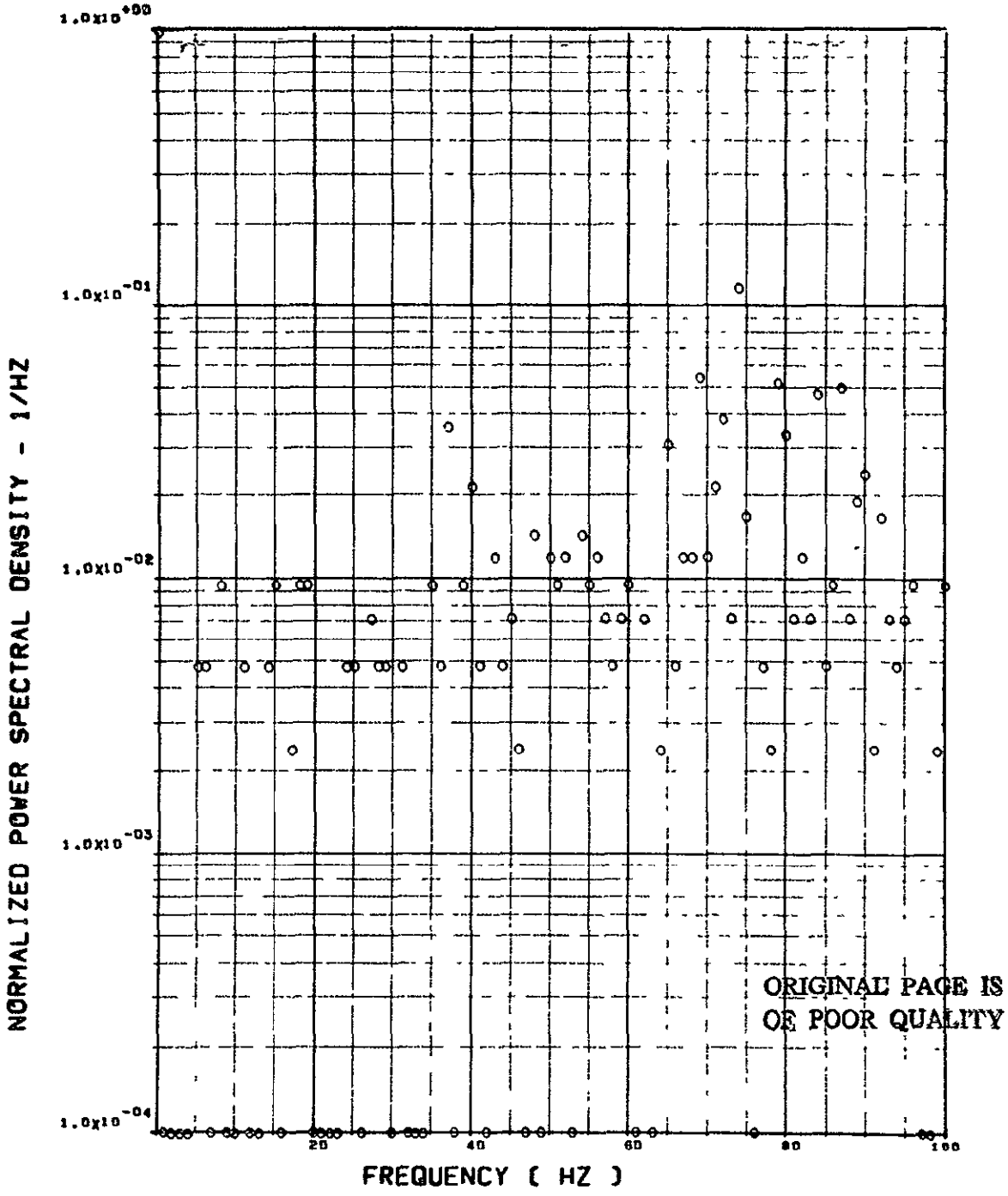

Figure 28. Continued

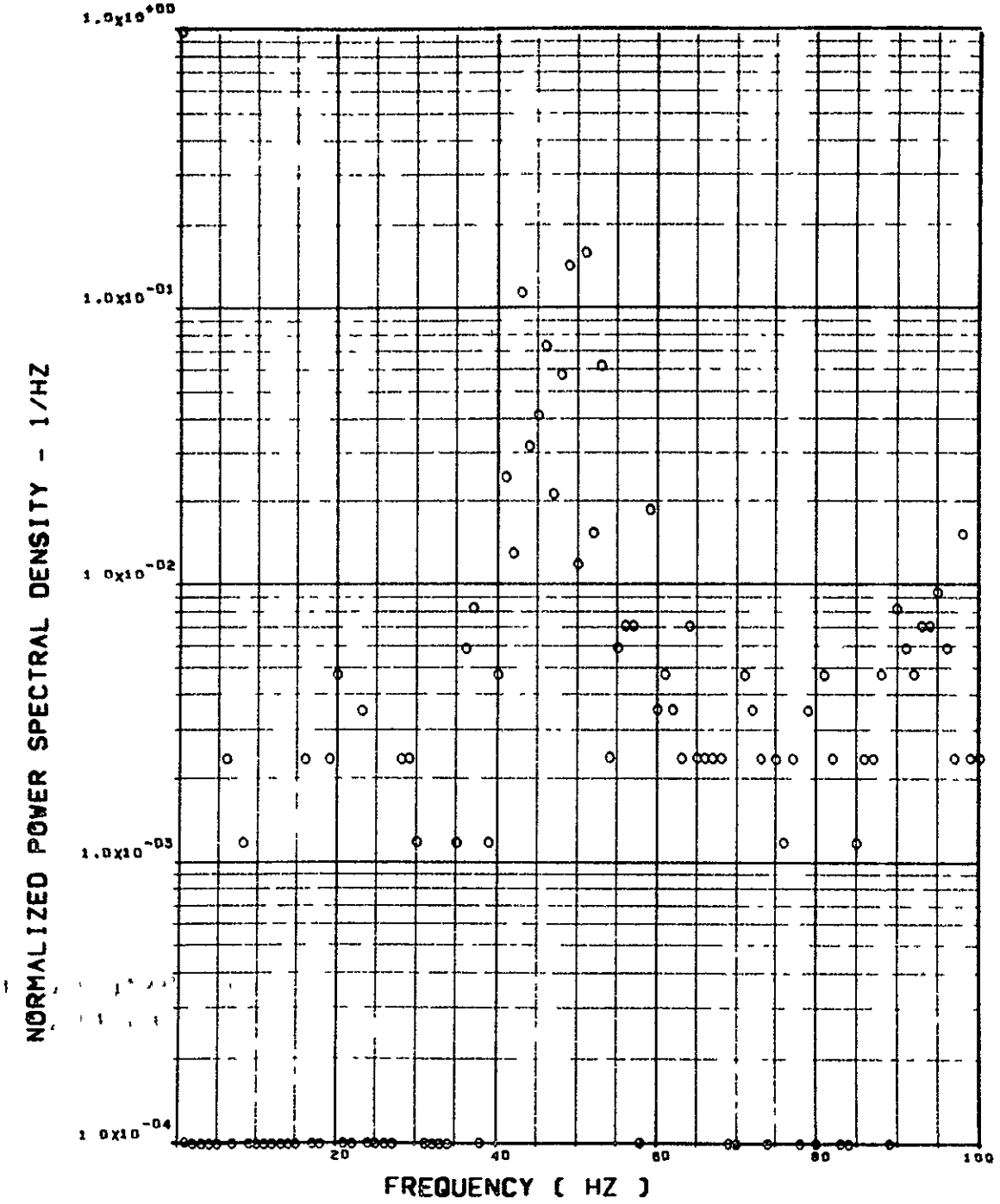

Figure 28. Continued

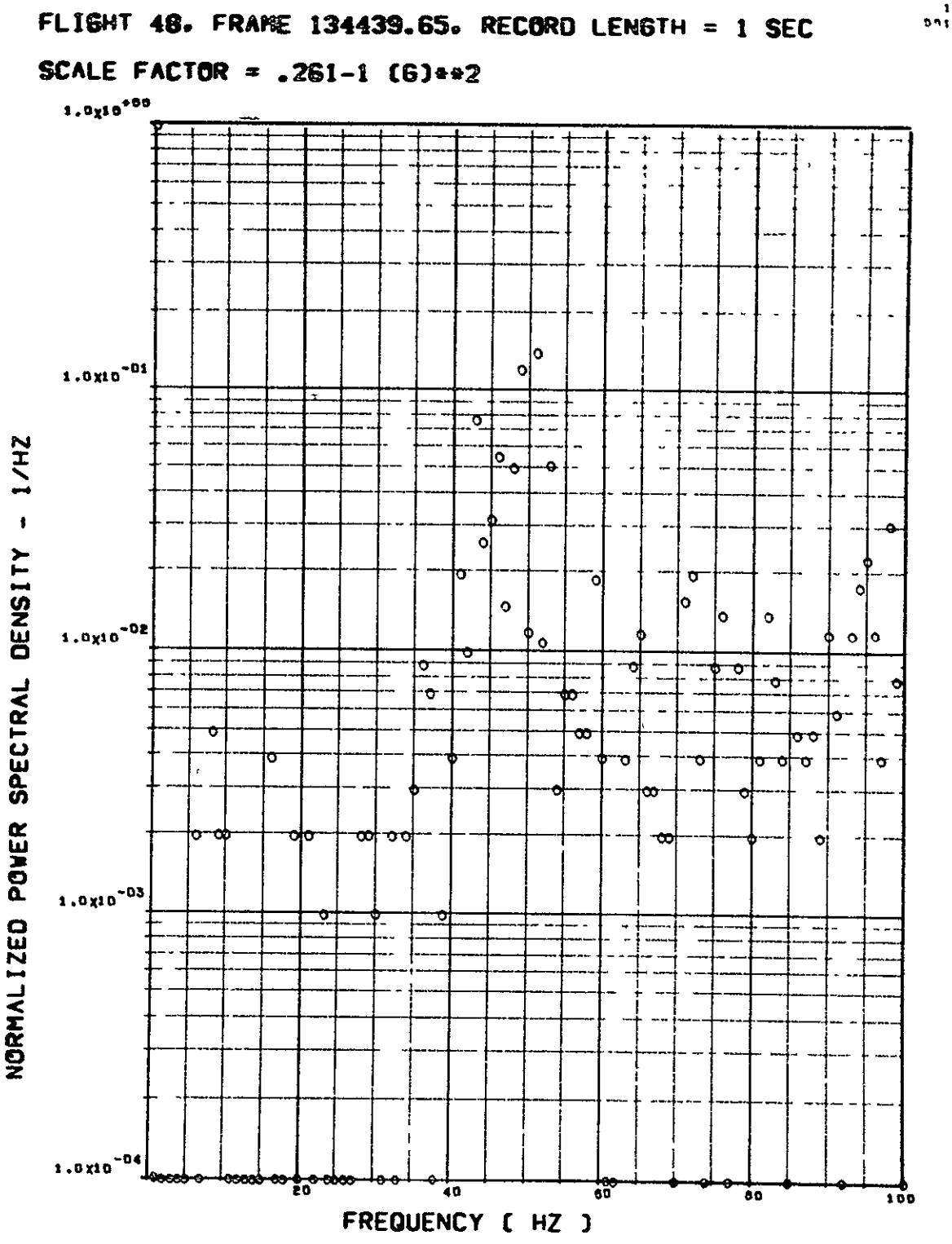

Figure 28. Continued

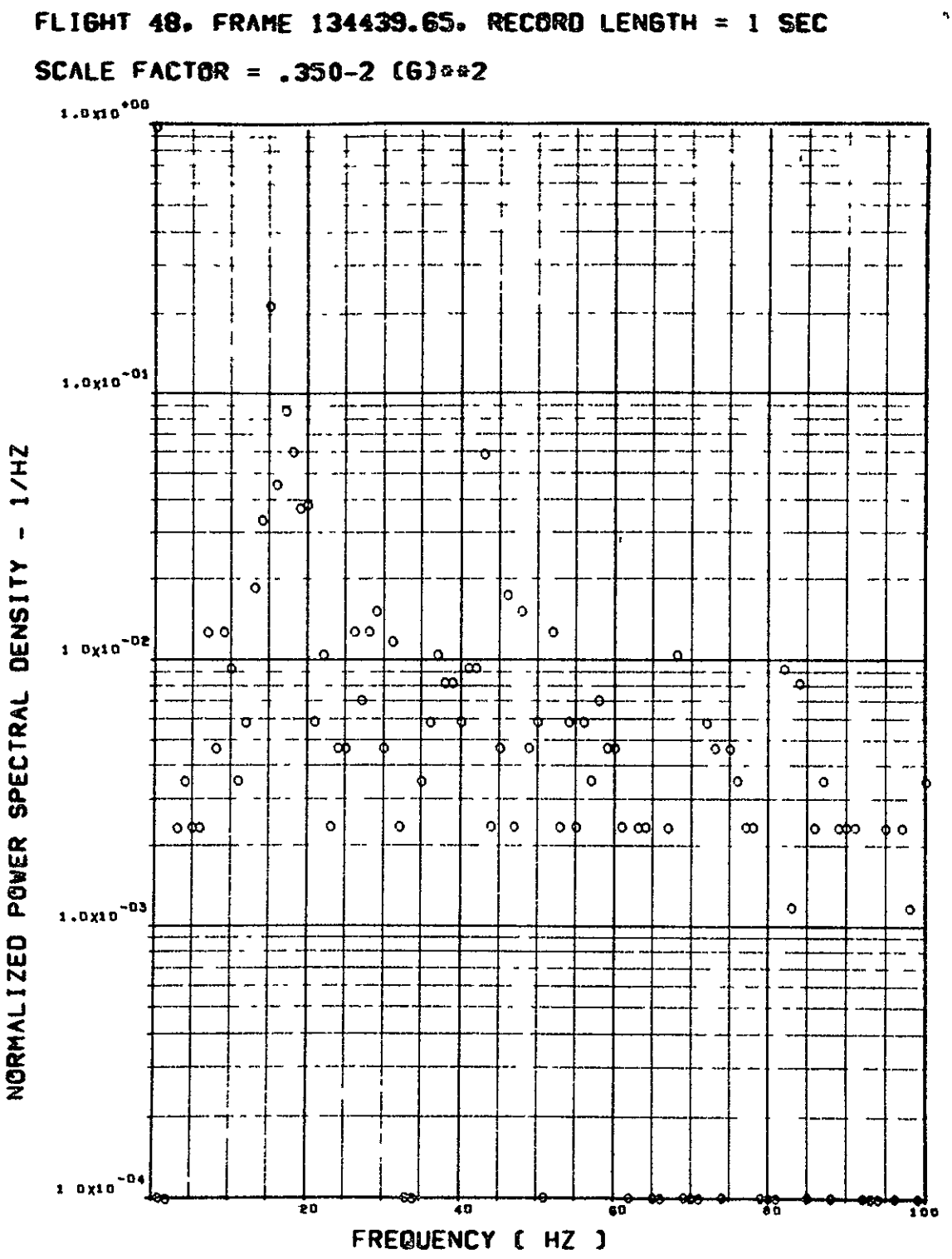

Figure 28. Continued

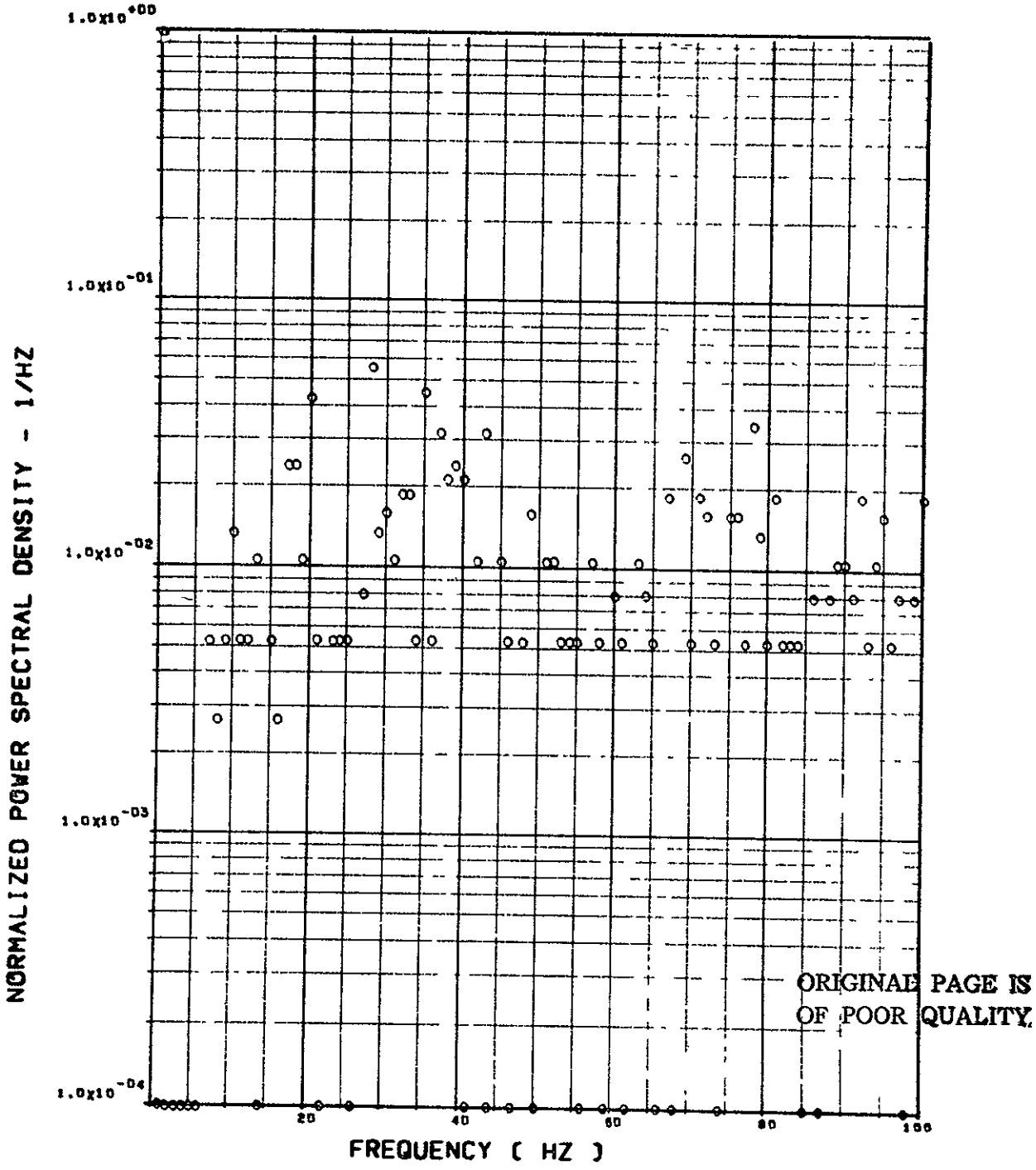

Figure 28. Continued

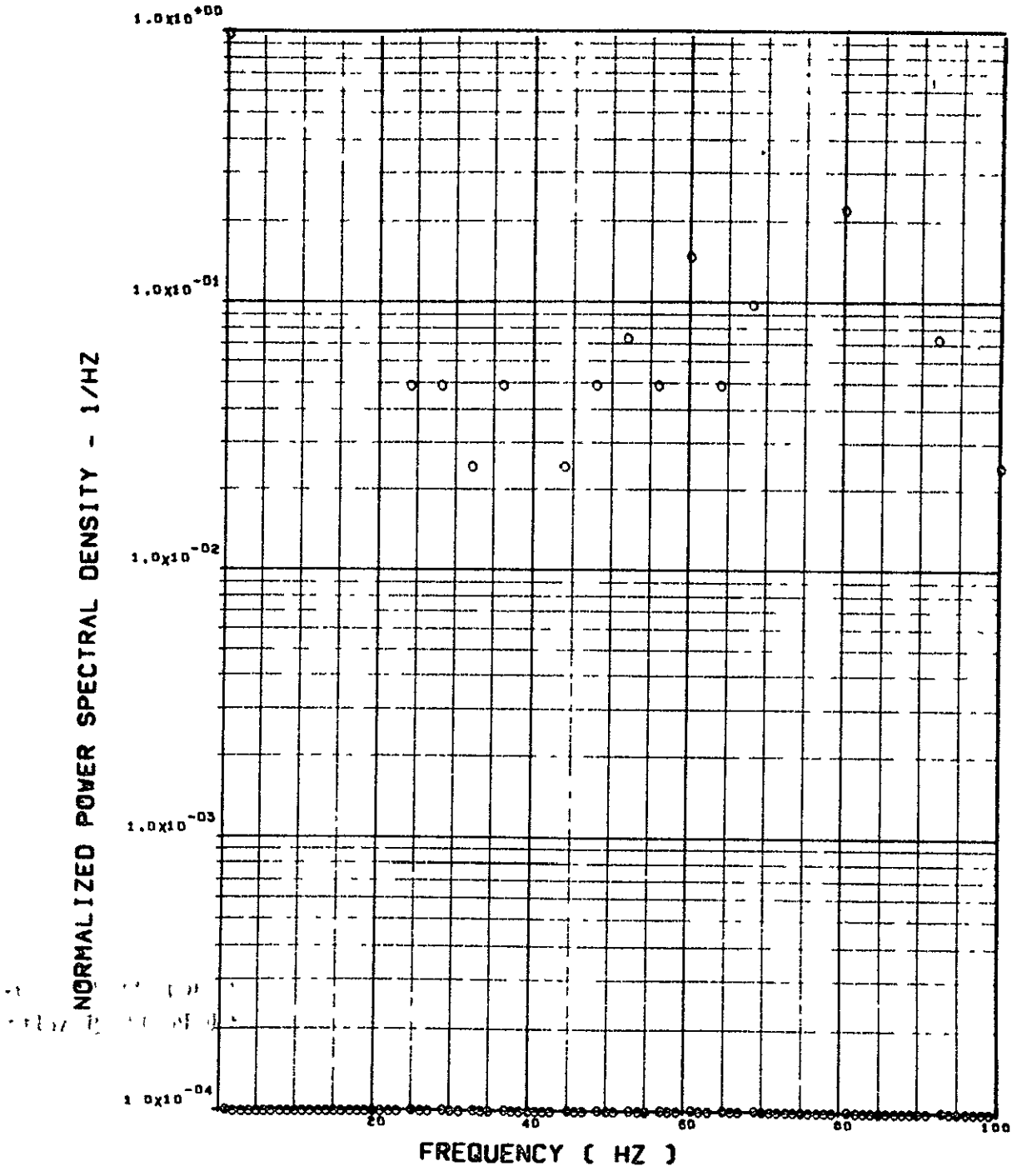

Figure 28. Continued

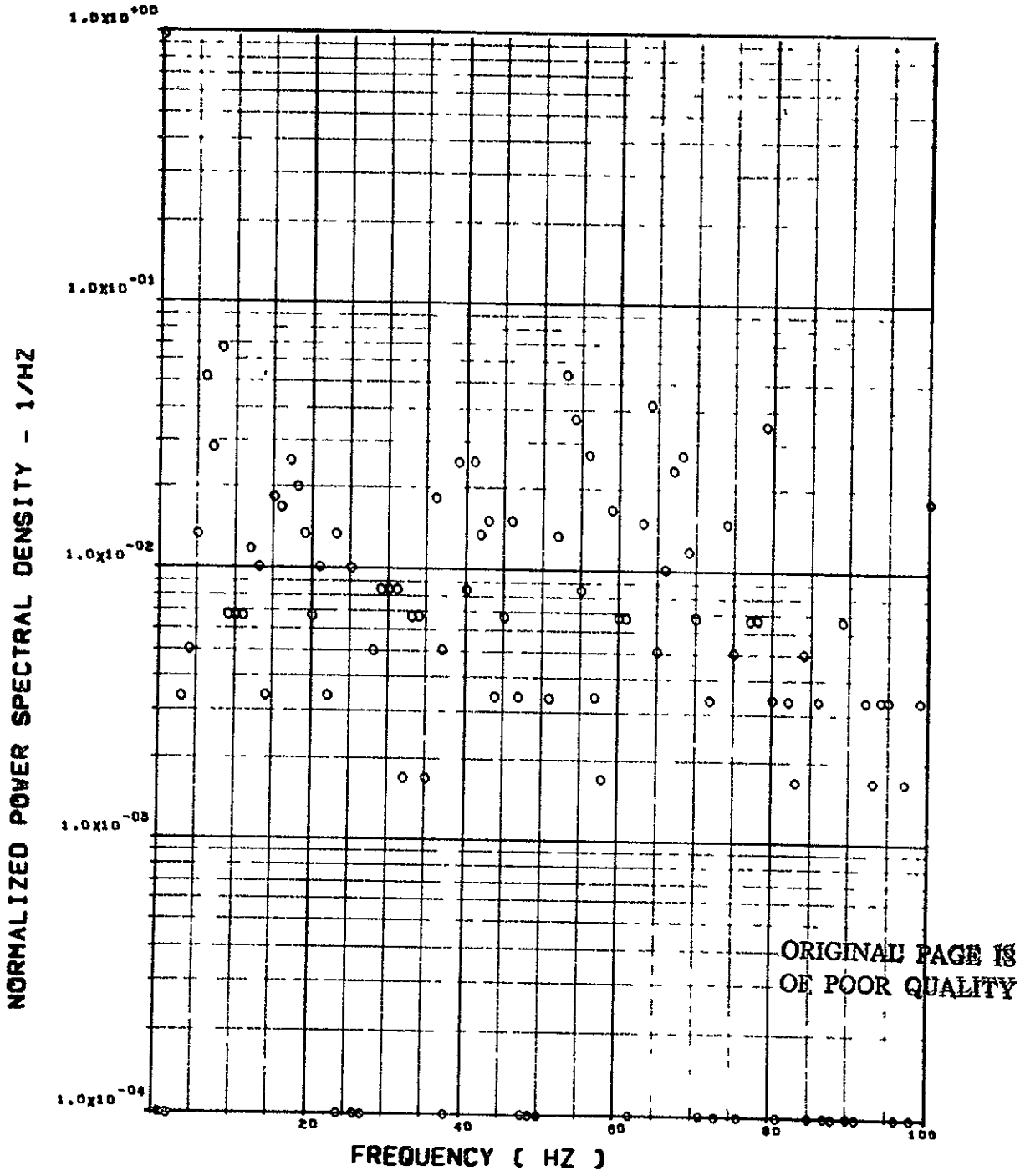

Figure 28. Continued

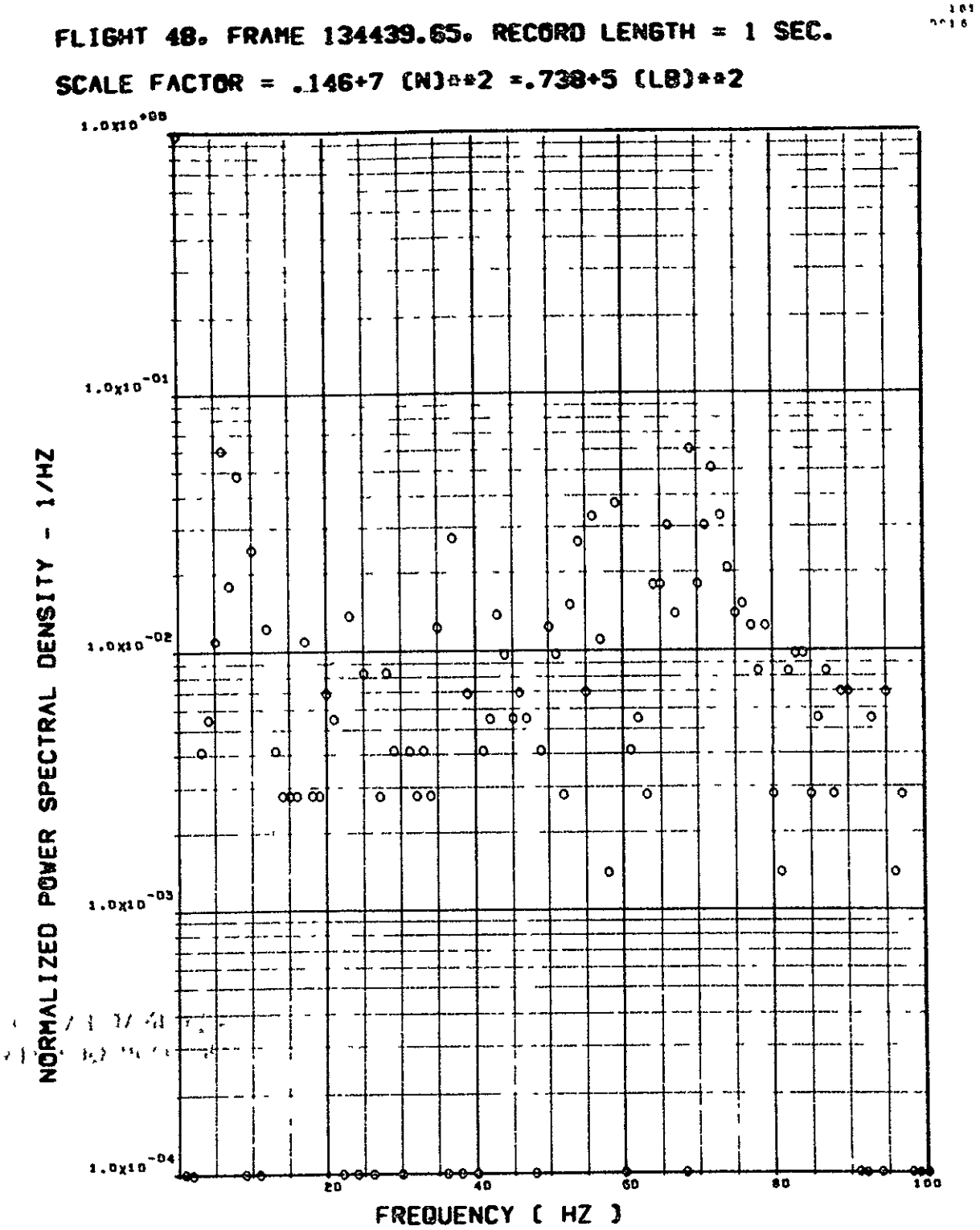

Figure 28. Continued

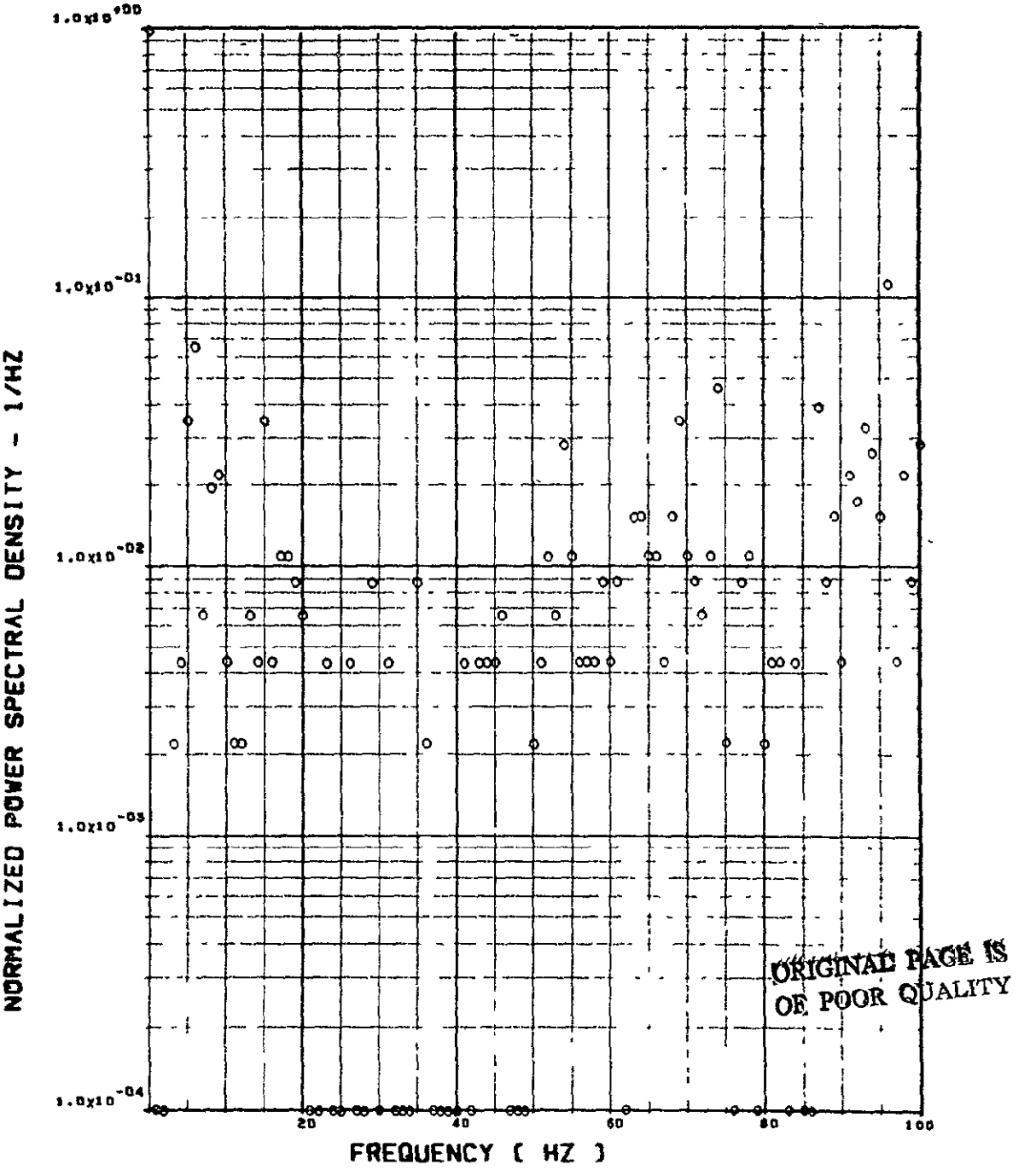

Figure 28. Continued

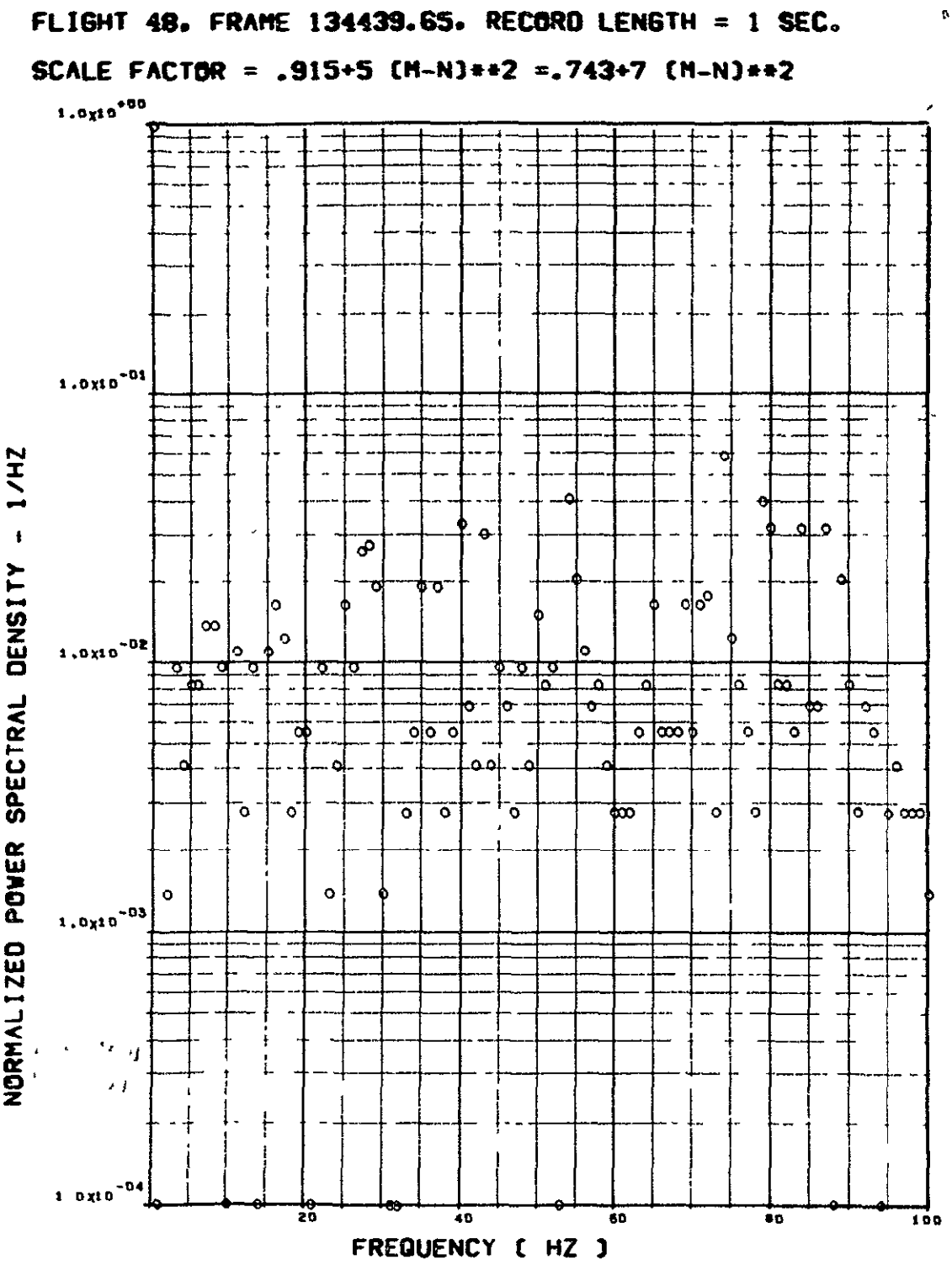

Figure 28. Continued

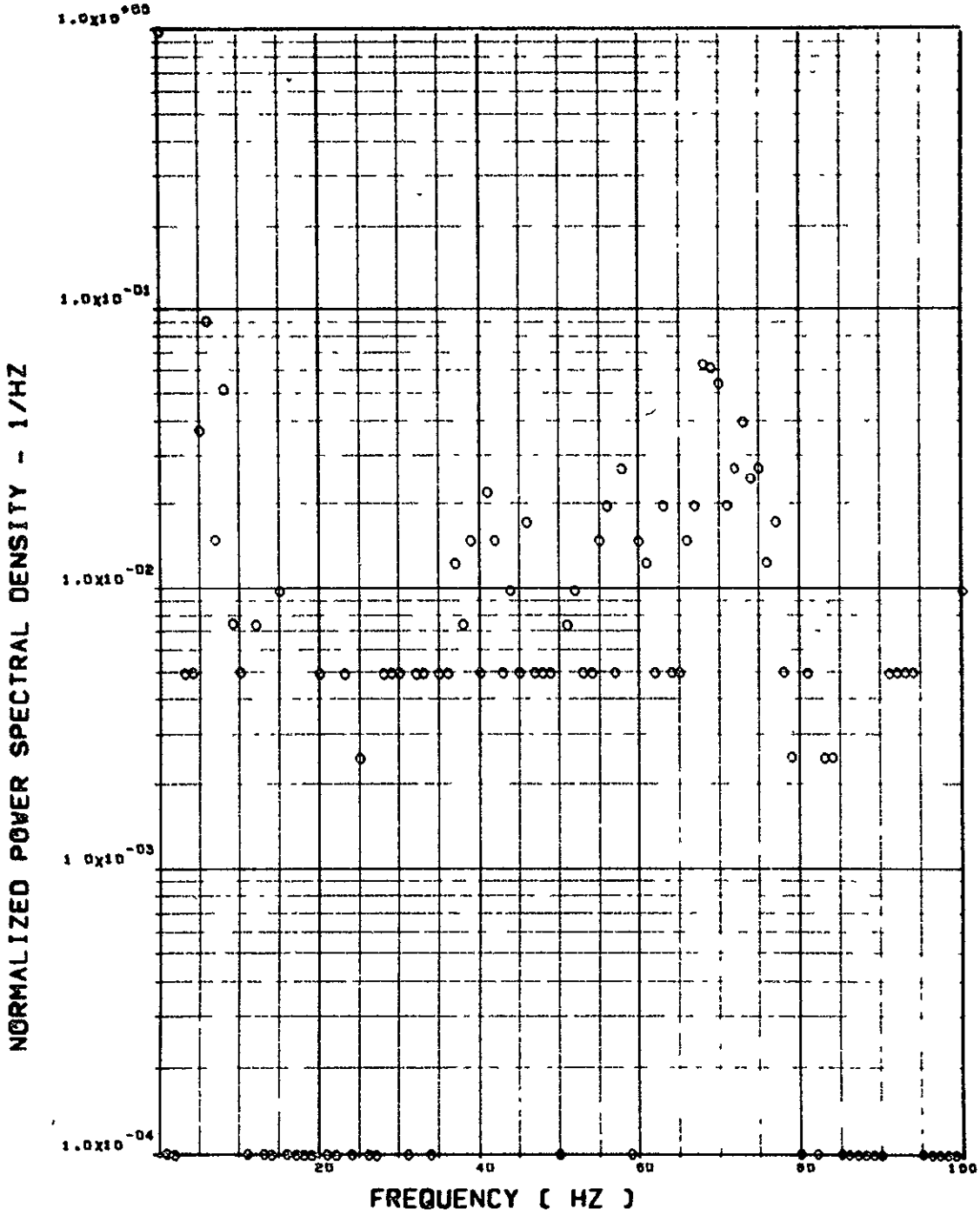

Figure 28. Continued

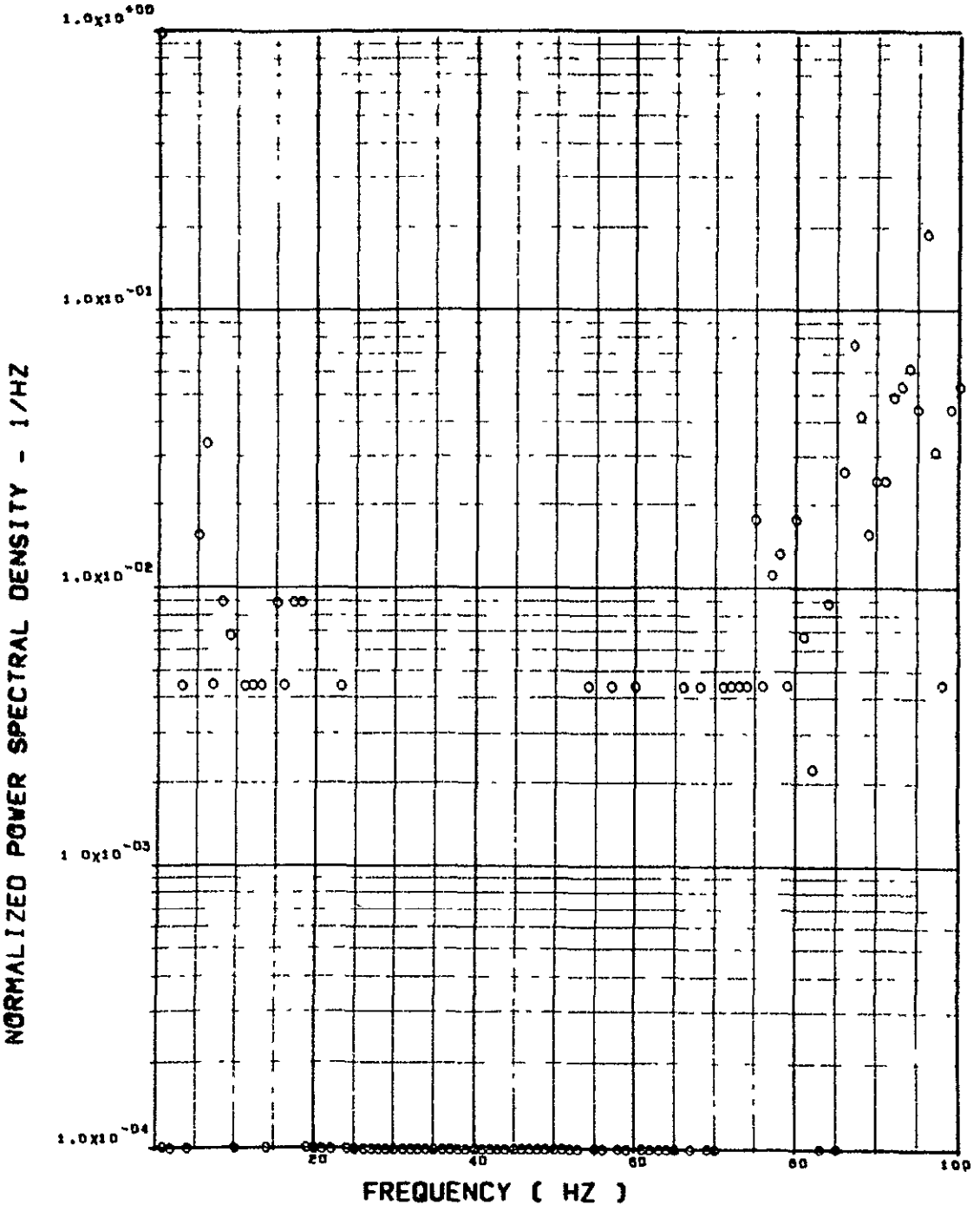

Figure 28. Continued

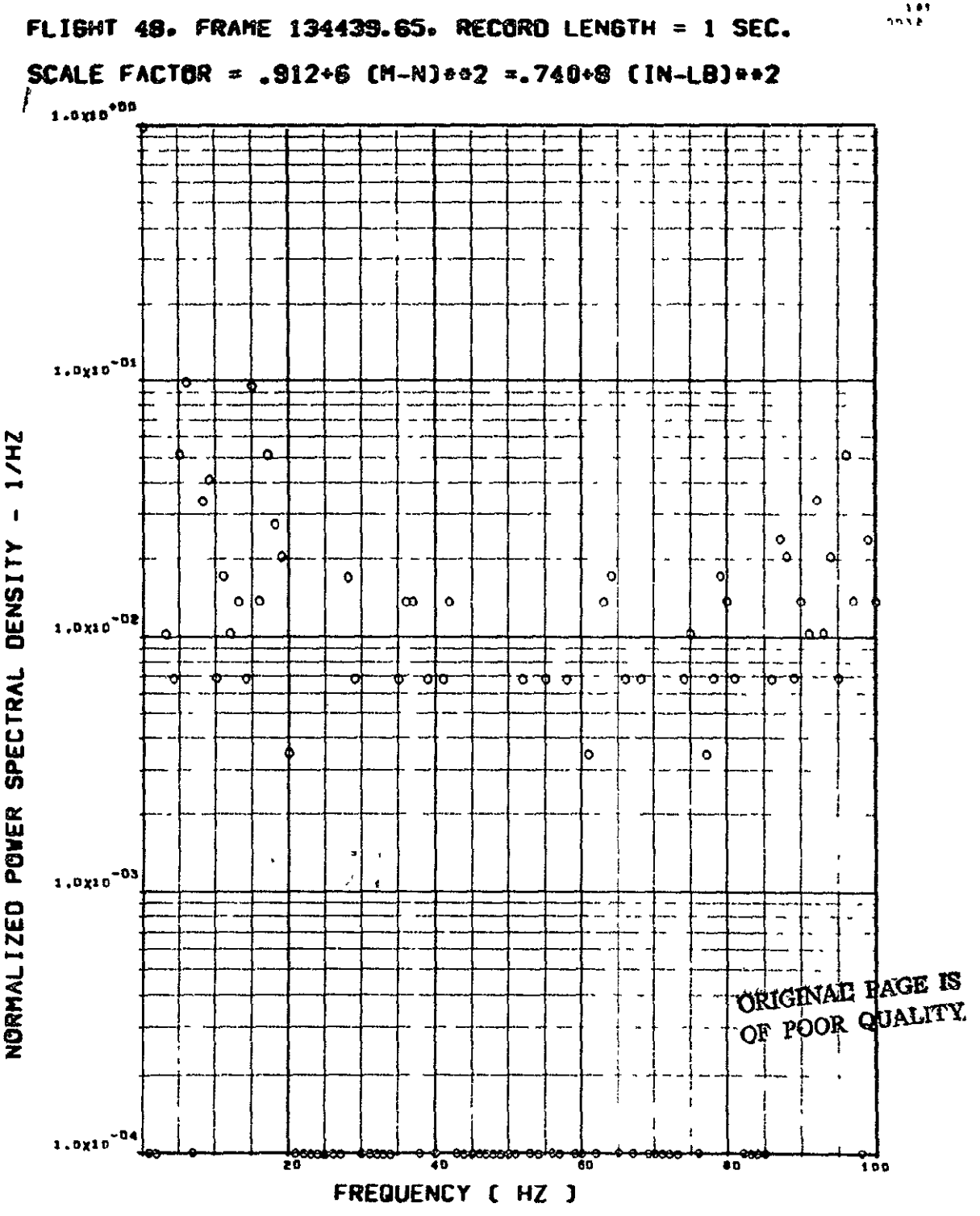

Figure 28. Continued

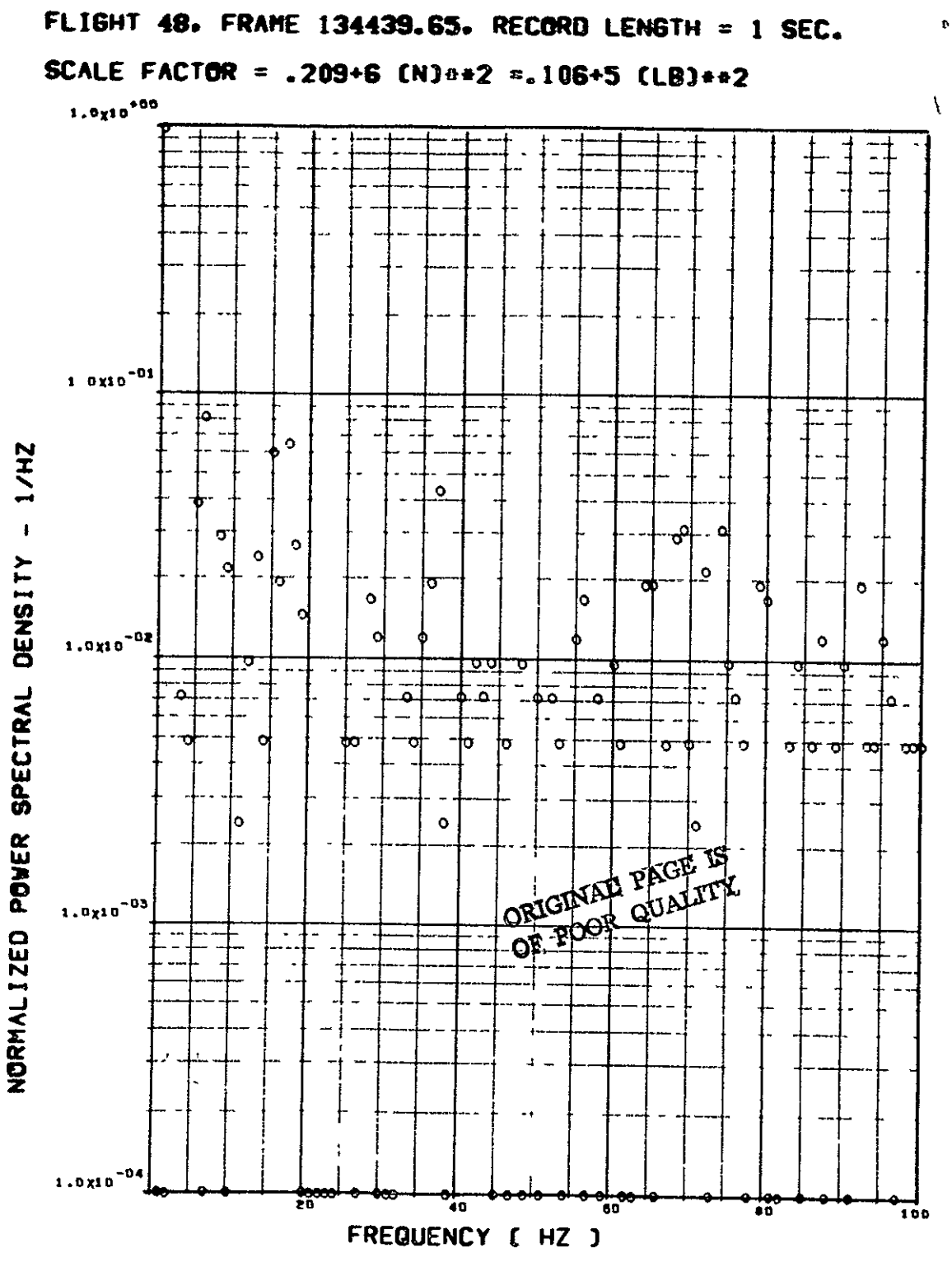

Figure 28. Continued

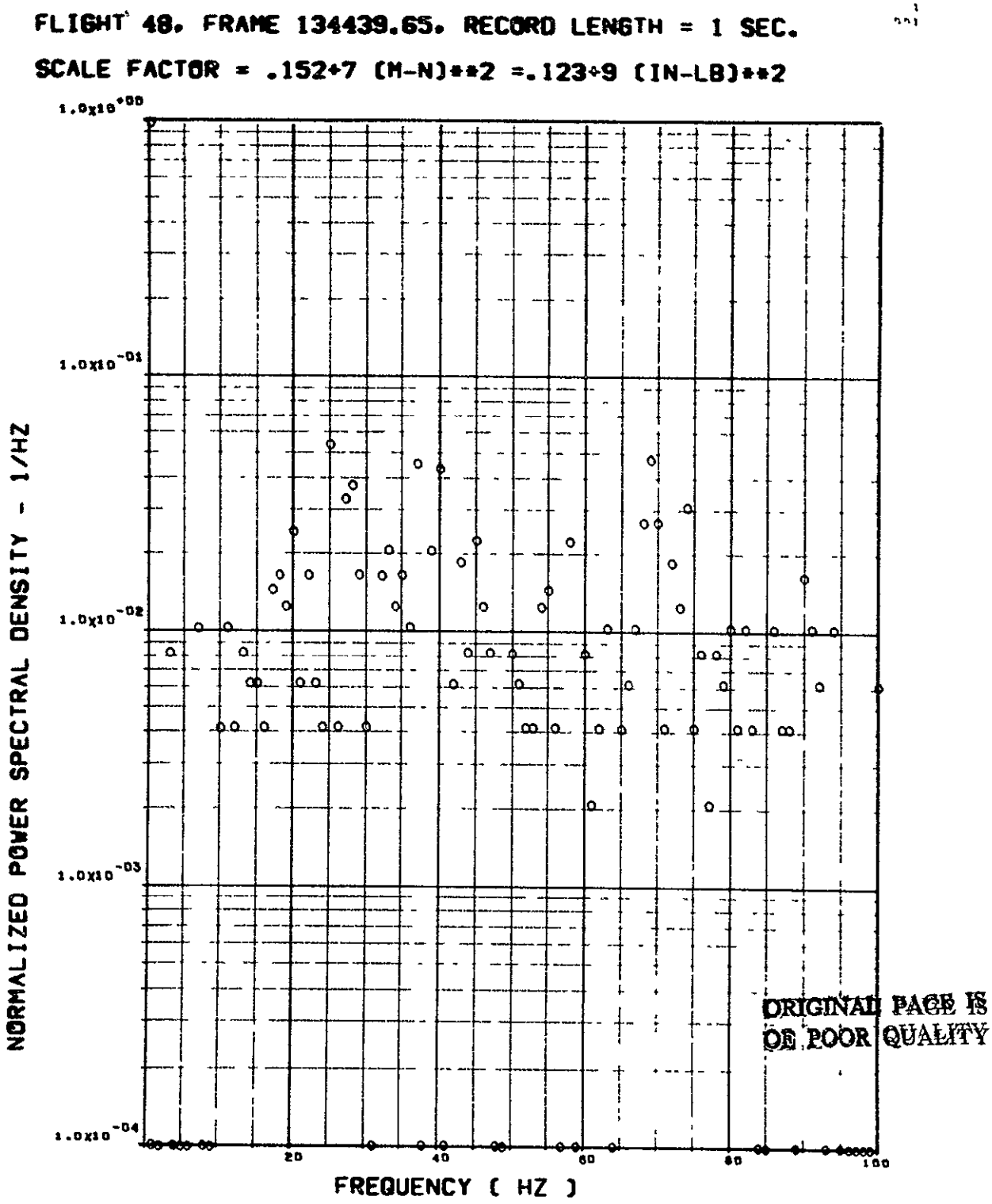

Figure 28. Continued

FLIGHT 48. FRAME 134439.65. RECORD LENGTH = 1 SEC.

SCALE FACTOR = .217+6 (M-N)**2 =.176+8 (IN-LB)**2

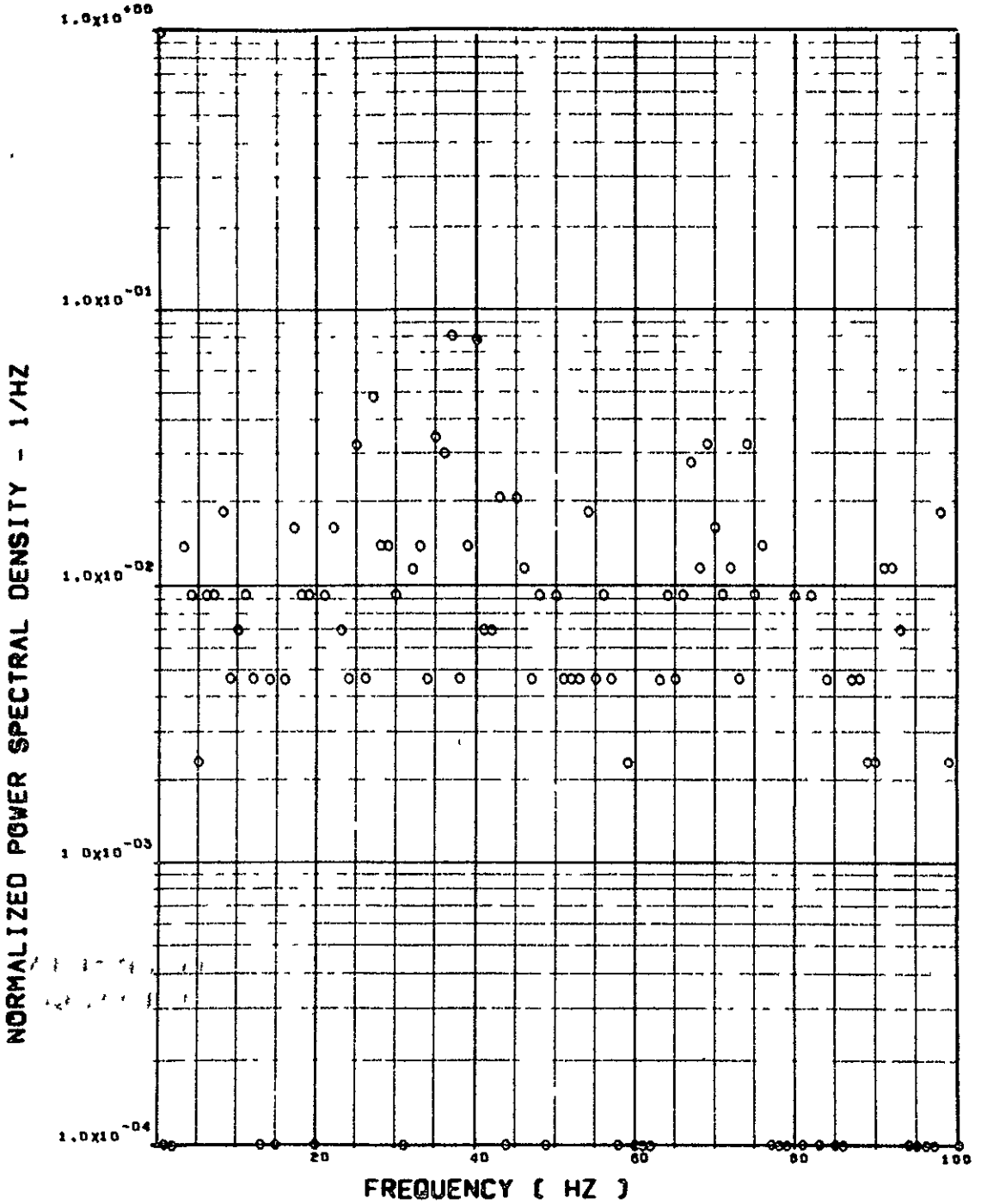

ITEM - SW128 TORSION AT WING STATION 2

Figure 28. Continued

C-7

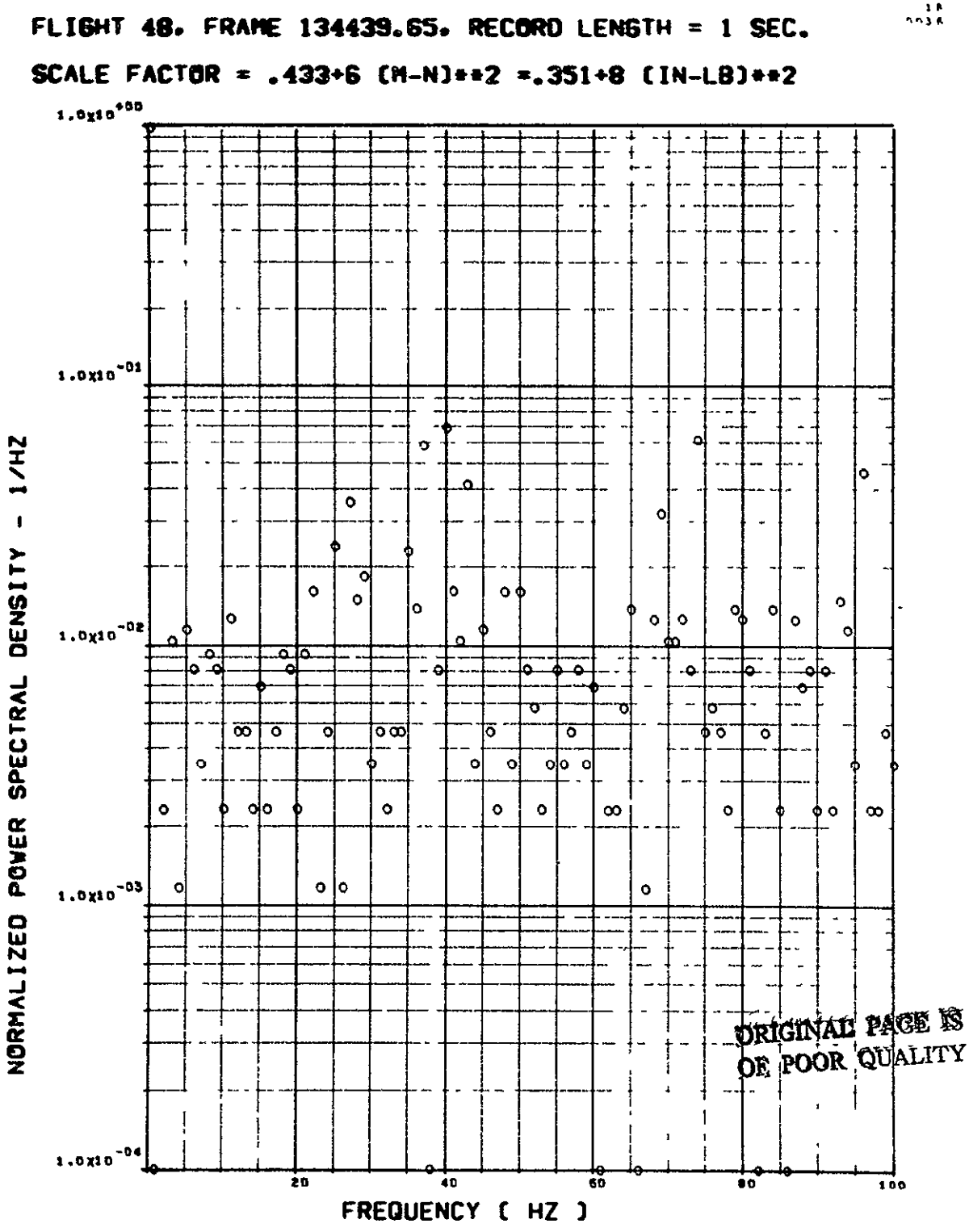

Figure 28. Continued

FLIGHT 48. FRAME 134439.65. RECORD LENGTH = 1 SEC.

SCALE FACTOR = .155+6 (M-N)**2 =.126+8 (M-N)**2

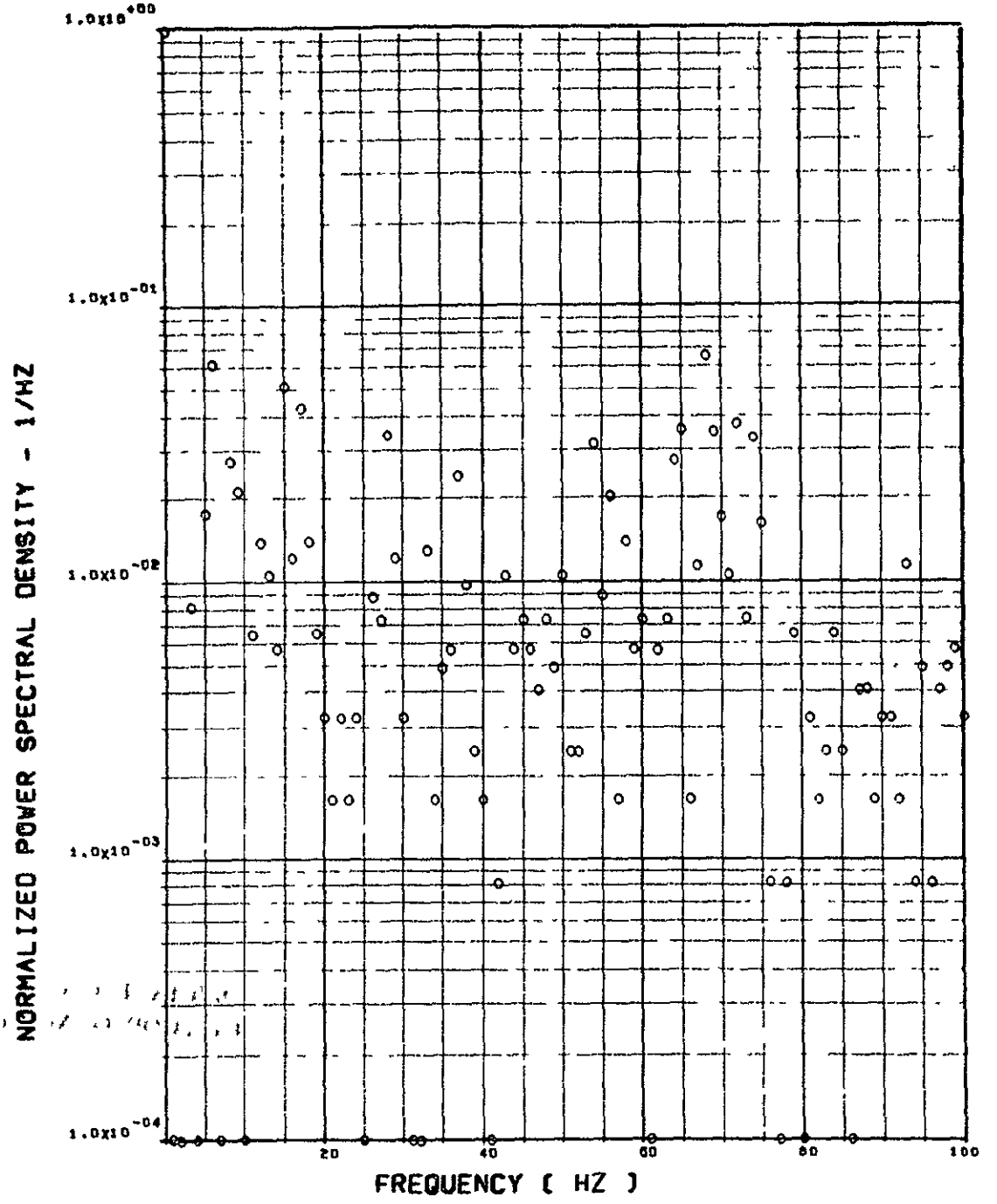

ITEM - SW134 TORSION AT WING STATION 4

Figure 28. Continued

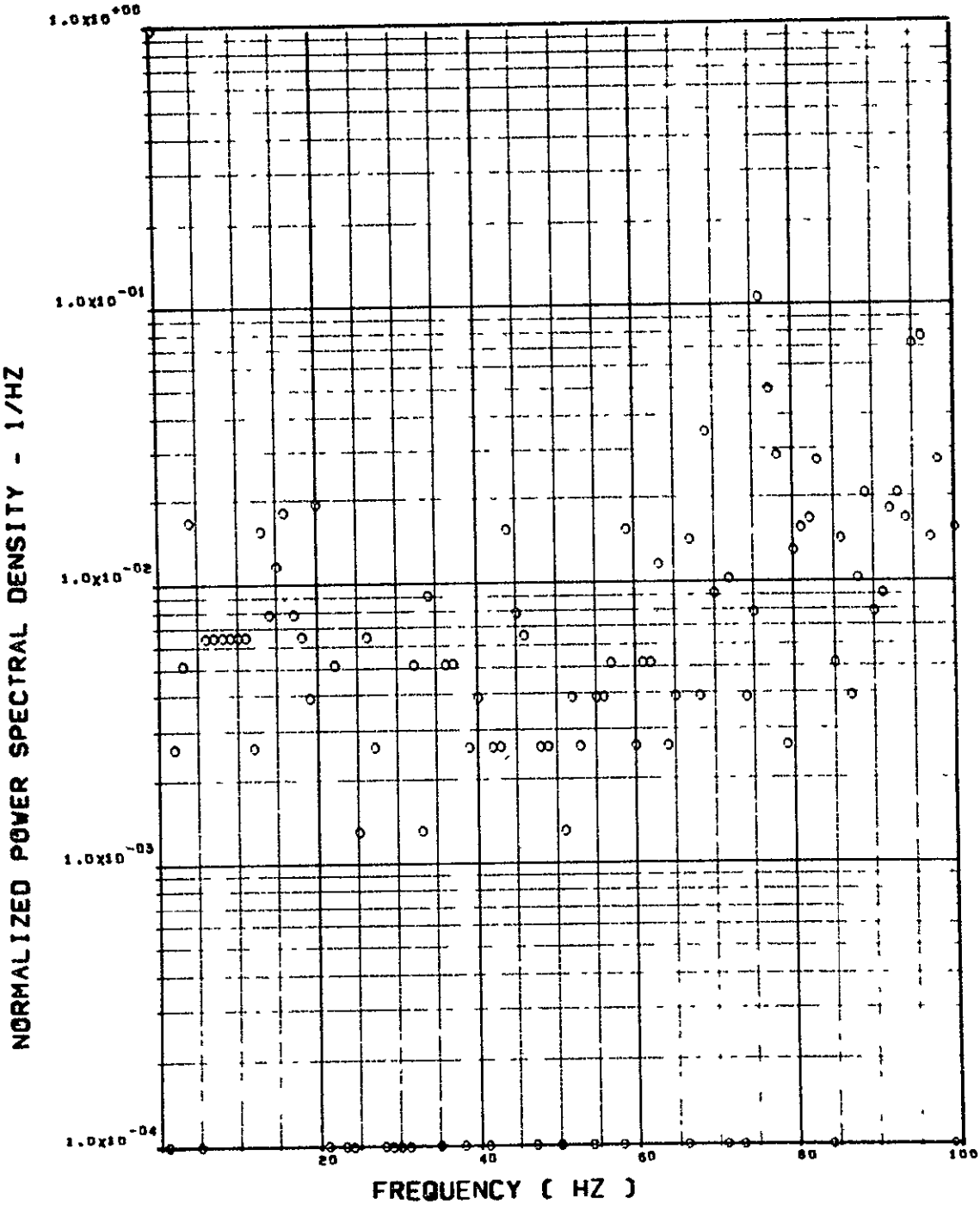

Figure 28. Continued

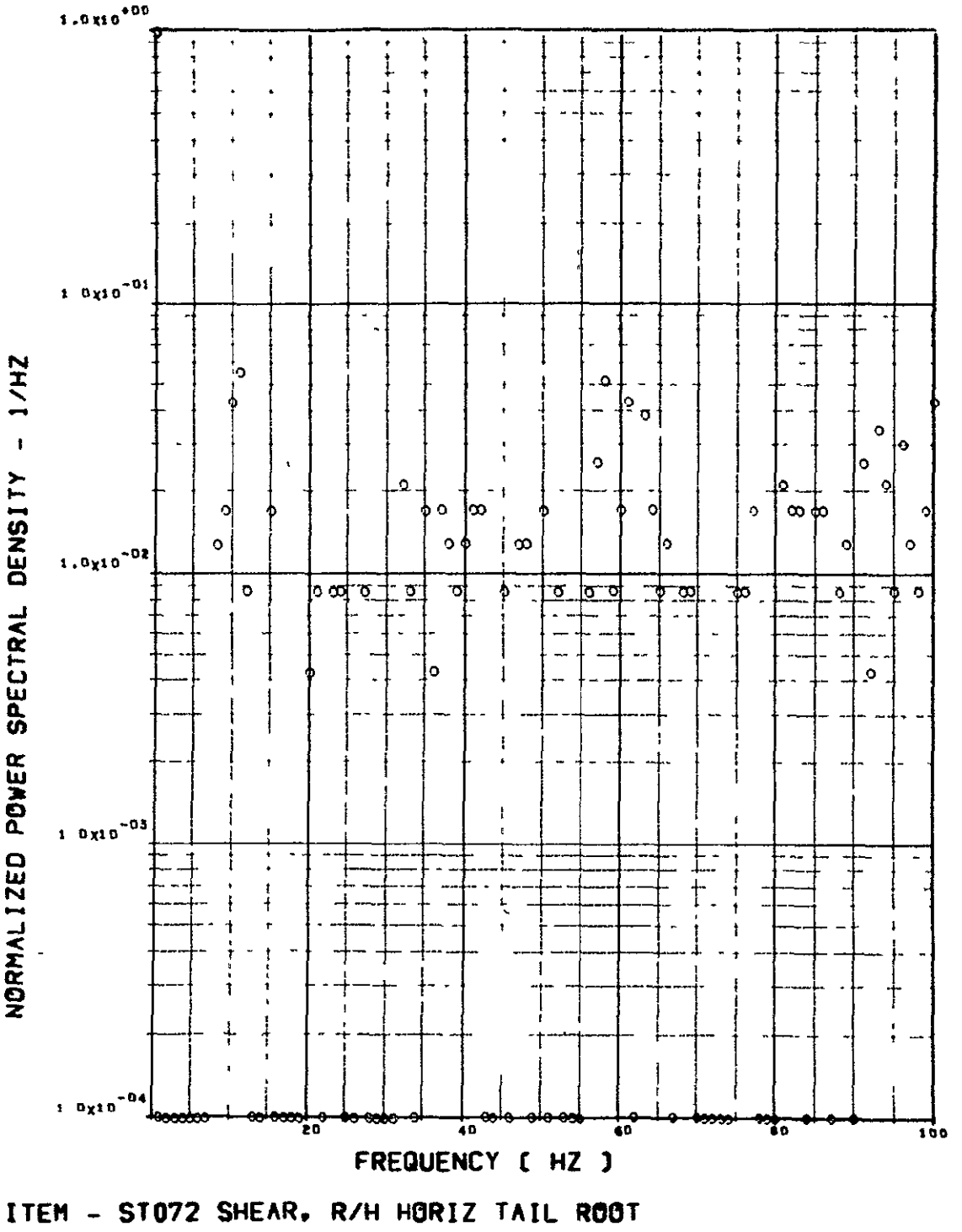

Figure 28. Continued

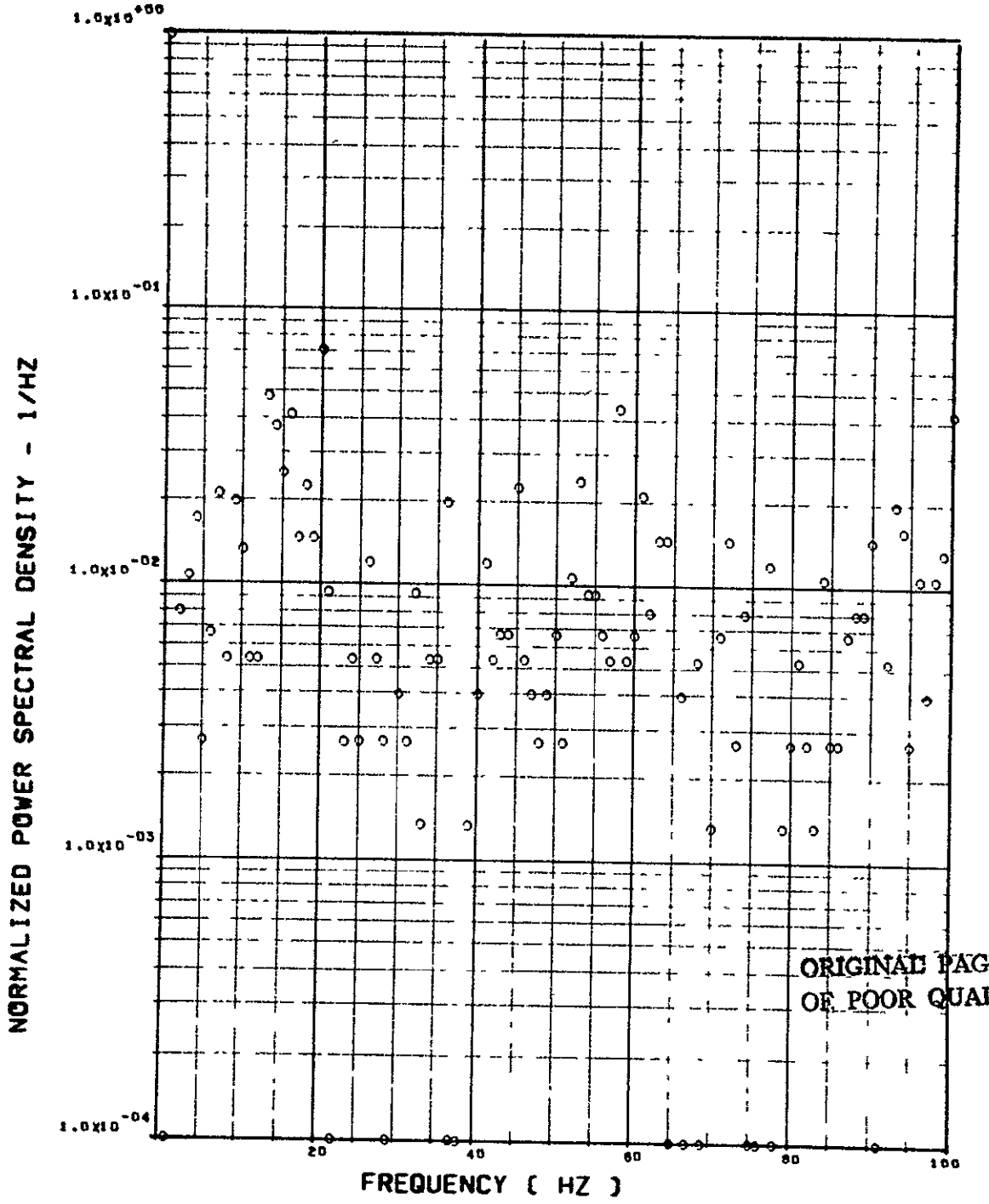

Figure 28. Continued

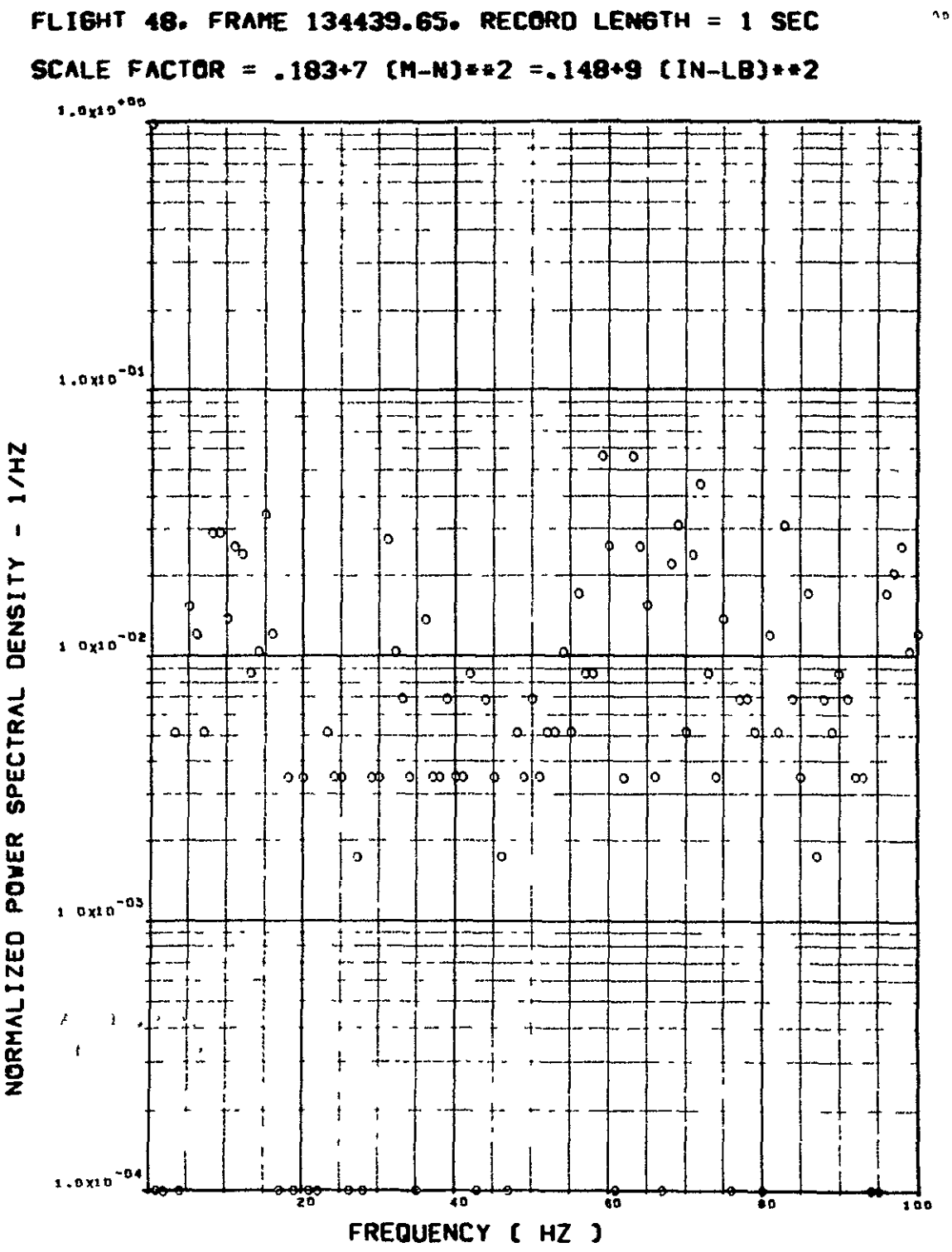

Figure 28. Continued

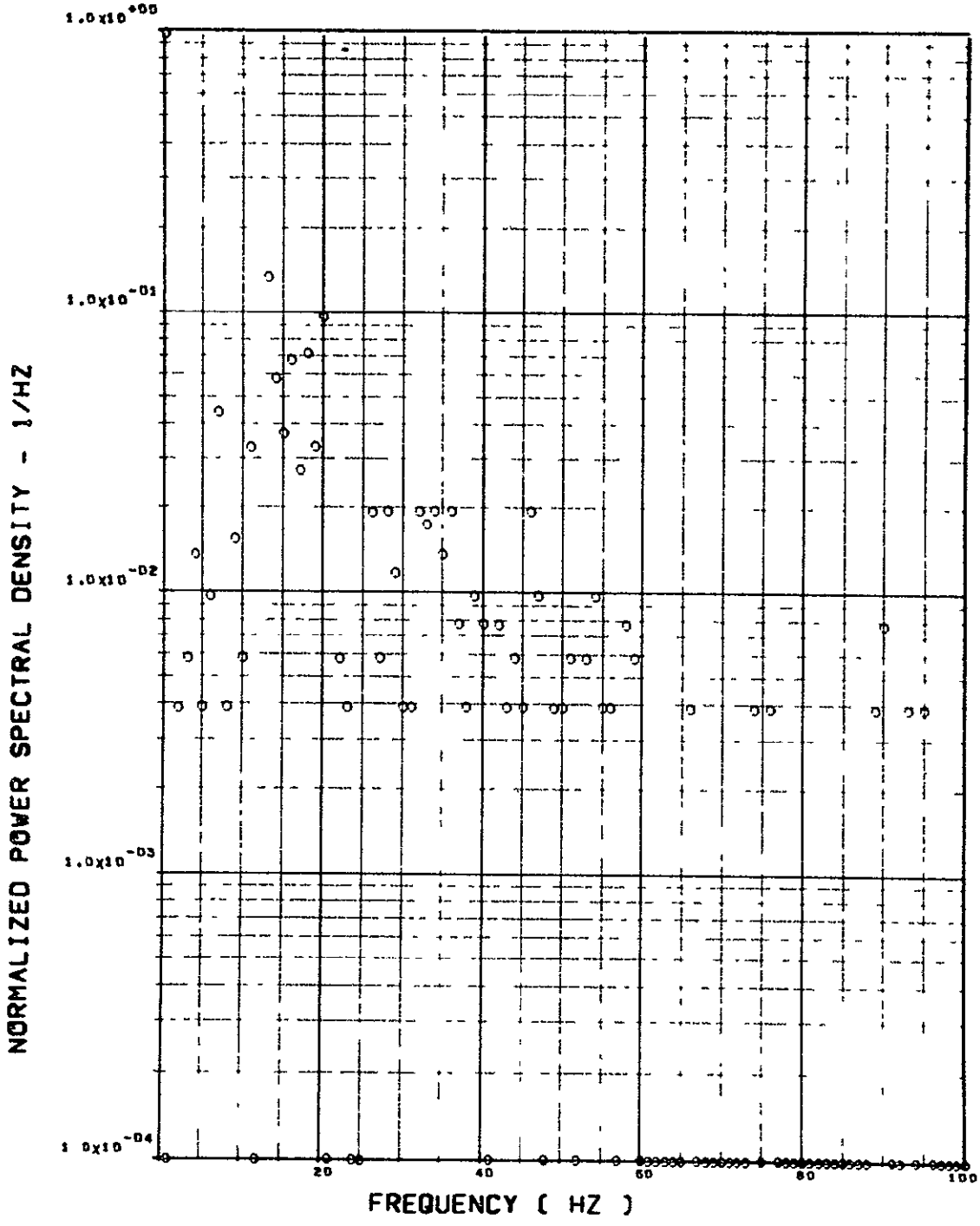

Figure 28. Continued

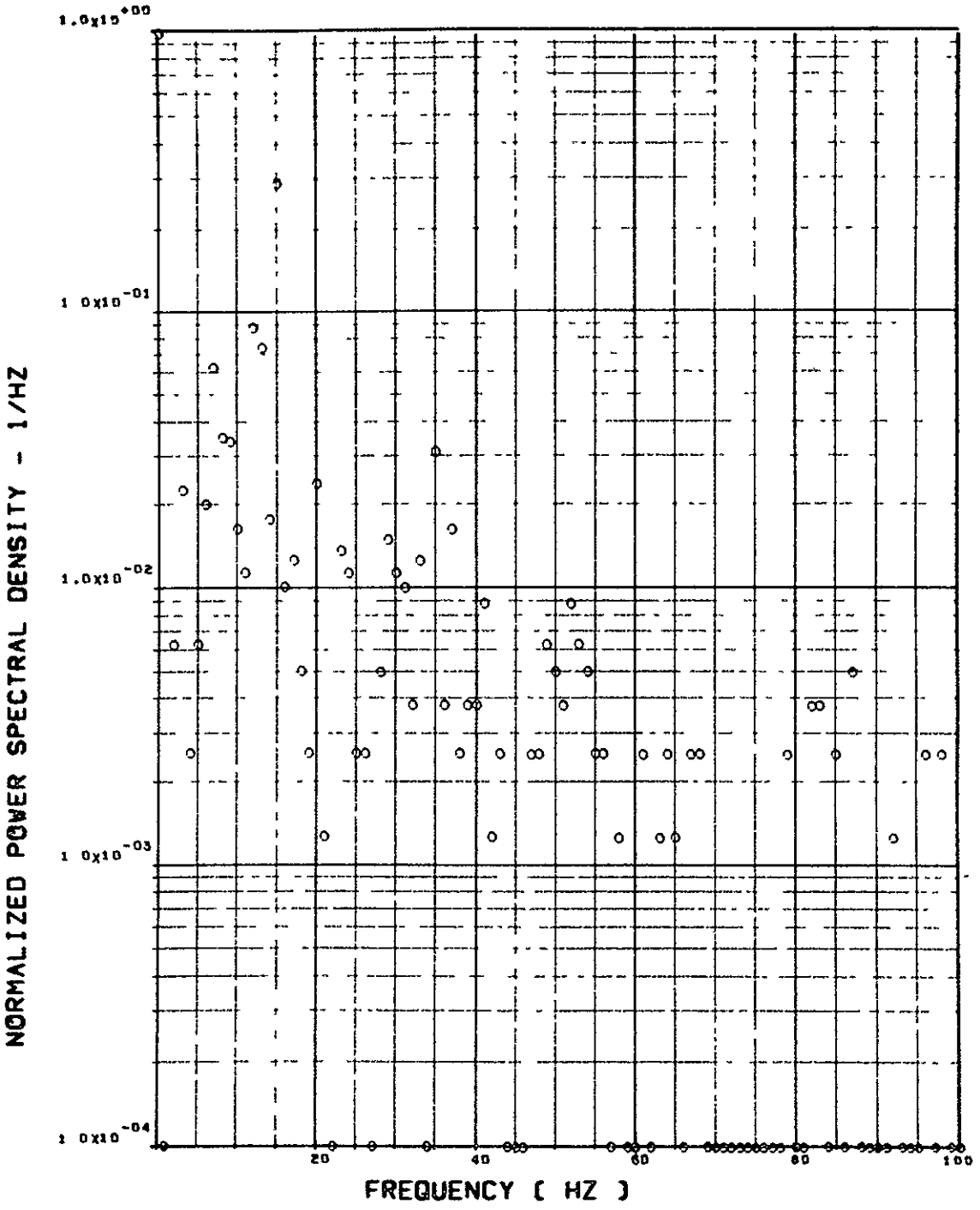

Figure 28. Concluded

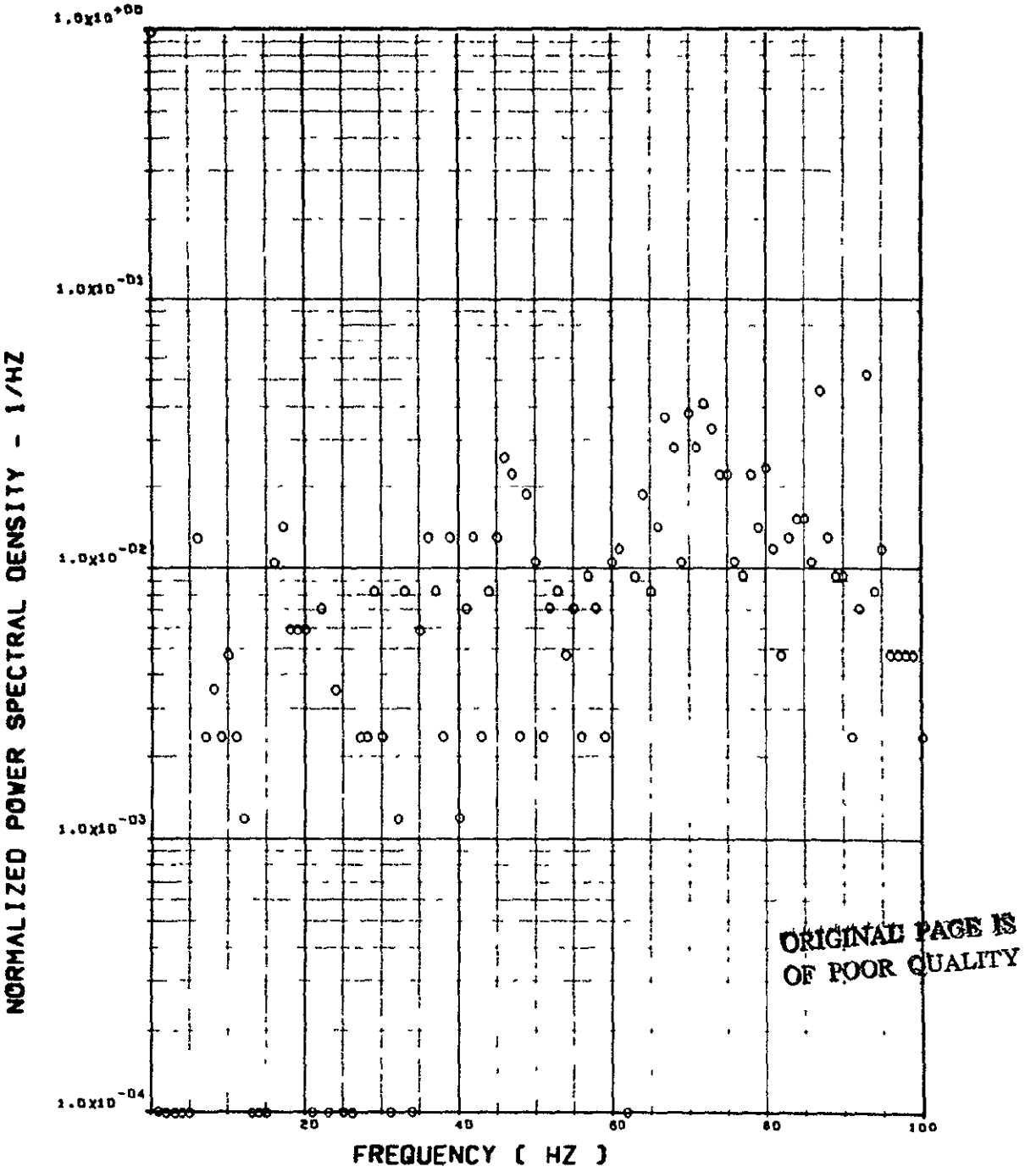

Figure 29. Power Spectra - Flight 59, Run S132R, Point 1
T_1 = 31901 0, ΔT = 2 Sec, α_{Nom} = 16.75 deg,
$\Delta\alpha$= 1.60 deg

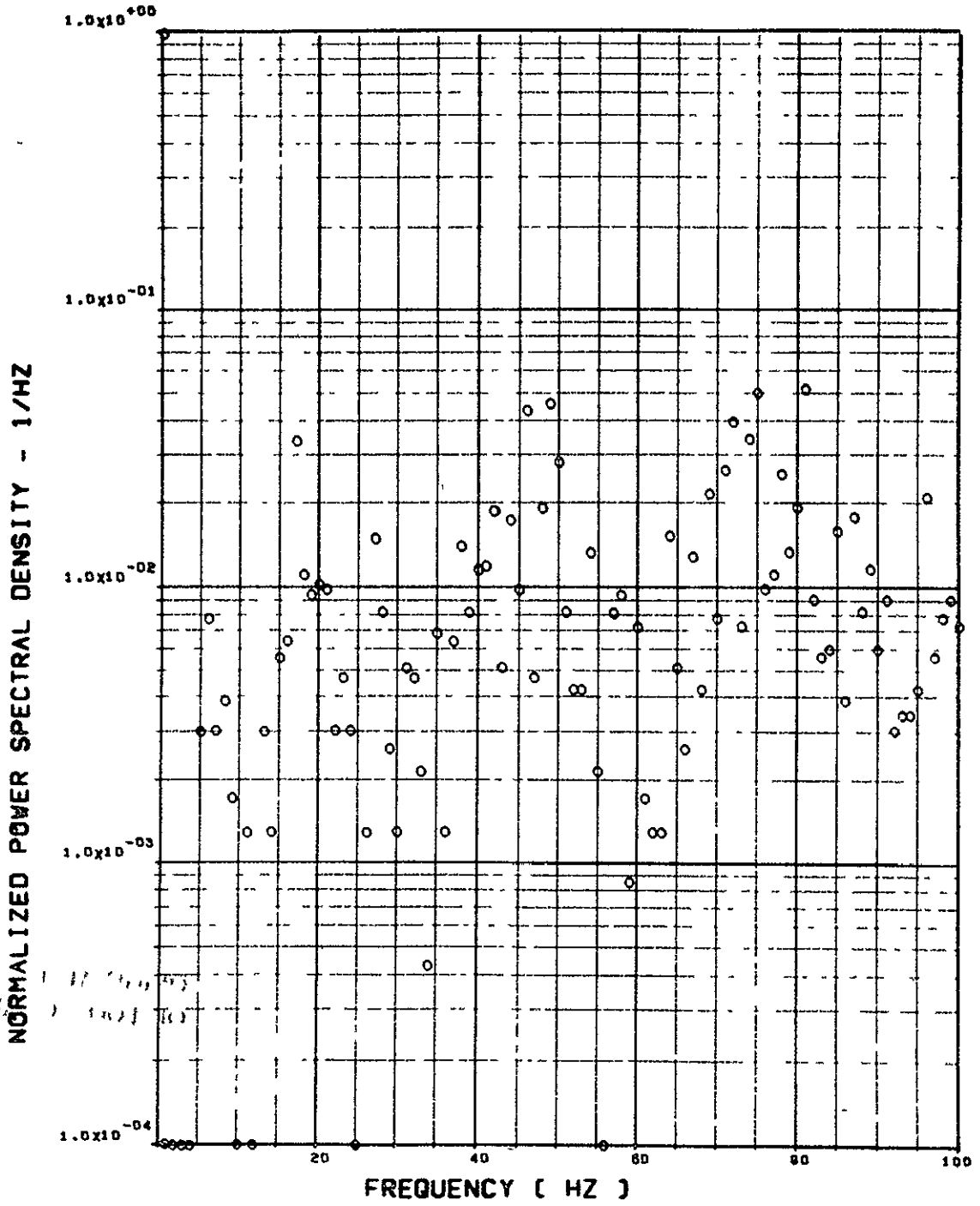

Figure 29. Continued

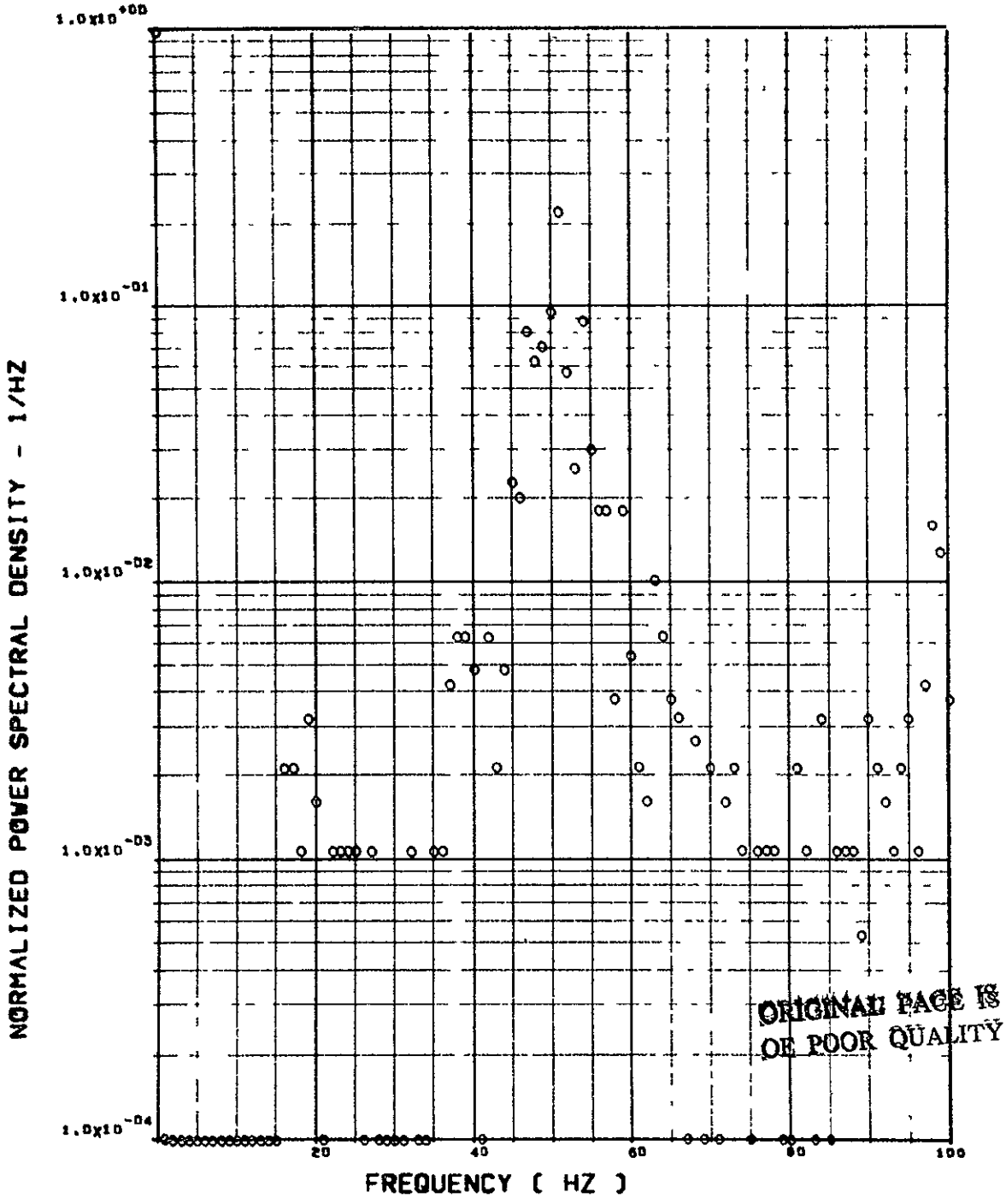

Figure 29. Continued

FLIGHT 59. FRAME 031901.00. RECORD LENGTH = 2 SEC

SCALE FACTOR = .141+0 (G)**2

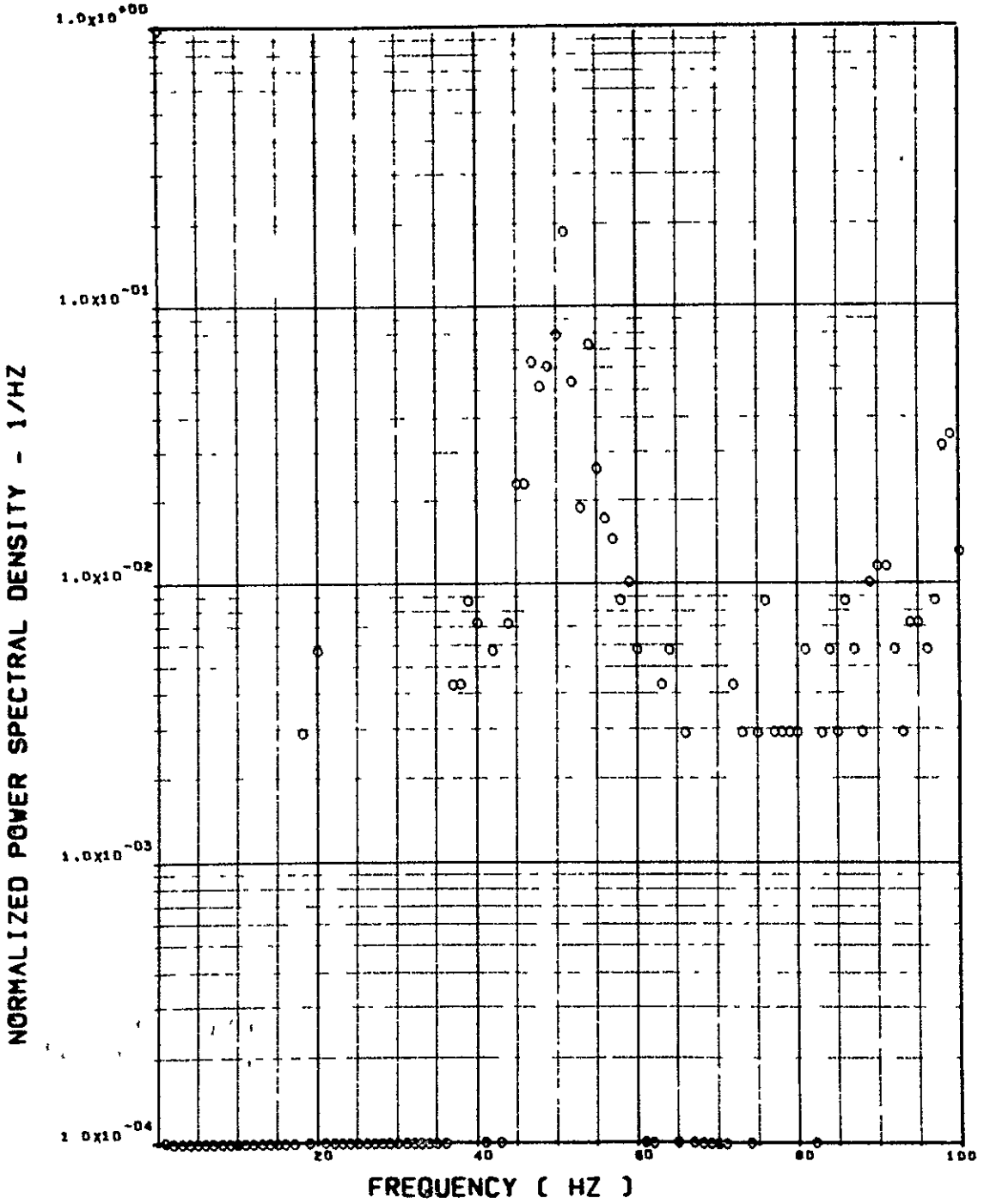

ITEM - AB019 C.G. VERTICAL ACCELEROMETER

Figure 29. Continued

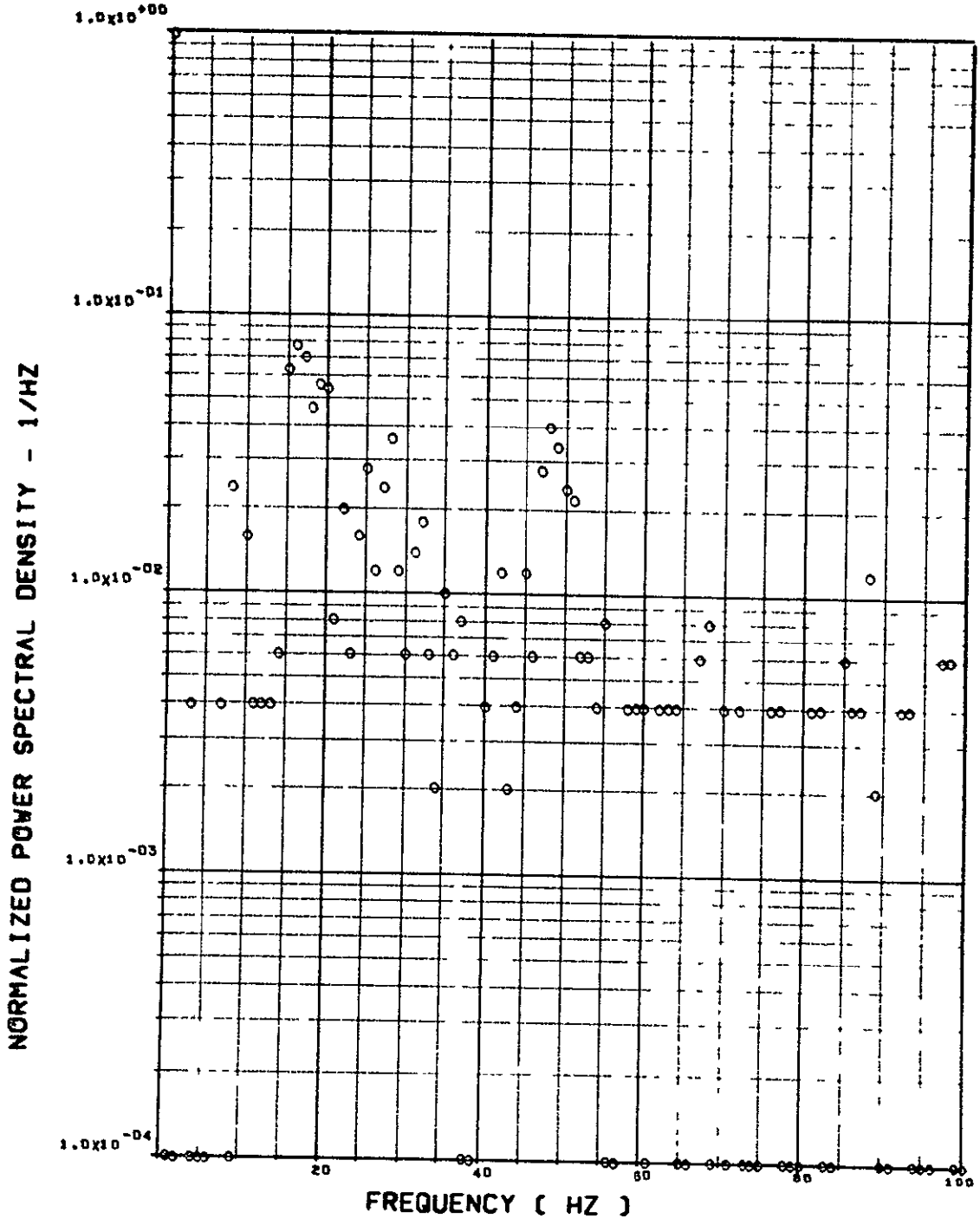

Figure 29. Continued

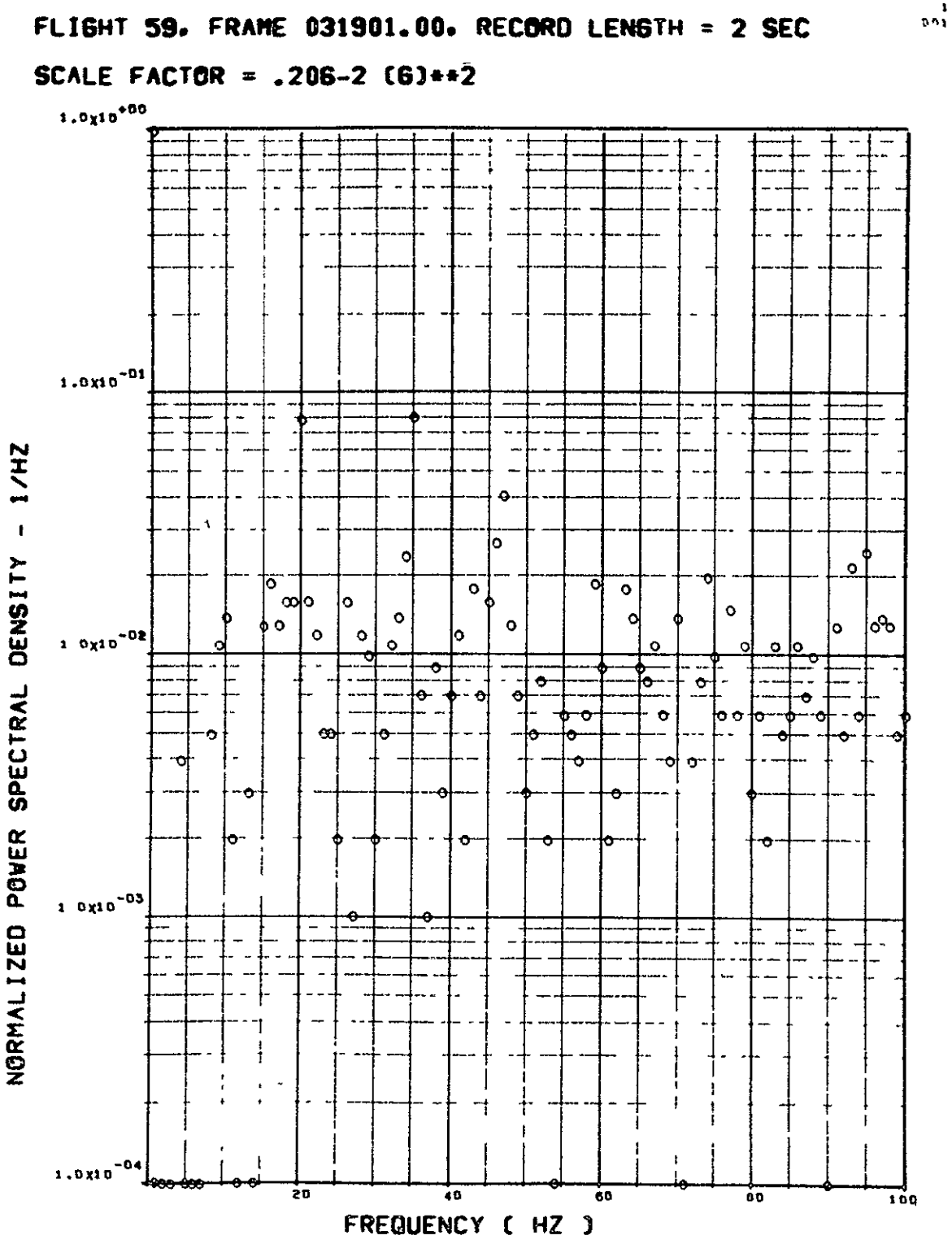

Figure 29. Continued

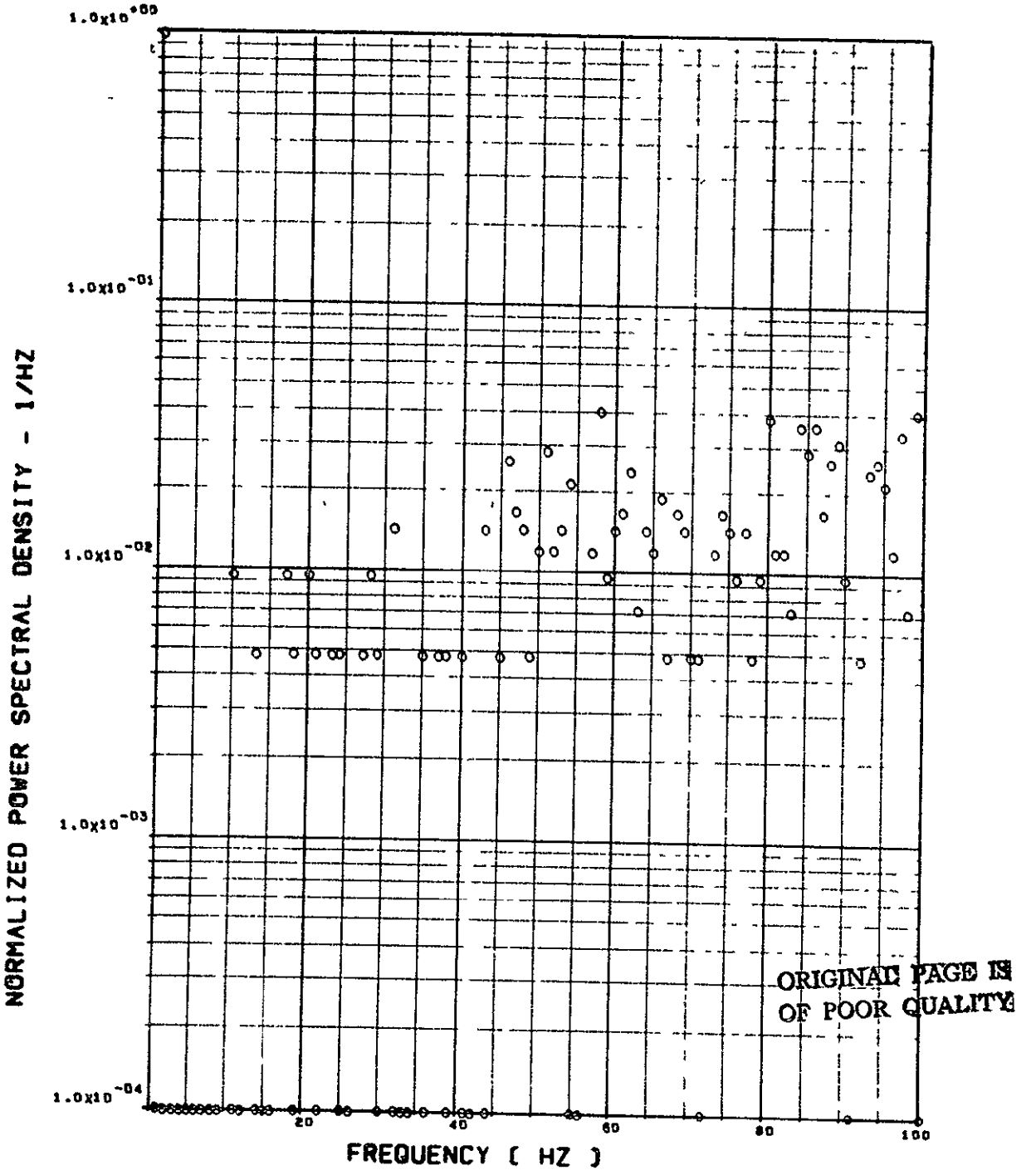

Figure 29. Continued

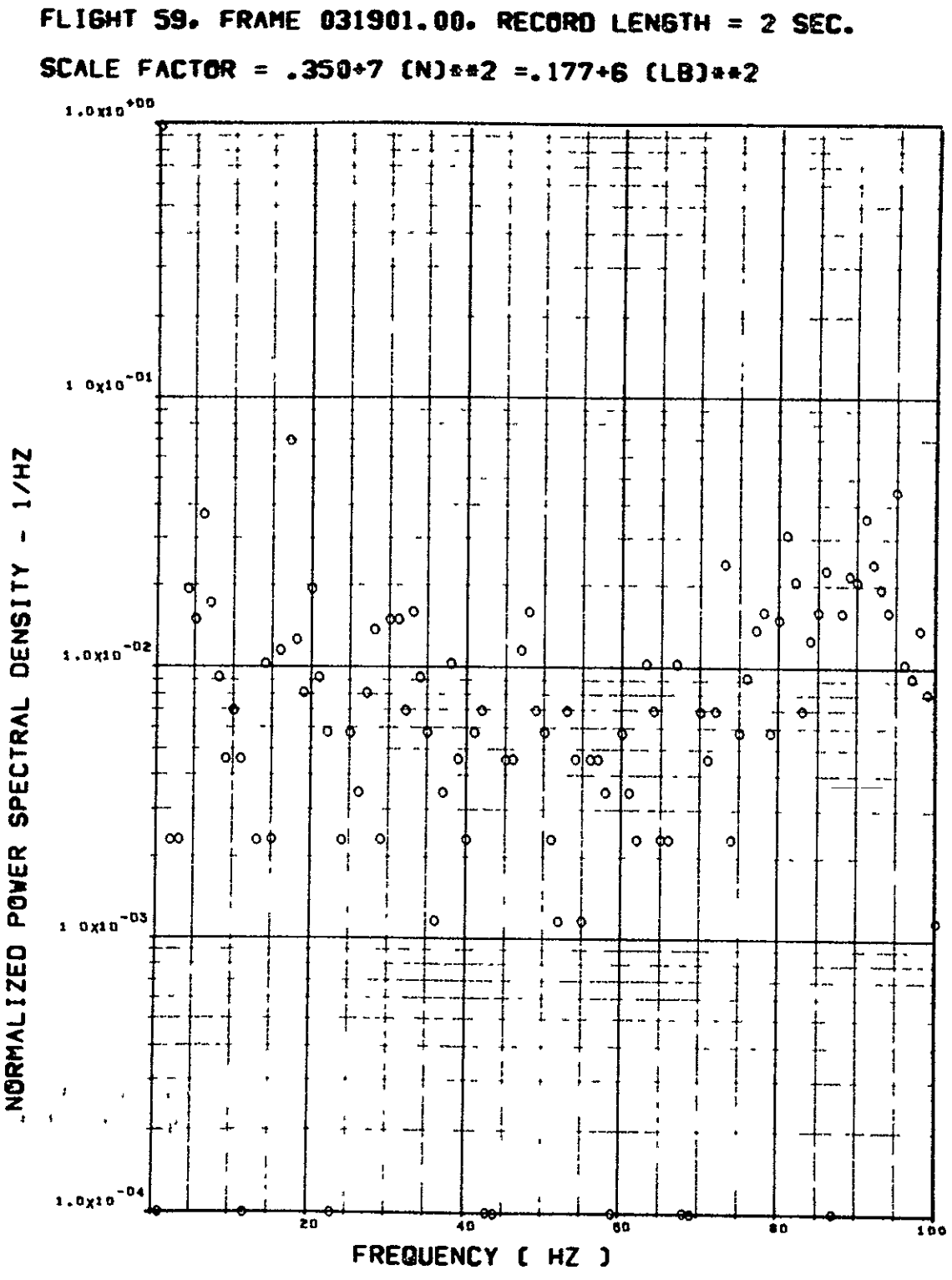

Figure 29. Continued

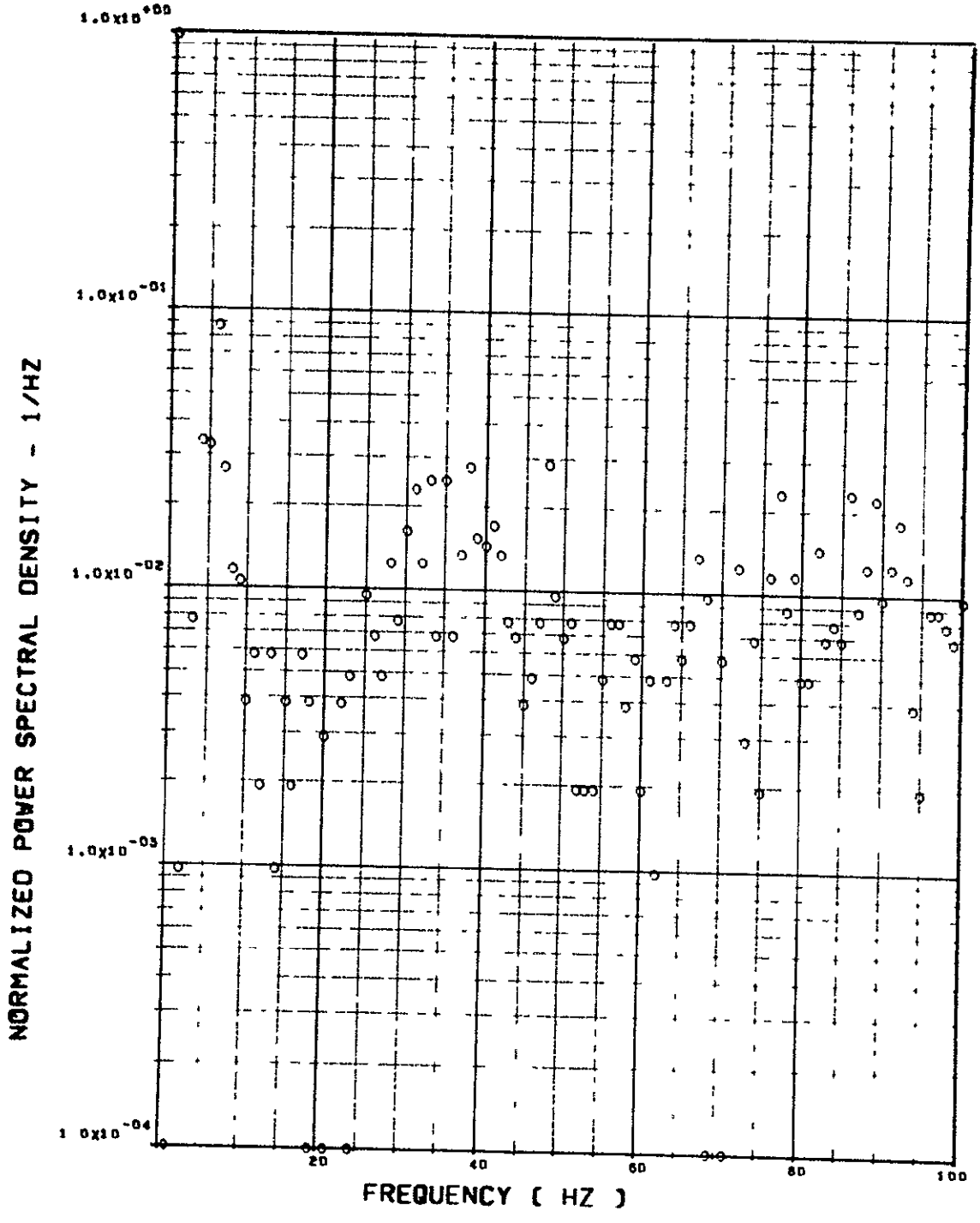

Figure 29. Continued

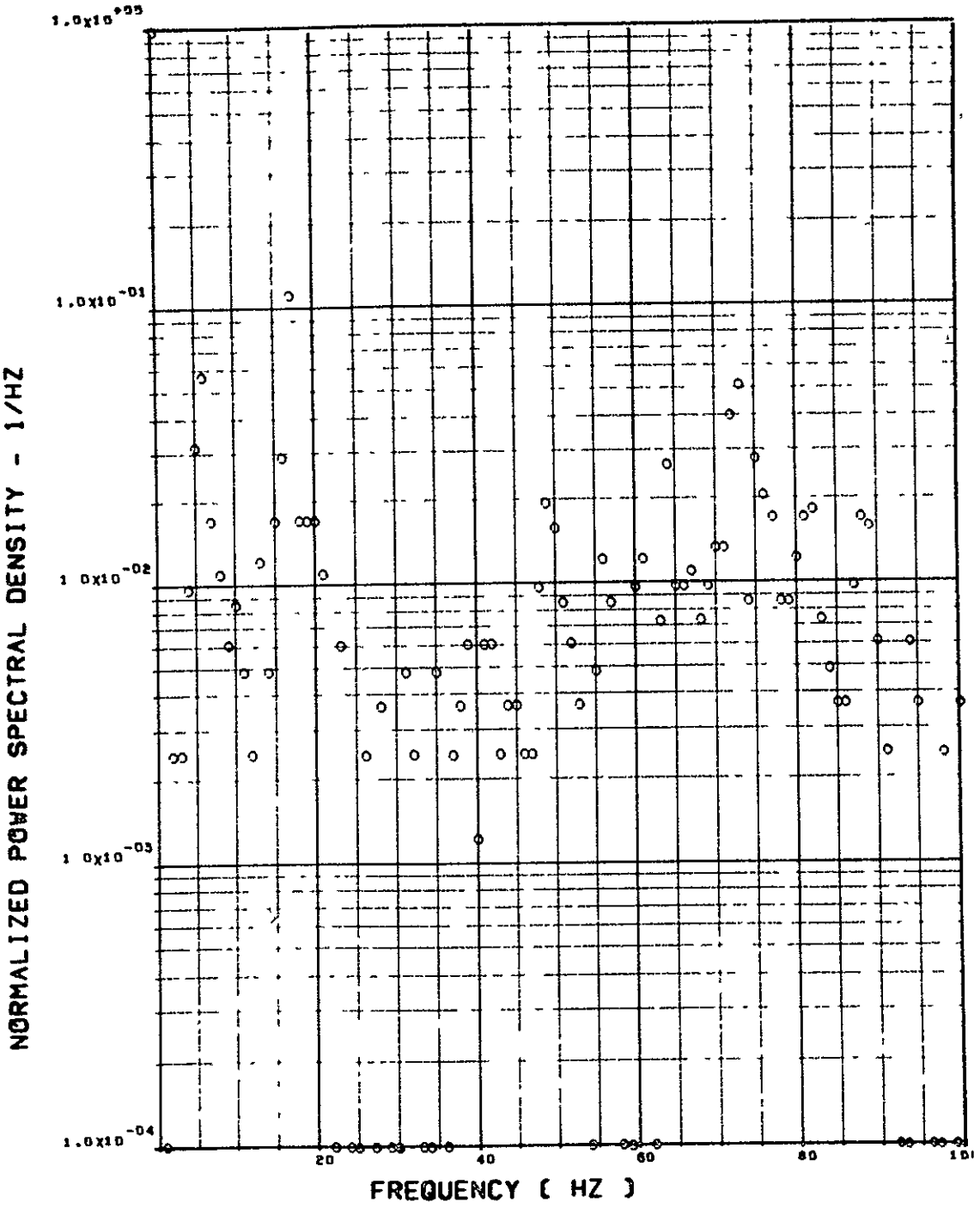

Figure 29. Continued

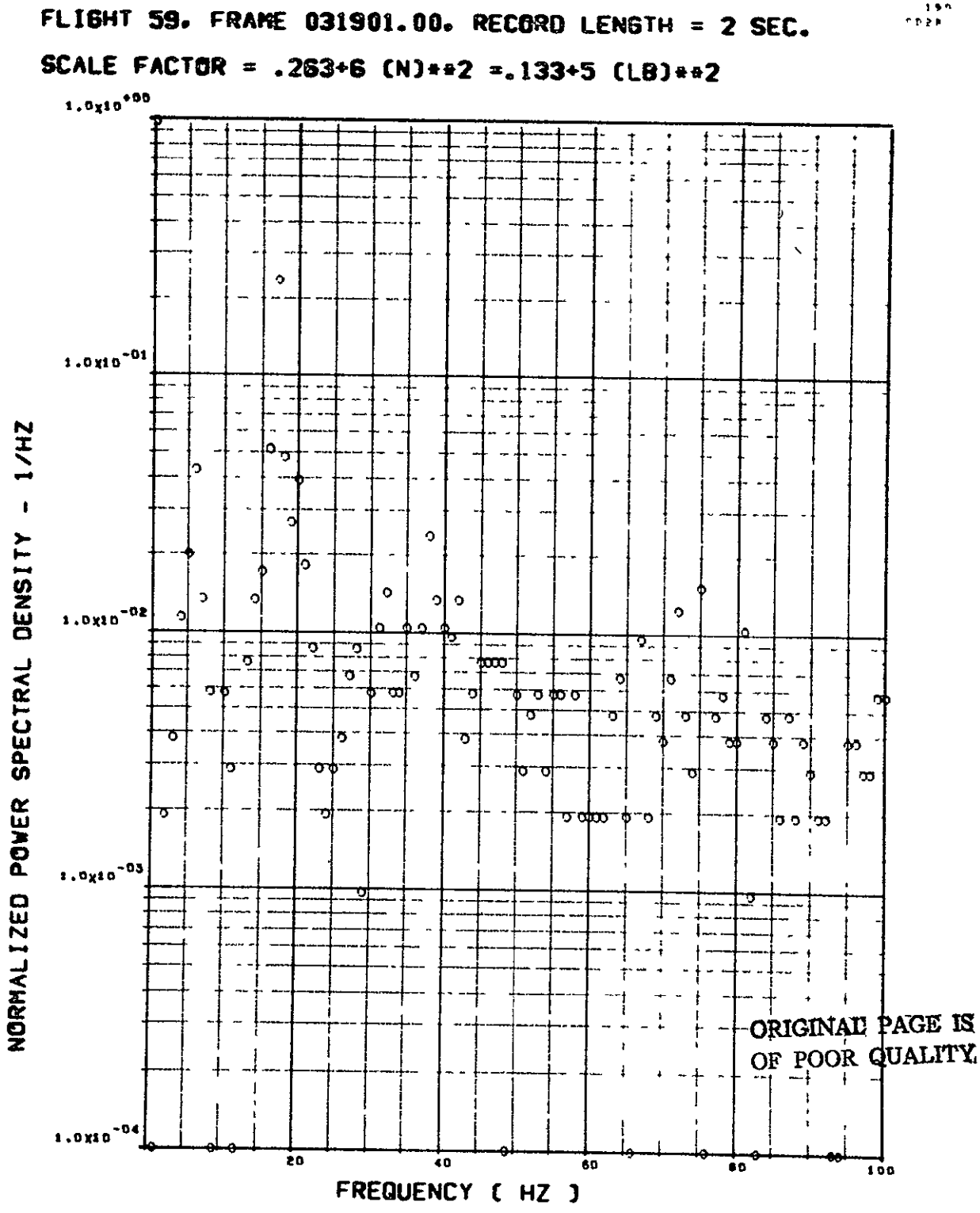

Figure 29. Continued

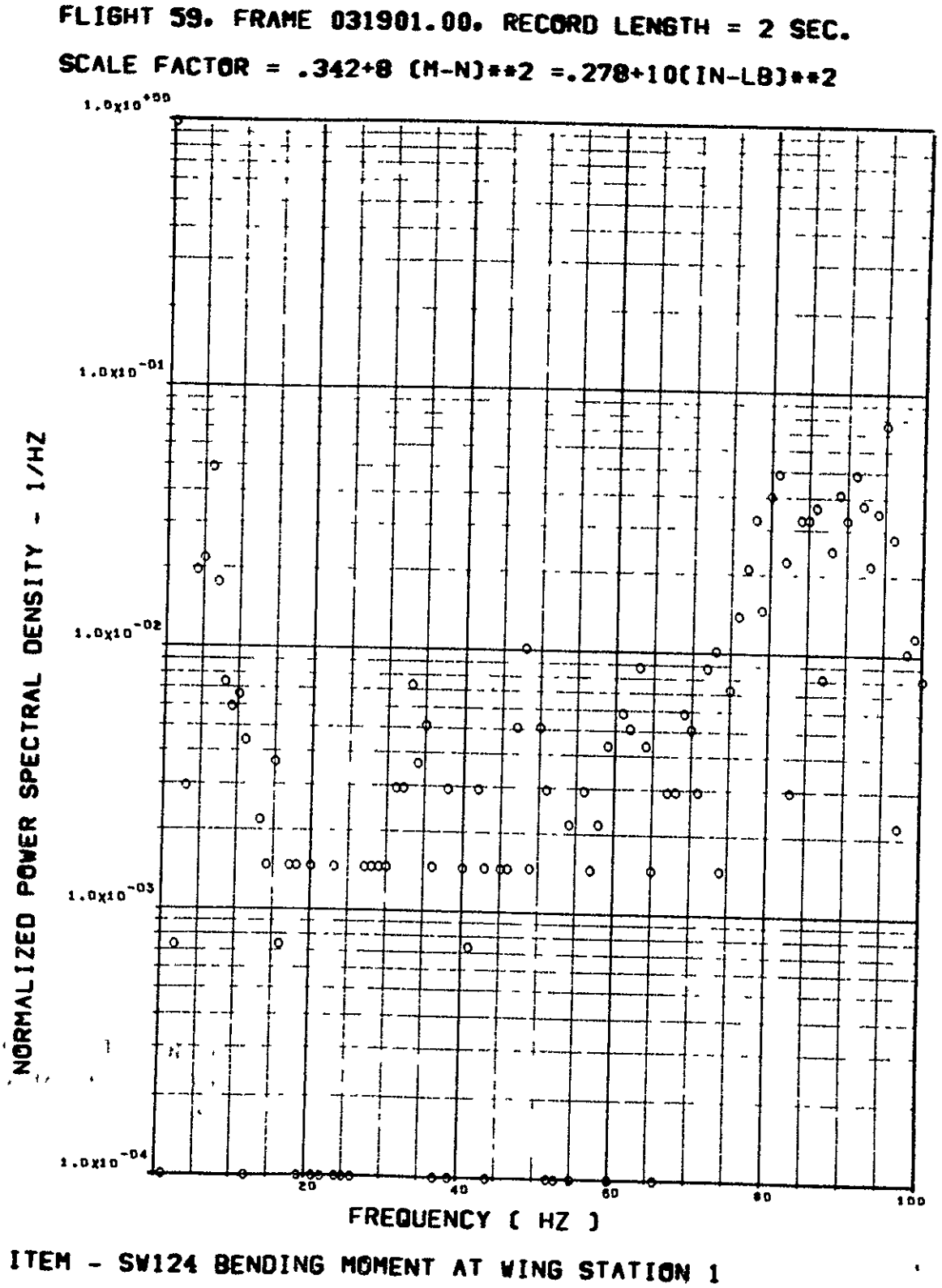

Figure 29. Continued

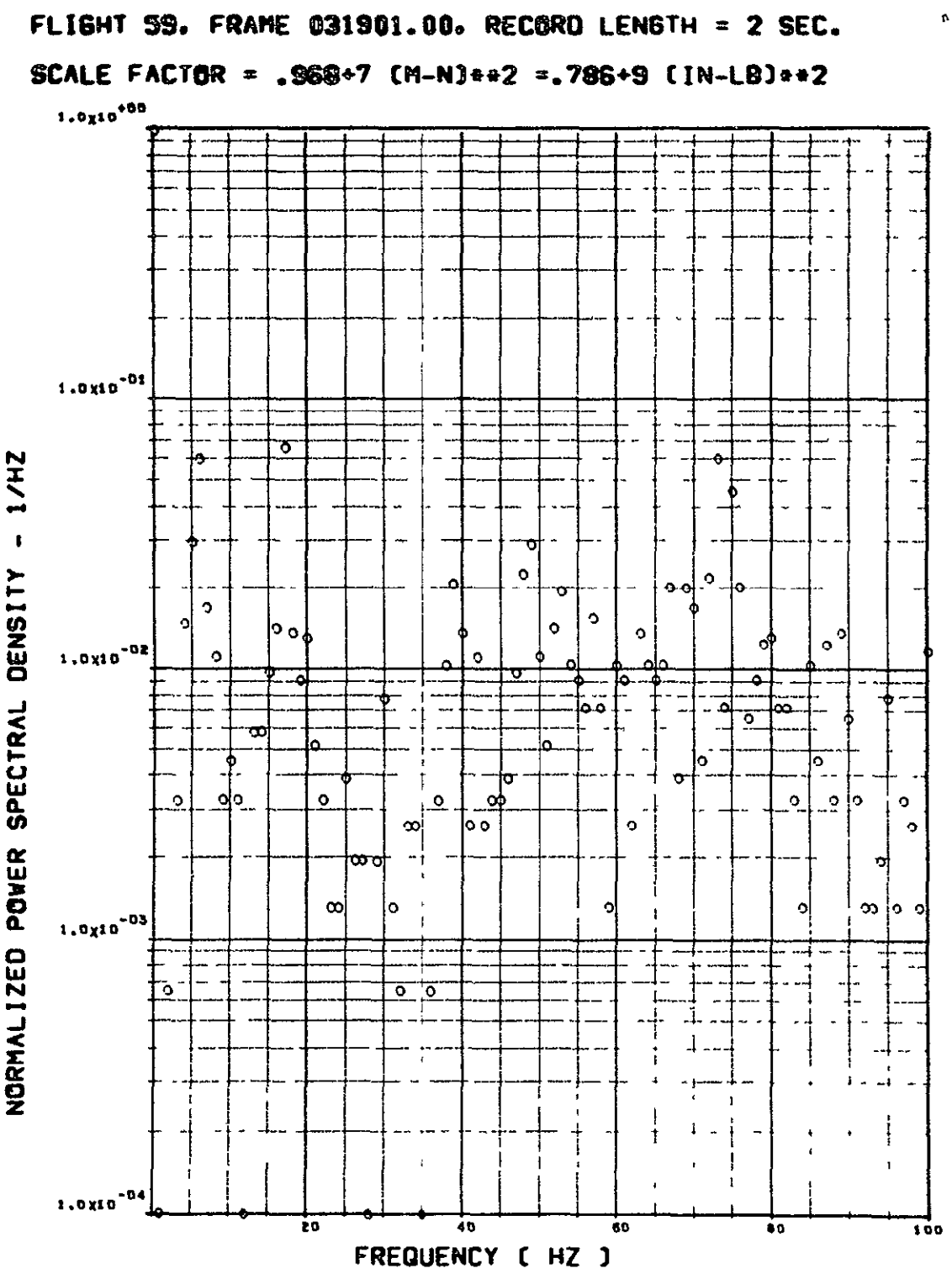

Figure 29. Continued

FLIGHT 59. FRAME 031901.00. RECORD LENGTH = 2 SEC.

SCALE FACTOR = .164+7 (M-N)**2 =.133+9 (IN-LB)**2

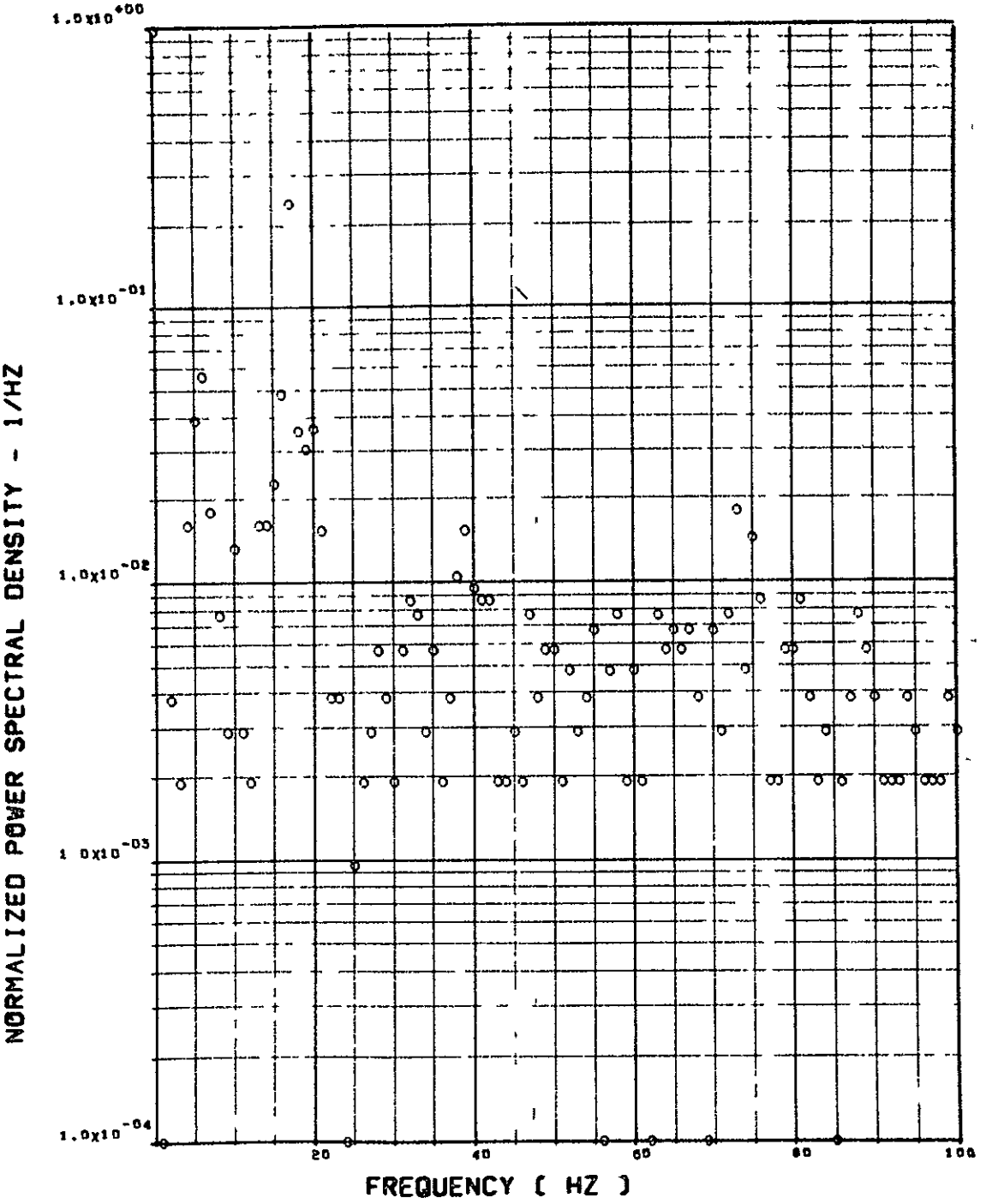

ITEM - SW130 BENDING MOMENT AT WING STATION 3

Figure 29. Continued

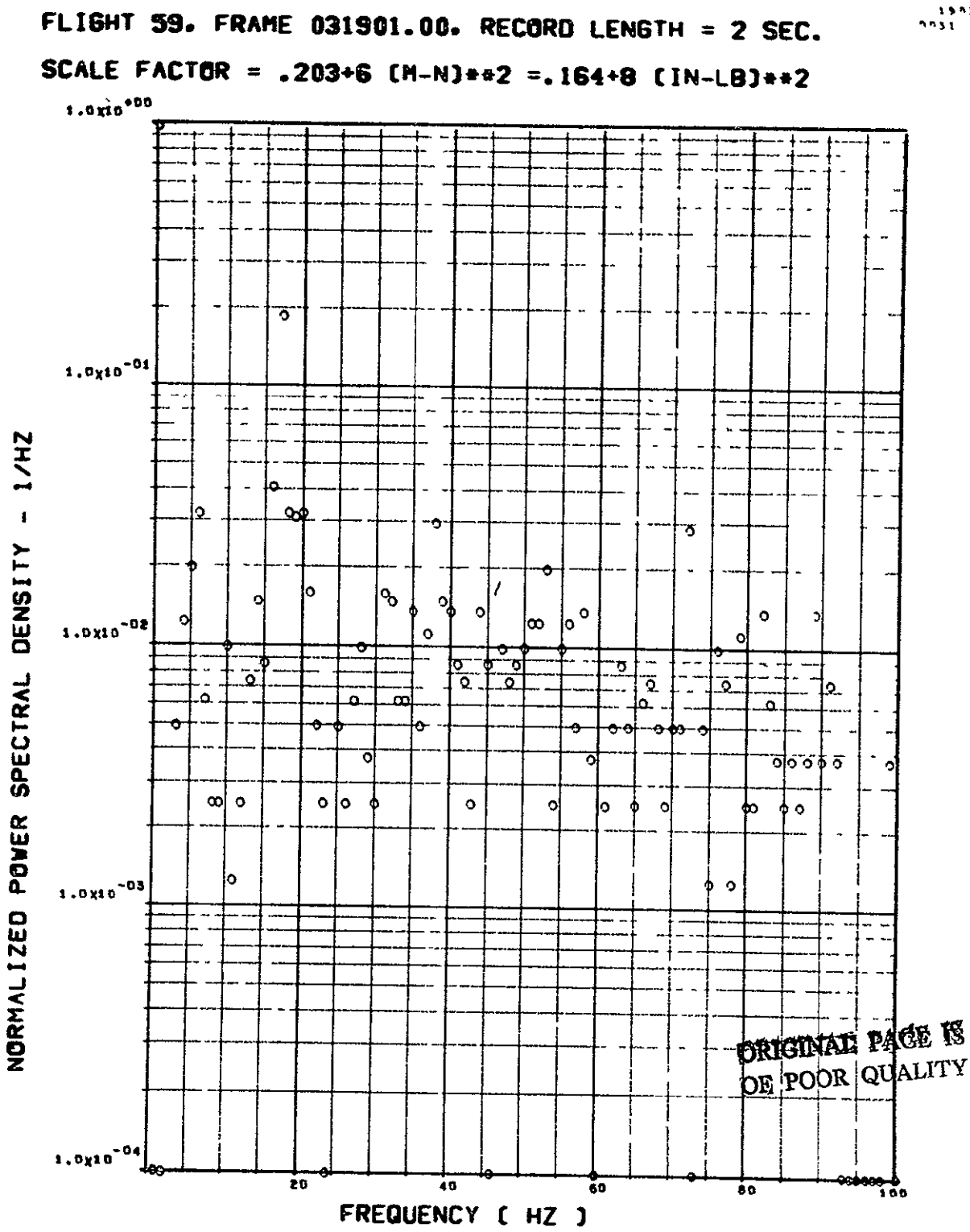

Figure 29. Continued

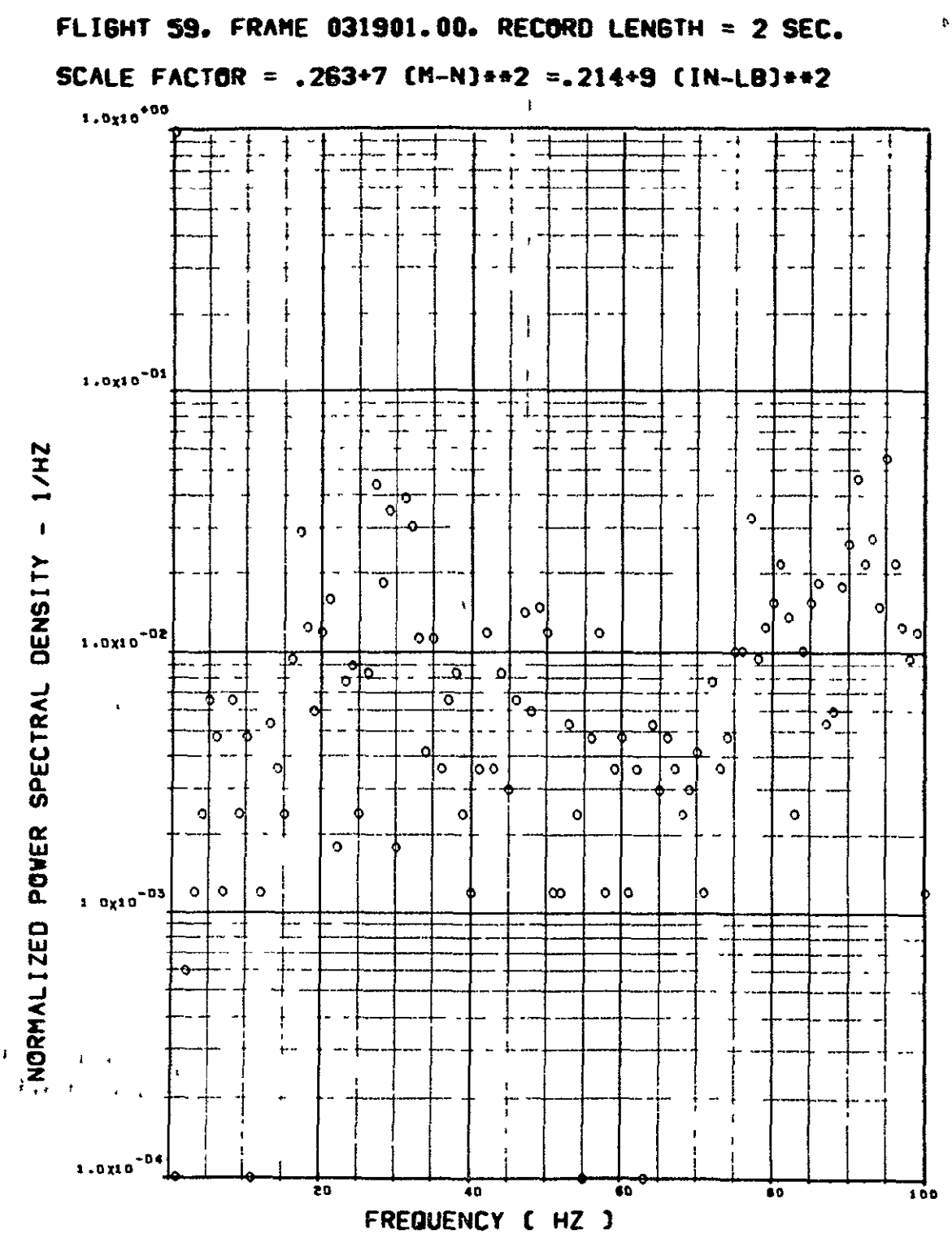

Figure 29. Continued

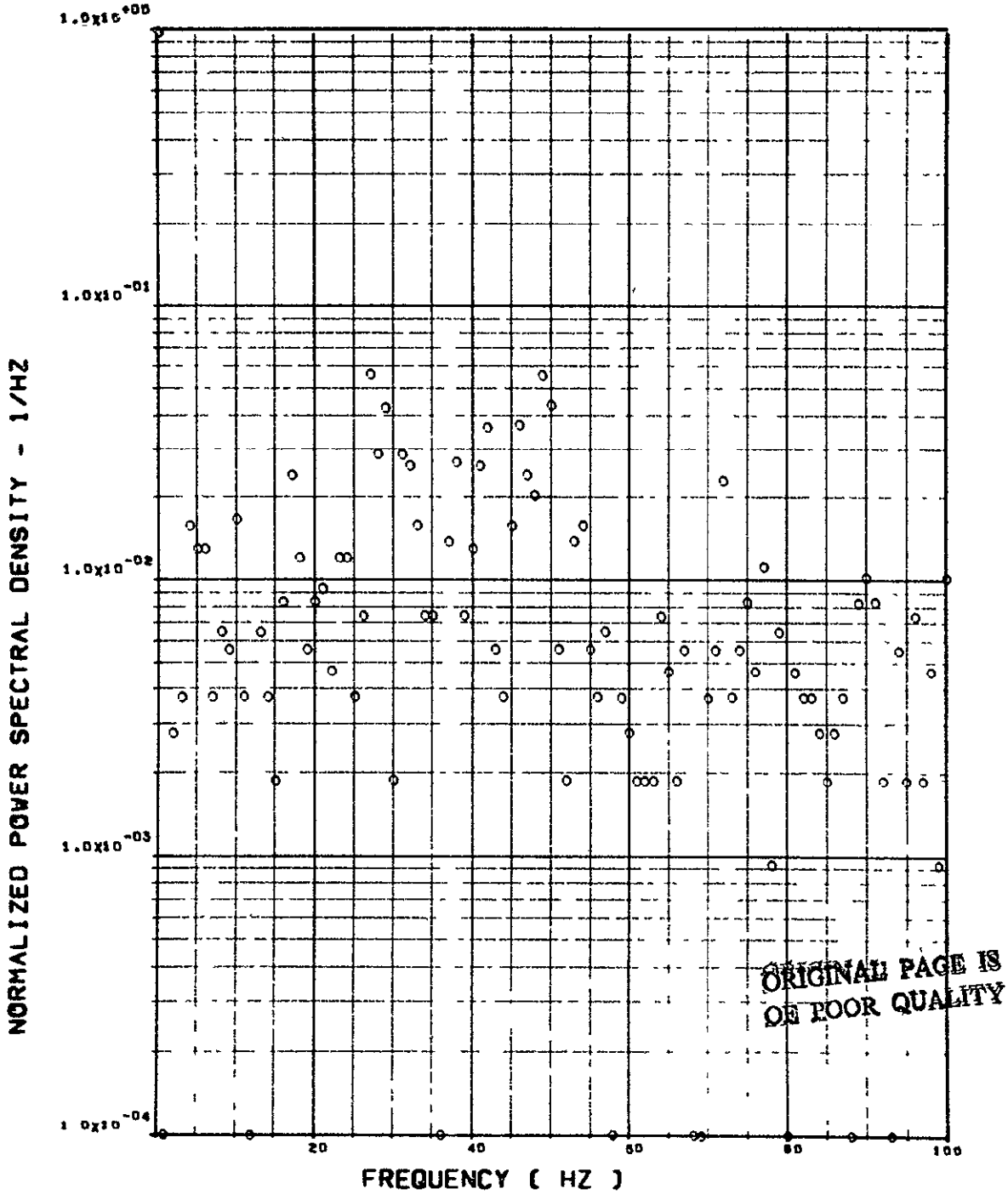

Figure 29. Continued

FLIGHT 59. FRAME 031901.00. RECORD LENGTH = 2 SEC.

SCALE FACTOR = .461+6 (M-N)**2 =.374+8 (IN-LB)**2

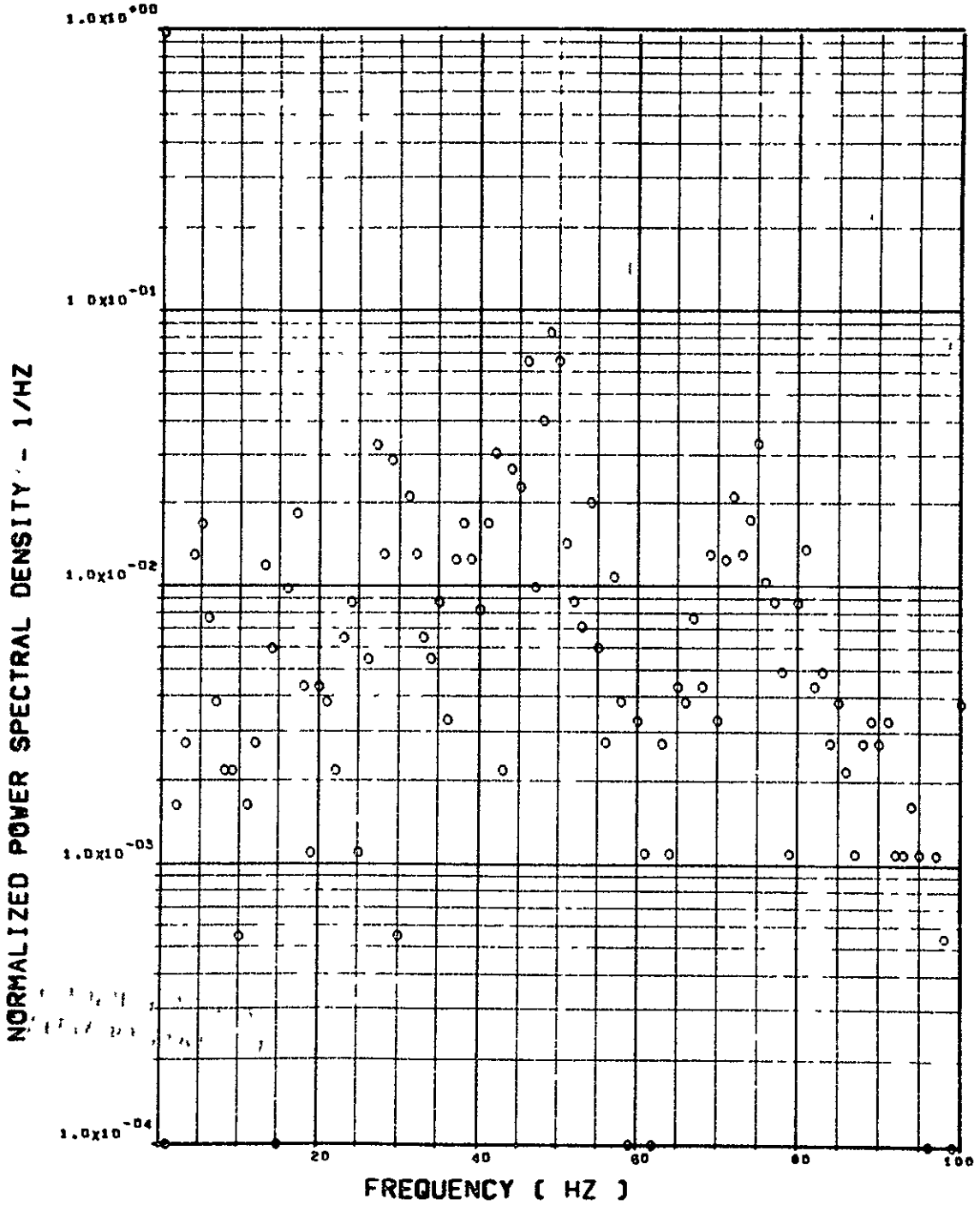

ITEM - SW131 TORSION AT WING STATION 3

Figure 29. Continued

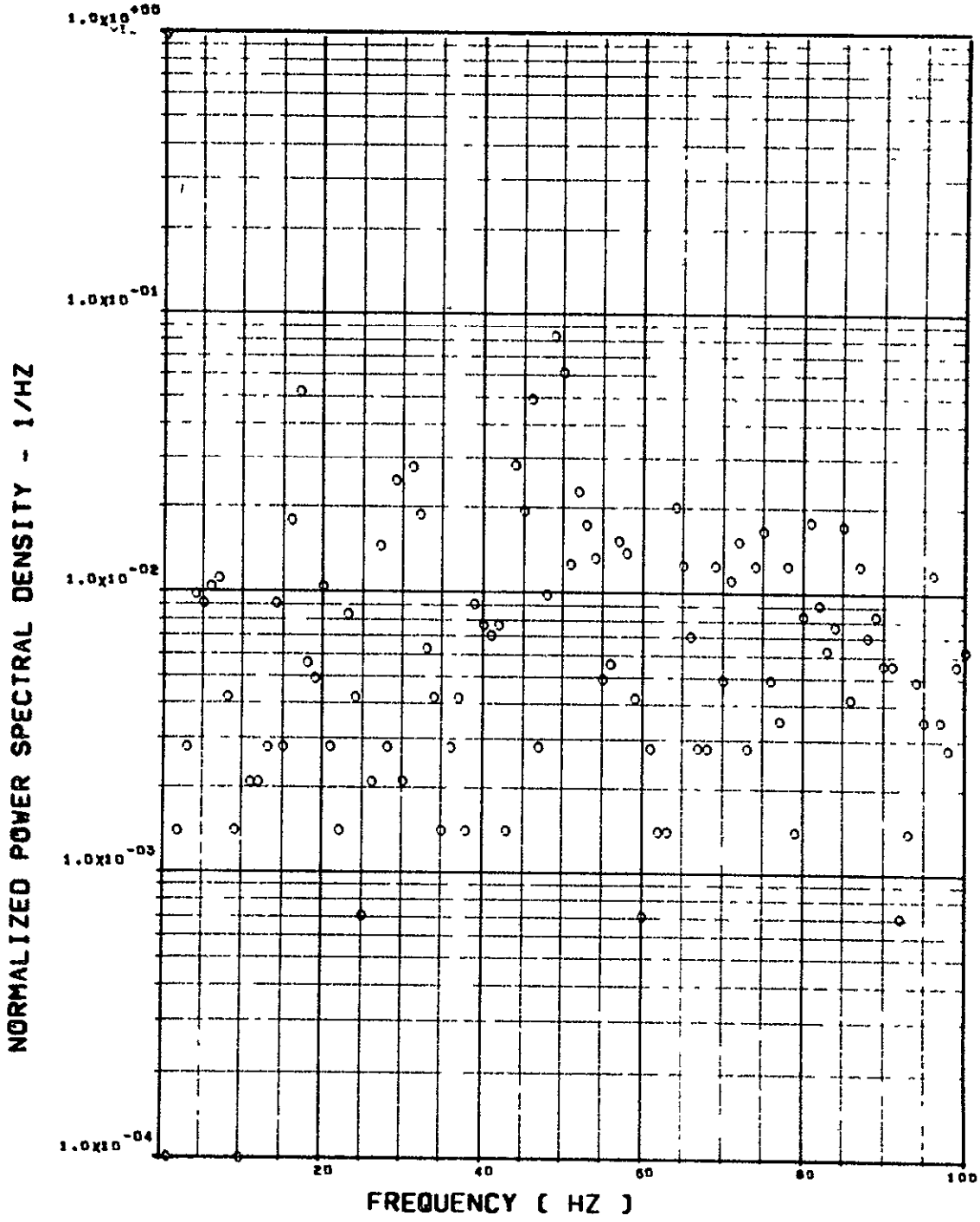

Figure 29. Continued

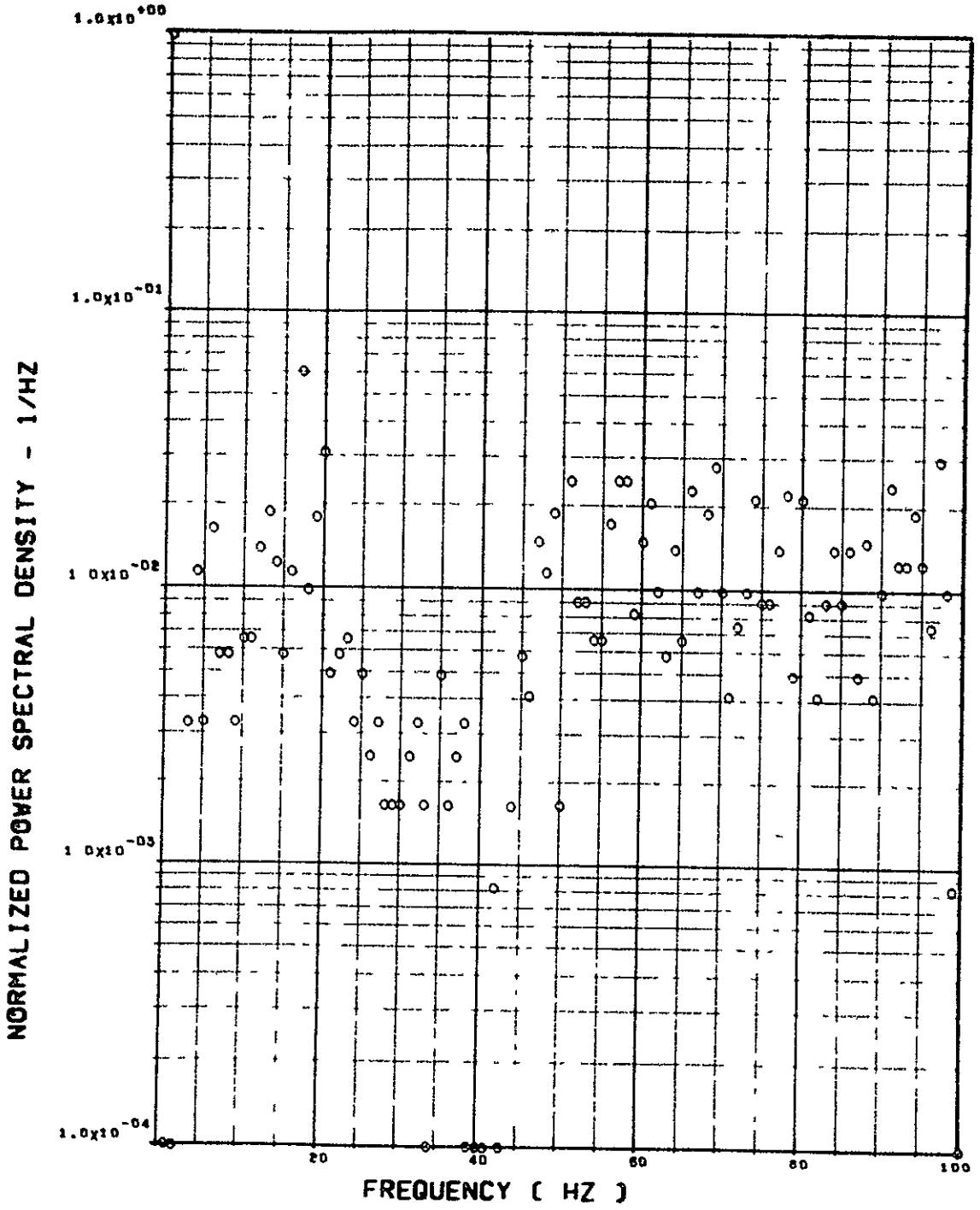

Figure 29. Continued

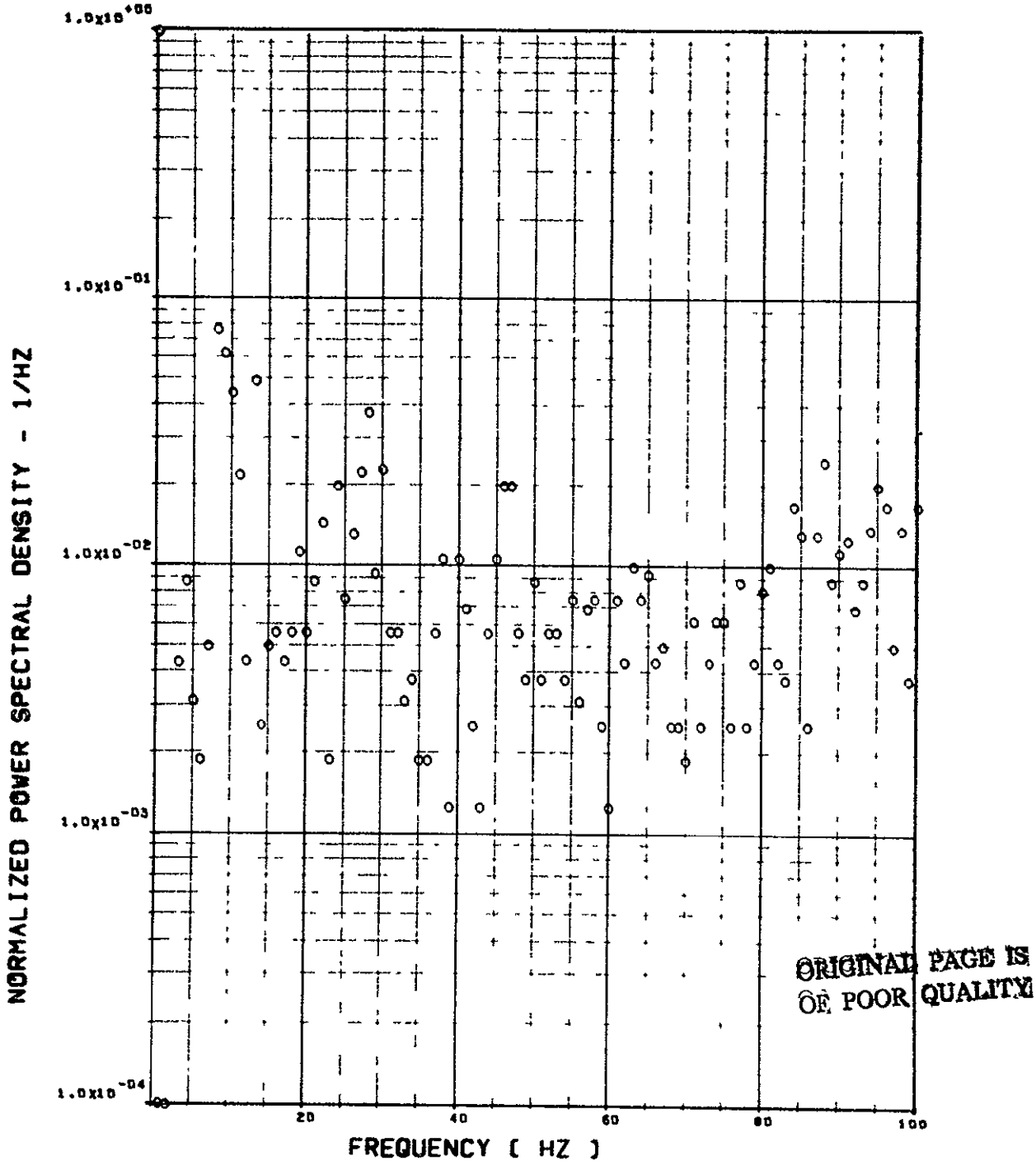

Figure 29. Continued

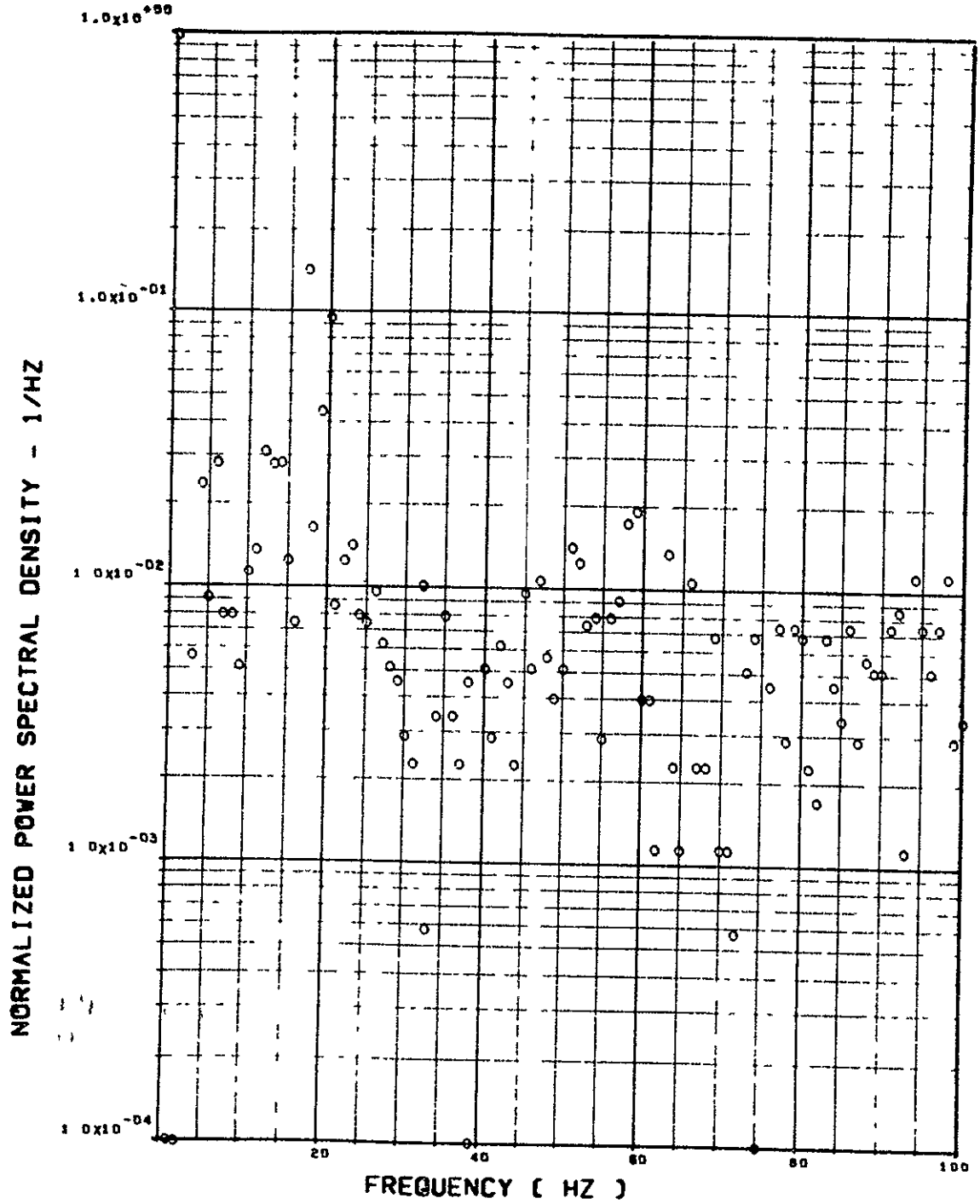

Figure 29. Continued

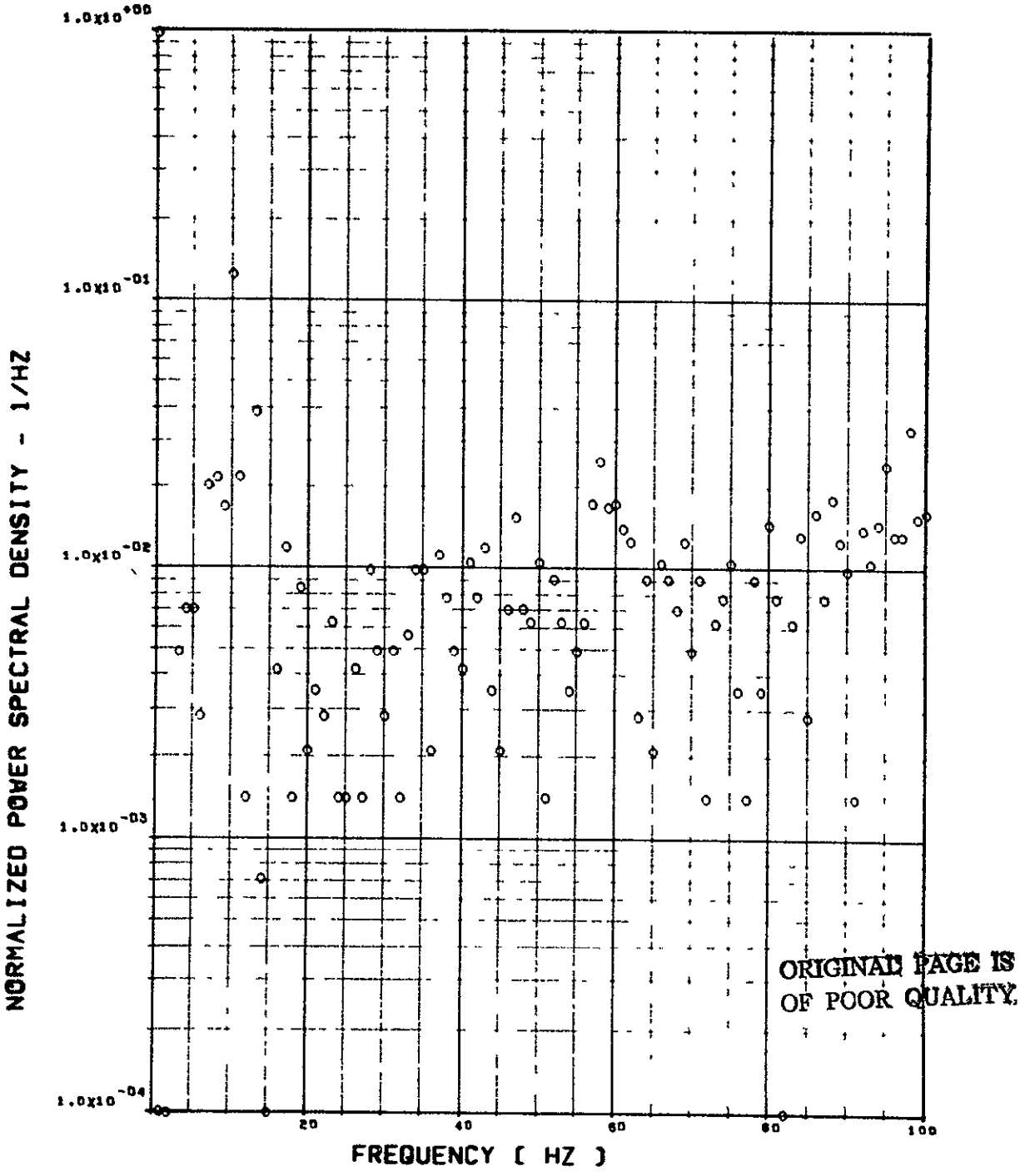

Figure 29. Continued

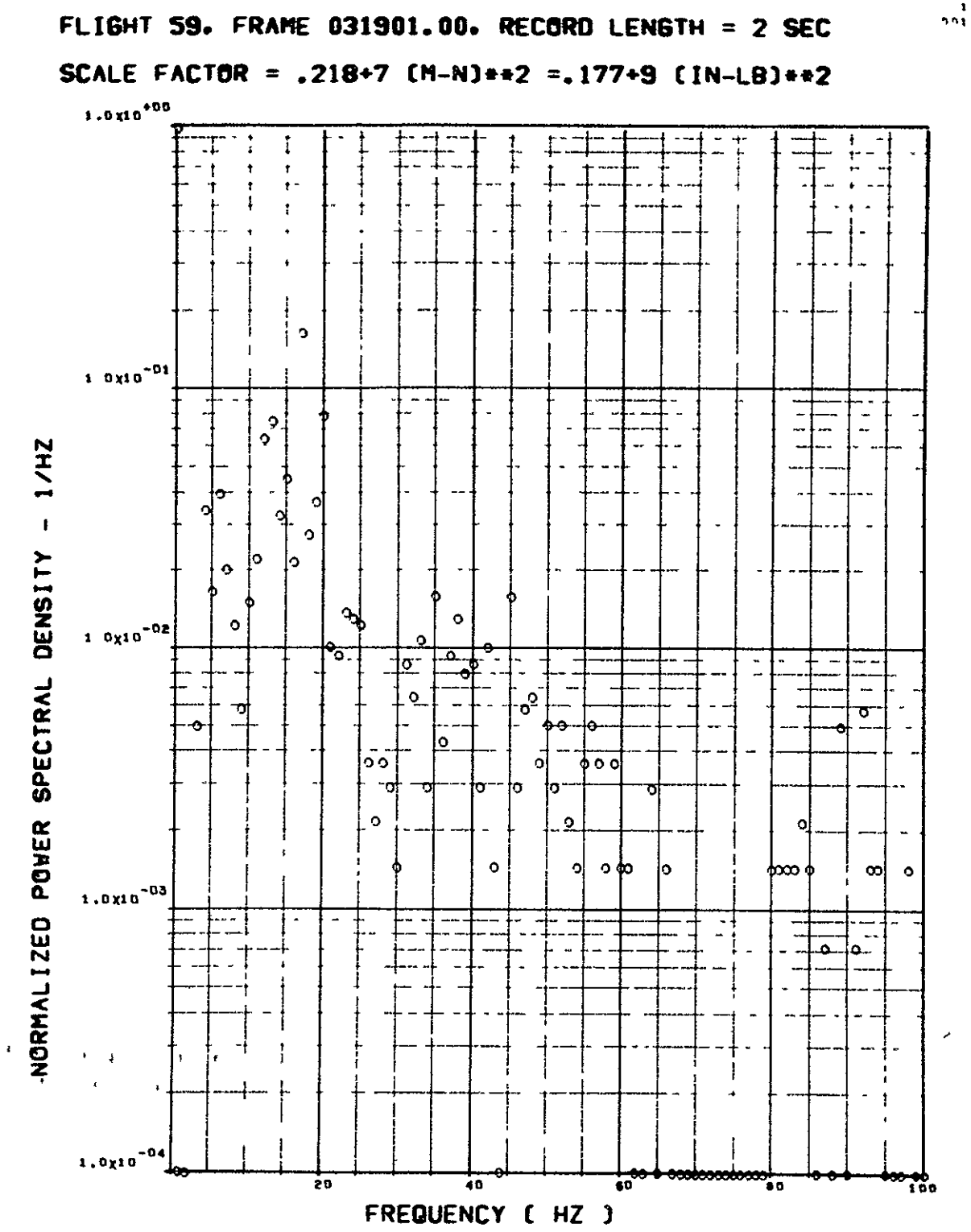

Figure 29. Continued

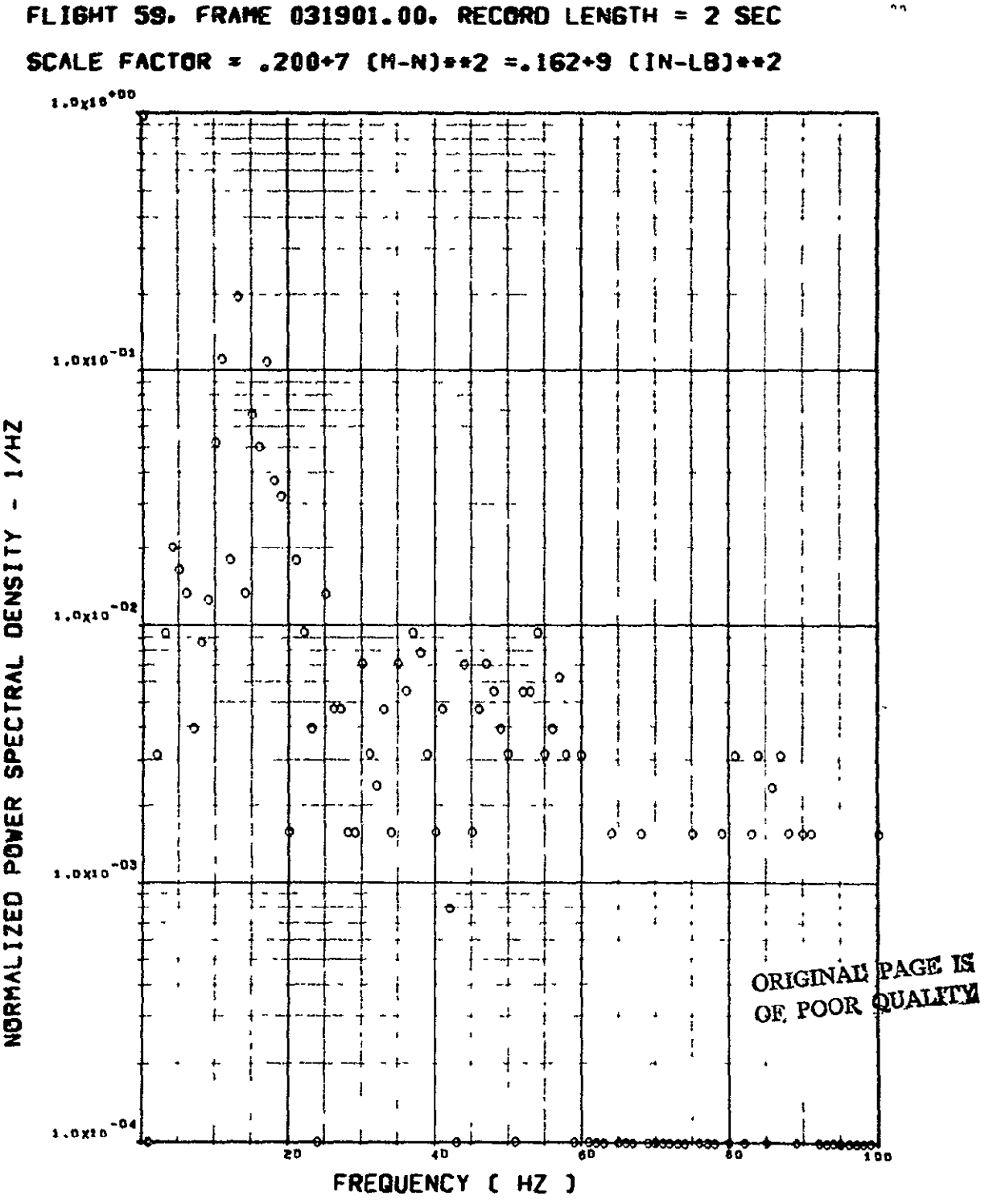

Figure 29. Concluded

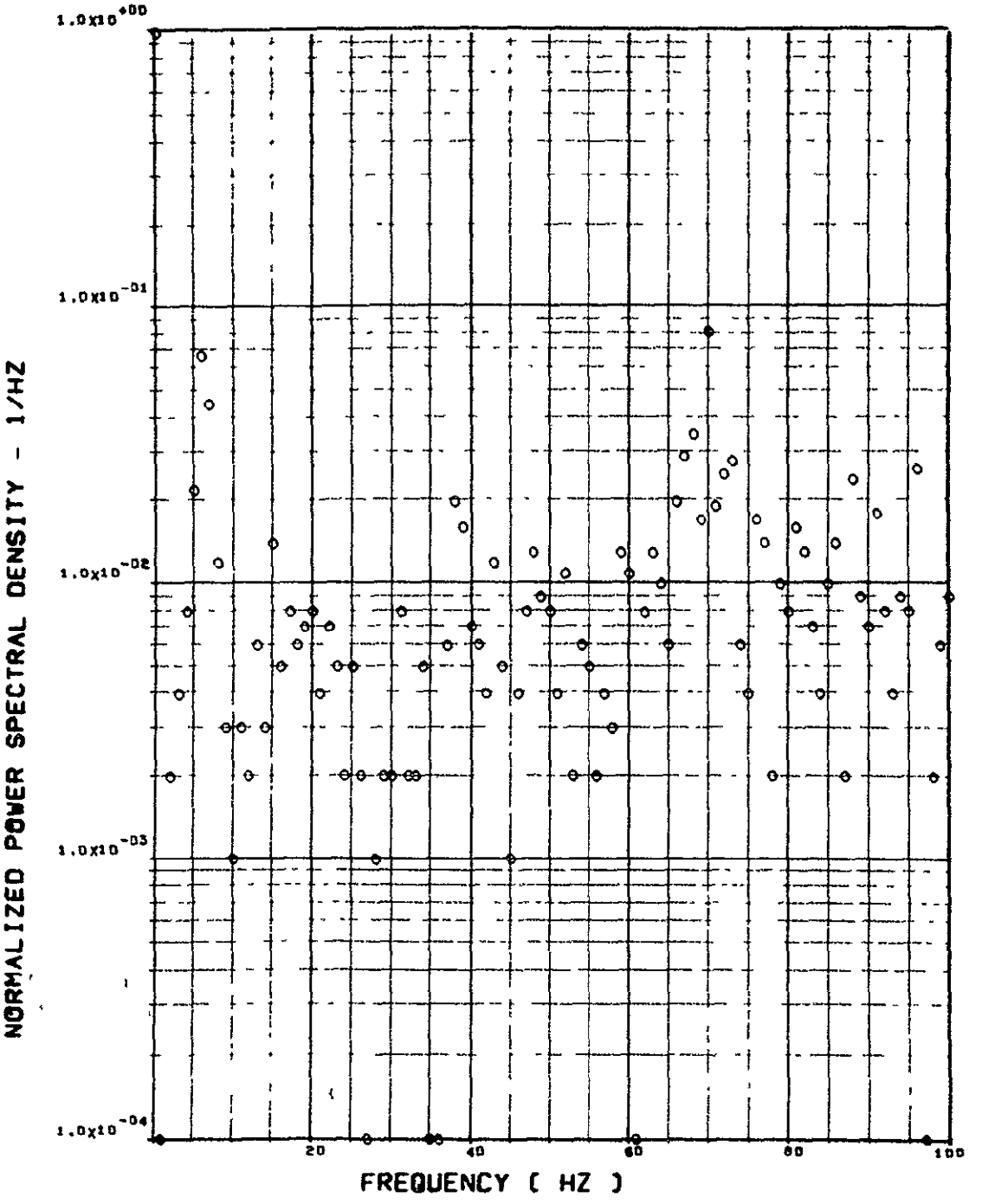

Figure 30. Power Spectra - Flight 59, Run S132R, Point 2 T_1 = 31903.0, ΔT = 2 Sec, α_{Nom} = 17.75 deg, $\Delta\alpha$= 0.63 deg

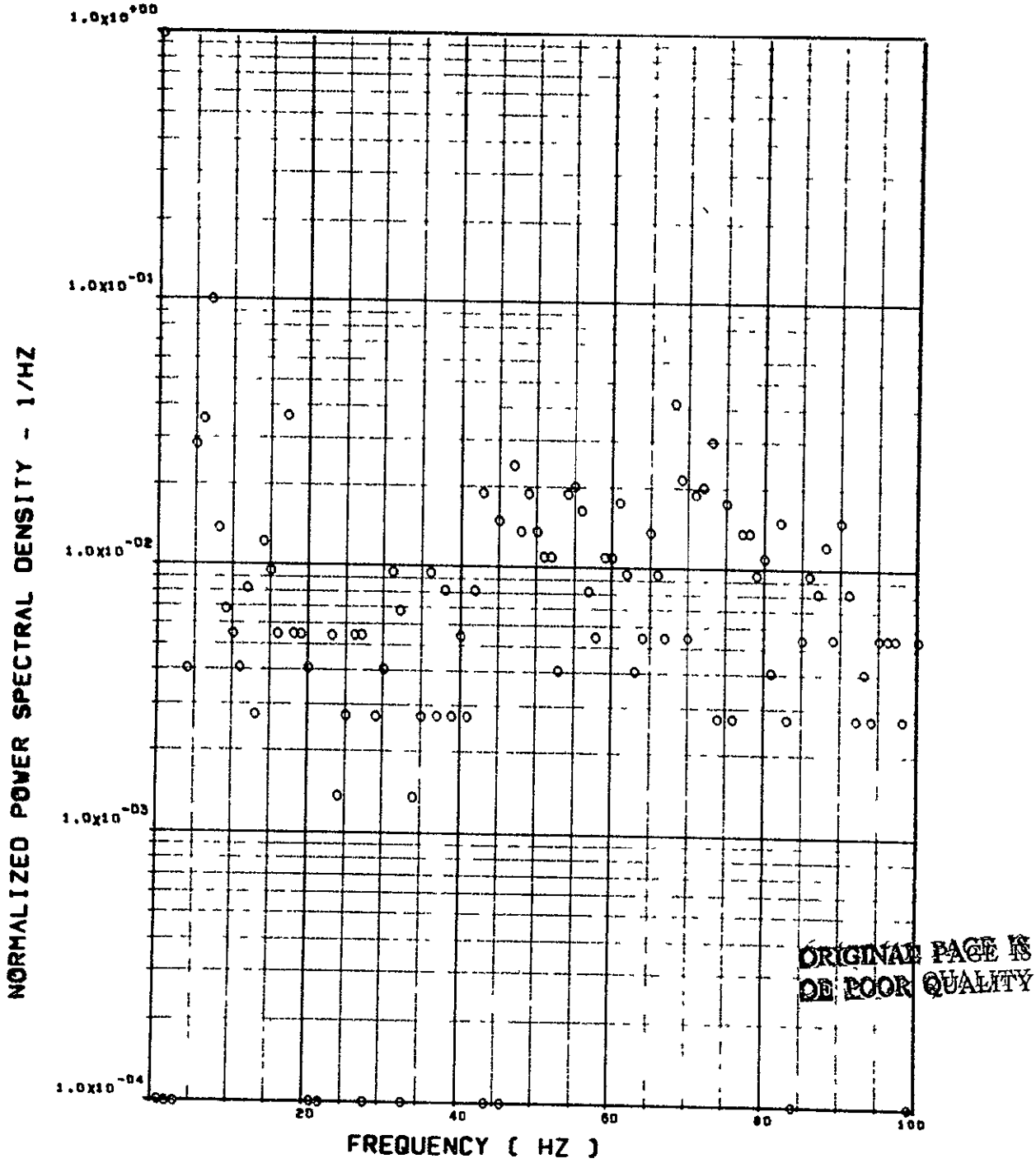

Figure 30. Continued

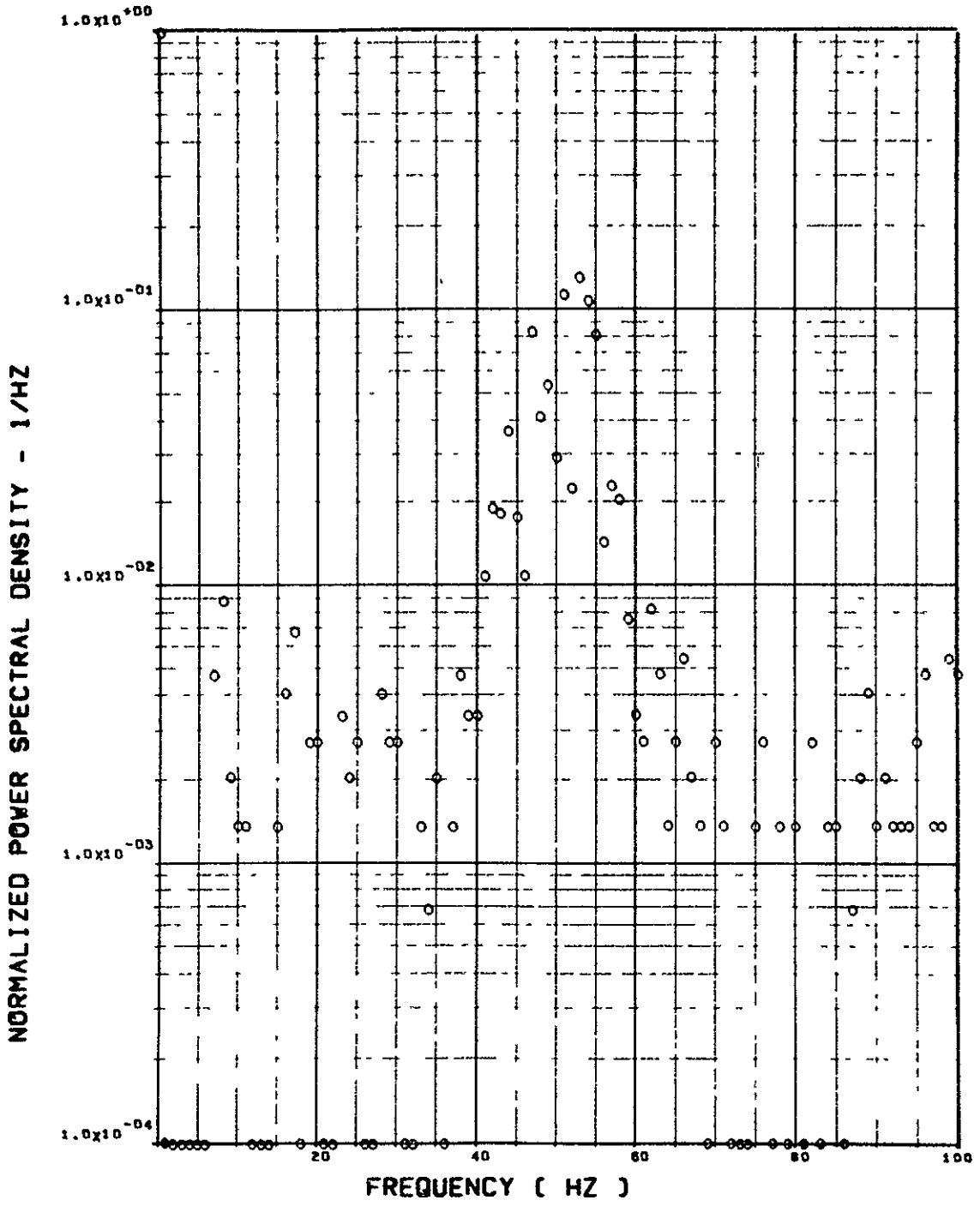

Figure 50. Continued

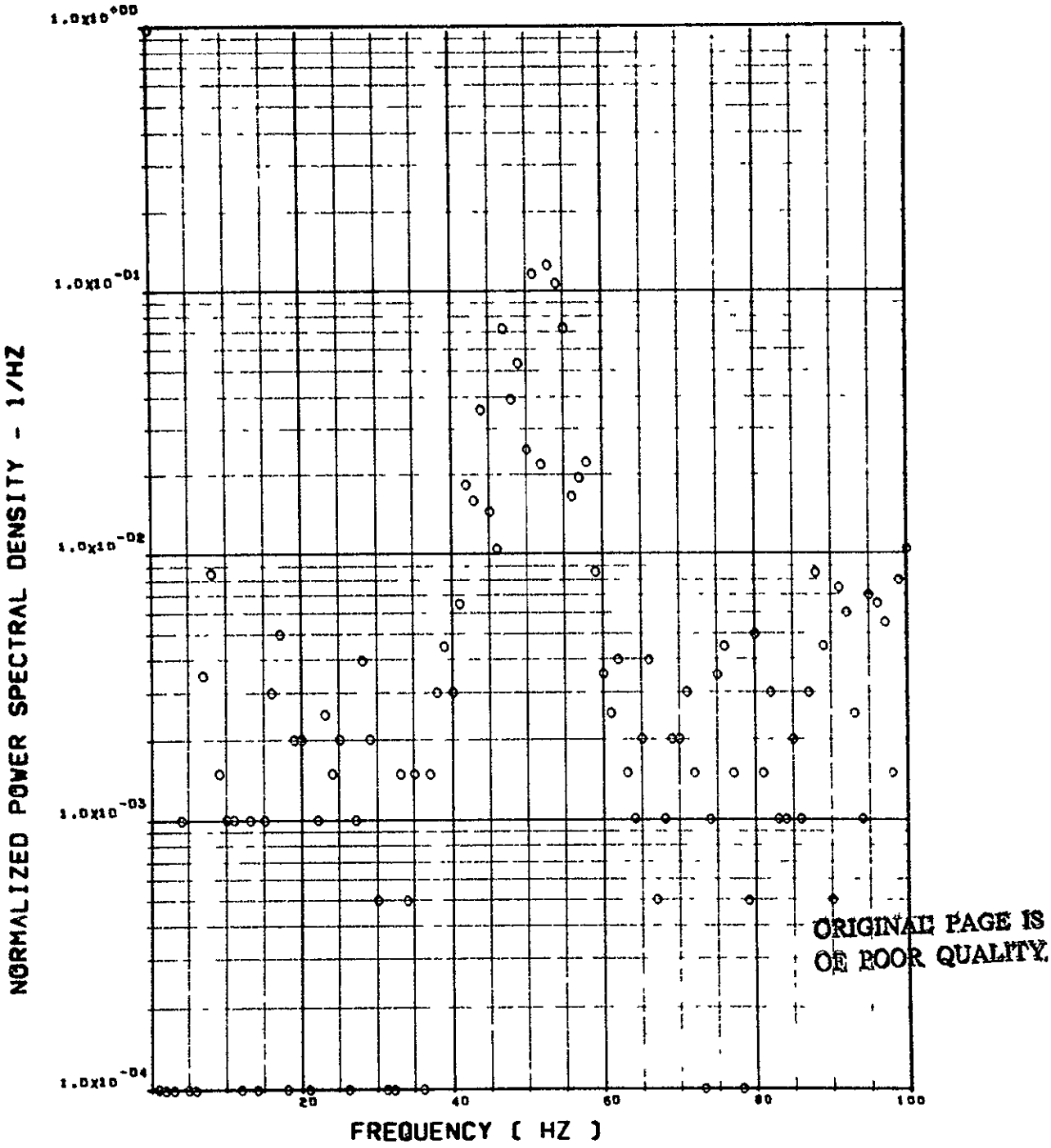

Figure 30. Continued

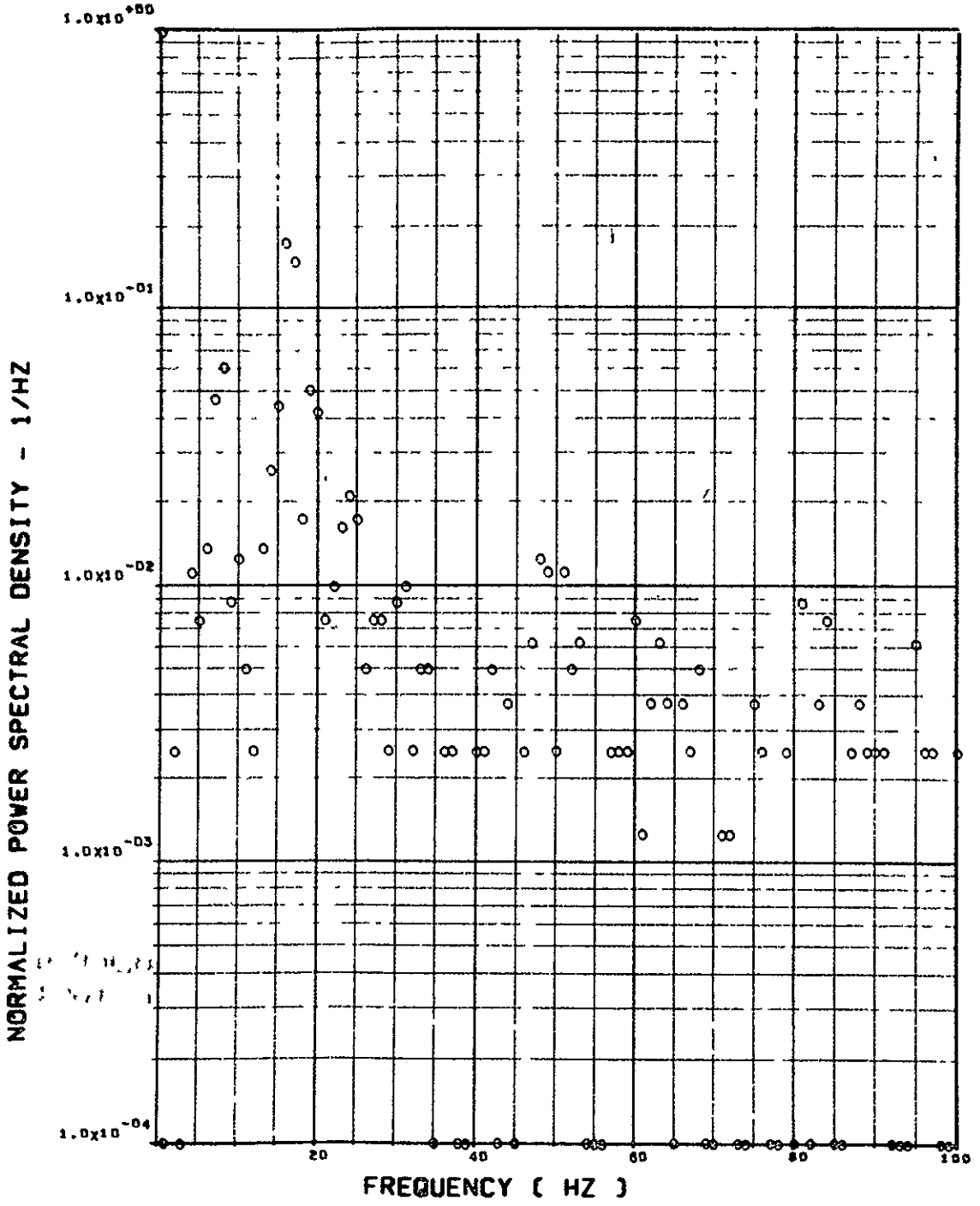

Figure 30. Continued

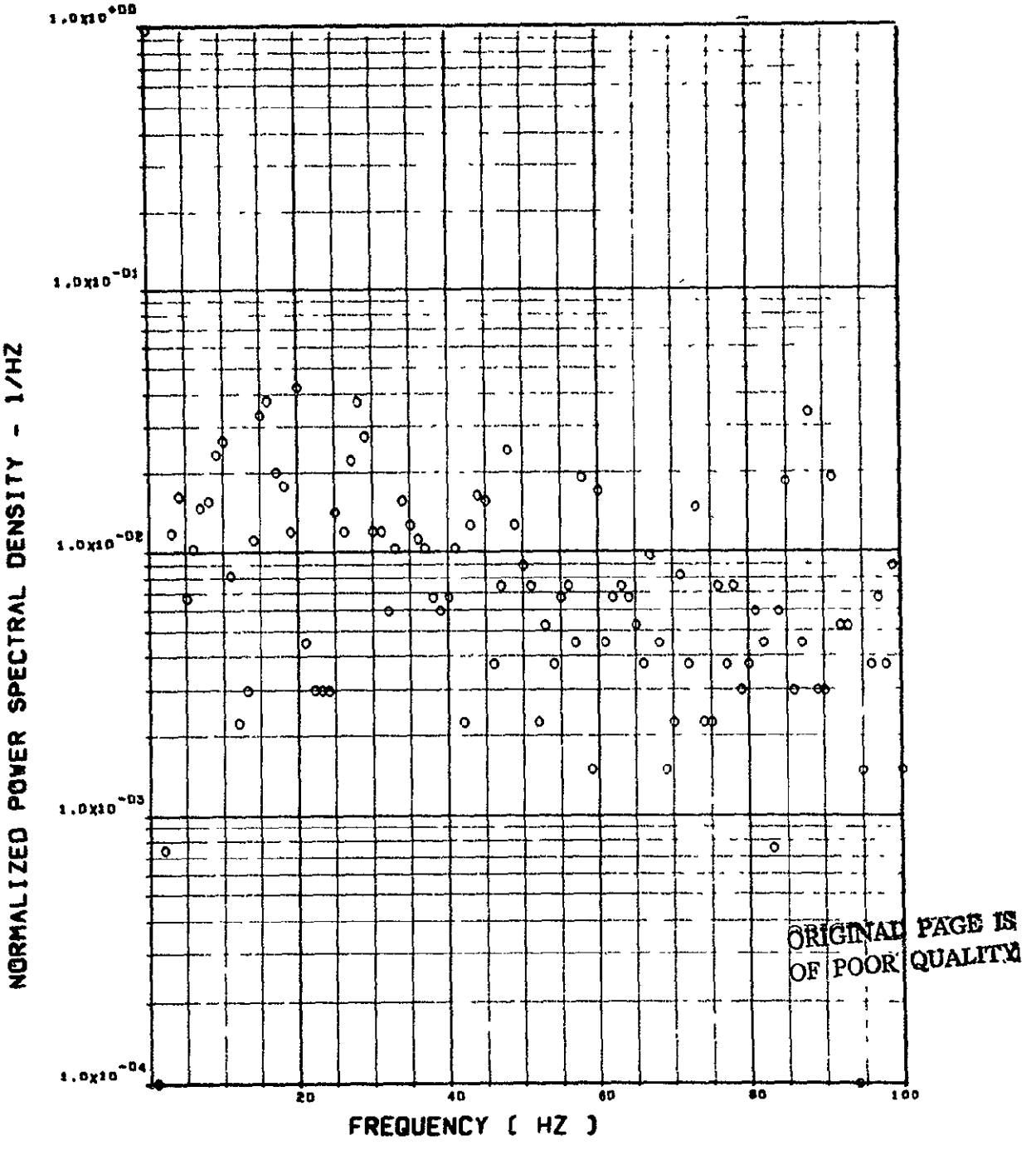

Figure 30. Continued

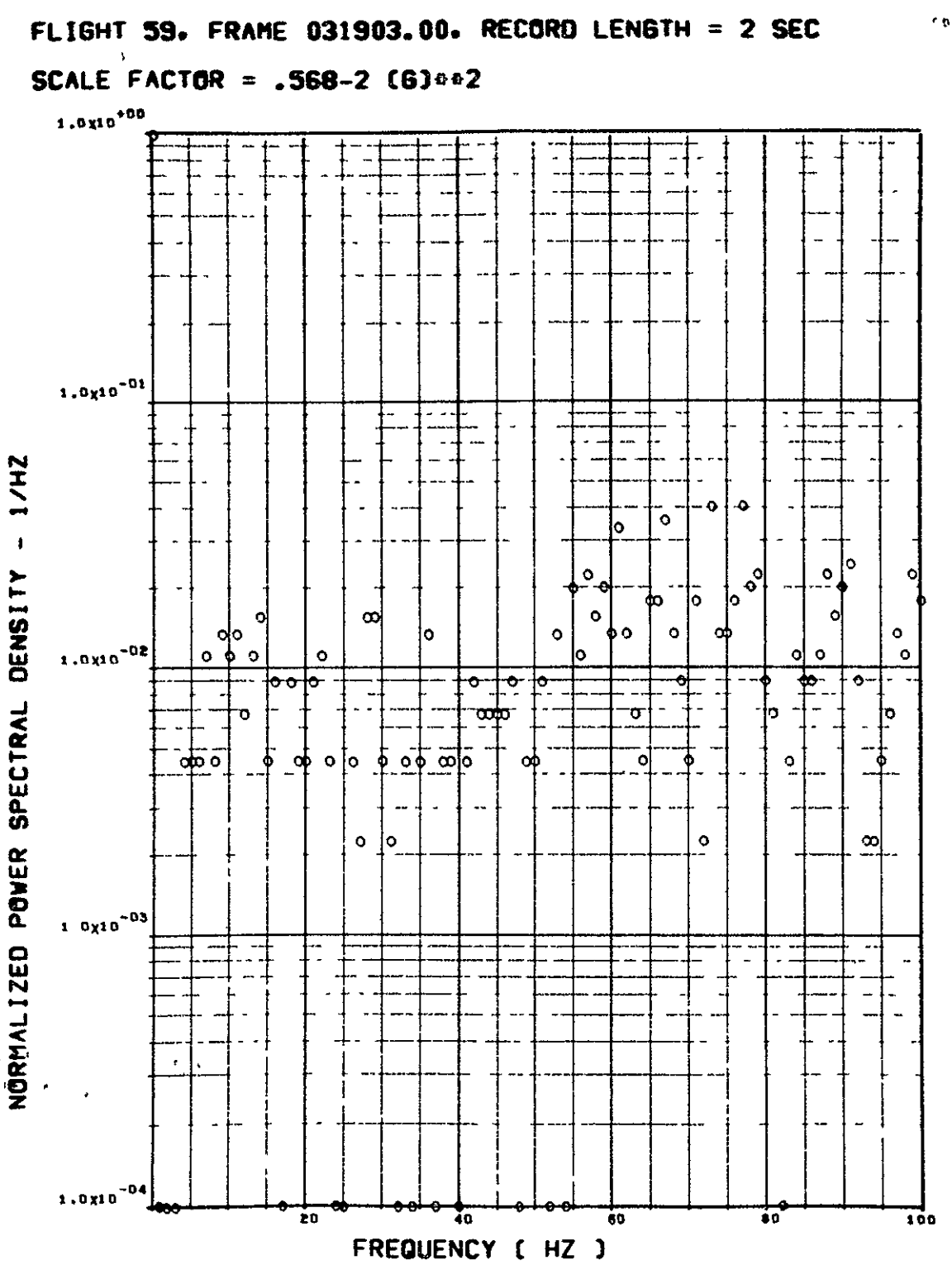

Figure 50. Continued

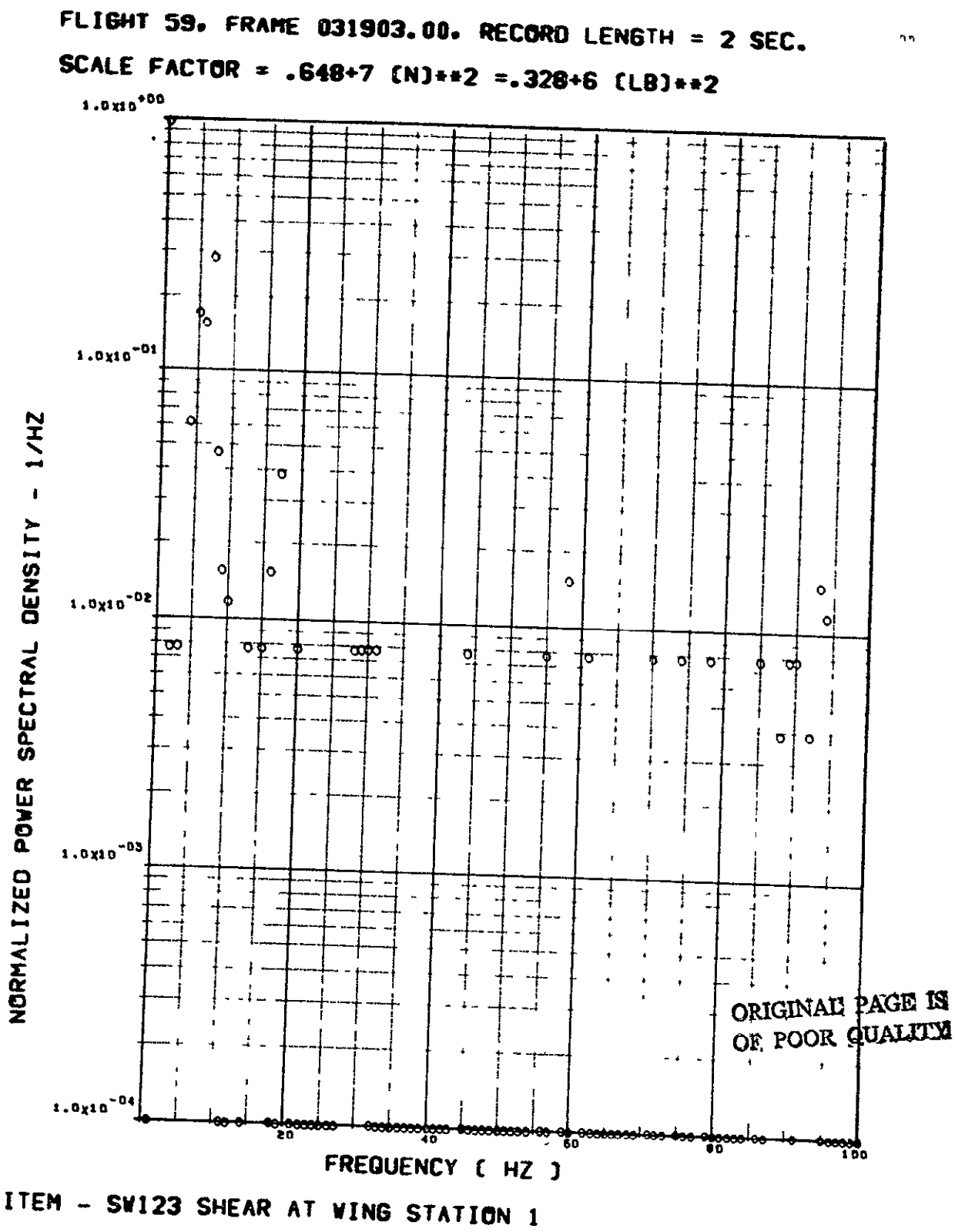

Figure 30. Continued

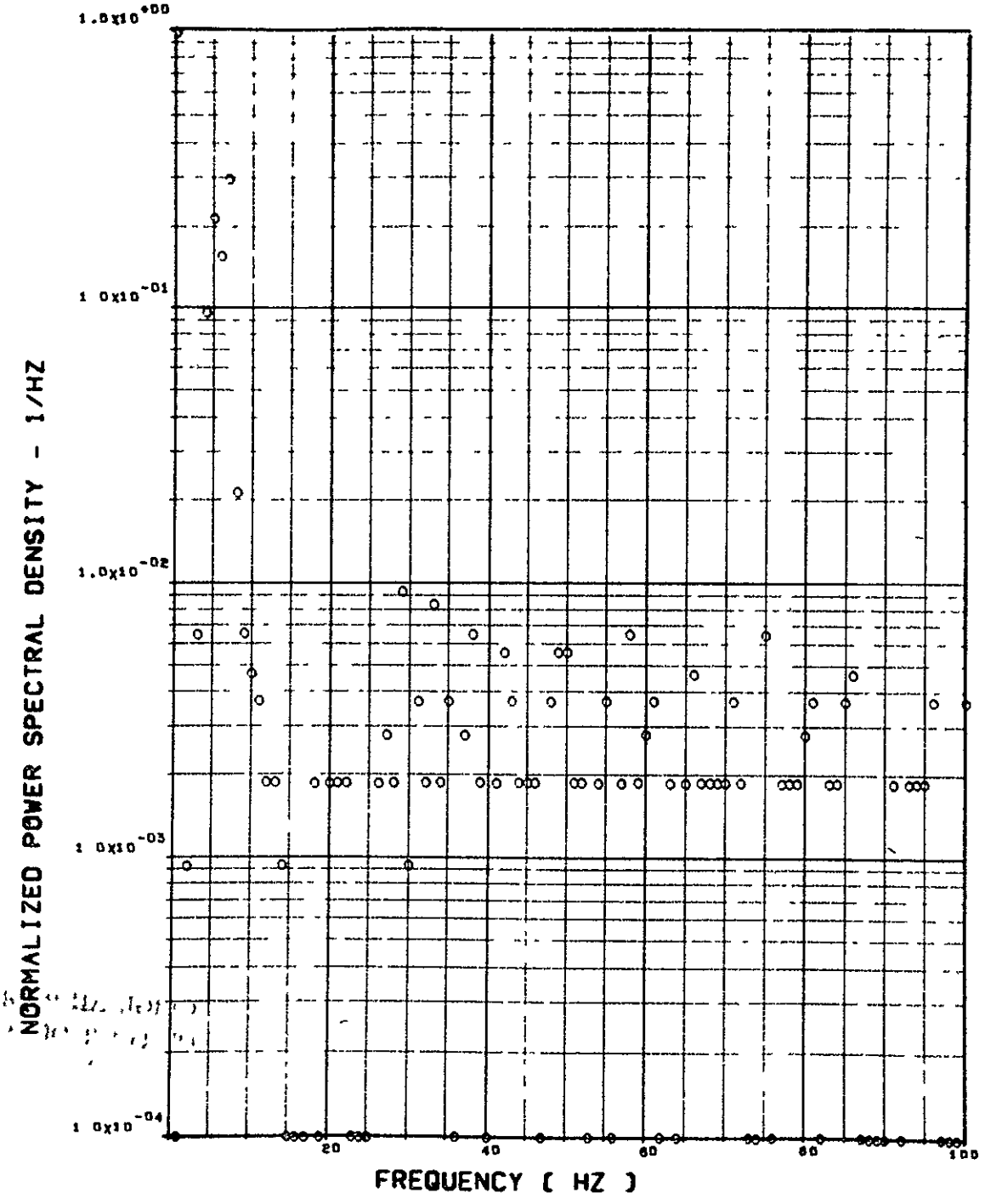

Figure 30. Continued

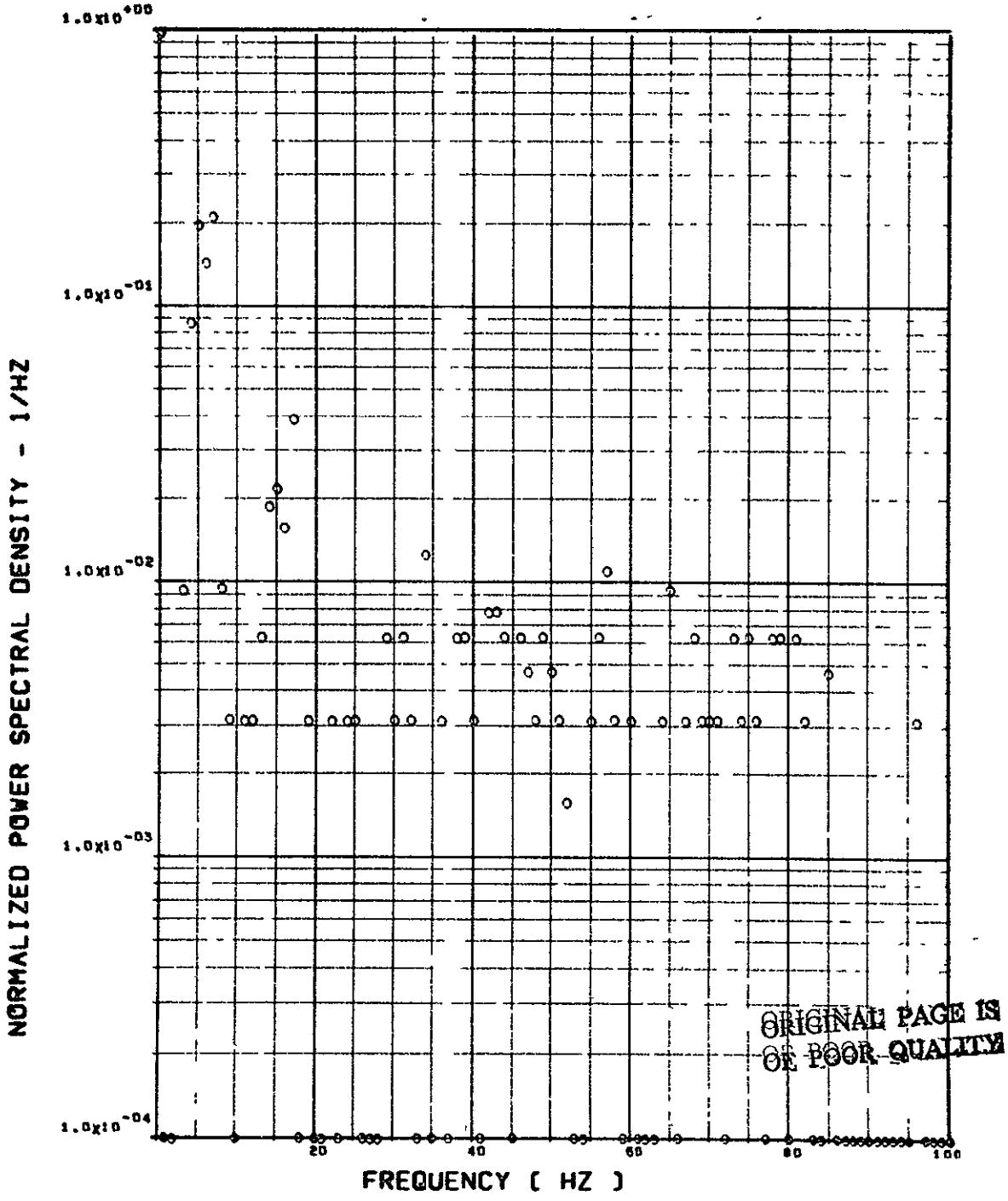

Figure 30. Continued

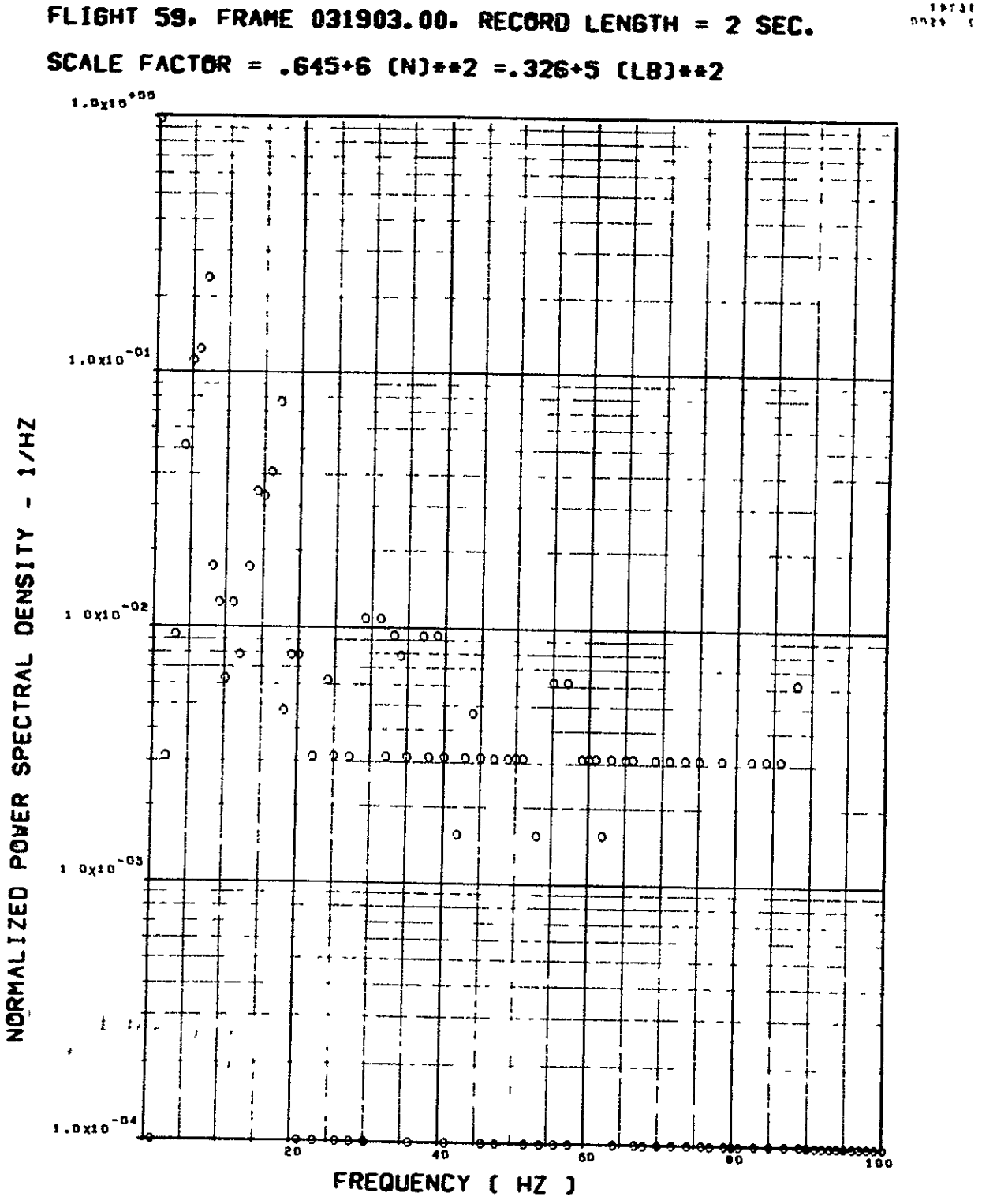

Figure 30. Continued

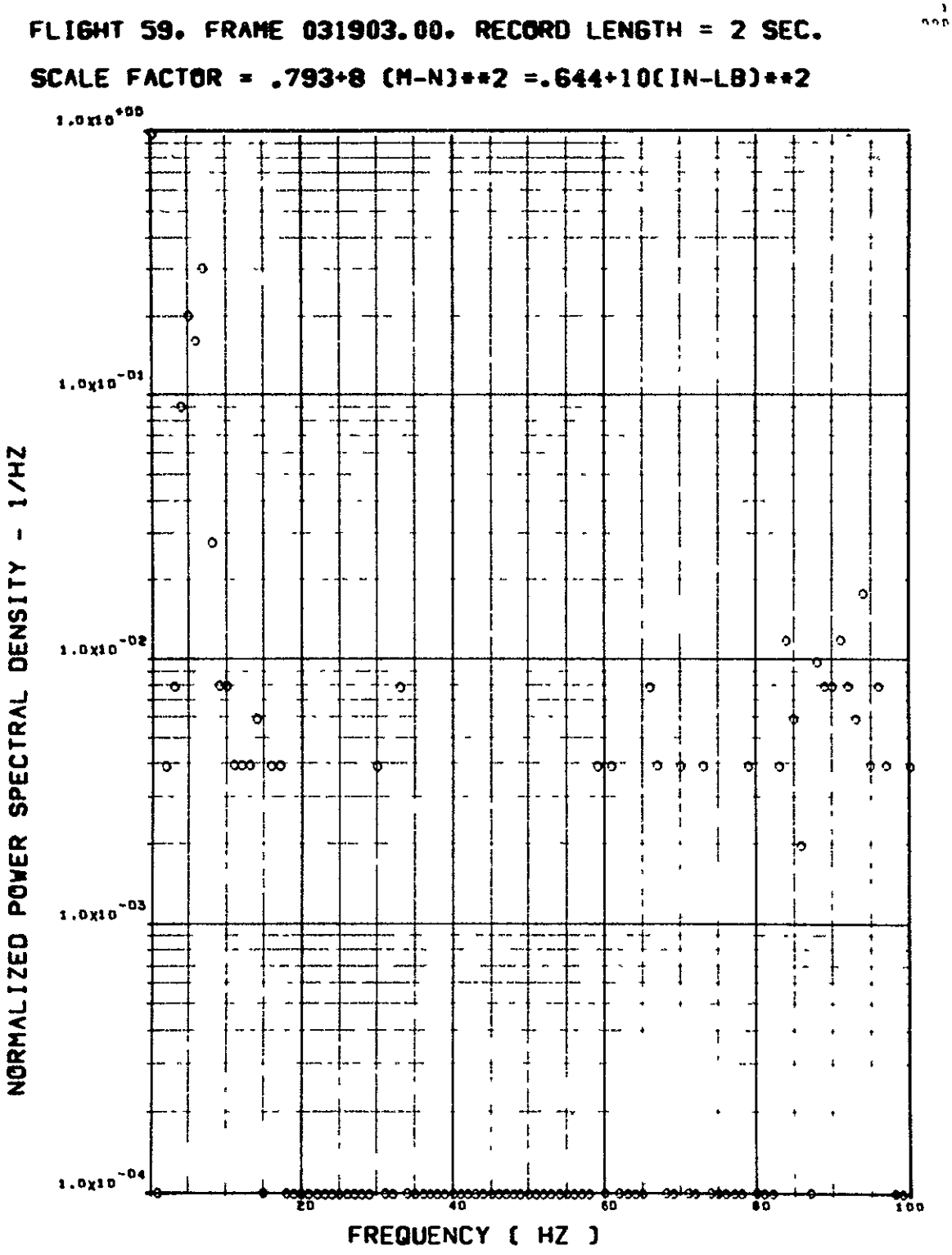

Figure 30. Continued

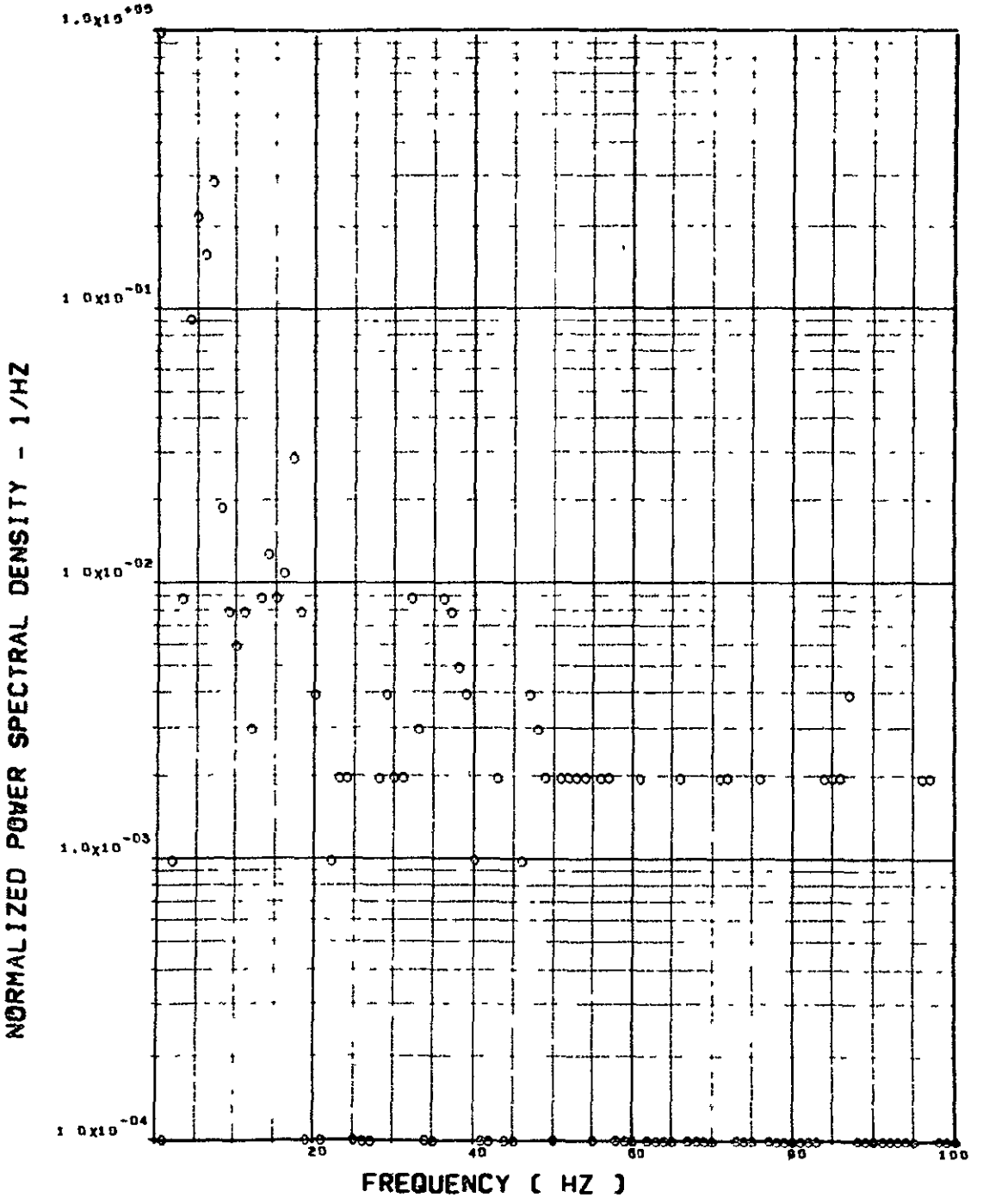

Figure 30. Continued

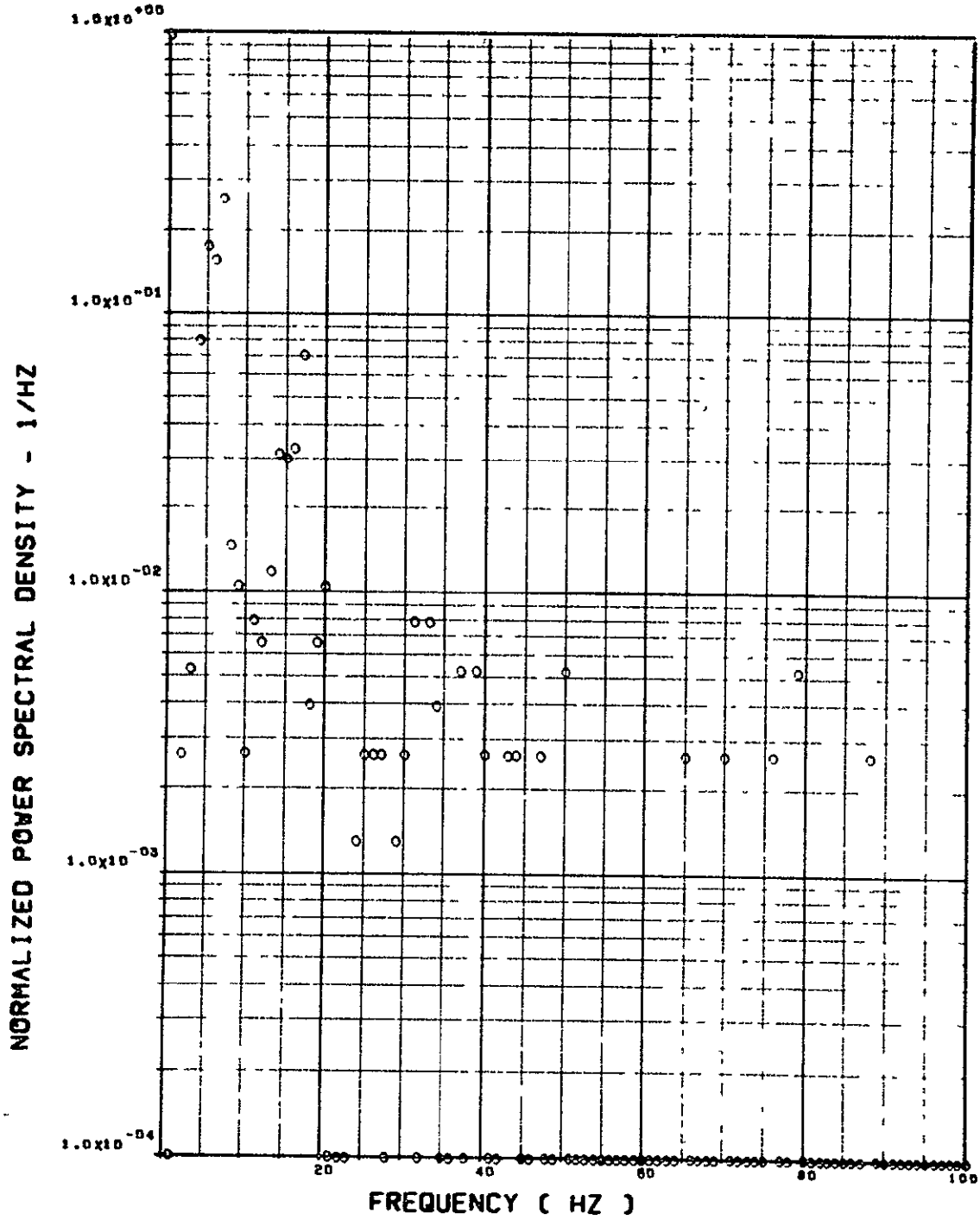

Figure 50. Continued

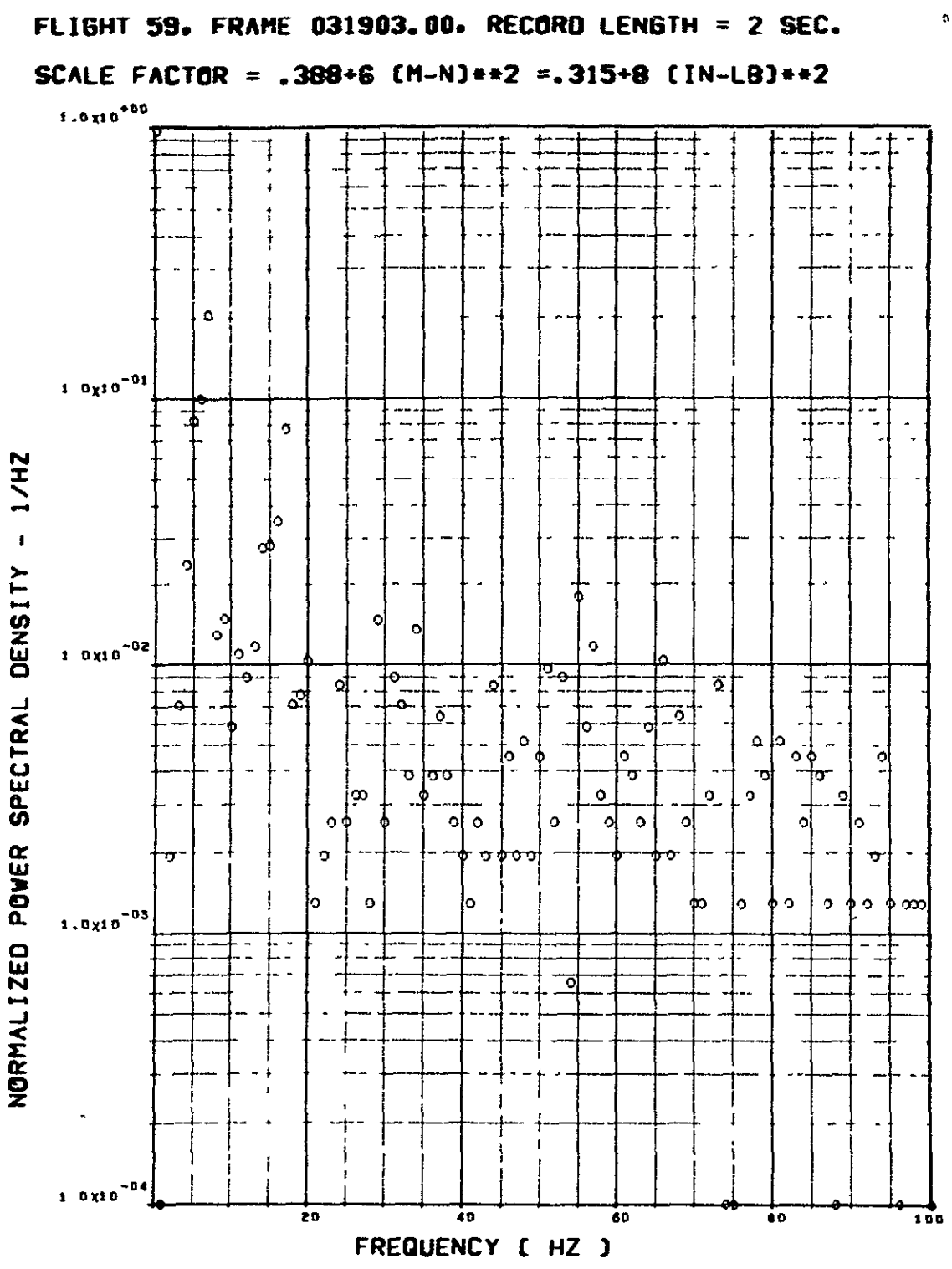

Figure 50. Continued

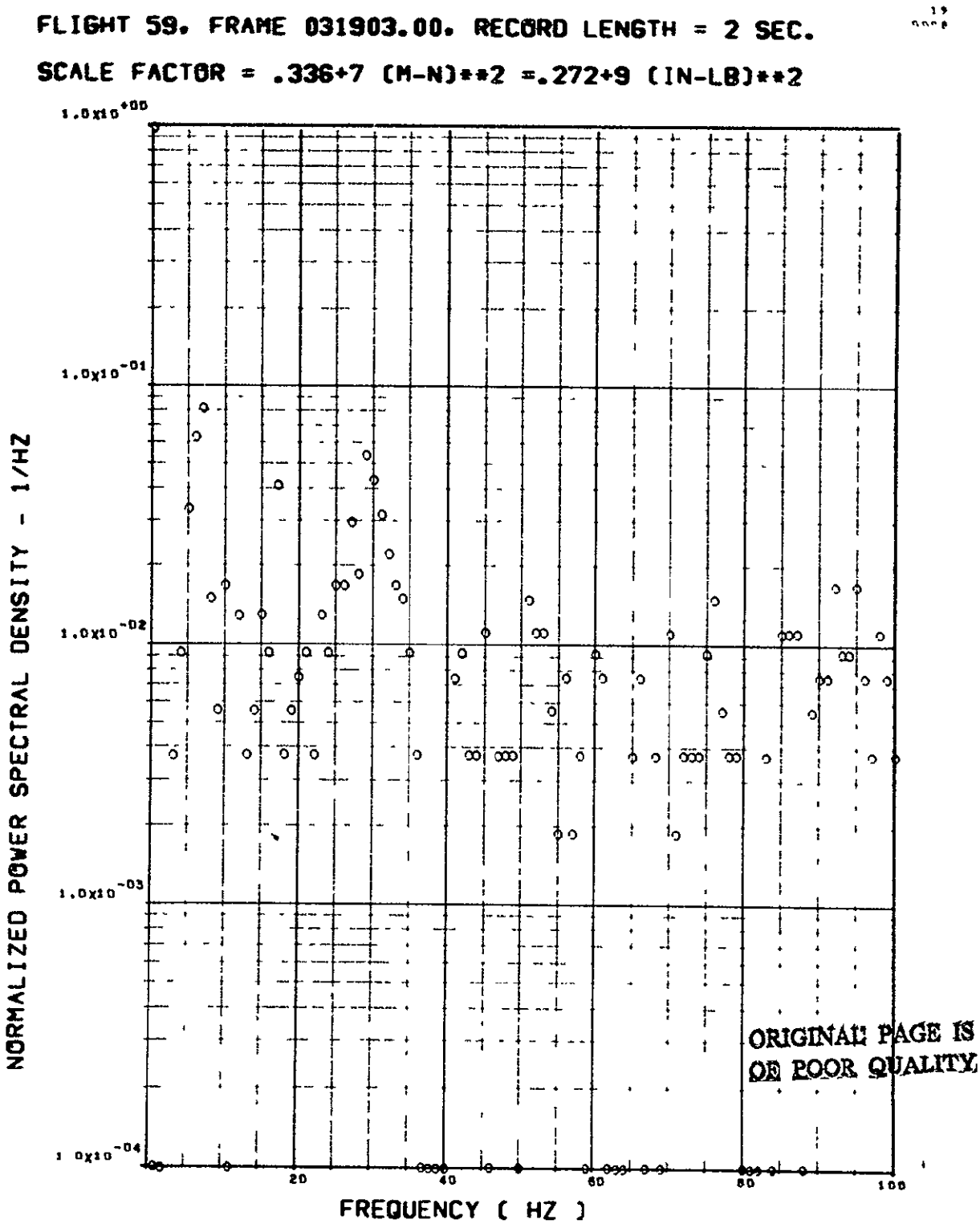

Figure 30. Continued

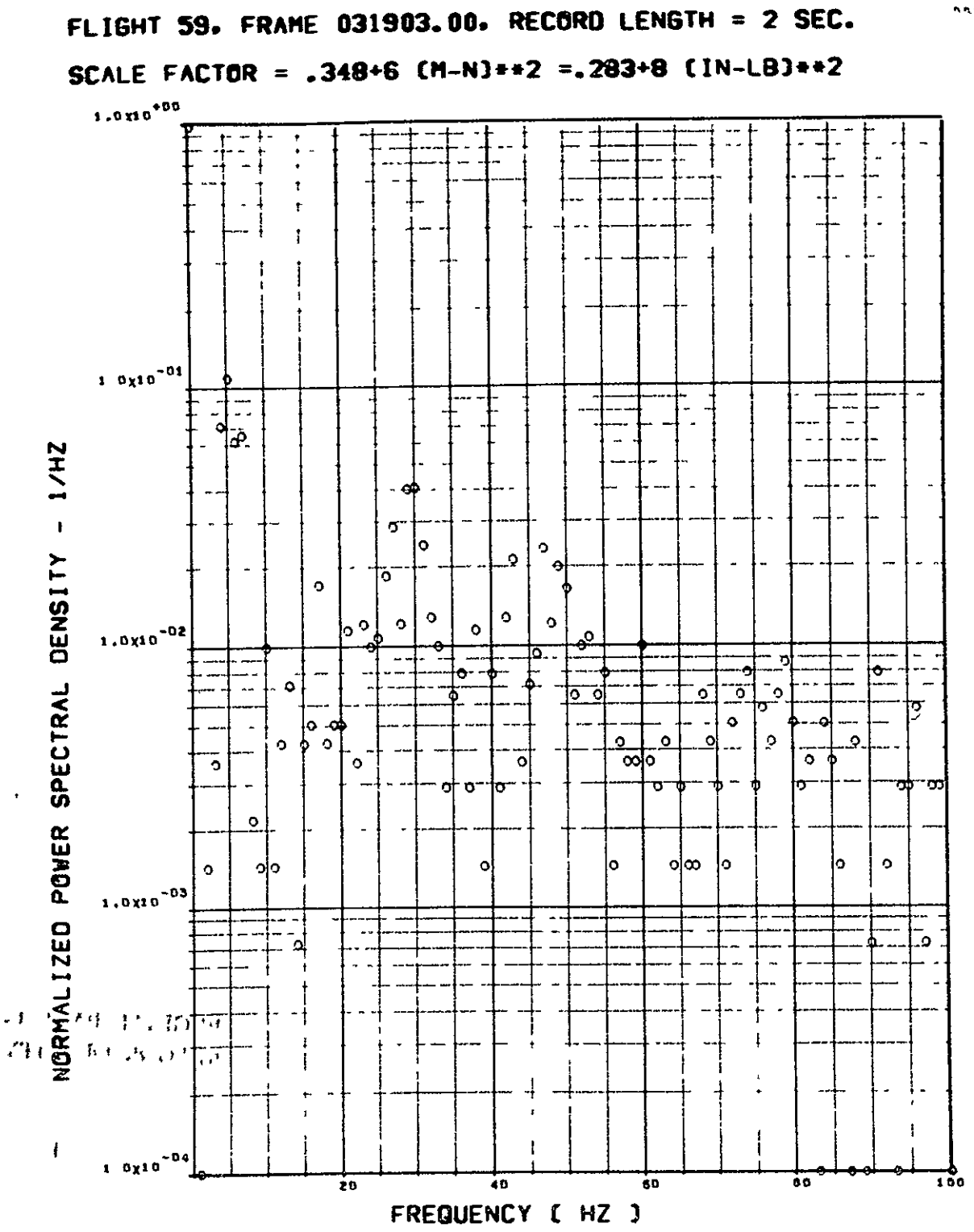

Figure 20. Continued

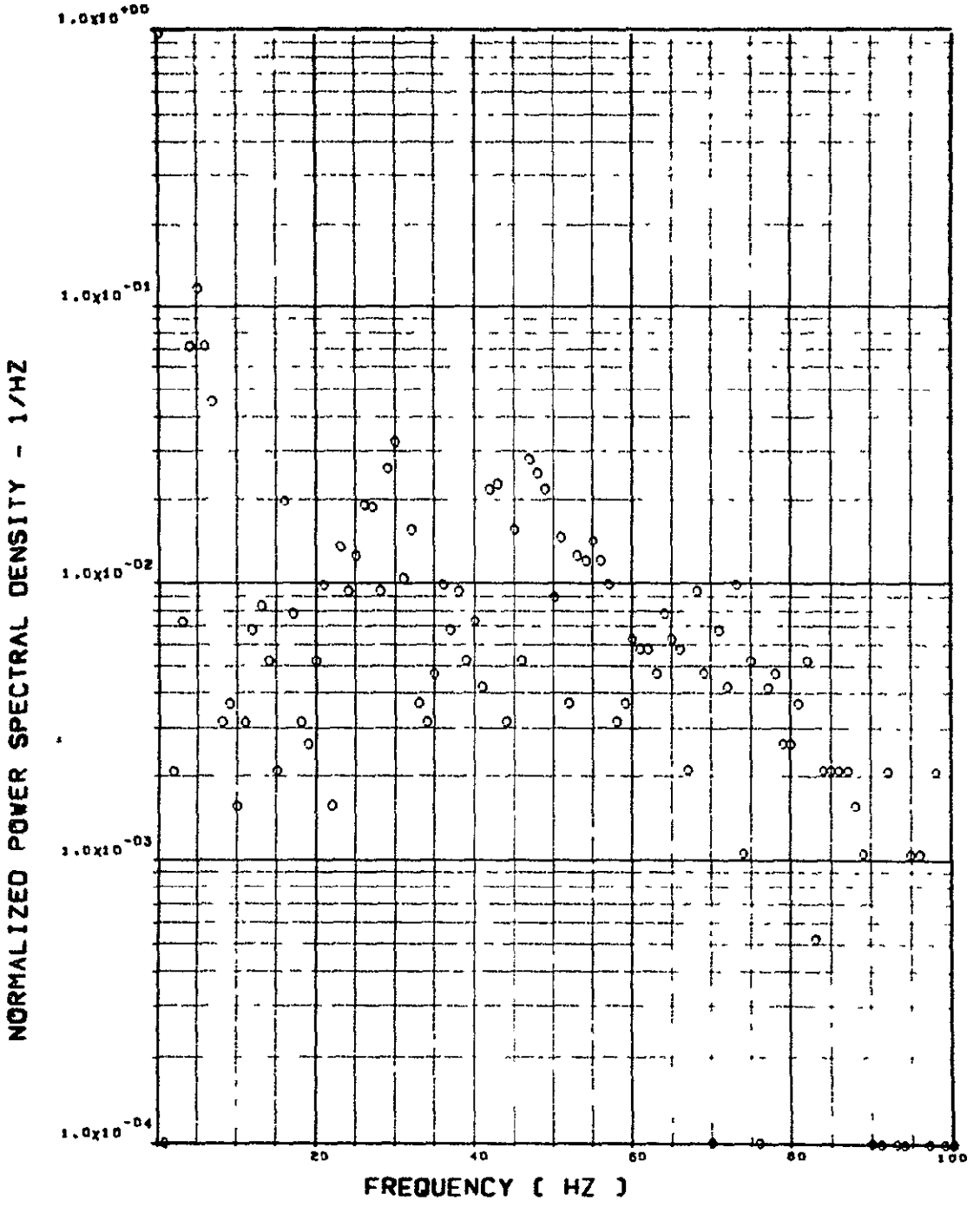

Figure 50. Continued

FLIGHT 59. FRAME 031903.00. RECORD LENGTH = 2 SEC.

SCALE FACTOR = .104+6 (M-N)**2 =.848+7 (IN-LB)**2

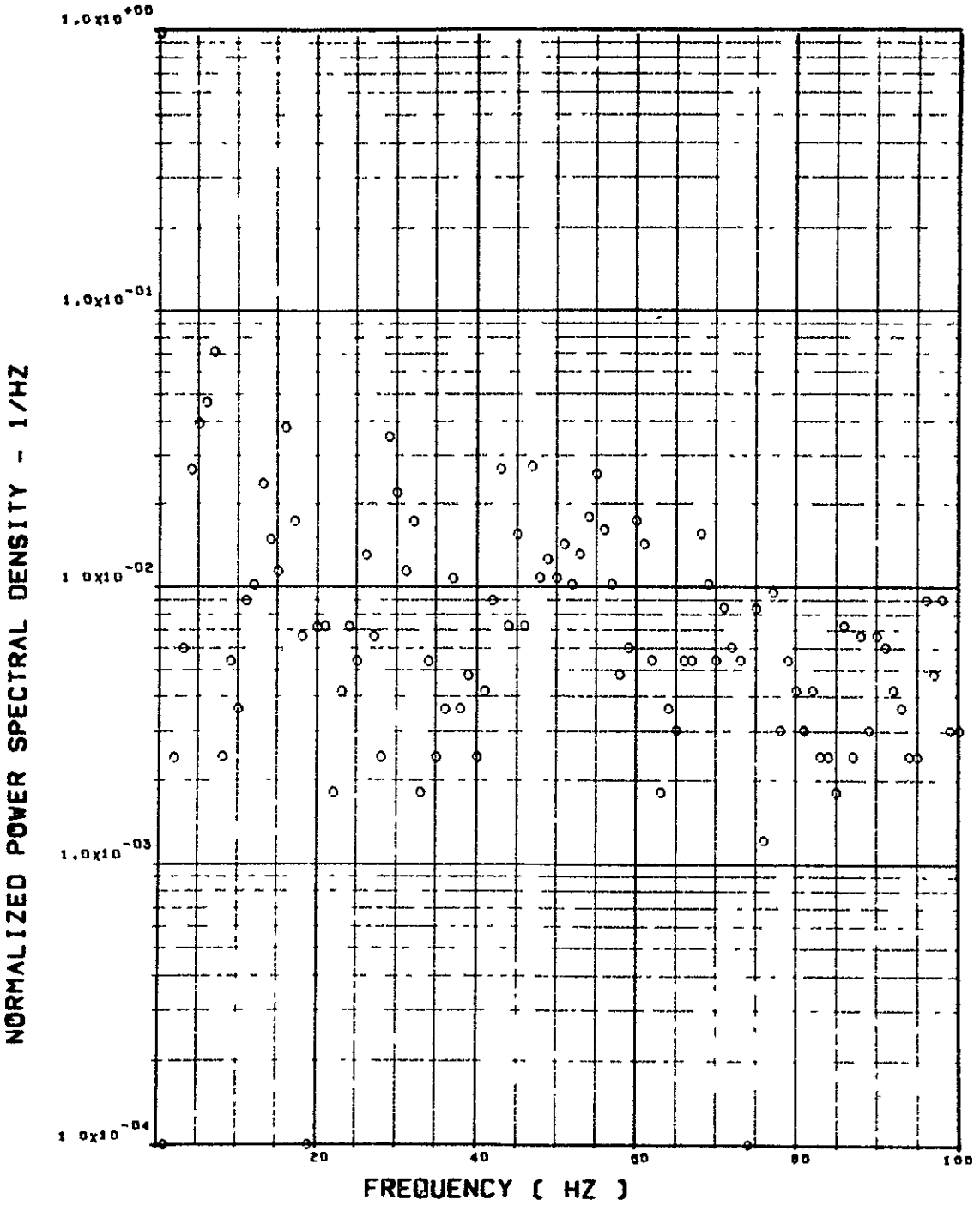

ITEM - SW134 TORSION AT WING STATION 4

Figure 50. Continued

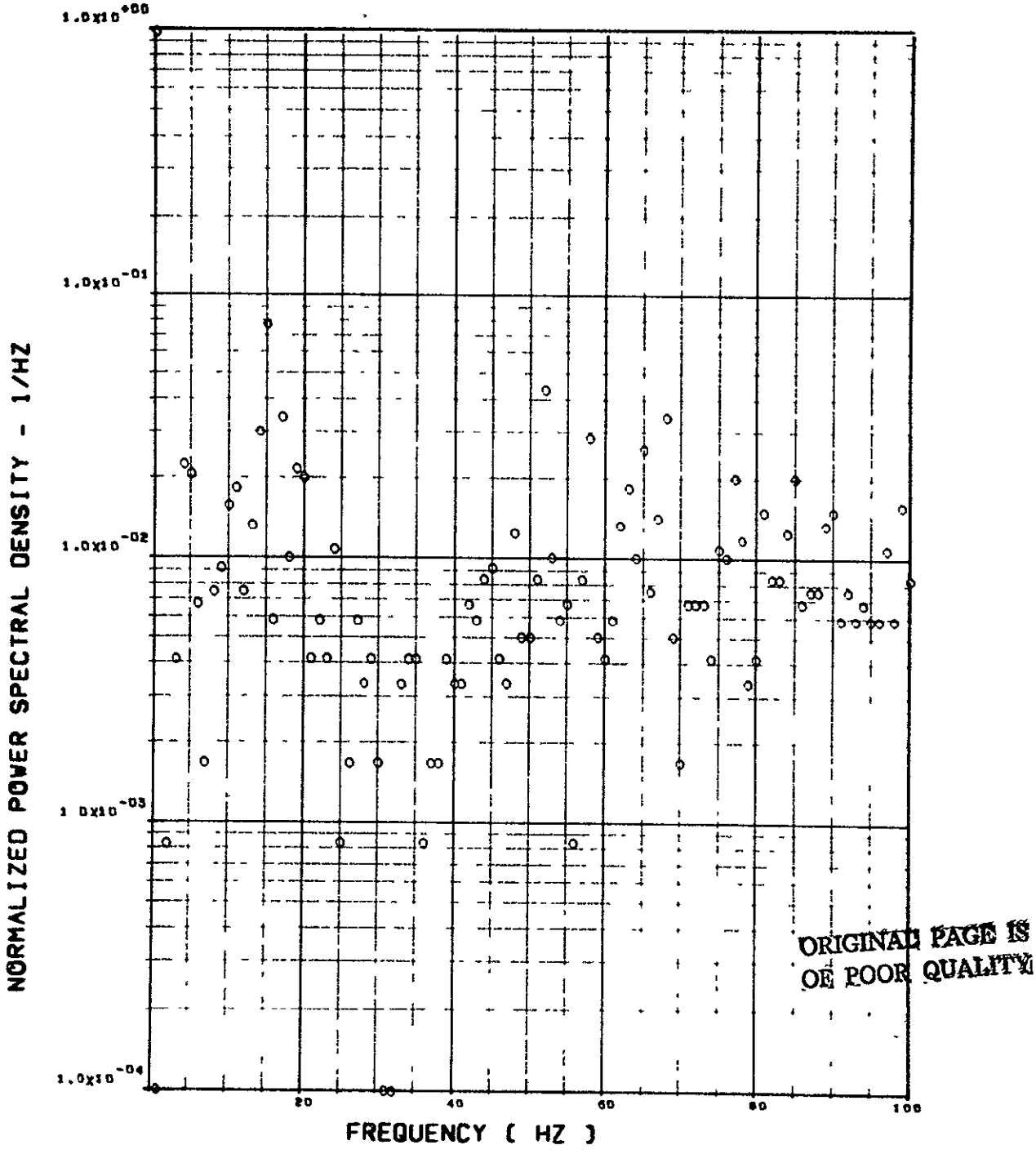

Figure 30. Continued

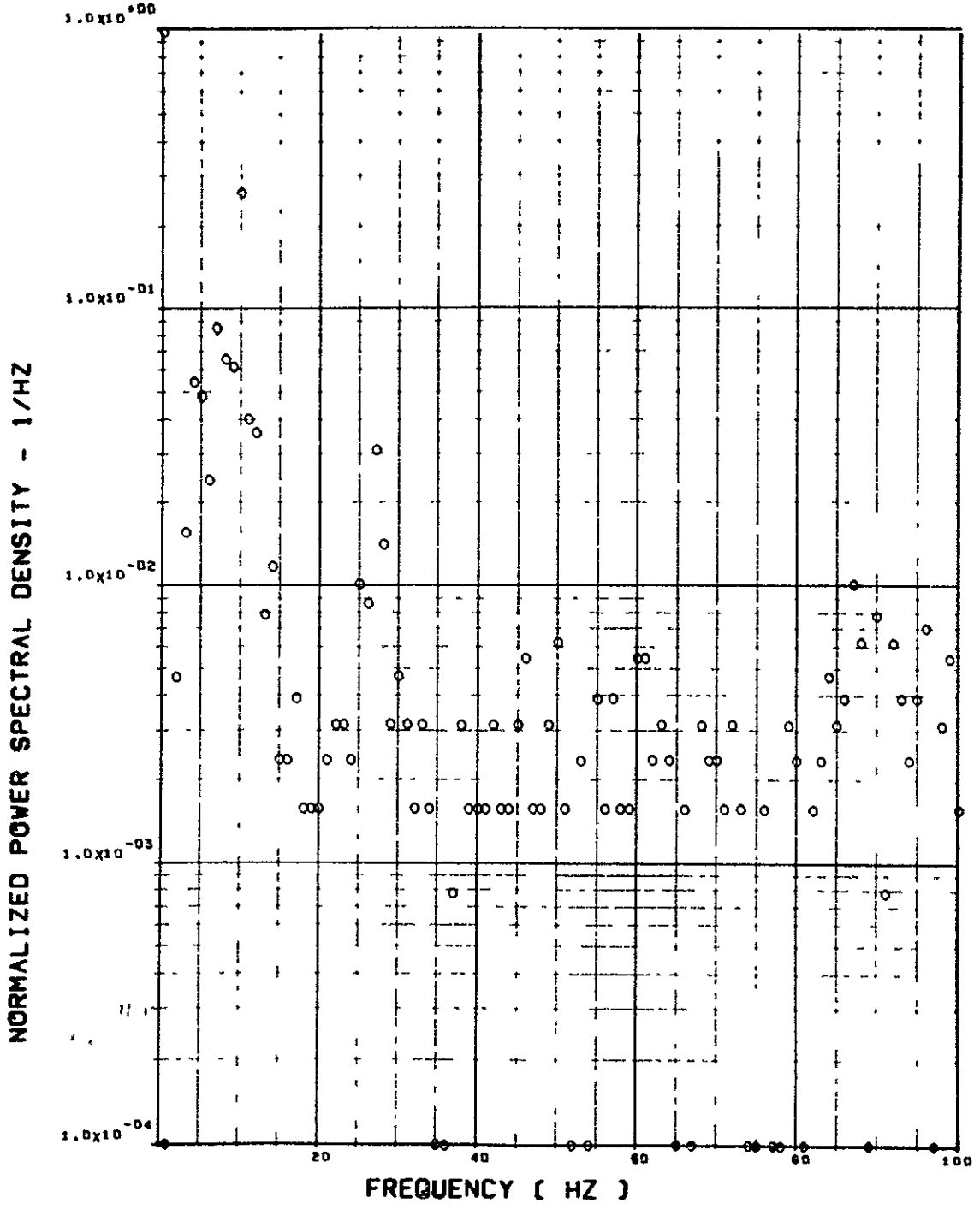

Figure 30. Continued

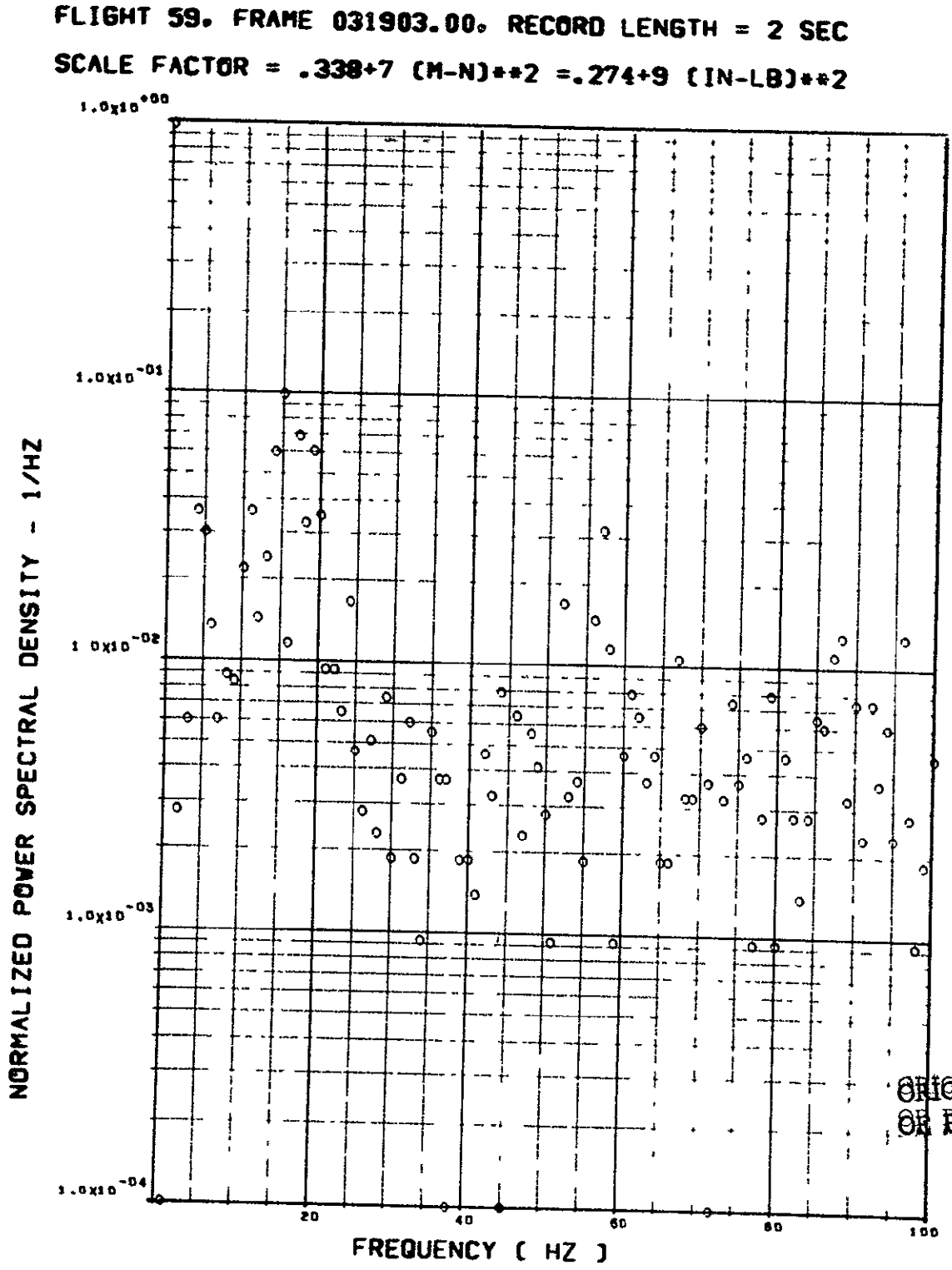

Figure 56. Continued

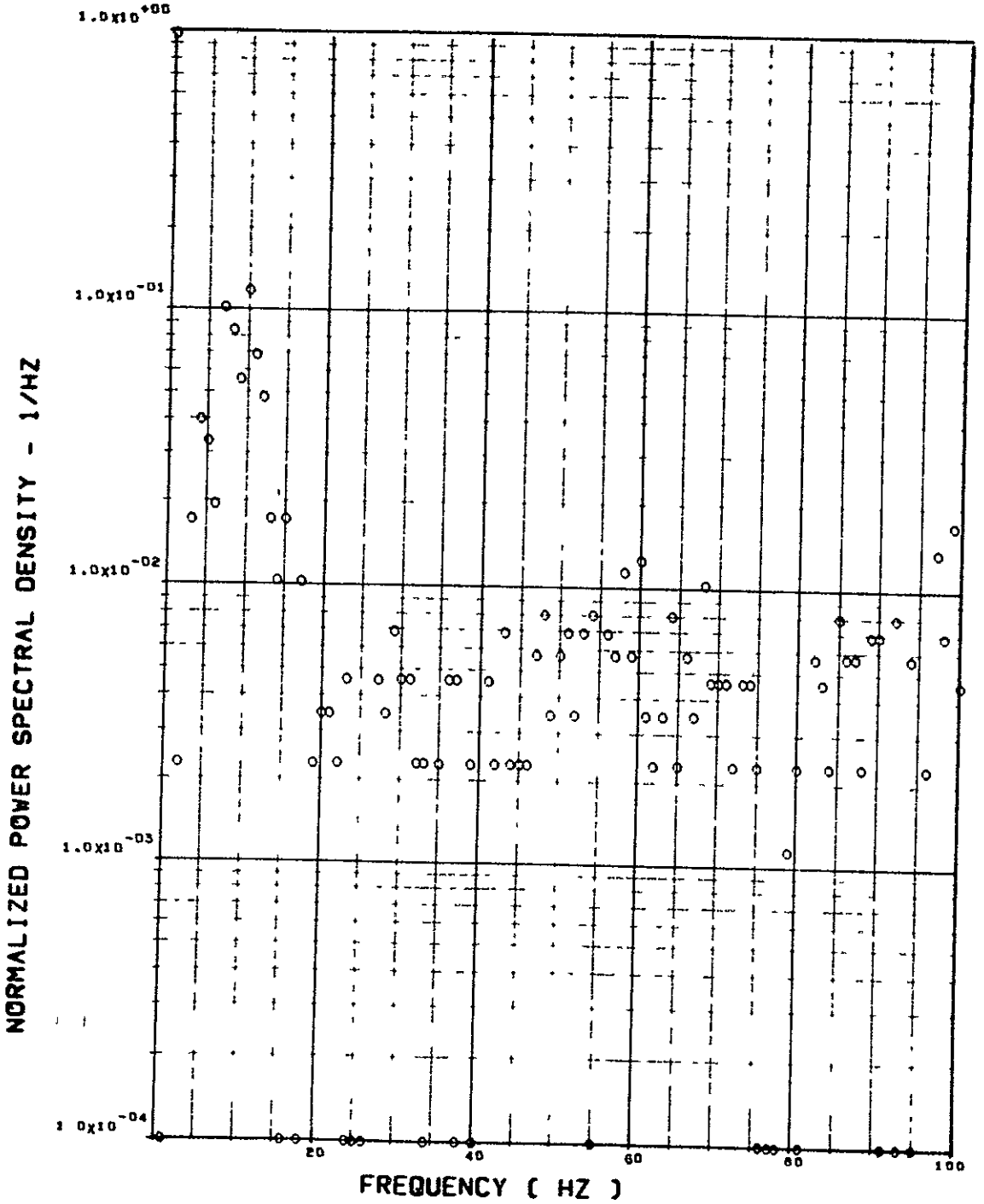

Figure 50. Continued

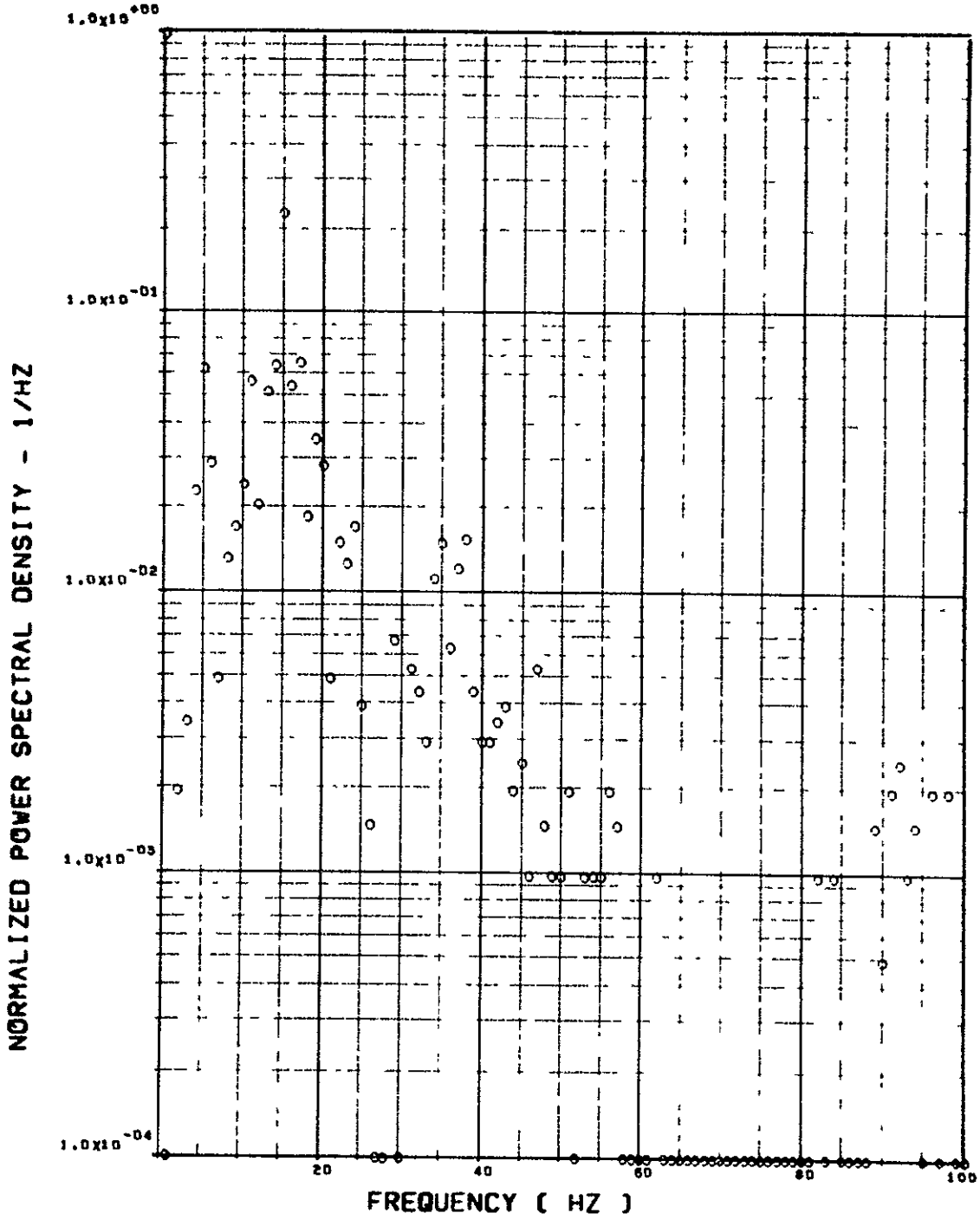

Figure 30. Continued

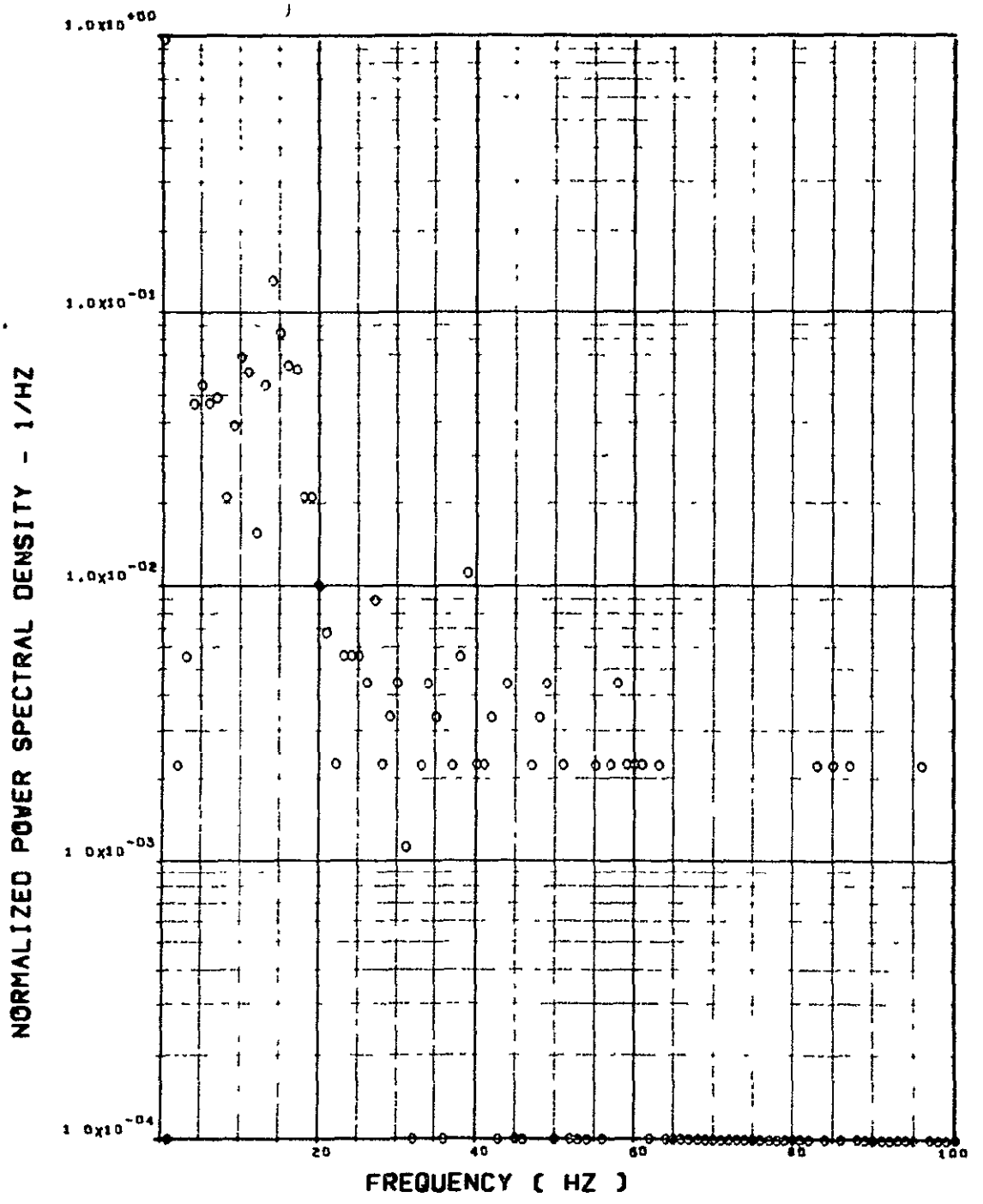

Figure 50. Concluded

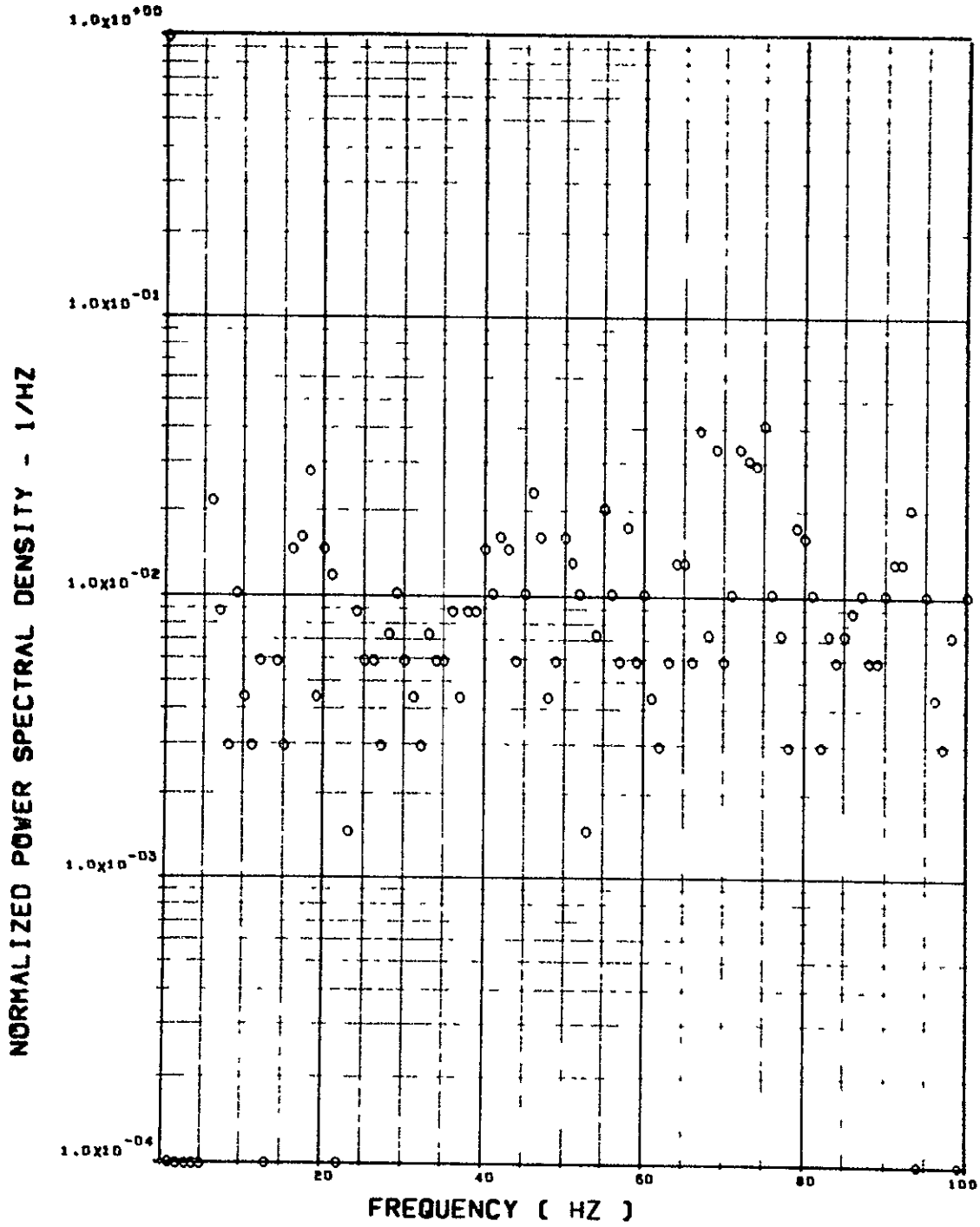

Figure 51. Power Spectra - Flight 59, Run S132R, Point 3 T_1 = 31907.0, ΔT = 2 Sec, α_{Nom} = 19.80 deg, $\Delta\alpha$= 0.45 deg.

FLIGHT 59. FRAME 031907.00. RECORD LENGTH = 2 SEC

SCALE FACTOR = .190+1 (G)**2

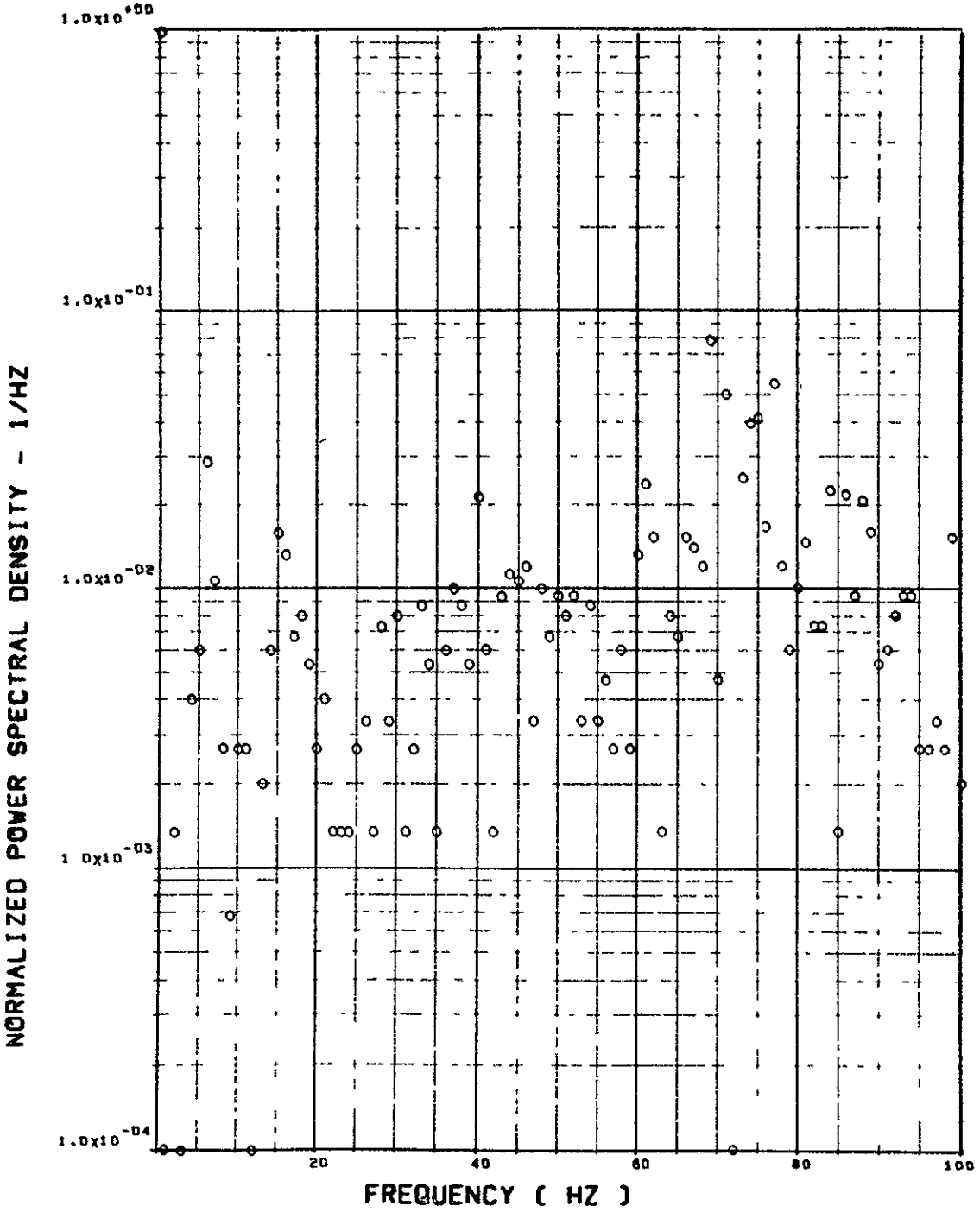

ITEM - AW002 R/H WING TIP VERTICAL ACCELERATION

Figure 51. Continued

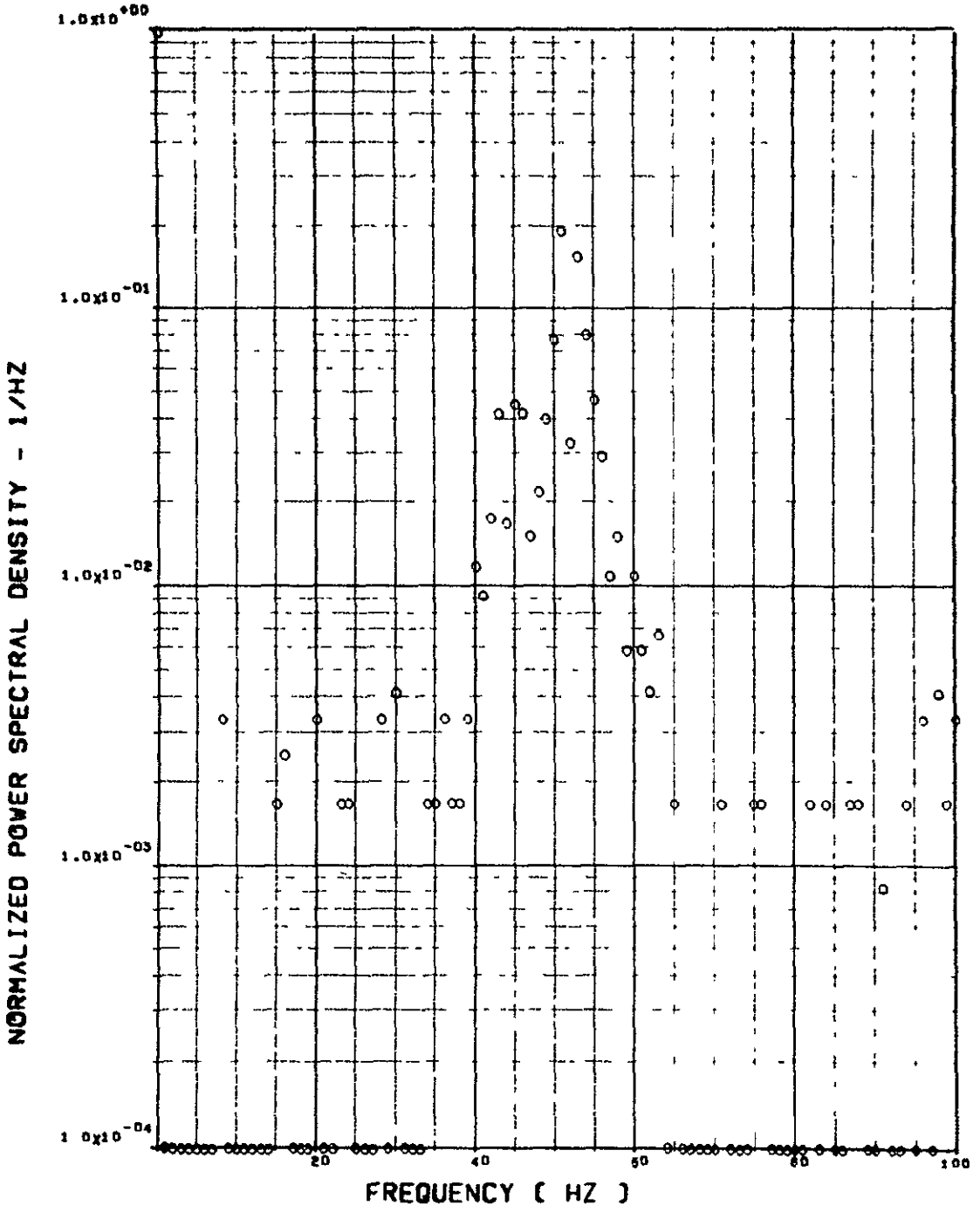

Figure 31. Continued

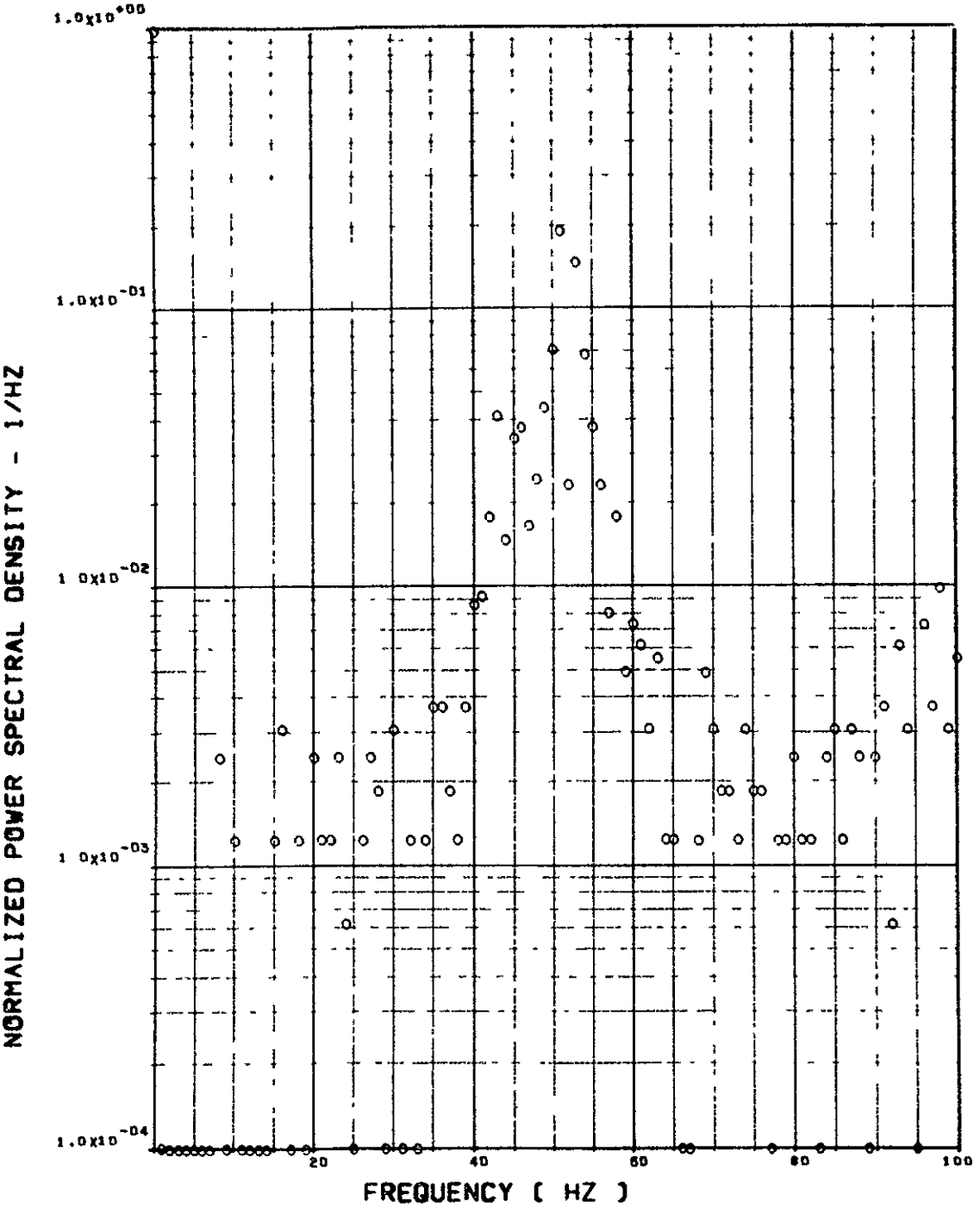

Figure 21. Continued

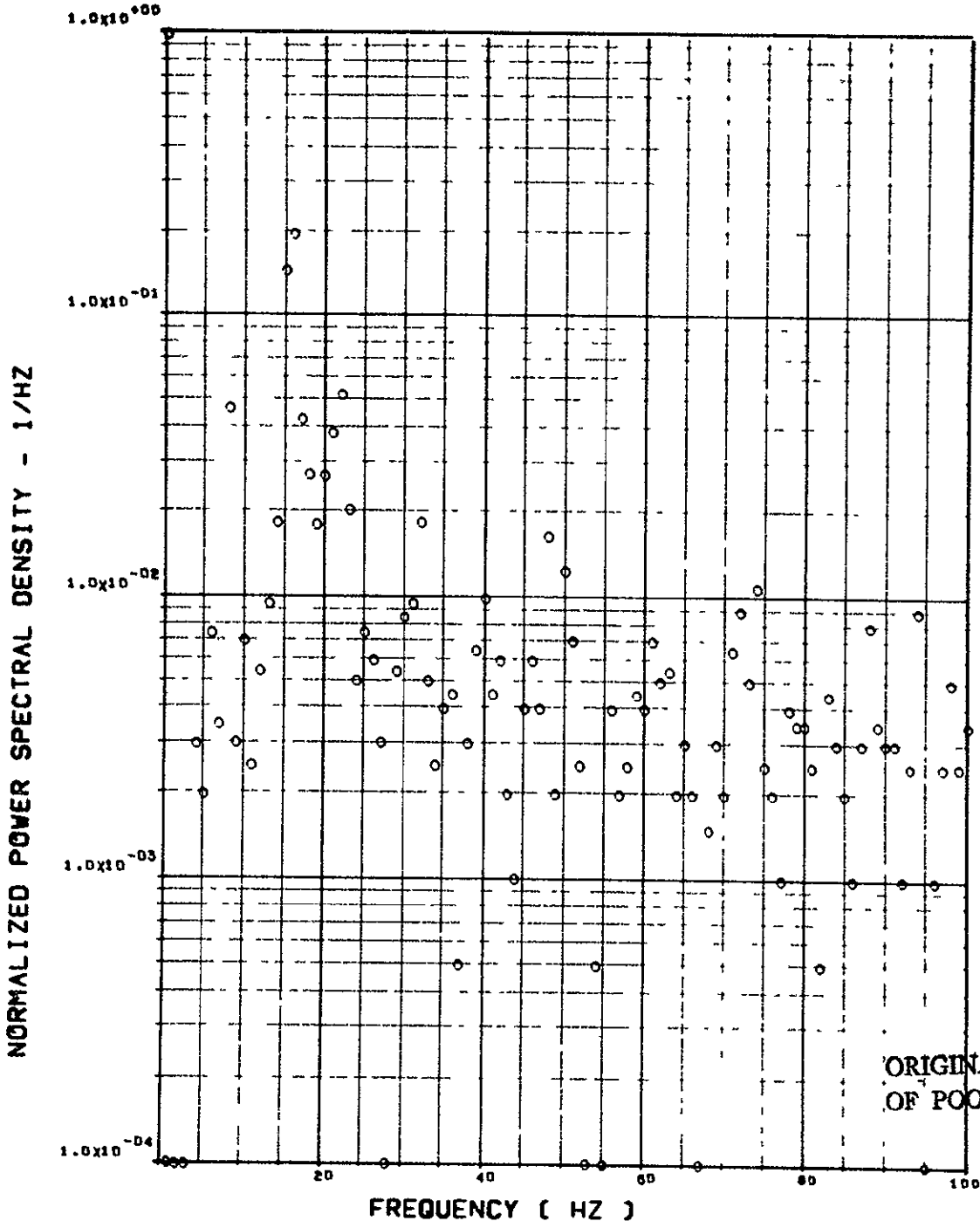

Figure 31. Continued

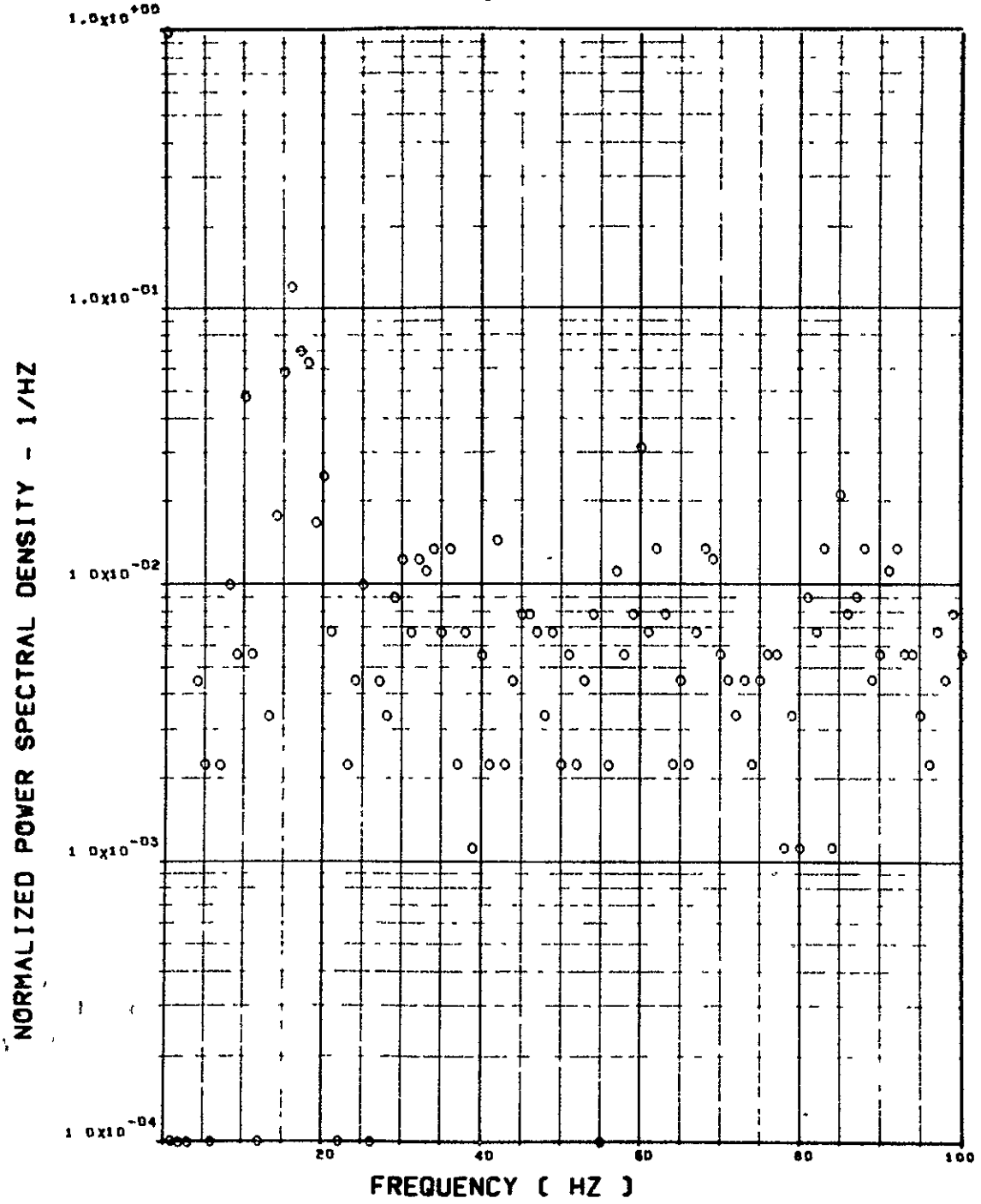

Figure 31. Continued

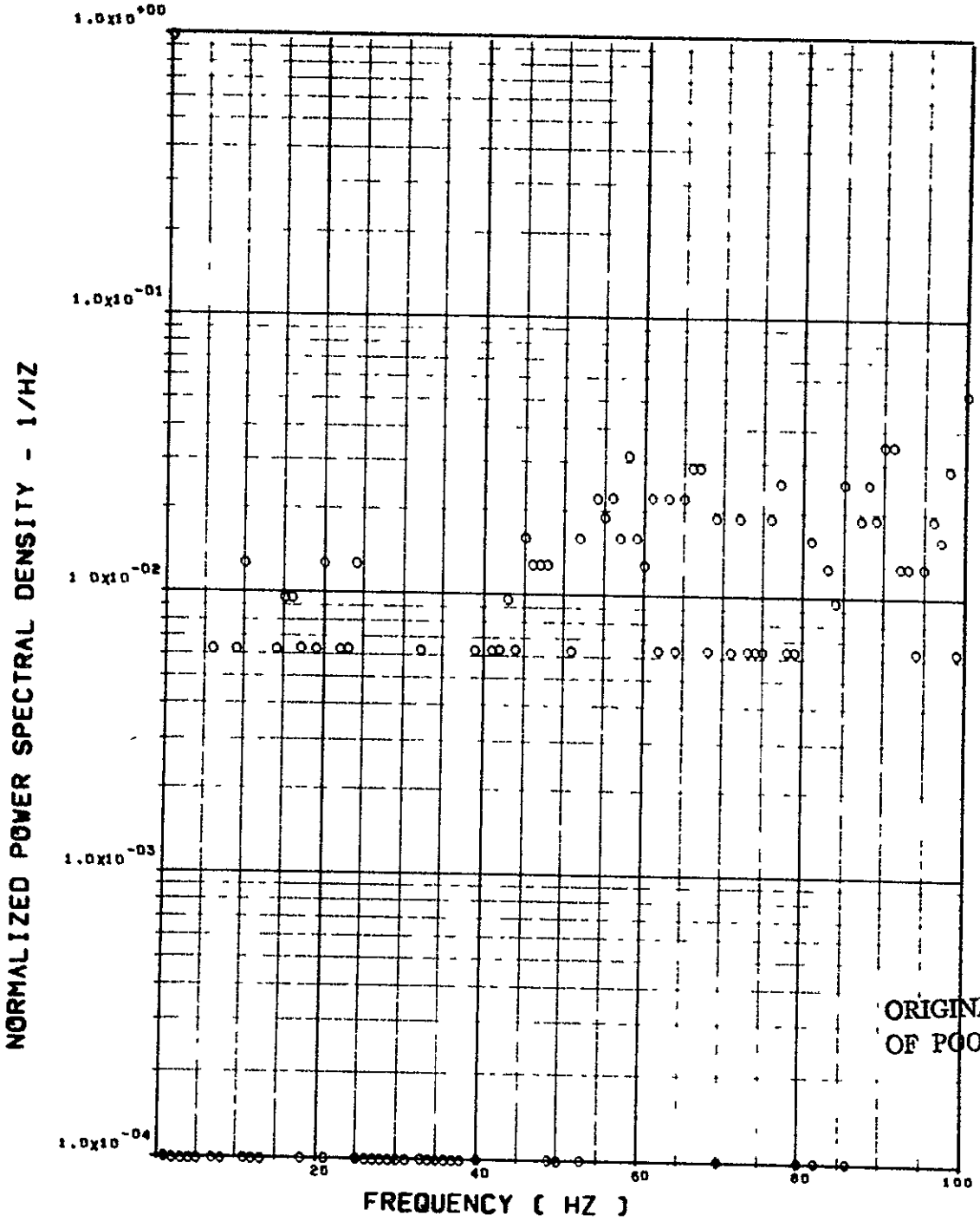

Figure 31. Continued

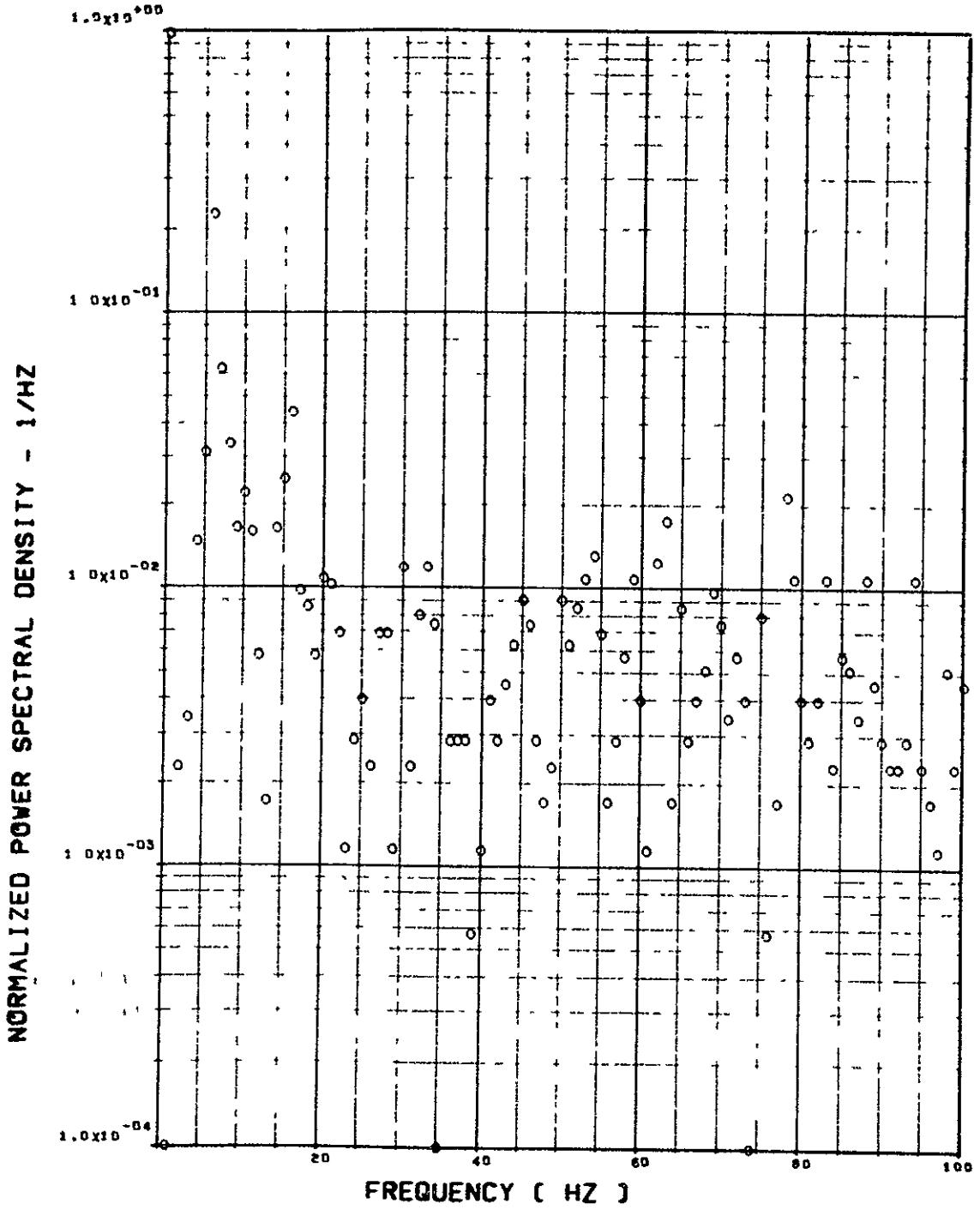

Figure 31. Continued

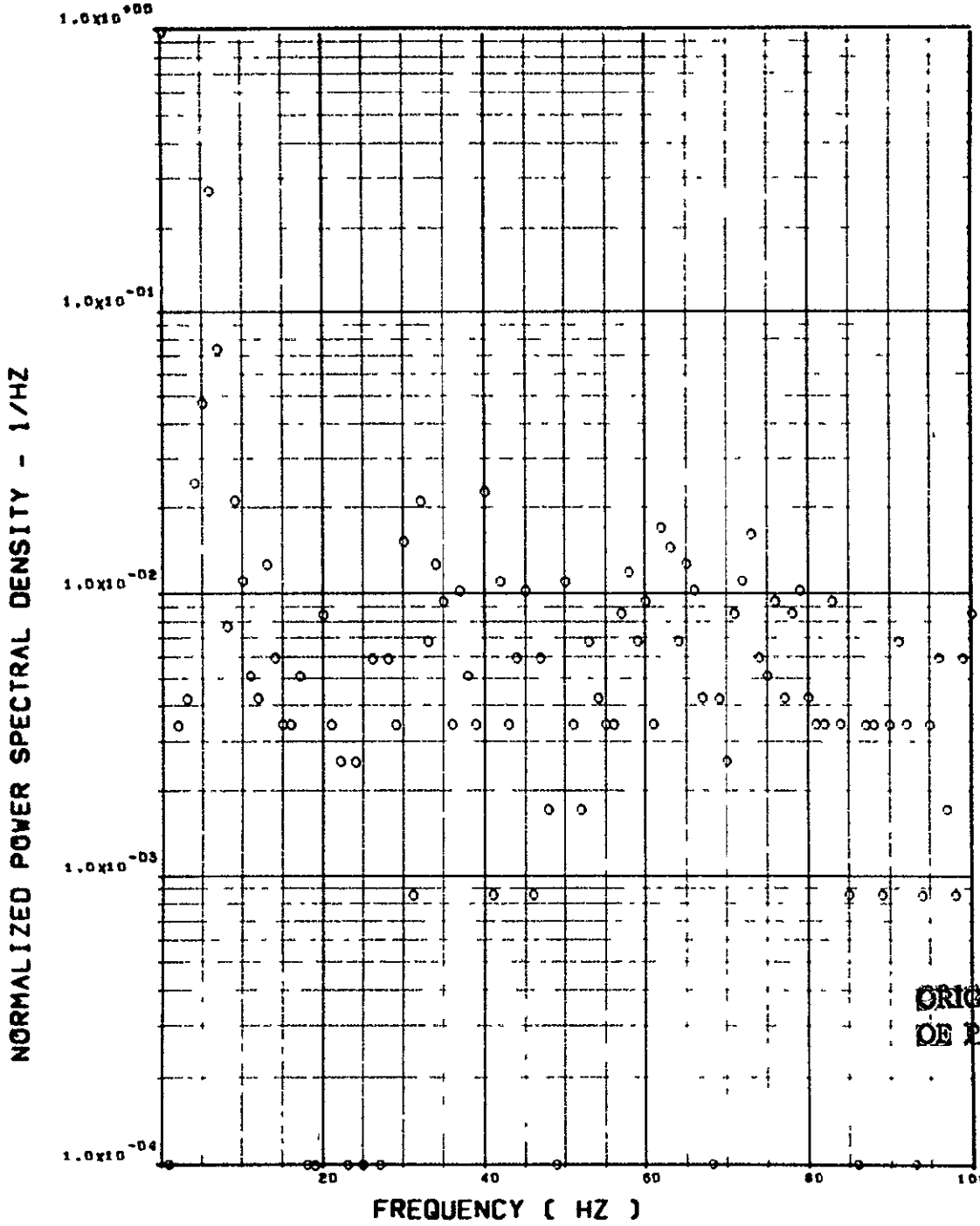

Figure 31. Continued

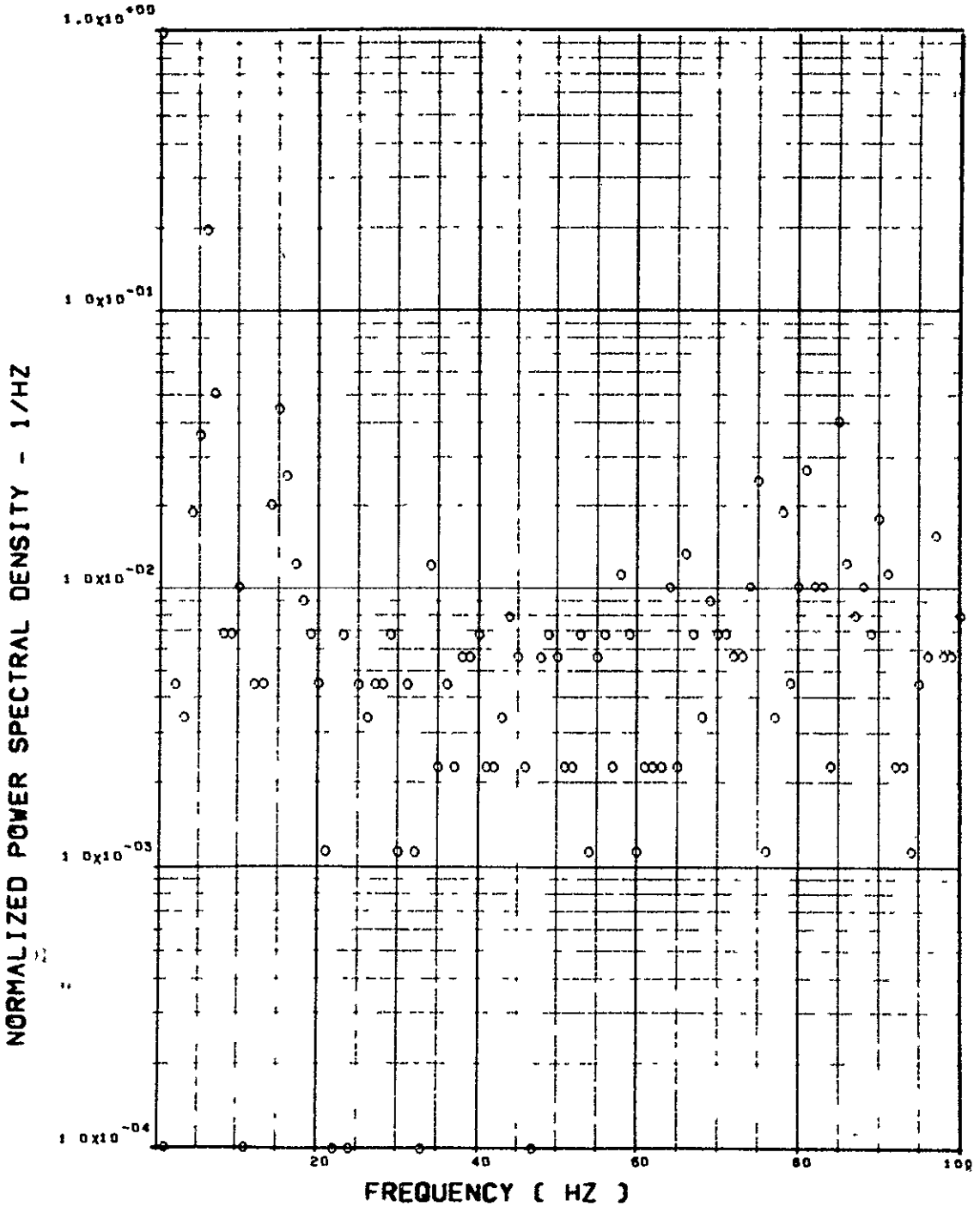

Figure 31. Continued

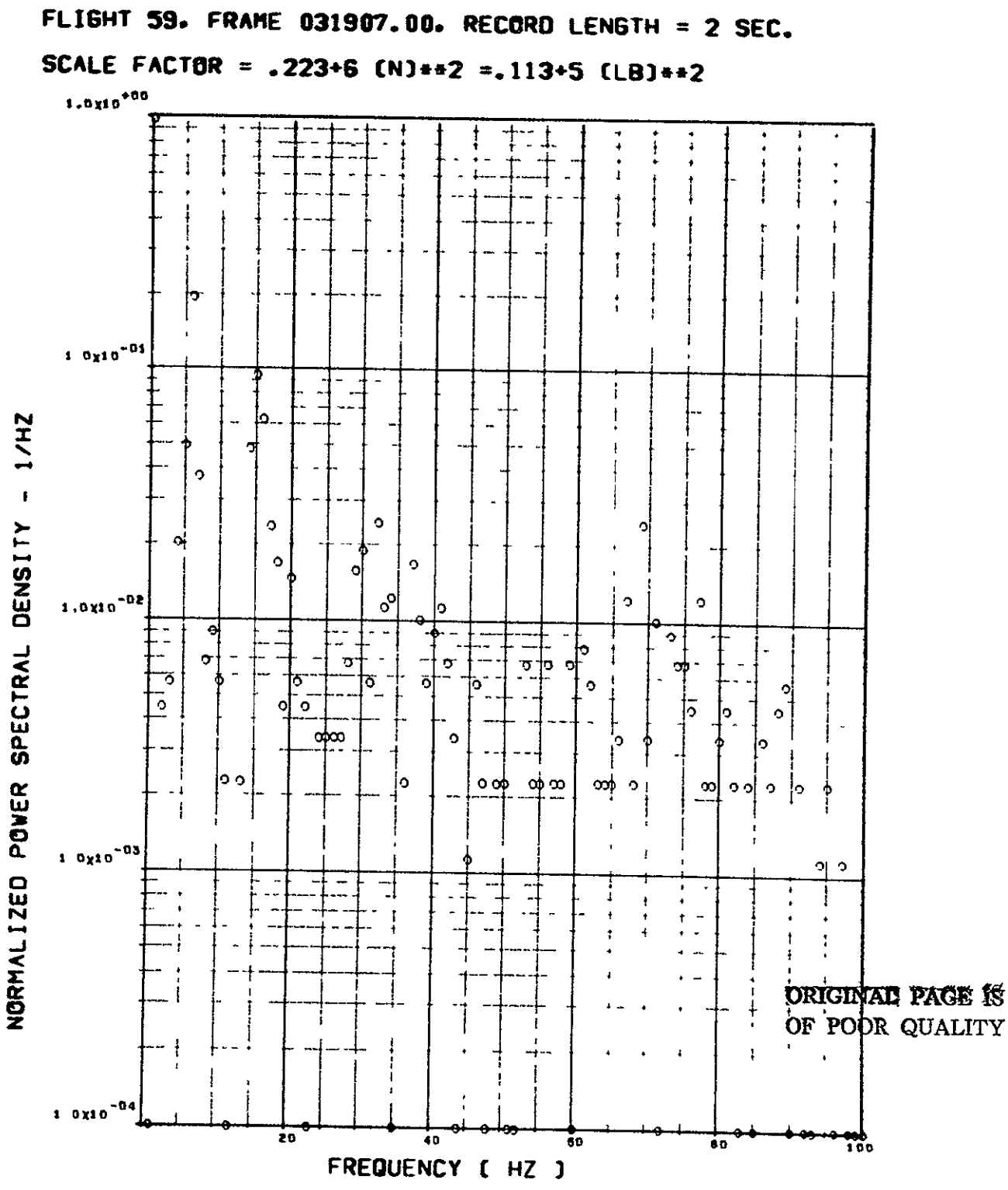

Figure 51. Continued

FLIGHT 59. FRAME 031907.00. RECORD LENGTH = 2 SEC.

SCALE FACTOR = .173+8 (M-N)**2 =.140+10(IN-LB)**2

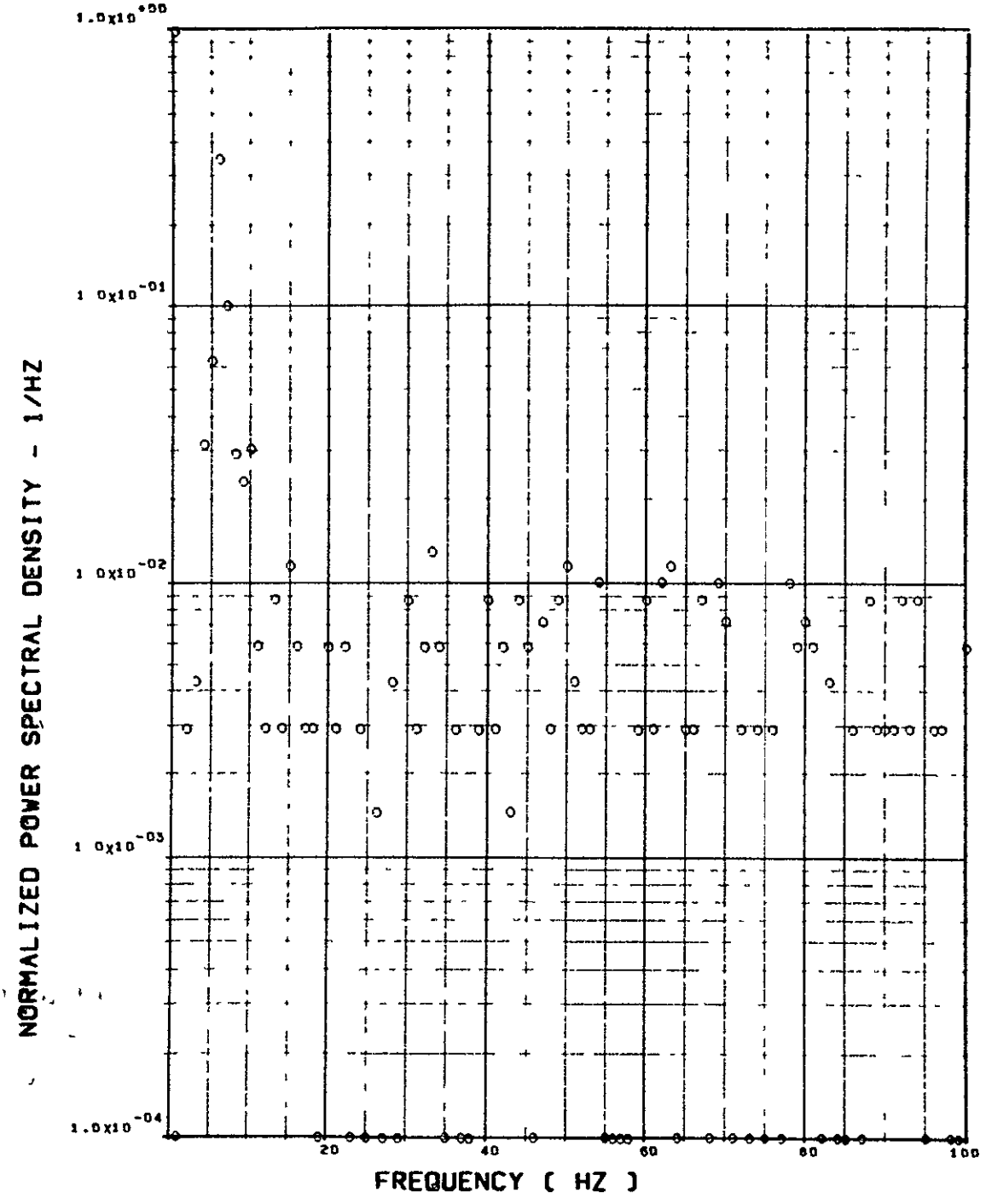

ITEM - SW124 BENDING MOMENT AT WING STATION 1

Figure 51. Continued

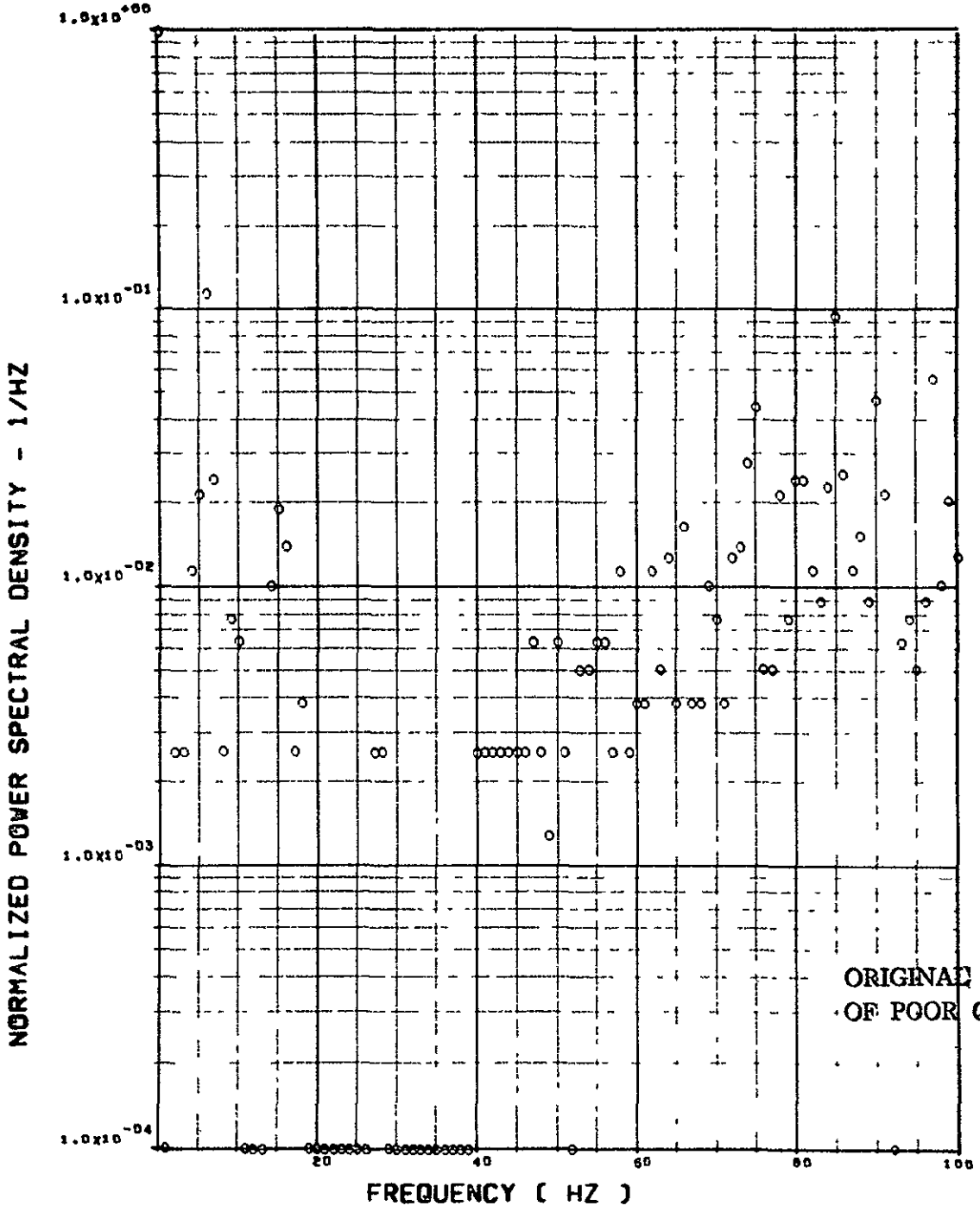

Figure 51. Continued

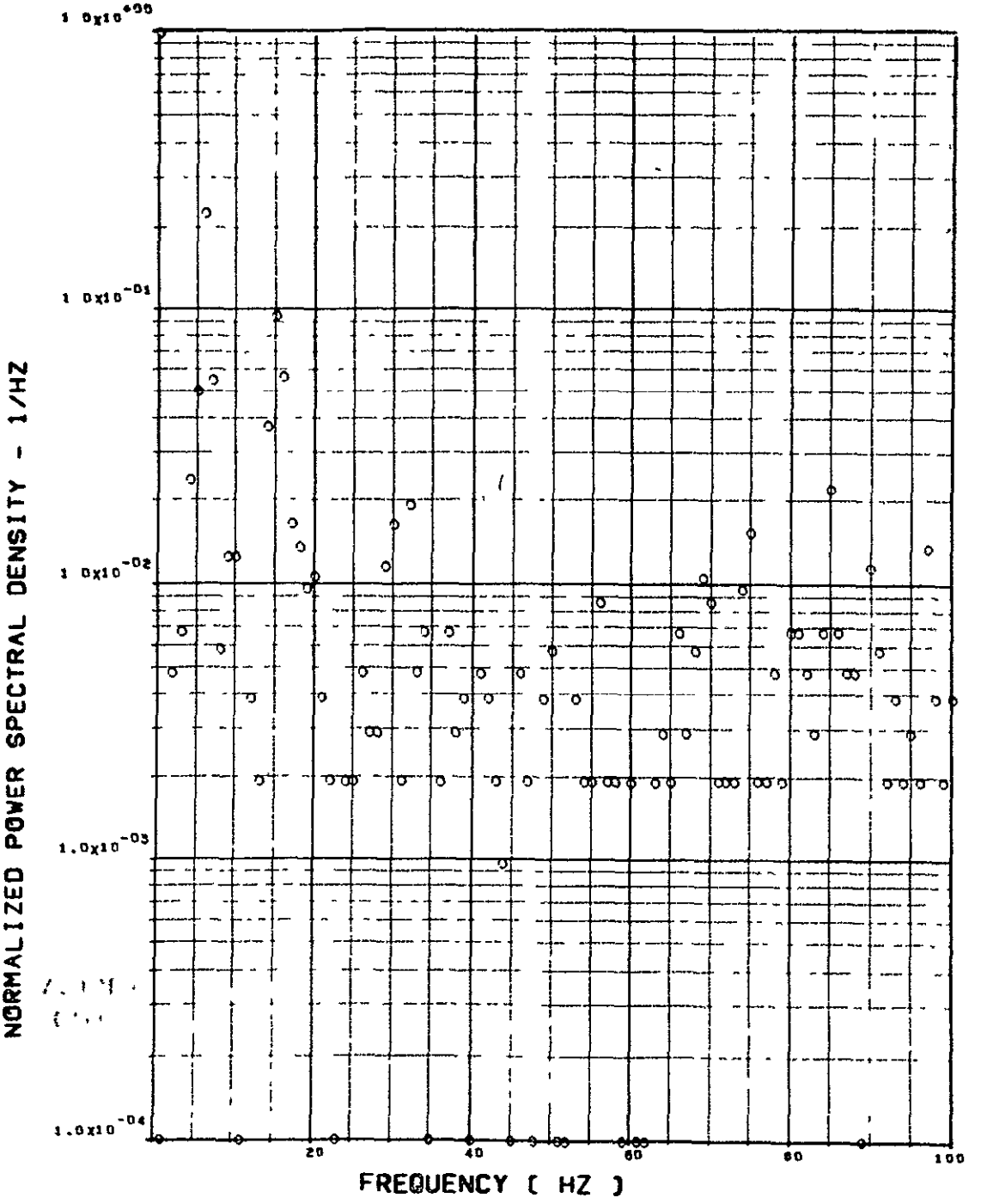

Figure 51. Continued

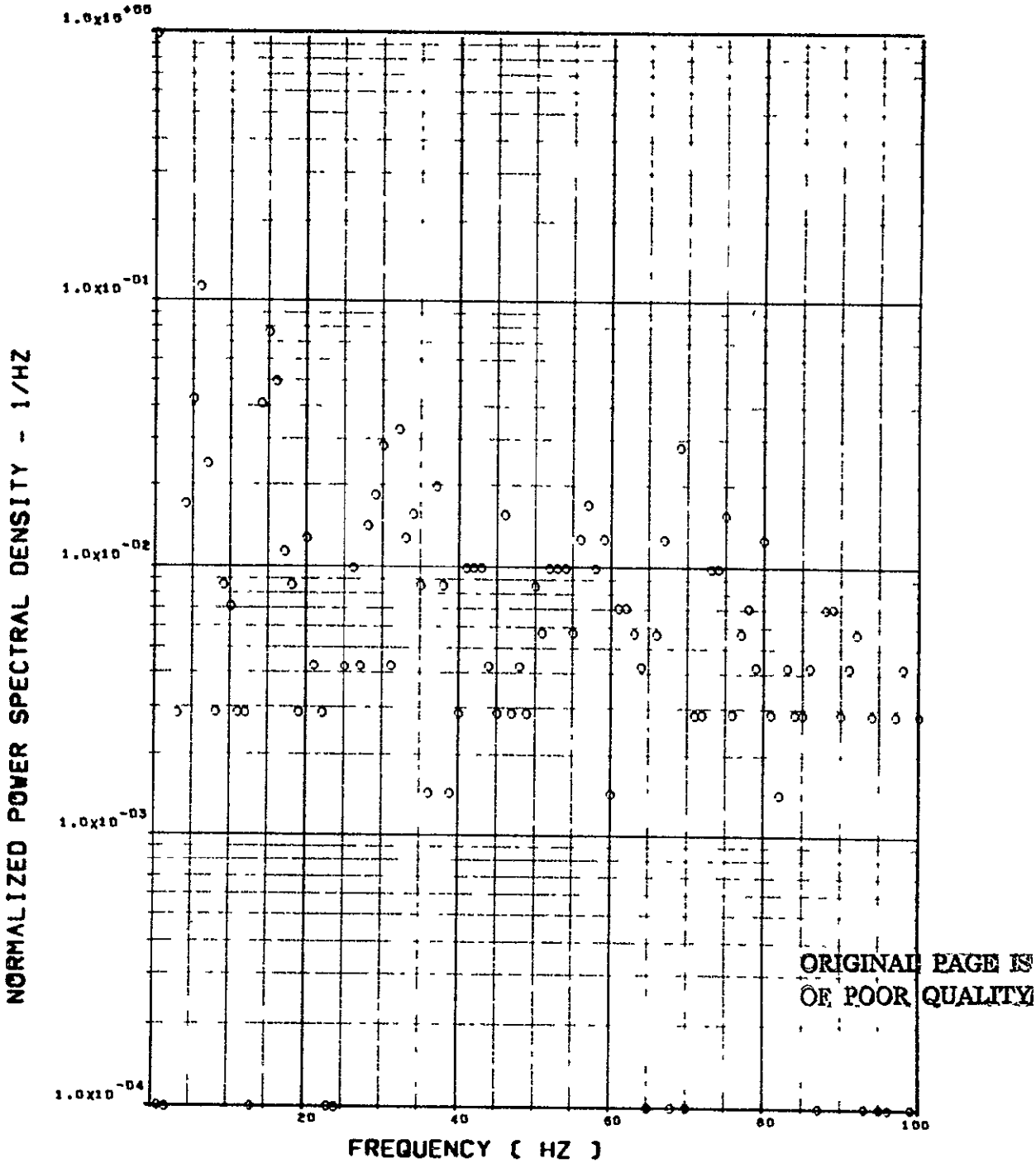

Figure 51. Continued

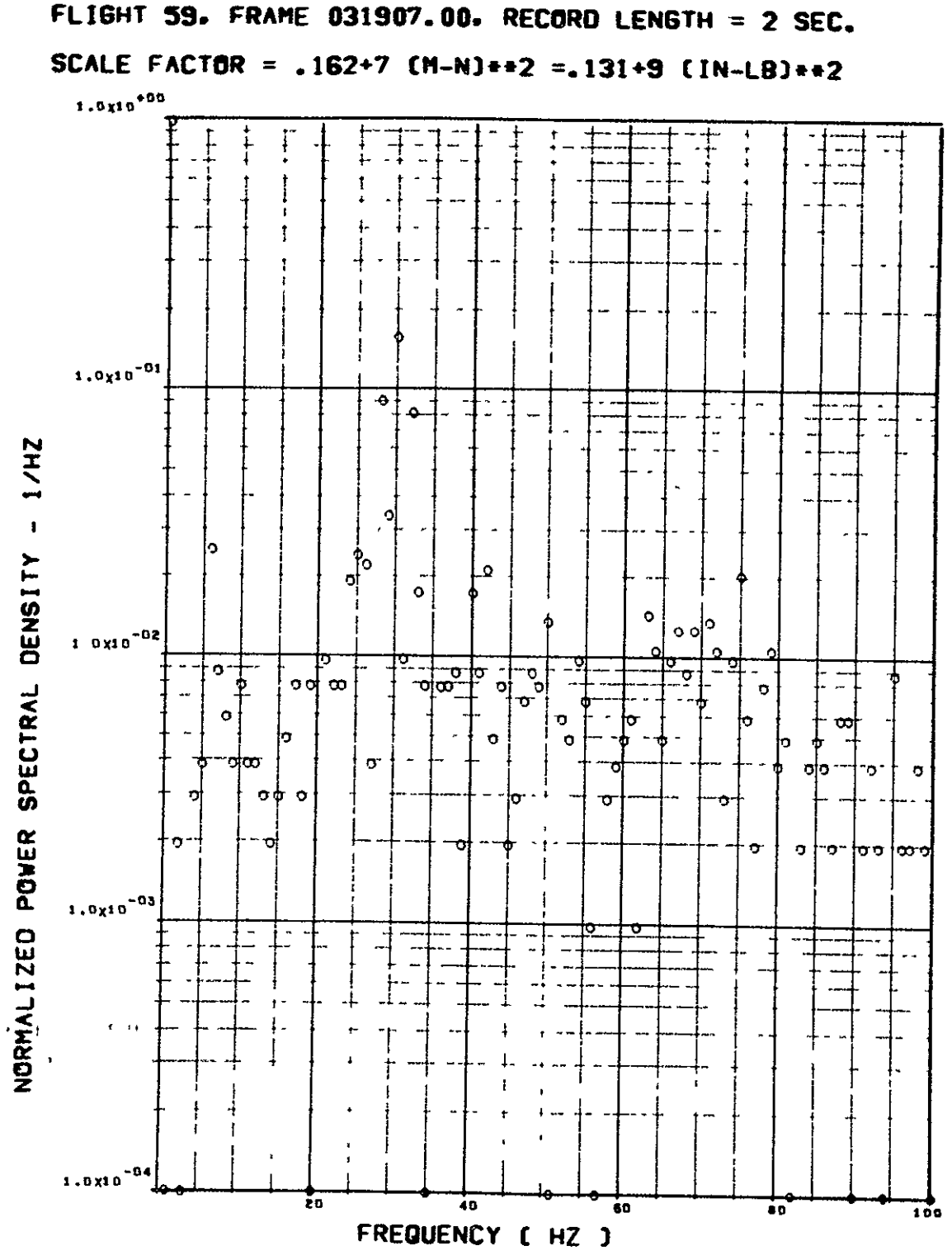

Figure 31. Continued

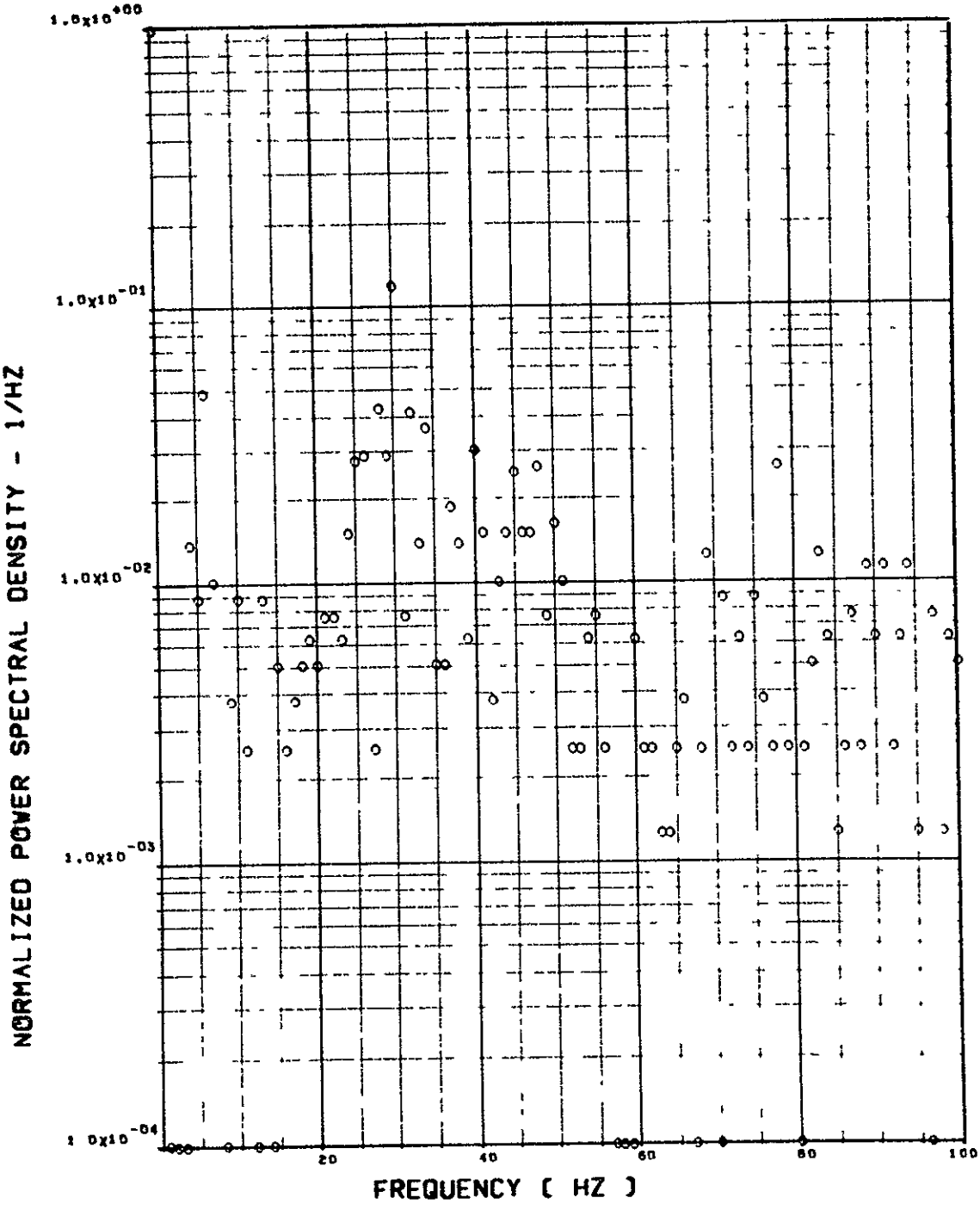

Figure 21. Continued

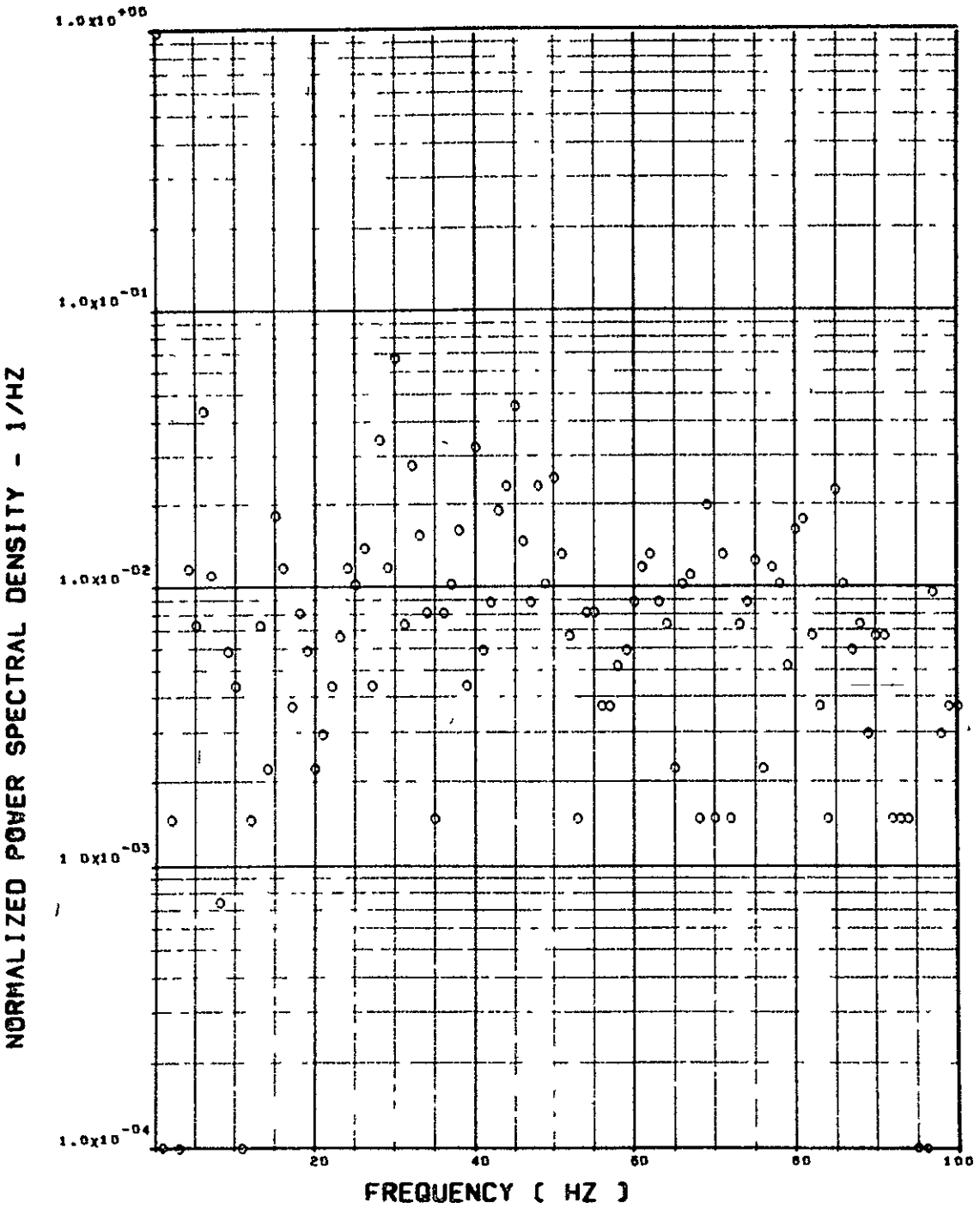

Figure 51. Continued

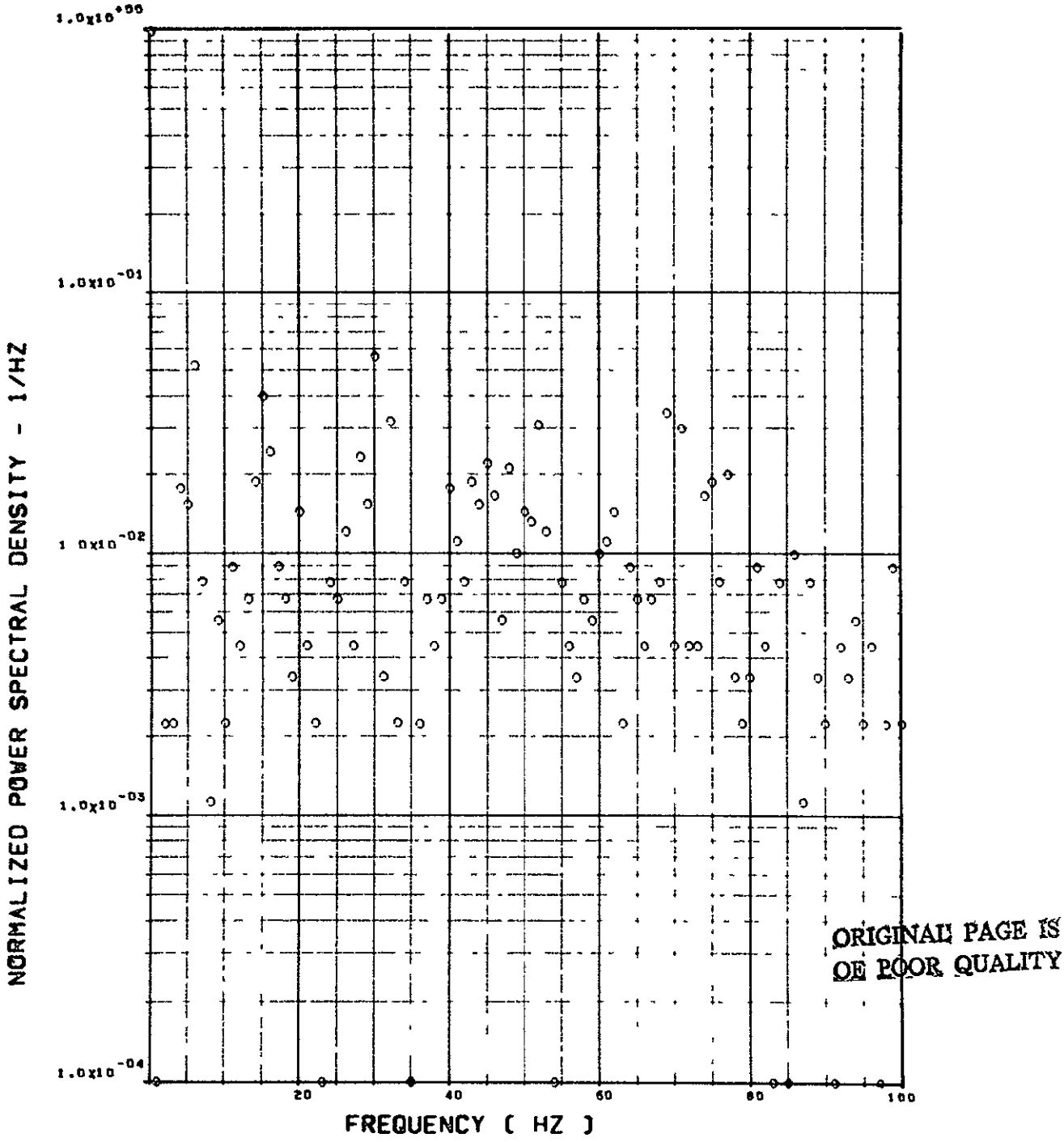

Figure 31. Continued

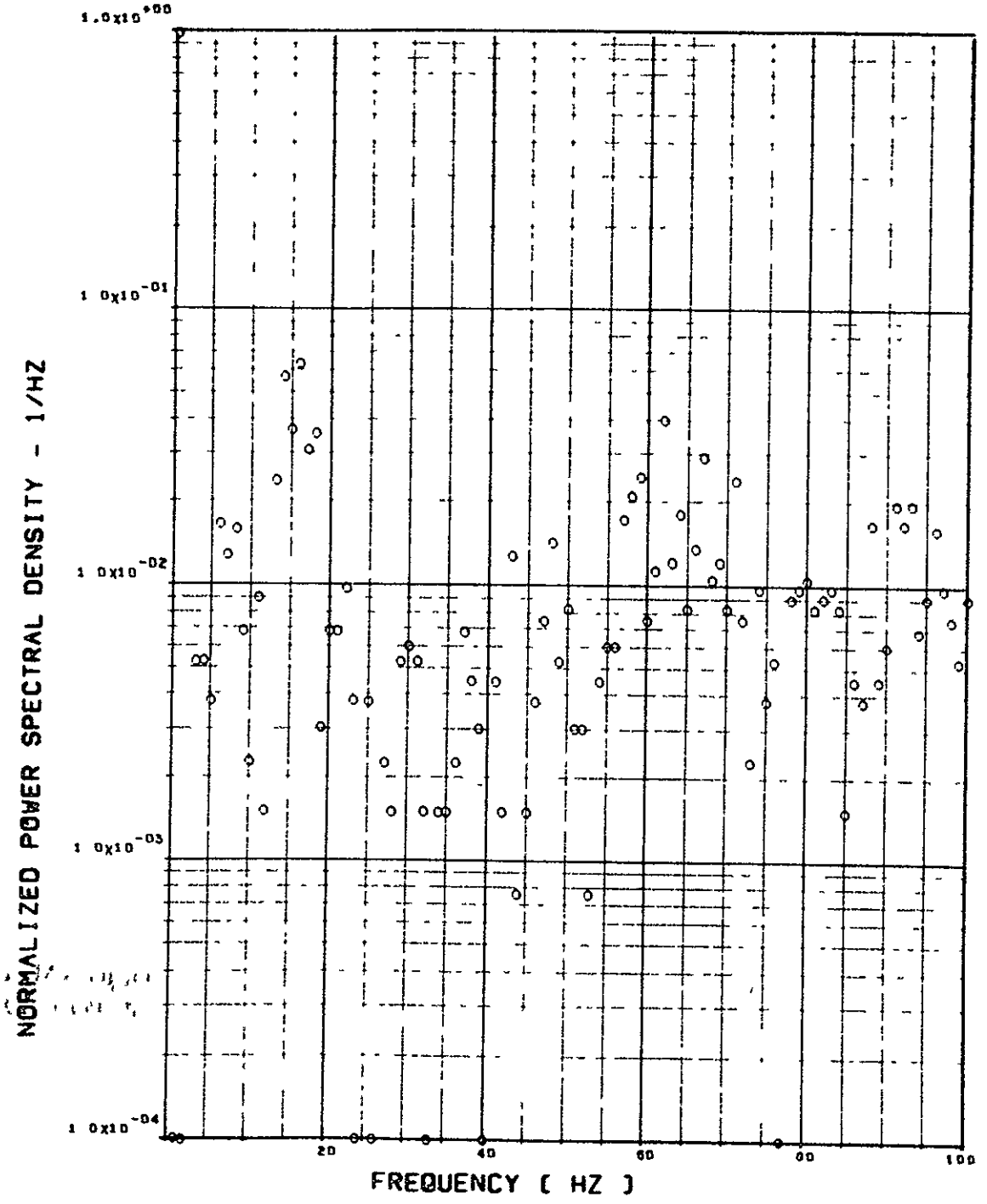

Figure 51. Continued

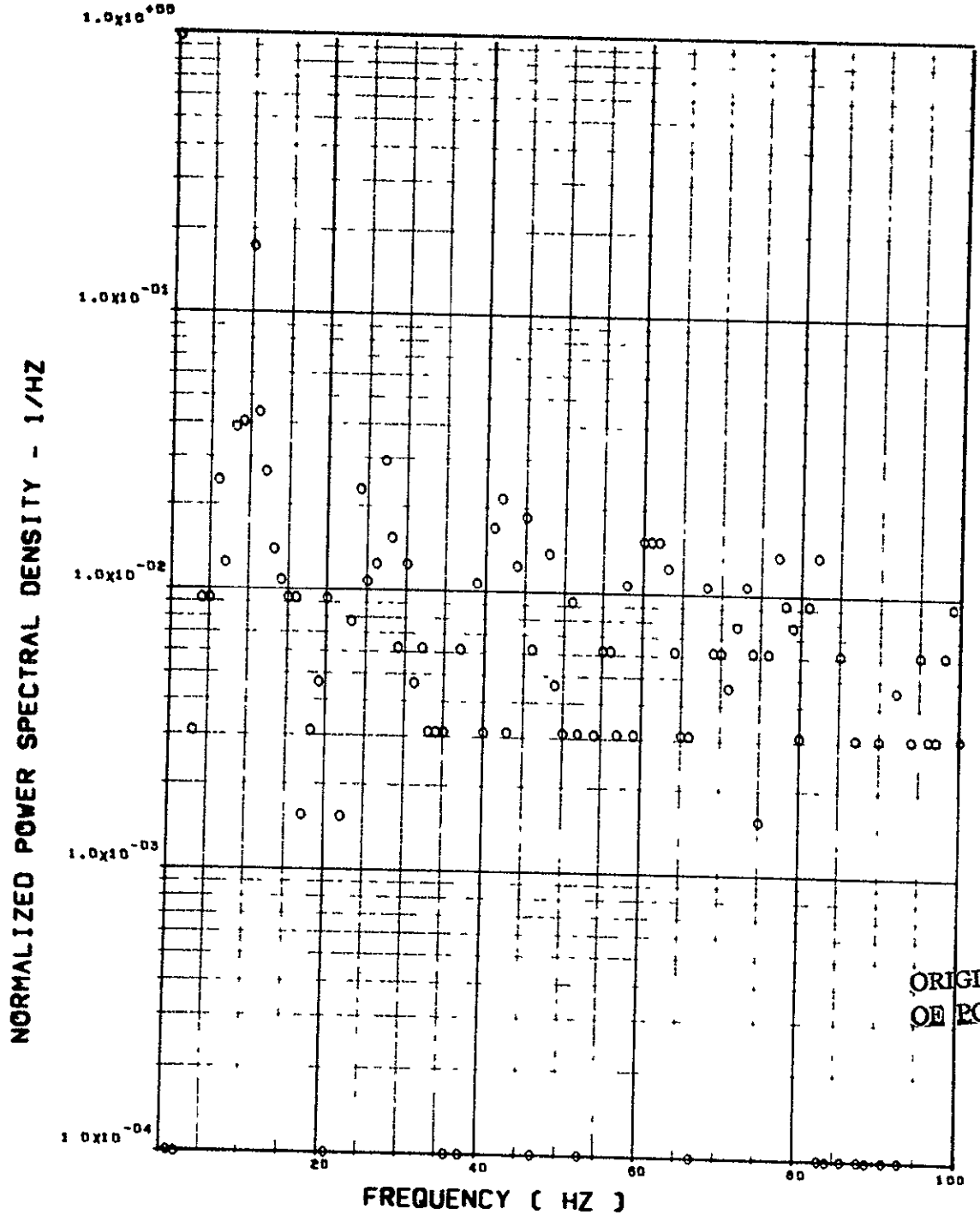

Figure 31. Continued

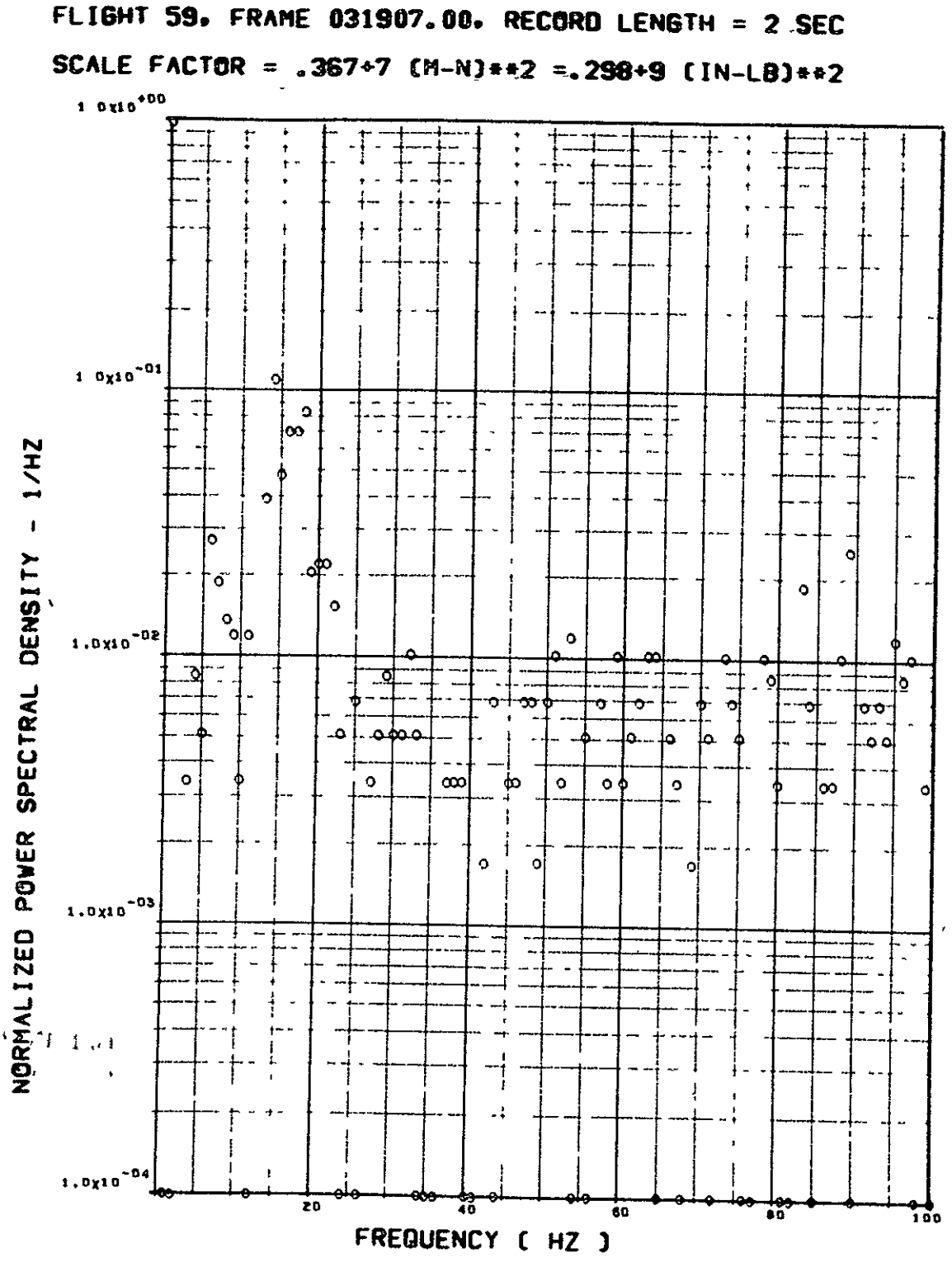

Figure 51. Continued

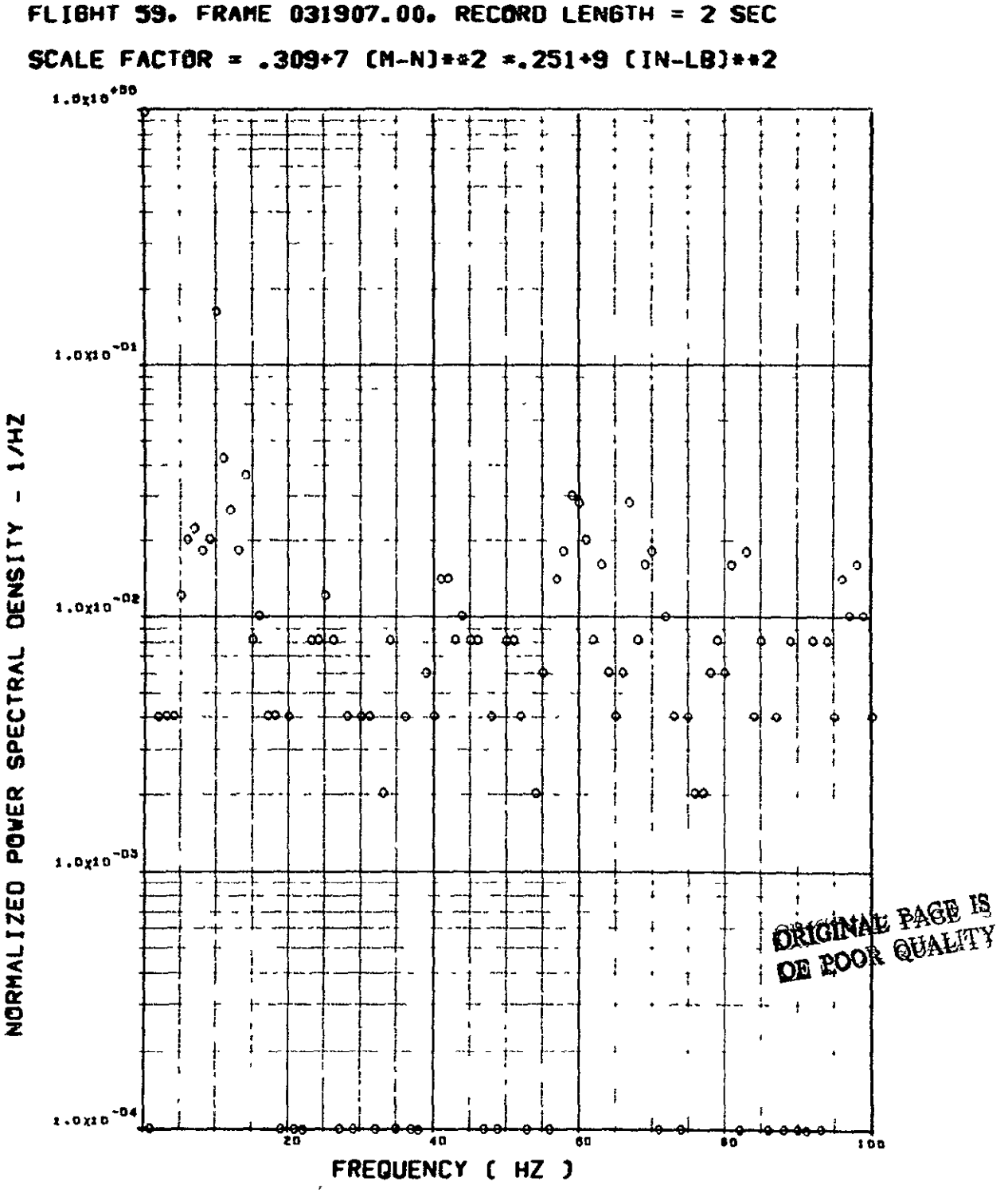

Figure 51. Continued

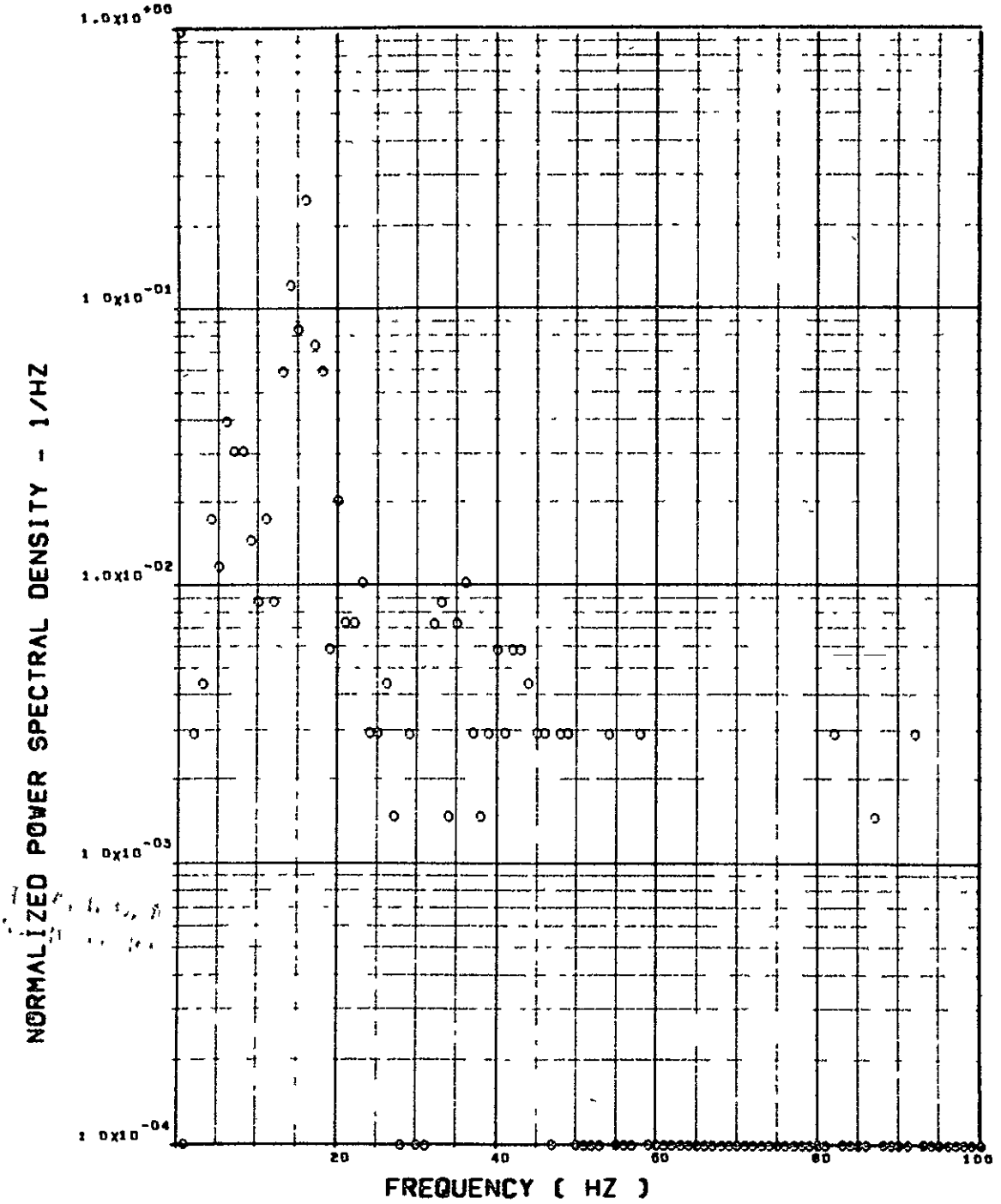

Figure 31. Continued

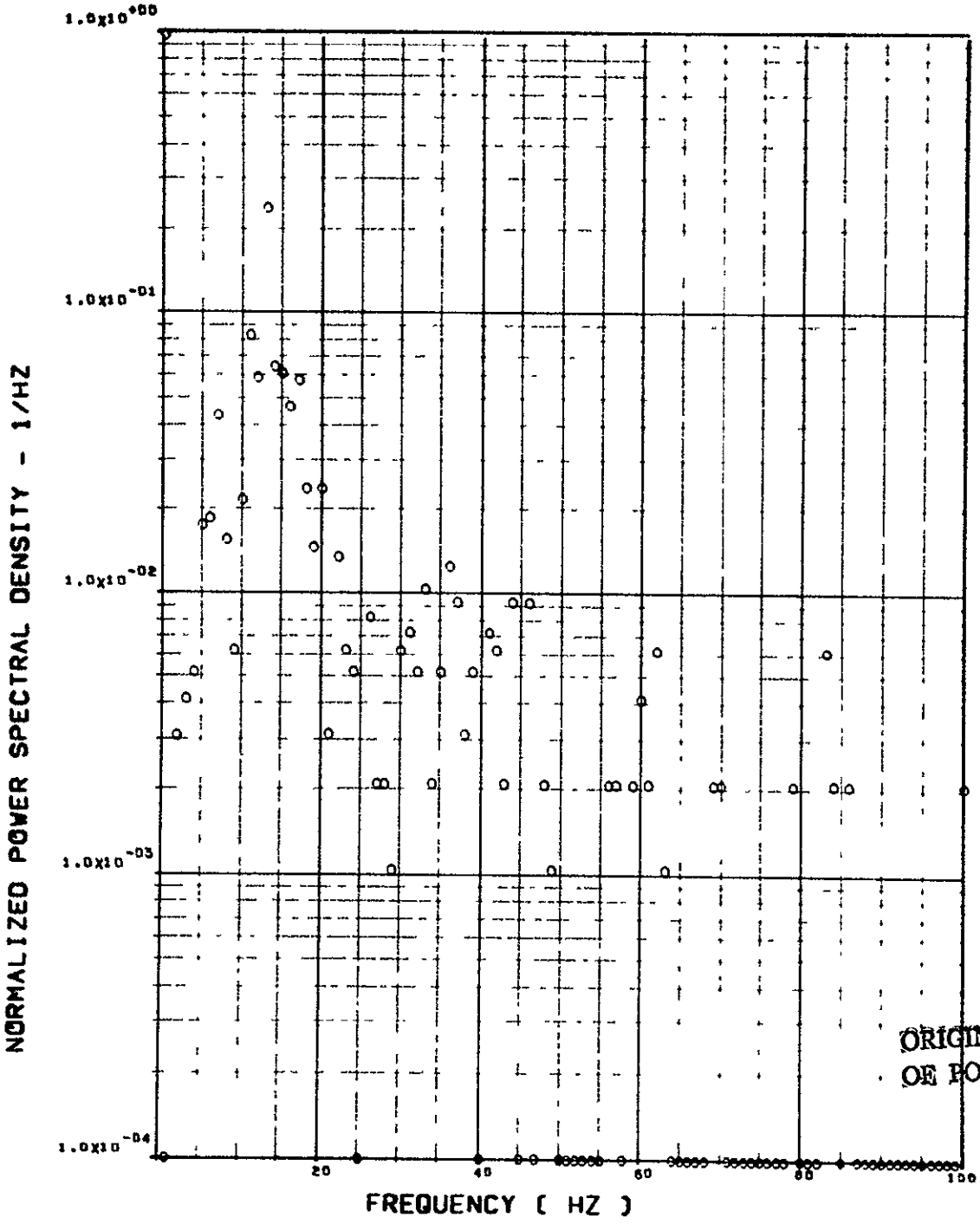

Figure 51. Concluded

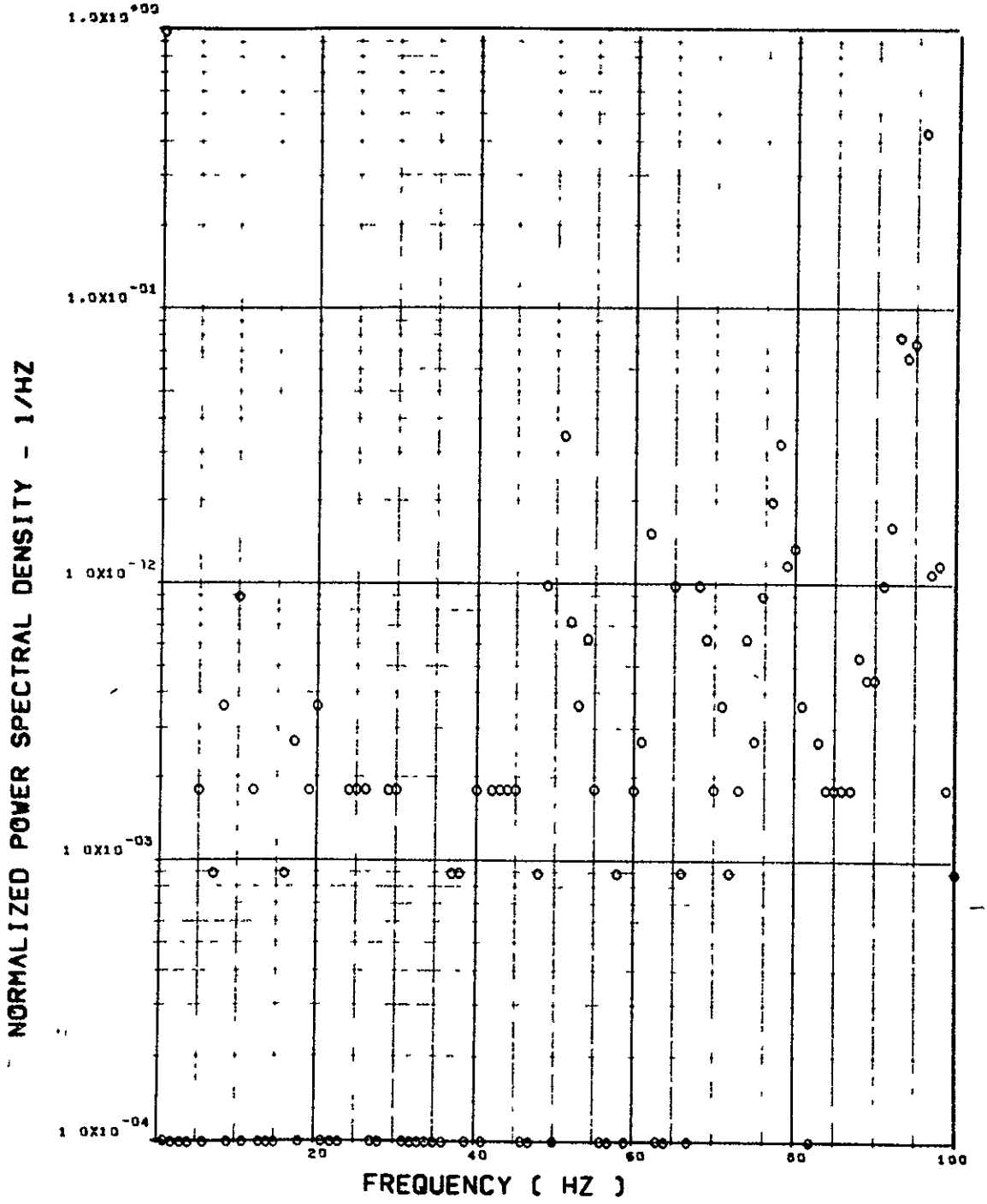

Figure 32. Power Spectra - Flight 48, Run 6, Point 3
T_1 = 133415 0, ΔT = 1 Sec, α_{Nom} = 9.1 deg,
$\Delta\alpha$ = 0 83 deg.

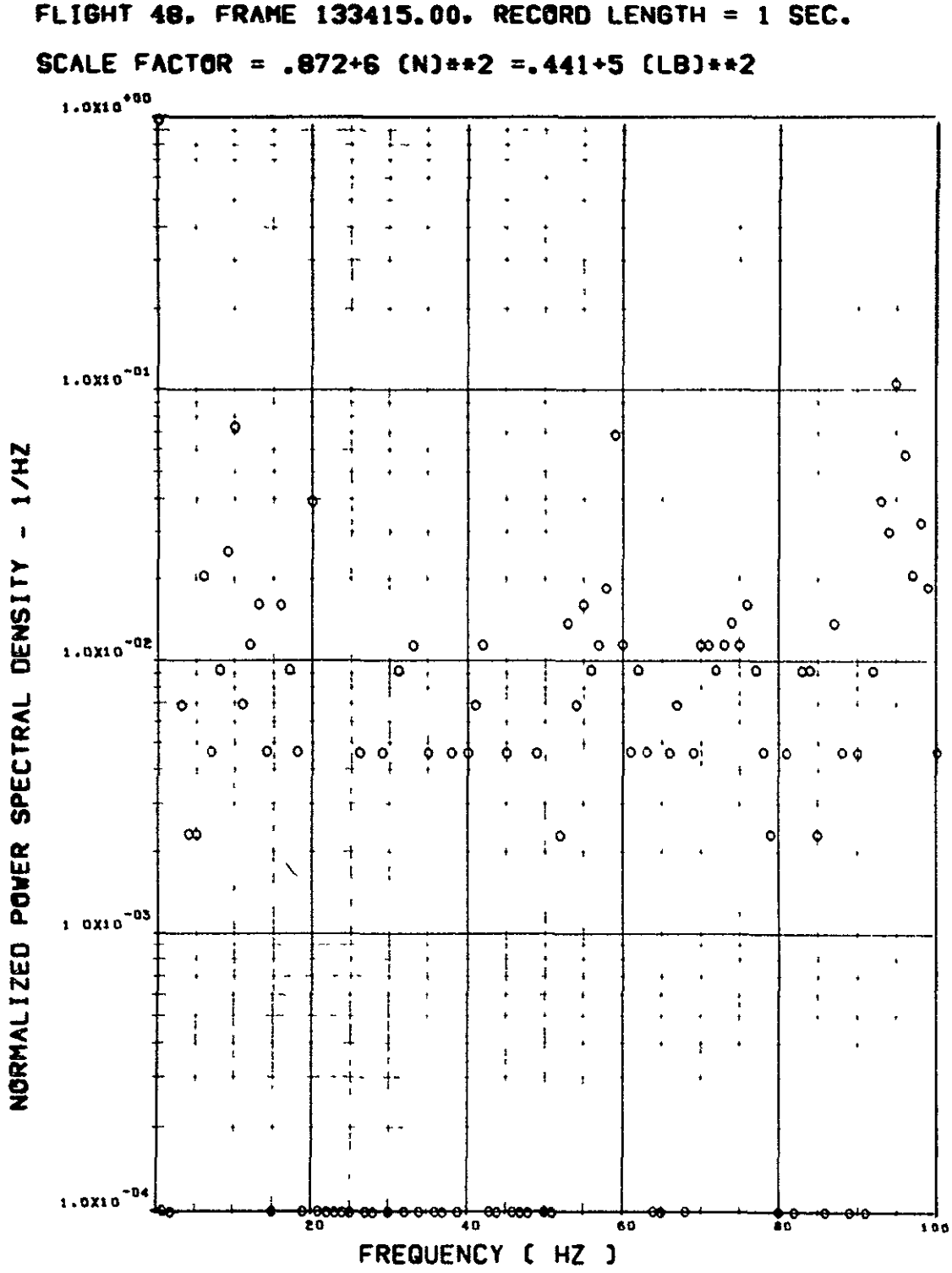

Figure 32. Continued

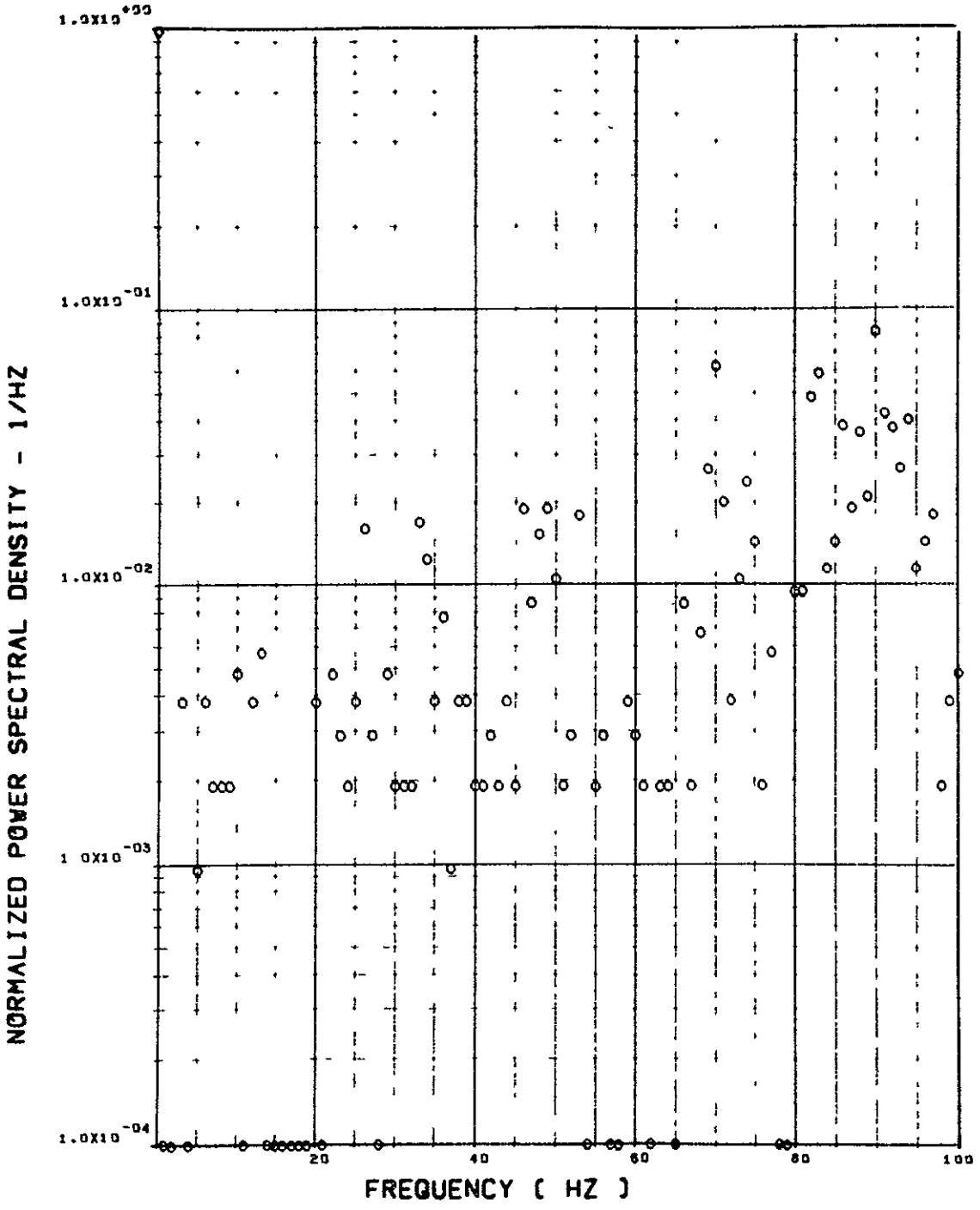

Figure 32. Continued

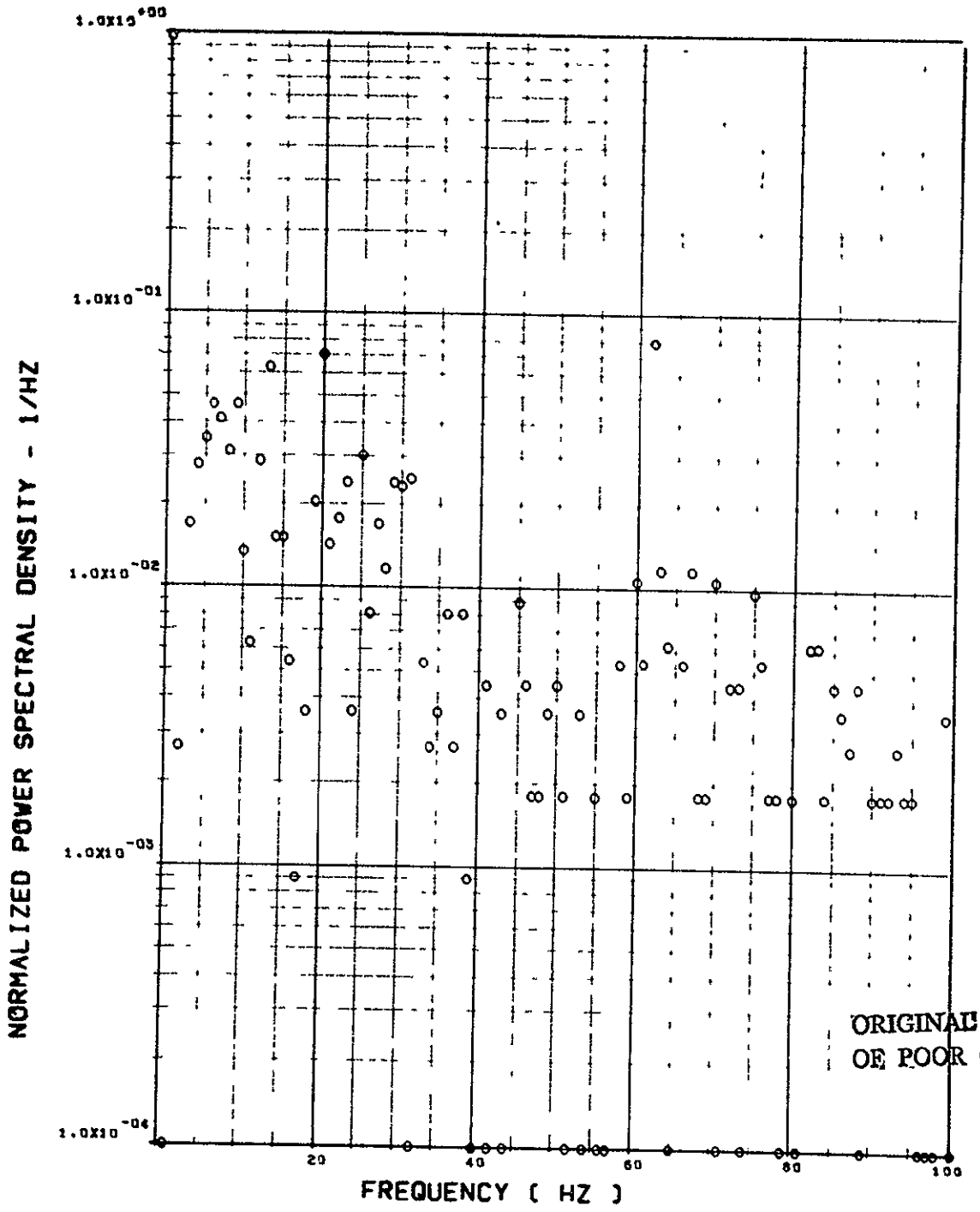

Figure 52. Continued

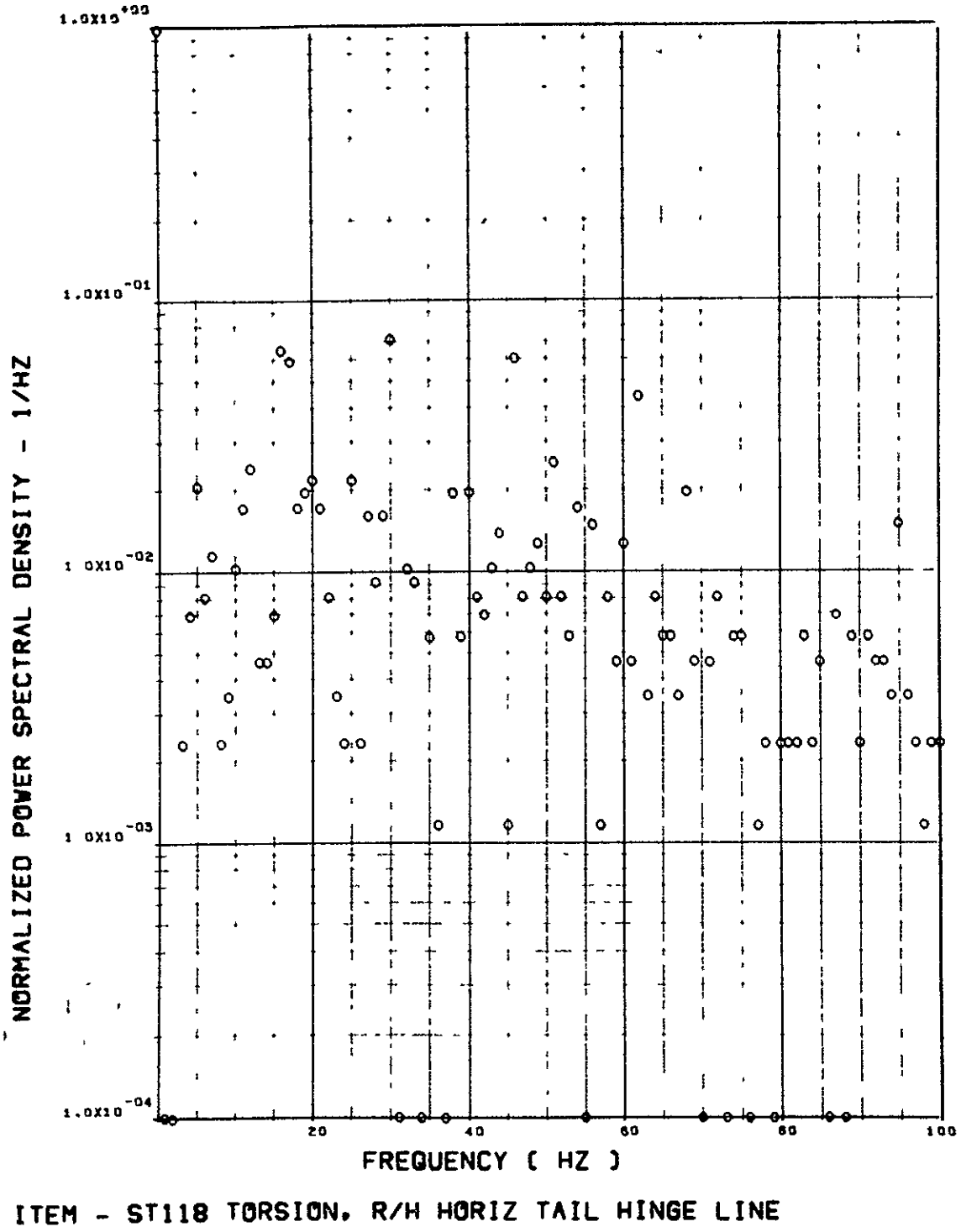

Figure 32. Concluded

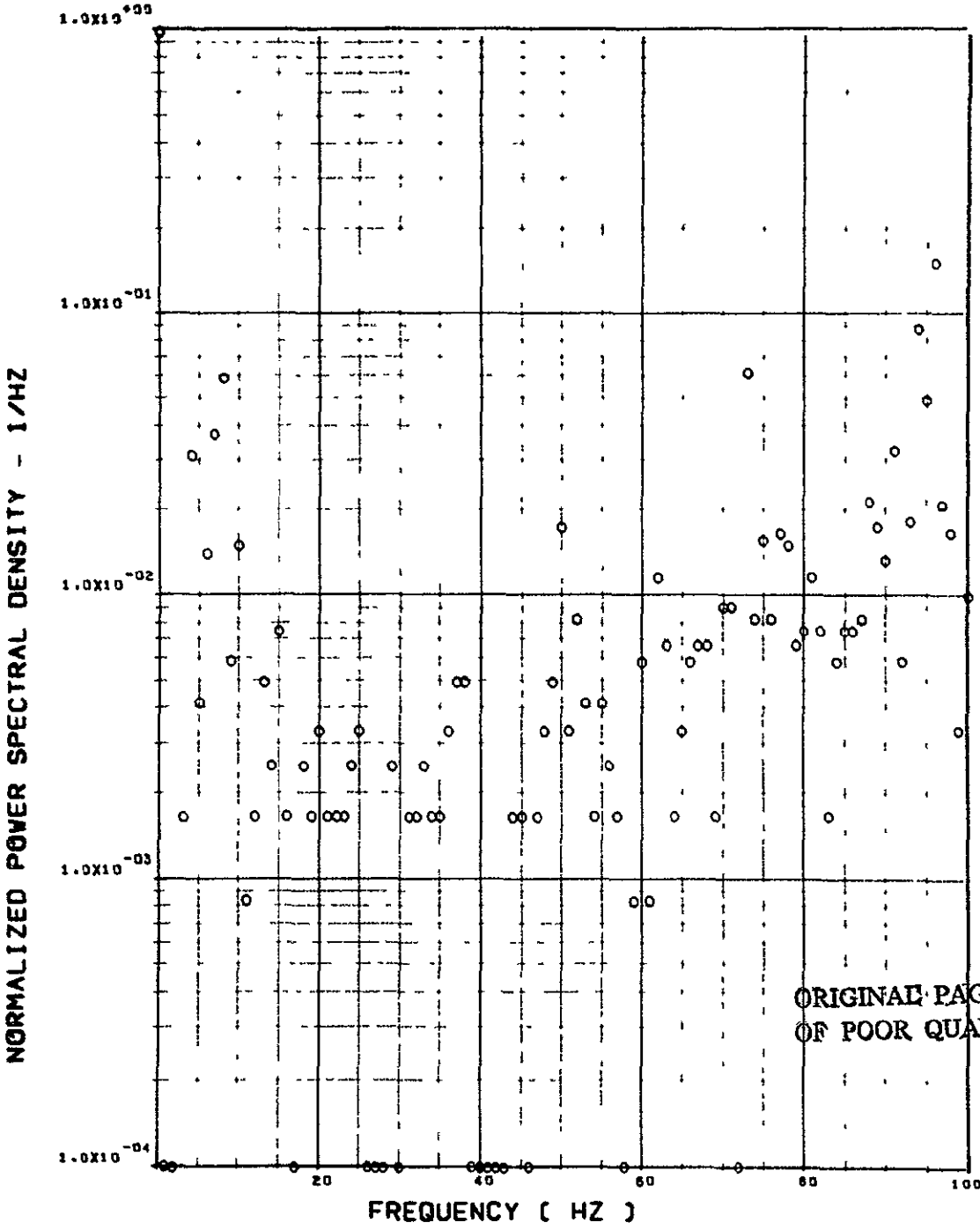

Figure 55. Power Spectra - Flight 48, Run 6, Point 4
T_1 = 133416.7, ΔT = 1 Sec, α_{Nom} = 10 2 deg,
$\Delta\alpha$= 1.05 deg.

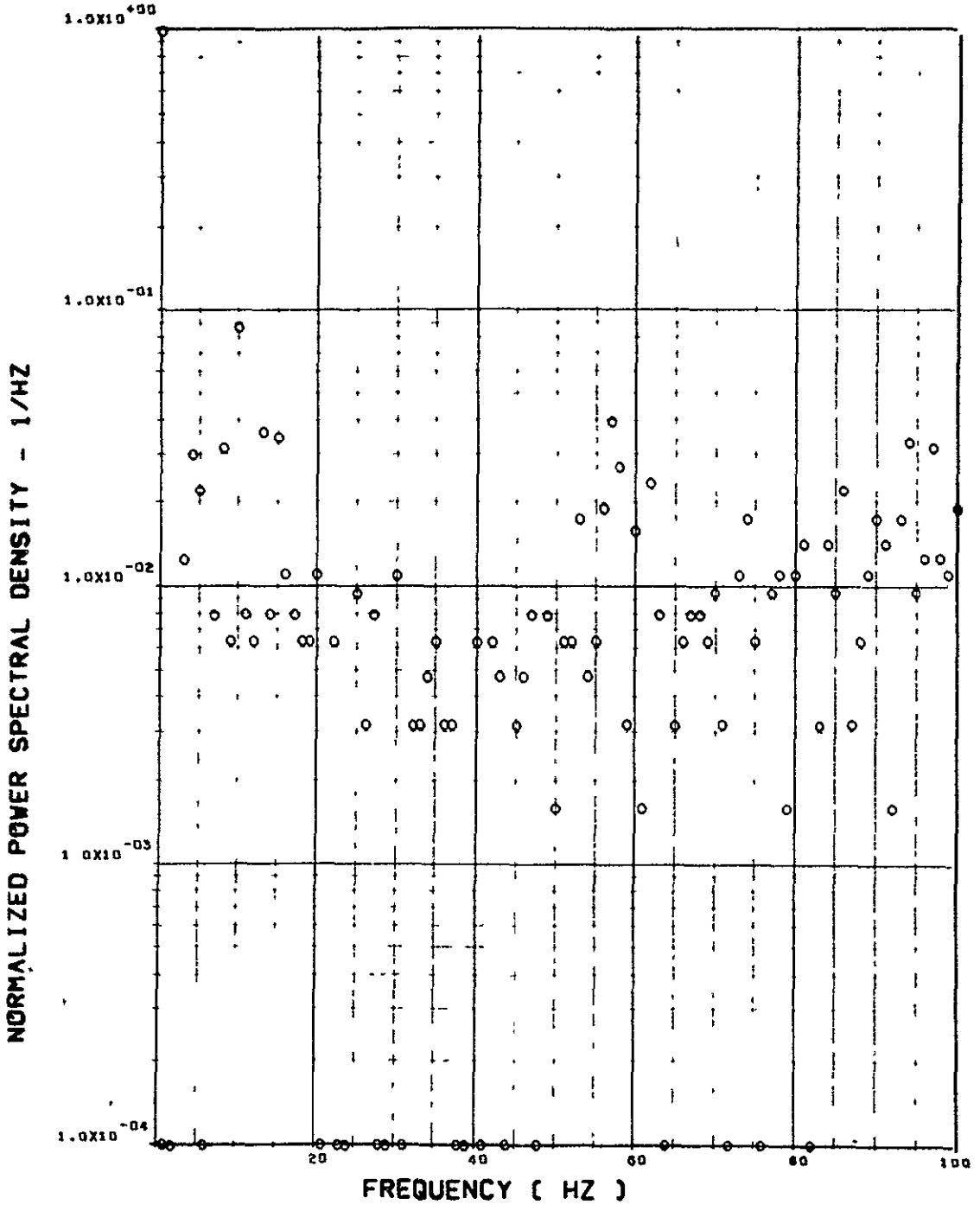

Figure 55. Continued

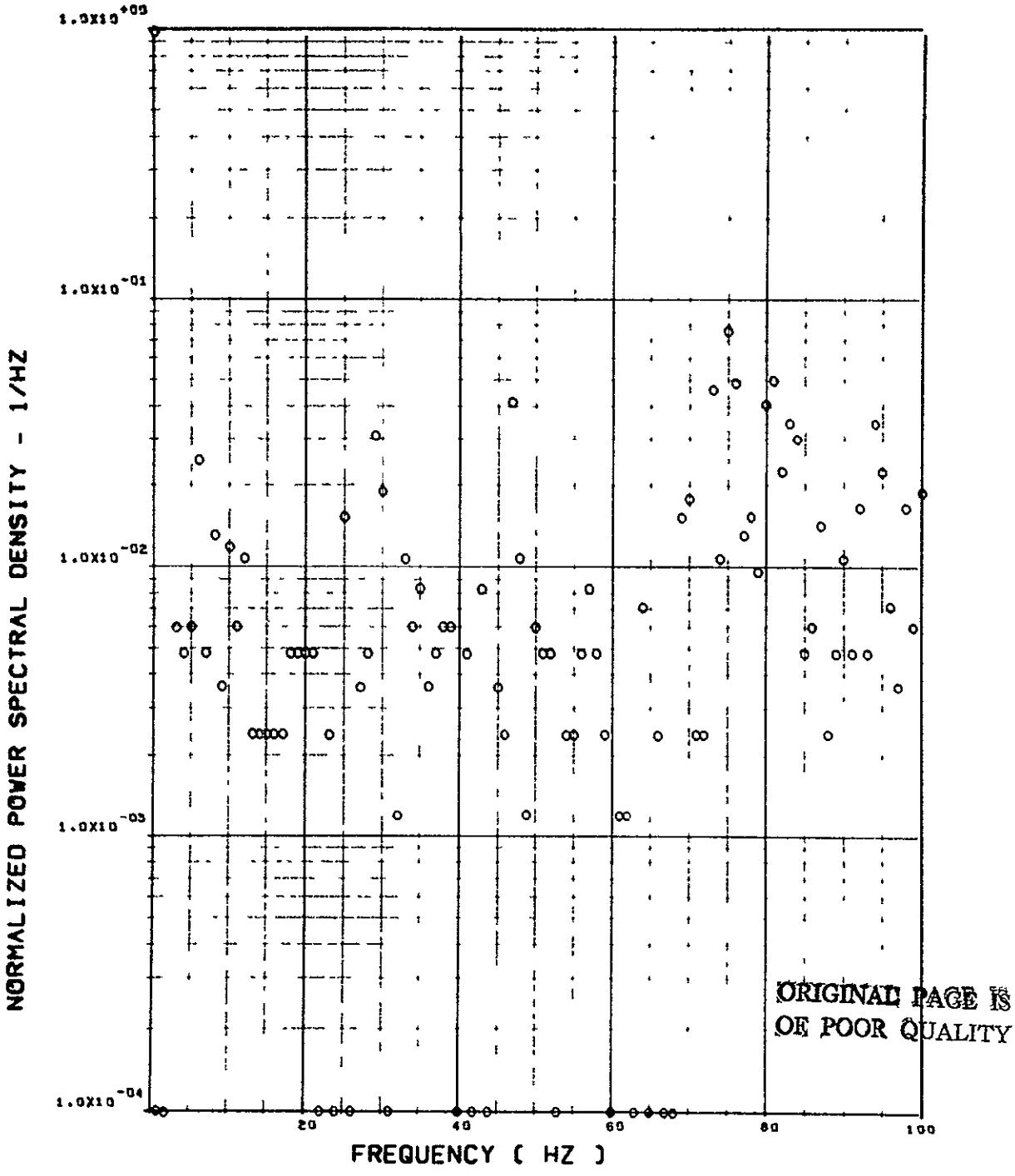

Figure 53. Continued

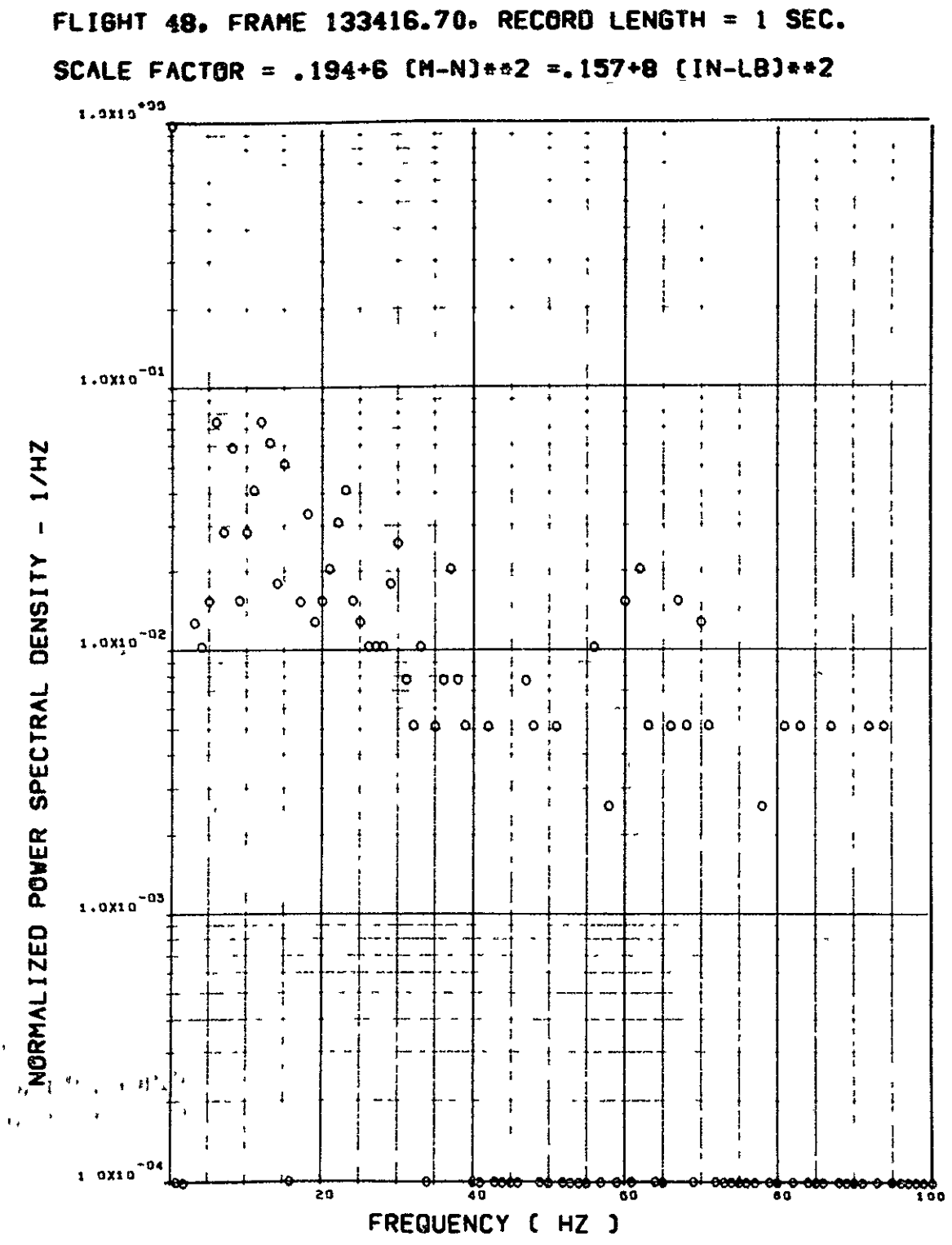

Figure 33. Continued

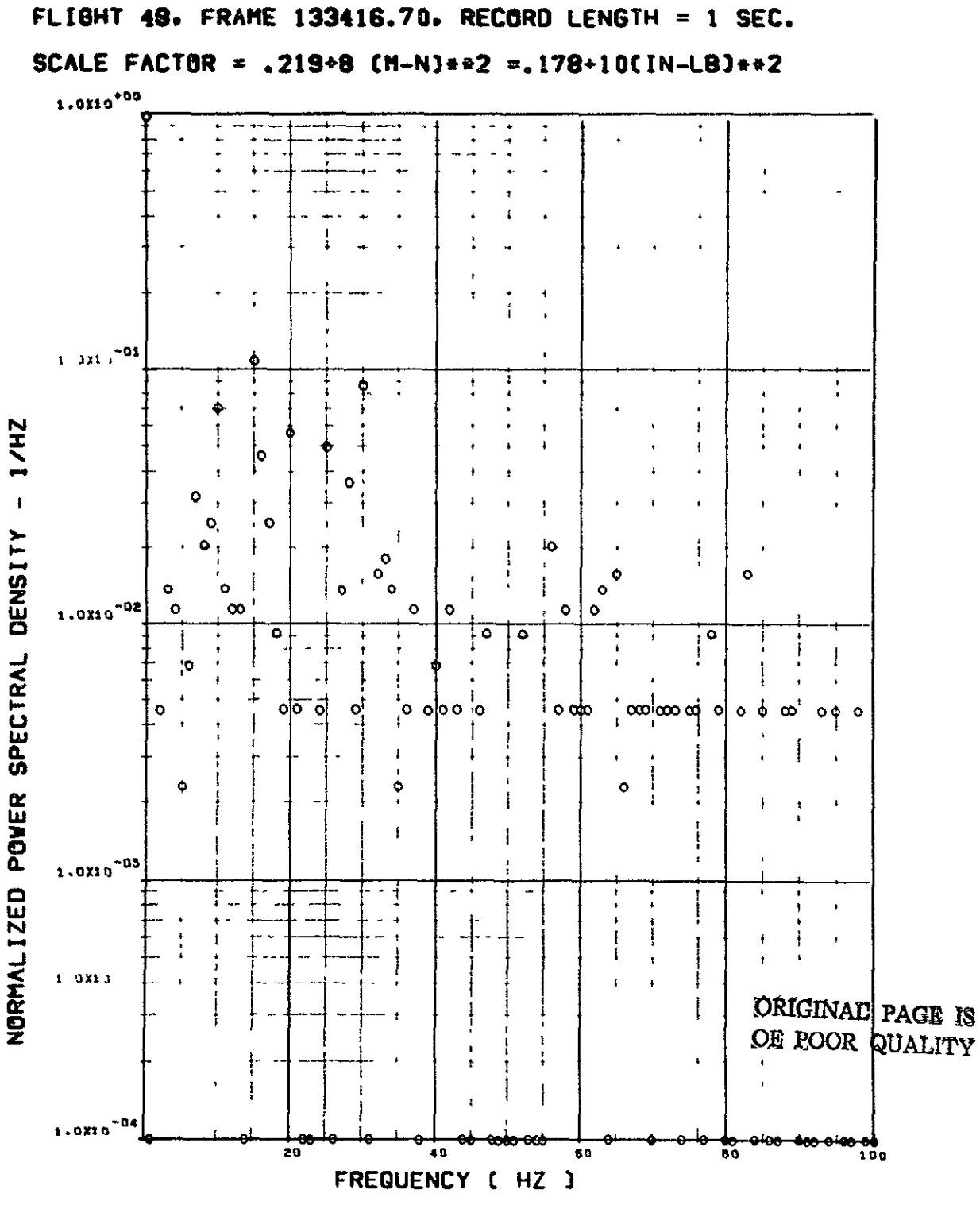

Figure 3b. Concluded

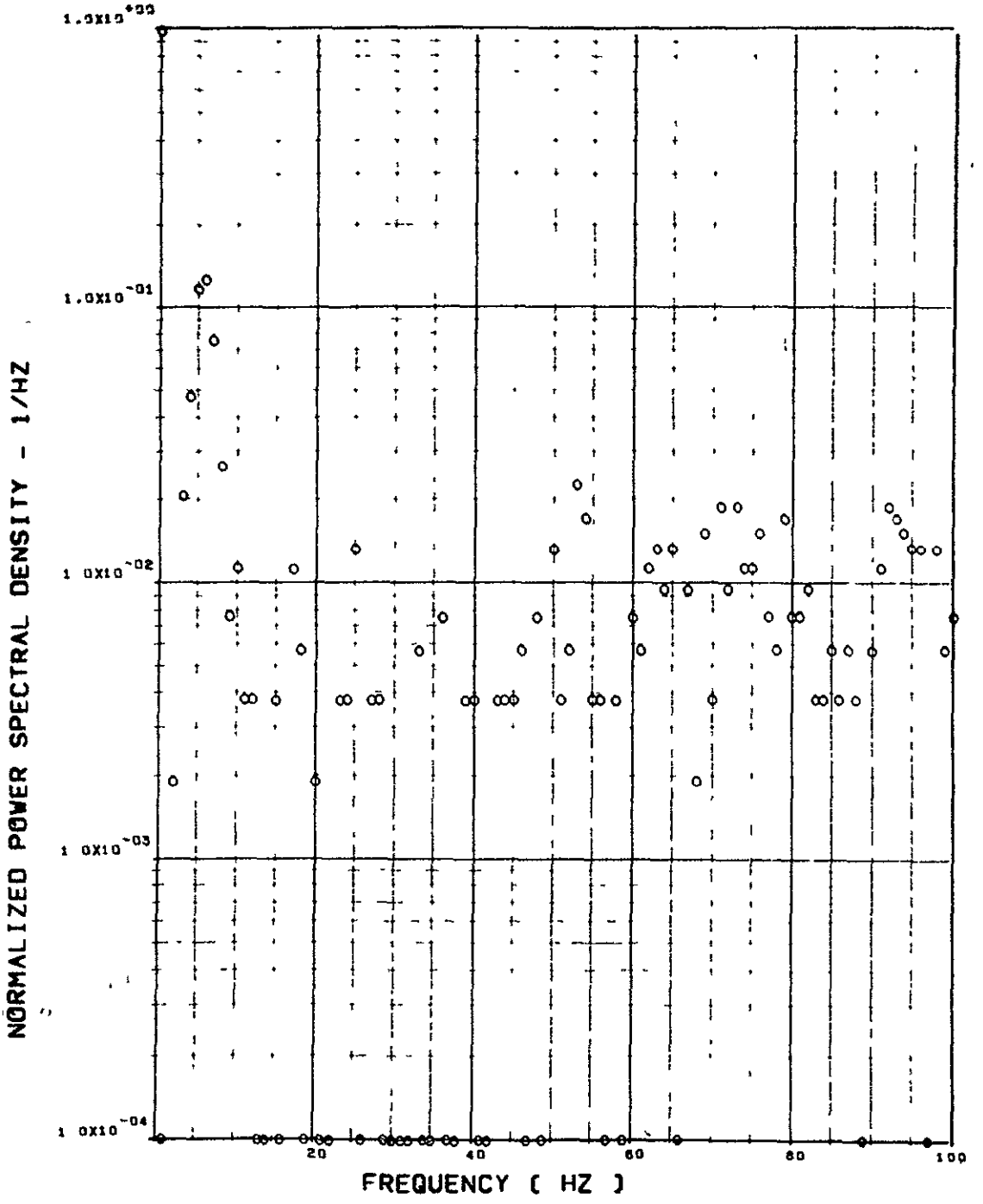

Figure 51. Power Spectra - Flight 48, Run 6, Point 5
T_1 = 133417 3, ΔT = 1 Sec, α_{Nom} = 11.1 deg,
$\Delta\alpha$= 1 45 deg

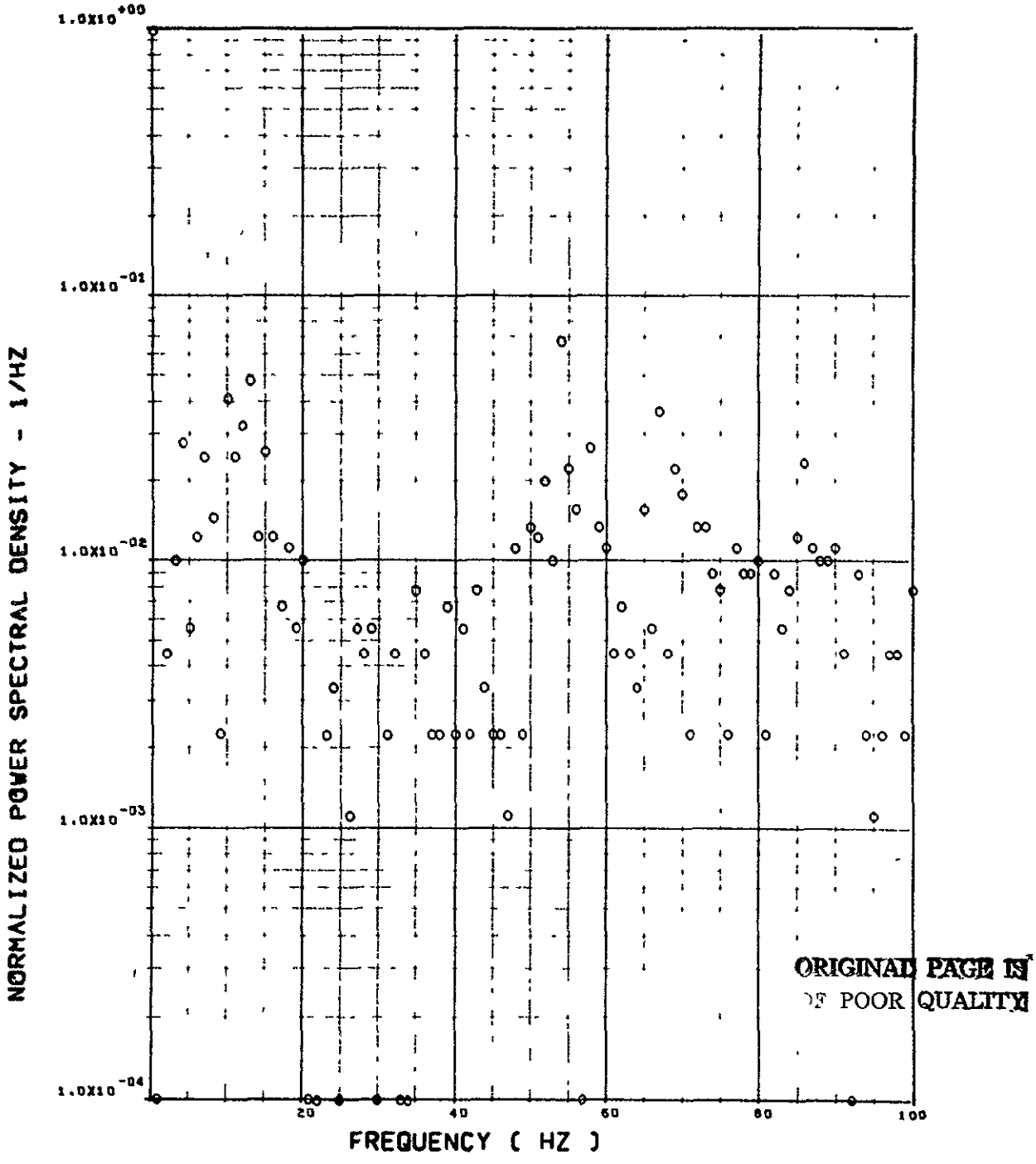

Figure 24. Continued

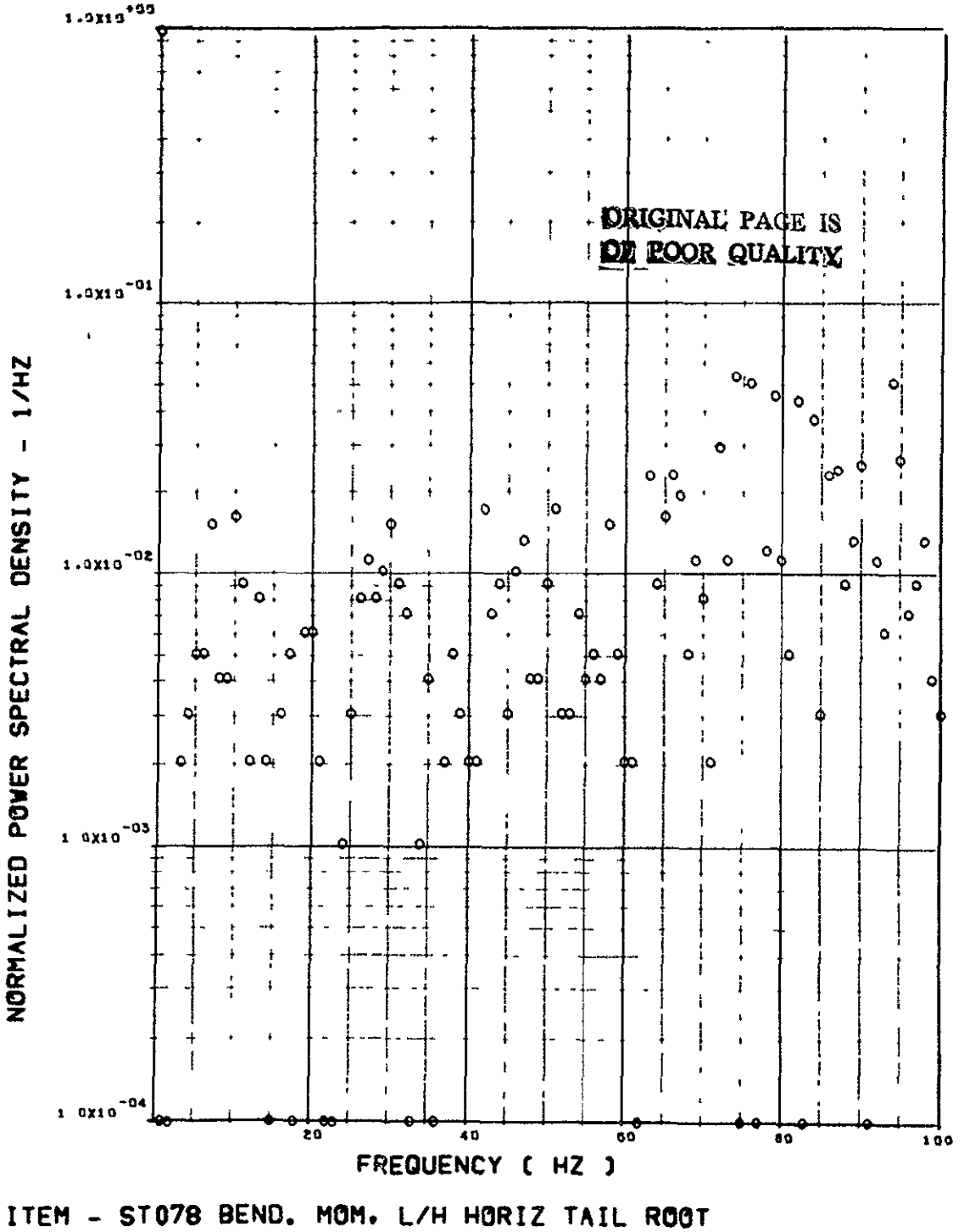

Figure 34. Continued

FLIGHT 48. FRAME 133417.30. RECORD LENGTH = 1 SEC.

SCALE FACTOR = .418+6 (M-N)**2 =.340+8 (IN-LB)**2

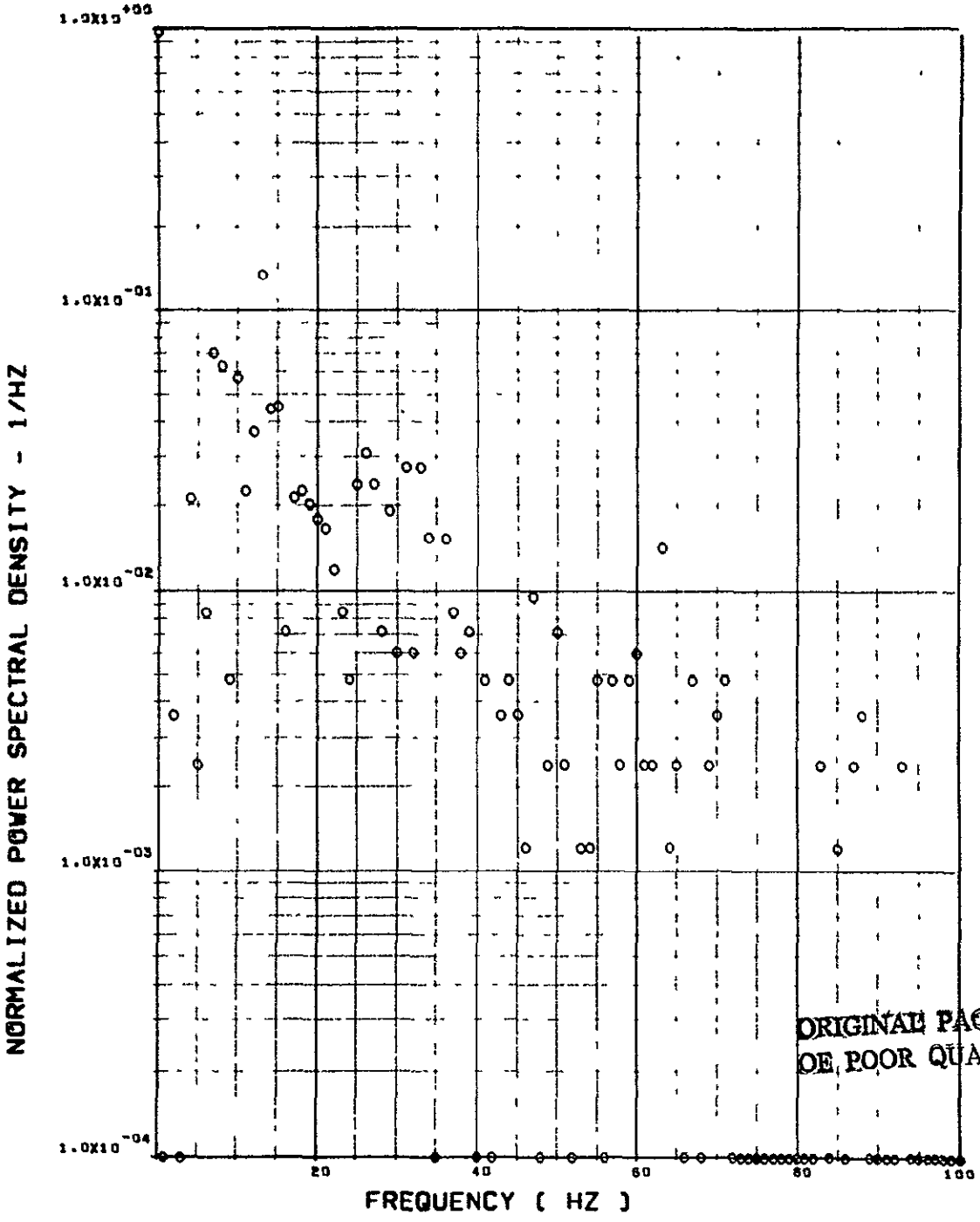

ITEM - ST135 TORSION. L/H HORIZ TAIL HINGE LINE

Figure 24. Continued

C-8

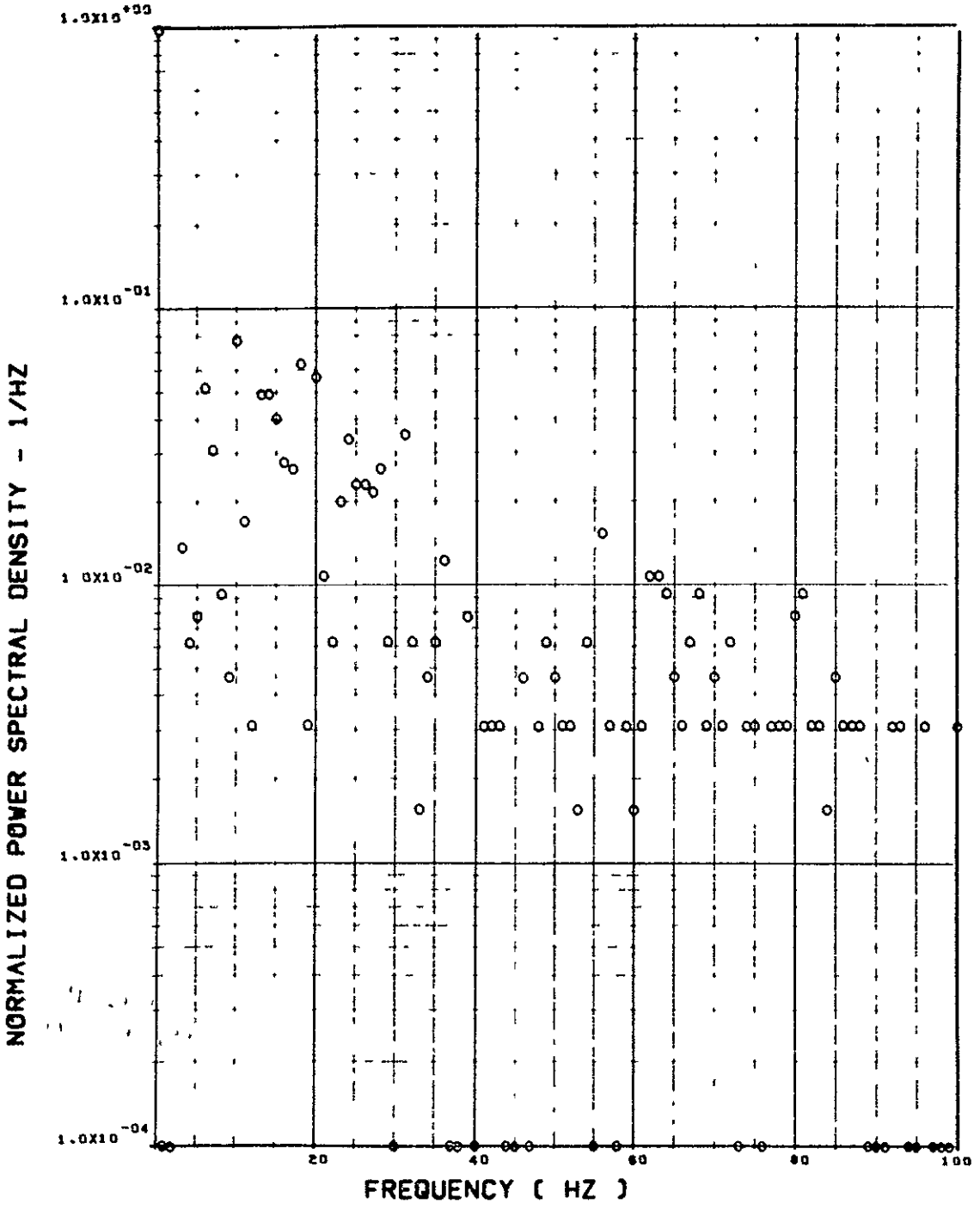

Figure 24. Concluded

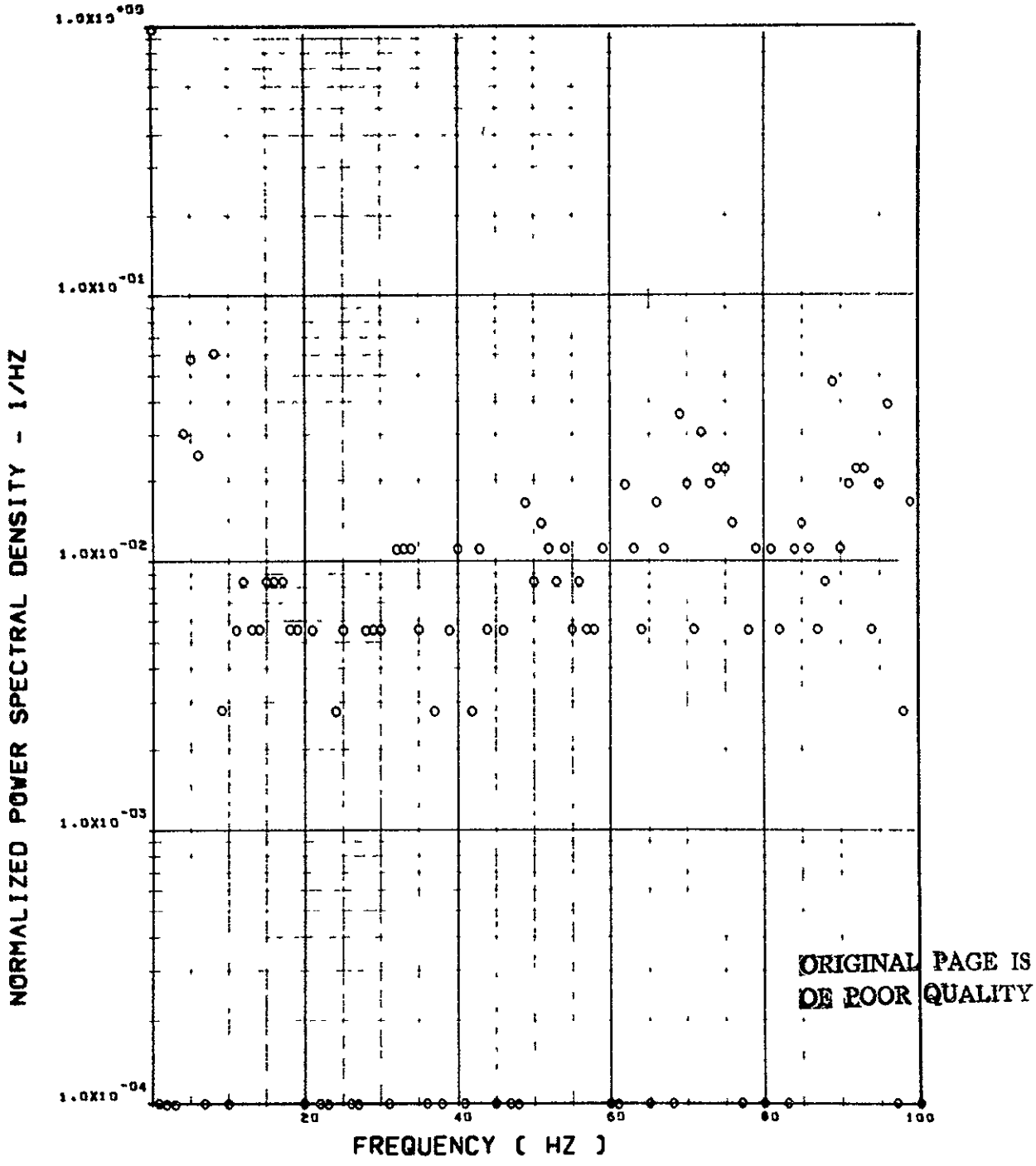

Figure 55. Power Spectra - Flight 48, Run 6, Point 6
T_1 = 133419.0, ΔT = 1 Sec, α_{Nom} = 12 3 deg.
$\Delta\alpha$= 2 40 deg.

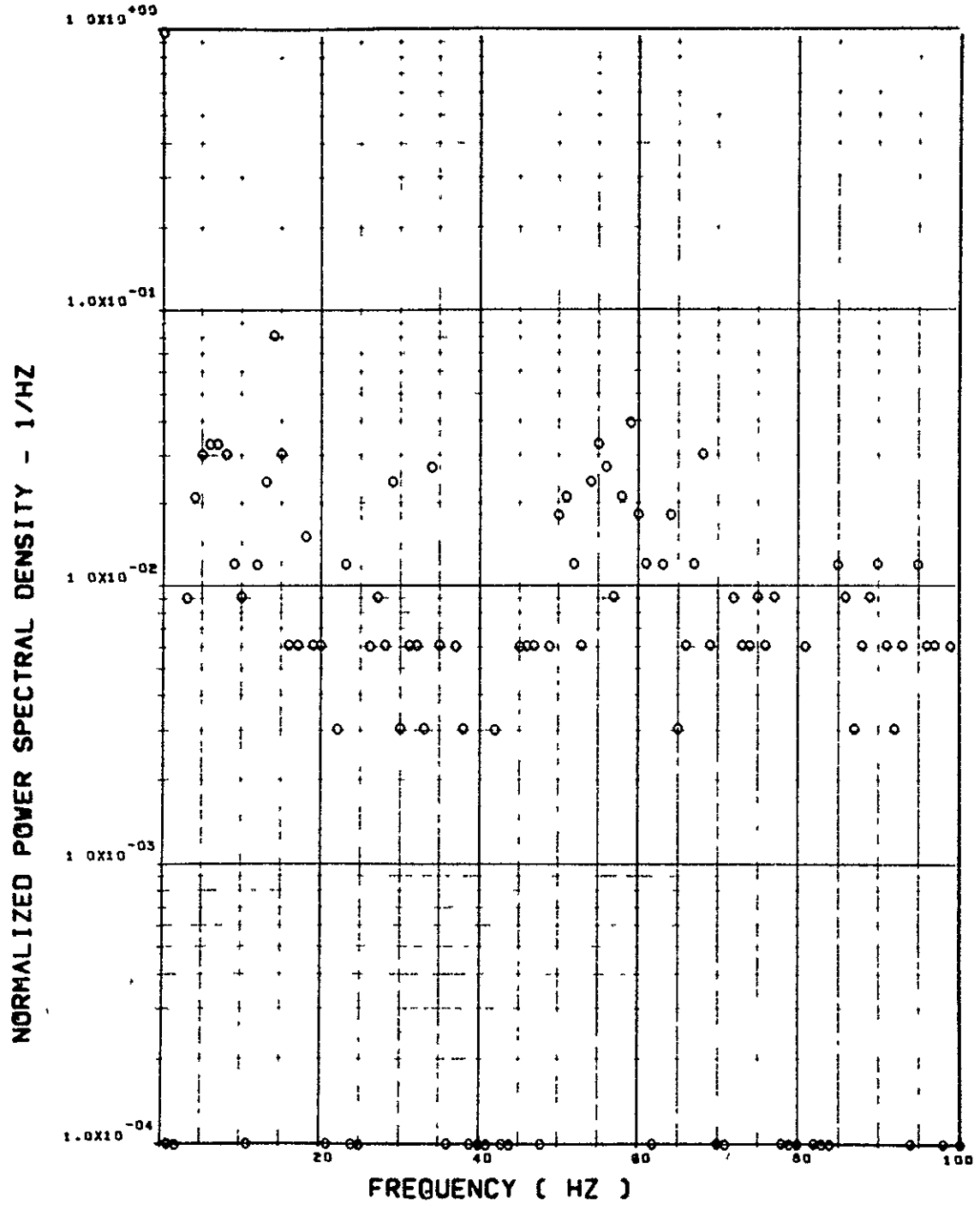

Figure 55. Continued

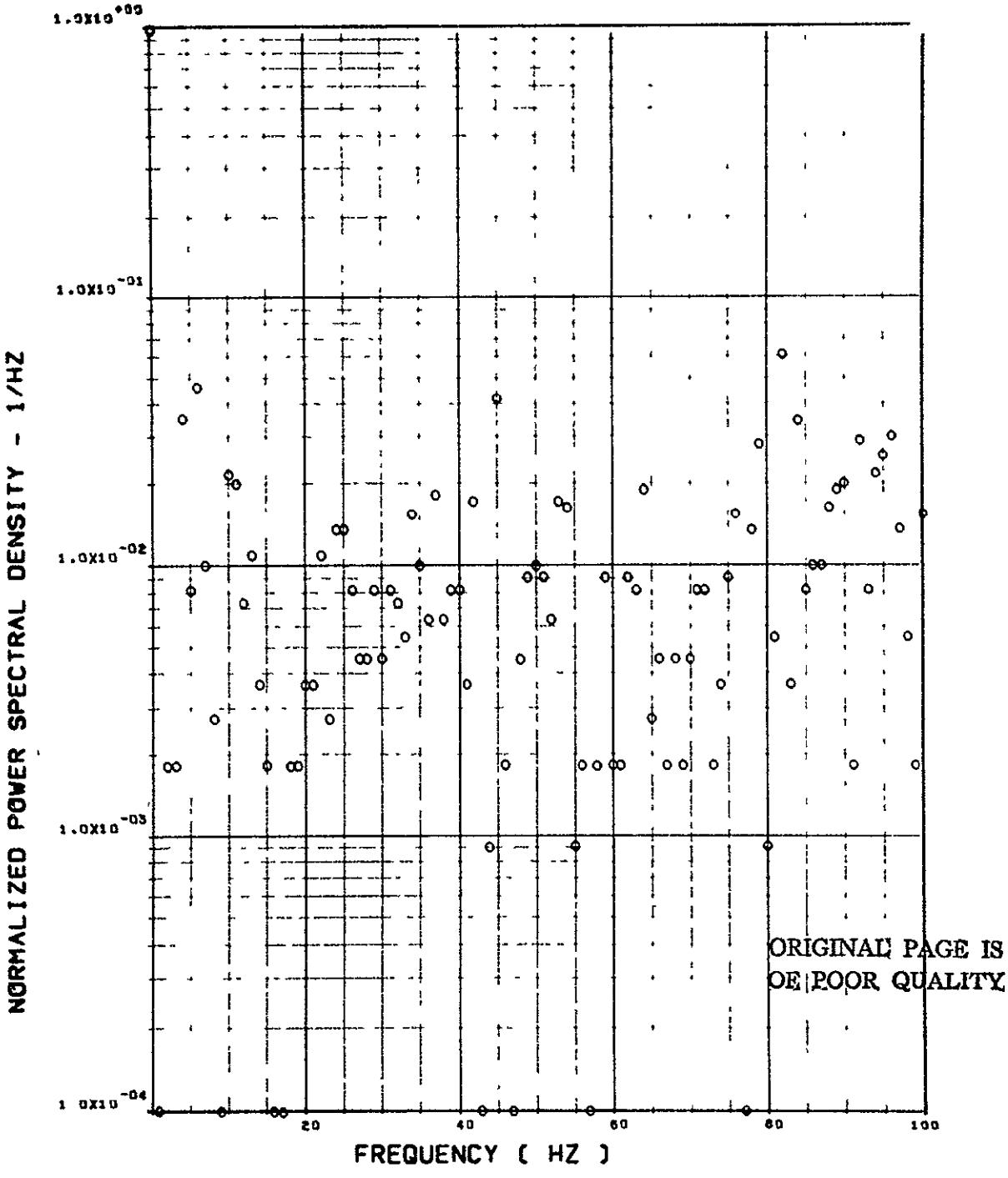

Figure 55. Continued

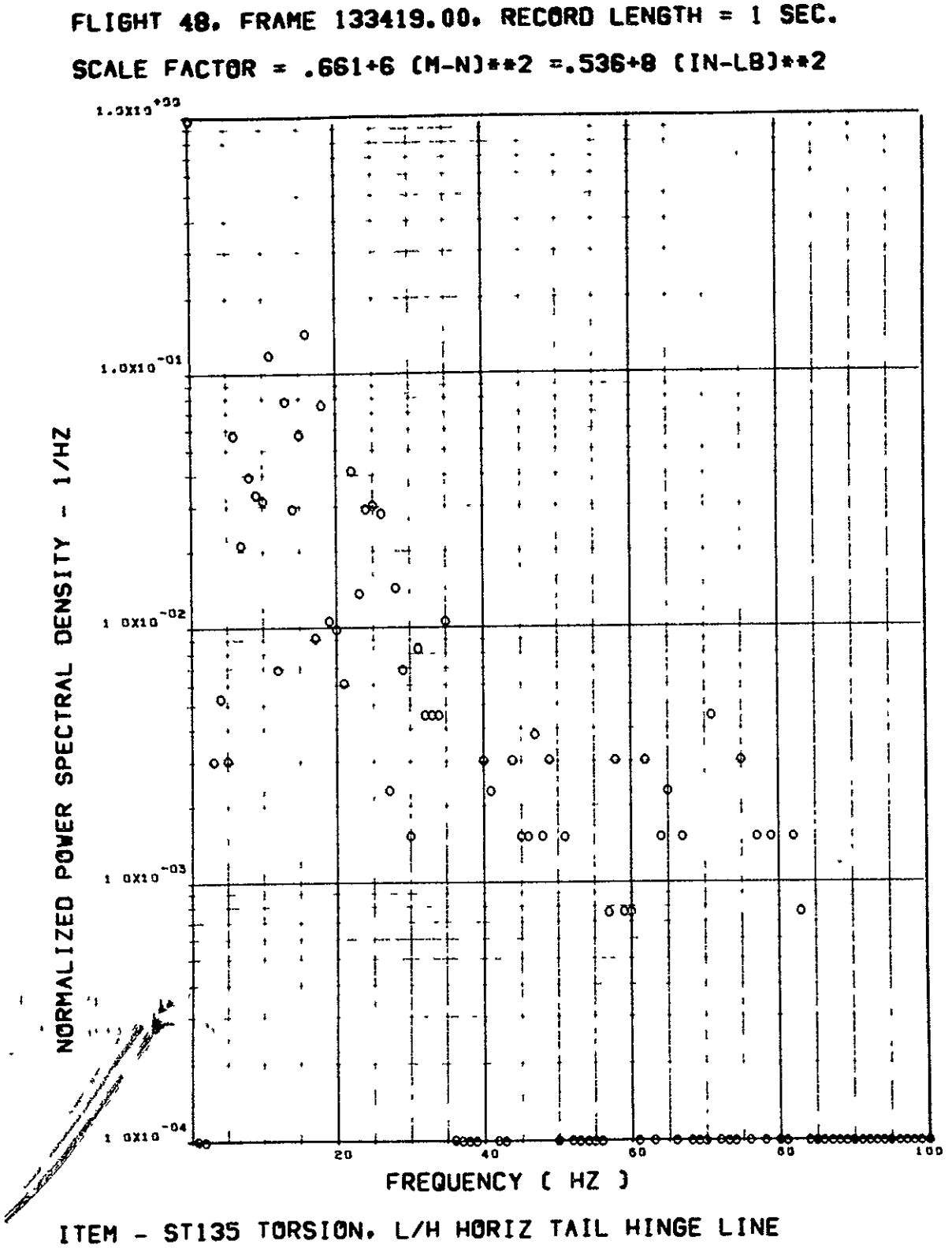

Figure 55. Continued

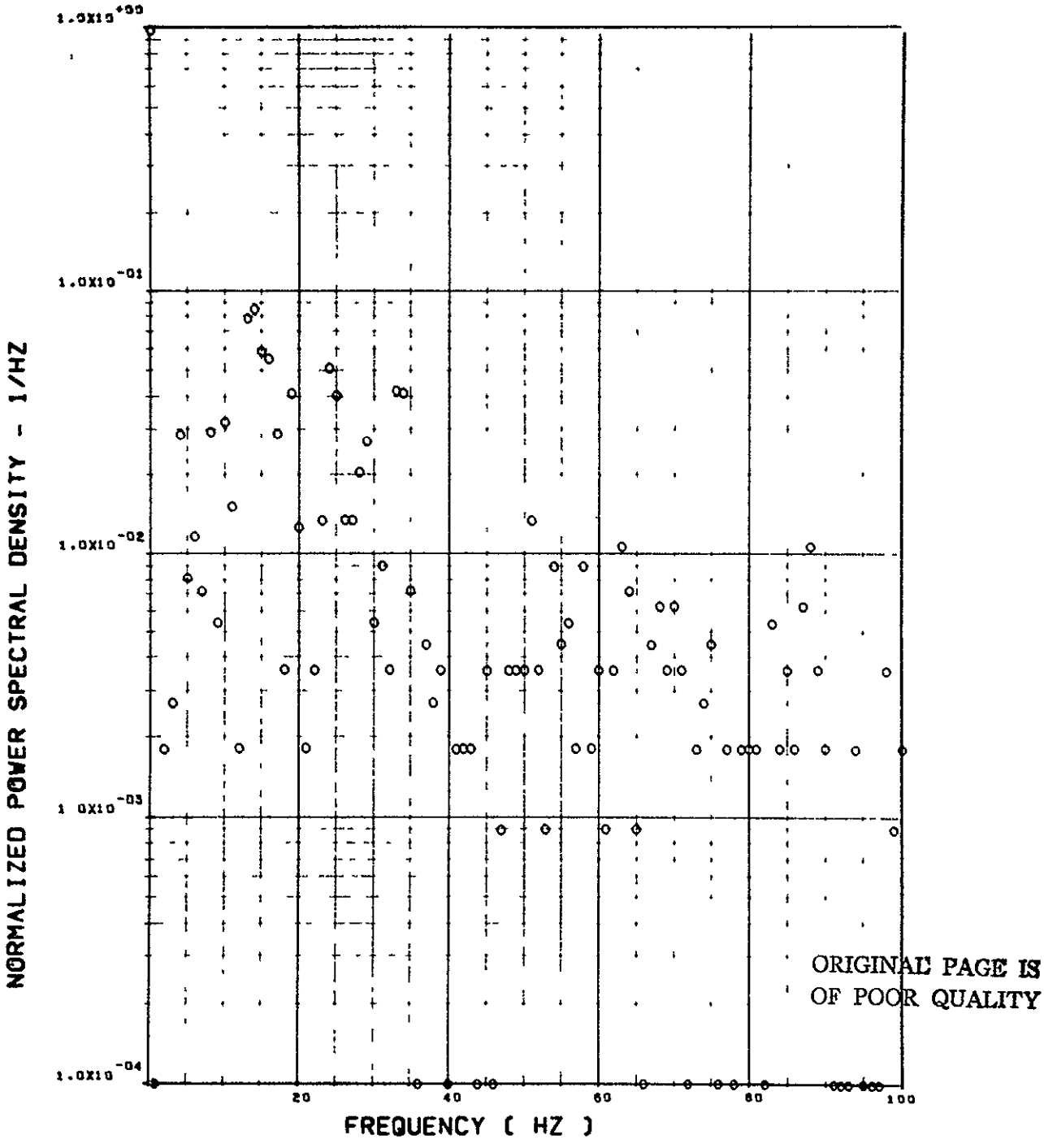

Figure 35. Concluded

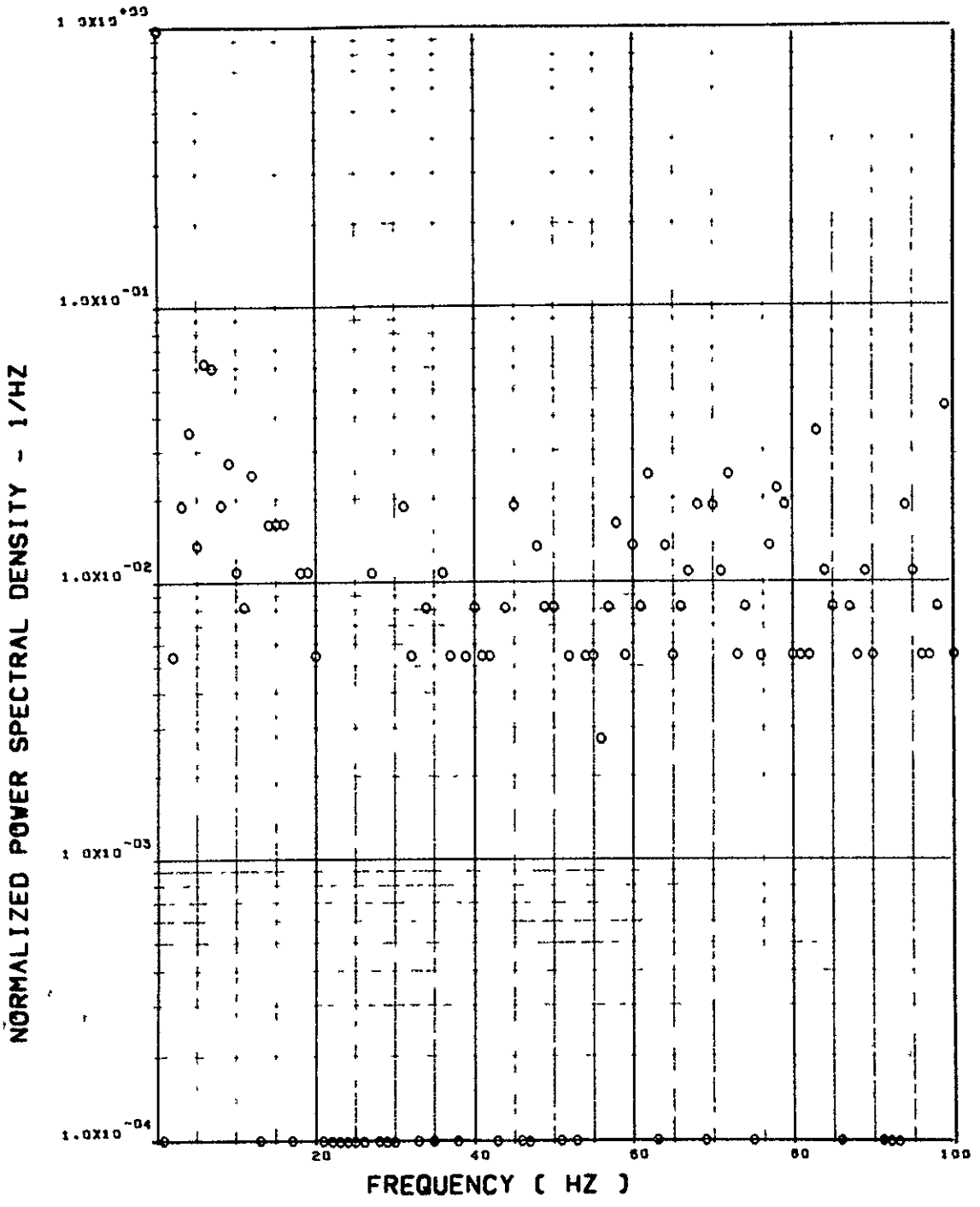

Figure 56. Power Spectra - Flight 48, Run 6, Point 7
T_1 = 133420 3, ΔT = 1 Sec, α_{Nom} = 15.3 deg,
$\Delta\alpha$= 2 35 deg

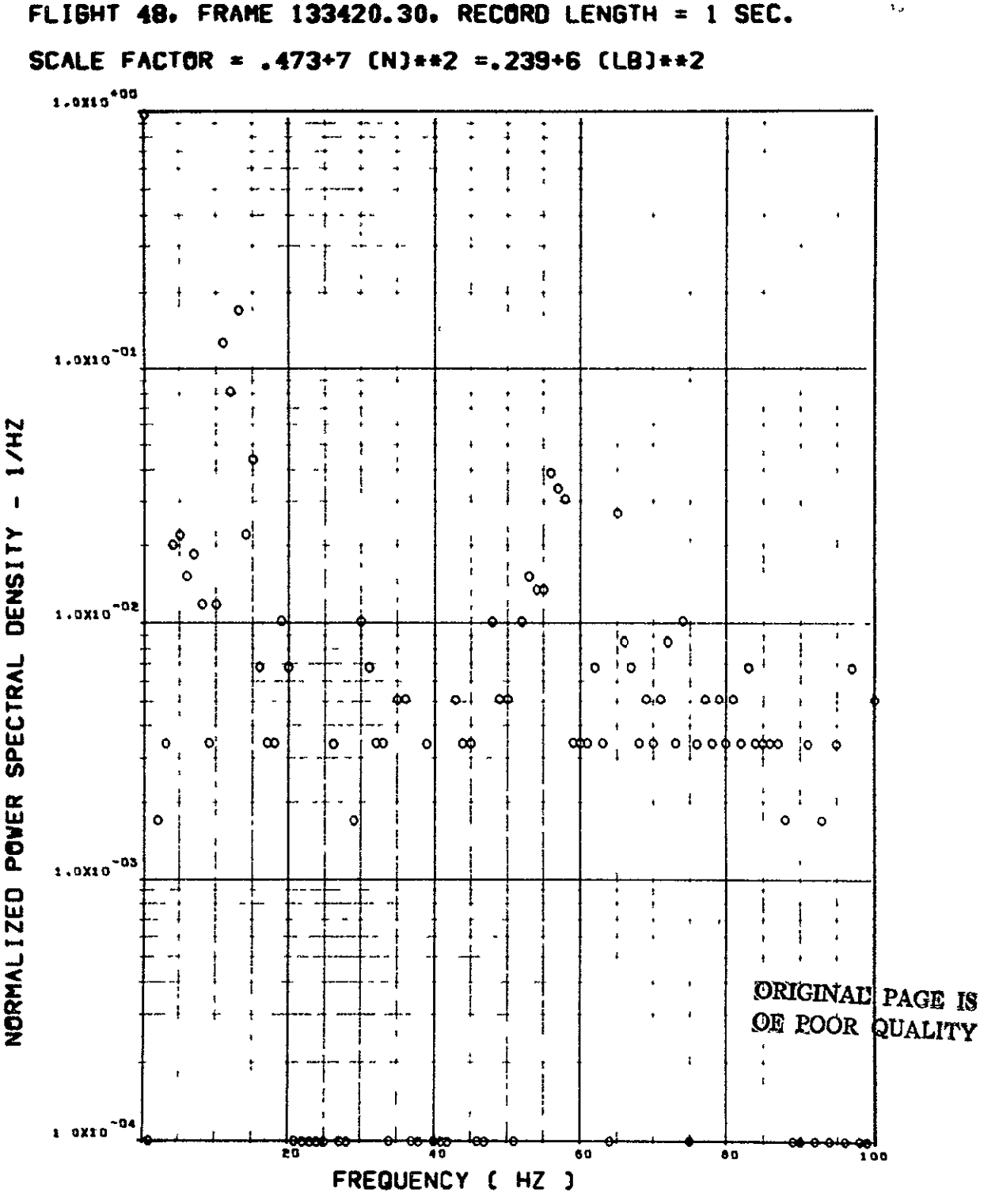

Figure 56. Continued

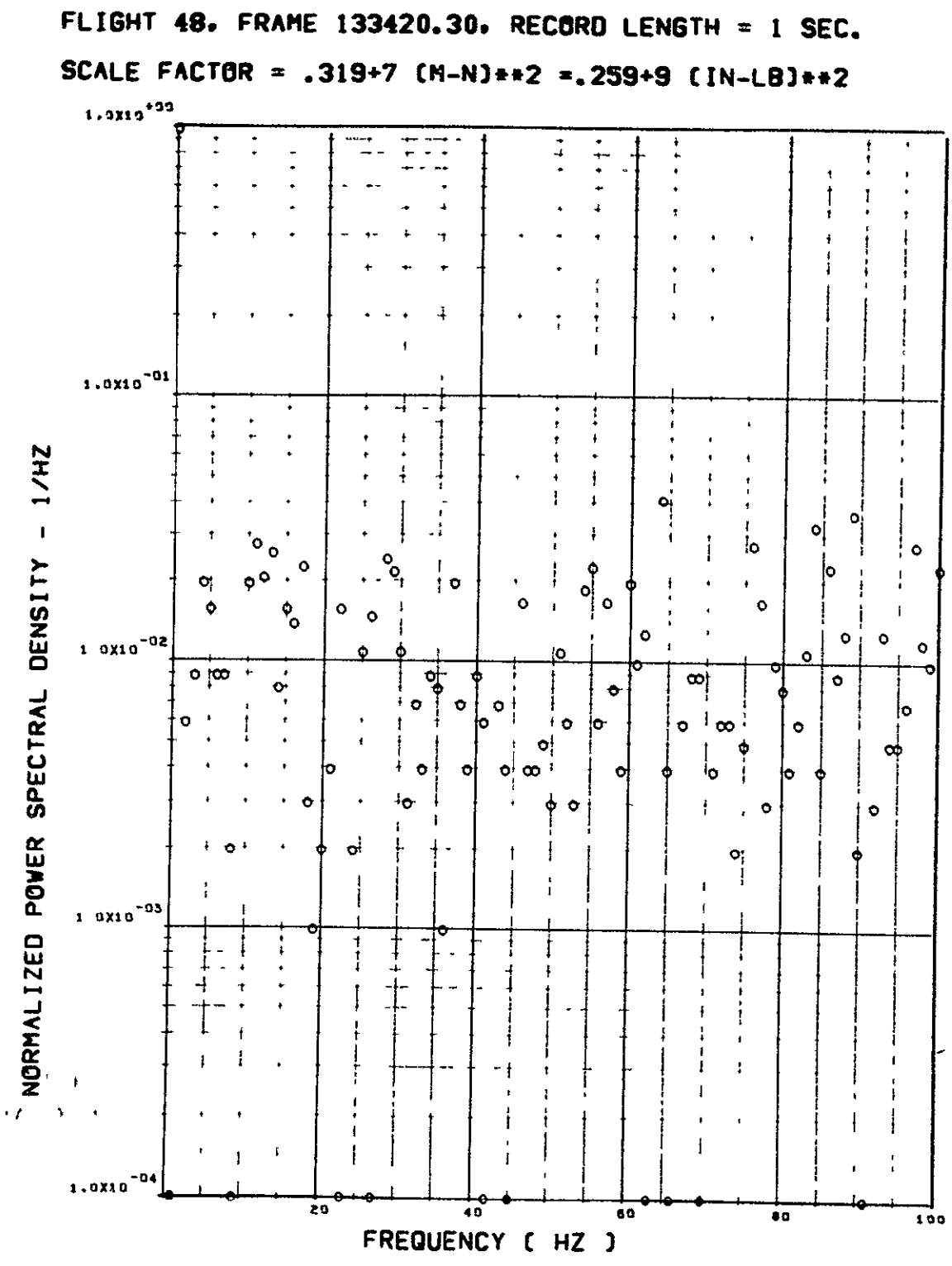

Figure 36. Continued

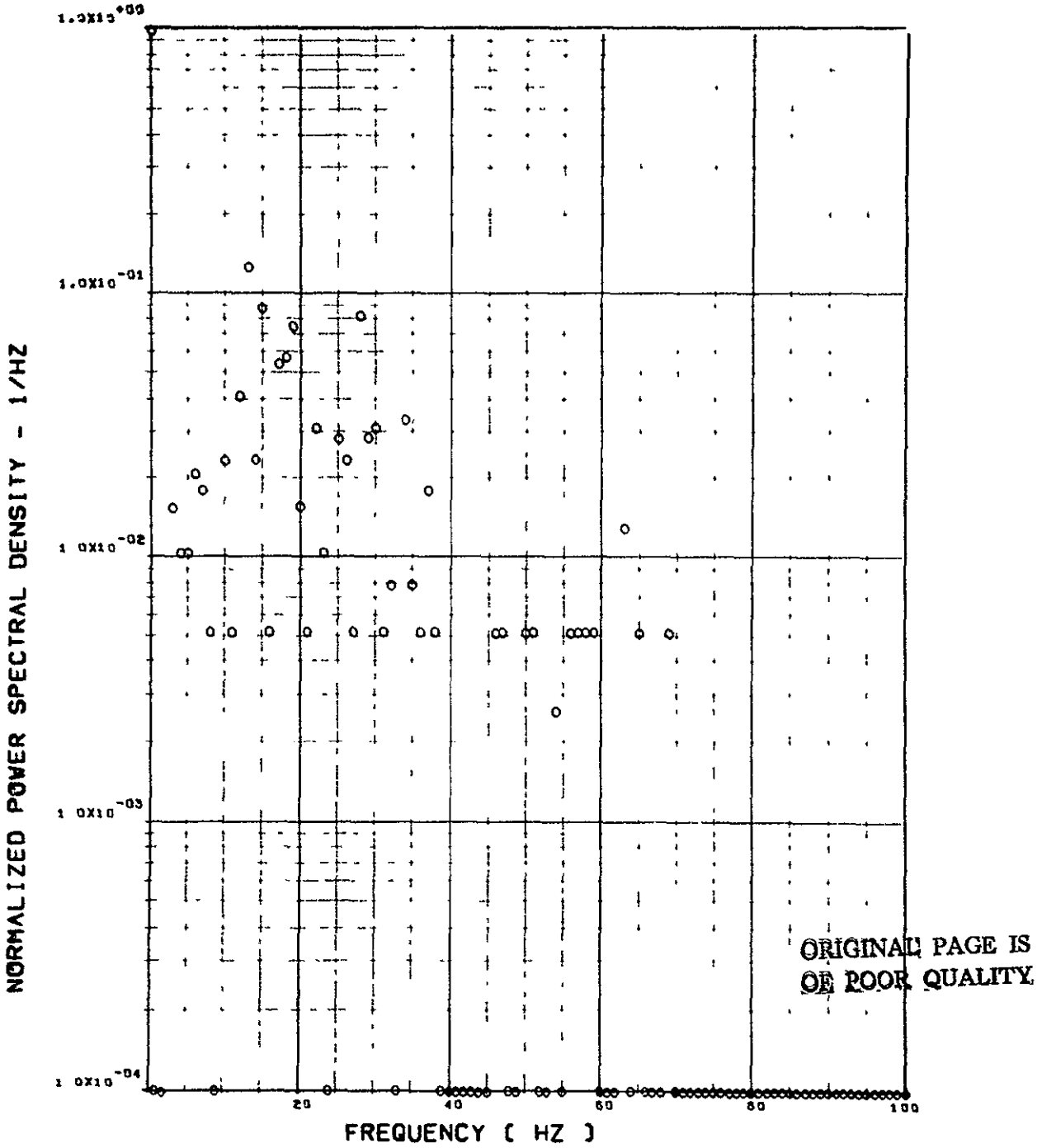

Figure 56. Continued

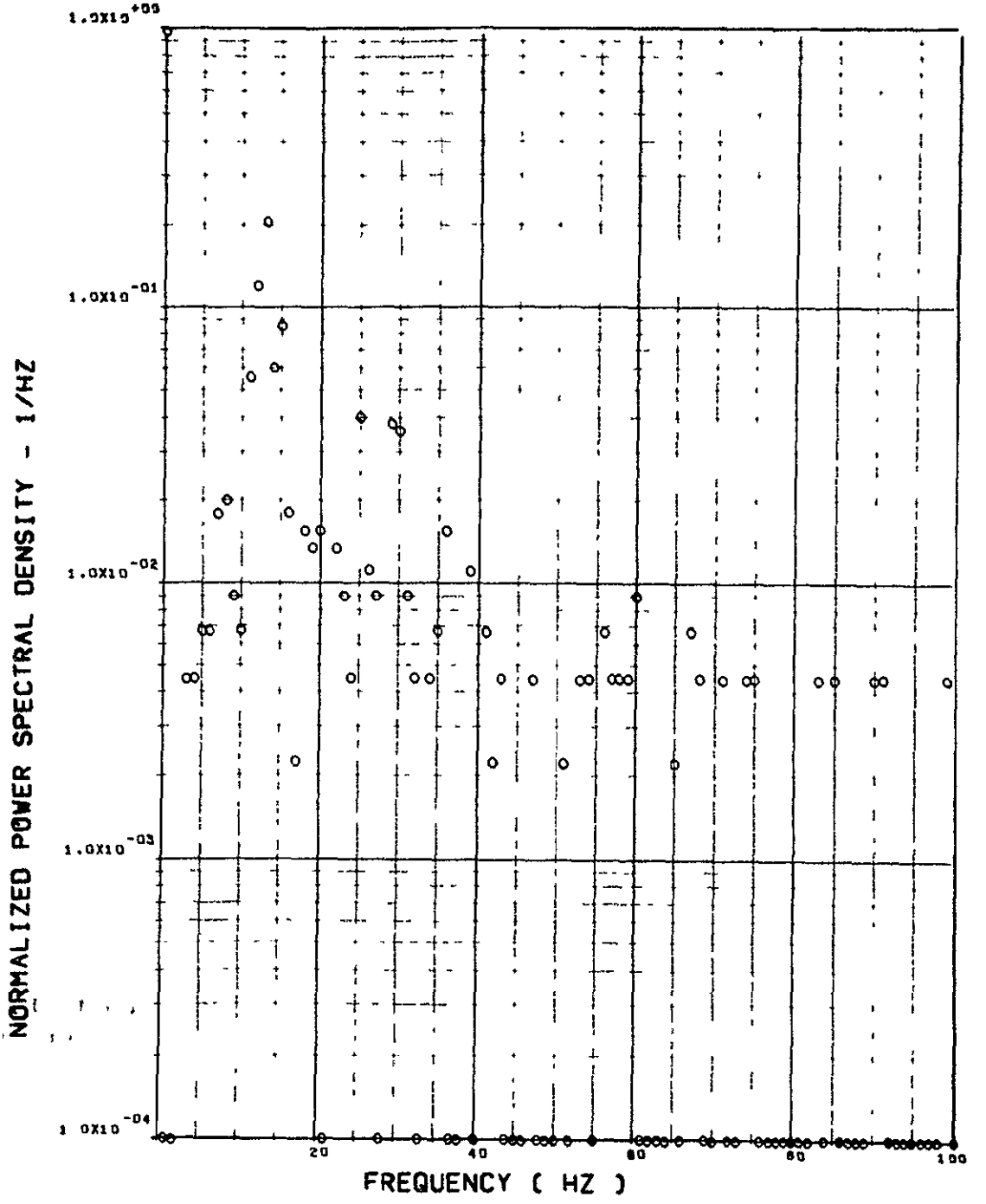

Figure 56. Concluded

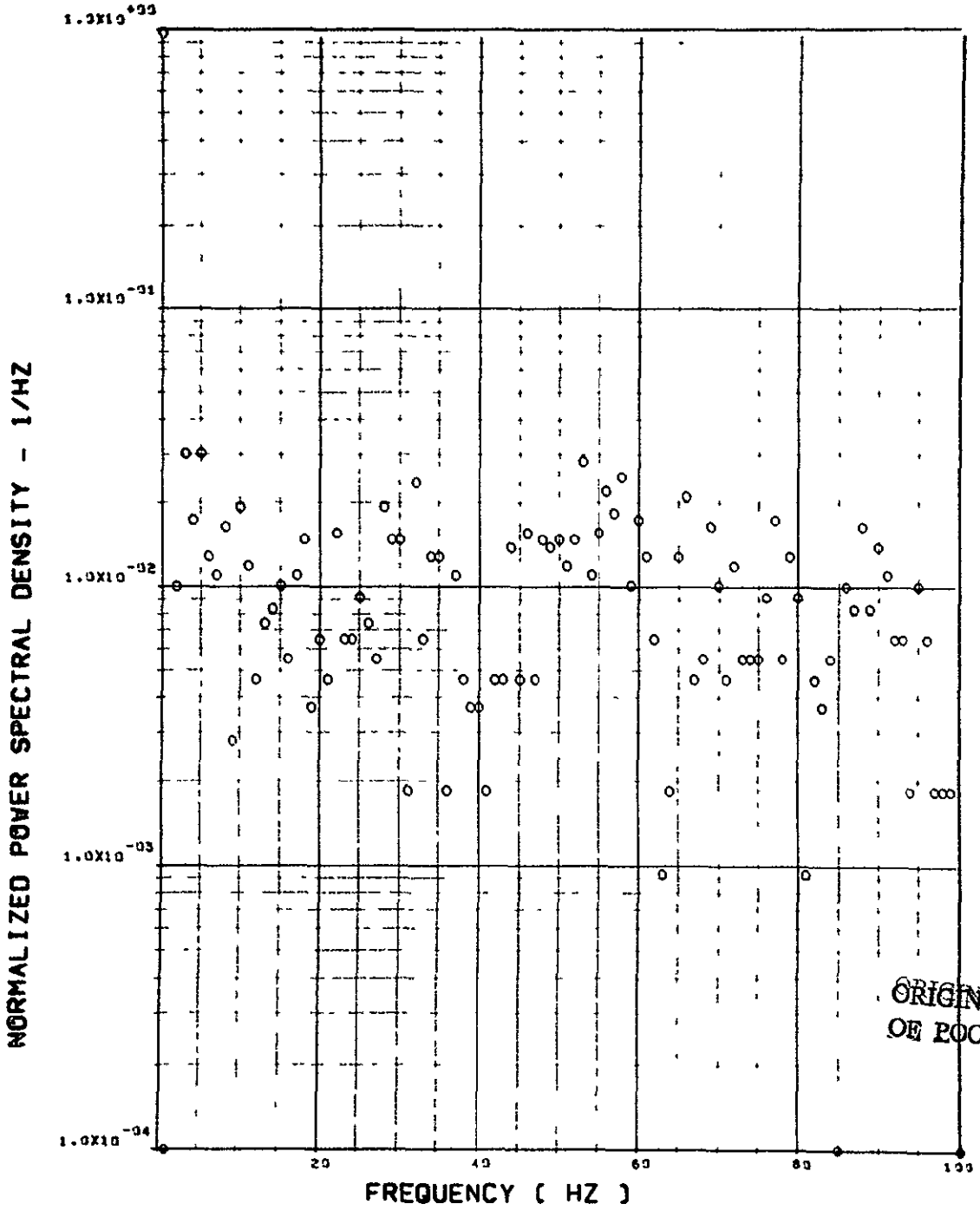

Figure 57. Power Spectra - Flight 77, Run S&C-R, Point 7
T_1 = 153311.0, ΔT = 2 Sec, α_{Nom} = 5.1 deg,
$\Delta\alpha$= 1 76 deg

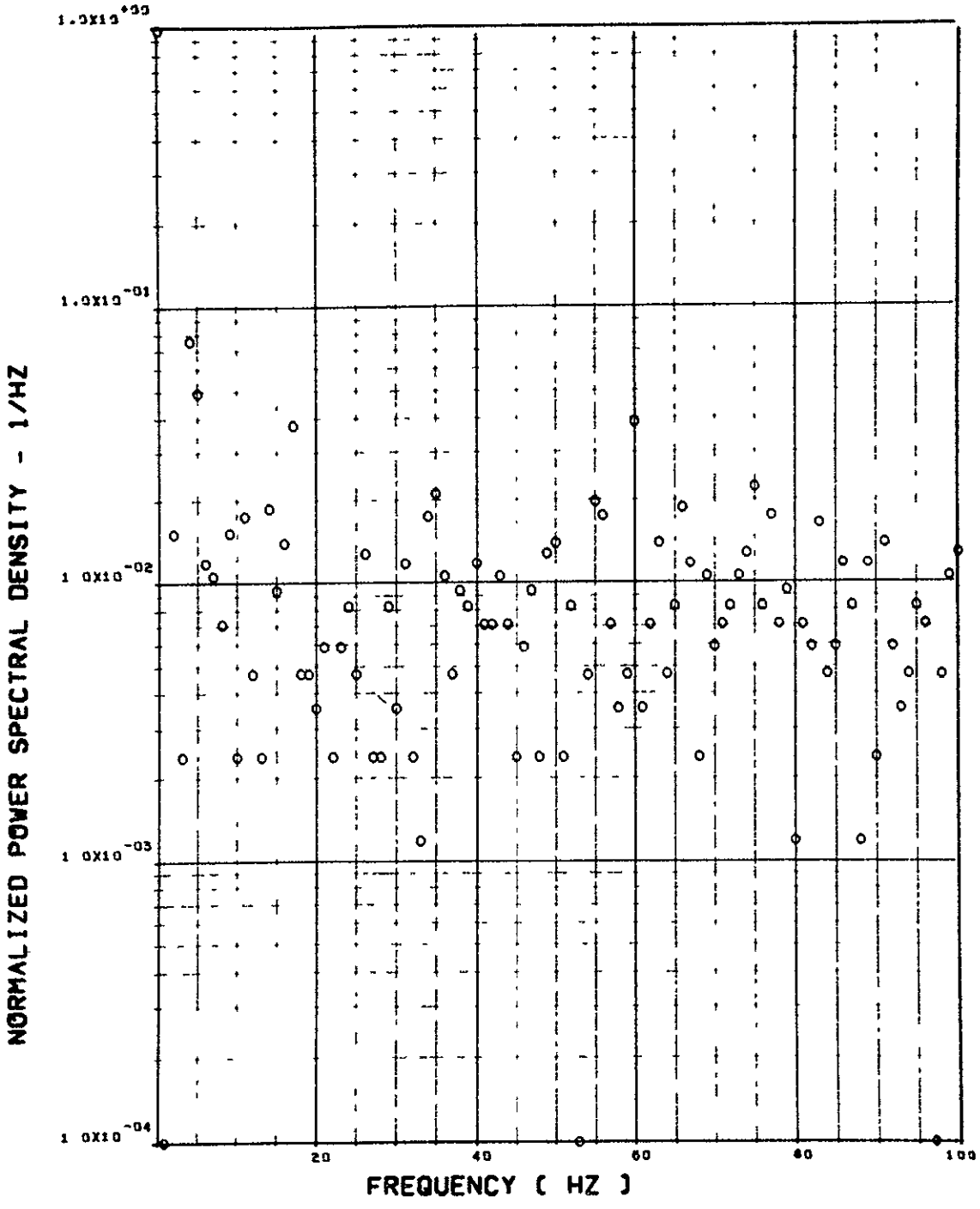

Figure 57. Continued

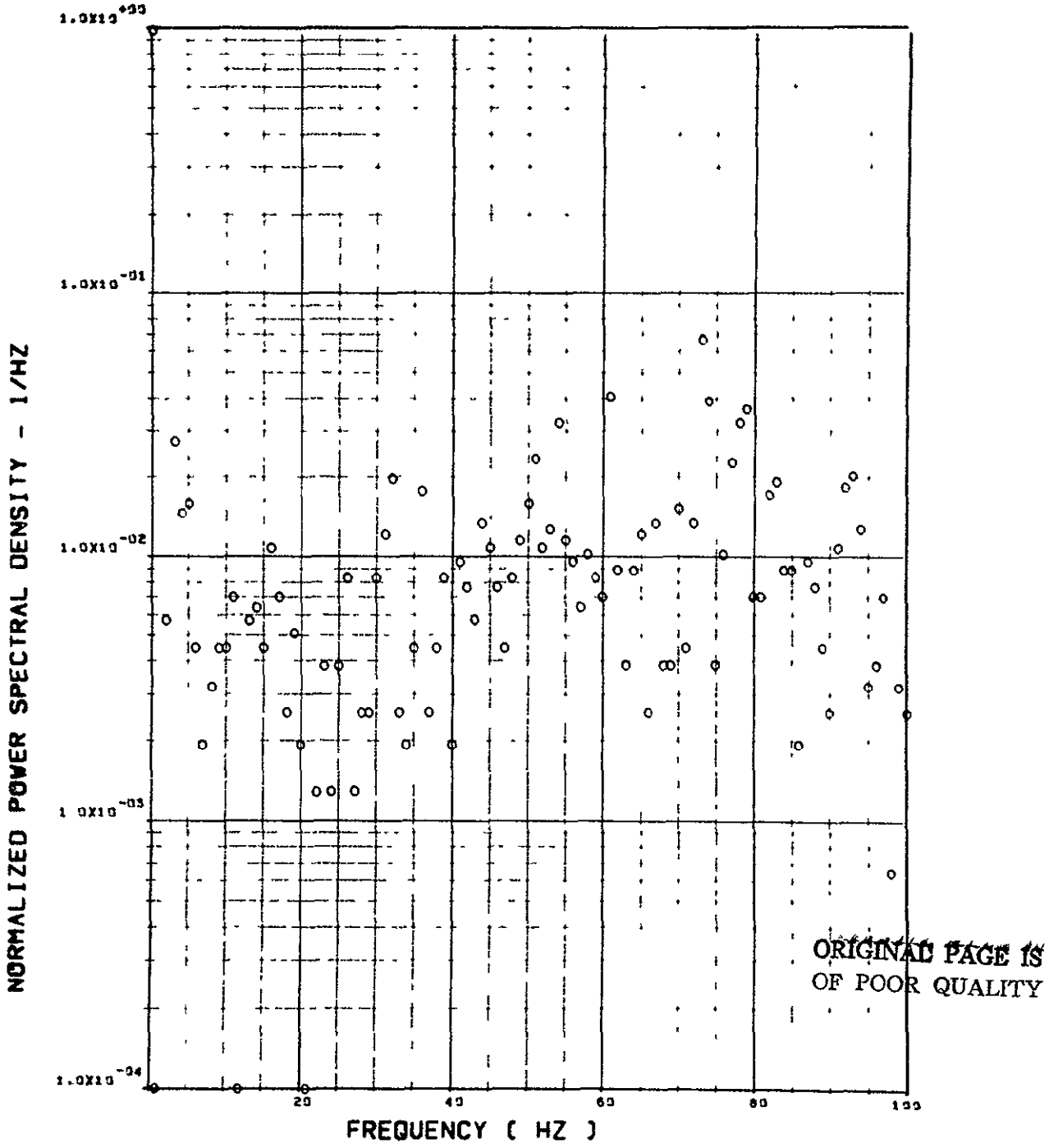

Figure 7. Continued

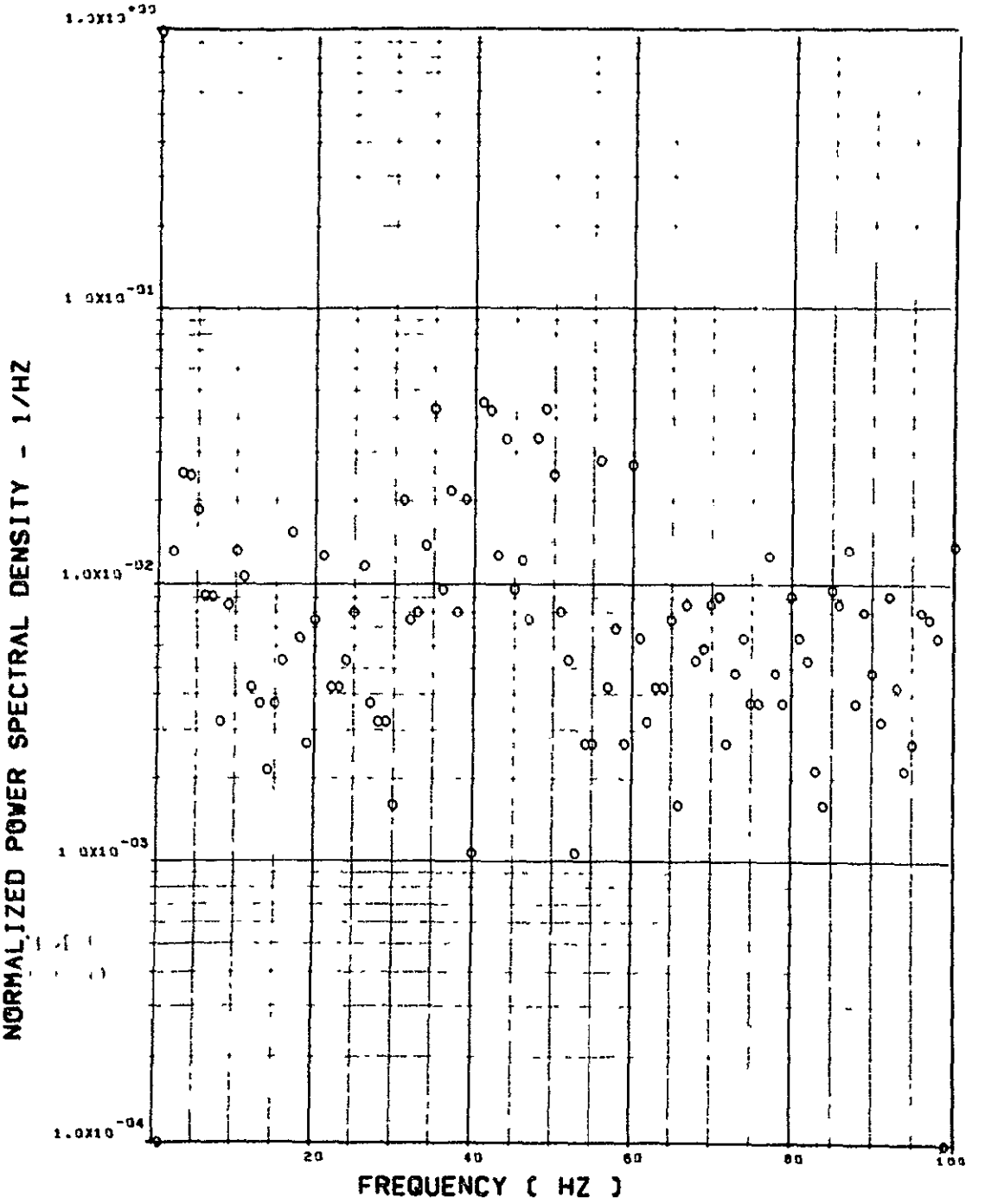

Figure 57. Continued

FLIGHT 77. FRAME 153311.00. RECORD LENGTH = 2 SEC.

SCALE FACTOR = .146+6 (M-N)**2 =.118+8 (IN-LB)**2

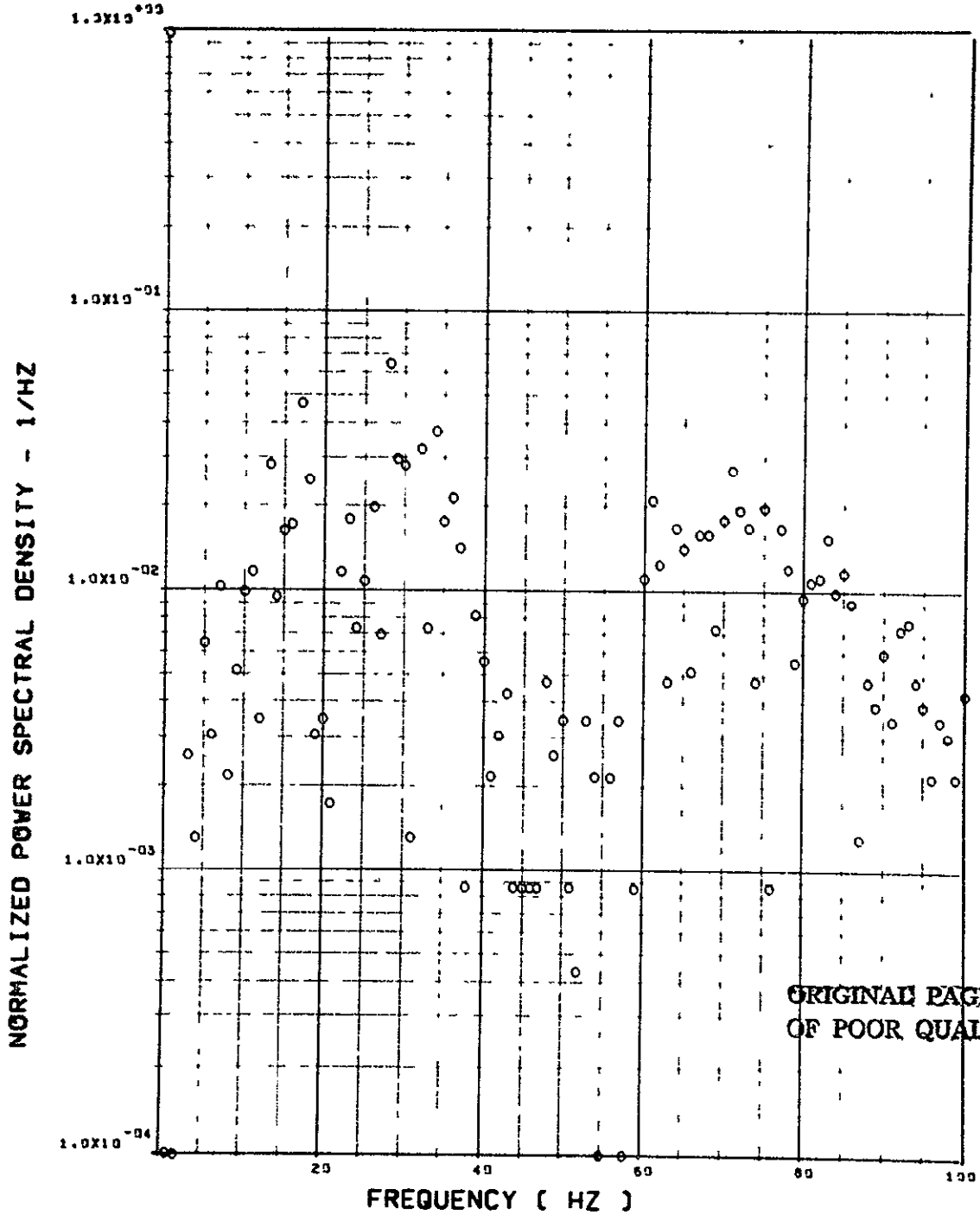

ITEM - ST135 TORSION. L/H HORIZ TAIL HINGE LINE

Figure 57. Continued

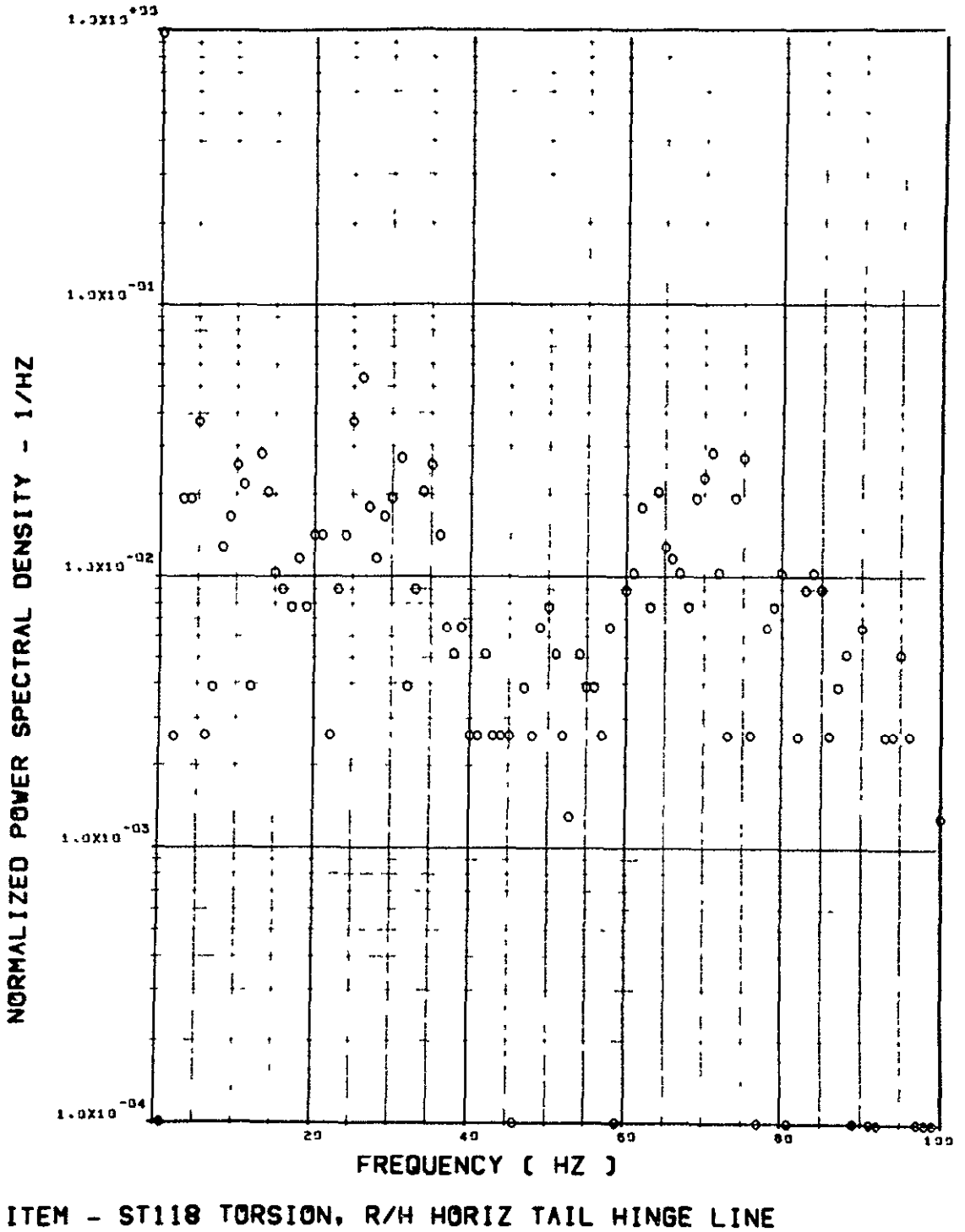

Figure 37. Concluded

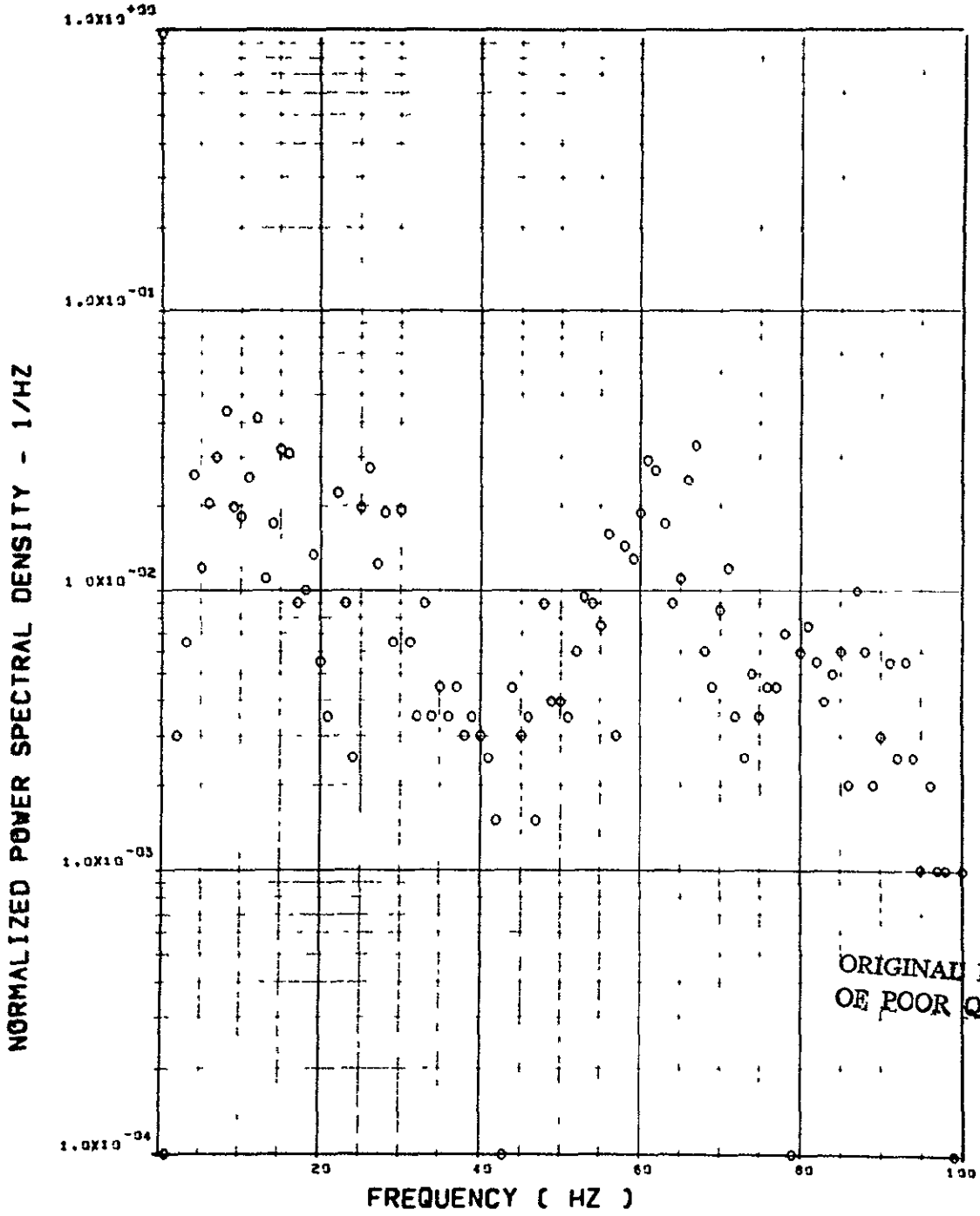

Figure 58. Power Spectra Flight 77, Run S&C-R, Point 8
T_1 = 153315 5, ΔT = 2 Sec, α_{Nom} = 7 1 deg,
$\Delta\alpha$= 0.32 deg

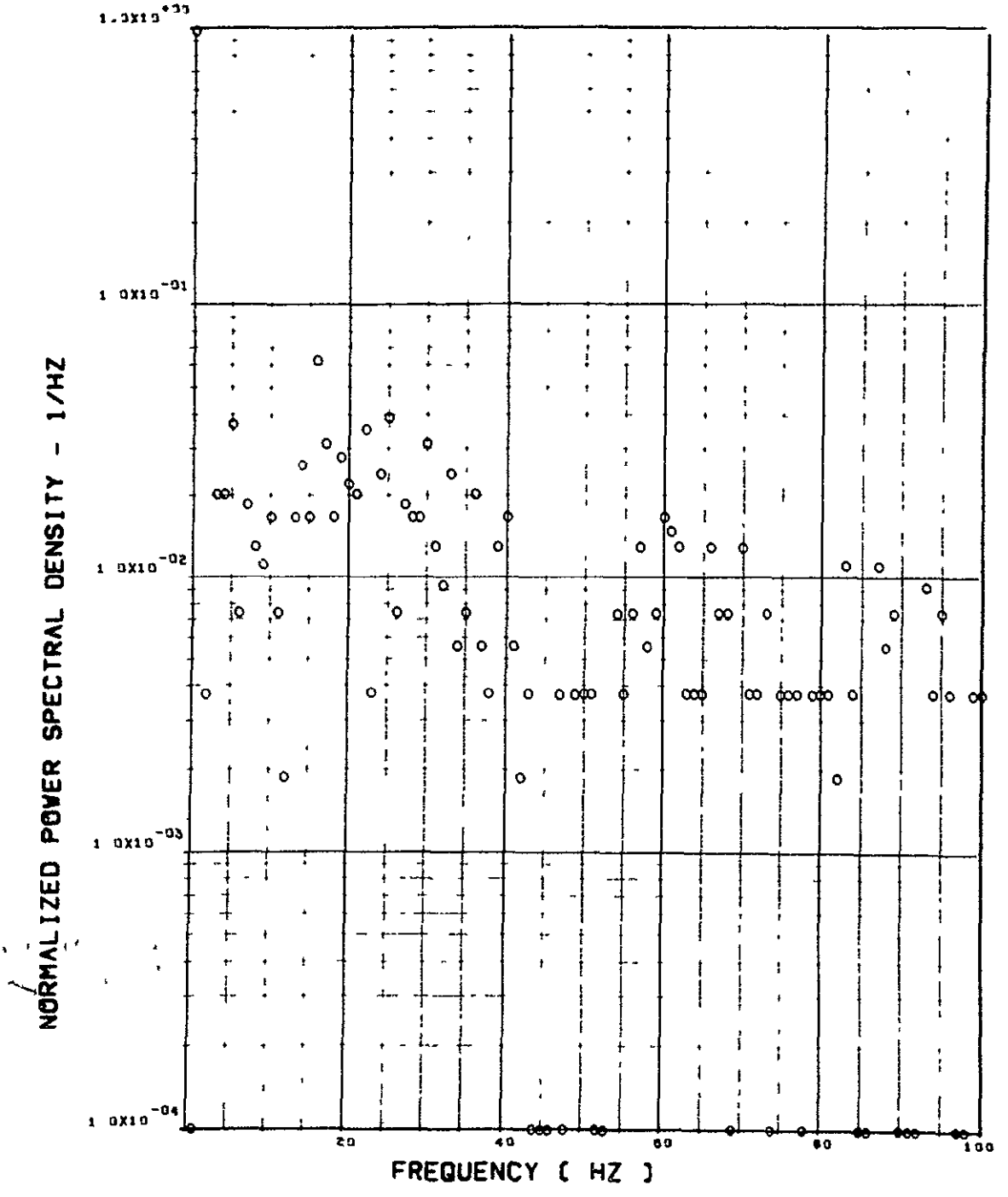

Figure 58. Continued

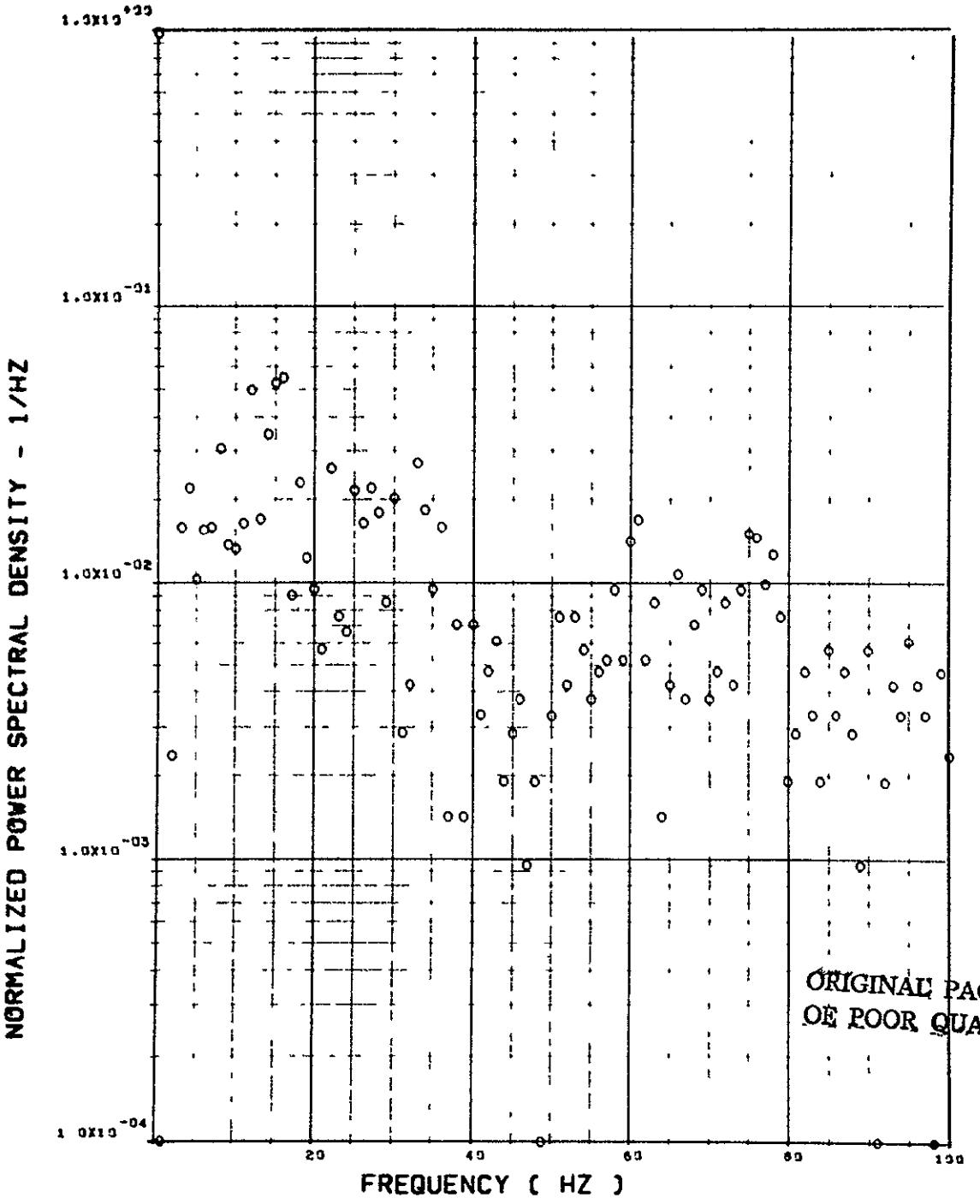

Figure 38. Continued

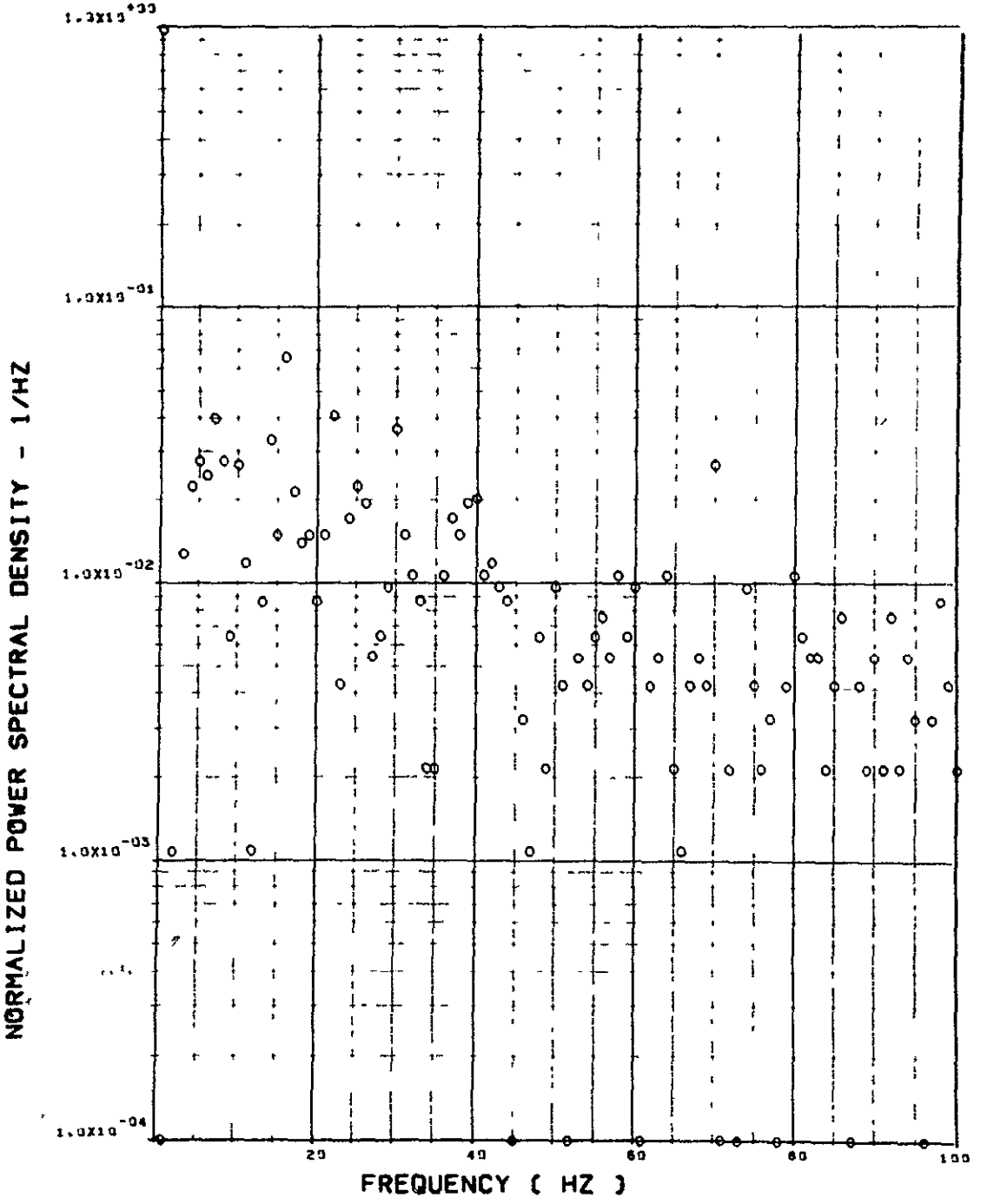

Figure 58. Continued

FLIGHT 77. FRAME 153315.50. RECORD LENGTH = 2 SEC.

SCALE FACTOR = .415+6 (M-N)**2 =.337+8 (IN-LB)**2

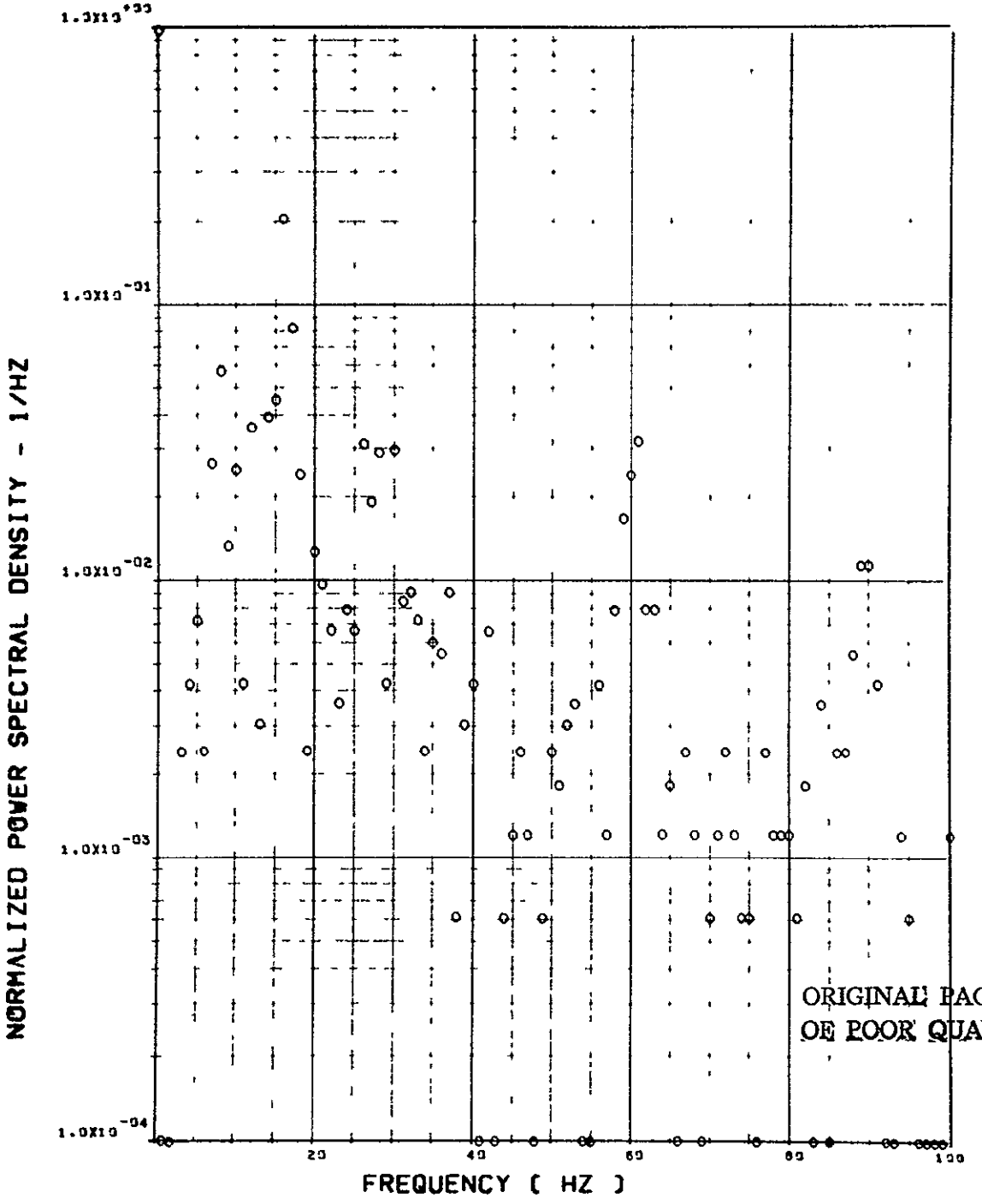

ITEM - ST135 TORSION. L/H HORIZ TAIL HINGE LINE

Figure 28. Continued

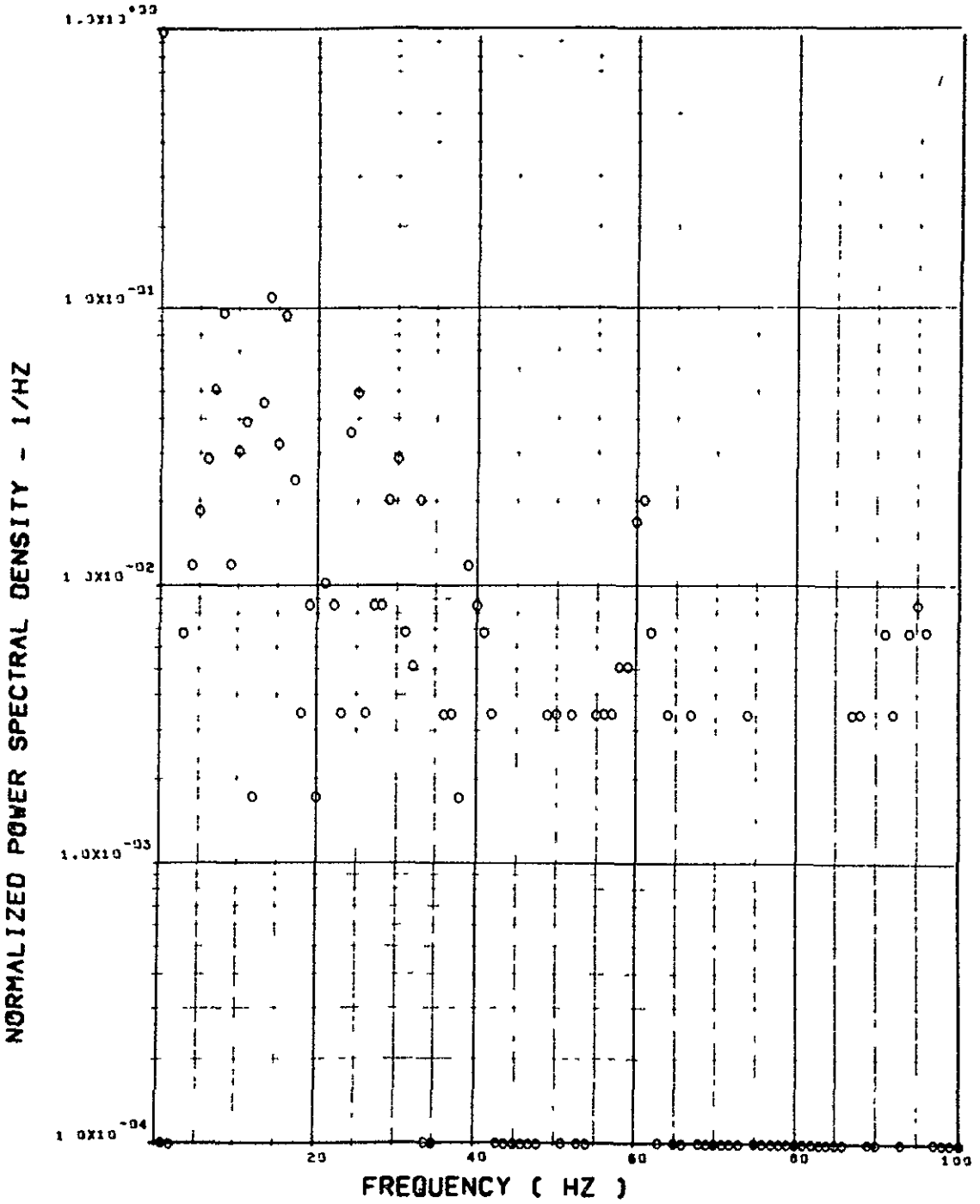

Figure 58. Concluded

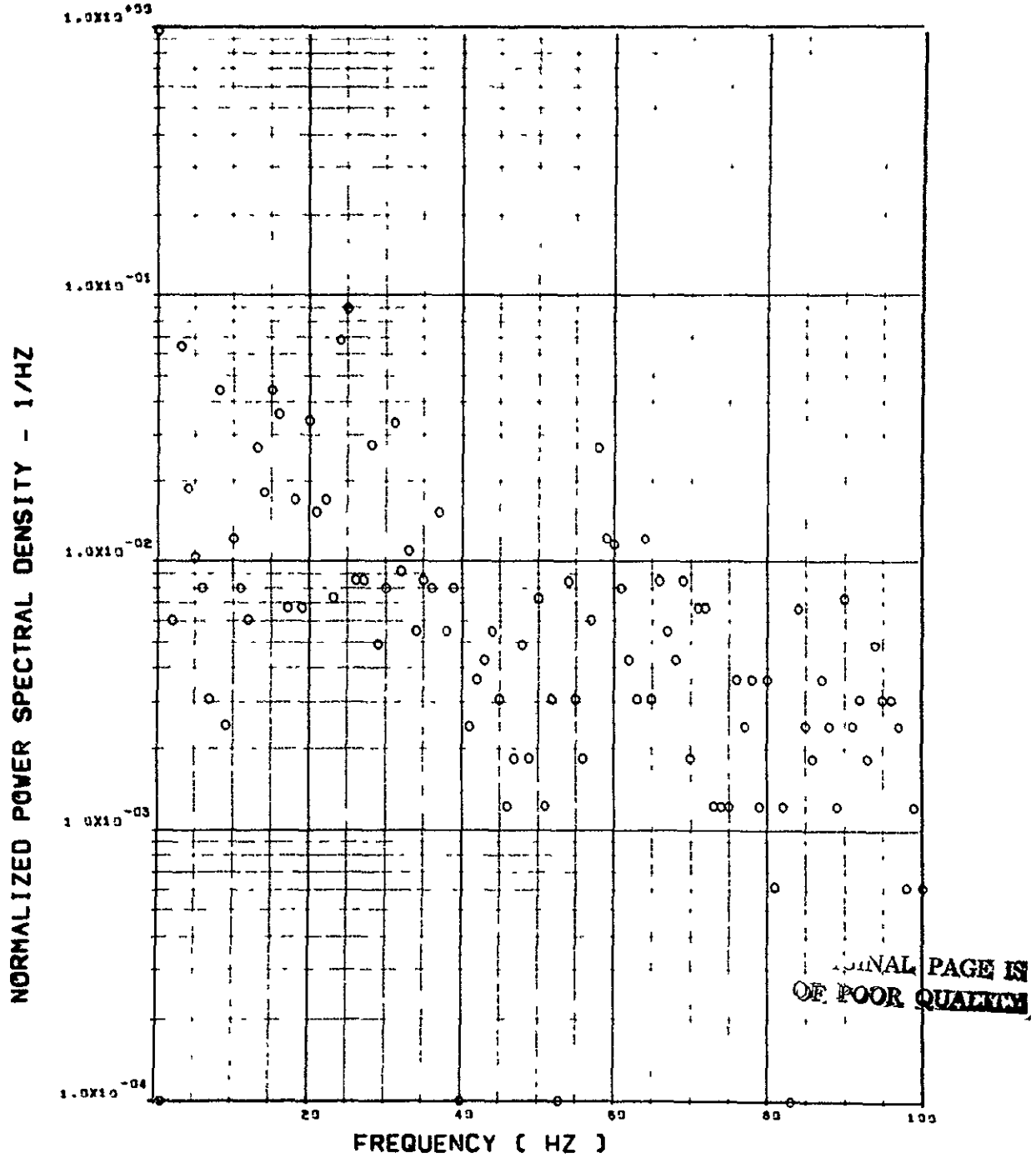

Figure 29. Power Spectra - Flight 77, Run S&C-R, Point 9
T_1 = 153318.5, ΔT = 2 Sec, α_{Nom} = 9 2 deg,
$\Delta\alpha$= 1.24 deg.

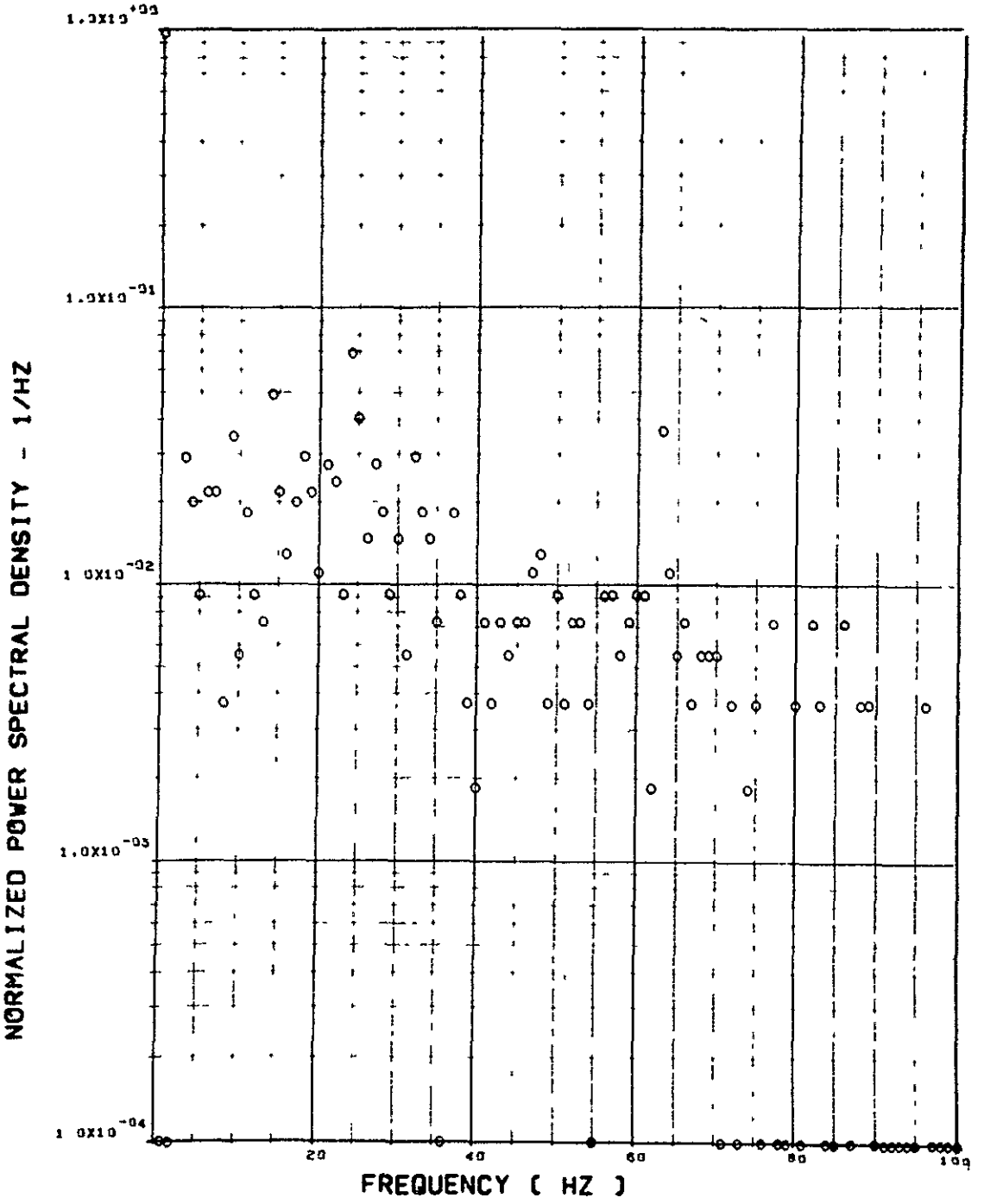

Figure 29. Continued

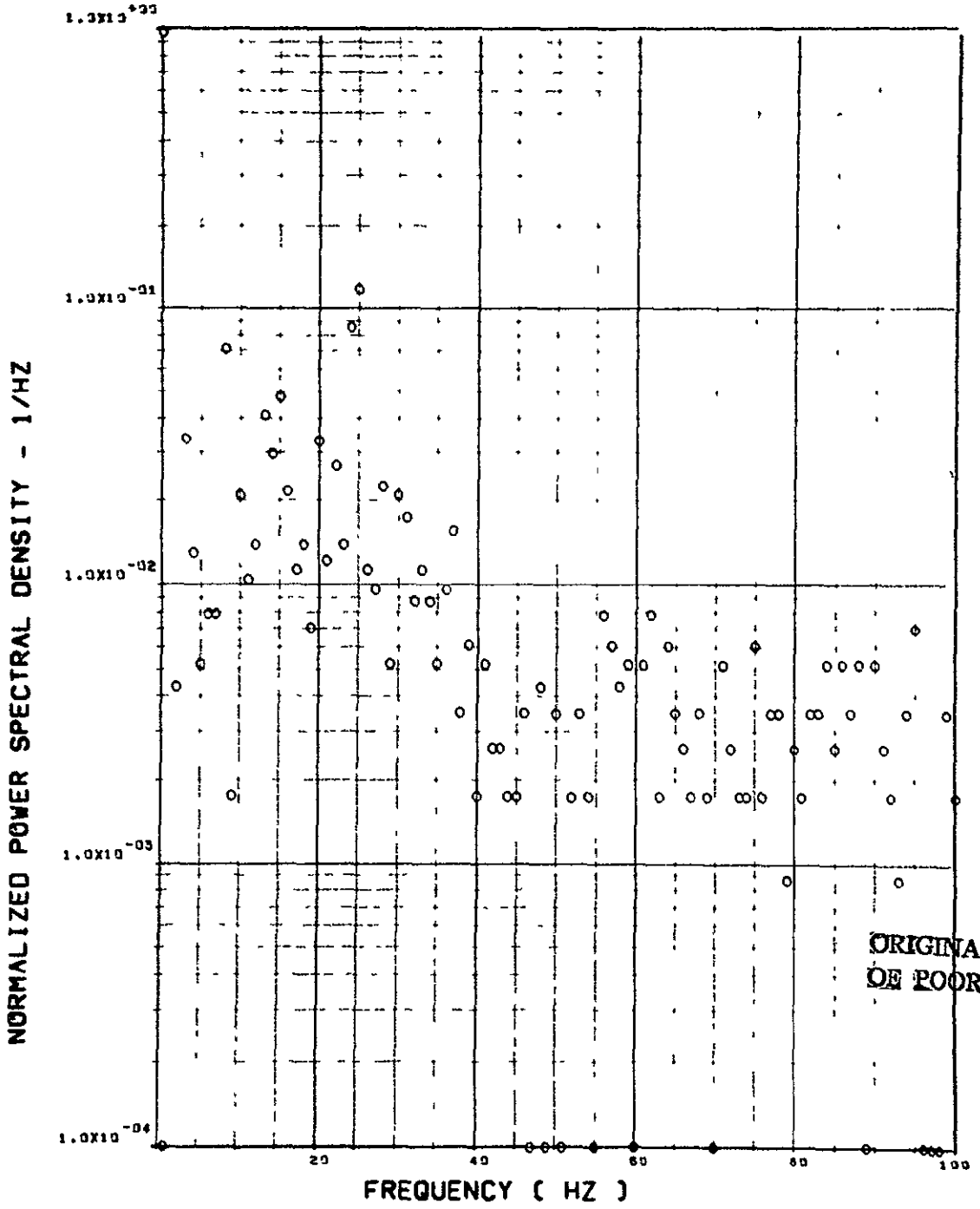

Figure 59. Continued

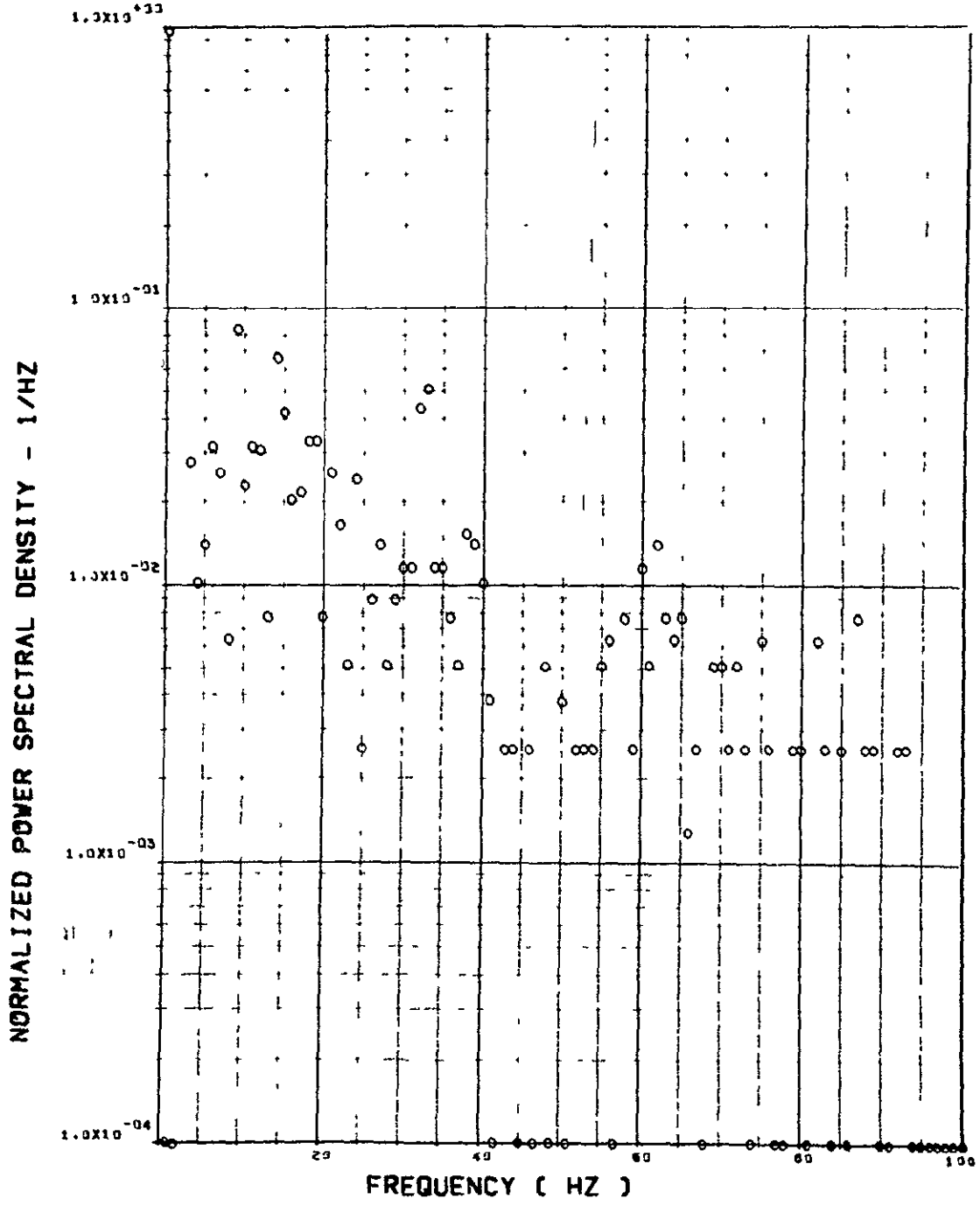

Figure 59. Continued

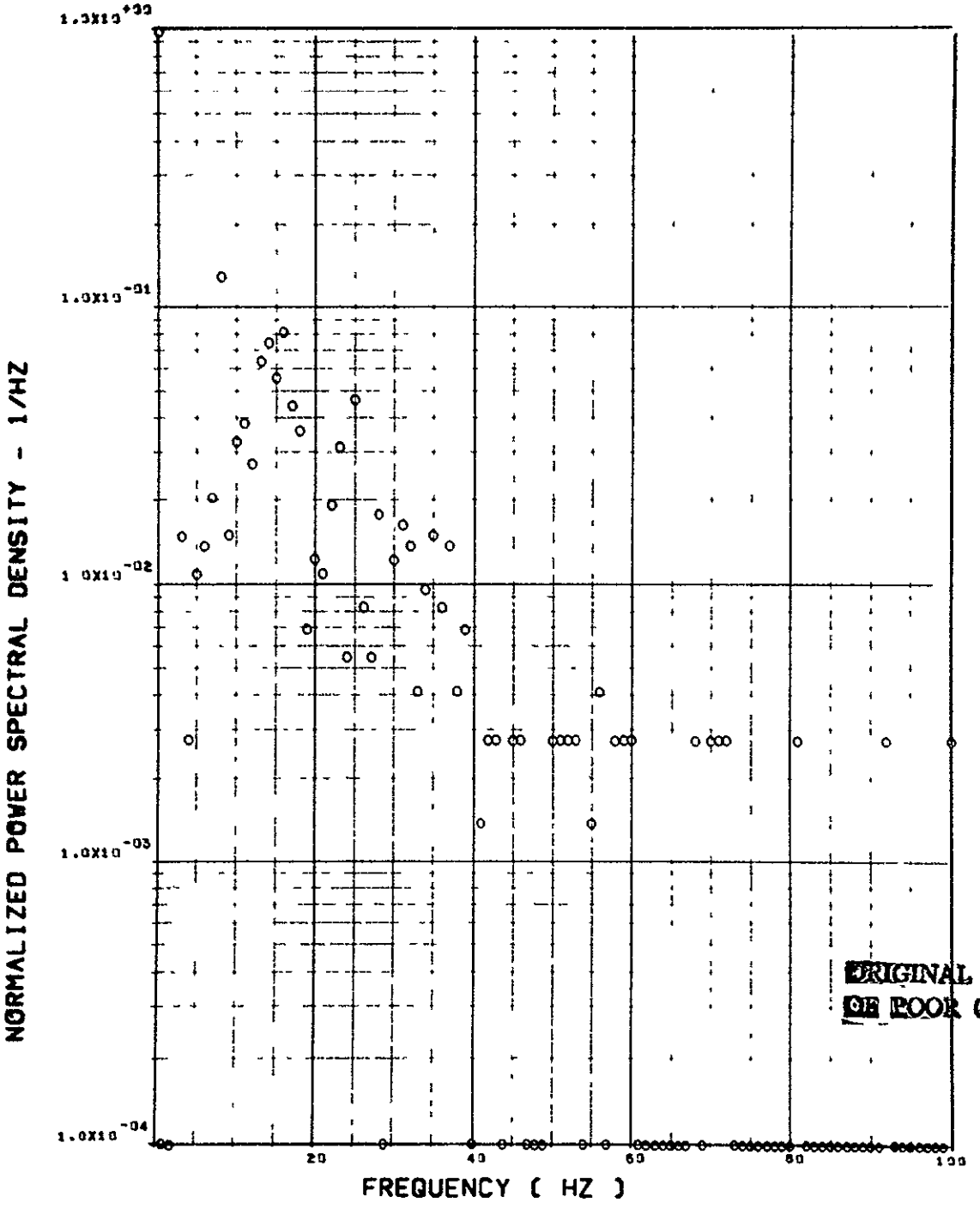

Figure 59. Continued

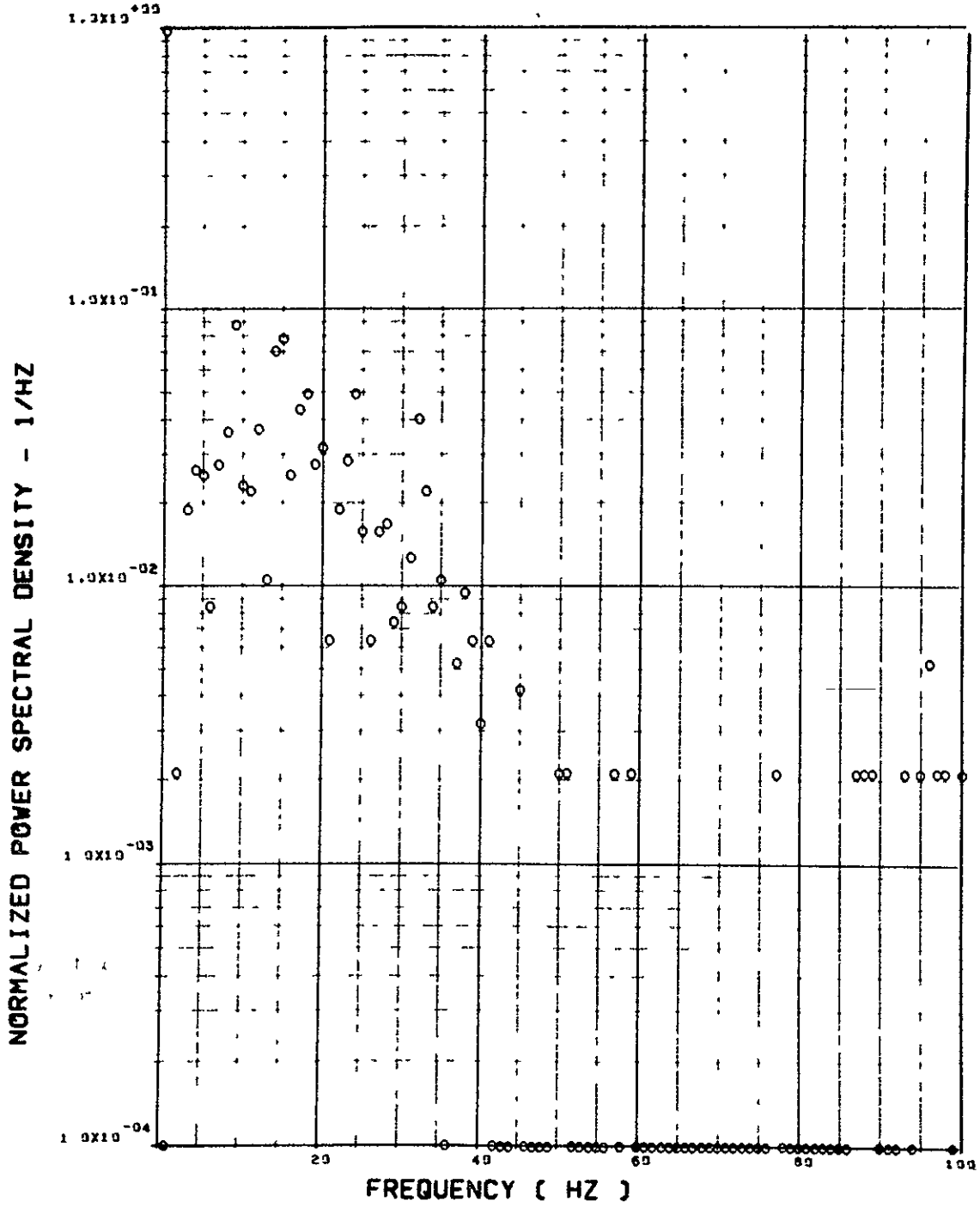

Figure 59. Concluded

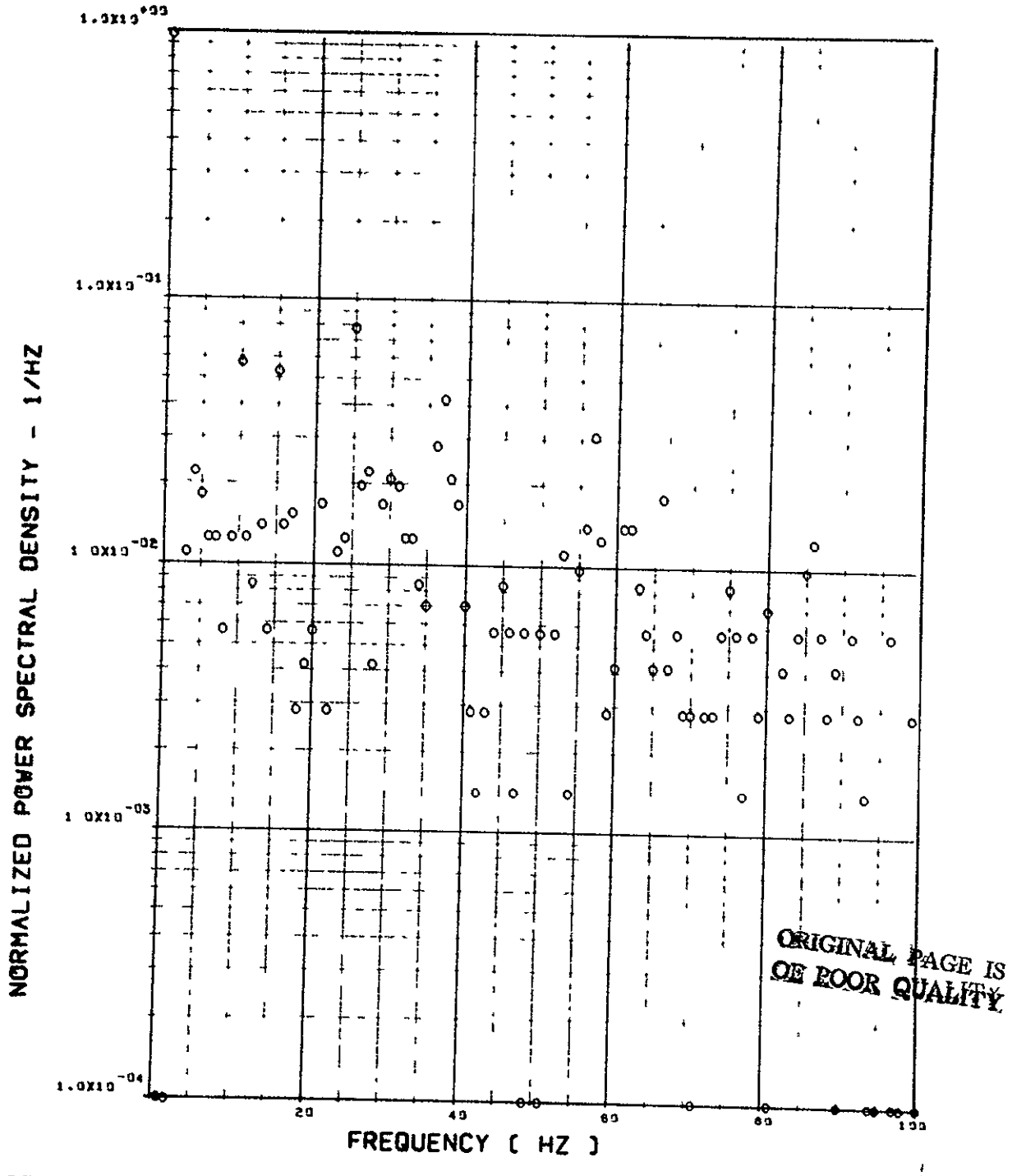

Figure 40. Power Spectra - Flight 77, Run S&C-R, Point 10
T_1 = 153322.35, ΔT = 2 Sec, α_{Nom} = 12.2 deg,
$\Delta\alpha$= 2 55 deg.

FLIGHT 77, FRAME 153322.35, RECORD LENGTH = 2 SEC.

SCALE FACTOR = .525+7 (N)**2 =.265+6 (LB)**2

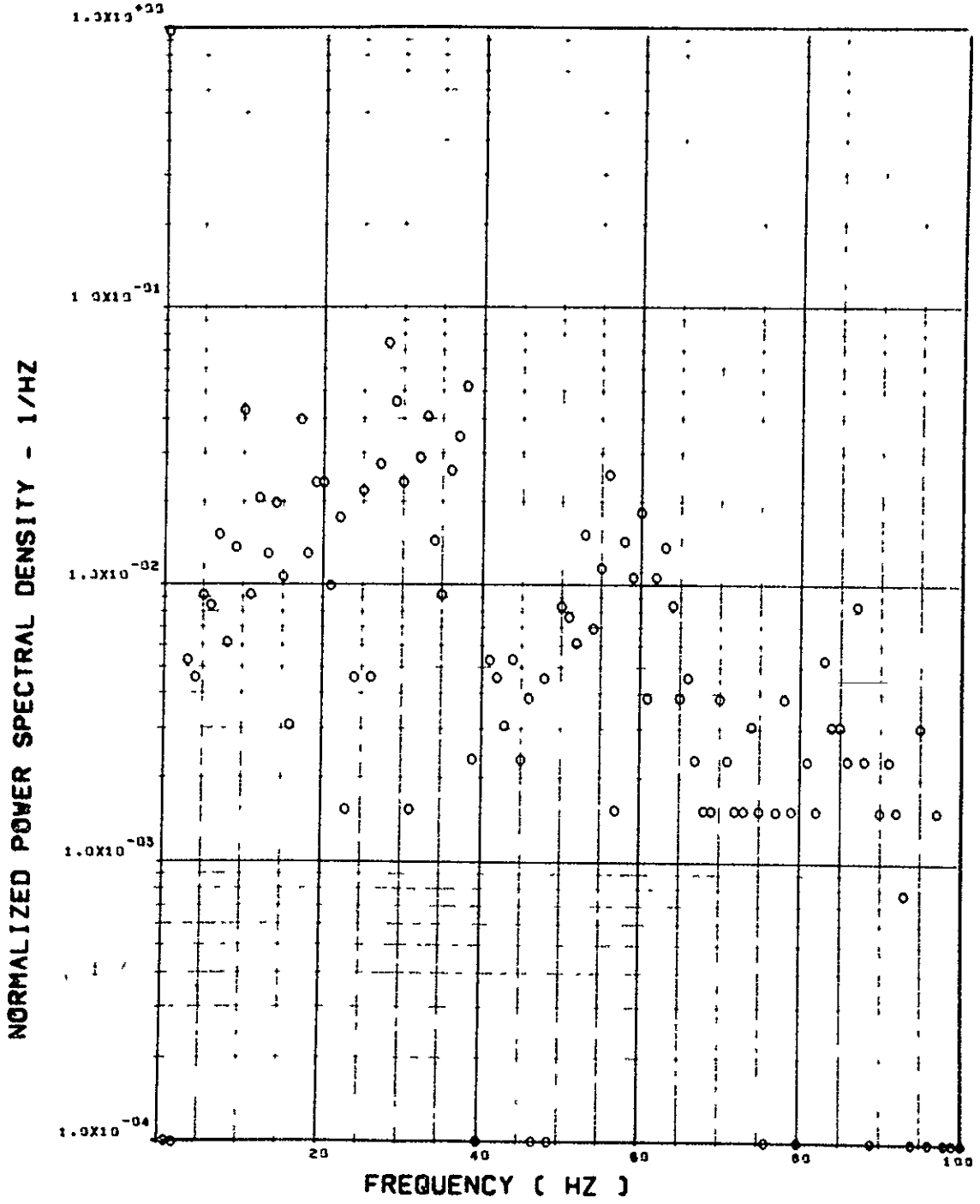

ITEM - ST072 SHEAR, R/H HORIZ TAIL ROOT

Figure 40. Continued

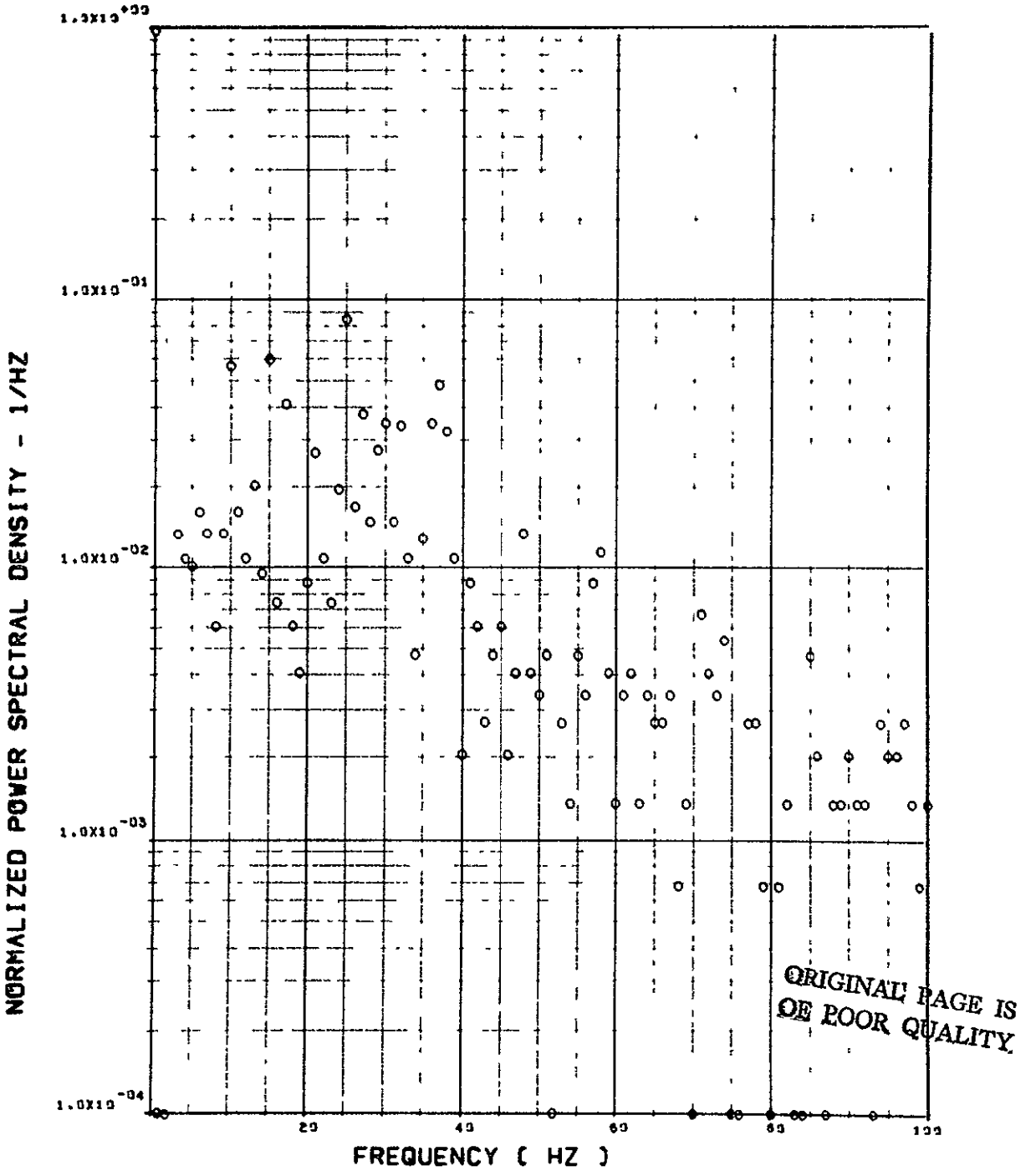

Figure 40. Continued

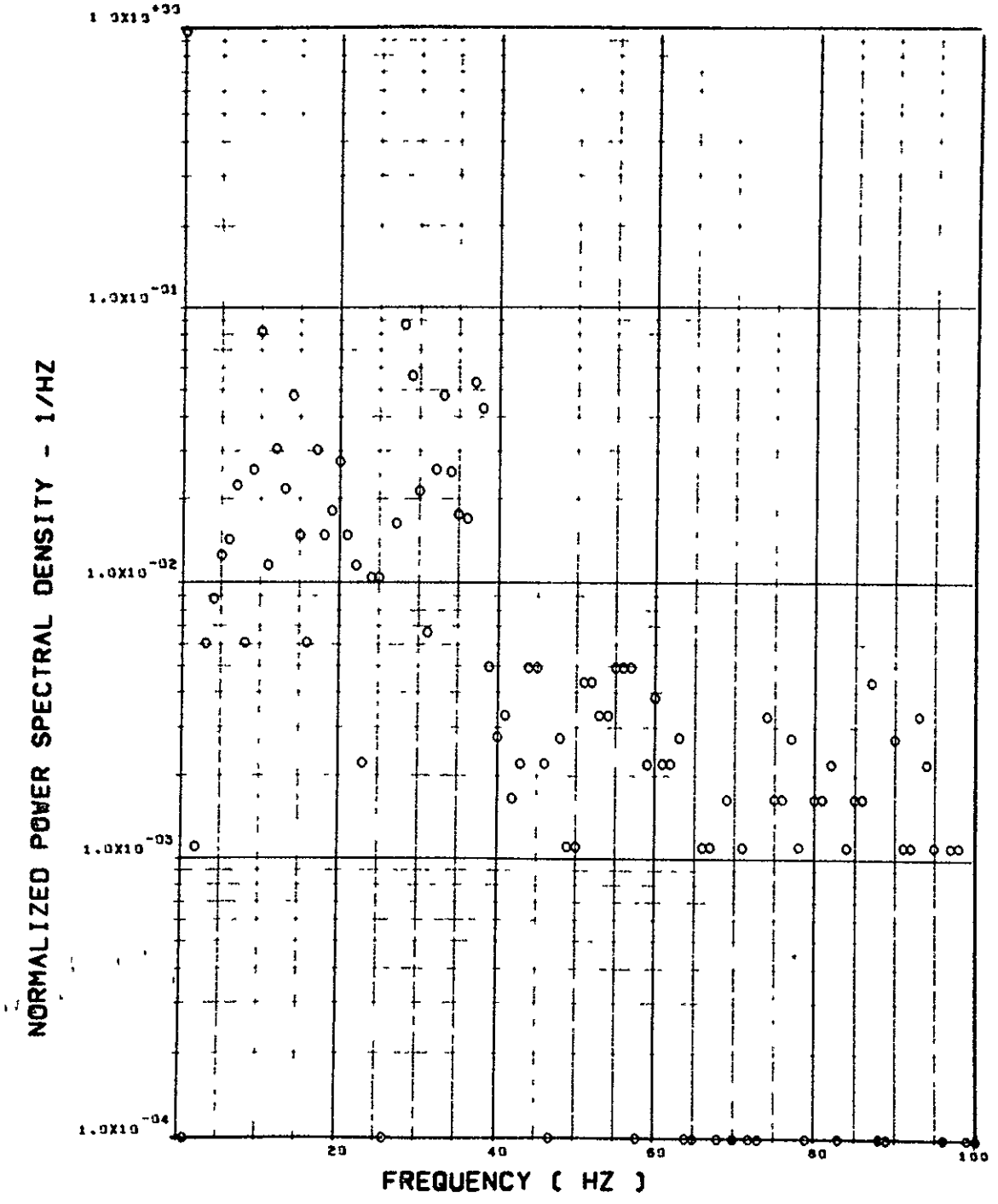

Figure 40. Continued

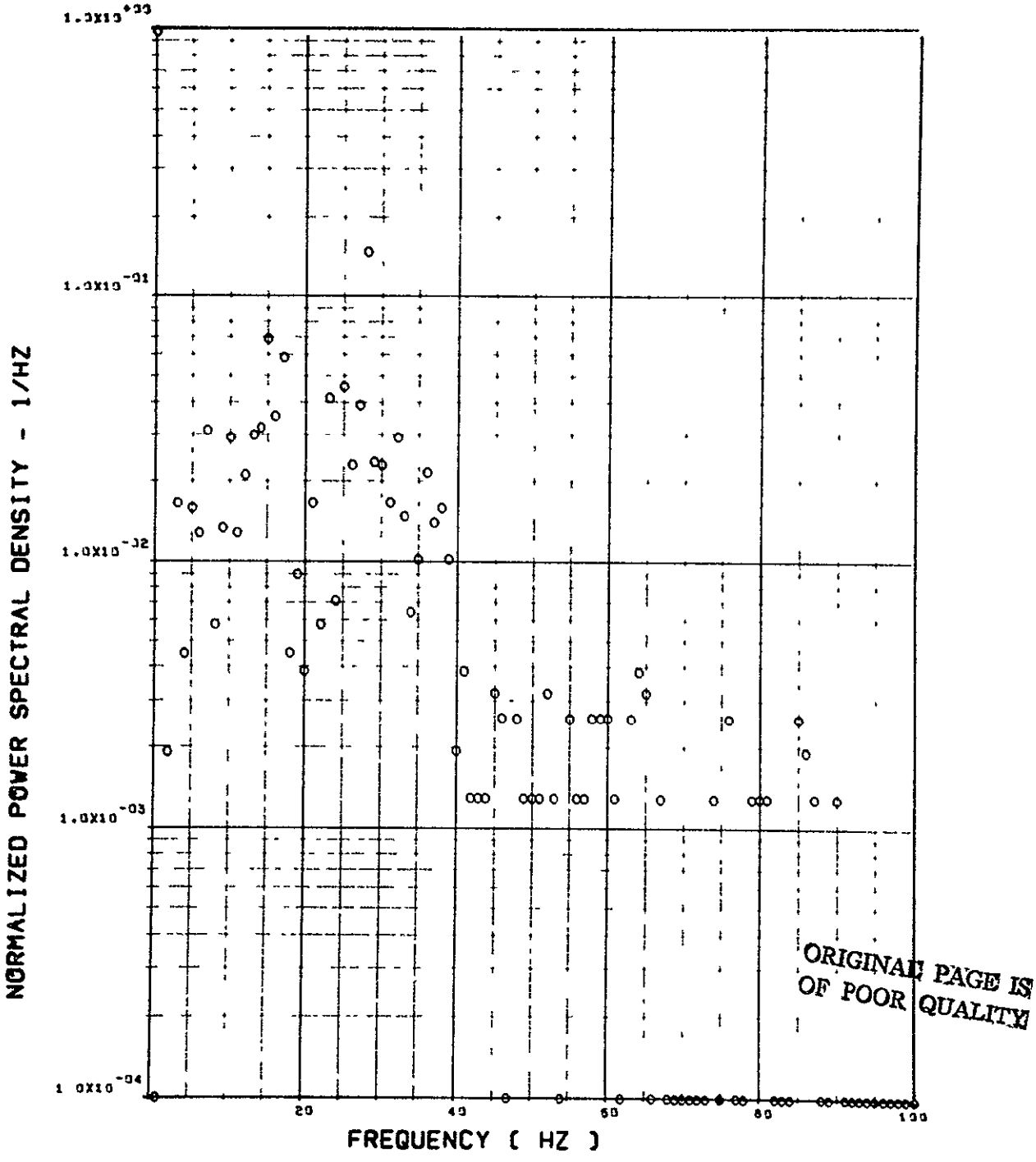

Figure 40. Continued

FLIGHT 77. FRAME 153322.35. RECORD LENGTH = 2 SEC.

SCALE FACTOR = .309+7 (M-N)**2 =.251+9 (IN-LB)**2

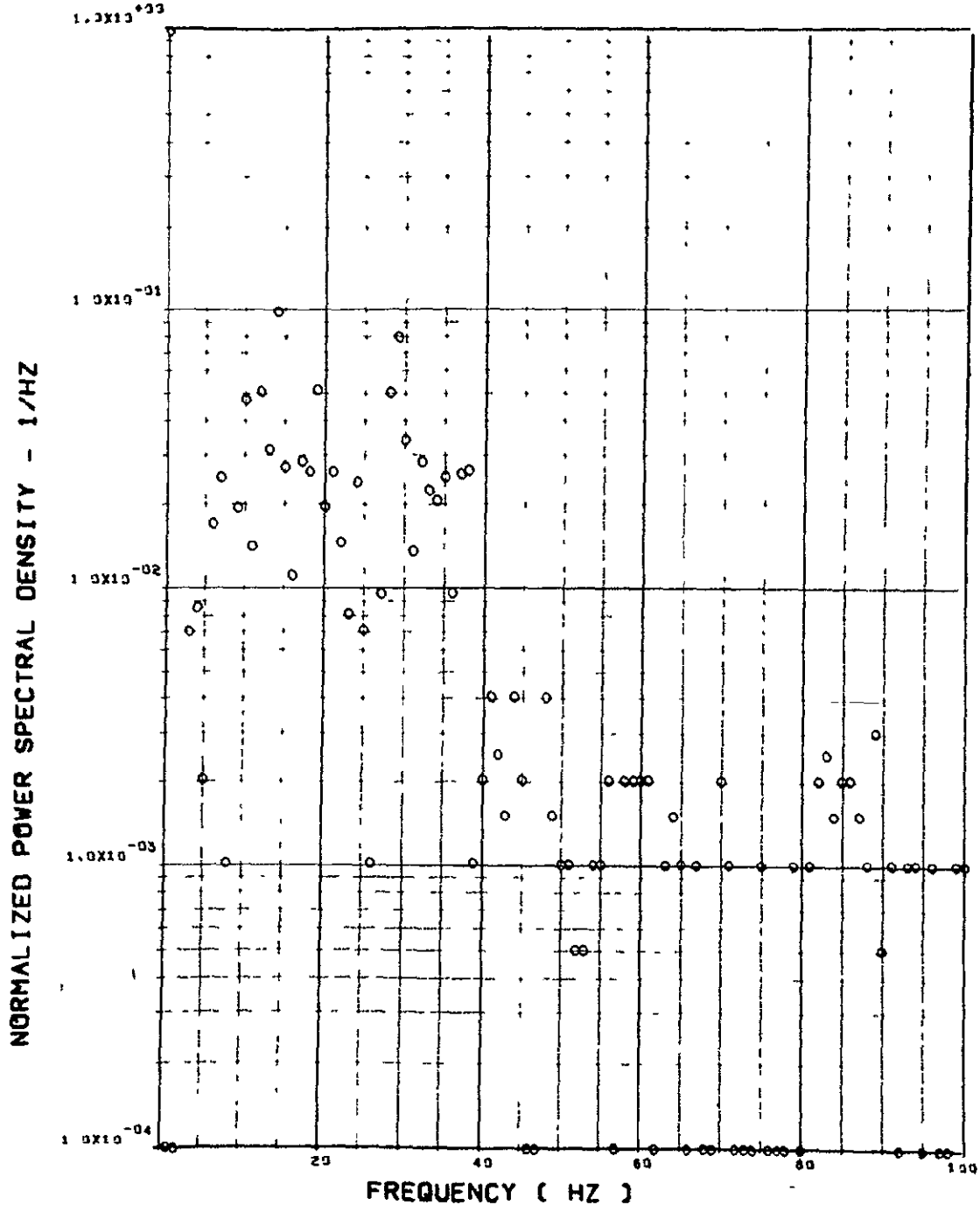

ITEM - ST118 TORSION. R/H HORIZ TAIL HINGE LINE

Figure 40. Concluded

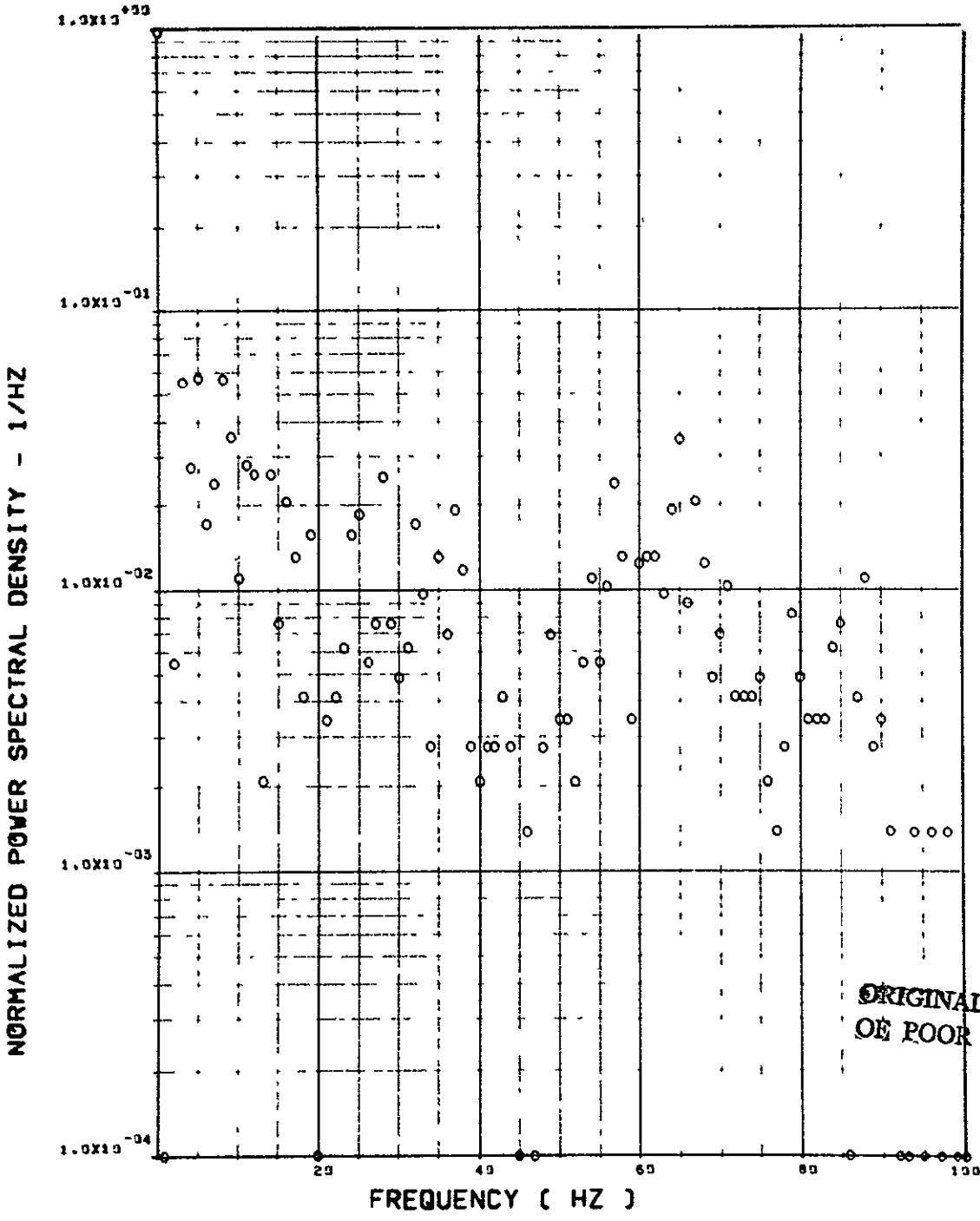

Figure 41. Power Spectra - Flight 77, Run S&C-R, Point 11
T_1 = 153324.35, ΔT = 2 Sec, α_{Nom} = 14.8 deg,
$\Delta\alpha$ = 2.15 deg.

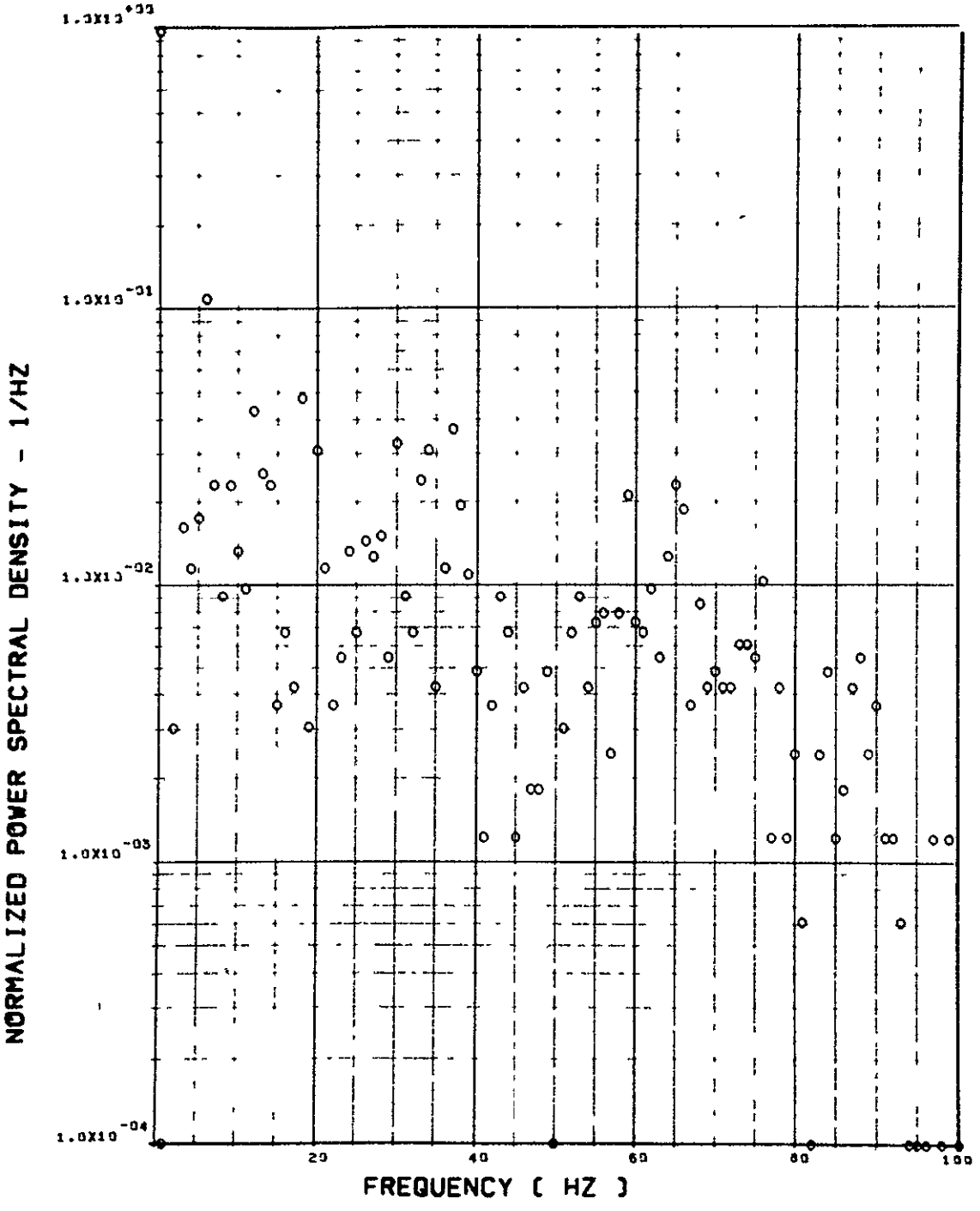

Figure 41. Continued

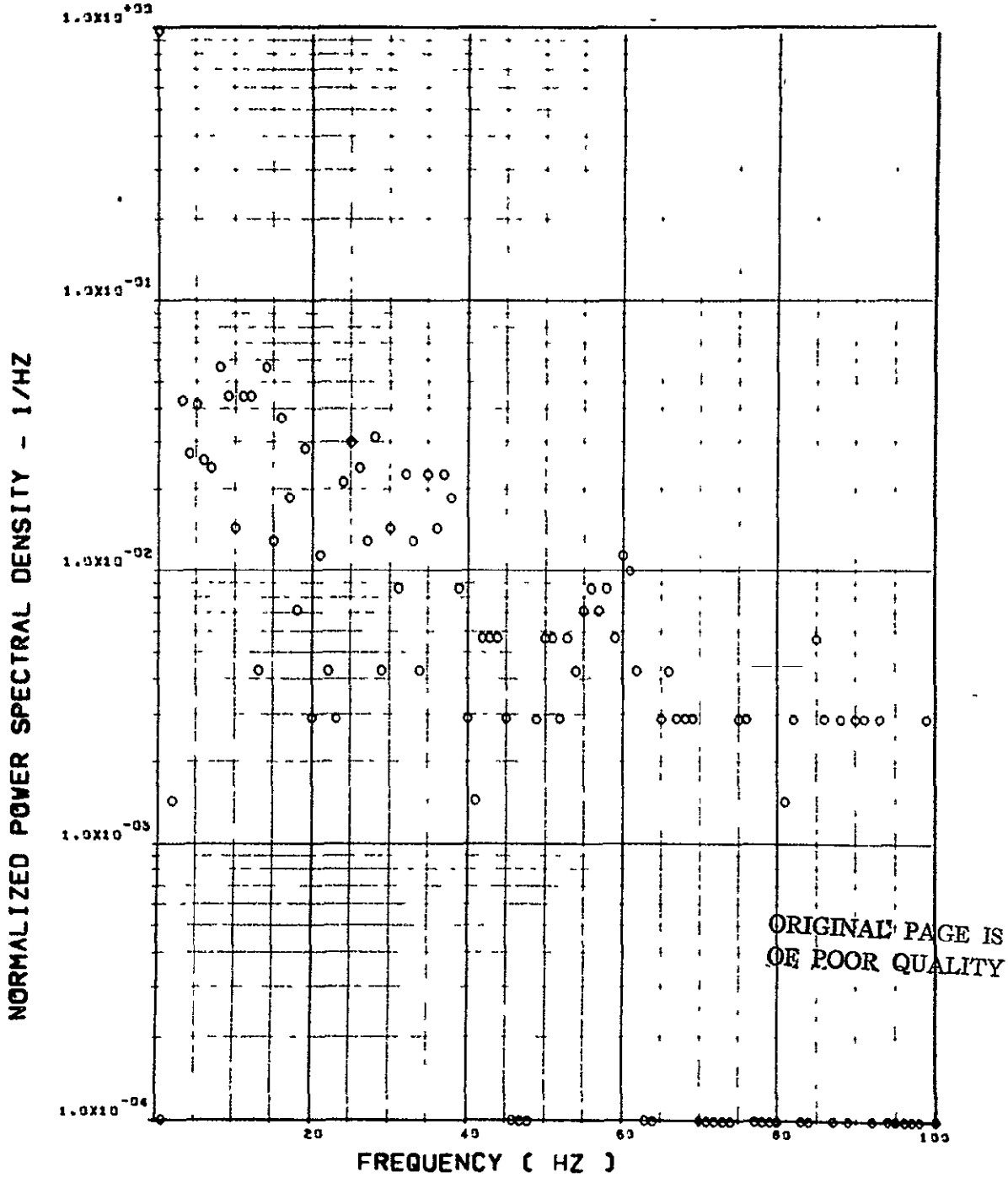

Figure 41. Continued

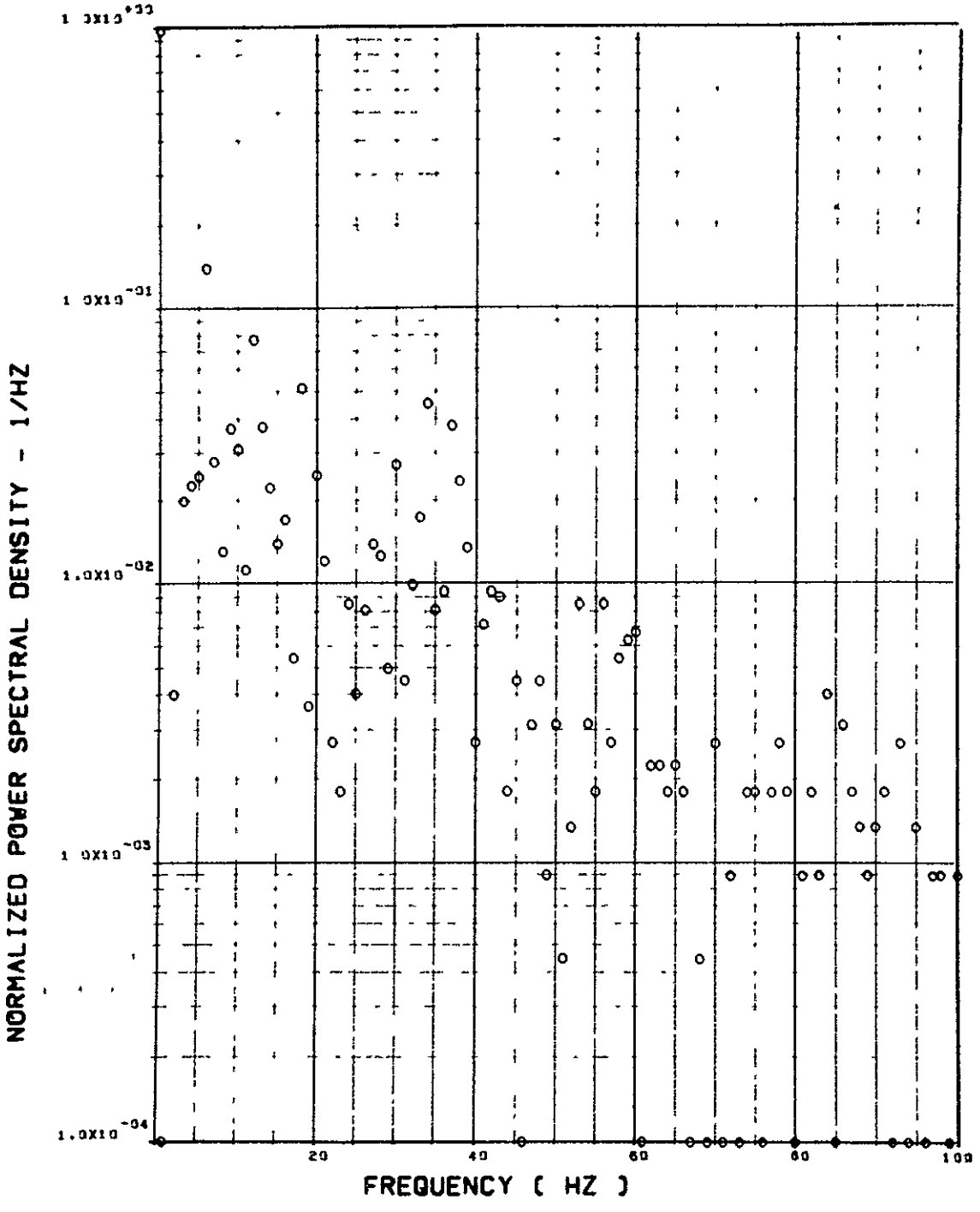

Figure 41. Continued

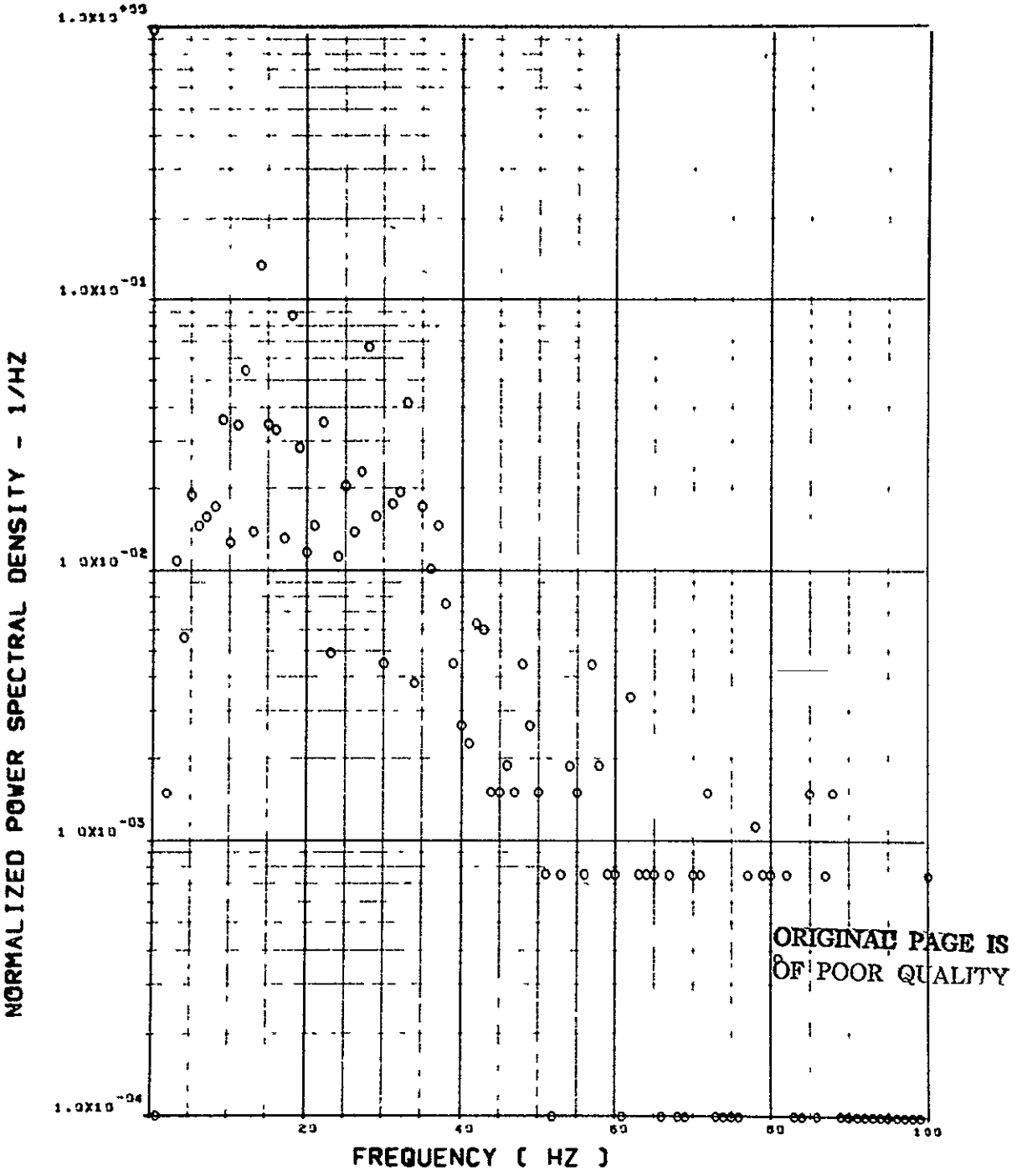

Figure 41. Continued

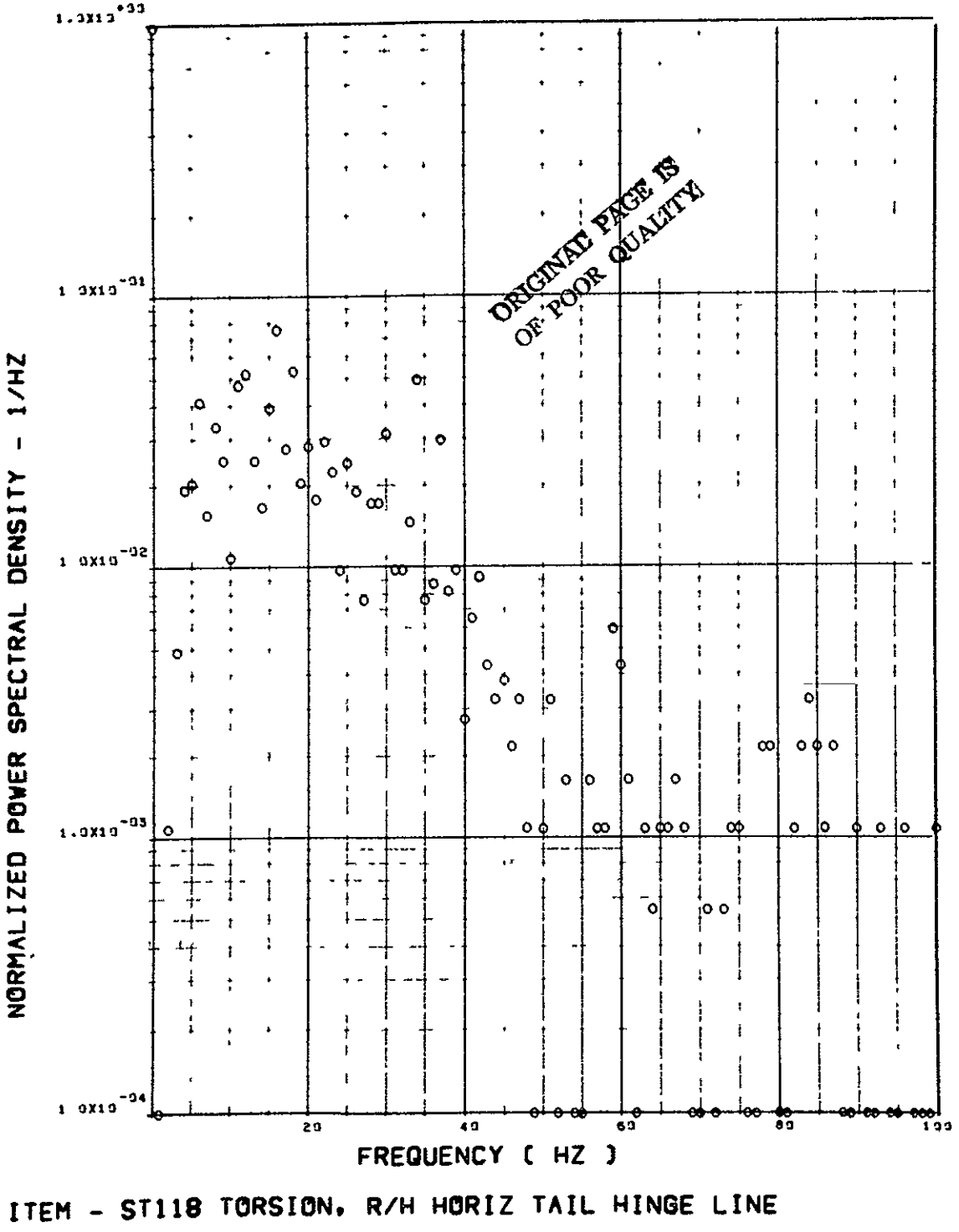

Figure 41. Concluded

REFERENCES

1. Benepe. D.B., Cunningham, A.M., Jr., and Dunmyer, W.D., "An Investigation of Wing Buffeting Response at Subsonic and Transonic Speeds: Phase I F-111A Flight Data Analysis," Volume I - Summary of Technical Approach, Results and Conclusions, NASA CR-152109, May 1978

2. Benepe, D.B., Cunningham, A.M., Jr., and Dunmyer, W.D., "An Investigation of Wing Buffeting Response at Subsonic and Transonic Speeds: Phase I F-111A Flight Data Analysis," Volume II - Plotted Power Spectra, NASA CR-152110, May 1978.

3. Benepe, D.B., Cunningham, A.M., Jr., and Dunmyer, W.D., "An Investigation of Wing Buffeting Response at Subsonic and Transonic Speeds: Phase I F-111A Flight Data Analysis," Volume III - Tabulated Power Spectra, NASA CR-152111, May 1978.

4. Nevius, H.E., F-111A Ground Vibration Test - No Wing Stores (Airplane 12), General Dynamics Fort Worth Division Report FZS-12-167, 5 August 1966, and Supplement 1, 1 August 1967.

5. Nevius, H.E., F-111A Ground Vibration Tests - No Wing Stores (Airplanes 1-11), General Dynamics Fort Worth Division Report FZS-12-060, 1 March 1965.

6. Cunningham, A.M., Jr., Waner, P.G., Watts, D., and Benepe, D.B., "Development and Evaluation of a New Method of Predicting Aircraft Buffet Response," AIAA Paper 75-69, Presented at the 13th AIAA Aerospace Sciences Meeting, Pasadena, California, 20-22 January 1975.

7. Cunningham, A.M., Jr., Benepe, D.B., Watts, D., and Waner, P.G., "A Method for Predicting Full-Scale Buffet Response with Rigid Wind Tunnel Model Fluctuating Pressure Data," Volume I - Prediction Method Development and Assessment, NASA CR-3035.

8. Cunningham, A.M., Jr., Benepe, D.B., Watts, D., and Waner, P.G., "A Method for Predicting Full-Scale Buffet Response with Rigid Wind Tunnel Model Fluctuating Pressure Data," Volume II - Power Spectral Densities for Method Assessment, NASA CR-3036.

GENERAL DYNAMICS

Fort Worth Division

P O. Box 748, Fort Worth, Texas 76101

FWP 2992B 6-74